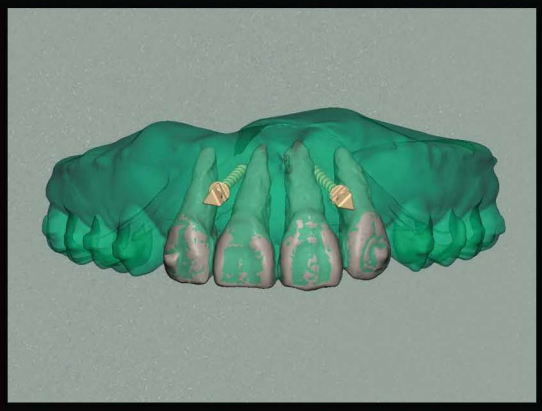
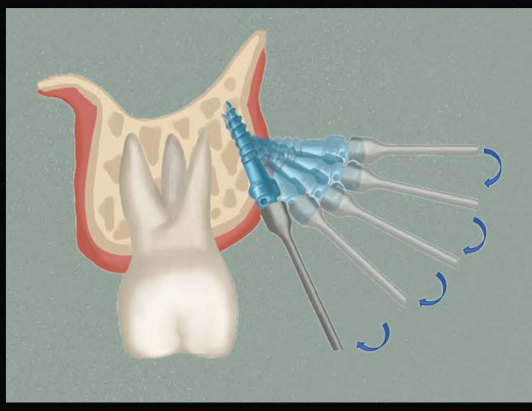
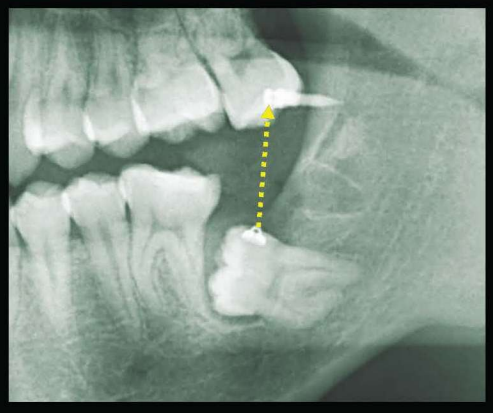
Clinical Insertion Techniques of Orthodontic Temporary Anchorage Devices

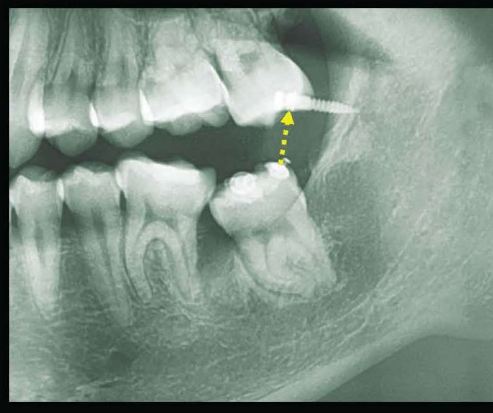
Edited by
Hu Long
Xianglong Han
Wenli Lai











WILEY Blackwell

Clinical Insertion Techniques of Orthodontic Temporary Anchorage Devices

t.me/Dr_Mouayyad_AlbtousH

Clinical Insertion Techniques of Orthodontic Temporary Anchorage Devices

Edited by

Hu Long
Department of Orthodontics
West China Hospital of Stomatology
Sichuan University
Chengdu, China

Xianglong Han
Department of Orthodontics
West China Hospital of Stomatology
Sichuan University
Chengdu, China

Wenli Lai
Department of Orthodontics
West China Hospital of Stomatology
Sichuan University
Chengdu, China

WILEY Blackwell

t.me/Dr_Mouayyad_AlbtousH

This edition first published 2024
© 2024 John Wiley & Sons Ltd

All rights reserved. No part of this publication may be reproduced, stored in a retrieval system, or transmitted, in any form or by any means, electronic, mechanical, photocopying, recording or otherwise, except as permitted by law. Advice on how to obtain permission to reuse material from this title is available at http://www.wiley.com/go/permissions.

The right of editor Hu Long, Xianglong Han, and Wenli Lai to be identified as the editorial material in this work has been asserted in accordance with law.

Registered Offices
John Wiley & Sons, Inc., 111 River Street, Hoboken, NJ 07030, USA
John Wiley & Sons Ltd, The Atrium, Southern Gate, Chichester, West Sussex, PO19 8SQ, UK

For details of our global editorial offices, customer services, and more information about Wiley products visit us at www.wiley.com.

Wiley also publishes its books in a variety of electronic formats and by print-on-demand. Some content that appears in standard print versions of this book may not be available in other formats.

Trademarks: Wiley and the Wiley logo are trademarks or registered trademarks of John Wiley & Sons, Inc. and/or its affiliates in the United States and other countries and may not be used without written permission. All other trademarks are the property of their respective owners. John Wiley & Sons, Inc. is not associated with any product or vendor mentioned in this book.

Limit of Liability/Disclaimer of Warranty
The contents of this work are intended to further general scientific research, understanding, and discussion only and are not intended and should not be relied upon as recommending or promoting scientific method, diagnosis, or treatment by physicians for any particular patient. In view of ongoing research, equipment modifications, changes in governmental regulations, and the constant flow of information relating to the use of medicines, equipment, and devices, the reader is urged to review and evaluate the information provided in the package insert or instructions for each medicine, equipment, or device for, among other things, any changes in the instructions or indication of usage and for added warnings and precautions. While the publisher and authors have used their best efforts in preparing this work, they make no representations or warranties with respect to the accuracy or completeness of the contents of this work and specifically disclaim all warranties, including without limitation any implied warranties of merchantability or fitness for a particular purpose. No warranty may be created or extended by sales representatives, written sales materials or promotional statements for this work. This work is sold with the understanding that the publisher is not engaged in rendering professional services. The advice and strategies contained herein may not be suitable for your situation. You should consult with a specialist where appropriate. The fact that an organization, website, or product is referred to in this work as a citation and/or potential source of further information does not mean that the publisher and authors endorse the information or services the organization, website, or product may provide or recommendations it may make. Further, readers should be aware that websites listed in this work may have changed or disappeared between when this work was written and when it is read. Neither the publisher nor authors shall be liable for any loss of profit or any other commercial damages, including but not limited to special, incidental, consequential, or other damages.

Library of Congress Cataloging-in-Publication Data
Names: Long, Hu, 1988– editor. | Han, Xianglong, editor. | Lai, Wenli, editor.
Title: Clinical insertion techniques of orthodontic temporary anchorage devices / edited by Hu Long, Xianglong Han, Wenli Lai.
Description: Hoboken, NJ : Wiley-Blackwell, 2024. | Includes index.
Identifiers: LCCN 2023032359 (print) | LCCN 2023032360 (ebook) | ISBN 9781119892236 (hardback) | ISBN 9781119892243 (adobe pdf) | ISBN 9781119892250 (epub)
Subjects: MESH: Orthodontic Anchorage Procedures–methods | Dental Implants | Bone Plates | Orthodontic Anchorage Procedures–adverse effects
Classification: LCC RK667.I45 (print) | LCC RK667.I45 (ebook) | NLM WU 426 | DDC 617.6/93–dc23/eng/20231113
LC record available at https://lccn.loc.gov/2023032359
LC ebook record available at https://lccn.loc.gov/2023032360

Cover Design: Wiley
Cover Images: © MirageC/Getty Images; Courtesy of Hu Long

Set in 9.5/12.5pt STIXTwoText by Straive, Pondicherry, India

t.me/Dr_Mouayyad_AlbtousH

Hu Long: I dedicate this book to my cherished wife Avril, my talented son Brian, and my parents for their unfailing love, enduring understanding, resourceful encouragement and unconditional support.

t.me/Dr_Mouayyad_AlbtousH

Contents

About the Editors *xv*
List of Contributors *xvii*
Foreword *xxi*
Preface *xxiii*
Acknowledgements *xxv*

1 An Overview of Orthodontic Temporary Anchorage Devices *1*
Hu Long, Xiaoqi Zhang, Xianglong Han, and Wenli Lai
1.1 Introduction *1*
1.2 Evolution of Orthodontic TADs *1*
1.3 Characteristics of Orthodontic TADs *2*
1.3.1 Materials *2*
1.3.2 Morphology *4*
1.3.3 Drilling Methods: Self-tapping versus Self-drilling *5*
1.4 Mechanical Retention of Orthodontic TADs *5*
1.4.1 Mechanical Retention *5*
1.4.2 Primary Stability and Secondary Stability *7*
1.4.3 Direct versus Indirect Anchorage *8*
1.5 Clinical Indications for Orthodontic TADs *9*
1.5.1 Sagittal Dimension *11*
1.5.2 Vertical Dimension *12*
1.5.3 Transverse Dimension *16*
1.6 Potential Complications *19*
1.7 Summary *21*
References *21*

2 Requirements for the Insertion of Orthodontic Temporary Anchorage Devices *25*
Lin Xiang, Ziwei Tang, Jing Zhou, Hong Zhou, Qingxuan Wang, Waseem S. Al-Gumaei, Hu Long, and Liang Zhang
2.1 Introduction *25*
2.2 Systemic Requirements *26*
2.2.1 Basic Conditions *26*
2.2.2 Systemic Diseases *28*
2.2.3 Drugs *28*
2.2.4 Habits *30*
2.3 Local Requirements *32*
2.3.1 Hard Tissue *32*
2.3.2 Soft Tissue *40*
2.4 Summary *51*
References *51*

t.me/Dr_Mouayyad_AlbtousH

3 General Principles for the Insertion of Orthodontic Temporary Anchorage Devices *55*
Hu Long, Xinyu Yan, Yanzi Gao, Qingxuan Wang, Chenghao Zhang, Rui Shu, Wen Liao, and Xianglong Han
3.1 Introduction *55*
3.2 Anatomy-driven Paradigm *56*
3.2.1 General Principles *56*
3.2.2 Available Anatomical Sites *64*
3.3 Biomechanics-driven Paradigm *75*
3.3.1 Maxillary Molar Uprighting *76*
3.3.2 Molar Intrusion *77*
3.3.3 Incisor Intrusion *79*
3.3.4 Orthodontic Traction of Impacted Molars *79*
3.3.5 Molar Protraction *82*
3.4 Clinical Procedures for Inserting Mini-implants *85*
3.4.1 Preinsertion Preparation *85*
3.4.2 Insertion of Mini-implants *86*
3.4.3 Post-insertion Examination *90*
3.5 Summary *92*
References *92*

4 Maxillary Labial Region *95*
Donger Lin, Huiyi Hong, Xiaolong Li, Jialun Li, Haoxin Zhang, Hong Zhou, Yan Wang, and Hu Long
4.1 Introduction *95*
4.2 Interradicular Sites *95*
4.2.1 Anatomic Features *95*
4.2.2 Biomechanical Considerations *103*
4.2.3 Selection of Appropriate Insertion Sites *107*
4.2.4 Insertion Techniques *107*
4.2.5 Clinical Applications *114*
4.3 Anterior Nasal Spine *125*
4.3.1 Anatomical Features *125*
4.3.2 Biomechanical Considerations *132*
4.3.3 Selection of Appropriate Insertion Sites *132*
4.3.4 Insertion Techniques *134*
4.3.5 Clinical Applications *136*
4.4 Summary *143*
References *143*

5 Maxillary Buccal Region *145*
Lingling Pu, Yanzi Gao, Qinxuan Song, Yang Zhou, Ying Jin, Yongwen Guo, Xianglong Han, and Hu Long
5.1 Introduction *145*
5.2 Interradicular Sites *145*
5.2.1 Anatomical Characteristics *145*
5.2.2 Biomechanical Considerations *156*
5.2.3 Selection of Appropriate Insertion Sites *158*
5.2.4 Insertion Techniques *160*
5.2.5 Clinical Applications *164*
5.3 Infrazygomatic Crest *183*
5.3.1 Anatomical Characteristics *183*
5.3.2 Biomechanical Considerations *194*
5.3.3 Selection of Appropriate Insertion Sites *196*
5.3.4 Insertion Techniques *196*
5.3.5 Clinical Applications *201*

t.me/Dr_Mouayyad_AlbtousH

5.4 Maxillary Tuberosity *223*
5.4.1 Anatomical Characteristics *223*
5.4.2 Biomechanical Considerations *228*
5.4.3 Selection of Appropriate Insertion Sites *229*
5.4.4 Insertion Techniques *229*
5.4.5 Clinical Applications *230*
5.5 Summary *232*
References *232*

6 Maxillary Palatal Region *235*
Jing Zhou, Xinwei Lyu, Hong Zhou, Jiabao Li, Wenqiang Ma, Heyi Tang, Tianjin Tao, Peipei Duan, and Hu Long
6.1 Introduction *235*
6.2 Interradicular Sites *238*
6.2.1 Anatomical Characteristics *238*
6.2.2 Biomechanical Considerations *248*
6.2.3 Selection of Appropriate Insertion Sites *248*
6.2.4 Insertion Techniques *248*
6.2.5 Clinical Applications *252*
6.3 Paramedian Sites *270*
6.3.1 Anatomical Characteristics *270*
6.3.2 Biomechanical Considerations *273*
6.3.3 Selection of Optimal Insertion Sites *273*
6.3.4 Insertion Techniques *273*
6.3.5 Clinical Applications *280*
6.4 Midpalatal Suture *296*
6.4.1 Anatomical Features *297*
6.4.2 Optimal Insertion Sites *298*
6.4.3 Insertion Techniques *299*
6.4.4 Clinical Applications *299*
6.5 Summary *301*
References *301*

7 Mandibular Labial Region *303*
Yi Yang, Donger Lin, Lingling Pu, Shizhen Zhang, Yan Wang, Erpan Alkam, and Hu Long
7.1 Introduction *303*
7.2 Interradicular Sites *305*
7.2.1 Anatomical Characteristics *305*
7.2.2 Biomechanical Perspectives *311*
7.2.3 Determining the Optimal Sites *312*
7.2.4 Insertion Techniques *313*
7.3 Mandibular Symphysis *320*
7.3.1 Anatomical Features *320*
7.3.2 Biomechanical Considerations *323*
7.3.3 Selection of Optimal Sites *325*
7.3.4 Insertion Techniques *325*
7.4 Summary *330*
References *330*

8 Mandibular Buccal Region *333*
Qi Fan, Lu Liu, Chaolun Mo, Xinxiong Xia, Yushi Zhang, Rui Shu, Liang Zhang, and Hu Long
8.1 Introduction *333*
8.2 Interradicular Sites *335*

t.me/Dr_Mouayyad_AlbtousH

8.2.1 Anatomical Characteristics *335*
8.2.2 Biomechanical Considerations *343*
8.2.3 Selection of Appropriate Insertion Sites *343*
8.2.4 Insertion Techniques *345*
8.2.5 Clinical Applications *350*
8.3 Buccal Shelf *364*
8.3.1 Anatomical Characteristics *364*
8.3.2 Biomechanical Considerations *369*
8.3.3 Selection of Appropriate Insertion Sites *371*
8.3.4 Insertion Techniques *372*
8.3.5 Clinical Applications *376*
8.4 Summary *386*
References *387*

9 Mandibular Ramus *389*
Qianyun Kuang, Qi Fan, Chengge Hua, Lingling Pu, and Hu Long
9.1 Introduction *389*
9.2 Anatomical Considerations *389*
9.2.1 Anatomical Location *389*
9.2.2 Hard Tissue Considerations *389*
9.2.3 Soft Tissue Considerations *391*
9.2.4 Optimal Insertion Sites *394*
9.3 Mini-implant Selection *396*
9.4 Insertion Procedure *397*
9.4.1 Insertion Procedures *397*
9.4.2 Insertion on Skulls *397*
9.4.3 Clinical Procedures *399*
9.4.4 Biomechanical Analysis *401*
9.5 Versatile Clinical Applications *402*
9.5.1 Uprighting Mesioangulated Impacted Mandibular Second Molars *402*
9.5.2 Orthodontic Traction of a Vertically Impacted Mandibular Second Molar *405*
9.5.3 Traction of a Lingually Angulated Impacted Mandibular Second Molar *405*
9.5.4 Traction of a Mandibular Third Molar Away from the Inferior Alveolar Canal *409*
9.6 Summary *413*
References *413*

10 The Placement of Miniplates *415*
Lingling Pu, Yi Yang, Xuechun Yuan, Hu Long, and Chengge Hua
10.1 Introduction *415*
10.2 Clinical Features *415*
10.2.1 Structure of Miniplates *415*
10.2.2 Advantages and Disadvantages *417*
10.2.3 Available Anatomical Sites *418*
10.3 Clinical Indications *420*
10.3.1 Orthopaedic Treatment for Skeletal Discrepancy *420*
10.3.2 Anatomical Factors Undesirable for Mini-implants *422*
10.3.3 Biomechanical Advantages *422*
10.4 Insertion Techniques *431*
10.5 Removal Techniques *433*
10.6 Summary *434*
References *435*

t.me/Dr_Mouayyad_AlbtousH

11 Three-dimensional Design and Manufacture of Insertion Guides *437*
Niansong Ye, Lingling Pu, Qi Fan, Wenqiang Ma, Yanqing Wu, Wenli Lai, and Hu Long
11.1 Introduction *437*
11.2 Evolution of Insertion Guides *437*
11.2.1 The Concept of Guided Surgery *437*
11.2.2 Evolution of Guided Insertion for Mini-implants *439*
11.3 Advantages and Disadvantages of Insertion Guides *446*
11.3.1 Advantages *446*
11.3.2 Disadvantages *449*
11.4 Three-dimensional Design of Insertion Guides for Mini-implants *451*
11.4.1 Reconstructing a Three-dimensional Dentition Model *451*
11.4.2 Establishing the Digital Data of Mini-implants and Screwdrivers *457*
11.4.3 Virtual Placement of Mini-implants *459*
11.4.4 Three-dimensional Design of Insertion Guides *461*
11.5 Manufacturing Insertion Guides *464*
11.5.1 Exporting the STL File *464*
11.5.2 Adding Supporting Components for the Insertion Guide *464*
11.5.3 Generating the Actual Insertion Guide Through 3-D Printing *464*
11.5.4 Removing the Supporting Components and Polishing the Insertion Guide *464*
11.5.5 Try-in on the Dental Model *464*
11.5.6 Examples of Insertion Guides for Different Anatomical Sites *466*
11.6 Summary *470*
References *470*

12 Clinical Techniques for Using Insertion Guides *473*
Lingling Pu, Qi Fan, Yuetian Li, Omar M. Ghaleb, Hu Long, and Niansong Ye
12.1 Introduction *473*
12.2 Clinical Procedures *473*
12.2.1 Verifying the Fit of Insertion Guides *473*
12.2.2 Anaesthesia *476*
12.2.3 Inserting Mini-implants *476*
12.2.4 Detaching Screwdrivers and Removing Insertion Guides *479*
12.3 Placement of Mini-implants with Insertion Guides at Different Sites *479*
12.3.1 Labial Interradicular Region *479*
12.3.2 Buccal Interradicular Region *480*
12.3.3 Palatal Region *480*
12.3.4 Buccal Shelf *481*
12.4 Summary *485*
References *485*

13 Root Contact *487*
Xinyu Yan, Yan Wang, Jianru Yi, Hu Long, Xianglong Han, and Wenli Lai
13.1 Introduction *487*
13.2 Clinical Manifestations *488*
13.3 Prognosis *490*
13.3.1 Mini-implants *490*
13.3.2 Periodontal Tissues and Dental Roots *491*
13.4 Risk Factors *493*
13.4.1 Insertion Site *493*
13.4.2 Limited Interradicular Space *493*
13.4.3 Insertion Height *494*

t.me/Dr_Mouayyad_AlbtousH

13.4.4 Insertion Angulation *495*
13.5 Prevention *496*
13.5.1 Prudent Selection of Insertion Sites *496*
13.5.2 Meticulous Design of Insertion Angulation *496*
13.5.3 Appropriate Anaesthesia and Insertion Technique *497*
13.6 Management of Root Contact *498*
13.7 Summary *499*
References *499*

14 Fractures of Orthodontic Temporary Anchorage Devices *501*
Hong Zhou, Jing Zhou, Fan Jian, Heyi Tang, Jianru Yi, Xiaolong Li, and Hu Long
14.1 Introduction *501*
14.2 Risk Factors for Mini-implant Fracture *504*
14.2.1 Operator-associated Factors *504*
14.2.2 Implant-associated Factors *505*
14.2.3 Insertion Site-associated Factors *507*
14.3 Prevention of Mini-implant Fracture *508*
14.3.1 Prudent Selection of Insertion Sites *508*
14.3.2 Judicious Selection of Appropriate Mini-implants *508*
14.3.3 Appropriate Insertion Techniques *508*
14.4 Management of Mini-implant Fracture *511*
14.4.1 Clinical Decisions in Different Clinical Scenarios *511*
14.4.2 Clinical Techniques for Removing Fractured Mini-implants *511*
14.5 Summary *512*
References *512*

15 Soft Tissue Complications *515*
Lin Xiang, Ziwei Tang, Jing Zhou, Heyi Tang, Hu Long, and Jianru Yi
15.1 Introduction *515*
15.2 Clinical Manifestations *516*
15.2.1 Soft Tissue Swelling *516*
15.2.2 Soft Tissue Hyperplasia *516*
15.2.3 Soft Tissue Infection *517*
15.2.4 Soft Tissue Lesion *517*
15.3 Adverse Consequences *519*
15.4 Risk Factors *520*
15.4.1 Patient Factors *520*
15.4.2 Operator Factors *522*
15.4.3 Factors Associated with the Mini-implant *523*
15.5 Prevention *525*
15.5.1 Meticulous Oral Hygiene Care *525*
15.5.2 Prudent Selection of Insertion Sites *525*
15.5.3 Sophisticated Insertion Techniques *525*
15.5.4 Prevention of Excessive Soft Tissue Trauma *526*
15.6 Treatment *528*
15.6.1 Peri-implant Irrigation and Scaling *528*
15.6.2 Removal of Causative Factors *528*
15.6.3 Local Debridement and Drainage *528*
15.6.4 Excision of Hypertrophic Soft Tissue *530*
15.7 Summary *530*
References *531*

t.me/Dr_Mouayyad_AlbtousH

16 Failure of Orthodontic Temporary Anchorage Devices *533*
Xinyu Yan, Xiaoqi Zhang, Jianru Yi, Chen Liang, Xi Du, Lingling Pu, and Hu Long
16.1 Introduction *533*
16.2 Primary Stability and Secondary Stability *534*
16.3 Risk Factors *537*
16.3.1 Patient-associated Factors *537*
16.3.2 Operator-associated Factors *538*
16.3.3 Implant-associated Factors *541*
16.4 Prevention of Mini-implant Failure *543*
16.4.1 Determining Optimal Insertion Sites *544*
16.4.2 Choosing Appropriate Mini-implants *544*
16.4.3 Appropriate Insertion Techniques *544*
16.4.4 Meticulous Oral Hygiene *544*
16.5 Management of Mini-implant Failure *544*
16.5.1 Tightening Mini-implants *In Situ* *544*
16.5.2 Inserting a New Mini-implant at a Neighbouring Site *544*
16.6 Summary *546*
References *546*

Index *549*

t.me/Dr_Mouayyad_AlbtousH

About the Editors





Dr Hu Long is Associate Professor of Orthodontics at the Department of Orthodontics, West China Hospital of Stomatology, Sichuan University. He completed a combined DDS/PhD programme on Orthodontics and obtained the DDS and PhD degree in 2014. He pursued postdoctoral study in Harvard Medical School, Boston, MA from 2016 to 2017.

Dr Long has received over ten research grants, including basic, translational and clinical research grants. He has conducted both basic and clinical studies related to orthodontics and has published over 90 basic and clinical articles in peer-reviewed scientific and orthodontic journals, including *AJO-DO*, *Angle Orthodontist*, *European Journal of Orthodontics* and *Progress in Orthodontics*. He lectures nationally and internationally on orthodontic TADs and clear aligner therapy. He has edited one book on orthodontic TADs (*Orthodontic Mini-Implants: Innovative Clinical Applications*) and authored chapters for a book on clear aligner therapy (*Invisalign Clear Aligner Technique*).

He holds five national invention patents on orthodontic appliances, including palatal mini-implant-assisted molar distalisation with clear aligner, Albert loop for mandibular molar protraction with mini-implants and Albert cantilever for molar protraction with clear aligner. He also invented the first evaluation system for appraising treatment difficulty with clear aligner – the Clear Aligner Treatment Complexity Assessment Tool (CAT-CAT).

Professor Xianglong Han serves as a professor, doctoral supervisor and Vice Dean of the West China Hospital of Stomatology, Sichuan University. He has received several international and national awards for both scientific and clinical excellence, including the IADR/Unilever Hatton award, ASBMR award, Webster Jee award and Sichuan Province Scientific and Technology Progress awards. Professor Han is a Fellow of the Edward H. Angle Society of Orthodontists and a Fellow of the International College of Dentists.

Professor Han has received several research grants, including five national research grants and five provincial grants, which have supported his scientific and clinical research. He has published over 100 publications in both basic and clinical peer-reviewed journals. Beyond his research and publications, Professor Han has actively contributed to the dissemination of knowledge in orthodontics. He has co-edited one book on orthodontic temporary anchorage devices entitled *Orthodontic Mini-Implants: Innovative Clinical Applications* and has authored book chapters for several textbooks.

Furthermore, Professor Han's innovative ideas have led to significant advancements in orthodontic technology. Holding 14 national invention patents on orthodontic appliances, he has demonstrated his commitment to improving orthodontic treatment methods. Notably, his pioneering efforts have resulted in the development of the DSA self-ligating brackets, translating his novel ideas into orthodontic products that positively impact patient care and treatment outcomes.

t.me/Dr_Mouayyad_AlbtousH



Professor Wenli Lai is Professor of Orthodontics at the Department of Orthodontics, West China Hospital of Stomatology, Sichuan University. She obtained her PhD degree in orthodontics in 1994 and was a postdoctoral fellow in Niigata University, Japan, from 1999 to 2001. Currently, Professor Lai is director of the Discipline of Orthodontics and Pediatric Dentistry, West China Hospital of Stomatology, Sichuan University. She is Chairman of the Professional Committee of Oral Sedation and Analgesia of Sichuan Stomatological Association, Vice Chairman of Orthodontic Professional Committee, Standing Committee of Orthodontic Professional Committee of Chinese Dental Association and a Fellow of the International College of Dentists.

Professor Lai has conducted both basic and clinical research on orthodontics and has published more than 160 publications in peer-reviewed journals. She lectures on clear aligner therapy nationally and internationally. She has edited one book on clear aligner therapy (*Invisalign Clear Aligner Technique*) and co-edited several textbooks on orthodontics. She co-invented the first evaluation system for appraising treatment difficulty with clear aligner – the Clear Aligner Treatment Complexity Assessment Tool (CAT-CAT).

t.me/Dr_Mouayyad_AlbtousH

List of Contributors

Waseem S. Al-Gumaei
Department of Orthodontics
State Key Laboratory of Oral Diseases and National Clinical Research Center for Oral Diseases
West China Hospital of Stomatology
Sichuan University, Chengdu, China

Erpan Alkam
Department of Orthodontics
State Key Laboratory of Oral Diseases and National Clinical Research Center for Oral Diseases
West China Hospital of Stomatology
Sichuan University, Chengdu, China

Xi Du
Department of Orthodontics
State Key Laboratory of Oral Diseases and National Clinical Research Center for Oral Diseases
West China Hospital of Stomatology
Sichuan University, Chengdu, China

Peipei Duan
Department of Orthodontics
State Key Laboratory of Oral Diseases and National Clinical Research Center for Oral Diseases
West China Hospital of Stomatology
Sichuan University, Chengdu, China

Qi Fan
Department of Orthodontics
State Key Laboratory of Oral Diseases and National Clinical Research Center for Oral Diseases
West China Hospital of Stomatology
Sichuan University, Chengdu, China

Yanzi Gao
Department of Orthodontics
State Key Laboratory of Oral Diseases and National Clinical Research Center for Oral Diseases
West China Hospital of Stomatology
Sichuan University, Chengdu, China

Omar M. Ghaleb
Department of Orthodontics
State Key Laboratory of Oral Diseases and National Clinical Research Center for Oral Diseases
West China Hospital of Stomatology
Sichuan University, Chengdu, China

Yongwen Guo
Department of Orthodontics
State Key Laboratory of Oral Diseases and National Clinical Research Center for Oral Diseases
West China Hospital of Stomatology
Sichuan University, Chengdu, China

Xianglong Han
Department of Orthodontics
State Key Laboratory of Oral Diseases and National Clinical Research Center for Oral Diseases
West China Hospital of Stomatology
Sichuan University, Chengdu, China

Huiyi Hong
Department of Orthodontics
State Key Laboratory of Oral Diseases and National Clinical Research Center for Oral Diseases
West China Hospital of Stomatology
Sichuan University, Chengdu, China

Chengge Hua
Department of General Dentistry
State Key Laboratory of Oral Diseases and National Clinical Research Center for Oral Diseases
West China Hospital of Stomatology
Sichuan University, Chengdu, China

Fan Jian
Department of Orthodontics
State Key Laboratory of Oral Diseases and National Clinical Research Center for Oral Diseases
West China Hospital of Stomatology
Sichuan University, Chengdu, China

t.me/Dr_Mouayyad_AlbtousH

Ying Jin
Department of Orthodontics
State Key Laboratory of Oral Diseases and National
Clinical Research Center for Oral Diseases
West China Hospital of Stomatology
Sichuan University, Chengdu, China

Qianyun Kuang
Department of Orthodontics
State Key Laboratory of Oral Diseases and National
Clinical Research Center for Oral Diseases
West China Hospital of Stomatology
Sichuan University, Chengdu, China

Wenli Lai
Department of Orthodontics
State Key Laboratory of Oral Diseases and National
Clinical Research Center for Oral Diseases
West China Hospital of Stomatology
Sichuan University, Chengdu, China

Jiabao Li
Department of General Dentistry
State Key Laboratory of Oral Diseases and National
Clinical Research Center for Oral Diseases
West China Hospital of Stomatology
Sichuan University, Chengdu, China

Private Practice, Chengdu, China

Jialun Li
Department of Orthodontics
State Key Laboratory of Oral Diseases and National
Clinical Research Center for Oral Diseases
West China Hospital of Stomatology
Sichuan University, Chengdu, China

Xiaolong Li
Department of Orthodontics
State Key Laboratory of Oral Diseases and National
Clinical Research Center for Oral Diseases
West China Hospital of Stomatology
Sichuan University, Chengdu, China

Yuetian Li
Department of Orthodontics
State Key Laboratory of Oral Diseases and National
Clinical Research Center for Oral Diseases
West China Hospital of Stomatology
Sichuan University, Chengdu, China

Chen Liang
Private Practice, Chengdu, China

Wen Liao
Department of Orthodontics
State Key Laboratory of Oral Diseases and National
Clinical Research Center for Oral Diseases
West China Hospital of Stomatology
Sichuan University, Chengdu, China

Donger Lin
Department of Orthodontics
State Key Laboratory of Oral Diseases and National
Clinical Research Center for Oral Diseases
West China Hospital of Stomatology
Sichuan University, Chengdu, China

Lu Liu
Department of Orthodontics
State Key Laboratory of Oral Diseases and National
Clinical Research Center for Oral Diseases
West China Hospital of Stomatology
Sichuan University, Chengdu, China

Department of Maxillofacial Orthognathics
Tokyo Medical and Dental University
Graduate School, Tokyo, Japan

Hu Long
Department of Orthodontics
State Key Laboratory of Oral Diseases and National
Clinical Research Center for Oral Diseases
West China Hospital of Stomatology
Sichuan University, Chengdu, China

Xinwei Lyu
Department of Orthodontics
Hospital of Stomatology
Sun Yat-Sen University, Guangzhou, China

Wenqiang Ma
Private Practice, Chengdu, China

Chaolun Mo
Department of Orthodontics
Stomatological Hospital of Guizhou Medical University
Guiyang, China

Lingling Pu
Department of Orthodontics
State Key Laboratory of Oral Diseases and National
Clinical Research Center for Oral Diseases
West China Hospital of Stomatology
Sichuan University, Chengdu, China

Private Practice, Chengdu, China

t.me/Dr_Mouayyad_AlbtousH

Rui Shu
Department of Pediatric Dentistry
State Key Laboratory of Oral Diseases and National Clinical Research Center for Oral Diseases
West China Hospital of Stomatology
Sichuan University, Chengdu, China

Qinxuan Song
Department of Prosthodontics
State Key Laboratory of Oral Diseases and National Clinical Research Center for Oral Diseases
West China Hospital of Stomatology
Sichuan University, Chengdu, China

Heyi Tang
Department of Head and Neck Oncology
State Key Laboratory of Oral Diseases and National Clinical Research Center for Oral Diseases
West China Hospital of Stomatology
Sichuan University, Chengdu, China

Ziwei Tang
Department of Orthodontics
State Key Laboratory of Oral Diseases and National Clinical Research Center for Oral Diseases
West China Hospital of Stomatology
Sichuan University, Chengdu, China

Tianjin Tao
Department of Orthodontics
State Key Laboratory of Oral Diseases and National Clinical Research Center for Oral Diseases
West China Hospital of Stomatology
Sichuan University, Chengdu, China

Qingxuan Wang
Department of Orthodontics
State Key Laboratory of Oral Diseases and National Clinical Research Center for Oral Diseases
West China Hospital of Stomatology
Sichuan University, Chengdu, China

Yan Wang
Department of Orthodontics
State Key Laboratory of Oral Diseases and National Clinical Research Center for Oral Diseases
West China Hospital of Stomatology
Sichuan University, Chengdu, China

Yanqing Wu
Private Practice, Chengdu, China

Xinxiong Xia
Private Practice, Chengdu, China

Lin Xiang
Department of Implantology
State Key Laboratory of Oral Diseases and National Clinical Research Center for Oral Diseases
West China Hospital of Stomatology
Sichuan University, Chengdu, China

Xinyu Yan
Department of Orthodontics
State Key Laboratory of Oral Diseases and National Clinical Research Center for Oral Diseases
West China Hospital of Stomatology
Sichuan University, Chengdu, China

Yi Yang
Department of Orthodontics
State Key Laboratory of Oral Diseases and National Clinical Research Center for Oral Diseases
West China Hospital of Stomatology
Sichuan University, Chengdu, China

Niansong Ye
Private Practice, Shanghai, China

Jianru Yi
Department of Orthodontics
State Key Laboratory of Oral Diseases and National Clinical Research Center for Oral Diseases
West China Hospital of Stomatology
Sichuan University, Chengdu, China

Xuechun Yuan
Department of Orthodontics
State Key Laboratory of Oral Diseases and National Clinical Research Center for Oral Diseases
West China Hospital of Stomatology
Sichuan University, Chengdu, China

Chenghao Zhang
Department of Orthodontics
State Key Laboratory of Oral Diseases and National Clinical Research Center for Oral Diseases
West China Hospital of Stomatology
Sichuan University, Chengdu, China

Haoxin Zhang
Department of Orthodontics
State Key Laboratory of Oral Diseases and National Clinical Research Center for Oral Diseases
West China Hospital of Stomatology
Sichuan University, Chengdu, China

t.me/Dr_Mouayyad_AlbtousH

Liang Zhang
Department of Implantology
State Key Laboratory of Oral Diseases and National Clinical Research Center for Oral Diseases
West China Hospital of Stomatology
Sichuan University, Chengdu, China

Center of Stomatology
West China Xiamen Hospital of Sichuan University
Xiamen, Fujian, China

Shizhen Zhang
Department of Orthodontics
State Key Laboratory of Oral Diseases and National Clinical Research Center for Oral Diseases
West China Hospital of Stomatology
Sichuan University, Chengdu, China

Faculty of Dentistry
The University of Hong Kong
Hong Kong, SAR, China

Yushi Zhang
Department of Orthodontics
State Key Laboratory of Oral Diseases and National Clinical Research Center for Oral Diseases
West China Hospital of Stomatology
Sichuan University, Chengdu, China

Xiaoqi Zhang
Department of Orthodontics
State Key Laboratory of Oral Diseases and National Clinical Research Center for Oral Diseases
West China Hospital of Stomatology
Sichuan University, Chengdu, China

Hong Zhou
Department of Orthodontics
State Key Laboratory of Oral Diseases and National Clinical Research Center for Oral Diseases
West China Hospital of Stomatology
Sichuan University, Chengdu, China

Private Practice, Chengdu, China

Jing Zhou
Department of Pediatric Dentistry
State Key Laboratory of Oral Diseases and National Clinical Research Center for Oral Diseases
West China Hospital of Stomatology
Sichuan University, Chengdu, China

Yang Zhou
Private Practice, Chengdu, China

t.me/Dr_Mouayyad_AlbtousH

Foreword

I am honoured and delighted to write the foreword for this monumental book on the clinical insertion techniques of orthodontic TADs. The introduction of TADs into orthodontic treatment has revolutionised the concept of orthodontic biomechanics. When TADs were initially applied in orthodontic treatment, they were primarily utilised as 'absolute' anchorage to achieve limited tooth movements, e.g. augmentation of molar anchorage for premolar extraction cases. Then, creative practitioners started to apply TADs in various ways to treat difficult cases and achieve challenging orthodontic tooth movements, which broadened the spectrum of the clinical applications of TADs. As a result, orthodontic TADs have become an essential tool in contemporary orthodontic practice.

Although some practitioners have a good understanding of the clinical applications of TADs, they may face difficulty inserting TADs themselves in clinical settings. Fortunately, this book is the first comprehensive guide primarily focusing on the detailed insertion techniques of orthodontic TADs. In addition to illustrating detailed insertion techniques, this book features associated anatomical characteristics and relevant clinical applications in a logical way. Thus, an appropriate balance, including both theoretical and practical applications, is presented in this book.

In addition to mini-implants, miniplates are presented and the step-by-step insertion techniques of miniplates are well displayed and illustrated in this book. Guided insertion techniques through 3D design and manufacturing are also included.

With over 800 beautifully illustrated figures, this book is indispensable for both orthodontic practitioners and students and enables readers to perform 'miraculous' orthodontic tooth movements with TADs, achieving results that were not possible in previous generations.

Steven J. Lindauer, DMD, MDentSc
Editor, *The Angle Orthodontist*
Paul Tucker Goad Professor and Chair
Department of Orthodontics
Virginia Commonwealth University
Richmond, Virginia, USA

t.me/Dr_Mouayyad_AlbtousH

Preface

Orthodontics is not a static discipline but is changing and developing all the time. This is not only due to the development of orthodontic materials but also the novel ideas and innovations that enthusiastic orthodontic practitioners suggest. Since the introduction of the concept of skeletal anchorage in 1945, orthodontic temporary anchorage devices (TADs) have revolutionised the concept of orthodontic anchorage and brought about tremendous paradigm shifts in contemporary orthodontic treatment. The envelope of orthodontic tooth movements has been largely expanded by orthodontic TADs. More predictable orthodontic treatment outcomes can be accomplished with TADs, such as correction of gummy smile and molar anchorage reinforcement. Moreover, practitioners are able to achieve challenging orthodontic tooth movements that were deemed impossible with conventional biomechanics, e.g. deeply impacted mandibular molars.

Nowadays, with numerous case reports showcasing the versatile applications of orthodontic TADs in the orthodontic literature, orthodontic practitioners, residents and students may gain a good understanding of the clinical applications of TADs for various challenging orthodontic tooth movements, e.g. incisor intrusion for the correction of gummy smile, molar distalisation, molar protraction, molar intrusion, skeletal expansion and maxillary skeletal protraction. However, practitioners may have difficulty in determining the optimal insertion sites of mini-implants for a particular tooth movement, e.g. palatal mini-implants for molar intrusion. Furthermore, even if some practitioners know the optimal anatomical sites of mini-implants for specific clinical scenarios (e.g. insertion of a mini-implant at the mandibular ramus region for a deeply impacted mandibular molar), they may eventually give up since they have no confidence in inserting mini-implants at these locations. This book offers solutions to these clinical problems.

This book is divided into five parts arranged in a logical way. The first part covers the general considerations of TADs and the second explores and offers detailed clinical insertion techniques for different anatomical sites. Specifically, a total of six anatomical regions (maxillary labial region, maxillary buccal region, palatal region, mandibular labial region, mandibular buccal region and mandibular ramus) are covered in this part. For each region, site-specific anatomical features, detailed and well-illustrated insertion techniques and site-specific clinical applications are sequentially presented. The third section delves into the insertion techniques of miniplates and the fourth part covers the cutting-edge guided insertion techniques of mini-implants. The adverse effects and complications associated with TADs are described in the fifth part.

We trust that this book will appeal to orthodontic practitioners who insert TADs by themselves and to implantologists who help orthodontists place TADs. We welcome potential readers to give us critical feedback so that the clinical insertion techniques of TADs can be advanced.

Hu Long, DDS, PhD
Associate Professor
Department of Orthodontics
West China Hospital of Stomatology
Sichuan University
Chengdu, 2023

t.me/Dr_Mouayyad_AlbtousH

Acknowledgements

My sincere thanks first go to my mentor, colleague, co-editor of this book and world-renowned clear aligner practitioner and educator, Professor Wenli Lai, for her enduring inspiration, encouragement and support. Her active and innovative incorporation of TADs into clear aligner therapy renders challenging tooth movements with clear aligner more predictable.

My gratitude also goes to the co-editor of this book, Professor Xianglong Han, for his kind help and inspiration. His complex and excellent clinical cases have always inspired me.

My special thanks go to Professor Chengge Hua for his kind patience in guiding me and my team to place miniplates and to Professor Zheng Yang for his resourceful encouragement that fosters my multidisciplinary thinking.

I also want to express my sincere thanks to all the contributors for their kind efforts and patience in writing this book and for their excellent contributions.

Lingling Pu and Jing Zhou deserve a special mention. I sincerely thank Lingling Pu, an irreplaceable colleague, for her enduring support in helping me at each step of preparing this book. She is an excellent orthodontist with an extraordinary vision, who will lead her orthodontic team to a bright future. I also would like to express my gratitude to Jing Zhou, an unparalleled collaborator, for her beautiful illustrations and for her constant support in writing and revising several book chapters. Her kind patience will make her an exceptional paediatric dentist and orthodontist.

My thanks also go to the entire Wiley team for their invaluable help in producing this book.

t.me/Dr_Mouayyad_AlbtousH

1

An Overview of Orthodontic Temporary Anchorage Devices

Hu Long, Xiaoqi Zhang, Xianglong Han, and Wenli Lai

Department of Orthodontics, State Key Laboratory of Oral Diseases and National Clinical Research Center for Oral Diseases, West China Hospital of Stomatology, Sichuan University, Chengdu, China

1.1 Introduction

The advent of orthodontic temporary anchorage devices (TADs) has revolutionised the concept of orthodontic anchorage and brought about tremendous paradigm shifts in contemporary orthodontic treatment. The range of orthodontic tooth movements has been expanded by the clinical applications of orthodontic TADs. Orthodontic tooth movements that were deemed difficult or even impossible with traditional anchorage modalities can now be accomplished through TADs. This chapter offers a brief overview of the evolution, characteristics, clinical indications and complications of TADs.

1.2 Evolution of Orthodontic TADs

The first attempt to apply TADs for orthodontic tooth movement can be traced back to 1945 when Gainsforth and Higley placed vitallium screws into the mandibular rami of dogs for *en masse* distalisation of the whole maxillary dentition (Figure 1.1).[1] Unfortunately, all the screws became loose and failed within one month. Examinations of mandibles from the sacrificed dogs displayed wide areas of bone destruction at the implantation site, which frustrated further exploration of using TADs in orthodontic treatments.

It was not until 1969 that the concept of TADs was revisited by Linkow.[2] He placed an endosseous blade-vent implant into an edentulous area in the mandibular posterior region of a patient. This blade-vent implant was used for upper anterior retraction by means of class II intermaxillary orthodontic traction (Figure 1.2). The stability of this blade-vent implant was demonstrated in a follow-up report by the same author.[3] In contrast to the vitallium screws used in 1945, the blade-vent implants were made of titanium alloy whose five-year long-term stability and high biocompatibility were evidenced by Branemark et al. in 1969.[4] This successful and stable application of blade-vent implants for orthodontic purposes opened up the possibility of TADs for orthodontic biomechanics.

In 1983, Creekmore et al. placed a mini-implant into the anterior nasal spine to offer intrusive force for deep bite correction.[5] An inspiring clinical success was noted as the upper incisors had been intruded for 6 mm without mini-implant failure (Figure 1.3), inspiring more practitioners to explore advanced and sophisticated biomechanical applications of TADs.

Later, with the development of implant materials, enthusiastic practitioners made repeated clinical attempts to expand the clinical scope of orthodontic TADs and to refine their sophisticated biomechanics. Specifically, clinical applications of TADs have evolved from *en masse* anterior retraction to sophisticated orthodontic movements (e.g. traction of impacted teeth), and even to orthopaedic movements (e.g. maxillary skeletal expansion) (Figure 1.4). Moreover, most insertion sites were initially limited to interradicular areas and have been expanded to extra-alveolar areas (e.g. infrazygomatic crest, buccal shelf and mandibular ramus) to fulfil advanced biomechanical requirements for treating complex and challenging orthodontic patients (Figure 1.5).

Clinical Insertion Techniques of Orthodontic Temporary Anchorage Devices, First Edition. Edited by Hu Long, Xianglong Han, and Wenli Lai.
© 2024 John Wiley & Sons Ltd. Published 2024 by John Wiley & Sons Ltd.

t.me/Dr_Mouayyad_AlbtousH

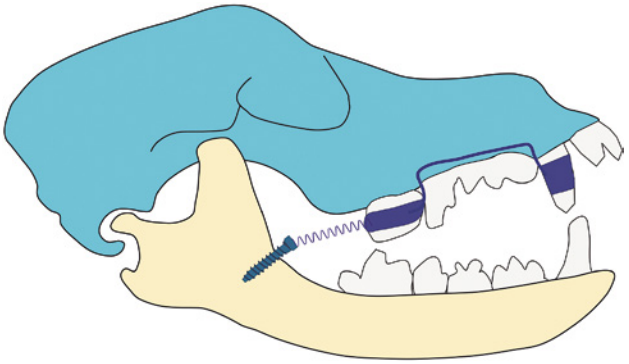


Figure 1.1 A vitallium screw was implanted into the mandibular ramus in a dog for *en masse* distalisation of the whole maxillary dentition.

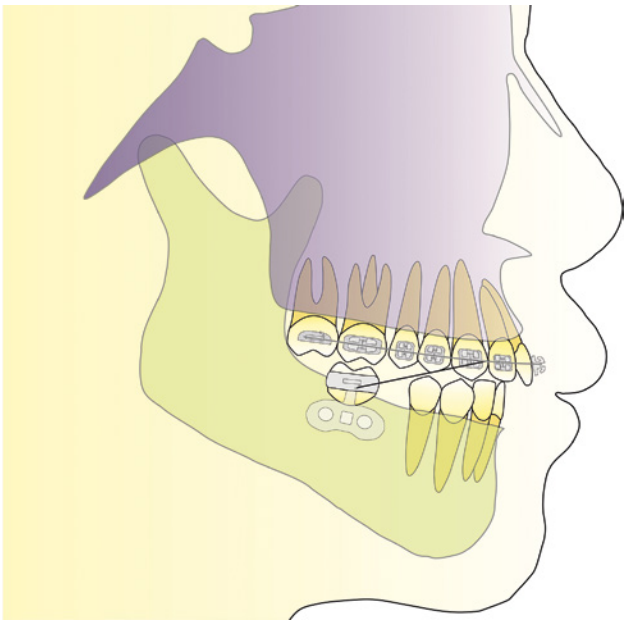


Figure 1.2 A blade-vent implant was inserted at the mandibular posterior region for upper anterior retraction.

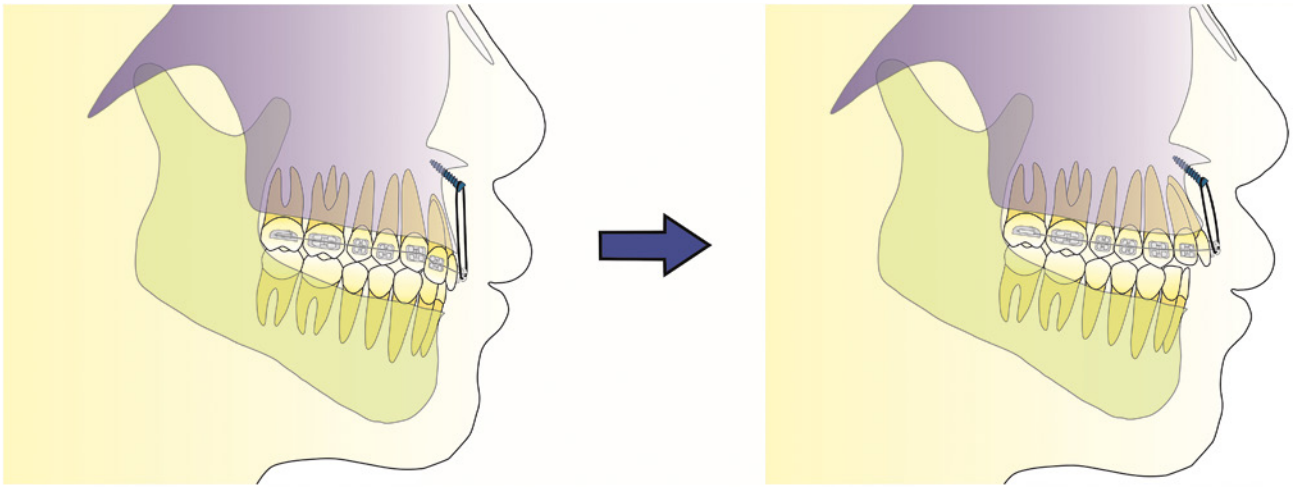


Figure 1.3 A schematic illustration demonstrating that the upper incisors are successfully intruded through a mini-implant at the anterior nasal spine region.

1.3 Characteristics of Orthodontic TADs

1.3.1 Materials

Orthodontic TADs must withstand orthodontic loading to accomplish various types of orthodontic tooth movements. Thus, orthodontic TADs are required to be stable, non-toxic, biocompatible and resistant to fracture. To meet these requirements, different materials have been investigated in order to determine the optimal materials for orthodontic TADs. To date, three types of materials have been used for orthodontic TADs: titanium alloy, stainless steel and vitallium. Vitallium was the first material used for orthodontic TADs.[1] However, due to undesirable biocompatibility and a higher failure rate, vitallium was gradually replaced by titanium alloy.[6] Stainless steel is also used for orthodontic mini-implants and recent evidence indicates that the success rate is similar between titanium alloy and stainless steel mini-implants.[7] Nowadays, due to high biocompatibility of titanium, orthodontic TADs made of titanium alloy are most frequently used in clinical practice.

t.me/Dr_Mouayyad_AlbtousH

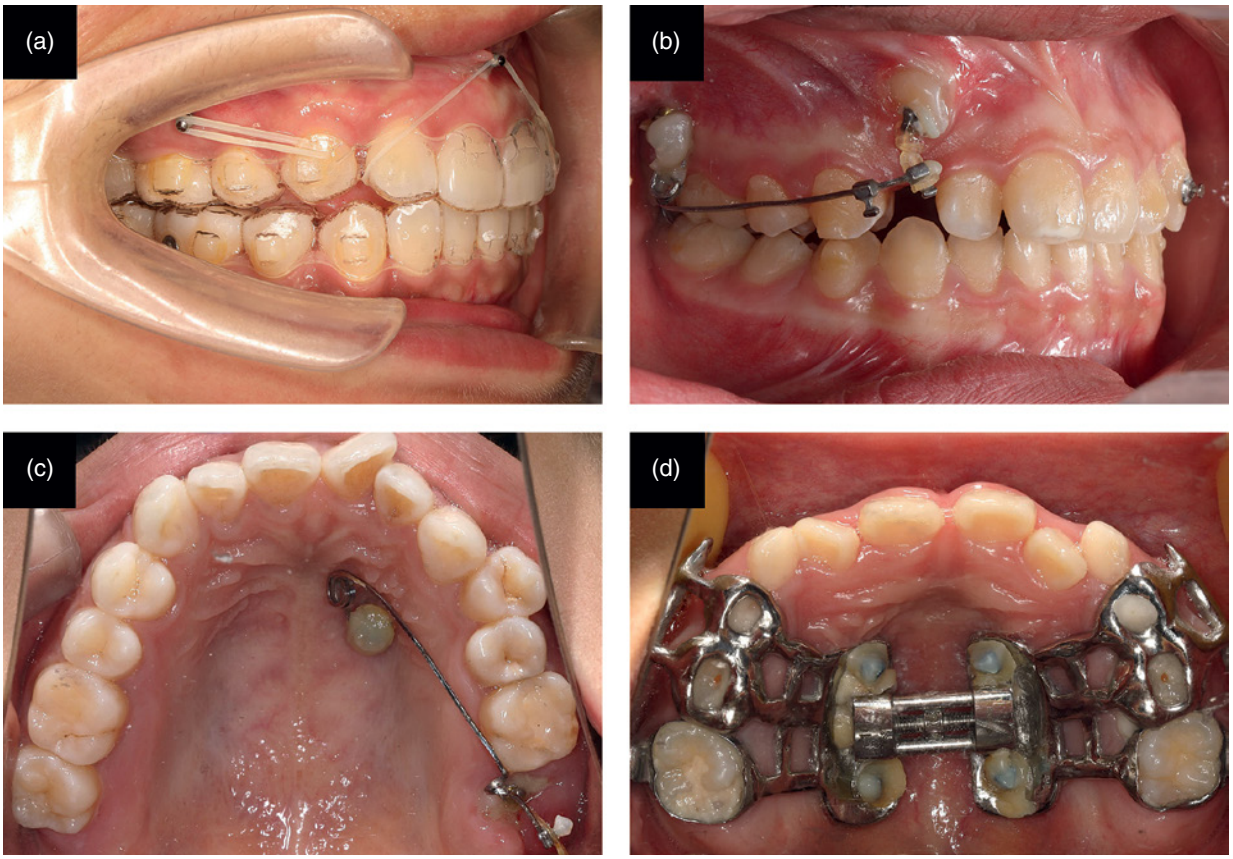


Figure 1.4 Versatile clinical applications of temporary anchorage devices (TADs). (a) Anterior retraction and incisor intrusion. (b) Orthodontic traction of an impacted canine. (c) Orthodontic traction of an impacted maxillary molar. (d) Maxillary skeletal expansion.

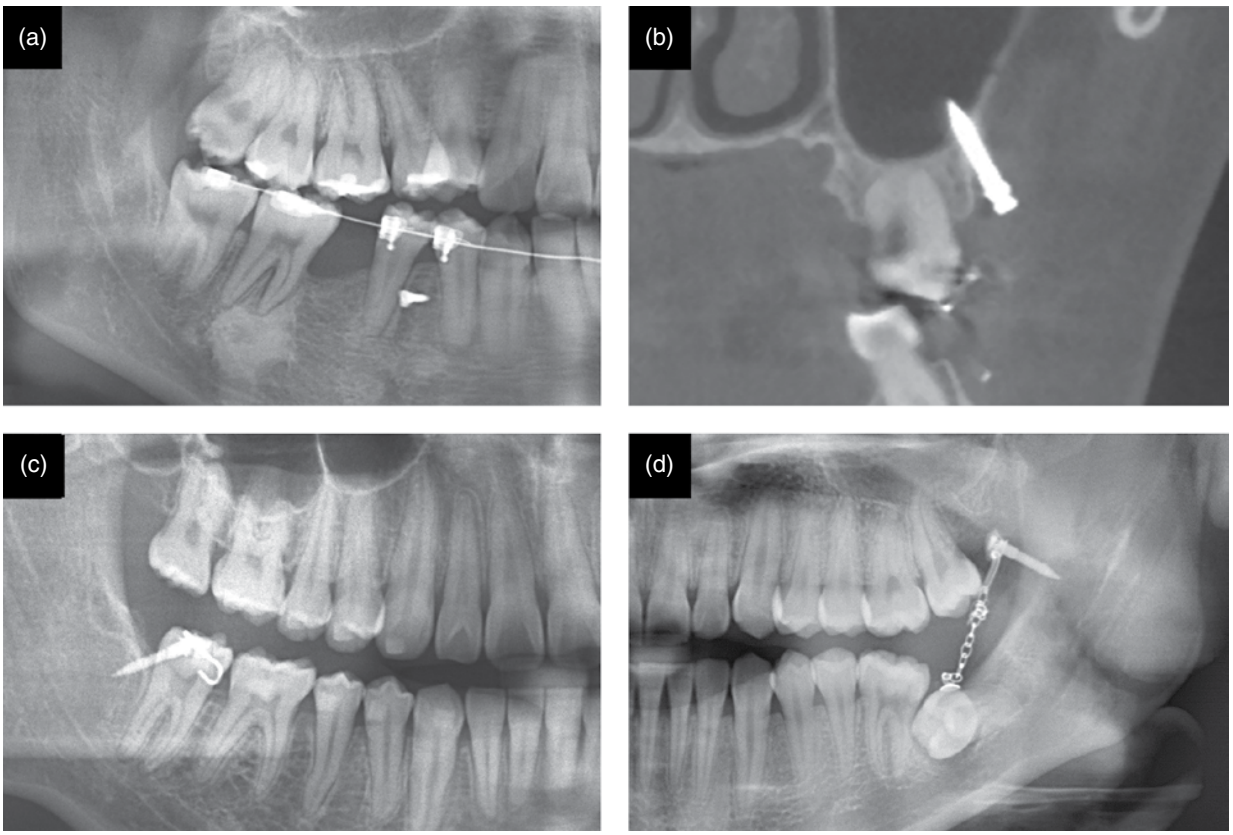


Figure 1.5 Various anatomical sites available for the placement of temporary anchorage devices (TADs). (a) Interradicular site. (b) Infrazygomatic crest. (c) Buccal shelf. (d) Mandibular ramus.

t.me/Dr_Mouayyad_AlbtousH

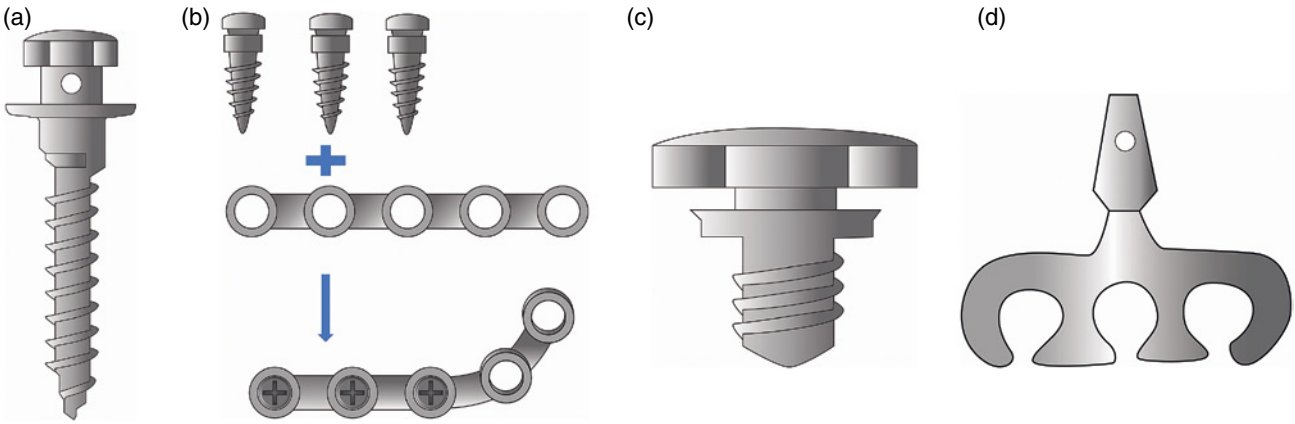


Figure 1.6 Different types of temporary anchorage devices (TADs). (a) Screw-shaped. (b) Plate-shaped. (c) Disc-shaped. (d) Blade-shaped.

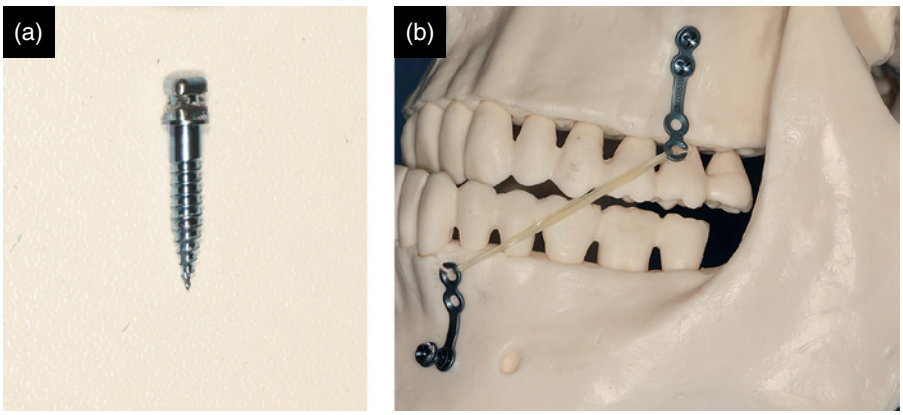


Figure 1.7 Most frequently used TADs in clinical practice. (a) Screw-shaped (mini-implant). (b) Plate-shaped (mini-plate).

1.3.2 Morphology

According to the different shapes of orthodontic TADs, currently available orthodontic TADs can be categorised into four types: screw, plate, disc and blade (Figure 1.6). Screw-shaped and plate-shaped TADs are most frequently used in clinical practice and will be discussed in this book (Figure 1.7). In current literature, various terminologies are used for screw-shaped TADs: mini-implant, miniscrew, mini-screw, micro-screw, micro-implant, etc. For the sake of disambiguity, the term 'mini-implants' is used for screw-shaped TADs in this book.

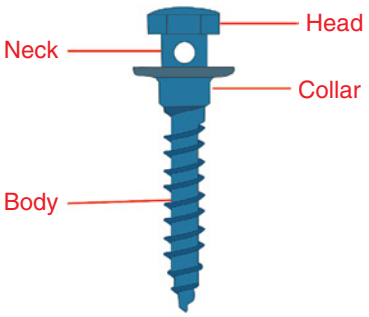


Figure 1.8 The structure of the mini-implant, including body, collar, neck and head.

Mini-implants

Mini-implants are composed of four distinct but contiguous segments: body, collar, neck and head (Figure 1.8). The body of a mini-implant is composed of a central core that ends in a sharp tip and a group of threads that spiral around the central core. Two types of mini-implants are currently available that have different shapes of central cores: tapered and cylindrical. The diameters of tapered mini-implants decrease from the head to the tip while those of cylindrical ones are constant throughout the whole length except for the tip (Figure 1.9).

t.me/Dr_Mouayyad_AlbtousH

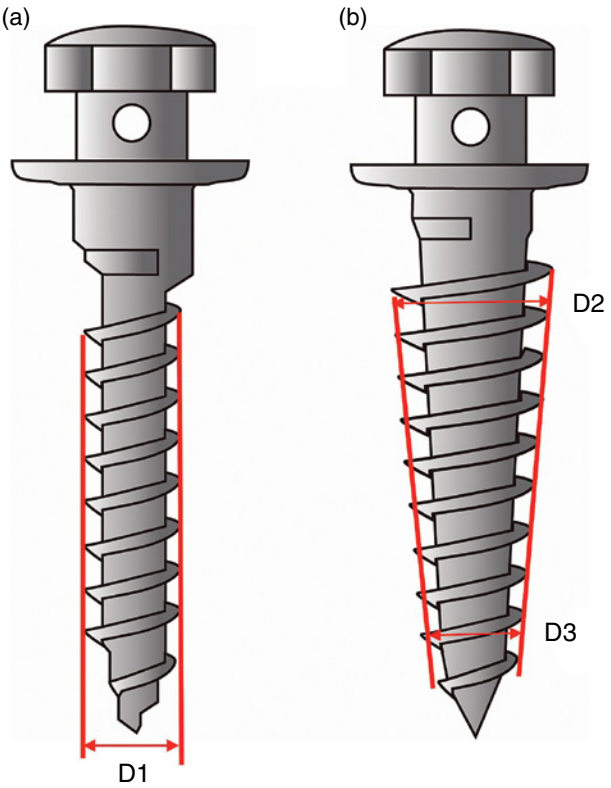


Figure 1.9 Two distinct types of mini-implants. (a) Cylindrical type. (b) Tapered type. Note the diameter of the mini-implant decreases gradually as it approaches the tip.

There are two parameters for thread design that may be different for mini-implants from different manufacturers: thread depth and pitch. Thread depth is the height of the thread and pitch refers to the distance between two nearby threads. Tight pitch means that threads are placed closely while loose pitch refers to threads with a greater distance between them (Figure 1.10). The collar of a mini-implant is a threadless and smooth transgingival portion above the body, ending in a flat plate that joins the collar with the neck. Furthermore, the head and neck lie above the flat plate and serve as a functional loading portion for the application of elastomeric chains, ligature wires or springs.

Mini-plates

Mini-plates are anchored to bone with anchor screws. Various designs of mini-plates are available to accommodate different biomechanical requirements in clinical scenarios. Flap surgery is indicated for the placement of mini-plates and mini-plates are partially embedded underneath soft tissues, with one portion extending out of soft tissue for orthodontic force loading (Figure 1.11).

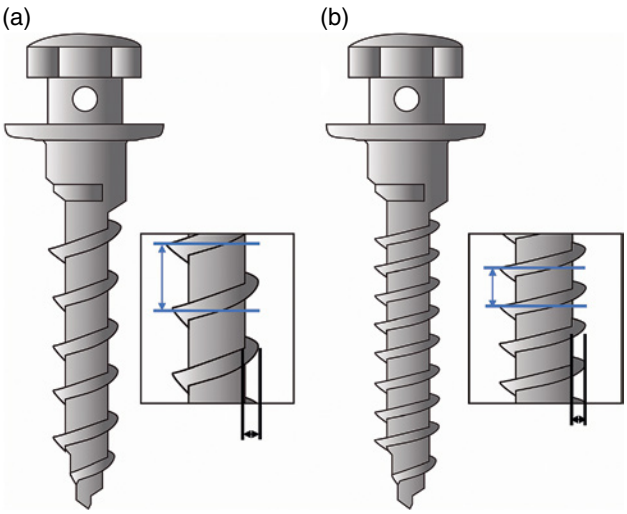


Figure 1.10 Thread design of mini-implants. (a) Loose pitch (the distance between the two blue lines) with greater thread depth (the distance between the two black lines). (b) Tight pitch with less thread pitch.

1.3.3 Drilling Methods: Self-tapping versus Self-drilling

Based on different drilling methods, mini-implants are categorised into self-tapping and self-drilling types. A self-tapping mini-implant requires predrilling at full length to form a pilot hole (Figure 1.12). The pilot hole is smaller than the diameter of the mini-implant and the primary stability of the implant is dependent on the compression of alveolar bone against the self-tapping mini-implant. In contrast, predrilling is not required for a self-drilling mini-implant that has a sharp tip for engaging alveolar bone.

1.4 Mechanical Retention of Orthodontic TADs

1.4.1 Mechanical Retention

It is the mechanical retention or interlocking between alveolar bone and mini-implant that is mainly responsible for the clinical stability of mini-implants. As a mini-implant is being inserted into alveolar bone, the implant engages the bone and the compression of the bone against the mini-implant creates resistance to lateral displacement. Moreover, the interlocking between the alveolar bone and threads prevents pull-out displacement of mini-implants (Figure 1.13). Thus, to improve the stability of mini-implants, special care should be taken to preserve the integration of the mechanical interlocking between bone and mini-implants. If alveolar bone is severely damaged during

t.me/Dr_Mouayyad_AlbtousH

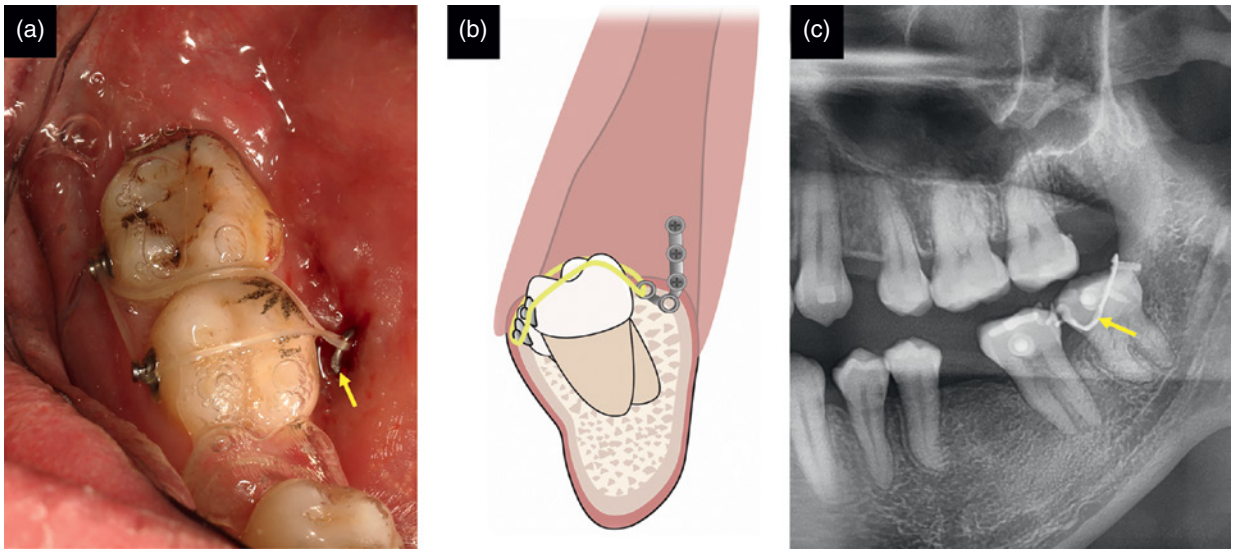


Figure 1.11 Clinical application of a mini-plate for molar uprighting. (a) The force-loading part (yellow arrow) of the mini-plate was utilised for the application of an orthodontic elastic rubber. (b) A schematic illustration showing the application of the mini-plate for molar uprighting. (c) Panoramic radiograph showing the mini-plate (yellow arrow).

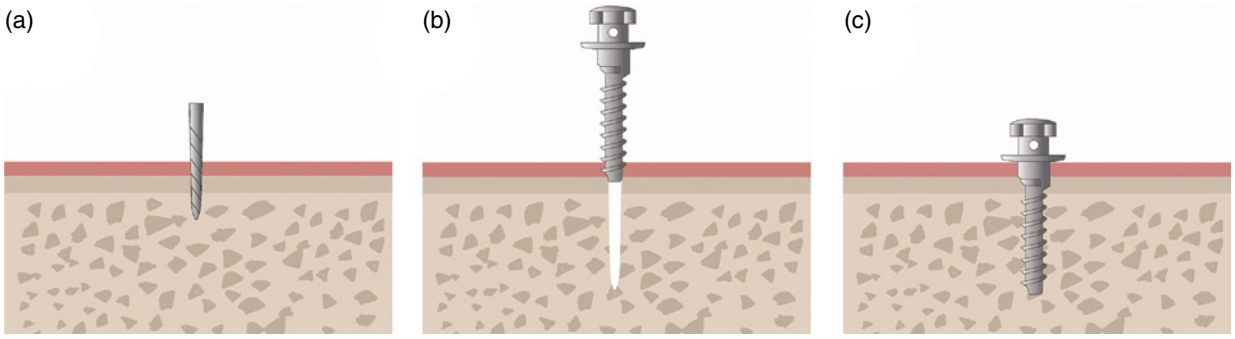


Figure 1.12 Predrilling for a self-tapping mini-implant. (a) Predrilling. (b) Insertion of a self-tapping mini-implant through the pilot hole. (c) Insertion completion.

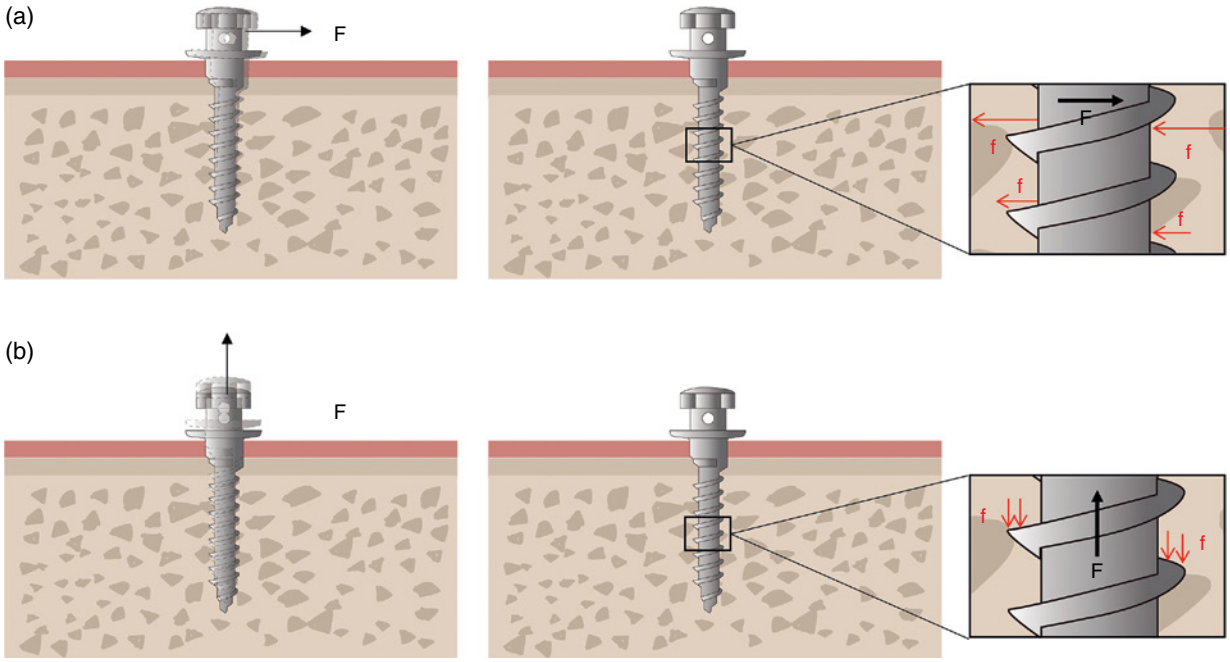


Figure 1.13 The mechanical interlocking between the alveolar bone and the mini-implant ensures the stability of the implant under force loading. (a) Lateral displacement force. When lateral displacement force (black arrow) is applied to the mini-implant, the alveolar bone resists mini-implant displacement by exerting an opposite force (red arrows) on the implant. (b) Pull-out displacement force. When pull-out force (black arrow) is applied to the mini-implant, the alveolar bone resists pull-out displacement by applying an opposite force (red arrows) on the threads of the mini-implant.

t.me/Dr_Mouayyad_AlbtousH

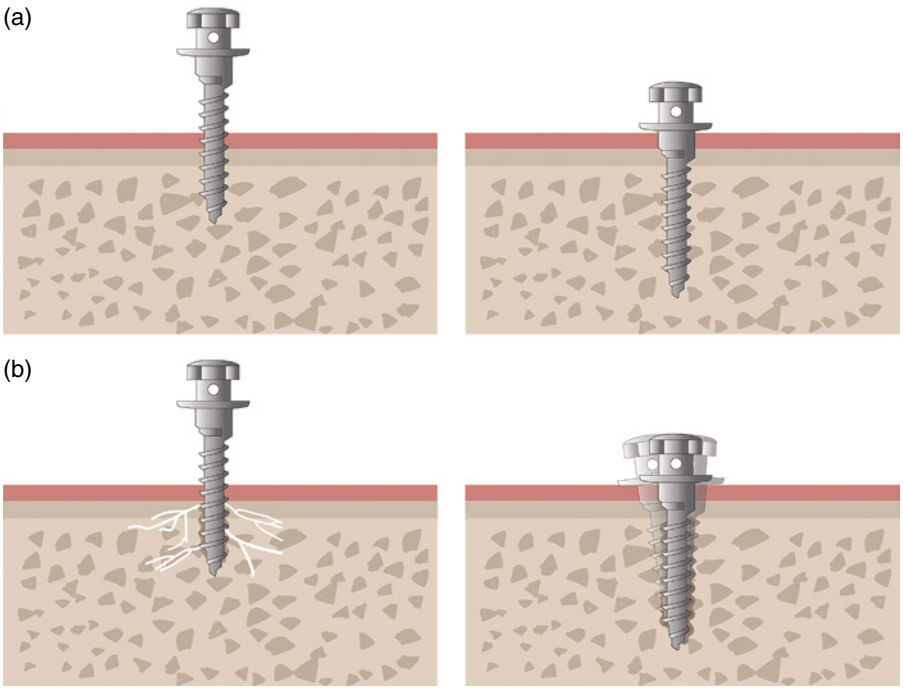


Figure 1.14 The effect of bone damage on mini-implant stability. (a) No or minimal bone damage occurs during insertion and adequate stability is achieved. (b) Extensive bone damage occurs during insertion and the mini-implant exhibits excessive mobility following insertion.

insertion, the stability of the mini-implant will be jeopardised, resulting in mobility of the mini-implant immediately after insertion (Figure 1.14).

1.4.2 Primary Stability and Secondary Stability

The stability that a mini-implant exhibits immediately after insertion is called primary stability and this is achieved by mechanical compression, interlocking and retention between alveolar bone and mini-implant. Although both cortical bone and cancellous bone contribute to primary stability,[8] recent evidence indicates that cortical bone plays a more important role in establishing primary stability.[9,10] It has been shown that alveolar bone damage is inevitable during insertion (Figure 1.15). Alveolar bone damage is manifested as mechanical damage (in the form of bone microcracks) and thermal damage (in the form of bone necrosis).[11,12] The damaged alveolar bone around mini-implants is subject to bone resorption and subsequent bone apposition. Thus, due to the resorption of damaged bone, primary stability that is built by the original (old) alveolar bone decreases gradually after insertion.

As bone remodelling progresses, bone apposition takes place and the newly formed alveolar bone strengthens

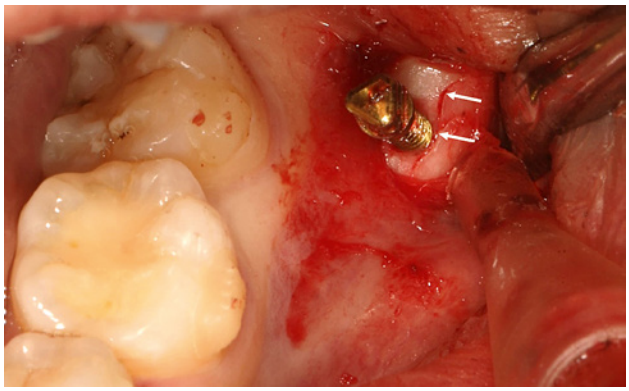


Figure 1.15 Bone damage during insertion of a buccal shelf mini-implant. Note the bone cracks (white arrows) in the vicinity of the insertion site.

mini-implant stability – this is called secondary stability.[13] Secondary stability that is achieved by newly formed alveolar bone increases gradually after the placement of mini-implants. Clinical stability (overall stability) of mini-implants is the sum of primary stability and secondary stability (Figure 1.16).

t.me/Dr_Mouayyad_AlbtousH

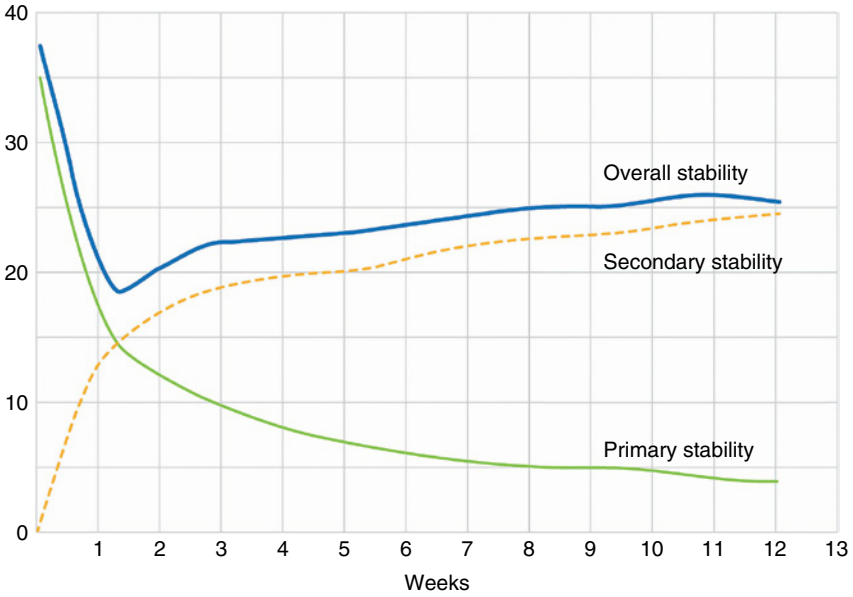


Figure 1.16 Clinical stability (overall stability) of a mini-implant is the sum of both primary and secondary stability. Primary stability decreases gradually following insertion while secondary stability increases after placement of the mini-implant.

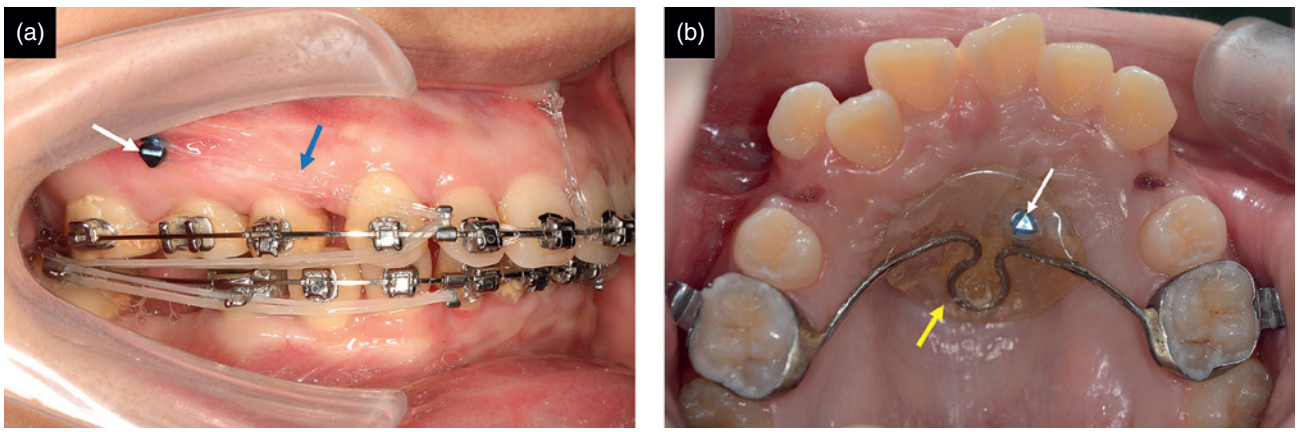


Figure 1.17 Direct versus indirect anchorage modes. (a) Direct anchorage mode. An elastomeric chain (blue arrow) was directly applied from the archwire hook to the mini-implant (white arrow). (b) Indirect anchorage mode. Maxillary bilateral first molars were stabilised and fixed onto a palatal mini-implant (white arrow) through a Nance holding arch (yellow arrow).

1.4.3 Direct versus Indirect Anchorage

A mini-implant serves as a functional and temporary device to withstand orthodontic force loading. Depending on the modality, force loading can be categorised into direct anchorage and indirect anchorage.

Direct anchorage refers to the force loading modality where required force loading is directly applied to a mini-implant with various appliances, such as elastomeric chains, elastics and closed-coil springs. In contrast, for indirect anchorage, force loading is exerted on anchorage teeth whose anchorage is reinforced by mini-implants (Figure 1.17).

It has been shown that mini-implants can migrate under force loading, due to elastic changes of alveolar bone (primary displacement) and subsequent bone remodelling in response to force loading (secondary displacement).[14,15] Thus, special attention should be paid to apply indirect anchorage in

t.me/Dr_Mouayyad_AlbtousH

clinical practice and the rigidity of the fixation between anchorage teeth and mini-implants should be thoroughly examined. Otherwise, anchorage teeth may move in undesired directions if mini-implant migration is overlooked (Figure 1.18).

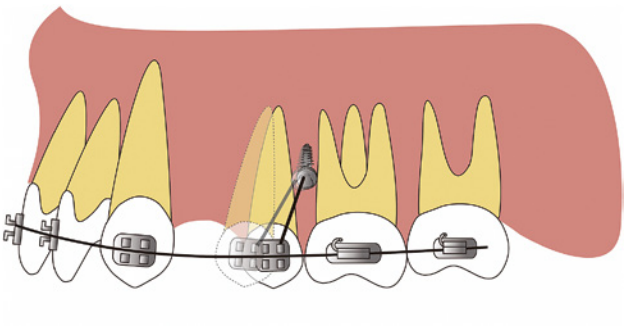


Figure 1.18 Migration of a mini-implant causes undesirable displacement of anchorage teeth. The maxillary second premolar is stabilised and fixed onto the mini-implant via a rigid stainless steel wire. Due to migration of the mini-implant, the second premolar moves in a mesial direction, resulting in anchorage loss.

1.5 Clinical Indications for Orthodontic TADs

Orthodontic TADs are compliance-free alternatives to traditional anchorage devices used in orthodontic treatment and prudent use of orthodontic TADs can efficiently achieve clinical outcomes (Figure 1.19). Orthodontic TADs can serve as strong anchorage units for difficult tooth movements (e.g. traction of deeply impacted teeth) with high anchorage requirements, thereby avoiding undesired movements of anchorage teeth (Figure 1.20). Furthermore, for patients requiring growth modifications, greater orthopaedic effects can be observed with the aid of orthodontic TADs (Figure 1.21).

In this section, the clinical indications of orthodontic TADs will be discussed in three different dimensions – sagittal, vertical and transverse. However, although the biomechanics of TADs is discussed separately in this chapter, the clinical biomechanics of orthodontic TADs in the three dimensions is not separate but should be integrated in clinical practice.

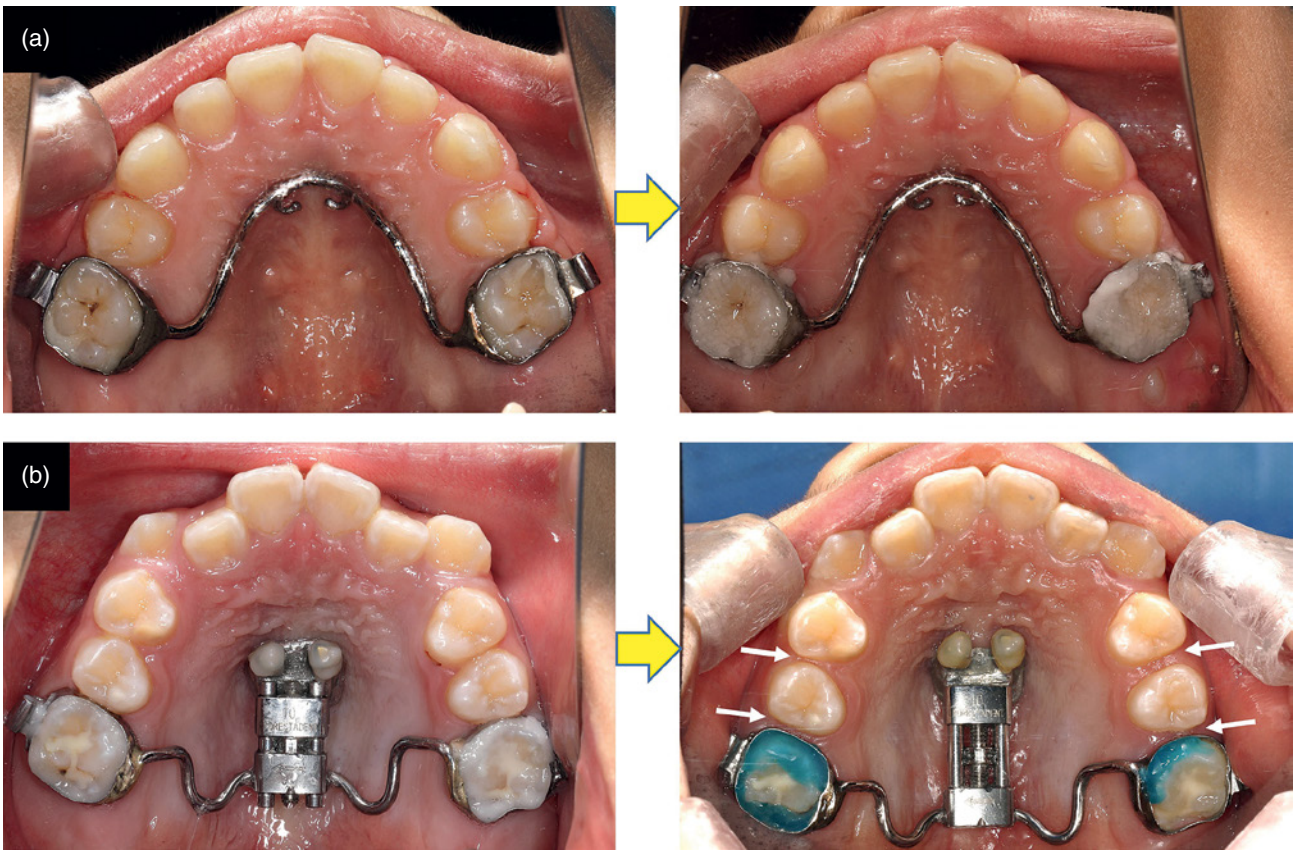


Figure 1.19 Upper molar distalisation with conventional versus TAD biomechanics. (a) Upper molar distalisation through headgear and facebow for seven months. Molar distalisation was inefficient. (b) Molar distalisation with palatal mini-implants and an expansion screw. The desired molar distalisation was achieved within two months. Note the spacings (white arrows) between the posterior teeth that were obtained through molar distalisation.

t.me/Dr_Mouayyad_AlbtousH

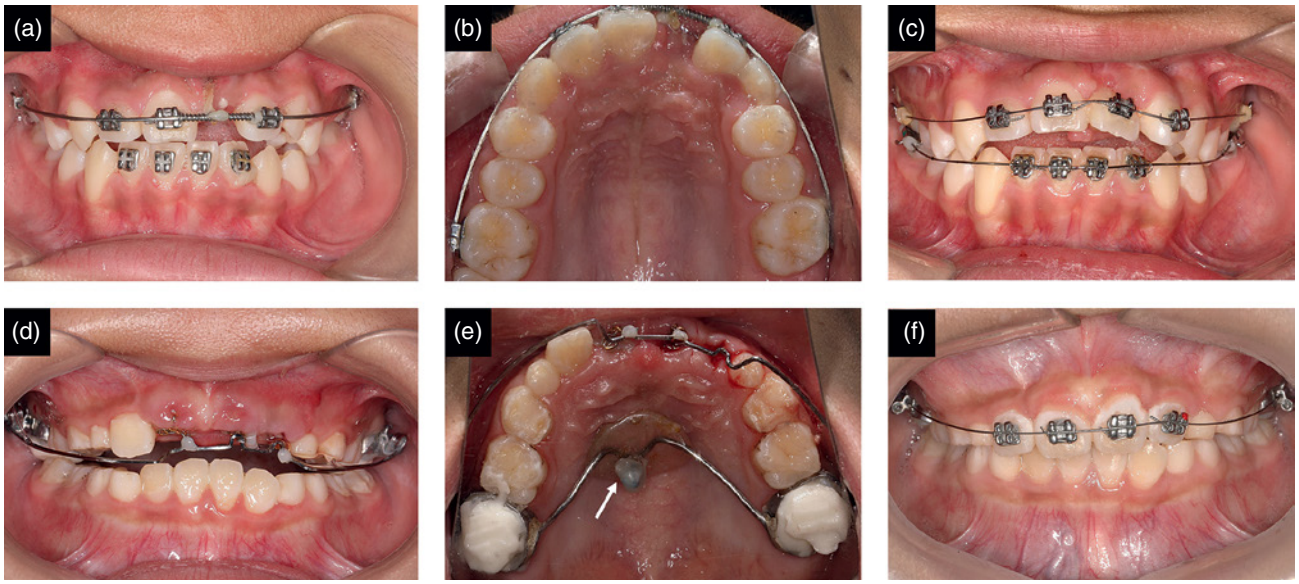


Figure 1.20 The role of TADs in preventing anchorage loss. (a–c) An impacted maxillary incisor was tractioned through an elastomeric chain on a 2*4 archwire. The reciprocal intrusive force acted on the anchorage teeth and resulted in anterior open bite. (d–f) Maxillary bilateral first molars were stabilised and fixed onto a palatal mini-implant (white arrow). The three impacted incisors were tractioned through cantilevers that were fixed onto the bilateral first molar bands. Note no incisor open bite occurred following successful traction of the three impacted incisors.

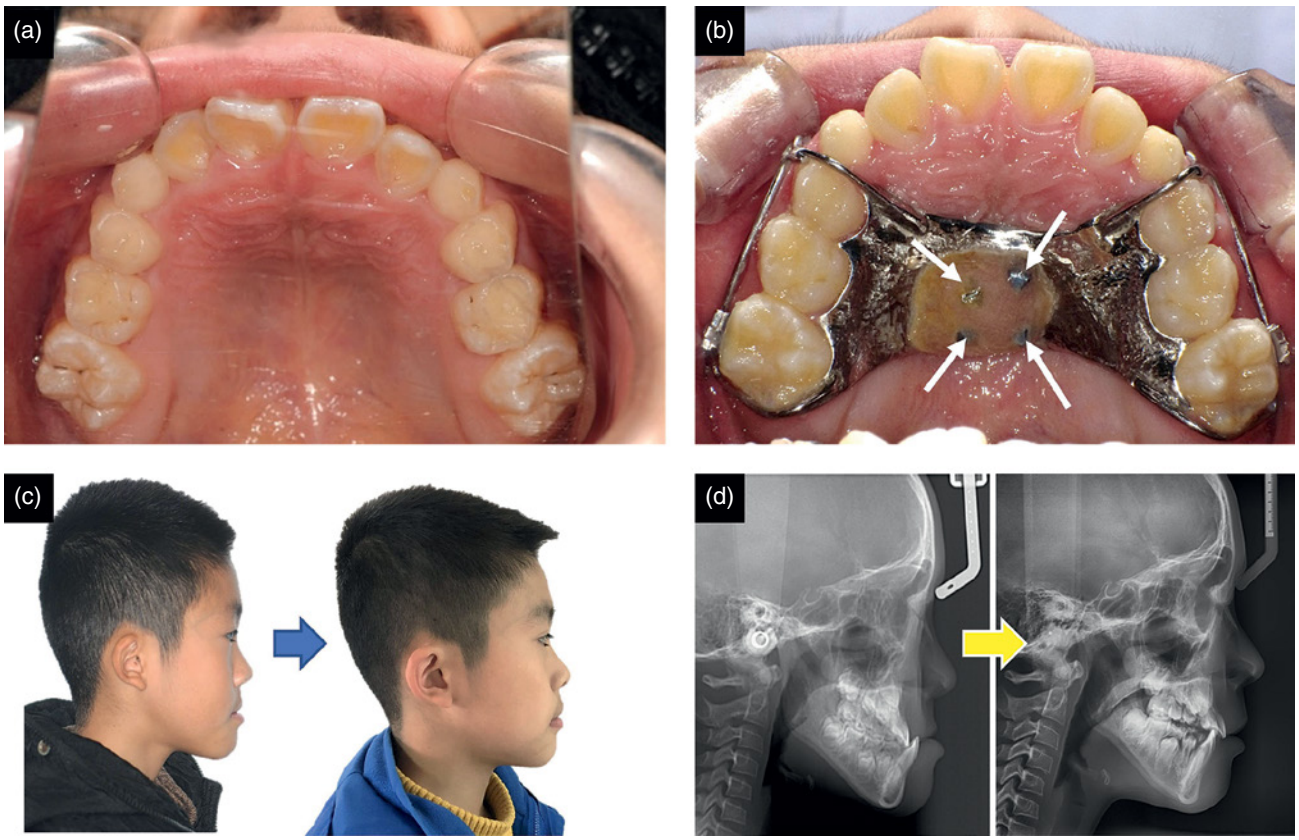


Figure 1.21 TADs are able to achieve satisfactory orthopaedic effects. (a) Pretreatment. (b) Four mini-implants (white arrows) were inserted to fix the protraction device onto the palatal bone. (c) Facial profiles before and after treatment. (d) Cephalometric radiographs before and after treatment.

t.me/Dr_Mouayyad_AlbtousH

1.5.1 Sagittal Dimension

Anterior Retraction

Anchorage control is of paramount importance in clinical practice. Among maximum anchorage cases, molar anchorage loss is often disastrous and leads to incisor proclination, undesirable molar relationship and unaesthetic facial profile. A seminal meta-analysis revealed that the mean difference of anchorage loss between a conventional anchorage group and a mini-implant group was 2.4 mm and that the pooled molar anchorage loss was 0.05 mm for the mini-implant group.[16] This notion has been endorsed by recent clinical trials and meta-analyses.[17-19] Moreover, it has been shown by a recent systematic review that a more favourable soft tissue profile was established by using mini-implants among maximum anchorage cases.[20] Therefore, compared to conventional anchorage devices, orthodontic mini-implants are better alternatives for preserving molar anchorage and in achieving desired facial profile for anterior retraction among maximum anchorage cases (Figure 1.22).

Molar Distalisation

Molar distalisation is clinically indicated among patients with mild skeletal discrepancy in the sagittal dimension, presenting as class II or class III molar relationship. To achieve molar distalisation, adequate anchorage from anterior teeth, palatal soft tissues and/or extraoral tissues is required for conventional anchorage biomechanics.[21] However, conventional anchorage devices (e.g. pendulum and headgear) for molar distalisation often result in less predicted molar distalisation and cause molar distal tipping and proclination or mesialisation of anchorage teeth.[22-24]

The advent of orthodontic mini-implants has led to their incorporation into the design of conventional distalisation devices (Figure 1.23).[25] More recently, mini-implants have been integrated into clear aligner therapy for molar distalisation (Figure 1.24).[26] Numerous seminal clinical studies have demonstrated that mini-implant-anchored molar distalisers were successful in achieving efficient molar distalisation without molar distal tipping or anterior anchorage loss.[25,27,28] This notion has been supported by recent systematic reviews and meta-analyses.[29,30]

Apart from the use of TADs in indirect anchorage form, orthodontic TADs can be applied for molar distalisation through direct anchorage modality. Both buccal and palatal mini-implants have been applied for molar distalisation. However, it has been revealed that the palatal approach resulted in greater molar distalisation and intrusion with less distal tipping compared to the buccal approach,[31] which may be attributed to biomechanical disadvantages obtained by the buccal approach due to vestibular soft tissue limitations. Therefore, orthodontic TADs can achieve more predictable molar distalisation, with the palatal approach being superior to the buccal approach (Figure 1.25).

Molar Protraction

Molar protraction is indicated for patients with missing molars who are reluctant to receive implant prostheses. Conventional biomechanics protracts molars mesially at the expense of reciprocally retracting anterior teeth,

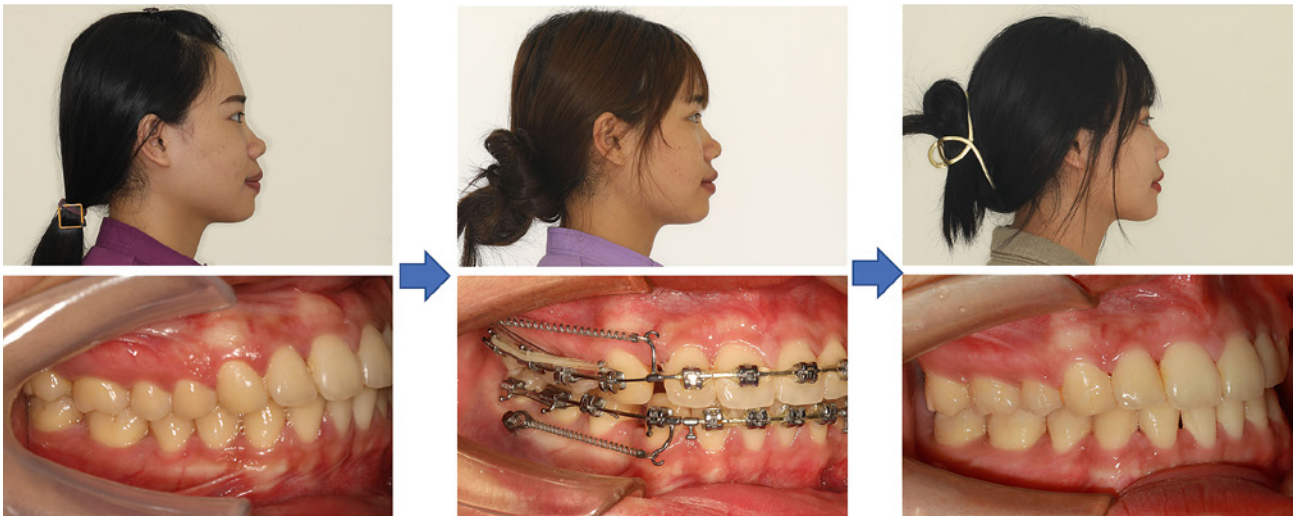


Figure 1.22 *En masse* retraction with the aid of mini-implants. Mini-implants were inserted at the buccal sides of both the maxilla and mandible. Class I molar relationship was maintained and facial profile was greatly improved after orthodontic treatment without molar anchorage loss.

t.me/Dr_Mouayyad_AlbtousH

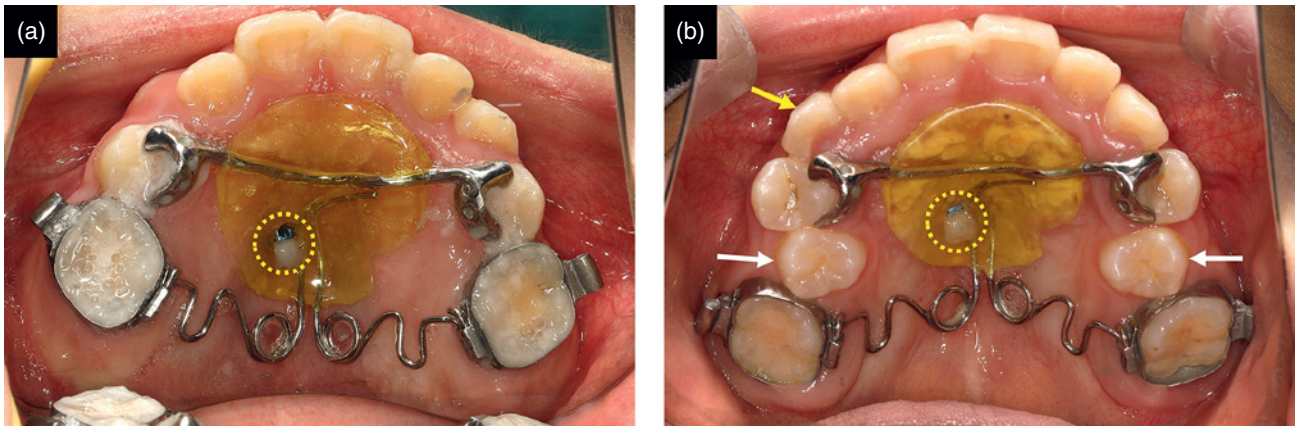


Figure 1.23 Mini-implant-anchored pendulum for upper molar distalisation. (a) A mini-implant was inserted at the palatal vault region and stabilised the pendulum appliance with ligature wire and flowable resin (yellow dashed circle). Note that the bilateral upper second premolars had not erupted due to the mesial drifting of the first molars. The treatment plan was to distalise bilateral first molars and regain space for the eruption of the second premolars. (b) Twelve months into treatment. Upper molar distalisation was efficient and effective. Following molar distalisation, the bilateral second premolars (white arrows) erupted spontaneously. Meanwhile, incorporation of the palatal mini-implant reinforced the anterior anchorage and prevented mesial tipping of the first premolars. Note the spontaneous eruption of the upper right canine (yellow arrow).



Figure 1.24 The incorporation of TADs into clear aligner therapy. (a) Pretreatment. The patient presented with class II canine and molar relationship. Molar distalisation was indicated to correct molar relationship. (b) Clear aligner was employed for upper molar distalisation with the aid of an infrazygomatic mini-implant. (c) Progress. Class I canine and molar relationships were obtained.

resulting in anchorage loss of anterior teeth (Figure 1.26). Moreover, due to higher bone density and more mesial inclination of molars in the mandible, protraction of mandibular molars is more challenging than that of maxillary molars.[32,33] Numerous clinical studies have revealed that orthodontic TADs are able to achieve predictable and efficient molar protraction without anchorage loss of anterior teeth.[34,35] Thus, orthodontic TADs are indicated to avoid anchorage loss of anterior teeth among patients demanding efficient and predictable molar protraction, especially for mandibular molars (Figures 1.27 and 1.28).

Skeletal Orthopaedics

Skeletal orthopaedic treatment is indicated for adolescent patients with maxillary deficiency or mandibular retrusion. It has been shown that conventional orthopaedic therapy can achieve some predicted skeletal effects at the expense of dental side-effects.[36,37] Specifically, bone-anchored maxillary protraction, in the form of either mini-implants or mini-plates, can promote greater maxillary forward growth and avoid labial inclination of maxillary incisors.[38,39] Thus, among patients demanding orthopaedic treatments, orthodontic TADs, either mini-plates or mini-implants, can be used to offer greater skeletal effects and avoid dental side-effects (Figure 1.29).

1.5.2 Vertical Dimension

Molar Intrusion

Orthodontic TADs are clinically indicated for molar intrusion in the following three clinical scenarios. First, for patients with severe open bite, molar intrusion through orthodontic TADs is highly indicated and recommended (Figure 1.30). Second, TADs are clinically demanded for molar overeruption due to the loss of opposing tooth, otherwise adjacent anchorage teeth will be extruded

t.me/Dr_Mouayyad_AlbtousH

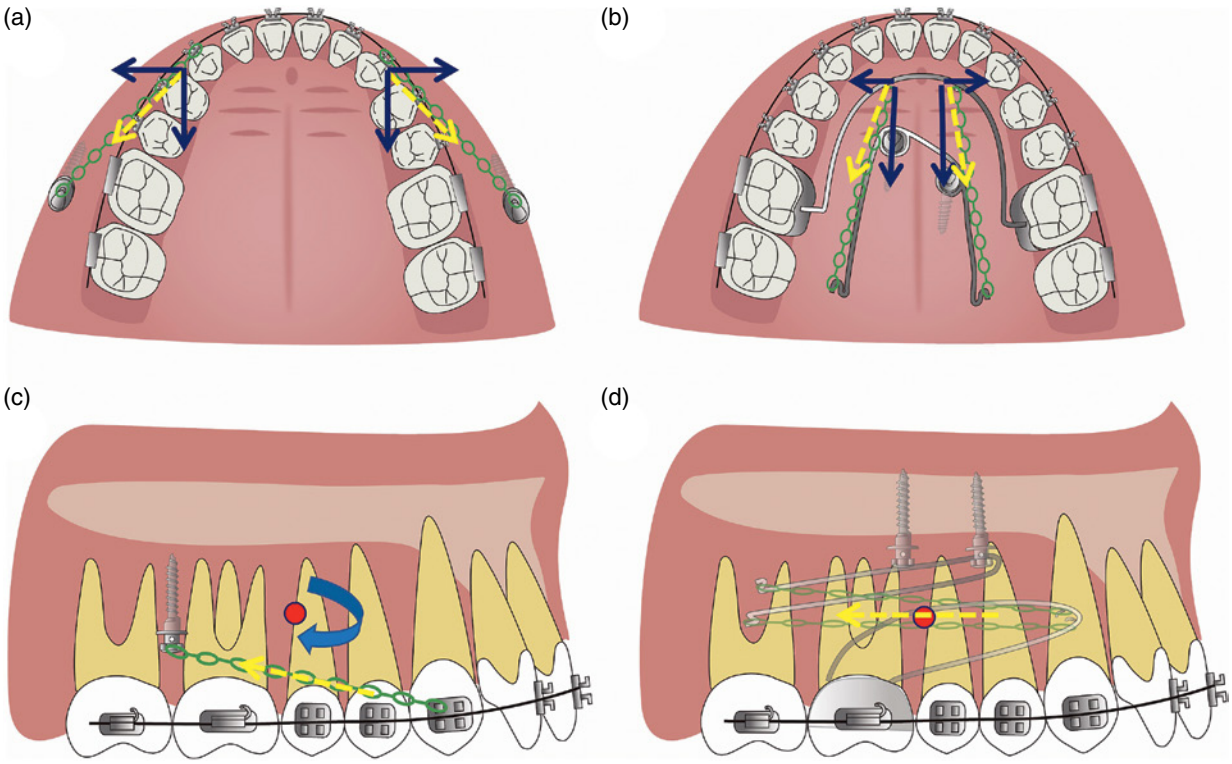


Figure 1.25 Biomechanics of molar distalisation with the buccal versus palatal approaches. (a) Occlusal view of molar distalisation with buccal mini-implants. The distalisation force can be split into sagittal and the coronal components. Specifically, the sagittal component force is responsible for molar distalisation while the coronal component force leads to arch expansion. (b) Molar distalisation with palatal mini-implants. Two extension hooks are stabilised by the two palatal mini-implants. The distalisation force can be split into sagittal and coronal components. Since the angle formed between the distalisation force and the sagittal plane is smaller for the palatal approach than for the buccal approach, the sagittal component is greater for the palatal approach, leading to more efficient molar distalisation than the buccal approach. Moreover, due to the smaller coronal component for the palatal approach and the stabilisation by the palatal arch, the effect of arch expansion is prevented for the palatal approach. (c) Due to the anatomical limitation at the buccal side, the head of the mini-implant is often occlusal to the centre of resistance (CoR) of the whole maxillary dentition. The distalisation force passes occlusally to the CoR, resulting in clockwise rotation of the maxillary occlusal plane. (d) Due to the adequate anatomical space at the palatal side, the extension hooks can be located at the same level of the CoR. Thus, the distalisation of the maxillary dentition can be bodily moved without any rotation of the maxillary occlusal plane.

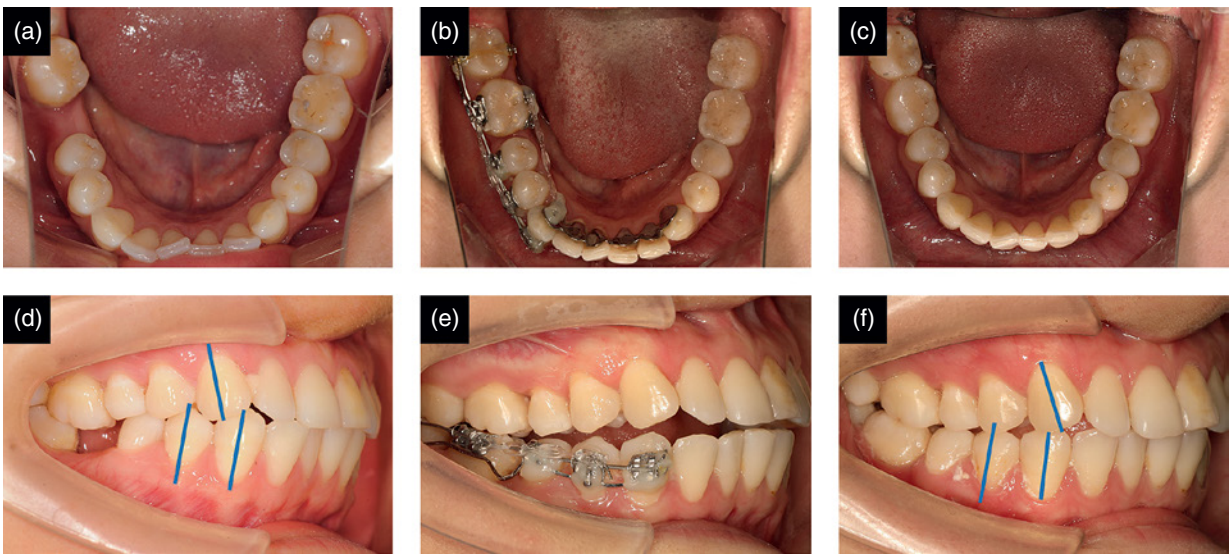


Figure 1.26 Anchorage loss in the anterior teeth with conventional biomechanics. (a) Pretreatment. The mandibular right first molar was missing and protraction of the second molar for substitution of the missing first molar was indicated. (b) Conventional biomechanics was used to protract the second molar. Note that the anchorage of the anterior teeth was augmented through a lingual appliance that was bonded on the six anterior teeth. (c) Posttreatment. Both the second and third molars were successfully protracted. (d–f) The lower anterior teeth were retracted in response to the reciprocal force of molar protraction. Note the changes of canine relationship before and after treatment. The canine relationship was class I before treatment and became class II during and after the treatment.

t.me/Dr_Mouayyad_AlbtousH

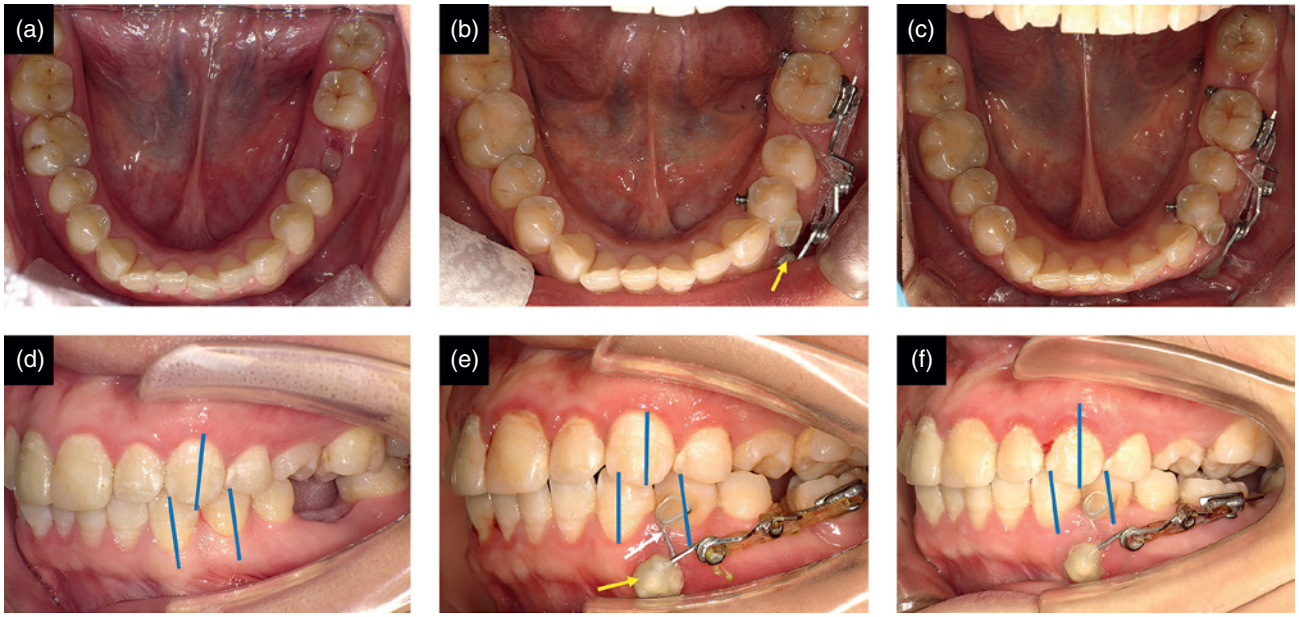


Figure 1.27 Molar protraction with the aid of a mini-implant. (a,d) Pretreatment. The mandibular left first molar was missing and molar protraction was indicated. Pretreatment canine relationship was class I. (b,e) The 'Albert loop' molar protraction appliance was used and anchored onto a buccal interradicular mini-implant (yellow arrow) inserted between the canine and first premolar. In addition, the adjacent first premolar was stabilised by the mini-implant through a stainless steel archwire (white arrow) with flowable resin. (c,f) Thes second molar was successfully protracted to substitute the missing first molar without anchorage loss in the anterior teeth. Note that the class I canine relationship was maintained.

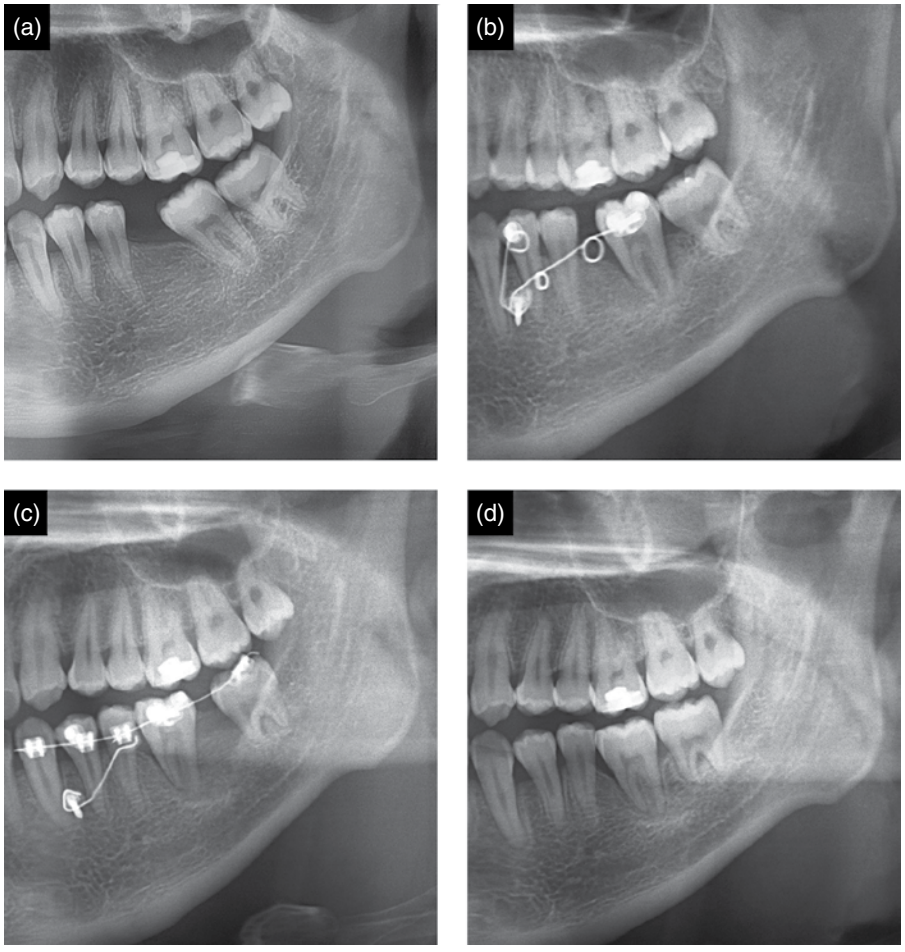


Figure 1.28 Efficient and predictable molar protraction can be achieved with the aid of TADs. (a) Pretreatment. The mandibular first molar was missing and protraction of the second and third molars was indicated. (b) A mini-implant was inserted between the canine and first premolar. The Albert loop molar protraction appliance was anchored onto the mini-implant for molar protraction. The first premolar was stabilised by the mini-implant for anchorage augmentation. (c) Following successful protraction of the second molar, protraction of the third molar was initiated. The second premolar was stabilised by the mini-implant for anchorage reinforcement. (d) Posttreatment. Both the second and third molars were successfully protracted.

t.me/Dr_Mouayyad_AlbtousH

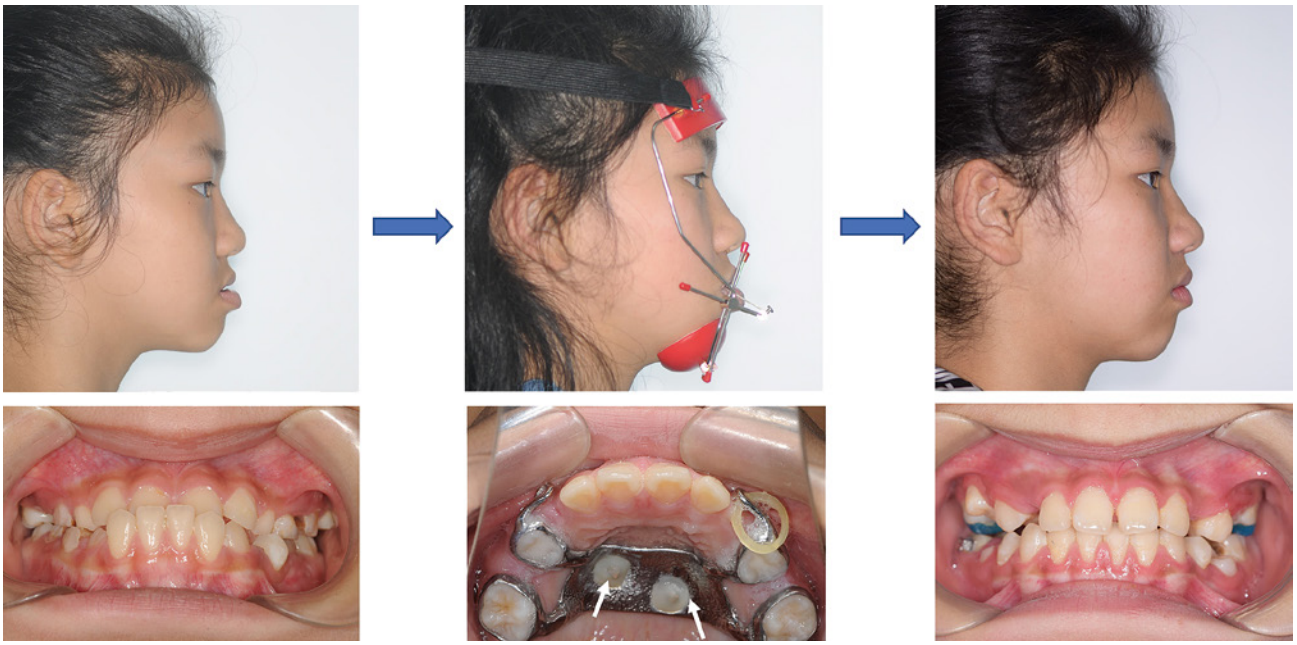


Figure 1.29 TAD-anchored maxillary protraction leads to significant skeletal effects. The protraction appliance was fixed and stabilised by two palatal mini-implants (white arrows).

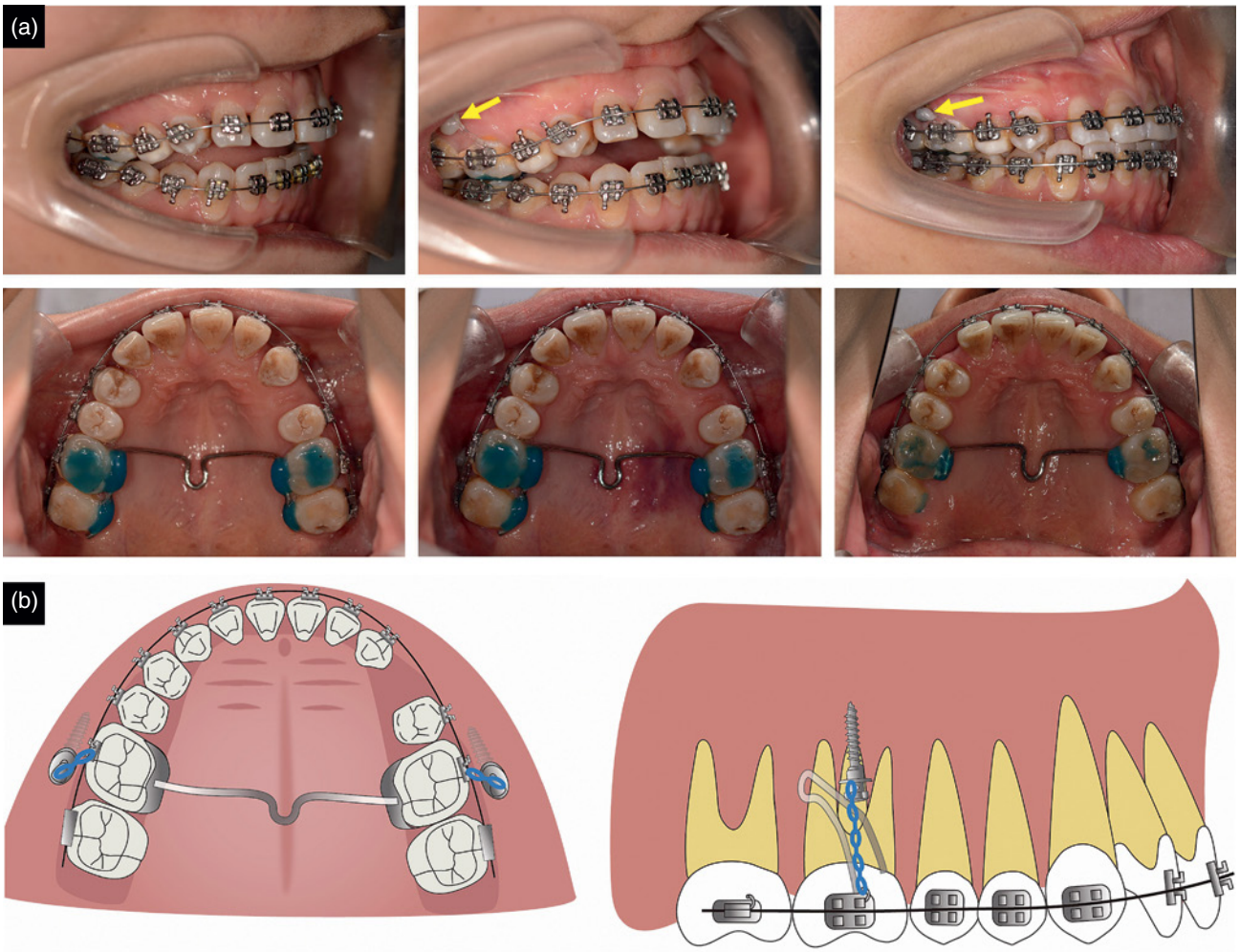


Figure 1.30 Molar intrusion with TADs for correcting severe open bite. (a) Treatment progresses. Two buccal mini-implants (yellow arrows) were placed to offer intrusive force on the molars. A transpalatal arch was used to maintain arch width and prevent buccal tipping of the molars. (b) Schematic illustrations.

t.me/Dr_Mouayyad_AlbtousH

(Figure 1.31). Lastly, for patients with class II skeletal base with high mandibular angle, adequate molar intrusion should be implemented to achieve mandibular anticlockwise rotation, thereby obtaining an aesthetic facial profile (Figure 1.32). Unless buccal or lingual tipping is indicated for selected patients, molars should be bodily intruded without buccal or lingual tipping. Thus, meticulous and prudent biomechanics should be implemented for molar intrusion (Figure 1.33).

Incisor Intrusion

A clinical study compared the intrusion effects of mini-implant, J-hook headgear and utility arch on incisor intrusion and revealed that mini-implants are the most effective approach for incisor intrusion with no side-effects (molar extrusion).[40] Moreover, with the intrusion of incisors, gummy smile can be well managed with aesthetic orthodontic treatment outcomes.[41,42] Therefore, orthodontic TADs are clinically indicated among patients with severe deep bite or gummy smile who require large amounts of incisor intrusion (Figure 1.34).

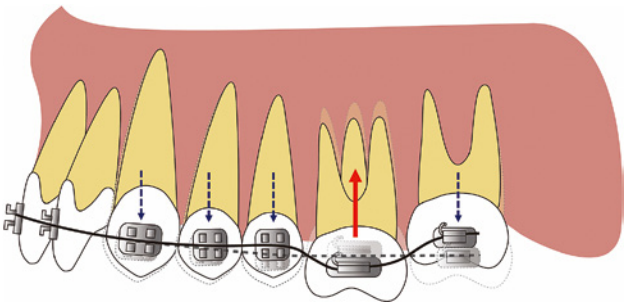


Figure 1.31 The overerupted maxillary first molar is intruded with conventional biomechanics, with adjacent teeth acting as the anchorage. During intrusion of the first molar, the adjacent anchorage teeth are being extruded in response to the reciprocal force.

Tooth Extrusion

When a large amount of tooth extrusion is required, complex appliances are necessary to offer extrusion force for conventional biomechanics, especially molar extrusion. Moreover, conventional biomechanics relies on anchorage teeth and these teeth are susceptible to reciprocal intrusion, resulting in open bite. Thus, orthodontic TADs are indicated in these clinical settings (Figure 1.35).

1.5.3 Transverse Dimension

Maxillary Arch Expansion

Maxillary arch expansion is indicated for patients with limited arch development, constricted maxillary arch or narrow maxillary skeletal base. However, conventional tooth-borne expansion appliances achieve limited skeletal expansion effects with significant dental side-effects, e.g. molar buccal tipping.[43] In contrast, a plethora of recent evidence indicates that, compared to tooth-borne appliances, bone-borne expansion appliances can achieve more predictable skeletal expansion effects and eliminate dental

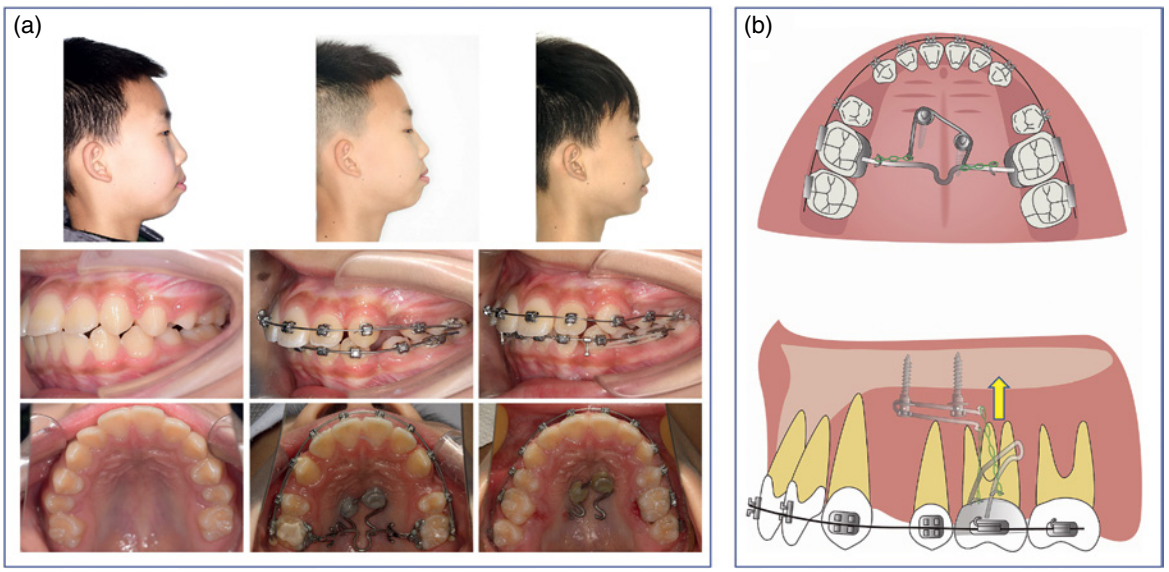


Figure 1.32 Molar intrusion with the aid of TADs for a class II patient with high mandibular angle. (a) Treatment starts. Two mini-implants were placed at the palatal vault region and two extension hooks were fixed onto the two palatal mini-implants. Molars were intruded and the mandible was rotated in an anticlockwise direction. Facial profile aesthetics was significantly improved and the chin gradually became prominent. (b) Schematic illustrations of the palatal appliances and palatal mini-implants.

t.me/Dr_Mouayyad_AlbtousH

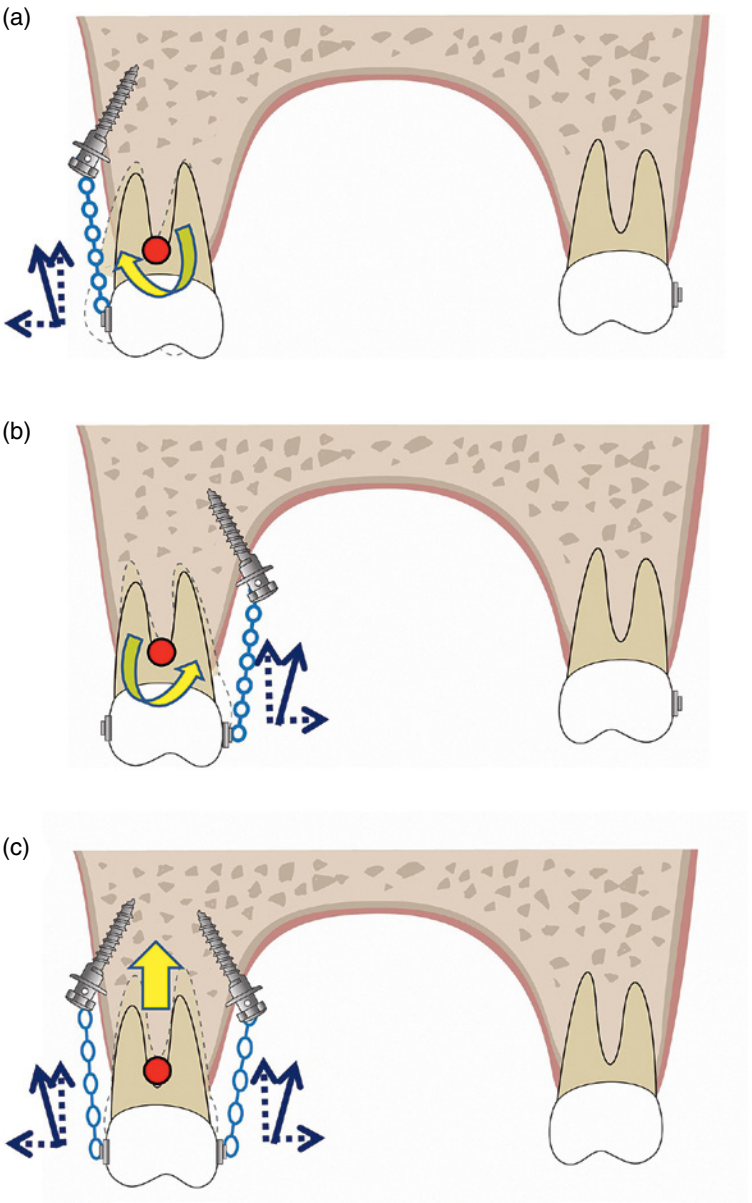


Figure 1.33 Biomechanical design for molar intrusion with TADs. (a) The molar is intruded by a buccal mini-implant. The intrusive force passes buccally to the centre of resistance and can be split into a vertical intrusive component and a transverse, buccally directed component. Thus, the molar exhibits both intrusion and buccal tipping. (b) The molar is intruded through a palatal mini-implant. Likewise, it exhibits intrusion and lingual tipping. (c) The molar is intruded through both buccal and palatal mini-implants. Buccal or lingual tipping can be prevented and pure intrusion can be achieved.

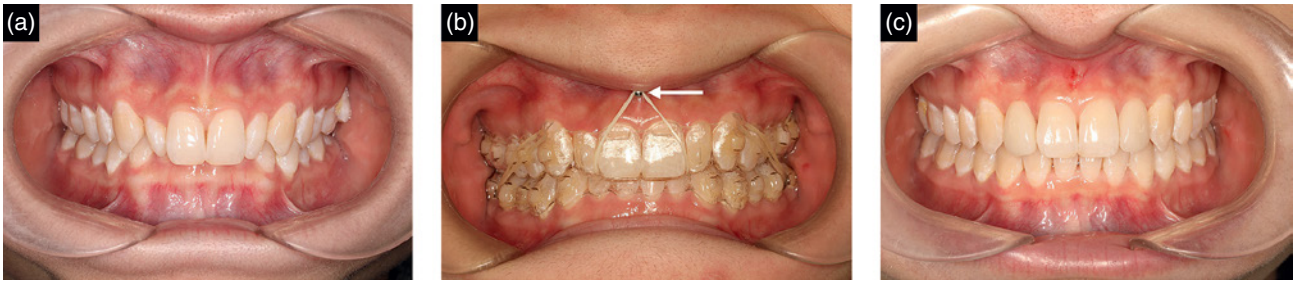


Figure 1.34 Incisor intrusion through a labial interradicular mini-implant. (a) Pretreatment. Severe deep bite was present. (b) The deep bite was treated by clear aligners with the aid of a labial interradicular mini-implant (white arrow). (c) Posttreatment. Deep bite was successfully corrected.

t.me/Dr_Mouayyad_AlbtousH

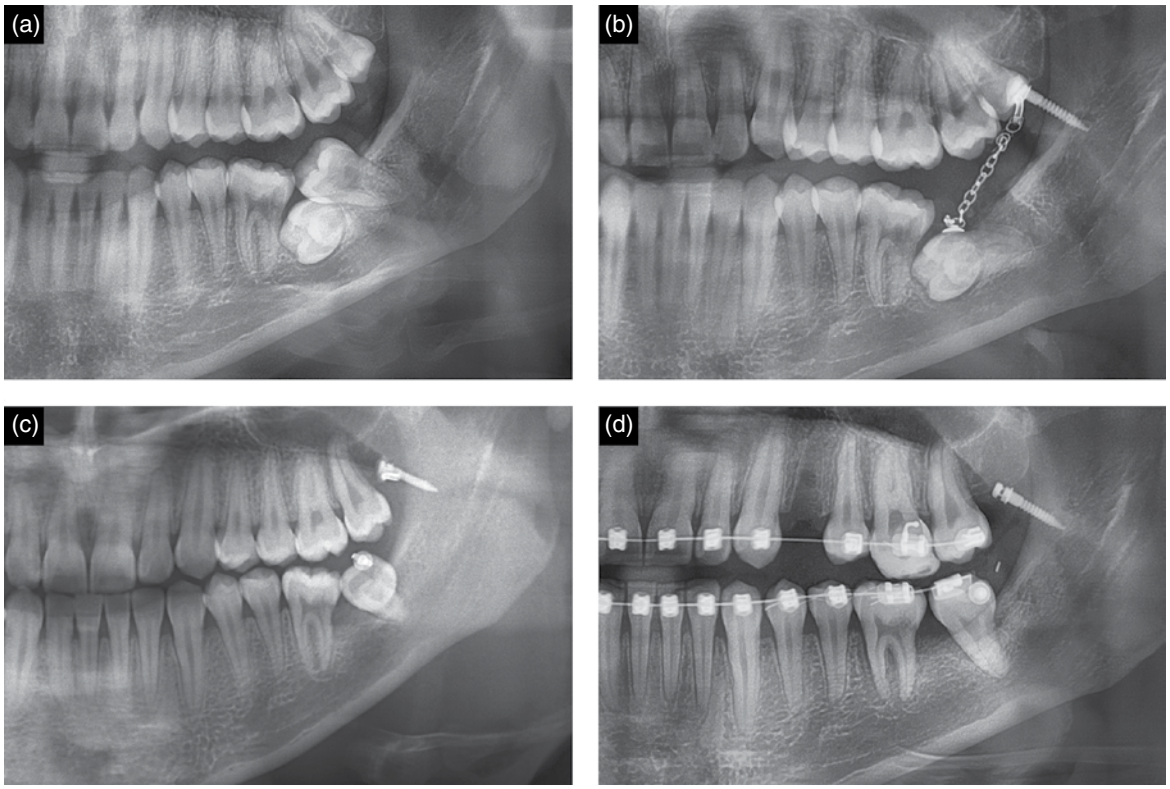


Figure 1.35 Orthodontic traction and extrusion of deeply impacted mandibular second molar. (a) Pretreatment. The mandibular left second molar was deeply impacted with an overlying third molar. (b) The overlying third molar was extracted and a mini-implant was placed at the mandibular ramus region to extrude the impacted second molar. The extrusion of the second molar would be refractory to conventional biomechanics. (c) The deeply impacted second molar was successfully extruded to the occlusal plane. (d) The second molar was being aligned.

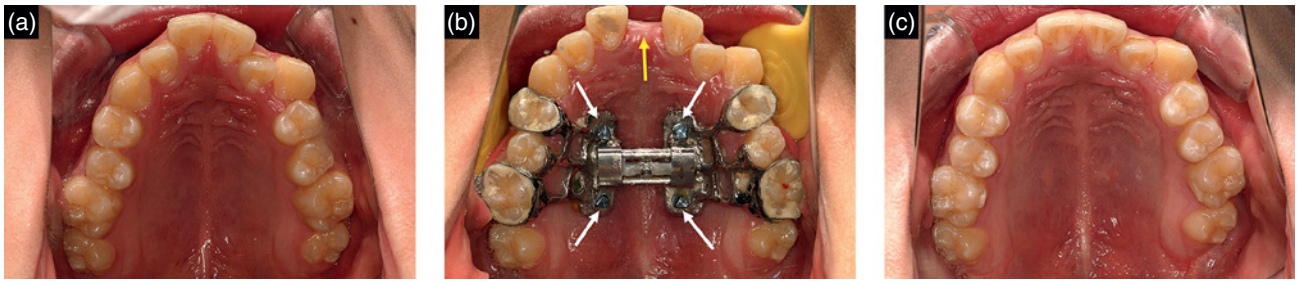


Figure 1.36 Skeletal expansion of the maxillae with mini-implants. (a) Pretreatment. Note the narrow dental arch. (b) The maxillary dental arch was expanded through mini-implant-assisted skeletal expansion. In total, four mini-implants were placed (white arrows). Note the large midline diastema (yellow arrow) that was indicative of successful skeletal expansion. (c) Posttreatment. The midline diastema was closed spontaneously through mesial drifting of the incisors. The narrowed dental arch was expanded.

side-effects.[44-46] Thus, mini-implants can be used for maxillary skeletal expansion in patients with narrow maxillary skeletal base (Figure 1.36).

Brodie Bite

This challenging transverse discrepancy manifests as the palatal cusps of maxillary molars lying buccally to the buccal cusps of mandibular antagonists.[47,48] Conventional biomechanics leverage crisscross elastics to correct Brodie bite by lingual tipping and buccal tipping of upper and lower molars, respectively. However, both the upper and lower molars are extruded by the crisscross elastics during correction of Brodie bite, resulting in open bite that requires further molar intrusion.

To reiterate, orthodontic biomechanics in all three dimensions should be designed and considered congruously.

t.me/Dr_Mouayyad_AlbtousH

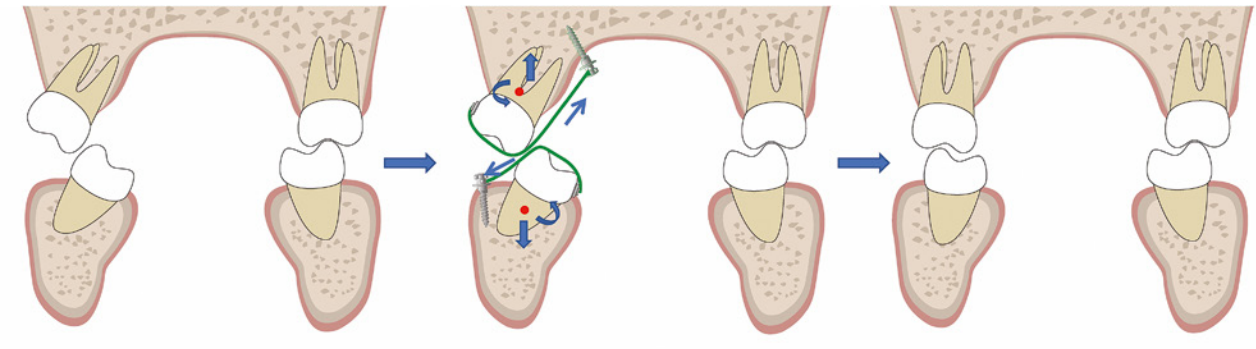


Figure 1.37 The biomechanics associated with Brodie bite correction through TADs. The traction force offered by the palatal mini-implant corrects the buccal tipping and intrudes the overerupted maxillary molar simultaneously. Likewise, the mandibular molar was buccally tipped and intruded at the same time. In this way, extrusion of the molars during correction of buccal or lingual tipping is prevented.

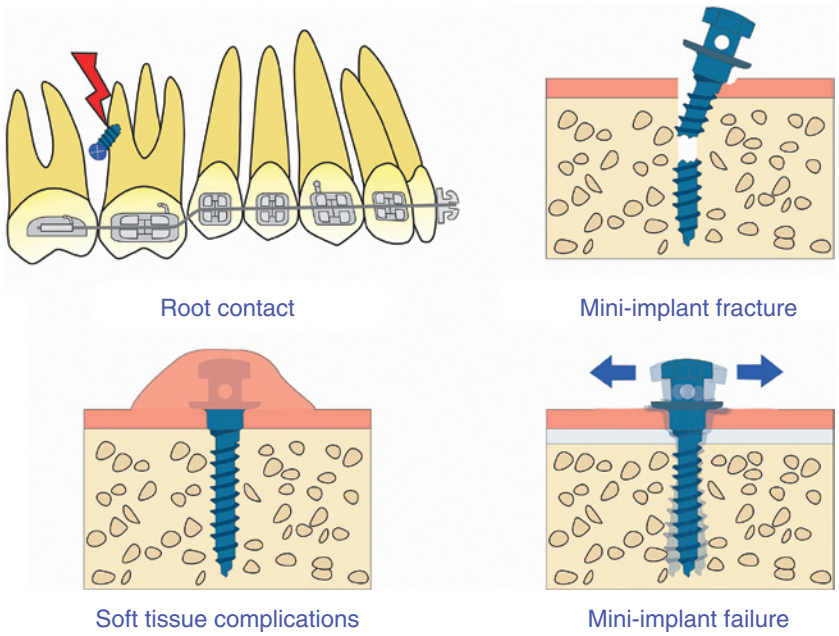


Figure 1.38 Potential complications associated with the placement of orthodontic TADs.

Orthodontic TADs are advantageous in correcting Brodie bite since molar intrusion can be accomplished with the correction of transverse discrepancy (Figure 1.37).

1.6 Potential Complications

The complications associated with the application of orthodontic TADs are not infrequently encountered in clinical practice. The four most frequently encountered complications of TADs are root contact or penetration, facture of orthodontic TADs, soft tissue inflammation and failure of orthodontic TADs (Figure 1.38).

Root contact or penetration refers to the situation where mini-implants contact or penetrate into dental roots during the insertion of orthodontic TADs (Figure 1.39), with an average incidence of 20%.[49] Main risk factors for root contact include limited interradicular space, inappropriate inclination of insertion direction and inadequate insertion height. Thus, preinsertion radiographic examinations, prudent planning of insertion site and appropriate insertion techniques are required to reduce the risk of root contact.

Fracture of a mini-implant occurs when insertion torque or removal torque exceeds the fracture torque of the implant (Figure 1.40). The overall incidence of mini-implant fracture is 1.7–3.5%.[50-53] To reduce the likelihood of mini-implant fracture, appropriate insertion techniques and selection of mini-implants with proper size are recommended. Notably, for insertion sites with high bone density and thick cortex,

t.me/Dr_Mouayyad_AlbtousH

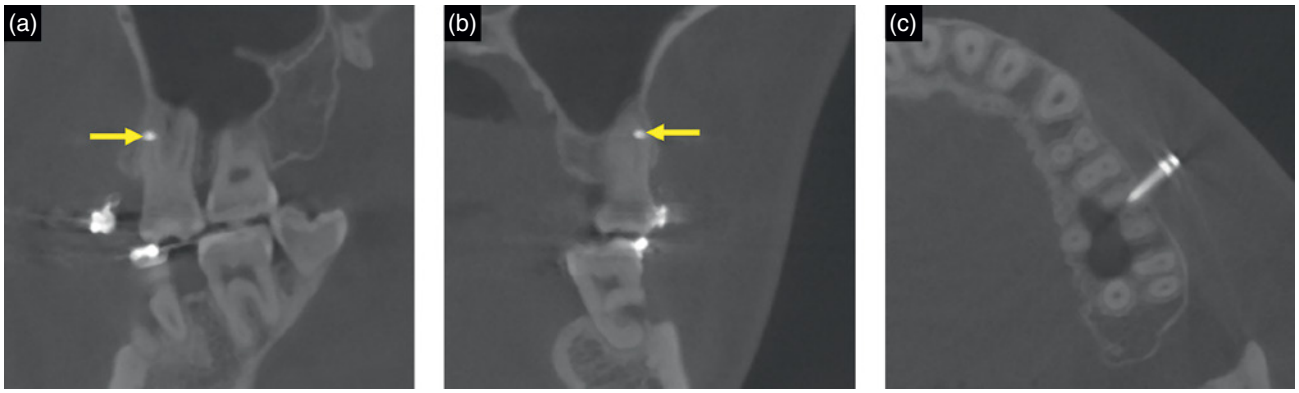


Figure 1.39 Root contact by a mini-implant. (a) Sagittal view. Note the proximity of the mini-implant (yellow arrow) and the root. (b) Coronal view. (c) Axial view.

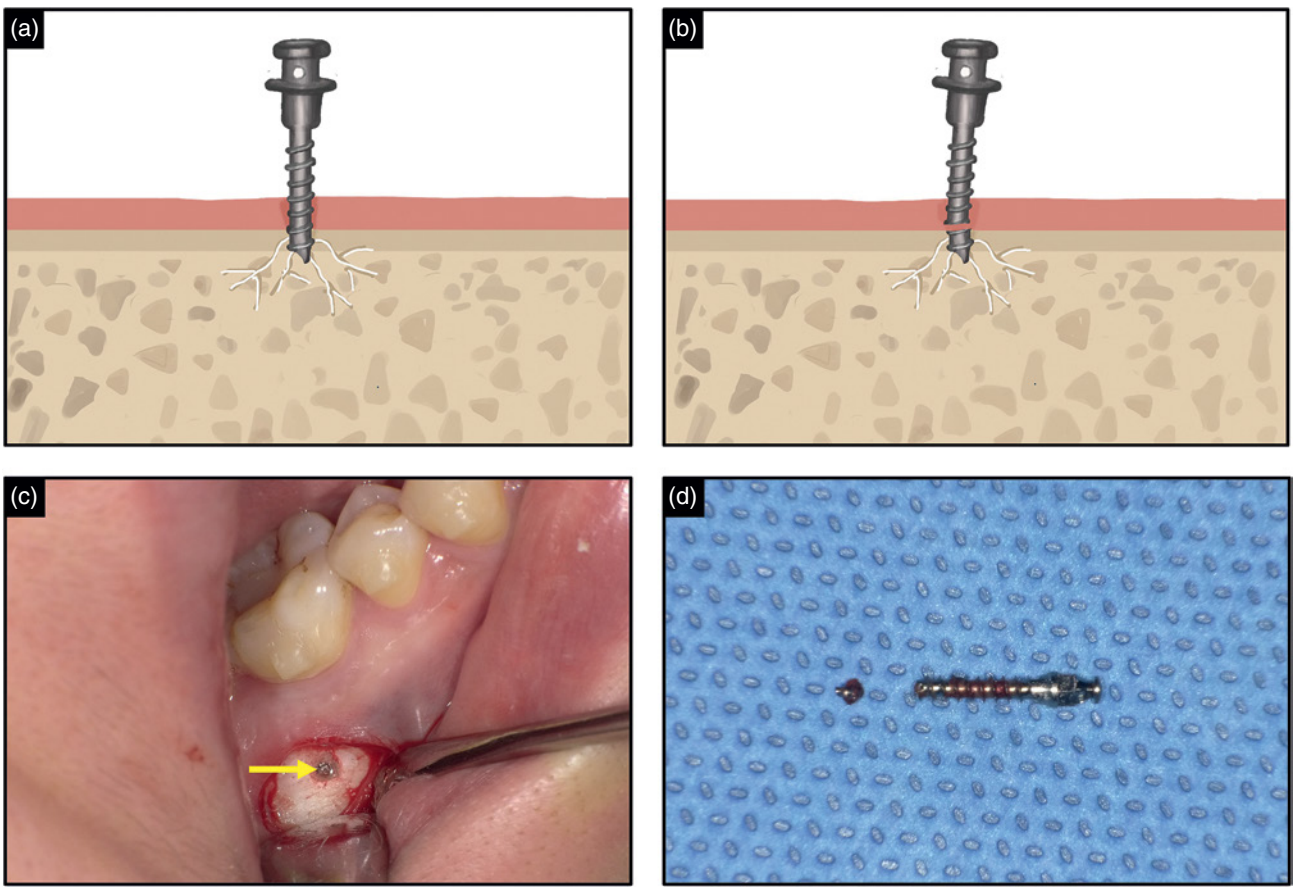


Figure 1.40 Mini-implant fracture. (a) A mini-implant is being inserted into a bone region with high density. Due to the high density of the cortex, bone cracks and fractures occur during the insertion procedure. (b) The tip of the mini-implant fractures during insertion due to high insertion torque. (c) The tip of a mini-implant (yellow arrow) fractured during insertion and was retained in the alveolar bone. Flap surgery was performed to remove the fractured tip. (d) Following the removal of the fractured tip.

t.me/Dr_Mouayyad_AlbtousH

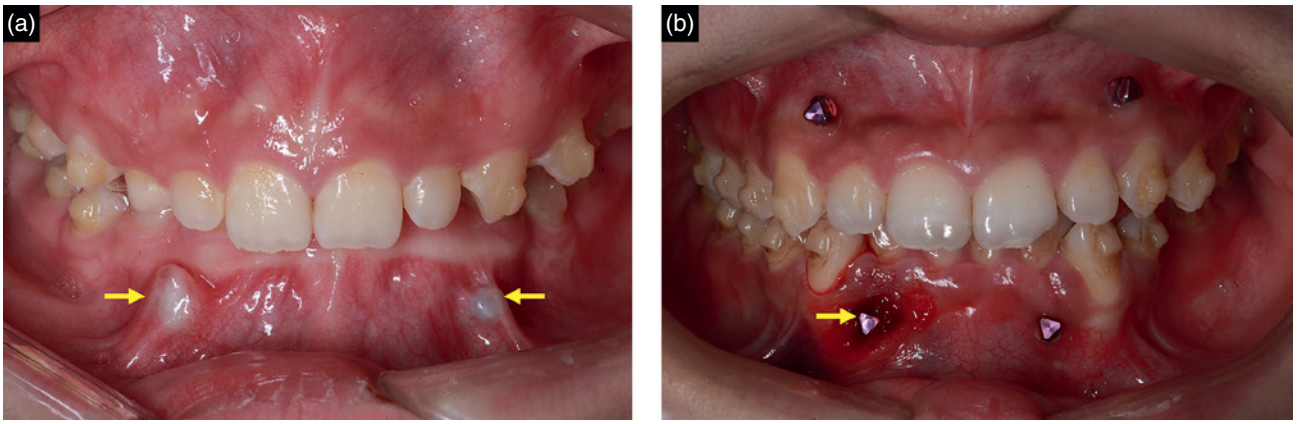


Figure 1.41 Soft tissue inflammation. (a) Overgrowth and hyperplasia of soft tissue around mini-implants (yellow arrows). (b) Inflammation of soft tissue around a mini-implant (yellow arrow). Note the redness and bleeding of the soft tissue around the mini-implant.

predrilling is recommended prior to insertion to reduce the incidence of mini-implant fracture.

Soft tissue inflammation is often manifested as soft tissue redness and swelling of soft tissue, with or without soft tissue hyperplasia (Figure 1.41). Its risk factors mainly include inadequate oral hygiene and insertion of mini-implants at the movable mucosa zone.

The failure of orthodontic TADs is defined as the clinical situation where TADs are unable to withstand orthodontic loading due to loosening or mobility (Figure 1.42). The risk of mini-implant failure is mainly associated with patient factors (e.g. low bone density), operator factors (e.g. root proximity) and implant-associated factors (e.g. diameter and length). If mini-implant failure is encountered in clinical practice, tightening the mini-implant *in situ* and reinsertion of a new mini-implant can be performed.

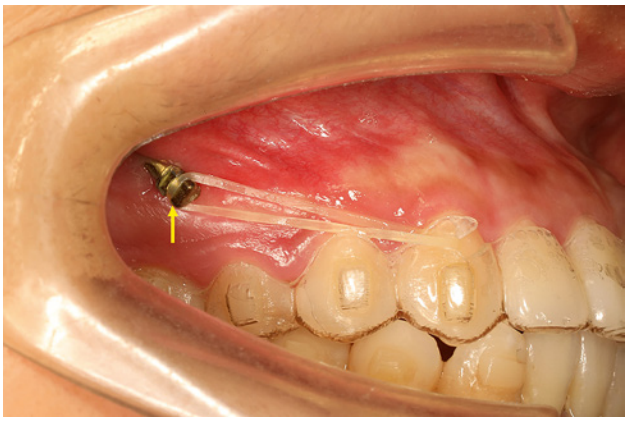


Figure 1.42 Mini-implant failure. The mini-implant became loose and was displaced by the elastic rubber.

1.7 Summary

The advent of orthodontic TADs has enabled practitioners to accomplish challenging orthodontic tooth movements that were deemed impossible with conventional biomechanics. Different materials and shapes of orthodontic TADs are being used in current clinical practice. With orthodontic TADs, practitioners are able to achieve orthodontic tooth movements in three dimensions – sagittal, vertical and horizontal. Potential complications are associated with the clinical application of orthodontic TADs and appropriate measures should be taken to prevent these complications.

References

1 Gainsforth BL, Higley LB. (1945). A study of orthodontic anchorage possibilities in basal bone. *Am. J. Orthod. Oral Surg.* 31(8): 406–417.
2 Linkow LI. (1969). The endosseous blade implant and its use in orthodontics. *Int. J. Orthod.* 7(4): 149–154.
3 Linkow LI. (1970). Endosseous blade-vent implants: a two-year report. *J. Prosthet. Dent.* 23(4): 441–448.
4 Branemark PI, Adell R, Breine U, Hansson BO, Lindstrom J, Ohlsson A. (1969). Intra-osseous anchorage of dental prostheses. I. Experimental studies. *Scand. J. Plast. Reconstr. Surg.* 3(2): 81–100.
5 Creekmore TD, Eklund MK. (1983). The possibility of skeletal anchorage. *J. Clin. Orthod.* 17(4): 266–269.

t.me/Dr_Mouayyad_AlbtousH

6 Linkow LI. (1970). The endosseous blade – a progress report. *Probe* 13(4): 105–106 passim.

7 Mecenas P, Espinosa DG, Cardoso PC, Normando D. (2020). Stainless steel or titanium mini-implants? *Angle Orthod.* 90(4): 587–597.

8 Mohlhenrich SC, Heussen N, Winterhalder P et al. (2019). Predicting primary stability of orthodontic mini-implants, according to position, screw-size, and bone quality, in the maxilla of aged patients: a cadaveric study. *Eur. J. Oral Sci.* 127(5): 462–471.

9 Alrbata RH, Yu W, Kyung HM. (2014). Biomechanical effectiveness of cortical bone thickness on orthodontic microimplant stability: an evaluation based on the load share between cortical and cancellous bone. *Am. J. Orthod. Dentofacial Orthop.* 2014;146(2): 175–182.

10 Motoyoshi M, Inaba M, Ono A, Ueno S, Shimizu N. (2009). The effect of cortical bone thickness on the stability of orthodontic mini-implants and on the stress distribution in surrounding bone. *Int. J. Oral Maxillofac. Surg.* 38(1): 13–18.

11 Liu SS, Cruz-Marroquin E, Sun J, Stewart KT, Allen MR. (2012). Orthodontic mini-implant diameter does not affect in-situ linear microcrack generation in the mandible or the maxilla. *Am. J. Orthod. Dentofacial Orthop.* 142(6): 768–773.

12 Mohlhenrich SC, Heussen N, Modabber A et al. (2021). Influence of bone density, screw size and surgical procedure on orthodontic mini-implant placement – part A: temperature development. *Int. J. Oral Maxillofac. Surg.* 50(4): 555–564.

13 Deguchi T, Yabuuchi T, Hasegawa M, Garetto LP, Roberts WE, Takano-Yamamoto T. (2011). Histomorphometric evaluation of cortical bone thickness surrounding miniscrew for orthodontic anchorage. *Clin. Implant Dent. Relat. Res.* 13(3): 197–205.

14 Becker K, Schwarz F, Rauch NJ, Khalaph S, Mihatovic I, Drescher D. (2019). Can implants move in bone? A longitudinal in vivo micro-CT analysis of implants under constant forces in rat vertebrae. *Clin. Oral Implants Res.* 30(12): 1179–1189.

15 Pittman JW, Navalgund A, Byun SH, Huang H, Kim AH, Kim DG. (2014). Primary migration of a mini-implant under a functional orthodontic loading. *Clin. Oral Invest.* 18(3): 721–728.

16 Papadopoulos MA, Papageorgiou SN, Zogakis IP. (2011). Clinical effectiveness of orthodontic miniscrew implants: a meta-analysis. *J. Dent. Res.* 90(8): 969–976.

17 Yassir YA, Nabbat SA, McIntyre GT, Bearn DR. (2022). Which anchorage device is the best during retraction of anterior teeth? An overview of systematic reviews. *Korean J. Orthod.* 52(3): 220–235.

18 Yin Y, Wang Z, Huang L et al. (2021). Orthodontic maximum anchorages in malocclusion treatment: a systematic review and network meta-analysis. *J. Evid. Based Med.* 14(4): 295–302.

19 El-Dawlatly MM, Mabrouk MA, ElDakroury A, Mostafa YA. (2021). The efficiency of mandibular mini-implants in reducing adverse effects of class II elastics in adolescent female patients: a single blinded, randomized controlled trial. *Prog. Orthod.* 22(1): 27.

20 Liu Y, Yang ZJ, Zhou J et al. (2019). Soft tissue changes in patients with dentoalveolar protrusion treated with maximum anchorage: a systematic review and meta-analysis. *J. Evid. Based Dent. Pract.* 19(4): 101310.

21 Santana LG, de Campos Franca E, Flores-Mir C, Abreu LG, Marques LS, Martins-Junior PA. (2020). Effects of lip bumper therapy on the mandibular arch dimensions of children and adolescents: a systematic review. *Am. J. Orthod. Dentofacial Orthop.* 157(4): 454–465 e451.

22 Kinzinger GSM, Hourfar J, Lisson JA. (2021). Efficiency of the skeletonized Pendulum K appliance for non-compliance maxillary molar distalization: a clinical pilot study. *J. Orofac. Orthop.* 82(6): 391–402.

23 Talvitie T, Helminen M, Karsila S et al. (2021). The impact of force magnitude on the first and second maxillary molars in cervical headgear therapy. *Eur. J. Orthod.* 43(6): 648–657.

24 Jambi S, Thiruvenkatachari B, O'Brien KD, Walsh T. (2013). Orthodontic treatment for distalising upper first molars in children and adolescents. *Cochrane Database Syst. Rev.* 10: CD008375.

25 Kircelli BH, Pektas ZO, Kircelli C. (2006). Maxillary molar distalization with a bone-anchored pendulum appliance. *Angle Orthod.* 76(4): 650–659.

26 Auladell A, De La Iglesia F, Quevedo O, Walter A, Puigdollers A. (2022). The efficiency of molar distalization using clear aligners and mini-implants: two clinical cases. *Int Orthod.* 20(1): 100604.

27 Gelgor IE, Buyukyilmaz T, Karaman AI, Dolanmaz D, Kalayci A. (2004). Intraosseous screw-supported upper molar distalization. *Angle Orthod.* 74(6): 838–850.

28 Polat-Ozsoy O, Kircelli BH, Arman-Ozcirpici A, Pektas ZO, Uckan S. (2008). Pendulum appliances with 2 anchorage designs: conventional anchorage vs bone anchorage. *Am. J. Orthod. Dentofacial Orthop.* 133(3): e339–339 e317.

29 Al-Thomali Y, Basha S, Mohamed RN. (2017). Pendulum and modified pendulum appliances for maxillary molar distalization in Class II malocclusion – a systematic review. *Acta Odontol. Scand.* 75(6): 394–401.

30 Mohamed RN, Basha S, Al-Thomali Y. (2018). Maxillary molar distalization with miniscrew-supported appliances

t.me/Dr_Mouayyad_AlbtousH

in Class II malocclusion: a systematic review. *Angle Orthod.* 88(4): 494–502.

31 Lee SK, Abbas NH, Bayome M et al. (2018). A comparison of treatment effects of total arch distalization using modified C-palatal plate vs buccal miniscrews. *Angle Orthod.* 88(1): 45–51.

32 Wu JC, Zheng YT, Dai YJ. (2020). Protraction of mandibular molars through a severely atrophic edentulous space in a case of juvenile periodontitis. *Korean J. Orthod.* 50(2): 145–154.

33 Choudhary S, Bhaumik B, Libang M, Kumar A. (2018). Uprighting and protraction of mandibular second and third molars into missing first molar spaces for a patient with T-loop and temporary anchorage device: a case report. *Acta Sci. Dent. Sci.* 2(2): 38–41.

34 Palone M, Casella S, De Sbrocchi A, Siciliani G, Lombardo L. (2022). Space closure by miniscrew-assisted mesialization of an upper third molar and partial vestibular fixed appliance: a case report. *Int. Orthod.* 20(1): 100602.

35 Wilhelmy L, Willmann JH, Tarraf NE, Wilmes B, Drescher D. (2022). Maxillary space closure using a digital manufactured Mesialslider in a single appointment workflow. *Korean J. Orthod.* 52(3): 236–245.

36 Liu L, Zhan Q, Zhou J et al. (2021). A comparison of the effects of Forsus appliances with and without temporary anchorage devices for skeletal Class II malocclusion. *Angle Orthod.* 91(2): 255–266.

37 Lee YS, Park JH, Kim J, Lee NK, Kim Y, Kook YA. (2022). Treatment effects of maxillary protraction with palatal plates vs conventional tooth-borne anchorage in growing patients with Class III malocclusion. *Am. J. Orthod. Dentofacial Orthop.* 162: 520–528.

38 Wang J, Yang Y, Wang Y et al. (2022). Clinical effectiveness of different types of bone-anchored maxillary protraction devices for skeletal Class III malocclusion: systematic review and network meta-analysis. *Korean J Orthod.* 52: 313–323.

39 Jahanbin A, Shafaee H, Pahlavan H, Bardideh E, Entezari M. (2023). Efficacy of different methods of bone-anchored maxillary protraction in cleft lip and palate children: a systematic review and meta-analysis. *J. Craniofac. Surg.* 34: 875–880.

40 Jain RK, Kumar SP, Manjula WS. (2014). Comparison of intrusion effects on maxillary incisors among mini implant anchorage, j-hook headgear and utility arch. *J. Clin. Diagn. Res.* 8(7): ZC21–24.

41 Saga AY, Araujo EA, Antelo OM, Meira TM, Tanaka OM. (2020). Nonsurgical treatment of skeletal maxillary protrusion with gummy smile using headgear for growth control, mini-implants as anchorage for maxillary incisor intrusion, and premolar extractions for incisor retraction. *Am. J. Orthod. Dentofacial Orthop.* 157(2): 245–258.

42 Qamruddin I, Shahid F, Alam MK, Zehra Jamal W. (2014). Camouflage of severe skeletal class II gummy smile patient treated nonsurgically with mini implants. *Case Rep. Dent.* 2014: 382367.

43 Zhou Y, Long H, Ye N et al. (2014). The effectiveness of non-surgical maxillary expansion: a meta-analysis. *Eur. J. Orthod.* 36(2): 233–242.

44 Inchingolo AD, Ferrara I, Viapiano F et al. (2022). Rapid maxillary expansion on the adolescent patient: systematic review and case report. *Children* 9(7): 1046.

45 Abu Arqub S, Gandhi V, Iverson MG et al. (2022). Radiographic and histological assessment of root resorption associated with conventional and mini-screw assisted rapid palatal expansion: a systematic review. *Eur. J. Orthod.* 44: 679–689.

46 Altieri F, Cassetta M. (2022). Comparison of changes in skeletal, dentoalveolar, periodontal, and nasal structures after tooth-borne or bone-borne rapid maxillary expansion: a parallel cohort study. *Am. J. Orthod. Dentofacial Orthop.* 161(4): e336–e344.

47 Deffrennes G, Deffrennes D. (2017). Management of Brodie bite: note on surgical treatment. *Int. Orthod.* 15(4): 640–676.

48 Agrawal A. (2020). Brodie bite: a clinical challenge. *Int. J. Clin. Pediatr. Dent.* 13(3): 288–294.

49 Shinohara A, Motoyoshi M, Uchida Y, Shimizu N. (2013). Root proximity and inclination of orthodontic mini-implants after placement: cone-beam computed tomography evaluation. *Am. J. Orthod. Dentofacial Orthop.* 144(1): 50–56.

50 Gurdan Z, Szalma J. (2018). Evaluation of the success and complication rates of self-drilling orthodontic mini-implants. *Niger J. Clin. Pract.* 21(5): 546–552.

51 Suzuki EY, Suzuki B. (2011). Placement and removal torque values of orthodontic miniscrew implants. *Am. J. Orthod. Dentofacial Orthop.* 139(5): 669–678.

52 Park HS, Jeong SH, Kwon OW. (2006). Factors affecting the clinical success of screw implants used as orthodontic anchorage. *Am. J. Orthod. Dentofacial Orthop.* 130(1): 18–25.

53 Fah R, Schatzle M. (2014). Complications and adverse patient reactions associated with the surgical insertion and removal of palatal implants: a retrospective study. *Clin. Oral Implants Res.* 25(6): 653–658.

t.me/Dr_Mouayyad_AlbtousH

2

Requirements for the Insertion of Orthodontic Temporary Anchorage Devices

Lin Xiang[1], Ziwei Tang[2], Jing Zhou[3], Hong Zhou[2,4], Qingxuan Wang[2], Waseem S. Al-Gumaei[2], Hu Long[2], and Liang Zhang[1,5]

[1] *Department of Implantology, State Key Laboratory of Oral Diseases and National Clinical Research Center for Oral Diseases, West China Hospital of Stomatology, Sichuan University, Chengdu, China*
[2] *Department of Orthodontics, State Key Laboratory of Oral Diseases and National Clinical Research Center for Oral Diseases, West China Hospital of Stomatology, Sichuan University, Chengdu, China*
[3] *Department of Pediatric Dentistry, State Key Laboratory of Oral Diseases and National Clinical Research Center for Oral Diseases, West China Hospital of Stomatology, Sichuan University, Chengdu, China*
[4] *Private Practice, Chengdu, China*
[5] *Center of Stomatology, West China Xiamen Hospital of Sichuan University, Xiamen, Fujian, China*

2.1 Introduction

When a clinical decision to insert orthodontic TADs for anchorage augmentation is made, the next step is to consider an optimal insertion site that meets both the biomechanical and anatomical requirements. It is intuitive to determine optimal insertion sites of orthodontic TADs from the perspective of biomechanics, e.g. insertion of interradicular mini-implants between buccal interradicular sites for anterior retraction (Figure 2.1a,b). However, due to the anatomical limitations of interradicular sites (e.g. inadequate bone volume or limited width of attached gingiva), mini-implants inserted at these regions are susceptible to failure (Figure 2.1c). Thus, alternative insertion sites may be chosen to optimise the clinical success of orthodontic TADs (Figure 2.1d). Moreover, systemic factors, such as osteoporosis, influence the success rates of orthodontic TADs. Thus, in this chapter, we will focus on both systemic (e.g. systemic factors) and local (both hard and soft tissues) requirements for the insertion of orthodontic TADs.

Clinical Insertion Techniques of Orthodontic Temporary Anchorage Devices, First Edition. Edited by Hu Long, Xianglong Han, and Wenli Lai.
© 2024 John Wiley & Sons Ltd. Published 2024 by John Wiley & Sons Ltd.

t.me/Dr_Mouayyad_AlbtousH

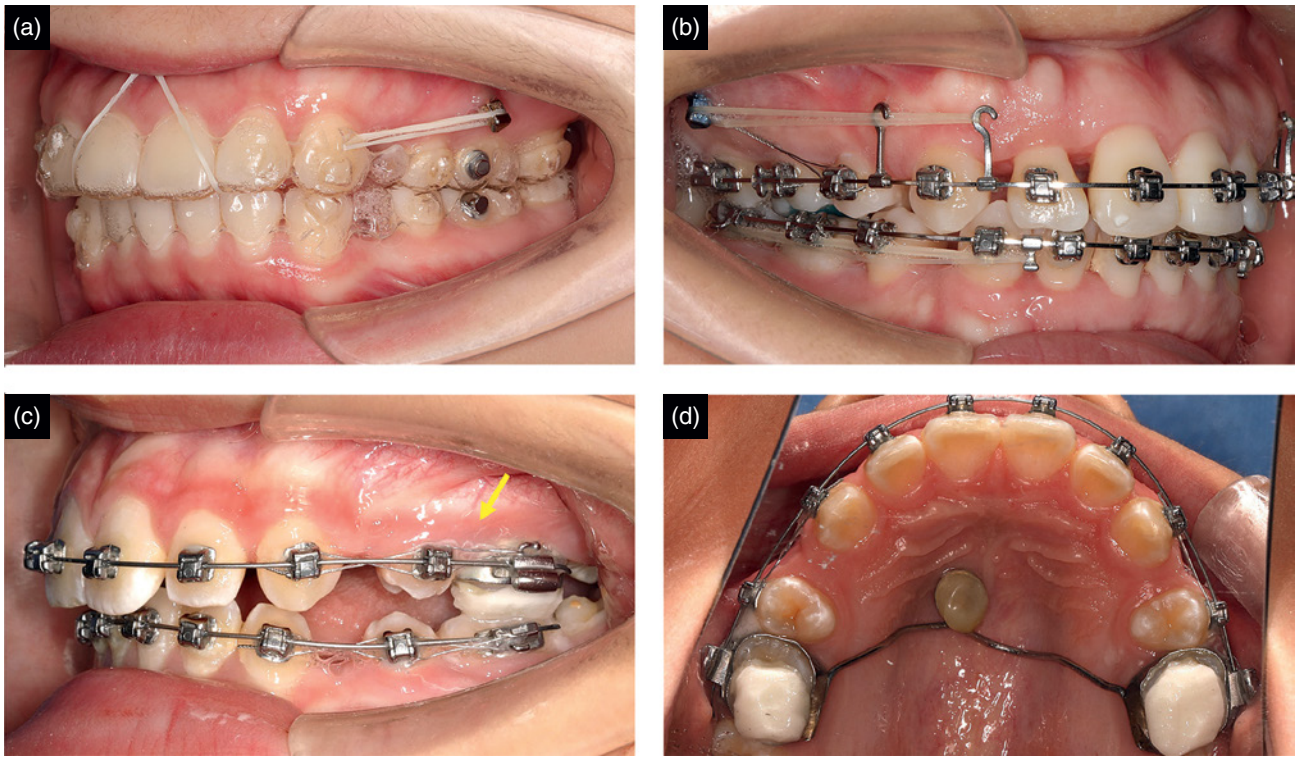


Figure 2.1 Determination of the optimal sites for mini-implants. (a) Insertion of a mini-implant at the buccal interradicular site for anterior retraction with clear aligner. (b) Insertion of a mini-implant at the infrazygomatic crest region for anterior retraction and molar anchorage reinforcement. (c,d) Insufficient width of attached gingiva (yellow arrow) at the buccal interradicular site rendered the insertion of mini-implants unsuitable. Thus, a mini-implant was inserted at the palatal vault region to reinforce molar anchorage through a palatal arch.

2.2 Systemic Requirements

The clinical success of orthodontic TADs is predominantly determined by the mechanical retention of alveolar bone. Alveolar bone is a living tissue composed of both cellular (i.e. precursor cells, osteoblasts, osteoclasts and osteocytes) and non-cellular components (i.e. hydroxyapatite crystals, collagens and non-collagenous proteins). Dynamic changes in bone quantity and quality (bone remodelling) take place in response to both physiological signals and pathological insults. Systemic factors that influence the process of alveolar bone remodelling in turn have an impact on the stability of orthodontic TADs (Figure 2.2). Thus, prior to insertion of orthodontic TADs, thorough examinations should be performed to verify that systemic requirements are met.

2.2.1 Basic Conditions

Age

Alveolar bone begins to develop following the eruption of teeth. In response to the increasing demands of occlusal force loading, alveolar bone remodelling takes place and results in an increase in bone quantity and quality. With the growth and development of alveolar bone from adolescence to adulthood, alveolar bone mass increases (Figure 2.3). Specifically, it has been revealed that both cortical bone thickness and density are greater among adults than among adolescents.[1-3] Moreover, recent studies have shown that total bone thickness (cortical bone thickness + cancellous bone thickness) of the palatal vault increases from adolescence to adulthood.[4] Thus, special care should be taken if orthodontic mini-implants are planned for adolescents with inadequate bone quantity or quality, since the failure rate of orthodontic TADs is higher among adolescents.[5,6]

Gender

Although alveolar bone mass is greater among males than females (Figure 2.3),[7,8] this difference in alveolar bone quantity and quality may not affect the success rate of orthodontic TADs.[9-12] Thus, in clinical settings, gender may not be an influencing factor in determining the success of orthodontic TADs.

t.me/Dr_Mouayyad_AlbtousH

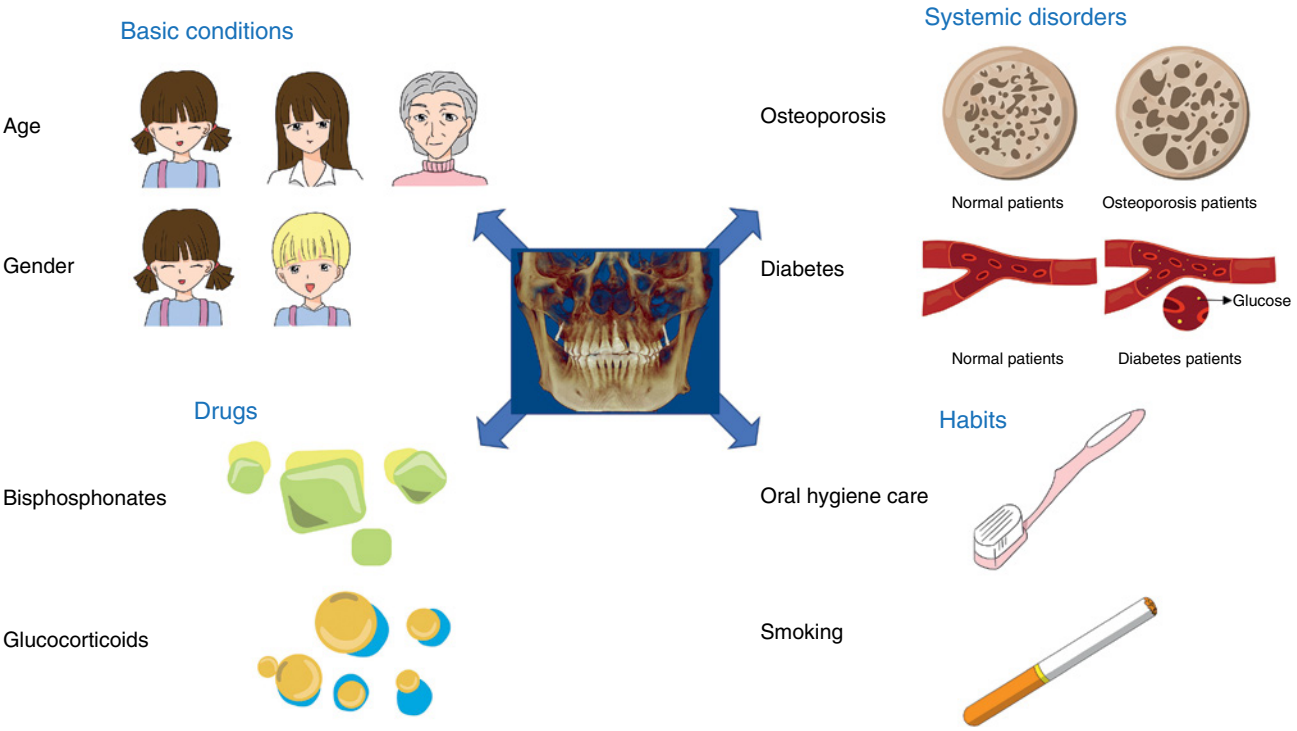


Figure 2.2 Systemic factors for the insertion of orthodontic TADs.

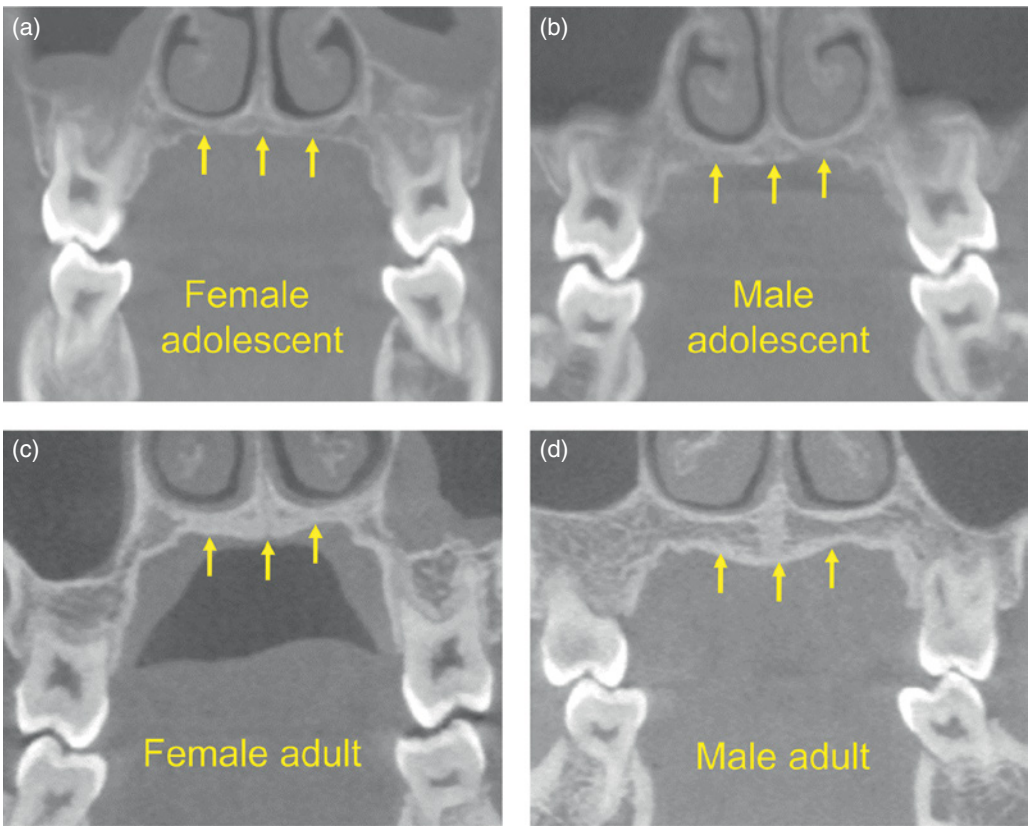


Figure 2.3 The influence of age and gender on bone quality and quantity. Note bone volume and density (yellow arrows) are greater and higher among male adults than female adolescents. (a) Female adolescent. (b) Male adolescent. (c) Female adult. (d) Male adult.

t.me/Dr_Mouayyad_AlbtousH

2.2.2 Systemic Diseases

Osteoporosis

To reiterate, bone remodelling occurs in response to both physiological and pathological signals. Thus, dynamic bone remodelling is taking place throughout individuals' whole lives. It has been revealed that the potential of bone remodeling is decreased among adults in comparison to adolescents,[13] which may explain the senescent or osteoporotic changes of alveolar bone with age. Bone becomes less dense and its structures deteriorate with age, leading to a clinical manifestation of osteoporosis. Being an integral part of skeletal bone, craniofacial bone is subject to hormone regulation (e.g. calcitonin), like the bones in other parts of the body.[14,15] The density of craniofacial and alveolar bone is positively correlated with that of the axial and lumbar skeleton. Moreover, it has been shown that the density of maxillary bone is significantly lower in osteoporotic individuals than in healthy people.[16] Thus, the decision to insert orthodontic TADs for patients with osteoporosis should be made with caution since alveolar bone density may be inadequate to support orthodontic TADs in individuals with osteoporosis (Figure 2.4).

Diabetes

It has been well documented that alveolar bone remodelling associated with implants is hindered in diabetic patients.[17] A histological study revealed that diabetic condition resulted in less bone-to-implant contact, indicative of compromised bone remodelling around implants.[18] As displayed in Figure 2.5, the underlying mechanisms are considered to be hyperglycaemia-induced accumulation of advanced glycation end-products that result in upregulation of inflammatory cytokines, e.g. IL-6, TNF-alpha, IL-8 and RANKL.[17,19] The inflammatory cytokines in turn lead to inhibition of osteoblasts and activation of osteoclasts,[19] resulting in compromised alveolar bone remodelling and undesirable secondary stability of orthodontic TADs. With insufficient secondary stability, orthodontic TADs applied in diabetic patients are more susceptible to failure and loosening than otherwise healthy orthodontic patients. Thus, diabetic condition should be considered when clinical applications of orthodontic TADs are planned.

Miscellaneous

As mentioned above, bone is an active organ subject to remodelling that is dependent on orchestrated interactions between osteoblasts and osteoclasts. The activities of osteoblasts and osteoclasts in the process of bone remodelling around orthodontic TADs are finely tuned by a variety of hormones, e.g. parathyroid hormone, calcitonin, growth hormone, glucocorticoid and oestrogen. In particular, the volume and thickness of alveolar bone decreased among menopausal females, indicating the significance of oestrogen in maintaining bone mass in females.[20] Thus, any disturbance in these aforementioned hormones may affect alveolar bone remodelling around orthodontic TADs, resulting in inadequate secondary stability. Thus, before insertion of orthodontic TADs, a thorough medical history should be taken and alternative biomechanics should be designed for those with severe endocrine disorders that contraindicate the use of TADs.

2.2.3 Drugs

Bisphosphonates

Since their clinical advent over three decades ago, bisphosphonates have been widely used to manage skeletal disorders.[21] Bisphosphonates are used for various clinical conditions, e.g. heritable skeletal disorders, osteoporosis due to menopause or glucocorticoid use, and malignancies with bone metastases.[21-23] Bisphosphonates can selectively concentrate in bone and inhibit bone resorption by inhibiting the activity of osteoclasts, resulting in slower bone

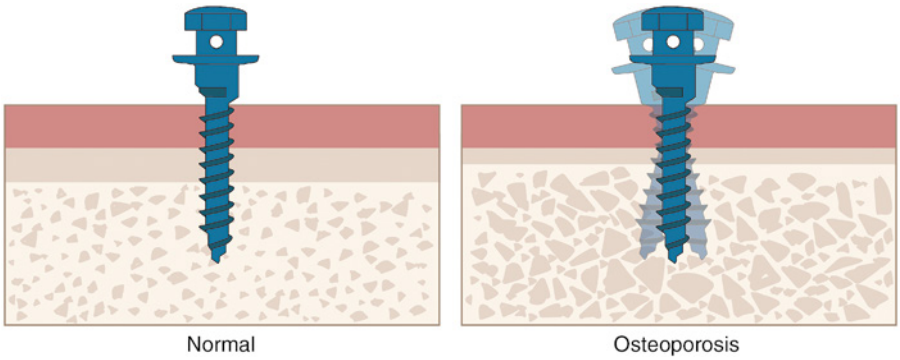


Figure 2.4 The stability of mini-implants inserted in an otherwise healthy orthodontic patient versus an osteoporotic patient. Note that the mini-implant inserted in the patient with osteoporosis exhibits excessive mobility.

t.me/Dr_Mouayyad_AlbtousH

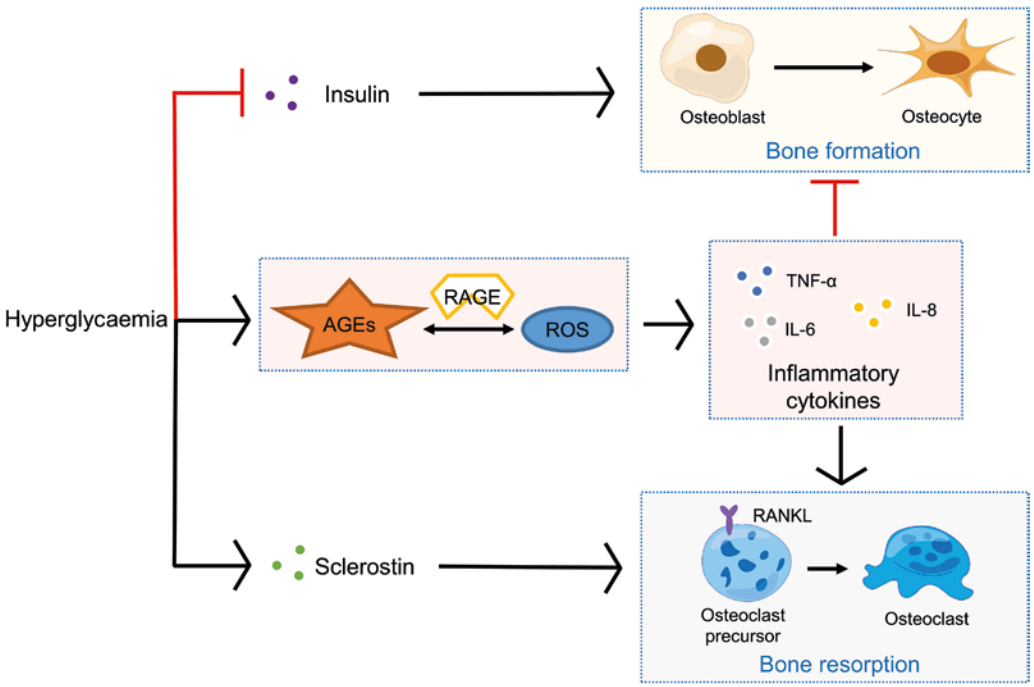


Figure 2.5 The mechanisms whereby hyperglycaemia influences bone remodelling. Elevated blood glucose level inhibits bone formation and promotes bone resorption through insulin inhibition, cytokine secretion stimulation and sclerostin upregulation. Notably, hyperglycaemia promotes the release of advanced glycation end-products (AGEs) that in turn upregulate reactive oxygen species (ROS) through the receptor for advanced glycation end-products (RAGE). The ROS further lead to inflammatory cascades and the release of inflammatory cytokines.

resorption and higher bone density (Figure 2.6). However, the increase in alveolar bone density but decrease in bone remodelling renders orthodontic TADs more susceptible to loosening and failure. This is similar to a clinical phenomenon in which mini-implants inserted at maxillae with lower density but higher bone remodelling levels have higher success rates than those inserted at mandibles with higher density but lower bone remodelling levels. Moreover, orthodontic TADs inserted in areas with higher bone density cause more pronounced mechanical and thermal trauma that demand postinsertion bone remodelling for healing (Figure 2.7). With reduced bone remodelling levels among patients taking bisphosphonates, secondary stability of orthodontic TADs is undesirable.

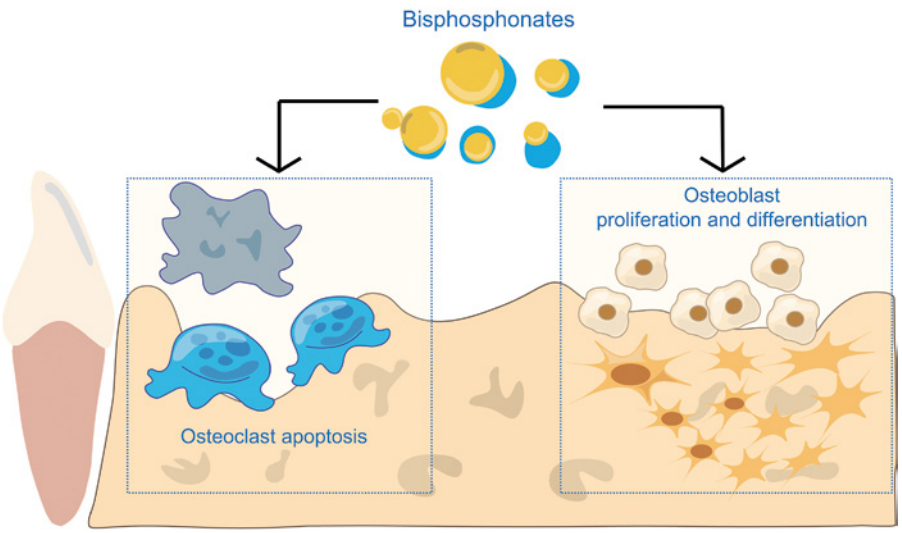


Figure 2.6 Bisphosphonates induce osteoclast apoptosis and promote osteoblast proliferation and differentiation.

t.me/Dr_Mouayyad_AlbtousH

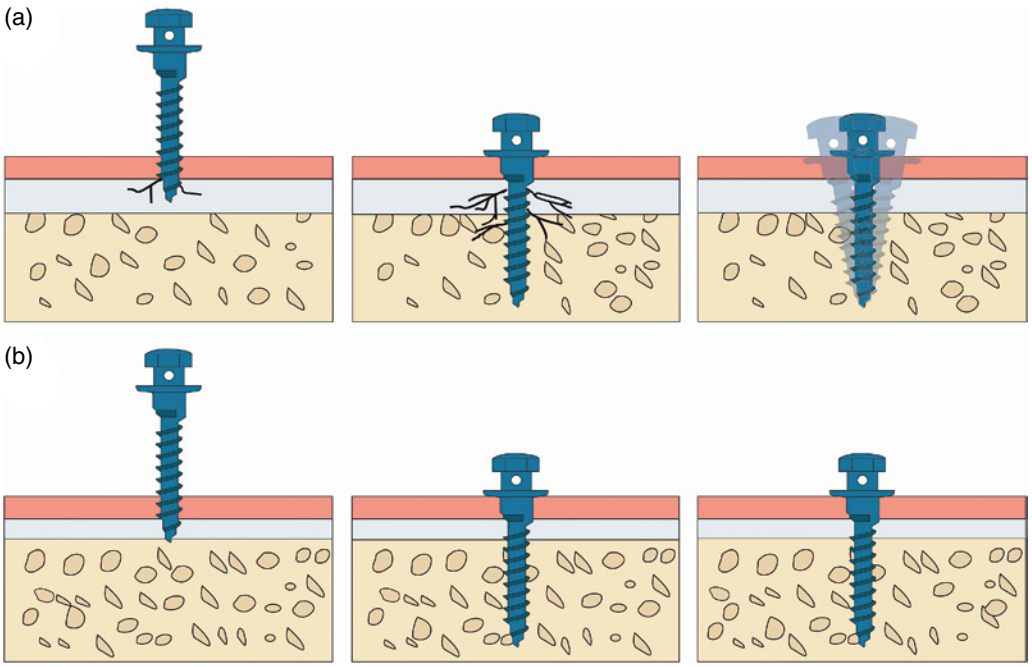


Figure 2.7 High bone density leads to bone fractures during insertion of the mini-implant. (a) Bone fracture occurs during the insertion of a mini-implant into alveolar bone with high bone density and thick cortex. Due to severe bone trauma, bone healing is undesirable and the mini-implant exhibits excessive mobility. (b) Minimal or no bone fracture occurs during insertion of a mini-implant into alveolar bone with lower bone density and thinner cortex. Postinsertion stability is adequate.

While intravenous bisphosphonates are strictly contraindicated for orthodontic TADs,[24,25] oral bisphosphonates are not absolutely contraindicated. After a six-month withdrawal of oral bisphosphonates, assessment of bone metabolism rate through C-terminal cross-linking telopeptide is recommended prior to the insertion of orthodontic TADs.[26] Therefore, the planning of orthodontic TADs should be cautious for patients who are taking or have taken bisphosphonates.

Glucocorticoids

Gluococorticoids are the treatment of choice for autoimmune and inflammatory diseases.[27] Glucocorticoid treatment has adverse effects on bone, leading to glucocorticoid-induced osteoporosis that is the most common type of secondary osteoporosis. Glucocorticoids contribute to secondary osteoporosis by acting on osteoblasts (interfering with recruitment and inducing apoptosis) and osteoclasts (enhancing osteoclast differentiation and maturation), and inhibits intestinal calcium absorption (Figure 2.8).[28,29] Thus, orthodontic TADs are relatively contraindicated for patients taking glucocorticoids.

Miscellaneous

Other medications, e.g. antiangiogenics (i.e. sorafenib, avastin, rapamycin, etc.), antihypertensives (i.e. loop diuretics) and levothyroxine, have an impact on bone metabolism and may interfere with bone remodelling around orthodontic TADs. Thus, a complete medical history and drug history should be taken in order to maximise the clinical success of orthodontic TADs.

2.2.4 Habits

Oral Hygiene Care

Individuals with inadequate oral hygiene are prone to periodontitis that in turn leads to decreased thickness and density of alveolar bone.[30] Clinical evidence indicates that the failure rate of orthodontic TADs is higher among patients with undesirable oral hygiene care.[31,32] Thus, prior to the insertion of orthodontic TADs, patients should be instructed to adhere to meticulous oral hygiene maintenance habits. Otherwise, placement of TADs should be postponed.

Smoking

Smoking is closely related to the occurrence of periodontitis, attachment loss and alveolar bone resorption (Figure 2.9). Clinical evidence reveals that smoking has a detrimental effect on the clinical success of orthodontic TADs.[33] Mechanistically, it has been demonstrated that smoking interferes with the process of alveolar bone remodelling through inhibiting a variety of molecules,

t.me/Dr_Mouayyad_AlbtousH

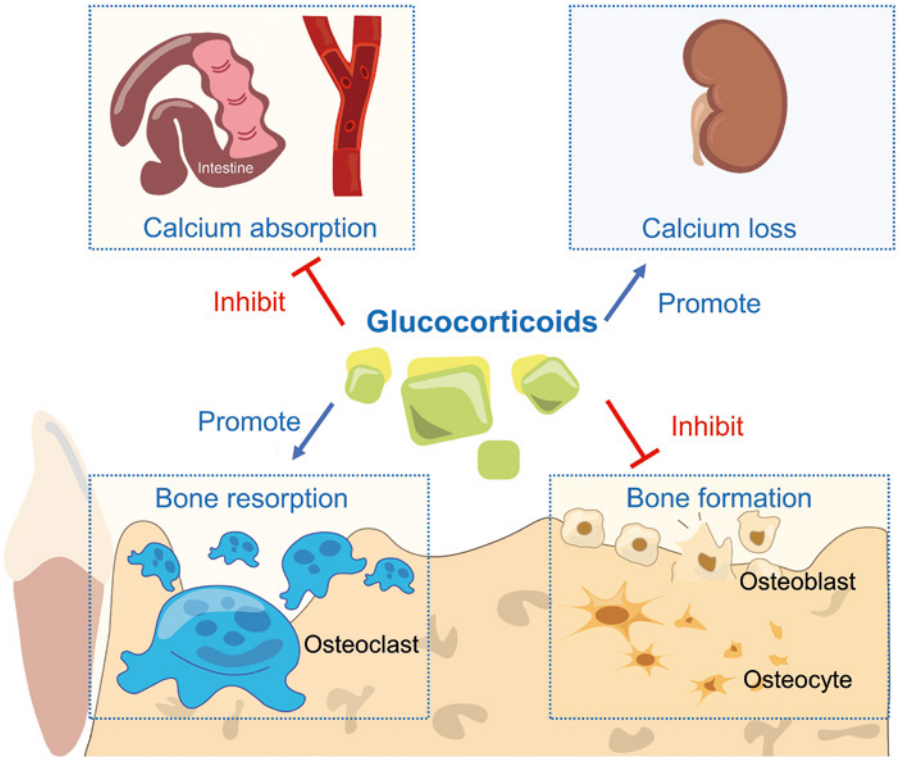


Figure 2.8 Glucocorticoids inhibit calcium absorption in the intestine and enhance calcium loss in the kidney. Moreover, they promote bone resorption by acting on osteoclasts and inhibit bone formation through acting on osteoblasts.

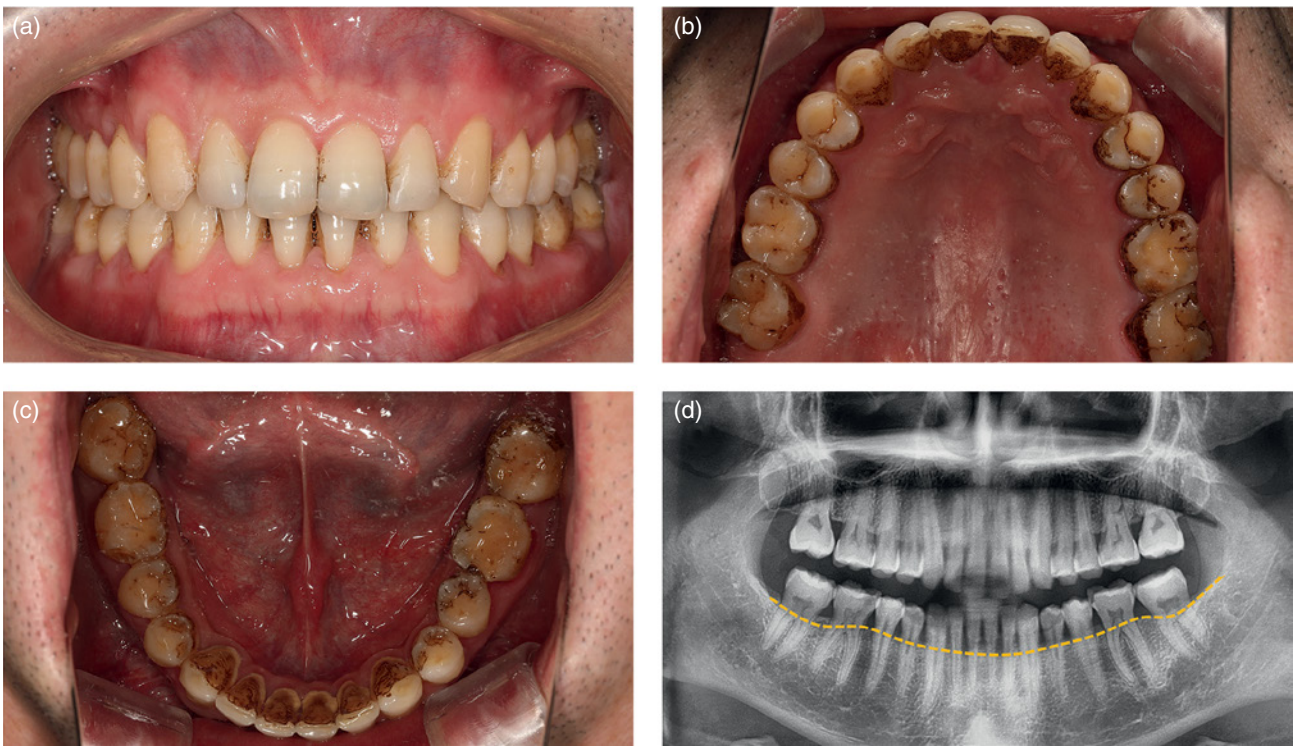


Figure 2.9 The influence of smoking habit on periodontal health. (a–c) Intraoral photographs are indicative of gingival recession and the presence of tartar. (d) The panoramic radiograph shows resorption of the alveolar bone. Note the position of the alveolar crest (yellow dashed line).

t.me/Dr_Mouayyad_AlbtousH

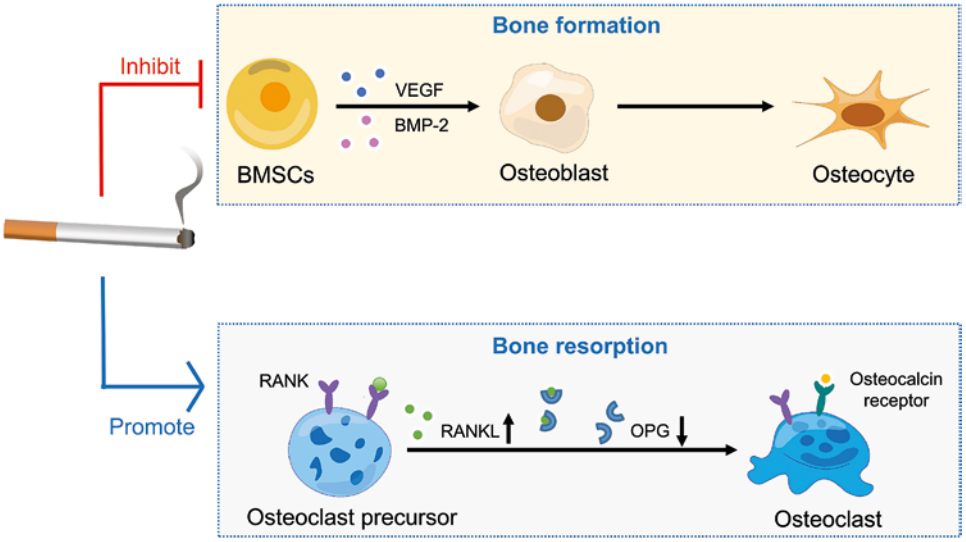


Figure 2.10 Smoking suppresses bone formation by inhibiting the proliferation and differentiation of osteoblasts and promotes bone resorption by enhancing osteoclast differentiation.

including osteoblast-related molecules (osteocalcin), osteoclast-related proteins (calcitonin receptor), bone remodelling molecules (RANKL, OPG and their ratio) and other molecules (VEGF and BMP-2) (Figure 2.10).[34] Thus, smoking cessation should be emphasised prior to the placement of orthodontic TADs.

2.3 Local Requirements

Orthodontic TADs should be stable enough to withstand orthodontic force loading, so that various difficult tooth movements can be achieved, e.g. molar protraction, anterior retraction with high anchorage requirements and molar intrusion. As displayed in Figure 2.11, once an orthodontic mini-implant is inserted into alveolar bone, it is surrounded and supported by both the hard tissue (alveolar bone) and soft tissue (gingiva or mucosa). Intuitively, the stability of mini-implants is predominantly determined by the mechanical retention of alveolar bone, indicating the significance of bone quantity and quality in ensuring the stability of mini-implants. However, soft tissue also plays an important role in maintaining the stability of mini-implants. For the ease of force applications, orthodontic mini-implants are required to penetrate through soft tissue and have a sufficient emergence profile, which demands adequate soft tissue seal around the mini-implants. Otherwise, inadequate soft tissue seal may cause local inflammation and subsequently interfere with bone remodelling, resulting in compromised secondary stability and mini-implant failure. Thus, both hard and soft tissues

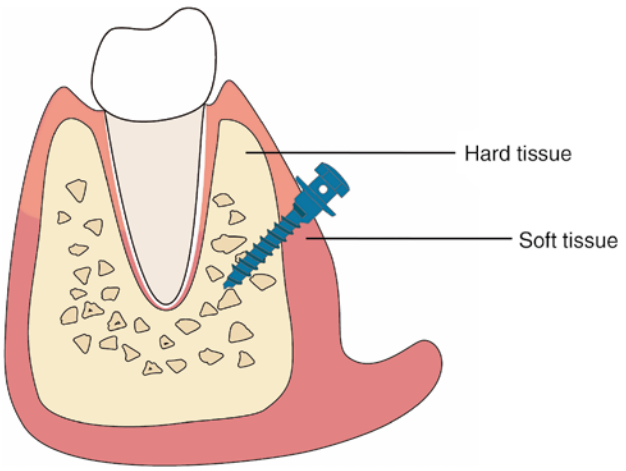


Figure 2.11 The mini-implant is supported by both the hard tissue and the soft tissue.

should satisfy certain requirements to guarantee the clinical success of orthodontic TADs.

2.3.1 Hard Tissue

Primary stability of an orthodontic mini-implant is governed by the mechanical retention resulting from the compression-tension state generated at the bone–implant interface. This mechanical retention is determined by the quantity and quality of bone that is influenced by a variety of factors, including bone density, bone depth, bone width and cortical thickness. Before delving into the details of influencing factors that affect bone quantity and quality,

t.me/Dr_Mouayyad_AlbtousH

we will first discuss two distinct types of bone clinically available for placing orthodontic TADs.

Alveolar Bone and Extra-alveolar Bone

Alveolar bone is formed and developed during and after tooth eruption from the alveolar process of maxillary and mandibular bone in order to accommodate dental roots. To put it simply, alveolar bone is the interradicular bone that surrounds dental roots while extra-alveolar bone is often referred to as the bone outside dental roots. Although alveolar bone is more commonly used for the placement of orthodontic mini-implants, extra-alveolar bone has been gaining popularity in the orthodontic community.[35,36] Extra-alveolar bone often benefits from the thickening of cortical bone and enjoys an advantage of better bone quality and greater bone quantity over alveolar bone.[3] Moreover, since extra-alveolar bone lies outside dental roots, the chance of root injury is negligible for mini-implants placed at this region.

Although alveolar bone and extra-alveolar bone differ in quality and quantity, they are not anatomically exclusive but continuous with each other. Interradicular sites are the targeted areas for mini-implants to be inserted at the alveolar bone region, while various extra-alveolar sites are clinically available for the placement of mini-implants, i.e. anterior nasal spine, infrazygomatic crest, hard palate, maxillary tuberosity, mandibular symphysis, buccal shelf and mandibular ramus (Figures 2.12 and 2.13). Although extra-alveolar sites enjoy the advantage of better bone quality and greater bone quantity over interradicular sites (alveolar bone), longer mini-implants and flap surgery may be indicated. The advantages and disadvantages of alveolar and extra-alveolar bone are summarised in Table 2.1.

Bone Density

To satisfy functional requirements, different parts of the maxilla and mandible are equipped with different bones of varying degrees of cortical thickness and mineralisation. Based on the ratio of cortical bone to cancellous bone and the macroscopic features of bone, a classification system of bone into five different densities was proposed by Misch in 1990 (Figure 2.14).[37] In particular, D5 bone is immature bone with a density less than 150 Hounsfield units (HU) and thus is not considered for the placement of orthodontic mini-implants. In contrast, D1–D4 bones are frequently used for mini-implants in clinical practice. D1 bone is predominantly composed of cortical bone with little cancellous bone and can be detected in the mandibular symphysis and buccal shelf, while D4 bone is characterised by little cortical bone, with the majority being cancellous bone, and can be found in the posterior region of the maxilla, i.e. maxillary tuberosity. Moreover, the features of D2 and D3 bones lie between those of D1 and D4 bones. The detailed characteristics and corresponding anatomical sites of D1–D5 bones are displayed in Table 2.2 and Figure 2.15.

The success rate of mini-implants is positively correlated with bone density.[38] Due to low density, D4 bone may not be indicated for the placement of orthodontic mini-implants. This is supported by a clinical study where a 74% success rate was observed at the maxillary tuberosity (D4 bone),[39] in contrast to a relatively higher success rate (91%) at interradicular sites (D2 or D3 bone).[40] However, paradoxically, orthodontic mini-implants inserted at D1 bone (e.g. infrazygomatic crest) fail to exhibit consistently higher success rates, ranging from 78% to 84%.[40,41] This could be attributed to thermal and mechanical damage of bone resulting from the thick and dense cortical bone where mini-implants must penetrate. The resulting bone damage interferes with bone remodelling processes, leading to compromised secondary stability. This notion could explain the clinical phenomenon where the success rate of mini-implants is higher in the maxilla than in the mandible, though bone density is higher in the mandible.[42]

Thus, in clinical practice, D2 and D3 bones are often selected for the placement of mini-implants. However, if mini-implants have to be inserted at D1 bone, measures can be taken to maximise clinical success through pilot drilling and copious irrigation with saline during insertion, so as to reduce mechanical and thermal damage of bone (Figure 2.16).

Bone Depth

Bone depth is defined as the distance from the cortical bone where the mini-implant initially penetrates to contralateral cortical bone or other limiting anatomical structures (e.g. palatal cortical plate, maxillary sinus and neurovascular bundles) (Figure 2.17). It is suggested that bone depth should be at least 4.5 mm to ensure adequate mini-implant stability.[43] A plethora of evidence indicates that the primary stability of mini-implants is positively correlated with the length of mini-implants.[44,45] Moreover, it is the intra-bony length of mini-implants that determines primary stability.[46] Thus, conceivably, with greater bone depth, a greater range of mini-implant length can be selected and longer mini-implants that may exhibit higher primary stability can be chosen (Figure 2.18).

However, increasing the length of mini-implant disproportionately to bone depth can be detrimental to stability and may lead to mini-implant failure. On one hand, with an increase in mini-implant length, insertion torque increases but fracture torque does not, rendering the mini-implant more susceptible to fracture.[45] On the other hand, increasing exposure length of the mini-implant (outside the bone) causes higher bone stress that may interfere with secondary bone remodelling and lead to eventual

t.me/Dr_Mouayyad_AlbtousH

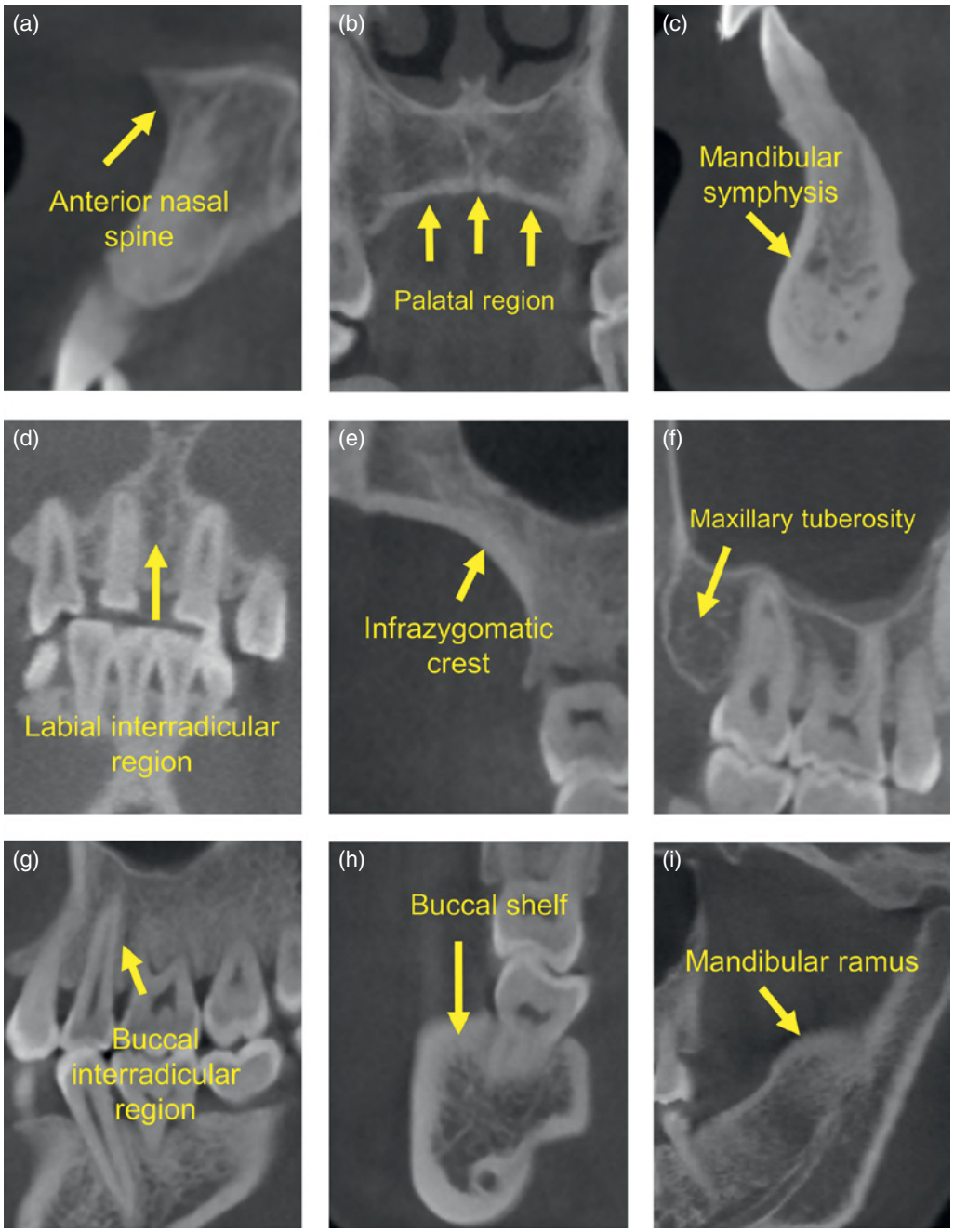


Figure 2.12 A variety of anatomical areas available for the placement of orthodontic TADs. (a) Anterior nasal spine. (b) Palatal region. (c) Mandibular symphysis. (d) Labial interradicular region. (e) Infrazygomatic crest. (f) Maxillary tuberosity. (g) Buccal interradicular region. (h) Buccal shelf. (i) Mandibular ramus.

failure.[47,48] Therefore, depending on different bone depths, the appropriate mini-implant length should be selected to maximise the clinical success of orthodontic mini-implants. For example, a 6 mm rather than 8 mm mini-implant is recommended for labial interradicular sites.

Occasionally, penetration of the contralateral cortical plate may be beneficial for increasing the primary stability of mini-implants, which is often encountered at the infrazygomatic crest and palatal vault (Figure 2.19). Penetration of two cortical plates gives the mini-implant bicortical engagement, which is more stable than and biomechanically superior to that with monocortical engagement (Figure 2.20). However, it has been suggested that penetration of the contralateral cortical plate may cause damage to the nasal cavity or maxillary sinus and should be avoided.[49] Recent clinical evidence and our personal

t.me/Dr_Mouayyad_AlbtousH

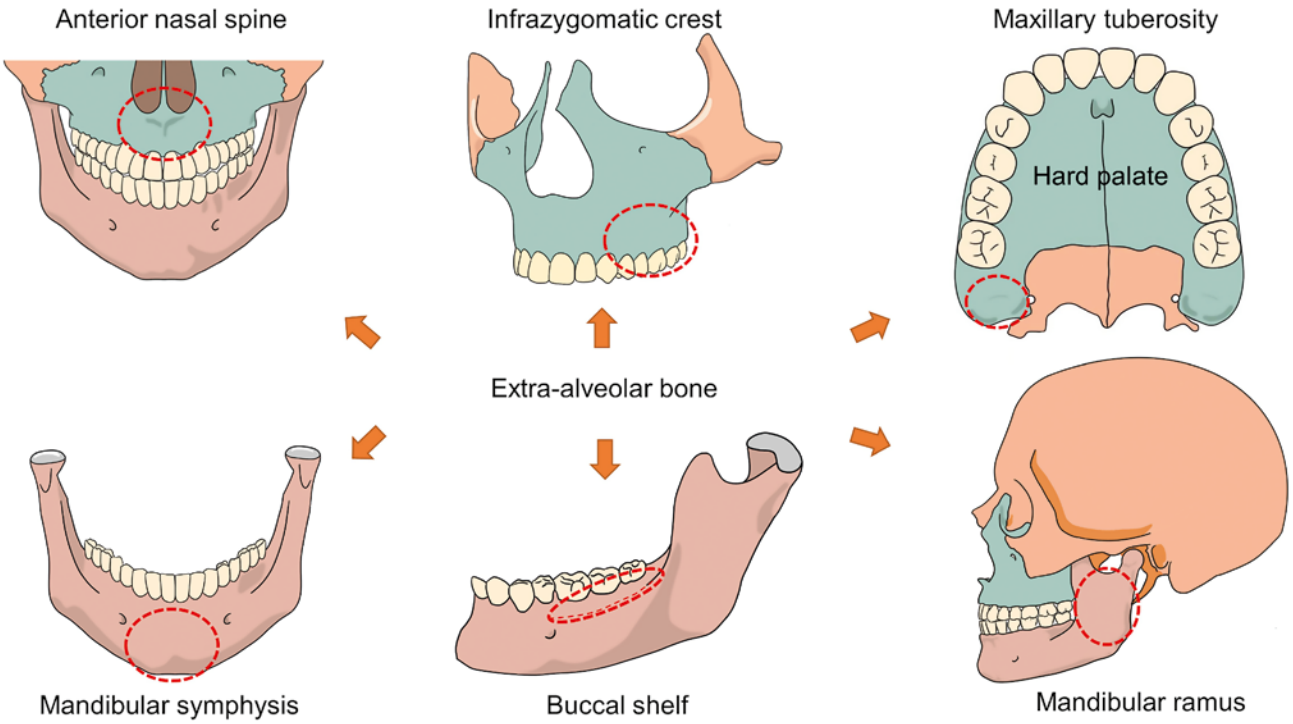
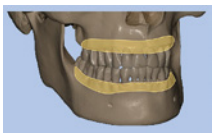
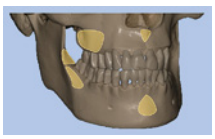


Figure 2.13 Schematic illustrations showing extra-alveolar regions for the placement of mini-implants.

Table 2.1 Advantages and disadvantages of alveolar and extra-alveolar bone.

	Advantage	Disadvantage
 Alveolar	Ease of insertion Less invasive	Risk of root damage Limited interradicular space
 Extra-alveolar	Better bone quality Greater bone quantity Greater primary stability	Flap surgery Soft tissue irritation

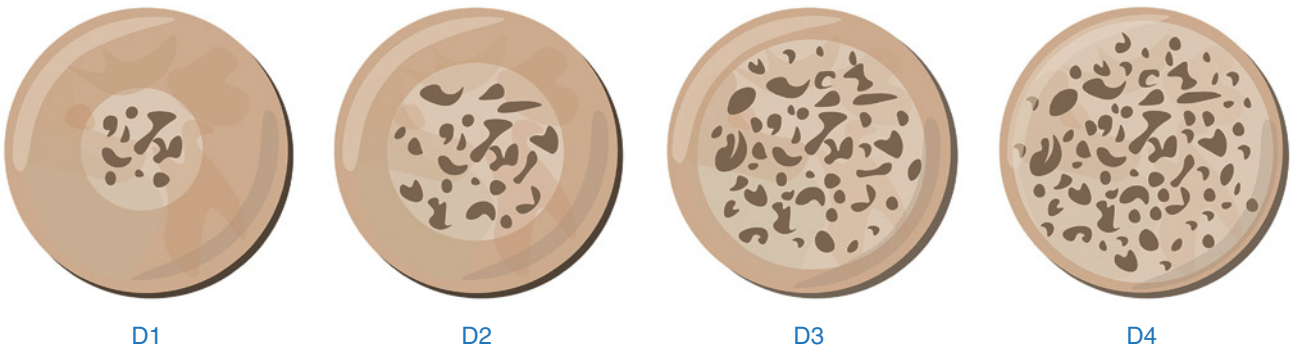


Figure 2.14 A schematic illustration showing the Misch classifications of bone according to different bone densities. D1 bone is almost entirely composed of cortical bone, with only a very small amount of dense trabecular bone. D2 bone has densely arranged trabecular bone surrounded by thick bone cortex. D3 bone exhibits densely arranged trabecular bone surrounded by thin bone cortex, while D4 bone has a thin layer of cortical bone and loosely arranged trabecular bone. D5 is immature bone and is not illustrated here.

t.me/Dr_Mouayyad_AlbtousH

Table 2.2 Detailed features and anatomic sites of D1–D5 bones.

Classification	Features	Anatomical sites
 **D1**	Predominantly composed of cortical bone with little trabecular bone	Mandibular symphysis Buccal shelf Mandibular ramus Midpalatal suture
 **D2**	Densely arranged trabecular bone surrounded by thick cortical bone	Anterior nasal spine Buccal shelf Palatal region Mandibular ramus Mandibular labial and buccal regions
 **D3**	Densely arranged trabecular bone surrounded by thin cortical bone	Maxillary labial and buccal region Mandibular buccal region
 **D4**	Loosely arranged trabecular bone surrounded by thin cortical bone	Maxillary posterior edentulous region Maxillary tuberosity
D5	Immature bone	Not suitable for insertion

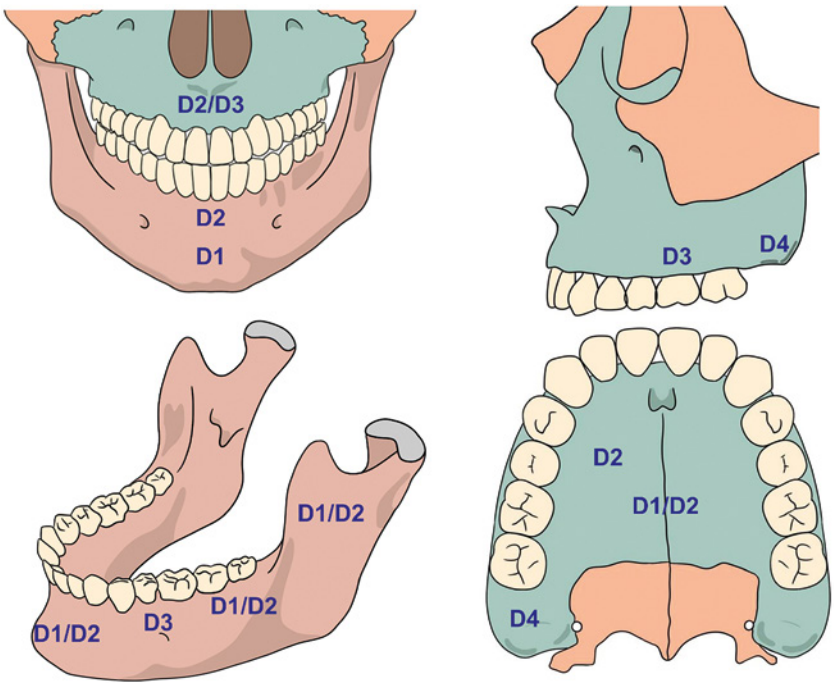


Figure 2.15 Schematic illustrations showing different anatomical sites corresponding to D1–D4 bones.

t.me/Dr_Mouayyad_AlbtousH

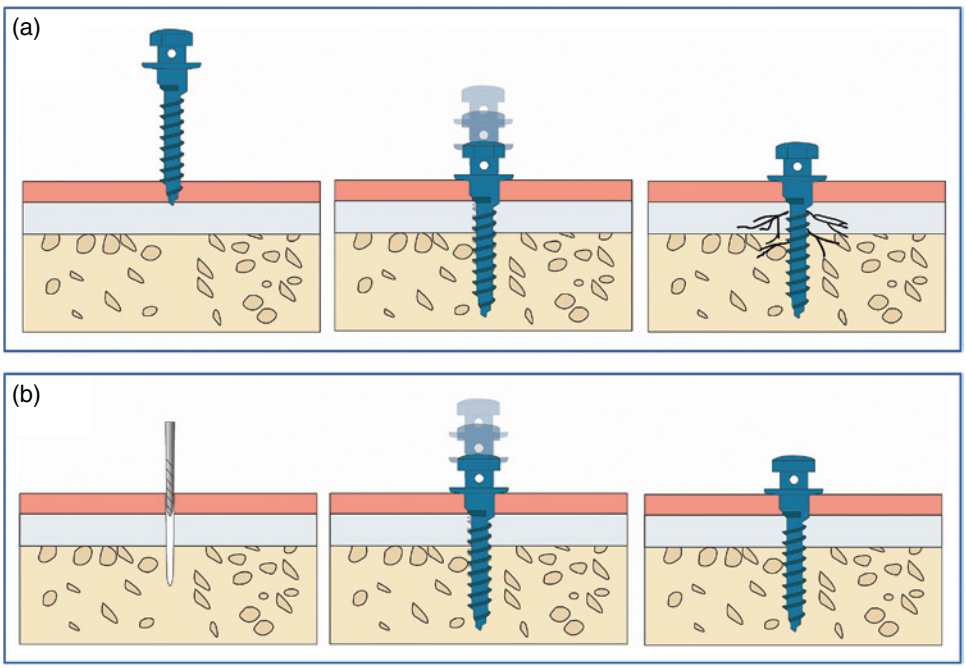


Figure 2.16 Predrilling is indicated for the insertion of mini-implants into D1 bone with thick cortex and high bone density. (a) Insertion of a mini-implant into a D1 bone area leads to bone fracture and damage. (b) Pilot drilling is performed before the insertion of a mini-implant. Note that minimal or no bone fracture occurs during and after the insertion.

clinical experiences suggest that unless pre-existing infection is present, penetration into the maxillary sinus or nasal cavity does not cause infection.[50] Thus, for the placement of mini-implants at the palatal vault and infrazygomatic crest, bicortical engagement mode is recommended for greater primary stability.

Bone Width

Bone width is the distance between two adjacent anatomical structures (e.g. two neighbouring roots) that limit the insertion of mini-implants in transverse dimension (Figure 2.17). As will be described in Chapter 3, at least 1 mm clearance from dental roots is highly recommended for mini-implants, as root proximity is associated with a high failure rate.[51-53] With inadequate bone width, smaller mini-implants have to be used to guarantee sufficient clearance from roots, which may result in compromised stability and subsequent loosening (Figure 2.21). Moreover, insufficient bone width increases the likelihood of root proximity and subsequent failure rate. Thus, bone width is recommended to be at least 2 mm greater than the diameter of the mini-implant.

As shown in Figure 2.22, bone width is influenced by various anatomical factors, such as anatomical site, buccal or palatal side and vertical position. Specifically, bone width varies at different anatomical sites, with the interradicular site between the second premolar and first molar being the widest and between the central and lateral incisors being the narrowest.

This finding is similar to that at the palatal side, but bone width is greater at the palatal side than the buccal side. In addition, vertical position has an impact on bone width that increases from crest to apex, suggesting insertion at a more apical level provides greater bone width and larger interradicular space (Figure 2.22 and 2.23).

Cortical Thickness

Cortical bone thickness is of great significance in ensuring the primary stability of mini-implants. Adequate primary stability offers a stable microenvironment for mini-implants to develop secondary stability (bone healing and remodelling). Otherwise, excessive micromovement of mini-implants results in excessive stress on alveolar bone around the implant and interferes with bone healing and remodelling, resulting in unacceptable secondary stability and mini-implant failure (Figure 2.24).

Both biomechanical and clinical studies suggest that cortical thickness should be at least 1 mm to guarantee adequate primary stability.[54,55] However, inevitable bone damage may be encountered if cortical bone is too thick,[56,57]

t.me/Dr_Mouayyad_AlbtousH

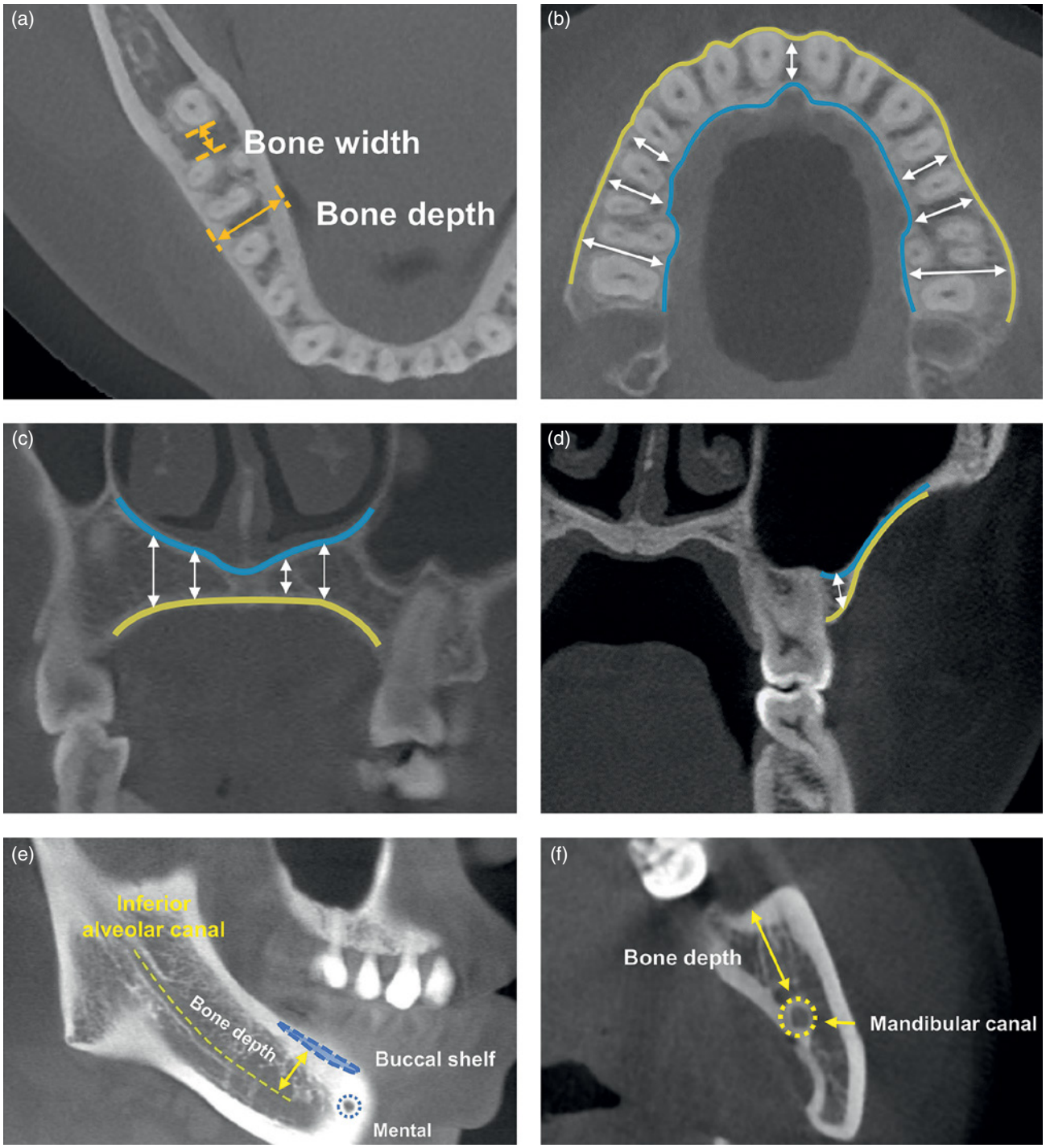


Figure 2.17 Bone depth and bone width. (a) Bone depth is the distance between the buccal and lingual cortical plates for interradicular sites while bone width is the distance between two adjacent roots. (b) Bone depth (between the buccal and lingual cortical plates) at different interradicular sites in the maxilla. (c) Bone depth (between the palatal cortex and nasal cortex) at the palatal vault. (d) Bone depth (between the buccal cortex and sinus cortex) at the infrazygomatic crest region. (e) Bone depth refers to the distance between the buccal cortex (blue dashed area) and the inferior alveolar canal (yellow dashed line) for the buccal shelf region. (f) Bone depth (between the buccal cortex and inferior alveolar canal) at the buccal shelf region.

t.me/Dr_Mouayyad_AlbtousH

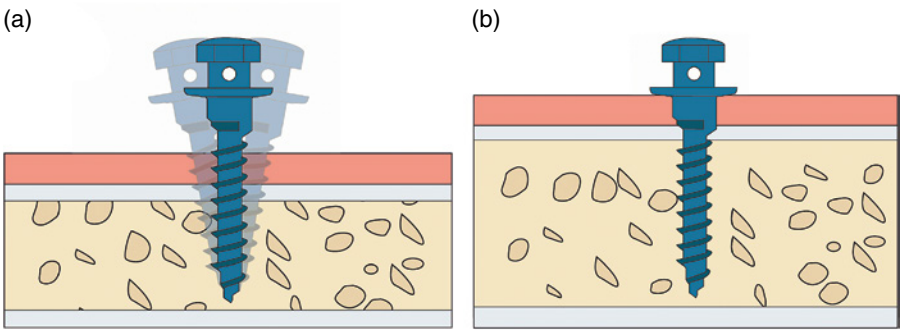


Figure 2.18 The influence of intra-bony length on the stability of a mini-implant. (a) A mini-implant with insufficient intra-bony length exhibits mobility. (b) A mini-implant with adequate intra-bony length exhibits sufficient stability.

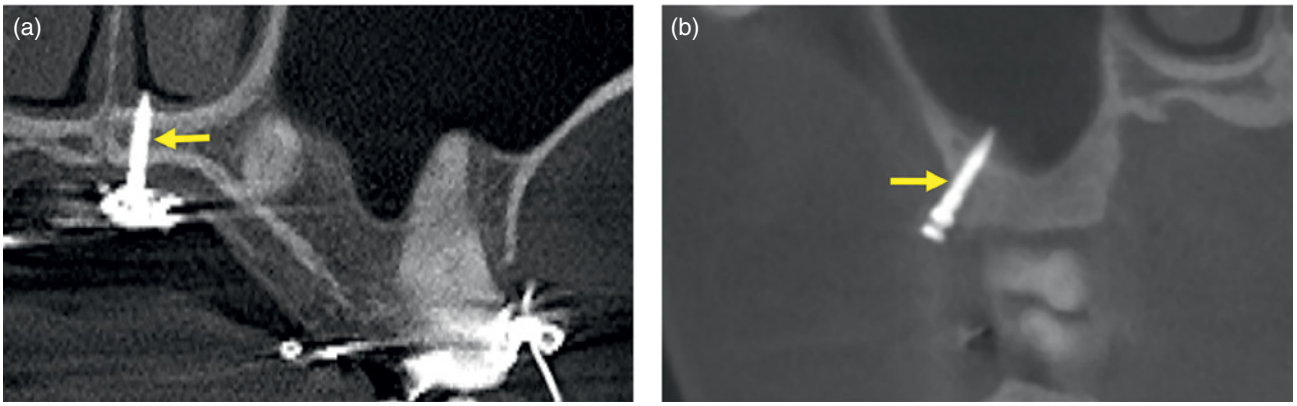


Figure 2.19 Penetration of the contralateral cortex by mini-implants and bicortical engagement mode is achieved. (a) Penetration of both the palatal cortex and the nasal cortex by a mini-implant (yellow arrow) inserted at the palatal vault region. (b) Penetration of both the buccal cortex and the sinus cortex by a mini-implant (yellow arrow) inserted at the infrazygomatic crest region.

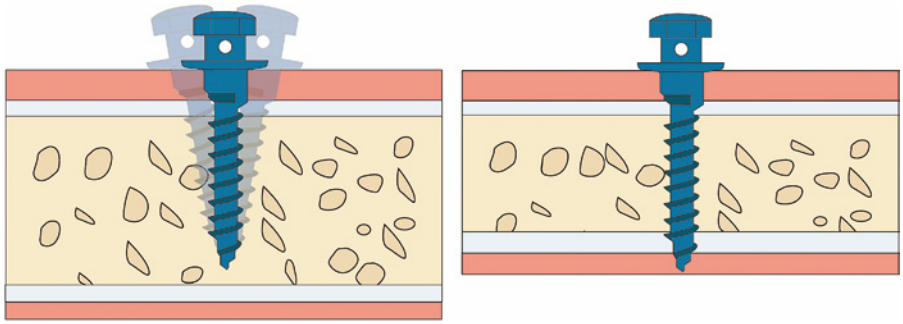


Figure 2.20 The bicortical engagement mode confers greater stability on the mini-implant.

which may interfere with bone remodelling and lead to poor secondary stability (Figure 2.25). Occasionally, mini-implants have to be inserted at anatomical sites with cortical thickness greater than 2 mm, so prudent measures should be taken to eliminate potential mechanical and thermal damage to bone. Nevertheless, we suggest that optimal cortical thickness is 1–2 mm.

Selection of Optimal Sites

We recommend that hard tissue should satisfy the following requirements (Figure 2.26): (1) bone density with D2 or D3 type; (2) bone depth greater than 4.5 mm; (3) bone width is adequate to insert mini-implants with 1 mm clearance from two adjacent roots; (4) cortical thickness is 1–2 mm.

t.me/Dr_Mouayyad_AlbtousH

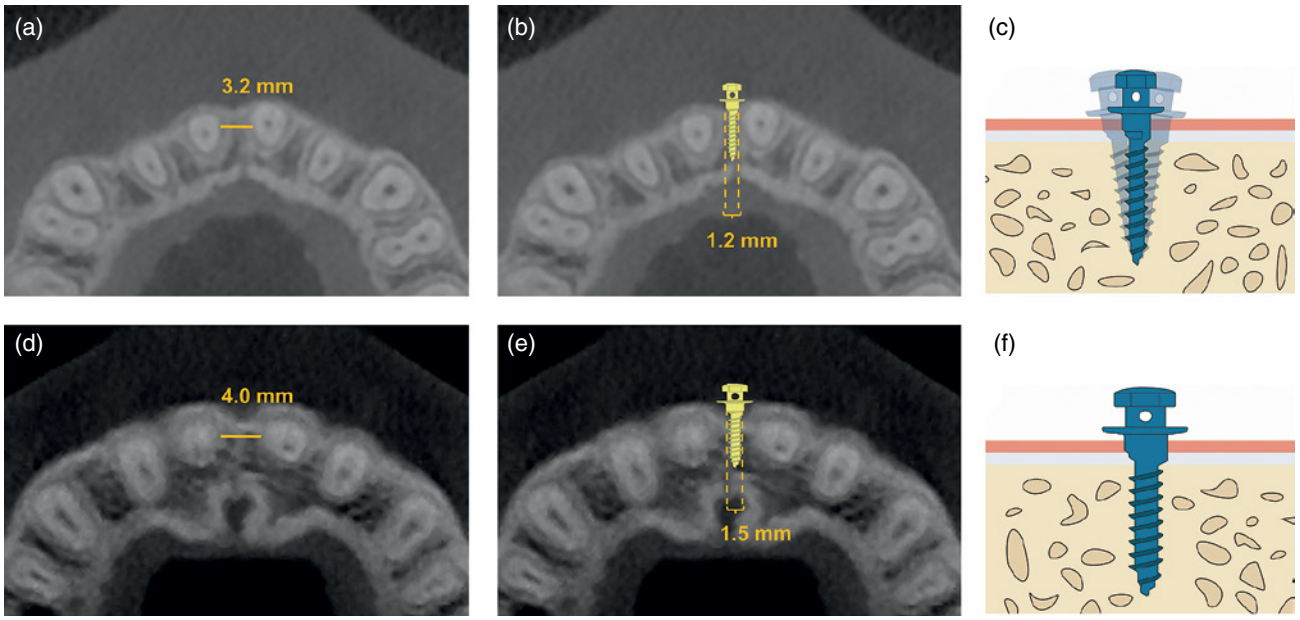


Figure 2.21 The influence of bone width on the selection of mini-implants and the resulting stability. (a,b) The limited interradicular space (3.2 mm) leads to selection of a small mini-implant (diameter: 1.2 mm). (c) The mini-implant may exhibit mobility. (d,e) Ample interradicular space (4.8 mm) offers a greater range of selection of mini-implants with different diameters. A larger mini-implant (diameter: 1.5 mm) is chosen. (f) The mini-implant exhibits greater stability.

2.3.2 Soft Tissue

The placement of mini-implants into bone elicits a reactive response from both the hard and soft tissues at implant–bone and implant–gingiva interfaces, respectively. In particular, soft tissue may incite varying degrees of response at the implant–gingiva interface, ranging from soft tissue healing with adequate soft tissue seal to soft infection with hyperplasia that may eventually cover the mini-implant head. As displayed in Figure 2.27, three distinct types of soft tissues can be encountered in clinical practice. The histological details of gingivae are depicted in Figure 2.28.

Types of Soft Tissue

Free gingiva refers to the gingiva between the gingival margin and the free gingival groove that is approximately at the level of the alveolar crest. It is keratinised in nature and pale pink in colour, rendering it difficult to differentiate from attached gingiva. Free gingiva is mobile and mini-implants should not be inserted here due to the lack of bone support (Figure 2.29).

Attached gingiva is defined as the gingiva between the free gingiva groove and mucogingival junction. Attached gingiva has a pale-pink appearance with stippling. With bone support, attached gingiva is fixed and immobile, rendering this area suitable for the placement of mini-implants. Specifically, good soft tissue adaptation will occur once mini-implants are inserted, resulting in an adequate soft tissue seal. Moreover, the keratinisation of attached gingiva renders it resistant to biological and mechanical insults.

Mobile mucosa refers to the soft tissue that is apical to the mucogingival junction. Since it is unattached and non-keratinised, alveolar mucosa is mobile and soft. It will move as functional movements occur, e.g. mastication. If mini-implants are inserted at this region, soft tissue may jiggle around the mini-implant and wrap around the threads, causing excessive soft tissue damage. Moreover, the mobile alveolar mucosa may be irritated by the mini-implant heads and adequate soft tissue seal will be difficult to achieve, resulting in undesirable soft tissue complications (e.g. infection, inflammation and hyperplasia).

Different anatomical sites exhibit different types of soft tissue. As shown in Figure 2.30, for interradicular sites, all the three types of soft tissue are present. Moreover, the hard palate and maxillary tuberosity are covered by attached gingiva only, while other extra-alveolar zones are covered by mobile mucosa.

Thickness of Soft Tissue

The thickness of soft tissue affects the clinical success of mini-implants in two ways (Figure 2.31). First, the thick soft tissue may easily wrap around the mini-implant heads and progress to soft tissue complications, e.g.

t.me/Dr_Mouayyad_AlbtousH

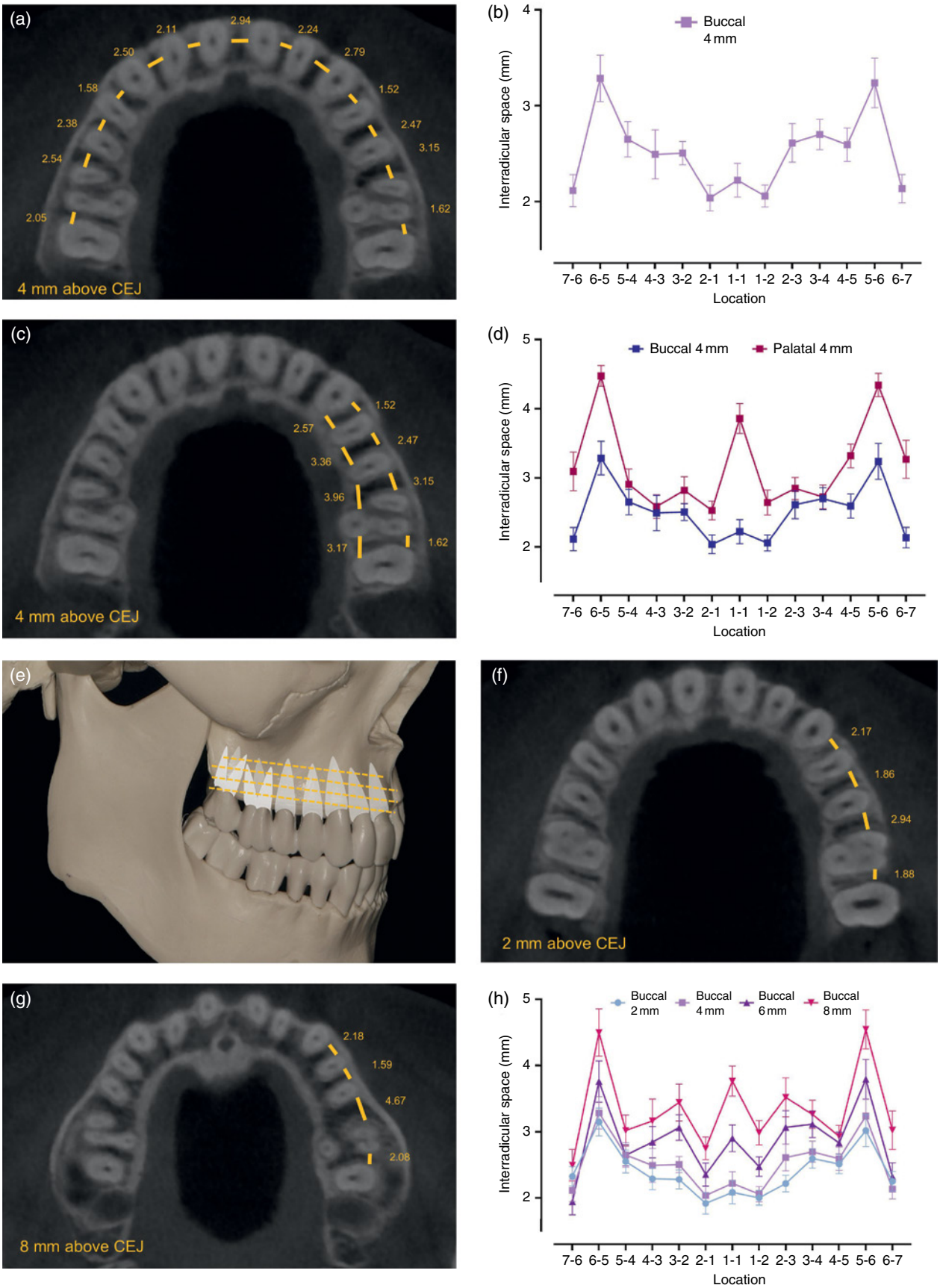


Figure 2.22 The influence of different interradicular sites, heights and sides (buccal versus palatal) on bone width. (a,b) Bone widths at different interradicular sites at the 4 mm level apical to the CEJ. Note that the interradicular site (U5–U6) exhibits the greatest bone width. (c,d) The differences in bone width at the buccal versus palatal sides. Note bone width is generally greater at the palatal side than at the buccal side. (e–h) The differences in bone width at different vertical levels. Note that bone width becomes greater as it approaches more apically.

t.me/Dr_Mouayyad_AlbtousH

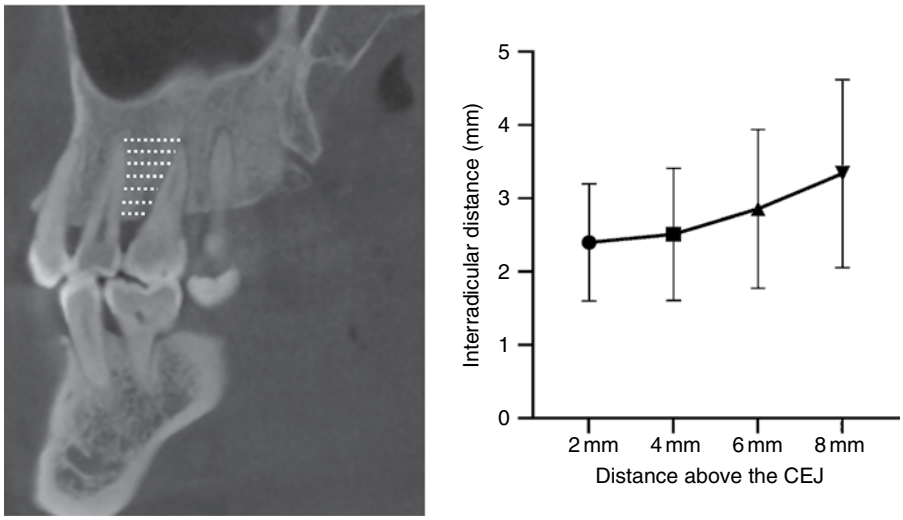


Figure 2.23 Differences in bone width at different vertical levels (2–8 mm apical to the CEJ). Note that the bone width is greater at more apical levels.

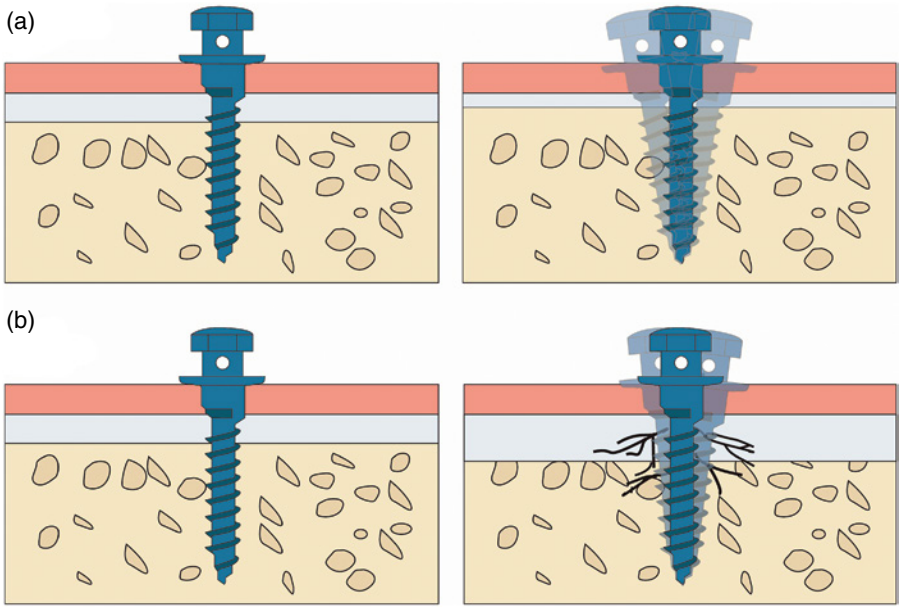


Figure 2.24 The influence of cortical thickness on the stability of the mini-implant. (a) The mini-implant inserted in alveolar bone with optimal cortical thickness (1–2 mm) displays adequate stability while that placed in alveolar bone with thin cortex exhibits excessive mobility. (b) Comparison of the stability between two mini-implants. One mini-implant is inserted in alveolar bone with optimal cortical thickness (1–2 mm) while the other is inserted at the bone region with thick cortex. Note that bone fractures and damage occur during the insertion and stability of the mini-implant is not desirable.

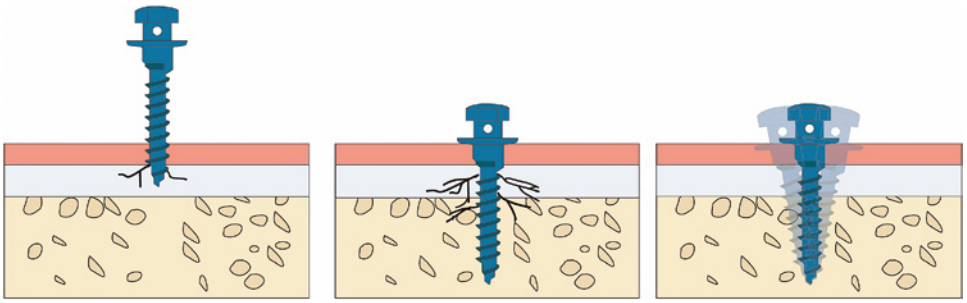


Figure 2.25 Bone damage may occur if cortical bone is too thick, which may interfere with bone remodelling and lead to poor secondary stability.

t.me/Dr_Mouayyad_AlbtousH

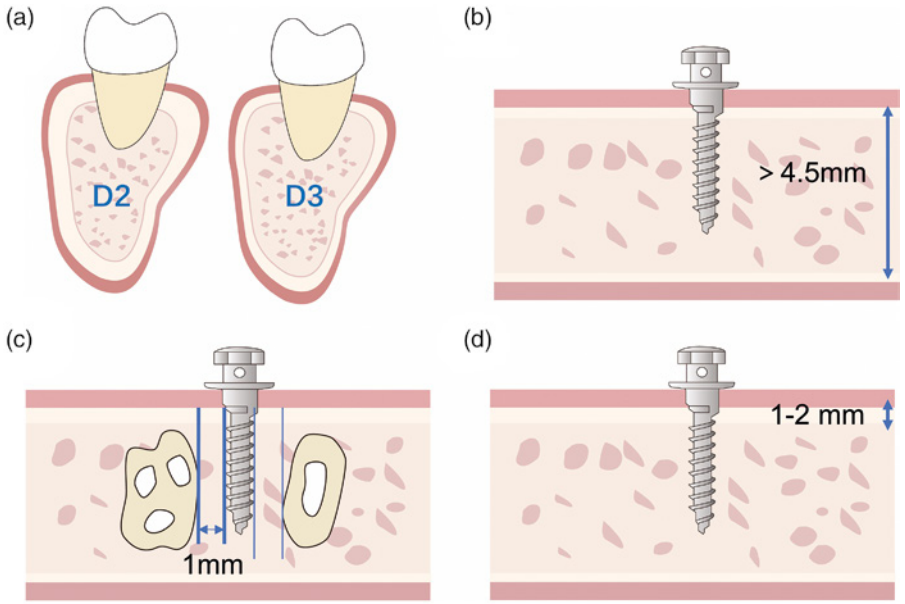


Figure 2.26 Recommended hard tissue characteristics for the placement of mini-implants. (a) D2 or D3 bone type. (b) Bone depth greater than 4.5 mm. (c) Bone width is adequate to allow mini-implants with 1 mm clearance from two adjacent roots. (d) Cortical thickness ranging between 1 and 2 mm.

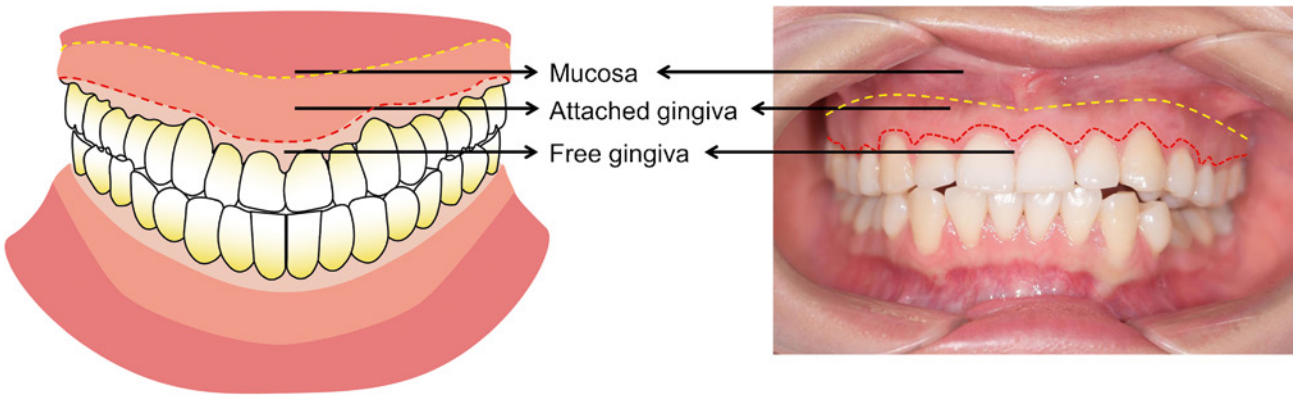


Figure 2.27 Three distinct types of soft tissues: free gingiva, attached gingiva and mucosa.

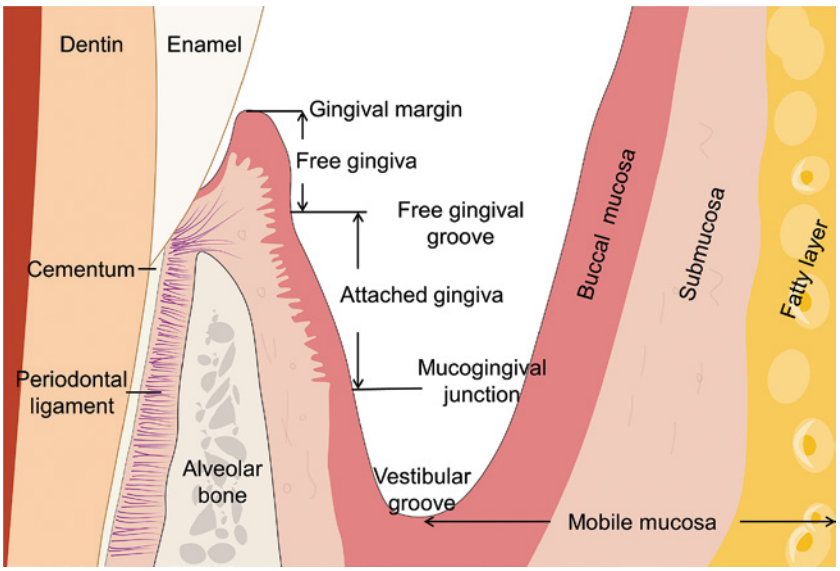


Figure 2.28 A schematic illustration showing the histological features of gingivae.

t.me/Dr_Mouayyad_AlbtousH

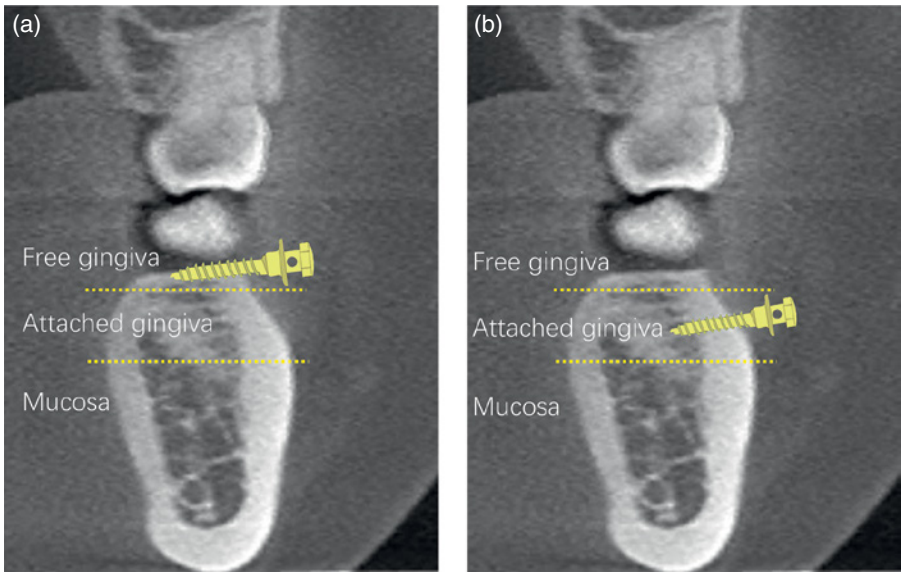


Figure 2.29 (a) The mini-implant is inserted at the free gingiva zone where bone support is minimal. (b) The mini-implant is placed at the attached gingiva zone with adequate bone support.

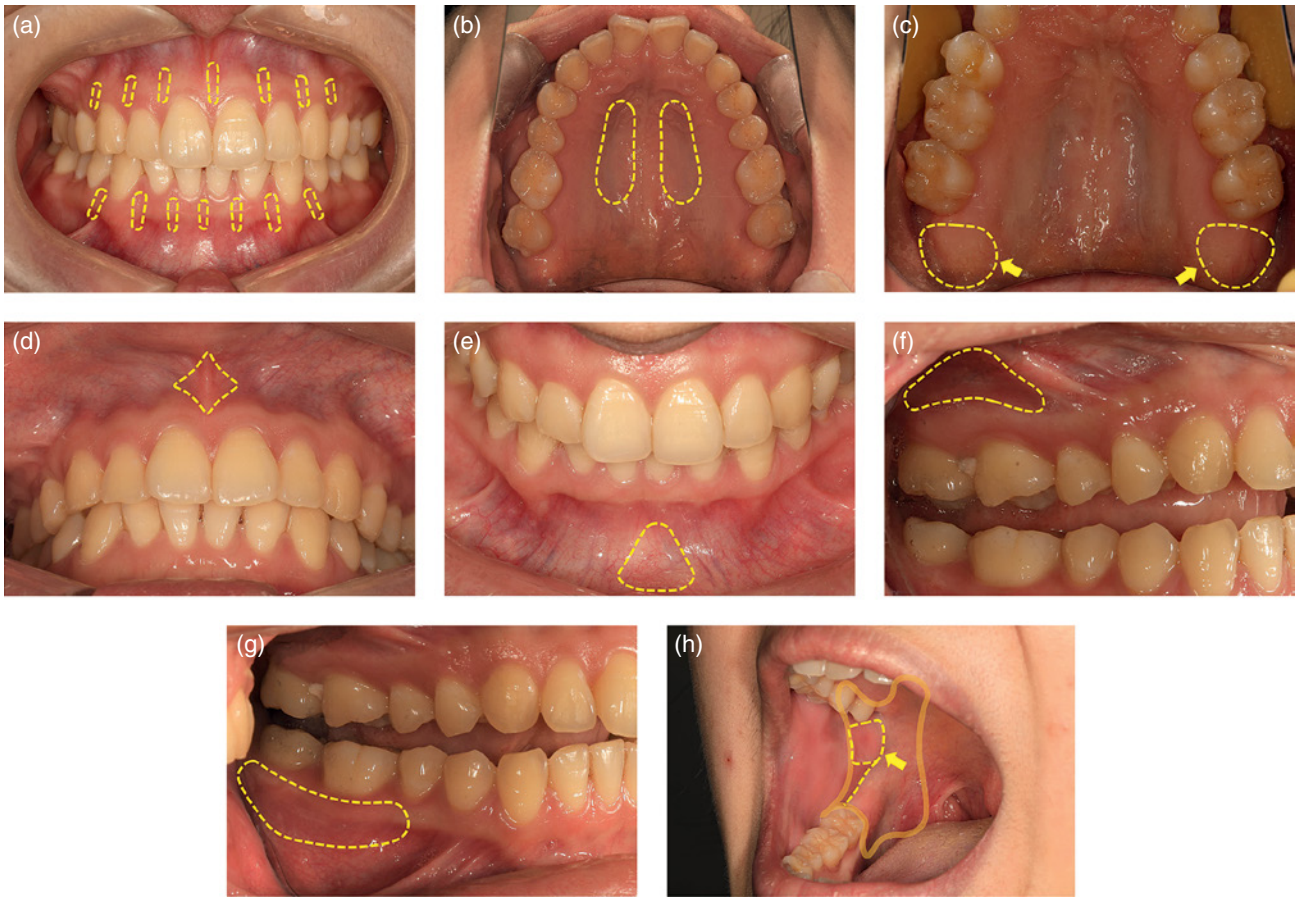


Figure 2.30 Different anatomical sites exhibit different types of soft tissue. (a) Interradicular sites with both attached gingiva and movable mucosa. (b) Palatal region with attached soft tissue. (c) Maxillary tuberosity with attached soft tissue. (d) Anterior nasal spine with movable mucosa. (e) Mandibular symphysis with movable mucosa. (f) Infrazygomatic crest with movable mucosa. (g) Buccal shelf with both attached gingiva and movable mucosa. (h) Mandibular ramus region with movable mucosa.

t.me/Dr_Mouayyad_AlbtousH

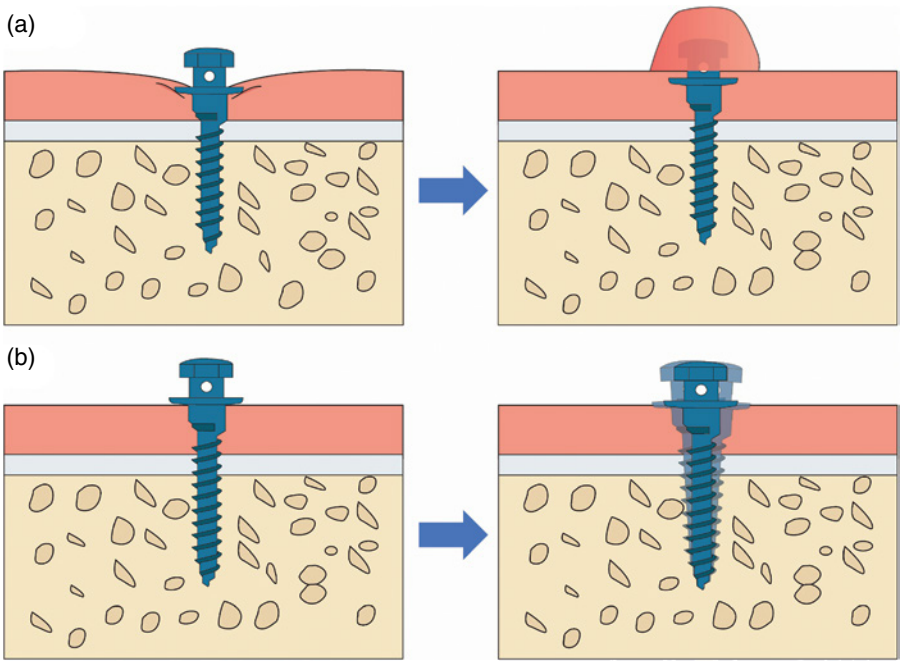


Figure 2.31 The influence of soft tissue thickness on the clinical success of mini-implants. (a) The mini-implant is inserted at a recommended depth. However, due to the thick soft tissue, the head of the mini-implant can be easily wrapped by the soft tissue, leading to soft tissue infection and hyperplasia. (b) A longer mini-implant is selected and inserted to obtain an adequate emergence profile. This leads to a smaller intra-bony to extra-bony length ratio and may jeopardise the stability of the mini-implant.

inflammation and hyperplasia. Second, to avoid soft tissue complications, longer mini-implants may be used at the expense of reducing the primary stability by increasing the length of mini-implants outside the bone.

For the alveolar zone, the thickness of soft tissue in buccal interradicular sites ranges from 1 mm to 2 mm, in different interradicular sites and heights.[58] In contrast, the thickness of soft tissue at interradicular sites is greater at the palatal side and ranges from 2 mm to 4 mm, with that between premolars being greater than that between molars.[59] Thus, optimal insertion sites require that soft tissue thickness is 1–2 mm. However, generally, mini-implants 6–8 mm in length are recommended for labial buccal interradicular sites while longer ones (8–10 mm) may be indicated for palatal interradicular sites.

For the extra-alveolar zone, the thickness of soft tissue varies greatly in different anatomical zones. Specifically, soft tissue is thinnest at the posterior midpalatal suture (average: 1.5 mm)[4,60] and thickest at the mandibular ramus (greater than 5 mm). For mini-implants inserted at anatomical sites with thick soft tissue, measures should be taken to avoid potential soft tissue complications. We recommend that longer mini-implants be selected for insertion or extension hooks be added on the heads of mini-implants (Figure 2.32).

Selection of Optimal Sites

For the alveolar zone where three types of soft tissue are present, the attached gingiva zone is the area of choice for insertion of mini-implants. Unlike mini-implants inserted in the attached gingiva, those placed in the mobile mucosa are susceptible to peri-implantitis, manifesting as soft tissue inflammation, irritation and hyperplasia (Figure 2.33). As a general rule, soft tissue thickness of 1–2 mm is optimal.

As mentioned above, bone width (interradicular distance) is greater if insertion is more apical, meaning that insertion is often indicated at the apical limit of the gingiva zone–mucogingival junction (Figure 2.34). However, among patients with limited height of attached gingiva, a clinical dilemma may be encountered (Figure 2.35): (1) if mini-implants are inserted at the level of the mucogingival junction, root damage is highly likely due to inadequate interradicular distance, or (2) if mini-implants are inserted apically to the mucogingival junction, soft tissue complications will probably occur. In these clinical situations, we recommend that oblique insertion be used to solve this problem. With oblique insertion, the mini-implant is able to engage wider interradicular bone at a more apical level while its head remains at the mucogingival junction with a lower risk of soft tissue complications (Figure 2.36).

t.me/Dr_Mouayyad_AlbtousH

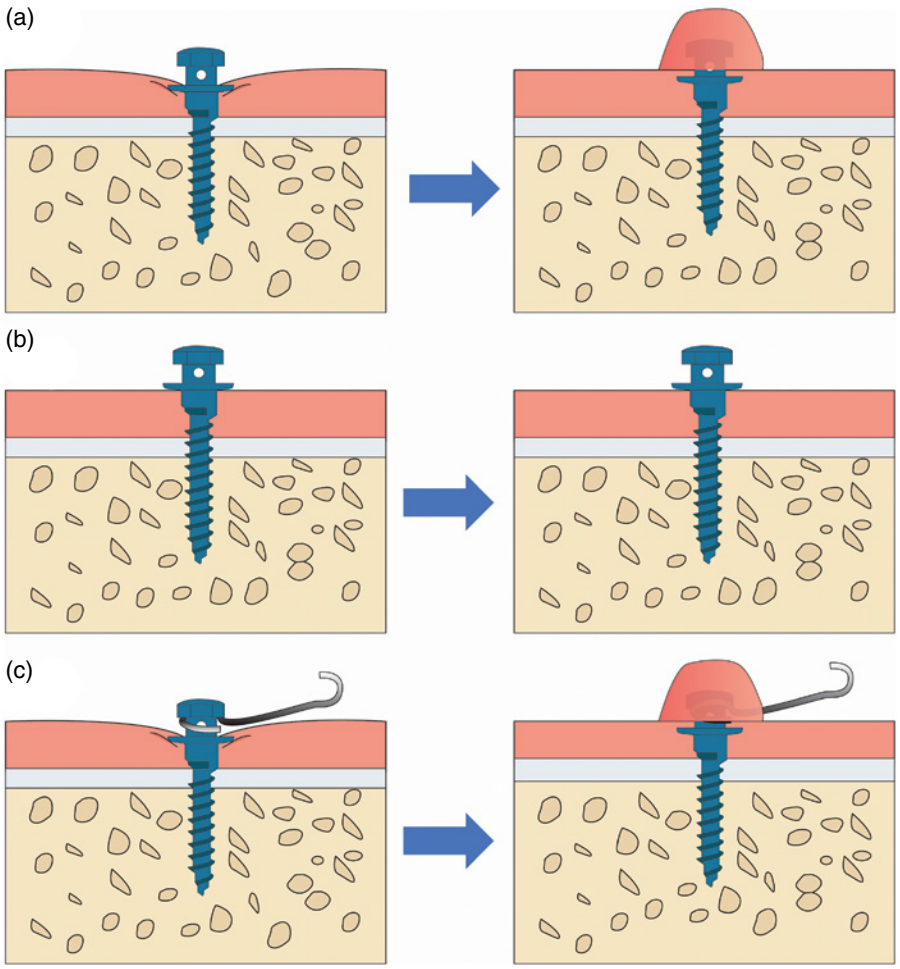


Figure 2.32 The selection of long mini-implants and application of extension hooks eliminate the influence of soft tissue complications on force loading. (a) Overinsertion of the mini-implant through thick soft tissue may result in soft tissue complications. (b) The utilisation of a long mini-implant obtains an adequate emergence profile and prevents the risk of soft tissue complications, facilitating the ease of force loading on the mini-implant. (c) The application of an extension hook on the head of the mini-implant facilitates the ease of force loading, although the head is wrapped by the hyperplastic soft tissue.

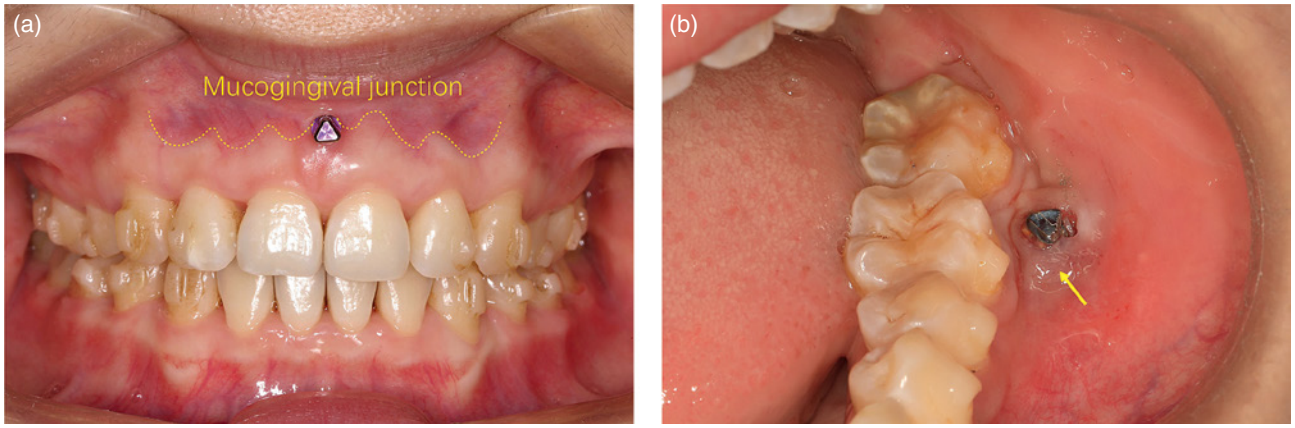


Figure 2.33 Selection of insertion sites according to types of soft tissues. (a) The mini-implant was inserted at the attached gingiva zone and was free from soft tissue complications, e.g. irritation and inflammation. (b) The mini-implant was inserted at the movable mucosa zone at the buccal shelf and soft tissue inflammation (yellow arrow) occurred around the mini-implant.

t.me/Dr_Mouayyad_AlbtousH

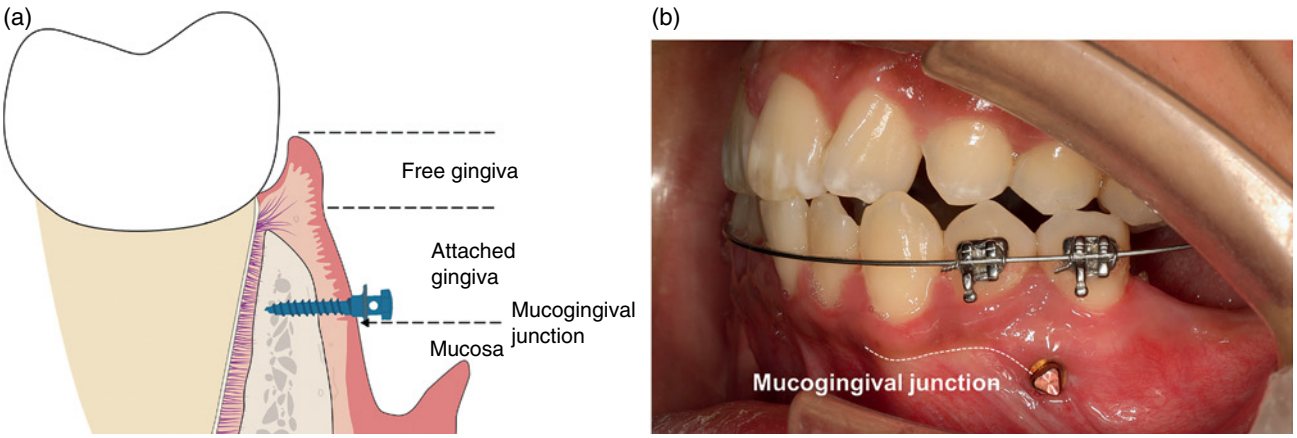


Figure 2.34 The mucogingival junction is recommended for the insertion of mini-implants. (a) A schematic illustration. (b) Intraoral photograph showing that the mini-implant is at the mucogingival junction.

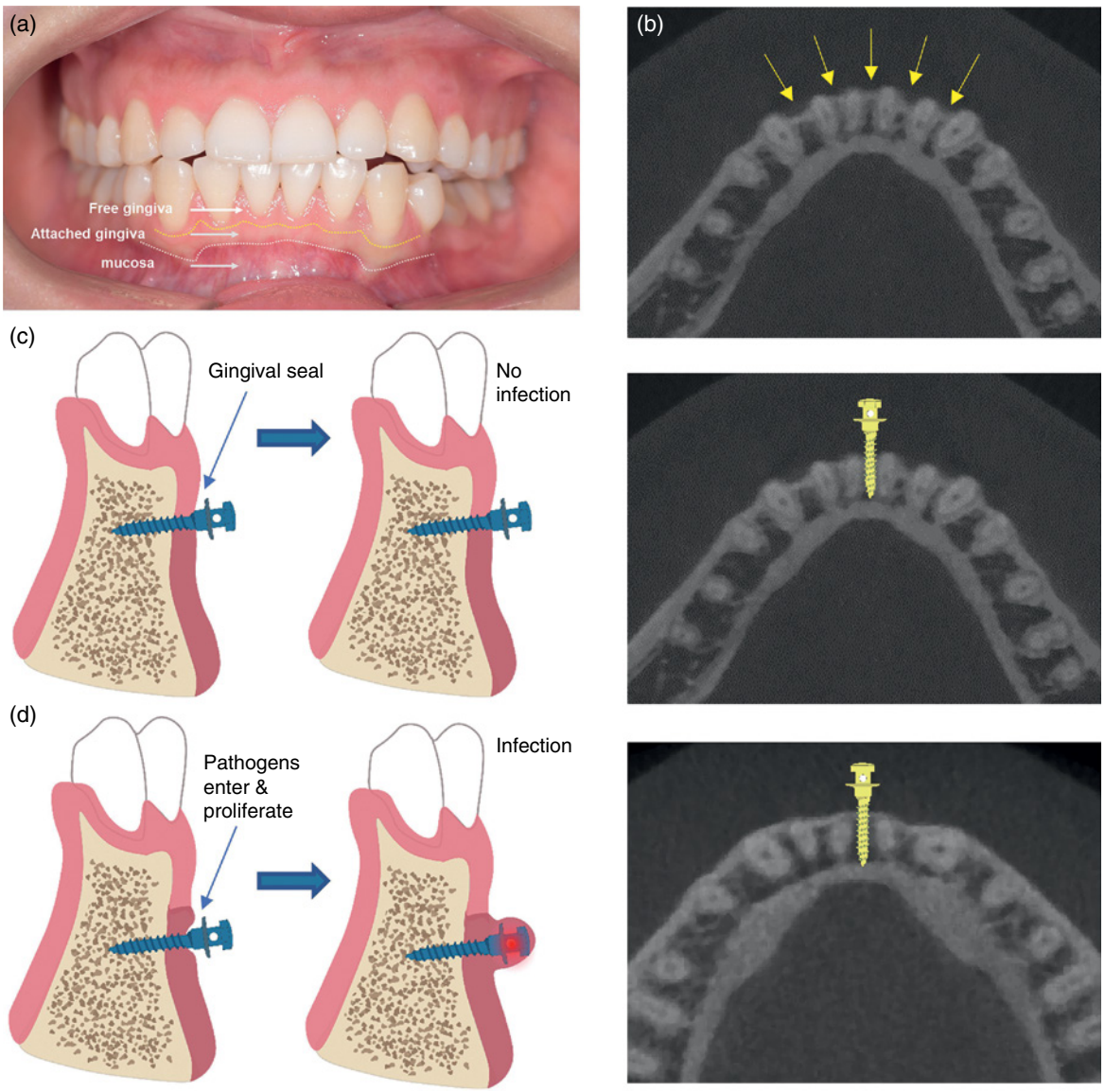


Figure 2.35 A clinical dilemma in selecting the optimal insertion site for interradicular sites with limited attached gingiva. (a) Limited width of attached gingiva. (b) CBCT axial section at the mucogingival junction showing insufficient interradicular space (yellow arrows) between adjacent roots. (c) If the mini-implant is inserted at the mucogingival junction, the risk of soft tissue inflammation is low. However, due to insufficient interradicular space, insertion of the mini-implant may lead to root contact or injury. (d) If the mini-implant is inserted apically to the mucogingival junction, the risk of root damage can be reduced at the expense of higher risk of soft tissue inflammation.

t.me/Dr_Mouayyad_AlbtousH

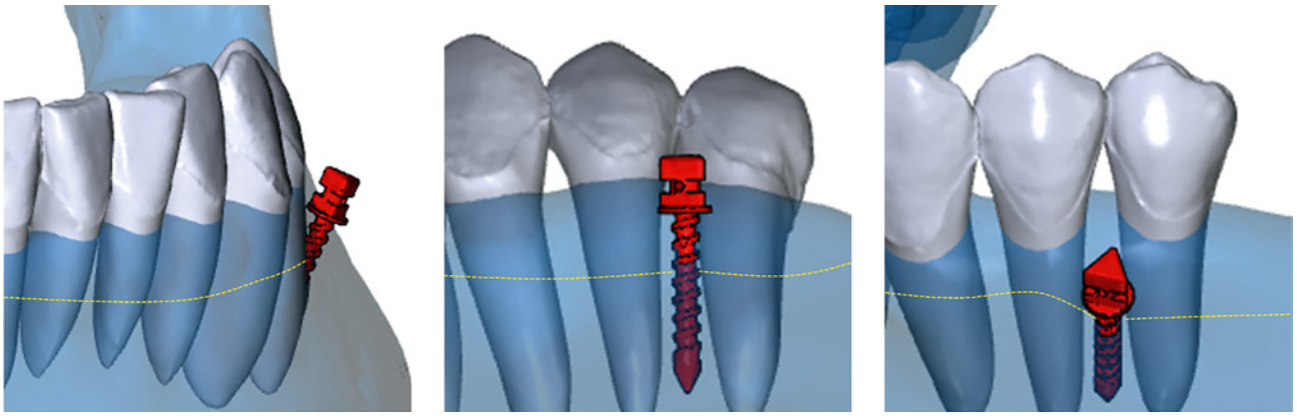


Figure 2.36 With oblique insertion, the mini-implant is able to engage wider interradicular bone at a more apical level while its head remains at the mucogingival junction (yellow dashed lines) with low risk of soft tissue complications.

For the extra-alveolar zone, except for the palatal vault and maxillary tuberosity where attached gingiva is present, all other anatomical zones (e.g. anterior nasal spine and mandibular ramus) possess mobile mucosa. For extra-alveolar zones with attached gingiva, the thickness of soft tissue should be assessed before insertion and mini-implants with appropriate length be selected (Figure 2.37). In contrast, for other extra-alveolar zones, both the thickness and the mobility of soft tissue should be taken into consideration. On one hand, for thick soft tissue, long mini-implants or extension hooks should be used to avoid soft tissue complications following the placement of mini-implants (Figures 2.38 and 2.39). On the other hand, during insertion, soft tissue flapping may be indicated to avoid soft tissue wrapping around the threads of mini-implants, reducing potential soft tissue damage (Figure 2.40).

The procedures for selecting an optimal insertion site are summarised in Figure 2.41. In brief, according to different types of soft tissue, attached gingiva is recommended. In cases of limited height of attached gingiva and/or insufficient interradicular space, oblique insertion technique may be indicated. Moreover, soft tissue thickness of 1–2 mm is recommended. However, in clinical practice, mini-implants may have to be inserted at anatomical sites with soft tissue thickness greater than 2 mm, in which case appropriate measures may be taken to avoid potential soft tissue complications. First, optimum length should be chosen based on the soft tissue thickness. Second, an extension arm may be used to gain clearance from the soft tissue. Lastly, during insertion, flapping may be indicated to avoid soft tissue wrapping around the threads of the mini-implants.

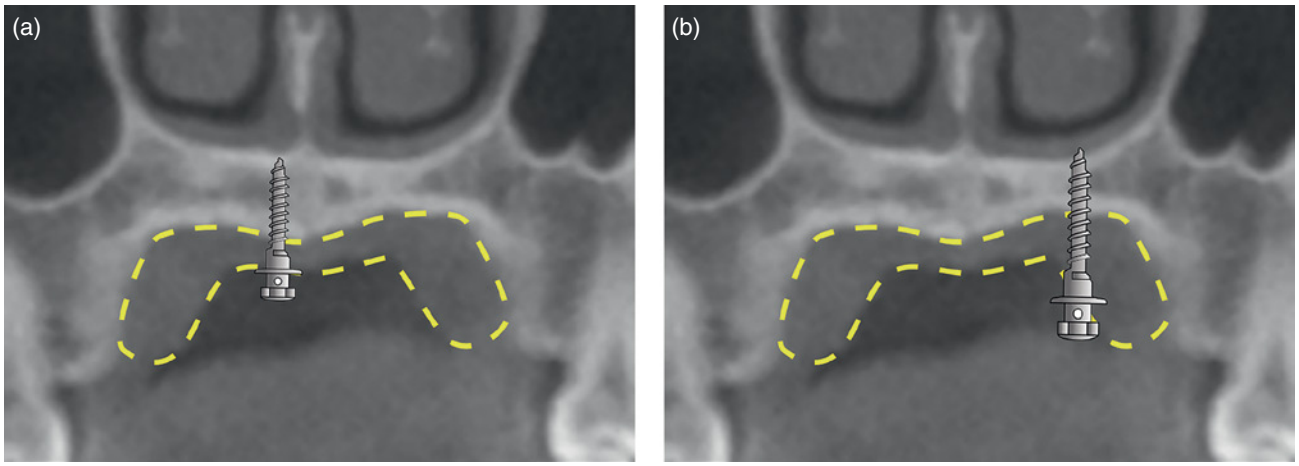


Figure 2.37 Site-specific selection of mini-implants with appropriate lengths. (a) A short mini-implant (8 mm) is adequate to obtain sufficient bone engagement at the paramedian region. (b) A longer mini-implant (10 mm) is required for the site that is 8 mm lateral to the midpalatal suture. The area encircled by the yellow dashed line indicates the soft tissue.

t.me/Dr_Mouayyad_AlbtousH

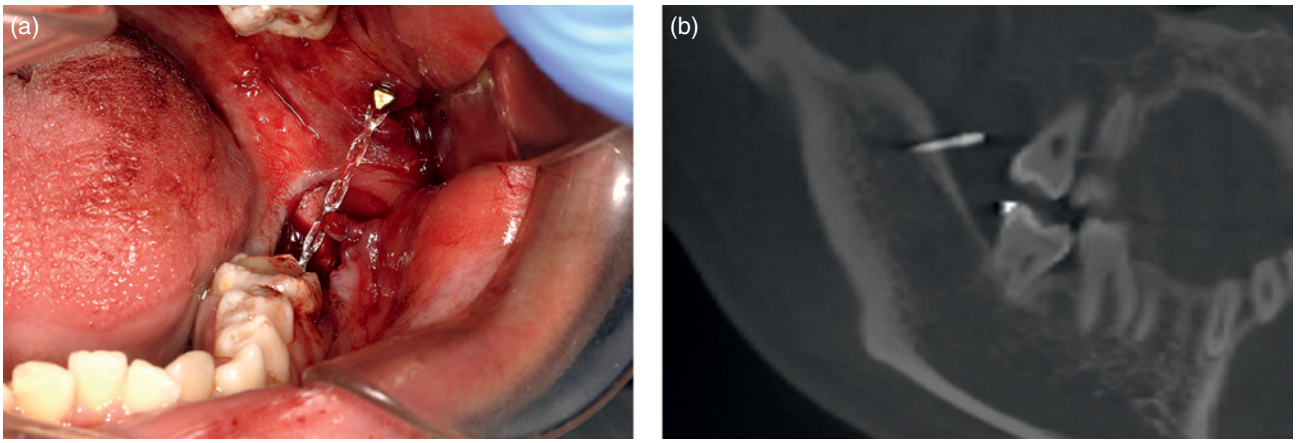


Figure 2.38 (a) A long mini-implant (12 mm) was inserted at the mandibular ramus region to upright a mesially impacted mandibular second molar. (b) The CBCT image showed that the majority of the mini-implant is outside the bone, so that the head of the implant can be exposed outside the soft tissue for ease of force application.

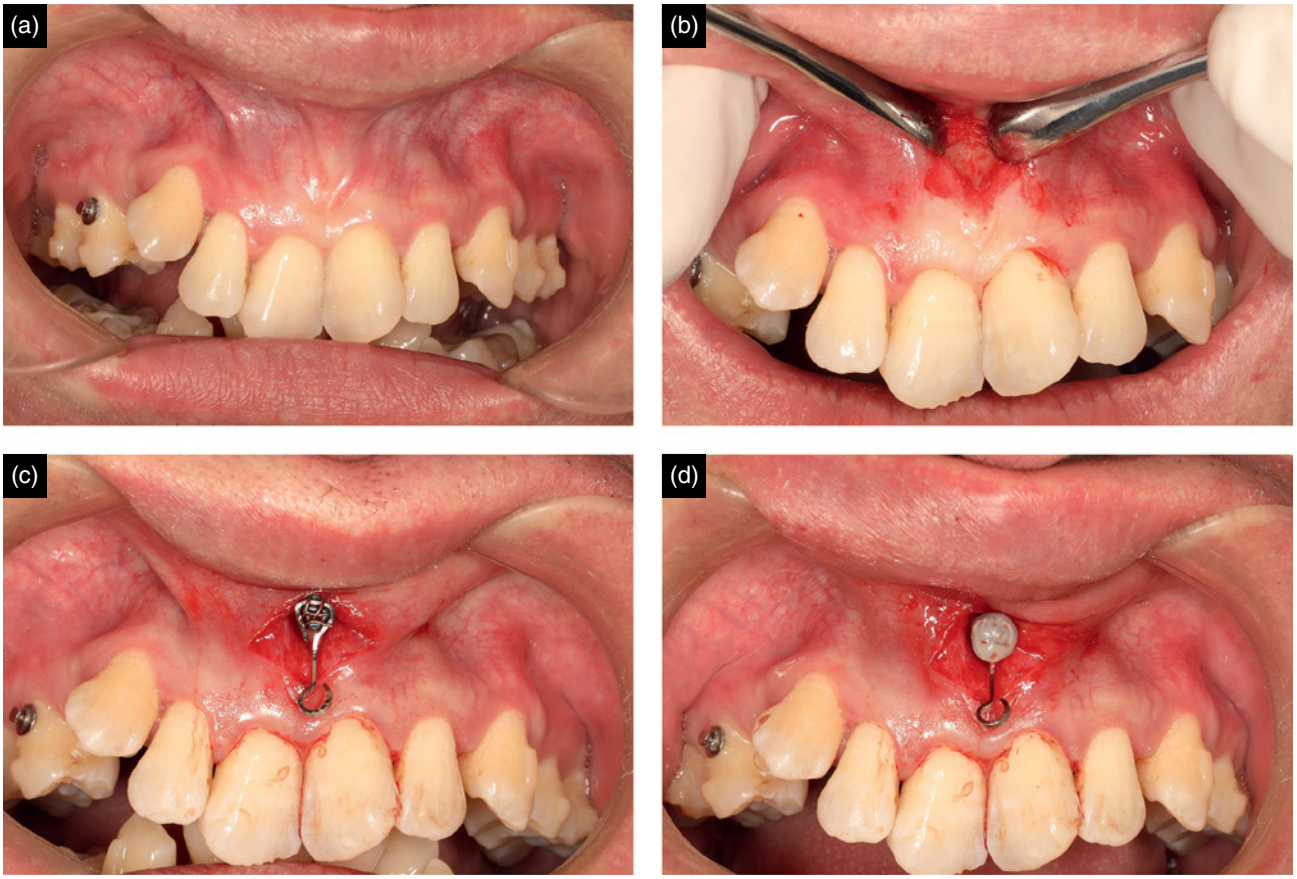


Figure 2.39 The application of an extension hook to avoid soft tissue complications. (a) Preinsertion. (b) Flap elevation to expose the bone surface. (c) A mini-implant was inserted at the anterior nasal spine and an extension hook was applied onto the implant. (d) The extension hook was fixed onto the mini-implant with flowable resin.

t.me/Dr_Mouayyad_AlbtousH

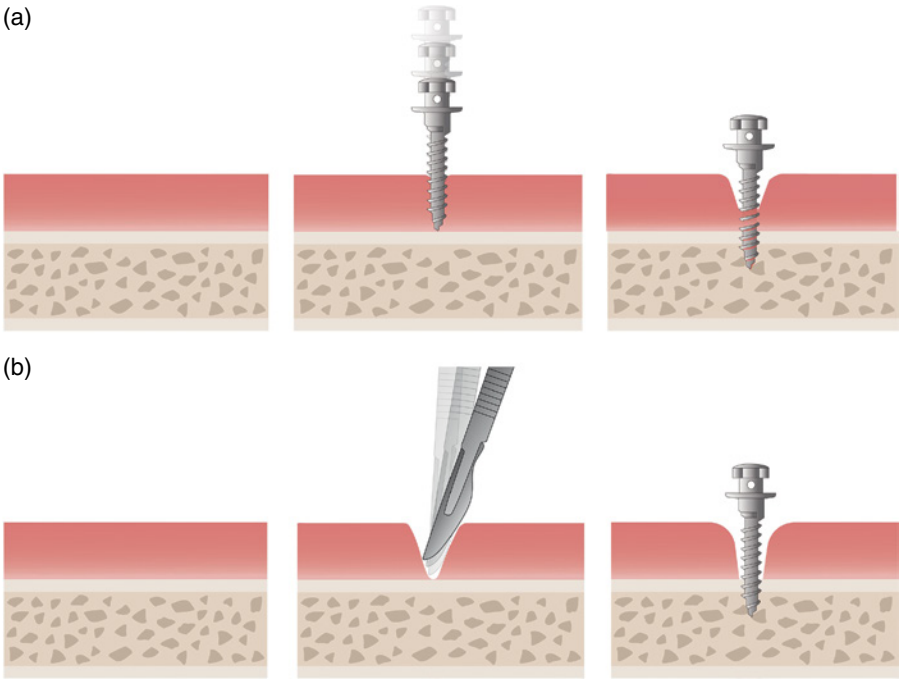


Figure 2.40 Soft tissue flapping for the placement of mini-implants into the movable mucosa region. (a) The mini-implant is inserted into the movable mucosa region. Soft tissue rolls around the threads of the mini-implant, leading to soft tissue damage. (b) Soft tissue flapping is performed prior to the insertion of the mini-implant and no soft tissue rolls around the threads of the mini-implant.

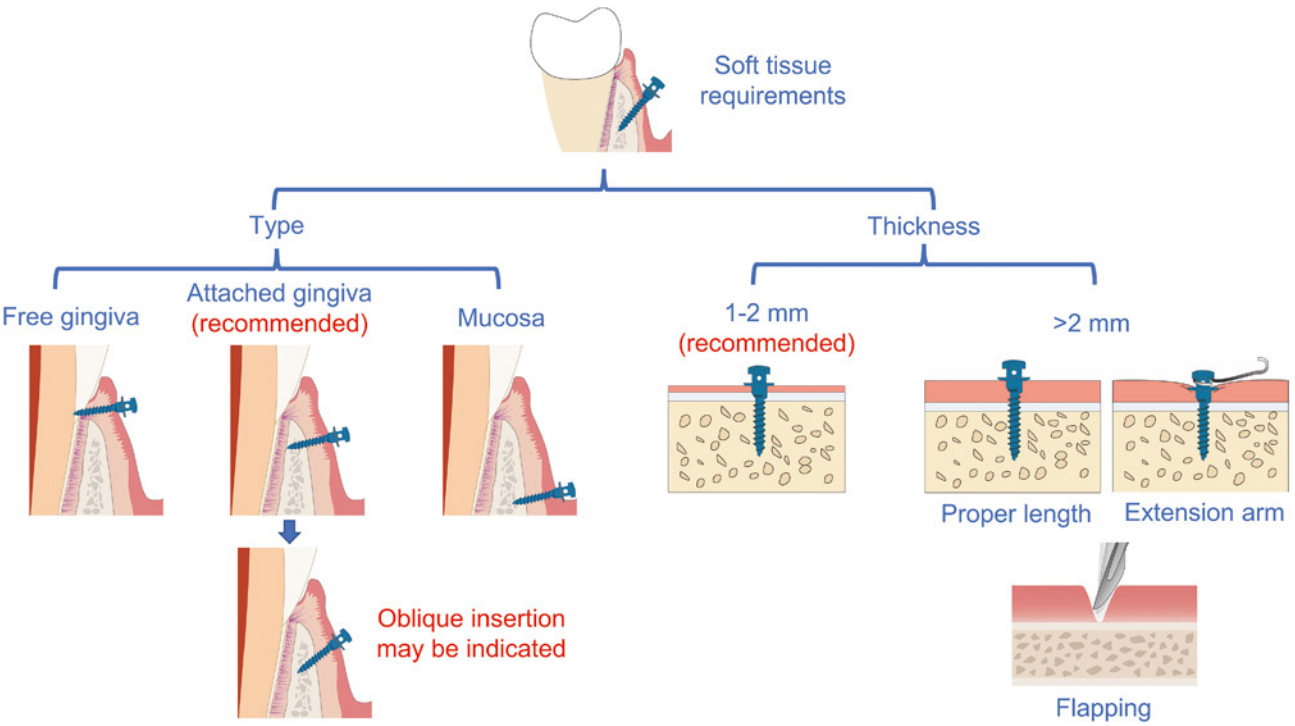


Figure 2.41 Selection of optimal insertion sites based on soft tissue characteristics.

t.me/Dr_Mouayyad_AlbtousH

2.4 Summary

In conclusion, prior to treatment planning, complete history taking and thorough examinations should be performed to assess whether a particular patient satisfies both the systemic and local requirements for the placement of orthodontic TADs. In addition to alveolar zone (interradicular sites), practitioners should be aware of the hard and soft tissues of extra-alveolar zones. As a general rule, mini-implants should be placed in systemically healthy patients, in anatomical areas with good bone quality and quantity and with thin soft tissue (1–2 mm).

References

1 Centeno ACT, Fensterseifer CK, Chami VO, Ferreira ES, Marquezan M, Ferrazzo VA. (2022). Correlation between cortical bone thickness at mini-implant insertion sites and age of patient. *Dental Press J. Orthod.* 27(1): e222098.

2 Rossi M, Bruno G, De Stefani A, Perri A, Gracco A. (2017). Quantitative CBCT evaluation of maxillary and mandibular cortical bone thickness and density variability for orthodontic miniplate placement. *Int. Orthod.* 15(4): 610–624.

3 Zhang S, Wei X, Wang L et al. (2022). Evaluation of optimal sites for the insertion of orthodontic mini implants at mandibular symphysis region through cone-beam computed tomography. *Diagnostics* 12(2): 285.

4 Lyu X, Guo J, Chen L et al. (2020). Assessment of available sites for palatal orthodontic mini-implants through cone-beam computed tomography. *Angle Orthod.* 90(4): 516–523.

5 Chen YJ, Chang HH, Huang CY, Hung HC, Lai EH, Yao CC. (2007). A retrospective analysis of the failure rate of three different orthodontic skeletal anchorage systems. *Clin. Oral Implants Res.* 18(6): 768–775.

6 Xin Y, Wu Y, Chen C, Wang C, Zhao L. Miniscrews for orthodontic anchorage: analysis of risk factors correlated with the progressive susceptibility to failure. *Am. J. Orthod. Dentofacial Orthop.* 162: e192–e202.

7 Aleshkina O, Suetenkov D, Dydykin S et al. (2021). Determination of sex dimorphisms of the thickness of the hard palate in adolescence using computed tomography: pilot study. *Ann. Anat.* 238: 151764.

8 Ning R, Guo J, Li Q, Martin D. (2021). Maxillary width and hard palate thickness in men and women with different vertical and sagittal skeletal patterns. *Am. J. Orthod. Dentofacial Orthop.* 159(5): 564–573.

9 Haddad R, Saadeh M. (2019). Distance to alveolar crestal bone: a critical factor in the success of orthodontic mini-implants. *Prog. Orthod.* 20(1): 19.

10 Tsai CC, Chang HP, Pan CY, Chou ST, Tseng YC. (2016). A prospective study of factors associated with orthodontic mini-implant survival. *J. Oral Sci.* 58(4): 515–521.

11 Yao CC, Chang HH, Chang JZ, Lai HH, Lu SC, Chen YJ. (2015). Revisiting the stability of mini-implants used for orthodontic anchorage. *J. Formos. Med. Assoc.* 114(11): 1122–1128.

12 Wu TY, Kuang SH, Wu CH. (2009). Factors associated with the stability of mini-implants for orthodontic anchorage: a study of 414 samples in Taiwan. *J. Oral Maxillofac. Surg.* 67(8): 1595–1599.

13 Zheng Y, Zhu C, Zhu M, Lei L. (2022). Difference in the alveolar bone remodeling between the adolescents and adults during upper incisor retraction: a retrospective study. *Sci. Rep.* 12(1): 9161.

14 Horner K, Devlin H, Alsop CW, Hodgkinson IM, Adams JE. (1996). Mandibular bone mineral density as a predictor of skeletal osteoporosis. *Br. J. Radiol.* 69(827): 1019–1025.

15 Drage NA, Palmer RM, Blake G, Wilson R, Crane F, Fogelman I. (2007). A comparison of bone mineral density in the spine, hip and jaws of edentulous subjects. *Clin. Oral Implants Res.* 18(4): 496–500.

16 Merheb J, Temmerman A, Coucke W et al. (2015). Relation between spongy bone density in the maxilla and skeletal bone density. *Clin. Implant Dent. Relat. Res.* 17(6): 1180–1187.

17 Lv X, Zou L, Zhang X, Zhang X, Lai H, Shi J. (2022). Effects of diabetes/hyperglycemia on peri-implant biomarkers and clinical and radiographic outcomes in patients with dental implant restorations: a systematic review and meta-analysis. *Clin. Oral Implants Res.* 33: 1183–1198.

18 Al Hezaimi K, Naghshbandi J, Nooh N, Schupbach P, Nevins M. (2021). Buccal bone remodeling around immediate implants in STZ-induced diabetic dogs: a histologic and microcomputed tomographic analysis. *Int. J. Periodont. Restorat. Dent.* 41(5): 683–690.

19 Sanches CP, Vianna AGD, Barreto FC. (2017). The impact of type 2 diabetes on bone metabolism. *Diabetol. Meta.b Syndr.* 9: 85.

20 Naghibi N, Fatemi K, Hoseini-Zarch SH, Sadeghi B, Fasihi Ramandi M. (2022). CBCT evaluation of buccal bone thickness in the aesthetic zone of menopausal women: a cross-sectional study. *Clin. Exp. Dent. Res.* 8(5): 1076–1081.

21 Drake MT, Clarke BL, Khosla S. (2008). Bisphosphonates: mechanism of action and role in clinical practice. *Mayo Clin. Proc.* 83(9): 1032–1045.

t.me/Dr_Mouayyad_AlbtousH

22 Allen CS, Yeung JH, Vandermeer B, Homik J. (2016). Bisphosphonates for steroid-induced osteoporosis. *Cochrane Database Syst. Rev.* 10: CD001347.

23 Dwan K, Phillipi CA, Steiner RD, Basel D. (2016). Bisphosphonate therapy for osteogenesis imperfecta. *Cochrane Database Syst. Rev.* 10: CD005088.

24 Bell BM, Bell RE. (2008). Oral bisphosphonates and dental implants: a retrospective study. *J. Oral Maxillofac. Surg.* 66(5): 1022–1024.

25 McLeod NM. (2009). Oral bisphosphonates and dental implants. *J. Oral Maxillofac. Surg.* 67(6): 1355.

26 Marx RE, Cillo JE Jr, Ulloa JJ. (2007). Oral bisphosphonate-induced osteonecrosis: risk factors, prediction of risk using serum CTX testing, prevention, and treatment. *J. Oral Maxillofac. Surg.* 65(12): 2397–2410.

27 Gensler LS. (2013). Glucocorticoids: complications to anticipate and prevent. *Neurohospitalist* 3(2): 92–97.

28 Gennari C. (1993). Differential effect of glucocorticoids on calcium absorption and bone mass. *Br. J. Rheumatol.* 32 Suppl 2: 11–14.

29 Wang L, Heckmann BL, Yang X, Long H. (2019). Osteoblast autophagy in glucocorticoid-induced osteoporosis. *J. Cell Physiol.* 234(4): 3207–3215.

30 Al-Sosowa AA, Alhajj MN, Abdulghani EA et al. (2022). Three-dimensional analysis of alveolar bone with and without periodontitis. *Int. Dent J.* 72(5): 634–640.

31 Azeem M, Saleem MM, Liaquat A, Ul Haq A, Ul Hamid W, Masood M. (2019). Failure rates of mini-implants inserted in the retromolar area. *Int. Orthod.* 17(1): 53–59.

32 Jing Z, Wu Y, Jiang W et al. (2016). Factors affecting the clinical success rate of miniscrew implants for orthodontic treatment. *Int. J. Oral Maxillofac. Implants.* 31(4): 835–841.

33 Bayat E, Bauss O. (2010). Effect of smoking on the failure rates of orthodontic miniscrews. *J. Orofac. Orthop.* 71(2): 117–124.

34 Sayardoust S, Omar O, Norderyd O, Thomsen P. (2018). Implant-associated gene expression in the jaw bone of smokers and nonsmokers: a human study using quantitative qPCR. *Clin. Oral Implants Res.* 29(9): 937–953.

35 Zhou J, Hong H, Zhou H et al. (2021). Orthodontic extraction of a high-risk impacted mandibular third molar contacting the inferior alveolar nerve, with the aid of a ramus mini-screw. *Quintessence Int.* 52(6): 538–546.

36 Pu L, Zhou J, Yan X et al. (2022). Orthodontic traction of an impacted maxillary third molar through a miniscrew-anchored cantilever spring to substitute the adjacent second molar with severe root resorption. *J. Am. Dent. Assoc.* 153(9): 884–892.

37 Misch CE. (1990). Density of bone: effect on treatment plans, surgical approach, healing, and progressive bone loading. *Int. J Oral Implantol.* 6(2): 23–31.

38 Lee MY, Park JH, Kim SC et al. (2016). Bone density effects on the success rate of orthodontic microimplants evaluated with cone-beam computed tomography. *Am. J. Orthod. Dentofacial Orthop.* 149(2): 217–224.

39 Azeem M, Haq AU, Awaisi ZH, Saleem MM, Tahir MW, Liaquat A. (2019). Failure rates of miniscrews inserted in the maxillary tuberosity. *Dental Press J. Orthod.* 24(5): 46–51.

40 Mohammed H, Wafaie K, Rizk MZ, Almuzian M, Sosly R, Bearn DR. (2018). Role of anatomical sites and correlated risk factors on the survival of orthodontic miniscrew implants: a systematic review and meta-analysis. *Prog. Orthod.* 19(1): 36.

41 Uribe F, Mehr R, Mathur A, Janakiraman N, Allareddy V. (2015). Failure rates of mini-implants placed in the infrazygomatic region. *Prog. Orthod.* 16: 31.

42 Zhang S, Choi Y, Li W et al. (2022). The effects of cortical bone thickness and miniscrew implant root proximity on the success rate of miniscrew implant: a retrospective study. *Orthod. Craniofac. Res.* 25(3): 342–350.

43 Ichinohe M, Motoyoshi M, Inaba M et al. (2019). Risk factors for failure of orthodontic mini-screws placed in the median palate. *J. Oral Sci.* 61(1): 13–18.

44 Mohlhenrich SC, Heussen N, Winterhalder P et al. (2019). Predicting primary stability of orthodontic mini-implants, according to position, screw-size, and bone quality, in the maxilla of aged patients: a cadaveric study. *Eur. J. Oral Sci.* 127(5): 462–471.

45 Pithon MM, Figueiredo DS, Oliveira DD. (2013). Mechanical evaluation of orthodontic mini-implants of different lengths. *J. Oral Maxillofac. Surg.* 71(3): 479–486.

46 Jin J, Kim GT, Kwon JS, Choi SH. (2020). Effects of intrabony length and cortical bone density on the primary stability of orthodontic miniscrews. *Materials* 13(24): 5615.

47 Lin TS, Tsai FD, Chen CY, Lin LW. (2013). Factorial analysis of variables affecting bone stress adjacent to the orthodontic anchorage mini-implant with finite element analysis. *Am. J. Orthod. Dentofacial Orthop.* 143(2): 182–189.

48 Kuroda S, Nishii Y, Okano S, Sueishi K. (2014). Stress distribution in the mini-screw and alveolar bone during orthodontic treatment: a finite element study analysis. *J. Orthod.* 41(4): 275–284.

49 Giudice AL, Rustico L, Longo M, Oteri G, Papadopoulos MA, Nucera R. (2021). Complications reported with the use of orthodontic miniscrews: a systematic review. *Korean J. Orthod.* 51(3): 199–216.

50 Jia X, Chen X, Huang X. (2018). Influence of orthodontic mini-implant penetration of the maxillary sinus in the infrazygomatic crest region. *Am. J. Orthod. Dentofacial Orthop.* 153(5): 656–661.

51 Chen YH, Chang HH, Chen YJ, Lee D, Chiang HH, Yao CC. (2008). Root contact during insertion of miniscrews for orthodontic anchorage increases the failure rate: an animal study. *Clin. Oral Implants Res.* 19(1): 99–106.

t.me/Dr_Mouayyad_AlbtousH

52 Ikenaka R, Koizumi S, Otsuka T, Yamaguchi T. (2022). Effects of root contact length on the failure rate of anchor screw. *J. Oral Sci.* 64(3): 232–235.

53 Lee Y, Choi SH, Yu HS, Erenebat T, Liu J, Cha JY. (2021). Stability and success rate of dual-thread miniscrews. *Angle Orthod.* 91(4): 509–514.

54 Motoyoshi M, Inaba M, Ono A, Ueno S, Shimizu N. (2009). The effect of cortical bone thickness on the stability of orthodontic mini-implants and on the stress distribution in surrounding bone. *Int. J. Oral Maxillofac Surg.* 38(1): 13–18.

55 Motoyoshi M, Yoshida T, Ono A, Shimizu N. (2007). Effect of cortical bone thickness and implant placement torque on stability of orthodontic mini-implants. *Int. J. Oral Maxillofac. Implants.* 22(5): 779–784.

56 Mohlhenrich SC, Heussen N, Modabber A et al. (2021). Influence of bone density, screw size and surgical procedure on orthodontic mini-implant placement – part A: temperature development. *Int. J. Oral Maxillofac. Surg.* 50(4): 555–564.

57 Liu SS, Cruz-Marroquin E, Sun J, Stewart KT, Allen MR. (2021). Orthodontic mini-implant diameter does not affect in-situ linear microcrack generation in the mandible or the maxilla. *Am. J. Orthod. Dentofacial Orthop.* 142(6): 768–773.

58 Lim WH, Lee SK, Wikesjo UM, Chun YS. (2007). A descriptive tissue evaluation at maxillary interradicular sites: implications for orthodontic mini-implant placement. *Clin. Anat.* 20(7): 760–765.

59 Lee JA, Ahn HW, Oh SH, Park KH, Kim SH, Nelson G. (2021). Evaluation of interradicular space, soft tissue, and hard tissue of the posterior palatal alveolar process for orthodontic mini-implant, using cone-beam computed tomography. *Am. J. Orthod. Dentofacial Orthop.* 159(4): 460–469.

60 Oh SH, Lee SR, Choi JY, Kim SH, Hwang EH, Nelson G. (2021). Quantitative cone-beam computed tomography evaluation of hard and soft tissue thicknesses in the midpalatal suture region to facilitate orthodontic mini-implant placement. *Korean J. Orthod.* 51(4): 260–269.

t.me/Dr_Mouayyad_AlbtousH

3

General Principles for the Insertion of Orthodontic Temporary Anchorage Devices

Hu Long[1], Xinyu Yan[1], Yanzi Gao[1], Qingxuan Wang[1], Chenghao Zhang[1], Rui Shu[2], Wen Liao[1], and Xianglong Han[1]

[1] *Department of Orthodontics, State Key Laboratory of Oral Diseases and National Clinical Research Center for Oral Diseases, West China Hospital of Stomatology, Sichuan University, Chengdu, China*
[2] *Department of Pediatric Dentistry, State Key Laboratory of Oral Diseases and National Clinical Research Center for Oral Diseases, West China Hospital of Stomatology, Sichuan University, Chengdu, China*

3.1 Introduction

Prudent selection of insertion sites for orthodontic TADs is fundamental to achieving the desired orthodontic biomechanical outcomes. The optimal insertion site varies greatly among different patients, different treatment plans for the same patient and even among different biomechanical designs for the same patient with the same treatment plan.

In general, site selection is determined by two main factors: biomechanics and anatomy. Thus, there are two different paradigms in site selection for orthodontic TADs: biomechanics-driven paradigm and anatomy-driven paradigm. The biomechanics-driven paradigm dictates site selection by biomechanical design while the anatomy-driven paradigm determines insertion sites based on ease of insertion and availability of both hard and soft tissues without injury to important anatomical structures (Figure 3.1). However, these two paradigms cannot always be perfectly combined. In these clinical scenarios, a compromised combination of the two paradigms can bring about a clinically acceptable trade-off result.

In this chapter, before delving into the biomechanics-driven paradigm, we will first discuss anatomical considerations in choosing insertion sites.

Clinical Insertion Techniques of Orthodontic Temporary Anchorage Devices, First Edition. Edited by Hu Long, Xianglong Han, and Wenli Lai.
© 2024 John Wiley & Sons Ltd. Published 2024 by John Wiley & Sons Ltd.

t.me/Dr_Mouayyad_AlbtousH

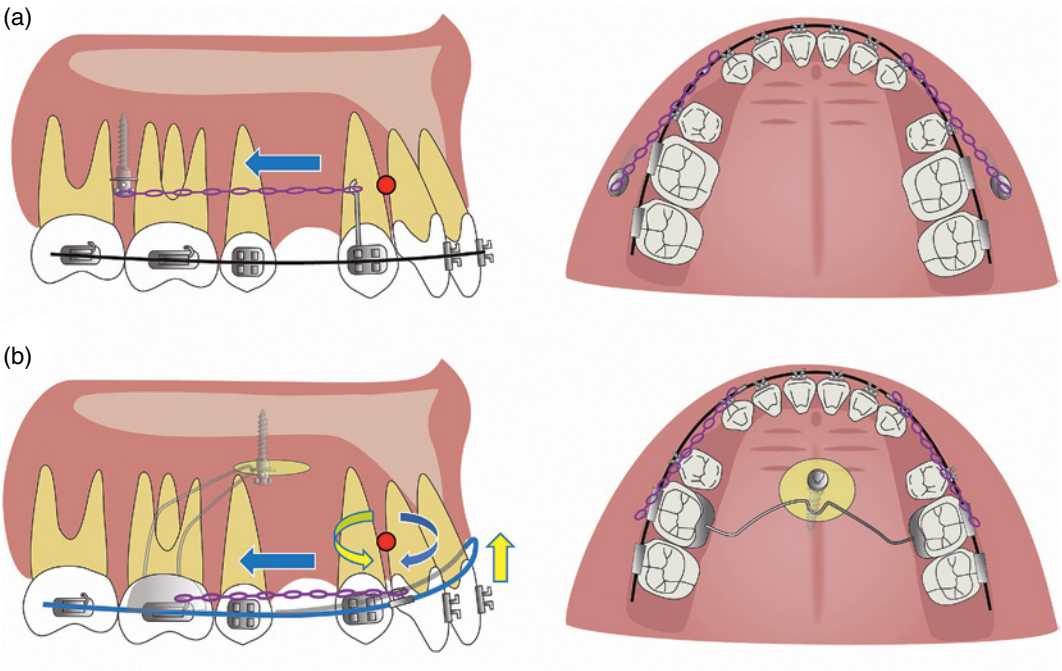


Figure 3.1 Biomechanics-driven versus anatomy-driven paradigm for the selection of mini-implant insertion sites. (a) Biomechanics-driven approach. An infrazygomatic mini-implant is inserted and applied for *en masse* anterior retraction. The retraction force (blue arrow) passes through the centre of resistance (red dot) of the anterior teeth and leads to bodily retraction of the anterior teeth. From the perspective of biomechanics, the infrazygomatic crest is the optimal insertion site. (b) Occasionally, the buccal side is not suitable for the placement of mini-implants due to a variety of reasons, e.g. inadequate bone quantity or limited interradicular space. From the perspective of anatomy, a palatal mini-implant is alternatively employed for molar anchorage augmentation. The bilateral molars are fixed and stabilised by the palatal mini-implant through a palatal arch. The retraction force (blue arrow) passes occlusally to the centre of resistance (red dot) and results in clockwise moment, leading to extrusion and lingual tipping of the incisors. To eliminate this adverse effect, a reverse curve of Spee archwire is used to offer intrusive force (yellow arrow) on incisors, which in turn generate an anticlockwise moment. The net effect is bodily retraction of the anterior teeth.

3.2 Anatomy-driven Paradigm

As a rule of thumb, mini-implants can be inserted to any anatomical site with adequate bone quality and quantity and without the risk of injury to important anatomical structures. As the requirements of both hard and soft tissues have been elaborated in Chapter 2, in this section, available and clinically frequently used anatomical sites will be discussed and illustrated without delving into their detailed requirements. In addition, proper size of mini-implants and potential injury to significant anatomical structures in each insertion site will be discussed in this section.

3.2.1 General Principles

As mentioned in the previous chapter, both the hard tissue (i.e. alveolar bone) and soft tissue should be considered. Four types of bone are described. Insertion sites of choice are those with D2 or D3 type, and sometimes D1 bone can be used due to biomechanical requirements. Moreover, it is recommended that mini-implants are inserted at the attached gingiva zone due to higher success rate.[1,2] However, if mini-implants have to be inserted at the movable mucosa zone due to biomechanical considerations, special care should be taken to avoid or eliminate soft tissue complications (e.g. inflammation and infection) following insertion. It has been reported that the success rates of mini-implants inserted at thick movable mucosa zones with excellent bone quality and quantity (e.g. buccal shelf and mandibular ramus) are around 95%,[3,4] comparable to those at palatal regions. Thus, bone quality and quantity are more predominant factors in determining the success rate of mini-implants than soft tissue factors.

When the placement of mini-implants is planned, injury of the following four types of anatomical structures should be avoided: dental roots, blood and nerve vessels, maxillary sinus and nasal cavity (Figure 3.2).

Dental Roots

It has been well documented that root proximity is a significant risk factor for mini-implant failure.[5-7] When a mini-implant is in contact with a root, high alveolar stress

t.me/Dr_Mouayyad_AlbtousH

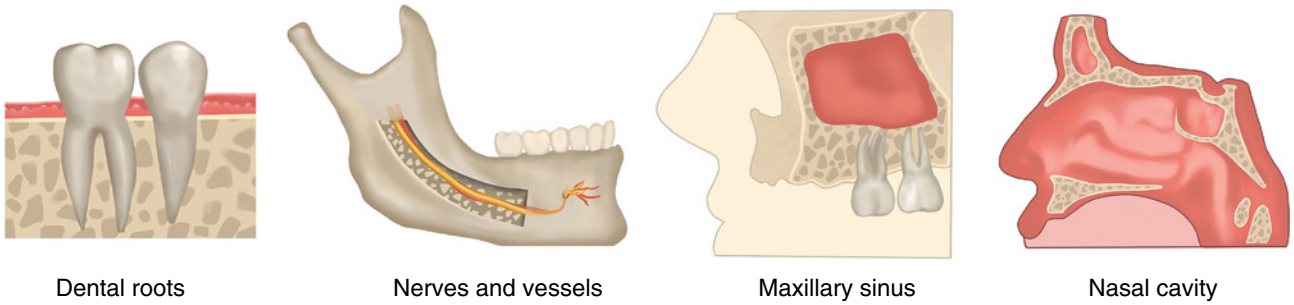


Figure 3.2 Vital anatomical structures (dental roots, nerves and vessels, maxillary sinus, and nasal cavity). Injury to these structures should be avoided.

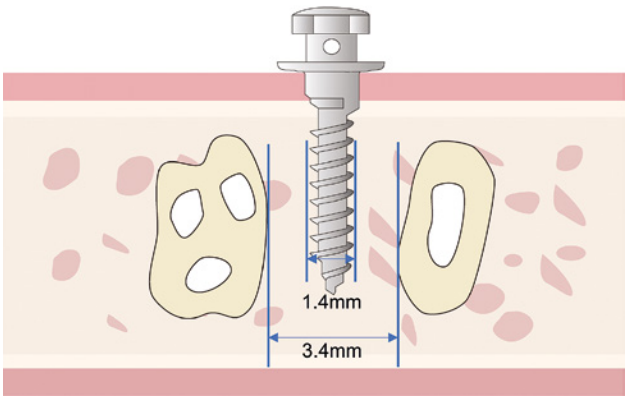


Figure 3.3 'Safe zone' between the mini-implant and the adjacent root. A 1 mm clearance from the adjacent root is required for clinical success of a mini-implant. For example, a 1.4 mm mini-implant is used for an interradicular site. This requires the interradicular distance to be at least 3.4 mm (1.4 + 1 + 1 mm).

and displacement of the mini-implant by masticatory force lead to undesirable development of secondary stability (bone remodelling) and subsequent mini-implant failure (Figure 3.3).[8-10] Even if the implant is not in direct contact with dental roots, the likelihood of implant failure is still high if it is in proximity to the roots,[7] which is mainly attributed to the following two reasons. First, periodical bite force can be transmitted to mini-implants that are close to dental roots, thereby interfering with secondary stability.[10] Second, both animal and human studies reveal that mini-implants are not stationary but can be displaced under continuous orthodontic force loading.[11,12] Thus, 1 mm clearance ('safe zone') from dental roots is highly recommended for orthodontic mini-implants.

In clinical practice, meticulous preinsertion assessment of interradicular space based on radiographic images is of great importance. According to the 1 mm clearance principle, the interradicular space should be at least 3.4 mm, which corresponds to a 1.4 mm diameter mini-implant leaving 1 mm clearance on each side from the roots of contiguous teeth (Figure 3.3).

For correct diagnosis of interradicular space before insertion, special care should be taken to choose the most appropriate diagnostic modality. It has been shown that the angulation of X-ray beam could significantly reduce interradicular space on two-dimensional radiographs.[13] Specifically, about 30% reduction in interradicular space was observed for every 10° of deviation from orthogonal projection. Thus, non-orthogonal two-dimensional radiographs often underestimate interradicular space and orthogonal periapical radiography or three-dimensional cone beam computed tomography (CBCT) is recommended to assess interradicular distance before insertion (Figure 3.4).

Panoramic radiography is a commonly used diagnostic modality in routine orthodontic treatment, but it is still susceptible to projection deviation and is not recommended for precise evaluation of interradicular space due to its misdiagnosis of root mesiodistal inclination.[14,15] A clinical study evaluated the diagnostic performance of panoramic radiography in comparision to CBCT (gold standard) and revealed that the agreement between panoramic radiography and CBCT was 65% (Table 3.1).[16] Specifically, after converting the outcome into a dichotomous one, we found that sensitivity and specificity of panoramic radiography were about 99.6% and 41.2% respectively, suggesting that panoramic radiography has high sensitivity in detecting root contact but low capability in ruling out non-contact. Moreover, the positive and negative predictive values were 54.4% and 99.3%, respectively. This finding suggests that, for a given patient who is diagnosed with root contact with panoramic radiography, we only have 54.4% confidence to establish the diagnosis of root contact, no better than chance. In contrast, for a given patient who is diagnosed with no root contact with panoramic radiography, we have 99.3% confidence to diagnose that the patient is really free from root contact (Figure 3.5). Therefore, panoramic radiography overestimates the likelihood of root contact but practitioners should

t.me/Dr_Mouayyad_AlbtousH

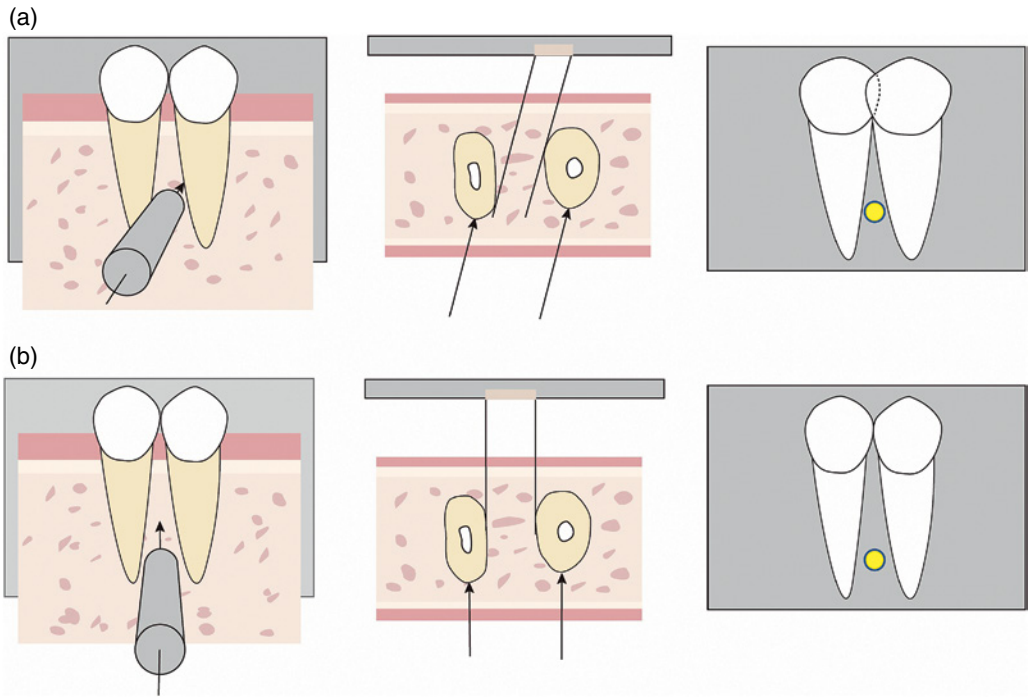


Figure 3.4 Potential errors in estimating interradicular distance based on 2-D radiography. (a) Non-orthogonal radiography is used and the interradicular distance is underestimated due to the projection angle. (b) The interradicular distance is correctly assessed through orthogonal radiography.

Table 3.1 Diagnostic performance of panoramic radiography.

	Contact (CBCT)	No contact (CBCT)
Contact (Panoramic)	247	207
No contact (Panoramic)	1	145

be confident in the diagnostic result of no root contact by panoramic radiography.

In clinical scenarios, interradicular space is often limited due to dental crowding and undesirable root parallelism between adjacent teeth.[17] Since interradicular space increases from the cervical to apical direction, mini-implants are often inserted at more apical levels to gain

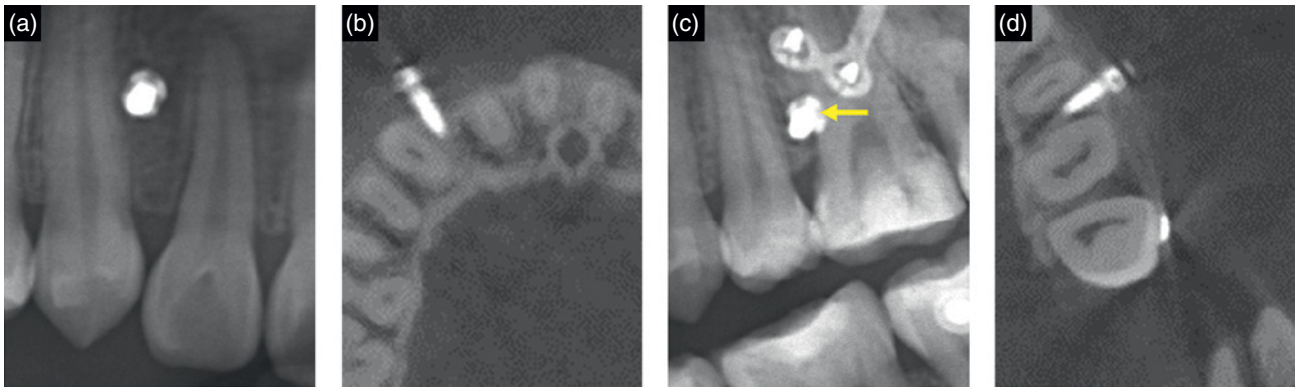


Figure 3.5 Root contact diagnosed with panoramic radiography. (a) Root contact is not evident on panoramic radiograph. (b) No root contact is confirmed by CBCT. (c) Root contact (yellow arrow) is evident on panoramic radiograph. (d) Root contact is ruled out through CBCT.

t.me/Dr_Mouayyad_AlbtousH

greater bone support.[18] However, there is a clinical paradox for this situation. On one hand, if a mini-implant is inserted too apically, although bone support is adequate, the implant is likely to cause soft tissue complications that may lead to implant failure. On the other hand, if a mini-implant is inserted close to the alveolar crest, although the mini-implant is inserted in the attached gingiva zone and the risk of soft tissue complications is reduced, it is prone to contact adjacent roots due to limited interradicular space near the alveolar crest. Thus, an oblique insertion technique has been proposed to solve these clinical problems. With the oblique insertion technique, a mini-implant is inserted in an oblique direction so that adequate bone support is assured and soft tissue complications can be avoided (Figure 3.6).

Furthermore, to reduce the risk of root injury, extra-alveolar bone has been proposed and the overall success rate of mini-implants inserted at these areas is high.[3,4,19] In clinical practice, the commonly used extra-alveolar sites are the infrazygomatic crest, anterior nasal spine, mandibular symphysis, buccal shelf and mandibular ramus (Figure 3.7).

Neurovascular Bundles

Vascular vessels and nerves often run in parallel. Thus, in this chapter, they will be discussed together. Blood vessels and nerves that are potentially prone to injury are the nasopalatine vessels and nerves, greater palatine vessels and nerves, and inferior alveolar vessels and nerves.

The nasopalatine vessels and nerves exist from the incisive foramen and may be injured when mini-implants are inserted at the anterior palatal region (Figure 3.8). Fortunately, injury to nasopalatine vessels and nerves does not result in any serious adverse effects. A clinical prospective study revealed that, among patients requiring the extraction of deeply palatally impacted canines, severing the nasopalatine vascular and nerve bundles only resulted in mild sensory disturbance within one week among all the patients (n = 59). Fortunately, the sensory disorder recovered among all the patients within four weeks.[20] Thus, although nasopalatine vessels and nerves are susceptible to injury from mini-implants inserted at the anterior palatal region, the injury is not severe and sensory disturbance should be readily recovered.

The greater palatine vessels and nerves emerge from the greater palatine foramina, run anteriorly on the palate and anastomose with the nasopalatine vascular and nerve bundles (Figure 3.9). Since the greater palatine foramina are located at a very apical level, the likelihood of direct injury to the greater palatine vascular and nerve bundles at that level is very low. Thus, it is more likely to damage the vascular and nerve bundles that run in the soft tissue. Fortunately, due to the elastic property of palatal soft tissue, the likelihood of injury to these vascular and nerve bundles is still low even if they are contacted by mini-implants (Figure 3.10). Nevertheless, care should be taken to avoid inserting a mini-implant at the greater foramen (dangerous zone) that is located distal and apical to the maxillary second molars (Figure 3.11).

Inferior alveolar vessels and nerves enter the mandibular bone through the mandibular foramina, run anteriorly inside the mandibular bone and exit from the mental foramina that are located apically to the second premolars (Figure 3.12). For average orthodontic patients, injury to these vascular and nerve bundles is unlikely for mini-implants inserted at either buccal shelf or interradicular sites between the first and second premolars. In contrast, for those with underdeveloped alveolar bone due to primary eruption disturbance, insertion of mini-implants at this region poses a high risk of injury to vascular and nerve bundles (Figure 3.13). Thus, meticulous

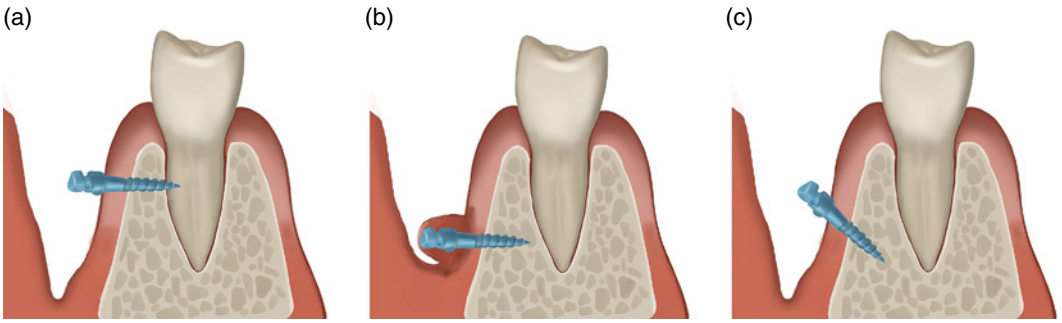


Figure 3.6 Oblique insertion technique. (a) The mini-implant is inserted at the attached gingiva zone in parallel to the occlusal plane. However, root injury occurs due to insufficient bone volume. (b) To gain greater bone support, the mini-implant is inserted more apically at the movable mucosa zone. Although bone quantity is adequate, soft tissue complications occur since the head of the mini-implant is located too apically. (c) The mini-implant is inserted in an oblique direction. On one hand, bone quantity is sufficient to support the mini-implant without root injury. On the other hand, the head of the mini-implant is located at the attached gingiva zone and the risk of soft tissue complications is low.

t.me/Dr_Mouayyad_AlbtousH

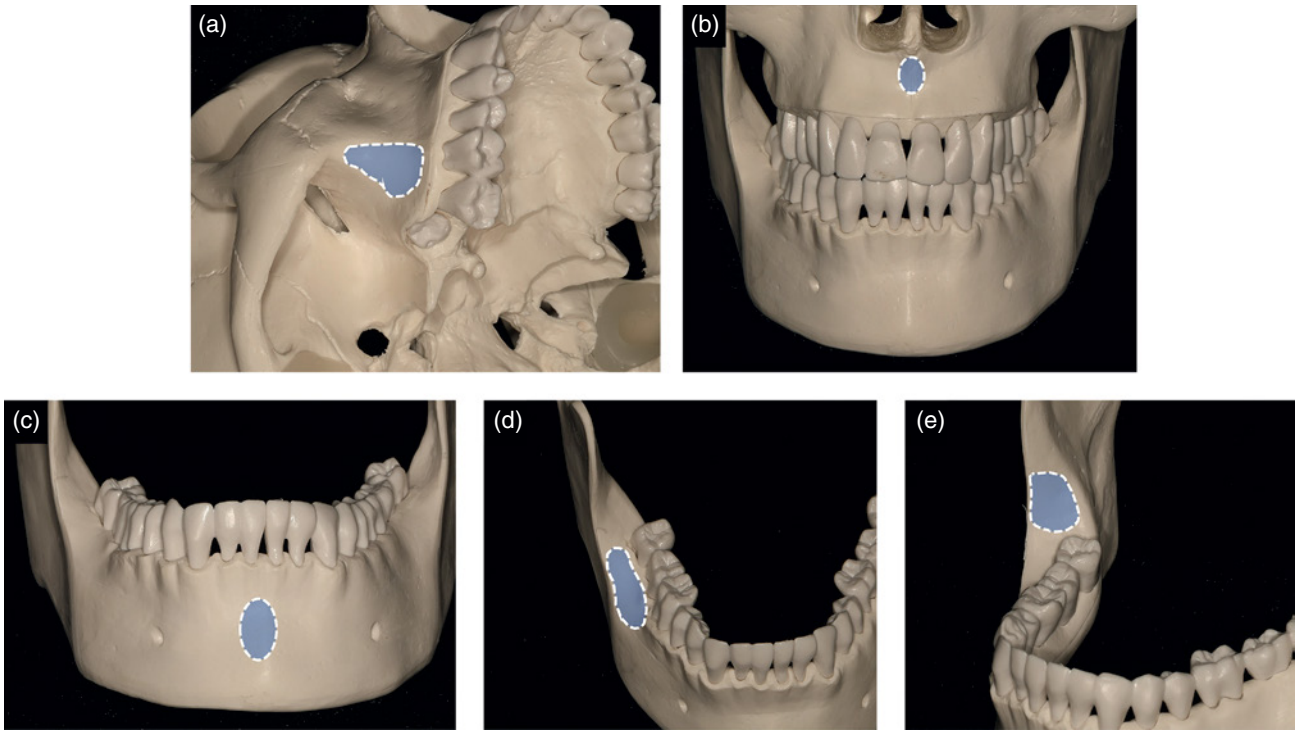


Figure 3.7 Commonly used extra-alveolar anatomical sites for the placement of mini-implants. (a) Infrazygomatic crest. (b) Anterior nasal spine. (c) Mandibular symphysis. (d) Buccal shelf. (e) Mandibular ramus.

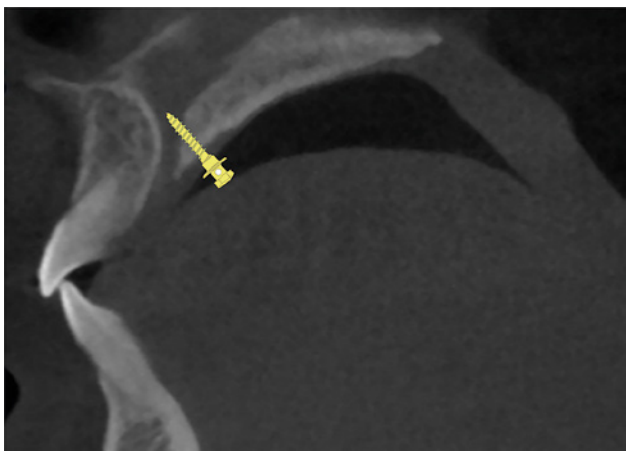


Figure 3.8 Simulated injury to the nasopalatine neurovascular bundles by a virtually placed mini-implant at the anterior palate region.

radiographic examinations are required to avoid injury to inferior alveolar bundles.

Maxillary Sinus

Maxillary sinus penetration by mini-implants inserted at the infrazygomatic crest is a concern for practitioners and efforts are made to reduce the risk of penetration, such as using digital insertion guides.[21,22] However, a clinical study of 32 patients revealed that 78% of mini-implants inserted at the infrazygomatic crest penetrated into the maxillary sinus and that the overall success rate of mini-implants with sinus penetration was 96% (45/47).[23] Specifically, the two failed mini-implants penetrated maxillary sinuses with a pre-existing membrane thickening of over 3 mm, suggesting that maxillary sinus with pre-existing inflammation (e.g. sinusitis) should not be penetrated by mini-implants. It was elaborated that, following sinus penetration, only slight local membrane thickening occurred around the tip of mini-implants (Figure 3.14). Moreover, from the perspective of biomechanics, sinus penetration offers greater primary stability of mini-implants due to bicortical engagement (Figure 3.15).[24] Thus, we suggest that maxillary sinus penetration is not a concern but renders greater primary stability to mini-implants unless pre-existing sinusitis is present (Figure 3.16).

Nasal Cavity

Penetration of the nasal cavity is likely to occur for mini-implants inserted at paramedian and midpalatal regions and nasal penetration was avoided by practitioners in the past.[25] However, current evidence reveals that nasal penetration can offer mini-implants a biomechanical advantage of bicortical engagement, resulting in improved

t.me/Dr_Mouayyad_AlbtousH

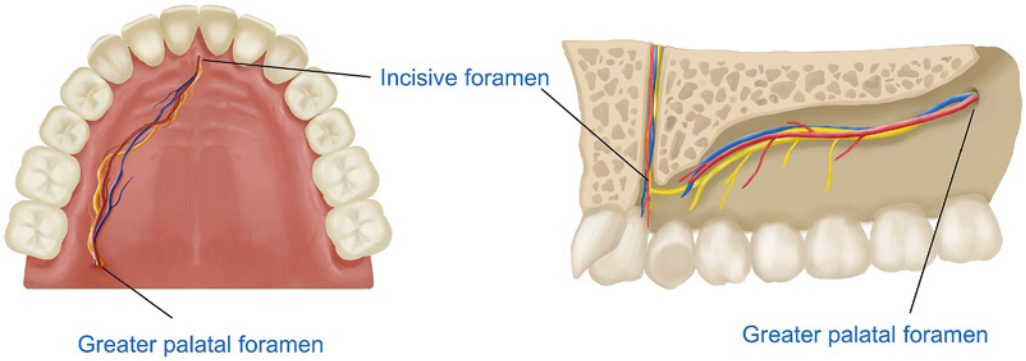


Figure 3.9 Greater palatine vessels and nerves. The greater palatine neurovascular bundles exit from the greater palatal foramen and run anteriorly to anastomose with nasopalatine bundles.

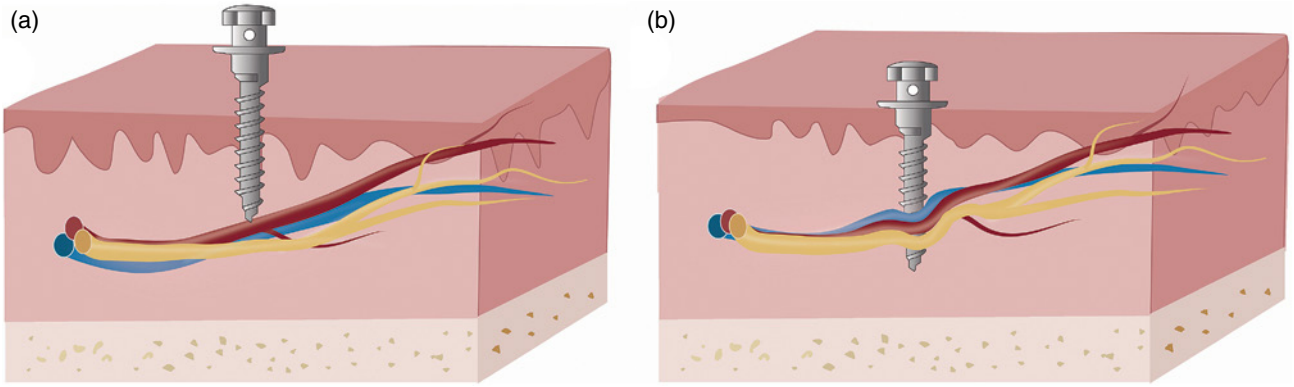


Figure 3.10 (a) The neurovascular bundle is contacted by the mini-implant during insertion. (b) The neurovascular bundle is displaced laterally by the mini-implant due to the soft and elastic property of the palatal soft tissue.

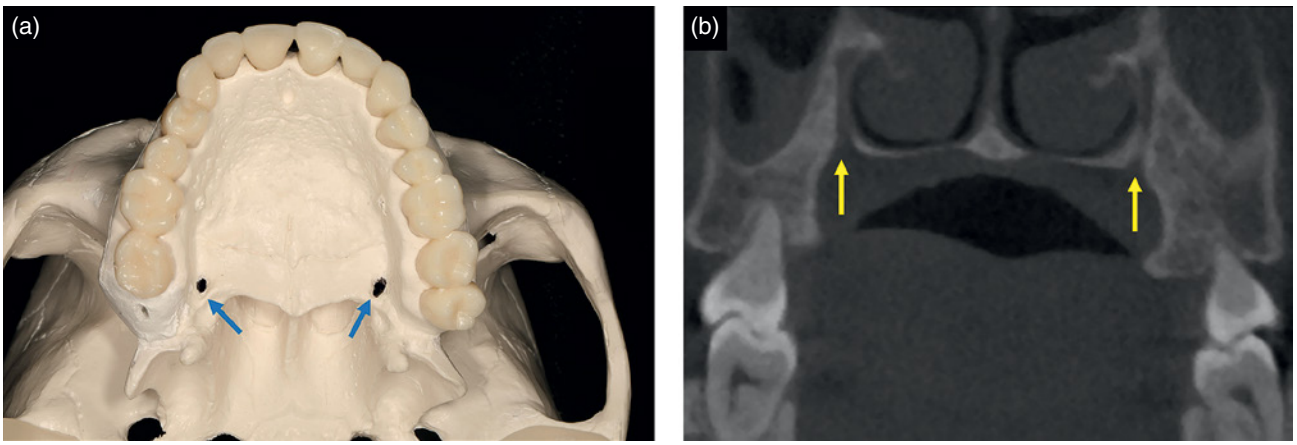


Figure 3.11 Greater palatine foramina. Injury to neurovascular bundles may occur if mini-implants are inserted at the greater palatine foramina since the neurovascular bundles are surrounded by hard tissue and cannot be displaced laterally to eliminate the injury. (a) Greater palatine foramina (blue arrows) shown in a skull. (b) Greater palatine foramina (yellow arrows) shown on a coronal CBCT image.

t.me/Dr_Mouayyad_AlbtousH

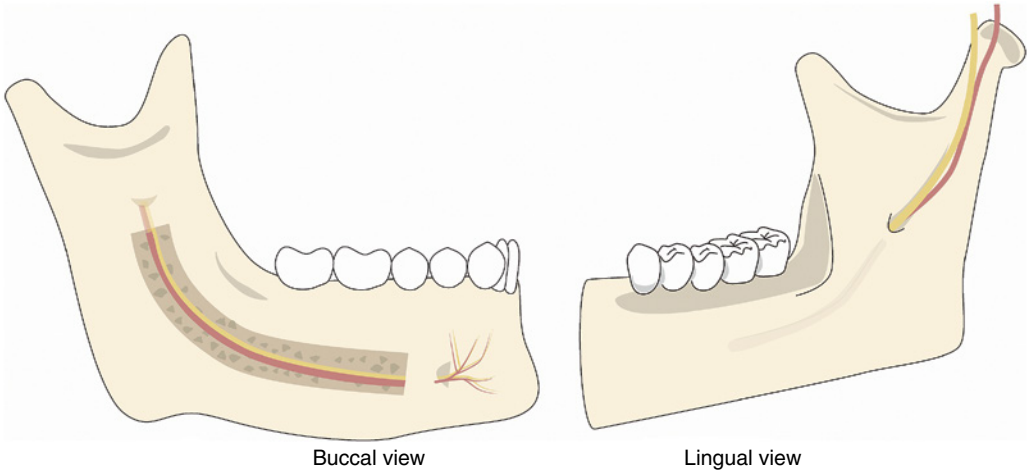


Figure 3.12 Inferior alveolar neurovascular bundles from both the buccal and lingual views.

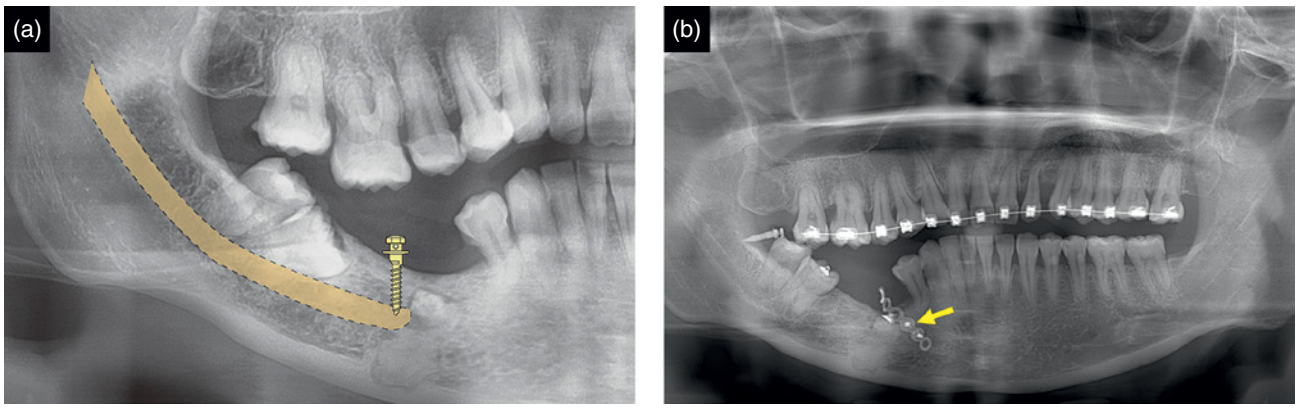


Figure 3.13 (a) Injury to the inferior alveolar neurovascular bundles is of high risk for the insertion of a mini-implant at the underdeveloped alveolar bone region due to tooth loss and primary eruption disturbance of the second premolar. (b) Alternatively, a miniplate (yellow arrow) was placed to avoid the injury.

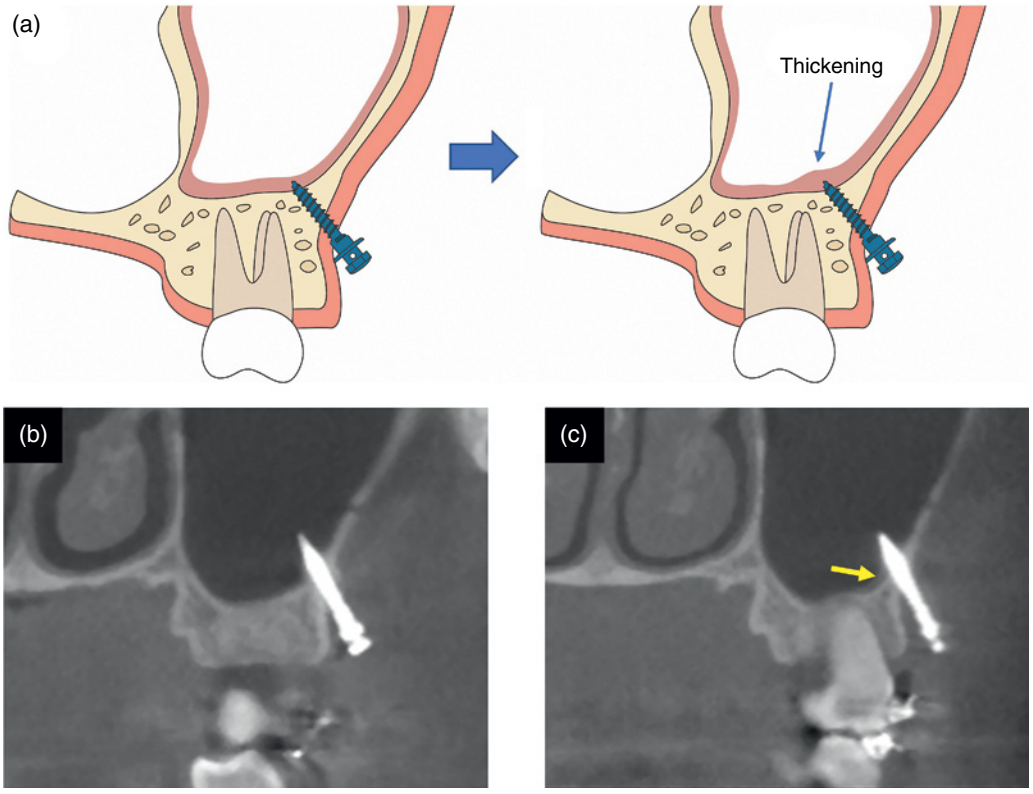


Figure 3.14 (a) A schematic illustration showing mucosa thickening following the insertion of a mini-implant that penetrates into the maxillary sinus. (b) Sinus penetration by a mini-implant immediately following insertion. (c) Slight mucosa thickening (yellow arrow) one year following placement of the mini-implant.

t.me/Dr_Mouayyad_AlbtousH

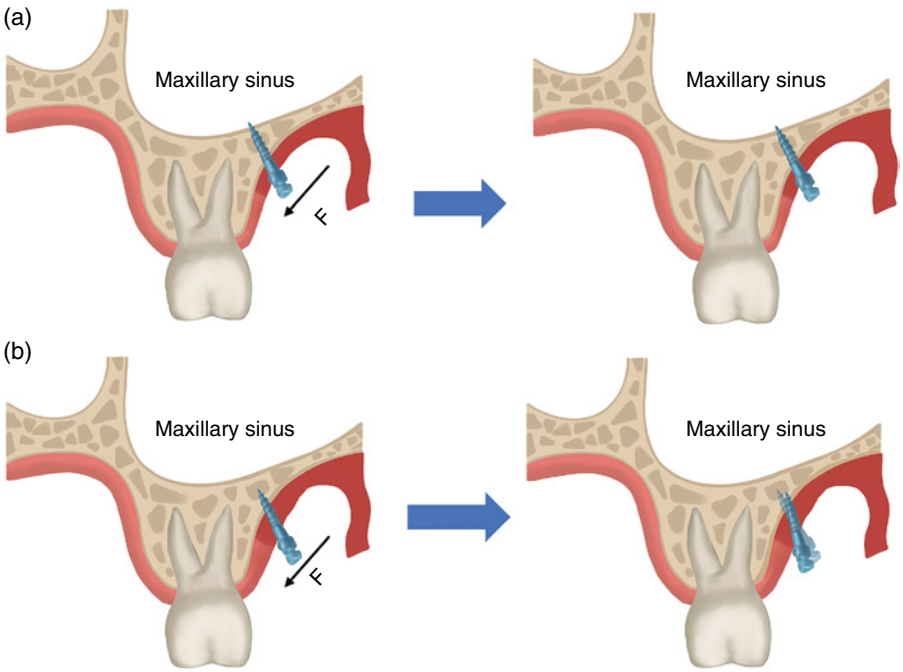


Figure 3.15 Bicortical versus monocortical anchorage modes. (a) Bicortical engagement. The mini-implant is anchored by the cortical plates at both the buccal and sinus sides. The mini-implant is stable in response to lateral displacement force. (b) Monocortical engagement. The mini-implant is only anchored by the cortical plate at the buccal side and may exhibit mobility in response to lateral displacement force.

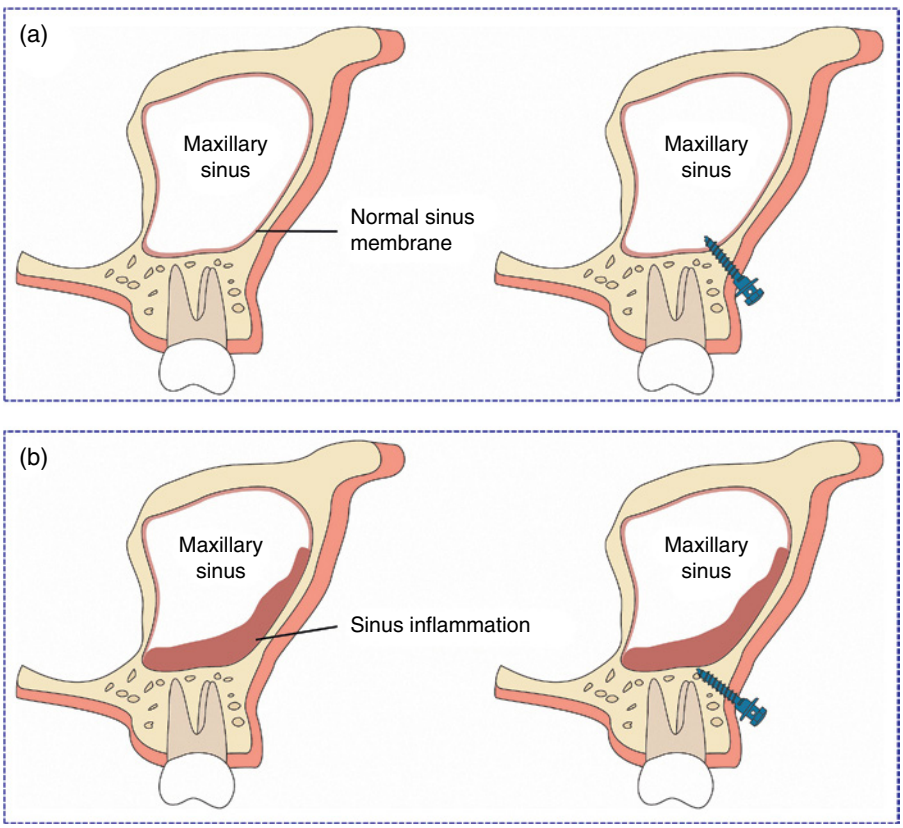


Figure 3.16 (a) Sinus penetration by the mini-implant is recommended if there is no pre-existing sinus inflammation. (b) Sinus penetration is not recommended in the presence of active sinus inflammation.

t.me/Dr_Mouayyad_AlbtousH

mini-implant stability, decreased mini-implant deformation and better treatment outcome for maxillary skeletal expansion. In our clinical experience, a few patients may complain of sneezing for one minute or so once their nasal cavities are penetrated (Figure 3.17). Therefore, unless nasal inflammation is present, penetration of nasal cavity by palatal mini-implants should not be a concern in clinical practice.

In summary, as illustrated in Figure 3.18, orthodontic TADs can be inserted into both alveolar and extra-alveolar sites with sufficient bone quality and quantity where injury to important anatomical structures should be avoided, including dental roots, blood vessels and nerve bundles but excluding maxillary sinus and nasal cavity (unless pre-existing inflammation is present).

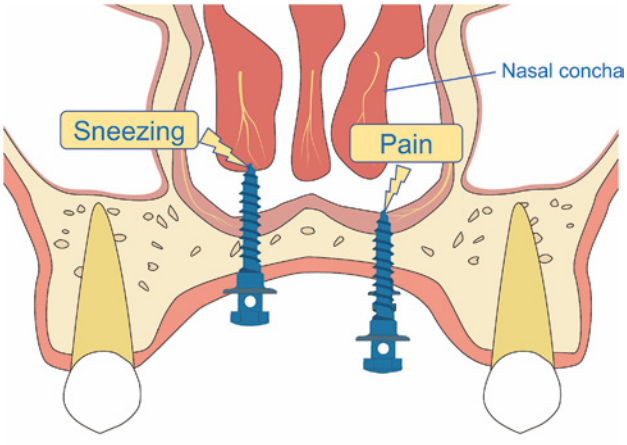


Figure 3.17 Penetration of the nasal mucosa by the mini-implant leads to painful sensation due to rich innervation. Transient sneezing may be experienced if the nasal concha is contacted by the mini-implant.

3.2.2 Available Anatomical Sites

In clinical practice, practitioners choose optimal insertion sites to achieve desired biomechanical results. There are numerous insertion sites that are frequently employed for orthodontic mini-implants (Table 3.2). Available insertion sites in both the maxilla and mandible will be described below.

Maxilla

Available insertion sites in the labial and buccal sides of maxilla are the anterior interradicular region, anterior nasal spine, posterior interradicular region, infrazygomatic crest, maxillary tuberosity and palatal region (Figure 3.19). Specifically, the anterior interradicular region is located at the labial side of the anterior teeth and orthodontic mini-implants are inserted between anterior dental roots. Mini-implants inserted at the anterior interradicular region are often indicated for intrusion of anterior teeth (Figure 3.20). For some orthodontic patients, the anterior interradicular region is contraindicated since interradicular space is limited due to crowding. In this situation, the anterior nasal spine may be a good alternative site. Since the anterior nasal spine is covered by thick mucosa,

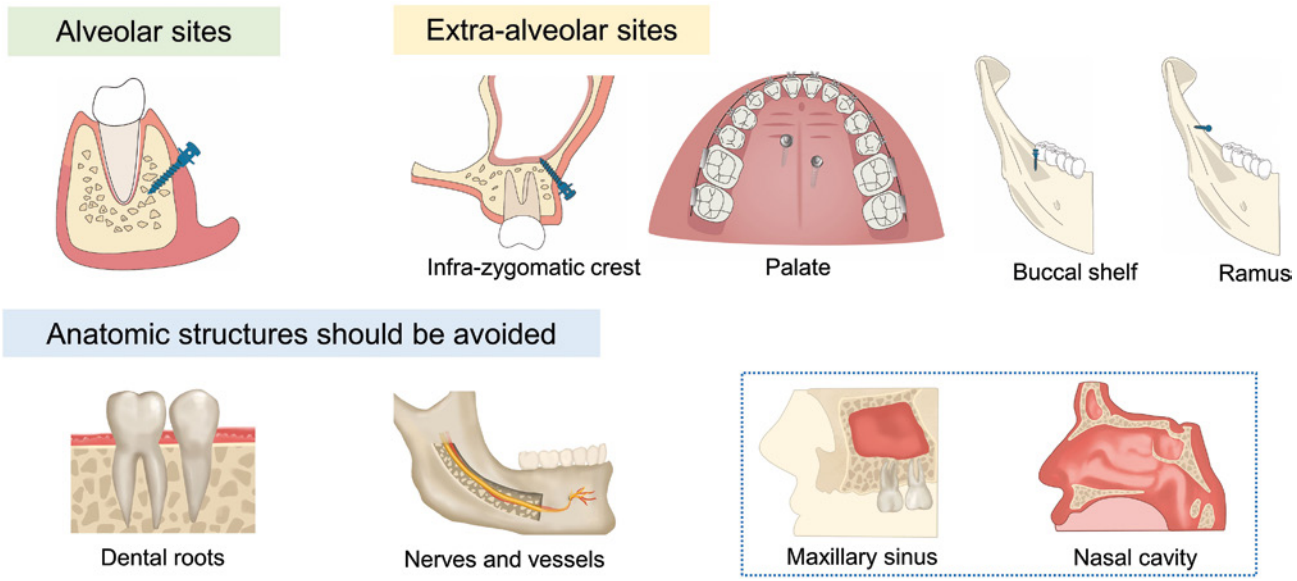


Figure 3.18 Available anatomical sites for the placement of orthodontic TADs. Both alveolar and extra-alveolar sites can be employed. Injury to dental roots and neurovascular bundles should be avoided. Penetration of the maxillary sinus or nasal cavity is not a concern unless pre-existing inflammation is present.

t.me/Dr_Mouayyad_AlbtousH

Table 3.2 Recommended sizes of mini-implants for different anatomical sites.

Jaw	Insertion sites		Recommended size
Maxilla	Alveolar sites	Labial interradicular sites	Diameter: 1.3–1.5 mm, length: 6–8 mm
		Buccal interradicular sites	Diameter: 1.3–1.5 mm, length: 8 mm
	Extra-alveolar sites	Anterior nasal spine	Diameter: 1.8–2 mm, length: 10–12 mm
		Tuberosity	Diameter: 2 mm, length: 10–12 mm
		Palatal region	Diameter: 1.4–2 mm, length: 8–12 mm
		Infrazygomatic crest	Diameter: 2mm, length: 12 mm
Mandible	Alveolar sites	Labial interradicular sites	Diameter: 1.3–1.5 mm, length: 6–8 mm
		Buccal interradicular sites	Diameter: 1.3–1.5 mm, length: 8 mm
	Extra-alveolar sites	Buccal shelf	Diameter: 2 mm, length: 10–12 mm
		Mandibular ramus	Diameter: 2 mm, length: 12–14 mm
		Mandibular symphysis	Diameter: 2 mm, length: 12–14 mm

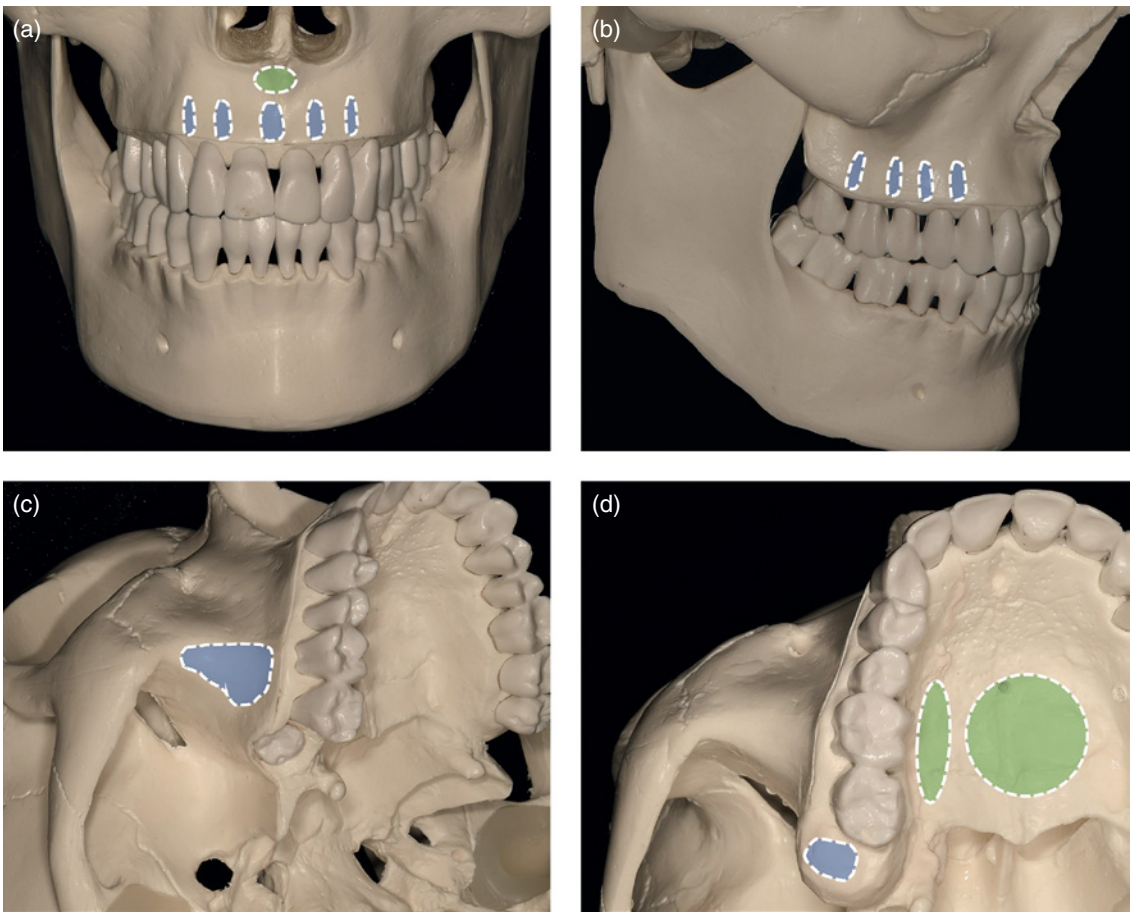


Figure 3.19 Available anatomical sites for the placement of orthodontic TADs in the maxilla. (a) Anterior interradicular regions (blue areas) and anterior nasal spine (green area). (b) Posterior interradicular regions (blue areas). (c) Infrazygomatic crest (blue area). (d) Maxillary tuberosity (blue area) and palatal regions (green areas).

t.me/Dr_Mouayyad_AlbtousH

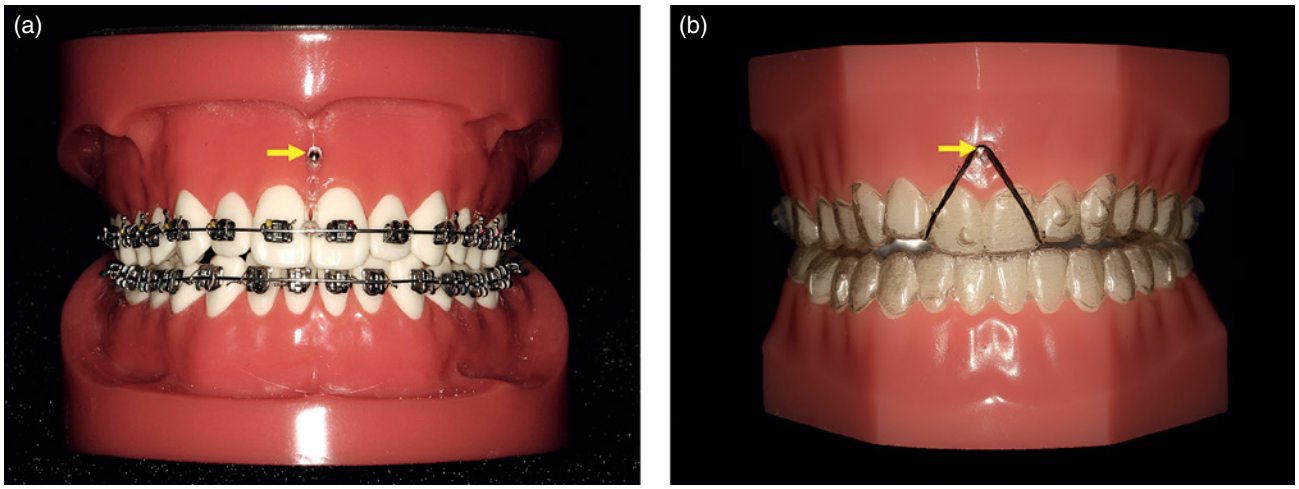


Figure 3.20 Mini-implants at the anterior interradicular region are used for incisor intrusion. (a) A mini-implant (yellow arrow) is inserted at the anterior interradicular site for incisor intrusion with fixed appliances. (b) Incisor intrusion is accomplished through an anterior interradicular mini-implant (yellow arrow) with clear aligner.

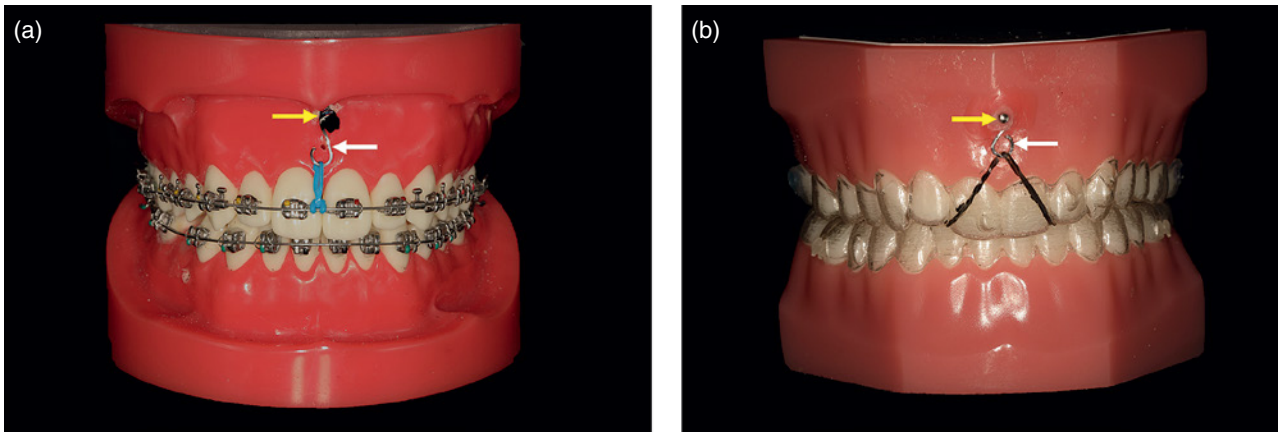


Figure 3.21 Mini-implants inserted at the anterior nasal spine are used for incisor intrusion. The mini-implants (yellow arrows) are used in conjunction with extension hooks (white arrows) to intrude anterior teeth. (a) Fixed appliances. (b) Clear aligner.

mini-implants inserted at this region should be used in conjunction with extension arms or hooks for orthodontic force loading (Figure 3.21).

The posterior interradicular region is one of the most frequently used insertion sites for orthodontic mini-implants that are often indicated for molar anchorage reinforcement and molar protraction (Figure 3.22). In particular, interradicular space is largest between the second premolars and first molars and this is most frequently employed among all the posterior interradicular sites. Moreover, for patients with insufficient space at posterior interradicular sites, interradicular sites may be contraindicated due to high risk of root injury and the infrazygomatic crest is a good alternative for these patients. The infrazygomatic crest is located buccally and apically to the first and second molars and mini-implants inserted at this region are often indicated for molar distalisation, anterior retraction and molar intrusion (Figure 3.23). More posteriorly located, the maxillary tuberosity is employed for maxillary uprighting and molar distalisation (Figure 3.24).

The palatal region of the maxilla offers good bone quality and quantity for the insertion of orthodontic mini-implants. Three commonly used insertion sites are the palatal posterior interradicular region, paramedian region and midpalatal suture (Figure 3.25). Mini-implants inserted at the posterior interradicular region are frequently used for anterior retraction with lingual appliances or molar intrusion (Figure 3.26). The paramedian region is located 5 mm away from the midpalatal suture and mini-implants inserted at this region are indicated for maxillary

t.me/Dr_Mouayyad_AlbtousH

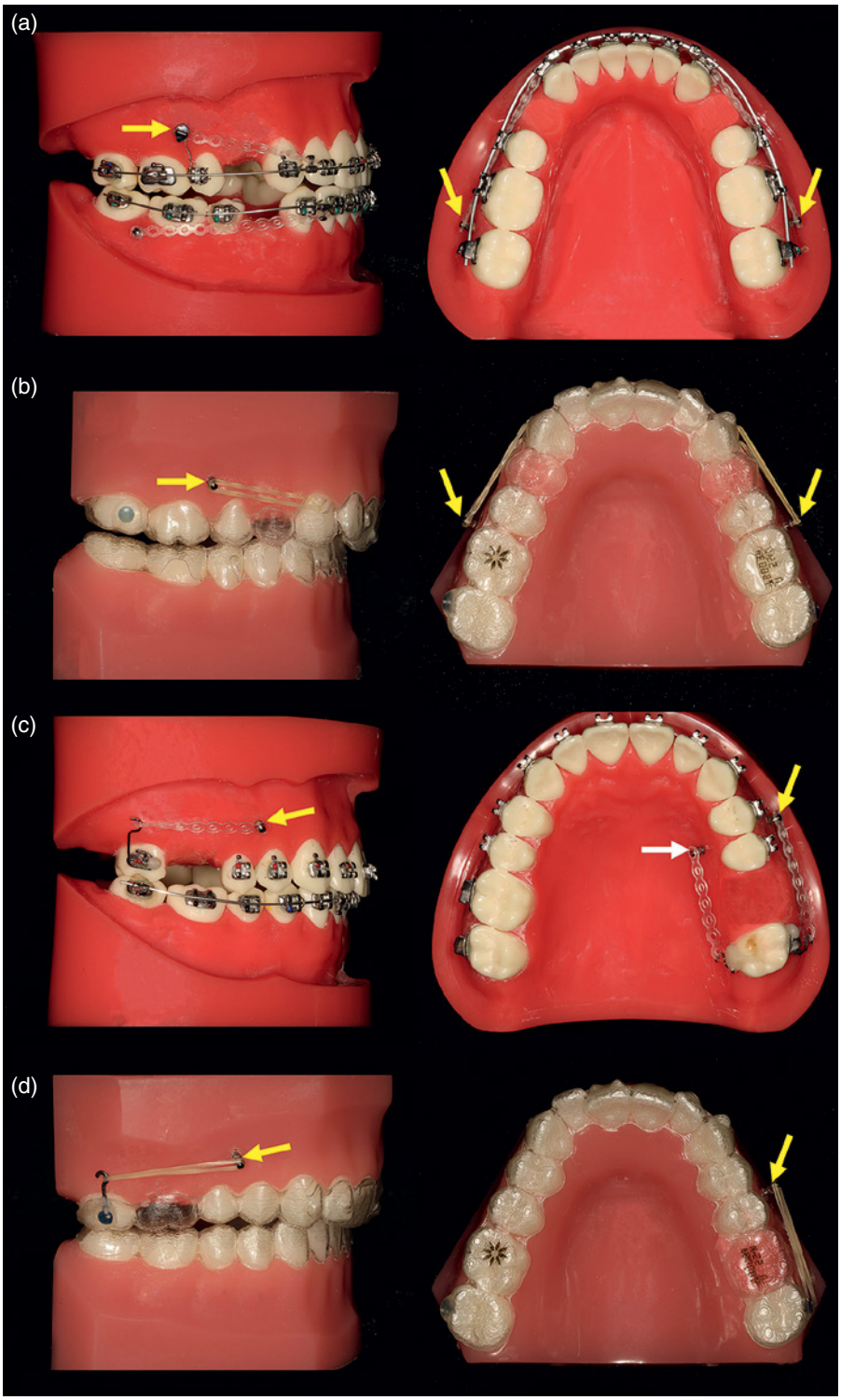


Figure 3.22 Versatile applications of mini-implants placed at the posterior interradicular region. (a) Interradicular mini-implants (yellow arrows) used for molar anchorage augmentation with fixed appliances. (b) Interradicular mini-implants (yellow arrows) for molar anchorage reinforcement with clear aligner. (c) A mini-implant (yellow arrow) inserted between the first and second premolars is used for molar protraction in conjunction with a palatal mini-implant (white arrow) for fixed appliance therapy. (d) A mini-implant (yellow arrow) between the first and second premolars is used for molar protraction for clear aligner therapy.

t.me/Dr_Mouayyad_AlbtousH

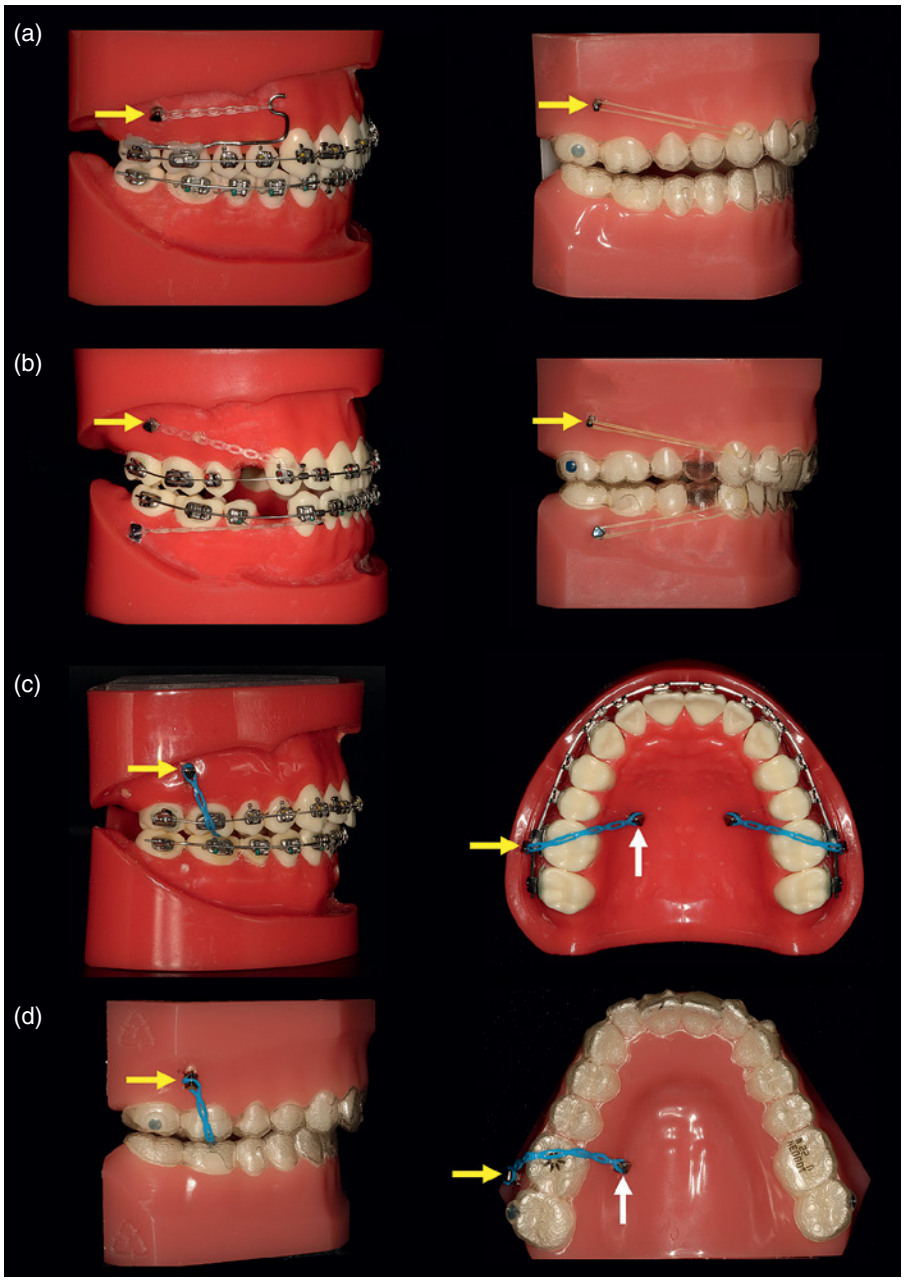


Figure 3.23 Versatile applications of infrazygomatic crest mini-implants. (a) Mini-implants (yellow arrows) inserted at the infrazygomatic crest (IZC) region are used for molar distalisation with both the fixed appliance and clear aligner. (b) IZC mini-implants are employed for anterior retraction with both the fixed appliance and clear aligner. (c) The IZC mini-implant (yellow arrow) is applied for molar intrusion in conjunction with a palatal mini-implant (white arrow) for fixed appliance therapy. (d) The IZC mini-implant (yellow arrow) is utilised for molar intrusion with a palatal mini-implant (white arrow) for clear aligner therapy.

skeletal expansion, molar intrusion, molar distalisation and traction of impacted teeth (Figure 3.27).

The midpalatal suture is available for orthodontic mini-implants that can be used for molar intrusion and molar distalisation (Figure 3.28). Since fusion of the midpalatal suture is not completed until adulthood, orthodontic mini-implants inserted at the midpalatal suture are often contraindicated in adolescents.

Mandible

Due to the high risk of injury to important anatomical structures and patient discomfort with mini-implants at the lingual side of the mandible, the labial and buccal sides are clinically employed. Commonly used insertion sites are the anterior interradicular region, mandibular symphysis, posterior interradicular region, buccal shelf and mandibular ramus (Figure 3.29).

t.me/Dr_Mouayyad_AlbtousH

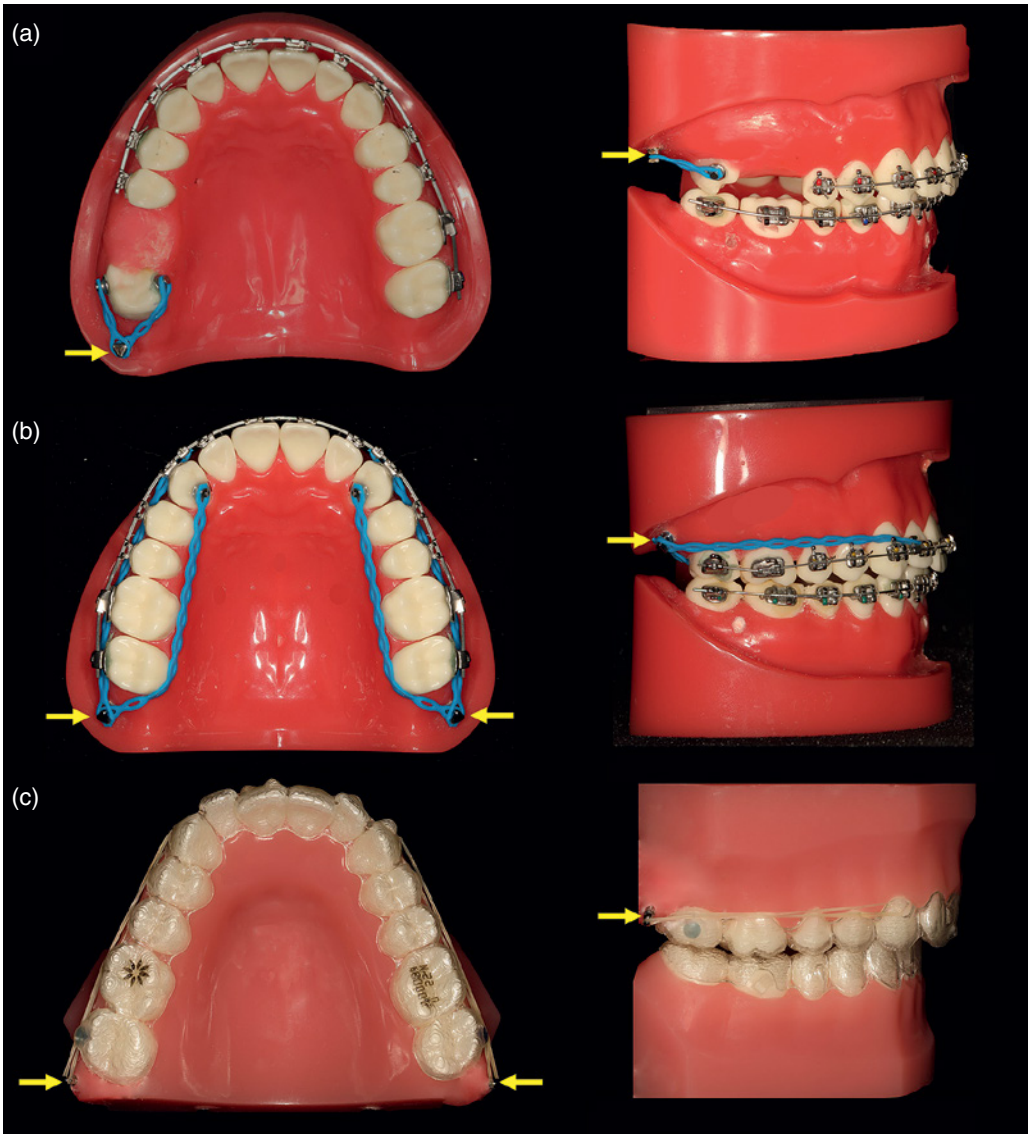
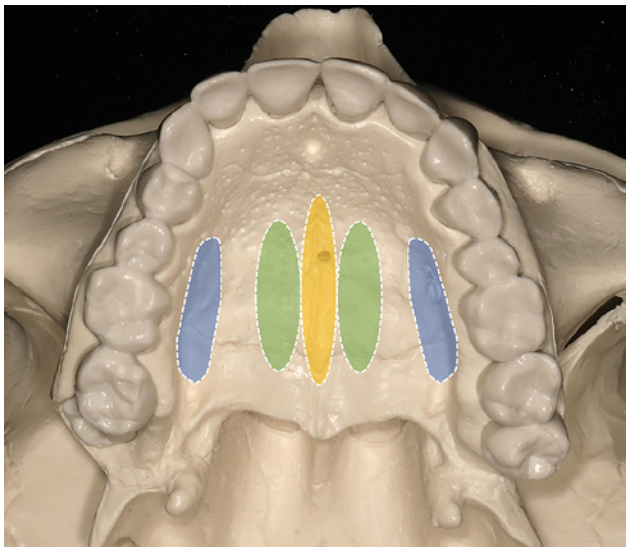


Figure 3.24 (a) The mini-implant (yellow arrow) placed at the maxillary tuberosity region is used for molar uprighting. (b) The mini-implants (yellow arrows) at the tuberosity region are employed for distalisation of the maxillary dentition with fixed appliances. (c) The mini-implants (yellow arrows) at the tuberosity region are employed for distalisation of the maxillary dentition with clear aligner.

Figure 3.25 Available anatomical sites for the placement of mini-implants at the palatal region include the interradicular region (blue area), paramedian region (green area) and midpalatal suture (yellow area).



t.me/Dr_Mouayyad_AlbtousH

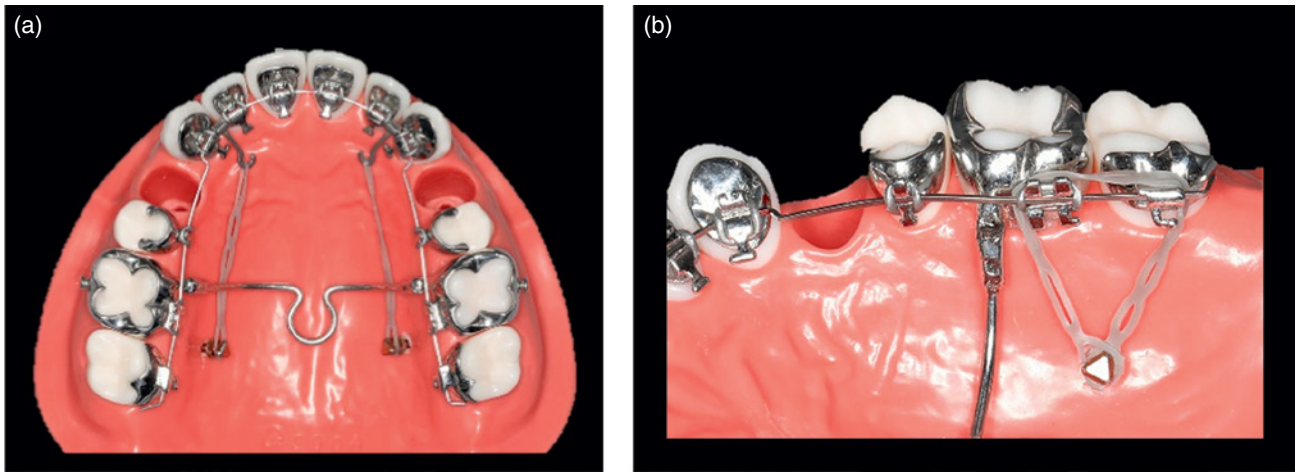


Figure 3.26 The clinical applications of palatal interradicular mini-implants with lingual appliances. (a) Anterior retraction. (b) Molar intrusion.

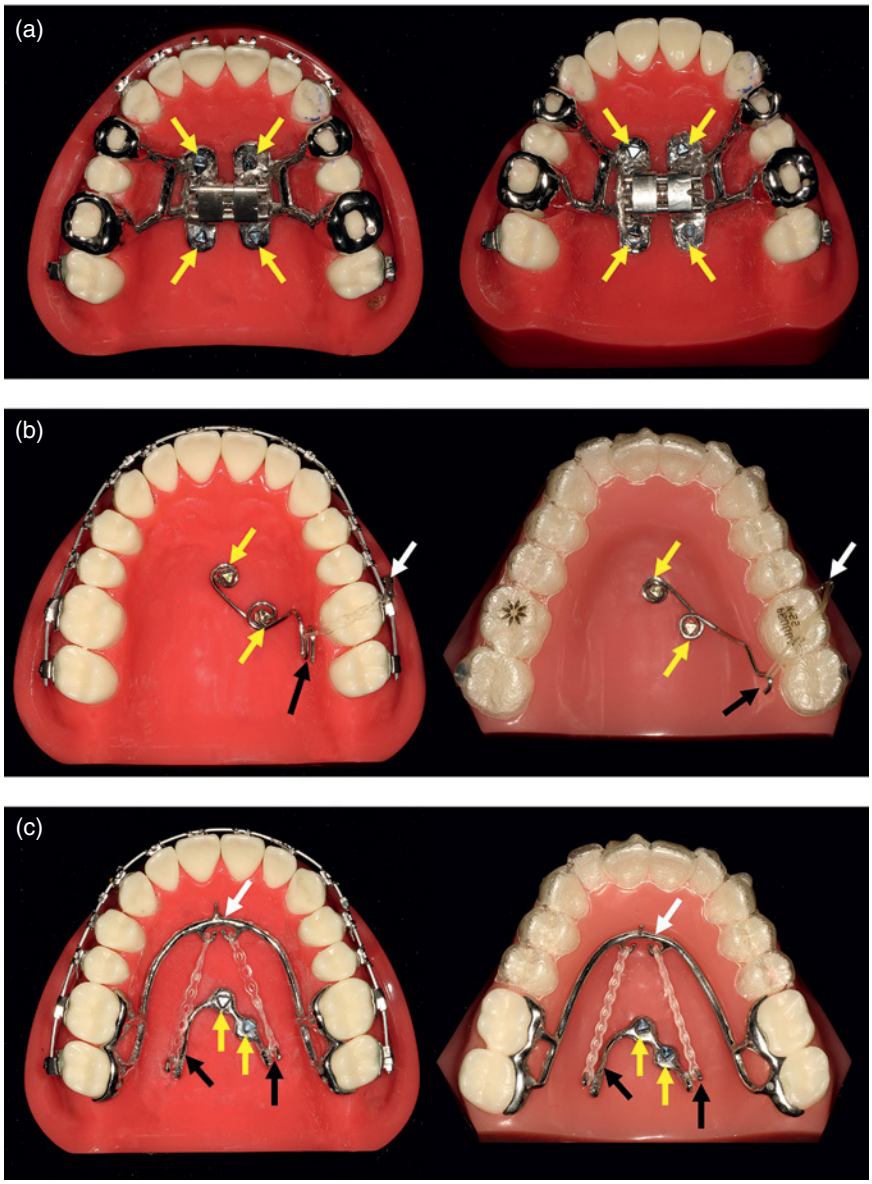


Figure 3.27 Versatile clinical applications of palatal mini-implants. (a) Mini-implants (yellow arrows) at the paramedian region are used for skeletal expansion. (b) Mini-implant-anchored extension hook (black arrow) is used for molar intrusion in conjunction with a buccal mini-implant (white arrow) for both fixed appliances and clear aligner. The palatal mini-implants are indicated by the yellow arrows. (c) Extension hooks (black arrows) fixed and anchored by two palatal mini-implants (yellow arrows) are used for molar distalisation. The bilateral molars are stabilised by a palatal arch (white arrow). (d) The palatal mini-implant (yellow arrow) is used for orthodontic traction of an impacted molar (black arrow). The cantilever appliance (white arrow) is fixed and anchored onto the palatal mini-implant.

t.me/Dr_Mouayyad_AlbtousH

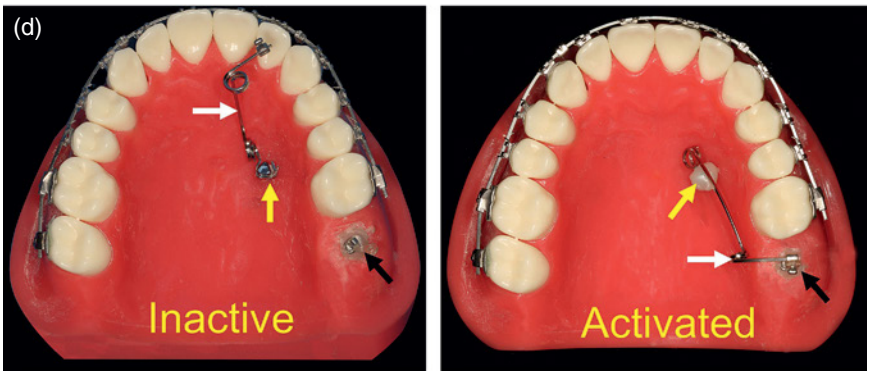


Figure 3.27 (Continued)

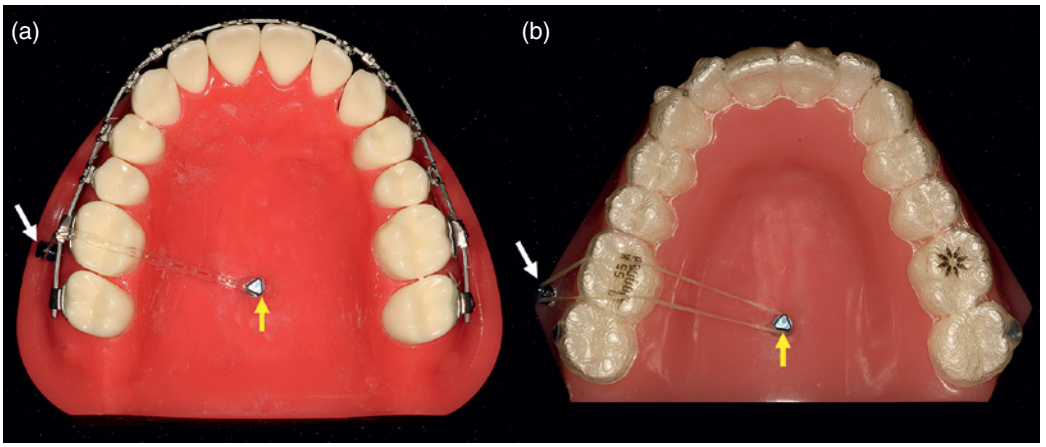


Figure 3.28 Mini-implants (yellow arrows) placed at the midpalatal suture are used for molar intrusion in conjunction with buccal mini-implants (white arrows). (a) Fixed appliance. (b) Clear aligner.

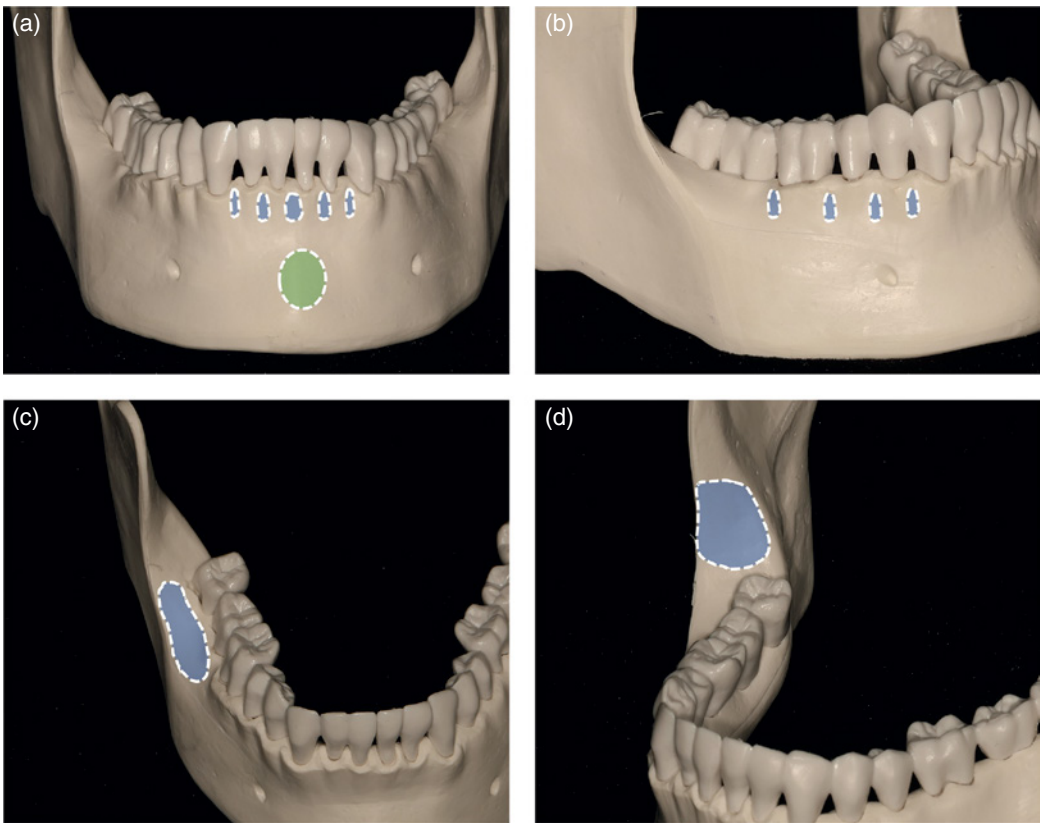


Figure 3.29 Commonly used insertion sites in the mandible. (a) Anterior interradicular region (blue area) and mandibular symphysis (green area). (b) Posterior interradicular region (blue area). (c) Buccal shelf (blue area). (d) Mandibular ramus (blue area).

t.me/Dr_Mouayyad_AlbtousH

The anterior interradicular region is seldom used for insertion of mini-implants due to limited space between the mandibular incisors. Occasionally, if interradicular space is adequate, mini-implants can be inserted at this region to intrude mandibular anterior teeth (Figure 3.30). Alternatively, the mandibular symphysis can be used for insertion of mini-implants indicated for anterior intrusion if anterior interradicular space is insufficient (Figure 3.31). As for its maxillary counterpart, the mandibular posterior interradicular region is often used for molar anchorage reinforcement and molar protraction (Figures 3.32 and 3.33). Buccal shelf is located buccally to the mandibular first and second molars and mini-implants inserted at this region are often indicated for anterior retraction, orthodontic traction of impacted teeth and mandibular molar distalisation (Figure 3.34). Furthermore, mini-implants inserted at the mandibular ramus region are often indicated for traction of deeply impacted teeth (Figure 3.35).

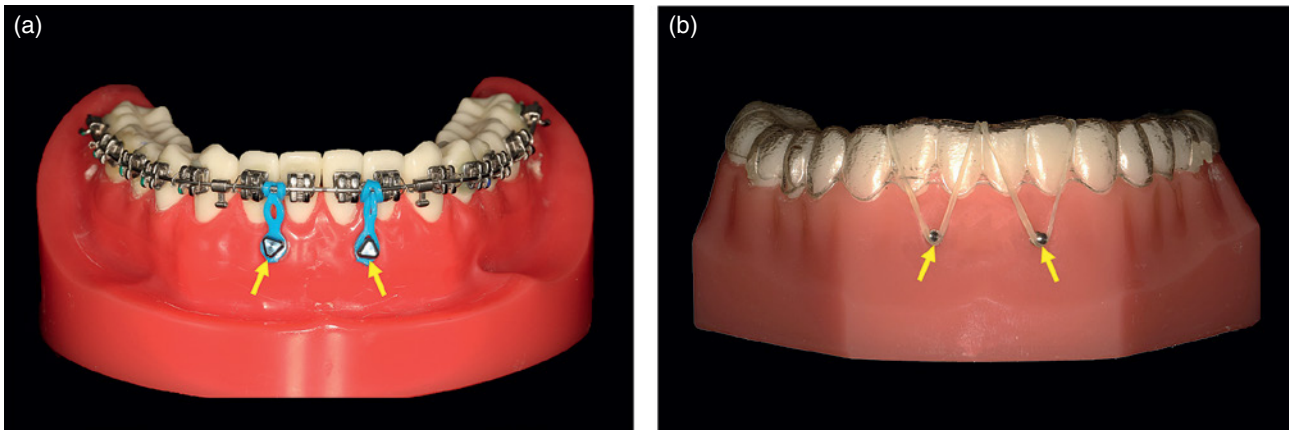


Figure 3.30 Anterior interradicular mini-implants (yellow arrows) used for molar intrusion. (a) Fixed appliances. (b) Clear aligner.

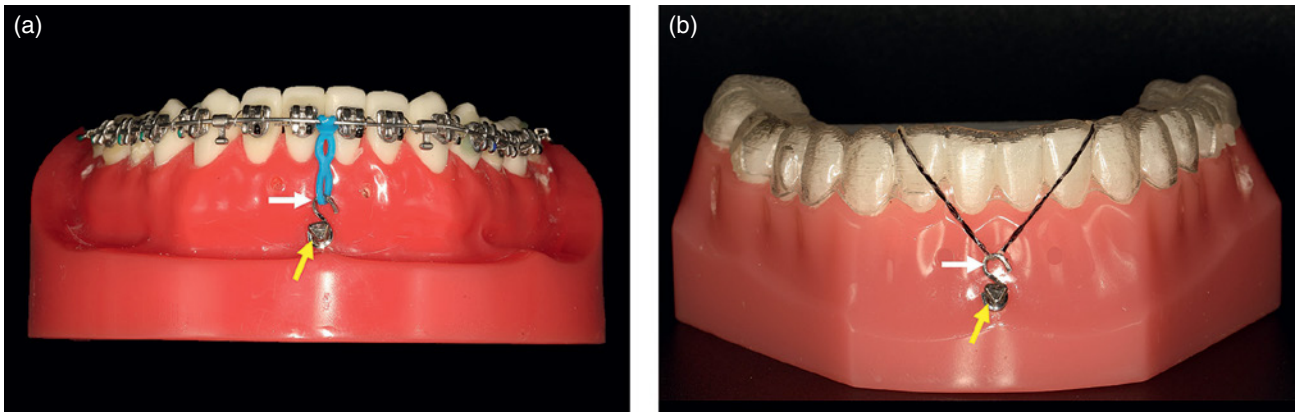


Figure 3.31 Mini-implants (yellow arrows) placed at the mandibular symphysis region are applied for incisor intrusion through extension hooks (white arrows). (a) Fixed appliances. (b) Clear aligner.

t.me/Dr_Mouayyad_AlbtousH

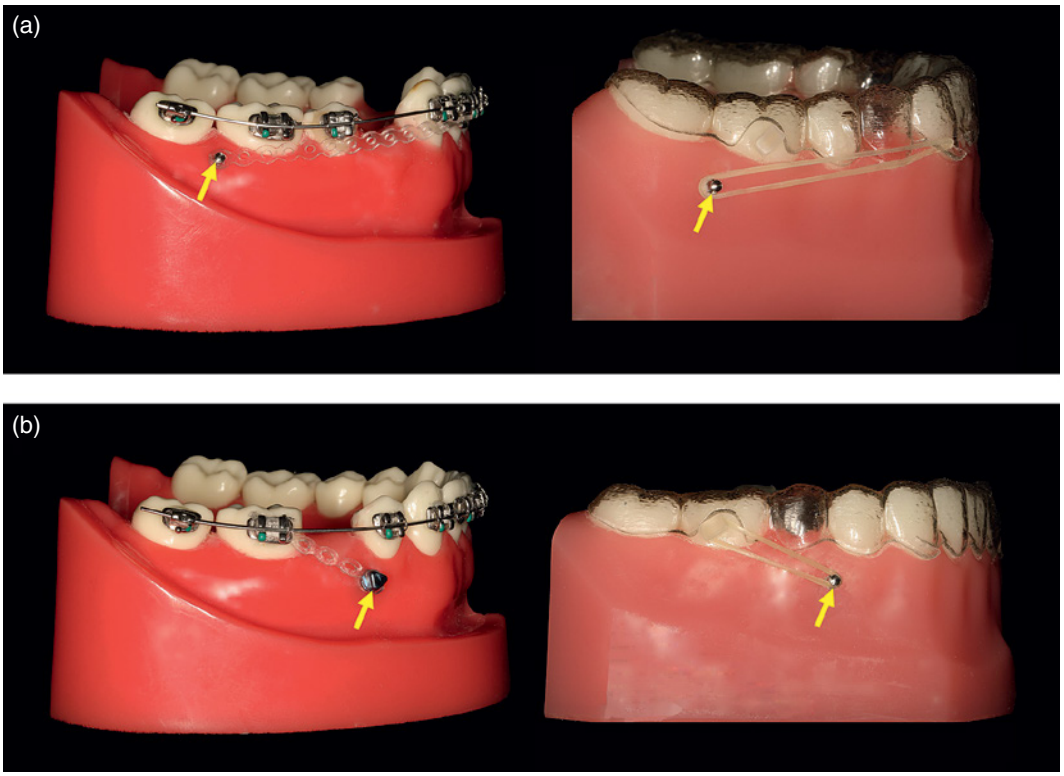


Figure 3.32 Versatile applications of mini-implants (yellow arrows) placed at the posterior interradicular sites. (a) Anterior retraction with both fixed appliances and clear aligner. (b) Molar protraction with both fixed appliances and clear aligner.

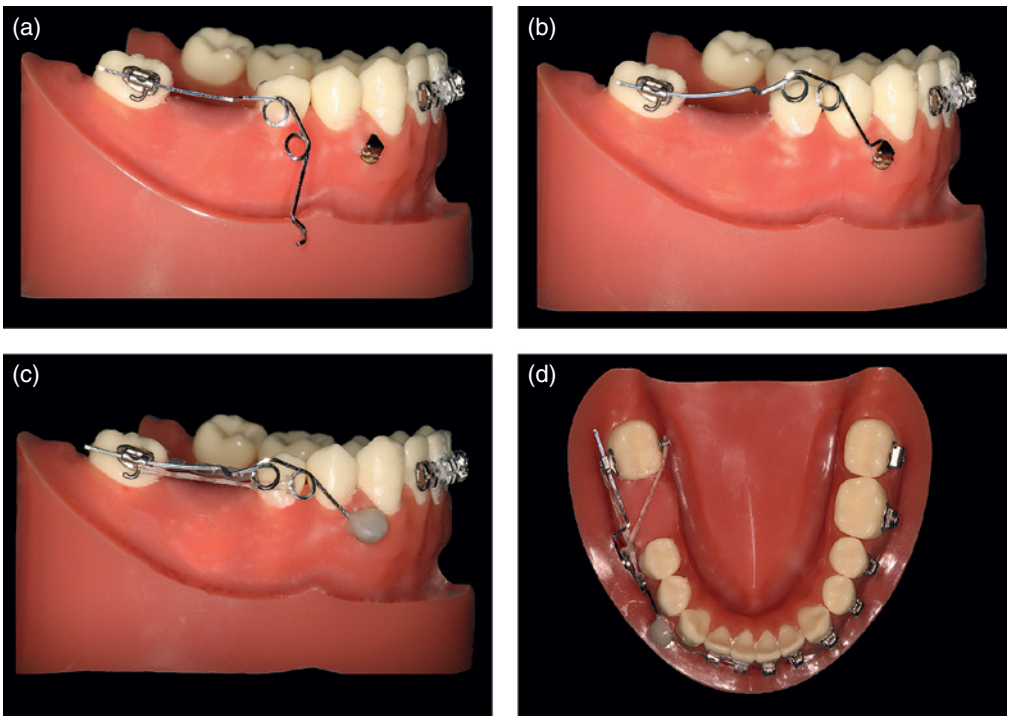


Figure 3.33 The mini-implant inserted at the posterior interradicular site is used for molar protraction through a protraction loop appliance (Albert protraction loop). (a) The Albert protraction loop is inserted into the molar tube (inactivated). (b) The loop is engaged onto the mini-implant (activated). (c) The loop is fixed onto the mini-implant with flowable resin. Elastomeric chain is used for molar protraction from the buccal side. (d) Elastomeric chain is applied between the lingual button on the molar and the loop. The two running loops offer anticlockwise moment that prevents mesial tipping of the molar and the elastomeric chain generates protraction forces from both the buccal and lingual sides. In this way, bodily protraction of the molar can be achieved. The whole biomechanical system is solely built on the mini-implant.

t.me/Dr_Mouayyad_AlbtousH

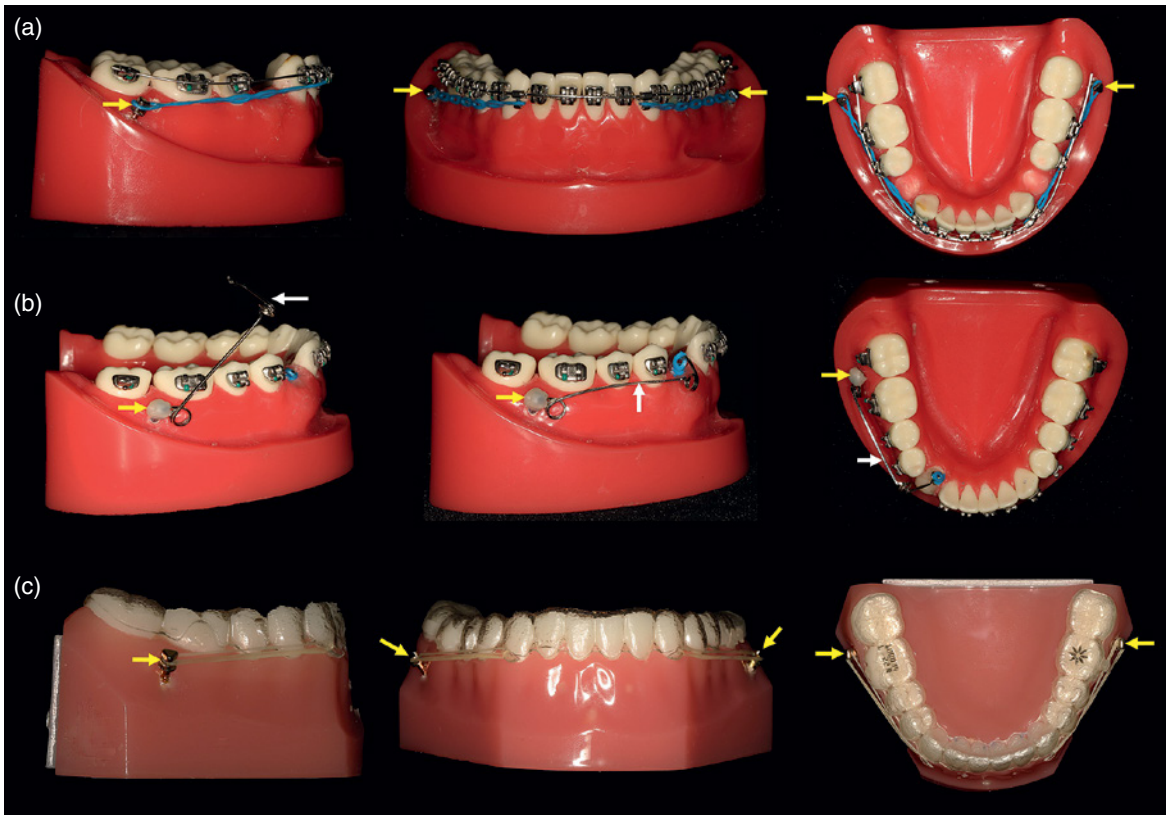


Figure 3.34 Versatile applications of mini-implants at the buccal shelf region. (a) Anterior retractions (mini-implants indicated by yellow arrows). (b) The cantilever appliance (white arrow) anchored by the buccal shelf mini-implant (yellow arrow) is used for traction of an impacted canine. (c) The mini-implants (yellow arrow) at the buccal shelf region are used for molar distalisation with clear aligner.

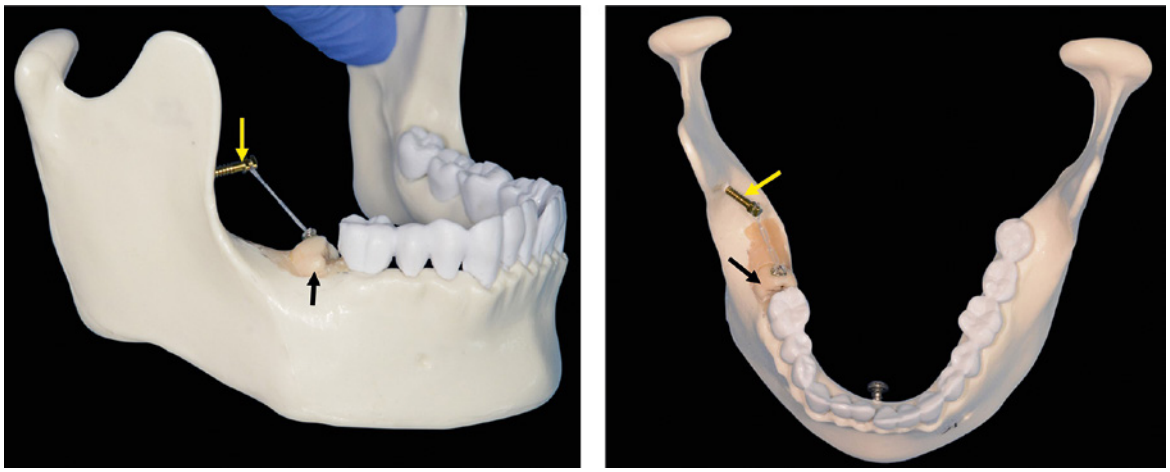


Figure 3.35 The mini-implant (yellow arrow) at the mandibular ramus region is used for orthodontic traction of a deeply impacted mandibular molar (black arrow).

t.me/Dr_Mouayyad_AlbtousH

3.3 Biomechanics-driven Paradigm

The biomechanics-driven paradigm determines insertion sites based on biomechanical requirements. If an optimal insertion site is available that meets the requirements of both the anatomy-driven and biomechanics-driven paradigms, it should be selected with no hesitation (Figure 3.36). However, in clinical practice, due to anatomical limitations, the optimal insertion site selected through the biomechanics-driven paradigm often does not coincide with that selected through the anatomy-driven paradigm. In these situations, equivalent biomechanical alternatives should be designed to fit the anatomy-driven paradigm. For example, from the biomechanics perspective, it is preferred to insert mini-implants at buccal interradicular sites for anterior retraction (Figure 3.37). However, for some patients, insufficient interradicular space limits the insertion of mini-implants at these sites. Thus, alternative anatomical sites could be chosen to fulfil the biomechanical requirements, e.g. palatal mini-implants in conjunction with palatal arches (Figure 3.38).

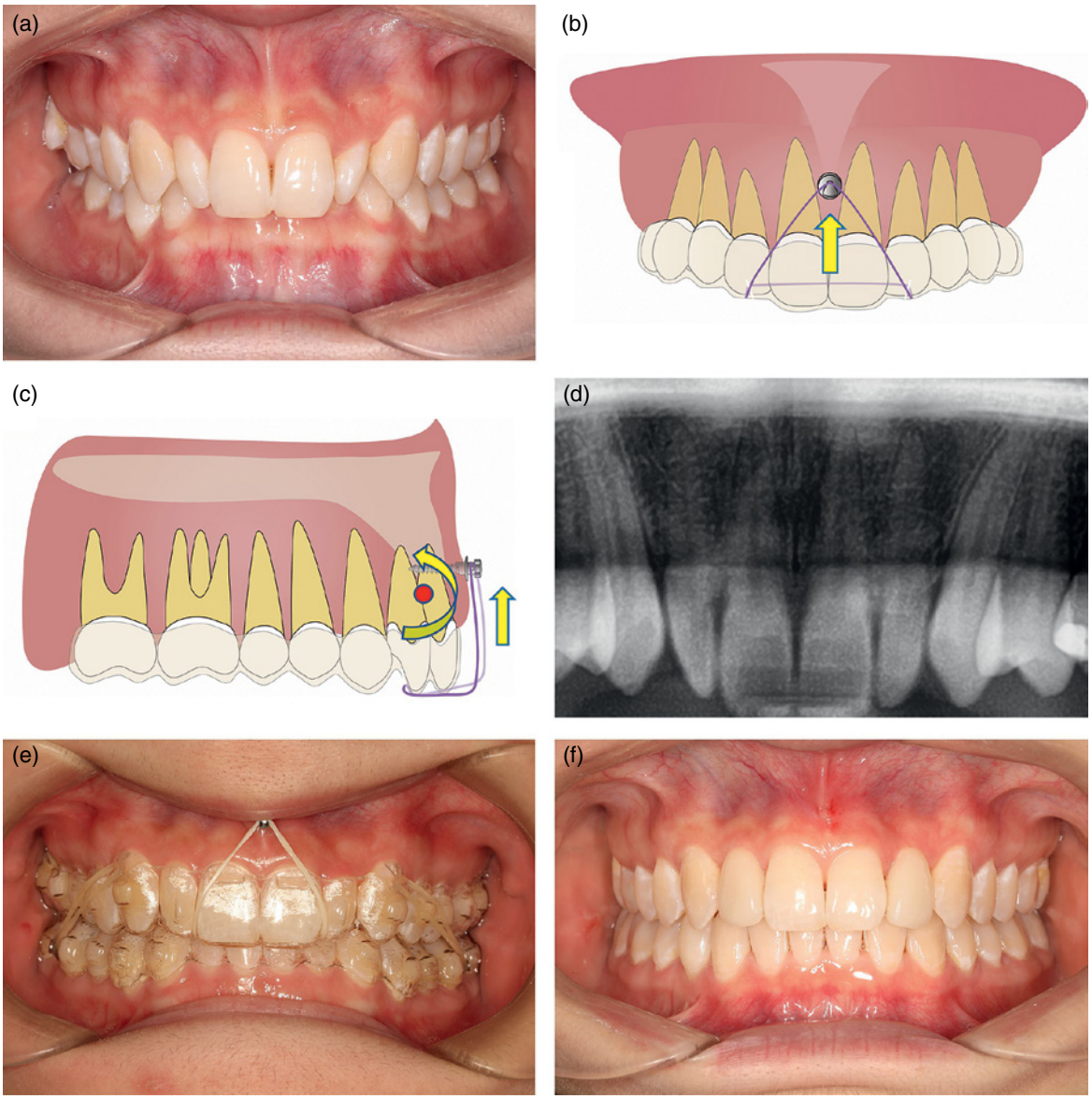


Figure 3.36 Selection of insertion sites according to the biomechanics-driven paradigm. (a) Severe deep bite with retroclined incisors (class II division 2 malocclusion). (b,c) From the biomechanical perspectives, a labial mini-implant is indicated for the clear aligner therapy since the intrusive force offered by the mini-implant generates an anticlockwise moment. The net effect is simultaneous intrusion and proclination of the incisors. (d) Radiography indicates that ample interradicular distance is present between the roots of the central incisors. (e) A mini-implant was inserted at the interradicular site between the central incisors to offer intrusive force with the clear aligner. (f) The deep bite was resolved.

t.me/Dr_Mouayyad_AlbtousH



Figure 3.37 *En masse* anterior retraction through mini-implants inserted at the buccal interradicular sites. (a) Facial profile changes. The patient presented with a convex and protrusive facial profile and the protrusion was resolved after treatment. (b) Pretreatment. (c) Progress. Note that two mini-implants (yellow arrows) were placed at the buccal interradicular sites and were used for *en masse* anterior retraction with the aid of long crimpable hooks. (d) Normal overjet and overbite as well as good buccal interdigitation were obtained.

Other clinical examples will be discussed below to demonstrate the philosophy of designing an equivalent biomechanical system when the anatomy-driven paradigm does not coincide with the biomechanics-driven paradigm.

3.3.1 Maxillary Molar Uprighting

Mesial tipping of maxillary molars often occurs due to missing their mesial adjacent teeth (Figure 3.39). For these patients, molar uprighting and subsequent implant restoration is the treatment option of choice. From the biomechanics perspective, distal force is desirable to upright the mesially tipped molars and the maxillary tuberosity is the most appropriate insertion site for orthodontic mini-implants (Figure 3.40). However, the failure rate of mini-implants inserted at the maxillary tuberosity is high due to low bone density and thin cortex.[26] Thus, in this clinical scenario, when the anatomy-driven approach

t.me/Dr_Mouayyad_AlbtousH

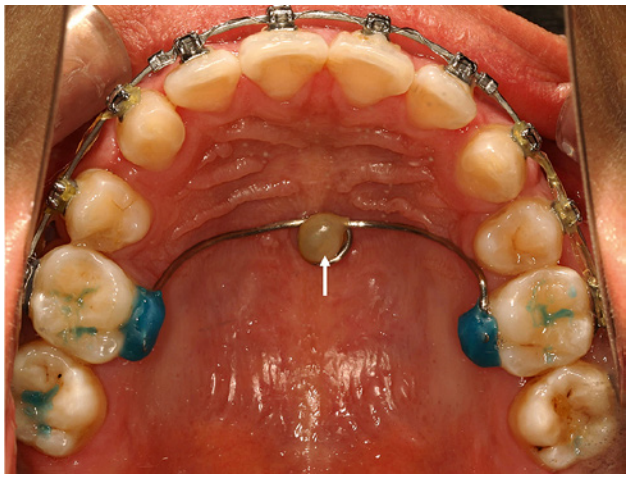


Figure 3.38 Molar anchorage was reinforced by the palatal mini-implant (white arrow) through a palatal arch. The mini-implant was embedded and covered by flowable resin.

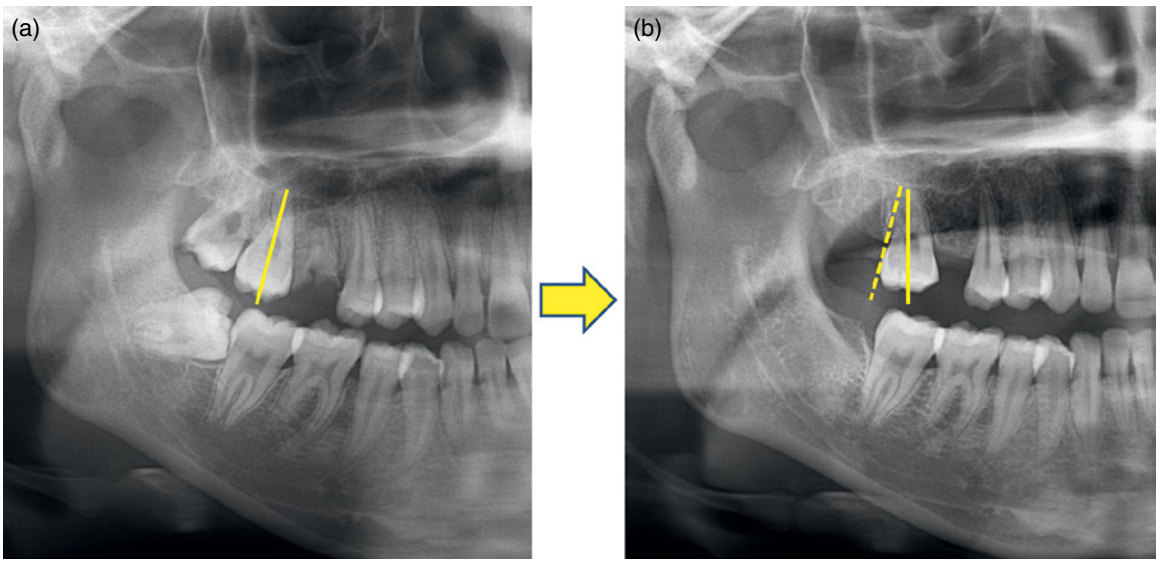


Figure 3.39 Mesial tipping of the maxillary second molar due to loss of the first molar. (a) Initial mesiodistal angulation of the second molar. The long axis of the second molar is indicated by the yellow line. The first molar was extracted for severe caries. (b) Follow-up after three years. Mesial tipping of the second molar has occurred. Compare the current long axis of the second molar (yellow line) with that three years ago (dashed yellow line).

does not coincide with the biomechanics-driven approach, an alternative equivalent biomechanical system could be designed. As displayed in a clinical case (Figure 3.41), indirect anchorage can be employed to upright the mesially tipped second molar through applying open-coil springs between the second molar and second premolar whose anchorage was reinforced by a mini-implant inserted at the edentulous region.

3.3.2 Molar Intrusion

Molar intrusion is indicated in orthodontic patients with overerupted molars or in dolichocephalic patients with open bite. Prudent biomechanics is a prerequisite for successful clinical outcomes.

Buccal or lingual tipping is frequently encountered in clinical practice if intrusive force lies at the buccal or lingual side of the molars requiring intrusion. Intrusive force should be applied at both the buccal and lingual sides to achieve bodily intrusion of molars with the help of a pair of mini-implants (one at the buccal side and the other at the lingual side) (Figure 3.42). From the occlusal view, this requires the line connecting the two mini-implants to pass through the centre of resistance of the molars, otherwise the molars will tip mesially or distally. However, this may not be accomplished due to anatomical limitations.

In this clinical scenario, one mini-implant could be inserted at the buccal side and two mini-implants inserted at the palatal side. With the help of an extension arm fixed on the two palatal mini-implants, the distal hook of the extension arm

t.me/Dr_Mouayyad_AlbtousH

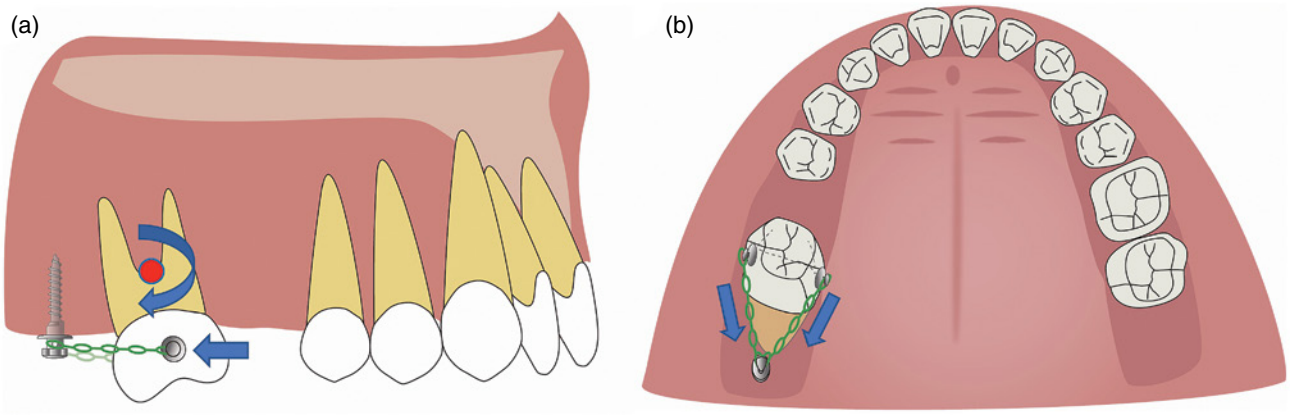


Figure 3.40 The mini-implant inserted at the maxillary tuberosity region is used for uprighting the mesially tipped molar. (a) Sagittal view. The distalisation force passes occlusally to the centre of resistance (red dot) and the molar will be distalised as well as distally tipped. (b) Occlusal view. Distalisation forces are applied from both the buccal and lingual sides, avoiding molar rotation.



Figure 3.41 Upper molar uprighting with indirect anchorage mode. (a) Pretreatment photographs and radiograph. Mesial tipping of the maxillary right second molar was present due to loss of the adjacent first molar. (b) Segmental archwire technique was applied for uprighting the mesially tipped second molar. An open-coil spring was mounted between the second premolar and the second molar for molar uprighting. A mini-implant was inserted to reinforce the anchorage of the anterior teeth. (c) The mesially tipped second molar was successfully uprighted and an implant placed for restoration of the missing first molar.

t.me/Dr_Mouayyad_AlbtousH

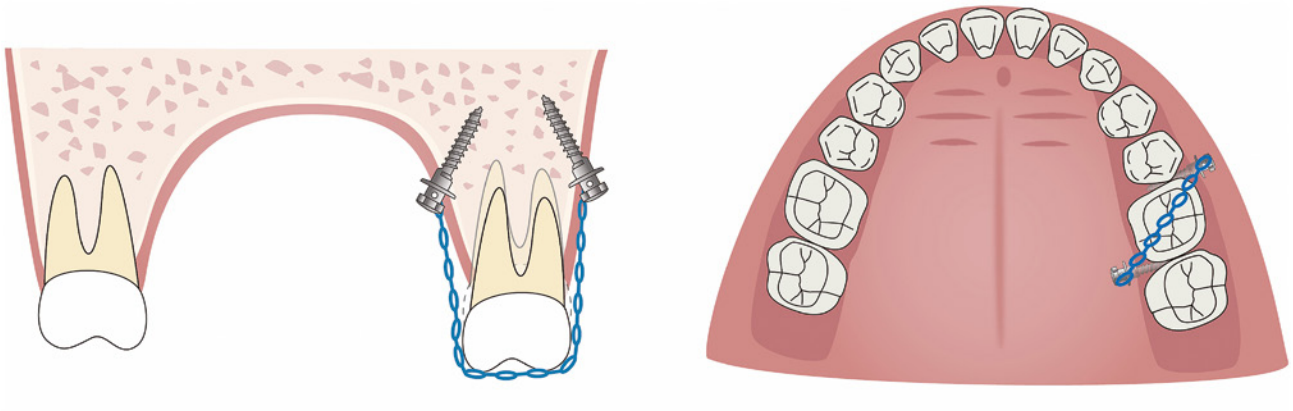


Figure 3.42 Bodily intrusion of the molar is achieved through two mini-implants. One mini-implant is inserted at the buccal side and the other at the palatal side.

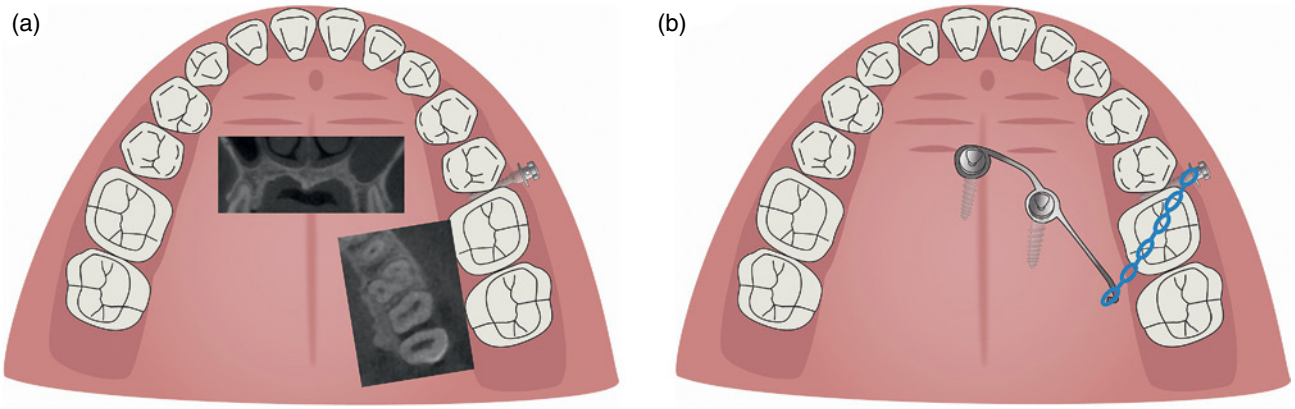


Figure 3.43 (a) Narrow interradicular space limits the insertion of a mini-implant at the palatal side, as indicated by the CBCT image. The CBCT image shows that bone quantity at the palatal vault is sufficient. (b) Two mini-implants are inserted at the paramedian region and an extension hook is fixed and anchored onto the palatal mini-implants. An elastomeric chain is applied between the buccal mini-implant and the extension hook for molar intrusion.

can be designed at the desired position to achieve bodily intrusion of molars in conjunction with the buccal mini-implant (Figure 3.43). Furthermore, when intrusion of mandibular molars is designed, due to anatomical limitations of the lingual side, mini-implants can only be inserted at the buccal side. Thus, when buccal mini-implants exert intrusive force on the mandibular molars, the mandibular molars will be buccally tipped (Figure 3.44a). To overcome this anatomical limitation, an equivalent biomechanical system could be designed by fixing a lingual arch on the bilateral molars to avoid buccal tipping (Figure 3.44b).

3.3.3 Incisor Intrusion

For patients with severe deep bite or gummy smile, the most appropriate insertion sites of mini-implants are labial interradicular sites from the perspective of biomechanics (Figure 3.45a). Labial mini-implants can offer intrusive force on incisors, but care should be taken to avoid potential labial flaring of incisors (Figure 3.45b). Occasionally, insertion sites determined through this biomechanics-driven paradigm may not be in line with those chosen through the anatomy-driven paradigm. For many patients, mini-implants cannot be inserted at the labial interradicular sites due to limited interradicular space. When anatomical limitations are encountered in practice, an equivalent biomechanical system can be designed: infrazygomatic crest mini-implants in conjunction with cantilever springs (Figure 3.45c). Moreover, incisor intrusion can be achieved through mini-implants placed at the buccal interradicular sites (Figures 3.46 and 3.47).[27] These alternative biomechanical systems can intrude maxillary incisors effectively.

3.3.4 Orthodontic Traction of Impacted Molars

In clinical practice, second molars are often subject to root resorption due to the impaction of adjacent third molars. In this scenario, extraction of second molars and

t.me/Dr_Mouayyad_AlbtousH

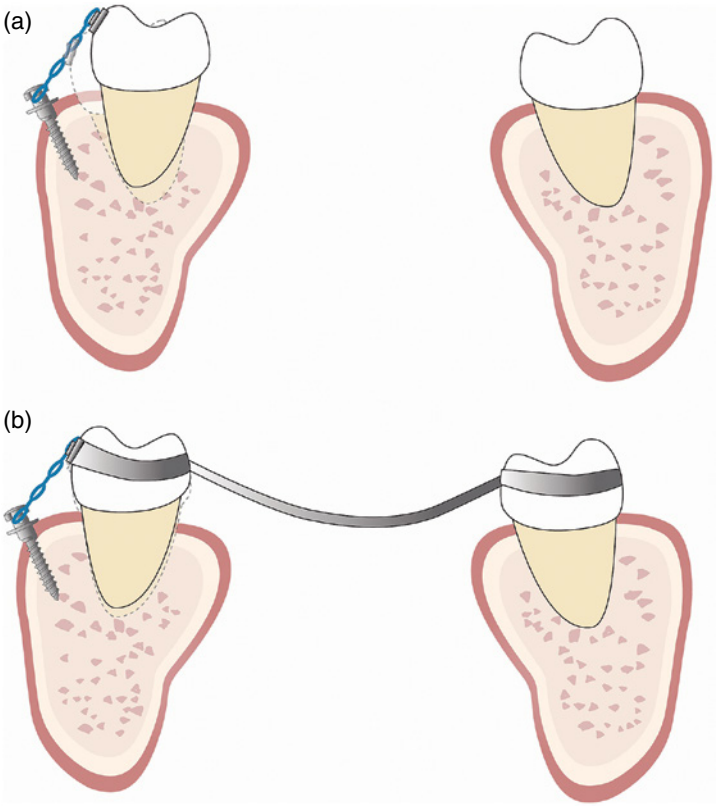


Figure 3.44 Intrusion of a mandibular molar through a mini-implant. (a) The buccal mini-implant offers intrusive force on the molar. Since the intrusive force passes buccally to the centre of resistance, the molar exhibits buccal tipping during the intrusion. (b) A lingual arch is applied on the molar to prevent buccal tipping of the molar during intrusion by the buccal mini-implant.

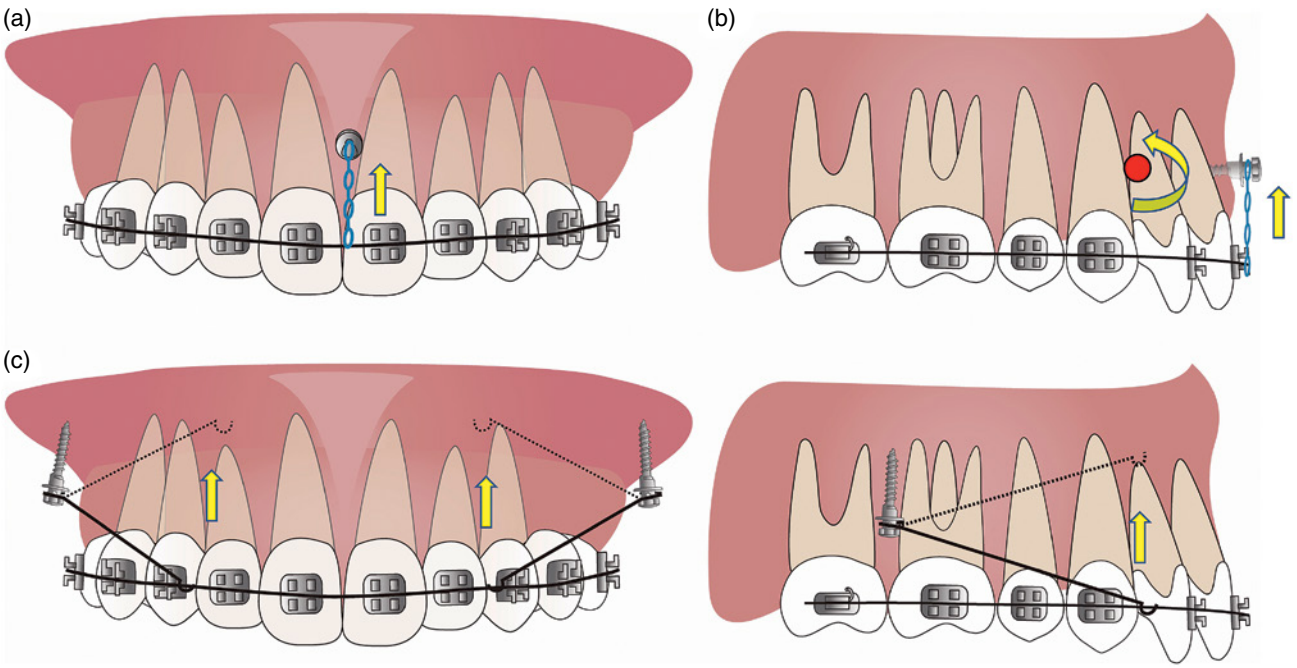


Figure 3.45 Incisor intrusion. (a) The labial mini-implant is desired for incisor intrusion from the perspective of biomechanics. (b) During intrusion of the incisors, since the intrusive force passes labially to the centre of resistance (red dot), the incisors exhibit labial flaring during intrusion. (c) An alternative biomechanical system based on an infrazygomatic mini-implant-anchored cantilever spring. The cantilever spring is at the apical level when inactive (black dashed line). It is activated after it is engaged onto the archwire. The spring-back force offered by the cantilever spring generates the intrusive force on incisors.

t.me/Dr_Mouayyad_AlbtousH

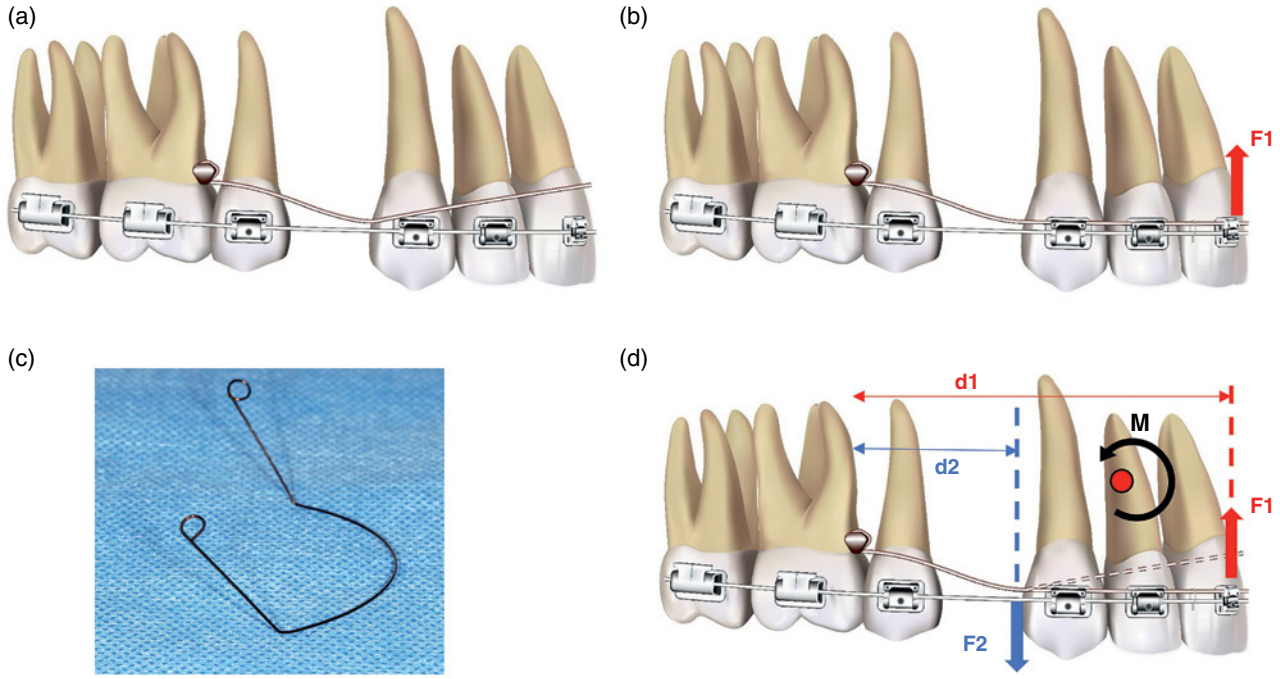


Figure 3.46 Schematic diagrams of the biomechanical system. (a) An intrusion lever arm is mounted onto the interradicular mini-implant and passively engaged onto the archwire. (b) The intrusion lever arm is actively engaged onto the archwire and offers intrusive force on the incisors. (c) The intrusion lever arm is formed with stainless steel wire (0.016 inch). (d) Biomechanical analysis. The intrusion lever arm offers intrusive force (F1) on incisors and extrusive force (F2) on the canine, generating an anticlockwise moment on anterior teeth (M = F1* d1 – F2 * d2). *Source:* Zhang et al.[27]/Wolters Kluwer Health, Inc./CC BY 4.0.



Figure 3.47 Incisor intrusion through an intrusion lever arm anchored on buccal mini-implants and canines. (a) Pretreatment. The patient presented with anterior deep bite. (b) Progress. Anterior deep bite was present. Upper incisors were being intruded through an intrusion lever arm. (c) Post-treatment. Note that the deep bite was resolved. *Source:* Zhang et al.[27]/Wolters Kluwer Health, Inc./CC BY 4.0.

t.me/Dr_Mouayyad_AlbtousH

subsequent orthodontic traction of third molars are indicated to substitute the second molars (Figure 3.48). From the perspective of biomechanics, the most desirable insertion site is the maxillary tuberosity and mandibular buccal shelf for maxillary and mandibular third molar, respectively. Specifically, the mini-implants should be inserted so that their heads are just occlusal to the impacted teeth. However, often this cannot be achieved due to anatomical limitations, e.g. undesirable bone quality and premature contacts of opposing teeth. Thus, equivalent alternative biomechanics could be accomplished through mini-implants inserted at more mesial sites with conjunction of cantilever springs (Figures 3.49 and 3.50).[28]

3.3.5 Molar Protraction

Molar protraction is challenging and successful clinical outcomes require meticulous and prudent biomechanical design. To achieve bodily movement of molar protraction, the protraction force should pass through the centre of resistance of the molar. Moreover, the protraction force should be available at both the buccal and lingual sides to avoid molar rotation. Thus, for protraction of maxillary molars, the most desirable insertion sites are interradicular sites between the first and second premolars. This requires the use of power arms on both the buccal and lingual sides of molars and the insertion of one mini-implant on the buccal side and one on the lingual side (Figure 3.51).

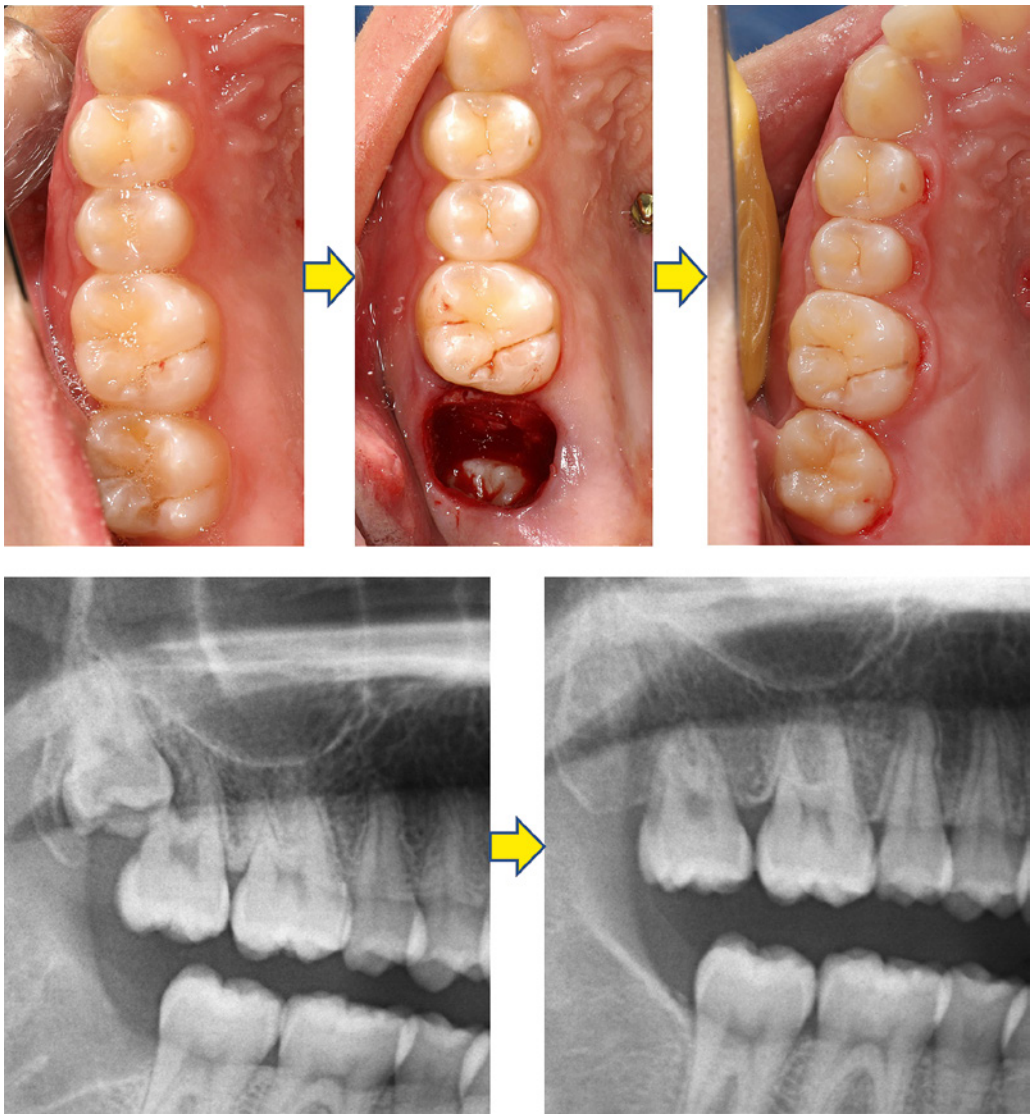


Figure 3.48 The second molar presented with severe root resorption due to the impinging adjacent third molar. The second molar was extracted and the adjacent third molar was tractioned to substitute the second molar.

t.me/Dr_Mouayyad_AlbtousH

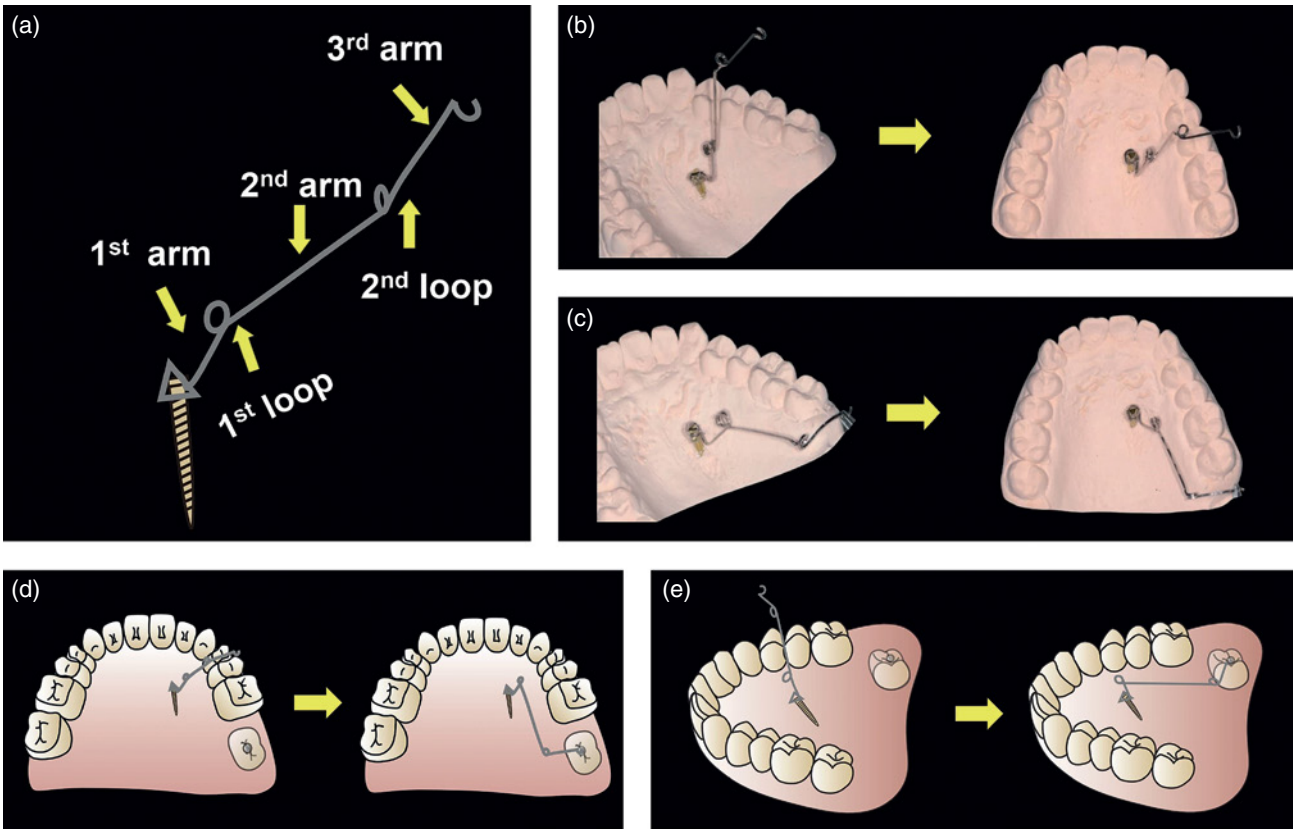
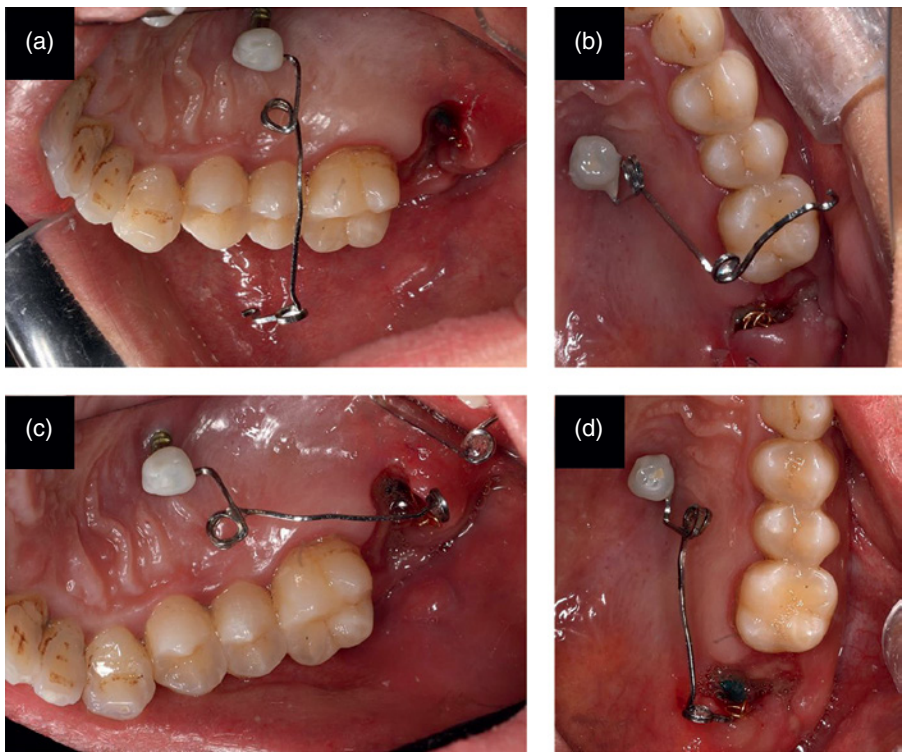


Figure 3.49 Mini-implant-anchored cantilever spring for orthodontic traction of impacted molars. (a) The cantilever system consists of two running loops and three arms. (b) The cantilever system is inactive. (c) The cantilever system is activated. (d) Occlusal view of the application of the mini-implant-anchored cantilever spring. (e) Lingual view of the application of the mini-implant-anchored cantilever spring. *Source:* Pu et al.[28]/Reprinted with permission from Elsevier.

Figure 3.50 Mini-implant-anchored cantilever spring for orthodontic traction of an impacted molar. Inactive cantilever spring. (a) Lingual view. (b) Occlusal view. Activated cantilever spring. (c) Lingual view. (b) Occlusal view. *Source:* Pu et al.[28]/ Reprinted with permission from Elsevier.



t.me/Dr_Mouayyad_AlbtousH

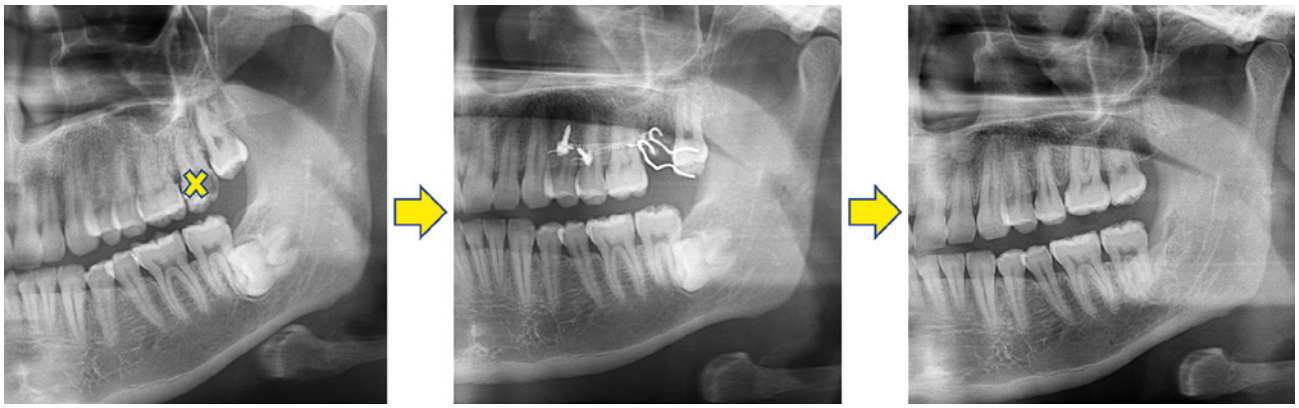


Figure 3.51 Molar protraction through power arms on both the buccal and palatal sides. The maxillary left second molar was extracted due to severe caries. One buccal and one palatal mini-implant were inserted between the first and second premolars. The third molar was protracted by the mini-implants through power arms. Finally, the third molar was protracted to substitute the second molar with good root parallelism.

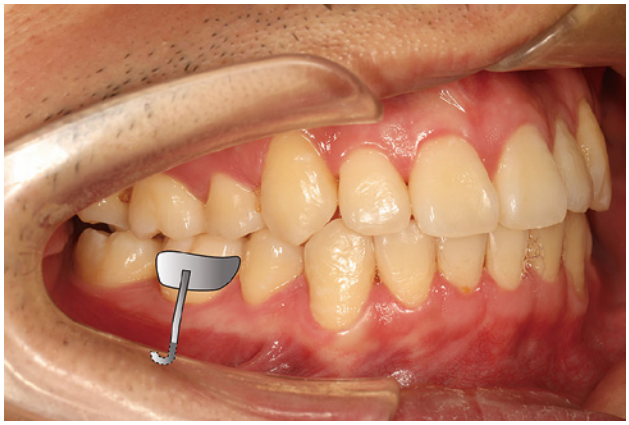


Figure 3.52 Power arm with adequate length is not applicable for mandibular molars due to insufficient vestibular space. Note the hook of the virtually placed power arm is covered by the soft tissue.

However, this does not apply for mandibular molars from the perspective of anatomy.

On one hand, a power arm with adequate length is not anatomically allowed on the buccal side due to insufficient vestibular space of mandibular molars (Figure 3.52). On the other hand, a lingual mini-implant is not clinically amenable due to anatomical limitations on the lingual side. Therefore, an equivalent alternative biomechanical system could be designed with a buccal mini-implant alone (Figures 3.33 and 3.53). We invented a molar protraction technique that employs a buccal mini-implant inserted at interradicular sites between first and second premolars (or between canines and first premolars) and an 'Albert' loop (Figures 3.33 and 3.53). Protraction force is applied at both the buccal and lingual sides of the molar though an elastomeric power chain. However, the protraction force passes occlusally to the centre of resistance, resulting in a mesial tipping tendency. Fortunately, this mesial tipping tendency is prevented by the tip-back bend of the distal part of the Albert loop. In this way, an alternative biomechanical system (a buccal mini-implant with Albert loop) is able to achieve mandibular molar protraction, which is equivalent to mini-implants and power arms on both the buccal and lingual sides.

Therefore, to select an optimal insertion site for a mini-implant, the biomechanics-driven paradigm should be considered first and several candidate sites that meet biomechanical requirements are selected, either through direct anchorage (e.g. direct force loading, cantilever, extension arms, etc.) or indirect anchorage (e.g. palatal mini-implants in conjunction with Nance arch) modes. Then, the suitability of these insertion sites is evaluated through the anatomy-driven paradigm and those insertion sites that meet the requirements of both paradigms can be selected for clinical use.

t.me/Dr_Mouayyad_AlbtousH

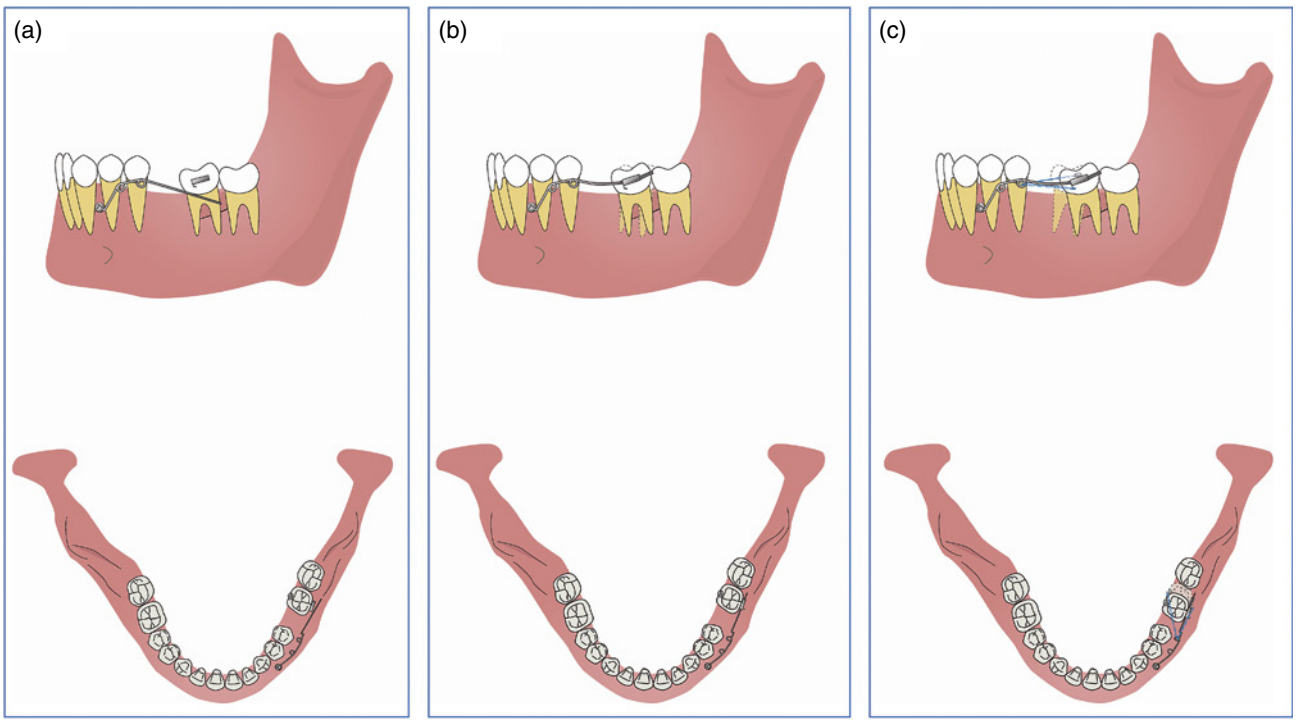


Figure 3.53 Albert protraction loop for mandibular molar protraction. (a) Inactivated. (b) Activated. (c) Application of elastomeric chain for molar protraction. Note that elastomeric chains are applied at both the buccal and lingual sides to prevent molar rotation.

3.4 Clinical Procedures for Inserting Mini-implants

3.4.1 Preinsertion Preparation

First, before insertion, an optimal site for an orthodontic mini-implant should be selected meticulously through the combination of biomechanics-driven and anatomy-driven approaches. Once the insertion site is determined, both the general and site-specific armamentarium (e.g. straight driver, contra-angle driver, mini-implants and pilot drill bits) should be prepared and sterilised before insertion (Figure 3.54).

Second, local anaesthesia is applied to anaesthetise the mucosa and periosteum where mini-implants penetrate, while periodontal tissues of adjacent teeth should not be anaesthetised but remain responsive. This can alert practitioners in case of root proximity during insertion. Since neither cortical bone nor cancellous bone has nerve innervation, superficial anaesthesia of mucosa and periosteum only is adequate for inserting mini-implants. Although both topical and infiltration anaesthetic agents are available for superficial anaesthesia, we recommend that infiltration anaesthesia is more effective than topical. Alternatively, topical anaesthesia plus subsequent infiltration anaesthesia is preferred for anxious patients. For infiltration anaesthesia, 0.2 ml of anaesthetic agent is adequate for anaesthetizing mucosa and periosteum but leaves dental roots responsive (Figure 3.55).

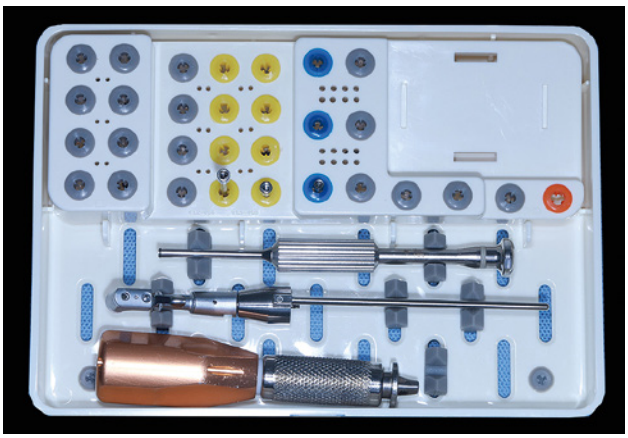


Figure 3.54 Armamentarium for the placement of mini-implants.

Third, chlorhexidine mouthrinse is required for antibacterial purposes at the insertion site immediately before the placement of mini-implants. Typically, chlorhexidine mouthrinse should be used at least for one minute to obtain sufficient antibacterial effects (Figure 3.56).

t.me/Dr_Mouayyad_AlbtousH

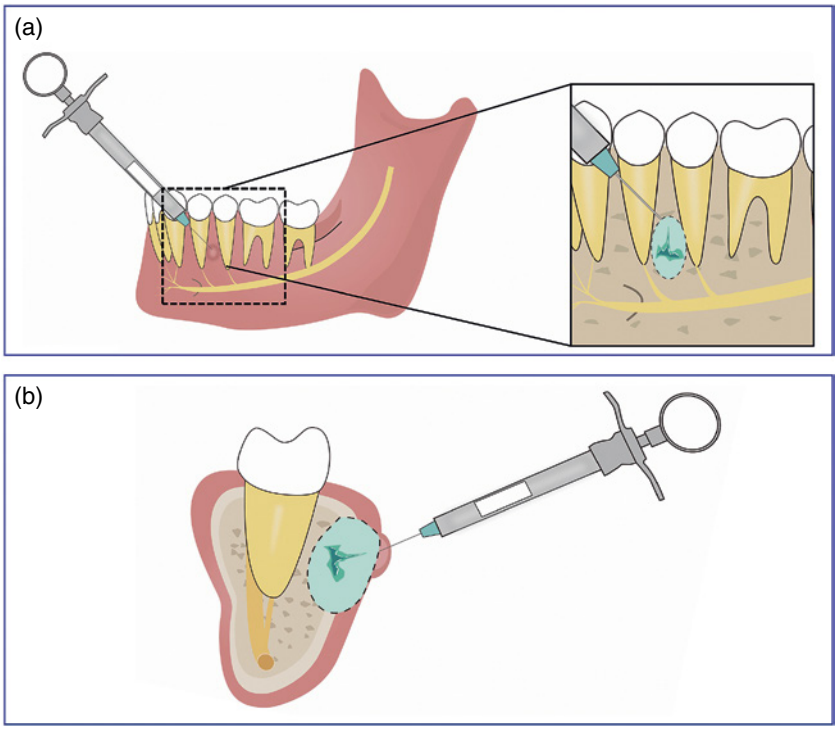


Figure 3.55 Infiltration anaesthesia is limited to the mucosa and periosteum and spares the dental roots, so that the roots are responsive to nociceptive stimuli during insertion, e.g. root contact. (a) Sagittal view. (b) Coronal view.



Figure 3.56 Mouthrinse with chlorhexidine.

The last aspect of preinsertion preparation is soft tissue indentation which is beneficial for accurate and precise location of the insertion point and direction. This procedure is exemplified through soft tissue indentation for interradicular mini-implants (Figure 3.57). To perform mucosa indentation or marking, a periodontal probe or explorer is placed against the mucosa in parallel to the dental long axis to form a vertical indentation on the soft tissue. The vertical indentation should be checked from the occlusal view with the help of a mouth mirror. From the occlusal view, the vertical indentation should be in parallel with the tooth's long axis and pass through the interproximal contact point. Then, a point marking is made on this vertical indentation and the exact location of the point marking is predetermined based on both biomechanical and anatomical requirements. The point marking is the site where the mini-implant penetrates mucosa and alveolar bone, and the vertical indentation is referenced for insertion direction (Figure 3.58).

3.4.2 Insertion of Mini-implants

First, an orthodontic mini-implant should be fully engaged into a mini-implant driver and this full engagement should be rechecked immediately before insertion (Figure 3.59). If a straight driver is used, the bottom of the driver should be held firmly against the palm and the shaft of the driver gripped stably by the fingers, thus preventing the mini-implant from wobbling around its axis while it is being inserted (Figure 3.60). If a contra-angle driver is employed to insert a mini-implant into an anatomical site that is difficult to access with a straight driver (e.g. hard palate), the contra-angle driver should be held stably with both hands (Figure 3.61). A mini-implant is engaged into a connecting bur that is mounted on a handpiece (Figure 3.62). Due to the inherent play between the connecting bur and the handpiece, the connecting bur may not be stable while the mini-implant is being inserted.

t.me/Dr_Mouayyad_AlbtousH

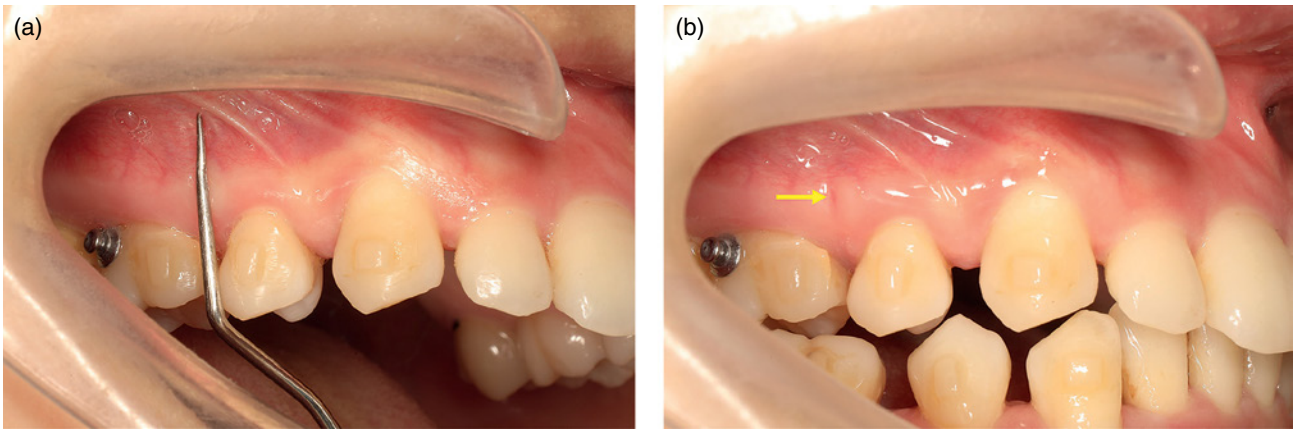


Figure 3.57 Soft tissue indentation. (a) An explorer is employed to perform a vertical indentation on the soft tissue. (b) The vertical soft tissue indentation (yellow arrow) is evident following removal of the explorer.

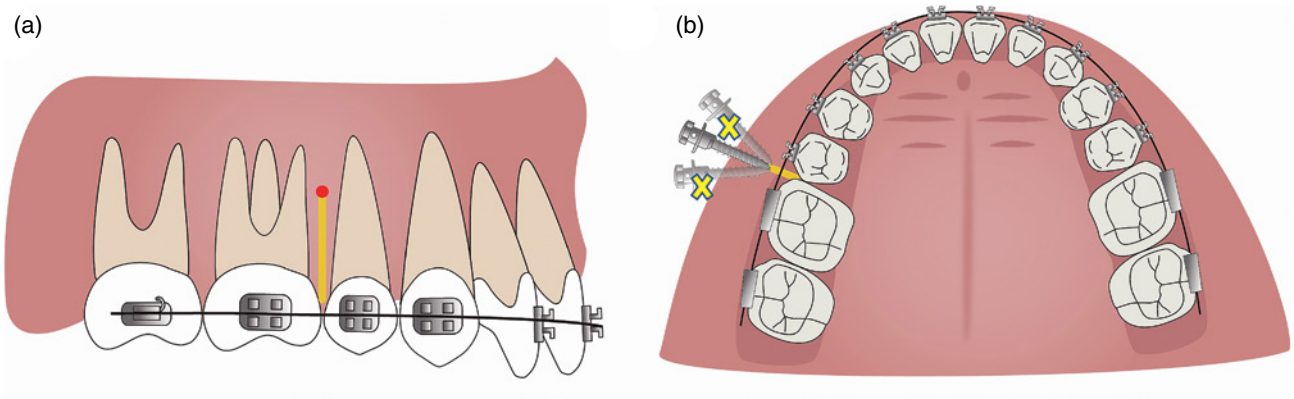


Figure 3.58 Vertical indentation and landmark on the soft tissue. (a) The point indicates the exact location where a mini-implant penetrates mucosa. (b) The vertical line dictates the insertion direction. Any deviation from the indentation indicates an incorrect insertion path and may cause root injury.

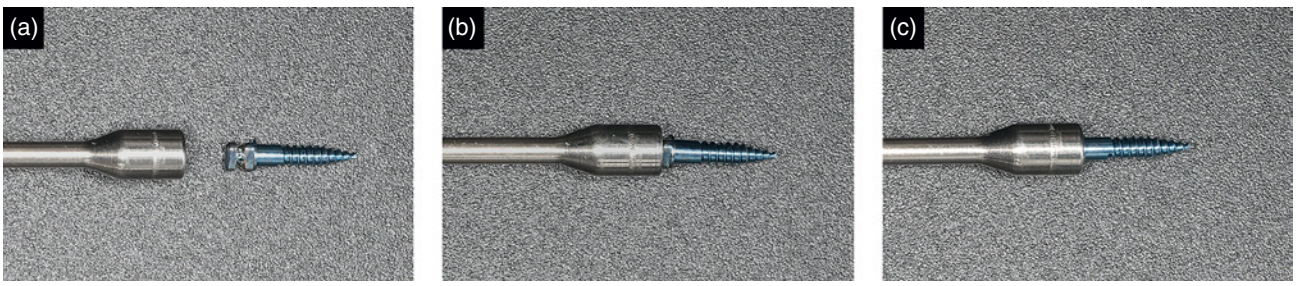


Figure 3.59 Engagement of the mini-implant into the screwdriver. (a) Before engagement. (b) Partial engagement. (c) Full engagement.

Second, the tip of the mini-implant is placed at the point marking and the driver is rotated to advance the mini-implant into alveolar bone. Before insertion, the insertion direction should be checked from the occlusal view through a mouth mirror to avoid root injury (Figure 3.63). Notably, the driver should only be rotated by the fingers rather than the wrist, since rotation through the wrist may exceed the maximal insertion torque and cause mini-implant fracture. During insertion, the driver should be held stably to prevent the mini-implant from wobbling which can cause bone

t.me/Dr_Mouayyad_AlbtousH



Figure 3.60 The bottom of the screwdriver is held firmly against the palm and the shaft is gripped stably by the fingers.



Figure 3.61 The contra-angle screwdriver is held firmly by both hands, with one hand holding the bottom and the other stabilising the shaft.

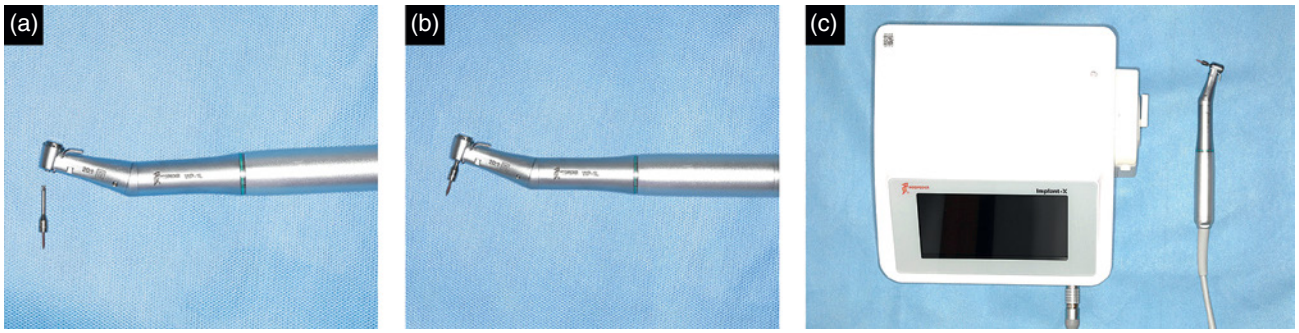


Figure 3.62 (a) The mini-implant is first engaged into the connecting bur. (b) The connecting bur is then mounted on a handpiece. (c) The handpiece is connected to the motor and ready for insertion of the mini-implant.

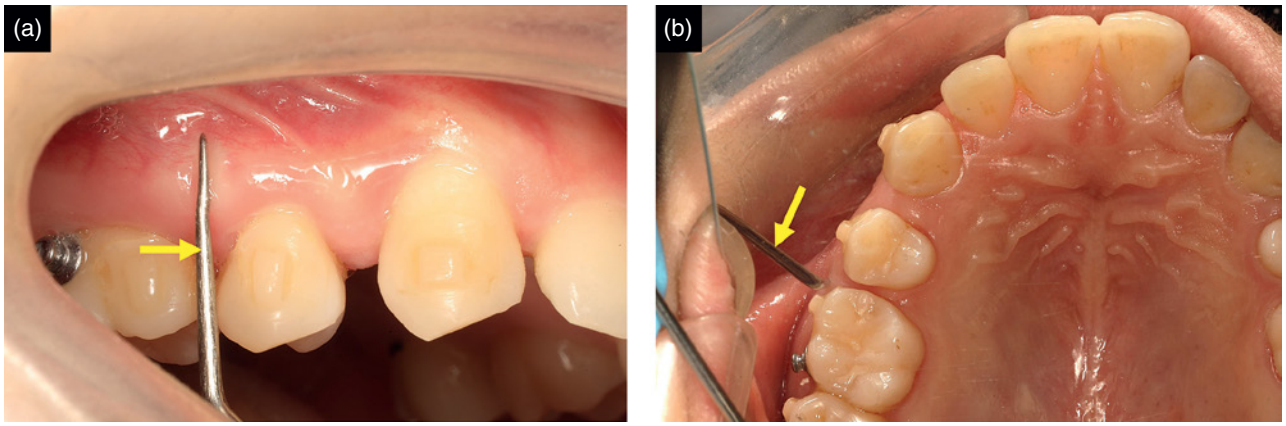


Figure 3.63 (a) Soft tissue indentation is being performed with an explorer (yellow arrow). (b) The insertion direction is confirmed from the occlusal side. The insertion path is simulated with the dental explorer (yellow arrow).

damage and compromise secondary stability. For a contra-angle driver, even if the driver is held stably with one hand, the shaft may rotate with the handle. This results in an undesirable lateral force that can be transmitted to the mini-implant and cause fracture. Thus, the contra-angle driver should be additionally stabilised with the other hand which can eliminate the undesirable lateral force (Figure 3.64).

t.me/Dr_Mouayyad_AlbtousH

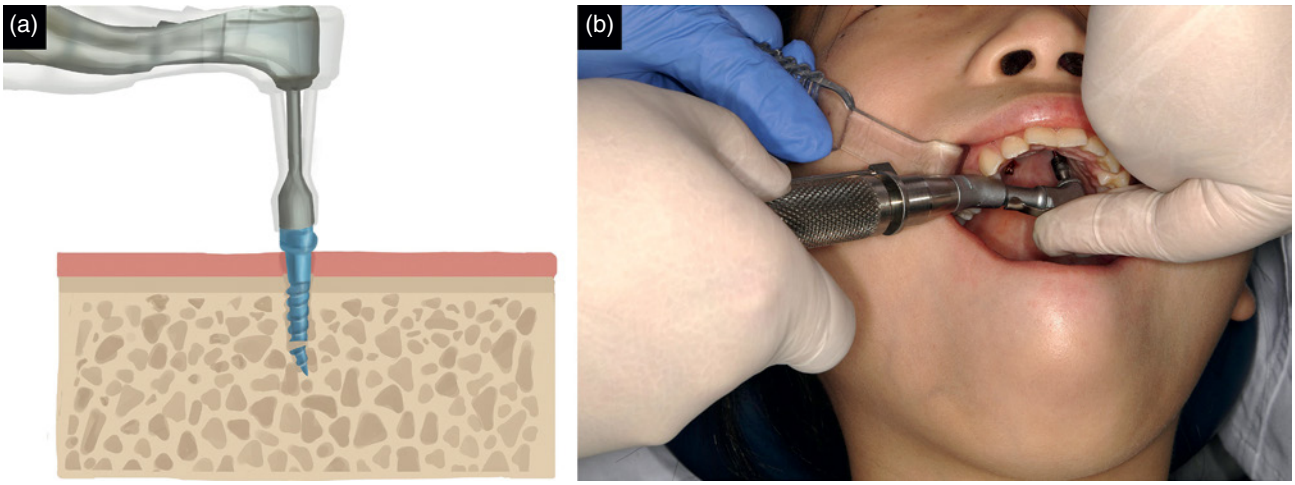


Figure 3.64 (a) A schematic illustration showing fracture of the mini-implant due to lateral displacement of the screwdriver. (b) The contra-angle screwdriver is stabilised by both hands, with one holding the bottom and the other stabilising the shaft.

Third, the mucosa and cortical bone should be perforated first; a sensation of loss of resistance may or may not be perceived by the operator, depending on different cortical thickness and the differences of density between cortical bone and cancellous bone. Once the cortex is penetrated, the mini-implant can be slightly unscrewed and the insertion direction can be changed to obtain an oblique insertion. While the mini-implant is being inserted obliquely, the long axis should be in line with the vertical indentation to guarantee the correct mesiodistal insertion direction (Figure 3.65).

The mini-implant should be advanced into alveolar bone gradually with slight palm pressure and the resistance to the rotation of the mini-implant driver increases gradually, but an abrupt increase in this resistance may herald root contact. If root contact is suspected due to either patient painful sensation or an abrupt increase in insertion torque, percussion can help the diagnosis. A negative percussion result can rule out the diagnosis of root contact, while a positive one may necessitate further radiographic examination. To reiterate, orthogonal periapical radiography rather than panoramic radiography is recommended for the diagnosis of root contact.

Once the desired insertion depth and emergence profile are reached, insertion of the mini-implant is complete. Overinsertion should be avoided, since it may cause

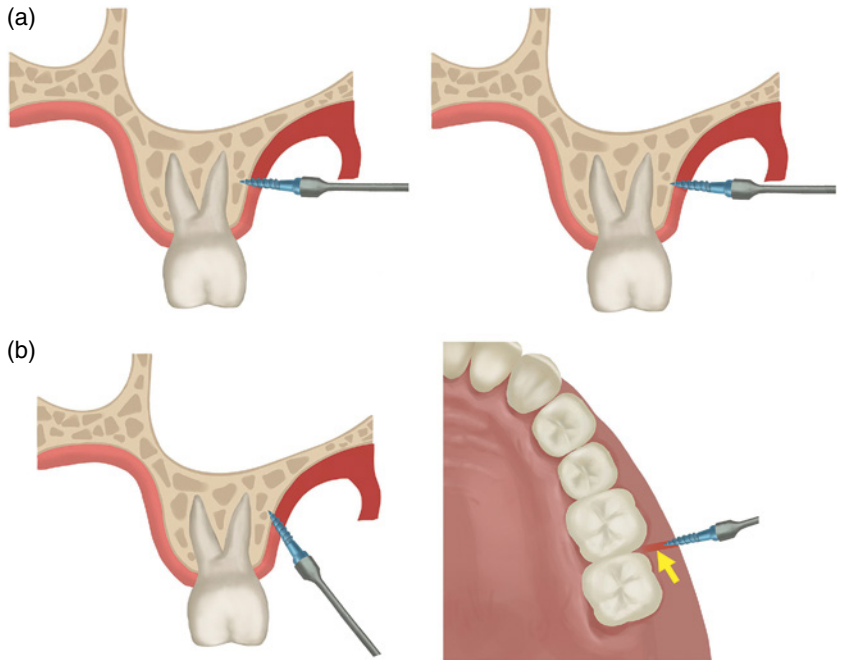


Figure 3.65 (a) Once the cortex is penetrated, the mini-implant can be slightly unscrewed to allow the change of insertion direction. (b) Once the desired oblique insertion direction is obtained, the long axis of the mini-implant should be consistent with the soft tissue indentation (yellow arrow) from the occlusal view.

t.me/Dr_Mouayyad_AlbtousH

insufficient head exposure or damage bone interlocking by rotating freely without further mini-implant advancement (Figure 3.66). Care should be taken to detach the driver from the mini-implant. If the first attempt fails, gentle separation of the shaft from its handle and subsequent removal of the shaft from the mini-implant is recommended (Figure 3.67). Wiggling the driver off the mini-implant should be avoided since this can damage the bone–implant interface and decrease primary stability (Figure 3.68).

3.4.3 Post-insertion Examination

Once the insertion is complete and the mini-implant driver removed, the position of the mini-implant should be examined from both the buccal/lingual side and the occlusal side to verify whether it was inserted in the correct direction as designed (Figure 3.69). If an incorrect insertion path and root contact are suspected, tooth percussion is recommended to rule out root contact. Finally, primary stability can be tested by using a tweezer or a specific instrument (Figure 3.70). If primary stability is not satisfactory, reinsertion may be considered.

Patients are encouraged to rinse with chlorhexidine after insertion to reduce bacterial levels around the mini-implant. Post-insertion instructions should be conveyed to patients regarding the importance of adequate oral hygiene maintenance.

A consensus has not yet been reached regarding choosing immediate or delayed force loading. However, in our clinical experience, no difference is noticed between the two loading

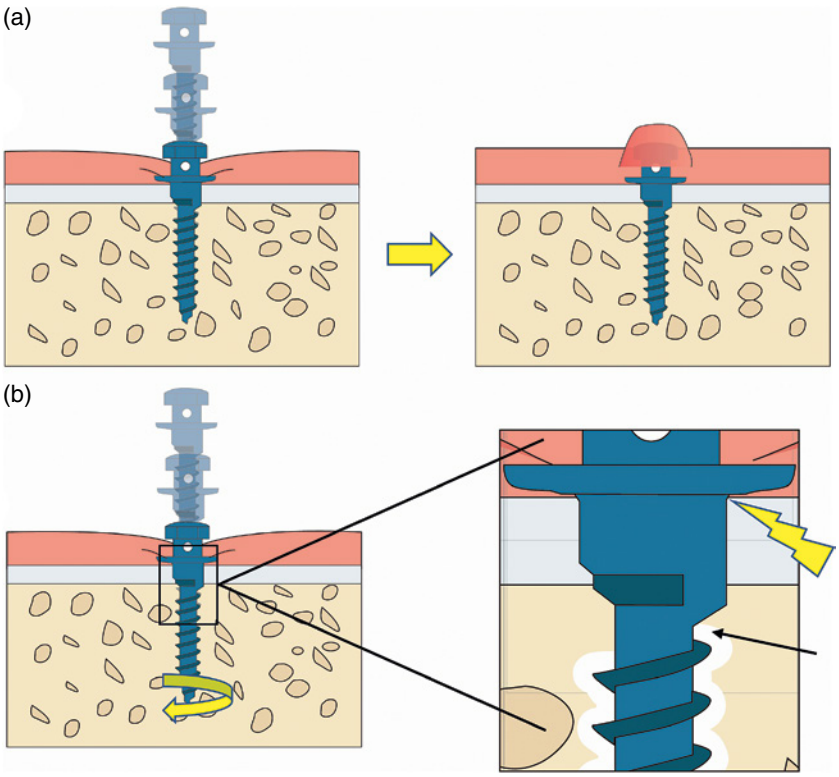


Figure 3.66 Overinsertion of mini-implants. (a) Overinsertion of the mini-implant leads to insufficient emergence profile and soft tissue hyperplasia. (b) Free rotation without further advancement is encountered when the cortex is contacting the platform of the mini-implant. The contact between the cortex and the platform prevents further advancement of the mini-implant. The free rotation often causes bone damage around the threads of the mini-implant, resulting in jeopardised stability of the mini-implant.

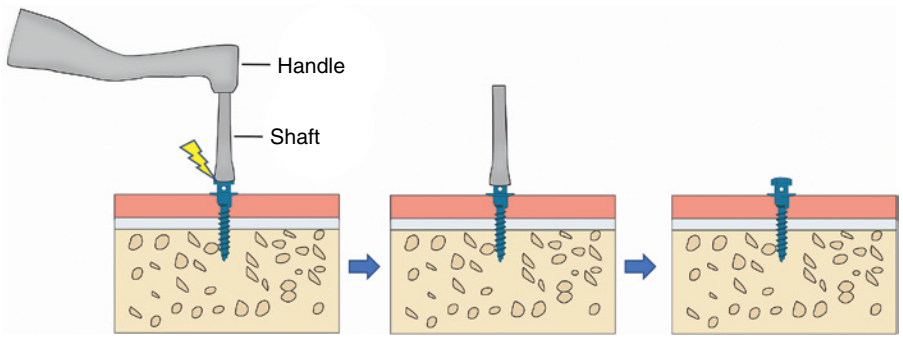


Figure 3.67 When it is difficult to detach the mini-implant from the screwdriver, the shaft is first separated from the handle and the shaft is then disengaged from the mini-implant.

t.me/Dr_Mouayyad_AlbtousH

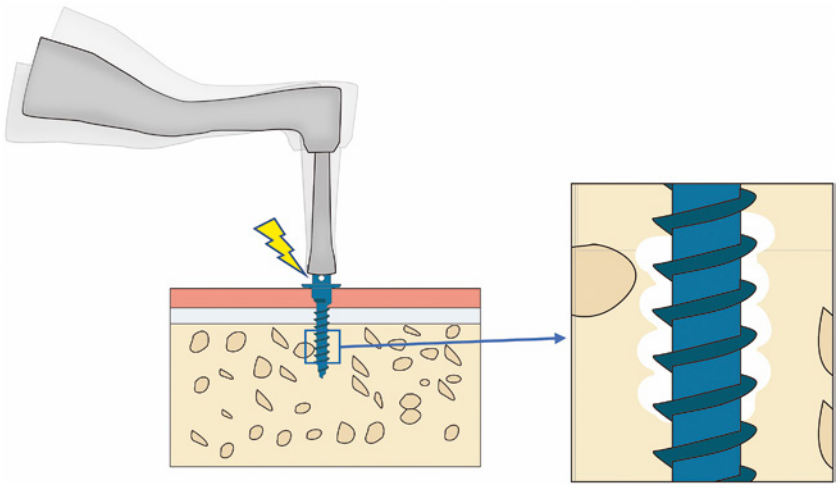


Figure 3.68 Bone damage is caused if the screwdriver is wiggled off the mini-implant.

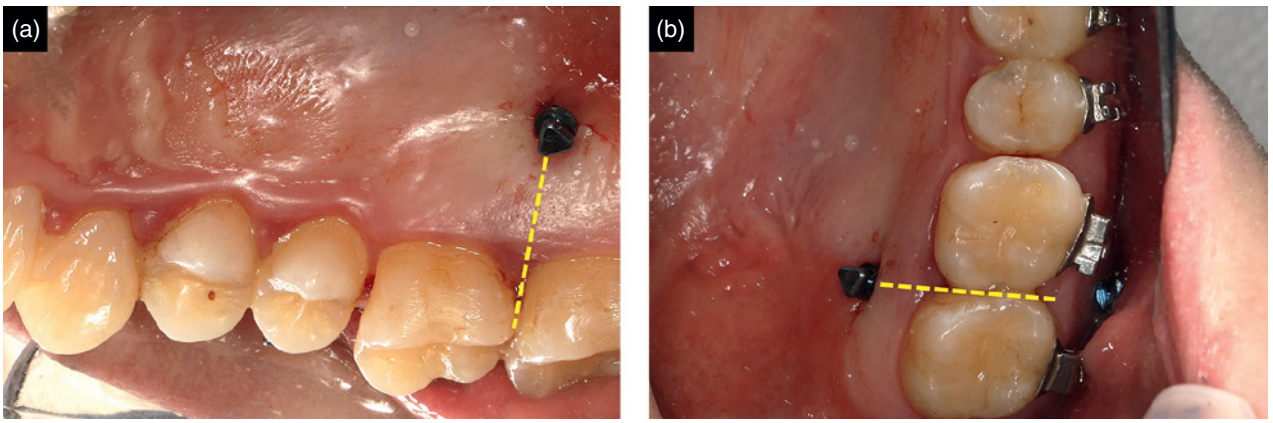


Figure 3.69 Examination of the insertion direction following insertion. (a) Examination from the lingual side. (b) Assessment from the occlusal side. The dashed yellow lines refer to the simulated long axis of the mini-implant.

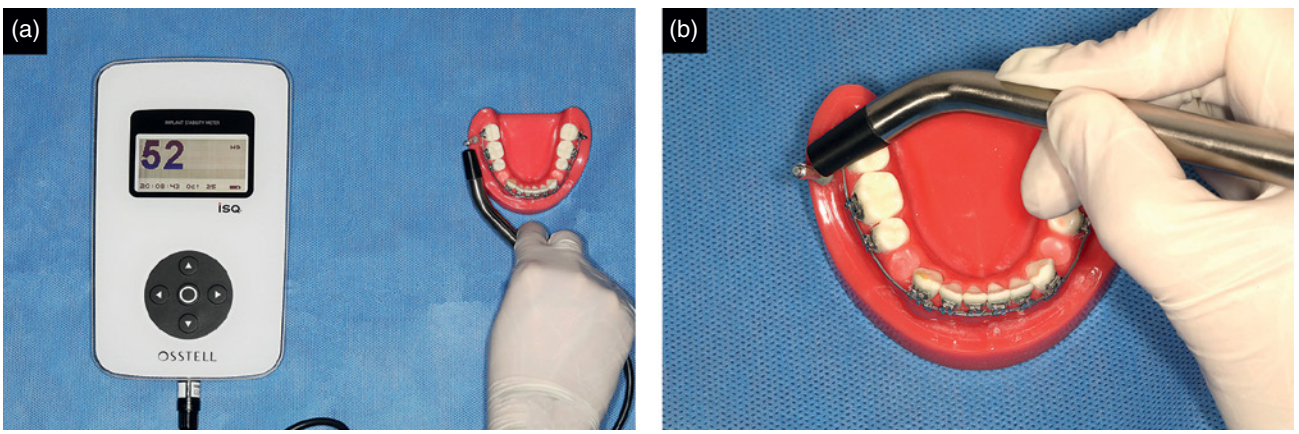


Figure 3.70 (a) The primary stability of a mini-implant is tested through an implant stability device. (b) Close-up view. The handle is approached towards the mini-implant for measurement of the stability.

t.me/Dr_Mouayyad_AlbtousH

strategies (for details, see Chapter 16). Thus, given that soft tissue healing generally takes 1–2 weeks, we recommend a two-week delay in force loading for the healing of soft tissue.

3.5 Summary

Judicious selection of insertion sites is crucial to the clinical success of orthodontic TADs. Two paradigms are available for practitioners to determine the optimal insertion site: anatomy-driven paradigm and biomechanics-driven paradigm. The two paradigms are not mutually exclusive but can be combined and integrated for selection of the optimal insertion site for orthodontic mini-implants. General procedures of inserting mini-implants include preinsertion preparation, insertion of mini-implants and postinsertion examination.

References

1 Manni A, Cozzani M, Tamborrino F, De Rinaldis S, Menini A. (2011). Factors influencing the stability of miniscrews. A retrospective study on 300 miniscrews. *Eur. J. Orthod.* 33(4): 388–395.

2 Antoszewska J, Papadopoulos MA, Park HS, Ludwig B. (2009). Five-year experience with orthodontic miniscrew implants: a retrospective investigation of factors influencing success rates. *Am. J. Orthod. Dentofacial Orthop.* 136(2): 158 e151–110; discussion 158–159.

3 Chang C, Lin SY, Roberts WE. (2016). Forty consecutive ramus bone screws used to correct horizontally impacted mandibular molars. *Int. J. Orthod. Implant.* 41: 60–72.

4 Chang C, Liu SS, Roberts WE. (2015). Primary failure rate for 1680 extra-alveolar mandibular buccal shelf mini-screws placed in movable mucosa or attached gingiva. *Angle Orthod.* 85(6): 905–910.

5 Chen YH, Chang HH, Chen YJ, Lee D, Chiang HH, Yao CC. (2008). Root contact during insertion of miniscrews for orthodontic anchorage increases the failure rate: an animal study. *Clin. Oral Implants Res.* 19(1): 99–106.

6 Ikenaka R, Koizumi S, Otsuka T, Yamaguchi T. (2022). Effects of root contact length on the failure rate of anchor screw. *J. Oral Sci.* 64(3): 232–235.

7 Lee Y, Choi SH, Yu HS, Erenebat T, Liu J, Cha JY. (2021). Stability and success rate of dual-thread miniscrews. *Angle Orthod.* 91(4): 509–514.

8 Motoyoshi M, Ueno S, Okazaki K, Shimizu N. (2009). Bone stress for a mini-implant close to the roots of adjacent teeth – 3D finite element analysis. *Int. J. Oral Maxillofac. Surg.* 38(4): 363–368.

9 Albogha MH, Kitahara T, Todo M, Hyakutake H, Takahashi I. (2016). Predisposing factors for orthodontic mini-implant failure defined by bone strains in patient-specific finite element models. *Ann. Biomed. Eng.* 44(10): 2948–2956.

10 Lee HJ, Lee KS, Kim MJ, Chun YS. (2013). Effect of bite force on orthodontic mini-implants in the molar region: finite element analysis. *Korean J. Orthod.* 43(5): 218–224.

11 Pittman JW, Navalgund A, Byun SH, Huang H, Kim AH, Kim DG. (2014). Primary migration of a mini-implant under a functional orthodontic loading. *Clin. Oral Invest.* 18(3): 721–728.

12 Becker K, Schwarz F, Rauch NJ, Khalaph S, Mihatovic I, Drescher D. (2019). Can implants move in bone? A longitudinal in vivo micro-CT analysis of implants under constant forces in rat vertebrae. *Clin. Oral Implants Res.* 30: 1179–1189.

13 Barros SE, Abella M, Janson G, Chiqueto K. (2019). X-ray beam angulation can compromise 2-dimensional diagnosis of interradicular space for mini-implants. *Am. J. Orthod. Dentofacial Orthop.* 156(5): 593–602.

14 Peck JL, Sameshima GT, Miller A, Worth P, Hatcher DC. (2007). Mesiodistal root angulation using panoramic and cone beam CT. *Angle Orthod.* 77(2): 206–213.

15 Bouwens DG, Cevidanes L, Ludlow JB, Phillips C. (2011). Comparison of mesiodistal root angulation with posttreatment panoramic radiographs and cone-beam computed tomography. *Am. J. Orthod. Dentofacial Orthop.* 139(1): 126–132.

16 An JH, Kim YI, Kim SS, Park SB, Son WS, Kim SH. (2019). Root proximity of miniscrews at a variety of maxillary and mandibular buccal sites: reliability of panoramic radiography. *Angle Orthod.* 89(4): 611–616.

17 Monnerat C, Restle L, Mucha JN. (2009). Tomographic mapping of mandibular interradicular spaces for placement of orthodontic mini-implants. *Am. J. Orthod. Dentofacial Orthop.* 135(4): 428 e421–429; discussion 428–429.

18 Moslemzadeh SH, Sohrabi A, Rafighi A, Kananizadeh Y, Nourizadeh A. (2017). Evaluation of interdental spaces of the mandibular posterior area for orthodontic mini-implants with cone-beam computed tomography. *J. Clin. Diagn. Res.* 11(4): ZC09–ZC12.

19 Chang CH, Lin JS, Roberts WE. (2018). Ramus screws: the ultimate solution for lower impacted molars. *Semin. Orthodont.* 24(1): 135–154.

t.me/Dr_Mouayyad_AlbtousH

20 Filippi A, Pohl Y, Tekin U. (1999). Sensory disorders after separation of the nasopalatine nerve during removal of palatal displaced canines: prospective investigation. *Br. J. Oral Maxillofac. Surg.* 37(2): 134–136.

21 Giudice AL, Rustico L, Longo M, Oteri G, Papadopoulos MA, Nucera R. (2021). Complications reported with the use of orthodontic miniscrews: a systematic review. *Korean J. Orthod.* 51(3): 199–216.

22 Su L, Song H, Huang X. (2022). Accuracy of two orthodontic mini-implant templates in the infrazygomatic crest zone: a prospective cohort study. *BMC Oral Health* 22(1): 252.

23 Jia X, Chen X, Huang X. (2018). Influence of orthodontic mini-implant penetration of the maxillary sinus in the infrazygomatic crest region. *Am. J. Orthod. Dentofacial Orthop.* 153(5): 656–661.

24 Brettin BT, Grosland NM, Qian F et al. (2008). Bicortical vs monocortical orthodontic skeletal anchorage. *Am. J. Orthod. Dentofacial Orthop.* 134(5): 625–635.

25 Arcuri C, Muzzi F, Santini F, Barlattani A, Giancotti A. (2007). Five years of experience using palatal mini-implants for orthodontic anchorage. *J. Oral Maxillofac. Surg.* 65(12): 2492–2497.

26 Azeem M, Haq AU, Awaisi ZH, Saleem MM, Tahir MW, Liaquat A. (2019). Failure rates of miniscrews inserted in the maxillary tuberosity. *Dental Press J. Orthod.* 24(5): 46–51.

27 Zhang C, Ji L, Liao W, Zhao Z. (2022). A novel biomechanical system to intrude the upper incisors and control overbite: posterior miniscrew-assisted lever arm and 2 cases report. *Medicine* 101(47): e31616.

28 Pu L, Zhou J, Yan X et al. (2022). Orthodontic traction of an impacted maxillary third molar through a miniscrew-anchored cantilever spring to substitute the adjacent second molar with severe root resorption. *J. Am. Dent. Assoc.* 153(9): 884–892.

t.me/Dr_Mouayyad_AlbtousH

4

Maxillary Labial Region

Donger Lin[1], Huiyi Hong[1], Xiaolong Li[1], Jialun Li[1], Haoxin Zhang[1], Hong Zhou[1,2], Yan Wang[1] and Hu Long[1]

[1] Department of Orthodontics, State Key Laboratory of Oral Diseases and National Clinical Research Center for Oral Diseases, West China Hospital of Stomatology, Sichuan University, Chengdu, China.
[2] Private Practice, Chengdu, China

4.1 Introduction

The clinical success of maxillary labial mini-implants in effective incisor intrusion was first evidenced in 1983 when Creekmore and colleagues placed a mini-implant at the maxillary labial region to correct a severe deep bite.[1] In their case report, a 6 mm incisor intrusion was achieved without any significant adverse effect, inspiring other enthusiastic practitioners to explore the therapeutic versatility of labial mini-implants.

As per the principle of biological width, soft tissue remodelling occurs following incisor intrusion. This justifies the clinical indication of labial mini-implants in improving smile aesthetics and broadens their clinical applications.

Nowadays, the maxillary labial region is frequently used for the placement of mini-implants for a variety of orthodontic purposes, such as incisor intrusion (Figure 4.1) and gummy smile correction (Figure 4.2).[2-4] Moreover, maxillary labial mini-implants can be employed to ensure bodily anterior retraction among premolar extraction patients.[5] Labial mini-implants can be used to intrude incisors for both fixed appliance (Figure 4.3) and clear aligner (Figure 4.4). Elastomeric chains, closed-coil springs and elastic rubbers are often applied to provide intrusive force between mini-implants and a fixed appliance. In contrast, only elastic rubbers can be used for clear aligners due to the nature of its removability.

Two anatomical sites are clinically available for the placement of mini-implants at the maxillary labial region: interradicular sites and anterior nasal spine (ANS) (Figure 4.5). Due to lower invasiveness, interradicular sites are more frequently used than the ANS. However, in patients with limited interradicular space, the ANS is a good alternative site where the risk of root damage by mini-implants can be reduced. Moreover, when great amount of incisor intrusion is clinically indicated, mini-implants placed at the ANS are superior to those inserted at interradicular sites in order to avoid root contact during incisor intrusion.

In this chapter, we will discuss the anatomical features, selection of insertion sites, step-by-step insertion techniques and clinical applications of maxillary labial mini-implants. For the sake of clarity, the interradicular region and ANS will be presented separately.

4.2 Interradicular Sites

4.2.1 Anatomic Features

For the maxillary labial interradicular region, three interradicular sites are clinically available: between two central incisors (U1-U1), between central and lateral incisors (U1-U2) and between lateral incisor and canine (U2-U3) (Figure 4.6). Distinct characteristics of both hard and soft tissues are featured for different interradicular sites. Both hard tissue (i.e. cortical thickness, bone depth, bone width and root prominence) and soft tissue (i.e. attached gingiva and labial frenum) factors should be considered in order to select the most appropriate site for placement of mini-implants at the maxillary labial region.

Clinical Insertion Techniques of Orthodontic Temporary Anchorage Devices, First Edition. Edited by Hu Long, Xianglong Han, and Wenli Lai.
© 2024 John Wiley & Sons Ltd. Published 2024 by John Wiley & Sons Ltd.

t.me/Dr_Mouayyad_AlbtousH

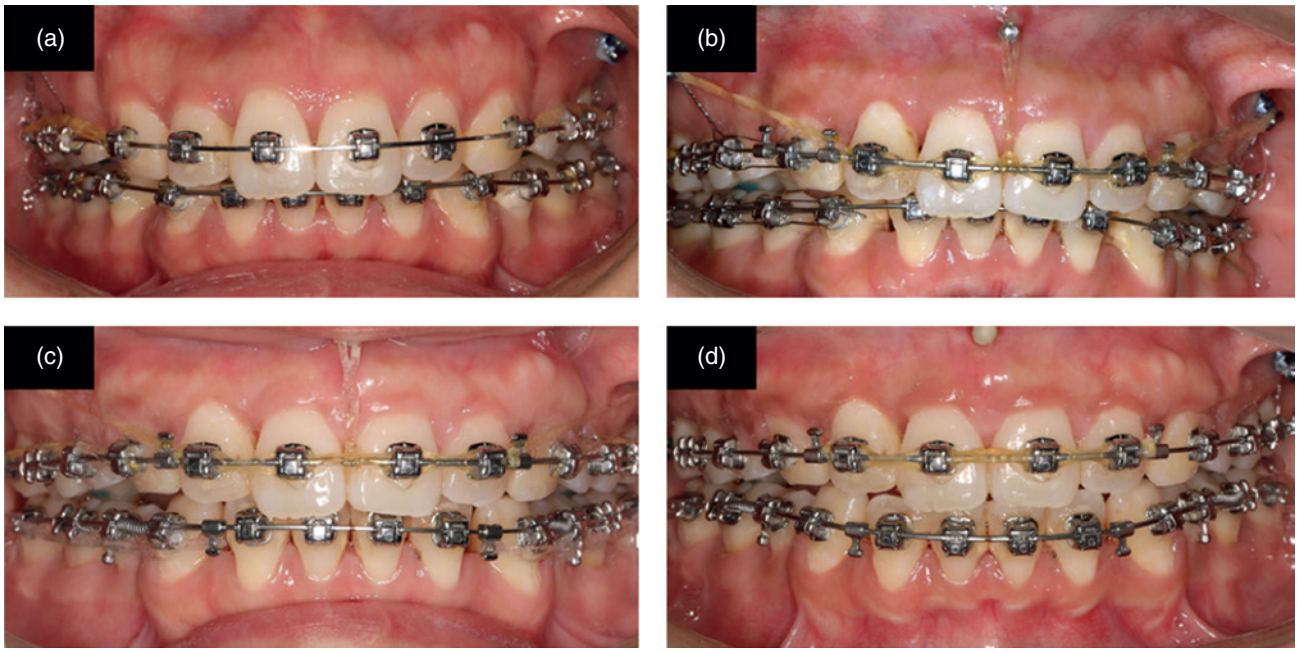


Figure 4.1 Incisor intrusion through a labial mini-implant. (a) Deep bite was present during treatment. (b) A mini-implant was inserted at the interradicular site between central incisors to achieve incisor intrusion. (c) Progress. Deep bite was partially resolved. (d) Incisors were intruded and the deep bite was completely resolved.

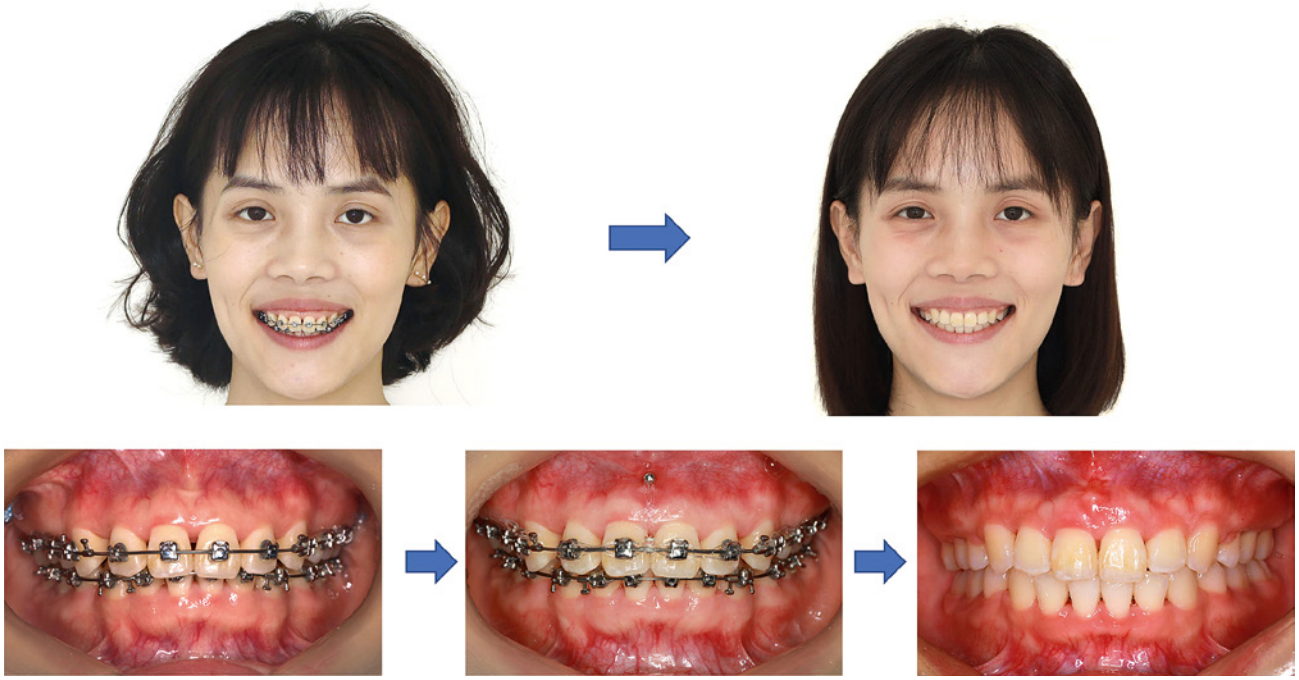


Figure 4.2 Gummy smile correction through a labial mini-implant. The patient exhibited gummy smile and deep bite. To correct gummy smile, a mini-implant was inserted at the labial interradicular site between two central incisors for the intrusion of the upper incisors. Finally, the upper incisors were successfully intruded and the gummy smile corrected.

t.me/Dr_Mouayyad_AlbtousH

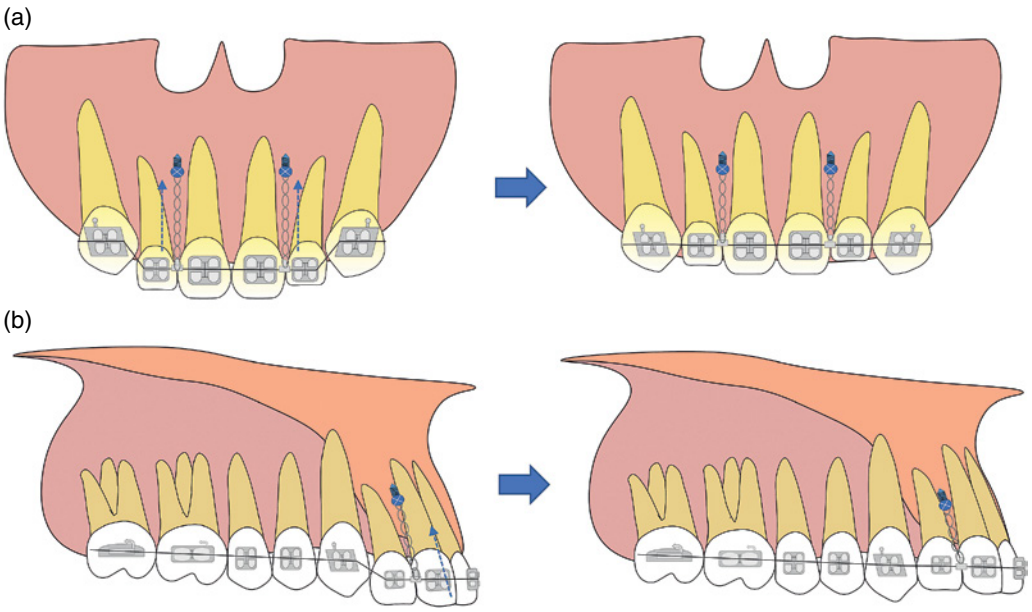


Figure 4.3 Mini-implants placed at the maxillary labial region are used for incisor intrusion with fixed appliance. Elastomeric chains are applied between the mini-implants and the archwire to offer intrusive force. (a) Frontal view. (b) Sagittal view.

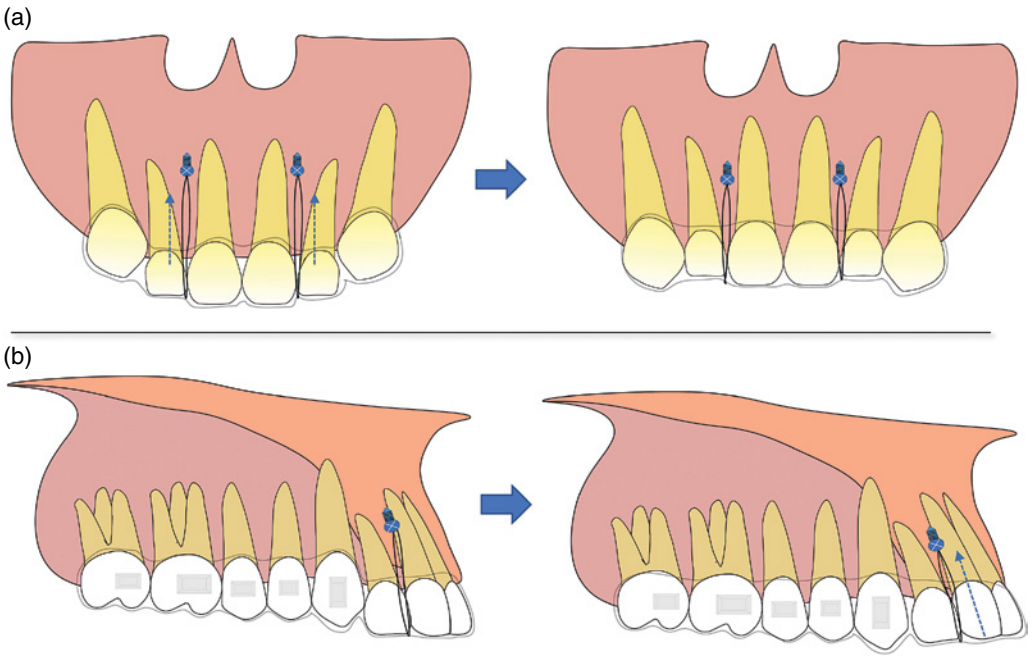


Figure 4.4 Labial mini-implants for anterior intrusion with clear aligner. Elastic rubbers are applied between the mini-implants and the clear aligner to generate intrusive force on maxillary incisors. (a) Frontal view. (b) Sagittal view.

t.me/Dr_Mouayyad_AlbtousH

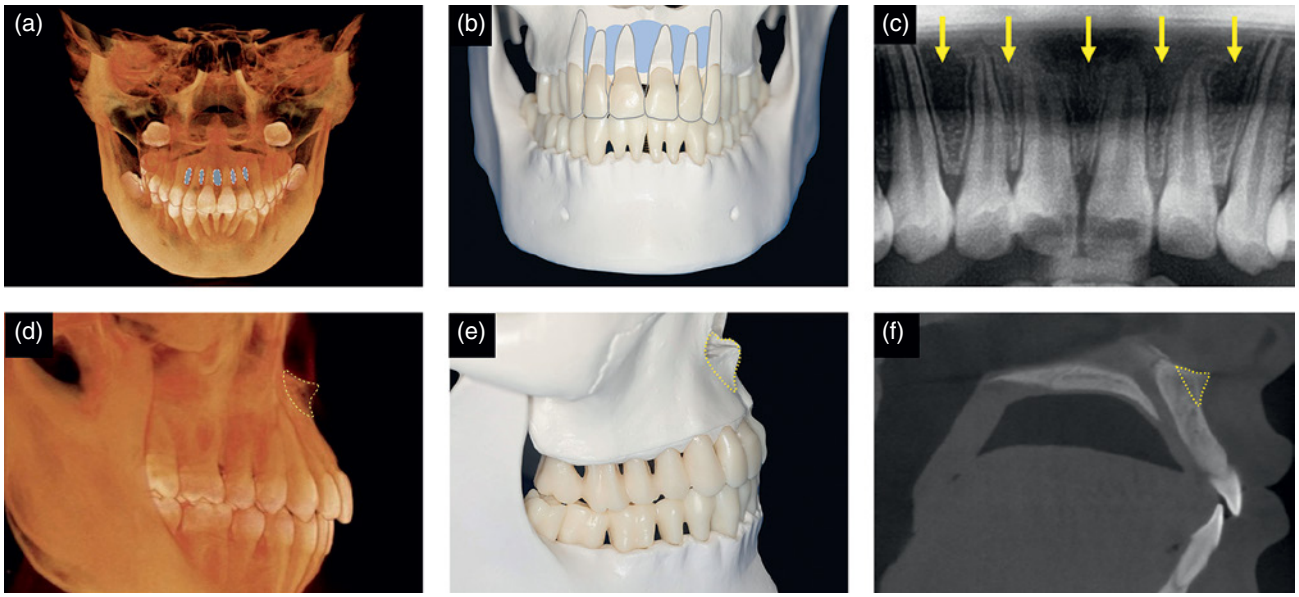


Figure 4.5 Labial interradicular sites and anterior nasal spine. (a) Labial interradicular sites (blue areas) shown in a 3-D reconstruction. (b) Labial interradicular sites (blue areas) shown on a skull. (c) Labial interradicular sites (yellow arrows) shown on a 2-D radiograph. (d) Anterior nasal spine (encircled by the yellow dashed line) shown in a 3-D reconstruction. (e) Anterior nasal spine (encircled by the yellow dashed line) shown on a skull. (f) Anterior nasal spine (encircled by the yellow dashed line) shown on a CBCT sagittal-section image.

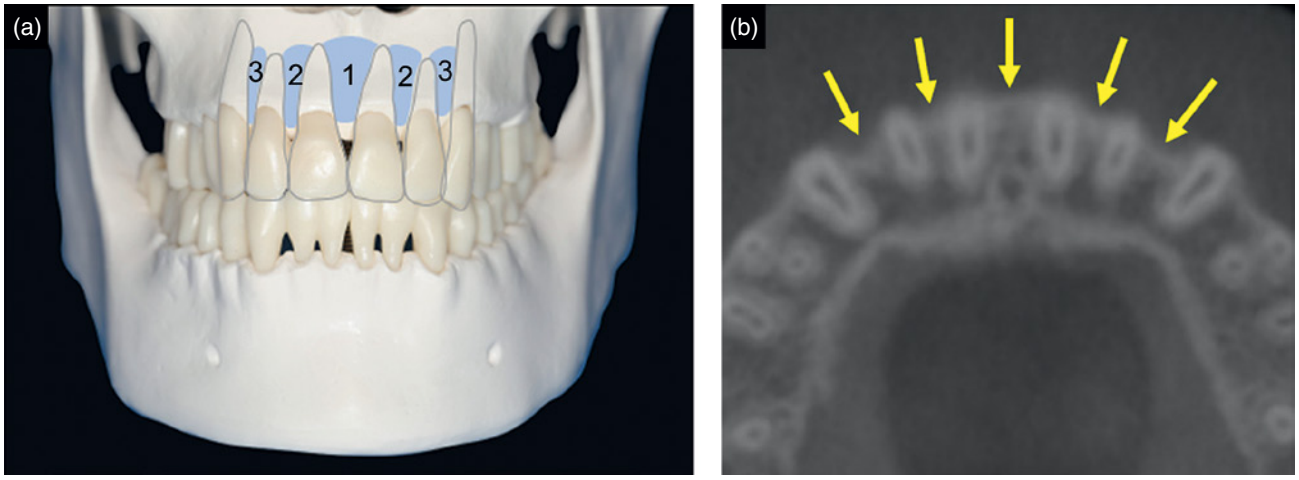


Figure 4.6 Three distinct interradicular sites available at the maxillary labial region. (a) Interradicular sites between two central incisors (1), between central and lateral incisors (2), and between lateral incisors and canines (3). (b) Axial view of the CBCT image showing the interradicular sites (yellow arrow) at the maxillary labial region.

Hard Tissue Factor: Cortical Thickness

As mentioned in previous chapters, cortical thickness is a pivotal factor in determining the stability of mini-implants and a minimum of 1 mm cortical thickness is recommended.[6,7] It has been shown that cortical thickness varies among different interradicular sites (e.g. U1-U1 versus U1-U2) and different insertion heights (4 mm versus 8 mm).[8] Moreover, cortical thickness is influenced by different vertical growth patterns and alveolar bone thickness is greater among hypodivergent subjects than hyperdivergent ones.[9] However, this difference does not alter the stability and success rate of mini-implants,[9] suggesting that vertical growth patterns need not be taken into consideration for this region.

t.me/Dr_Mouayyad_AlbtousH

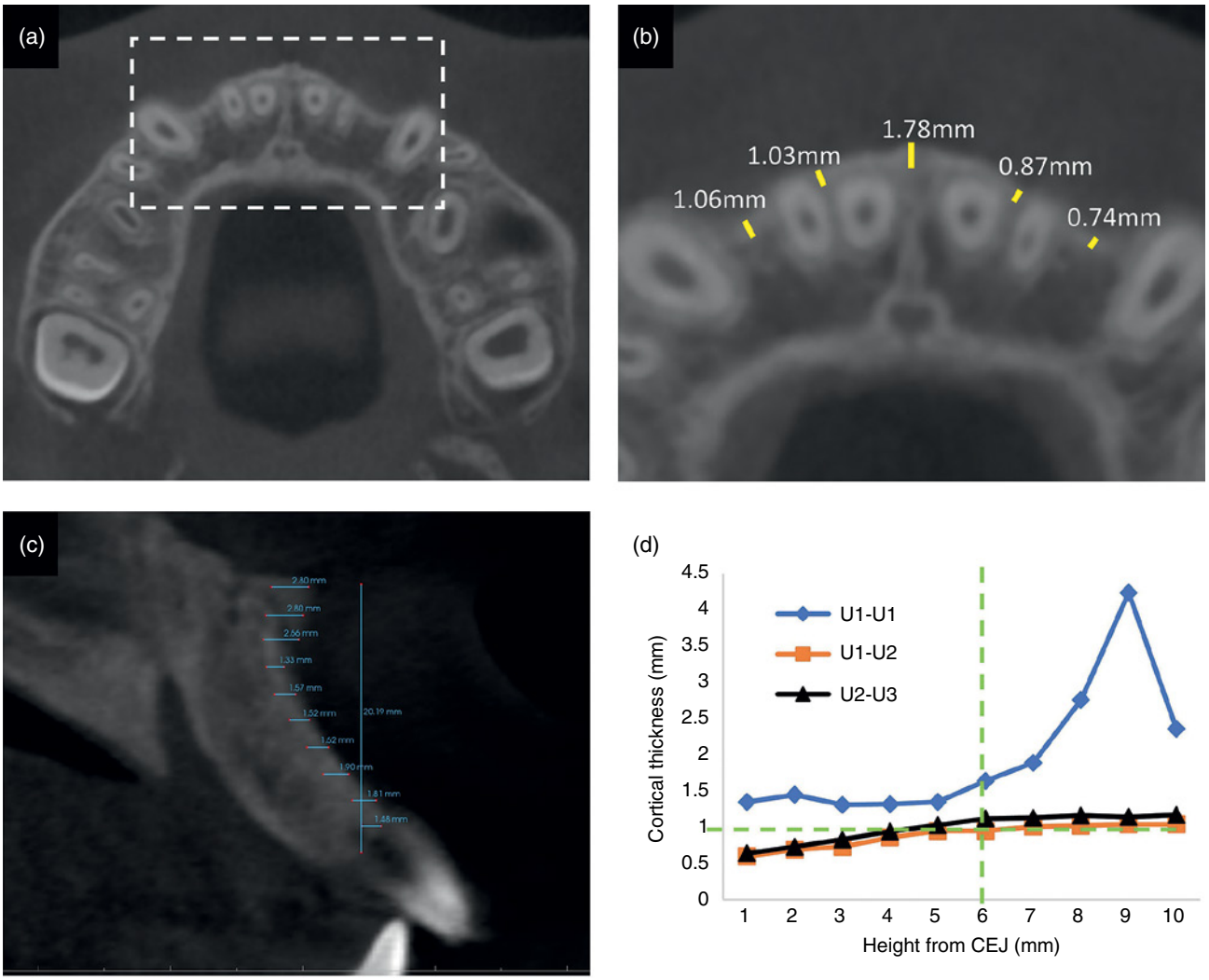


Figure 4.7 Comparison of cortical thickness among the three interradicular sites. (a) Axial section of the CBCT image. (b) The differences in cortical thickness among the three sites on one axial section. (c) Measurement of cortical thickness at different heights from the CEJ with 1 mm increment among 20 orthodontic patients. (d) The changes of cortical thickness at each interradicular site with changes in height from CEJ. Cortical thickness becomes greater with an increase in height for all three interradicular sites. Among the three sites, the site between two central incisors (U1-U1) exhibits the greatest cortical thickness. For the other two sites, cortical thickness becomes greater than 1 mm when the insertion height reaches 6 mm.

Cortical thickness differs among the three interradicular sites, with that of the U1-U1 site being slightly greater than that of U1-U2 and U2-U3 sites (Figure 4.7). Moreover, the fact that cortical thickness increases with an increase in insertion height from the cementoenamel junction (CEJ) holds true for all three interradicular sites, except for U1-U1 at the height of 9–10 mm. The cortical thickness peaks at the 9 mm level and is mainly attributed to the presence of the ANS, which could further explain the abrupt decrease of cortical thickness beyond 9 mm. According to the minimum requirements of cortical thickness (1 mm), placement of mini-implants at the 6 mm height is recommended for U1-U2 and U2-U3 sites, while mini-implants can be inserted at all insertion heights for the U1-U1 site, provided that other requirements (e.g. interradicular distance) are satisfied.

Hard Tissue Factor: Bone Depth

Bone depth is defined as the distance between labial and palatal cortical plates and is a key factor for ensuring the stability of mini-implants. Bone depth of at least 4.5 mm is recommended, otherwise sufficient primary stability cannot be guaranteed. As shown in Figure 4.8, bone depth increases with increasing insertion height from the

t.me/Dr_Mouayyad_AlbtousH

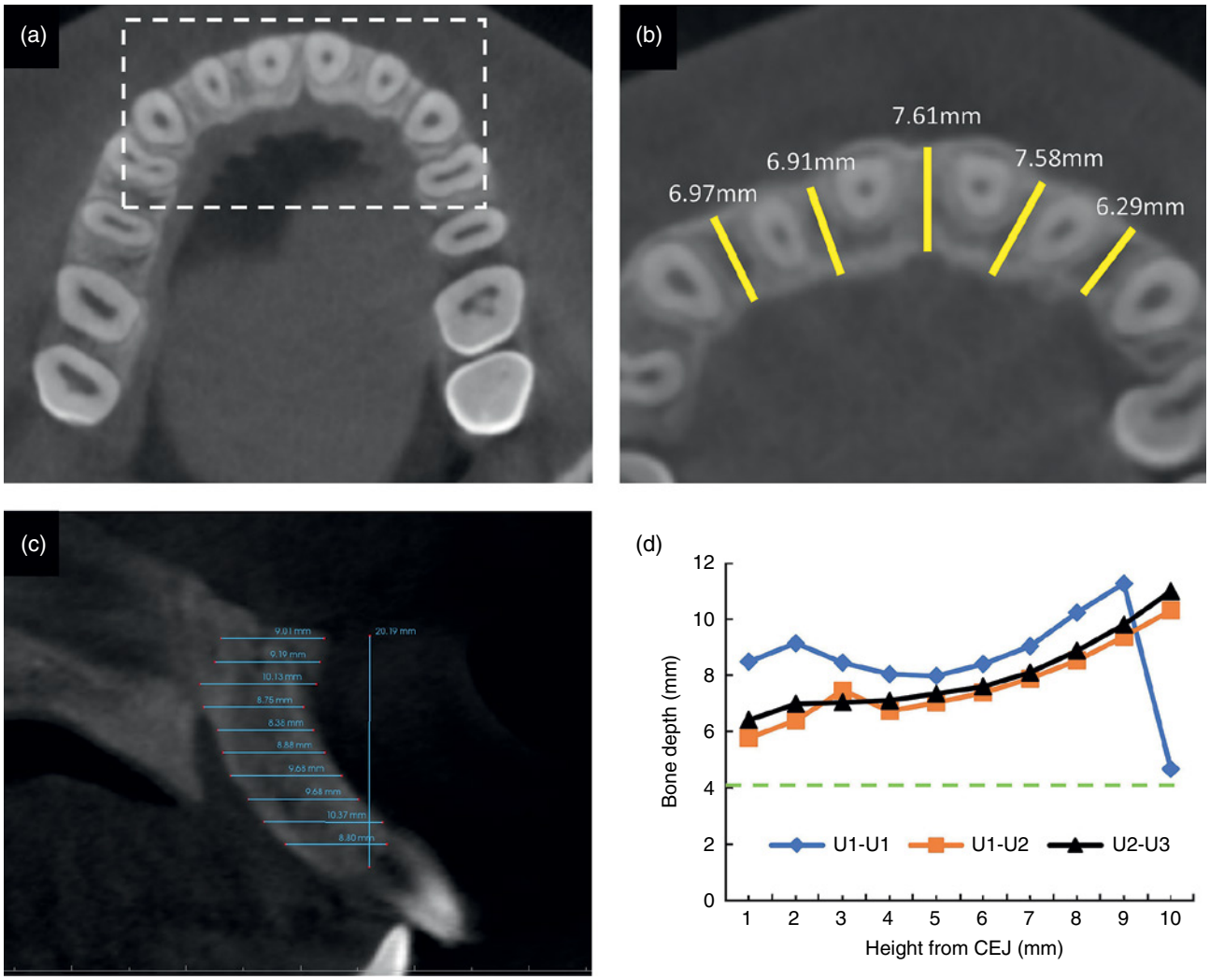


Figure 4.8 Comparison of bone depth among the three interradicular sites. (a) Axial section of the CBCT image. (b) The differences in bone depth among the three sites on one axial section. (c) Measurement of bone depth at different heights from the CEJ with 1 mm increment among 20 orthodontic patients. (d) The changes in bone depth at each interradicular site with changes in height from the CEJ. Bone depth becomes greater with an increase in the height for all three interradicular sites. Among the three sites, the site between two central incisors (U1-U1) exhibits the greatest bone depth.

CEJ. Moreover, bone depth is greater at the U1-U1 site than the U1-U2 and U2-U3 sites, which is mainly due to the bony projection formed by the fusion of two maxillary halves at the U1-U1 site (midline) (Figure 4.9). However, the greater bone depth at the U1-U1 site has no clinical significance since the minimum requirement (4.5 mm) of bone depth is satisfied at all three interradicular sites. Thus, this anatomical factor need not be considered since almost all interradicular sites are qualified in terms of adequacy of bone depth.

Hard Tissue Factor: Bone Width

Bone width is the amount of available bone between two adjacent roots and the term is often used interchangeably with interradicular distance. As displayed in Figure 4.10, bone width is greater if insertion entry point is more apical. Moreover, bone width is greater at the U1-U1 and U2-U3 sites than at the U1-U2 site. According to the 1 mm clearance principle, the minimum distance of mini-implants from adjacent roots should be at least 1 mm to prevent high stress around the implants that may lead to failure. If a

t.me/Dr_Mouayyad_AlbtousH

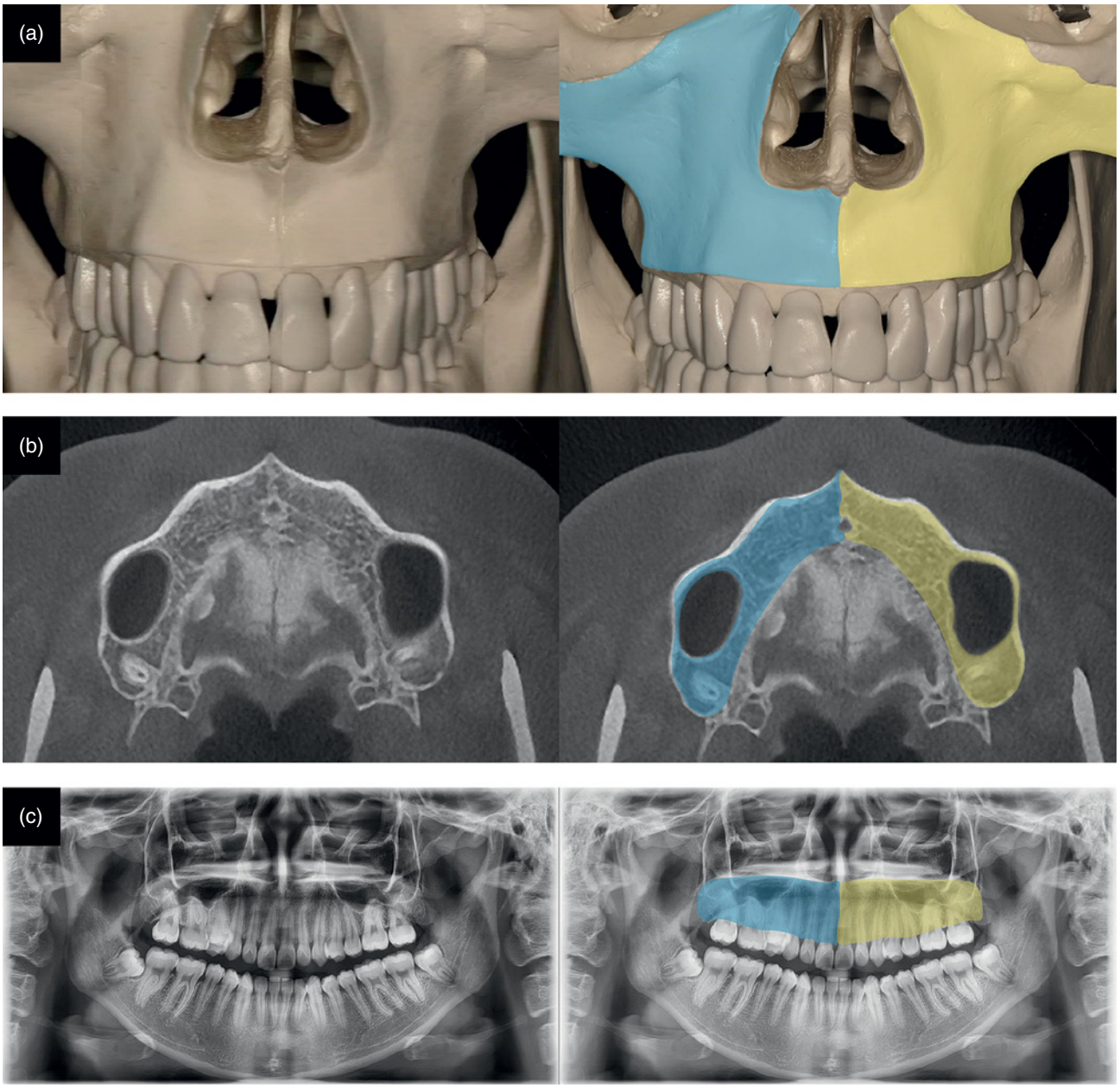


Figure 4.9 The maxillae are formed by the fusion of the left (yellow area) and right (blue area) halves. (a) Skull. (b) CBCT axial section. (c) Panoramic radiograph.

mini-implant with a 1.4 mm diameter is used, a minimum bone width of 3.4 mm (1.4 mm + 1 mm +1 mm) is required according to this principle. This means that only a few sites can be selected for the placement of labial mini-implants, i.e. U1-U1 and U2-U3 regions at the insertion height of 8 mm. To overcome this limitation, an oblique insertion technique can be used for mini-implants to engage a greater amount of bone apically (Figures 4.11 and 4.12). This broadens the anatomical areas for the placement of labial mini-implants and all the three interradicular regions at various heights (i.e. 6 mm and 8 mm) can be selected for mini-implant placement.

A clinical caveat should be borne in mind in that oblique insertion with exaggerated angles (e.g. 45°) may lead to

t.me/Dr_Mouayyad_AlbtousH

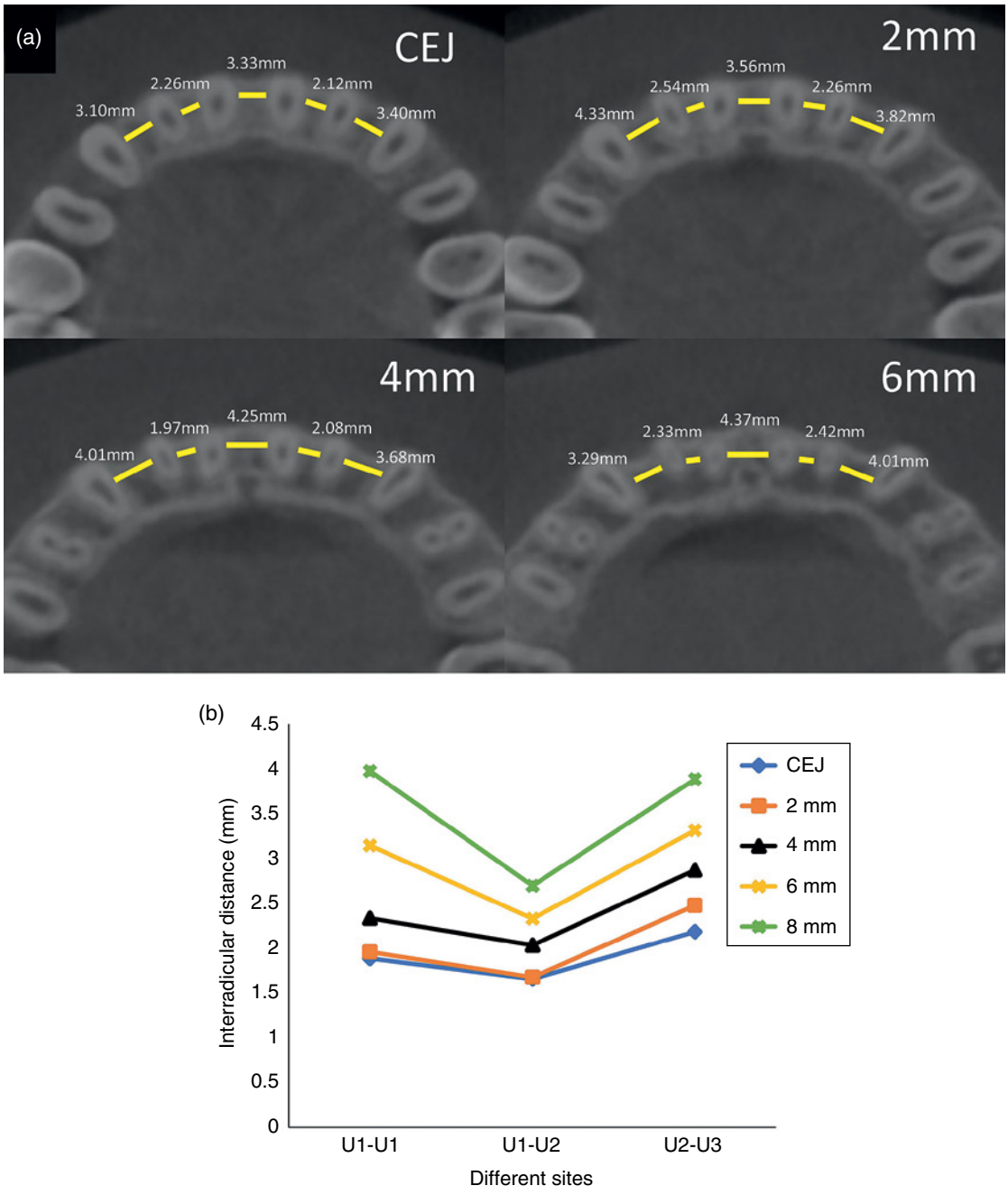


Figure 4.10 Comparison of bone width among the three interradicular sites at different heights based on 20 orthodontic patients. (a) Axial section of CBCT images showing bone width at different heights and among different interradicular sites in an exemplified patient. (b) Line chart showing the differences in bone width at different heights among the three interradicular sites. Bone width becomes greater with an increase in insertion height for all three sites. Among the three sites, the interradicular site between the central and lateral incisors exhibits the smallest bone width.

slippage of mini-implants during insertion and subsequent soft tissue damage (e.g. laceration) (Figure 4.13). Thus, we recommend that oblique insertion technique (0–30° to occlusal planes) be applied for the placement of labial mini-implants. Moreover, among patients with severe crowding, bone width may not follow the aforementioned rule and appropriate insertion sites should be individualised (Figure 4.14). Nevertheless, as a general rule, in terms of bone width, we recommend that mini-implants be placed with oblique insertion technique (0–30° to occlusal planes) at a height of 6–8 mm for the U1-U1 and U2-U3 sites or 8 mm for the U1-U2 site.

t.me/Dr_Mouayyad_AlbtousH

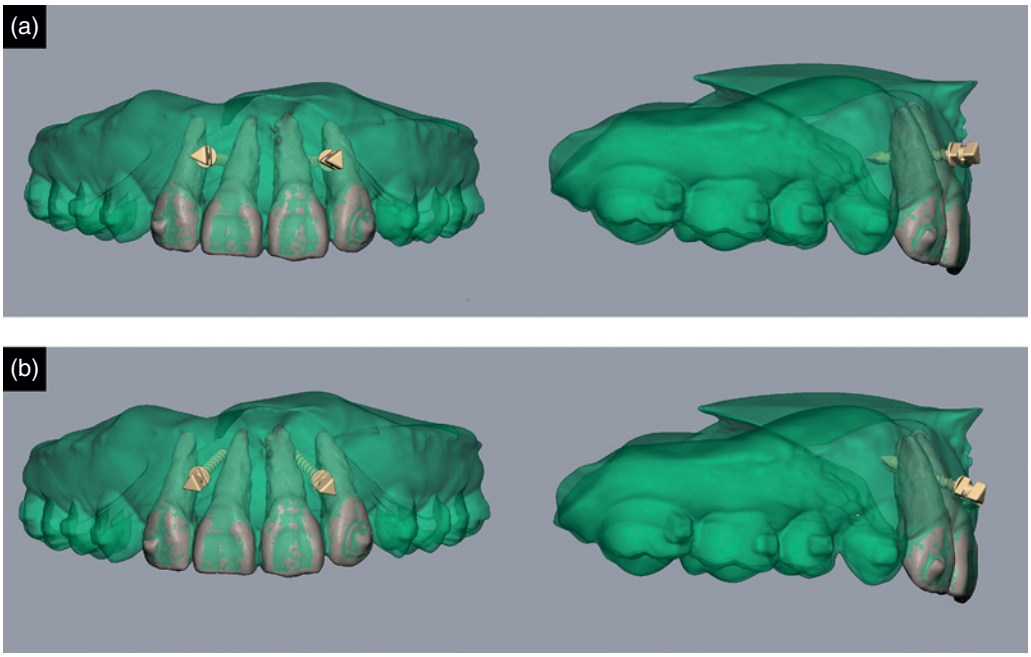


Figure 4.11 Greater bone width is obtained for oblique insertion. (a) Horizontal insertion. (b) Oblique insertion. Note that greater bone width is engaged if the mini-implants are inserted obliquely.

Hard Tissue Factor: Root Prominence

Root prominence makes it easier to locate mini-implant entry points (Figure 4.15). By palpating the depression areas between two adjacent root prominences, practitioners are able to accurately locate midpoints between two adjacent roots. However, for some patients, non-apparent root prominence makes it more difficult to locate the correct entry point.

Soft Tissue Factor: Labial Frenum

The presence of the labial frenum at the U1-U1 site may interfere with insertion of mini-implants (Figure 4.16). Due to the removability of the frenum, frenectomy is indicated to avoid soft tissue wrapping around mini-implants during insertion and to reduce soft tissue complications following insertion. Due to its invasive nature, frenectomy renders mini-implant placement more invasive at the U1-U1 site than at the other two sites. However, following frenectomy and flapping, the intermaxillary suture can be readily observed and detected, making entry points easily and confidently located since this bone fissure is at the centre of the U1-U1 interradicular site (Figure 4.17).

Soft Tissue Factor: Mucogingival Junction

It is preferable to insert mini-implants at the mucogingival junction to prevent potential soft tissue complications. If the junction is located too occlusally, root injury may be caused by mini-implants placed at the mucogingival junction. Thus, mini-implants should be preferably placed at interradicular regions with adequate height of mucogingival junction. Among the three available interradicular sites, the mucogingival junction is highest at the U2-U3 site and lowest at the U1-U1 site due to the presence of the labial frenum (Figure 4.18).

4.2.2 Biomechanical Considerations

From the perspective of biomechanics, the three different interradicular sites have distinct biomechanical advantages. If the six anterior teeth are taken as a whole, the centre of resistance of the anterior teeth lies at the interradicular space between lateral incisors and canines in the sagittal plane, rendering the distance between the mini-implant heads and centre of resistance different among the three sites (Figure 4.19). This distance is largest for the mini-implant inserted at the U1-U1 site and smallest for that inserted at the U2-U3 site. Thus, mini-implants placed at the three sites differ in their effectiveness in producing proclination effects. Specifically, if incisor proclination and intrusion are both required, mini-implants are preferable to be placed at the U1-U1 site. In contrast, the U2-U3 site is recommended if bodily intrusion without incisor proclination is clinically indicated.

t.me/Dr_Mouayyad_AlbtousH

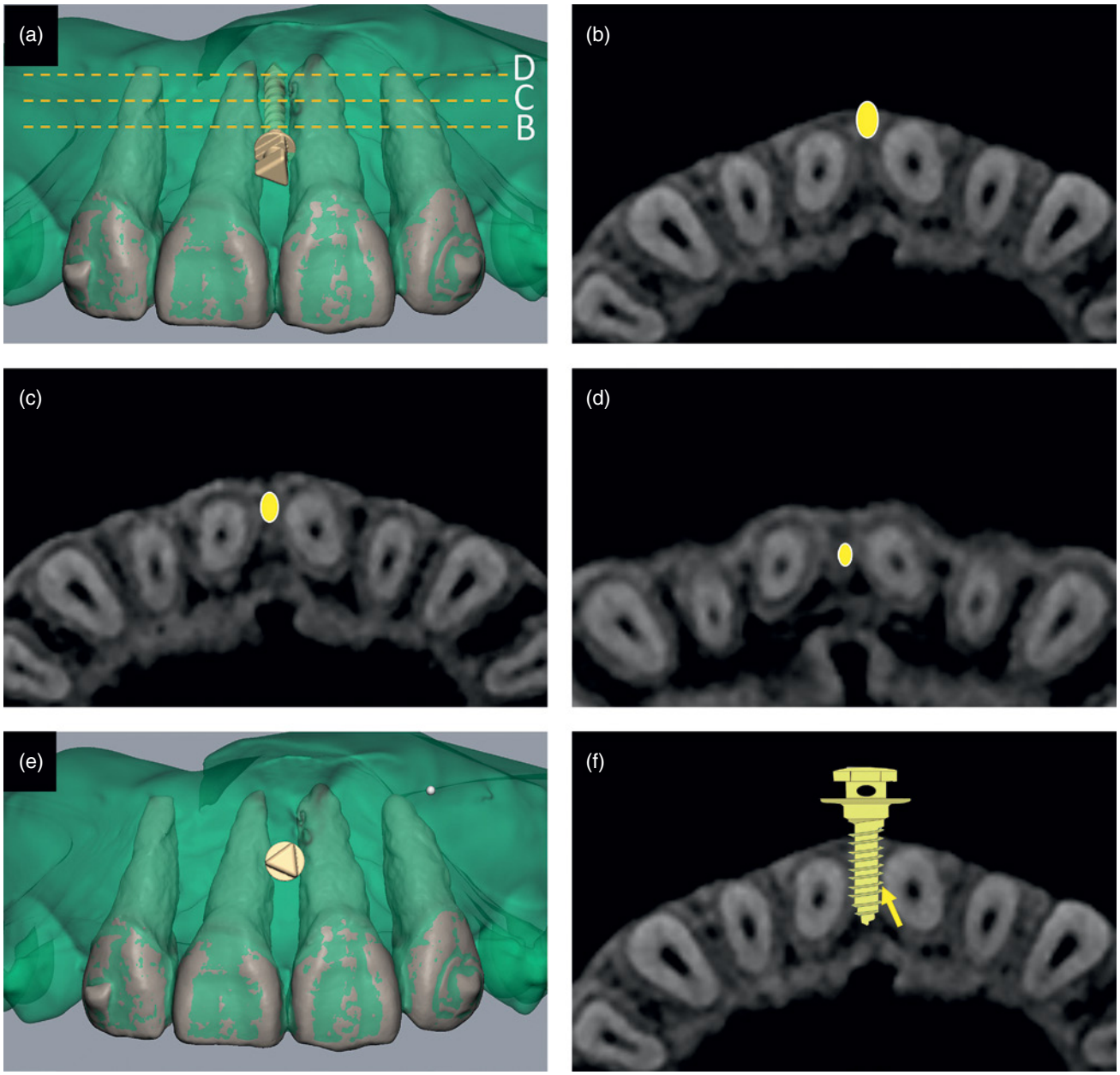


Figure 4.12 Illustrations and CBCT images showing spatial relationship between the mini-implant and adjacent central incisors. (a) 3-D reconstruction of the dentition and alveolar bone. A mini-implant is virtually inserted in an oblique direction. The three dashed lines correspond to the axial sections in the images below. (b–d) Bone width becomes greater as it approaches more apically, resulting in greater clearance between the mini-implant and the adjacent roots. The ellipsoid yellow dot represents the mini-implant image on each of the sections. (e) A mini-implant is virtually inserted in a horizontal direction. (f) Bone width is limited and root contact by the mini-implant occurs (yellow arrow).

t.me/Dr_Mouayyad_AlbtousH

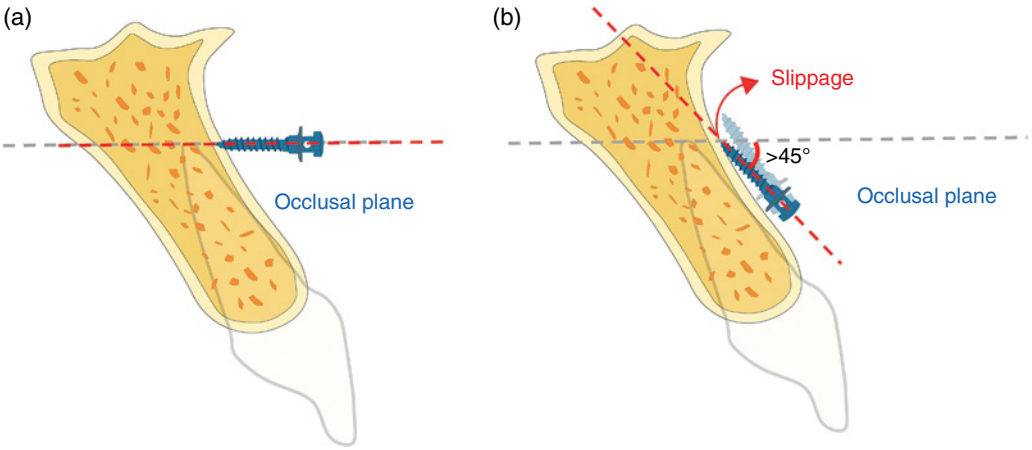


Figure 4.13 Schematic illustrations showing slippage of a mini-implant during insertion. (a) The mini-implant is inserted with an insertion path that is in line with the occlusal plane. No slippage of the mini-implant occurs. (b) The mini-implant is inserted at an insertion angle greater than 45° to the occlusal plane. Slippage of the mini-implant occurs during insertion.

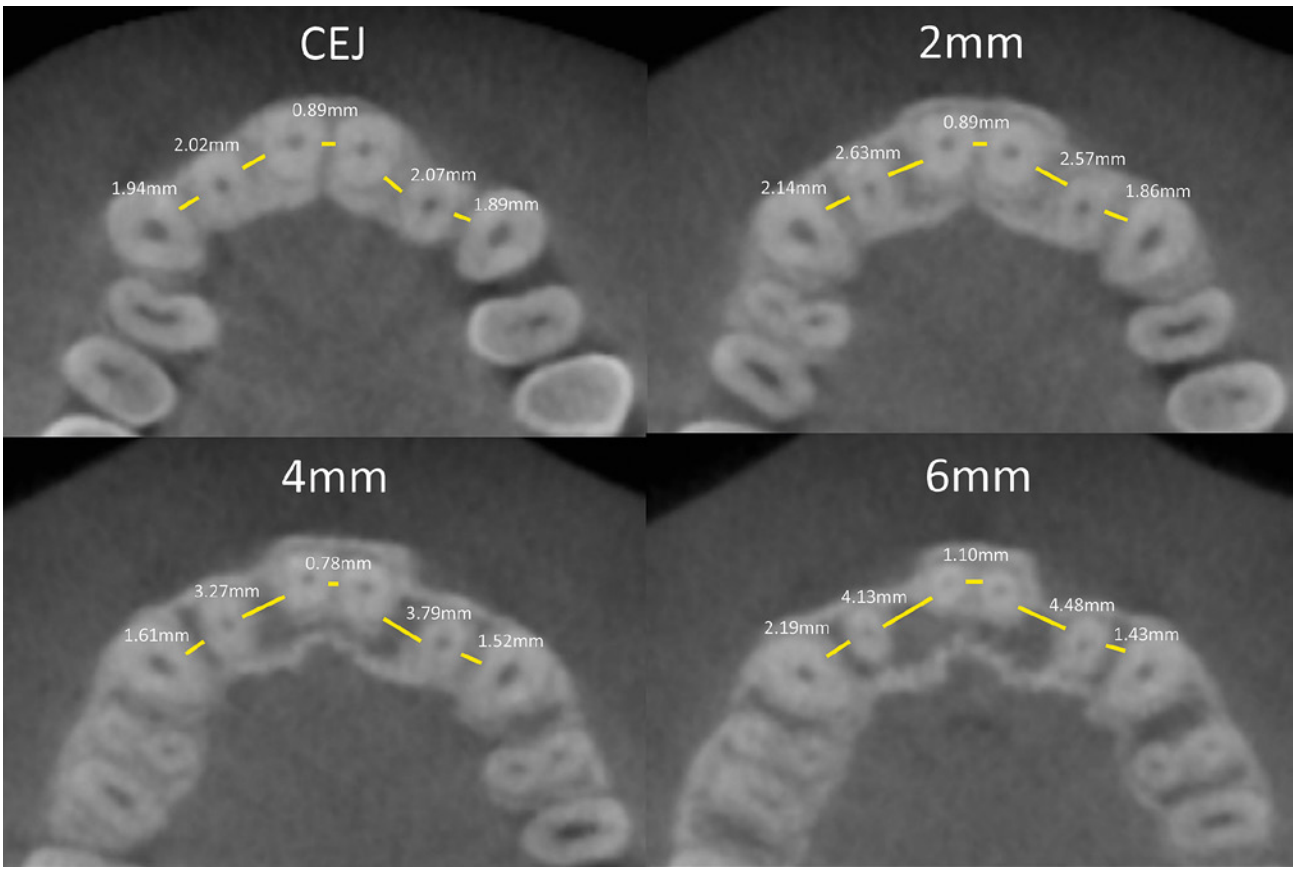


Figure 4.14 Axial sections of CBCT images showing bone width at different interradicular sites at different heights from the CEJ in an individual. Note that the bone width is limited at the interradicular site between the two central incisors.

t.me/Dr_Mouayyad_AlbtousH

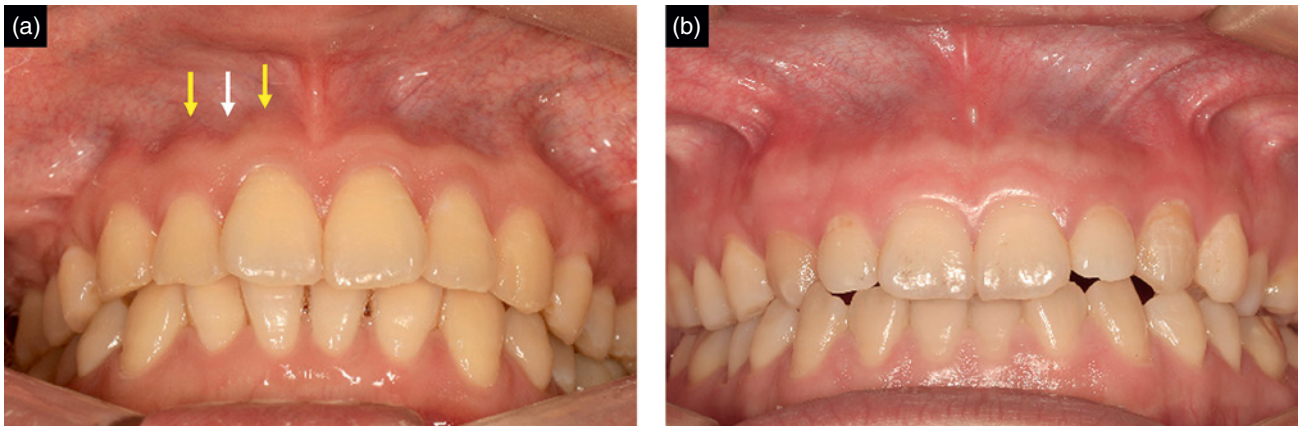


Figure 4.15 Root prominence. (a) Root prominences (yellow arrows) are prominent and noticeable. The noticeable root prominences allow operators to locate the interradicular depression (white arrow) with ease. (b) Root prominences are not apparent and noticeable.



Figure 4.16 Prominent labial frenum. The presence of a prominent labial frenum (yellow arrow) may interfere with insertion of a mini-implant at the interradicular site between central incisors.

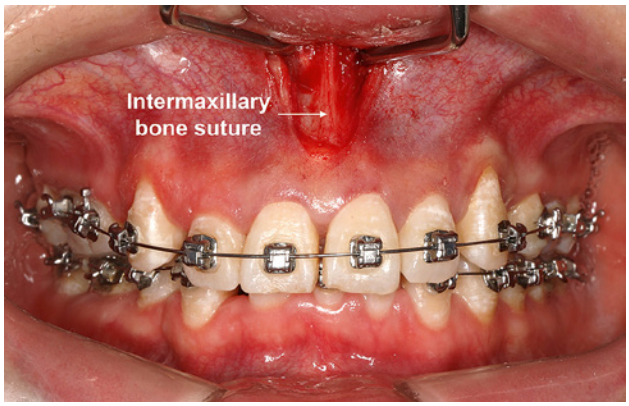


Figure 4.17 Intermaxillary suture. The intermaxillary suture is easily noticeable following flap elevation. This bone fissure indicates the centre of the U1-U1 interradicular site.

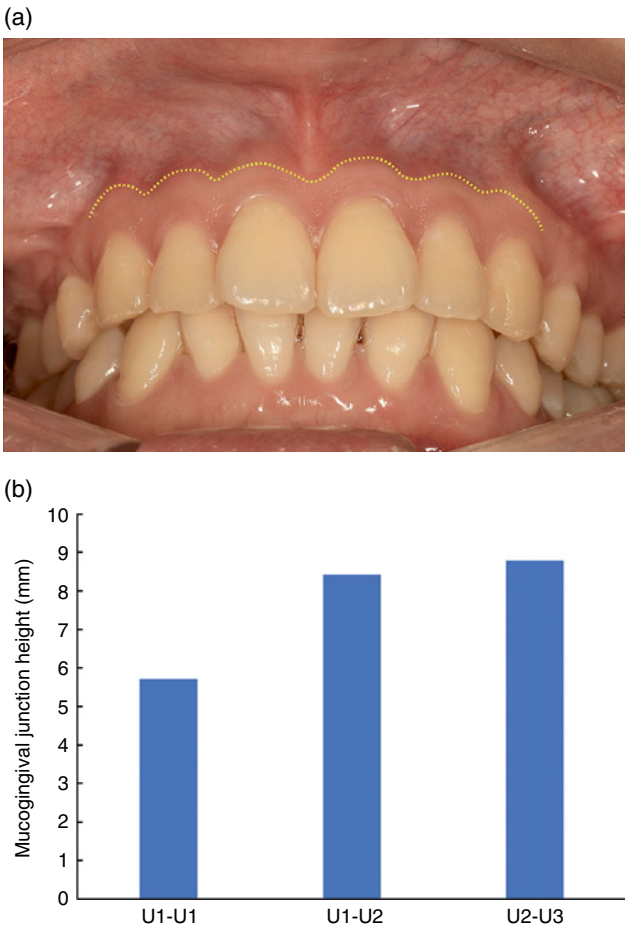


Figure 4.18 Comparison of the height of the mucogingival junction among the three interradicular sites. The U2-U3 interradicular site exhibits the greatest mucogingival junction height while the U1-U1 site has the smallest mucogingival junction height. (a) Intraoral photograph showing the mucogingival junction (yellow dashed line). (b) Bar chart showing the differences of mucogingival junction heights among the three sites.

t.me/Dr_Mouayyad_AlbtousH

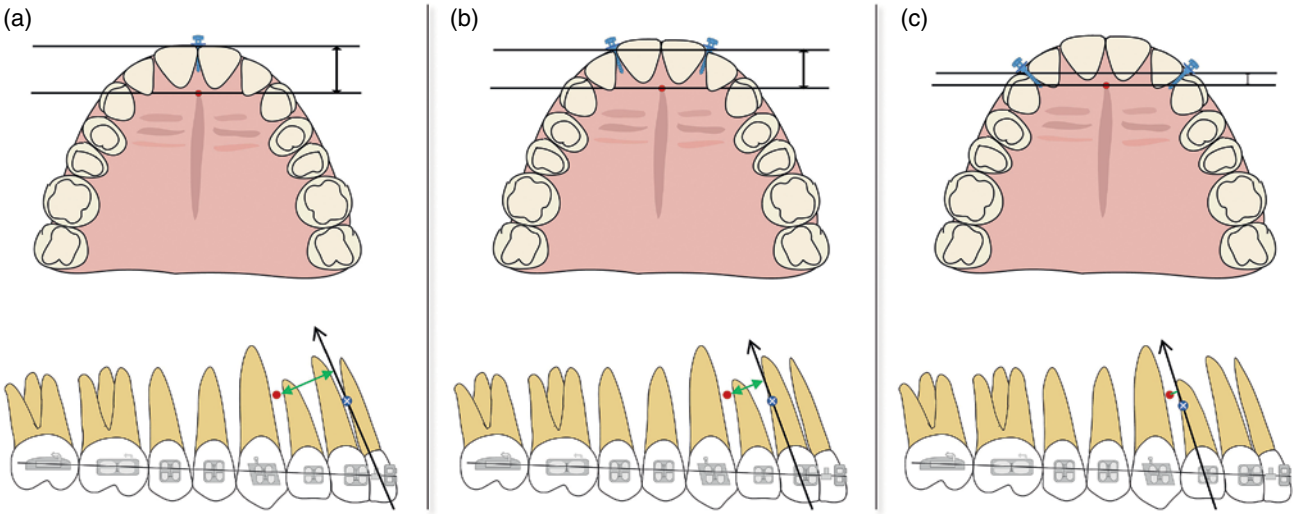


Figure 4.19 Biomechanical analyses for incisor intrusion with mini-implants at different interradicular sites. (a) U1-U1 interradicular site. (b) U1-U2 interradicular site. (c) U2-U3 interradicular site. Note that the distance from the centre of resistance to the line of force is greatest for the mini-implant at the U1-U1 site and smallest for the one at the U2-U3 site. With the same magnitude of intrusion force, different magnitudes of moments will be generated.

Table 4.1 Comparison of anatomical and biomechanical features among the three sites.

	Anatomy						Biomechanics		
Site	Bone width	Bone depth	Cortical thickness	Mucogingival height	Frenectomy	Ease of location	Proclination	Intrusion	M/F ratio
1-1	Wide	Sufficient	Thick	Low	Yes	Easy	Very efficient	Efficient	High
1-2	Narrow	Sufficient	Thin	Medium	No	Relatively difficult	Efficient	Efficient	Medium
2-3	Wide	Sufficient	Thin	High	No	Relatively difficult	Inefficient	Efficient	Low

4.2.3 Selection of Appropriate Insertion Sites

Appropriate insertion sites are selected based on both anatomical factors and biomechanical factors. In Table 4.1, anatomical factors and biomechanical considerations are demonstrated and compared among the three interradicular sites. Appropriate interradicular sites can be selected and individualised case by case according to anatomical characteristics and biomechanical requirements among different orthodontic patients. As a general rule, we recommend that labial mini-implants be obliquely inserted (0–30° to occlusal planes) at the height of 6–8 mm apical to the CEJ.

4.2.4 Insertion Techniques

Due to the presence of the labial frenum and the need for frenectomy among some patients, the insertion techniques differ between the U1-U1 site and the two other sites. Thus, the insertion techniques will be presented separately.

U1-U1 Site

For the placement of mini-implants into the interradicular site between two central incisors, the first step is to evaluate the adequacy of the interradicular space and the position of frenum attachment. If the frenum attaches too occlusally, frenectomy is indicated to avoid soft tissue wrapping around mini-implants during insertion and to prevent soft tissue complications following insertion. The entry point is generally 6–8 mm apical to the CEJ of central incisors. If the interradicular distance at this level is adequate, horizontal insertion of mini-implants is indicated. Otherwise, angled insertion with an insertion angle of 0–30° is recommended to avoid root damage (Figure 4.20). Once the insertion height and angle are determined, insertion can be implemented. The detailed procedures of inserting a mini-implant at the U1-U1 site are displayed in Figure 4.21.

Second, infiltration anaesthesia is performed following mucosal disinfection with iodophor. The amount of anaesthetic used should not be too much in order to maintain

t.me/Dr_Mouayyad_AlbtousH

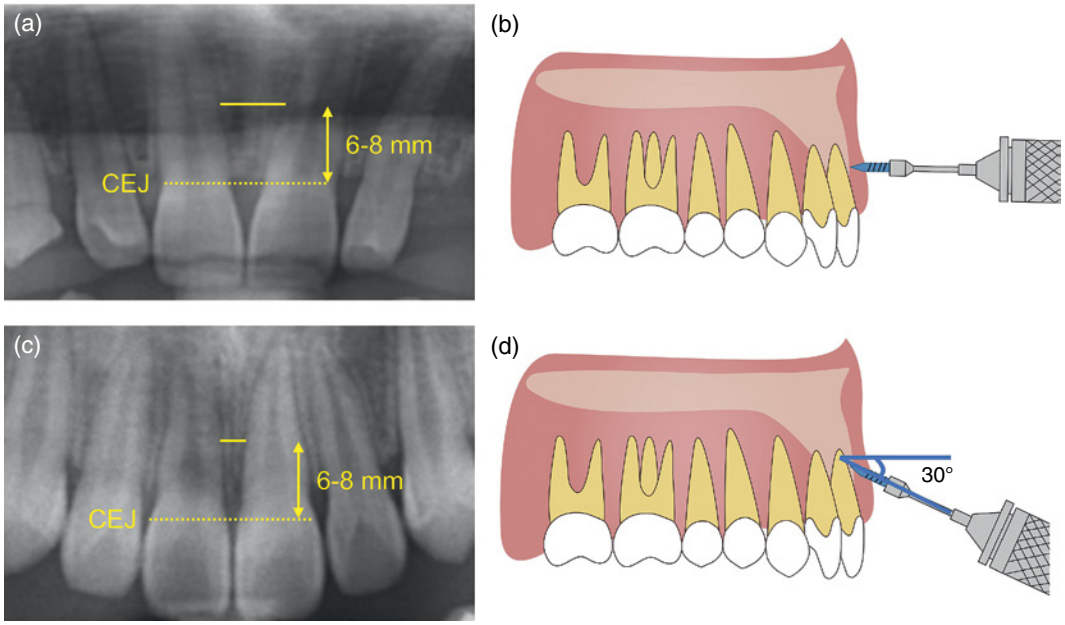


Figure 4.20 (a) Bone width is evaluated at the height of 6–8 mm. Sufficient interradicular space is present. (b) The mini-implant is inserted in a horizontal direction due to ample interradicular space. (c) Limited interradicular space is present at the height of 6–8 mm. (d) The mini-implant is inserted in an oblique direction (30° to the occlusal plane).

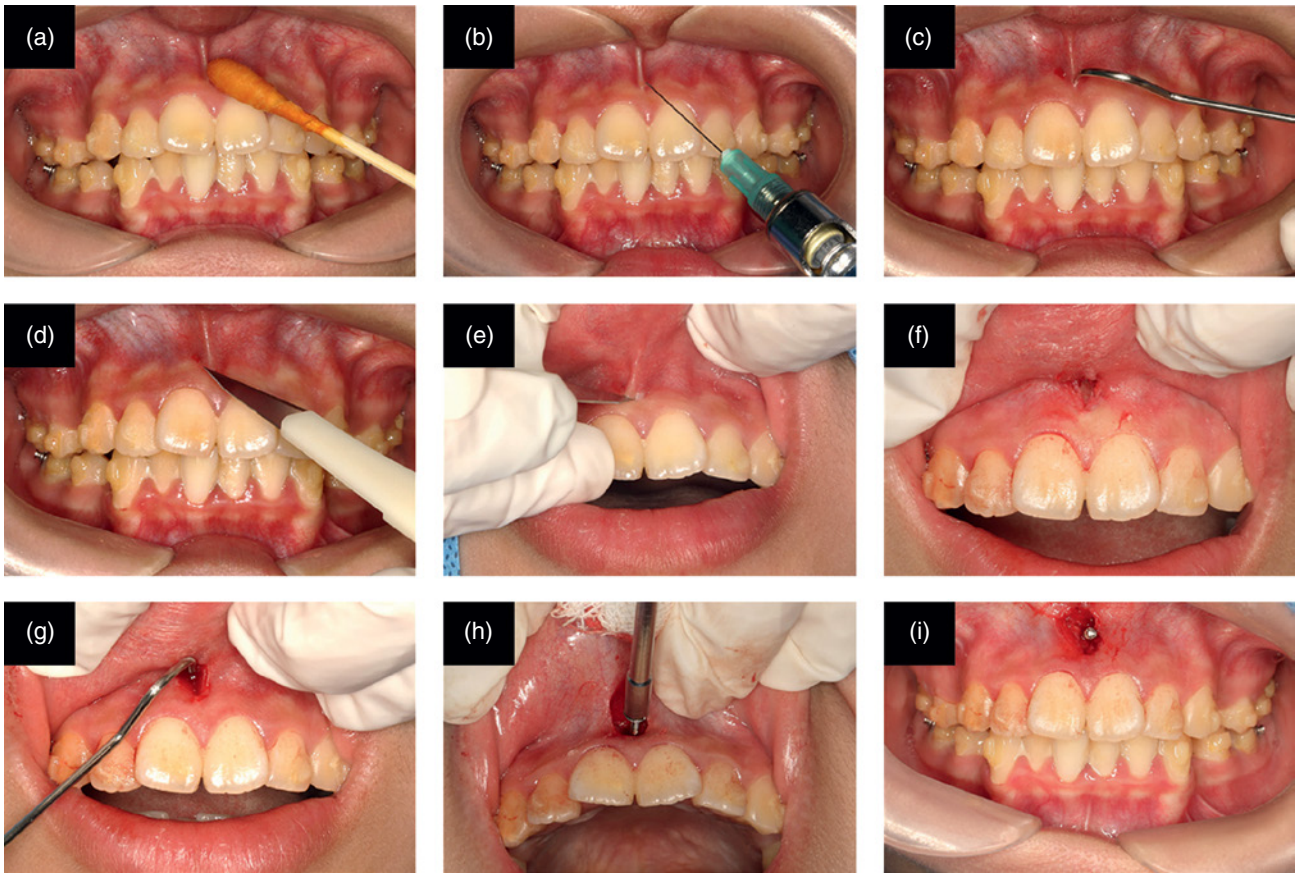


Figure 4.21 The clinical procedures of inserting a mini-implant at the U1-U1 interradicular site. (a) Mucosal disinfection with iodophor. (b) Local infiltration anaesthesia. (c) Mark the desired entry point with an explorer. (d,e) Perform a horizontal incision on the labial frenum (frenectomy). (f) Postfrenectomy. (g) Locate the optimal entry point on the bone surface. (h) Insertion of a mini-implant. (i) Postinsertion.

t.me/Dr_Mouayyad_AlbtousH

the sensory perception of periodontal tissues, so that the practitioner will be alerted if root proximity is encountered during insertion. Generally, 0.2–0.5 ml anaesthetic is sufficient. However, if frenectomy is indicated, additional anaesthetic should be injected submucosally at the frenum.

Third, the optimal entry point is marked with an explorer, followed by frenectomy at this marked point. For frenectomy, horizontal incision is made to reduce soft tissue tension and expose the bony surface of the interradicular area between the two central incisors. As mentioned above, the optimal entry point is easily located at the intermaxillary bony suture that can be readily observed following frenectomy and flap elevation (Figure 4.22).

Fourth, the entry point is marked at the bony suture based on the predetermined insertion height (6–8 mm apical to CEJ) with an explorer. The mark should be made by expanding the suture slightly with the explorer so that a pilot hole is formed (Figure 4.23). The presence of the pilot hole, on one hand, facilitates location of the entry point and on the other hand, prevents slippage of mini-implants during insertion.

Lastly, the mini-implant is inserted through the pilot hole. To gain greater interradicular space and to prevent root damage, angled insertion (0–30° to the occlusal plane) is recommended. Moreover, the mini-implant should be inserted perpendicularly to the tangent line of the dental arch at the midpoint between two central incisors (Figure 4.24). However, operators often sit at the 11 o'clock position and their eyes are not in the midsagittal plane, rendering the mini-implant to be placed towards the right side (Figure 4.25).



Figure 4.22 The presence of the intermaxillary suture (yellow arrow) facilitates accurate location of the optimal entry point.

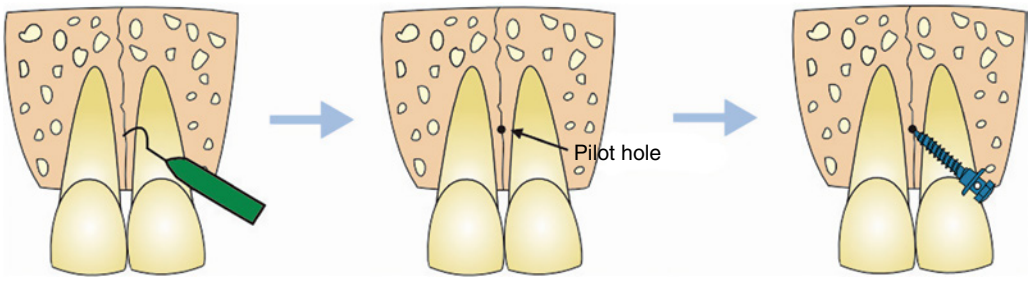


Figure 4.23 The intermaxillary suture can be expanded through an explorer or a probe so that a pilot hole is obtained. The presence of the pilot hole can prevent slippage of the mini-implant.

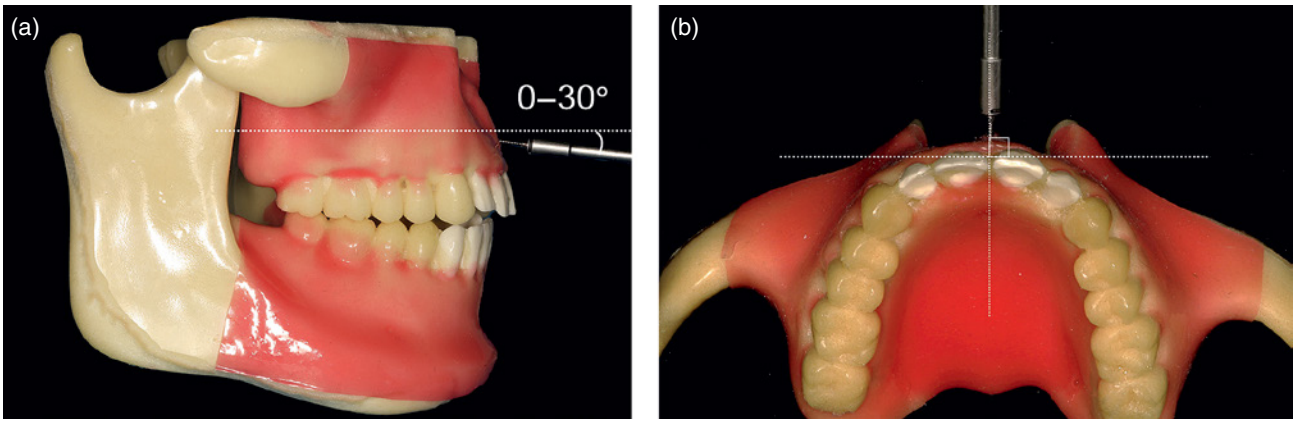


Figure 4.24 (a) The mini-implant is inserted at an angle of 30° to the occlusal plane. (b) From the occlusal view, the mini-implant is inserted perpendicularly to the tangent line of the dental arch at the entry point (between two central incisors).

t.me/Dr_Mouayyad_AlbtousH

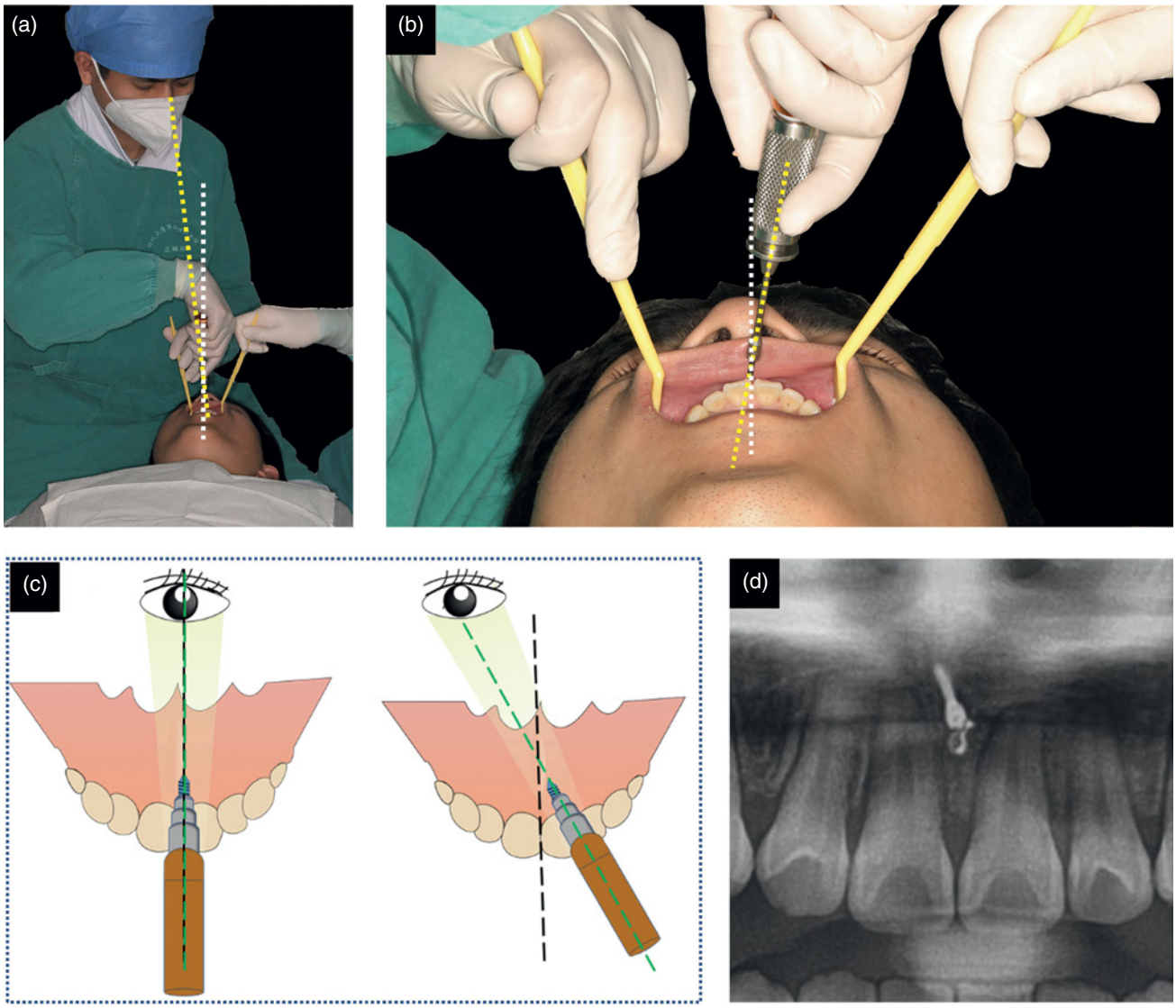


Figure 4.25 Deviated insertion path due to the operator's deviated line of view. (a) The operator sat at the 11 o'clock position and his line of view (dashed yellow line) was not in the midsagittal plane (white dashed line). (b) Close-up photograph. The insertion path was deviated to the right side. (c) Schematic illustrations showing the influence of eye position on the insertion path. (d) Radiographic image showing that the mini-implant was deviated to the right side.

Thus, to avoid this error, we recommend operators sit at the 12 o'clock position to keep their eyes in the midsagittal plane so that perpendicular insertion to the tangent line of the dental arch can be guaranteed. Alternatively, the operator can sit at the 11 o'clock but patients should be asked to tilt their head towards the operator so that the operator's eyes are in the midsagittal plane (Figure 4.26).

Depending on the extent of incision made for frenectomy, sutures may or may not be placed. Following the healing of soft tissues for one or two weeks, force loading can be applied.

For patients with non-apparent labial frenum, frenectomy is not indicated and insertion techniques are similar to those with frenectomy, except frenectomy is not performed. The clinical procedures are displayed in a case example in Figure 4.27.

The detailed clinical procedures for the placement of mini-implants at the U1-U1 site are illustrated in Figure 4.28.

U1-U2 or U2-U3 Site

Due to the absence of labial frenum at these two sites, frenectomy is not needed. However, unlike the U1-U1 site

t.me/Dr_Mouayyad_AlbtousH

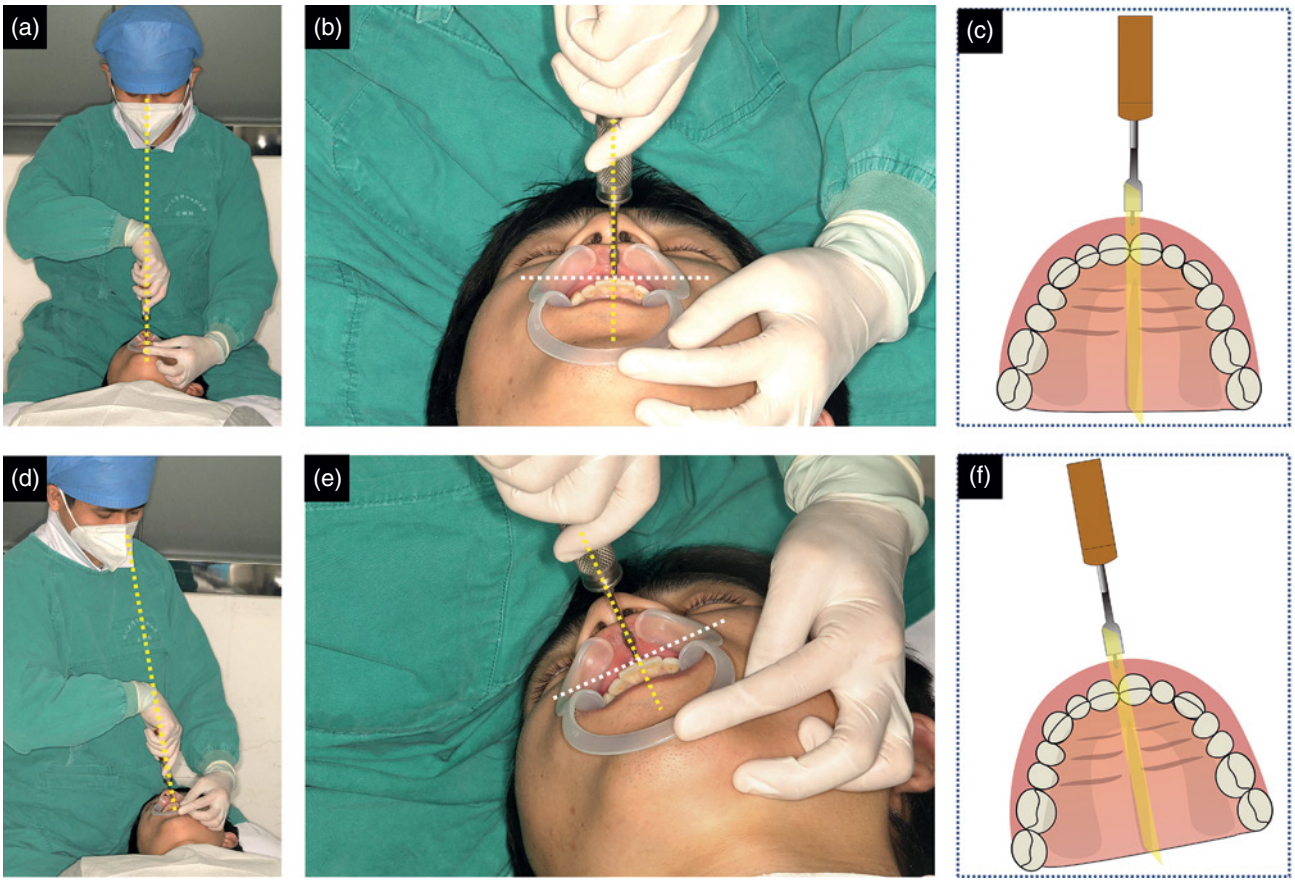


Figure 4.26 (a) If the operator sits at the 12 o'clock position, the line of view is consistent with the midsagittal plane. (b) Close-up view. The insertion path (yellow dashed line) is perpendicular to the tangent line (dashed white line) of the dental arch passing the entry point (the midpoint between the two roots). (c) A schematic illustration showing the insertion path that is desired. (d) If the operator sits at the 11 o'clock position, the patient is also instructed to tilt his head towards the operator so that the operator's line of view coincides with the midsagittal plane. (e) Close-up view. The insertion path (yellow dashed line) is perpendicular to the tangent line (dashed white line) of the dental arch passing the entry point (the midpoint between the two roots). (f) A schematic illustration showing the insertion path that is desired.

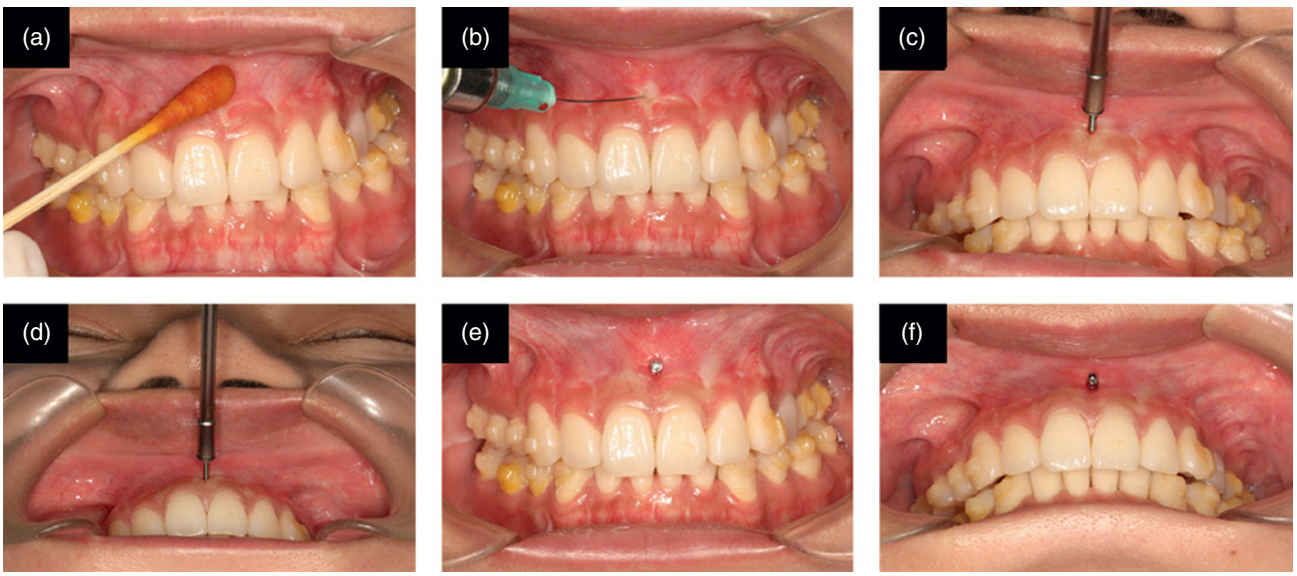


Figure 4.27 Detailed procedures for inserting a mini-implant at the U1-U1 interradicular site where frenectomy is not required. (a) Mucosal disinfection with iodophor. (b) Local infiltration anaesthesia. (c) Insert a mini-implant through the designated entry point. (d) Confirm the insertion path. (e) Postinsertion. (f) Check the position of the mini-implant.

t.me/Dr_Mouayyad_AlbtousH

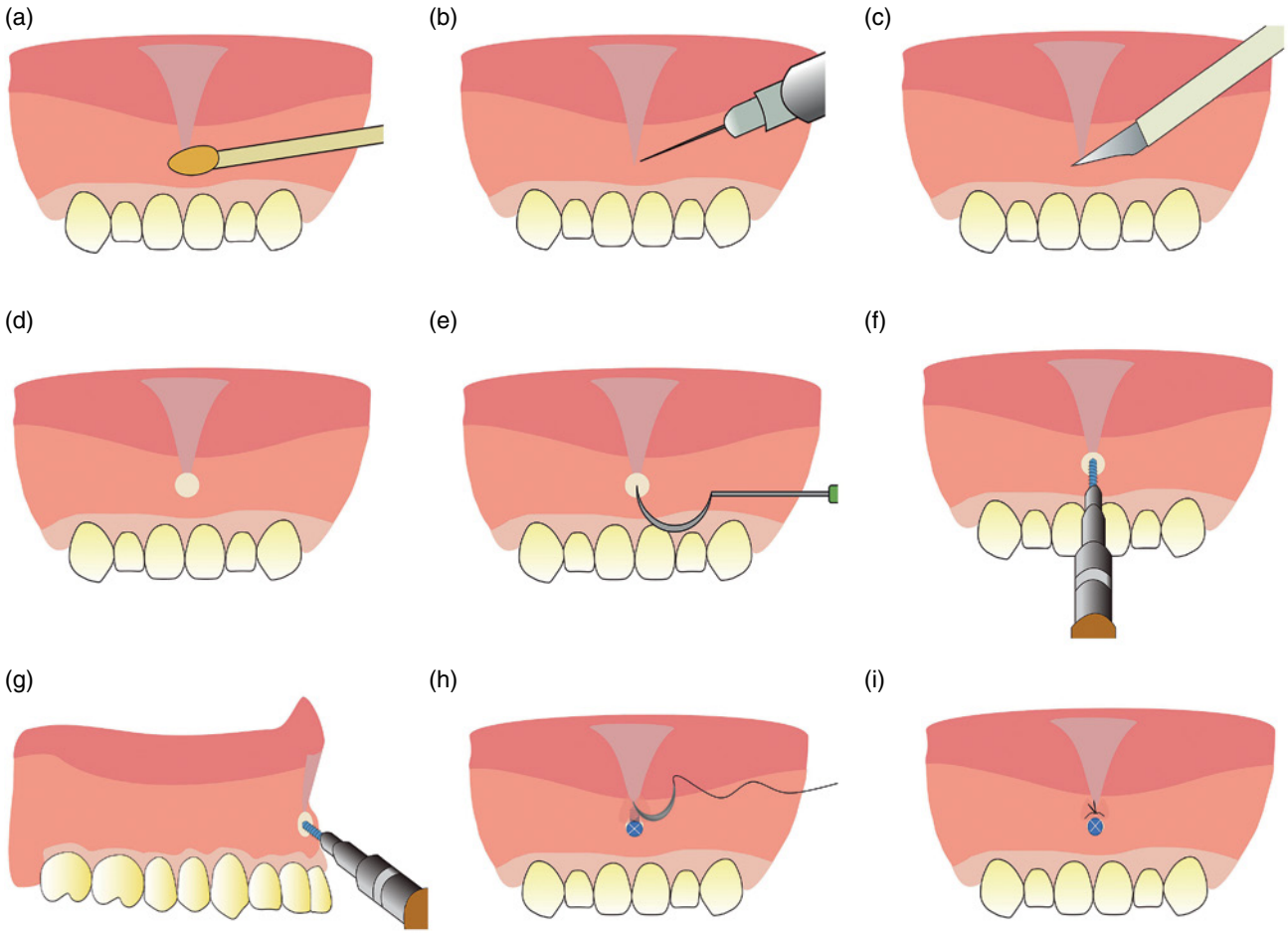


Figure 4.28 Schematic illustrations showing detailed procedures for inserting a mini-implant at the U1-U1 interradicular site. (a) Mucosal disinfection. (b) Local infiltration anaesthesia. (c) Frenectomy. (d) Flap elevation to expose the intermaxillary suture. (e) Expand the suture with an explorer to form a pilot hole. (f) Insert a mini-implant through the designated pilot hole. (g) Insert the mini-implant. (h) Primary suture. (i) Postinsertion.

where the intermaxillary suture can be used for location of the entry point, the U1-U2 or U2-U3 site has no obvious landmarks for locating the mesiodistal positions of entry points. Thus, special care should be taken to determine the mesiodistal positions of entry points so that root injury can be avoided.

First, the height of the entry point and the insertion angle should be determined based on clinical and radiographic examinations. Due to the smaller interradicular distance at the U1-U2 site, the entry point for this site may be slightly more apical than that for the U1-U1 and U2-U3 sites. Moreover, insertion angles may be greater for the U1-U2 site, in order to reduce the risk of root damage. Generally, the insertion heights are 8 mm or more for the U1-U2 site and 6–8 mm for the U2-U3 site. However, occasionally, for patients with limited width of attached gingiva, mini-implants can still be placed through the recommended entry points but should be inserted with greater insertion angles in order to leave their heads at the mucogingival junction, so that the risk of soft tissue complications is reduced (Figure 4.29). This increase in insertion angles can reduce the risk of root damage and soft tissue complications at the expense of probable mini-implant slippage during insertion and limited bone quantity on the labial side.

Second, due to the lower amount of soft tissue at these two sites, the recommended amount of infiltration anaesthetic is about 0.2–0.5 ml and the anaesthetic area should be limited to the entry point.

t.me/Dr_Mouayyad_AlbtousH

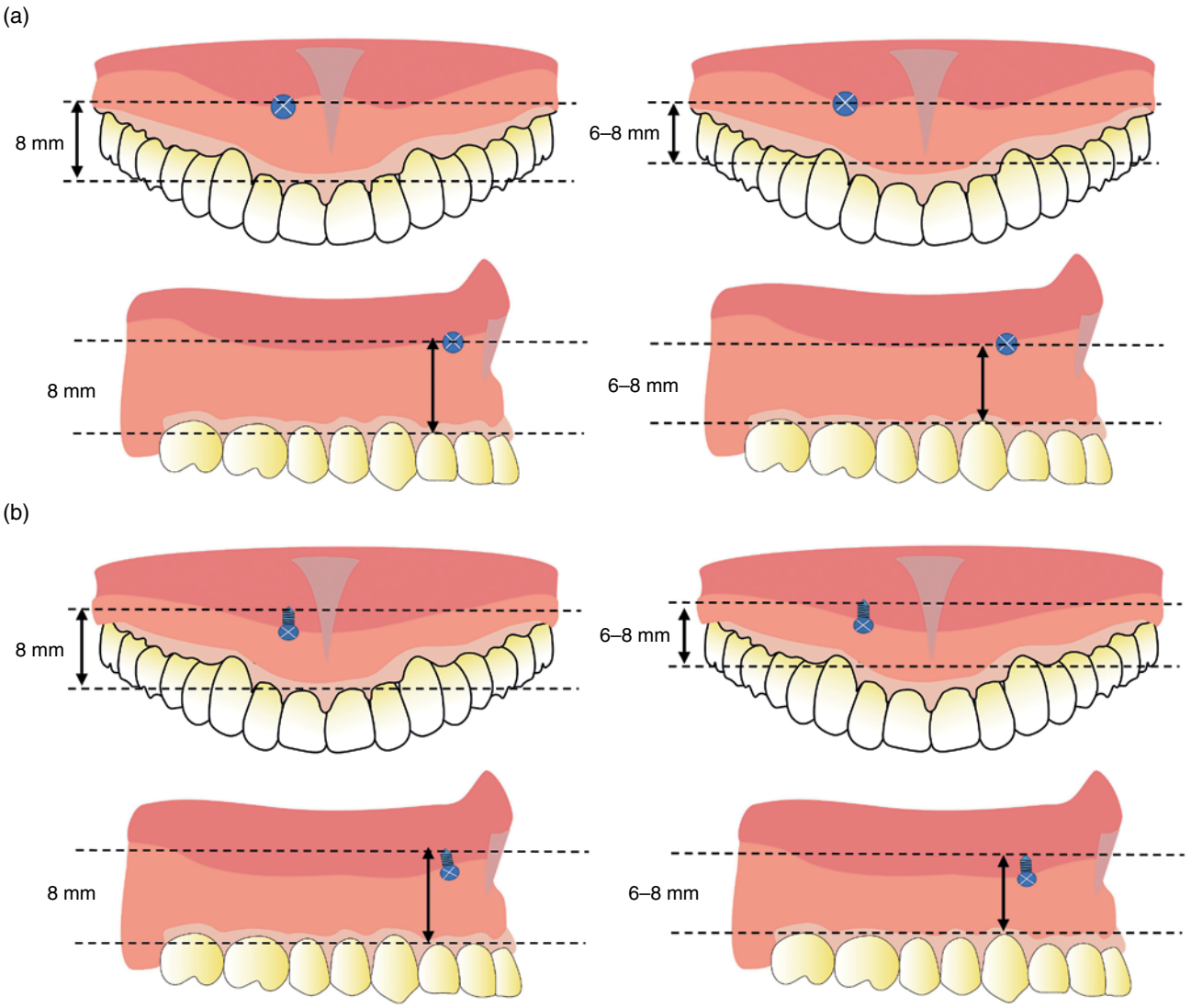


Figure 4.29 (a) Mini-implants are horizontally inserted through the recommended entry points (8 mm for the U1-U2 site and 6–8 mm for the U2-U3 site) in patients with adequate attached gingiva. (b) Mini-implants are inserted obliquely through the recommended entry points in patients with limited attached gingiva. With the oblique insertion technique, the heads of the mini-implants can be left at the mucogingival junction.

Third, the mesiodistal position of the entry point can be readily determined by palpating the depression between two adjacent root prominences. Even for patients with non-visually detectable root prominences, the root prominences of anterior teeth can be palpated. The deepest point of the depression indicates the middle point between the two adjacent roots. Then, the entry point is marked with an explorer or probe, and an indentation is made on the gingiva, followed by visual confirmation of the mesiodistal position of the entry point from the occlusal side (Figure 4.30). Specifically, the soft tissue indentation should be parallel to the long axes of the two adjacent teeth. If the designated entry point is apical to the mucogingival junction, special attention should be paid to keep the marked entry point stable during the whole procedure due to the removability of the soft tissue beyond mucogingival junction.

Lastly, the mini-implant is inserted through the determined entry point. Angled insertion is recommended with the insertion angulation being 0–30° (Figure 4.31). Moreover, the mini-implant should be inserted perpendicular to the tangent line at the midpoint between two

t.me/Dr_Mouayyad_AlbtousH

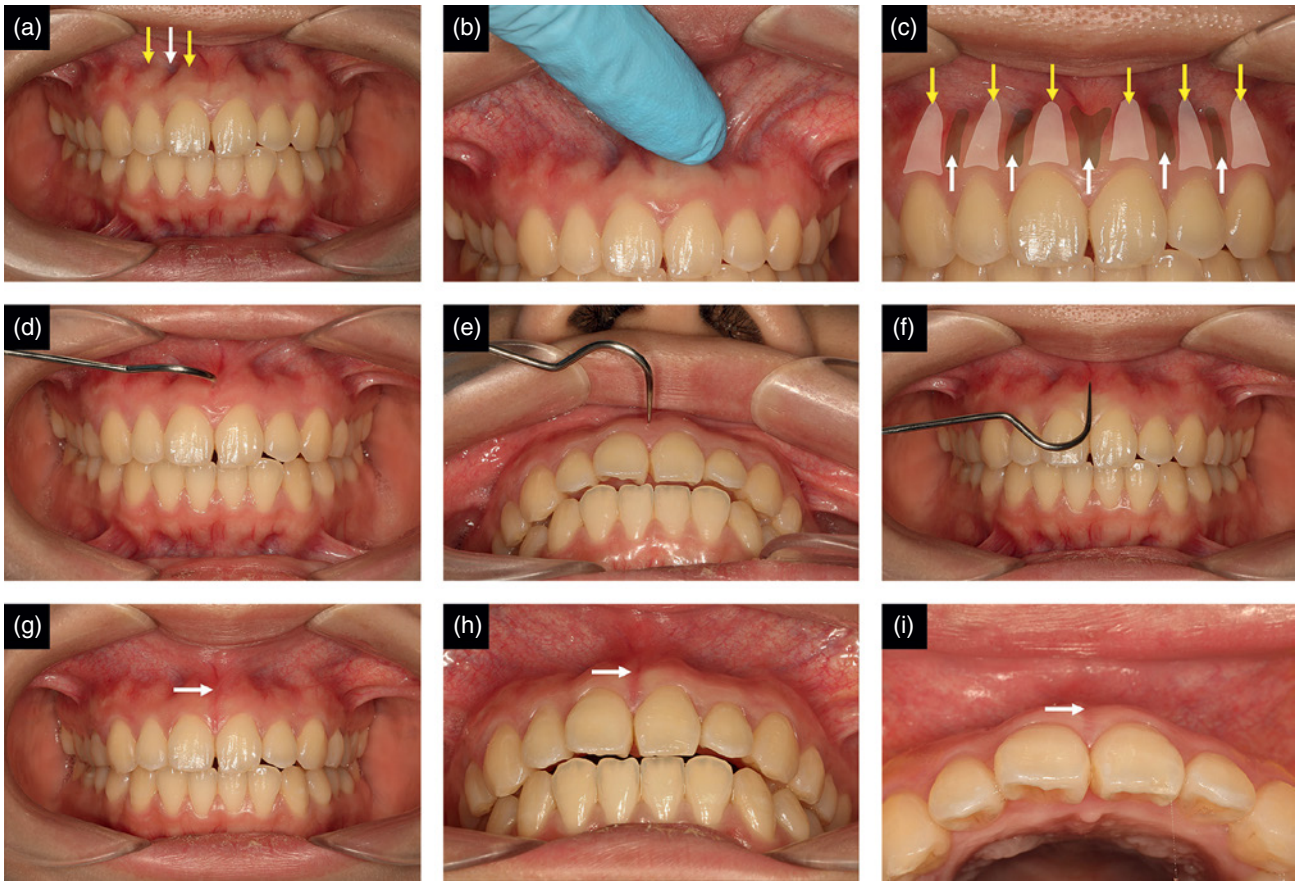


Figure 4.30 Determination and marking of the desired entry point. (a) The frontal intraoral photograph showing root prominences (yellow arrows) and interradicular depressions (white arrow). (b) Manual palpation of root prominences and interradicular depressions. (c) Close-up view of root prominences (yellow arrow) and interradicular depressions (white arrow). (d,e) Mark the entry point with an explorer. (f) Mark a vertical soft tissue indentation. (g–i) Check the orientation of the soft tissue indentation (white arrow) from all directions.

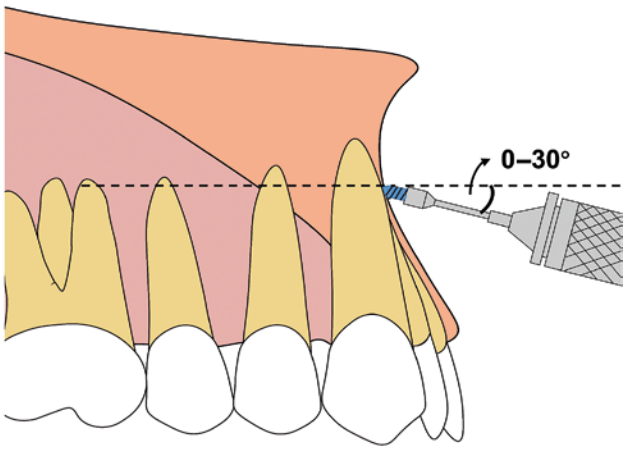


Figure 4.31 A schematic illustration showing the recommended insertion angulation. The mini-implant is inserted at an angle of 0–30° to the occlusal plane.

adjacent teeth (Figure 4.32). We recommend the operator sit at the 11 o'clock position and ask the patient to adjust his or her head to allow the operator's line of view to coincide with the normal line of the dental arch passing through the entry point (Figure 4.33). Once insertion is complete, both the vertical and mesiodistal positions of mini-implants should be checked.

The procedures of inserting a mini-implant at this region are displayed in Figures 4.34 and 4.35.

4.2.5 Clinical Applications

Incisor Intrusion

A female adult patient presented to the orthodontic department with a chief complaint of deep bite. As shown in Figure 4.36, this patient had a straight facial profile, with

t.me/Dr_Mouayyad_AlbtousH

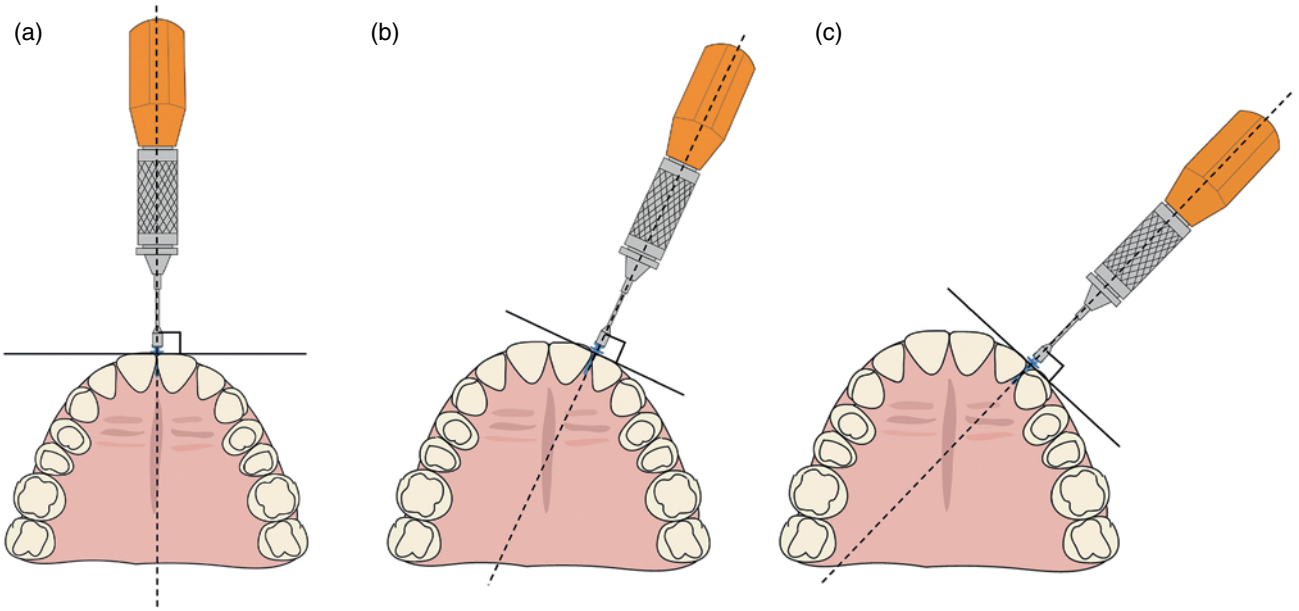


Figure 4.32 The insertion path (dashed line) should be perpendicular to the tangent line (solid line). (a) U1-U1 site. (b) U1-U2 site. (c) U2-U3 site.

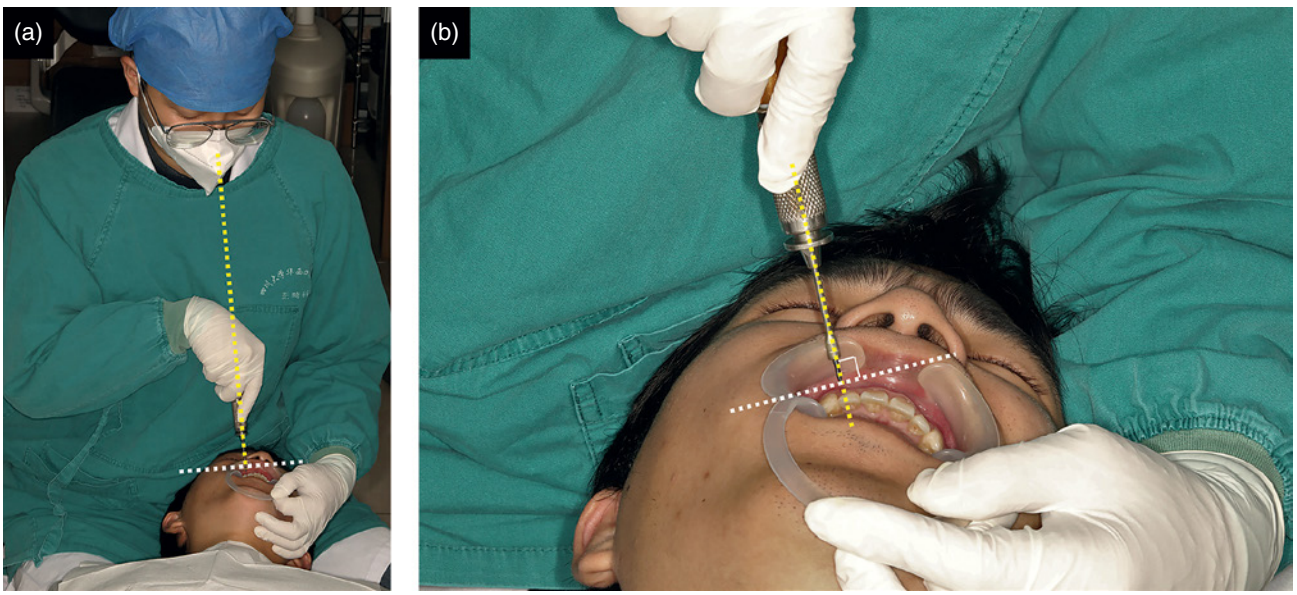


Figure 4.33 Adjustment of the patient's head to allow the operator's line of view to coincide with the normal line of the dental arch passing through the entry point. (a) The operator sat at the 11 o'clock position and the patient was instructed to tilt his head to the left side so that the operator's line of view (yellow dashed line) passed through the midpoint between the two adjacent roots. (b) Close-up view. The operator's line of view (yellow dashed line) was perpendicular to the tangent line of the dental arch.

both the upper and lower lips on the E-line. She had a slight class II molar relationship at both sides with severe deep bite and mild crowding in both arches. The left maxillary second molar and left mandibular second molar were in Brodie bite. She had two peg-shaped maxillary lateral incisors with an abnormal Bolton ratio for anterior teeth (0.88). The lateral cephalometry was indicative of class I skeletal base (ANB = 2.1), average mandibular plane angle

t.me/Dr_Mouayyad_AlbtousH

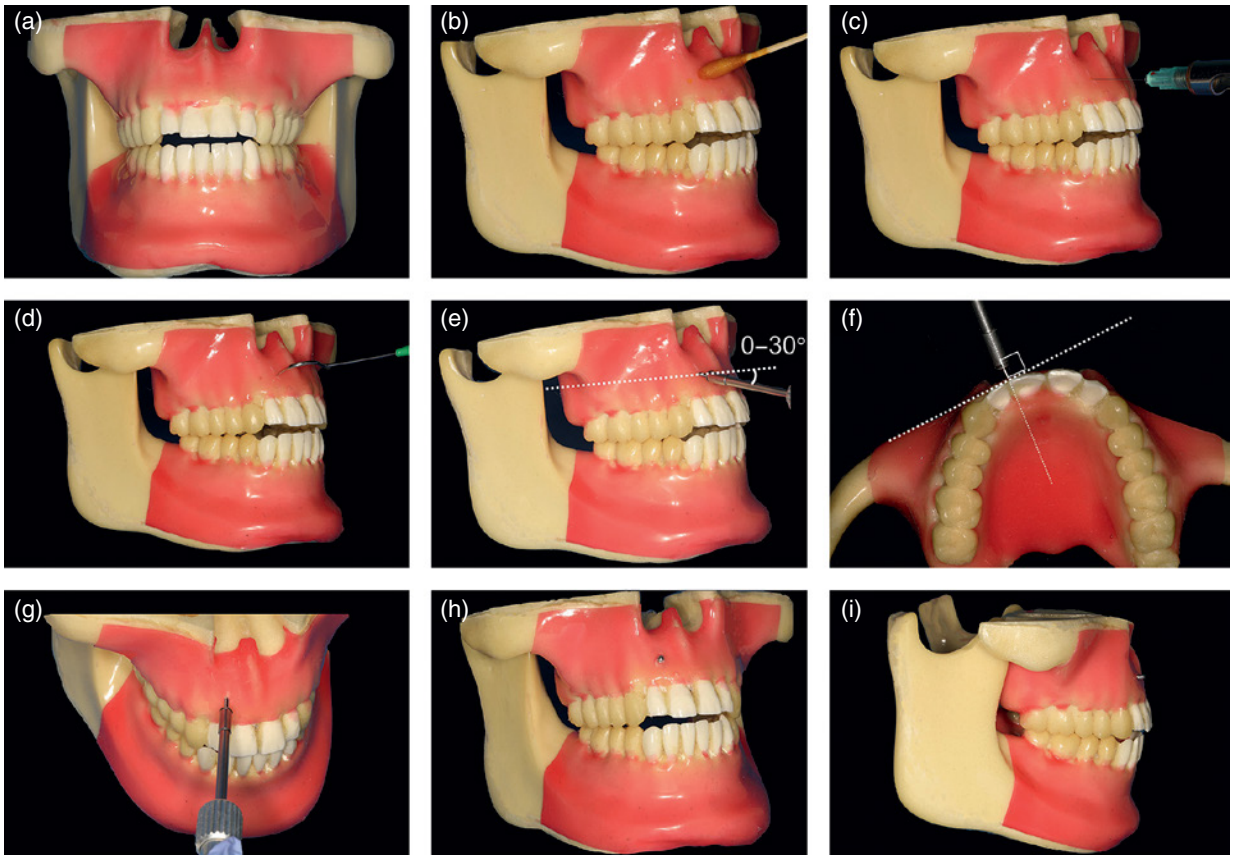


Figure 4.34 Detailed procedures for inserting a mini-implant at the U1-U2 interradicular site on a skull model. (a) Before insertion. (b) Mucosal disinfection. (c) Local infiltration anaesthesia. (d) Mark the entry point with an explorer. (e) Insert a mini-implant at an angle of 0–30° to the occlusal plane. (f) The insertion path is perpendicular to the tangent line of the arch passing through the entry point. (g) Mini-implant insertion and advancement. (h) Postinsertion (frontal view). (i) Postinsertion (sagittal view).

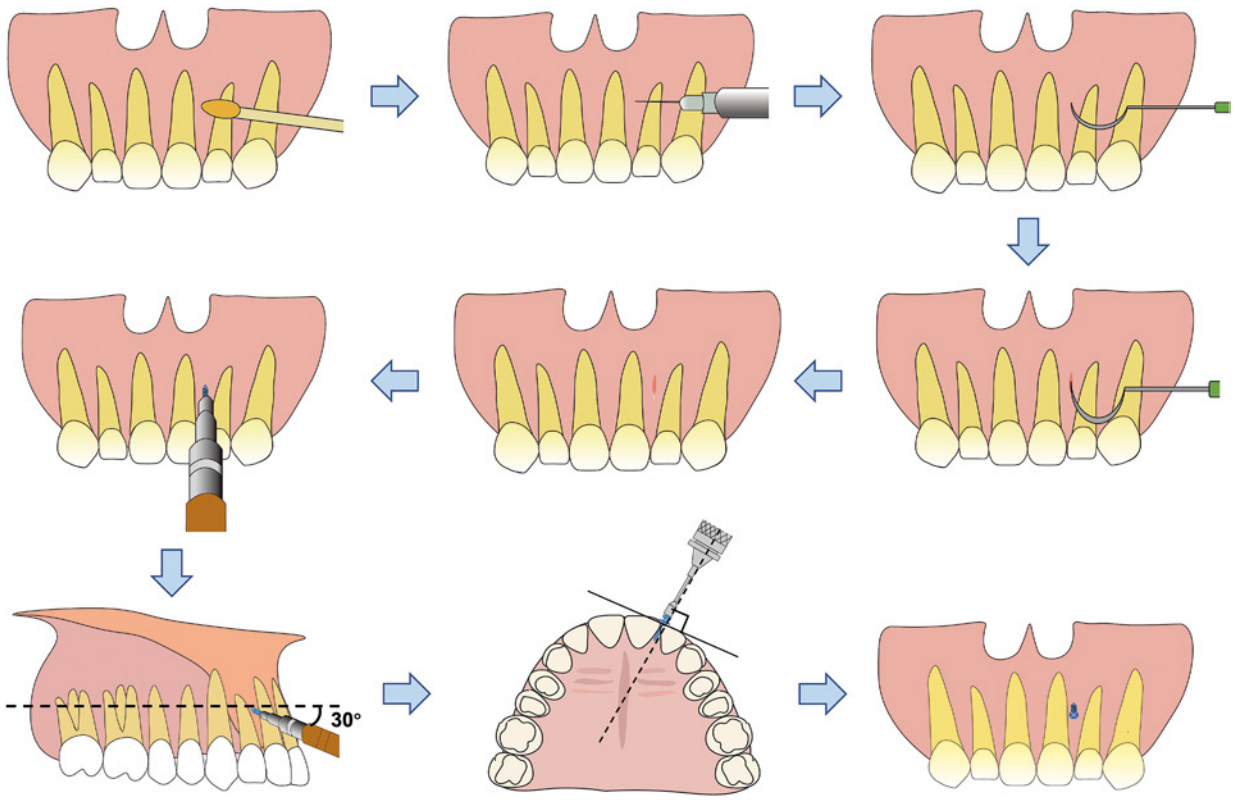


Figure 4.35 Schematic illustrations displaying detailed procedures for the insertion of a mini-implant at the labial interradicular site.

t.me/Dr_Mouayyad_AlbtousH



Figure 4.36 Pretreatment photographs and radiographs.

t.me/Dr_Mouayyad_AlbtousH

(SN-MP = 33.4) and retroclined upper incisors (U1-SN = 86.9) (Table 4.2). The treatment plan was molar distalisation with clear aligner to correct the class II molar relationship and incisor intrusion through a labial mini-implant to resolve the severe deep bite. Moreover, space was regained on both the mesial and distal sides of the lateral incisors for final veneer restoration following the active orthodontic treatment.

Table 4.2 Pretreatment cephalometric values.

Item	Case	Normal	SD
SNA	78.1	83.0	4.0
SNB	76.0	84.0	3.0
ANB	2.1	3.0	2.0
MP-SN	33.4	33.0	4.0
MP-FH	18.8	28.0	4.0
S-Go/N-Me	66.2	66.0	4.0
Y-axis	69.6	64.0	4.0
U1-L1	151.2	127.0	8.0
U1-SN	86.9	105.0	6.7
FMIA (L1-FH)	72.8	57.0	6.0
IMPA (L1-MP)	88.4	95.0	6.0
Wits value	−4.8	0.0	1.0
Upper lip E-plane (mm)	−2.3	2.0	2.0
Lower lip E-plane (mm)	−0.4	3.0	2.0

The clear aligner treatment included an initial stage of incisor intrusion and proclination, and the correction of posterior Brodie bite, followed by molar distalisation with alternate lower incisor and canine intrusion for lower arch levelling (Figure 4.37). A labial mini-implant was inserted at the interradicular site between the two central incisors to aid use of a clear aligner for incisor intrusion through elastic rubbers (Figure 4.38). With the aid of the labial mini-implant, additional intrusive force was applied onto the upper incisors, with an anticlockwise moment that is beneficial for torquing incisor roots lingually.

The designed tooth movement progressed smoothly during the treatment with the deep bite corrected gradually (Figure 4.39). Following the active orthodontic treatment, veneer restoration was performed for the bilateral peg-shaped lateral incisors. A good buccal interdigitation and normal incisor overbite were finally achieved (Figure 4.40).

Correction of Gummy Smile

A female adult patient sought orthodontic treatment with a chief complaint of crooked teeth and lip protrusion. As shown in Figure 4.41, clinical and radiographic

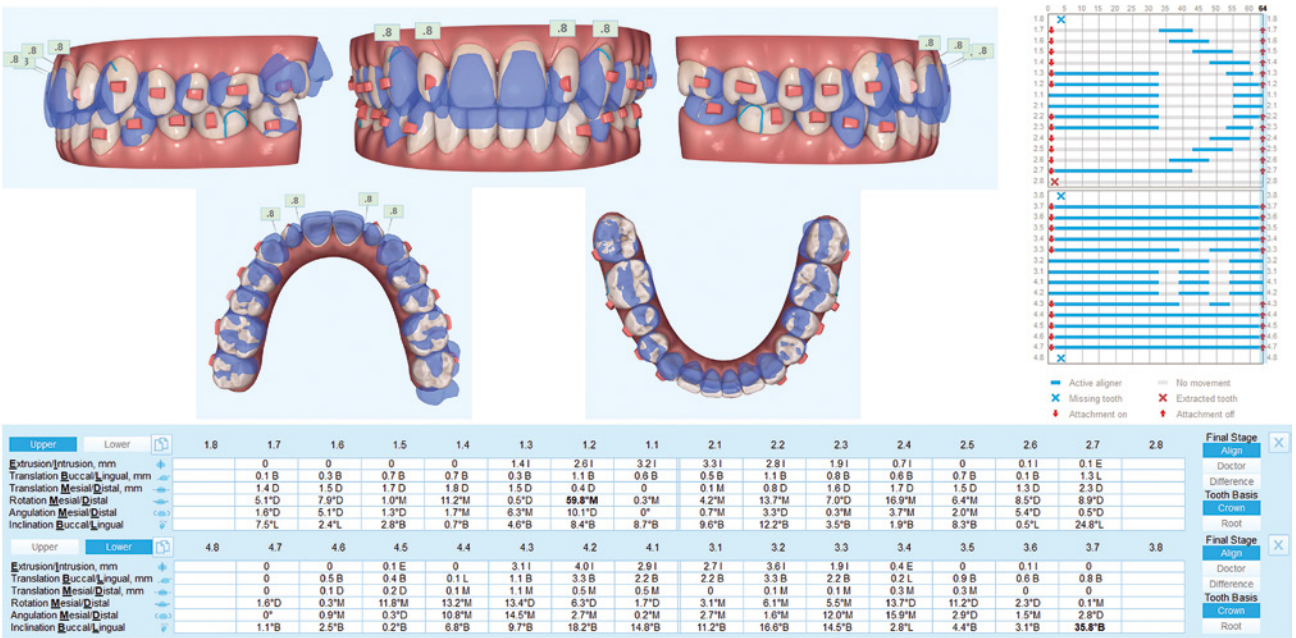


Figure 4.37 Pretreatment versus posttreatment superimposition, treatment staging and planned tooth movements.

t.me/Dr_Mouayyad_AlbtousH

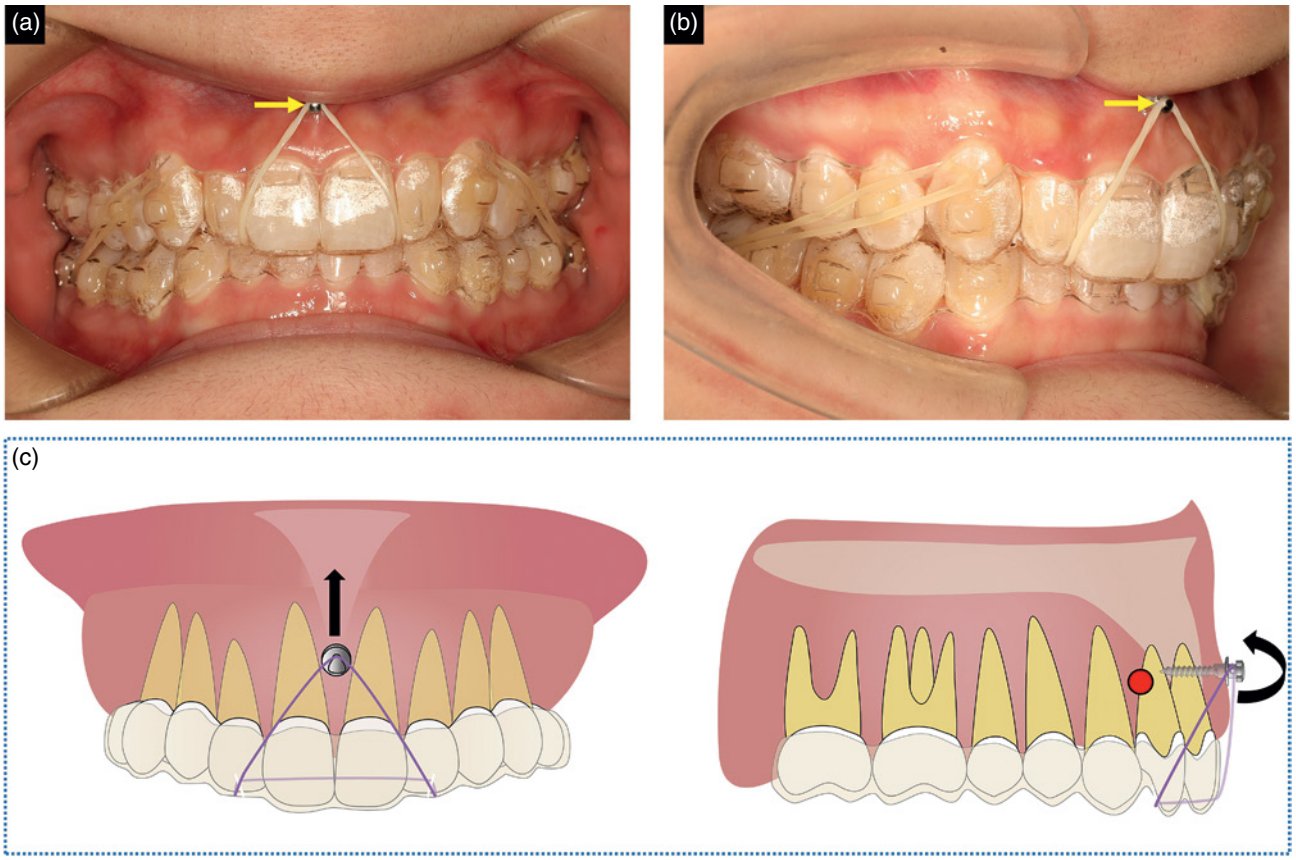


Figure 4.38 Anterior intrusion using a labial interradicular mini-implant with clear aligner. (a,b) An elastic rubber was applied between the clear aligner and the labial mini-implant (yellow arrow). (c) Biomechanical analysis. As the intrusion force passes labially to the centre of resistance (red dot) for the anterior teeth, an anticlockwise moment is generated, resulting in simultaneous intrusion and proclination of the maxillary anterior teeth.

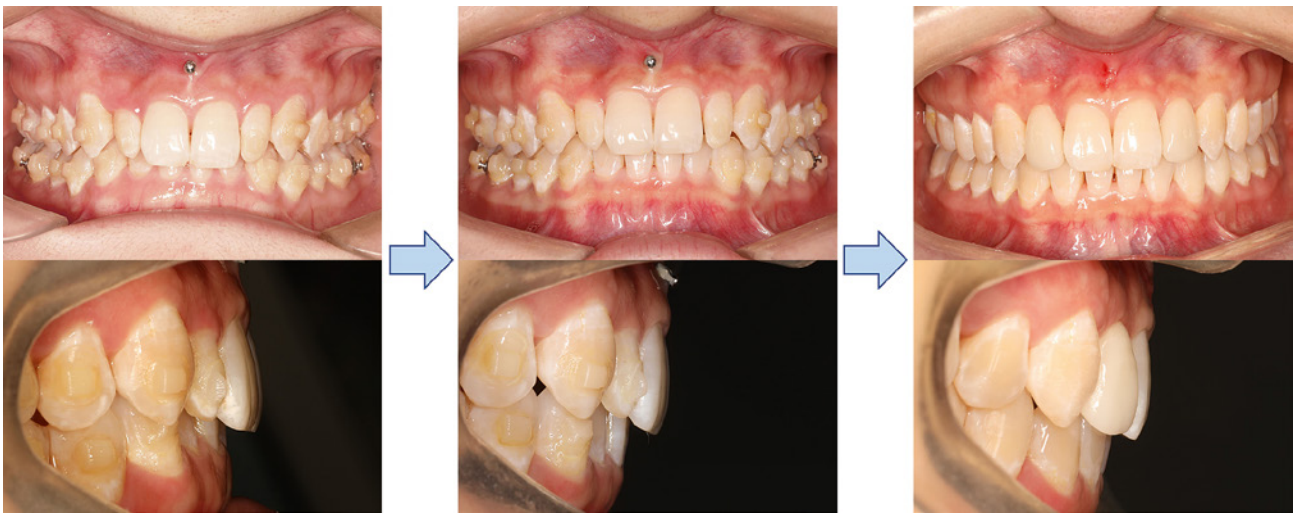


Figure 4.39 The severe deep bite was gradually corrected.

t.me/Dr_Mouayyad_AlbtousH



Figure 4.40 Posttreatment photographs and radiographs.

t.me/Dr_Mouayyad_AlbtousH



Figure 4.41 Pretreatment photographs and radiographs.

t.me/Dr_Mouayyad_AlbtousH

examinations were indicative of convex facial profile and chin deficiency with slight lip incompetence and mentalis strain. She had a class II molar relationship on both sides with mild upper arch crowding and moderate lower arch crowding. Lateral cephalometric analysis revealed that she had a class II skeletal base (ANB = 7.1), mandibular deficiency (SNB = 70.1), high angle (SN-MP = 45.3), retroclined upper incisors and proclined lower incisors (U1-SN = 93.9; L1-MP = 101.7) (Table 4.3). The treatment plan was extractions of four first premolars and anterior retraction with the aid of two buccal mini-implants. With anterior retraction, the convex facial profile would be resolved.

Table 4.3 Pretreatment cephalometric values.

Item	Case	Normal	SD
SNA	77.2	82	3
SNB	70.1	78	3
ANB	7.1	4	2
MP-SN	45.3	35.0	4
MP-FH	32.0	29.0	4
S-Go/N-Me	56.7	67.0	4
Y-Axis	79.8	65.0	4
U1-L1	119.2	121.0	9
U1-SN	93.9	107.0	6
FMIA (L1-FH)	46.3	58.8	6
IMPA (L1-MP)	101.7	95.6	6
Wits Value	2.9	0.8	1
Upper lip-E plane (mm)	0.6	0.8	2
Lower lip-E plane (mm)	3.8	1.4	3

The buccal mini-implants were on one hand to reinforce molar anchorage and on the other hand to intrude molars through the clockwise rotation of the upper dentition so that anticlockwise rotation of mandible would be achieved (Figure 4.42). The adverse effect of this biomechanical design was the occurrence of bite deepening and the patient was informed of this adverse effect and the possible insertion of a labial mini-implant for deep bite correction.

During the anterior retraction stage, the patient presented with severe deep bite with gummy smile. Thus, a labial mini-implant was placed at the interradicular site between central incisors (Figure 4.43). With the aid of the labial mini-implant, the anterior deep bite and gummy smile were resolved gradually (Figure 4.44).

Following orthodontic treatment, class I molar relationship and normal overbite and overjet were achieved. Straight facial profile and smile aesthetics were accomplished with absence of gummy smile and mentalis strain (Figure 4.45). The comparison of the pre- and posttreatment cephalometric values is displayed in Table 4.4.

Correction of Occlusal Canting

A female adolescent presented to the orthodontic department with a chief complaint of deep bite and crooked

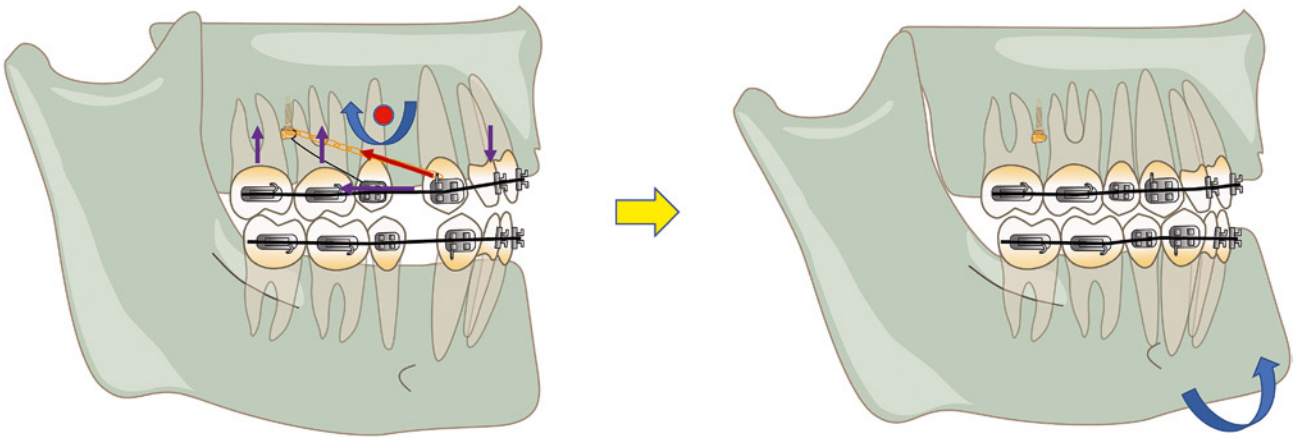


Figure 4.42 Biomechanical analysis. As the retraction force passes occlusally to the centre of resistance for the whole maxillary dentition, clockwise moment is generated. This leads to clockwise rotation of the maxillary dentition, resulting in extrusion of the maxillary anterior teeth, intrusion of the maxillary posterior teeth and subsequent anticlockwise rotation of the mandible.

t.me/Dr_Mouayyad_AlbtousH

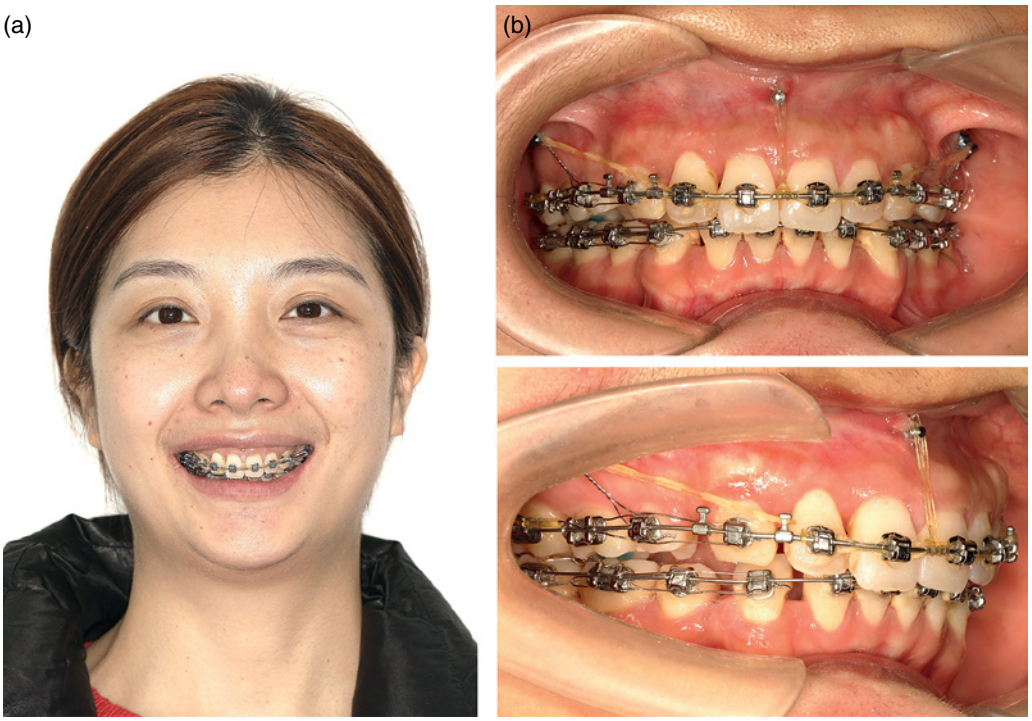


Figure 4.43 Progress photographs. (a) The patient presented with deep bite with gummy smile. (b) A labial interradicular mini-implant was inserted to aid in the correction of deep bite and gummy smile.



Figure 4.44 Deep bite and gummy smile were gradually resolved.

t.me/Dr_Mouayyad_AlbtousH



Figure 4.45 Posttreatment photographs and radiographs.

t.me/Dr_Mouayyad_AlbtousH

Table 4.4 Comparison of pretreatment versus posttreatment cephalometric values.

Item	Pretreatment	Posttreatment
SNA	77.2	77.3
SNB	70.1	70.7
ANB	7.1	6.6
MP-SN	45.3	43.7
MP-FH	32.0	31.1
S-Go/N-Me	56.7	59.0
Y-axis	79.8	77.8
U1-LI	119.2	129
U1-SN	93.9	84.0
FMIA (L1-FH)	46.3	55.6
IMPA (L1-MP)	101.7	93.3
Wits value	2.9	−0.2
Upper lip E-plane (mm)	0.6	−0.8
Lower lip E-plane (mm)	3.8	−0.7

teeth. As shown in Figure 4.46, upon clinical examination, we found that she had a class I molar relationship on both sides with mild upper arch crowding and moderate lower arch crowding. She had a convex facial profile and upper and lower lips protruding beyond the E-line. In particular, an obvious occlusal canting was noticeable. Lateral cephalometry was indicative of class II skeletal base (ANB = 5.8), normal mandibular angle (SN-MP = 34.9) and normoclined upper incisors and proclined lower incisors (U1-SN = 107.5; L1-MP = 101.2) (Table 4.5).

The treatment plan was extraction of four first premolars and anterior retraction with moderate molar anchorage. Following extraction of the four first premolars, anterior crowding was resolved but the occlusal canting was still present (Figure 4.47). A labial mini-implant at the interradicular site between the right lateral incisor and canine was planned for correction of the occlusal canting (Figure 4.48). Then, a labial mini-implant was placed at the interradicular site between the right upper lateral incisor and canine to correct occlusal canting. The occlusal canting was corrected gradually with the aid of this labial mini-implant (Figure 4.49).

4.3 Anterior Nasal Spine

4.3.1 Anatomical Features

The anterior nasal spine (ANS) is a bony protuberance of the maxilla at the base of the nose and is formed by the fusion of two maxillary halves at the intermaxillary suture (Figure 4.50). It is located apically to the root apices of the maxillary central incisors and starts at the 10 mm height apical to the CEJ. It is a viable alternative anatomical site for labial mini-implants if limited interradicular space prevents placement at interradicular sites. Due to the absence of dental roots at this region, this region belongs to the extra-alveolar zone and is covered by thick soft tissue. Thus, oblique insertion with large insertion angles is required to achieve adequate emergence profile of mini-implants so that ease of force loading can be guaranteed. When evaluating the optimal insertion site for mini-implants placed at this region, optimal insertion angle should be taken into consideration.

Hard Tissue Factor: Cortical Thickness

The cortical thickness increases with increase in insertion height, indicating that greater cortical engagement can be obtained with a more apical entry (Figure 4.51). However, cortical thickness peaks at the 22 mm level and then drops down at the height of 24 mm. The 22 mm height level with greatest cortical thickness corresponds to the sharp edge of the ANS. Moreover, increasing the insertion angle results in greater cortical engagement, with the cortical thickness being the greatest at an insertion angle of 45°. The requirement of cortical thickness (>1 mm) is satisfied for all the insertion heights and insertion angles. Thus, all insertion heights and angles can be clinically employed in terms of cortical thickness.

Hard Tissue Factor: Bone Depth

For horizontal insertion, bone depth remains constant (greater than 8 mm) at all heights and is adequate for mini-implant insertion (Figure 4.52). In contrast, bone depth decreases with an increase in insertion height, starting from the 10 mm height level for angled insertion and bone depth may be inadequate for insertion heights greater than 18 mm. However, bone depth may be inadequate for the insertion angle of 60° at the 16–24 mm levels. This general

t.me/Dr_Mouayyad_AlbtousH

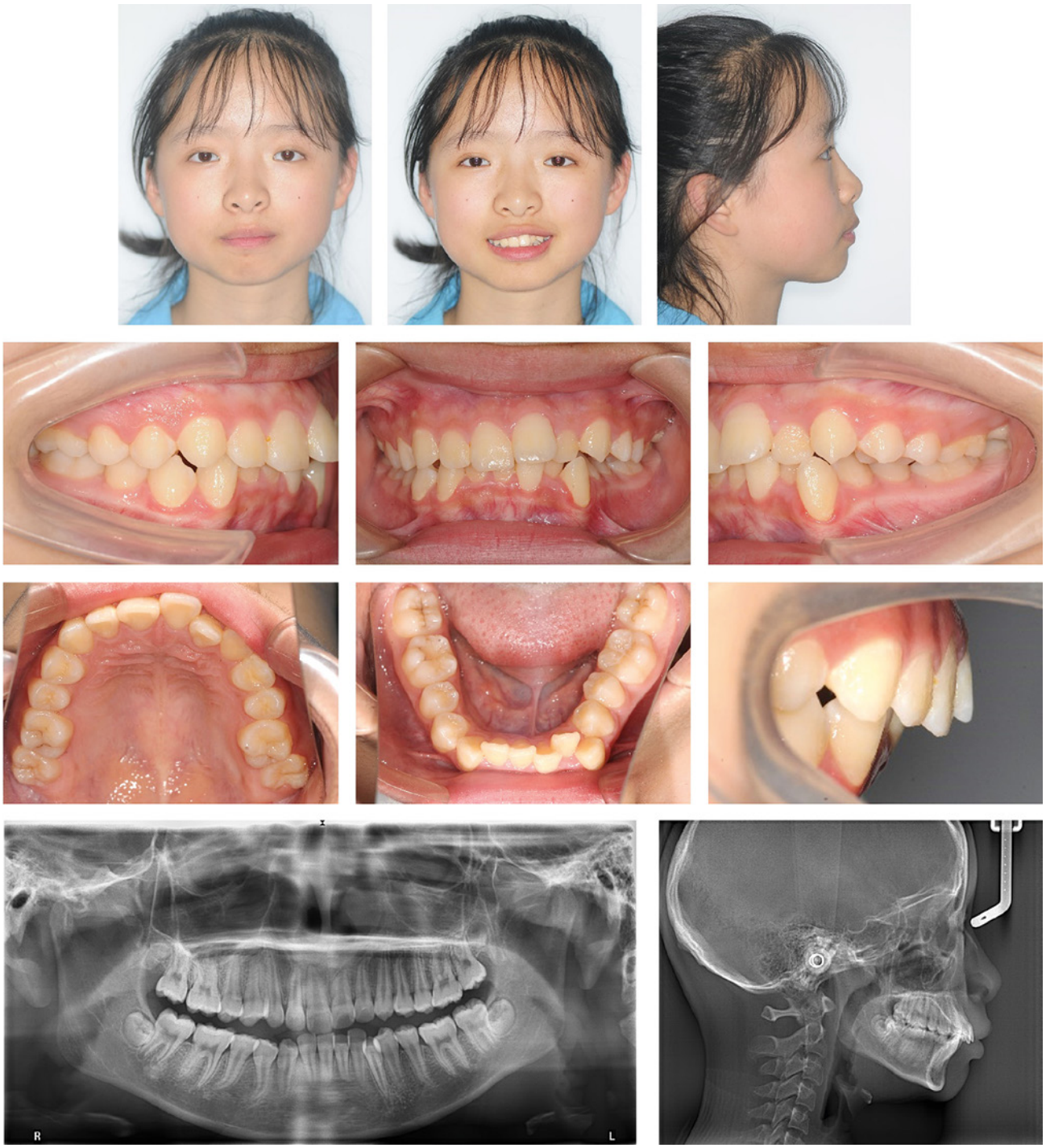


Figure 4.46 Pretreatment photographs and radiographs.

t.me/Dr_Mouayyad_AlbtousH

trend of reduction in bone depth with increasing insertion angle may be attributed to the limitation of contralateral nasal cortex. Thus, in terms of bone depth, all insertion angles (except for 60°) and insertion heights of 12–18 mm can be chosen.

Table 4.5 Pretreatment cephalometric values.

Item	Case	Normal	SD
SNA	82.0	83.0	4.0
SNB	76.2	84.0	3.0
ANB	5.8	3.0	2.0
MP-SN	34.9	33.0	4.0
MP-FH	22.3	28.0	4.0
S-Go/N-Me	63.3	66.0	4.0
Y-axis	71.3	64.0	4.0
U1-L1	116.4	127.0	8.0
U1-SN	107.5	105.0	6.0
FMIA (L1-FH)	56.5	57.0	6.0
IMPA (L1-MP)	101.2	95.0	6.0
Wits value	0.5	0.0	1.0
Upper lip E-plane (mm)	3.3	2.0	2.0
Lower lip E-plane (mm)	3.9	3.0	2.0

Hard Tissue Factor: Bone Width

The ANS is a blade-shaped bony protuberance projecting anteriorly (Figure 4.53). Due to the sharp edge of the ANS, slippage of a mini-implant may occur during placement (Figure 4.54). Moreover, cortical fractures or cracks may be encountered if mini-implants are placed at the ANS with sharp edges (Figure 4.55). Thus, measures should be taken to avoid bone fractures due to the presence of sharp edges. Specifically, prior to insertion, sharp edges can be removed to form a bone platform with at least 2 mm width. Since a bony platform of 2 mm width can accommodate commonly used mini-implants (diameter: 2 mm), bone fractures and slippage of mini-implants can be avoided (Figure 4.56).

Soft Tissue Factor: Labial Frenum

Due to the deep location of the ANS and the presence of thick soft tissues, frenectomy and flapping surgery are indicated to expose this region and facilitate insertion (Figure 4.57).

Soft Tissue Factor: Mucogingival Junction

Due to the presence of labial frenum and thick soft tissue covering the ANS, long mini-implants (10 mm or 12 mm) should be used to achieve adequate bone engagement and adequate emergence profile simultaneously. To prevent soft tissue complications, the heads of mini-implants should be located at the level of the mucogingival junction

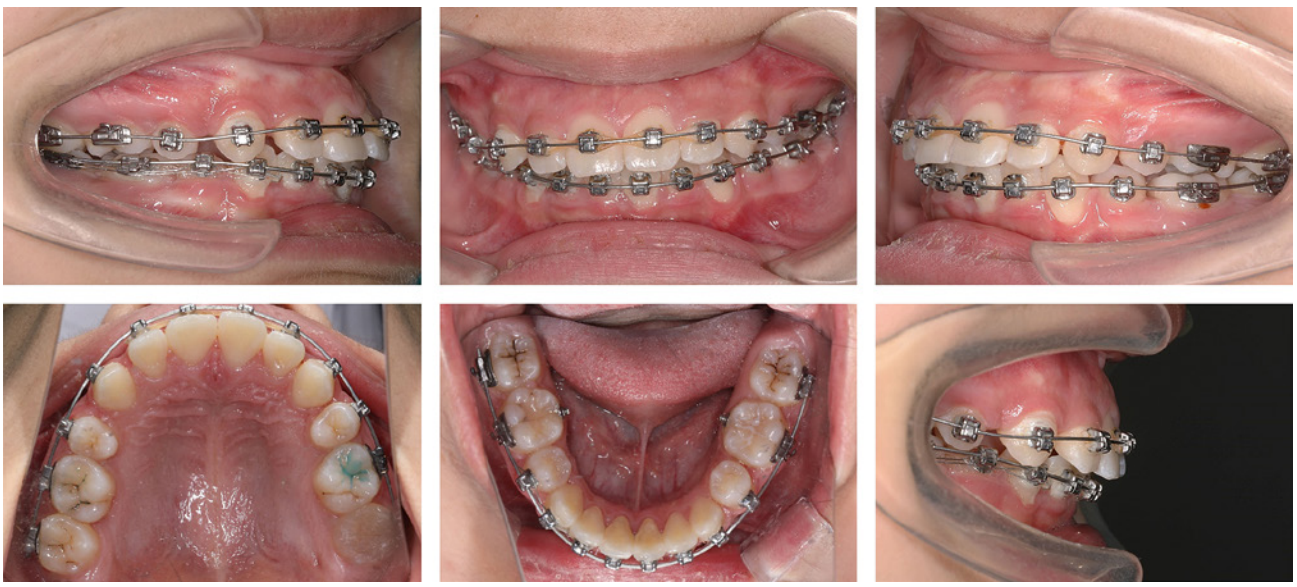


Figure 4.47 Progress photographs. The occlusal canting was still present.

t.me/Dr_Mouayyad_AlbtousH

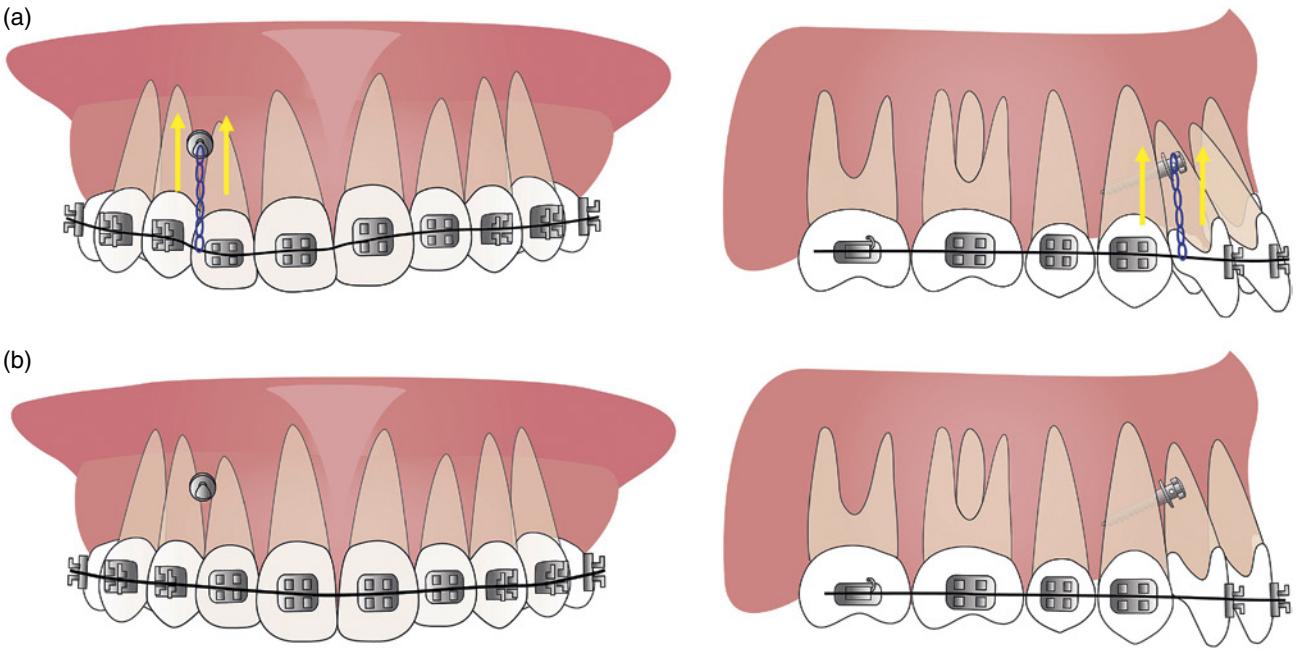


Figure 4.48 A schematic illustration of the correction of the occlusal canting through a mini-implant at the U2-U3 interradicular site. (a) A mini-implant is inserted at the U2-U3 interradicular site and an elastomeric chain is applied for intrusion of the lateral incisor and canine. The intrusive force is indicated by the yellow arrows. (b) The correction of the occlusal canting.

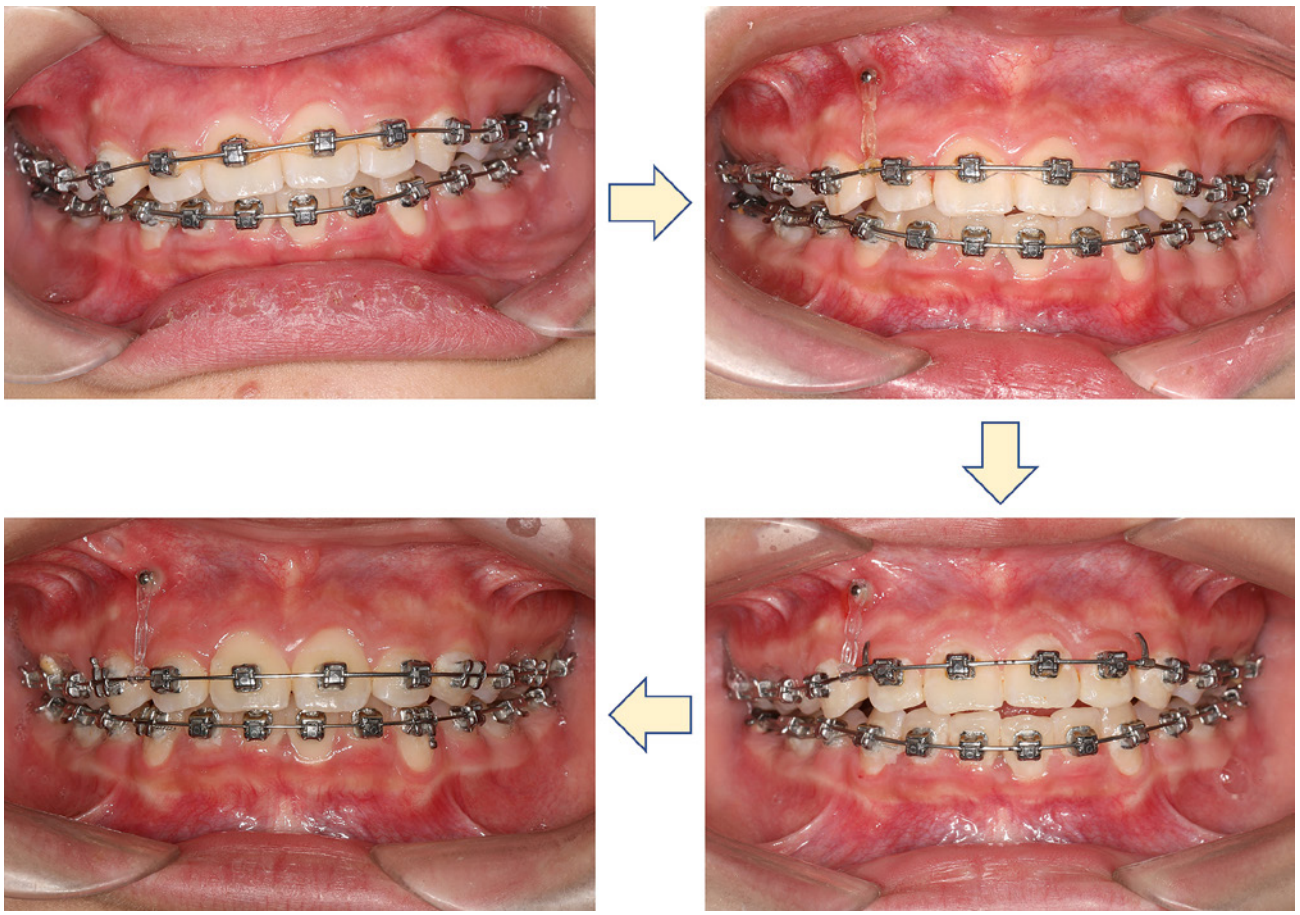
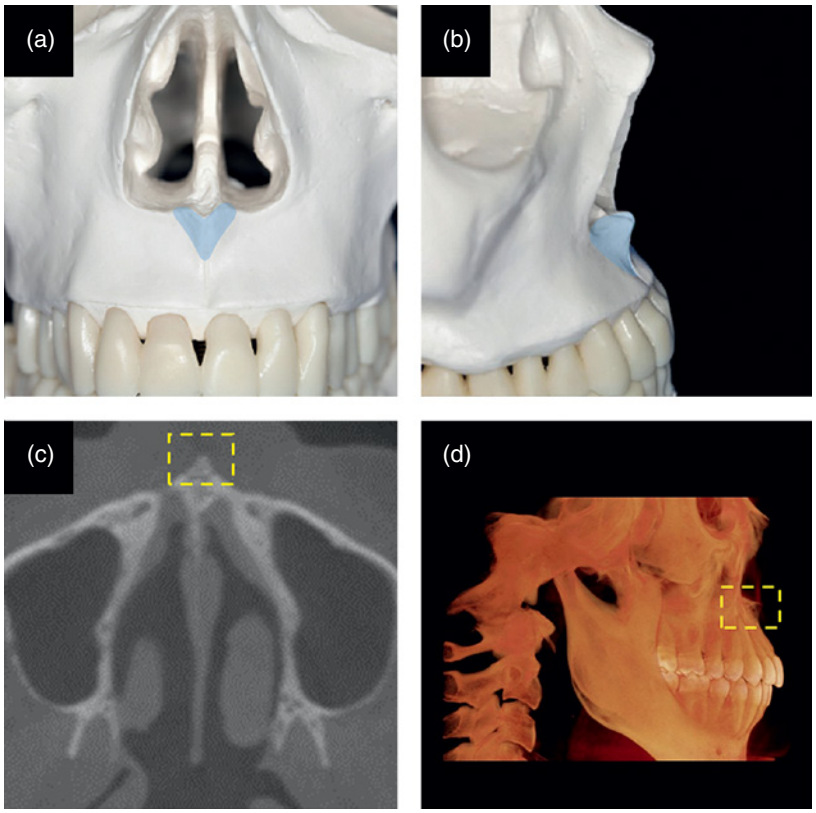
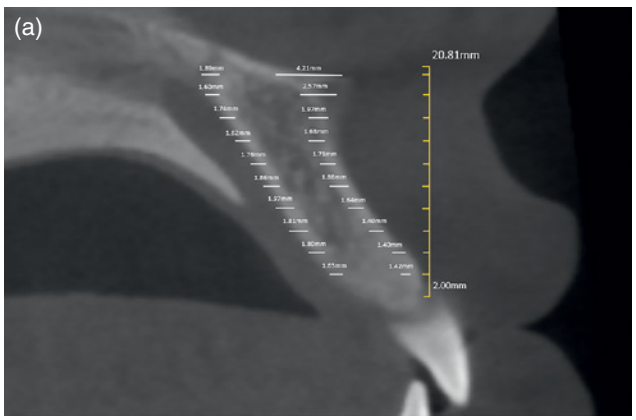


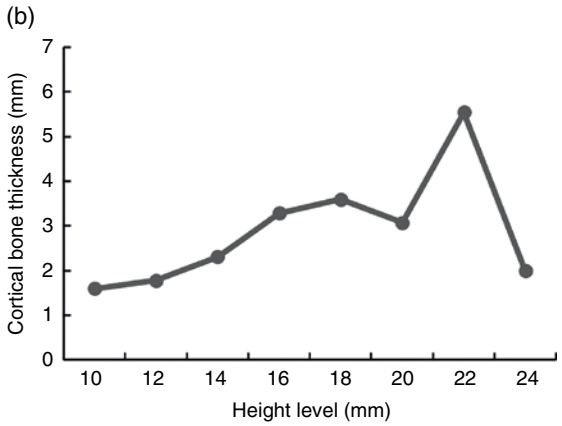
Figure 4.49 The occlusal canting was gradually resolved.

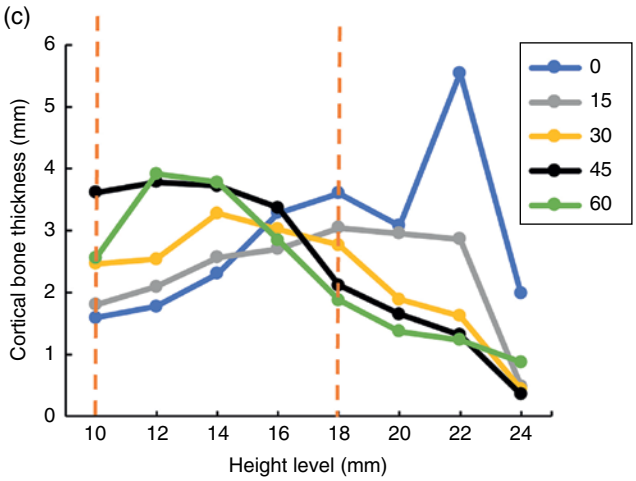
t.me/Dr_Mouayyad_AlbtousH

Figure 4.50 Anterior nasal spine. (a) Anterior nasal spine (blue area) shown on a skull (frontal view). (b) Anterior nasal spine (blue area) shown on a skull (side view). (c) Anterior nasal spine (yellow dashed rectangle) shown in a CBCT image (axial view). (d) Anterior nasal spine (yellow dashed rectangle) shown in a 3-D reconstruction.









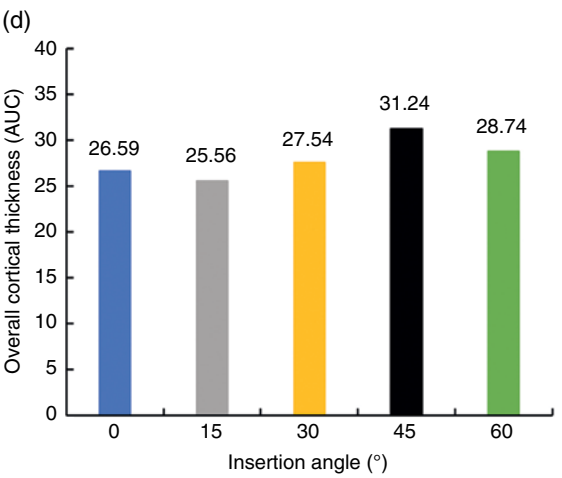


Figure 4.51 Cortical thickness of the anterior nasal spine. (a) Measurement of the cortical thickness based on CBCT image. (b) The changes of cortical thickness with the increase in insertion height (insertion angle: 0° to the occlusal plane). (c) The influence of insertion height and angle on cortical thickness. (d) Comparison of the overall cortical thickness (area under curve) between 10 mm and 18 mm among different insertion angles.

t.me/Dr_Mouayyad_AlbtousH

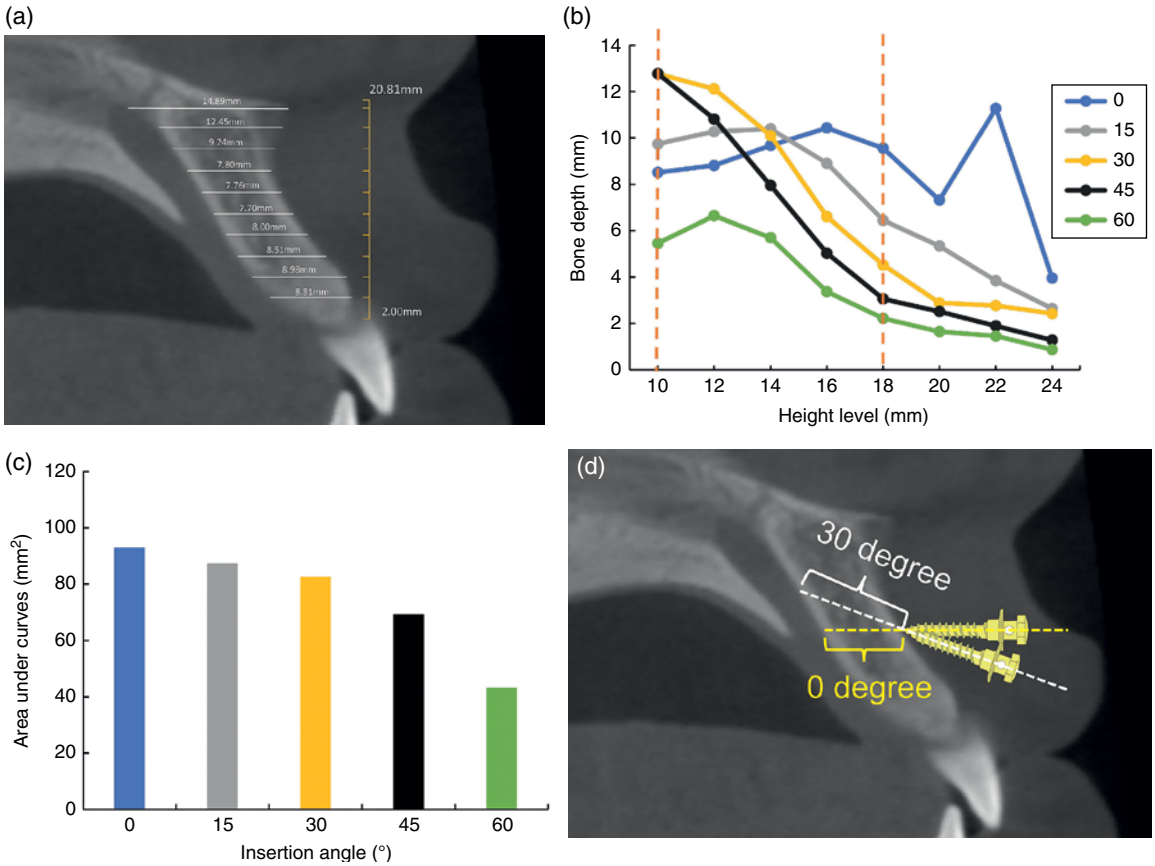


Figure 4.52 Bone depth of the anterior nasal spine. (a) Measurement of the bone depth based on CBCT image. (b) The influence of insertion height and angle on bone depth. (c) Comparison of the overall bone depth (area under curve) between 10 mm and 18 mm among different insertion angles. (d) An illustration showing different bone depths obtained with different insertion angles.

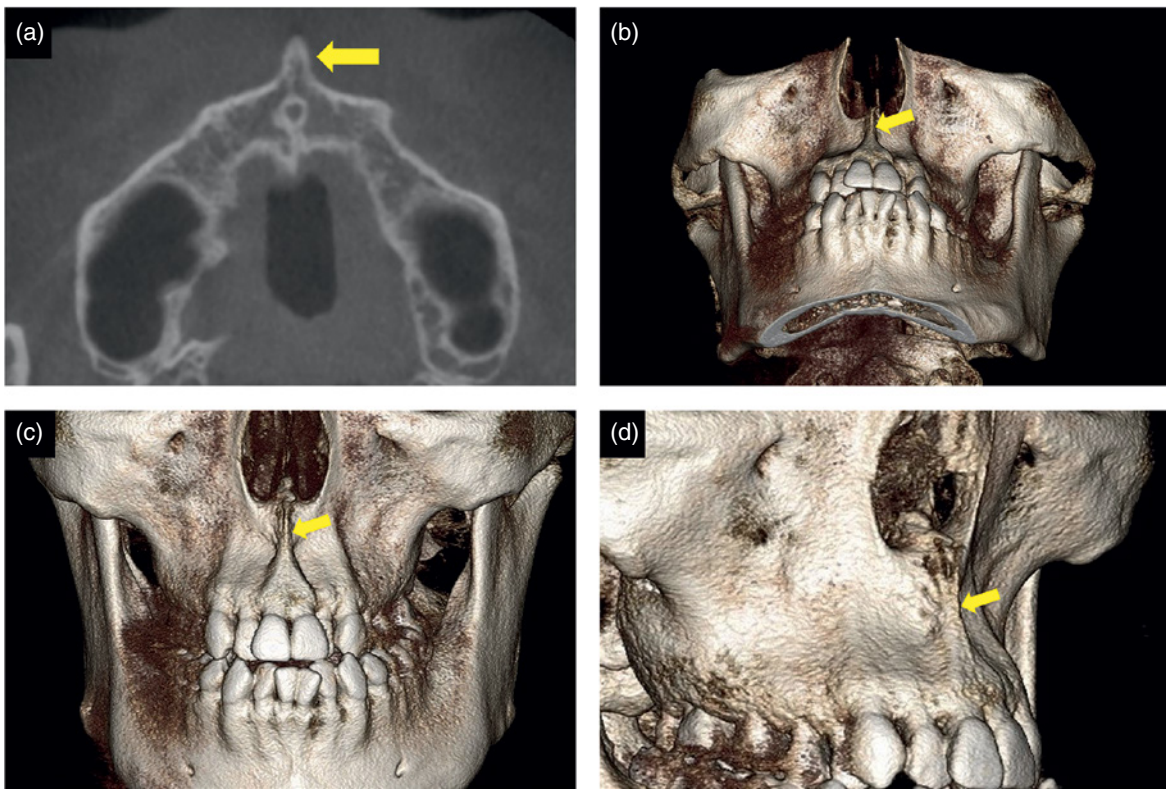


Figure 4.53 The anterior nasal spine is a blade-shaped bony protuberance protruding labially. (a) A CBCT image showing the anterior nasal spine (yellow arrow) (axial view). (b–d) 3-D reconstructions showing the anterior nasal spine (yellow arrow).

t.me/Dr_Mouayyad_AlbtousH

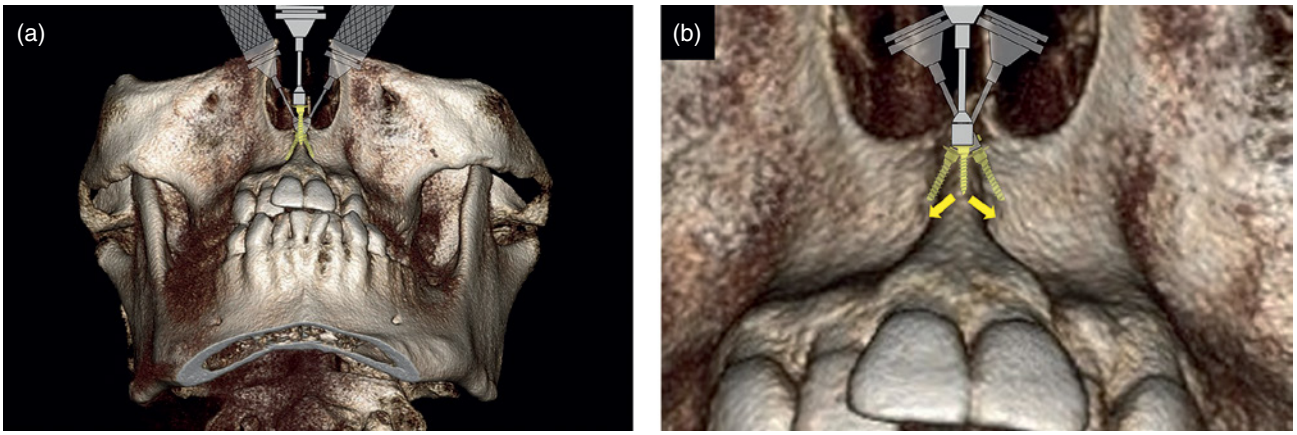


Figure 4.54 (a) An illustration showing the slippage of mini-implants that are inserted through the sharp edge of the anterior nasal spine. (b) Close-up view.

Figure 4.55 Cortical fractures and bone cracks during insertion. (a) Axial view. (b) Sagittal view.

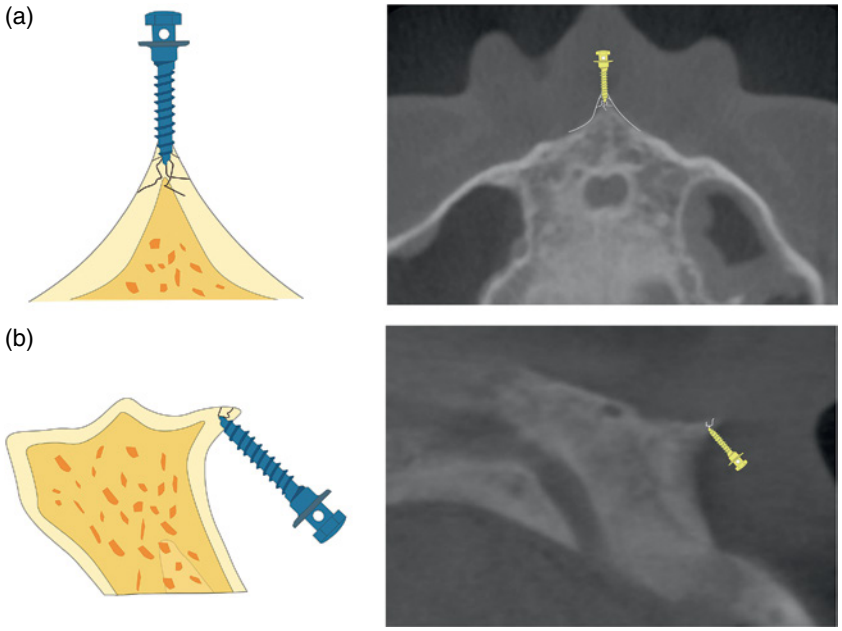
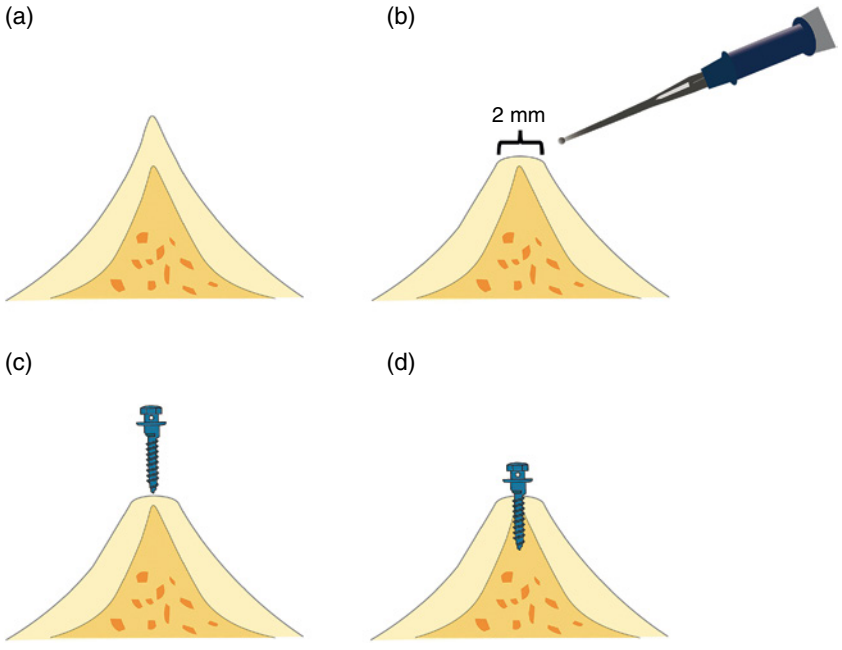


Figure 4.56 Prevention of mini-implant slippage and cortical fracture by removal of the sharp edge. (a) Preinsertion. Note the sharp edge of the anterior nasal spine. (b) Removal of the sharp edge of the anterior nasal spine. (c) Insertion of a mini-implant through the bony platform. (d) Postinsertion. Note that no or minimal cortical fractures are present.



t.me/Dr_Mouayyad_AlbtousH



Figure 4.57 Anterior nasal spine (yellow arrow) following frenectomy and flap elevation.

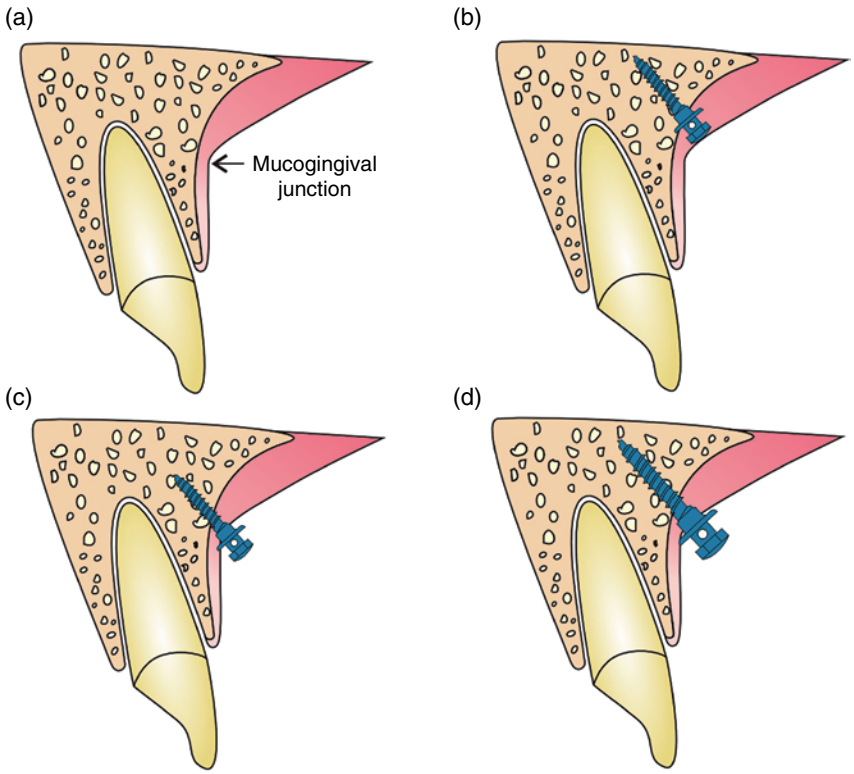


Figure 4.58 Mini-implants with adequate length are recommended. (a) Sagittal view of the alveolar bone, incisors and soft tissue. Note the position of the mucogingival junction. (b) A short mini-implant is inserted. The head is apical to the mucogingival junction and embedded into the soft tissue to obtain adequate bone engagement, which may lead to soft tissue complications. (c) To achieve adequate emergence profile, the short mini-implant is partially inserted into the bone. This may lead to mini-implant loosening or failure. (d) A long mini-implant is inserted with adequate bone engagement and sufficient emergence profile.

(Figure 4.58). Moreover, this requires angled insertion with sufficient insertion angle (45°) to be implemented since the ANS is located apically to the mucogingival junction (Figure 4.59).

4.3.2 Biomechanical Considerations

Due to similar anatomical location with the U1-U1 site, mini-implants placed at the ANS share similar biomechanical features with those inserted at the interradicular site between the two central incisors. However, due to greater versatility, the sagittal positions of the heads of ANS mini-implants can be changed by altering the insertion depth and angle (Figure 4.60). Thus, based on different requirements of the moment/force ratio of incisors, the sagittal positions of mini-implant heads can be adjusted in an acceptable range.

4.3.3 Selection of Appropriate Insertion Sites

Based on the anatomical features mentioned above, ANS mini-implants are recommended to be placed at the labial midline areas 12–18 mm apical to the CEJ with the insertion angle being 45° (Figure 4.61).

t.me/Dr_Mouayyad_AlbtousH

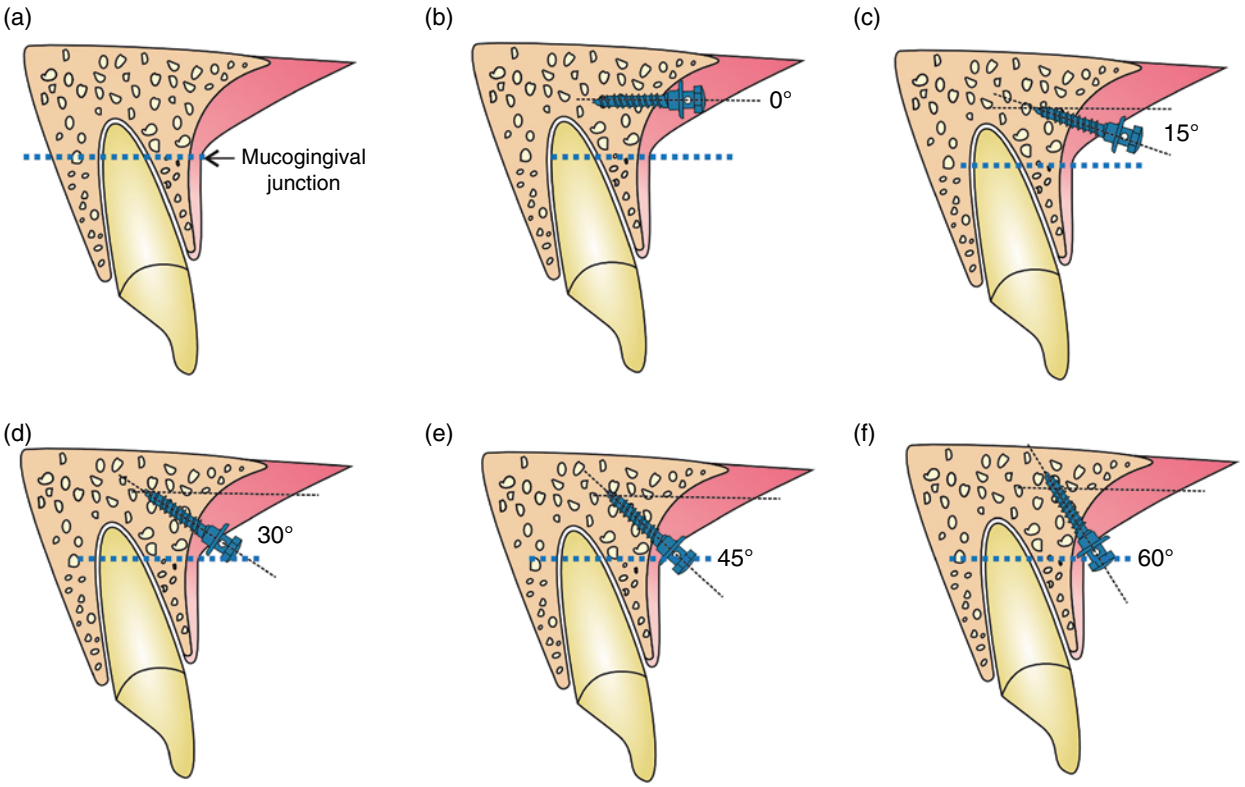


Figure 4.59 Angled technique for the insertion of mini-implants at the anterior nasal spine. (a) A schematic illustration showing alveolar bone, the maxillary central incisor and the mucogingival junction. (b) A mini-implant is inserted with an angle of 0° to the occlusal plane and the head is located apically to the mucogingival junction. Postinsertion soft tissue complications are highly likely. (c) A mini-implant is inserted with an angle of 15° to the occlusal plane and the head is located apically to the mucogingival junction. (d) A mini-implant is inserted with an angle of 30° to the occlusal plane and the head is located slightly apically to the level of the mucogingival junction. The risk of soft tissue complications is still likely. (e) A mini-implant is inserted with an angle of 45° to the occlusal plane and the head is located at the mucogingival junction. The risk of soft tissue complications is low. (f) A mini-implant is inserted with an angle of 60° to the occlusal plane and the head is located at the mucogingival junction. The risk of soft tissue complications is low.

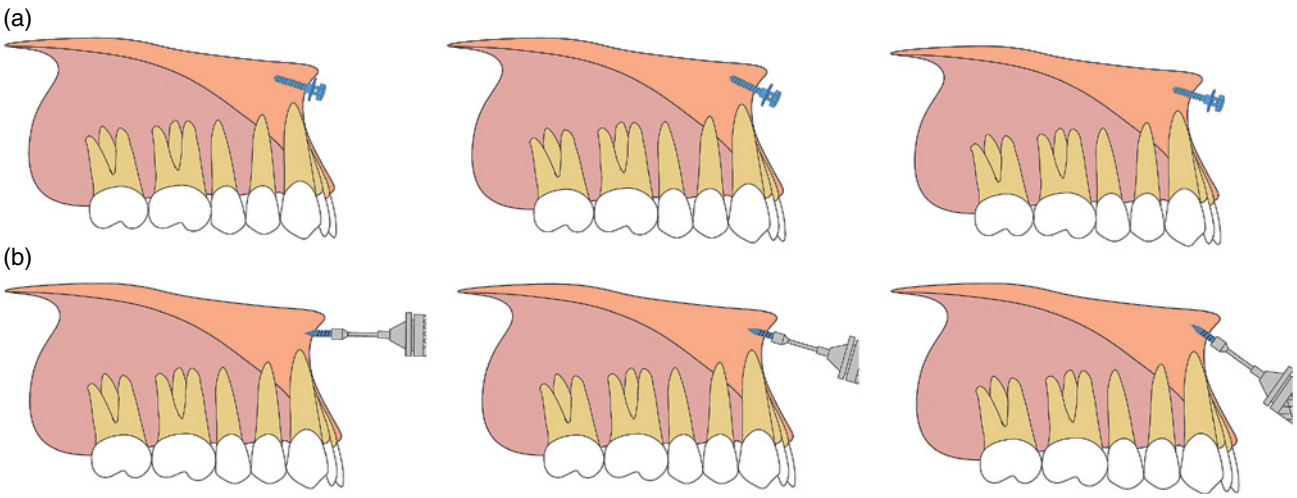


Figure 4.60 (a) The sagittal positions of the mini-implant head can be adjusted by controlling the insertion depth of the mini-implant. (b) The vertical positions of the mini-implant head can be changed by adjusting the insertion angle of the mini-implant.

t.me/Dr_Mouayyad_AlbtousH

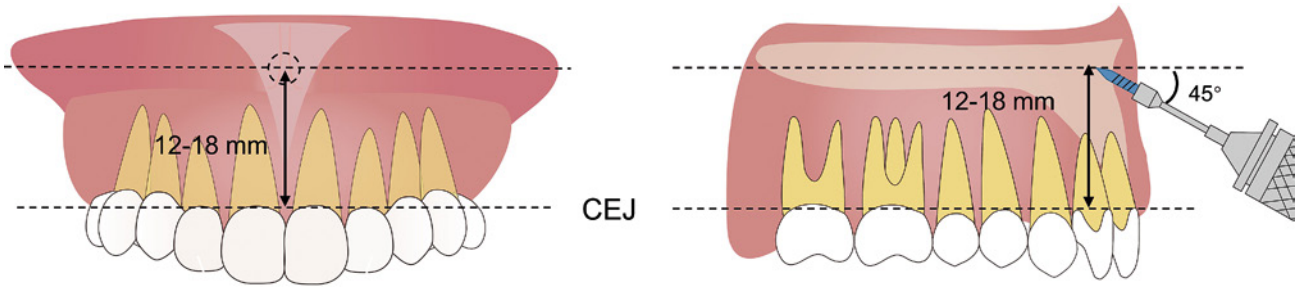


Figure 4.61 Recommended insertion height and angle for insertion of the mini-implant at the anterior nasal spine. The recommended insertion height is 12–18 mm apical to the cementoenamel junction (CEJ) with an insertion angle of 45° to the occlusal plane.

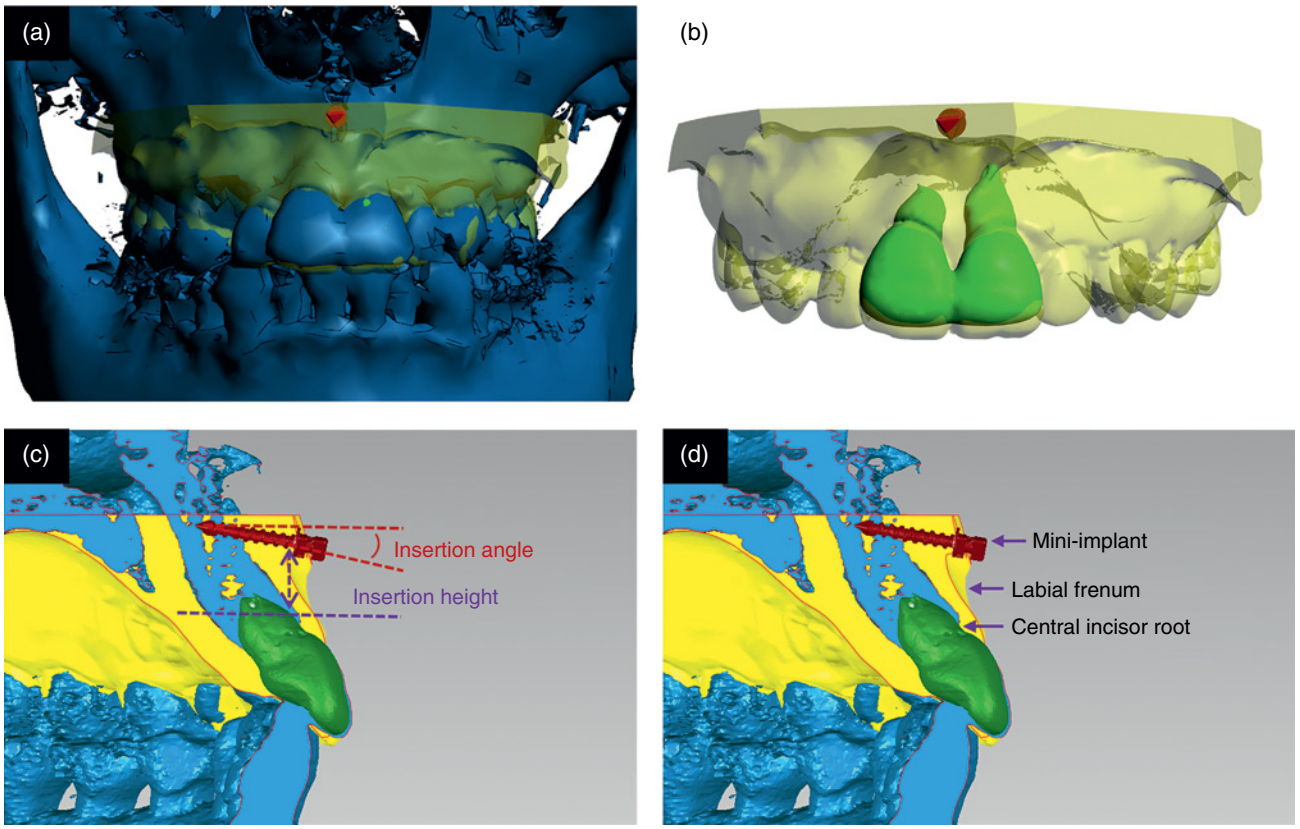


Figure 4.62 Virtual placement of a mini-implant on a digital model. (a) A mini-implant is virtually placed at the anterior nasal spine. (b) The mini-implant is virtually inserted at the anterior nasal spine that is apical to the roots of central incisors. (c) Determination of the insertion height and angle based on the sagittal view of the 3-D reconstructed image. (d) The section view shows bone engagement by the mini-implant.

4.3.4 Insertion Techniques

Since the ANS is located apical to the U1-U1 interradicular site and covered by thick soft tissue, frenectomy and flap elevation are indicated to expose this area for direct visualisation. Moreover, due to the thick soft tissue, long mini-implants (10 mm or 12 mm) are required to achieve adequate emergence profile of mini-implant heads. Occasionally, extension hooks may be needed for patients with very thick soft tissue covering the ANS.

Generally, the recommended entry point is located 12–18 mm apical to the CEJ of the central incisors. The insertion angle is recommended to be 45° to the occlusal plane. However, the entry point and insertion angle should be determined individually based on clinical radiographic examinations. With computer-aided design (CAD), both hard and soft tissues can be included in a 3D-reconstructed model and a mini-implant can be virtually placed into this model. This simulation allows practitioners to directly visualise the anatomical site and the mini-implant and to determine the optimal entry point and insertion angle (Figure 4.62).

t.me/Dr_Mouayyad_AlbtousH

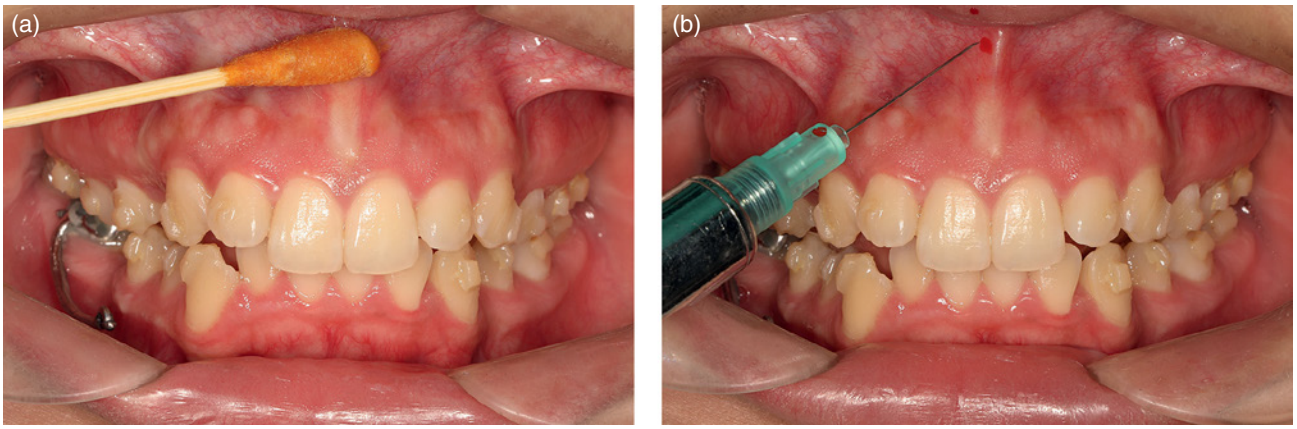


Figure 4.63 (a) Mucosal disinfection with iodophor. (b) Local infiltration anaesthesia.

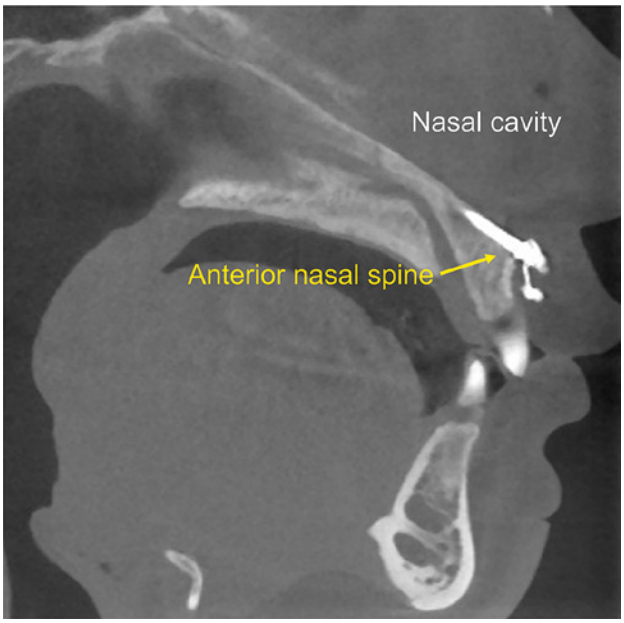


Figure 4.64 The mini-implant is inserted at the anterior nasal spine region that is close to the nasal cavity.

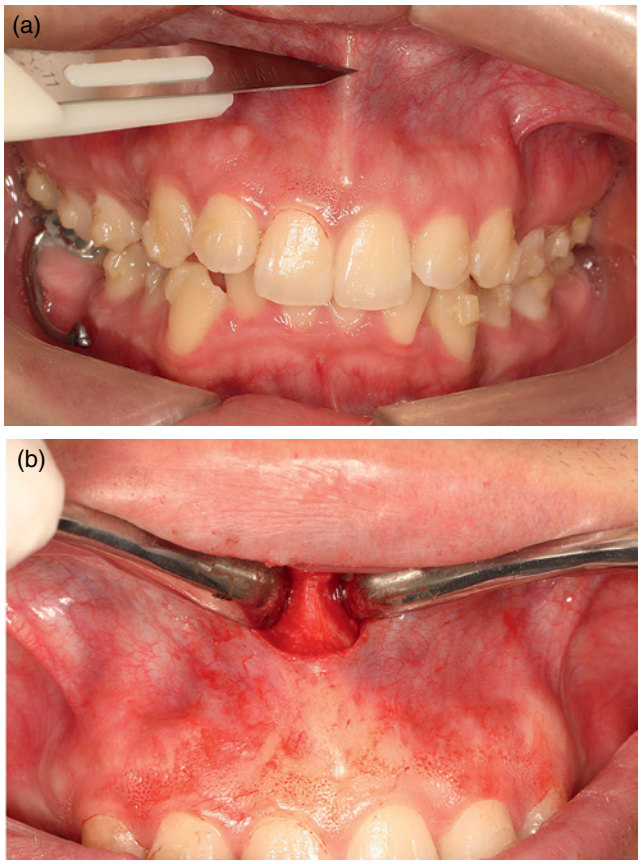


Figure 4.65 (a) Frenectomy. (b) Flap elevation for exposure of the anterior nasal spine.

Second, infiltration anaesthesia is performed following mucosal disinfection (Figure 4.63). Due to the deep location of the ANS and lack of dental roots in this area, infiltration anaesthesia should be adequate. Moreover, this area is close to the nasal cavity and the insertion of mini-implants may irritate the nasal mucosa (Figure 4.64), further justifying the need of profound anaesthesia. Thus, it is recommended that 1.0 ml or more anaesthetic is applied before mini-implant placement.

Third, frenectomy and flap elevation are performed to expose the ANS area (Figure 4.65). Specifically, a horizontal incision is made on the labial frenum to reduce soft tissue tension, followed by a vertical incision on the underlying soft tissue to expose the intermaxillary suture. Then, soft tissue undermining and full-thickness flap elevation are performed to surgically expose the ANS area. For patients with a sharp ANS edge, removing the sharp edge to form a bone platform is recommended in order to prevent mini-implant slippage and cortical fractures.

Fourth, the designated entry point is marked with an explorer on the intermaxillary suture. To mark the entry

t.me/Dr_Mouayyad_AlbtousH

point, the explorer is pressed against the suture and the sharp tip of the explorer is wedged into the suture to form a pilot hole. The presence of the pilot hole facilitates mini-implant insertion through the marked entry point. Once the entry point is marked and confirmed, the mini-implant is inserted through the entry point (Figure 4.66). As displayed in Figure 4.67, the mini-implant is initially inserted in a direction perpendicular to the bone surface for cortical penetration. Then, the insertion angle is gradually changed to reach a final angle that is 45° to the occlusal plane. Given that the bone surface is inclined, this gradual change in the insertion angle is able to prevent apical slippage of the mini-implant during insertion.

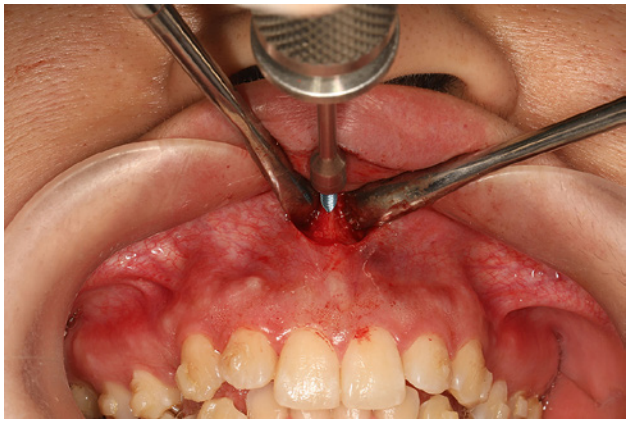


Figure 4.66 The mini-implant was inserted through the entry point at the anterior nasal spine region.

Lastly, based on the thickness of soft tissue, insertion of the mini-implant is stopped once an adequate emergence profile is achieved. However, for patients with very thick soft tissue, the heads of mini-implants cannot be exposed. For these patients, adding an extension hook facilitates force loading and avoids potential soft tissue irritation (Figure 4.68). Once the extension hook is fixed onto the mini-implant head, primary suture of the flap is performed (Figure 4.69).

The procedures for placing the ANS mini-implant are illustrated in Figure 4.70.

4.3.5 Clinical Applications

Mini-implants inserted at the ANS region are most frequently applied for incisor intrusion and gummy smile correction. A case example will be discussed below to demonstrate the clinical applications of ANS mini-implants for simultaneous incisor intrusion and gummy smile correction.

An adult male patient sought orthodontic treatment with a chief complaint of lip protrusion and gummy smile. As shown in Figure 4.71, the clinical and radiographic examinations were indicative of convex facial profile, gummy smile, excessive incisor display and mentalis strain. Moreover, he had a class I molar relationship on both sides, deep bite and mild dental crowding. The lateral cephalometric analysis revealed that he had class II skeletal base (ANB = 6.3), mandibular deficiency (SNB = 75.6), normal mandibular angle (SN-MP = 34.1),

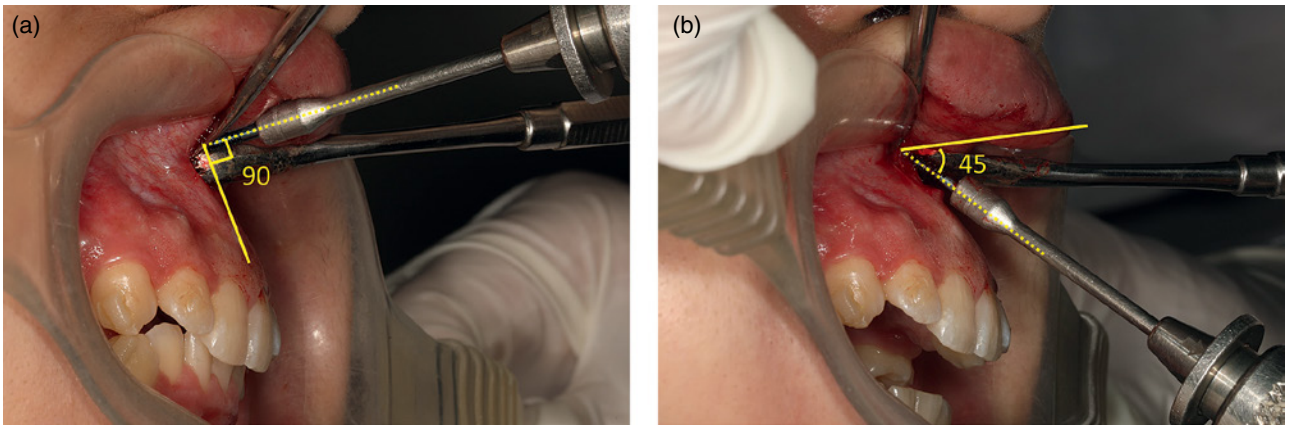


Figure 4.67 (a) The mini-implant was initially inserted perpendicularly to the bone surface. The dashed line and solid lines indicate the insertion path and bone surface, respectively. (b) The mini-implant was finally advanced with an insertion angle of 45° to the occlusal plane.

t.me/Dr_Mouayyad_AlbtousH

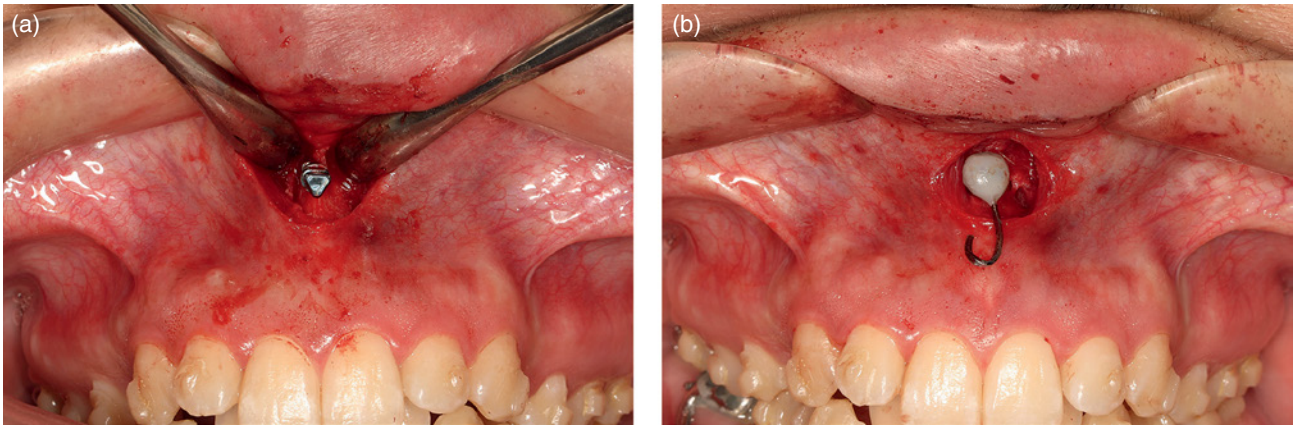


Figure 4.68 (a) Postinsertion. The mini-implant had been inserted with an adequate insertion depth. (b) An extension hook was fabricated and fixed onto the mini-implant.

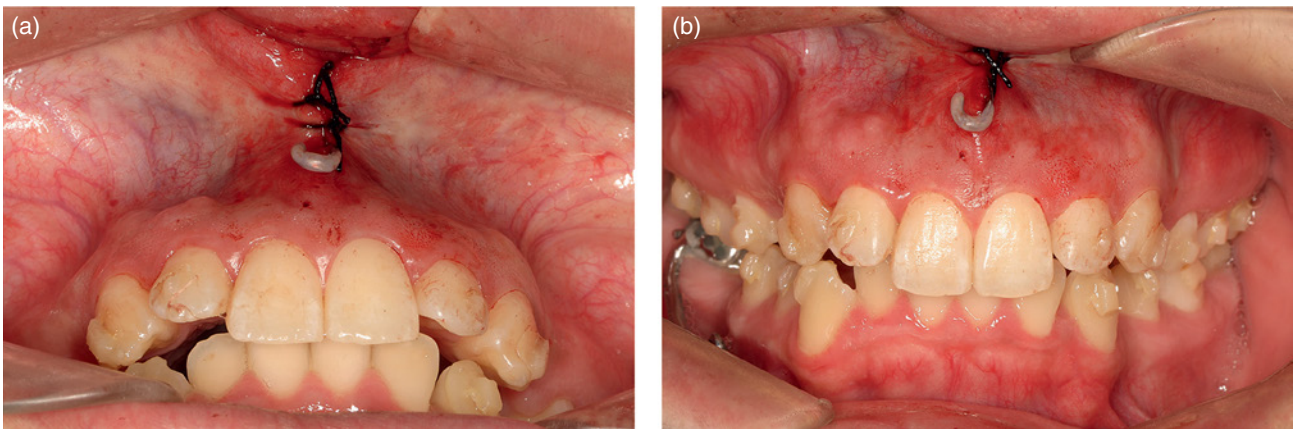


Figure 4.69 Primary suture of the elevated flap. (a) The upper lip was retracted to allow the primary suture. (b) Frontal view of the intraoral photograph showing the extension hook that was fixed onto the mini-implant.

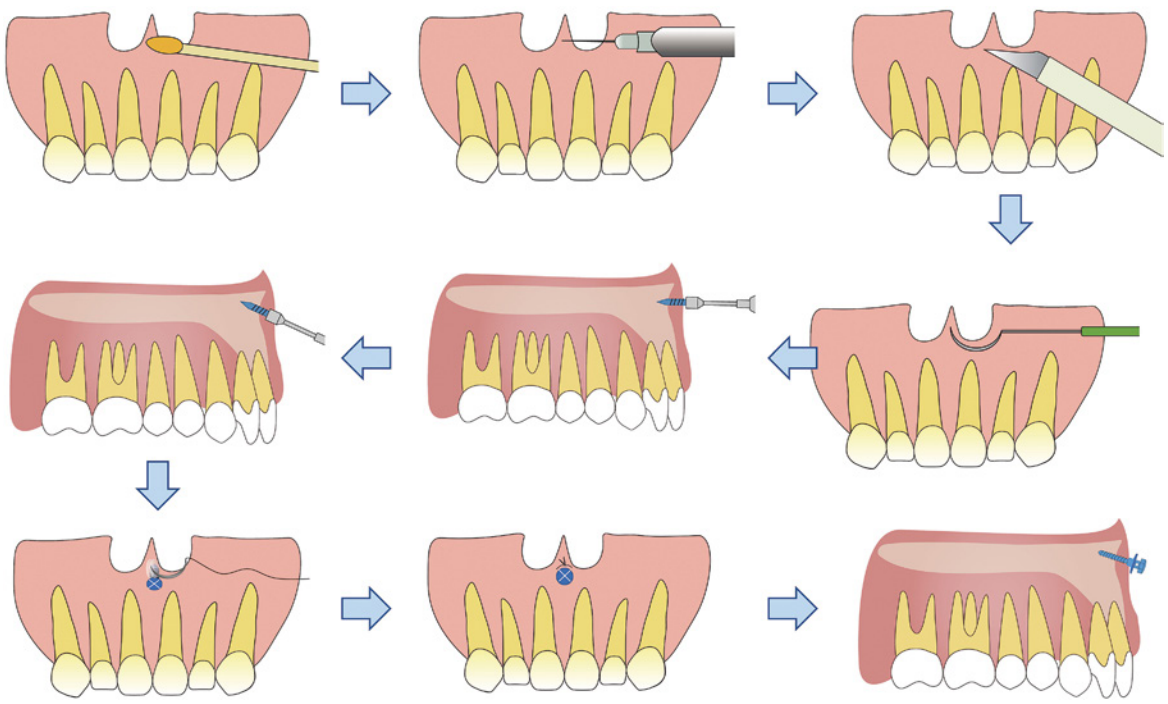


Figure 4.70 Schematic illustrations displaying the detailed procedures for inserting a mini-implant at the anterior nasal spine.

t.me/Dr_Mouayyad_AlbtousH

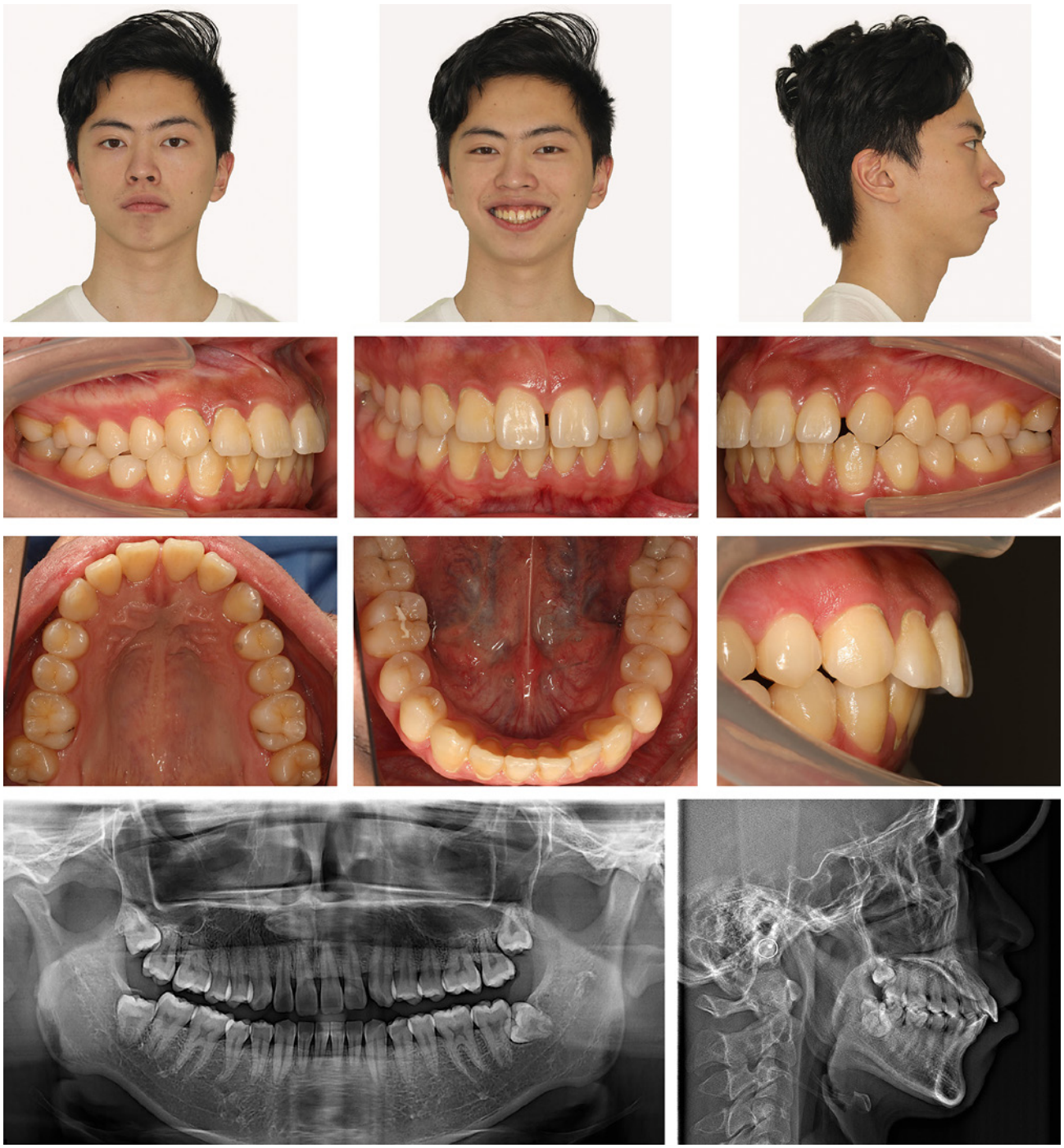


Figure 4.71 Pretreatment photographs and radiographs.

normal buccolingual inclination of the upper incisors and labial proclination of the lower incisors (U1-SN = 104.9; L1-MP = 107.6) (Table 4.6).

The treatment plan was extraction of the four first premolars and retraction of the anterior teeth with maximal molar anchorage with a clear aligner to resolve his convex and protrusive facial profile. The correction of the gummy smile was by clear aligner with the aid of a labial mini-implant. Due to a large amount of incisor intrusion, an ANS mini-implant was planned.

t.me/Dr_Mouayyad_AlbtousH

As displayed in Figure 4.72, following extraction of the four first premolars, retraction of the upper anterior teeth was designed with overtreatment in incisor intrusion and lingual root torque, resulting in an open bite in the virtually planned dental model. For the lower arch, canines were initially distalised and intruded, followed by incisor intrusion and *en masse* retraction of the anterior six teeth.

Table 4.6 Pretreatment cephalometric values.

Item	Case	Normal	SD
SNA	82.0	84.0	3.0
SNB	75.6	80.0	3.0
ANB	6.3	4.0	2.0
MP-SN	34.1	35.0	4.0
MP-FH	25.9	29.0	4.0
S-Go/N-Me	67.8	67.0	4.0
Y-axis	71.5	65.0	4.0
U1-L1	113.4	121.0	9.0
U1-SN	104.9	107.0	6.0
FMIA (L1-FH)	46.5	58.8	6.0
IMPA (L1-MP)	107.6	95.6	6.0
Wits value	2.1	0.8	1.0
Upper lip E-plane (mm)	2.8	0.8	2.0
Lower lip E-plane (mm)	6.5	1.4	3.0

An orthodontic mini-implant was placed at the ANS region and an extension hook was fixed onto the mini-implant to prevent soft tissue irritation and facilitate force loading (Figure 4.73). Incisor intrusion was achieved through applying an elastic rubber from the aligner to the extension hook fixed on the ANS mini-implant (Figure 4.74). From the biomechanical perspective, the elastic rubber offers an intrusive force that produces an anticlockwise moment, leading to incisor labial flaring (Figure 4.75). Thus, to prevent incisor flaring and achieve molar maximal anchorage, two buccal mini-implants were inserted. Elastic rubbers were applied from the aligner to the buccal mini-implants, so that bodily *en masse* retraction could be achieved (Figure 4.76).

Incisor intrusion and anterior retraction progressed smoothly (Figure 4.77). Following the active orthodontic treatment, a class I molar relationship was achieved on both sides with normal overjet and overbite. Moreover, straight facial profile was obtained and gummy smile was corrected (Figure 4.78). The comparison of the pre- and posttreatment cephalometric values is displayed in Table 4.7.

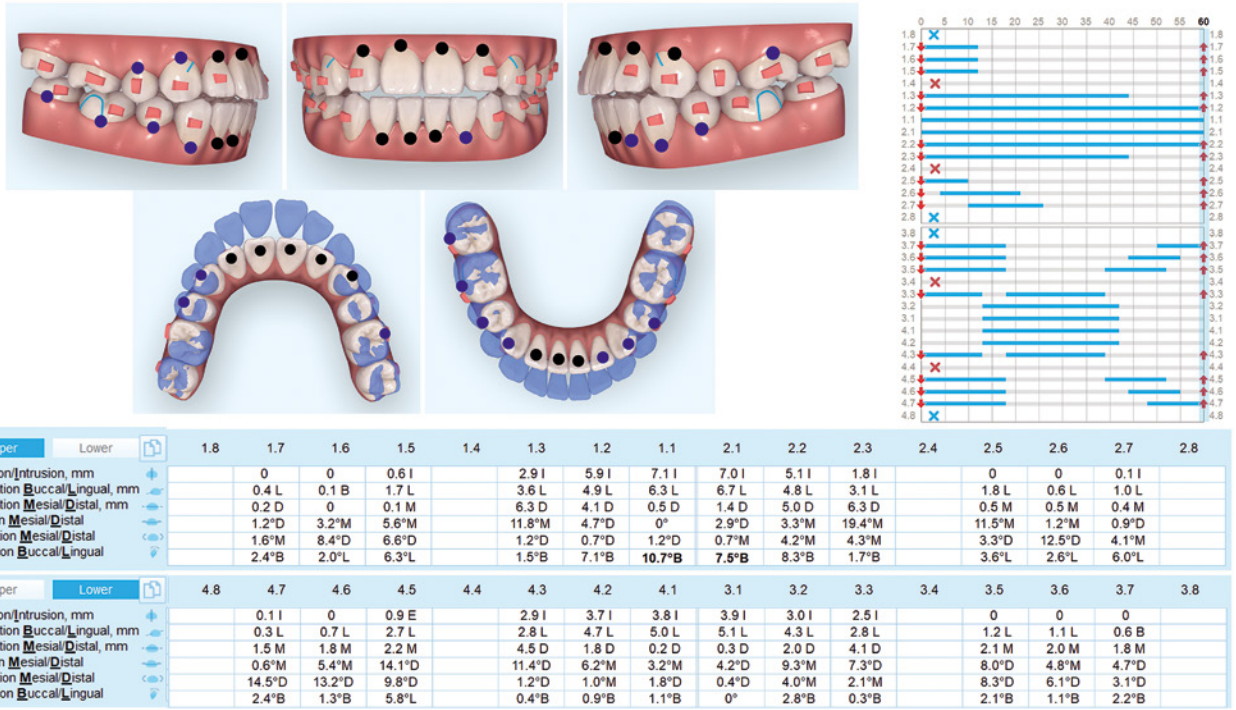


Figure 4.72 Pretreatment versus posttreatment superimposition, treatment staging and distances of tooth movements. Note that additional lingual root torque and intrusion of maxillary incisors were designed.

t.me/Dr_Mouayyad_AlbtousH



Figure 4.73 A mini-implant had been inserted and an extension hook (yellow arrow) was fixed onto the mini-implant head to facilitate force application.



Figure 4.74 Incisor intrusion was achieved by applying an elastic rubber from the clear aligner to the extension hook fixed onto the ANS mini-implant.

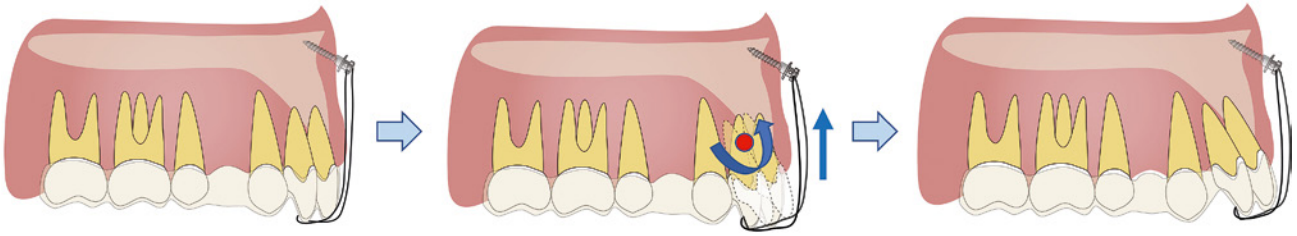


Figure 4.75 The intrusive force (blue arrow) offered by the ANS mini-implant passes labially to the centre of resistance (red dot) for the anterior teeth, generating an anticlockwise moment (blue curved arrow). This eventually causes labial flaring of the upper incisors.

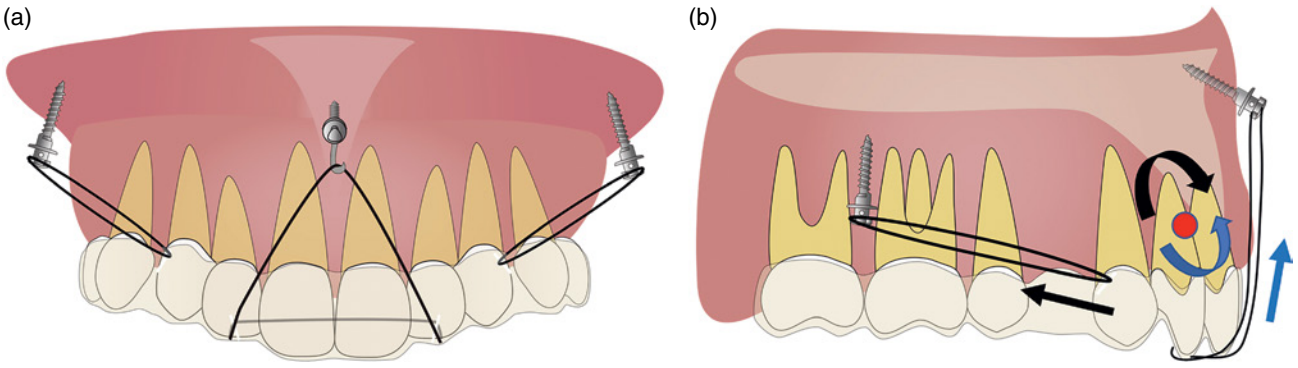


Figure 4.76 (a) Two elastic rubbers are applied from the clear aligner to the bilateral buccal mini-implants, in addition to the elastic rubber applied between the aligner and the ANS mini-implant. (b) Biomechanical analysis. The intrusive force offered by the ANS mini-implant generates an anticlockwise moment that is offset by the moment generated by the retraction force offered by the buccal mini-implants. The net effect is bodily retraction of the upper anterior teeth with simultaneous intrusion and retraction.

t.me/Dr_Mouayyad_AlbtousH

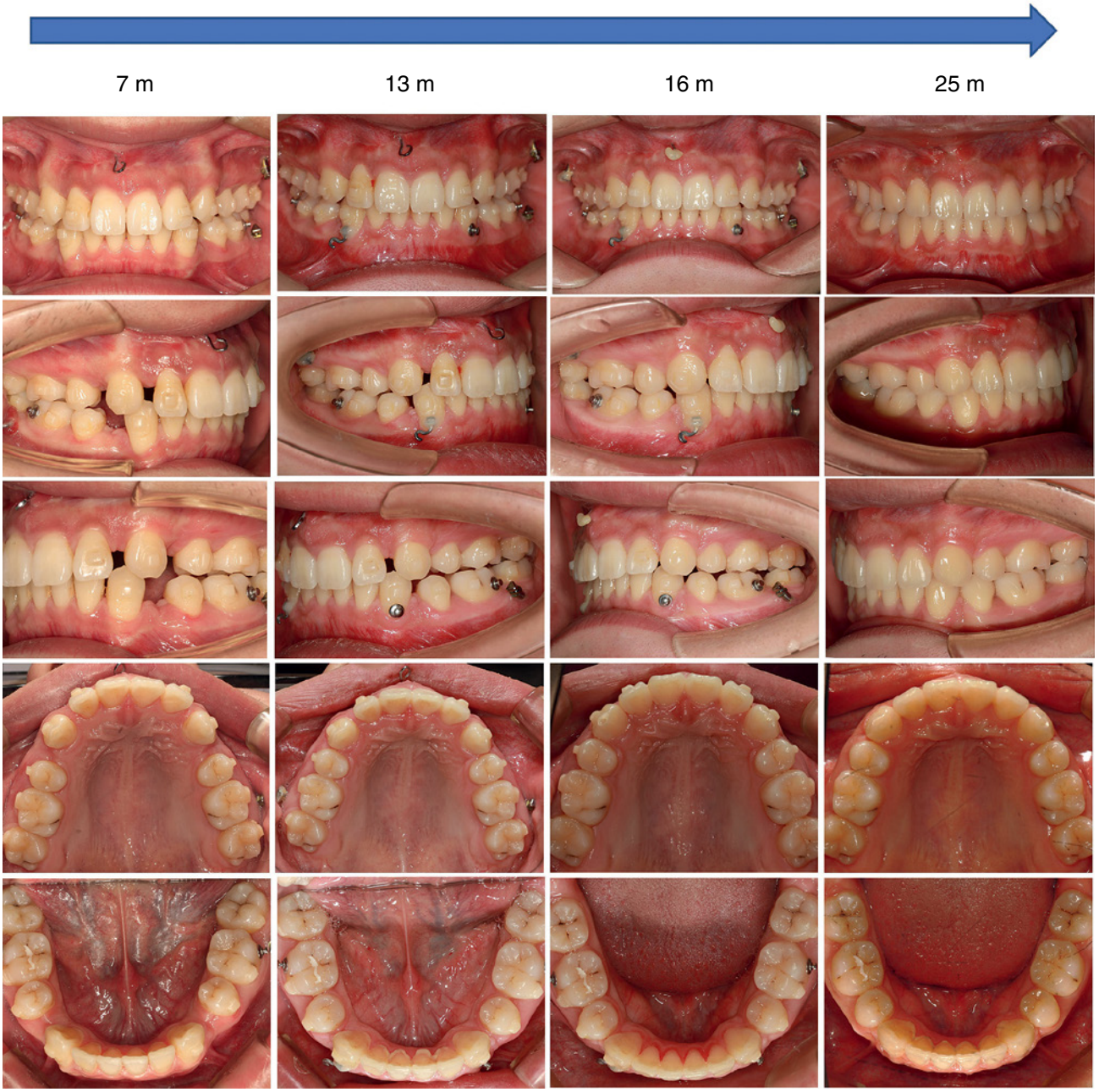


Figure 4.77 The deep bite was gradually corrected with efficient retraction of the anterior teeth.

t.me/Dr_Mouayyad_AlbtousH

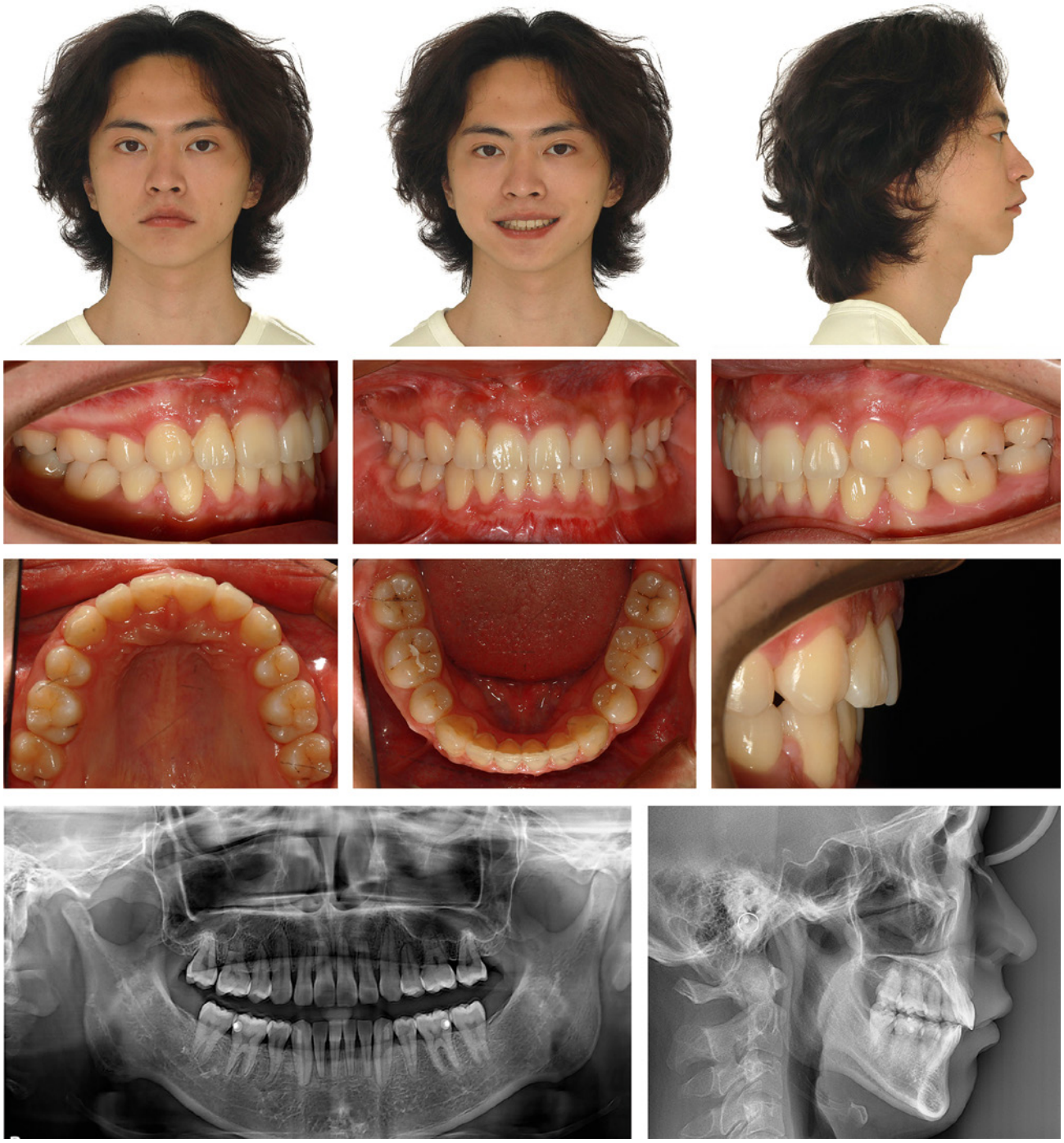


Figure 4.78 Posttreatment photographs and radiographs.

t.me/Dr_Mouayyad_AlbtousH

Table 4.7 Comparison of pretreatment and posttreatment cephalometric values.

Item	Pretreatment	Posttreatment
SNA	82.0	80.2
SNB	75.6	75.8
ANB	6.3	4.4
MP-SN	34.1	33.3
MP-FH	25.9	25.6
S-Go/N-Me	67.8	69.7
Y-axis	71.5	71.2
U1-L1	113.4	134.7
U1-SN	104.9	96.4
FMIA (L1-FH)	46.5	58.8
IMPA (L1-MP)	107.6	95.6
Wits value	2.1	0.8
Upper lip E-plane (mm)	2.8	0.8
Lower lip E-plane (mm)	6.5	1.4

4.4 Summary

The maxillary labial region has two distinct anatomical areas: interradicular sites and anterior nasal spine. Mini-implants inserted at the maxillary labial region have versatile clinical applications, for incisor intrusion and gummy smile correction. Thorough clinical and radiographic examinations are required to determine the optimal insertion sites and angles. Delicate insertion techniques should be employed to ensure the clinical success of maxillary labial mini-implants.

References

1 Creekmore TD, Eklund MK. (1983). The possibility of skeletal anchorage. *J. Clin. Orthod.* 17(4):266–269.

2 Saga AY, Araujo EA, Antelo OM, Meira TM, Tanaka OM. (2020). Nonsurgical treatment of skeletal maxillary protrusion with gummy smile using headgear for growth control, mini-implants as anchorage for maxillary incisor intrusion, and premolar extractions for incisor retraction. *Am. J. Orthod. Dentofacial Orthop.* 157(2):245–258.

3 Atalla AI, Aboul Fotouh MH, Fahim FH, Foda MY. (2019). Effectiveness of orthodontic mini-screw implants in adult deep bite patients during incisor intrusion: a systematic review. *Contemp. Clin. Dent.* 10(2):372–381.

4 Reddy S, Jonnalagadda VNS. (2021). Mini-implant assisted gummy smile and deep bite correction. *Contemp. Clin. Dent.* 12(2):199–204.

5 Namburi M, Nagothu S, Kumar CS, Chakrapani N, Hanumantharao CH, Kumar SK. (2017). Evaluating the effects of consolidation on intrusion and retraction using temporary anchorage devices – a FEM study. *Prog. Orthod.* 18(1):2.

6 Motoyoshi M, Inaba M, Ono A, Ueno S, Shimizu N. (2009). The effect of cortical bone thickness on the stability of orthodontic mini-implants and on the stress distribution in surrounding bone. *Int. J. Oral Maxillofac. Surg.* 38(1):13–18.

7 Motoyoshi M, Yoshida T, Ono A, Shimizu N. (2007). Effect of cortical bone thickness and implant placement torque on stability of orthodontic mini-implants. *Int. J. Oral Maxillofac. Implants* 22(5):779–784.

8 Murugesan A, Dinesh SPS, Muthuswamy Pandian S et al. (2022). Evaluation of orthodontic mini-implant placement in the maxillary anterior alveolar region in 15 patients by cone beam computed tomography at a single center in south India. *Med. Sci. Monit.* 28:e937949.

9 Menezes CC, Barros SE, Tonello DL et al. (2020). Influence of the growth pattern on cortical bone thickness and mini-implant stability. *Dental Press J. Orthod.* 25(6):33–42.

t.me/Dr_Mouayyad_AlbtousH

5

Maxillary Buccal Region

Lingling Pu[1,2], Yanzi Gao[1], Qinxuan Song[3], Yang Zhou[2], Ying Jin[1], Yongwen Guo[1], Xianglong Han[1], and Hu Long[1]

[1] *Department of Orthodontics, State Key Laboratory of Oral Diseases and National Clinical Research Center for Oral Diseases, West China Hospital of Stomatology, Sichuan University, Chengdu, China*
[2] *Private Practice, Chengdu, China*
[3] *Department of Prosthodontics, State Key Laboratory of Oral Diseases and National Clinical Research Center for Oral Diseases, West China Hospital of Stomatology, Sichuan University, Chengdu, China*

5.1 Introduction

The maxillary buccal region is one of the most frequently used anatomical regions for the placement of mini-implants and the most frequent clinical application is anterior *en masse* retraction.[1] Anteroposteriorly, the maxillary buccal region spans from the canine root to the maxillary tuberosity, and it is continuous with the zygomatic buttress superiorly and limited by the alveolar crest inferiorly (Figure 5.1).

From the anatomical perspective, the maxillary buccal region consists of three continuous but functionally distinct sites: interradicular sites, infrazygomatic crest (IZC) and maxillary tuberosity (Figure 5.2). Specifically, the interradicular sites are the alveolar bone areas between posterior teeth (e.g. between the second premolar and first molar). The IZC is a palpable bony ridge running between the buccal alveolar process and the zygomatic buttress, and it is located buccally and apically to the roots of the posterior teeth (e.g. first molars and second molars). Furthermore, the maxillary tuberosity is the alveolar bone distal to the most posterior tooth (e.g. maxillary second molars). As mentioned in previous chapters, the maxillary tuberosity has loosely arranged trabecular bone surrounded by thin cortical bone and belongs to the D4 classification,[2] while the infrazygomatic crest and interradicular sites exhibit D2 or D3 bone. Thus, in clinical practice, the infrazygomatic crest and interradicular sites are more frequently used than the maxillary tuberosity.

Mini-implants inserted at the maxillary buccal region are versatile in a variety of orthodontic tooth movements, e.g. anterior retraction, molar distalisation, molar protraction and the traction of impacted teeth (Figure 5.3). In this chapter, anatomical characteristics, selection of optimal insertion sites, step-by-step clinical insertion techniques and clinical applications of mini-implants in the maxillary buccal region will be described.

5.2 Interradicular Sites

5.2.1 Anatomical Characteristics

The interradicular sites refer to the alveolar bone between two adjacent teeth in the buccal region. As shown in Figure 5.4, four interradicular sites are available for the insertion of mini-implants: between the canine and first premolar (U3-U4), between the first and second premolars (U4-U5), between the second premolar and first molar (U5-U6) and between the first and second molars (U6-U7). To maximise the clinical success of mini-implants inserted at the maxillary buccal region, the following anatomical features should be taken into consideration when choosing an optimal insertion site. Both hard tissue factors (i.e. bone density, cortical thickness, bone depth, bone width and buccal exostosis) and soft tissue factors (i.e. soft tissue type and buccal frenum) should be thoroughly evaluated prior to the insertion of mini-implants.

Clinical Insertion Techniques of Orthodontic Temporary Anchorage Devices, First Edition. Edited by Hu Long, Xianglong Han, and Wenli Lai.
© 2024 John Wiley & Sons Ltd. Published 2024 by John Wiley & Sons Ltd.

t.me/Dr_Mouayyad_AlbtousH

Hard Tissue Factor: Bone Density

The success of orthodontic mini-implants requires an adequate bone quantity and good bone quality, and the stability of mini-implants is mainly dependent on bone engagement. Thus, bone density is a pivotal factor in determining the stability and success of mini-implants. Bone density at the maxillary buccal region differs among subjects with different vertical patterns, with hypodivergent subjects exhibiting higher bone density than normodivergent and hyperdivergent subjects.[3] Moreover, alveolar bone in the maxillary buccal region has a lower density than basal bone,[3] indicating that basal bone areas (e.g. infrazygomatic crest) may possess denser bone than the interradicular sites. As displayed in Figure 5.5, among the interradicular sites, the highest density of cortical bone was detected at the U5-U6 and U6-U7 sites.[2] In contrast, the density of trabecular bone was similar among the four interradicular sites.[2] Thus, in terms of bone density, the U5-U6 and U6-U7 sites are recommended for the placement of mini-implants.

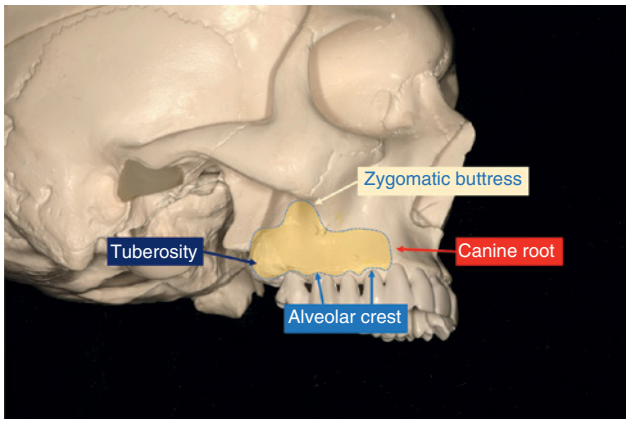


Figure 5.1 A skull model showing the maxillary buccal region (encircled by the blue dashed line). Anteroposteriorly, this region spans from the canine root to the maxillary tuberosity. Superoinferiorly, this region is continuous with the zygomatic buttress superiorly and limited inferiorly by the alveolar crest.

Hard Tissue Factor: Cortical Thickness

Cortical bone plays an indispensable role in maintaining the primary stability of mini-implants.[4] Moreover, following the placement of mini-implants, cortical bone acts as a functional 'cushion' in resisting stress in the trabecular bone, resulting in a satisfactory microenvironment for the

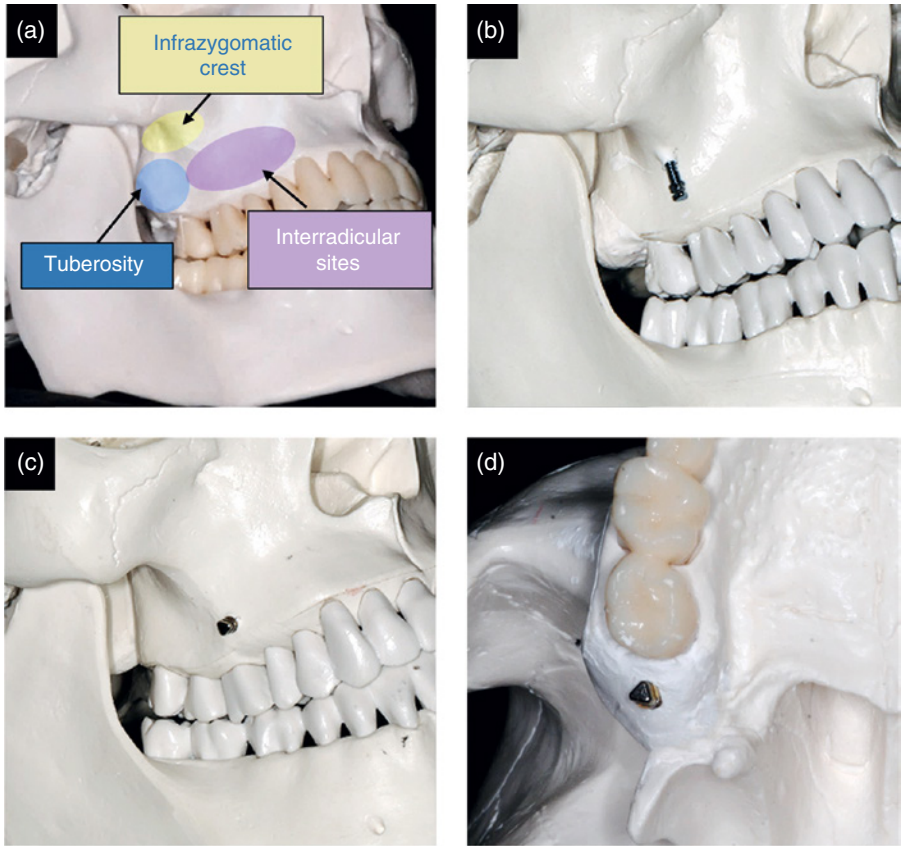


Figure 5.2 (a) Three anatomical sites in the maxillary buccal region. (b) A mini-implant inserted at the infrazygomatic crest region (buccal view). (c) A mini-implant placed at the U5-U6 interradicular site. (d) A mini-implant inserted at the maxillary tuberosity area.

t.me/Dr_Mouayyad_AlbtousH

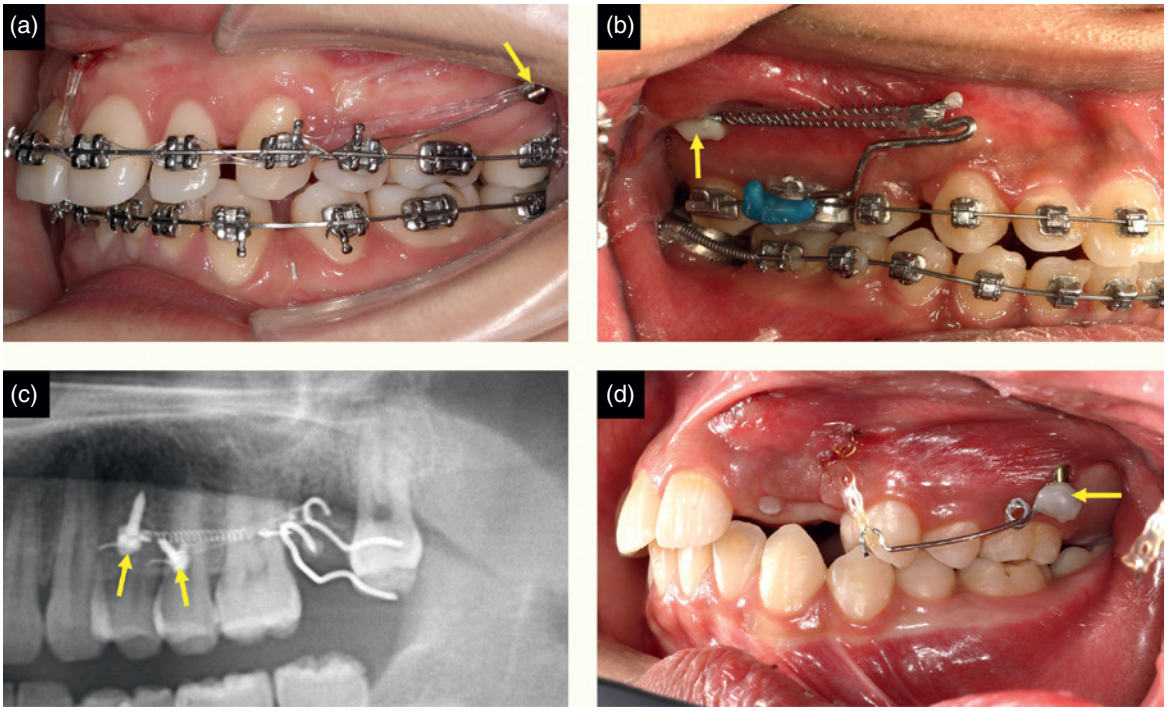


Figure 5.3 Versatile clinical applications of mini-implants (yellow arrows) placed at the maxillary buccal region. (a) Anterior retraction. (b) Molar distalisation. (c) Molar protraction. (d) Traction of an impacted canine.

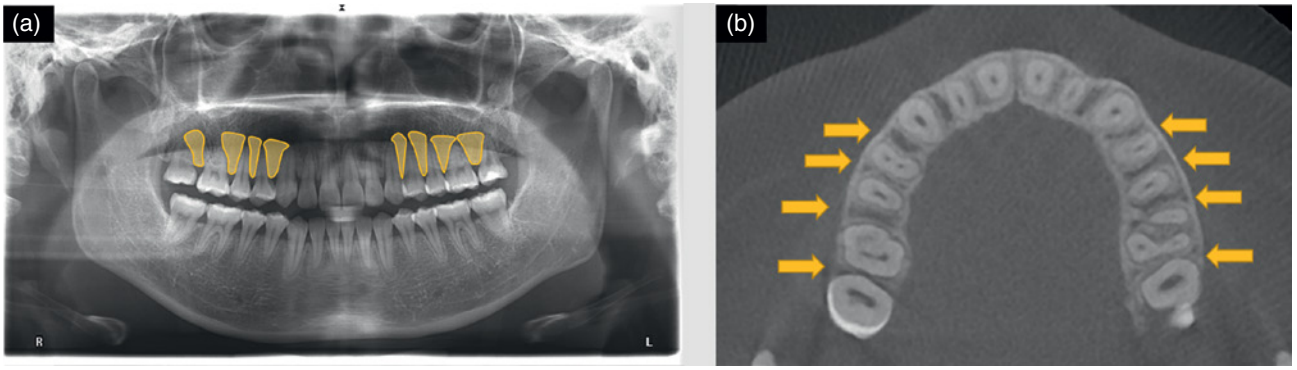


Figure 5.4 Maxillary buccal interradicular sites. (a) A panoramic radiograph showing the interradicular sites (yellow areas). (b) A CBCT image demonstrating the interradicular sites (yellow arrows).

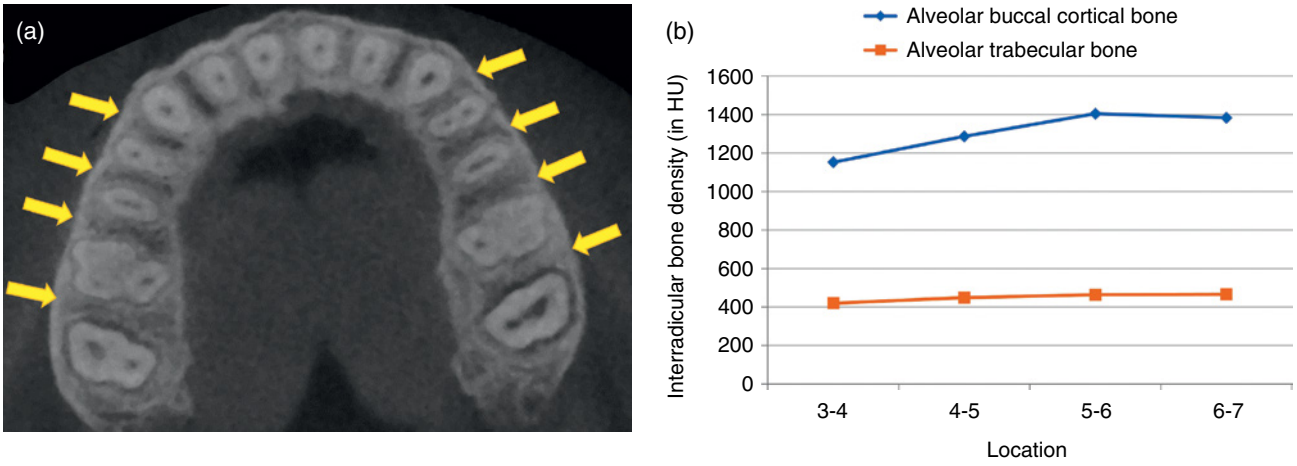


Figure 5.5 The differences of bone density at different interradicular sites. (a) Four interradicular sites (indicated by yellow arrows). (b) The density of cortical bone and trabecular bone at different interradicular sites. *Source:* Adapted from Chugh et al. [2].

t.me/Dr_Mouayyad_AlbtousH

development of secondary stability (alveolar bone remodelling). It has been revealed that stress is mainly exerted on trabecular bone when cortical thickness is less than 1 mm.[5] If the cortical thickness is 1.5 mm, 95% of the stress is concentrated on the cortical bone, leaving only 5% stress acting on trabecular bone.[5] Thus, cortical thickness should be at least 1 mm so that adequate stability of mini-implants can be anticipated.

Males exhibit greater cortical thickness than females.[6] Cortical thickness is associated with age and vertical skeletal patterns. Adults possess thicker cortical bone than adolescents, and hypodivergent patients exhibit thicker cortical bone than normodivergent and hyperdivergent patients.[7,8] Furthermore, cortical thickness is influenced by anatomical location; specifically, the thickness of cortical bone increases from alveolar crest to alveolar base (Figure 5.6), suggesting that greater cortical engagement can be achieved with more apical entry.[6,7]

However, cortical thickness is similar among different interradicular sites (Figure 5.7).[9] Since the U5-U6 and

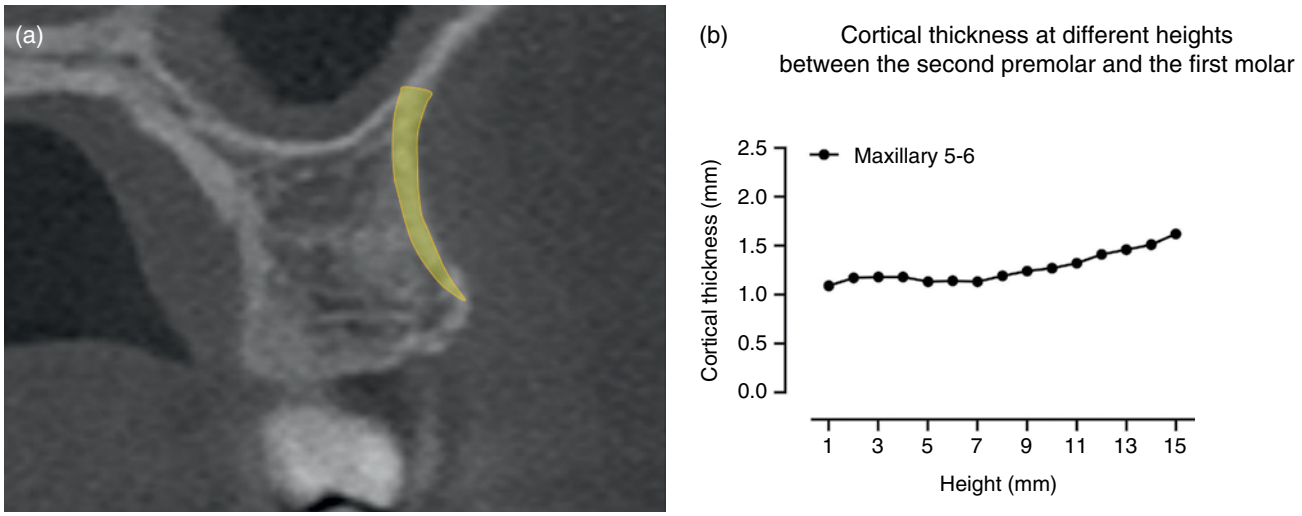


Figure 5.6 The influence of insertion height on cortical thickness. (a) The coronal section of a CBCT image demonstrating the differences in thickness of the cortical bone (yellow area) at different insertion heights. (b) The changes of cortical thickness with an increase in the insertion height. *Source:* Data from Ono et al. [6].

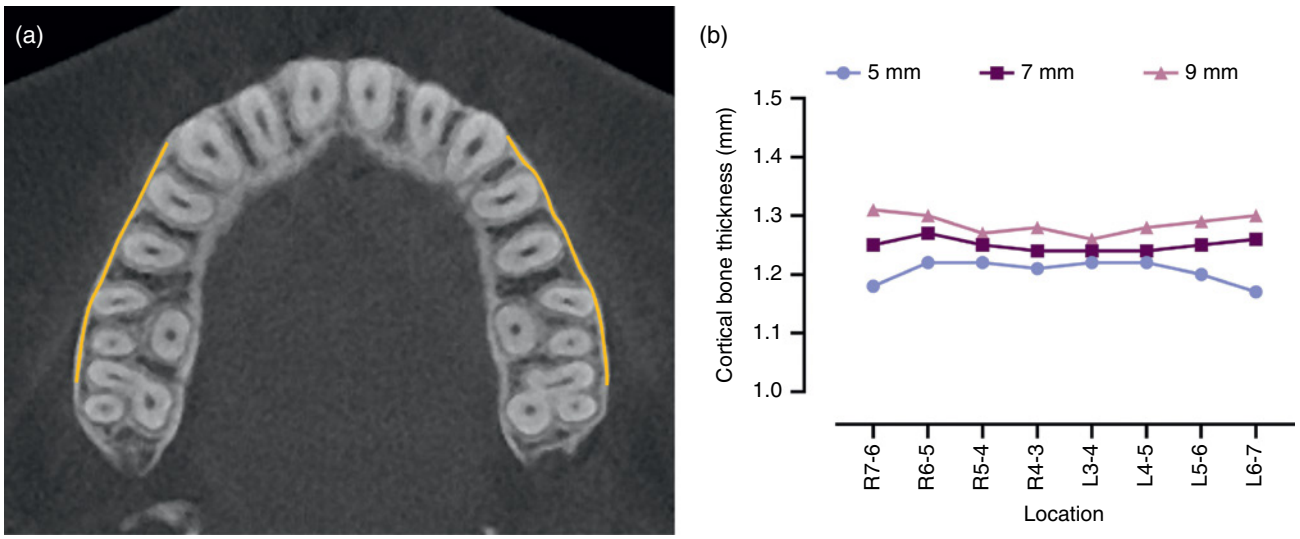


Figure 5.7 Cortical thickness at different interradicular sites and insertion heights. (a) Axial view of a CBCT image demonstrating that cortical thickness is similar among different sites. (b) Line chart showing the thickness of cortical bone among different interradicular sites. *Source:* Data from Park and Cho [9].

t.me/Dr_Mouayyad_AlbtousH

U6-U7 interradicular sites are the most frequently used for inserting mini-implants, more details will be elaborated below. It has been shown that the average cortical thickness ranges from 1.1 mm to 1.6 mm at the U5-U6 site and from 1.1 mm to 2.1 mm at the U6-U7 site,[6] suggesting that cortical bone at these two interradicular sites is suitable for the placement of mini-implants. As displayed in Figure 5.8, the percentage of patients with cortical bone greater than 1 mm is 56–97% and 67–100% for the U5-U6 and U6-U7 sites, respectively. Moreover, if cortical thickness is unsatisfactory, angled insertion can help obtain greater cortical engagement (Figure 5.9). It has been shown that changing the insertion angle from 90° to 45° increased the cortical engagement by 47%.[10] However, a further increase in insertion angle poses a high risk of mini-implant slippage. Thus, the recommended insertion angle is 45–60° to the alveolar bone surface. Considering that the inclination of the maxillary buccal alveolar bone surface is almost perpendicular to the occlusal surface,[11] the recommended insertion angle is 30–45° to the occlusal plane for mini-implants to be inserted at the interradicular sites.

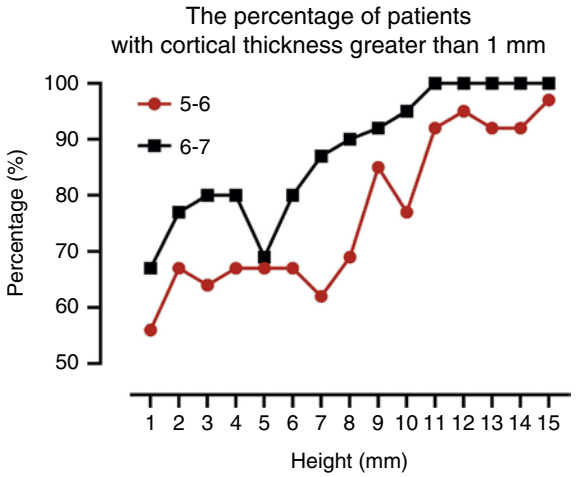


Figure 5.8 The percentage of patients with cortical thickness greater than 1 mm at different insertion heights. Note that the percentage increases with an increase in the insertion height for both the U5-U6 and U6-U7 interradicular sites. *Source:* Adapted from Ono et al. [6].

Therefore, since cortical thickness is influenced by various factors (i.e. gender, age, vertical skeletal pattern, insertion height), pretreatment radiographic examinations are indispensable and judicious selection of optimal sites (cortical thickness greater than 1 mm) is recommended. Moreover, greater cortical engagement can be anticipated with more apical entry and angled insertions (insertion angle: 30–45° to the occlusal plane).

Hard Tissue Factor: Bone Depth

Bone depth refers to the distance between the buccal cortical plate and the palatal cortical plate or between the buccal cortical plate and the sinus cortex. Usually, the distance between the buccal and palatal cortical plates is sufficient to accommodate 8 mm mini-implants. The distance between the buccal cortical plate and the sinus cortex varies greatly among patients and should be taken into consideration for individualised planning of optimal insertion sites. As depicted in Figure 5.10, the height of the sinus floor differs among patients and the risk of sinus penetration varies.

The height of the sinus floor differs among patients with different vertical skeletal patterns, with hyperdivergent subjects possessing higher sinus floor than normodivergent and hypodivergent subjects (Figure 5.11).[12] Moreover, the height of the sinus floor differs among different interradicular sites, with the highest sinus floor found at the U4-U5 site (Figure 5.11). With sinus penetration, the quantity of bone surrounding the mini-implant is reduced, resulting in inadequate bone depth. Sinus penetration was encountered among 10% of patients who received placement of mini-implants at the U5-U6 interradicular site and sinus penetration had no impact on the survival rate of mini-implants.[13] This may be attributed to the fact that reduction of bone depth due to sinus penetration is offset by the

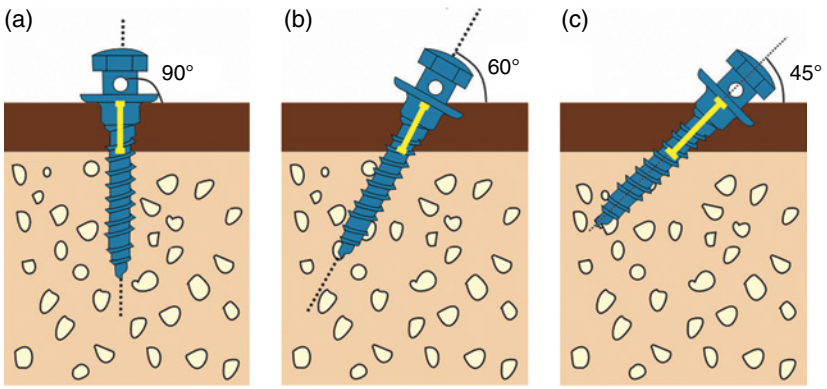


Figure 5.9 Angled insertion increases cortical engagement. (a) Perpendicular insertion (90°). (b) Angled insertion (60°). (c) Angled insertion (45°).

t.me/Dr_Mouayyad_AlbtousH

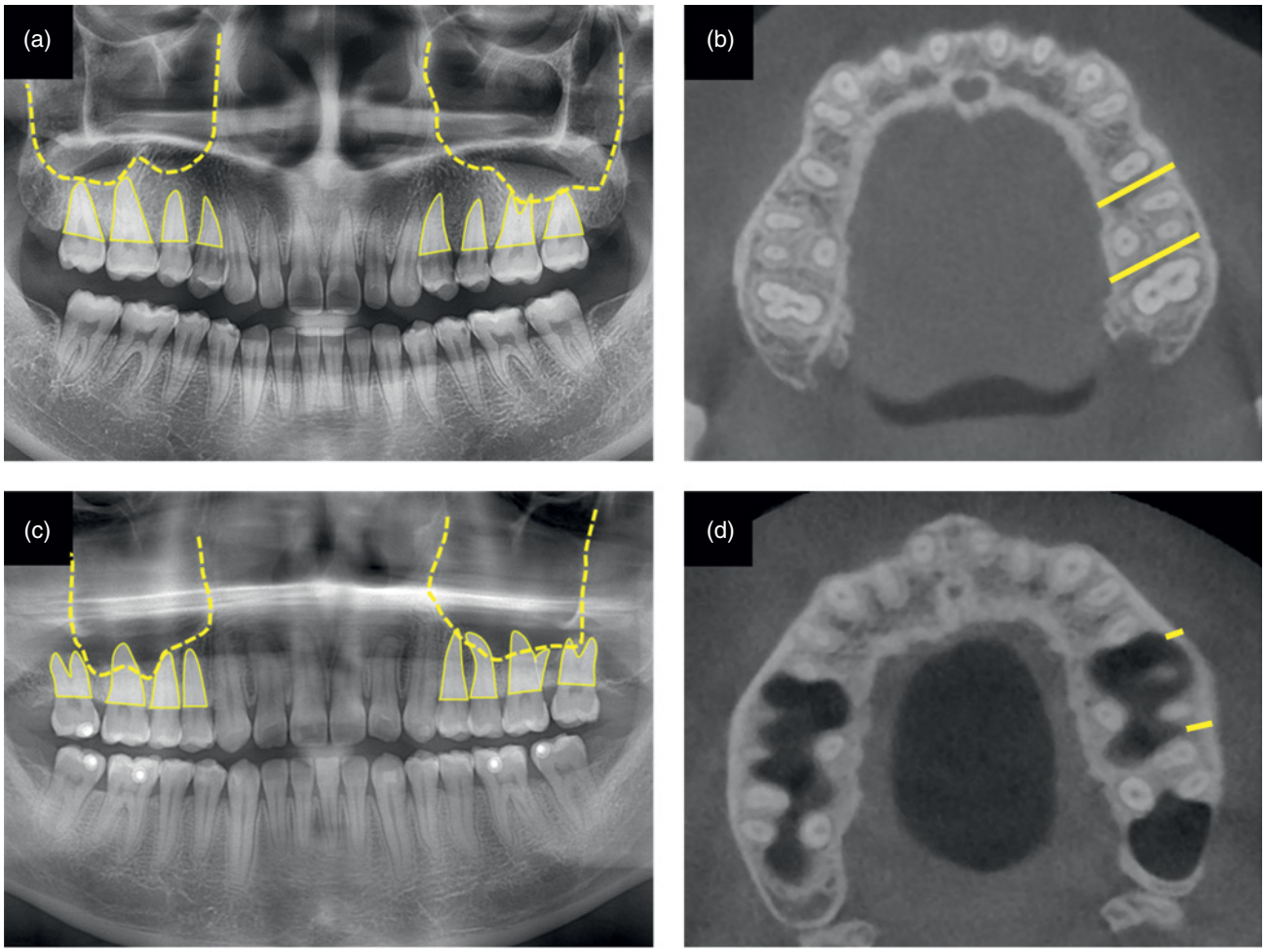


Figure 5.10 The influence of different heights of sinus floor on bone depth. (a) A panoramic radiograph showing that the heights of sinus floors are normal. (b) A CBCT image (axial view) showing the absence of sinus and bone depth is not influenced (bone depth is indicated by the yellow line). (c) A panoramic radiograph showing sinus pneumatisation and low sinus floor. (d) CBCT image (axial view) showing the presence of sinus that reduces the bone depth (indicated by the yellow line).

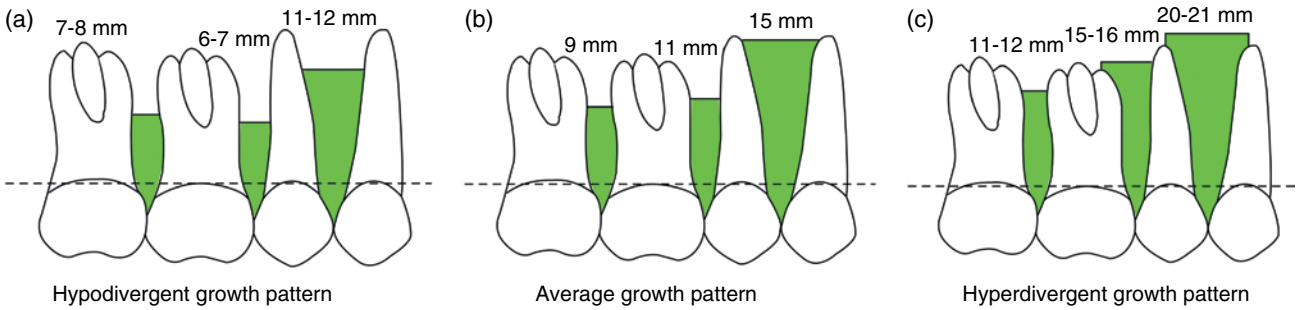


Figure 5.11 Different heights of sinus floor at different interradicular sites and among patients with different vertical skeletal patterns. (a) Hypodivergent growth pattern. (b) Average growth pattern. (c) Hyperdivergent growth pattern. *Source:* Adapted from Vibhute et al. [12].

t.me/Dr_Mouayyad_AlbtousH

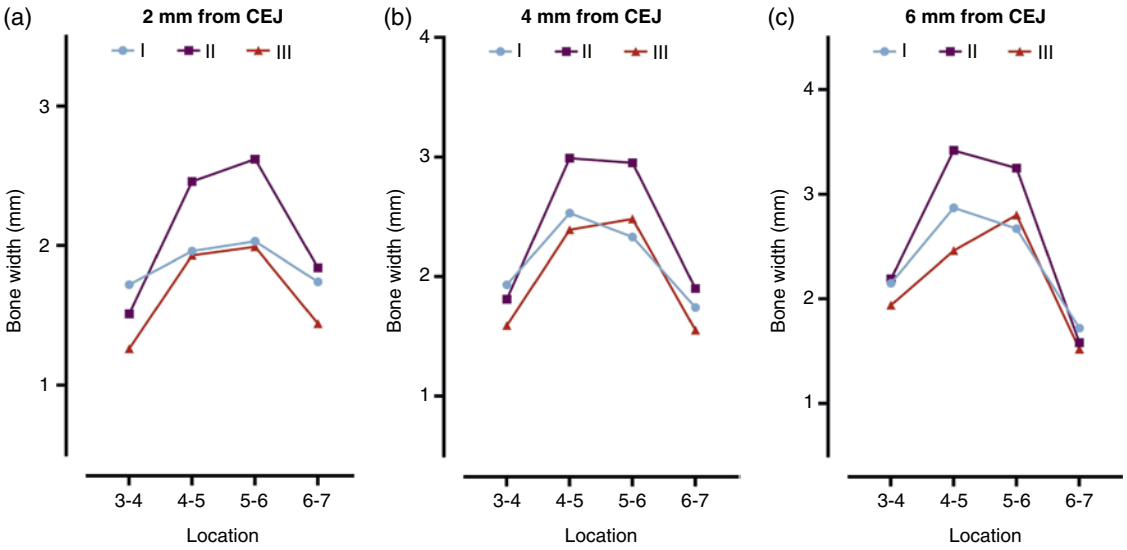


Figure 5.12 Comparison of bone width at different insertion heights and different interradicular sites among patients with different sagittal skeletal patterns. (a) Bone width at the 2 mm level from the CEJ. (b) Bone width at the 4 mm level from the CEJ. (c) Bone width at the 6 mm level from the CEJ. *Source:* Adapted from Golshah et al. [17].

better bone quality offered by the sinus cortical plate (bicortical engagement). Thus, unless severe sinus pneumatisation is present, bone depth is adequate for the placement of mini-implants at the interradicular sites.

Hard Tissue Factor: Bone Width

Bone width is defined as the mesiodistal width of alveolar bone that is available for the insertion of mini-implants. Bone width is determined by two adjacent roots and also refers to interradicular distance. A large body of evidence reveals that root proximity is a detrimental factor for the stability of mini-implants,[14-16] so it is recommended that 1 mm clearance from the root be implemented to reduce the failure rate of mini-implants. As per the 1 mm clearance principle, for a mini-implant with a diameter of 1.4 mm, at least 3.4 mm bone width is required (1 + 1.4 + 1 = 3.4 mm). Usually, due to limited interradicular space and wide individual variations, the recommended diameter of a mini-implant ranges from 1.2 to 1.6 mm for the maxillary buccal interradicular sites.[9] Thus, we recommend that meticulous evaluation of bone width and judicious selection of optimal mini-implants and insertion sites be performed prior to the placement of mini-implants.

Bone width at the maxillary buccal region differs among subjects with different sagittal skeletal patterns. Specifically, greater bone width is exhibited among class II subjects than class I and class III patients (Figure 5.12),[17,18] probably due to larger and wilder maxillae among class II patients.

Since the roots are tapered and become smaller apically, the bone width increases from the alveolar crest to alveolar base (Figure 5.13). Notably, the curvature of the mesiobuccal root of the maxillary first molars may limit the insertion of mini-implants at its corresponding height. It has been shown that the majority (two-thirds) of patients had curved mesiobuccal roots of first molars and that 95% of them were curved distally with the convexity facing anteriorly (Figure 5.14).[19] Although the most curved point of the root curvature was 6.4 ± 0.7 mm apical to the CEJ (Figure 5.14),[20] the exact height of the most curved point exhibits intersubject variation and careful and thorough radiographic examinations are required to pinpoint its specific location.

Bone width differs among different interradicular sites (Figure 5.15). A plethora of evidence indicates that the U5-U6 site exhibits the largest interradicular space and is the most appropriate interradicular site for the placement of mini-implants.[9,18,21-23] Moreover, as shown in Figure 5.16, the bone widths differ among the buccal, middle and palatal sides, with the middle being the smallest. This is attributed to the specific morphology of the roots on the horizontal plane. Although CBCT scanning is the most accurate and reliable modality to measure the interradicular distances, 2-D radiography is often used in clinical settings for

t.me/Dr_Mouayyad_AlbtousH

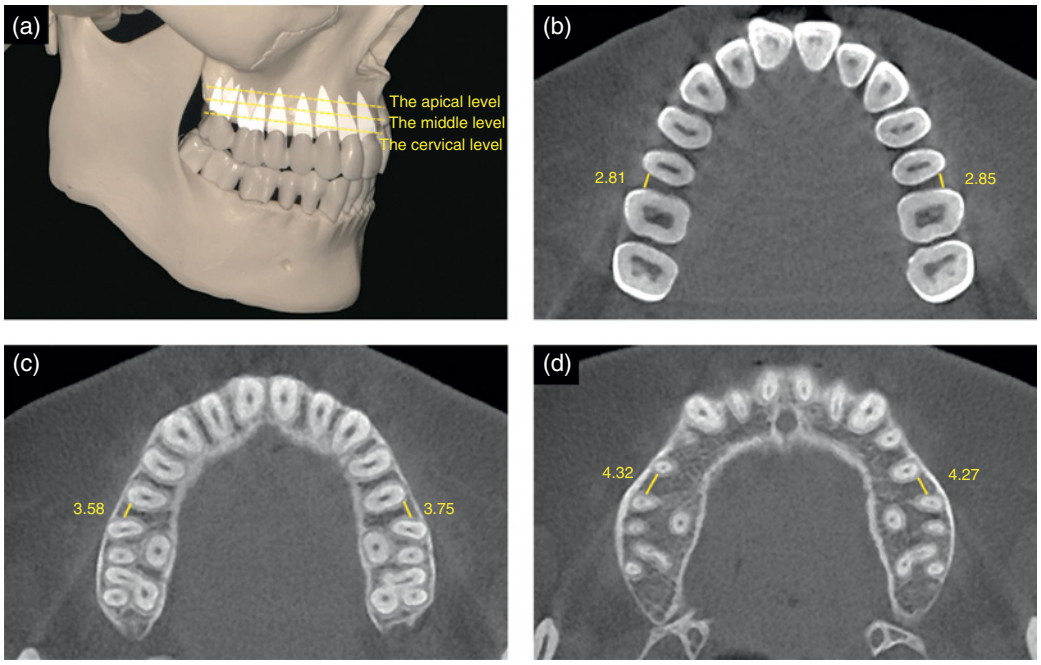


Figure 5.13 Bone widths at different heights. (a) Illustration of three levels sectioning the roots: cervical level, middle level and apical level. (b) Bone widths at the cervical level. (c) Bone widths at the middle level. (d) Bone widths at the apical level. Note that the bone width increases from the cervical level to the apical level.

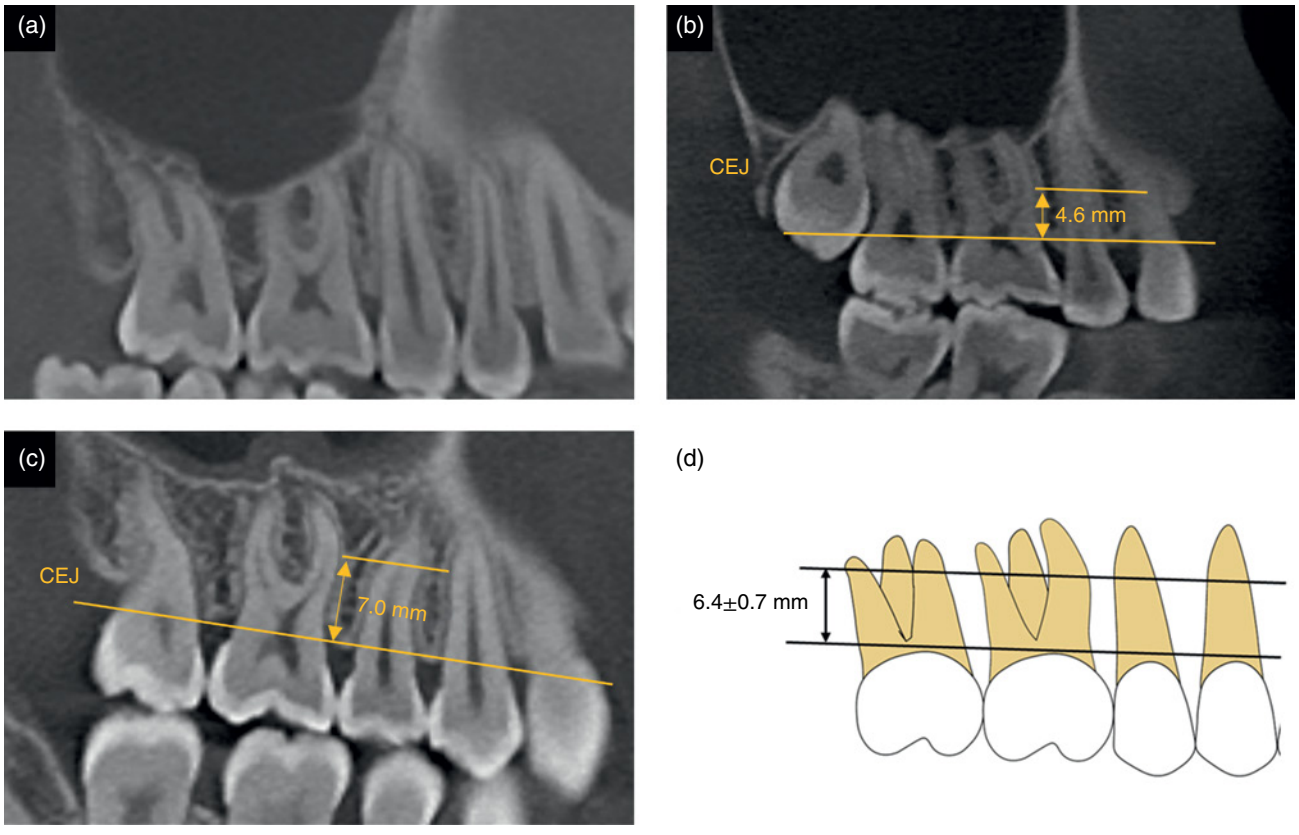


Figure 5.14 Root curvature of the mesiobuccal root of the first molar. (a) No root curvature is present. (b) Root curvature is present, with the convexity facing anteriorly. The most curved point is 4.6 mm apical to the CEJ. (c) Root curvature is present, with the convexity facing anteriorly. The most curved point is 7.0 mm apical to the CEJ. (d) A schematic illustration showing that the averaged height of the most curved point is 6.4 mm apical to the CEJ.

t.me/Dr_Mouayyad_AlbtousH

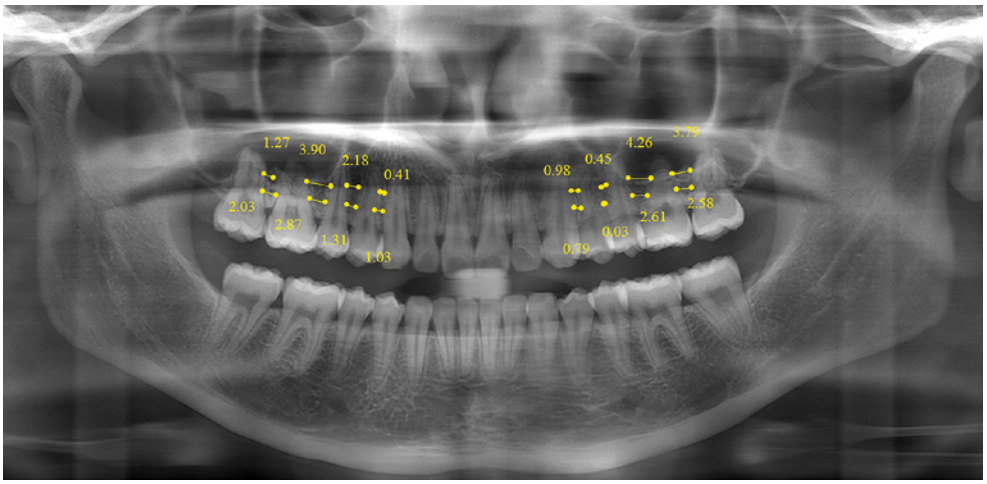
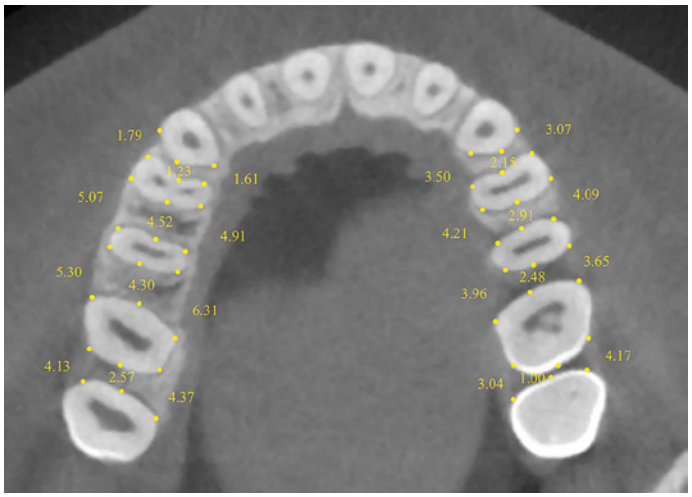


Figure 5.15 A panoramic radiograph demonstrating the differences in bone width among different interradicular sites. Note that the U5-U6 site exhibits the largest interradicular distance.

Figure 5.16 Axial section view of a CBCT image showing the differences of interradicular distances at the buccal, middle and palatal sides.



preliminary and rapid evaluation due to lower radiation and reduced cost.[24,25] However, it is noteworthy that panoramic radiography may underestimate interradicular space due to its possible oblique projections (Figure 5.17). Thus, orthogonal periapical radiography or CBCT is recommended to evaluate bone width for the insertion of mini-implants.

Bone widths at different interradicular sites and at different heights are summarised in Figure 5.18 (data from our preliminary unpublished study). As per the 1 mm root clearance principle, the minimum bone width should be 3.4 mm if a 1.4 mm-wide mini-implant is used. The recommended site is the U5-U6 site with the insertion height being 6–8 mm apical to the CEJ. Moreover, the specific position of the root curvature should be taken into consideration in determining the optimal height of entry.

Hard Tissue Factor: Buccal Exostosis

Exostosis is a benign nodular bony protuberance that is often present in the premolar and molar regions of the maxilla (Figure 5.19).[26] The buccal exostosis is palpated as a hard bony mass and the overlying mucosa is often intact and painless. It is proposed that buccal exostosis enlarges in response to increased and abnormal masticatory force.[27,28] It may develop during adolescence and enlarges in adulthood. Since it is often asymptomatic, no specific treatment is required but the presence of buccal exostosis may interfere with the insertion of mini-implants (Figure 5.20). Thus, prior to insertion, thorough clinical and radiographic examinations should be performed to check the presence and location of the buccal exostosis. If the buccal exostosis is suspected to hinder the insertion of mini-implants, surgical excision of the exostosis is recommended prior to the placement of mini-implants.

t.me/Dr_Mouayyad_AlbtousH

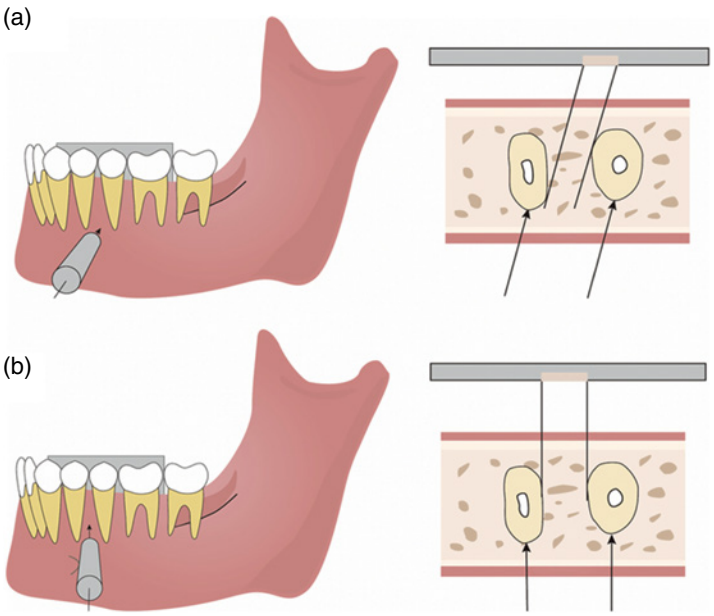


Figure 5.17 Two-dimensional radiographs often underestimate interradicular space. (a) Oblique projection. (b) Orthogonal projection. The interradicular space is underestimated due to the oblique projection.

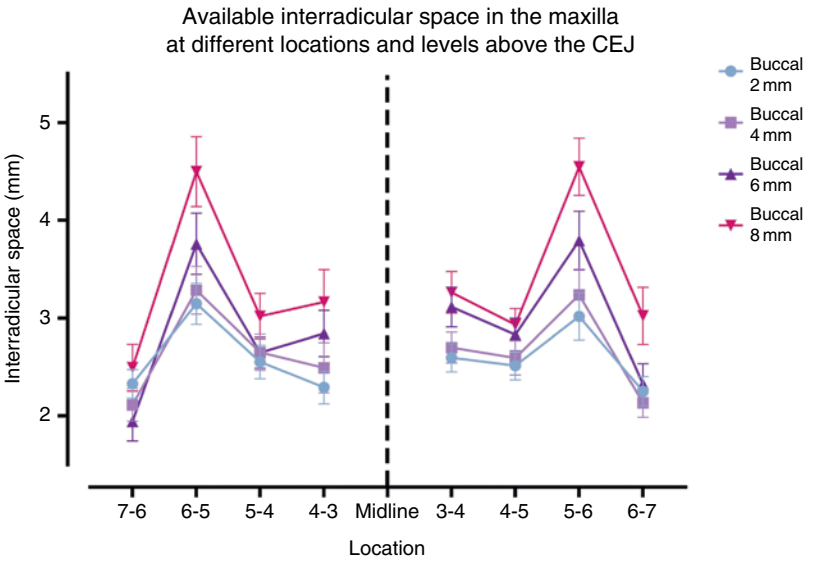


Figure 5.18 Bone widths at different interradicular sites and at different heights (2, 4, 6 and 8 mm apical to the CEJ).



Figure 5.19 The presence of buccal exostosis that is manifested as a benign nodular bony protuberance (yellow arrow).

Soft Tissue Factor: Soft Tissue Type

The placement of mini-implants may lead to soft tissue irritation, evoke soft tissue inflammation and infection, and even cause soft tissue overgrowth around the heads of mini-implants, especially for insertions at the non-keratinised movable mucosa zone.[29,30] Since the attached gingiva is keratinised and fixed onto the alveolar bone, it is more resistant to mechanical trauma and inflammation than movable mucosa. Thus, it is recommended to place mini-implants at the attached gingiva zone rather than the movable mucosa zone, so that the risk of soft tissue complications can be reduced.[31-33] In order to exploit the alveolar bone at a more apical level where bone quality and quantity are more desirable, operators are advised to place

t.me/Dr_Mouayyad_AlbtousH

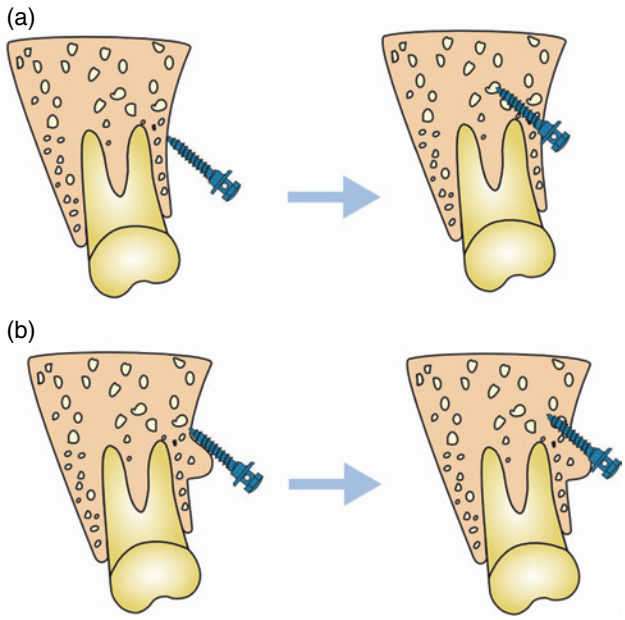


Figure 5.20 The presence of buccal exostosis interferes with the insertion of mini-implants. (a) The mini-implant can be inserted at appropriate depth if no exostosis is present. (b) The presence of a buccal exostosis prevents advancement of the mini-implant and leads to inadequate insertion depth.

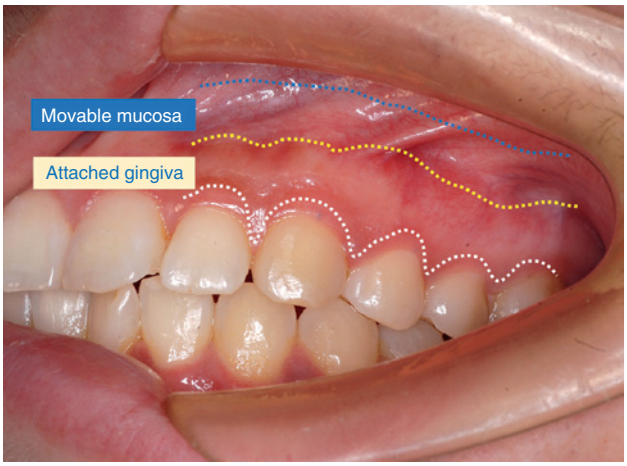


Figure 5.21 Mini-implants should be placed at the apical limit of the attached gingiva (indicated by the yellow dashed line). The apical limit of the free gingiva is indicated by the white dashed line and the vestibular sulcus by the blue dashed line.

mini-implants at the most apical limit of the attached gingiva, i.e. mucogingival junction (Figure 5.21).

The width of attached gingiva is defined as the distance from the gingival sulcus to the mucogingival junction. The width of attached gingiva is influenced by age and increases with an increase in patient age.[34] The width of attached gingiva is greater in the permanent dentition

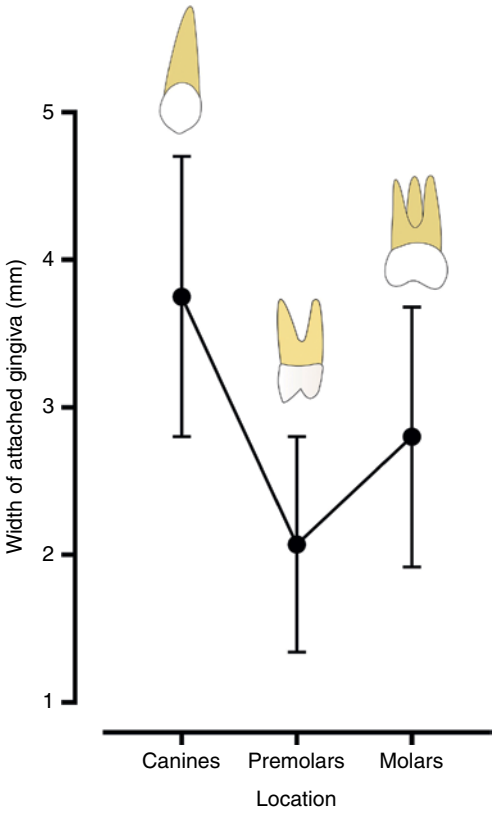


Figure 5.22 The width of attached gingiva at different buccal regions. Note that the averaged width of attached gingiva is greatest at the canine region and least at the premolar region. The width of attached gingiva exhibits great individual variations. *Source:* Adapted from Bhatia et al. [38].

than in the mixed dentition.[35] Moreover, it differs among different interradicular sites and fluctuates from the canine region to the second molar region.[36,37] Specifically, it decreases from the canine region to the premolar region and then increases gradually to the molar region (Figure 5.22), with the average value being 2–3 mm.[38] As depicted in Figure 5.22, great variations among different individuals are present, so this factor should be assessed case by case.

For interradicular sites with suboptimal height of mucogingival junction, slight apical movement of the entry point from the mucogingival junction with angled insertion technique (30–45° to the occlusal plane) can still leave the mini-implant head at the attached gingiva zone (Figure 5.23). However, for interradicular sites with very limited width of attached gingiva (especially in adolescents), the insertion angle should be greater than 45° so that the mini-implant heads can be left at the attached gingiva zone. In this clinical scenario, it is not recommended to pursue the placement of mini-implants in this area since slippage of mini-implants and cortical fracture may occur

t.me/Dr_Mouayyad_AlbtousH

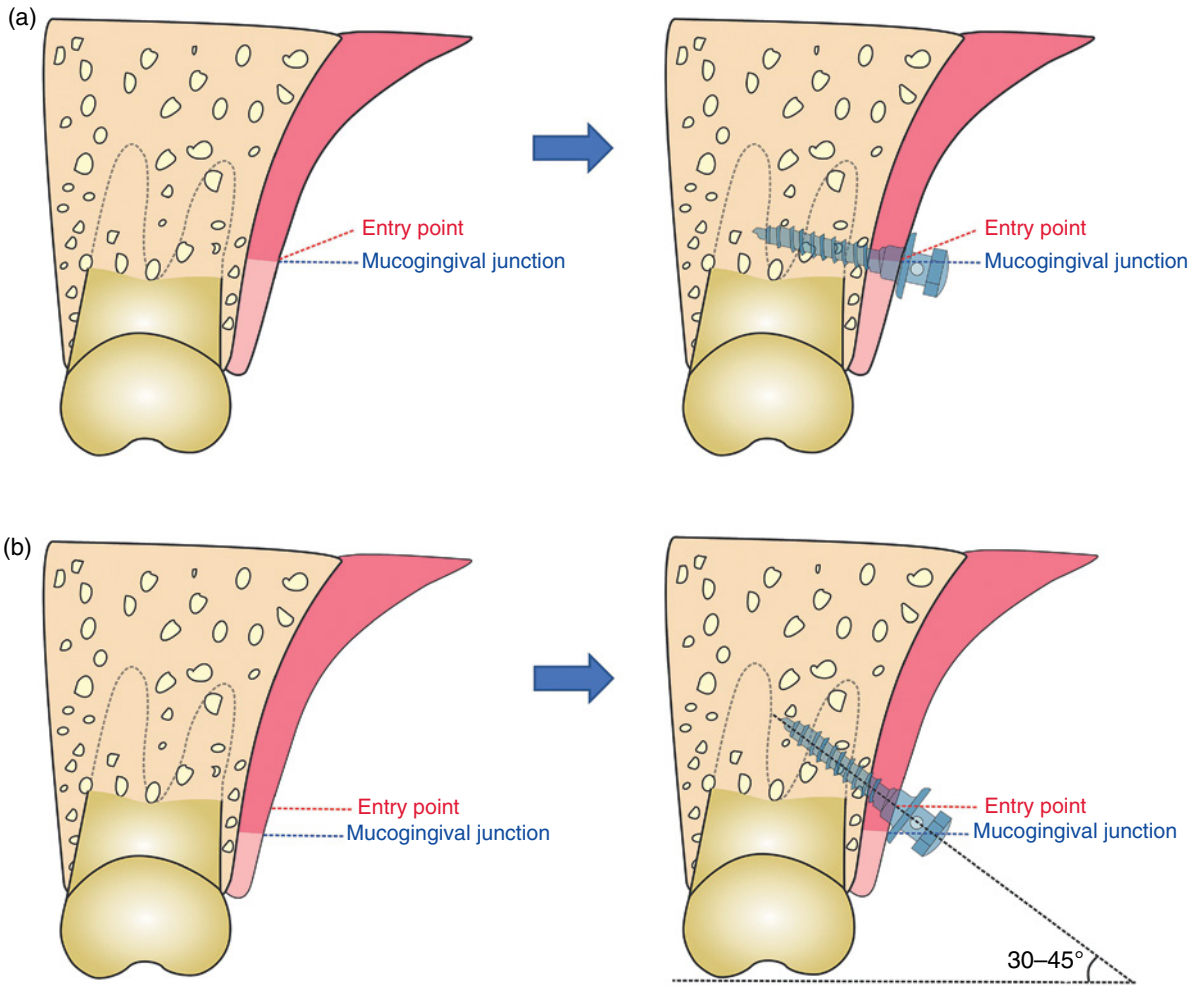


Figure 5.23 Angled insertion technique. (a) The amount of attached gingiva is sufficient at the insertion site with an adequate height of mucogingival junction. A mini-implant is inserted through an entry point that coincides with the mucogingival junction. (b) Attached gingiva is inadequate at the insertion site and the mucogingival junction is more occlusal. To prevent root injury and soft tissue complications, angled insertion technique (30–45° to the occlusal plane) is employed and the mini-implant is inserted through the entry point that is 2–3 mm apical to the mucogingival junction. No root contact occurs and the head of the mini-implant still lies in the attached gingiva zone, resulting in a low likelihood of soft tissue complications.

if the insertion angle is too large. Alternative anatomical regions can be considered to fulfil the biomechanical demands, e.g. infrazygomatic crest.

Furthermore, the thickness of attached gingiva ranges from 1.2 mm to 1.5 mm at the maxillary buccal region.[39] Thus, to guarantee adequate intrabony depth of mini-implants, the length of mini-implants is recommended to be 7–8 mm.

Soft Tissue Factor: Buccal Frenum

The presence of buccal frenum may complicate the insertion of mini-implants (Figure 5.24). It may lead to soft tissue irritation and trauma after mini-implants are placed due to its movability during functional movements, e.g. swallowing and speech. Thus, if the presented buccal frenum attaches too occlusally at the determined insertion site, frenectomy is recommended prior to the insertion of mini-implants.

5.2.2 Biomechanical Considerations

Mini-implants at the maxillary buccal region are versatile in achieving a variety of orthodontic tooth movements. Mini-implants inserted at different interradicular sites fulfil different biomechanical demands (Table 5.1). Specifically, mini-implants inserted at the U3-U4 and U4-U5 sites are applied for premolar intrusion and molar protraction while

t.me/Dr_Mouayyad_AlbtousH

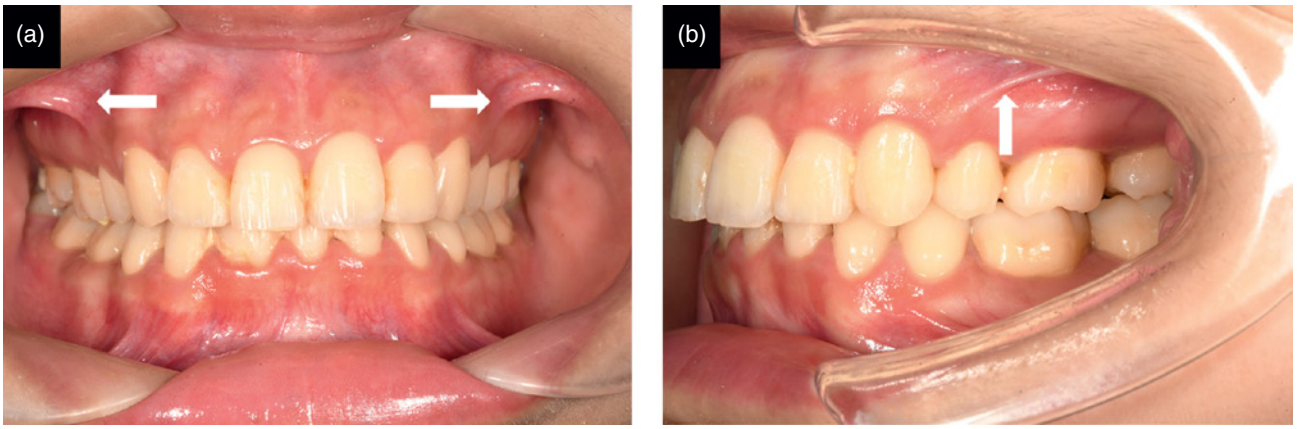
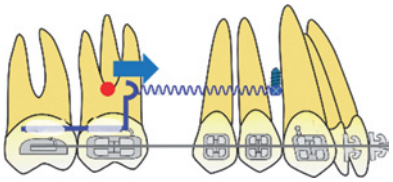
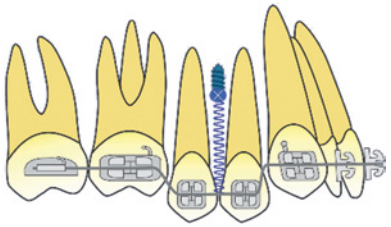
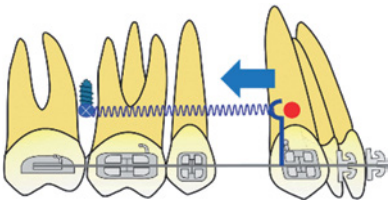
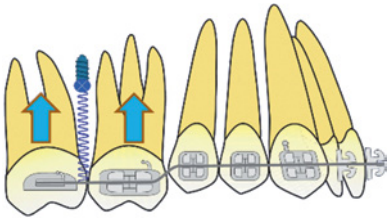
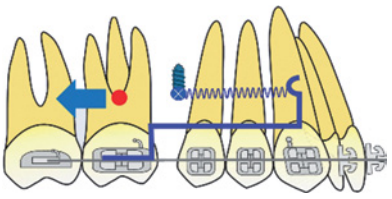


Figure 5.24 Buccal frenum may complicate the insertion process. (a) Frontal view. The buccal frena are indicated by white arrows. (b) Buccal view. The buccal frenum is indicated by the white arrow.

Table 5.1 The application of mini-implants at different interradicular sites.

Location	Application	
U3-U4 and U4-U5	Molar protraction	
	Premolar intrusion	
U5-U6 and U6-U7	Anterior retraction	
	Molar intrusion	
	Molar distalization	

t.me/Dr_Mouayyad_AlbtousH

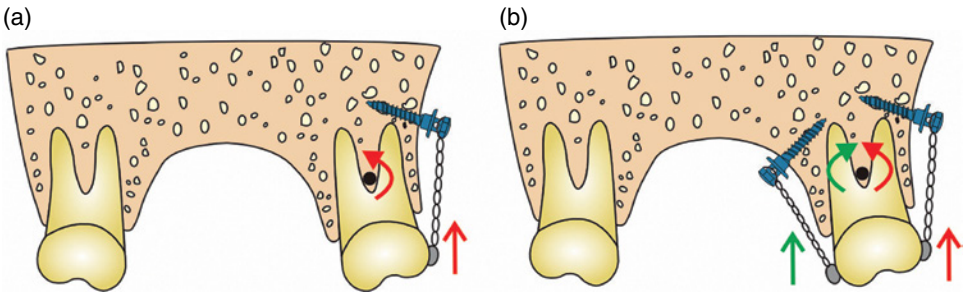


Figure 5.25 Biomechanics of molar intrusion with TADs. (a) A mini-implant is inserted at the buccal side for molar intrusion. The intrusive force passes buccally to the centre of resistance of the molar, resulting in buccal tipping of the molar during intrusion. (b) Mini-implants are inserted at both the buccal and palatal sides. Intrusive force is offered at both sides, so bodily intrusion of the molar occurs.

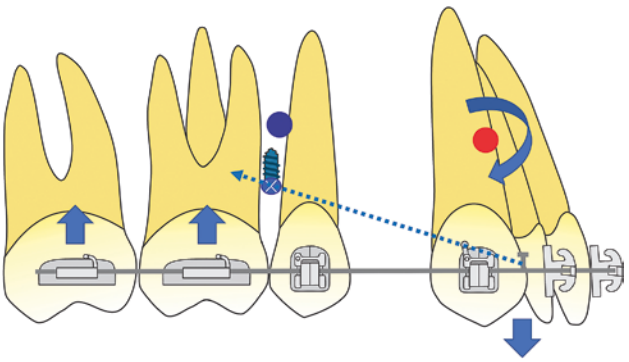


Figure 5.26 The retraction force (blue dashed arrow) offered by the mini-implant passes occlusally to the centre of resistance (red dot) of the anterior teeth. Thus, this retraction force generates a clockwise moment on the anterior teeth that leads to extrusion and lingual tipping of the anterior teeth. If the maxillary dentition is considered as a whole, the retraction force also passes occlusally to the centre of resistance (blue dot) of the maxillary dentition, leading to intrusion of the posterior teeth.

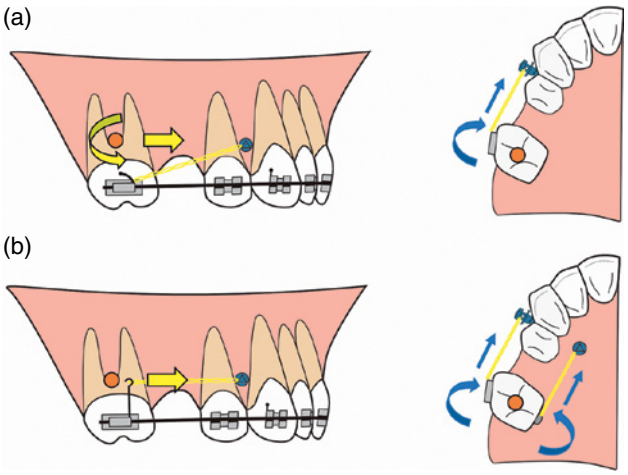


Figure 5.27 Molar protraction with mini-implants inserted at the interradicular site between the first and second premolars. (a) An elastomeric chain is applied between the buccal mini-implant and the molar. Sagittally, since the protraction force passes occlusally to the centre of resistance of the molar, the molar exhibits mesial tipping. Transversely, mesial-in rotation of the molar occurs as the protraction force passes buccally to the centre of resistance of the molar. (b) The molar is protracted through long hooks on both the buccal and palatal sides. Sagittally, as the protraction forces pass through the centre of resistance, the molar exhibits bodily movement during protraction. Transversely, since the molar is protracted from both the buccal and palatal sides, no rotation of the molar occurs.

those placed at the U5-U6 and U6-U7 sites are exploited for achieving *en masse* anterior retraction, molar distalisation and molar intrusion. For the intrusion of premolars or molars, the buccal mini-implant offers intrusive force at the buccal side, resulting in buccal tipping of premolars or molars. Thus, this biomechanical side-effect should be borne in mind and adding a mini-implant at the palatal side can resolve this biomechanical drawback (Figure 5.25).

For anterior retraction through bilateral mini-implants inserted at the U5-U6 or U6-U7 site, since the retraction force passes occlusally to the centre of resistance, lingual tipping and extrusion of anterior teeth and intrusion of molars may occur (Figure 5.26). Depending on orthodontic treatment planning, if this biomechanical effect is desired (e.g. open bite), further biomechanics is not needed. Otherwise, appropriate measures should be taken to avoid this adverse effect, e.g. incisor intrusion through a labial mini-implant and molar extrusion through vertical elastics. For molar protraction, mesial tipping and rotation of molars may occur and mini-implants at both buccal and palatal sides with power arms are able to avoid these biomechanical disadvantages (Figure 5.27).

5.2.3 Selection of Appropriate Insertion Sites

Based on hard tissue factors, the most appropriate interradicular site is U5-U6 where sufficient interradicular distance is present, with the insertion height being 6–8 mm apical to the CEJ. Moreover, angled insertion (30–45° to the

t.me/Dr_Mouayyad_AlbtousH

occlusal plane) is recommended to exploit alveolar bone at more apical levels. Assuming that an 8 mm mini-implant is used and the thickness of soft tissue is 2 mm, the intra-bony length of the mini-implant will be 6 mm (Figure 5.28). If the insertion angle is 30° to the occlusal plane, the tip of the mini-implant is 3 mm apical to the entry point. In the axial view, the distance between the buccolingual midpoints between two adjacent roots is the narrowest compared to that between buccal or lingual points, and is considered to be the limiting factor in determining the availability of placing a mini-implant (Figure 5.29). Depending on the buccolingual positions of dental roots, the point where the long axis of the mini-implant intersects with the plane passing through the midpoints of two adjacent roots is usually 2–3 mm (defined as the apical-gaining distance) apical to the entry point (Figure 5.30). Thus, with an insertion angle being 30°, the recommended entry point is the subtraction of the apical-gaining distance (2–3 mm) from the recommended insertion height (6–8 mm), rendering the recommended entry point to be 3–6 mm.

Moreover, the positions of the root curvature of the mesiobuccal roots of the first molars should be carefully determined in order to reduce the risk of root injury. Based on soft tissue factors, the height of the mucogingival junction should be meticulously evaluated. For suboptimal width of attached gingiva, angled insertion is able to move the entry point apically while keeping the mini-implant head at the attached gingiva zone. In contrast, for other interradicular sites (i.e. U3-U4, U4-U5 and U6-U7), the suitability of placing mini-implants should be determined on a case-by-case basis according to the individual's hard tissue and soft tissue factors.

Therefore, we recommend that practitioners place mini-implants at the U5-U6 interradicular site at the height of 3–6 mm apical to the CEJ with the insertion angle being 30–45° to the occlusal plane (Figure 5.31).

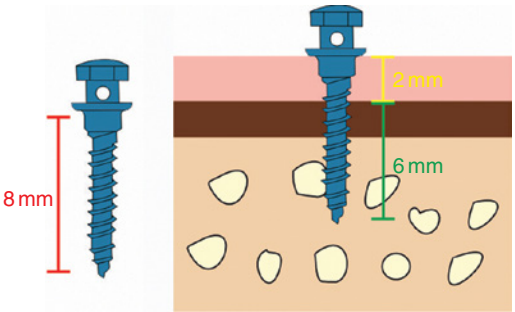


Figure 5.28 For a mini-implant with a length of 8 mm, the intra-bony length of the mini-implant will be 6 mm if the thickness of the soft tissue is 2 mm.

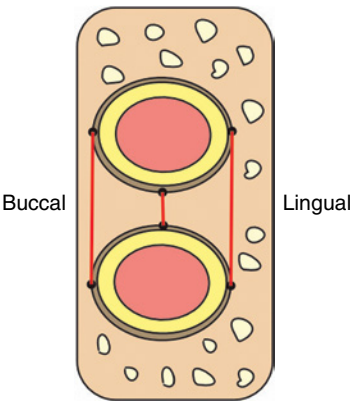
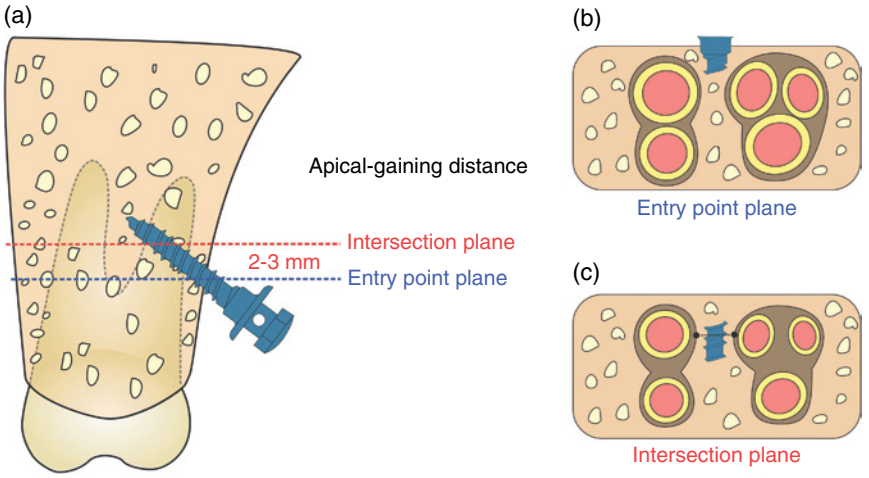


Figure 5.29 The distance between the buccolingual midpoints between two adjacent roots is narrower compared to that between buccal or lingual points.

Figure 5.30 (a) The intersection plane is the plane where the mini-implant passes through the narrowest space between the two adjacent buccal roots (e.g. between the buccal root of the second premolar and the mesiobuccal root of the first molar).The intersection plane is usually 2–3 mm apical to the entry point plane and the distance between the two planes is defined as the apical gaining distance. (b) Axial view of the mini-implant and the two adjacent roots at the entry point plane. (c) Axial view of the mini-implant and the two adjacent roots at the intersection plane. Note that the mini-implant passes through the narrowest space (between the buccolingual midpoints of the buccal adjacent roots) between the two adjacent roots.



t.me/Dr_Mouayyad_AlbtousH

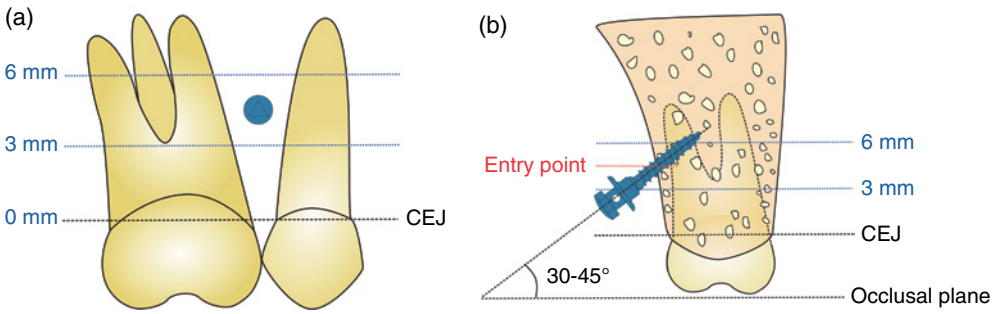


Figure 5.31 Recommended insertion heights and angle for the insertion of a mini-implant at the U5-U6 interradicular site. (a) The mini-implant is recommended to be inserted at the height of 3–6 mm apical to the CEJ. (b) The mini-implant is recommended to be inserted with an angle of 30–45° to the occlusal plane.

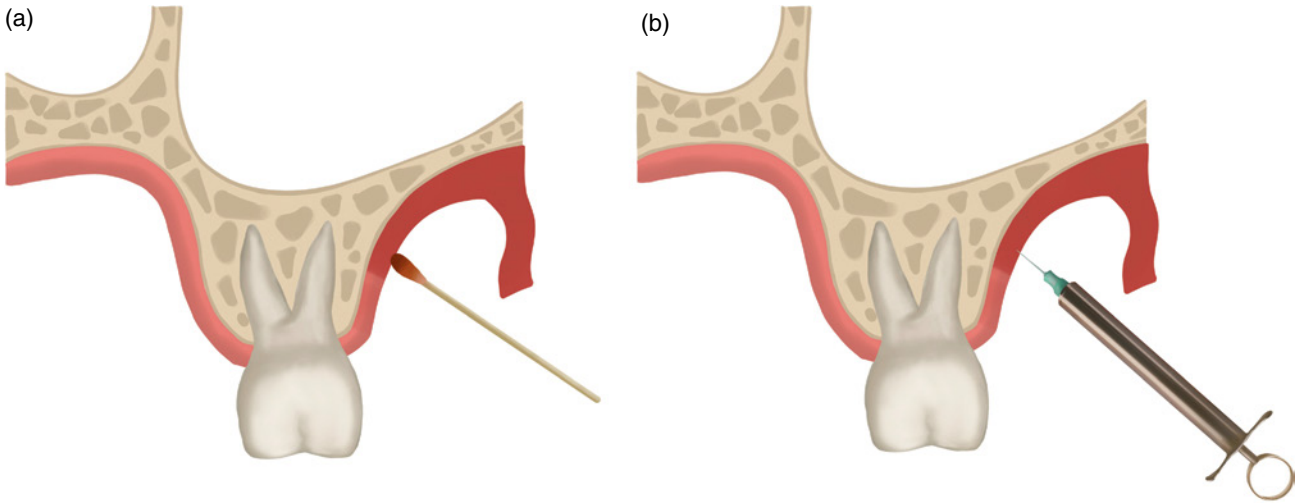


Figure 5.32 (a) Mucosa disinfection with iodophor. (b) Local infiltration anaesthesia. Note the injection point is 1–2 mm apical to the mucogingival junction.

5.2.4 Insertion Techniques

Preinsertion

Based on pretreatment examinations, anchorage requirements and biomechanical designs, the specific interradicular site of choice is selected. Insertion height and angle are determined based on meticulous pretreatment radiographic evaluations. Moreover, mini-implants with appropriate diameters and lengths are determined, and insertion armamentaria are sterilised and prepared. The use of 3-D insertion guides is recommended for placement of mini-implants with high demands of accuracy and precision.

Insertion Procedures

First, local infiltration anaesthesia is performed following mucosa disinfection with iodophor (Figure 5.32). Notably, since the attached gingiva is keratinised and fixed onto the alveolar bone, injection through the attached gingiva or even at the mucogingival junction elicits an acutely painful response. Thus, we recommend that the injection point is located 1–2 mm apical to the mucogingival junction where the mucosa is loose. In order to maintain adjacent roots sensitive to nociceptive stimuli, a small amount of anesthetic agent (0.2–0.5 ml) is recommended so that operators can be alerted to root contact by mini-implants. To reduce patients' painful perception, slow injection of the anaesthetic agents is recommended with manual injection.

Alternatively, the clinical availability of the painless single tooth anaesthesia (STA) system has enabled the delivery of anaesthetic agent through computer-controlled injection. Less painful perception was reported by patients receiving the STA system than those receiving traditional manual injection.[40,41] For patients with low pain threshold or dental treatment phobia, the STA system can be used. Following the confirmation of satisfactory anaesthesia, patients are instructed to rinse with chlorhexidine for 30–60 seconds to reduce microbial levels.

t.me/Dr_Mouayyad_AlbtousH

Second, the predetermined entry point is marked with an explorer or dental probe, and the mesiodistal position of the entry point should be checked from both the buccal and occlusal sides (Figure 5.33). In particular, confirmation of the mesiodistal position of the entry point from the occlusal side is very important. Since the operator's line of view is often oblique to the insertion site, checking the entry point with the naked eye from the chairside may lead to an entry point that is distal to the desired one (Figure 5.34). Then, a vertical mucosa indentation is made and the mesiodistal inclination of the vertical indentation is confirmed from the occlusal side (Figure 5.35). The vertical mucosa indentation is helpful in guiding the insertion so that the correct mesiodistal insertion angle can be followed.

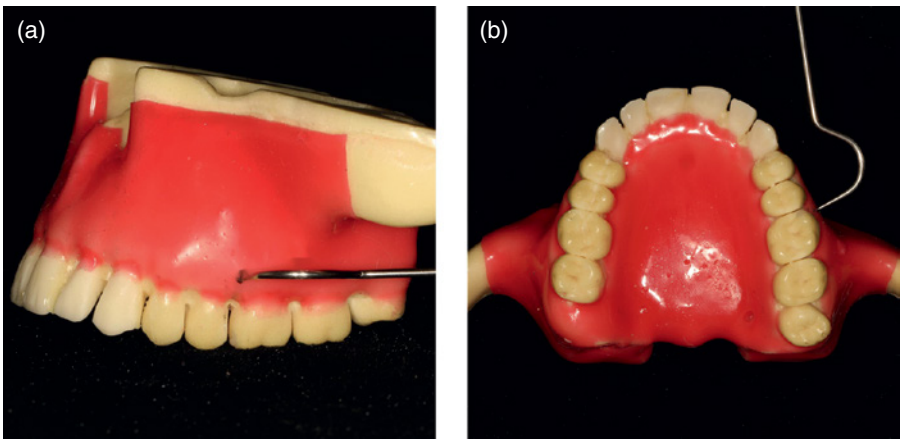


Figure 5.33 (a) The entry point is marked with an explorer (buccal view). (b) Confirm the mesiodistal position of the entry point from the occlusal side.

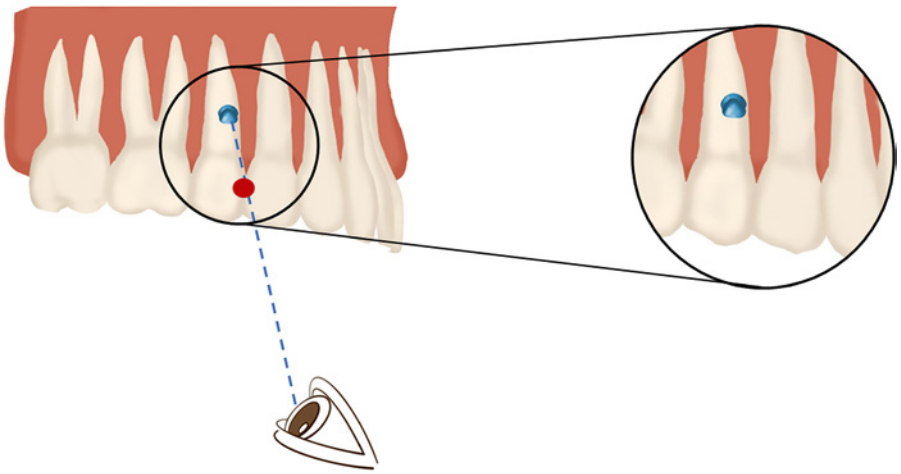


Figure 5.34 Oblique line of view leads to an entry point that is distal to the desired one. The distally positioned entry point may lead to root contact by the mini-implant with the distal tooth.

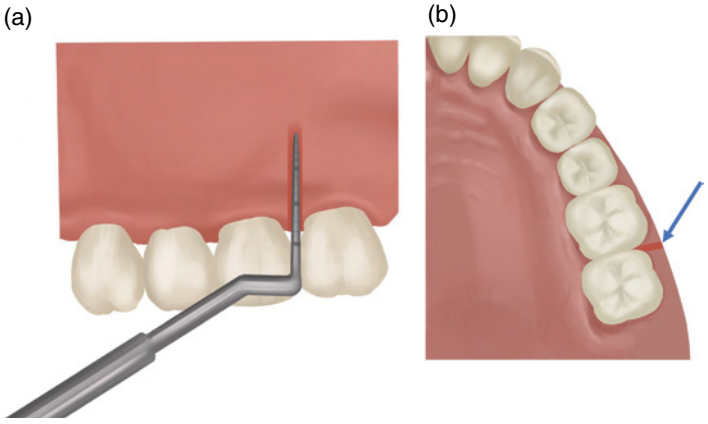


Figure 5.35 (a) A vertical mucosa indentation is made with a dental probe; the indentation should be in the middle of the interradicular space. (b) The mesiodistal inclination of the vertical indentation is confirmed from the occlusal side.

t.me/Dr_Mouayyad_AlbtousH

Third, once the entry point and the vertical mucosa indentation are correctly marked, the next procedure is to insert the mini-implant through the entry point. After mounting the mini-implant onto the screwdriver, the operator should hold the screwdriver firmly and the mini-implant should be placed against the bone surface in parallel with the occlusal plane (Figure 5.36). Then, the mini-implant is slowly advanced to penetrate the bone cortex by rotating the screwdriver (Figure 5.37a). Notably, due to the relatively high density of the cortex, slow rotation (less than 30 rpm) is recommended so as to reduce any possible thermal and mechanical damage to the bone cortex. Once the cortex is penetrated, slight derotation (1–2 turns) of the screwdriver is performed so that the mini-implant is slightly moved away from the cortex (Figure 5.37b), rendering the change of insertion angle to be applicable (Figure 5.37c,d).

Fourth, once the bone cortex is penetrated, angled insertion technique is implemented. Specifically, the insertion angle is 30–45° to the occlusal plane (Figure 5.38). Before insertion of the mini-implant, confirmation of the mesiodistal orientation of the insertion is mandatory, in order to reduce the likelihood of root injury (Figure 5.39). Due to the limited access for the posterior interradicular sites, the desired mesiodistal inclination of the insertion may not be

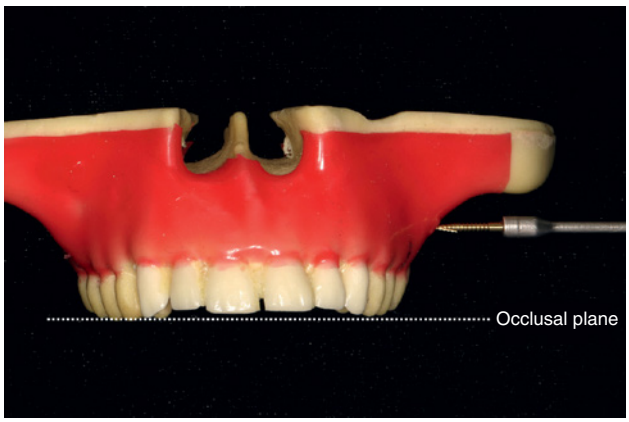


Figure 5.36 A mini-implant is placed against the buccal bone surface for cortex penetration. Note that the insertion path is parallel to the occlusal plane.

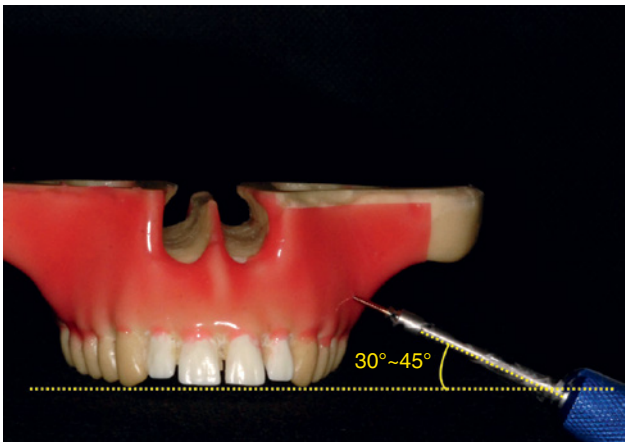


Figure 5.38 The recommended insertion angle is 30–45° to the occlusal plane.

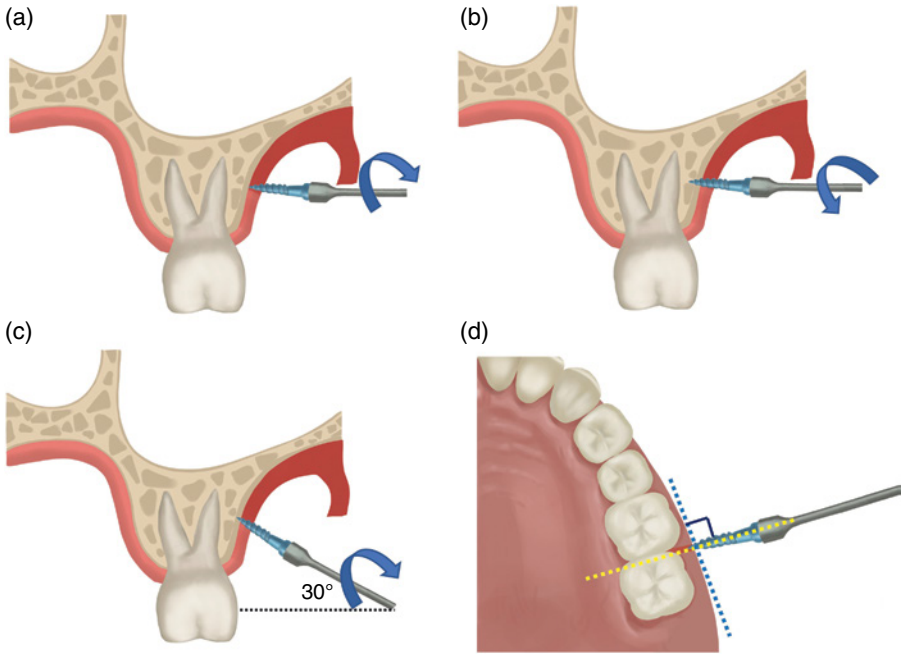


Figure 5.37 (a) Cortex penetration. (b) Derotation of the mini-implant once the cortex has been penetrated. (c) The desired insertion angle (e.g. 30° to the occlusal plane) is obtained by changing the insertion path. (d) Confirm the insertion path from the occlusal side. Notably, the insertion path is perpendicular to the tangent line of the dental arch passing through the entry point.

t.me/Dr_Mouayyad_AlbtousH

executed. Specifically, cheek or lip tension often leads to distal orientation of the insertion, resulting in a high risk of root injury (Figure 5.40). If this is encountered in clinical practice, two solutions are recommended to solve this problem: reduction in mouth opening and the use of a contra-angle screwdriver. Specifically, the decrease in mouth opening is able to reduce lip or cheek tension so that the desirable mesiodistal insertion angle can be implemented. Moreover, the contra-angle screwdriver is able to overcome this anatomical limitation due to its different configuration from the straight screwdriver. Once the mesiodistal orientation is confirmed from the occlusal view, the mini-implant is advanced lowly (less than 30 rpm) until there is firm contact between the mini-implant platform and the soft tissue (Figure 5.41). Notably, overinsertion is prohibited since it may lead to soft tissue complications, e.g. mucosa overgrowth.

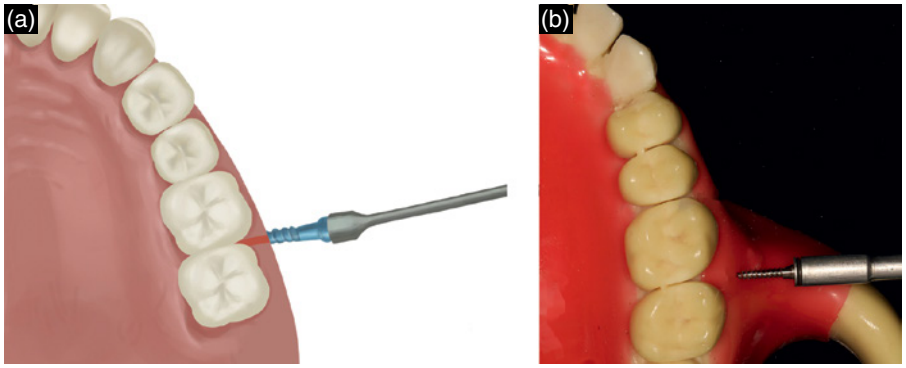


Figure 5.39 Confirmation of the insertion path from the occlusal side. (a) Schematic illustration. (b) A skull model.

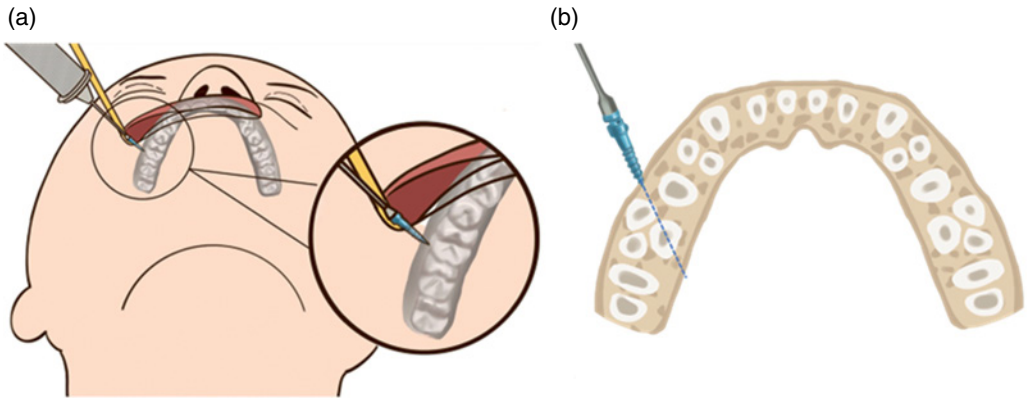


Figure 5.40 Anatomical limitations lead to a distal orientation of the insertion path. (a) Soft tissue tension, especially cheek tension, limits perpendicular insertion of the mini-implant to the bone surface and leads to distal inclination of the insertion. (b) The distal orientation of the insertion may result in root injury, especially for the root of the distal tooth.

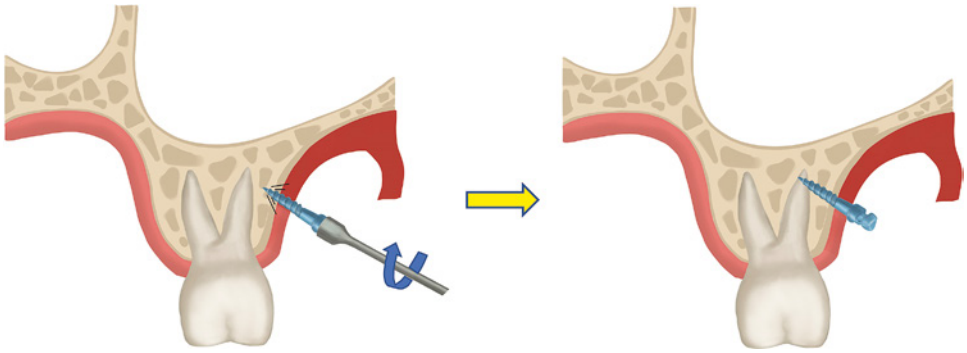


Figure 5.41 Advancement of the mini-implant with the confirmed insertion path.

t.me/Dr_Mouayyad_AlbtousH

Lastly, once the insertion is complete, the position and orientation of the mini-implants should be checked from both the buccal and occlusal sides. Primary stability is evaluated and reinsertion may be indicated if insufficient primary stability is detected. Moreover, patients should be asked about any discomfort, while sharp pain may suggest the presence of root contact. Percussion testing and further radiographic examinations may be performed to rule out root contact.

The detailed clinical procedures of placing an interradicular mini-implant at the maxillary buccal region is displayed in Figures 5.42–5.46.

5.2.5 Clinical Applications

En Masse Anterior Retraction

Bimaxillary protrusion is a common dentofacial condition associated with proclination of maxillary and mandibular incisors relative to the dental and cranial bases, resulting in soft tissue procumbence and undesirable facial aesthetics.[42] The treatment goal is to retract the proclined anterior teeth following premolar extractions, so that protrusive profile is resolved and facial aesthetics improved. For these cases, maximal anchorage is often indicated and orthodontic TADs are recommended to reinforce molar anchorage and to accomplish *en masse* anterior retraction. Usually, mini-implants inserted at the U5-U6 and U6-U7 interradicular sites are recommended. Two case examples are presented below to demonstrate the clinical applications of mini-implants for **en masse** anterior retraction.

Case 1 A female adult sought orthodontic treatment with a chief complaint of lip protrusion and crooked teeth. Her extraoral and intraoral examinations were indicative of class II canine and molar relationships on both sides, anterior deep bite, mild dental crowding in both arches and convex facial profile (Figure 5.47). Cephalometric analysis revealed that she had class II skeletal base (ANB = 6.5), low mandibular plane angle (SN-MP = 27.9),

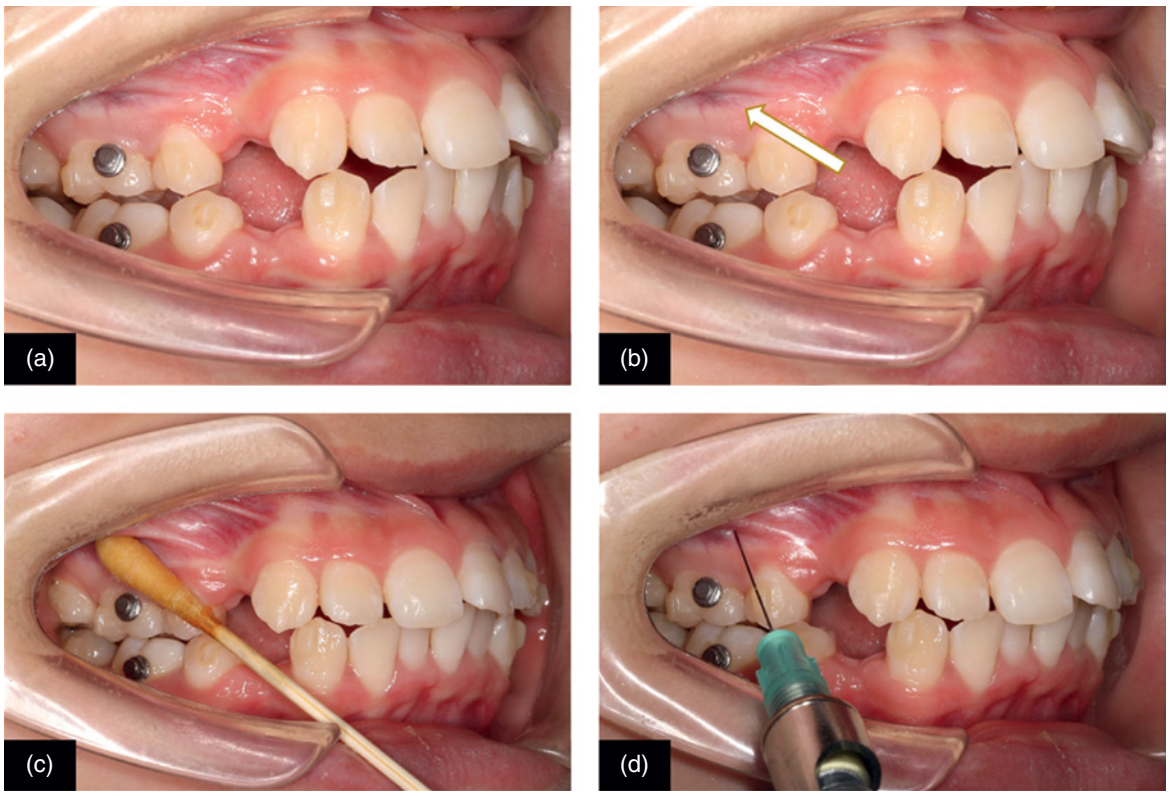


Figure 5.42 The detailed clinical procedures of placing a mini-implant at the interradicular region between the second premolar and the first molar. (a,b) Determine the desired entry point (white arrow). (c) Mucosa disinfection with iodophor. (d) Local infiltration anaesthesia.

t.me/Dr_Mouayyad_AlbtousH

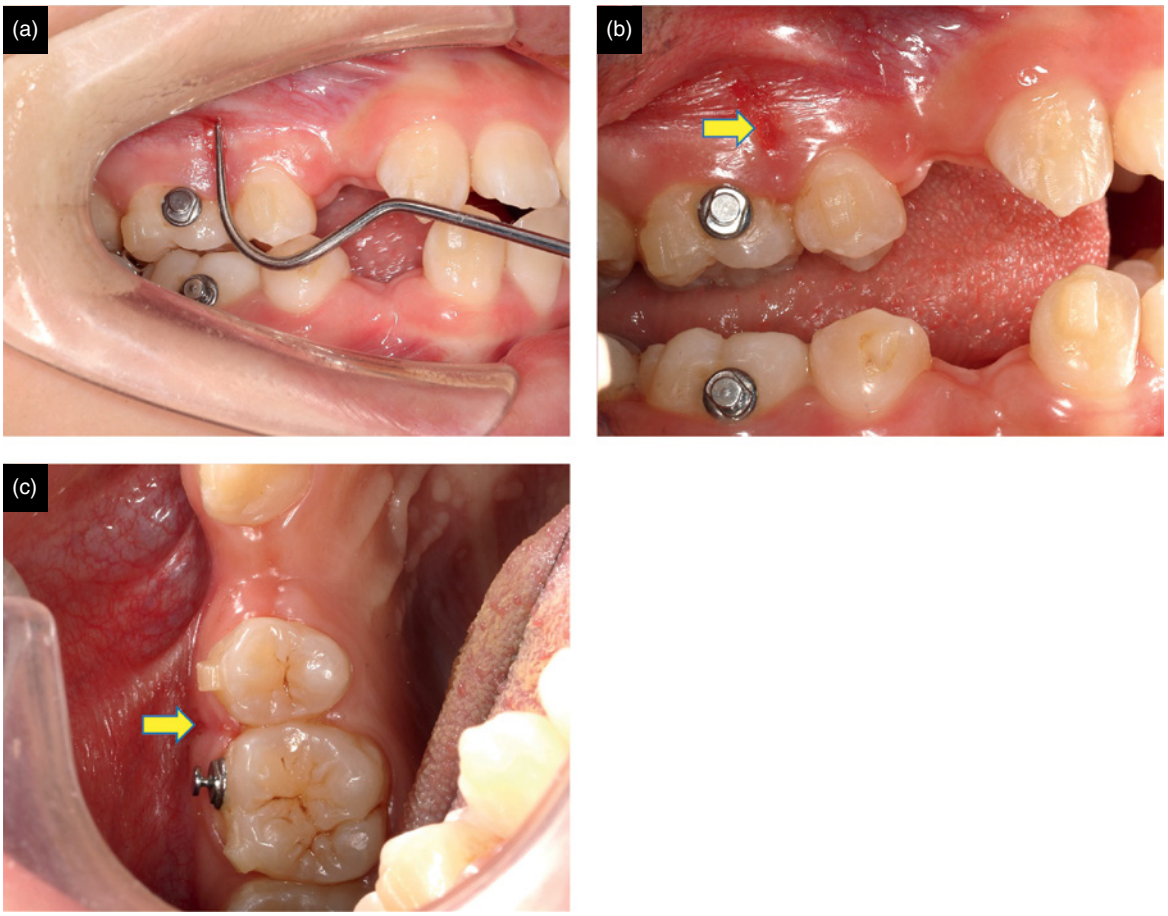


Figure 5.43 (a) Create a vertical indentation with an explorer. (b) Check the orientation of the vertical indentation (yellow arrow) from the buccal side. (c) Confirm the orientation of the vertical indentation (yellow arrow) from the occlusal side.

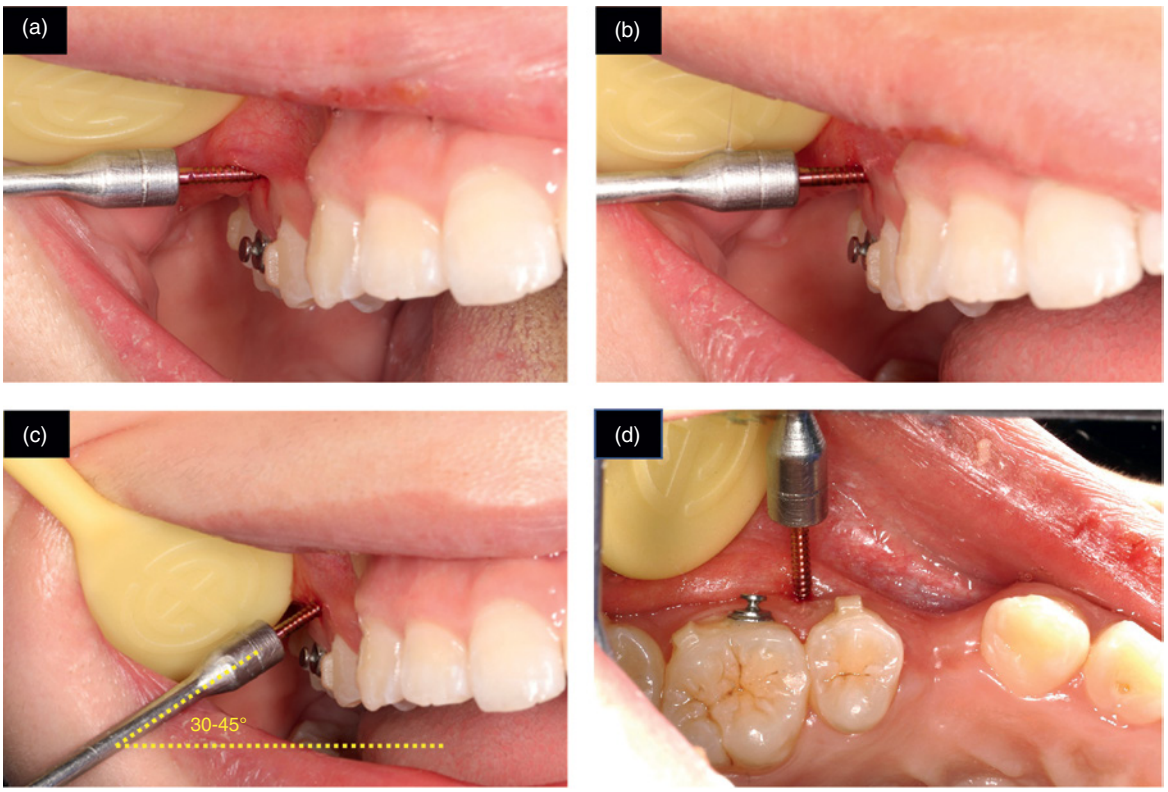


Figure 5.44 (a) Insert the mini-implant through the designated entry point. (b) Cortex penetration. (c) Change the insertion path to obtain an angled insertion (30° to the occlusal plane). (d) Confirm the mesiodistal orientation of the insertion path from the occlusal side.

t.me/Dr_Mouayyad_AlbtousH

normal labiolingual inclination of the upper incisors (U1-SN = 104.1) and proclined lower incisors (L1-MP = 107.5) (Table 5.2).

To resolve lip protrusion, extractions of the four first premolars were planned, with requirements of maximal molar anchorage. To reinforce molar anchorage and facilitate *en masse* anterior retraction, two mini-implants were inserted at the bilateral maxillary interradicular sites between the second premolars and first molars, and long crimpable hooks were used for anterior retraction (Figure 5.48). Following active orthodontic treatment, bilateral class I canine and molar relationships were obtained, and normal incisor overjet and overbite were achieved. Moreover, following retraction of the anterior teeth, a convex facial profile was resolved and a straight facial profile was achieved (Figure 5.49). The pre- and posttreatment cephalometric analyses are presented in Table 5.3.

Case 2 An adult female presented with a chief complaint of incisor proclination and protrusive facial profile. The clinical examinations were indicative of bilateral class I molar relationship, anterior open bite, mild crowding in both arches and convex facial profile (Figure 5.50). Moreover, the panoramic radiography revealed that three third molars (28, 38 and 48) were impacted, with the lower two being horizontally impacted. The lateral cephalometry indicated that the patient had class I skeletal base (ANB = 3.9), average mandibular plane (SN-MP = 35.2) and incisor proclination in both arches (U1-SN = 119.8; L1-MP = 108.2) (Table 5.4).

Based on the pretreatment evaluations, extractions of the impacted third molars and four first premolars were planned, followed by *en masse* anterior retraction with maximal molar anchorage. The treatment goal was to resolve lip incompetence and improve profile aesthetics. To reinforce molar anchorage, insertion of two mini-implants at the bilateral U6-U7 sites was planned.

The proclined anterior teeth were retracted by applying orthodontic elastics between crimpable hooks on the archwire and the mini-implants at the maxillary buccal region. From the perspective of biomechanics, since the retraction force passed occlusally to the centre of resistance of the anterior teeth, a clockwise moment was generated during the anterior retraction. This moment would lead to incisor extrusion and lingual tipping, which can be leveraged to correct anterior open bite and incisor proclination (Figure 5.51).

The orthodontic treatment progressed smoothly and efficiently, with open bite and incisor proclination being corrected in the middle of the treatment (Figure 5.52). Following the active orthodontic treatment, bilateral class I canine and molar relationships were maintained, with incisor proclination and anterior open bite resolved (Figure 5.53). Normal anterior overbite and overjet were achieved. Moreover, following anterior retraction, good facial profile aesthetics was accomplished. The superimposition of



Figure 5.45 The insertion is complete once the platform of the mini-implant is in slightly firm contact with the soft tissue.



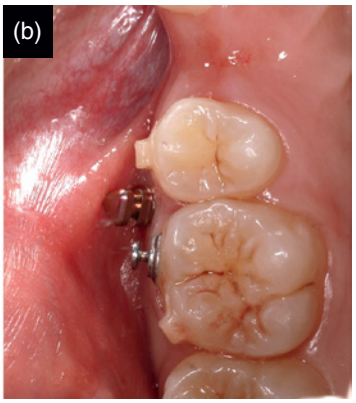


Figure 5.46 Check the position and orientation of the mini-implant following insertion. (a) Buccal view. (b) Occlusal view.

t.me/Dr_Mouayyad_AlbtousH

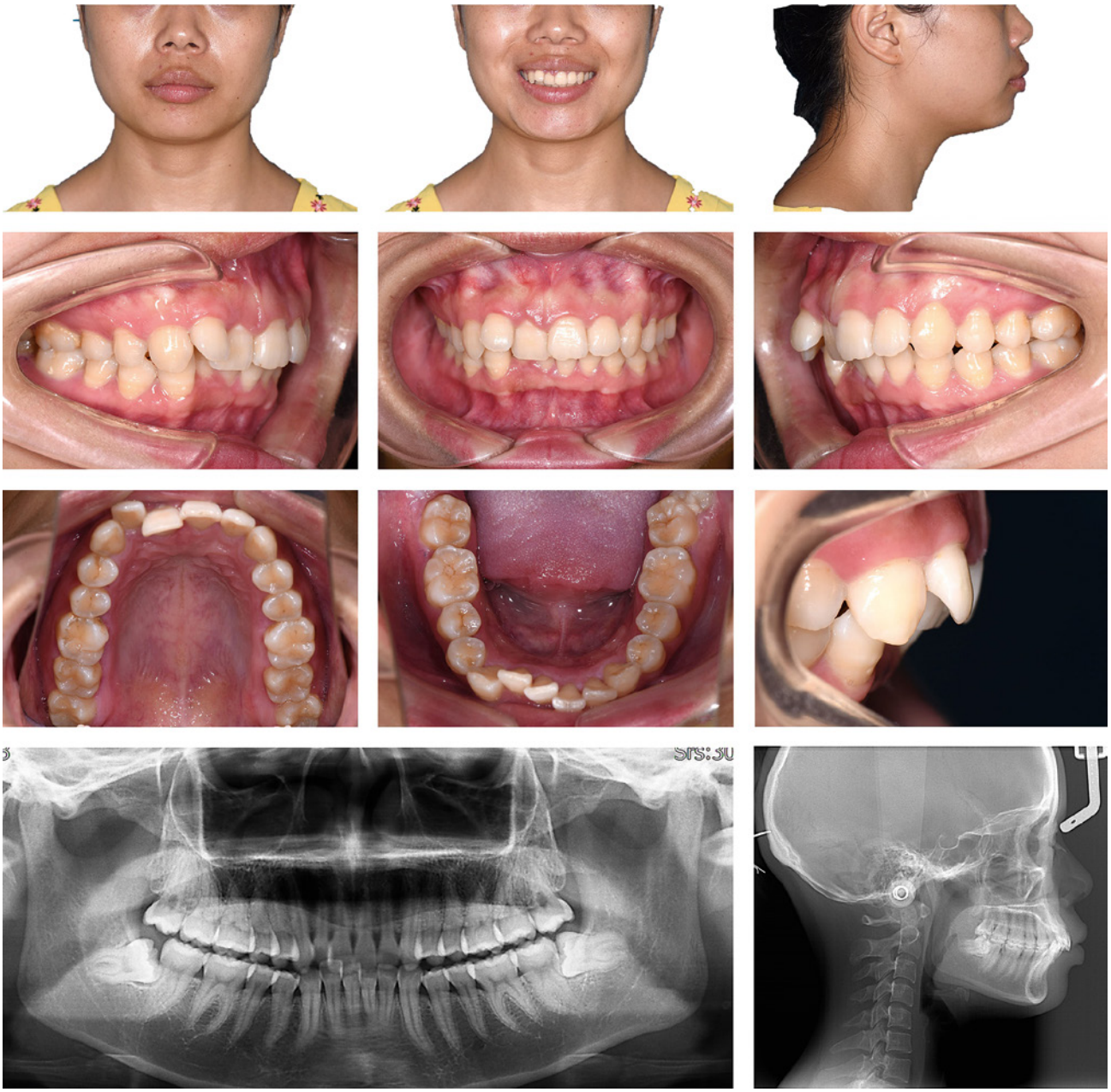


Figure 5.47 Pretreatment photographs and radiographs.

t.me/Dr_Mouayyad_AlbtousH

Table 5.2 Pretreatment lateral cephalometric analysis.

Measurement	Norm	Pretreatment
Skeletal (°)		
SNA	83.0±4.0	83.5
SNB	80.0±4.0	77
ANB	2.0±2.0	6.5
FMA	28.0±4.0	18.6
SN-MP	35.0±4.0	27.9
Dental (°)		
U1-SN	105.7±6.3	104.1
L1-MP	97.0±7.1	107.5
FMIA	65.0±6.0	53.9
U1-L1	124.0±8.0	120.6
Soft tissue (mm)		
UL-EP	2.0±2.0	3.1
LL-EP	3.0±2.0	5.2
Wits (mm)		
Wits	–1.0	5.9

pre- and posttreatment lateral cephalometry revealed that anterior retraction with maximal molar anchorage was achieved (Figure 5.54 and Table 5.5).

Molar Protraction

Molar protraction is often indicated among patients with missing first or second molars and the presence of well-developed third molars. The molars to be protracted are susceptible to mesial tipping and rotation if inappropriate biomechanics is applied. Thus, molar protraction is very challenging and demands meticulous and judicious biomechanical designs. To overcome frequently encountered biomechanical limitations, we recommend two mini-implants be inserted at the interradicular sites at the premolar regions (one on the buccal side and the other on the palatal side). Moreover, power arms can be leveraged so that the protraction force passes through the centre of resistance of molars (Figure 5.55). In this way, mesial tipping of the molars will be eliminated and bodily protraction of molars can be achieved. A case example is presented below.

An adult male presented to the multidisciplinary department with a chief complaint of multidisciplinary



Figure 5.48 Treatment progress. Two mini-implants were placed bilaterally between the second premolars and first molars to reinforce molar anchorage and facilitate *en masse* anterior retraction through long crimpable hooks.

t.me/Dr_Mouayyad_AlbtousH

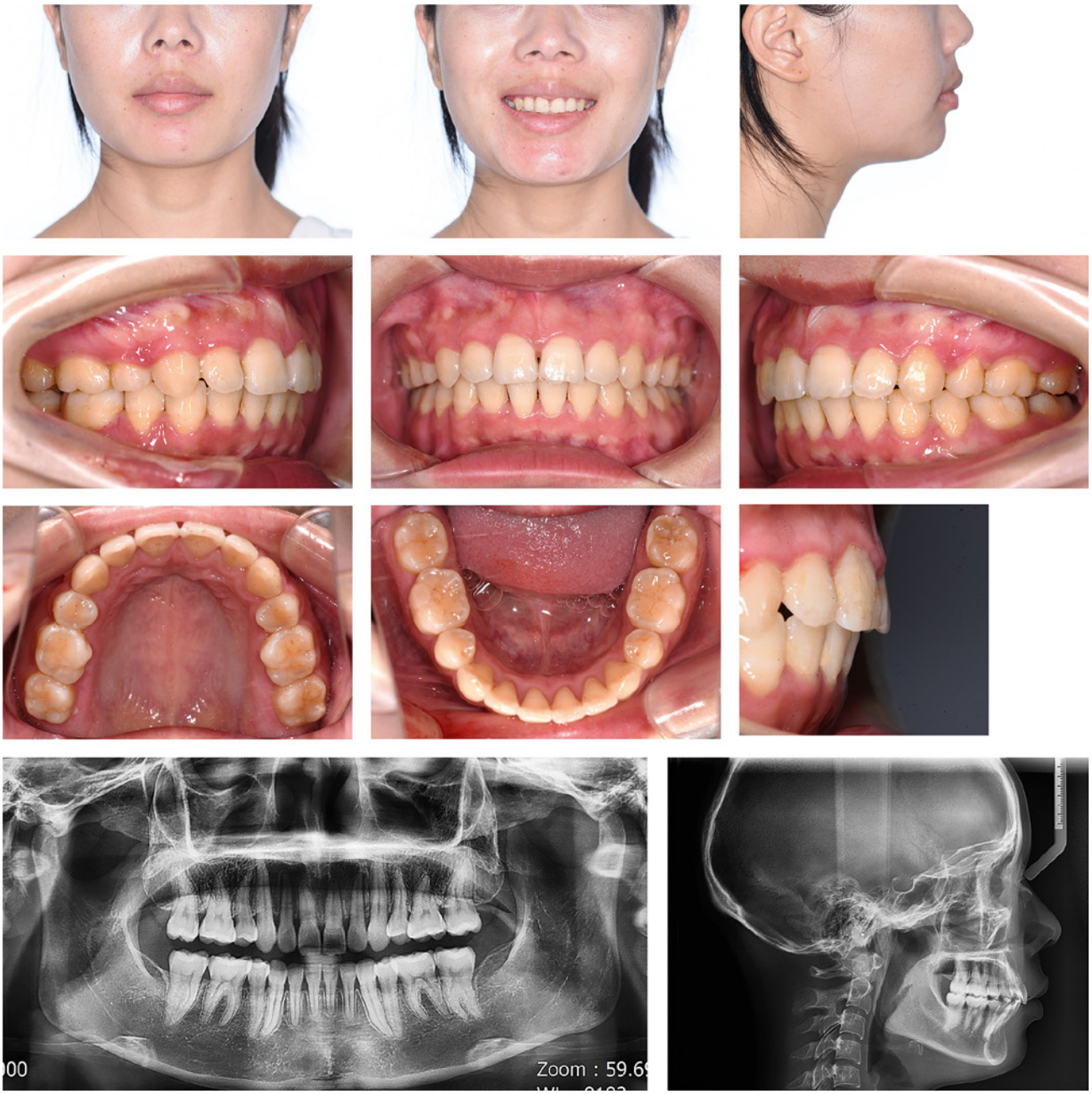


Figure 5.49 Posttreatment photographs and radiographs.

t.me/Dr_Mouayyad_AlbtousH

Table 5.3 Pre- and posttreatment lateral cephalometric analysis.

Measurement	Norm	Pretreatment	Posttreatment
Skeletal (°)			
SNA	83.0±4.0	83.5	81.6
SNB	80.0±4.0	77	76.4
ANB	2.0±2.0	6.5	5.2
FMA	28.0±4.0	18.6	20.2
SN-MP	35.0±4.0	27.9	28.4
Dental (°)			
U1-SN	105.7±6.3	104.1	101.2
L1-MP	97.0±7.1	107.5	103.3
FMIA	65.0±6.0	53.9	56.5
U1-L1	124.0±8.0	120.6	127
Soft tissue (mm)			
UL-EP	2.0±2.0	3.1	1.5
LL-EP	3.0±2.0	5.2	3.2
Wits (mm)			
Wits	–1.0	5.9	3.5

treatment advice. As displayed in Figure 5.56, the clinical and radiographic examinations revealed that the maxillary left second molar was subject to severe caries. The adjacent maxillary third molar was present intraorally with good root development.

Two multidisciplinary treatment alternatives were established following multidisciplinary consultation and thorough discussion. The first treatment plan was to perform root canal therapy for the maxillary second molar (27) and prosthetic crown restoration would be performed following post build-up. The second treatment alternative was to extract the second molar (27) and protract the adjacent third molar (28) for substitution of the second molar (27). After discussion with the patient, he finally chose the second treatment plan.

Two mini-implants were inserted at the U4-U5 interradicular sites, with one on the buccal side and the other on the palatal side (Figure 5.57). Molar protraction progressed efficiently and smoothly, and segmental archwire technique was applied for final tooth alignment (Figure 5.58). Finally, the maxillary left third molar was successfully protracted mesially with good root parallelism with the adjacent first molar (Figure 5.59).

Molar Intrusion

Molar intrusion is indicated among patients with molar overeruption or among open bite patients demanding adequate vertical control. Molar intrusion can be accomplished through mini-implants inserted at interradicular sites. However, prudent biomechanical designs should be implemented, otherwise adverse effects may occur due to inappropriate intrusive biomechanics. From the biomechanics perspective, intrusive force generated from either the buccal or palatal side may lead to inadvertent buccal or lingual tipping of molars (Figure 5.60). To overcome this biomechanical shortcoming, two mini-implants (one on the buccal side and the other on the palatal side) are applied to offer intrusive forces on both sides (Figure 5.61). Moreover, if bilateral molars require intrusion simultaneously, bilateral mini-implants on the buccal sides with a stabilisation transpalatal arch are recommended to prevent buccal or lingual tipping (Figure 5.62).

Two case examples are given below to demonstrate the clinical applications of interradicular mini-implants for molar intrusion.

Case 1 A female adult presented with a chief complaint of a missing molar in her lower right quadrant. Panoramic radiography indicated the loss of the mandibular right second molar (47) and overeruption of the opposing maxillary right second molar (17) (Figure 5.63). For the missing lower second molar, implant restoration was the treatment of choice and was planned for this patient. However, due to the overeruption of the opposing maxillary second molar, direct implant restoration was not possible because of insufficient vertical space. Thus, intrusion of the overerupted maxillary right second molar was planned through orthodontic mini-implants.

Two interradicular mini-implants were inserted, with one placed at the U6-U7 site buccally and the other inserted at the U7-U8 site palatally (Figure 5.64). A closed-coil spring was applied for molar intrusion. To avoid displacement, the spring was fixed onto the occlusal surface of the molar with flowable resin. The molar intrusion progressed efficiently and successfully, resulting in adequate vertical space for implant restoration (Figure 5.65).

Case 2 A premolar extraction case presented with severe anterior open bite during treatment (Figure 5.66). To correct the anterior open bite, molar intrusion was designed. Two mini-implants were inserted at the U6-U7 interradicular sites bilaterally and elastomeric chain was

t.me/Dr_Mouayyad_AlbtousH



Figure 5.50 Pretreatment photographs and radiographs.

applied between the archwire and mini-implants for molar intrusion (Figure 5.67). To avoid buccal tipping of the maxillary molars, a transpalatal arch was used so that bodily intrusion of molars could be achieved. The molar intrusion progressed smoothly and the anterior open bite was finally corrected (Figure 5.68).

Occlusal Canting

Occlusal canting manifests as canted occlusal plane from the frontal view and is often refractory to conventional orthodontic biomechanics, jeopardising patients' smile aesthetics. Fortunately, application of orthodontic TADs has enabled the treatment of occlusal canting more

t.me/Dr_Mouayyad_AlbtousH

Table 5.4 Pretreatment lateral cephalometric analysis.

Measurement	Norm	Pretreatment
Skeletal (°)		
SNA	83.0±4.0	81.2
SNB	80.0±4.0	77.1
ANB	2.0±2.0	3.9
FMA	28.0±4.0	24.4
SN-MP	35.0±4.0	35.2
Dental (°)		
U1-SN	105.7±6.3	119.8
L1-MP	97.0±7.1	108.2
FMIA	65.0±6.0	47.4
U1-L1	124.0±8.0	96.8
Soft tissue (mm)		
UL-EP	2.0±2.0	1.6
LL-EP	3.0±2.0	4.1
Wits (mm)		
Wits	–1.0	3

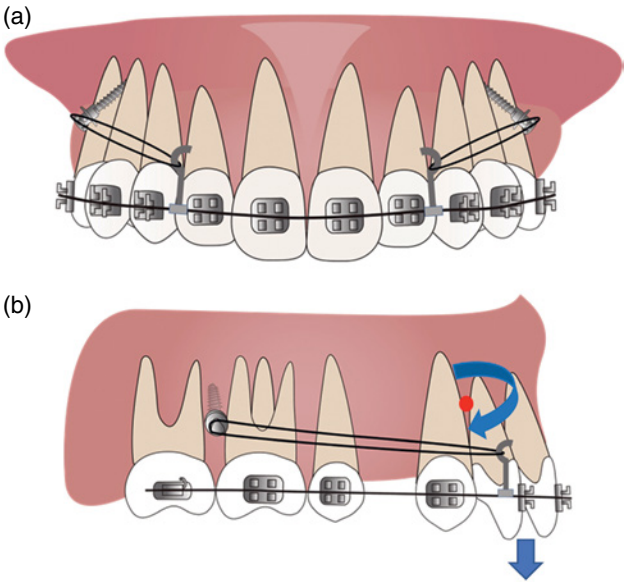


Figure 5.51 Schematic illustrations demonstrating the biomechanics of anterior retraction through bilateral mini-implants at the U6-U7 interradicular sites. (a) Frontal view. (b) Buccal view. Since the retraction force offered by the mini-implant passes occlusally to the centre of resistance of the anterior teeth, a clockwise moment is generated, leading to incisor extrusion and lingual tipping of the incisors.

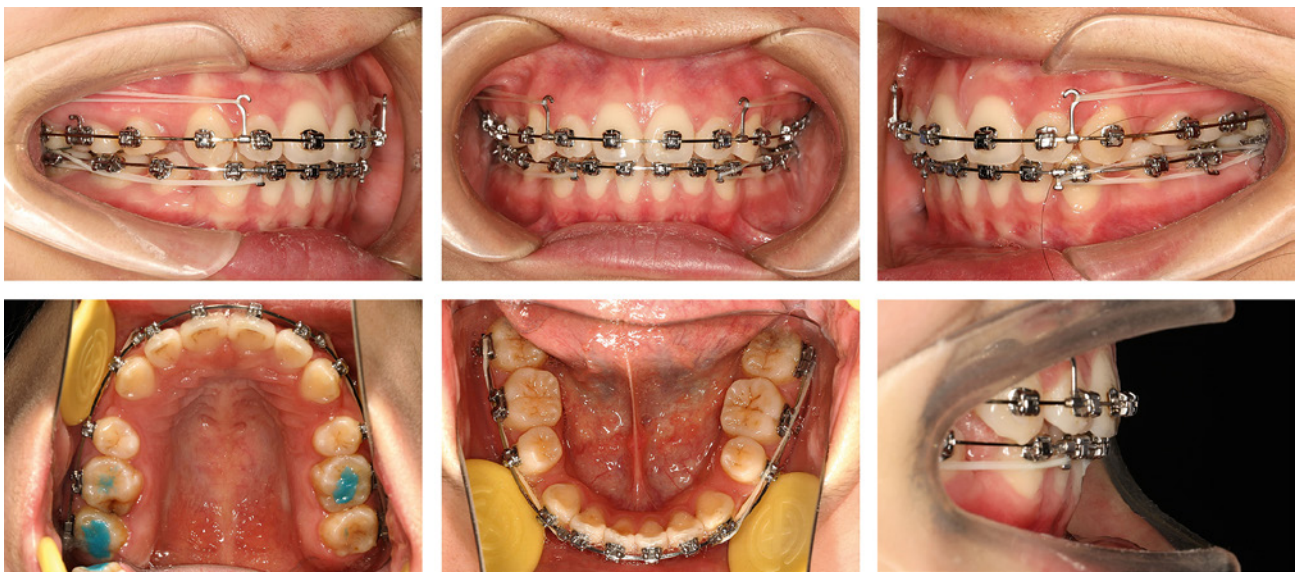


Figure 5.52 Treatment progress. Elastic rubbers were applied between the mini-implants and the long crimpable hooks on the archwire.

t.me/Dr_Mouayyad_AlbtousH



Figure 5.53 Posttreatment photographs and radiographs.

t.me/Dr_Mouayyad_AlbtousH

efficiently than conventional biomechanics.[43] Depending on the requirements of vertical control for different individuals, two distinct biomechanical approaches can be applied (Figures 5.69 and 5.70). A case example is given below.

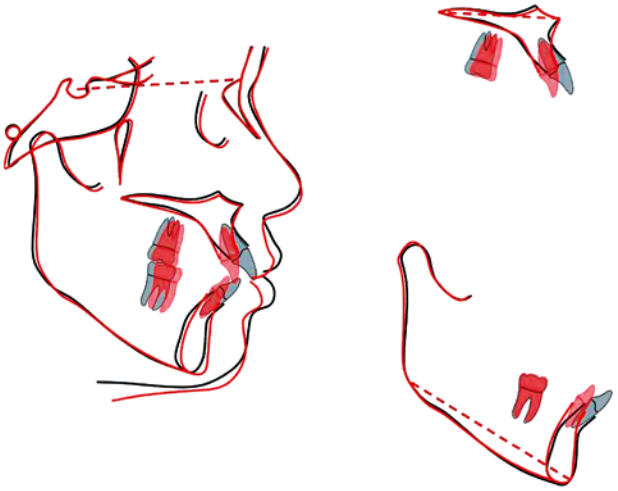


Figure 5.54 Superimposition of pre- and posttreatment cephalometric radiographs.

A female adult presented to the orthodontic department with a chief complaint of unaesthetic frontal smile. Her clinical examinations were indicative of slight class II canine and molar relationship on both sides, mild crowding and straight facial profile with normal chin prominence (Figure 5.71). A close-up examination revealed that the patient had a canted occlusal plane (Figure 5.72). The cephalometric analysis showed that she had a class II skeletal base (ANB = 5.8), high mandibular angle (SN-MP = 41.7) and retroclined upper and lower incisors (U1-SN = 94.0; L1-MP = 89.2) (Table 5.6).

The treatment plan was to align and level the upper and lower arches. Although the patient was a high-angle case, maintenance of the vertical dimension was indicated due to her normal chin prominence before treatment. Thus, the first biomechanical approach was employed, i.e. intrusion of the maxillary right quadrant and extrusion of the mandibular right quadrant. Two buccal mini-implants were placed at the interradicular sites (U4-U5 and U5-U6 sites) and one palatal mini-implant was inserted at the palatal side. The intrusion of the maxillary right quadrant was achieved through mini-implants on both the buccal and palatal sides (Figure 5.73). The intrusion of the maxillary right quadrant resulted in right buccal open bite that was further corrected by extrusion of the mandibular opposing teeth (Figure 5.74).

Table 5.5 Pre- and posttreatment lateral cephalometric analysis.

Measurement	Norm	Pretreatment	Posttreatment
Skeletal (°)			
SNA	83.0±4.0	81.2	81.2
SNB	80.0±4.0	77.1	79.8
ANB	2.0±2.0	3.9	1.4
FMA	28.0±4.0	24.4	25.1
SN-MP	35.0±4.0	35.2	34.5
Dental (°)			
U1-SN	105.7±6.3	119.8	102.4
L1-MP	97.0±7.1	108.2	93.5
FMIA	65.0±6.0	47.4	61.4
U1-L1	124.0±8.0	96.8	129.6
Soft tissue (mm)			
UL-EP	2.0±2.0	1.6	–2.4
LL-EP	3.0±2.0	4.1	–1.7
Wits (mm)			
Wits	–1.0	3	1

t.me/Dr_Mouayyad_AlbtousH

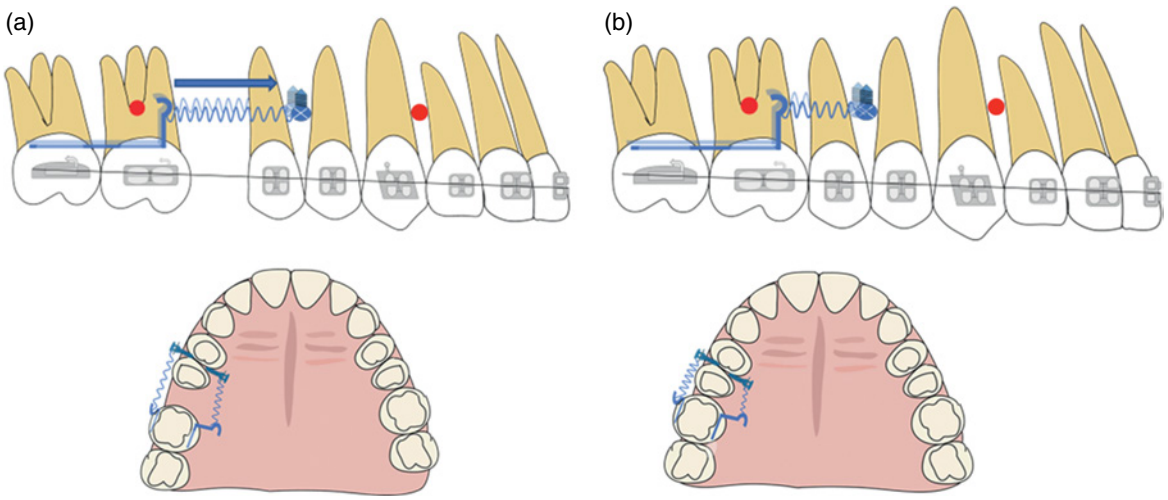


Figure 5.55 Schematic illustrations demonstrating the biomechanics of molar protraction with mini-implants at the interradicular sites between the first and second premolars. (a) Long hooks are bonded onto both the buccal and palatal sides of the maxillary molars. Mini-implants are placed at the interradicular sites between the first and second premolars on both the buccal and palatal sides. Thus, the molars are protracted from both sides. (b) Bodily protraction of the molars occurs without rotations.

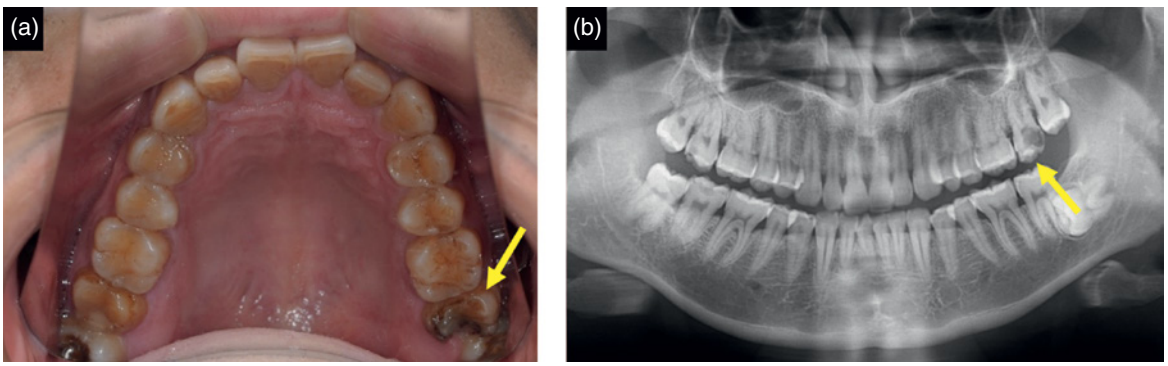


Figure 5.56 (a) Intraoral photograph showing that severe caries (yellow arrow) was found for the maxillary left second molar. (b) Panoramic radiograph demonstrating the large area of decay (yellow arrow) in the maxillary left second molar and the adjacent well-developed third molar.



Figure 5.57 Long hooks were bonded onto both the buccal and palatal sides of the maxillary third molar. Two mini-implants were inserted at both the buccal and palatal sides between the first and second premolars. Closed-coil springs were applied for molar protraction between the long hooks and the mini-implants.

t.me/Dr_Mouayyad_AlbtousH

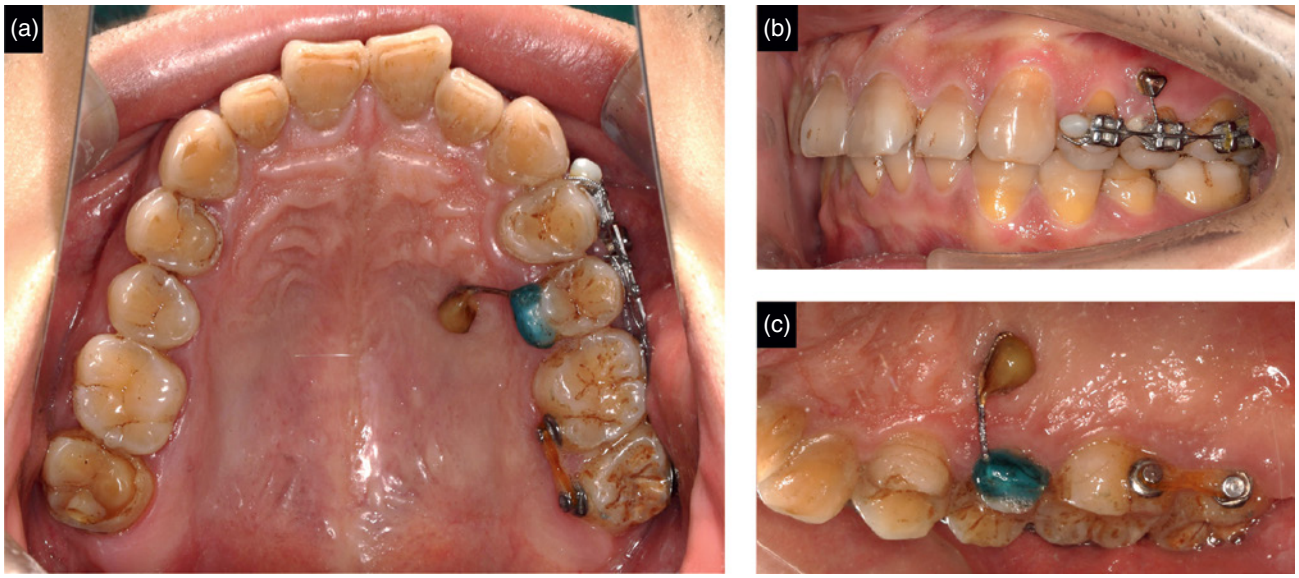


Figure 5.58 Segmental archwire technique was used for segmental tooth alignment. (a) Occlusal view. (b) Buccal view. (c) Lingual view.



Figure 5.59 Posttreatment photographs and panoramic radiograph. The third molar was protracted successfully with good root parallelism with the adjacent first molar.

t.me/Dr_Mouayyad_AlbtousH

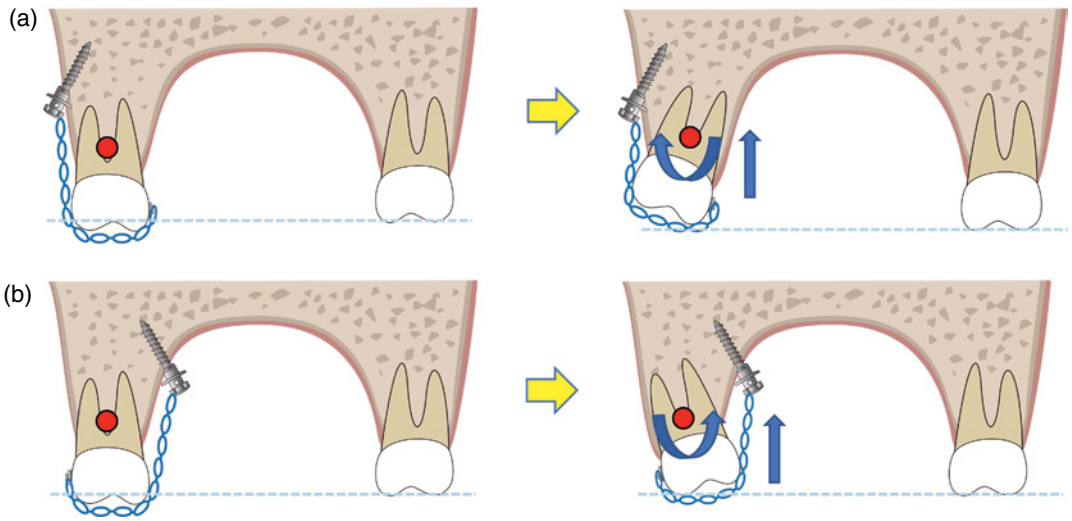


Figure 5.60 Injudicious biomechanical design. (a) One mini-implant is placed at the buccal side and the buccal intrusion force passes buccally to the centre of resistance (red dot), leading to buccal tippling of the molar. (b) One mini-implant is inserted at the palatal side and the intrusion force passes lingually to the centre of resistance (red dot), resulting in lingual tipping of the molar.

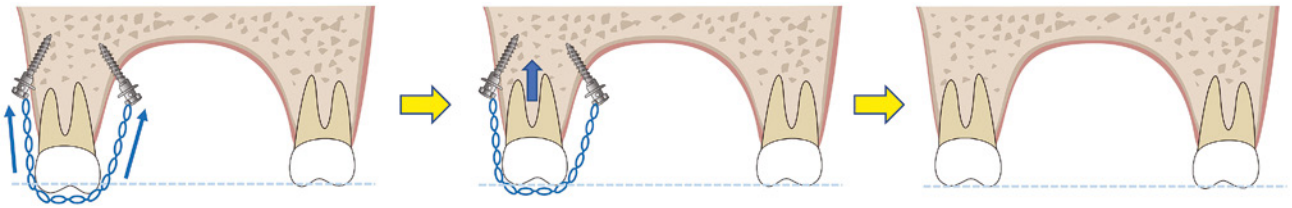


Figure 5.61 Mini-implants are placed at both the buccal and palatal sides. Intrusion forces are applied on both sides and bodily intrusion occurs.

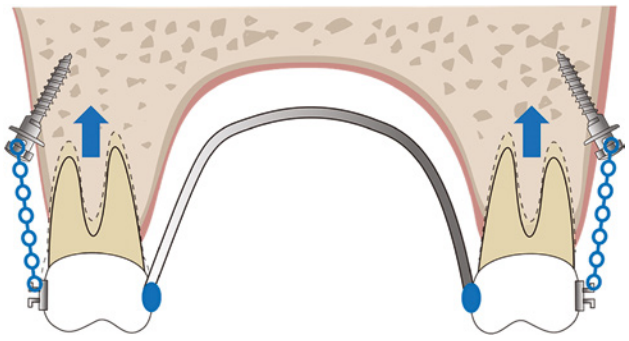


Figure 5.62 A transpalatal arch is able to stabilise the arch width if bilateral molars are intruded with mini-implants only on the buccal sides.



Figure 5.63 The panoramic radiograph is indicative of the loss of the mandibular right second molar and the overeruption of the maxillary right second molar. Note the vertical difference of the occlusal surfaces between the maxillary right second molar and the adjacent first molar.

t.me/Dr_Mouayyad_AlbtousH



Figure 5.64 One mini-implant was inserted at the interradicular site between the first and second molars at the buccal side and one mini-implant was placed at the palatal side. A closed-coil spring was employed for molar intrusion. (a) Buccal view. (b) Occlusal view. (c) Palatal view.

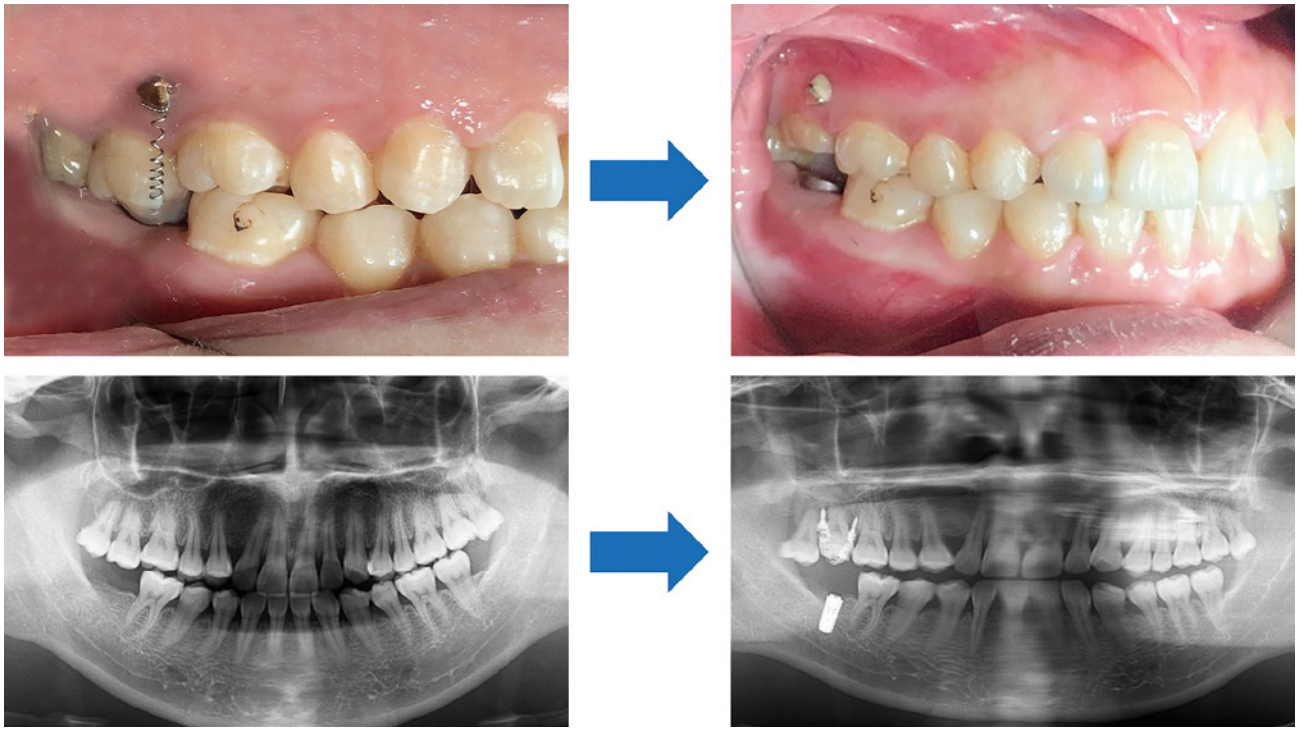


Figure 5.65 Molar intrusion progressed smoothly and successfully. Once the maxillary right second molar had been intruded, an implant was placed in the mandible to restore the missing mandibular right second molar.

t.me/Dr_Mouayyad_AlbtousH



Figure 5.66 Anterior open bite during orthodontic treatment.



Figure 5.67 Two mini-implants (yellow arrows) were inserted at the interradicular sites between the first and second molars. A transpalatal arch was used to prevent buccal tipping of the molar during intrusion.

t.me/Dr_Mouayyad_AlbtousH

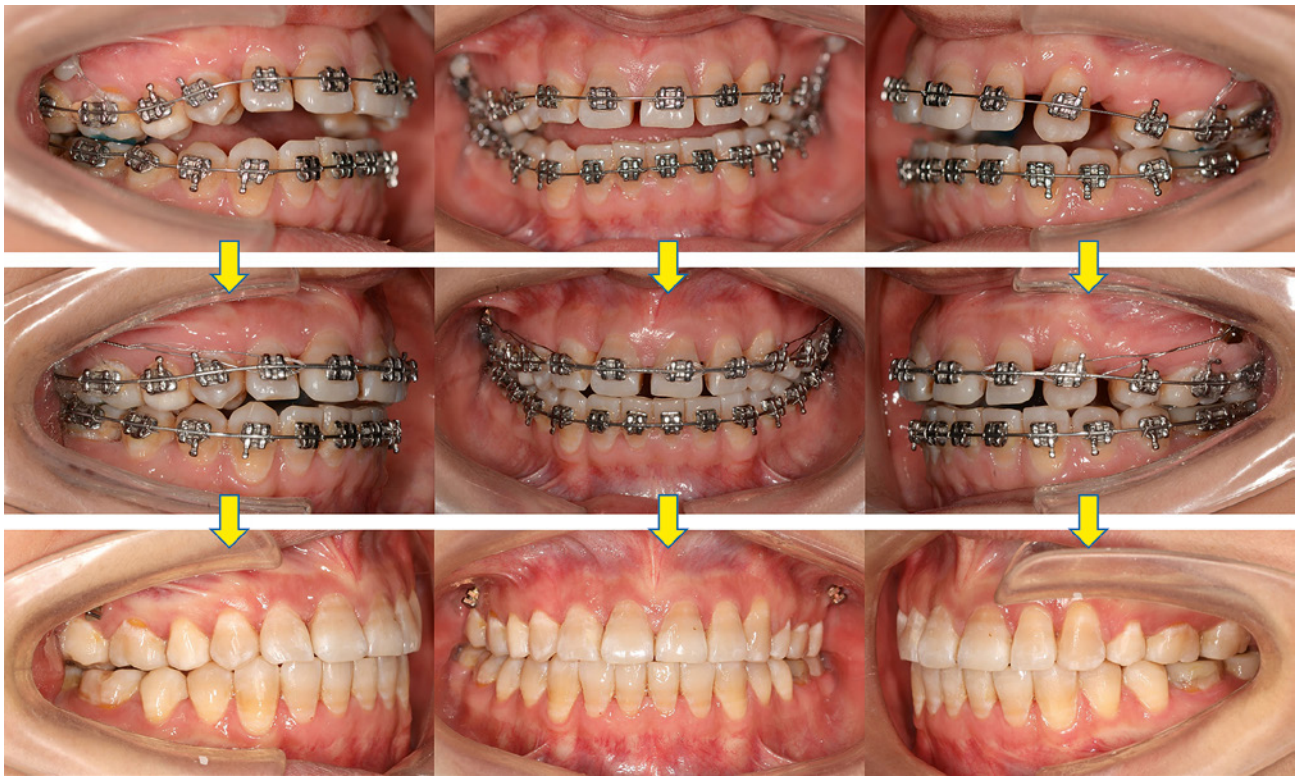


Figure 5.68 Anterior open bite was resolved gradually.

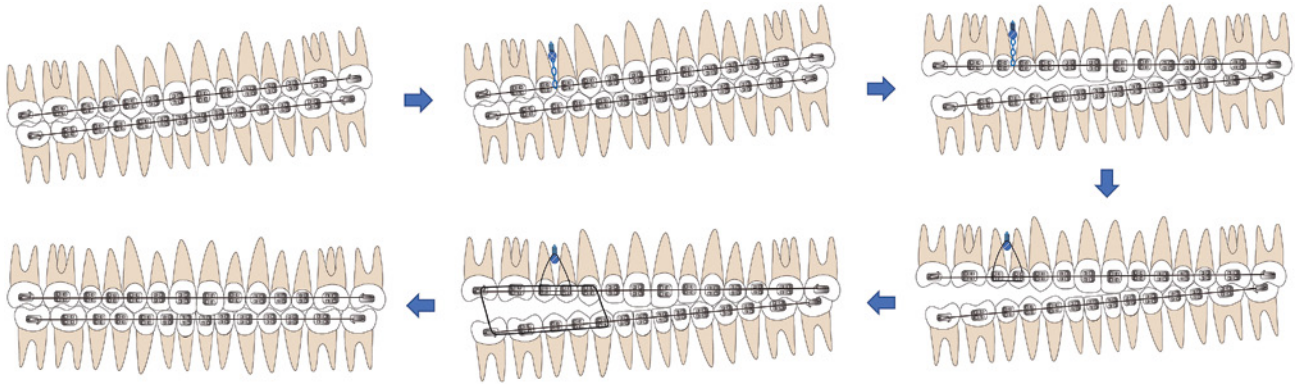


Figure 5.69 The application of a mini-implant for correcting occlusal canting for a patient not requiring vertical control.

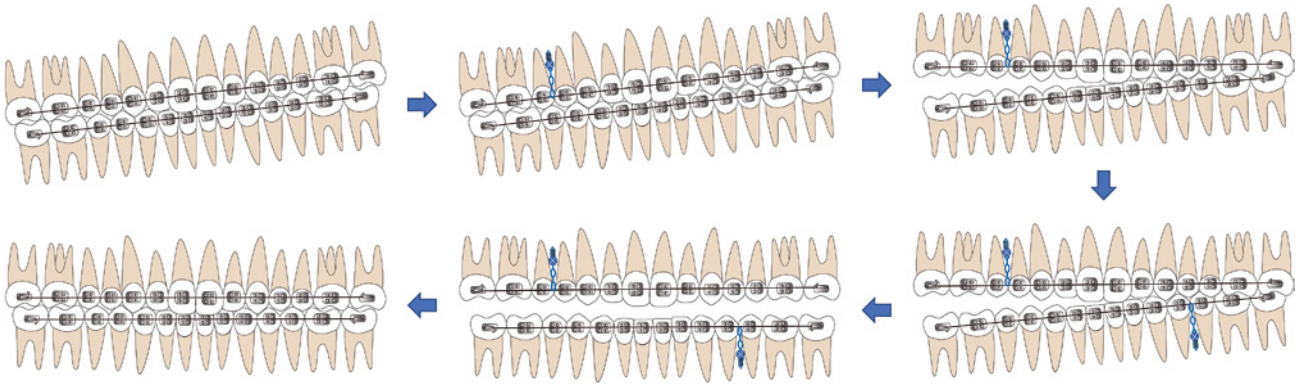


Figure 5.70 The application of mini-implants for correcting occlusal canting for a patient requiring vertical control.

t.me/Dr_Mouayyad_AlbtousH



Figure 5.71 Pretreatment photographs and radiographs.

t.me/Dr_Mouayyad_AlbtousH

At the end of the orthodontic treatment, the pretreatment occlusal canting had been completely resolved (Figure 5.75). Class I canine and molar relationships, normal overjet and overbite, and good buccal interdigitation were obtained following orthodontic treatment (Figure 5.76). The mini-implants were to be retained for at least one year in case of relapse of the occlusal canting. The pre- and posttreatment cephalometric values are presented in Table 5.7.

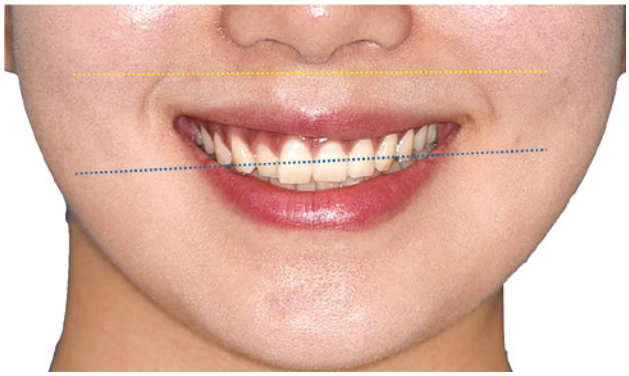


Figure 5.72 From the frontal view, the occlusal plane (blue dashed line) was canted in reference to the horizontal plane (yellow dashed line).

Table 5.6 Pretreatment lateral cephalometric analysis.

Measurement	Norm	Pretreatment
Skeletal (°)		
SNA	83.0±4.0	83.9
SNB	80.0±4.0	78.1
ANB	2.0±2.0	5.8
FMA	28.0±4.0	33.0
SN-MP	35.0±4.0	41.7
Dental (°)		
U1-SN	105.7±6.3	94.0
L1-MP	97.0±7.1	89.2
FMIA	65.0±6.0	57.9
U1-L1	124.0±8.0	135.2
Soft tissue (mm)		
UL-EP	2.0±2.0	0.8
LL-EP	3.0±2.0	1.0
Wits (mm)		
Wits	–1.0	–0.8

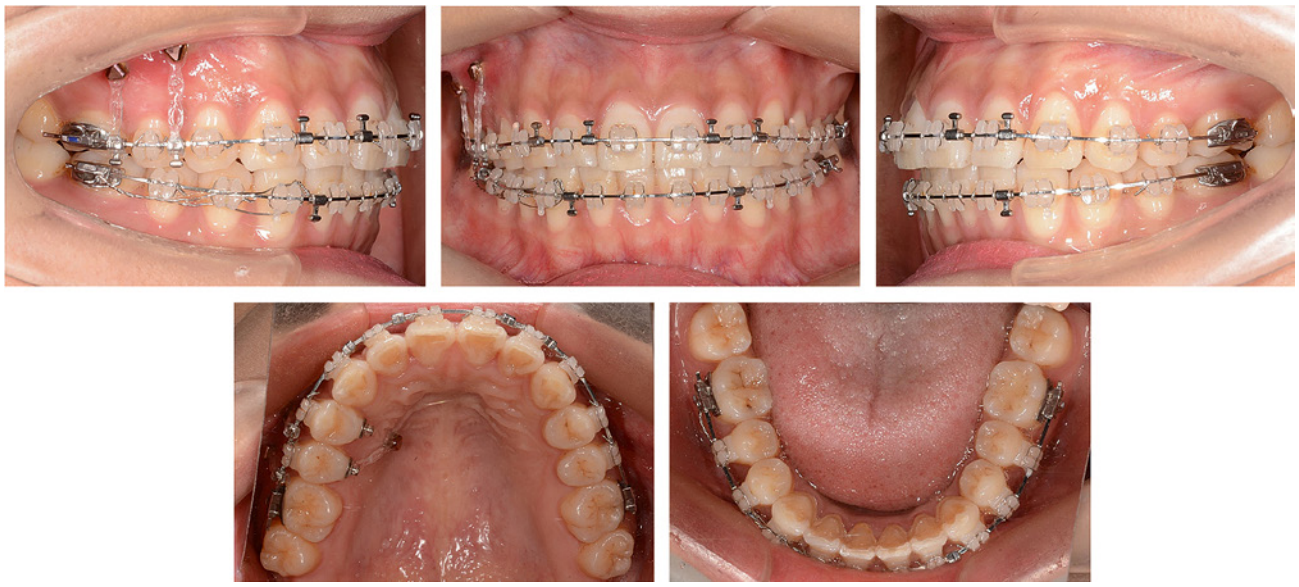


Figure 5.73 The intrusion of the maxillary right quadrant was achieved by mini-implants on both the buccal and palatal sides.

t.me/Dr_Mouayyad_AlbtousH

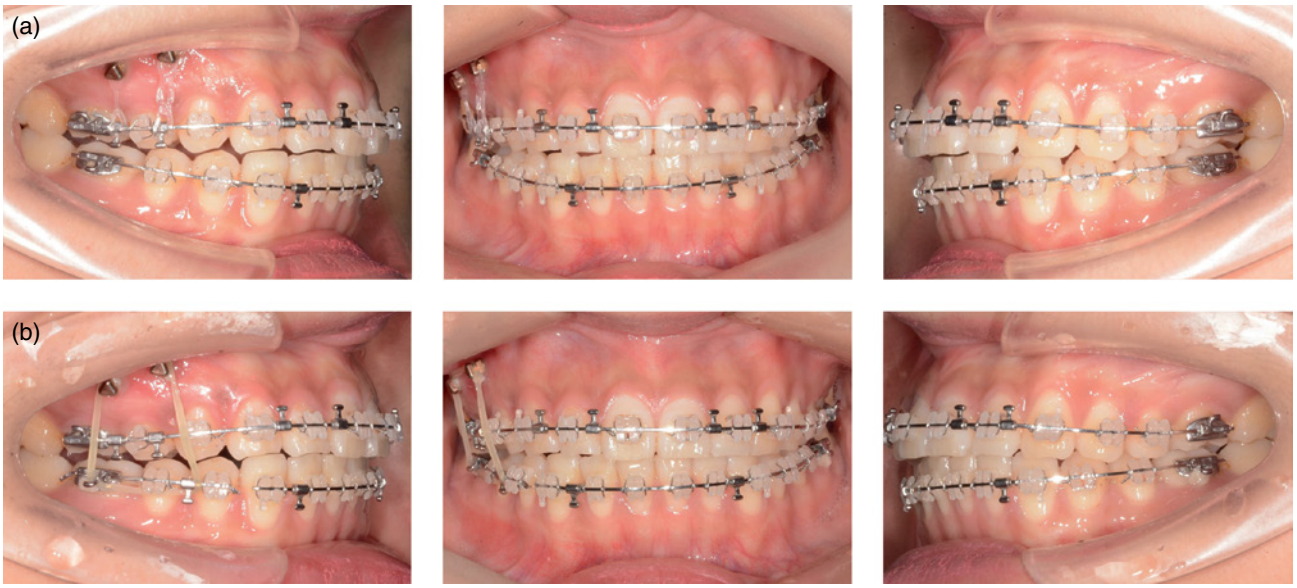


Figure 5.74 (a) The intrusion of the maxillary right quadrant resulted in buccal open bite on the right side. (b) The buccal open bite on the right side was resolved by applying a vertical elastic rubber.

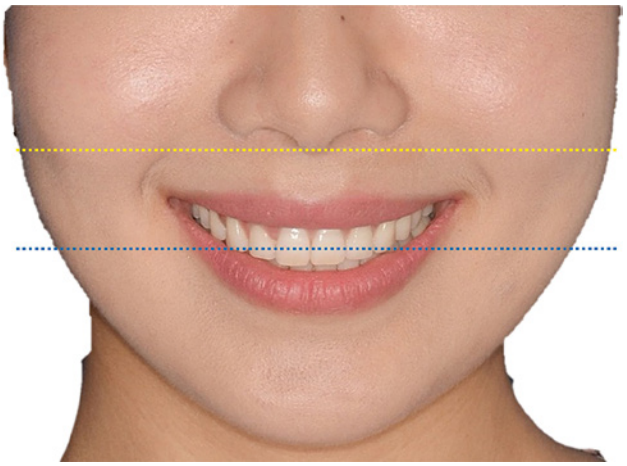


Figure 5.75 The occlusal canting has been completely resolved. Note that the occlusal plane (blue dashed line) is parallel with the horizontal plane (yellow dashed line).

5.3 Infrazygomatic Crest

5.3.1 Anatomical Characteristics

The infrazygomatic crest (IZC) is a palpable bony curvature running between the alveolar and zygomatic processes (Figure 5.77). Anatomically, the IZC is located apically to the region between the maxillary second premolar and the first molar in adolescents and apically to the maxillary first molar in adults.[44] Since the IZC is located buccally and apically to dental roots, this anatomical area is regarded as an extra-alveolar region. Due to the presence of adequate bone quantity and good bone quality in this region, the IZC is an ideal anatomical region for the insertion of mini-implants.[45] Different forms of orthodontic TADs can be placed at the IZC region, i.e. mini-implants and miniplates. However, since miniplates will be discussed in Chapter 10, only mini-implants are described in this chapter.

The IZC mini-implants are clinically versatile in accomplishing a variety of orthodontic tooth movements, e.g. anterior retraction, distalisation of maxillary dentition, molar distalisation and orthodontic traction of impacted teeth (Figure 5.78). To achieve successful applications of IZC mini-implants, hard tissue factors, soft tissue factors and vital anatomical structures should be thoroughly evaluated in order to determine the optimal insertion site.

We performed a three-dimensional radiographic analysis of the IZC anatomical region based on CBCT images from 32 orthodontic patients.[46] Both the cortical thickness and bone depth were measured and analysed (Figure 5.79). Moreover, the measurements were performed at different insertion sites and insertion heights, and with different insertion angles (Figure 5.80). The results from this study regarding the hard tissue factors will be elaborated below.

t.me/Dr_Mouayyad_AlbtousH



Figure 5.76 Posttreatment photographs and radiographs.

t.me/Dr_Mouayyad_AlbtousH

Table 5.7 Pre- and posttreatment lateral cephalometric analysis.

Measurement	Norm	Pretreatment	Posttreatment
Skeletal (°)			
SNA	83.0±4.0	83.9	82.4
SNB	80.0±4.0	78.1	77.4
ANB	2.0±2.0	5.8	5.0
FMA	28.0±4.0	33.0	34.0
SN-MP	35.0±4.0	41.7	44.5
Dental (°)			
U1-SN	105.7±6.3	94.0	97.2
L1-MP	97.0±7.1	89.2	90.5
FMIA	65.0±6.0	57.9	55.5
U1-L1	124.0±8.0	135.2	127.8
Soft tissue (mm)			
UL-EP	2.0±2.0	0.8	–0.1
LL-EP	3.0±2.0	1.0	–0.2
Wits (mm)			
Wits	–1.0	–0.8	–0.7

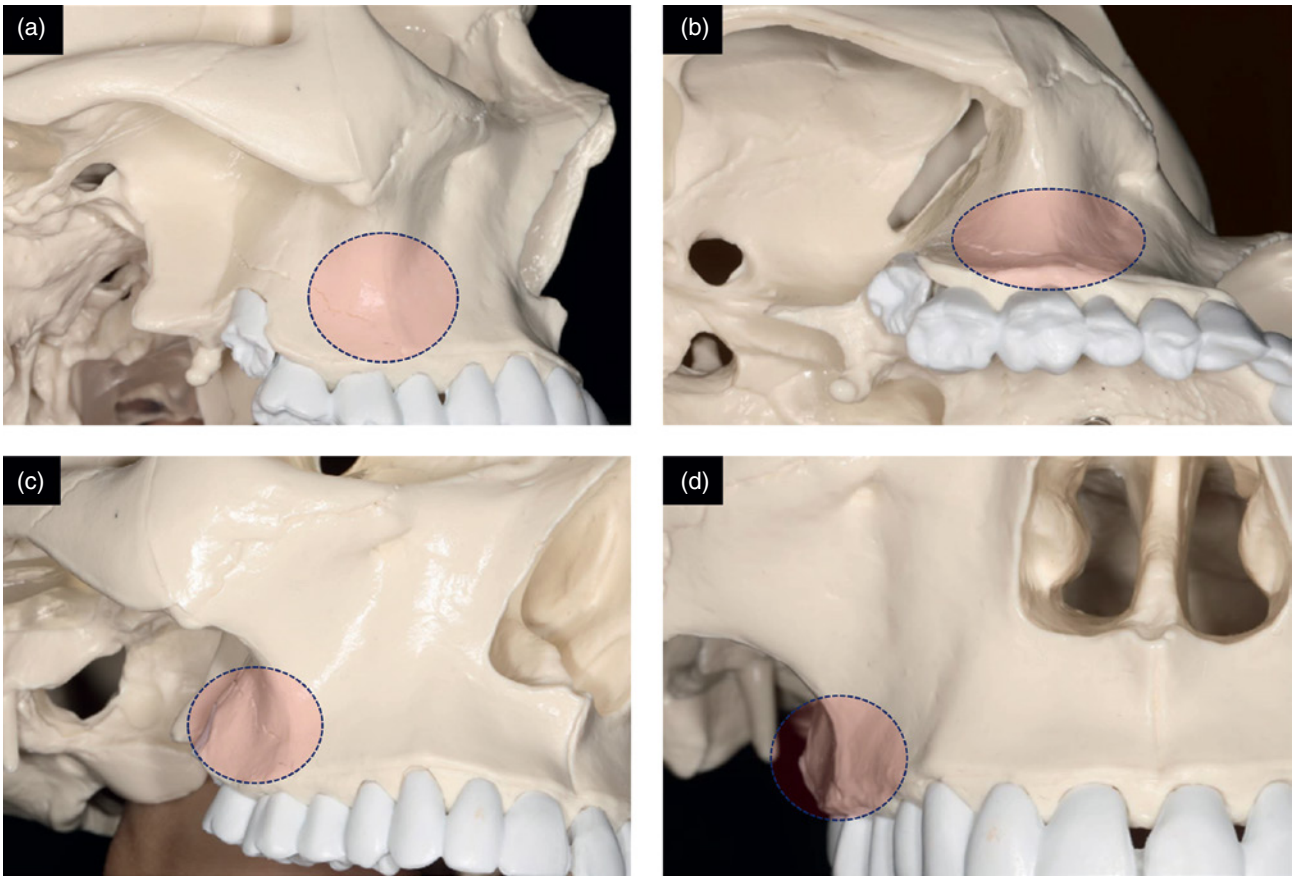


Figure 5.77 Infrazygomatic crest (encircled by the dashed line). (a) Buccal view. (b) Inferior view. (c) Frontal oblique view. (d) Frontal view.

t.me/Dr_Mouayyad_AlbtousH

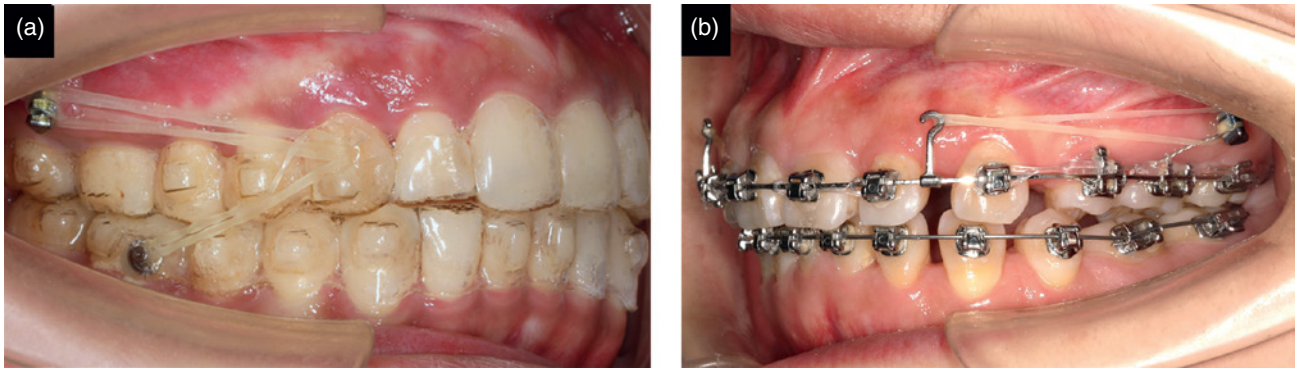


Figure 5.78 (a) A mini-implant inserted at the infrazygomatic crest was used for molar distalisation with clear aligner. (b) A mini-implant at the infrazygomatic crest was employed for reinforcing molar anchorage and facilitating *en masse* anterior retraction.

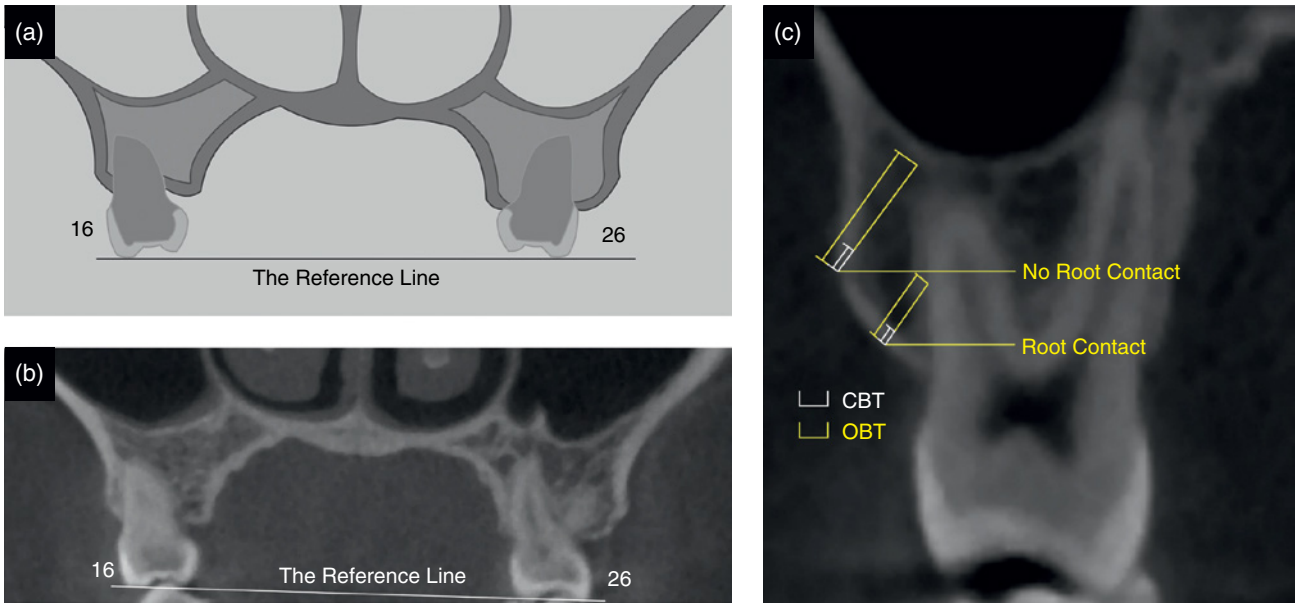


Figure 5.79 Measurement of overall bone thickness (OBT) and cortical bone thickness (CBT) based on CBCT images. (a) A schematic illustration showing the reference line passing through the mesiobuccal cusps of the bilateral first molars. (b) A coronal section of CBCT image demonstrating the reference line. (c) The definition of OBT and CBT in case of root contact and no root contact. *Source:* Song et al. [46]/e-Century Publishing Corporation.

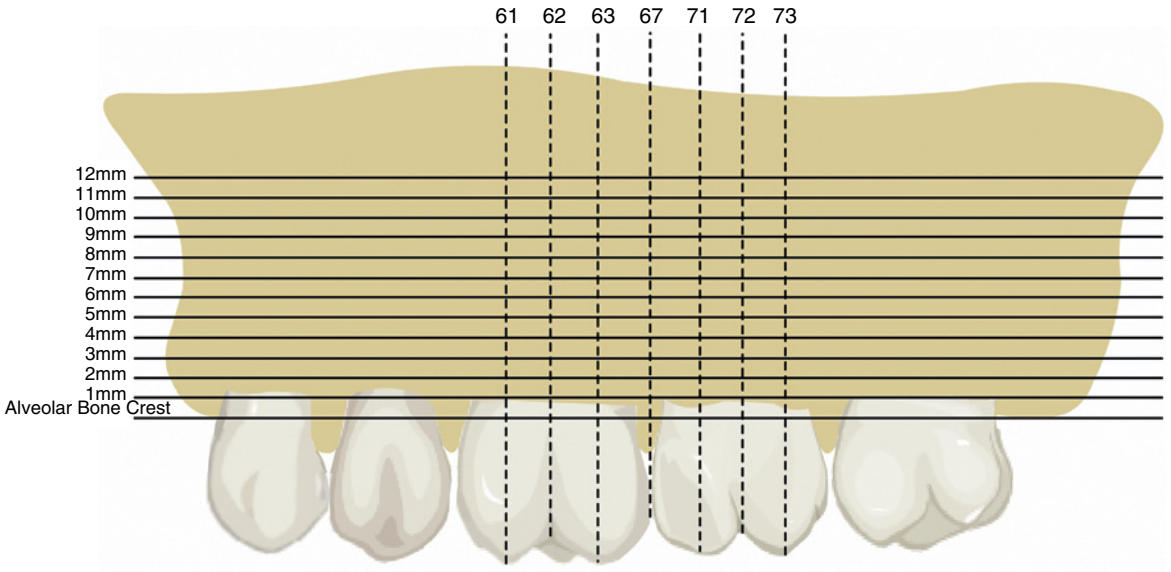


Figure 5.80 Measurements were performed at different coronal planes (61, 62, 63. . ., 73) and at different heights (1 mm to 12 mm) from the alveolar crest. *Source:* Song et al. [46]/e-Century Publishing Corporation.

t.me/Dr_Mouayyad_AlbtousH

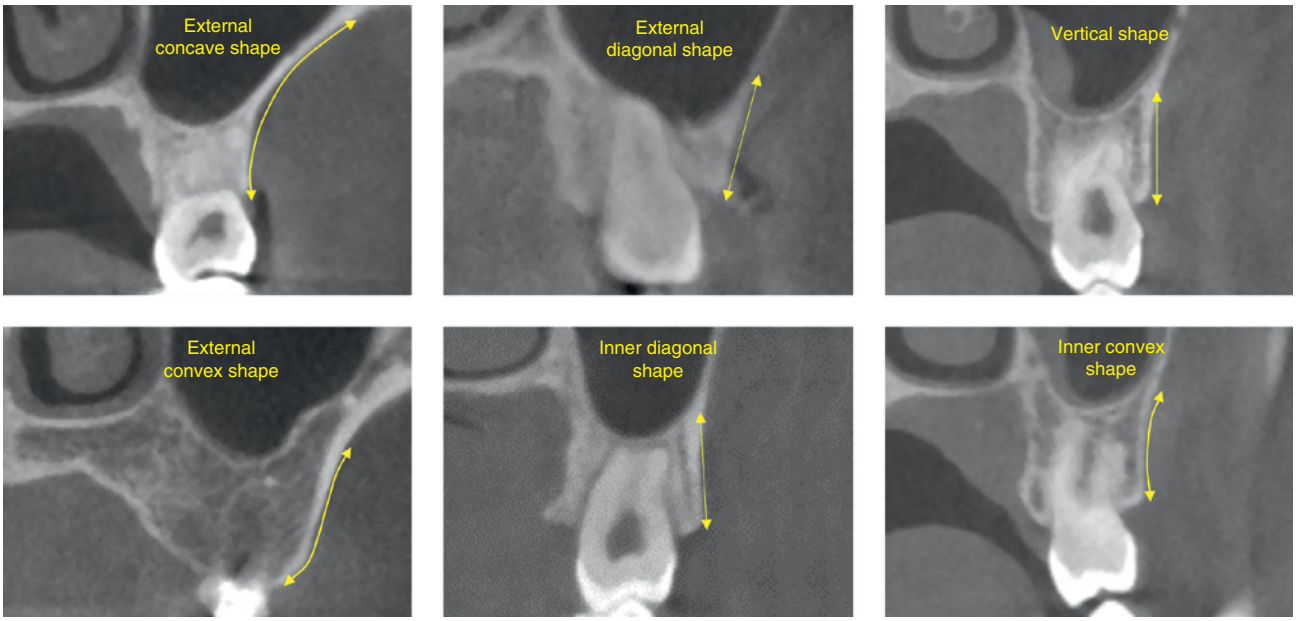


Figure 5.81 Different shapes of infrazygomatic crest shown on CBCT images.

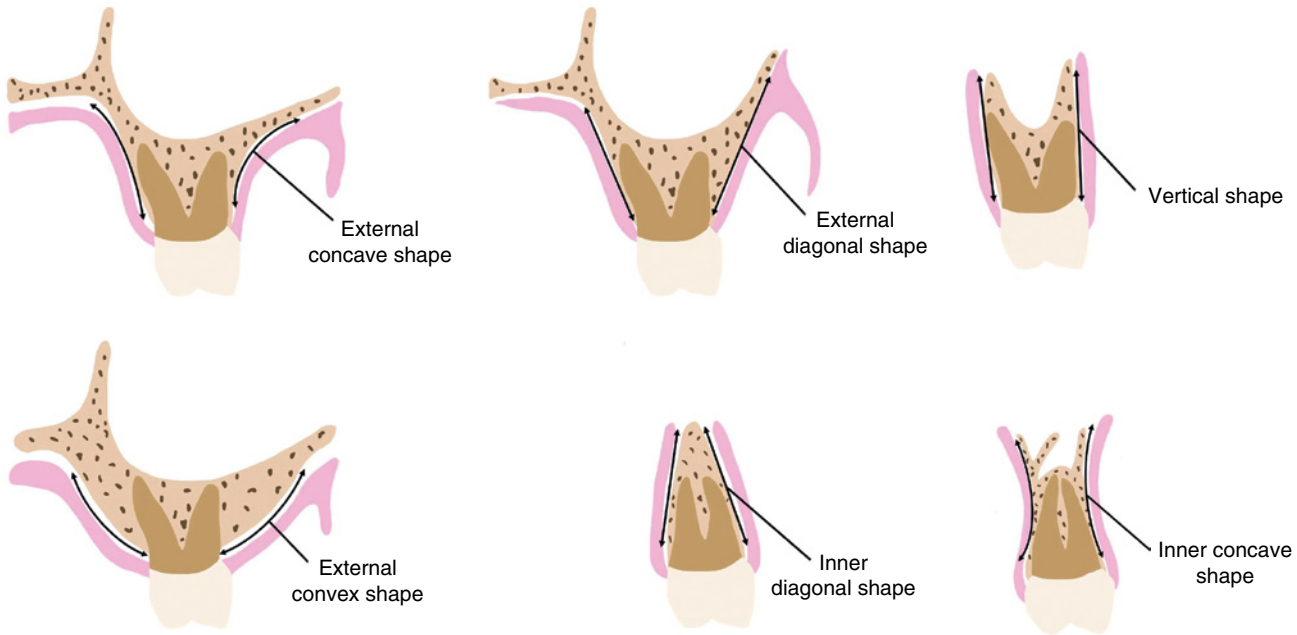


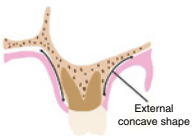
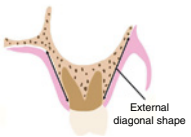
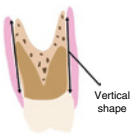
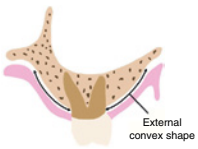
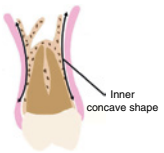
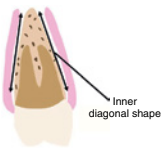
Figure 5.82 Schematic illustrations showing six distinct shapes of the infrazygomatic crest on the buccal side. *Source:* Song et al. [46]/e-Century Publishing Corporation.

Hard Tissue Factor: Crest Shape

On the coronal view, the IZC exhibits different morphologies depending on the bone quantity on the buccal side (Figure 5.81). Six distinct shapes are present clinically: (1) external concave; (2) external diagonal; (3) vertical; (4) external convex; (5) inner diagonal; (6) inner concave (Figure 5.82). Among them, the external concave, external diagonal and vertical shapes are mostly frequently encountered and comprise 94% of the IZC shapes in clinical practice (Table 5.8). Due to the excellent bone quantity at the buccal side, the IZC with external convex shape is the most favourable one for the placement of mini-implants,

t.me/Dr_Mouayyad_AlbtousH

Table 5.8 Distribution of the infrazygomatic crest (IZC) shape among seven sites. *Source:* Song et al. [46].

Shape	External concave shape	External diagonal shape	Vertical shape	External convex shape	Inner concave shape	Inner diagonal shape
						
61	50	6	0	3	4	1
62	47	15	0	2	0	0
63	36	17	9	2	0	0
67	12	26	25	1	0	0
71	7	19	36	1	0	1
72	2	17	40	0	0	5
73	1	18	36	0	0	9
Total	155	118	146	9	4	16

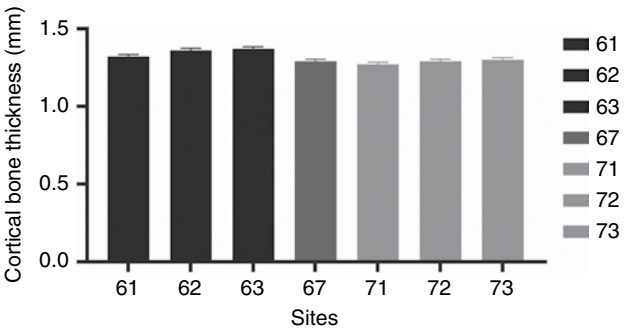


Figure 5.83 Cortical thickness at different coronal planes. *Source:* Song et al. [46]/e-Century Publishing Corporation.

followed by those with the external concave and external diagonal shapes. The IZC with inner diagonal shape is the least desirable one for inserting mini-implants.

According to our study, almost 90% of IZCs at the maxillary first molar region exhibit external concave and external diagonal shapes. Moreover, the external diagonal shape and the vertical shape predominate among IZC shapes (80%) at the site between the first and second molars and at the second molar region (86%). Thus, in terms of bone morphology, most IZC regions corresponding to the maxillary first and second molar regions are suitable for the placement of mini-implants.

Hard Tissue Factor: Cortical Thickness

Cortical thickness is a determining anatomical factor for the stability of mini-implants. The bone density of the IZC may differ among patients with different vertical skeletal patterns, with hypodivergent subjects exhibiting higher density than normodivergent and hyperdivergent subjects.[3] In contrast, cortical thickness is similar among subjects with different vertical skeletal patterns.[47] Moreover, our study revealed that different coronal sections of IZC exhibit similar cortical thickness, with the average value being 1.0–1.5 mm (Figure 5.83).[46] These findings indicate that cortical thickness is constant and not influenced by different vertical patterns or different sagittal insertion sites.

Cortical thickness is influenced by insertion height, insertion angle and their interactions. Specifically, cortical thickness remains relatively constant for different insertion heights when the insertion angle is 0–30°, but differs among different insertion heights when the insertion angle is greater than 30° (Figure 5.84). Moreover, the maximum value of cortical thickness reaches 2 mm when the insertion angle exceeds 60°. However, the likelihood of mini-implant slippage is very high if the insertion angle is 80° or greater.

Thus, in terms of cortical thickness, the recommended insertion angle is 60–70°, with the insertion height being 3–9 mm above the alveolar crest.

Hard Tissue Factor: Bone Depth

Bone depth is the distance between the buccal cortical plate and the sinus cortex, and is an important factor in determining the stability of the mini-implant at the IZC region. Bone depth exhibits great individual variations (Figure 5.85). Moreover, it is influenced by gender and age.

t.me/Dr_Mouayyad_AlbtousH

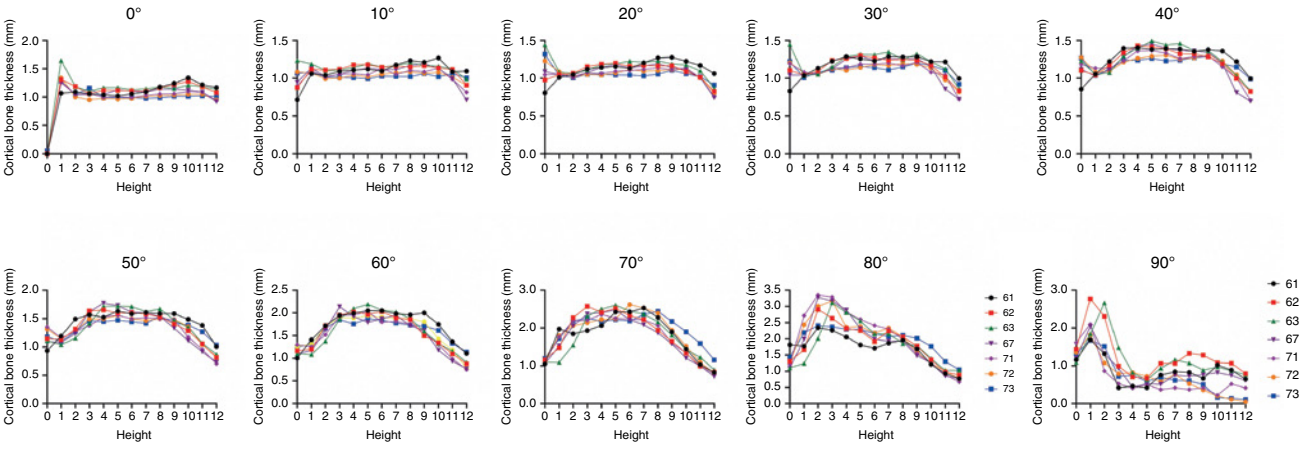


Figure 5.84 The influence of insertion height and insertion angle on cortical thickness at different coronal planes. *Source:* Song et al. [46]/e-Century Publishing Corporation.

t.me/Dr_Mouayyad_AlbtousH

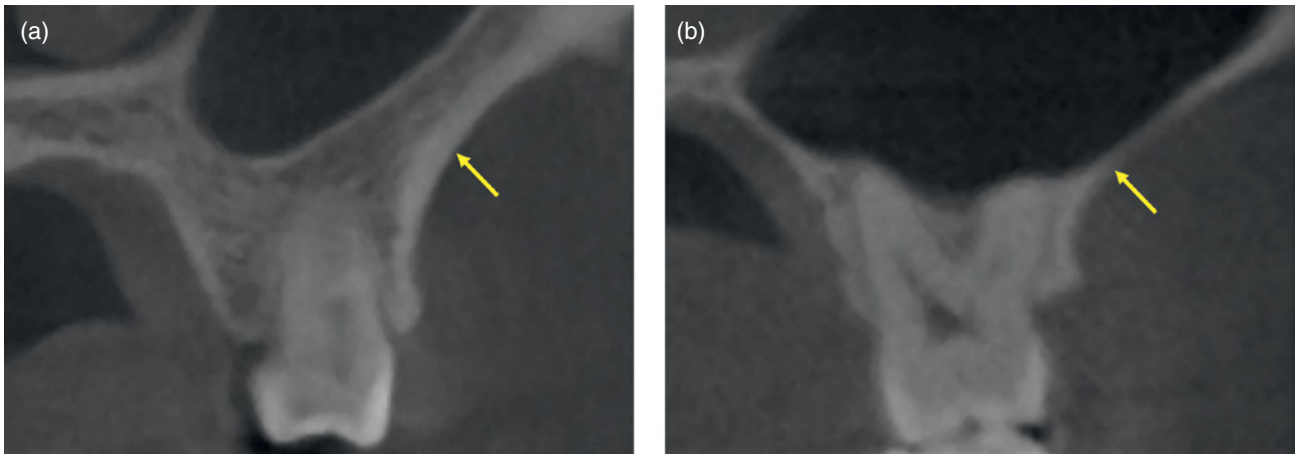


Figure 5.85 Great variations are exhibited among different patients. (a) A patient with adequate bone depth at the infrazygomatic crest. (b) A patient with a thin infrazygomatic crest.

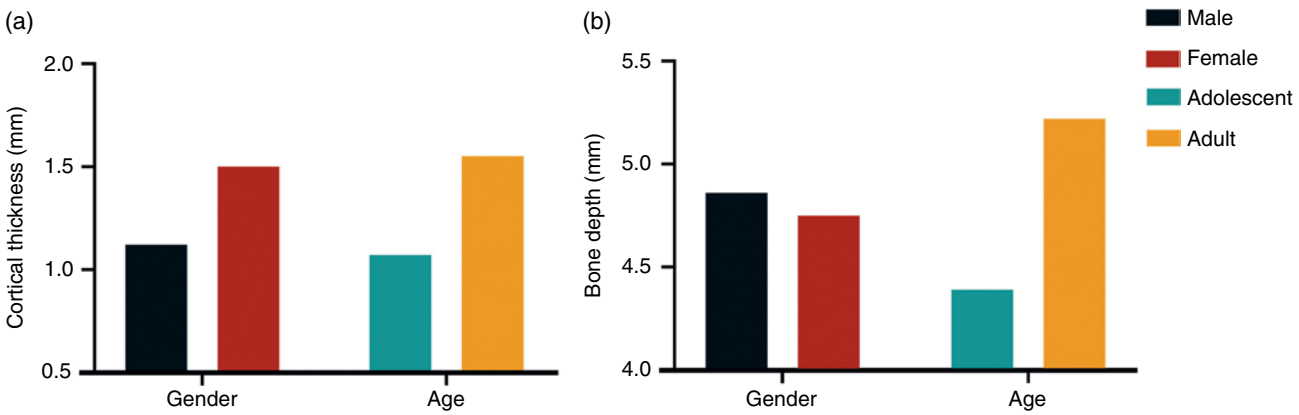


Figure 5.86 (a) The comparison of cortical bone thickness (CBT) between adults and adolescents and between males and females. (b) The comparison of overall bone thickness (OBT) between adults and adolescents and between males and females. *Source:* Song et al. [46]/e-Century Publishing Corporation.

Specifically, our study reveals that bone depth is greater among males than females and that adults possess greater bone depth than adolescents (Figure 5.86).

Bone depth is influenced by different sagittal positions. Specifically, bone depth is greatest at the coronal plane that corresponds to the distobuccal cusp of the first molar and the least at the area corresponding to the mesiobuccal cusp of the first molar (Figure 5.87).

Furthermore, bone depth is influenced by insertion height, insertion angle and their interactions (Figure 5.88). Specifically, bone depth increases with an increase in the insertion height if the insertion is almost in parallel to the occlusal plane (insertion angle: 0–10°), while it

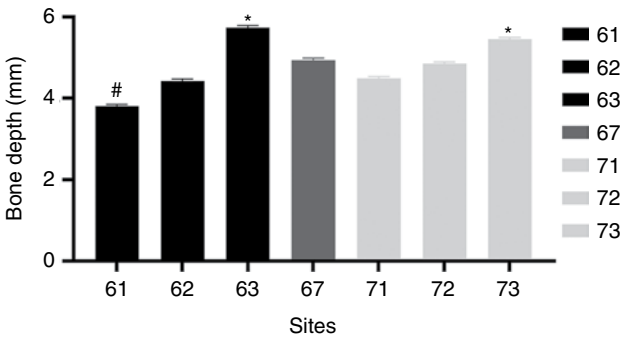


Figure 5.87 The overall bone depth at different coronal planes. *Source:* Song et al. [46].

t.me/Dr_Mouayyad_AlbtousH

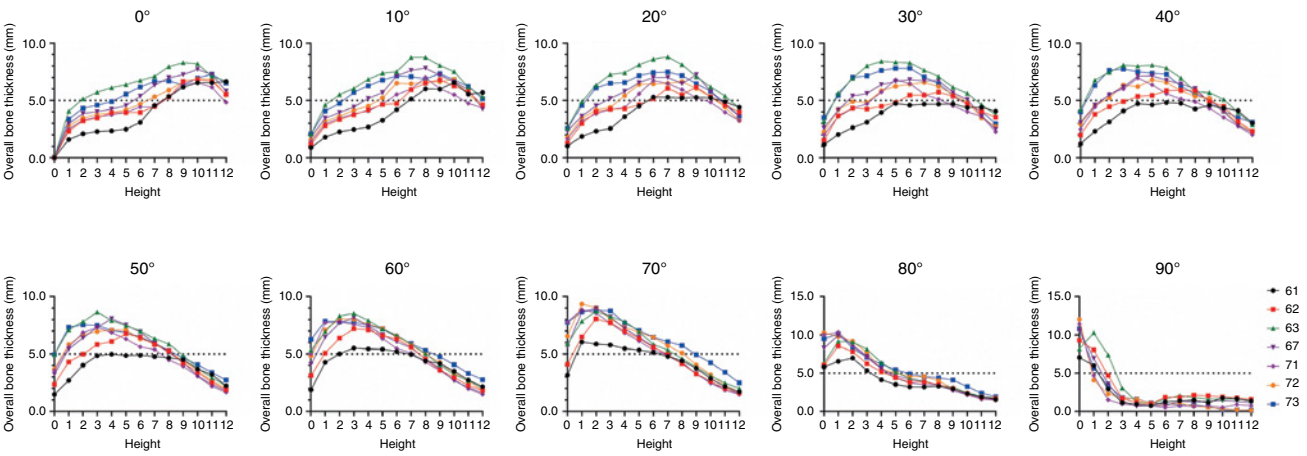


Figure 5.88 The influence of insertion height and insertion angle on bone depth at different coronal planes. *Source:* Song et al. [46]/e-Century Publishing Corporation.

t.me/Dr_Mouayyad_AlbtousH

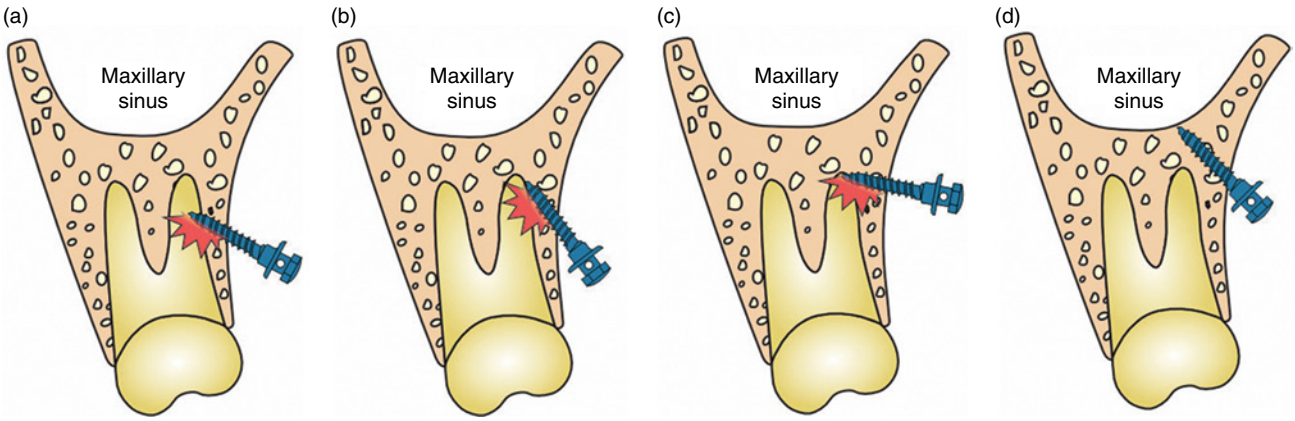


Figure 5.89 (a) Inadequate insertion height and insertion angle lead to root contact. (b) Even if the insertion angle is sufficient, root contact still occurs with inadequate insertion height. (c) Root contact occurs with inadequate insertion angle, even if the mini-implant is placed at a sufficient height. (d) Root contact can be avoided with sufficient insertion height and adequate insertion angle.

decreases with an increase in the insertion height if the insertion is almost perpendicular to the occlusal plane (insertion angle: 80–90°). In contrast, the change of bone depth in response to insertion height displays an inverted 'V' pattern for the insertion angle being 20–70°, and the insertion height corresponding to the peak bone depth decreases with an increase in the insertion angle. This indicates that a mini-implant could be placed at a lower insertion height with a greater insertion angle to obtain a similar bone depth. Generally, the minimum required bone depth is considered to be 5 mm. Thus, different combinations of insertion height and insertion angle that result in bone depth greater than 5 mm are displayed in Figure 5.88.

Hard Tissue Factor: Dental Roots

Since the IZC region lies buccally and apically to the molar roots, injudicious placement of a mini-implant with inappropriate insertion height and angle may result in root contact by the mini-implant (Figure 5.89). Thus, a good combination of insertion height and angle should be selected in order to reduce the likelihood of root contact (Figure 5.90). The likelihood of root contact by the mini-implant is displayed in Figure 5.91, and the risk of root contact is reduced with an increase in the insertion height and angle.

Soft Tissue Factor: Soft Tissue Type

As mentioned above, limited keratinised attached gingiva is present at the maxillary molar region and the IZC region

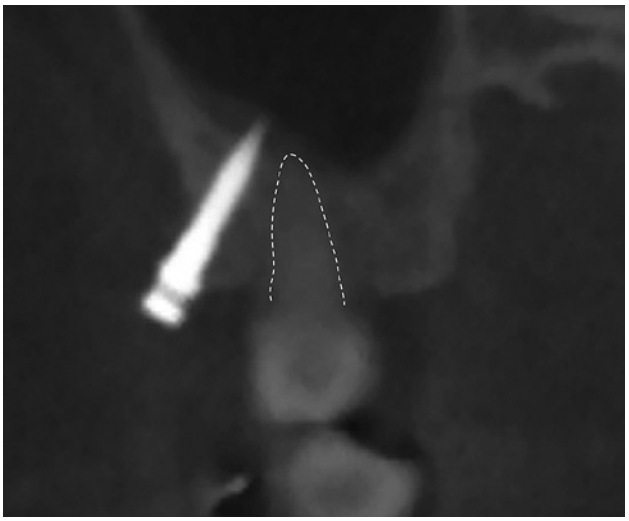


Figure 5.90 No root contact is present with a good combination of insertion height and insertion angle.

is primarily covered by movable mucosa (Figure 5.92). Thus, mini-implants have to penetrate through movable mucosa and should be long enough so that the heads can be located at the attached gingiva zone (Figure 5.93). In this way, the risk of soft tissue irritation and complications can be greatly reduced. Due to the thick movable mucosa at the IZC region, 10 mm or 12 mm mini-implants are recommended. From our personal clinical experience, we prefer to the 12 mm mini-implants that have adequate length in order to avoid soft tissue irritation around the mini-implant heads.

t.me/Dr_Mouayyad_AlbtousH

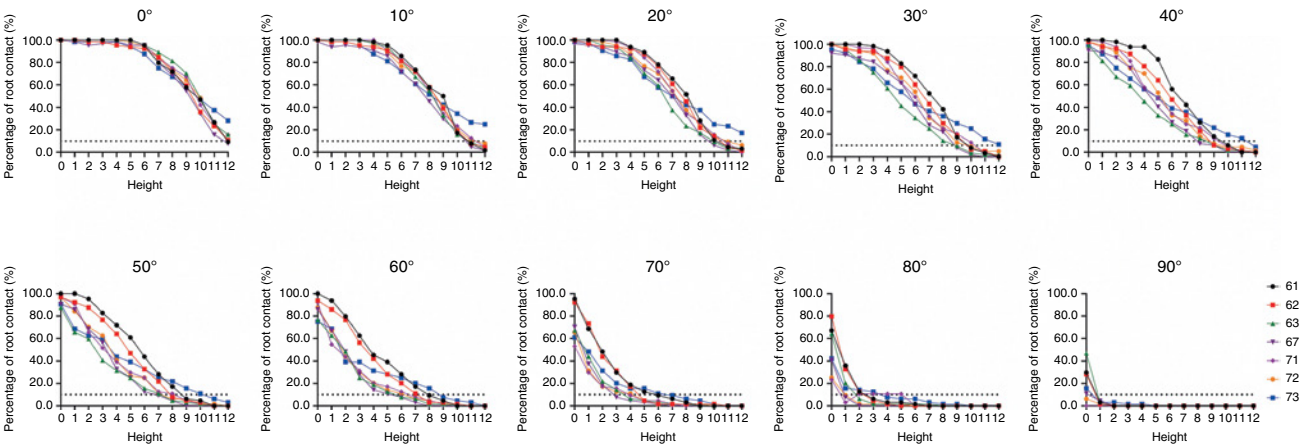


Figure 5.91 The influence of insertion height and insertion angle on the likelihood of root contact at different coronal planes. *Source:* Song et al. [46]/e-Century Publishing Corporation.

t.me/Dr_Mouayyad_AlbtousH

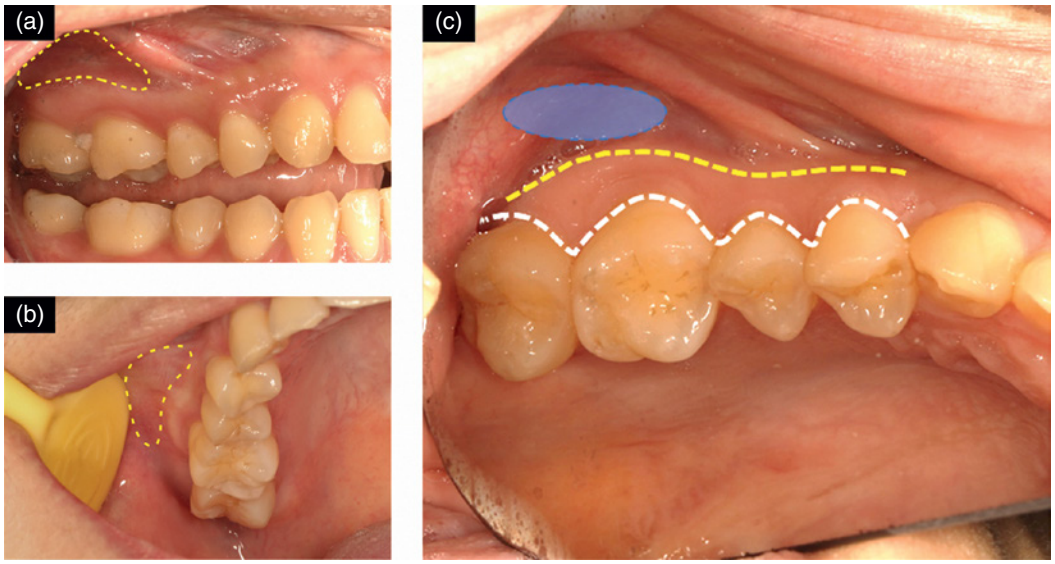


Figure 5.92 Limited keratinised attached gingiva is present at the maxillary molar region and the infrazygomatic (IZC) region is primarily covered by the movable mucosa. (a,b) The IZC regions are encircled by the yellow dashed lines. (c) The IZC region (blue area) is located apically to the mucogingival junction (yellow dashed line) and is primarily covered by movable mucosa. The white dashed line indicates the free gingival margin.

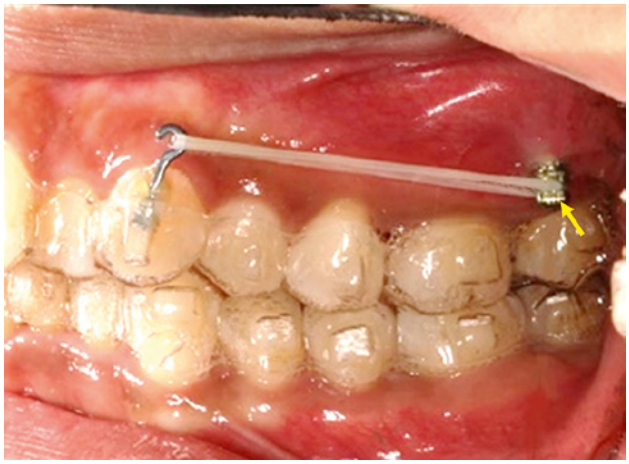


Figure 5.93 The head of the mini-implant (yellow arrow) inserted at the infrazygomatic crest is located at the attached gingiva zone. This mini-implant can be applied for force loading with low risk of soft tissue complications.

Vital Anatomical Structures: Maxillary Sinus

The presence of the maxillary sinus in the vicinity of the IZC region may complicate the placement of IZC mini-implants, and clinical efforts (e.g. fabrication of digital insertion guides) can be made to reduce the likelihood of sinus penetration.[48,49] Sinus penetration by orthodontic mini-implants is concerning for the possible occurrence of sinusitis and mucocoele. However, clinical studies reveal that sinus penetration is not associated with mini-implant stability or sinusitis, unless pre-existing sinusitis is present.[50,51] Although sinus penetration leads to insufficient bone engagement by the mini-implant, the stability of the mini-implant is not influenced since the less bone engagement is offset by better bone quality provided by the sinus cortex (bicortical engagement).[51]

From the perspectives of biomechanics, mini-implants with bicortical engagement exhibit higher stability, less deformation and lower risk of fracture than those with monocortical engagement (Figure 5.94).[52] Thus, for mini-implants to be inserted at the IZC region, sinus penetration is recommended for greater stability (Figure 5.95).

Therefore, sinus penetration is not a concern and, unless pre-existing sinusitis is present, sinus penetration is recommended for the bicortical engagement mode.

5.3.2 Biomechanical Considerations

The IZC mini-implants are often applied for anterior retraction and molar distalisation. Since the line of force passes occlusally to the center of resistance of the dentition, clockwise rotation of the dentition and occlusal plane may occur even if power arms are used (Figure 5.96). This often leads to extrusion and lingual tipping of anterior teeth, and intrusion of and buccal tipping of molars, resulting in deepening of anterior bite (Figure 5.97). Thus, this consequence

t.me/Dr_Mouayyad_AlbtousH

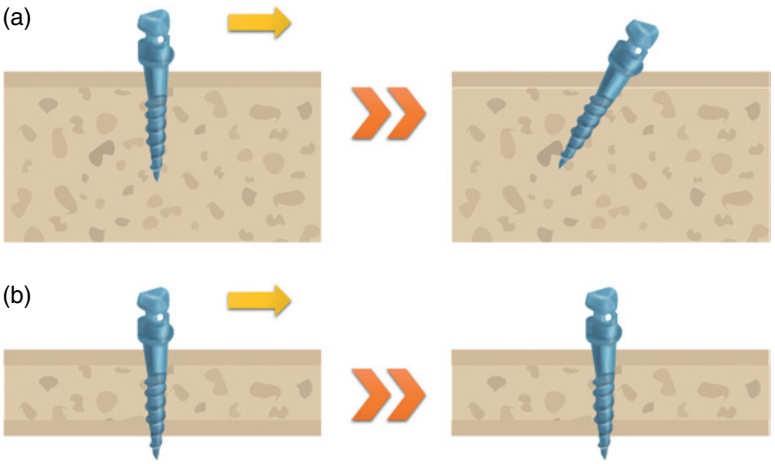


Figure 5.94 (a) Monocortical engagement. The mini-implant is displaced in response to force loading. (b) Bicortical engagement. Displacement of the mini-implant in response to force loading is minimal.

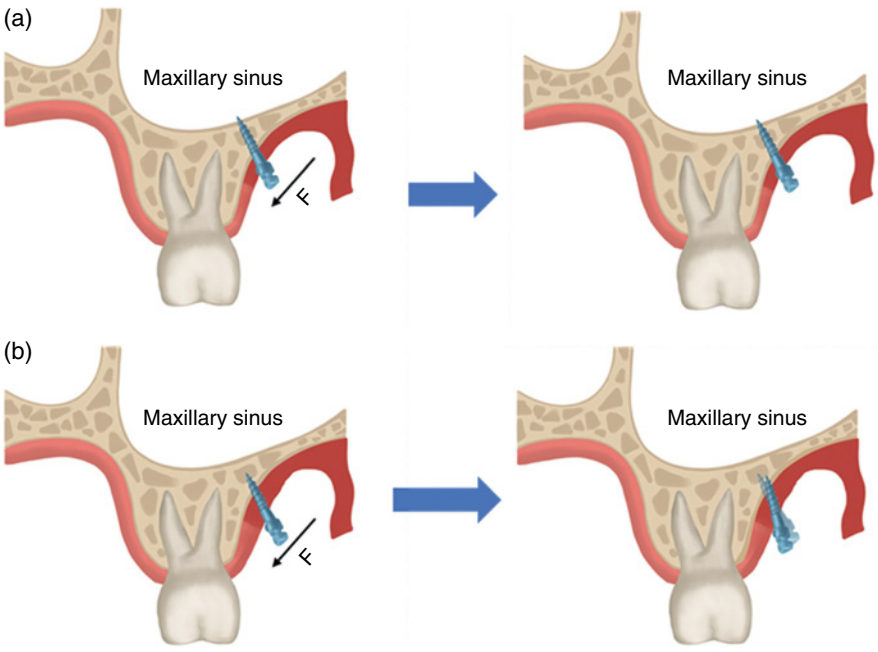


Figure 5.95 Bicortical versus monocortical engagement. (a) Bicortical engagement is achieved by penetrating into the sinus. The mini-implant is stable and displays minimal displacement in response to force loading. (b) Monocortical engagement. The mini-implant exhibits greater displacement under force loading.

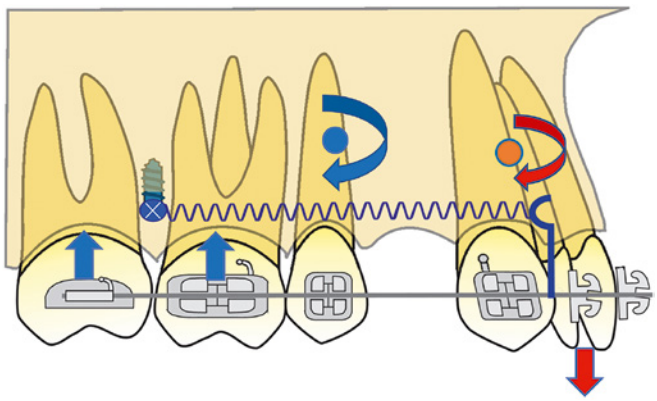


Figure 5.96 Biomechanical analysis of anterior retraction with a mini-implant at the infrazygomatic crest region. Even if a long crimpable hook is used, the retraction force passes occlusally to the centre of resistance of the anterior teeth (red dot), and the anterior teeth exhibit extrusion and lingual tipping due to the clockwise moment generated by the retraction force. If the maxillary dentition is considered as a whole, it is subject to clockwise moment that leads to clockwise rotation of the occlusal plane. Thus, intrusion of the molars occurs.

t.me/Dr_Mouayyad_AlbtousH

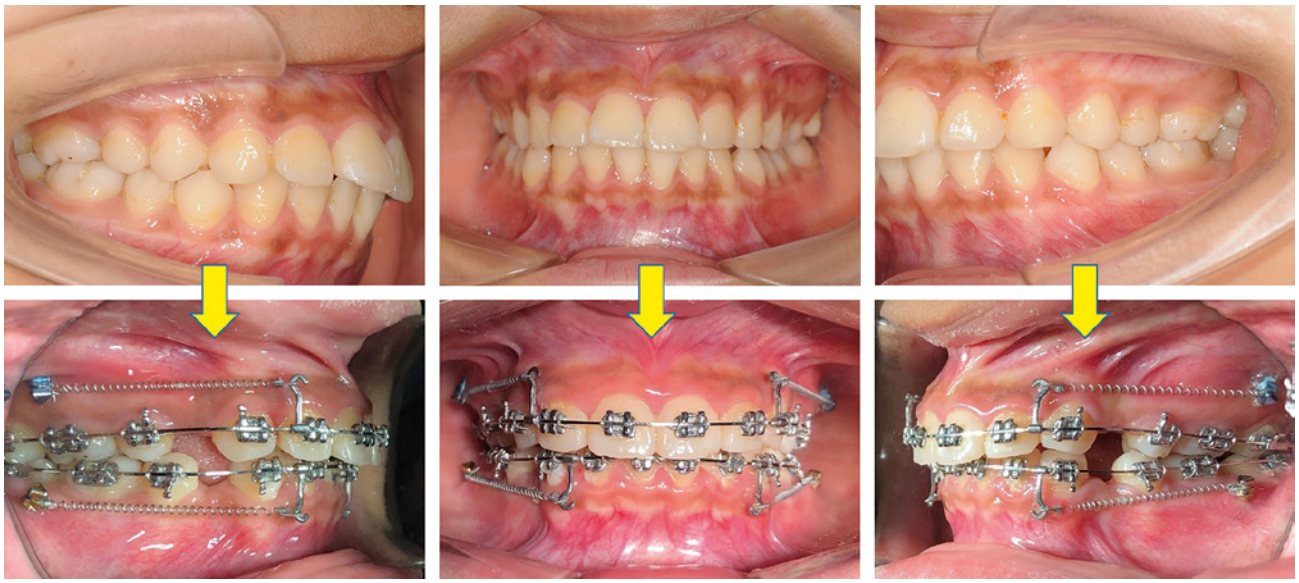


Figure 5.97 The mini-implants inserted at the infrazygomatic crest region were used for anterior retraction. Bite deepening occurred during anterior retraction.

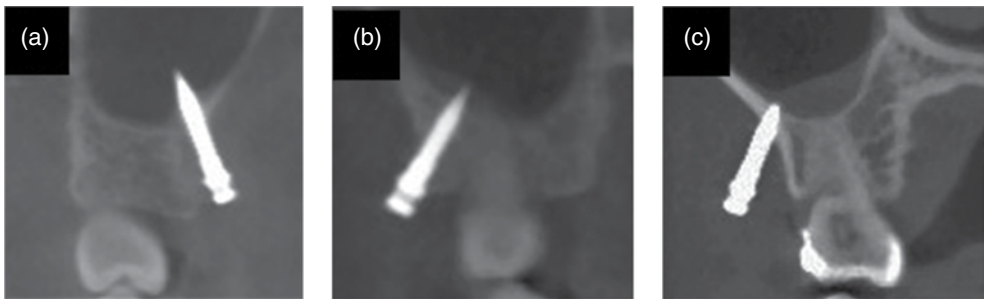


Figure 5.98 The influence of cortical thickness and bone depth on stability of mini-implants. (a) Neither bone depth nor cortical thickness was adequate and the mini-implant became loose and was dislodged one month following insertion. (b) Bone depth was adequate while cortical thickness was insufficient. The stability of the mini-implant was not high and it was displaced in response to orthodontic force. (c) The cortical thickness is sufficient with inadequate bone depth, but the mini-implant was stable during the whole orthodontic treatment phase.

should be taken into consideration during the biomechanical design and appropriate measures taken.

5.3.3 Selection of Appropriate Insertion Sites

The selection of appropriate insertion sites is based on both hard tissue and soft tissue factors. Specifically, cortical thickness is more important than bone depth for stability of mini-implants, and bicortical engagement is recommended (Figure 5.98). Based on the following criteria: (1) bone depth greater than 5 mm, (2) likelihood of root contact less than 10%, we previously proposed the optimal insertion height and insertion angle to be 12–18 mm apical to the occlusal plane and 40–70° to the occlusal plane at the first-second molar region.[46] However, if we further refine this region by taking the requirement of cortical thickness (greater than 2 mm) into consideration, the insertion angle is recommended to be 60–70°. Thus, we recommend that the IZC mini-implant be inserted at the entry point that is 12–18 mm above the occlusal plane with the insertion angle being 60–70° to the occlusal plane (Figures 5.99 and 5.100).

5.3.4 Insertion Techniques

Preinsertion

A thorough radiographic examination should be performed based on CBCT images. Based on biomechanical demands, the desired sagittal position for the insertion, and the optimal entry point and associated insertion

t.me/Dr_Mouayyad_AlbtousH

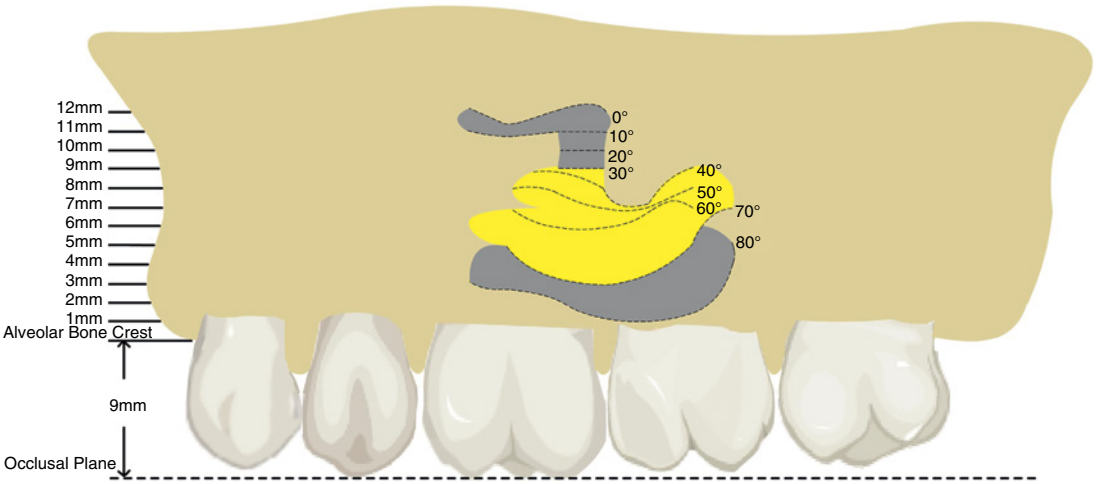


Figure 5.99 Recommended region for the insertion of mini-implants at the infrazygomatic crest region (optimal area: yellow; suboptimal area: grey). *Source:* Song et al. [46]/e-Century Publishing Corporation.

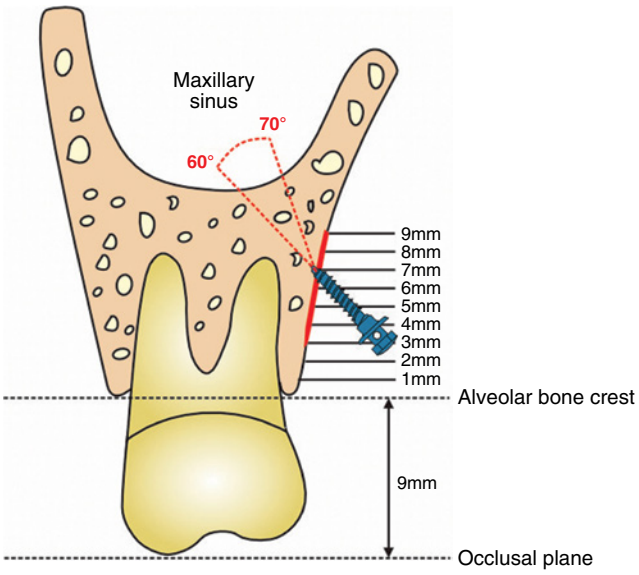


Figure 5.100 It is recommended that the IZC mini-implants be inserted at the entry point 12–18 mm above the occlusal plane with the insertion angle being 60–70° to the occlusal plane.

angle should be determined. The spatial relationship between vital structures (i.e. sinus and dental roots) and the buccal cortical plate should be meticulously evaluated in order to obtain bicortical engagement. Moreover, based on the clinical evaluation of soft tissue thickness, mini-implants with appropriate lengths and diameters should be selected.

Insertion Procedures

First, local infiltration anaesthesia is performed following mucosal disinfection with iodophor (Figure 5.101). To achieve greater mini-implant stability, sinus penetration is recommended. Since the inner surface of the maxillary sinus is covered by the richly innervated Schneiderian membrane, sinus penetration by the mini-implant often elicits intense pain perception. Thus, this demands profound local anaesthesia. However, profound anaesthesia may extend to molar roots and render them unresponsive to root contact, resulting in a clinical dilemma for practitioners in applying local anaesthesia.

To solve this problem, we recommend a 'two-point injection' anaesthesia technique for placement of the mini-implant at the IZC region (Figure 5.102). Specifically, the first injection point is the entry point where the mini-implant will penetrate the soft tissue. At the first injection point, a limited amount (0.2–0.5 ml) of anaesthetic agent is needed to anaesthetize the soft tissue and the periosteum but spare the neighbouring dental roots, so that operators can be alerted if root contact occurs during the insertion. The second injection point is 5–8 mm apical to the first injection point and profound anaesthetic agent (1.0 ml) is required to anaesthetise the Schneiderian membrane covering the inner surface of the sinus. In this way, both the soft tissues around the entry point and the sinus membrane are anaesthetised, with the dental roots being spared and responsive to nociceptive stimuli of root contact. Following the verification of satisfactory anaesthetic effect, the patient is instructed to rinse with chlorhexidine for 30–60 seconds to decrease intraoral microbial levels.

Second, the predetermined optimal entry point is transferred to the patient's actual IZC region. The specific entry point and a soft tissue indentation are marked with a probe based on the predetermined height from the occlusal plane (Figure 5.103). Due to the posterior location of the IZC region, the entry point is located posteriorly and

t.me/Dr_Mouayyad_AlbtousH

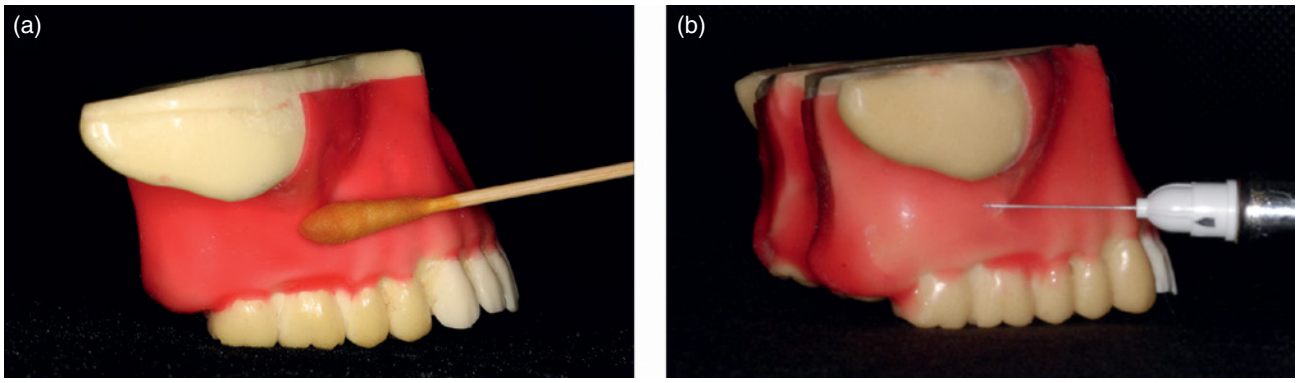


Figure 5.101 (a) Mucosa disinfection with iodophor. (b) Local infiltration anaesthesia.

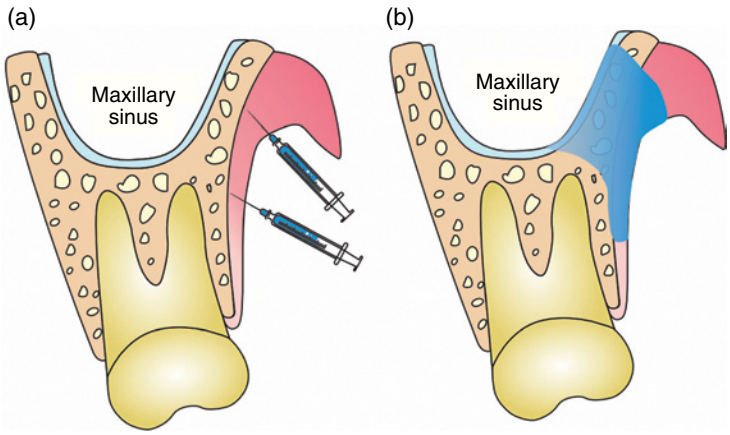


Figure 5.102 'Two-point injection' anaesthesia technique for the placement of mini-implant at the IZC region. (a) The first injection point is the entry point where the mini-implant will penetrate the soft tissue, and a limited amount (0.2–0.5 ml) of anaesthetic agent is needed. The second injection point is 5–8 mm apical to the first injection point and profound anaesthetic agent (1.0 ml) is required. (b) After the two-point injection anaesthesia, the soft tissues around the entry point and the sinus membrane are anaesthetised, with the dental roots being spared. The blue area indicates the anaesthetised region.

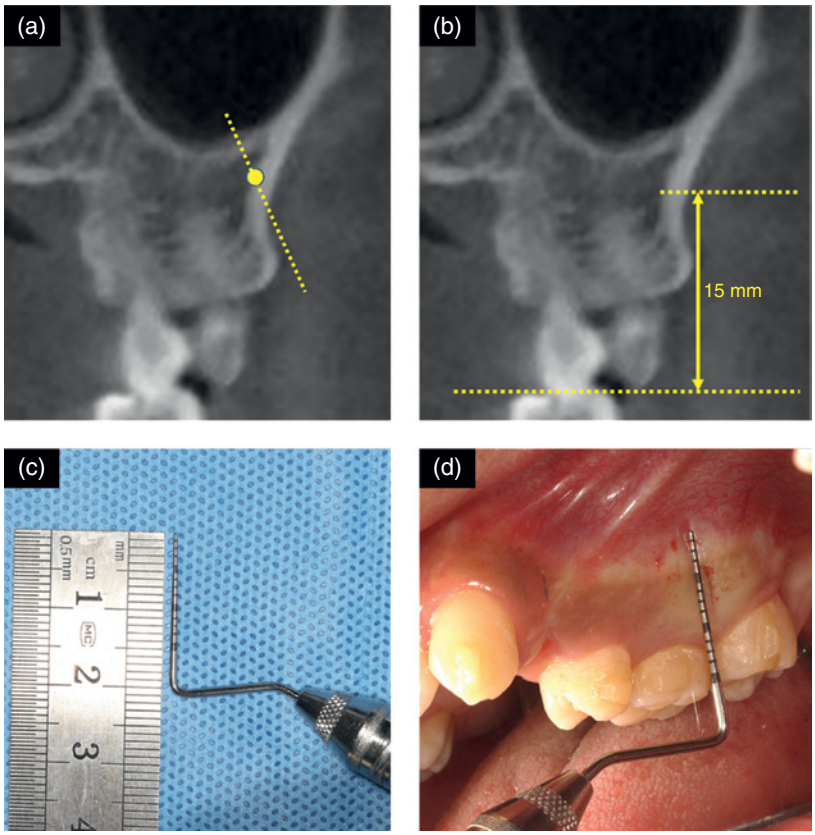


Figure 5.103 (a) Virtual insertion. The desired entry point (yellow dot) is determined based on a virtual placement. The virtual insertion path is indicated by the yellow dashed line. (b) The distance from the designated entry point to the occlusal plane is measured on the CBCT image (e.g. 15 mm). (c,d) A periodontal probe is employed to mark the designated entry point.

t.me/Dr_Mouayyad_AlbtousH

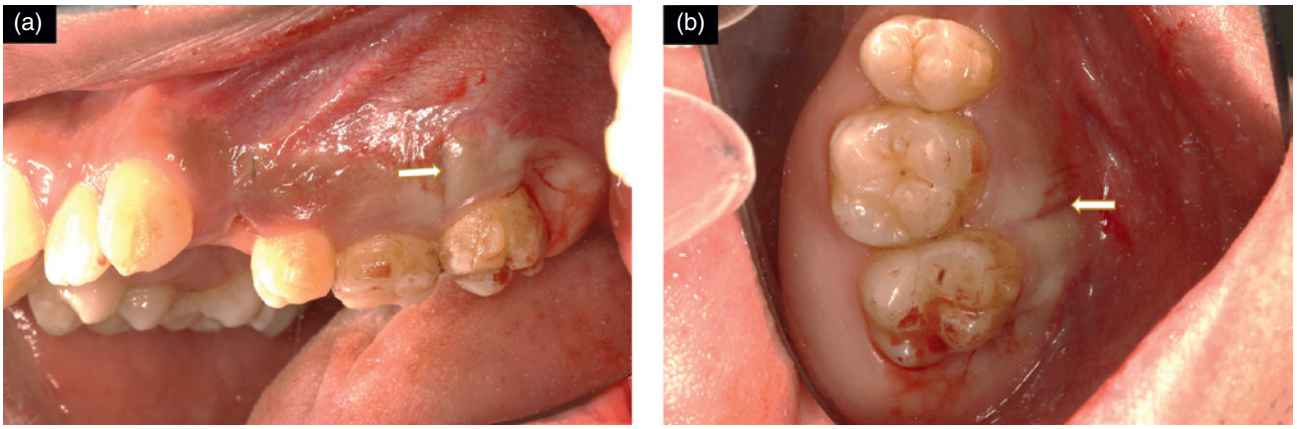


Figure 5.104 The marked vertical indentations (white arrows) are checked from both the buccal and occlusal sides. (a) Buccal side. (b) Occlusal side.

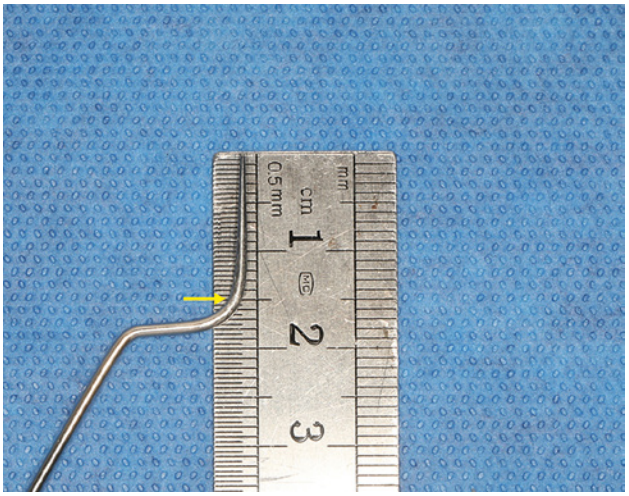


Figure 5.105 A dental explorer is used for marking the soft tissue indentation by bending at the designated point (yellow arrow).

access is often limited. Thus, adequate soft tissue retraction is required to clearly expose the IZC region. The patient should be instructed not to open their mouth too widely, as operative access would be further limited by the coronoid process that is moved anteriorly during mouth opening. Since the operator's line of view is often oblique to the insertion site, the marked entry point may be located distally to the desired one. Thus, the vertical indentation on the soft tissue should be checked from both the buccal and occlusal sides (Figure 5.104). Alternatively, a dental explorer can be used for marking the soft tissue indentation by bending at the designated point (Figure 5.105). Similar techniques are employed for the soft tissue indentation with the dental explorer (Figure 5.106). The soft tissue indentation helps guide the insertion so that correct mesiodistal angulation is guaranteed.

Third, once the soft tissue indentation is correctly marked, the next step is to insert the mini-implant through the marked entry point. Since the entry point is often located in the movable mucosa zone, it may be displaced with the movement of mucosa. Thus, retraction of the soft tissue should be stable throughout the whole insertion procedure, otherwise an incorrect entry point may be penetrated by the mini-implant.

After the mini-implant is mounted into the straight screwdriver, it is held against the bone surface at the designated entry point. Then, the mesiodistal angulation should be checked from the occlusal side and an insertion path that is perpendicular to the line connecting the two adjacent teeth is often recommended (Figure 5.107). Once the desired mesiodistal angle is verified, the mini-implant is slowly advanced to penetrate the cortex. Due to the thick cortex at the IZC region, cortex penetration should be slow (less than 30 rpm) and 1–2 minutes may be required for cortex penetration. Following cortex penetration, the mini-implant is slightly derotated to allow the change in the insertion angle (Figure 5.108).

t.me/Dr_Mouayyad_AlbtousH

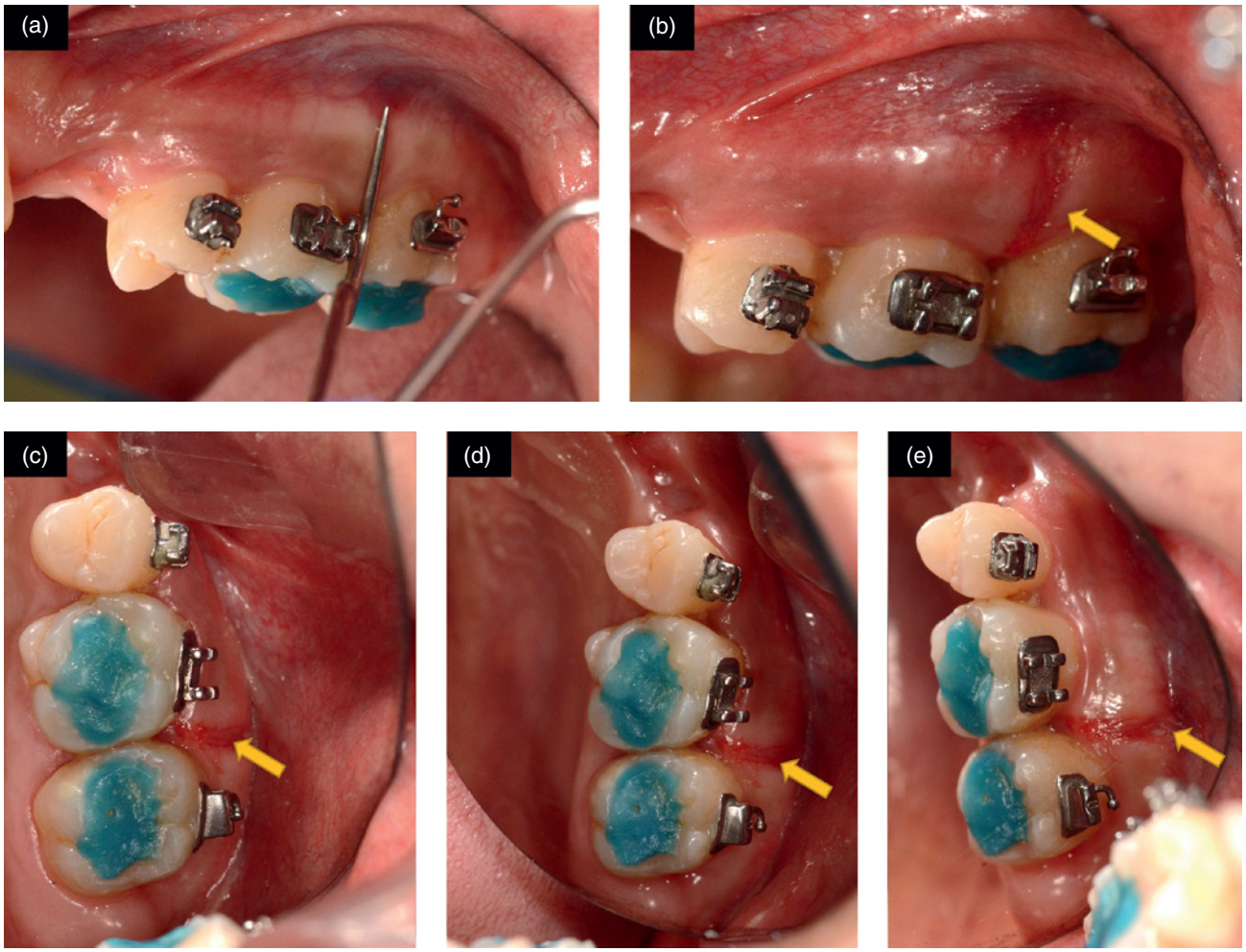


Figure 5.106 (a) Perform a vertical indentation on the soft tissue with an explorer. (b) Check the orientation of the vertical indentation (yellow arrow) from the buccal side. (c–e) Check the position and orientation of the vertical indentation from the occlusal side.

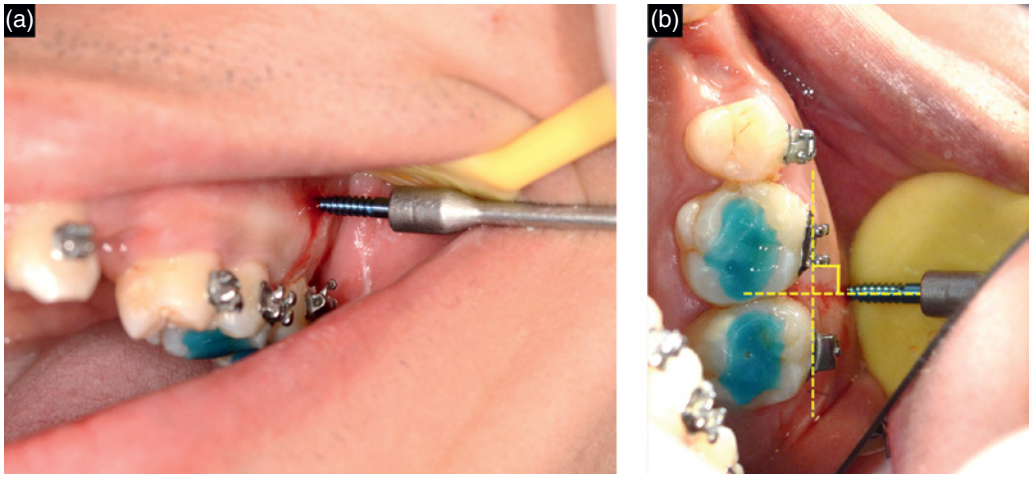


Figure 5.107 (a) The mini-implant is being inserted through the designated entry point. (b) The insertion path is perpendicular to the line connecting the two adjacent teeth (occlusal view).

t.me/Dr_Mouayyad_AlbtousH

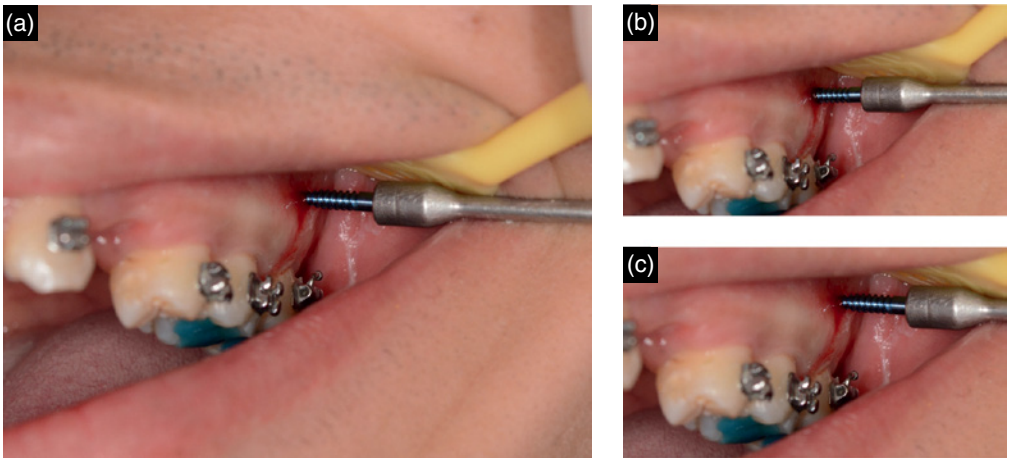


Figure 5.108 (a) Initial contact of the mini-implant with the bone surface. (b) The mini-implant is slightly advanced so that the cortex has been penetrated. (c) Following cortex penetration, the mini-implant is slightly derotated to allow the change in the insertion angle.

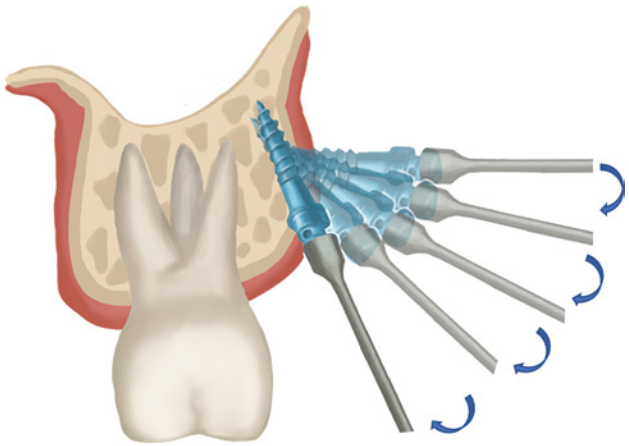


Figure 5.109 'Gradual angulation change' technique. In this technique, the insertion angle is gradually increased while the mini-implant is being advanced.

Fourth, the mini-implant is inserted at an angle of 60–70° to the occlusal plane. Unlike the mini-implant inserted at the buccal interradicular site where the insertion angle is small (30–45°), here the mini-implant is inserted with greater angulation (60–70°) at the IZC region. A direct change to the desired insertion angle (60–70°) for the mini-implant at the IZC region may lead to mini-implant slippage and soft tissue trauma, resulting in insertion failure. Thus, a 'gradual angulation change' technique should be followed for the placement of mini-implants at the IZC region (Figure 5.109). This technique requires the operator to slowly advance the mini-implant with a gradual increase in the insertion angle, until the desired angle is reached (60–70°). Once the desired angle is obtained, the screwdriver is disengaged and the angle is confirmed from the frontal view (Figure 5.110). Then, the mini-implant is advanced into the IZC region until adequate bone engagement is reached and sufficient emergence profile is obtained.

Lastly, once insertion is complete, the positions and orientations of the mini-implant should be checked from both the buccal and occlusal sides, and force loading can be applied if adequate primary stability is confirmed (Figure 5.111).

The procedures of inserting a mini-implant at the IZC region are illustrated in Figure 5.112.

5.3.5 Clinical Applications

Molar Distalisation

Since IZC mini-implants are located buccally and apically to molar roots, they do not impede the sagittal movement of those roots and are frequently employed for maxillary molar distalisation. IZC mini-implants can distalise maxillary molars through both direct and indirect anchorage modes. Two case examples are presented below.

t.me/Dr_Mouayyad_AlbtousH

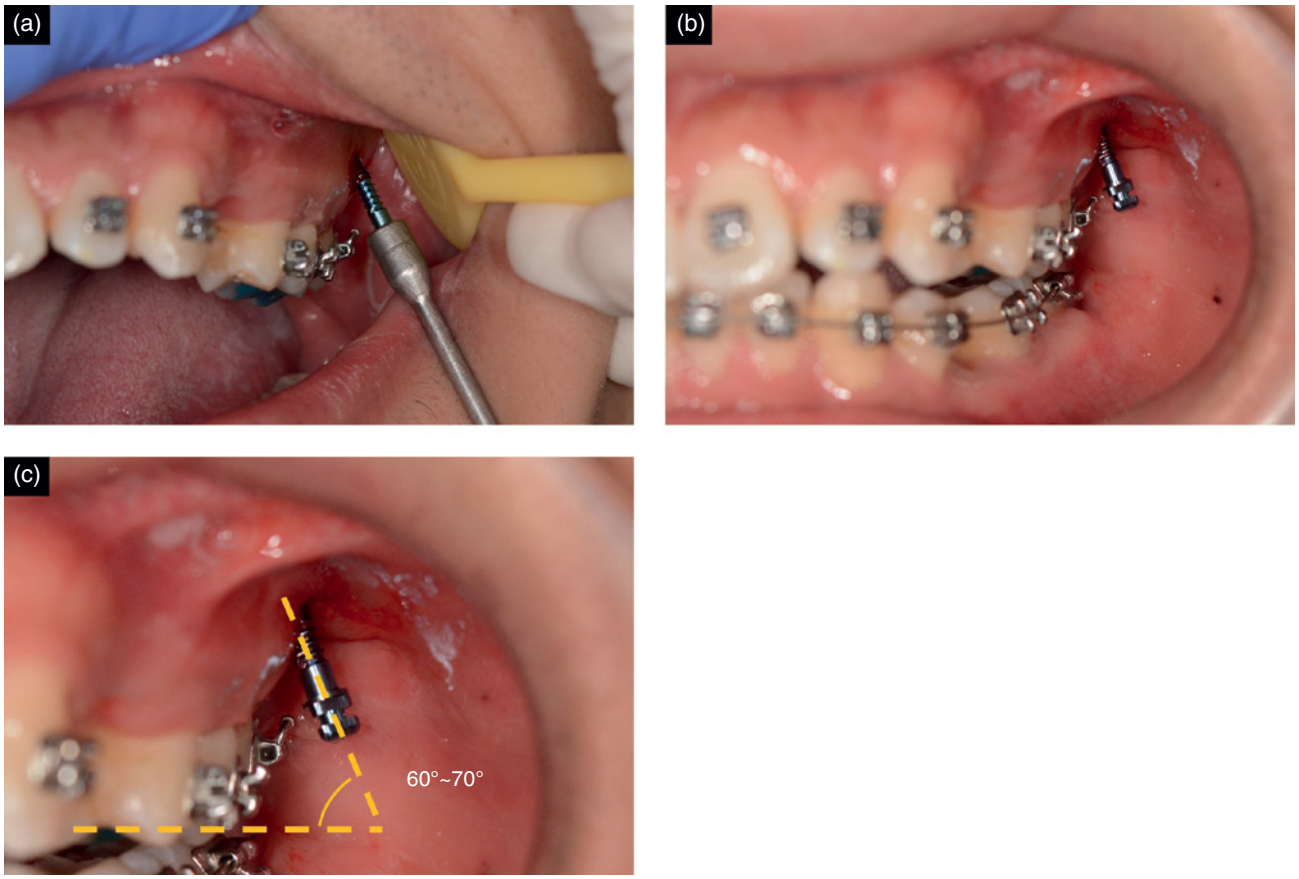


Figure 5.110 (a) The desired insertion angle is obtained. (b) The screwdriver is disengaged and the insertion angle is confirmed from the frontal view. (c) Confirm the insertion angle from the frontal side.

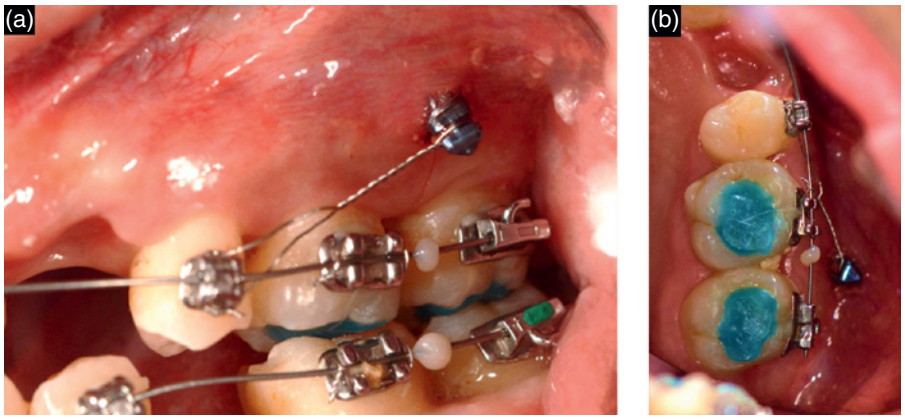


Figure 5.111 Force loading is applied onto the mini-implant. (a) Buccal view. (b) Occlusal view.

Case 1 A female adult presented with a chief complaint of dental crowding and deep bite. As displayed in Figure 5.113, her clinical and radiographic examinations revealed that she had a class II canine and molar relationship on both sides ('end-to-end' class II on the left side and slight class II on the right side). She had anterior deep bite with moderate crowding in the upper arch and mild crowding in the lower arch. Her upper and lower dental midlines were not coincident, with the upper one deviating to the right side by 3 mm. Sha had a straight facial profile and the panoramic radiograph was indicative of erupted bilateral maxillary third molars and horizontally impacted mandibular third molars. As shown in Table 5.9, the lateral cephalometric analysis revealed that the patient had class II skeletal base (ANB = 4.6) with normal mandibular plane angle (SN-MP = 34.8). Moreover, the labiolingual inclinations of both the

t.me/Dr_Mouayyad_AlbtousH

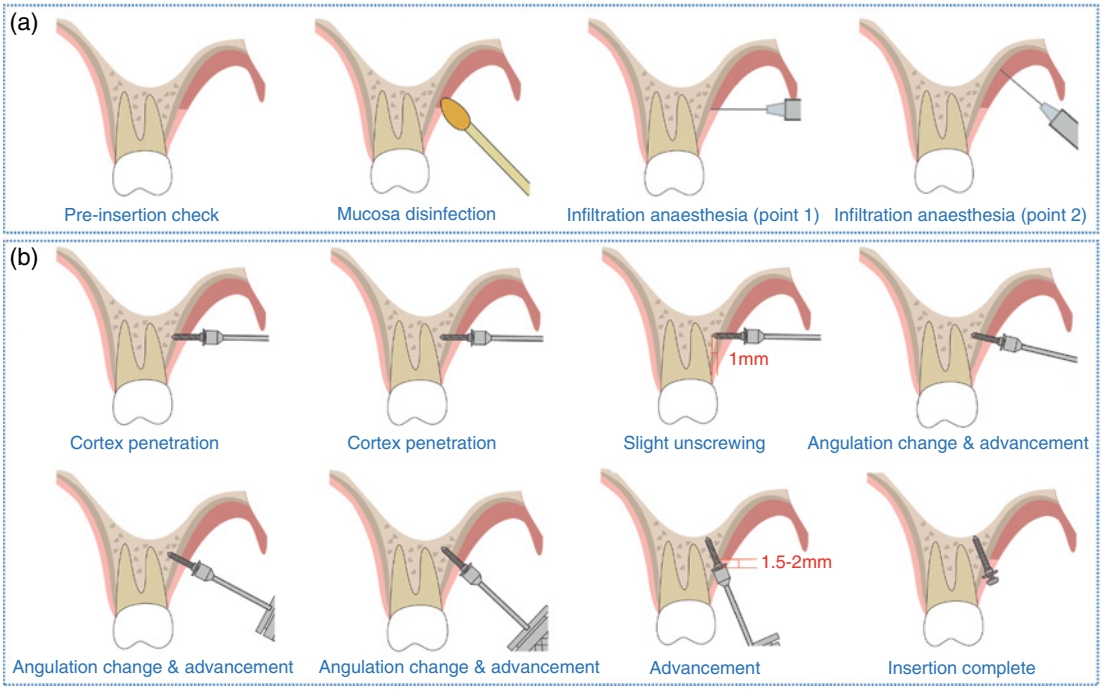


Figure 5.112 Schematic illustrations demonstrating the procedure of inserting a mini-implant at the infrazygomatic crest. (a) Preinsertion examination, disinfection and local infiltration anaesthesia. (b) Insert the mini-implant through the designated entry point.



Figure 5.113 Pretreatment photographs and radiographs.

t.me/Dr_Mouayyad_AlbtousH

Table 5.9 Pretreatment lateral cephalometric analysis.

Measurement	Norm	Pretreatment
Skeletal (°)		
SNA	83.0±4.0	80.6
SNB	80.0±4.0	76.0
ANB	2.0±2.0	4.6
FMA	28.0±4.0	25.9
SN-MP	35.0±4.0	34.8
Dental (°)		
U1-SN	105.7±6.3	100.5
L1-MP	97.0±7.1	95.1
FMIA	65.0±6.0	59.1
U1-L1	124.0±8.0	129.6
Soft tissue (mm)		
UL-EP	2.0±2.0	–1.5
LL-EP	3.0±2.0	–0.9
Wits (mm)		
Wits	–1.0	1.4

upper and lower incisors are within the normal ranges (U1-SN = 100.5; L1-MP = 95.1).

In view of the pretreatment data, upper molar distalisation was planned to correct the class II molar relationship and gain space for anterior crowding in the upper arch. In addition, aligning and levelling were designed for the lower arch. To achieve efficient molar distalisation, two mini-implants were placed at the bilateral IZC regions and power-arm hooks that extended anteriorly were welded onto the molar bands (Figure 5.114). The power-arm hooks were exploited to ensure that the distalising force passed through the centres of resistance of the molars, so that bodily distalisation of molars could be achieved. The bilateral molar bands were stabilised by a palatal arch, otherwise mesial-out rotation of the molars would occur.

Once the molar distalisation was complete and class I molar relationship achieved, the power-arm hooks were removed and fixed appliances used for alignment and levelling (Figure 5.115). Finally, bilateral class I canine and molar relationships were achieved with dental crowding resolved. The patient's straight profile was maintained (Figure 5.116). The pre- and posttreatment cephalometric analyses are displayed in Table 5.10.

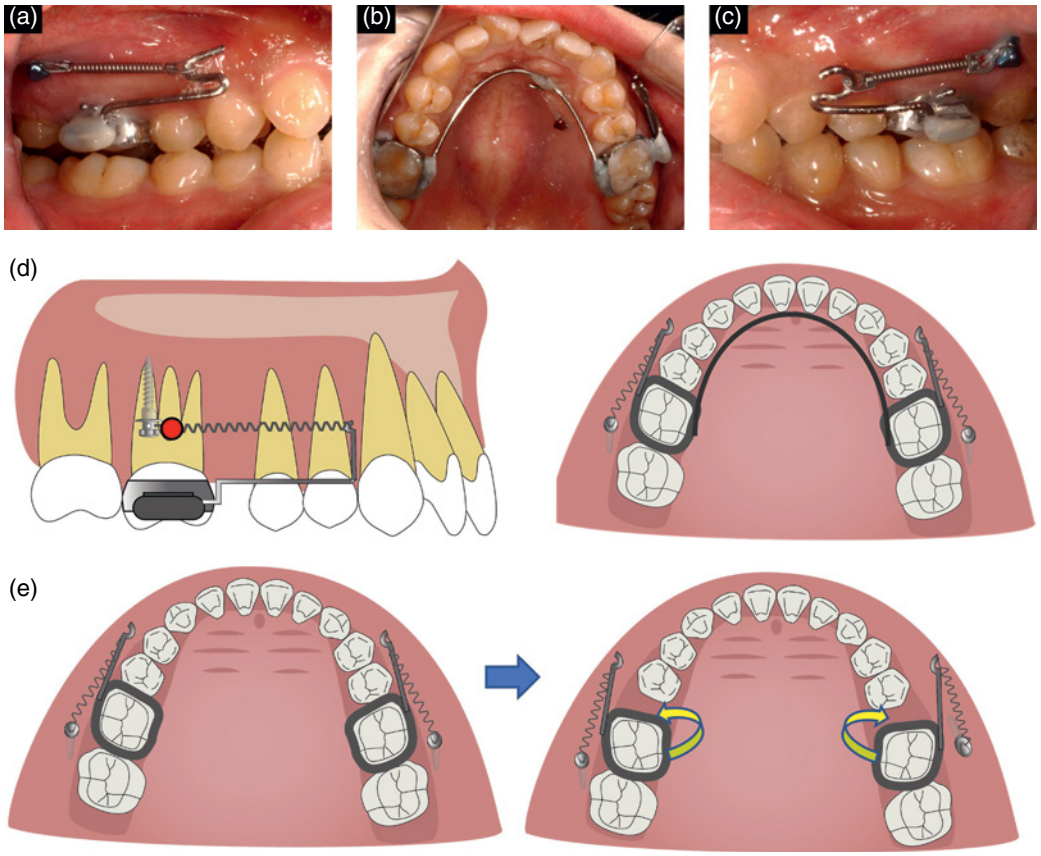


Figure 5.114 Molar distalisation with mini-implants inserted at bilateral infrazygomatic crests. (a–c) Intraoral photographs showing that molars were distalised through closed-coil springs from the mini-implants to the buccal long hooks on the molar bands. (d) The distalisation force passes through the centre of resistance, leading to bodily distalisation of the molars. The bilateral molars were stabilised by a transpalatal arch. (e) If no transpalatal arch is designed, molars exhibit mesial-out rotation.

t.me/Dr_Mouayyad_AlbtousH

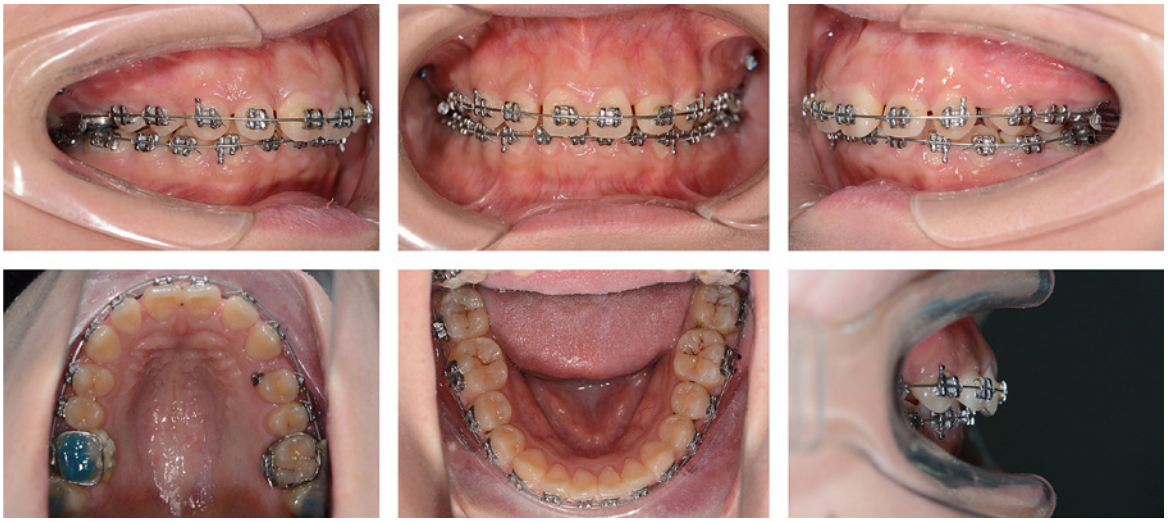


Figure 5.115 Fixed appliances were employed for tooth alignment and levelling once the molar distalisation was complete.



Figure 5.116 Posttreatment photographs and radiographs.

t.me/Dr_Mouayyad_AlbtousH

Table 5.10 Pre- and posttreatment lateral cephalometric analysis.

Measurement	Norm	Pretreatment	Posttreatment
Skeletal (°)			
SNA	83.0±4.0	80.6	80.3
SNB	80.0±4.0	76.0	76.3
ANB	2.0±2.0	4.6	4.0
FMA	28.0±4.0	25.9	26.9
SN-MP	35.0±4.0	34.8	33.8
Dental (°)			
U1-SN	105.7±6.3	100.5	96.1
L1-MP	97.0±7.1	95.1	98.8
FMIA	65.0±6.0	59.1	54.3
U1-L1	124.0±8.0	129.6	131.4
Soft tissue (mm)			
UL-EP	2.0±2.0	−1.5	−0.2
LL-EP	3.0±2.0	−0.9	−0.5
Wits (mm)			
Wits	−1.0	1.4	0.1

Case 2 A male adult patient presented to the orthodontic department with a chief complaint of dental crowding. As displayed in Figure 5.117, the clinical and radiographic examinations indicated class I canine and molar relationships at both sides with moderate dental crowding in both the upper and lower arches, with four third molars normally erupted. He had a straight facial profile. As displayed in Table 5.11, the lateral cephalometric analysis revealed that the patient had class I skeletal base (ANB = 6.5) with normal mandibular plane angle (SN-MP = 35.1). Moreover, the labiolingual inclinations of both the upper and lower incisors were within normal ranges (U1-SN = 106.4; L1-MP = 104).

Molar distalisation in both the upper and lower arches was planned to gain space to resolve anterior dental crowding. The patient chose clear aligners for his orthodontic treatment. Two mini-implants were inserted at the bilateral IZC regions and two more placed at the bilateral buccal shelf regions. Indirect anchorage mode was employed by applying orthodontic elastics between the mini-implant at each quadrant and the corresponding canine hook on the clear aligner (Figure 5.118).

Molar distalisation progressed smoothly and anterior crowding resolved efficiently (Figures 5.119–5.121). Bilateral class I canine and molar relationships as well as the straight facial profile were maintained (Figure 5.122). The pre- and posttreatment cephalometric analyses are displayed in Table 5.12.

Case 3 A female adult sought orthodontic treatment with a chief complaint of crooked teeth. Upon examination, we found that the patient had class II molar relationships on both sides, retained upper primary canines and mild crowding in both arches (Figure 5.123). The radiographic examinations were indicative of palatally impacted canines on both sides (Figures 5.123 and 5.124). The cephalometric analysis is presented in Table 5.13.

The treatment plan was to extract the retained primary canines and distalise upper molars to gain space for the permanent canines. Since the impacted canines were impinging on the roots of the maxillary incisors, orthodontic traction of the impacted canines would be distalisation followed by labial movement. The primary canines would not be extracted until enough space was created

t.me/Dr_Mouayyad_AlbtousH

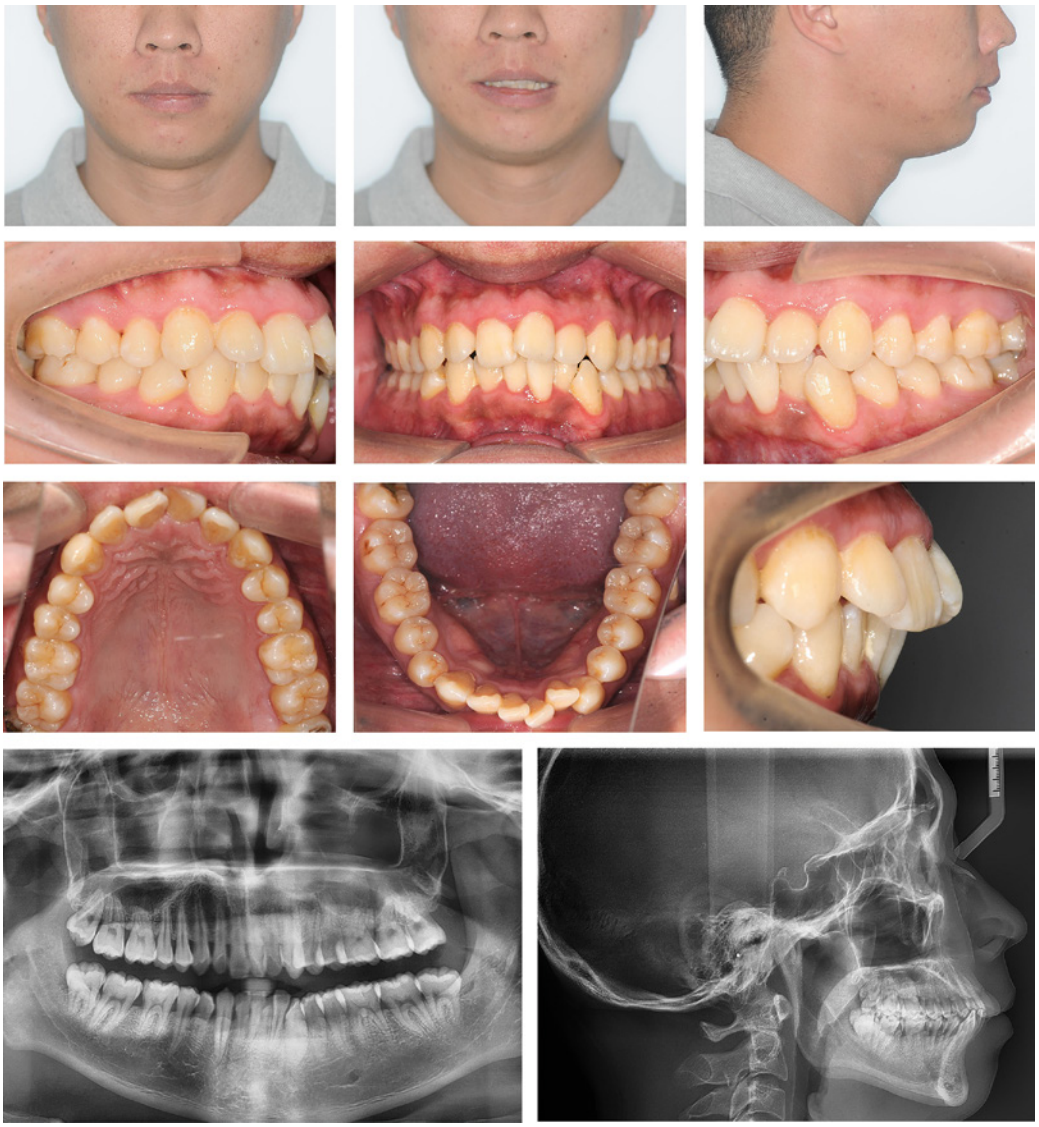


Figure 5.117 Pretreatment photographs and radiographs.

for labial movement of the permanent canines, so that traction of the impacted permanent canines would be more efficient due to regional acceleratory phenomena. To achieve molar distalisation, two mini-implants were placed at the bilateral infrazygomatic crest regions and extension hooks secured onto the main archwire were fixed on the molar bands (Figure 5.125). The upper molars were distalised by applying closed-coil springs between the mini-implants and the extension hooks that can be slid distally along the main archwire. The biomechanical features of this appliance are illustrated in Figure 5.126.

The molar distalisation progressed smoothly and efficiently, and the impacted canines were distalised away from the incisors by applying elastomeric chains between the lingual buttons on the canines and the palatal hooks on the first molars (Figure 5.127). Once the molar distalisation was complete and adequate space was gained for the permanent canines, the primary canines were extracted and labial movement of the palatally impacted

t.me/Dr_Mouayyad_AlbtousH

Table 5.11 Pretreatment lateral cephalometric analysis.

Measurement	Norm	Pretreatment
Skeletal (°)		
SNA	83.0±4.0	82.5
SNB	80.0±4.0	76.0
ANB	2.0±2.0	6.5
FMA	28.0±4.0	25.7
SN-MP	35.0±4.0	35.1
Dental (°)		
U1-SN	105.7±6.3	106.4
L1-MP	97.0±7.1	104.0
FMIA	65.0±6.0	50.3
U1-L1	124.0±8.0	114.5
Soft tissue (mm)		
UL-EP	2.0±2.0	0.9
LL-EP	3.0±2.0	3.6
Wits (mm)		
Wits	−1.0	5.4

canines was initiated (Figure 5.128). After the palatally impacted canines were moved labially, brackets were bonded on the canines and alignment was started (Figure 5.129). At the end of treatment, the palatally impacted canines were successfully aligned into the dental arch, and bilateral class I molar relationship, normal overjet and overbite were achieved (Figure 5.130). The pre- and posttreatment cephalometric analyses are displayed in Table 5.14.

Anterior Intrusion

The IZC mini-implants can be utilised for incisor intrusion through a specific cantilever spring. As illustrated in Figure 5.131, cantilever springs are fixed and anchored onto the IZC mini-implants, with the anterior hooks being apical to the archwire during the inactivation phase. While the implant-anchored cantilever springs are activated onto the archwire, the anterior teeth are subject to intrusive force that leads to anterior intrusion.

As depicted in Figure 5.132, the anterior hooks of the implant-anchored cantilever springs were located at the



Figure 5.118 For molar distalisation in the upper arch, mini-implants (yellow arrows) were placed at the infrazygomatic crest region. Mini-implants (white arrows) were inserted at the buccal shelf region for distalisation of molars for the lower arch. Indirect anchorage mode was employed by applying orthodontic elastics between the mini-implant at each quadrant and the corresponding canine hook on the clear aligner. (a) Right side view. (b) Frontal view. (c) Left side view.

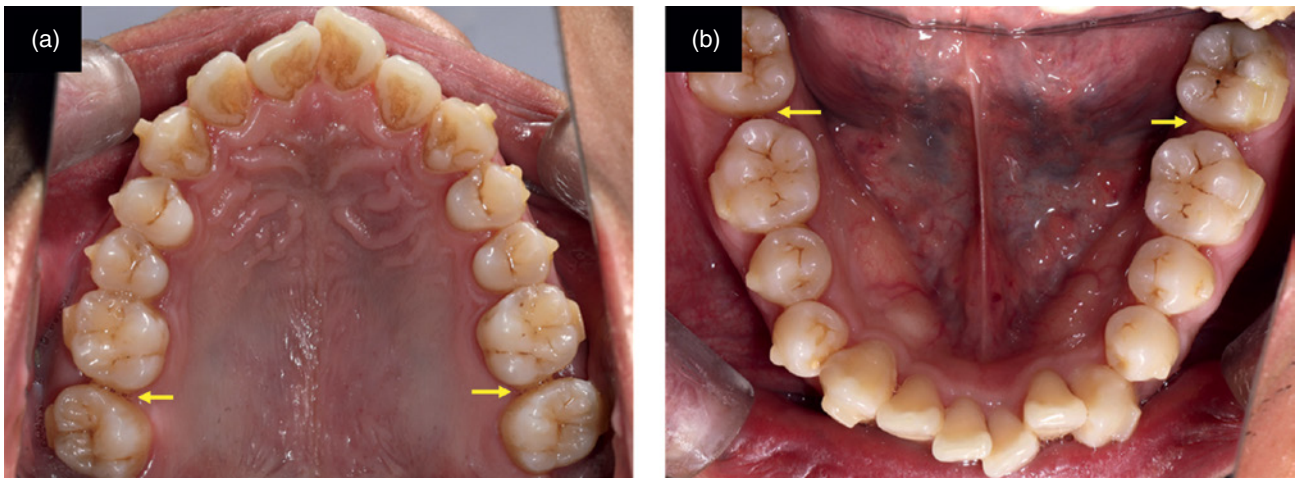


Figure 5.119 Treatment progress. Note the presence of spacings (yellow arrows) between the first and second molars. This indicates that both the upper molars and lower molars had been distalised. (a) Upper arch (occlusal view). (b) Lower arch (occlusal view).

t.me/Dr_Mouayyad_AlbtousH

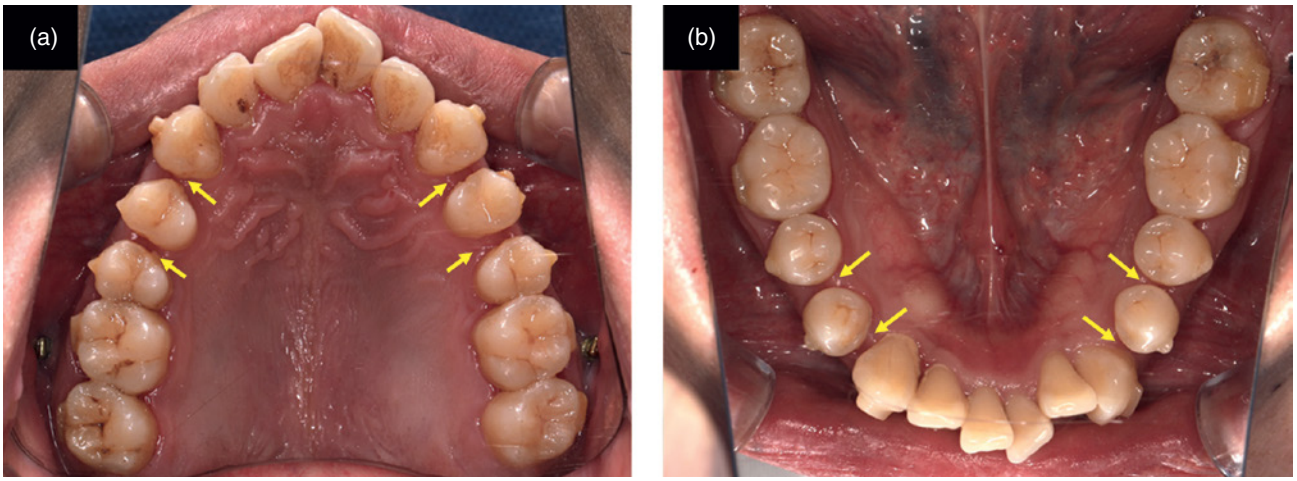


Figure 5.120 Treatment progress. Canines and premolars are being distalised. Note the spacings (yellow arrows) at the canine premolar region. (a) Upper arch (occlusal view). (b) Lower arch (occlusal view).

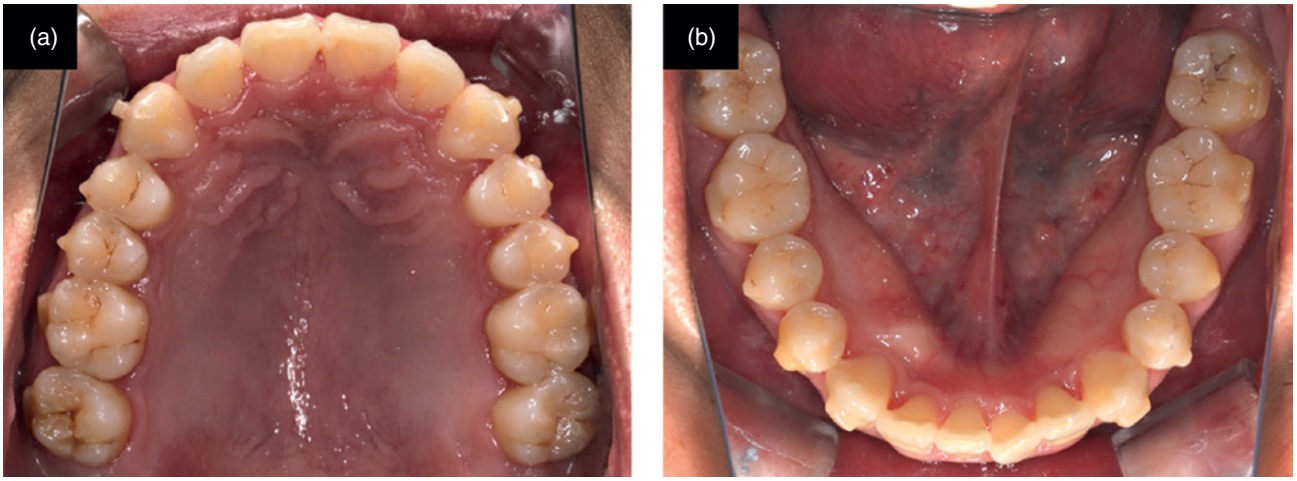


Figure 5.121 Treatment progress. The space gained through molar distalisation is being used to resolve anterior crowding. (a) Upper arch (occlusal view). (b) Lower arch (occlusal view).

vestibular sulcus during inactivation. The anterior hooks were secured onto the archwire to deliver intrusive force on the anterior teeth. The intrusive biomechanics offered by this system was efficient and effective (Figure 5.133).

Molar Intrusion

Since the mini-implants inserted at the IZC region are located buccally and apically to molar roots, they do not impede root movements, allowing a great amount of molar intrusion to be accomplished. Thus, maxillary molars, especially overerupted molars, can be effectively intruded by IZC mini-implants. However, inappropriate biomechanical design may lead to inadvertent buccal tipping and judicious design of biomechanics is very important. In addition to the intrusion force from the IZC mini-implant, an intrusion force from the palatal side should be implemented in order to achieve bodily intrusion of molars (Figure 5.134). A case example is presented below.

t.me/Dr_Mouayyad_AlbtousH

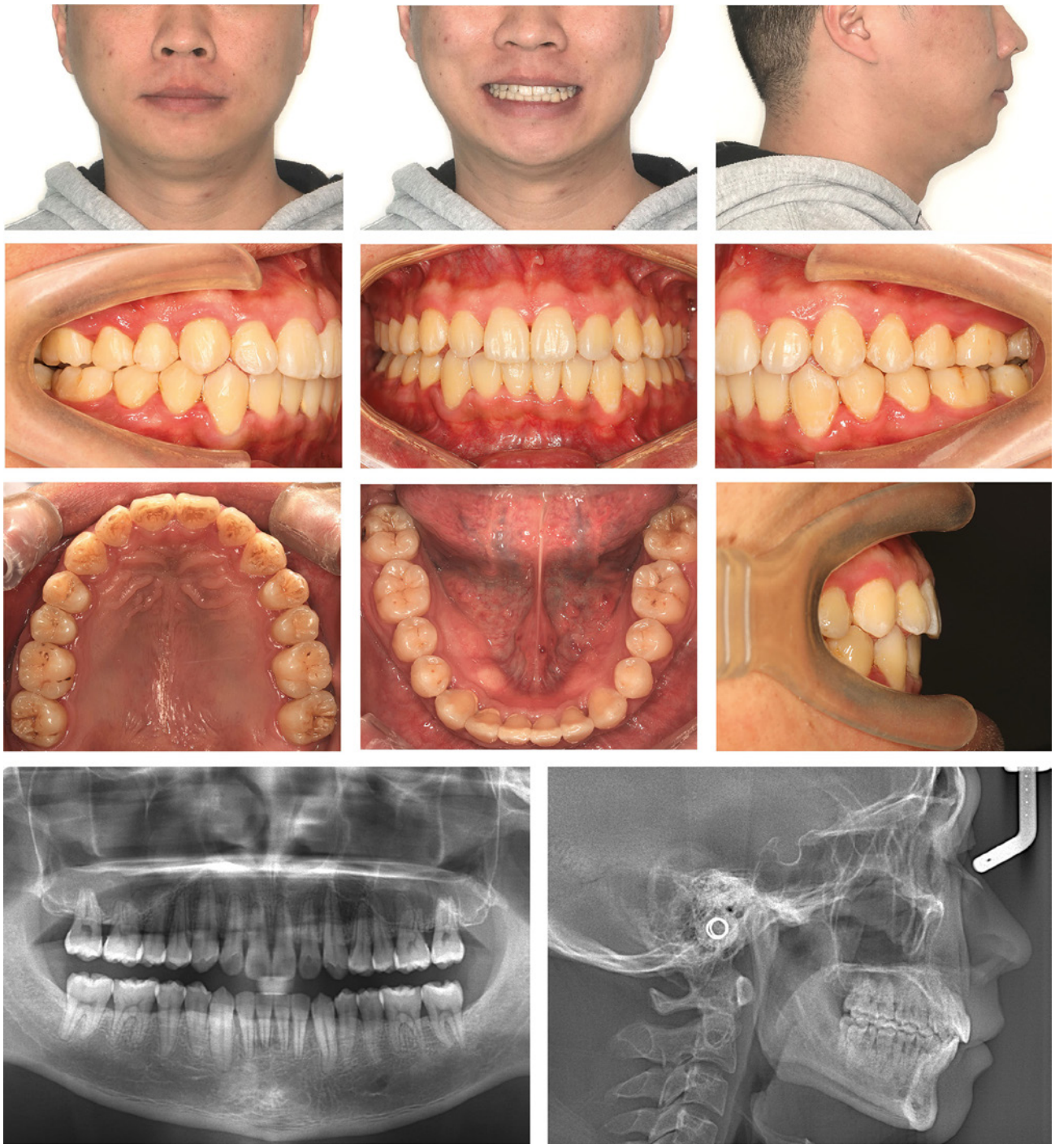


Figure 5.122 Posttreatment photographs and radiographs.

t.me/Dr_Mouayyad_AlbtousH

Table 5.12 Pre- and posttreatment lateral cephalometric analysis.

Measurement	Norm	Pretreatment	Posttreatment
Skeletal (°)			
SNA	83.0±4.0	82.5	82.2
SNB	80.0±4.0	76.0	77.0
ANB	2.0±2.0	6.5	5.2
FMA	28.0±4.0	25.7	24.4
SN-MP	35.0±4.0	35.1	33.2
Dental (°)			
U1-SN	105.7±6.3	106.4	99.4
L1-MP	97.0±7.1	104.0	101.7
FMIA	65.0±6.0	50.3	53.9
U1-L1	124.0±8.0	114.5	125.7
Soft tissue (mm)			
UL-EP	2.0±2.0	0.9	0.4
LL-EP	3.0±2.0	3.6	1.6
Wits (mm)			
Wits	−1.0	5.4	0.5



Figure 5.123 Pretreatment photographs and radiographs.

t.me/Dr_Mouayyad_AlbtousH

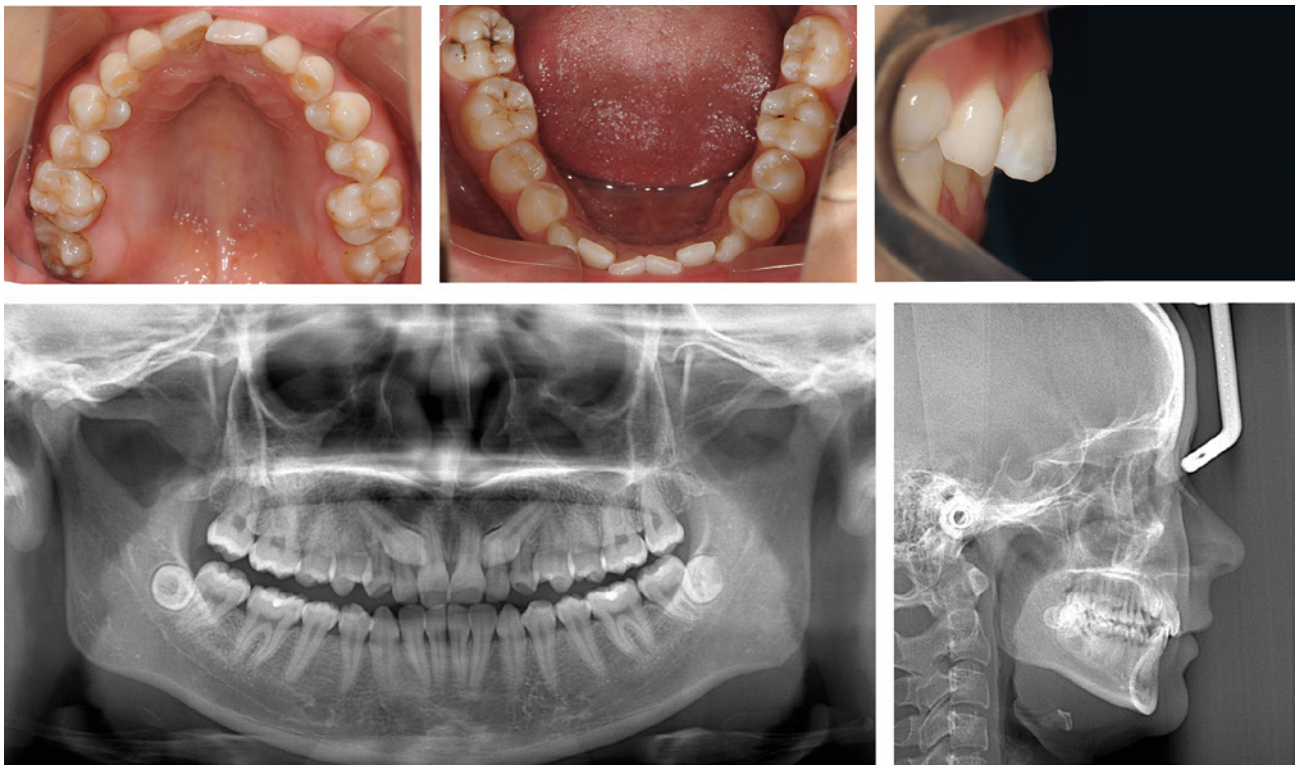


Figure 5.123 (Continued)

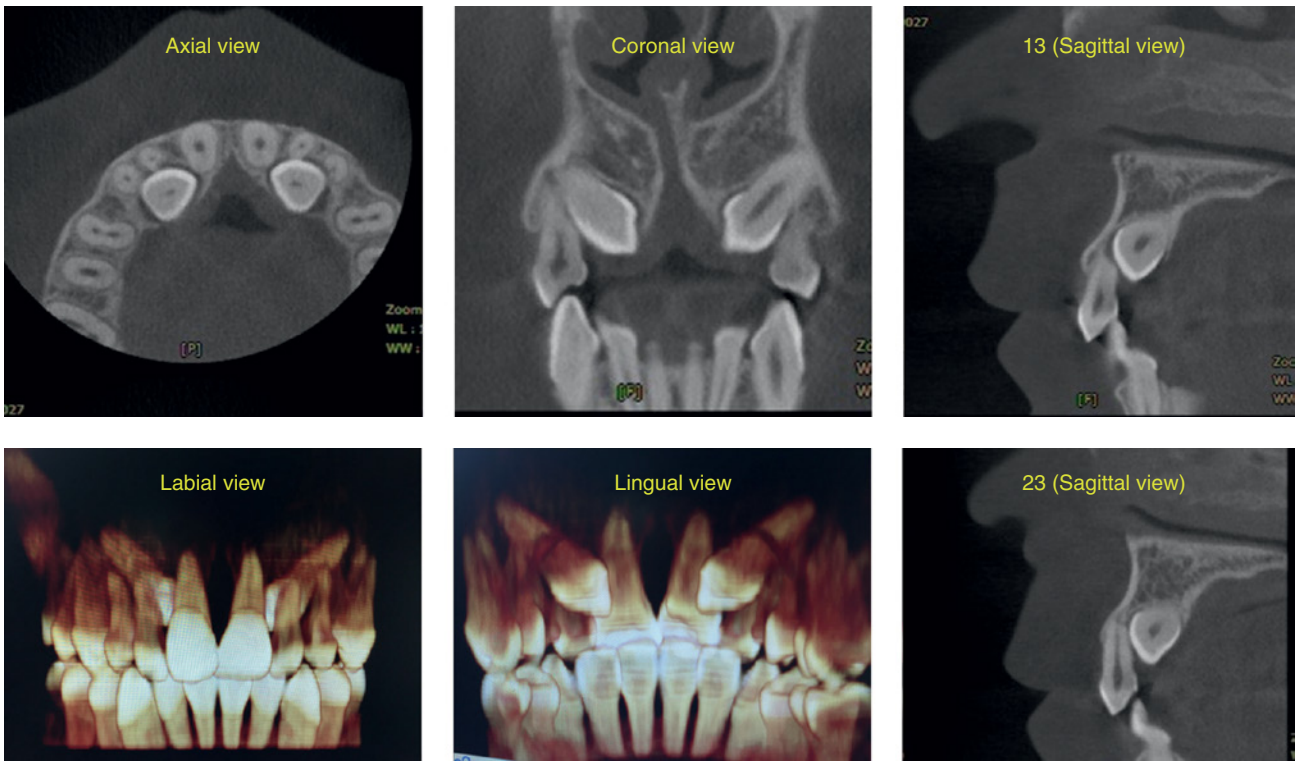


Figure 5.124 CBCT examinations indicated palatally impacted permanent canines.

t.me/Dr_Mouayyad_AlbtousH

Table 5.13 Pretreatment lateral cephalometric analysis.

Measurement	Norm	Pretreatment
Skeletal (°)		
SNA	83.0±4.0	83.1
SNB	80.0±4.0	78.6
ANB	2.0±2.0	4.5
FMA	28.0±4.0	18.4
SN-MP	35.0±4.0	30.2
Dental (°)		
U1-SN	105.7±6.3	98.4
L1-MP	97.0±7.1	91.6
FMIA	65.0±6.0	70.1
U1-L1	124.0±8.0	139.8
Soft tissue (mm)		
UL-EP	2.0±2.0	−4.2
LL-EP	3.0±2.0	−6.6
Wits (mm)		
Wits	−1.0	2.0

A male adult presented to the multidisciplinary treatment department with a chief complaint of missing teeth in his lower left quadrant. His clinical and radiographic examinations revealed that his mandibular left first and second molars were missing, with overeruption of the opposing maxillary left first and second molars (Figure 5.135). The treatment plan was to intrude the overerupted maxillary first and second molars to regain the vertical space and restore the missing mandibular molars with implants. However, a compromised treatment plan was made that only the mandibular first molar would be restored with implant since the patient did not want to have two implants (Figure 5.136). To intrude the overerupted maxillary molars, two mini-implants were placed: the buccal one at the IZC and the palatal one at the midpalatal suture. The overerupted molars were intruded by applying an elastomeric chain anchored on the buccal and palatal mini-implants (Figure 5.137). The intrusion of the maxillary molars progressed smoothly and efficiently. At the end of the minor tooth movement, the overerupted maxillary molars were successfully intruded and the mandibular first molar was restored with an implant (Figure 5.138).

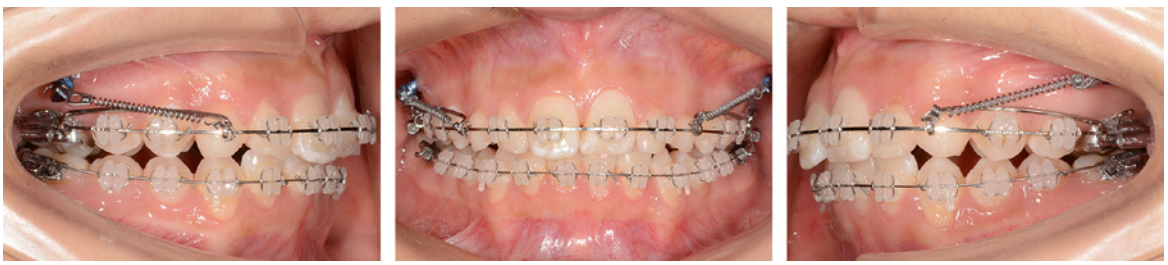


Figure 5.125 Treatment progress. Two mini-implants were placed at the bilateral infrazygomatic crest regions. Extension hooks were fixed on the molar bands and secured onto the main archwire. Closed-coil springs were applied between the mini-implants and the extension hooks that can be slid distally along the main archwire.

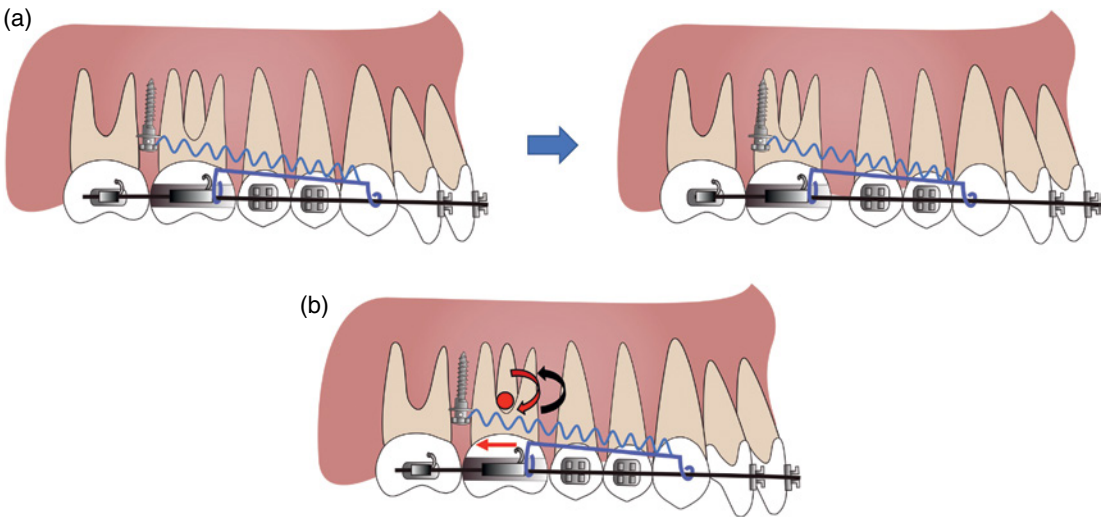


Figure 5.126 The distalisation force (red arrow) passes occlusally to the centre of resistance of the molar and generates a clockwise moment (red curved arrow), leading to distal tipping of the molar. This effect is counterbalanced by the main archwire that offers an anticlockwise moment (black curved arrow), so that the molar exhibits almost bodily distalisation. (a) Before and after molar distalisation. (b) Biomechanical analysis.

t.me/Dr_Mouayyad_AlbtousH

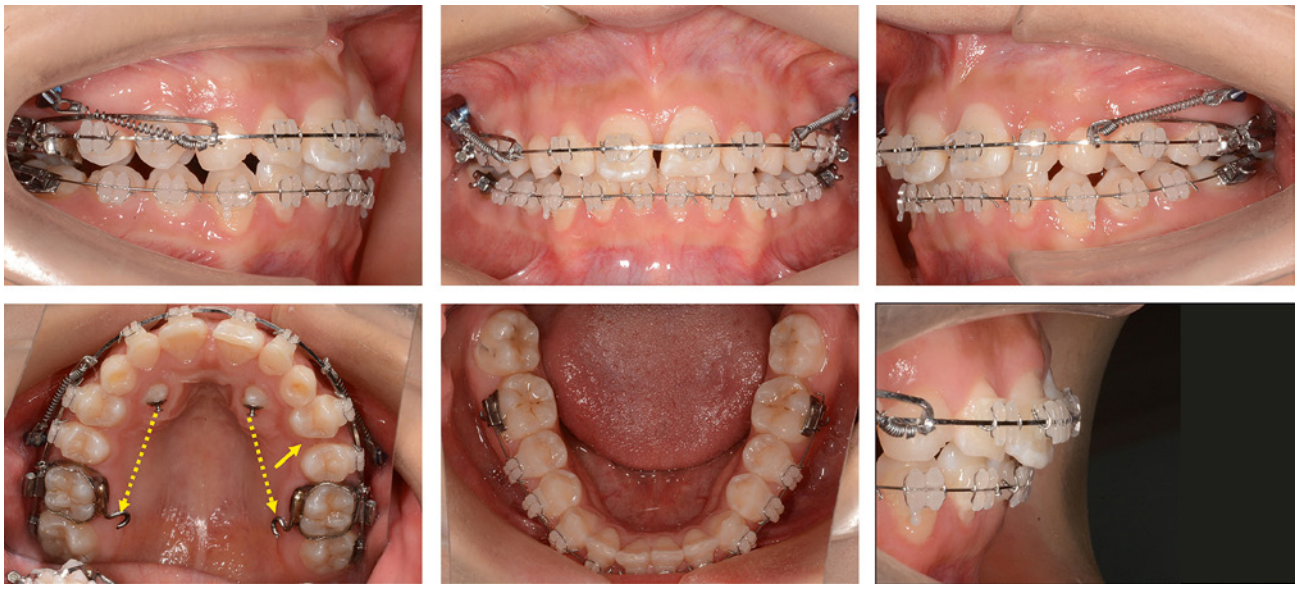


Figure 5.127 Treatment progress. Space was gained during molar distalisation. Note the space (yellow arrow) between the maxillary left first and second premolars. During molar distalisation, the impacted canines were distalised by applying elastomeric chains (illustrated by dashed yellow arrows) between the lingual buttons on the canines and the palatal hooks on the first molars.

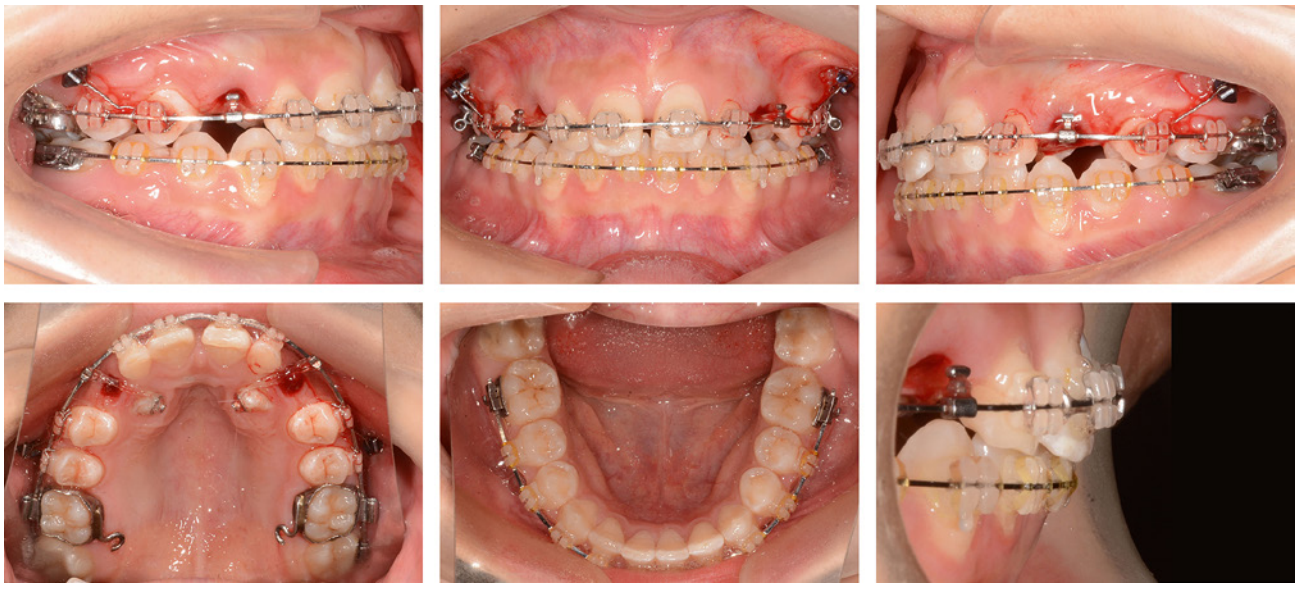


Figure 5.128 Treatment progress. Molar distalisation was complete and class I molar relationship was obtained on both sides. The primary canines had been extracted and the palatally impacted canines are being tractioned.

Orthodontic Traction of Impacted Teeth

Infrazygomatic crest mini-implants are effective in the traction of impacted teeth, provided that prudent biomechanics is designed. A case example is given below to demonstrate the clinical applications of the IZC mini-implant for traction of an impacted maxillary canine.

A male adolescent was referred to the orthodontic department for impacted teeth. As displayed in Figure 5.139, the maxillary left lateral incisor and canine were impacted with retained primary lateral incisor and canine. A supernumerary tooth was impacted mesially to the adjacent first premolar.

t.me/Dr_Mouayyad_AlbtousH

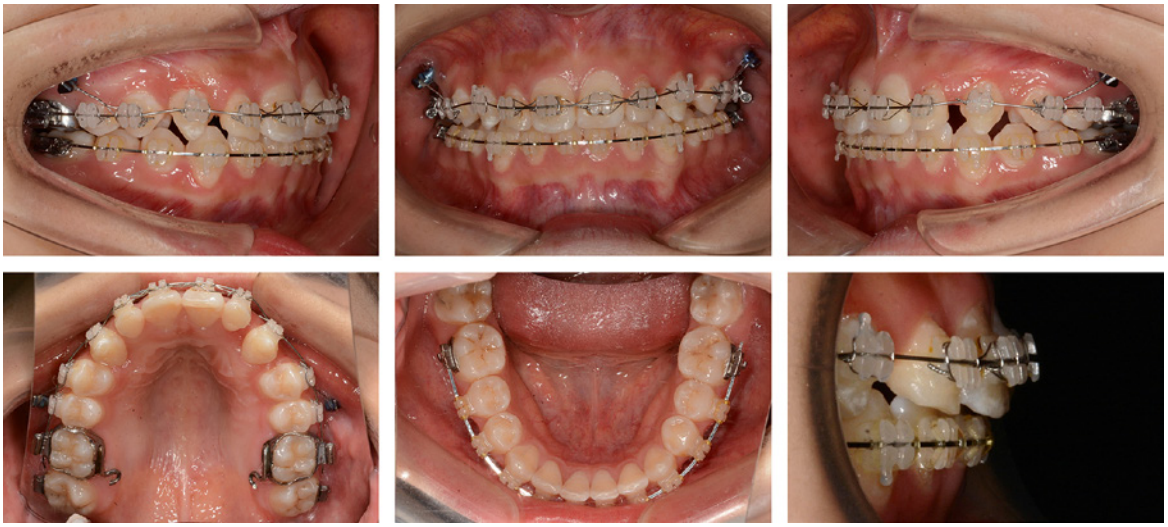


Figure 5.129 After the canines were tractioned labially, the alignment was started.

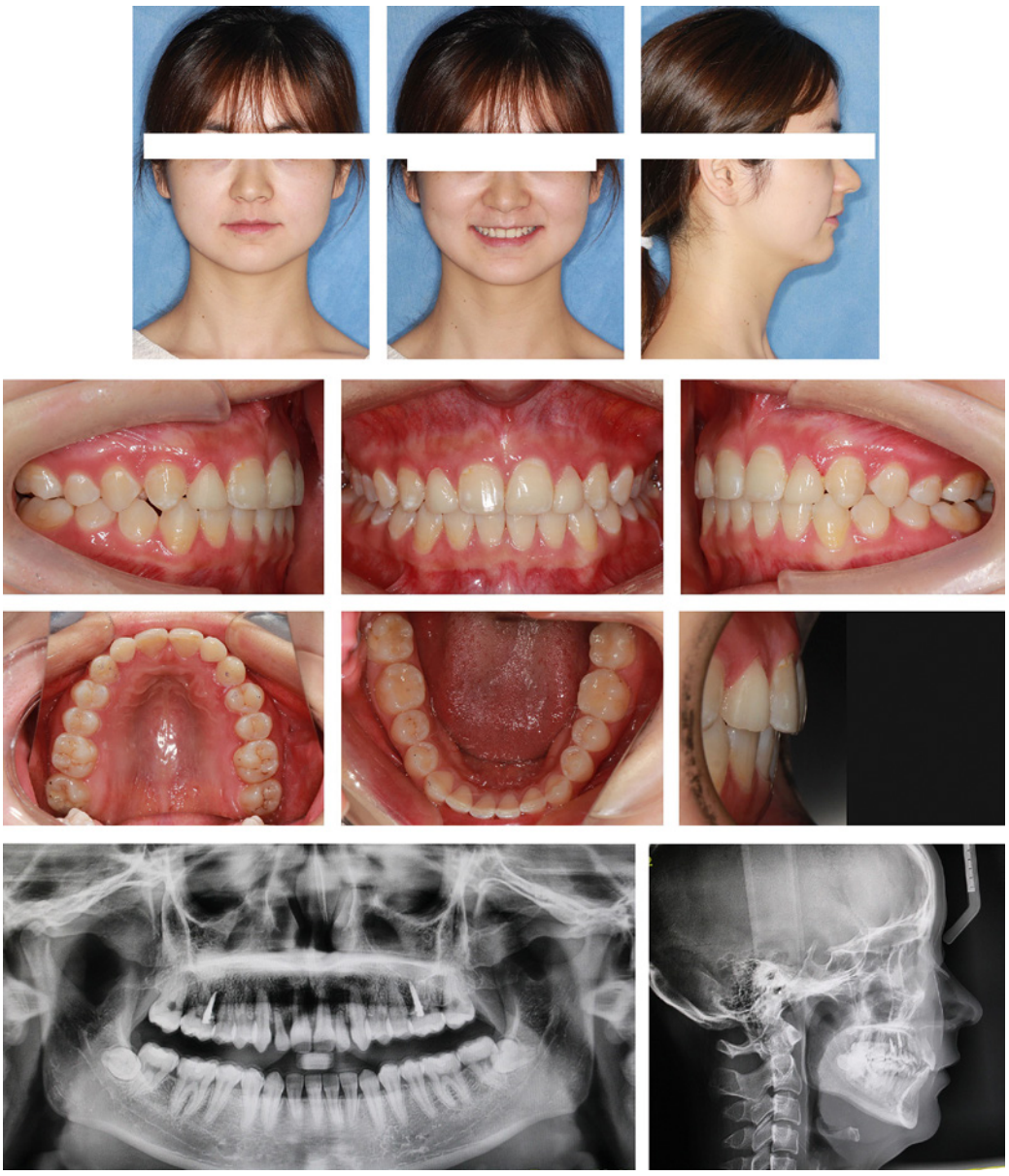


Figure 5.130 Posttreatment photographs and radiographs.

t.me/Dr_Mouayyad_AlbtousH

Table 5.14 Pre- and posttreatment lateral cephalometric analysis.

Measurement	Norm	Pretreatment	Posttreatment
Skeletal (°)			
SNA	83.0±4.0	83.1	81.8
SNB	80.0±4.0	78.6	76.6
ANB	2.0±2.0	4.5	5.2
FMA	28.0±4.0	18.4	19.7
SN-MP	35.0±4.0	30.2	32.2
Dental (°)			
U1-SN	105.7±6.3	98.4	95.5
L1-MP	97.0±7.1	91.6	98.3
FMIA	65.0±6.0	70.1	61.9
U1-L1	124.0±8.0	139.8	133.9
Soft tissue (mm)			
UL-EP	2.0±2.0	−4.2	−2.4
LL-EP	3.0±2.0	−6.6	−2.5
Wits (mm)			
Wits	−1.0	2.0	1.6

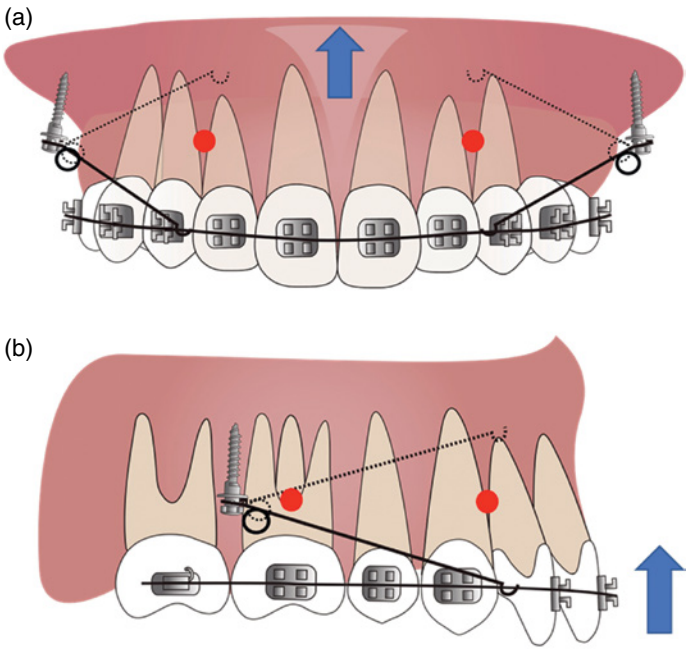


Figure 5.131 Schematic illustrations demonstrating the biomechanics of mini-implant-anchored cantilever springs for incisor intrusion. (a) The cantilever springs are fixed onto the mini-implants at the infrazygomatic crest region. The inactivated cantilever springs (dashed) are located at the vestibular sulcus and are activated (solid) by being engaged onto the archwire, so that intrusion force is generated on the anterior teeth (frontal view). (b) Buccal view.

t.me/Dr_Mouayyad_AlbtousH

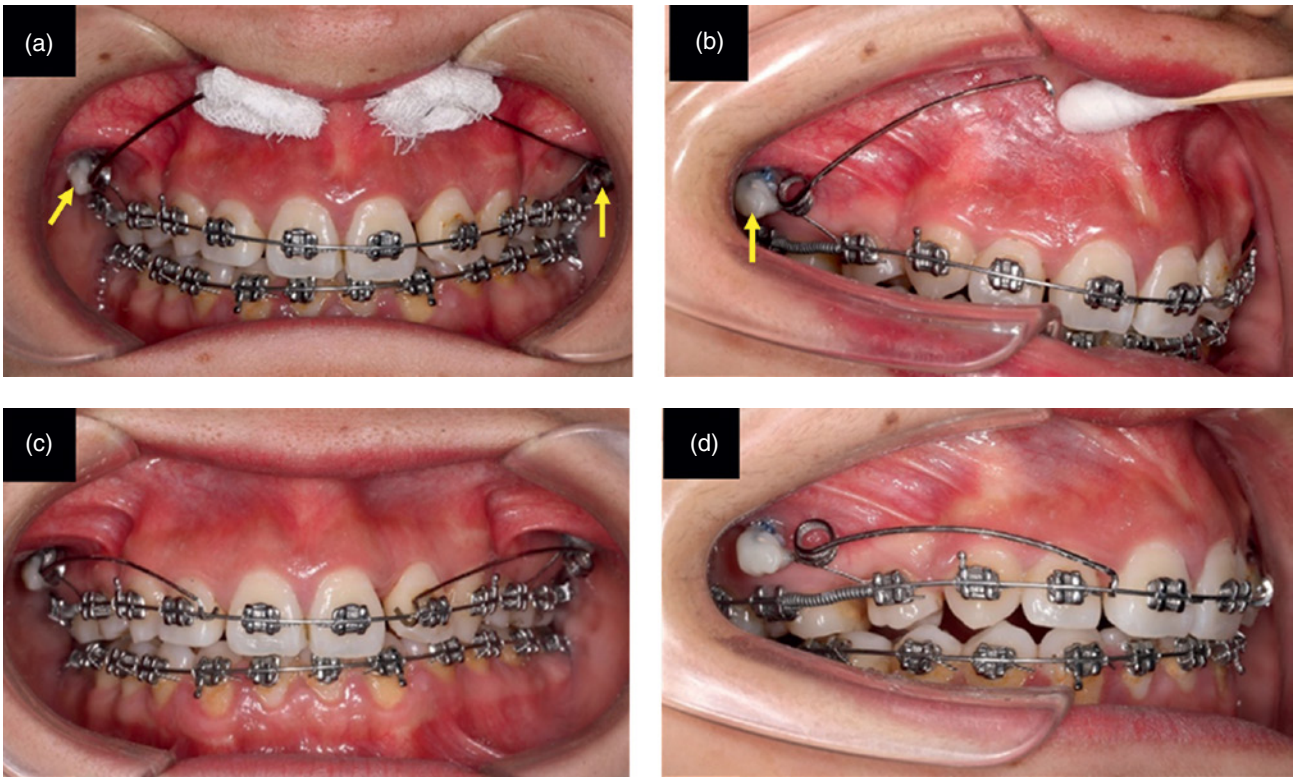


Figure 5.132 (a,b) Inactivated form of the cantilever springs. Cantilevers were fixed onto the infrazygomatic mini-implants with flowable resin (yellow arrows). (c,d) The cantilever springs were activated by being engaged onto the archwire, so that intrusion force was generated on the anterior teeth.

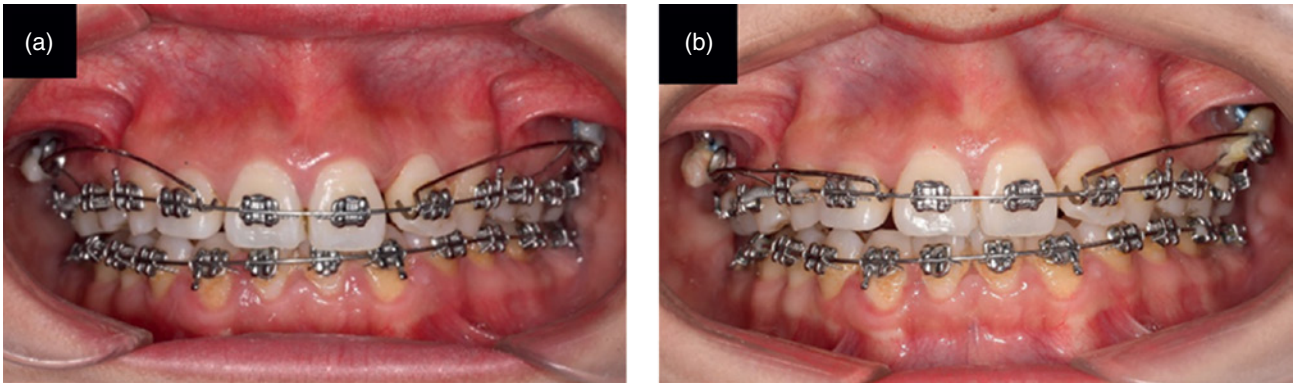


Figure 5.133 The upper incisors had been intruded successfully. (a) Before intrusion. (b) After intrusion.

t.me/Dr_Mouayyad_AlbtousH

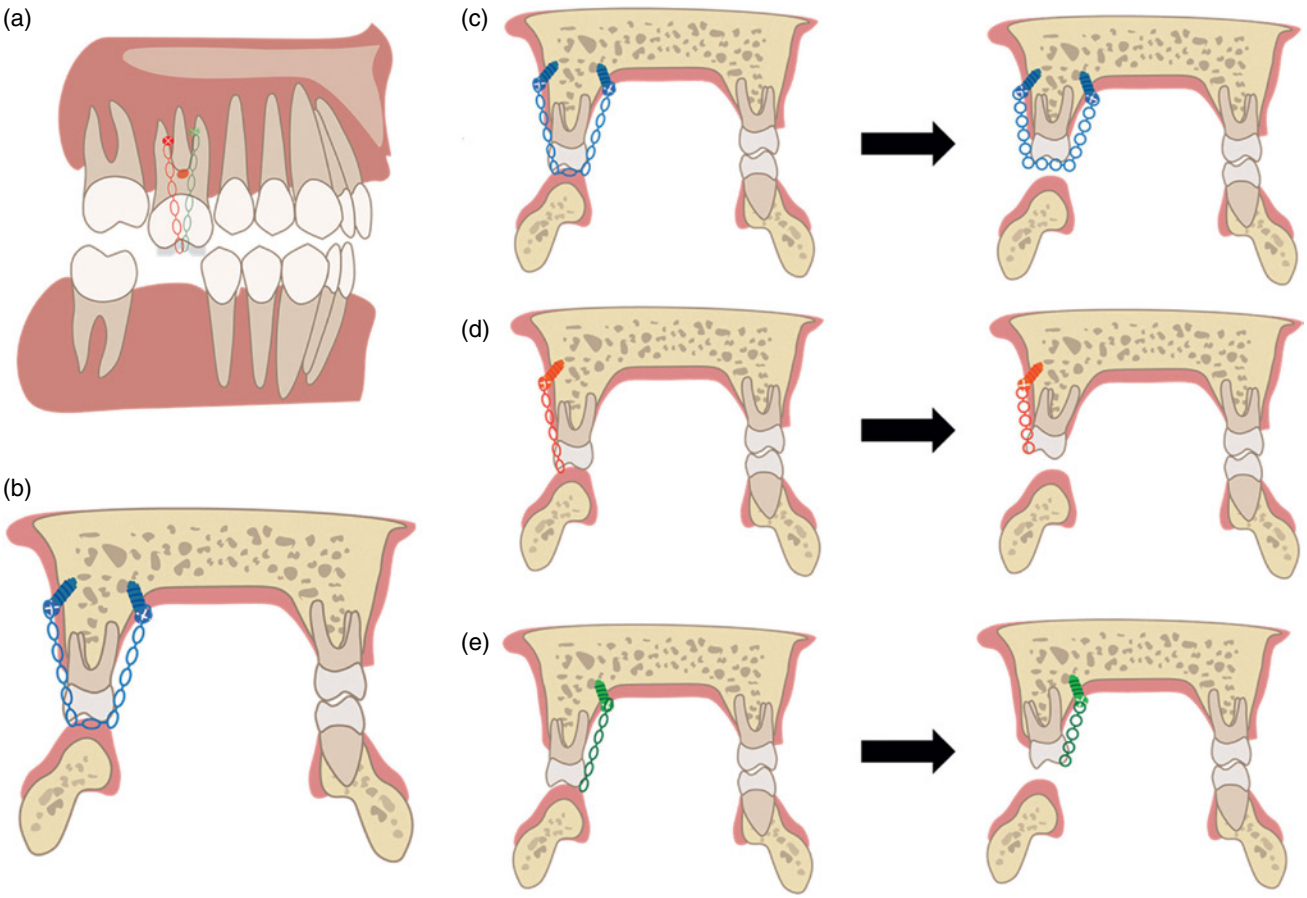


Figure 5.134 Biomechanics of molar intrusion. (a,b) Molar intrusion on both the buccal and palatal sides. (c) Bodily intrusion occurs if the intrusion force is offered on both the buccal and palatal sides. (d) The molar exhibits buccal tipping if the intrusion force is offered only on the buccal side. (e) The molar is lingually tipped if the intrusion force is offered only on the palatal side.

The treatment plan was to extract the retained primary teeth and the supernumerary tooth and to traction the impacted lateral incisor and canine. To traction the deeply impacted canine, a buccal, occlusal and distal force vector was required. Thus, an IZC mini-implant was planned and the traction would be achieved through a cantilever spring anchored onto the IZC mini-implant. The implant-anchored cantilever system offers the necessary buccal, distal and occlusal force vector (Figure 5.140).

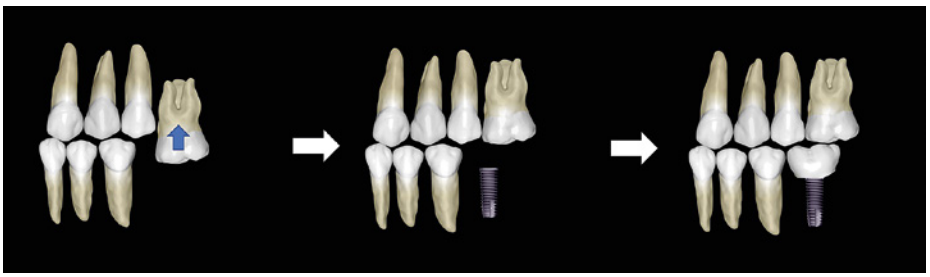
The anterior hook of the cantilever spring was located buccally, distally and occlusally to the impacted canine and delivered the required biomechanics for orthodontic traction when the cantilever spring was activated (Figure 5.141). At each appointment, the operator reactivated the cantilever spring by stretching the powerchain and moving the anterior hook to the adjacent loop that was more apical to the current one (Figure 5.142). Finally, the impacted canine was tractioned successfully and efficiently (Figure 5.143).

t.me/Dr_Mouayyad_AlbtousH



Figure 5.135 Pretreatment photographs and panoramic radiograph. Note that the maxillary left first and second molars were overerupted due to loss of the mandibular opposing teeth. The maxillary left second premolar was in the undercut region of the adjacent first molar.

Figure 5.136 Treatment planning.



t.me/Dr_Mouayyad_AlbtousH

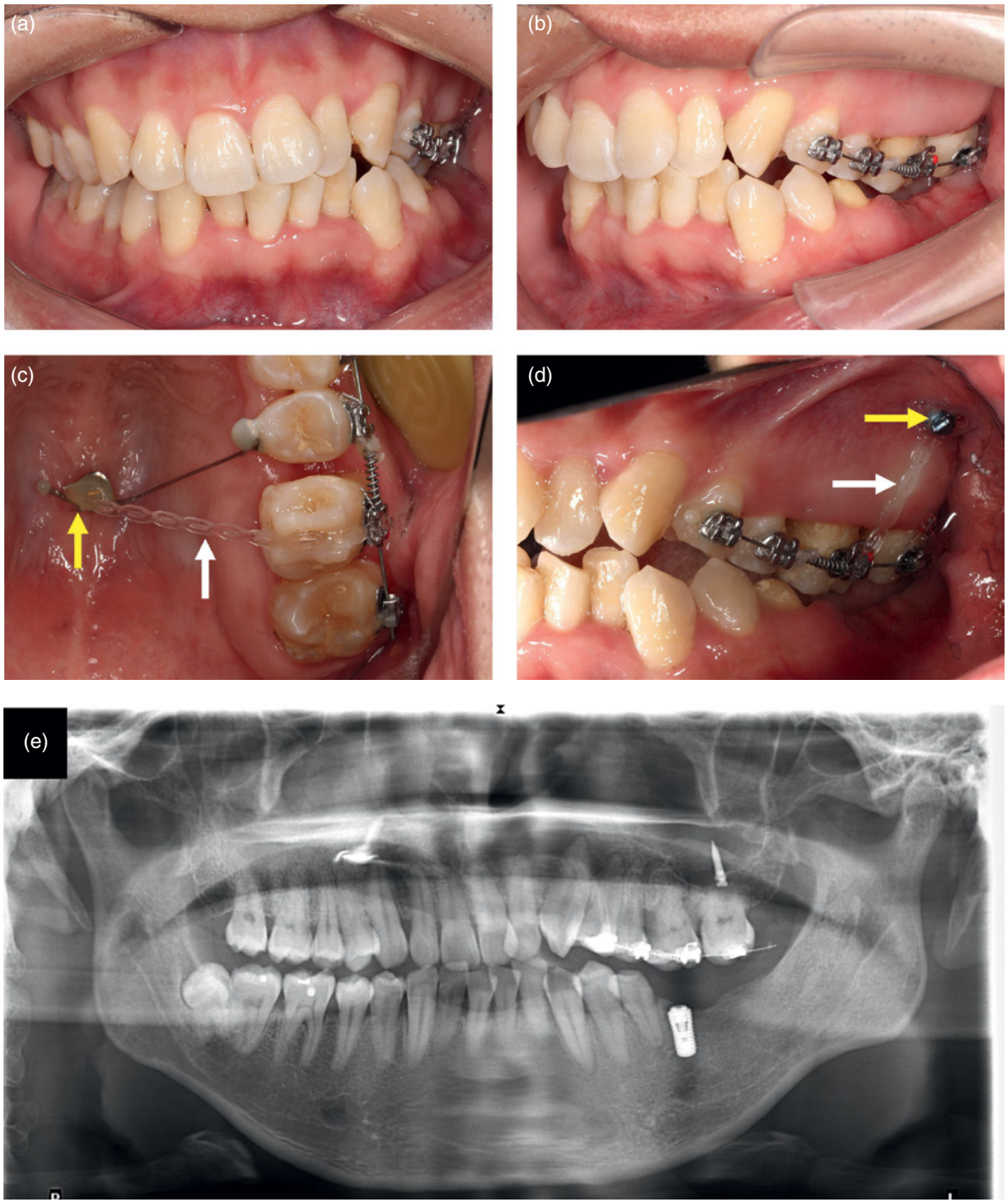


Figure 5.137 Treatment progress. (a,b) Segmental archwire technique was employed for *en masse* intrusion of the first and second molars. (c) Occlusal view. A mini-implant (yellow arrow) was inserted at the midpalatal suture region and the maxillary left second premolar was fixed and stabilised by the palatal mini-implant. An elastomeric chain was used for molar intrusion. An open-coil spring was mounted between the second premolar and first molar to prevent intrusion of the second premolar since the second premolar was in the undercut region of the first molar before treatment. (d) Buccal view. A mini-implant (yellow arrow) was inserted at the infrazygomatic crest and an elastomeric chain (white arrow) was used for molar intrusion. (e) Panoramic radiograph showing that the maxillary left molars have been partially intruded and an implant was placed in the mandible.

t.me/Dr_Mouayyad_AlbtousH

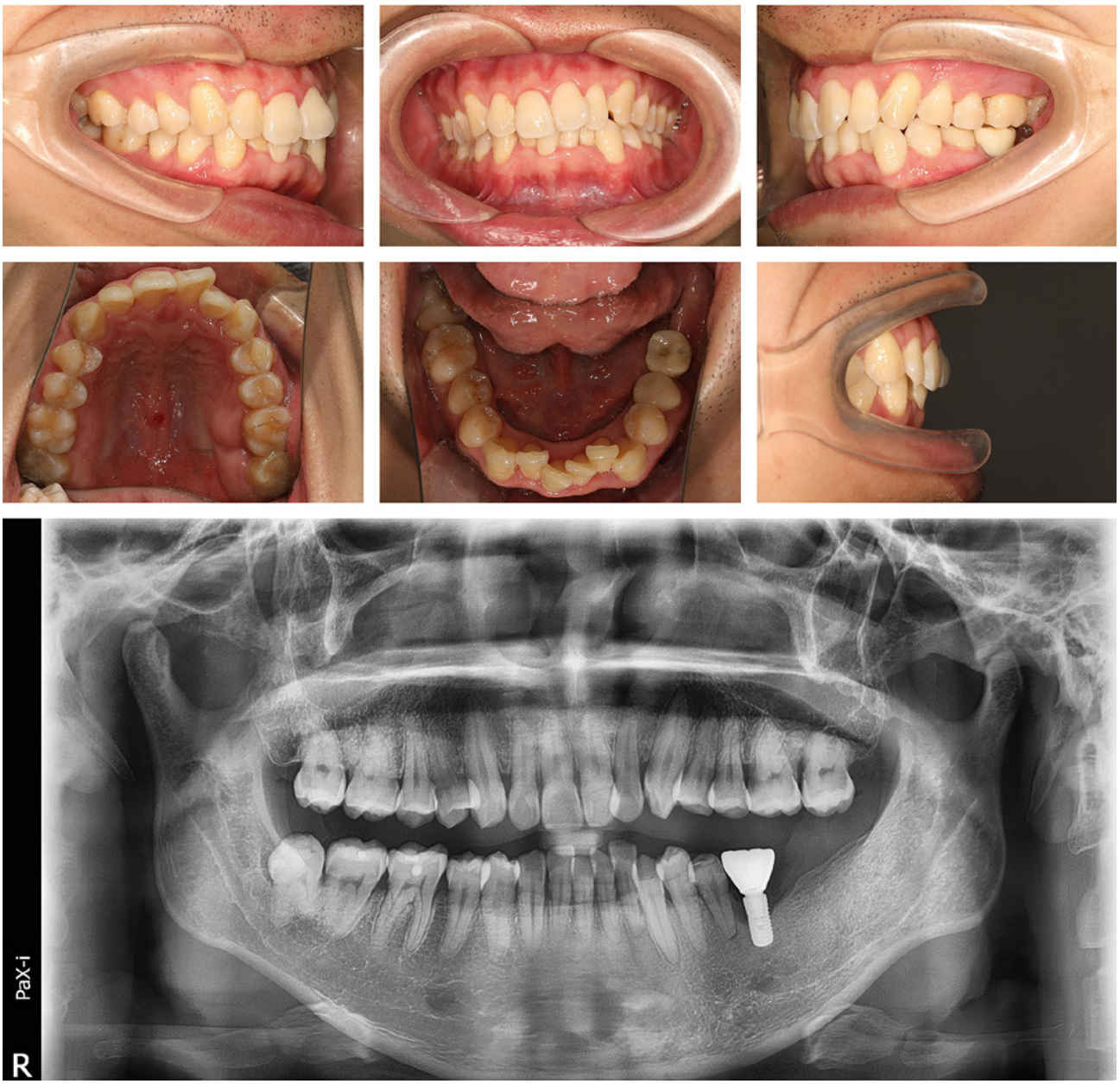


Figure 5.138 Posttreatment photographs and panoramic radiograph.

t.me/Dr_Mouayyad_AlbtousH

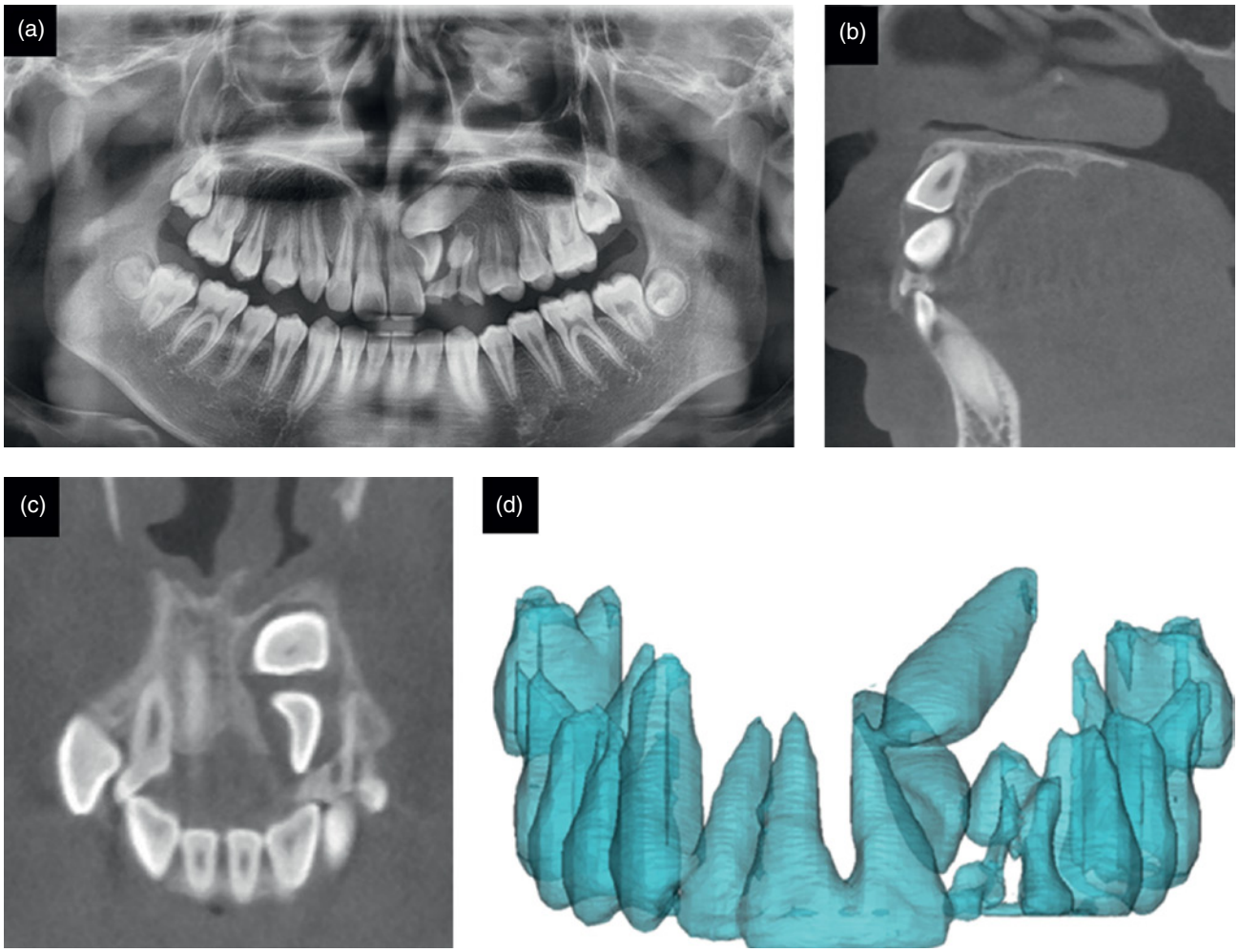


Figure 5.139 Radiographic examinations indicated the impacted lateral incisor and canine. (a) Panoramic radiograph. (b) CBCT image (sagittal view). (c) CBCT image (coronal view). (d) 3-D reconstruction image.

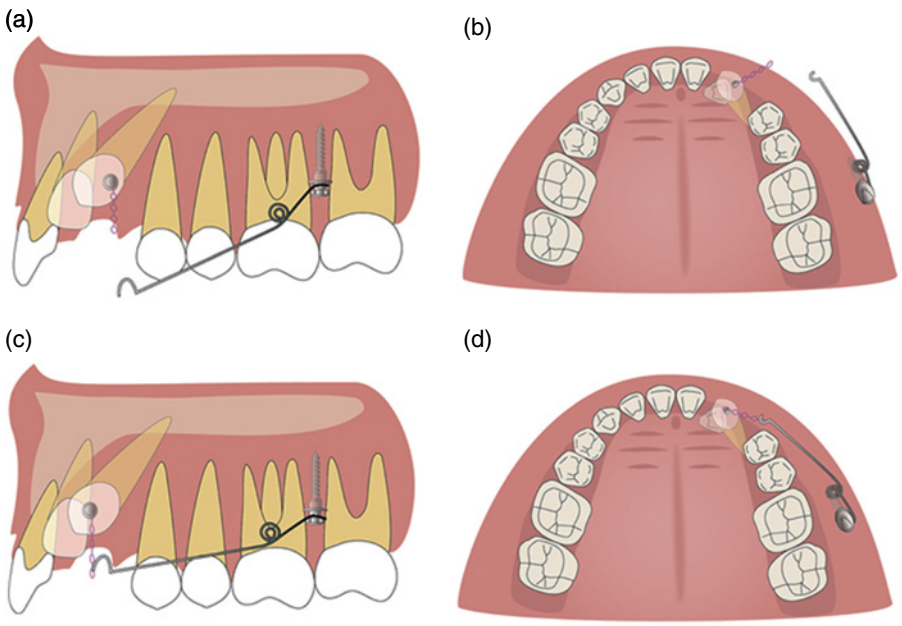


Figure 5.140 Schematic illustrations demonstrating the mini-implant-anchored cantilever spring. (a,b) Inactivated form. (c,d) Activated form.

t.me/Dr_Mouayyad_AlbtousH

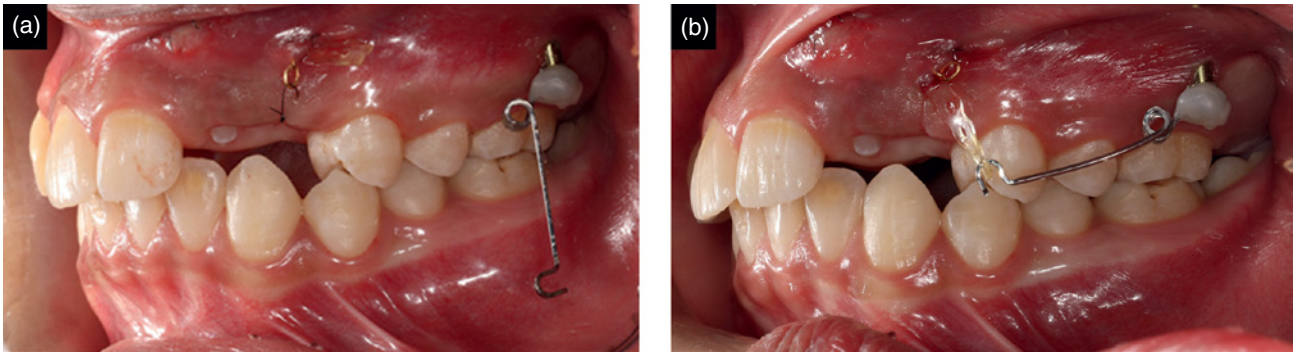


Figure 5.141 A mini-implant was inserted at the left infrazygomatic crest region and a cantilever spring was fixed onto the mini-implant. (a) Inactivated form. (b) Activated form.



Figure 5.142 Traction of the impacted lateral incisor and canine progressed smoothly. (a) Before traction. (b) During traction. (c) After traction.

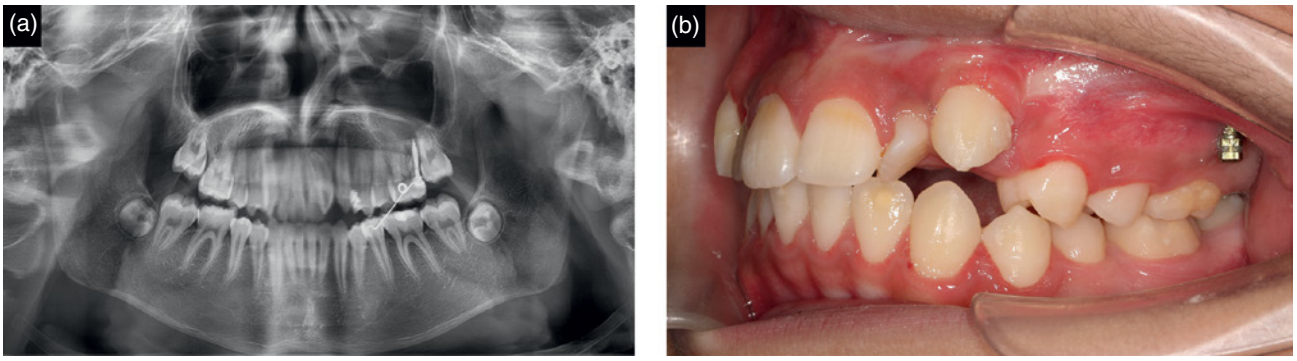


Figure 5.143 The impacted lateral incisor and canine were tractioned efficiently and successfully. (a) Panoramic radiograph. (b) Intraoral photograph.

5.4 Maxillary Tuberosity

5.4.1 Anatomical Characteristics

The maxillary tuberosity is a rounded bony eminence at the most posterior part of the maxilla (Figure 5.144). It is bounded by the most posterior maxillary molar mesially and the maxillary sinus superiorly (Figure 5.145a). It articulates with the pyramidal process of the palatine bone posteriorly (Figure 5.145b).[53,54] The maxillary tuberosity grows from six to 20 years of age and its growth accounts for 36% of the increase in maxillary length.[55] The maxillary tuberosity becomes prominent after the eruption of the maxillary third molar. However, the availability of bone at this region is influenced by the presence of maxillary third molars. Bone quantity is significantly smaller among patients with

t.me/Dr_Mouayyad_AlbtousH

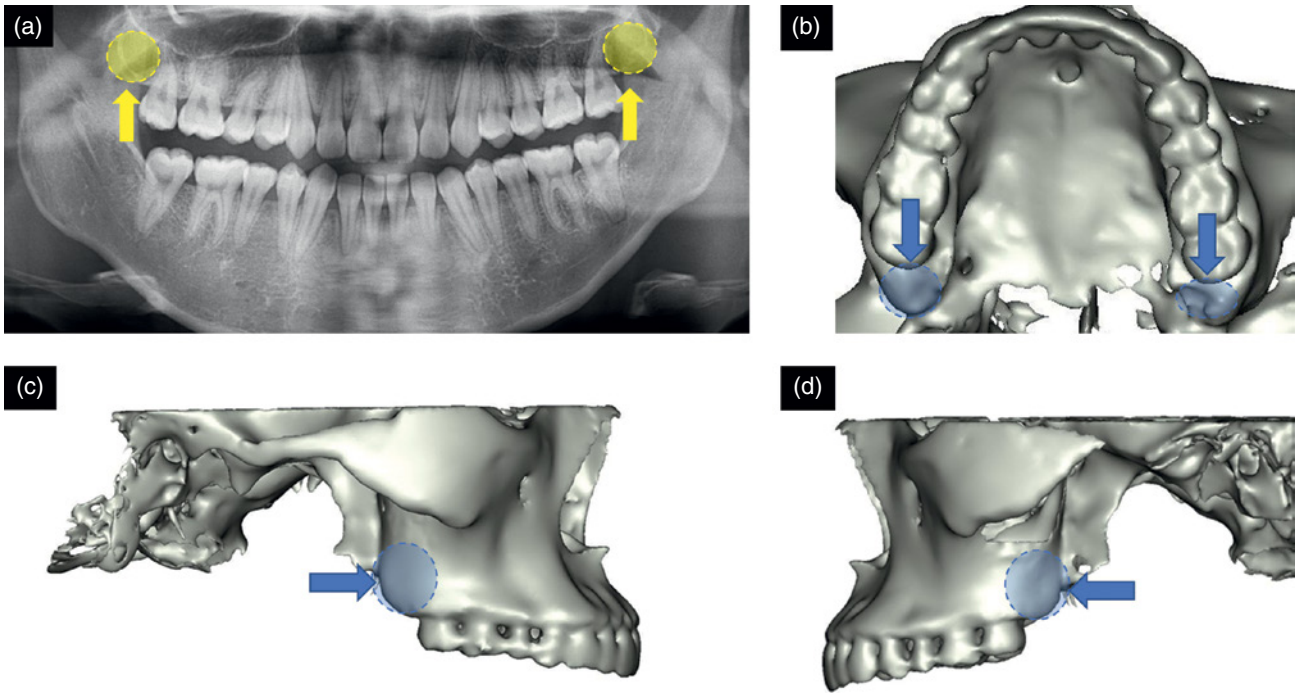


Figure 5.144 Maxillary tuberosity. (a) Panoramic radiograph. The tuberosity regions (yellow areas) are indicated by yellow arrows. (b) 3-D reconstructed image (occlusal view). The tuberosity regions (blue areas) are indicated by the blue arrows. (c) 3-D reconstructed image (right-side view). The tuberosity region (blue area) is indicated by the blue arrow. (d) 3-D reconstructed image (left-side view). The tuberosity region (blue area) is indicated by the blue arrow.

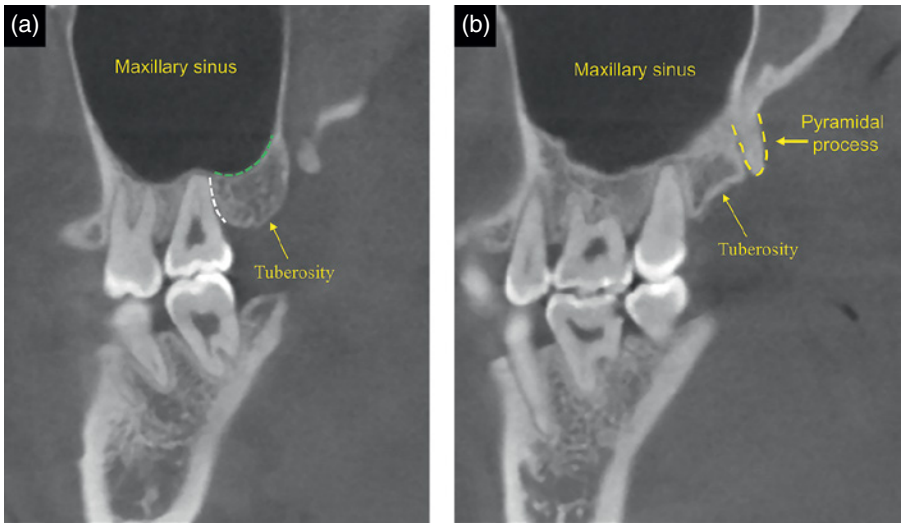


Figure 5.145 The boundaries of the maxillary tuberosity. (a) The maxillary tuberosity is bounded by the maxillary molar anteriorly and the maxillary sinus superiorly. (b) The tuberosity is bounded by the pyramidal process of the palatine bone posteriorly.

maxillary third molars than those without (Figure 5.146). Thus, among patients with maxillary third molars that preclude the insertion of mini-implants, extraction of the maxillary third molars is recommended before the placement of mini-implants at the tuberosity region (Figure 5.147).

Mini-implants inserted at the maxillary tuberosity can be applied for *en masse* distalisation of the entire maxillary dentition and molar uprighting. Unfortunately, the success rate of mini-implants at the tuberosity region is relatively lower (74%) compared to those at other anatomical sites,[56] probably due to low bone density. Therefore, to maximise the clinical success of mini-implants, both hard tissue and soft tissue anatomical factors should be thoroughly evaluated prior to the insertion.

t.me/Dr_Mouayyad_AlbtousH

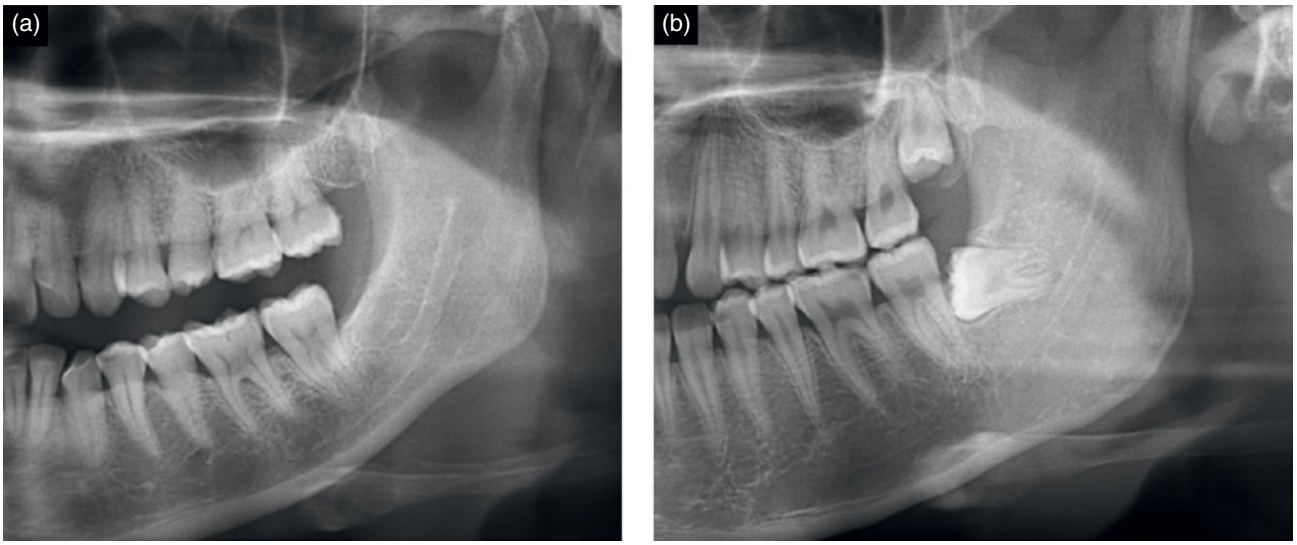


Figure 5.146 Bone quantity of the maxillary tuberosity among patients with versus without maxillary third molars. (a) The bone quantity of the left tuberosity is sufficient in a patient without the maxillary left third molar. (b) The bone quantity of the left tuberosity is limited in a patient with the maxillary left third molar.

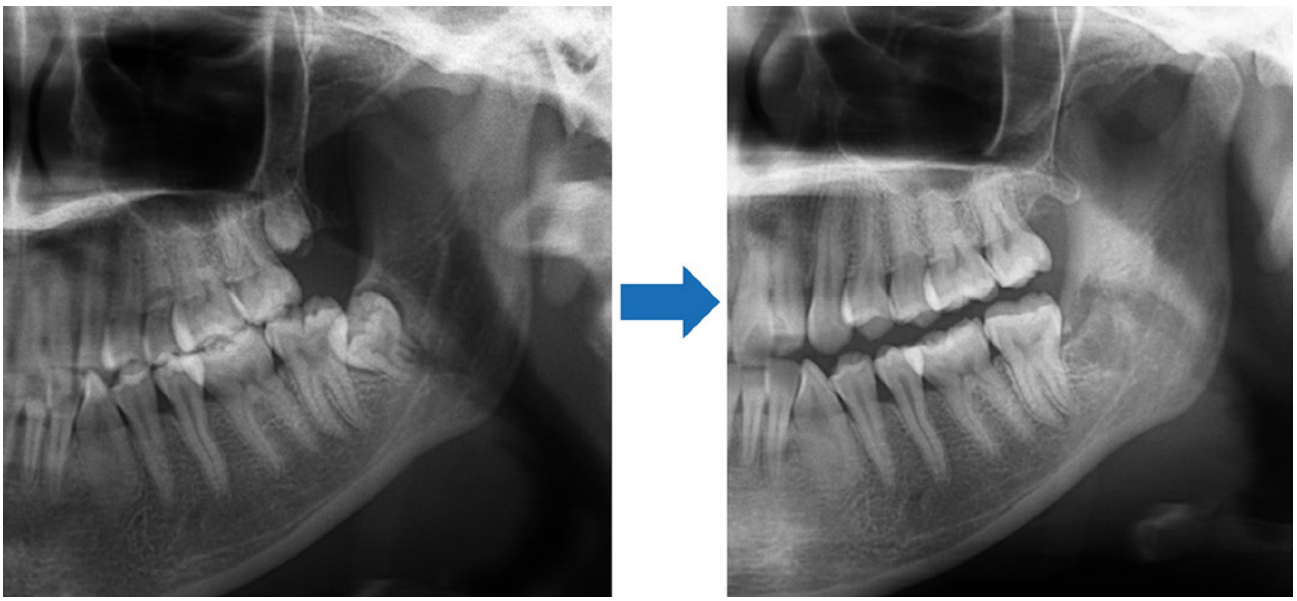


Figure 5.147 Greater bone availability at the tuberosity region was obtained following extraction of the maxillary third molar.

Hard Tissue Factor: Bone Density

Bone density is a pivotal factor in determining the primary stability of a mini-implant. It has been revealed that the density of both cortical and trabecular bones was lowest in the tuberosity region (Figures 5.148 and 5.149).[57] Specifically, the density of trabecular bone is 150 HU at the maxillary tuberosity, compared to 500 HU at the labial interradicular region. Moreover, cortical bone density in the tuberosity region is only half of that in the buccal interradicular region. According to the Misch classification, the bone in the maxillary tuberosity is considered to be type 4 and the primary stability of mini-implants at this region may not be satisfactory. Thus, given that the bone density varies greatly among different subjects, the suitability of inserting a mini-implant at the tuberosity region should be carefully evaluated according to radiographic examinations on a case-by-case basis. Moreover, mini-implants with large diameters (2 mm) are recommended to ensure adequate primary stability.

t.me/Dr_Mouayyad_AlbtousH

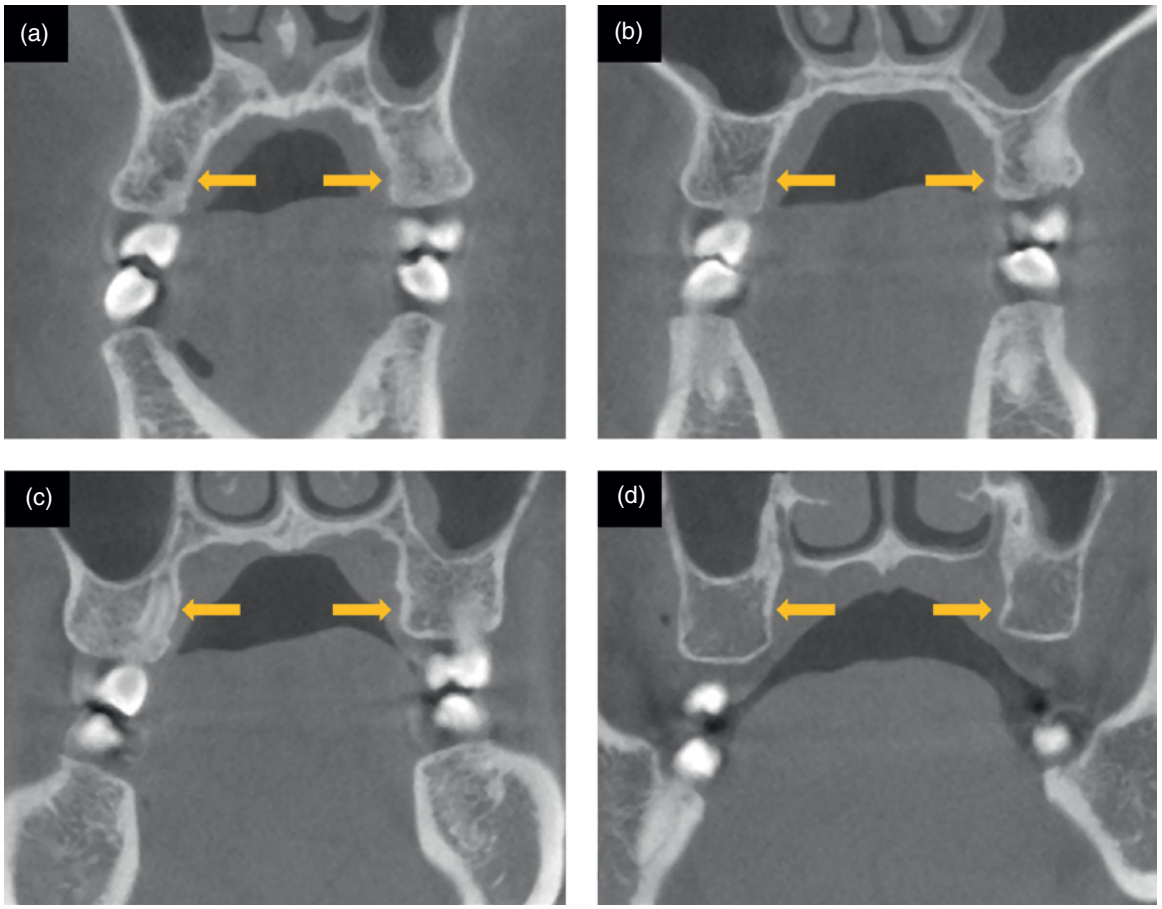


Figure 5.148 Alveolar bone density at different anteroposterior sites of the maxilla. (a) Second premolar region. (b) First molar region. (c) Second molar region. (d) Tuberosity region. Note that the bone density is lowest at the tuberosity region.

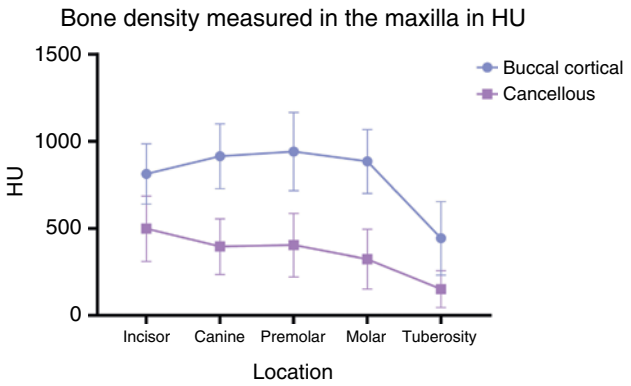


Figure 5.149 The differences in bone density at different anteroposterior sites of the maxilla in HU. *Source:* Adapted from Park et al. [57].

Hard Tissue Factor: Cortical Thickness

Cortical thickness is an essential factor that governs primary stability and ensures a satisfactory microenvironment for the development of secondary stability. It has been shown that buccal cortical thickness at the tuberosity region is not influenced by either age or gender, indicating that cortical thickness of the maxillary tuberosity is relatively stable. Notably, buccal cortical thickness is relatively thin at the incisor region, becomes thicker at the canine region (due to the canine prominence) and decreases slightly in the premolar region, becomes thicker in the molar region, and finally decreases in the tuberosity region (Figure 5.150).[58] Although the average cortical thickness at the tuberosity region was above 1 mm,[58] individual variations should be taken into consideration and the suitability of placing mini-implants at this region should be determined individually.

Hard Tissue Factor: Bone Dimension

At the maxillary tuberosity region, bone dimension consists of three indices: bone width, bone depth and bone length (Figure 5.151). As mini-implants are often inserted perpendicularly to the occlusal plane at the tuberosity region, bone width refers to the vestibulolingual distance measured on the axial plane. Bone depth is defined as the distance from the alveolar crest to the most apical point of the basal bone.

t.me/Dr_Mouayyad_AlbtousH

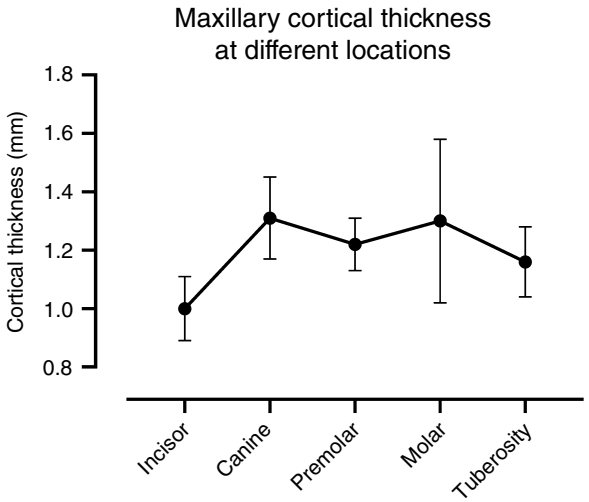
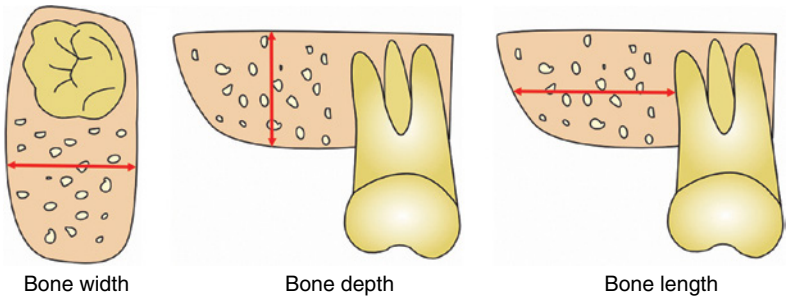


Figure 5.150 The differences in maxillary cortical thickness at different anteroposterior locations. *Source:* Adapted from Sathapana et al. [58].

Bone length is defined as the mesiodistal distance from the most distal point of the upper second molar to the distal limit of the maxillary tuberosity on the sagittal plane.

As displayed in Figure 5.152, although bone width gradually decreases as it approaches distally,[54] bone width at the tuberosity region is adequate for the insertion of mini-implants. In addition, since the mean value of bone depth ranges from 10 to 12 mm, the tuberosity region exhibits sufficient bone depth for the insertion of mini-implants (Figure 5.153). Notably, as shown in Figure 5.154, bone depth becomes smaller as it approaches posteriorly and this change should be borne in mind by operators. Bone length becomes greater at more apical levels, with the mean values being 9 mm and 11 mm at the 3 mm and 9 mm levels respectively.[54] This indicates that bone length is also adequate for the placement of mini-implants at the maxillary tuberosity region.

Figure 5.151 Illustration of bone width, bone depth and bone length of the maxillary tuberosity.



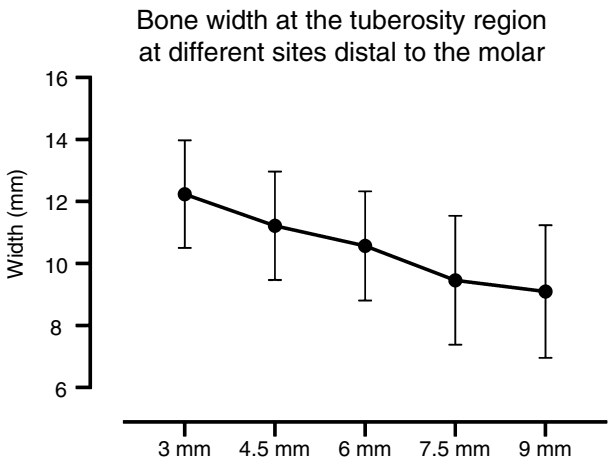


Figure 5.152 Bone width of the tuberosity at different sites distal to the molar. *Source:* Adapted from Manzanera et al. [54].

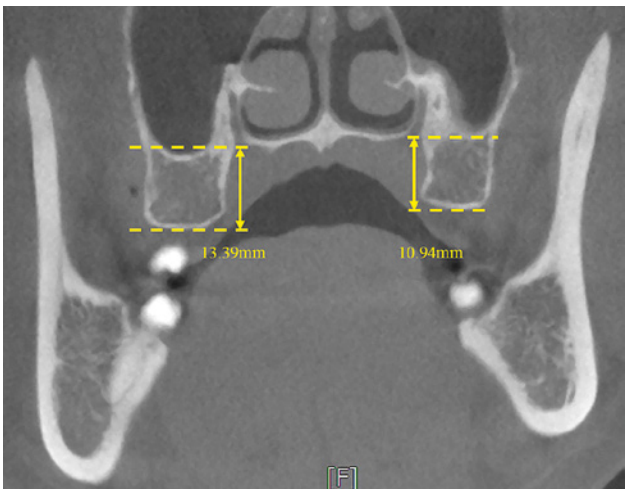


Figure 5.153 CBCT image (coronal view) demonstrating adequate bone depth for the insertion of mini-implants at the maxillary tuberosity region.

t.me/Dr_Mouayyad_AlbtousH

Soft Tissue Factor: Types of Soft Tissue

The soft tissue covering the maxillary tuberosity region is mainly composed of attached and keratinised tissue that is more resistant to mechanical irritation than movable mucosa (Figure 5.155). Thus, due to the presence of attached mucosa, the risk of soft tissue complications associated with mini-implants is low. However, overinsertion of mini-implants should be avoided, as soft tissue complications may still occur.

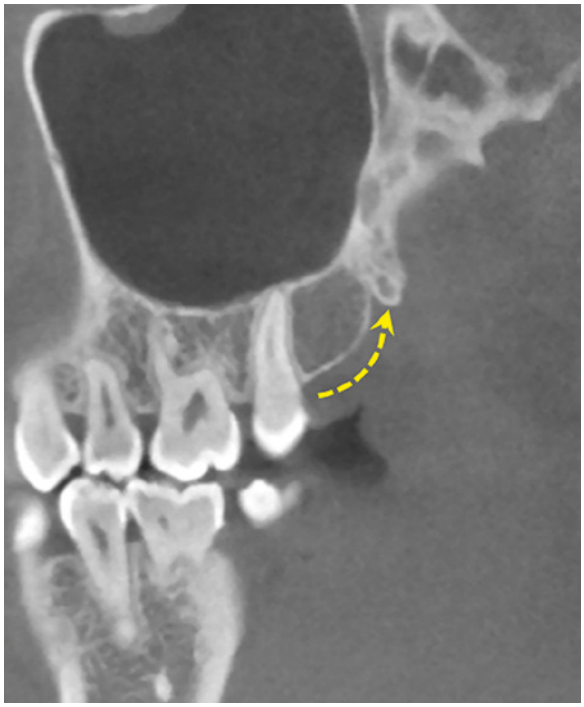


Figure 5.154 CBCT image (sagittal view) demonstrating that the bone depth becomes smaller as it approaches posteriorly.

Soft Tissue Factor: Soft Tissue Thickness

Soft tissue thickness is an important anatomical factor for mini-implants since it determines the selection of appropriate implant length. It has been shown that soft tissue thickness differs among different sites of the maxillary tuberosity region.[59] Specifically, the soft tissue thickness ranges from 1.6 mm to 2 mm at the buccal aspect, 2.5 mm to 4 mm at the occlusal side, and 2 mm to 3.5 mm on the palatal side.[59] Thus, based on soft tissue thickness, 10 mm or 12 mm mini-implants are recommended for the tuberosity region.

5.4.2 Biomechanical Considerations

Mini-implants inserted at the maxillary tuberosity region are often utilised for maxillary molar uprighting. As illustrated in Figure 5.156, the uprighting force offered by the mini-implant generates a distal force vector and a clockwise moment that helps to upright the mesially tipped molar.

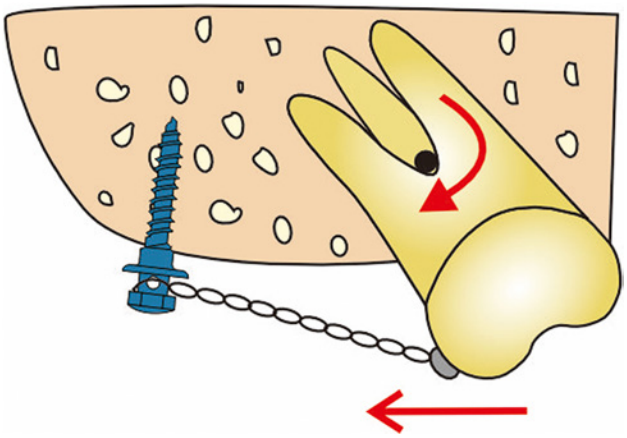


Figure 5.156 The mini-implant inserted at the maxillary tuberosity provides a distal force that is occlusal to the centre of resistance of the molar. Thus, a clockwise moment is generated.



Figure 5.155 The maxillary tuberosity is primarily covered by attached and keratinised mucosa. (a) Occlusal view. (b) Lingual view. (c) Buccal view.

t.me/Dr_Mouayyad_AlbtousH

5.4.3 Selection of Appropriate Insertion Sites

The optimal insertion sites for the maxillary tuberosity should be meticulously determined in all three dimensions. Buccolingually, the optimal entry point could be at the crestal ridge, the buccal side or the palatal side, depending on biomechanical demands. In the mesiodistal dimension, the optimal entry point should be determined based on both anatomical factors and biomechanical requirements. Especially for molar uprighting, mini-implants should be inserted as distally as possible so that sufficient clearance is present, otherwise the mini-implants may interfere with molar uprighting. Moreover, the positions of molar roots should be thoroughly evaluated prior to insertion, so that root contact can be prevented (Figure 5.157).

5.4.4 Insertion Techniques

Preinsertion

Before insertion, anatomical characteristics and biomechanics of the maxillary tuberosity should be thoroughly examined and properly designed. The placement of mini-implants at the maxillary tuberosity is applicable only when bone quality is satisfactory. Moreover, the mesiodistal position of the entry point should be determined based on biomechanical requirements and anatomical features. Specifically, clearance for the opposing mandibular teeth or mucosa should be evaluated carefully in order to avoid premature contact with the opposing teeth or mucosa trauma.

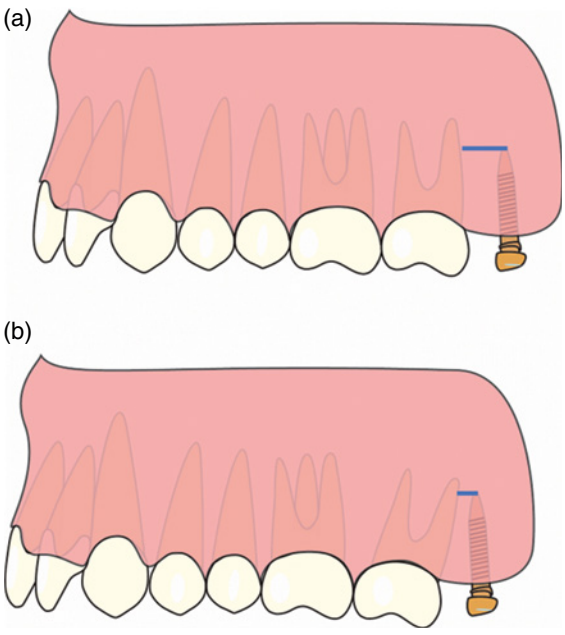


Figure 5.157 The mesiodistal inclination of the maxillary second molar should be meticulously evaluated prior to insertion of the mini-implant at the tuberosity. (a) The second molar has normal mesiodistal inclination and the risk of root contact is low. (b) The second molar exhibits mesial tipping and the root is distally positioned. The risk of root contact is high if the mini-implant is inserted too closely to the second molar.

Insertion Procedures

First, local infiltration anaesthesia is performed following mucosal disinfection with iodophor (Figure 5.158). Although the maxillary tuberosity is an extra-alveolar region, root contact may still occur if the insertion path is directed mesially. Thus, anaesthesia should not be too profound, otherwise the nociceptive sensation may not be perceived by the patient. Generally, 0.5 ml anaesthetic agent is adequate to anaesthetise the mucosa and spare the adjacent roots.

Second, the desired entry point is marked with an explorer or dental probe (Figure 5.159). Then, the marked

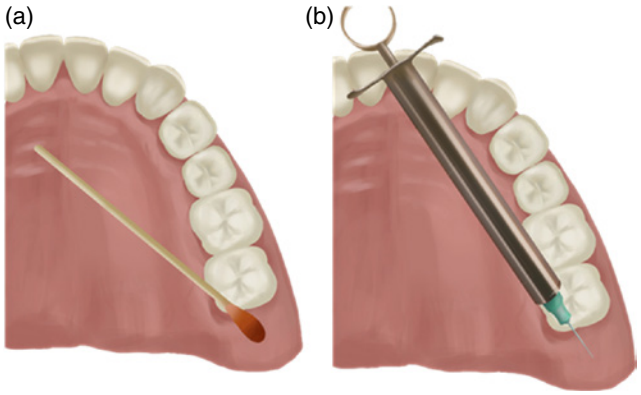


Figure 5.158 (a) Mucosa disinfection with iodophor. (b) Local infiltration anaesthesia.

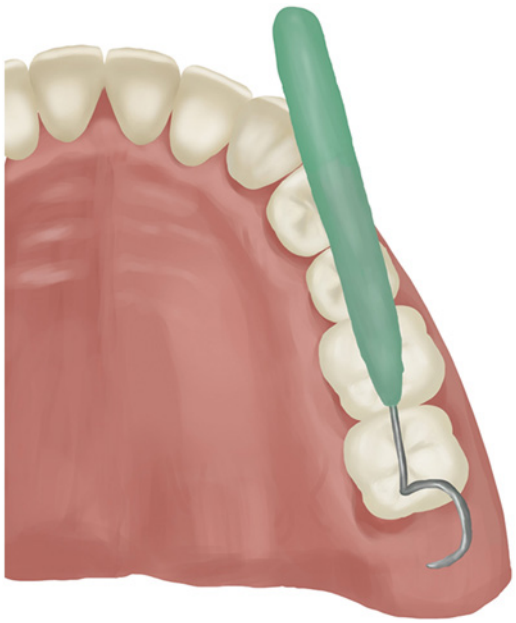


Figure 5.159 The entry point is marked with an explorer.

t.me/Dr_Mouayyad_AlbtousH

entry point should be examined and checked from the occlusal side (Figure 5.160). Specifically, the distance between the entry point and the distal surface of the molar crown should be carefully evaluated to verify that sufficient space is present to allow for molar uprighting.

Third, once the desired entry point is correctly marked, the next step is to insert the mini-implant through the marked entry point. Due to the limitation in mouth opening, a contra-angle screwdriver rather than a straight one is preferred. The insertion is often recommended to be perpendicular to the occlusal plane (Figure 5.161).

Lastly, the insertion should be stopped once an appropriate insertion depth is achieved. To guarantee that an optimal insertion depth is reached, the operator is advised not to insert the mini-implant all the way to the desired depth. We recommend the operator disengage the mini-implant and check the spatial position of the mini-implant head during insertion. If premature contact between the head and the opposing teeth or buccal mucosa impingement by the head is present, further advancement of the mini-implant is recommended. After the desired insertion depth is reached, the patient should be instructed to perform mandibular movements in all directions to rule out any premature contact with opposing teeth or soft tissue impingement. Then, the position of the mini-implant is checked from both the occlusal and buccal sides (Figure 5.162).

The clinical procedures of inserting a mini-implant at the maxillary tuberosity region are displayed in Figure 5.163.

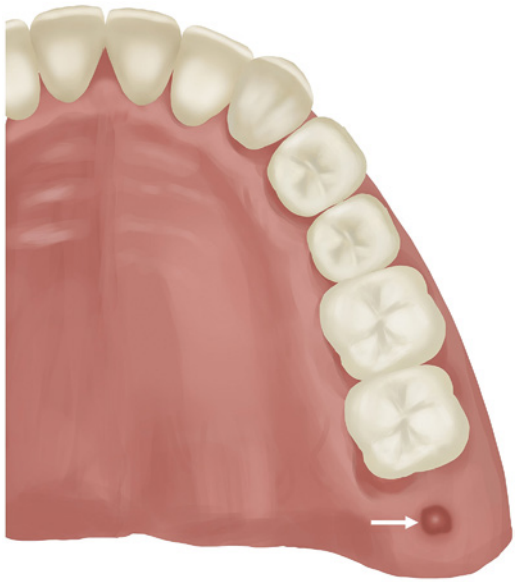


Figure 5.160 The marked entry point (white arrow) is checked from the occlusal side.

Postinsertion

Following insertion, the primary stability of the mini-implant should be checked. If the primary stability is insufficient, replacing the mini-implant with a larger one is recommended. Alternatively, reimplanting the mini-implant at other anatomical sites may be indicated.

5.4.5 Clinical Applications

Mini-implants that are inserted at the tuberosity region are often applied for maxillary molar uprighting. Since the tuberosity mini-implant is located distally to the mesially tipped molar, the distalising force offered by the mini-implant passes occlusally to the centre of resistance and a clockwise moment is generated. Thus, the molar is distalised and uprighted simultaneously (Figures 5.164 and 5.165).

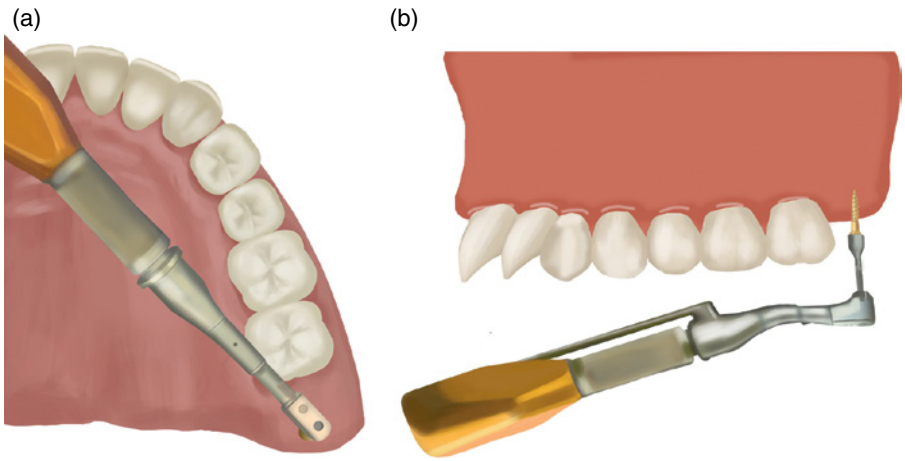


Figure 5.161 The recommended insertion path is perpendicular to the occlusal plane. A contra-angle screwdriver is recommended. (a) Occlusal view. (b) Lingual view.

t.me/Dr_Mouayyad_AlbtousH

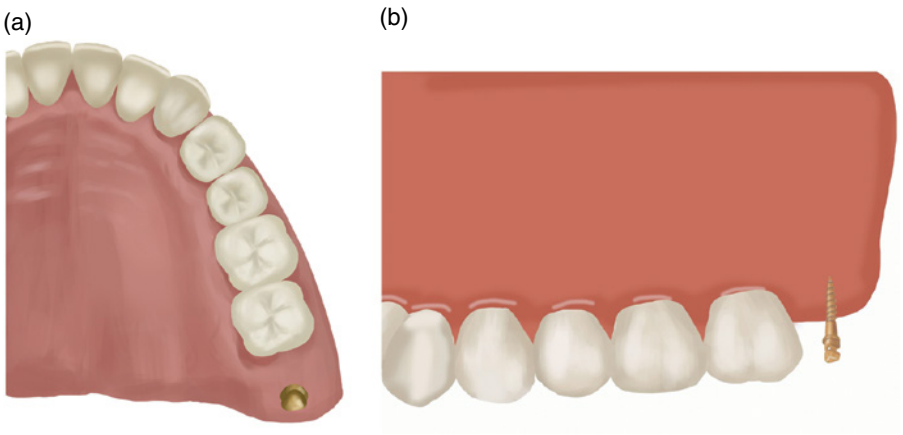


Figure 5.162 Examination of the position and orientation of the mini-implant. (a) Occlusal view. (b) Lingual view.

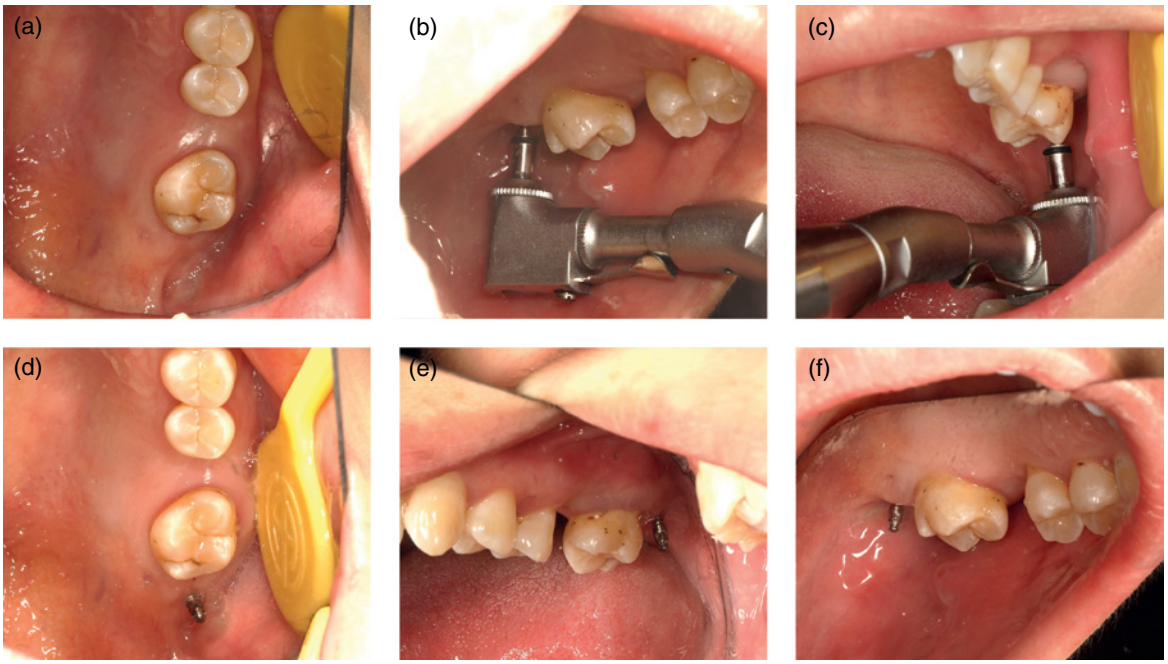


Figure 5.163 Clinical procedure for inserting a mini-implant at the maxillary tuberosity region. (a) Occlusal view of the tuberosity region. (b) Insertion of a mini-implant (lingual view). (c) Insertion of a mini-implant (frontal view). (d) Examination of the position and orientation of the mini-implant (occlusal view). (e) Examination of the position and orientation of the mini-implant (buccal view). (f) Examination of the position and orientation of the mini-implant (lingual view).

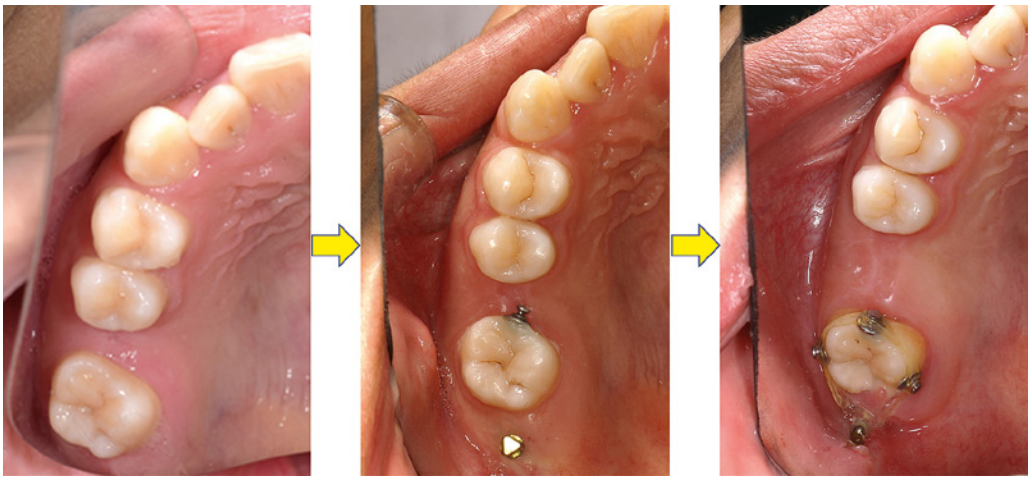


Figure 5.164 The mesially tipped maxillary second molar was uprighted efficiently by a mini-implant at the tuberosity region.

t.me/Dr_Mouayyad_AlbtousH

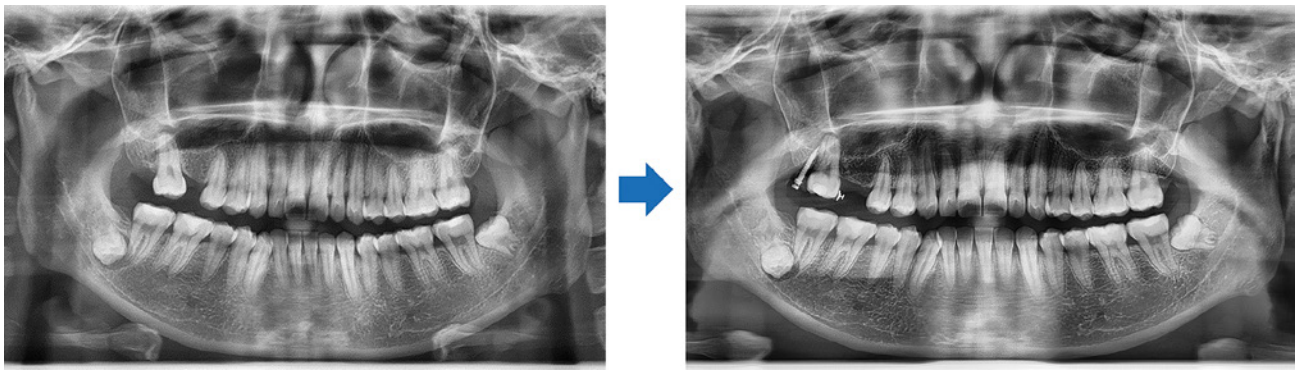


Figure 5.165 The mesially tipped maxillary second molar was successfully uprighted by a tuberosity mini-implant.

5.5 Summary

The maxillary buccal region contains three distinct anatomical regions that can be employed for the placement of mini-implants: interradicular region, IZC region and maxillary tuberosity. Mini-implants inserted at the three anatomical regions are able to accomplish a variety of both conventional and challenging orthodontic tooth movements. Different anatomical features are present at the three anatomical regions and should be meticulously examined prior to insertion. Site-specific insertion techniques should be adhered to for these three regions.

References

1 Shirck JM, Firestone AR, Beck FM, Vig KW, Huja SS. (2011). Temporary anchorage device utilization: comparison of usage in orthodontic programs and private practice. *Orthodontics* 12(3): 222–231.

2 Chugh T, Ganeshkar SV, Revankar AV, Jain AK. (2013). Quantitative assessment of interradicular bone density in the maxilla and mandible: implications in clinical orthodontics. *Prog. Orthod.* 14(1): 38.

3 Arvind Tr P, Jain RK. (2021). Computed tomography assessment of maxillary bone density for orthodontic mini-implant placement with respect to vertical growth patterns. *J. Orthod.* 48(4): 392–402.

4 Vilani GN, Ruellas AC, Mattos CT, Fernandes DJ, Elias CN. (2015). Influence of cortical thickness on the stability of mini-implants with microthreads. *Braz. Oral Res.* 29: S1806.

5 Alrbata RH, Yu W, Kyung HM. (2014). Biomechanical effectiveness of cortical bone thickness on orthodontic microimplant stability: an evaluation based on the load share between cortical and cancellous bone. *Am. J. Orthod. Dentofacial Orthop.* 146(2): 175–182.

6 Ono A, Motoyoshi M, Shimizu N. (2008). Cortical bone thickness in the buccal posterior region for orthodontic mini-implants. *Int. J. Oral Maxillofac. Surg.* 37(4): 334–340.

7 Cassetta M, Sofan AA, Altieri F, Barbato E. (2013). Evaluation of alveolar cortical bone thickness and density for orthodontic mini-implant placement. *J. Clin. Exp. Dent.* 5(5): e245–252.

8 Ozdemir F, Tozlu M, Germec-Cakan D. (2013). Cortical bone thickness of the alveolar process measured with cone-beam computed tomography in patients with different facial types. *Am. J. Orthod. Dentofacial Orthop.* 143(2): 190–196.

9 Park J, Cho HJ. (2009). Three-dimensional evaluation of interradicular spaces and cortical bone thickness for the placement and initial stability of microimplants in adults. *Am. J. Orthod. Dentofacial Orthop.* 136(3): e311–312; discussion 314–315.

10 Laursen MG, Melsen B, Cattaneo PM. (2013). An evaluation of insertion sites for mini-implants: a micro-CT study of human autopsy material. *Angle Orthod.* 83(2): 222–229.

11 Tozlu M, Germec Cakan D, Ulkur F, Ozdemir F. (2015). Maxillary buccal cortical plate inclination at mini-screw insertion sites. *Angle Orthod.* 85(5): 868–873.

12 Vibhute PJ, Patil PA. (2014). Inferior level of maxillary sinus and cortical bone thickness at maxillary posterior quadrant, in three different growth patterns: 3D-computed tomographic study. *J. Oral Implants* 2014: 870193.

13 Motoyoshi M, Sanuki-Suzuki R, Uchida Y, Saiki A, Shimizu N. (2015). Maxillary sinus perforation by orthodontic anchor screws. *J. Oral Sci.* 57(2): 95–100.

14 Lee Y, Choi SH, Yu HS, Erenebat T, Liu J, Cha JY. (2021). Stability and success rate of dual-thread miniscrews. *Angle Orthod.* 91(4): 509–514.

t.me/Dr_Mouayyad_AlbtousH

15 Chen YH, Chang HH, Chen YJ, Lee D, Chiang HH, Yao CC. (2008). Root contact during insertion of miniscrews for orthodontic anchorage increases the failure rate: an animal study. *Clin. Oral Implants Res.* 19(1): 99–106.

16 Ikenaka R, Koizumi S, Otsuka T, Yamaguchi T. (2022). Effects of root contact length on the failure rate of anchor screw. *J. Oral Sci.* 64(3): 232–235.

17 Golshah A, Salahshour M, Nikkerdar N. (2021). Interradicular distance and alveolar bone thickness for miniscrew insertion: a CBCT study of Persian adults with different sagittal skeletal patterns. *BMC Oral Health* 21(1): 534.

18 Khumsarn N, Patanaporn V, Janhom A, Jotikasthira D. (2016). Comparison of interradicular distances and cortical bone thickness in Thai patients with Class I and Class II skeletal patterns using cone-beam computed tomography. *Imaging Sci. Dent.* 46(2): 117–125.

19 Nyaga JM, Maina SW, Gathece LW, Okoth J. (2016). Root curvature in the maxillary first permanent molars in a Kenyan population. *Afr. J. Oral Health Sci.* 6(1): 12–14.

20 Jeong S-R, Yu S-K, Kim M-S, Lim S-H. (2018). Interradicular distance between the maxillary second premolar and the first molar. *Oral Biol. Res.* 42(2): 73–78.

21 Fayed MM, Pazera P, Katsaros C. (2010). Optimal sites for orthodontic mini-implant placement assessed by cone beam computed tomography. *Angle Orthod.* 80(5): 939–951.

22 Monnerat C, Restle L, Mucha JN. (2009). Tomographic mapping of mandibular interradicular spaces for placement of orthodontic mini-implants. *Am. J. Orthod. Dentofacial Orthop.* 135(4): e421–429; discussion 428–429.

23 Sawada K, Nakahara K, Matsunaga S, Abe S, Ide Y. (2013). Evaluation of cortical bone thickness and root proximity at maxillary interradicular sites for mini-implant placement. *Clin. Oral Implants Res.* 24 Suppl A100: 1–7.

24 Kalra S, Tripathi T, Rai P, Kanase A. (2014). Evaluation of orthodontic mini-implant placement: a CBCT study. *Prog. Orthod.* 15(1): 1–9.

25 Yu J-J, Kim G-T, Choi Y-S et al. (2012). Accuracy of a cone beam computed tomography-guided surgical stent for orthodontic mini-implant placement. *Angle Orthod.* 82(2): 275–283.

26 Gomes GH, Pegoraro GO, Mazzetti T, Martos J. (2020). Esthetic treatment of buccal exostoses: a case report. *Gen. Dent.* 68(6): 75–77.

27 Shamim T. (2017). Bilateral maxillary and mandibular buccal exostosis: a self reported case and a proposal to include buccal exostosis under miscellaneous disorders of revised working classification of the psychosomatic disorders pertaining to dental practice. *Korean J. Pain* 30(2): 151–152.

28 Medsinge SV, Kohad R, Budhiraja H, Singh A, Gurha S, Sharma A. (2015). Buccal exostosis: a rare entity. *J. Int. Oral Health* 7(5): 62–64.

29 Giudice AL, Rustico L, Longo M, Oteri G, Nucera R. (2021). Complications reported with the use of orthodontic miniscrews: a systematic review. *Korean J. Orthod.* 51(3): 199–216.

30 Baumgaertel S. (2014). Hard and soft tissue considerations at mini-implant insertion sites. *J. Orthod.* 41(1 suppl): s3–s7.

31 Manni A, Cozzani M, Tamborrino F, De Rinaldis S, Menini A. (2011). Factors influencing the stability of miniscrews. A retrospective study on 300 miniscrews. *Eur. J. Orthod.* 33(4): 388–395.

32 Antoszewska J, Papadopoulos MA, Park HS, Ludwig B. (2009). Five-year experience with orthodontic miniscrew implants: a retrospective investigation of factors influencing success rates. *Am. J. Orthod. Dentofacial Orthop.* 136(2): 158.e1–10; discussion 158–159.

33 Cheng SJ, Tseng IY, Lee JJ, Kok SH. (2004). A prospective study of the risk factors associated with failure of mini-implants used for orthodontic anchorage. *Int. J. Oral Maxillofac. Implants* 19(1): 100–106.

34 Ainamo J, Talari A. (1976). The increase with age of the width of attached gingiva. *J. Periodontal Res.* 11(4): 182–188.

35 Singh S, Vandana K. (2017). Assessment of width of attached gingiva in primary, mixed, and permanent dentition: Part 2. *SRM J. Res. Dent. Sci.* 8(4): 157–161.

36 Bowers GM. (1963). A study of the width of attached gingiva. *J. Periodontol.* 34(3): 201–209.

37 Tenenbaum H, Tenenbaum M. (1986). A clinical study of the width of the attached gingiva in the deciduous, transitional and permanent dentitions. *J. Clin. Periodontol.* 13(4): 270–275.

38 Bhatia G, Kumar A, Khatri M, Bansal M, Saxena S. (2015). Assessment of the width of attached gingiva using different methods in various age groups: a clinical study. *J. Indian Soc. Periodontol.* 19(2): 199–202.

39 Alkan O, Kaya Y. (2019). The thickness of posterior buccal attached gingiva at common miniscrew insertion sites in subjects with different facial types. *Am. J. Orthod. Dentofacial Orthop.* 156(6): 800–807.

40 Patini R, Coviello V, Raffaelli L et al. (2012). Subjective pain response to two anesthetic systems in dental surgery: traditional syringe vs. a computer controlled delivery system. *J. Biol. Regul. Homeost. Agents.* 26(2 Suppl): 89–97.

41 Feng L, Wang H, Lin M. (2018). Effect of painless STA on tooth extraction of elderly patients with periodontal diseases. *Exp. Ther. Med.* 15(3): 2956–2960.

42 Alqahtani ND, Alshammari R, Almoammar K, Almosa N, Almahdy A, Albarakati SF. (2019). Post-orthodontic cephalometric variations in bimaxillary protrusion cases managed by premolar extraction – a retrospective study. *Niger. J. Clin. Pract.* 22(11): 1530–1538.

t.me/Dr_Mouayyad_AlbtousH

43 Yanez-Vico RM, Iglesias-Linares A, Cadenas de Llano-Perula M, Solano-Reina A, Solano-Reina E. (2014). Management of occlusal canting with miniscrews. *Angle Orthod.* 84(4): 737–747.

44 Liou EJ, Chen PH, Wang YC, Lin JC. (2007). A computed tomographic image study on the thickness of the infrazygomatic crest of the maxilla and its clinical implications for miniscrew insertion. *Am. J. Orthod. Dentofacial Orthop.* 131(3): 352–356.

45 Lima A Jr, Domingos RG, Cunha Ribeiro AN, Rino Neto J, de Paiva JB. (2022). Safe sites for orthodontic miniscrew insertion in the infrazygomatic crest area in different facial types: a tomographic study. *Am. J. Orthod. Dentofacial Orthop.* 161(1): 3–45.

46 Song Q, Jiang F, Zhou M et al. (2022). Optimal sites and angles for the insertion of orthodontic mini-implants at infrazygomatic crest: a cone beam computed tomography (CBCT)-based study. *Am. J. Transl. Res.* 14(12): 8893–8902.

47 Matias M, Flores-Mir C, Almeida MR et al. (2021). Miniscrew insertion sites of infrazygomatic crest and mandibular buccal shelf in different vertical craniofacial patterns: a cone-beam computed tomography study. *Korean J. Orthod.* 51(6): 387–396.

48 Giudice AL, Rustico L, Longo M, Oteri G, Papadopoulos MA, Nucera R. (2021). Complications reported with the use of orthodontic miniscrews: a systematic review. *Korean J. Orthod.* 51(3): 199–216.

49 Su L, Song H, Huang X. (2022). Accuracy of two orthodontic mini-implant templates in the infrazygomatic crest zone: a prospective cohort study. *BMC Oral Health* 22(1): 252.

50 Jia X, Chen X, Huang X. (2018). Influence of orthodontic mini-implant penetration of the maxillary sinus in the infrazygomatic crest region. *Am. J. Orthod. Dentofacial Orthop.* 153(5): 656–661.

51 Chang CH, Lin JH, Roberts WE. (2022). Success of infrazygomatic crest bone screws: patient age, insertion angle, sinus penetration, and terminal insertion torque. *Am. J. Orthod. Dentofacial Orthop.* 161(6): 783–790.

52 Lee RJ, Moon W, Hong C. (2017). Effects of monocortical and bicortical mini-implant anchorage on bone-borne palatal expansion using finite element analysis. *Am. J. Orthod. Dentofacial Orthop.* 151(5): 887–897.

53 Apinhasmit W, Chompoopong S, Methathrathip D, Sangvichien S, Karuwanarint S. (2005). Clinical anatomy of the posterior maxilla pertaining to Le Fort I osteotomy in Thais. *Clin. Anat.* 18(5): 323–329.

54 Manzanera E, Llorca P, Manzanera D, Garcia-Sanz V, Sada V, Paredes-Gallardo V. (2018). Anatomical study of the maxillary tuberosity using cone beam computed tomography. *Oral Radiol.* 34(1): 56–65.

55 Vardimon AD, Shoshani K, Shpack N, Reimann S, Bourauel C, Brosh T. (2010). Incremental growth of the maxillary tuberosity from 6 to 20 years – a cross-sectional study. *Arch. Oral Biol.* 55(9): 655–662.

56 Azeem M, Haq AU, Awaisi ZH, Saleem MM, Tahir MW, Liaquat A. (2019). Failure rates of miniscrews inserted in the maxillary tuberosity. *Dental Press J. Orthod.* 24(5): 46–51.

57 Park HS, Lee YJ, Jeong SH, Kwon TG. (2008). Density of the alveolar and basal bones of the maxilla and the mandible. *Am. J. Orthod. Dentofacial Orthop.* 133(1): 30–37.

58 Sathapana S, Forrest A, Monsour P, Naser-ud-Din S. (2013). Age-related changes in maxillary and mandibular cortical bone thickness in relation to temporary anchorage device placement. *Aust. Dent. J.* 58(1): 67–74.

59 Gapski R, Satheesh K, Cobb CM. (2006). Histomorphometric analysis of bone density in the maxillary tuberosity of cadavers: a pilot study. *J. Periodontol.* 77(6): 1085–1090.

t.me/Dr_Mouayyad_AlbtousH

6

Maxillary Palatal Region

Jing Zhou[1], Xinwei Lyu[2], Hong Zhou[3,5], Jiabao Li[4,5], Wenqiang Ma[5], Heyi Tang[6], Tianjin Tao[3], Peipei Duan[3], and Hu Long[3]

[1] *Department of Pediatric Dentistry, State Key Laboratory of Oral Diseases and National Clinical Research Center for Oral Diseases, West China Hospital of Stomatology, Sichuan University, Chengdu, China*
[2] *Department of Orthodontics, Hospital of Stomatology, Sun Yat-Sen University, Guangzhou, China*
[3] *Department of Orthodontics, State Key Laboratory of Oral Diseases and National Clinical Research Center for Oral Diseases, West China Hospital of Stomatology, Sichuan University, Chengdu, China*
[4] *Department of General Dentistry, State Key Laboratory of Oral Diseases and National Clinical Research Center for Oral Diseases, West China Hospital of Stomatology, Sichuan University, Chengdu, China*
[5] *Private Practice, Chengdu, China*
[6] *Department of Head and Neck Oncology, State Key Laboratory of Oral Diseases and National Clinical Research Center for Oral Diseases, West China Hospital of Stomatology, Sichuan University, Chengdu, China*

6.1 Introduction

The maxillary palatal region, formed by the palatal process of the maxillae and the horizontal plates of the palatine bone, is commonly used for the placement of orthodontic TADs due to its good bone quality, sufficient bone quantity and low risk of root damage.[1,2] Being a vault-like anatomical area, the palatal region is mostly covered by keratinised and attached mucosa (Figure 6.1a), rendering soft tissues around mini-implants more resistant to irritation, swelling and hyperplasia. Recent evidence indicates that mini-implants placed at the palatal region display good stability in both adults and adolescents, with a success rate of 95%.[3,4] The success rate of mini-implants is higher in the palatal region than in the buccal region.[5] Moreover, the palatal region is considered to be a back-up anatomical region for secondary insertion in case of mini-implant failure in the buccal region.[6]

The palatal vault region is continuous with the palatal alveolar process of the maxillae, resulting in several anatomical sites that are available for mini-implant placement (Figure 6.1b). In the palatal region, there are three anatomical sites available for the placement of orthodontic mini-implants in clinical practice: interradicular sites, paramedian sites and midpalatal suture (Figure 6.2). Although sufficient bone with excellent soft tissue can be found at these three anatomical sites, special care should be taken to avoid potential damage to neurovascular bundles. Specifically, greater palatal neurovascular bundles exit from the bilateral greater palatine foramina, run anteriorly and anastomose with nasopalatine bundles exiting from the nasopalatine foramen (Figures 6.3 and 6.4).

Mini-implants placed in the palatal region are often applied for many orthodontic purposes, e.g. mini-implant-assisted maxillary expansion, maxillary molar distalisation, molar anchorage augmentation and traction of impacted teeth (Figure 6.5). In this chapter, we will discuss the anatomical characteristics, site selection, biomechanical considerations, detailed insertion techniques and clinical applications of palatal mini-implants.

Clinical Insertion Techniques of Orthodontic Temporary Anchorage Devices, First Edition. Edited by Hu Long, Xianglong Han, and Wenli Lai.
© 2024 John Wiley & Sons Ltd. Published 2024 by John Wiley & Sons Ltd.

t.me/Dr_Mouayyad_AlbtousH

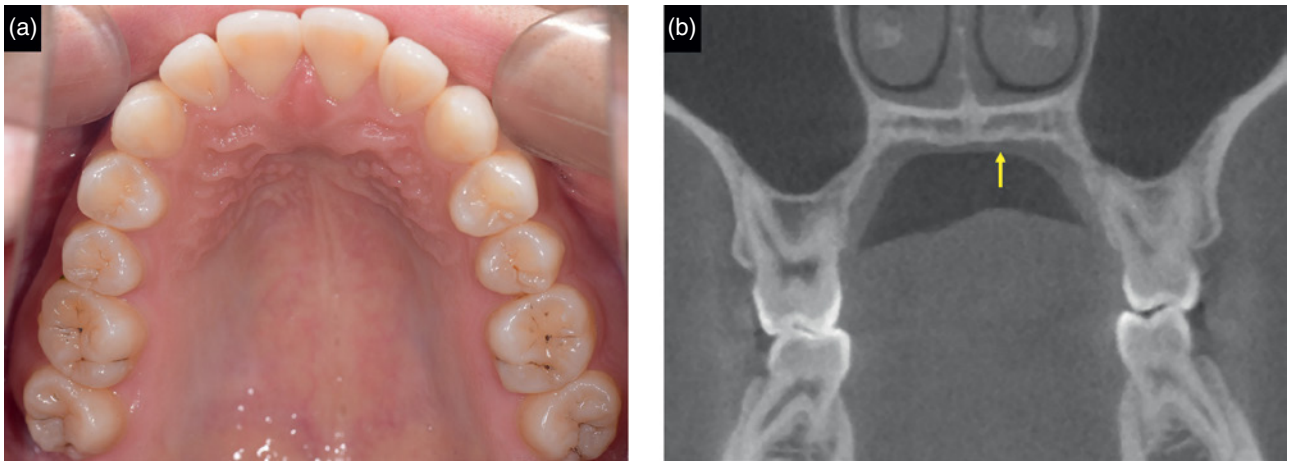


Figure 6.1 Maxillary palatal region. (a) The palatal region is mostly covered by keratinised and attached mucosa. (b) A CBCT image (coronal view) showing sufficient bone quantity and thin soft tissue (yellow arrow) at the palatal region.

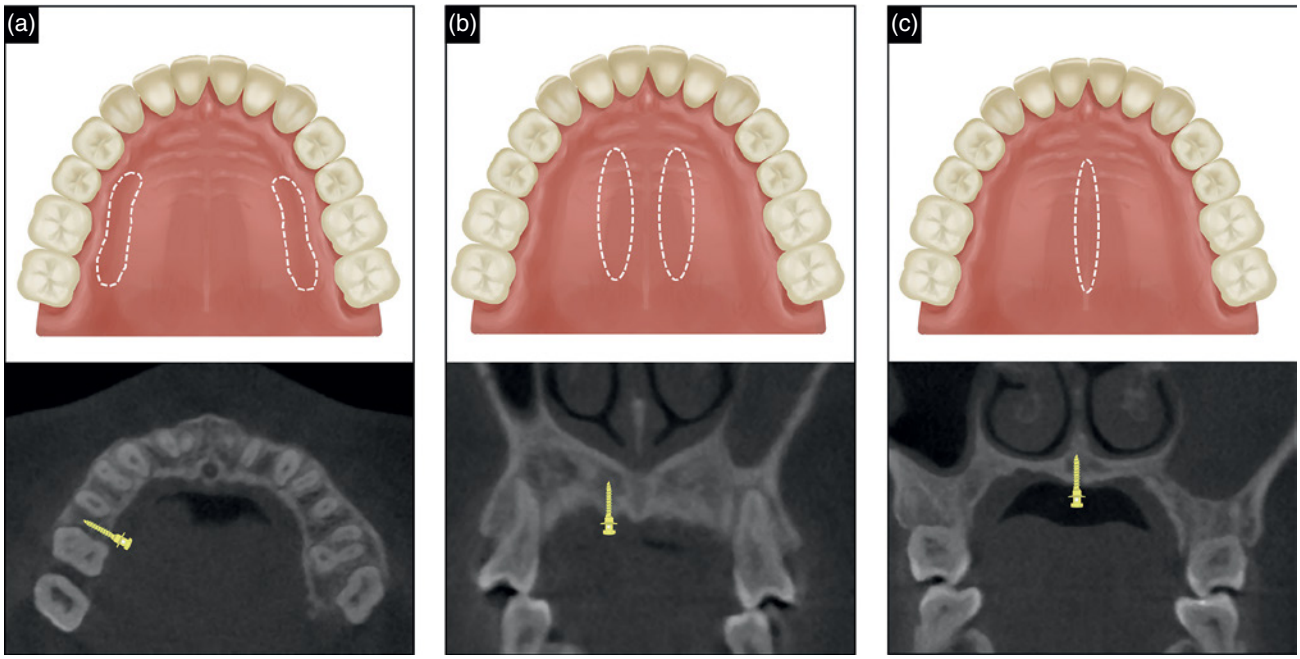


Figure 6.2 Three anatomical sites available for placement of orthodontic mini-implants in clinical practice. (a) Interradicular sites. (b) Paramedian sites. (c) Midpalatal suture.

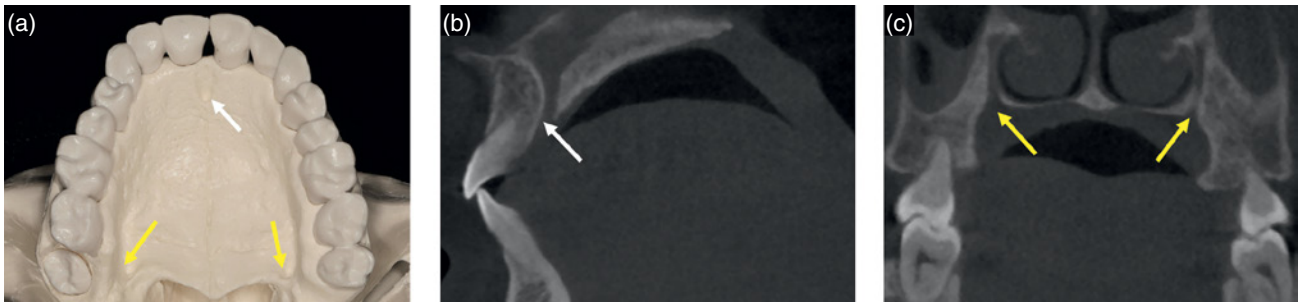


Figure 6.3 Anatomical structures accommodating neurovascular bundles at the palatal region. (a) Greater palatal foramina (yellow arrows) and nasopalatine foramen (white arrow) shown on a skull model. (b) Nasopalatine foramen (white arrow) shown on a CBCT image (sagittal view). (c) Greater palatal foramina (yellow arrows) shown on a CBCT image (coronal view).

t.me/Dr_Mouayyad_AlbtousH

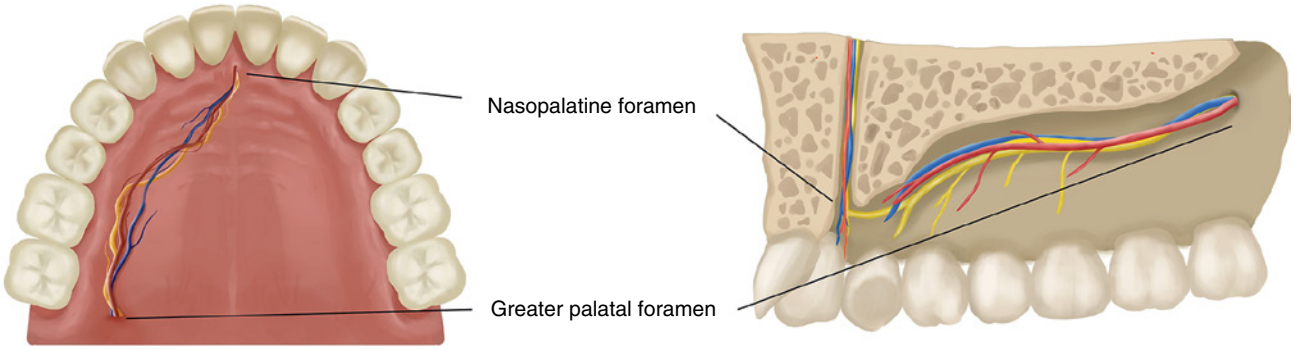


Figure 6.4 Schematic illustrations of neurovascular bundles at the palatal region. The greater palatal vascular bundles exit from the greater palatine foramen, run anteriorly at the lateral wall of the palatal vault, and anastomose with the nasopalatine bundles that exit from the nasopalatine foramen.

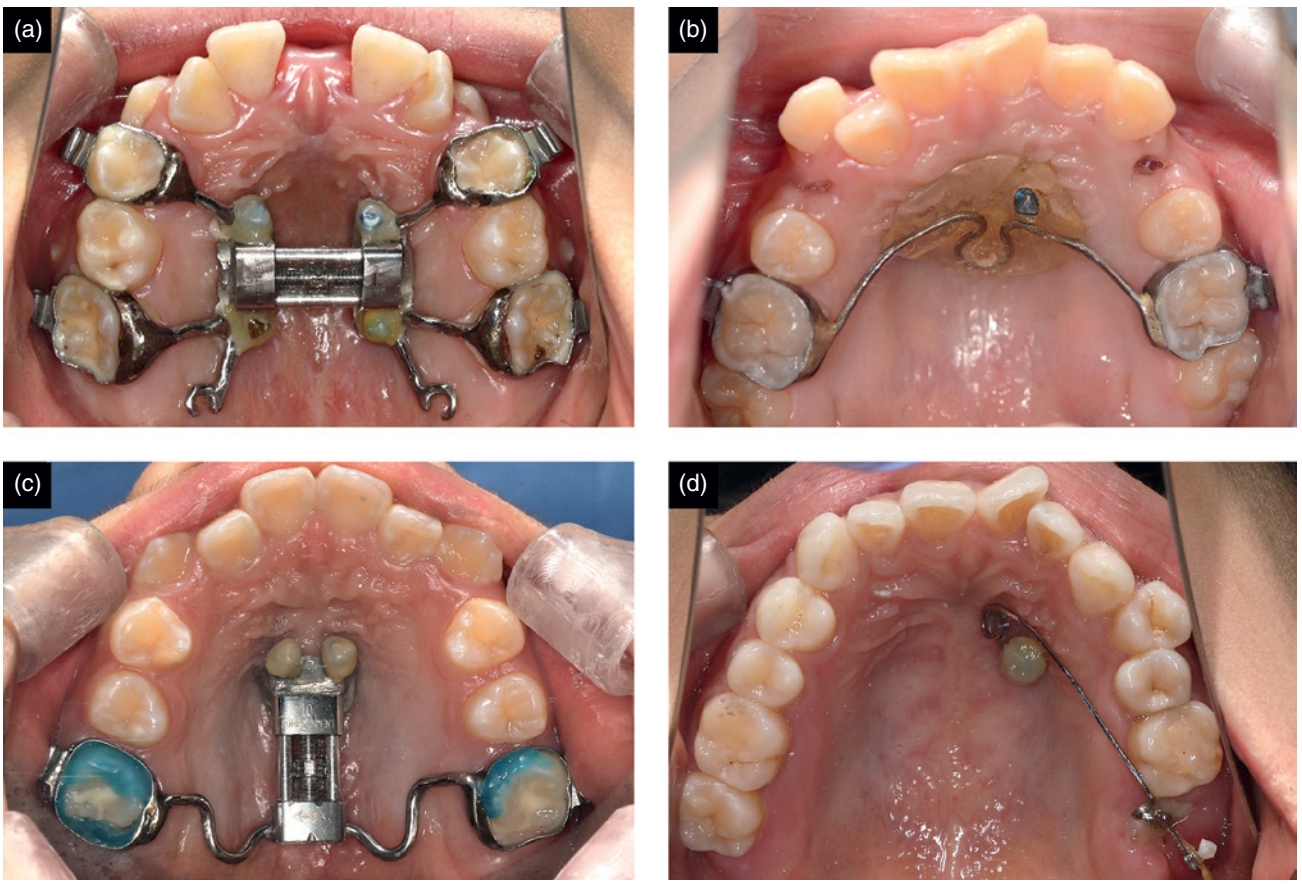


Figure 6.5 Versatile clinical applications of palatal mini-implants. (a) Maxillary skeletal expansion. (b) Molar anchorage reinforcement. (c) Molar distalisation. (d) Orthodontic traction of an impacted maxillary molar.

t.me/Dr_Mouayyad_AlbtousH

6.2 Interradicular Sites

6.2.1 Anatomical Characteristics

The palatal interradicular region is located at the interradicular sites in the palatal region, spanning from first premolars to second molars (Figures 6.6 and 6.7). Similar to buccal interradicular sites, palatal interradicular sites can be used for the placement of mini-implants. Mini-implants placed at interradicular sites in the palatal region are often employed for a variety of orthodontic purposes, e.g. anterior retraction and molar intrusion (Figure 6.8). For successful placement of mini-implants at palatal interradicular sites, hard tissue factors (i.e. cortical thickness, bone depth, bone width and inclination of cortical plate), soft tissue factors (i.e. soft tissue type and soft tissue thickness) and vital structures should be considered in order to choose the most appropriate site.

Hard Tissue Factor: Cortical Thickness

Cortical thickness is a significant contributing factor in determining the primary stability of mini-implants; the optimal thickness of the cortical plate is considered to be 1–2 mm. In general, cortical thickness is greater at the palatal side than at the buccal side.[7] The thickness of the palatal cortical plate is influenced by both gender and age factors (Figure 6.9).[7] Specifically, males possess thicker and denser palatal cortical plates than females, and palatal cortical thickness is greater among adults than adolescents.

An increase in cortical thickness is exhibited from alveolar crest to alveolar base (Figure 6.10). This indicates that

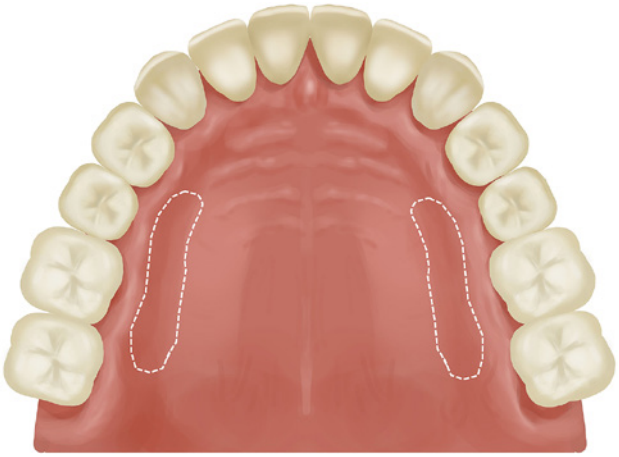


Figure 6.6 A schematic illustration of the palatal interradicular region, encircled by the dashed lines.

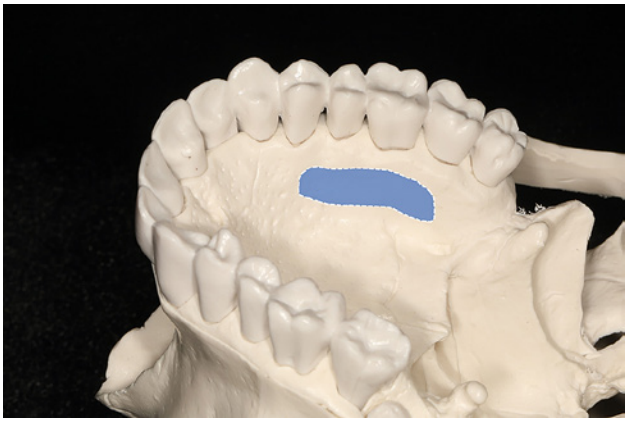


Figure 6.7 Palatal interradicular region (blue area) shown on a skull model.

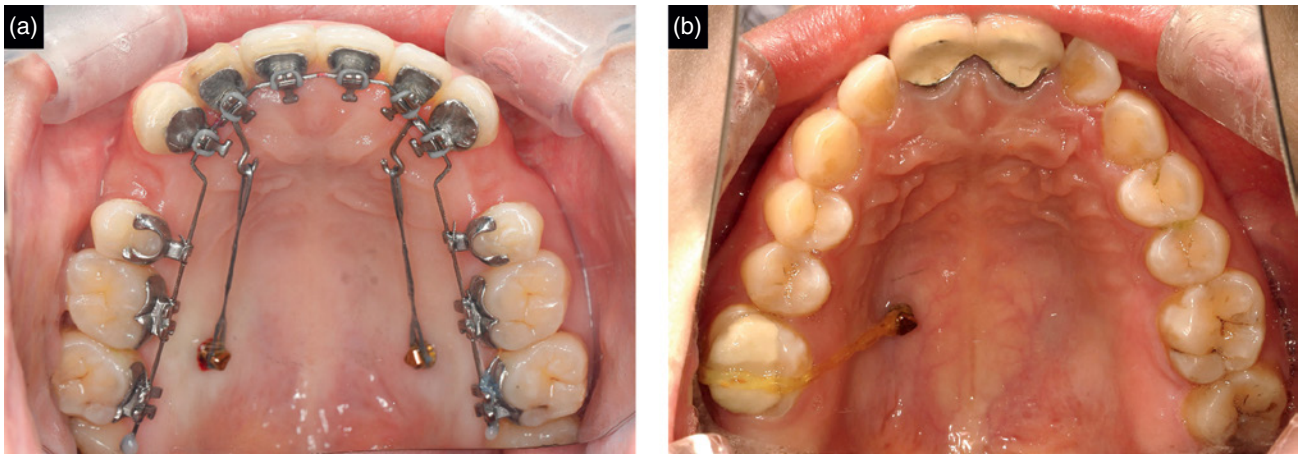


Figure 6.8 Clinical applications of mini-implants placed at the palatal interradicular region. (a) *En masse* anterior retraction. (b) Molar intrusion through mini-implants at both the buccal and palatal regions.

t.me/Dr_Mouayyad_AlbtousH

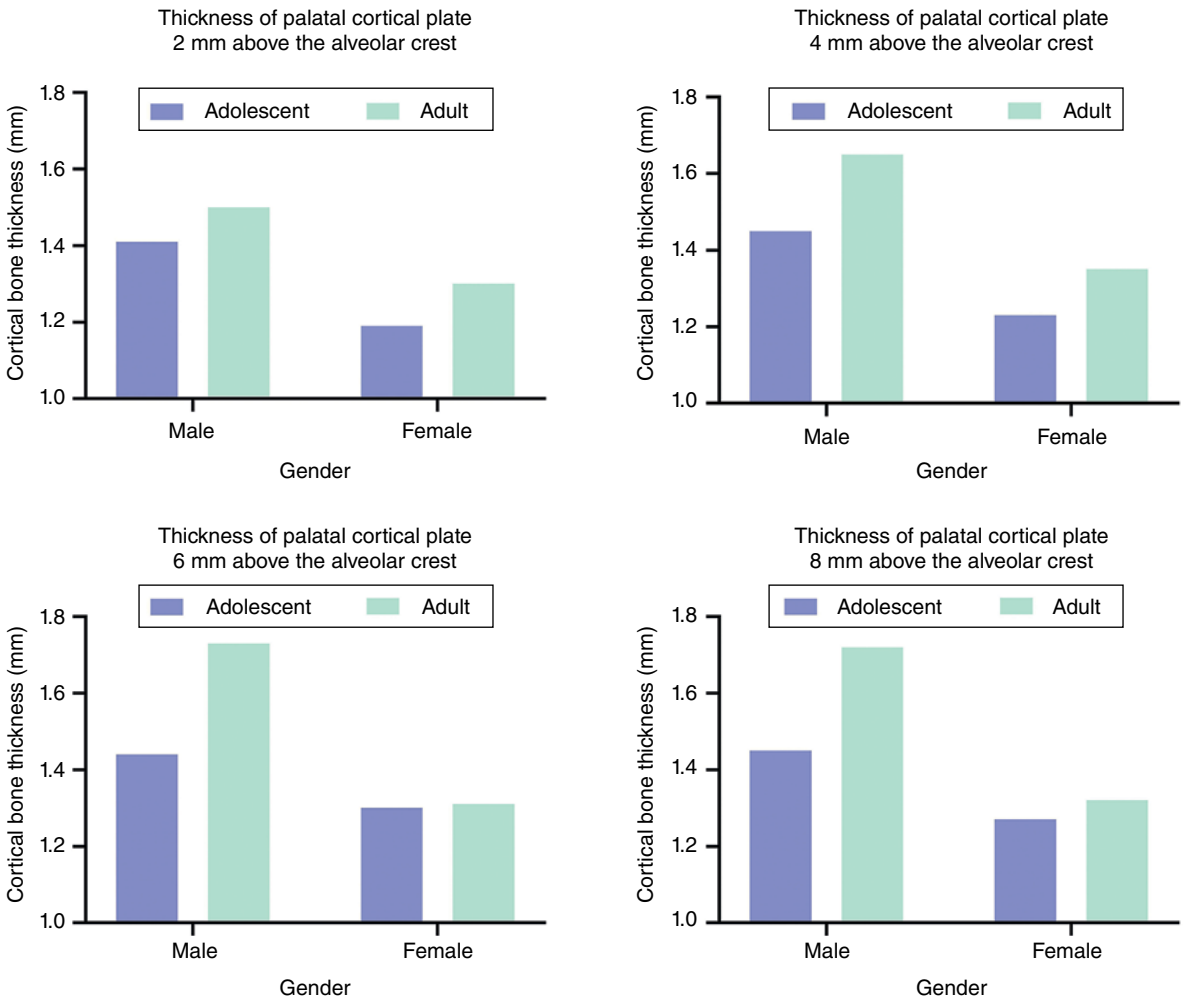


Figure 6.9 The influence of gender and age on cortical thickness at the palatal interradicular region. *Source:* Adapted from Cassetta et al. [7].

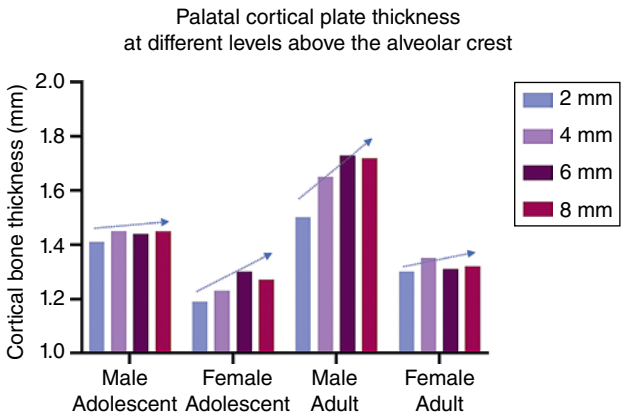


Figure 6.10 The thickness of the palatal cortical plate at different heights apical to the alveolar crest. The palatal cortical thickness increases with increases in the vertical height. *Source:* Adapted from Cassetta et al. [7].

different vertical entry points of mini-implants result in different cortical engagements. However, cortical thickness at all vertical levels is within the optimal range (1–2 mm) and this increase may not be clinically significant. Moreover, different vertical skeletal patterns have an impact on palatal cortical thickness. Specifically, low-angle subjects exhibit thicker palatal cortical plates than normal-angle and high-angle subjects (Figure 6.11).[8] Cortical thickness differs among different interradicular sites, and cortical thickness decreases anteroposteriorly. Specifically, cortical thickness is greatest at the U3-U4 site and least at the U6-U7 site (Figure 6.12).[9]

Although cortical thickness is influenced by many factors (i.e. age, gender, vertical skeletal pattern, vertical level), cortical thickness at the palatal interradicular sites among different subjects is within the optimal range

t.me/Dr_Mouayyad_AlbtousH

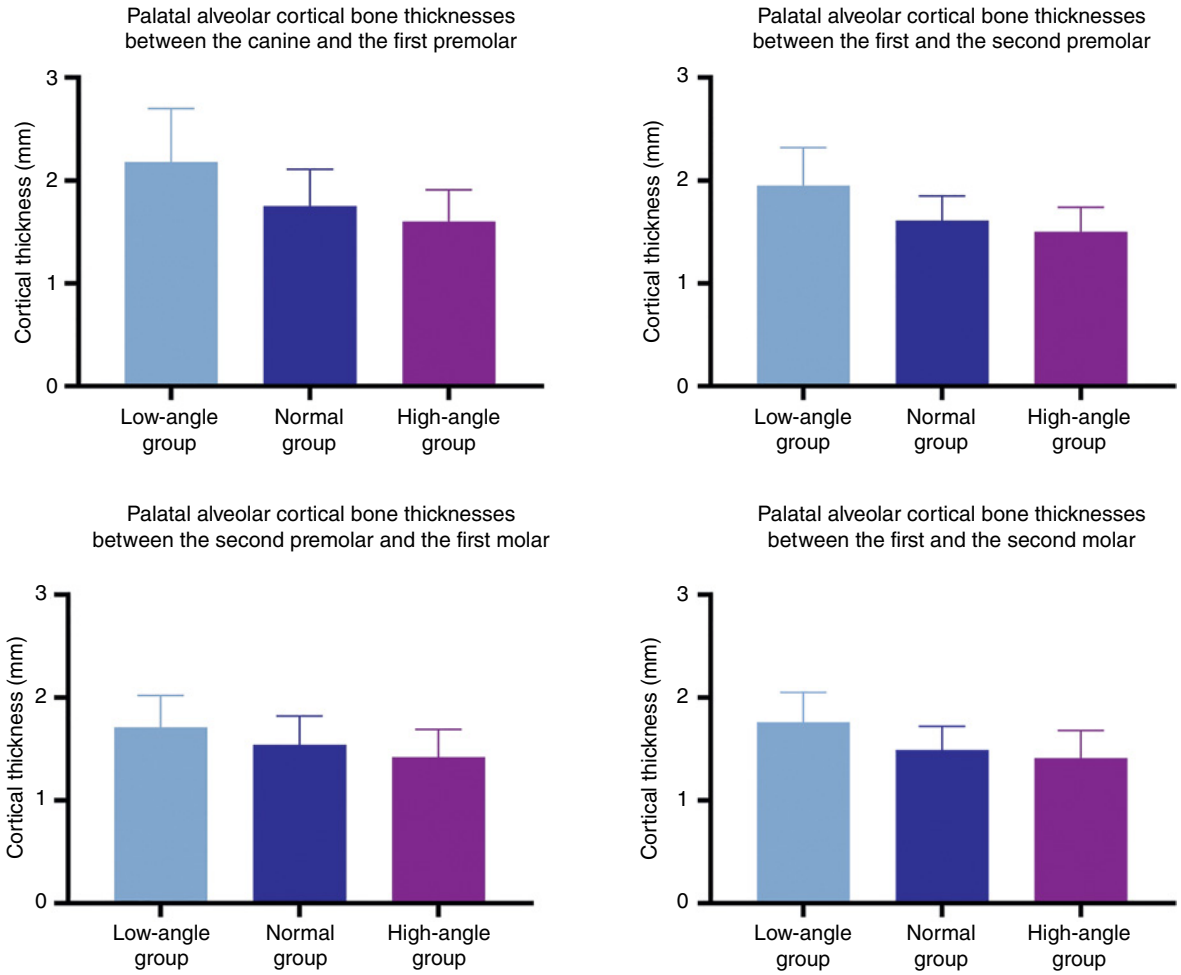


Figure 6.11 The thickness of the palatal cortical plate among patients with different vertical skeletal patterns. Low-angle subjects exhibited thicker cortical plates than normal-angle and high-angle patients. *Source:* Date from Ozdemir et al. [8].

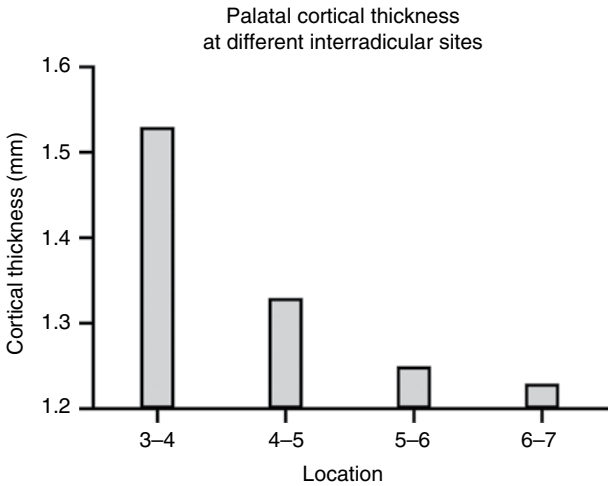


Figure 6.12 The thickness of palatal cortical plates at different interradicular sites. *Source:* Adapted from Tepedino et al. [9].

(1–2 mm). Therefore, the requirements of cortical thickness are satisfied among different clinical individuals, so cortical thickness need not be considered in determining the optimal insertion site.

Hard Tissue Factor: Bone Depth

Bone depth is defined as the distance between the palatal cortical plate and its buccal counterpart, and a minimum bone depth of 4.5 mm is recommended to ensure adequate primary stability of mini-implants. Bone depth increases from alveolar crest to alveolar base and this indicates that greater bone engagement can be obtained with an increase in insertion height (Figure 6.13). Moreover, bone depth increases from anterior to posterior interradicular sites, with bone depth being least at the U3-U4 site and greatest

t.me/Dr_Mouayyad_AlbtousH

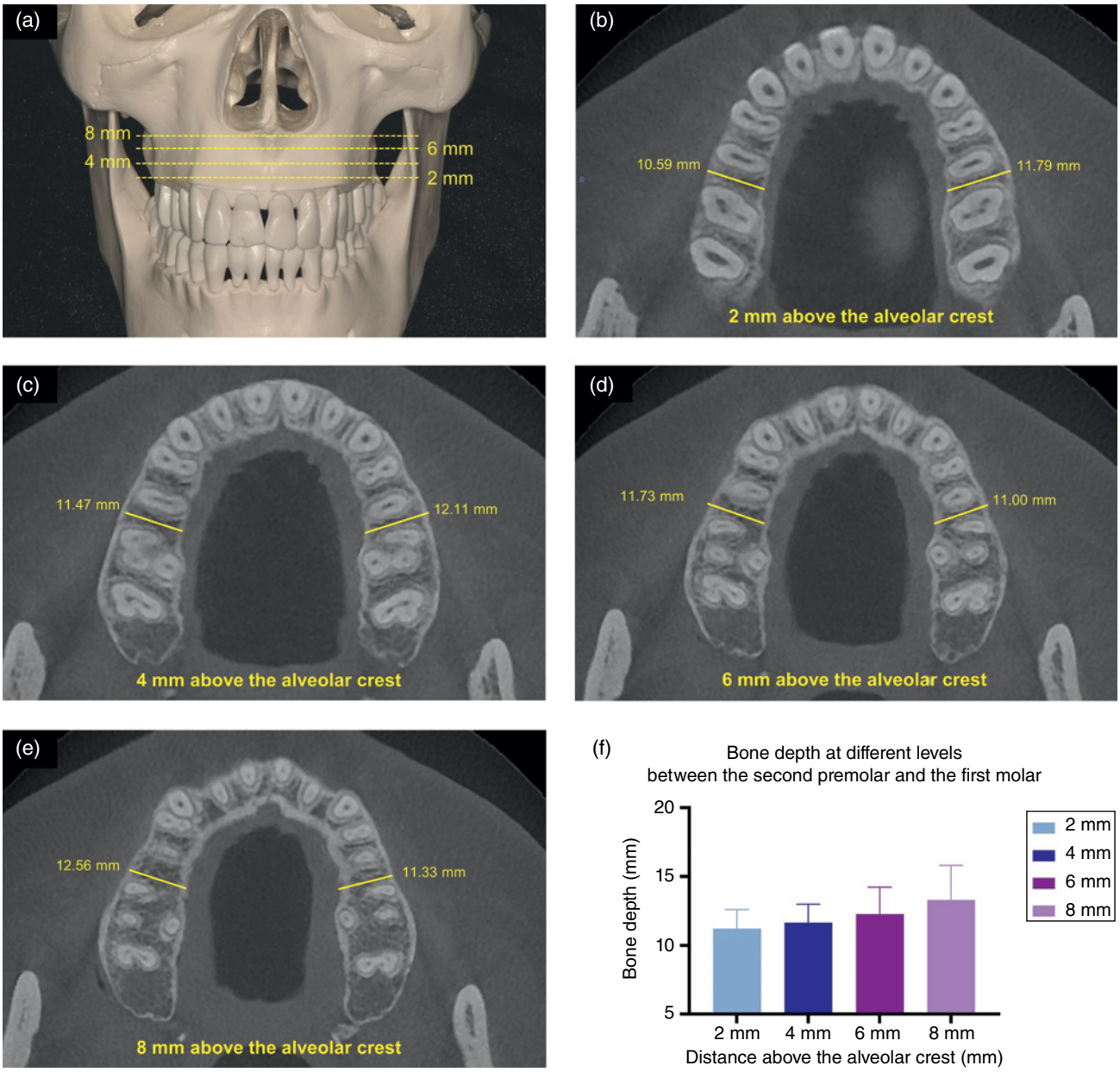


Figure 6.13 Bone depth at different heights above the alveolar crest at the interradicular site between the second premolar and first molar. (a) Illustration of the section planes above the alveolar crest on the skull. (b–e) Bone depth at different heights shown on CBCT images (axial view). (f) Comparison of bone depth among different heights.

at the U6-U7 site (Figure 6.14). The minimum requirement (4.5 mm) of bone depth is satisfied at all the interradicular sites at all insertion heights. Therefore, this anatomical factor need not be considered since all interradicular sites are qualified for mini-implant placement.

Hard Tissue Factor: Bone Width

Bone width refers to the mesiodistal interradicular distance between two adjacent roots. Interradicular space is greater at palatal interradicular sites than buccal sites due to the presence of fewer roots at the palatal side (Figure 6.15), resulting in a lower likelihood of root

t.me/Dr_Mouayyad_AlbtousH

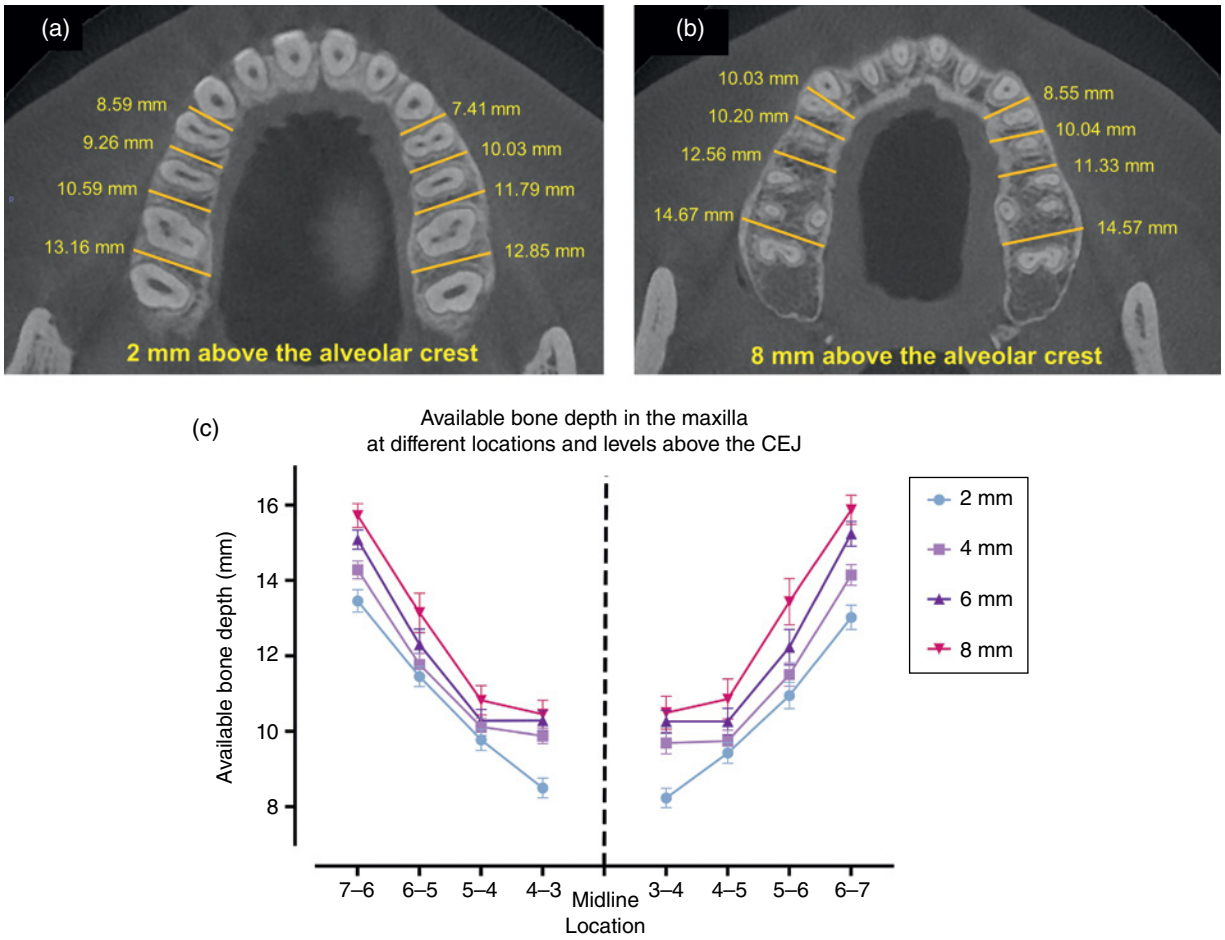


Figure 6.14 Bone depths at different heights and different interradicular sites. (a) Bone depths at different interradicular sites at the 2 mm level above the alveolar crest shown on a CBCT image (axial view). (b) Bone depths at different interradicular sites at the 8 mm level above the alveolar crest shown on a CBCT image (axial view). (c) Comparison of bone depth among different heights and different interradicular sites.

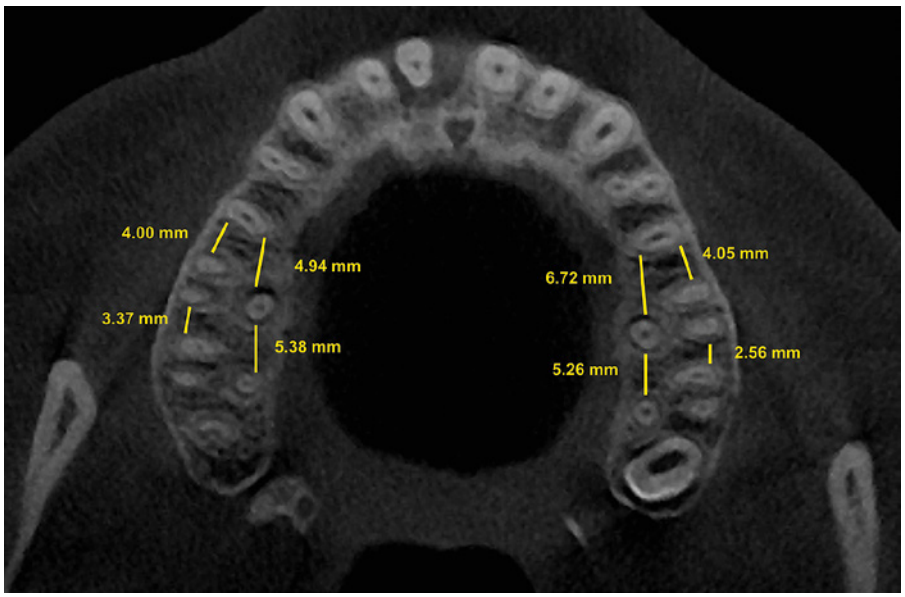


Figure 6.15 Comparison of bone width at the buccal versus the palatal sides.

t.me/Dr_Mouayyad_AlbtousH

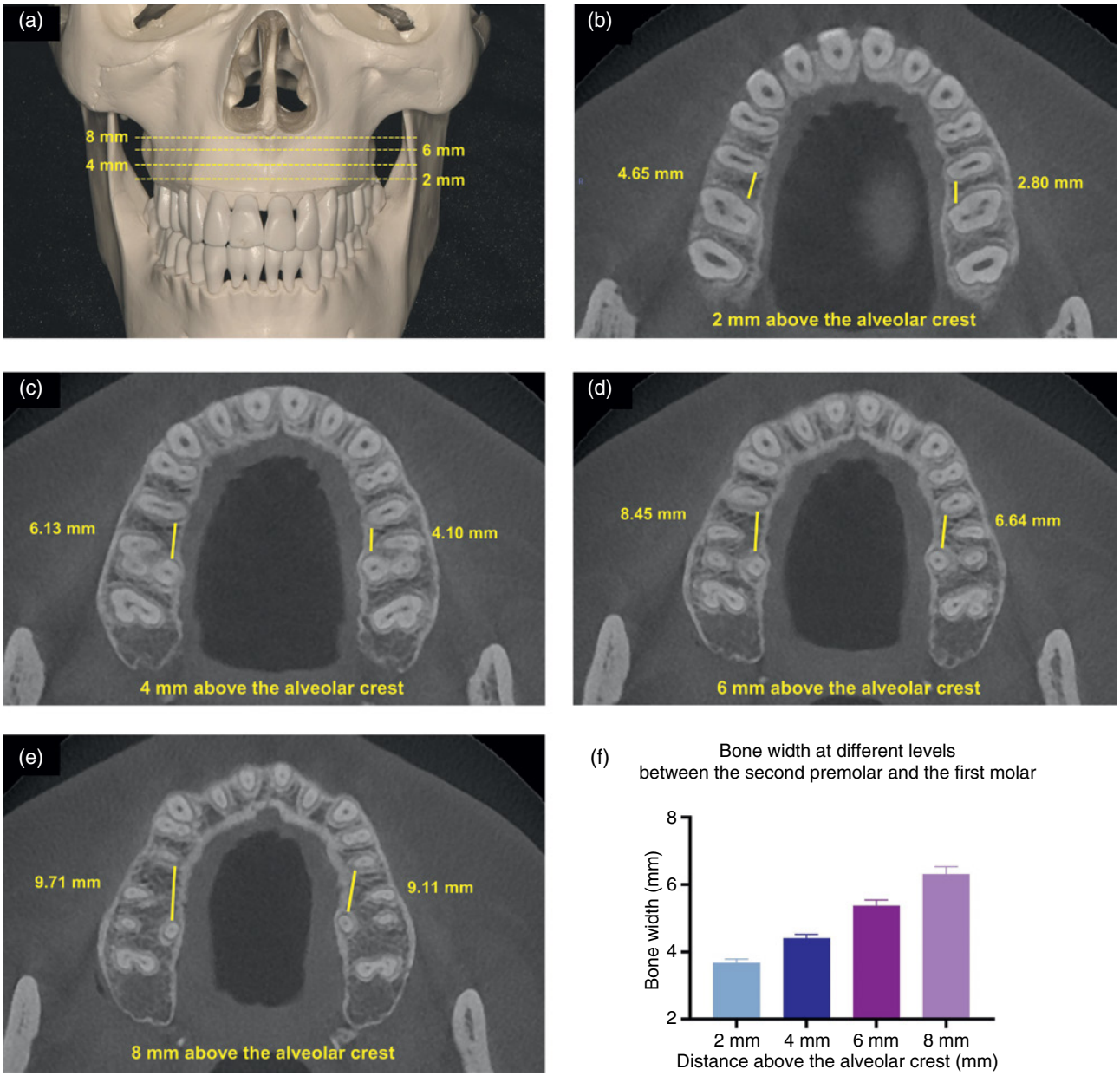


Figure 6.16 Bone width at different heights above the alveolar crest at the interradicular site between the second premolar and first molar. (a) Illustration of the section planes above the alveolar crest on the skull. (b–e) Bone widths at different heights shown on CBCT images (axial view). (f) Comparison of bone width among different heights.

contact in the palatal region.[10,11] Due to the tapered shape of roots, bone width becomes greater from alveolar crest to alveolar base (Figure 6.16). Moreover, bone width differs among different interradicular sites, being the greatest at the U5-U6 site (Figure 6.17). As per the 1 mm clearance principle, interradicular space should be at least 3.5 mm (1 + 1.5 + 1 = 3.5 mm) if a mini-implant with a diameter of 1.5 mm is placed. The U5-U6 site at all insertion heights is recommended for mini-implant placement. However, it is recommended that the insertion should be at least 2 mm from the alveolar crest since mini-implants placed close to the alveolar crest exhibit a high risk of failure.[12,13] Thus, it is recommended to place mini-implants at the U5-U6 site 4–8 mm apical to the CEJ.

For other interradicular sites with limited interradicular space, interradicular distance should be carefully assessed to determine the suitability of mini-implant placement.

t.me/Dr_Mouayyad_AlbtousH

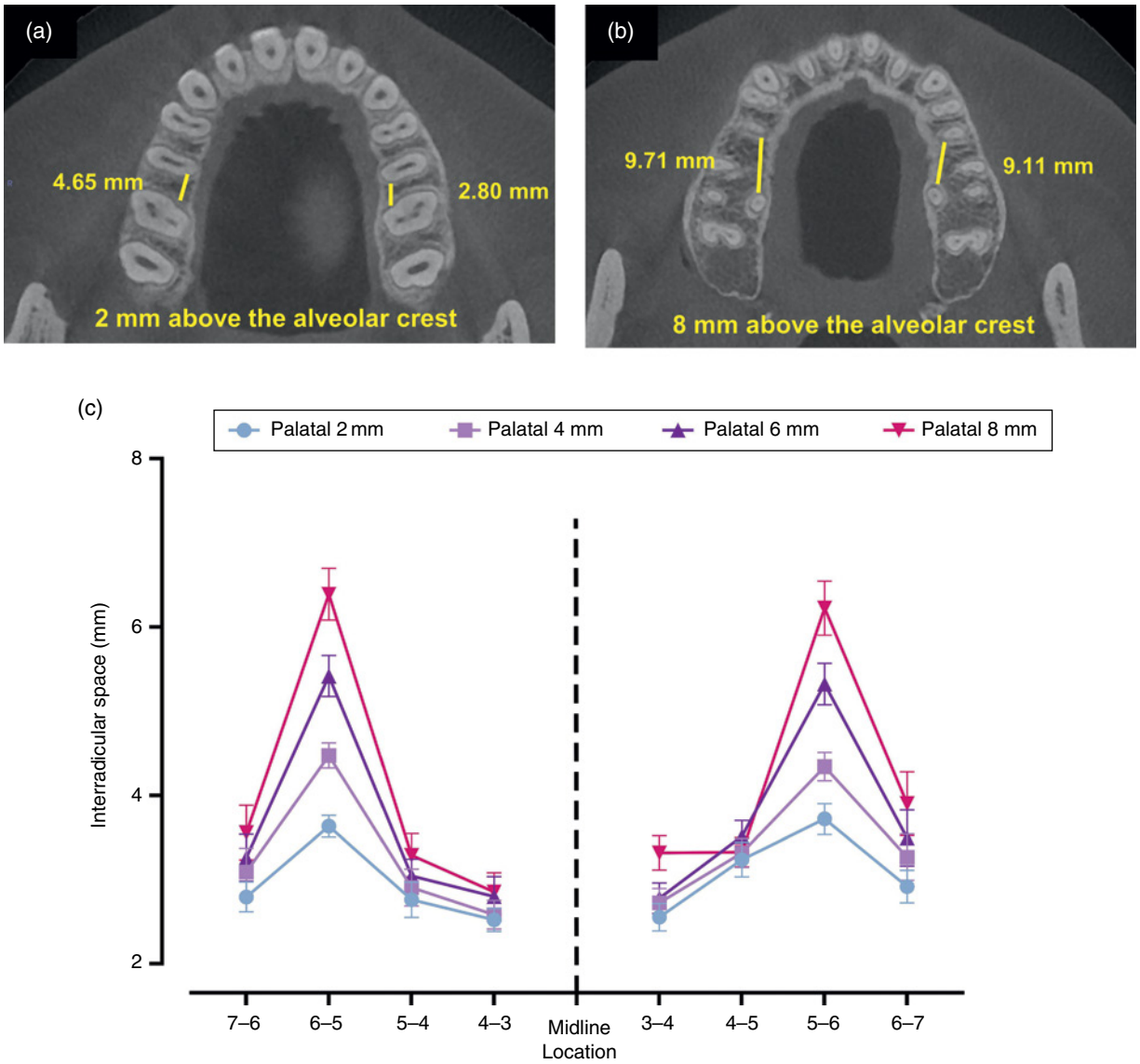


Figure 6.17 Bone widths at different heights and different interradicular sites. (a) Bone width at the 2 mm level above the alveolar crest shown on a CBCT image (axial view). (b) Bone depth at the 8 mm level above the alveolar crest shown on a CBCT image (axial view). (c) Comparison of bone depth among different heights and different interradicular sites. Bone width is greatest at the interradicular site between the second premolar and first molar.

Hard Tissue Factor: Inclination of Cortical Plate

Due to the vault-like shape of the palatal region, the palatal cortical plate is not perpendicular to the occlusal plane and the inclination of the palatal cortical plate should be taken into consideration for determining the insertion angle. The inclination angle of the palatal cortical plate increases from anterior to posterior sites (Figure 6.18). The average inclination angle of the cortical plate at the U5-U6 is about 60° to the occlusal plane. Generally, it is recommended to place mini-implants at 15-30° to the bone surface, in order to avoid root injury and to obtain greater cortical engagement. Thus, for the U5-U6 interradicular site, the insertion angle is recommended to be 30-45° to the occlusal plane (Figure 6.19). In contrast, the insertion angle may be greater for the U3-U4 site and the U4-U5 site while smaller for the U6-U7 site. However, due to the limited interradicular space at the U6-U7 site, the insertion angle is still recommended to be 30-45° in order to avoid root damage.

t.me/Dr_Mouayyad_AlbtousH

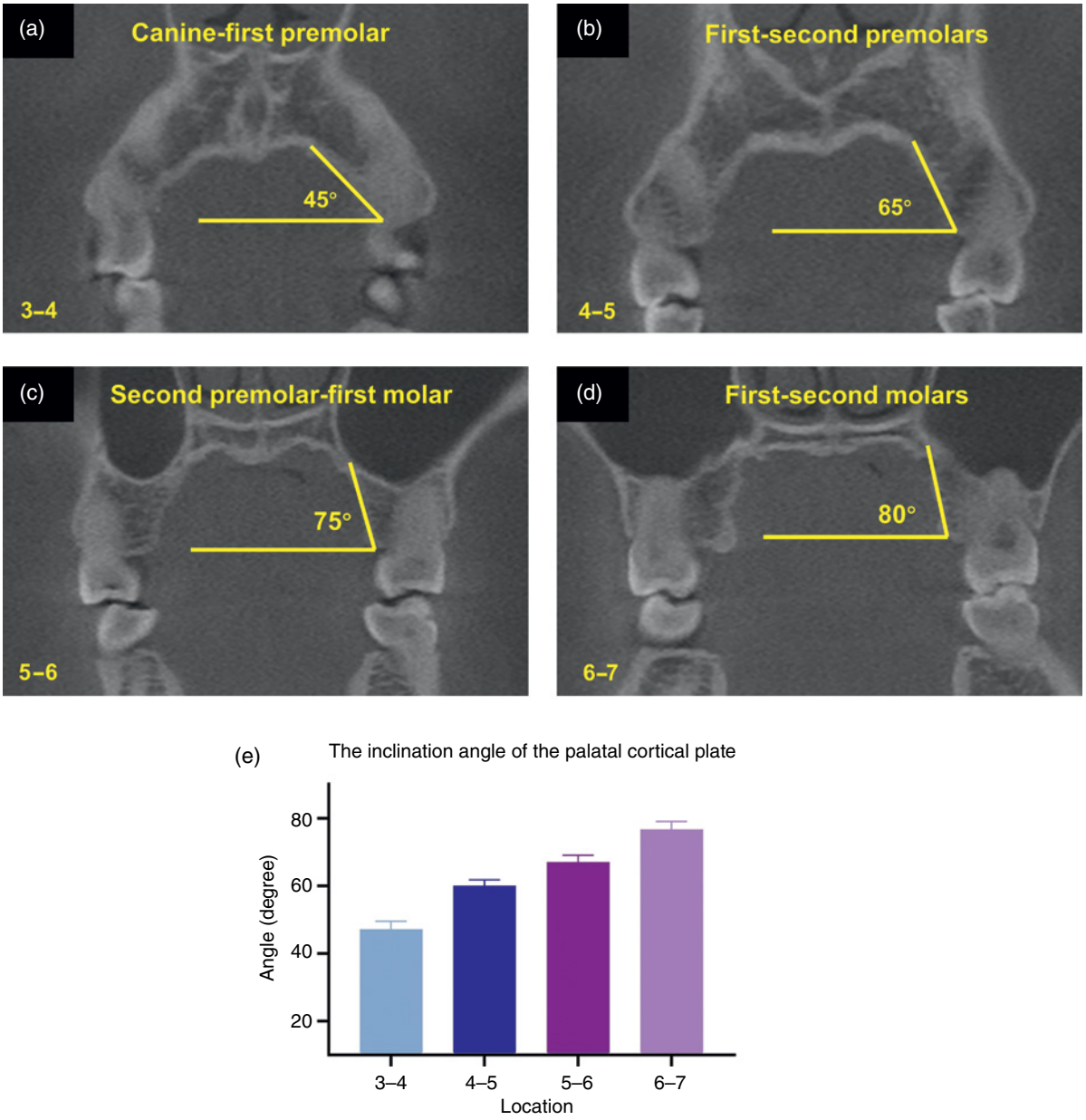


Figure 6.18 Inclination of the palatal cortical plate at different interradicular sites. (a–d) Measurements of the inclination angle of the palatal cortical plate in reference to the occlusal plane at different interradicular sites. (e) Comparison of the inclination angle of the palatal cortical plate at different interradicular sites.

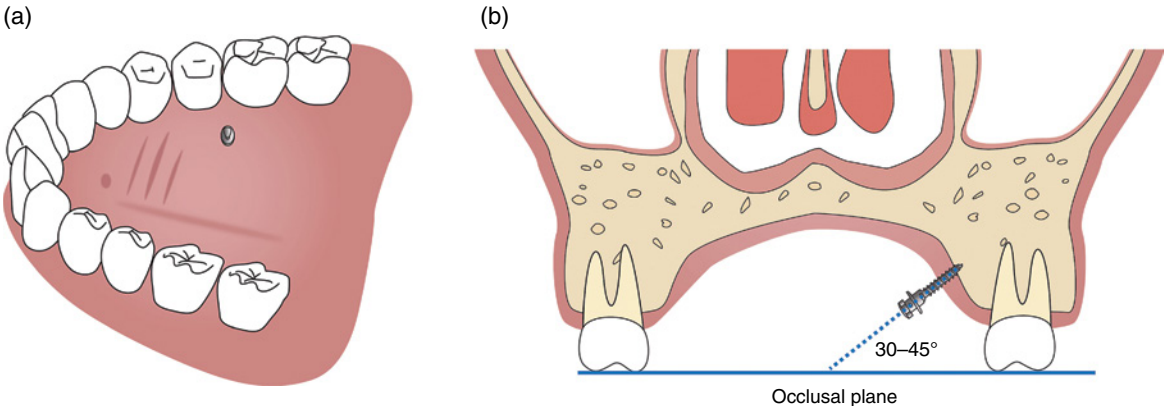


Figure 6.19 Recommended insertion site and insertion angle for the palatal interradicular region. (a) The interradicular site between the second premolar and first molar is the recommended insertion site for the palatal interradicular region. (b) The insertion angle is 30–45° to the occlusal plane.

t.me/Dr_Mouayyad_AlbtousH

Soft Tissue Factor: Soft Tissue Type

The soft tissue in the palatal region is keratinised and attached (Figure 6.20), rendering the soft tissue around mini-implants resistant to irritation, swelling and hyperplasia. However, soft tissue complications do occur if meticulous oral hygiene maintenance is not implemented or mini-implants with inappropriate lengths are used (Figure 6.21). Thus, although attached and keratinised soft tissue is present at the palatal interradicular sites, care should be taken to avoid any potential soft tissue complication.

Soft Tissue Factor: Soft Tissue Thickness

Soft tissue thickness is an important factor in determining the suitability of anatomical sites for the placement of mini-implants. If soft tissue is too thick, the transgingival part of the mini-implant is long. On one hand, this is a biomechanical disadvantage for mini-implants since the ratio of extra-bony to intra-bony length is high. On the other hand, thick soft tissue around mini-implants is susceptible to soft tissue complications. The thickness of soft tissue covering the palatal interradicular sites is influenced by the vertical level, the anteroposterior location and their interactions (Figure 6.22). Specifically, soft tissue thickness is increased from alveolar crest to alveolar base, indicating that inserting mini-implants at a more apical level is accompanied by thicker soft tissue and is associated with higher risk of soft tissue complications around mini-implants. Moreover, at the 2 mm and 4 mm levels, soft tissue becomes thinner if the entry point is located more posteriorly. In contrast, at the 8 mm level, soft tissue thickness becomes greater if the entry point is at a more posterior location.

Generally, mini-implants are inserted at the 8 mm level and we suggest that longer mini-implants should be used for the U6-U7 site due to the presence of thick soft tissue at this site. Thus, in consideration of the average soft tissue thickness at different interradicular sites, we recommend that 8 mm mini-implants be inserted at the U3-U4, U4-U5 and U5-U6 sites while 10 mm mini-implants be placed at the U6-U7 site.



Figure 6.20 Keratinised and attached mucosa (yellow arrow) at the palatal interradicular region.

Vital Structures

At the palatal interradicular sites, greater palatine neurovascular bundles are vital structures that should be considered when planning the locations of mini-implants. Mini-implants should be meticulously placed away from

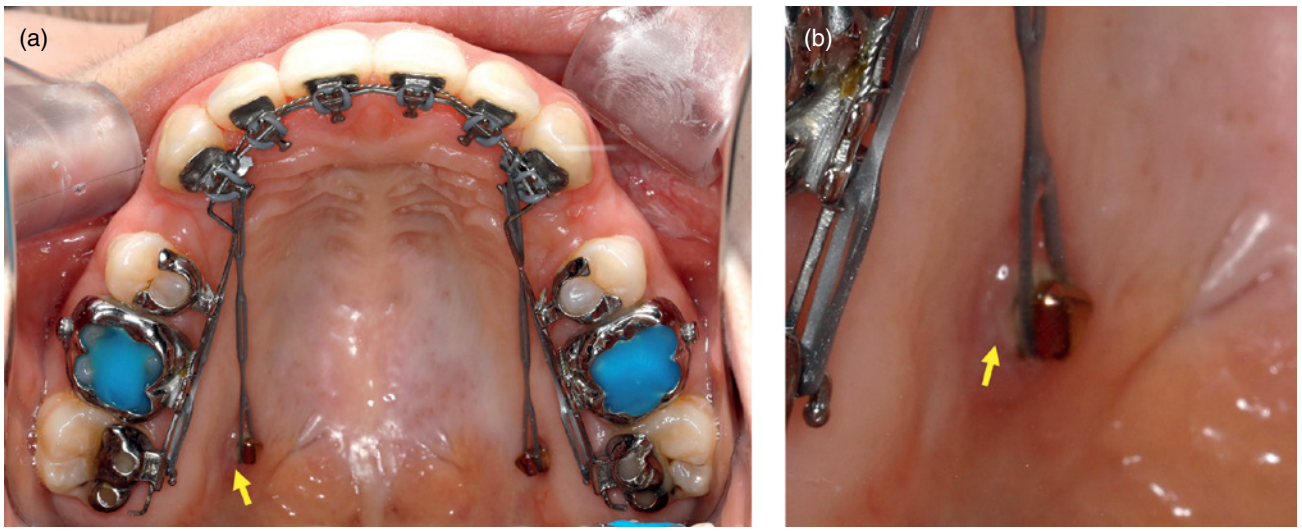


Figure 6.21 (a) Soft tissue inflammation (yellow arrow) associated with a mini-implant placed at the right palatal interradicular region. (b) A close-up photograph showing the soft tissue inflammation. Note the reddish and swollen inflamed soft tissue (yellow arrow) around the mini-implant.

t.me/Dr_Mouayyad_AlbtousH

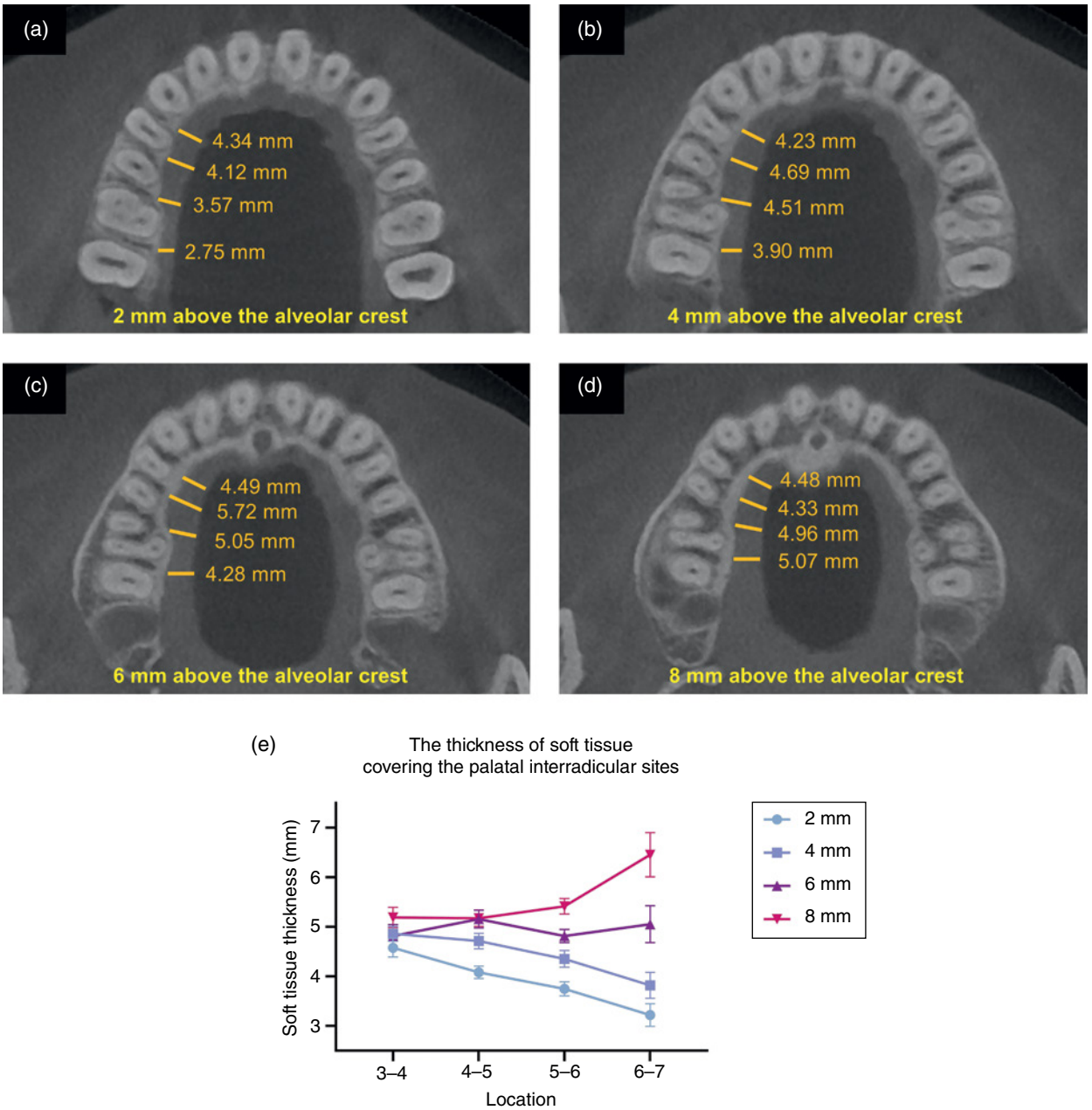


Figure 6.22 The thickness of soft tissue covering the palatal interradicular region. (a) Soft tissue thickness at different anteroposterior interradicular sites 2 mm above the alveolar crest shown on a CBCT image (axial view). (b) Soft tissue thickness at different anteroposterior interradicular sites 4 mm above the alveolar crest shown on a CBCT image (axial view). (c) Soft tissue thickness at different anteroposterior interradicular sites 6 mm above the alveolar crest shown on a CBCT image (axial view). (d) Soft tissue thickness at different anteroposterior interradicular sites 8 mm above the alveolar crest shown on a CBCT image (axial view). (e) Comparison of soft tissue thickness at different heights and different interradicular sites.

the greater palatine neurovascular bundles to avoid bleeding and nerve injury.

The greater palatine bundles exit from the greater palatine foramen, run anteriorly and anastomose with nasopalatine vessels. A recent systematic review reveals that the greater palatine foramen is located 4 mm and 15 mm away from the posterior border of the hard palate and midsagittal suture, respectively (Figure 6.23).[14] After exiting from the greater palatine foramen, the greater palatine bundles run 10–14 mm apical to the CEJ of the posterior teeth. Specifically, the distances from the greater palatine vessels to the CEJ are 10 mm, 12 mm, 14 mm, 13 mm and 14 mm for the canine, first premolar, second premolar, first molar and second molar, respectively (Figure 6.24). Thus,

t.me/Dr_Mouayyad_AlbtousH

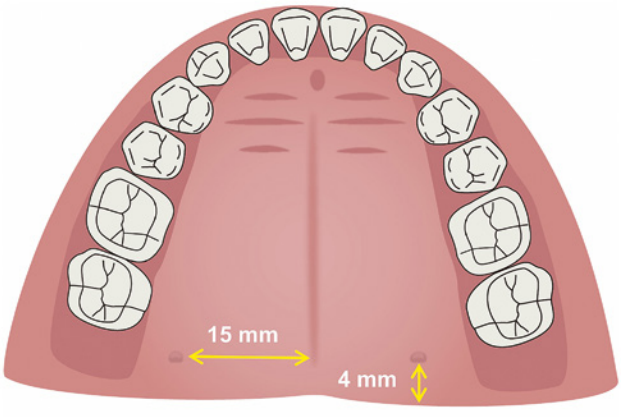


Figure 6.23 The greater palatine foramen is located 15 mm away from the midsagittal suture and 4 mm anterior to the posterior border of the hard palate.

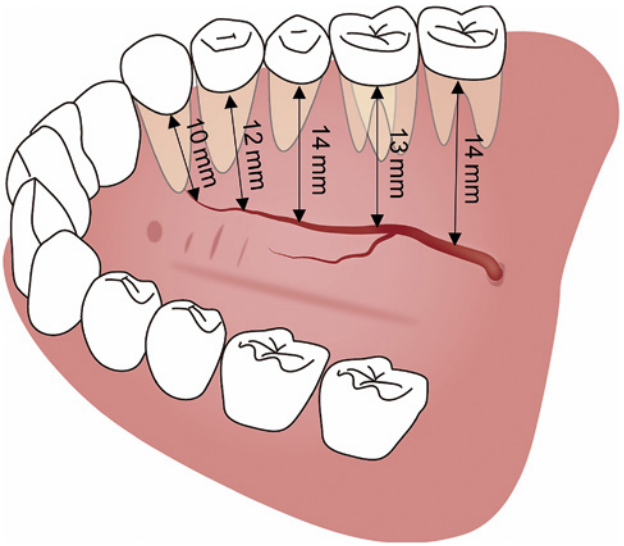


Figure 6.24 Location of the greater palatine neurovascular bundles.

considering individual variations, we recommend mini-implants not be placed beyond 10 mm apical to the CEJ of posterior teeth in order to avoid potential injury to greater palatine neurovascular bundles.

6.2.2 Biomechanical Considerations

Mini-implants are placed at different interradicular sites for different orthodontic purposes (Table 6.1). Specifically, mini-implants placed at the U3-U4 and U4-U5 sites are often employed for molar protraction and premolar intrusion, while those inserted at the U5-U6 site are used for anterior retraction with lingual appliances and for premolar or molar intrusion. Furthermore, mini-implants at the U6-U7 site are often utilised for anterior retraction and molar intrusion. Depending on the clinical indications and biomechanical requirements, different interradicular sites can be chosen, provided that anatomical or biological requirements (e.g. 1 mm root clearance) are not violated.

Table 6.1 Mini-implants inserted at different sites for different applications.

Interradicular site	Orthodontic application
U3-U4	Molar protraction; premolar intrusion
U4-U5	Molar protraction; premolar intrusion
U5-U6	Anterior retraction; premolar or molar intrusion
U6-U7	Anterior retraction; molar intrusion

6.2.3 Selection of Appropriate Insertion Sites

Based on anatomical features of the palatal interradicular sites, the most appropriate interradicular site is the U5-U6 site where the largest interradicular space is present. The insertion height is 4-8 mm apical to the CEJ of posterior teeth, with the insertion angle being 30-45° to the occlusal plane (Figure 6.25). In clinical practice, other interradicular sites may be indicated for biomechanical purposes other than anterior retraction, e.g. molar protraction. For other interradicular sites (U3-U4, U4-U5 and U6-U7) where limited interradicular space is present, meticulous evaluation of anatomical characteristics should be performed. If interradicular space is too limited, a mini-implant may not be placed at these interradicular sites and an alternative biomechanical system with mini-implants placed at other anatomical sites should be designed. If interradicular space is not ample but permits mini-implant placement, judicious selection of entry points and insertion angles should be implemented.

6.2.4 Insertion Techniques

For the placement of mini-implants at the palatal interradicular sites, the first step is to determine the most appropriate insertion site, height and angle based on anatomical features and biomechanical requirements.

Second, once the entry point is determined, the next step is to perform local anaesthesia following mucosal disinfection with iodophor (Figure 6.26). Block anaesthesia of the greater palatine nerve is not recommended and local infiltration anaesthesia around the entry point is suggested. This is to retain sensory perception of dental roots during the insertion of mini-implants, so that inadvertent root contact can be perceived by the patient and the practitioner alerted. To perform local infiltration anaesthesia, 0.2–0.5 ml

t.me/Dr_Mouayyad_AlbtousH

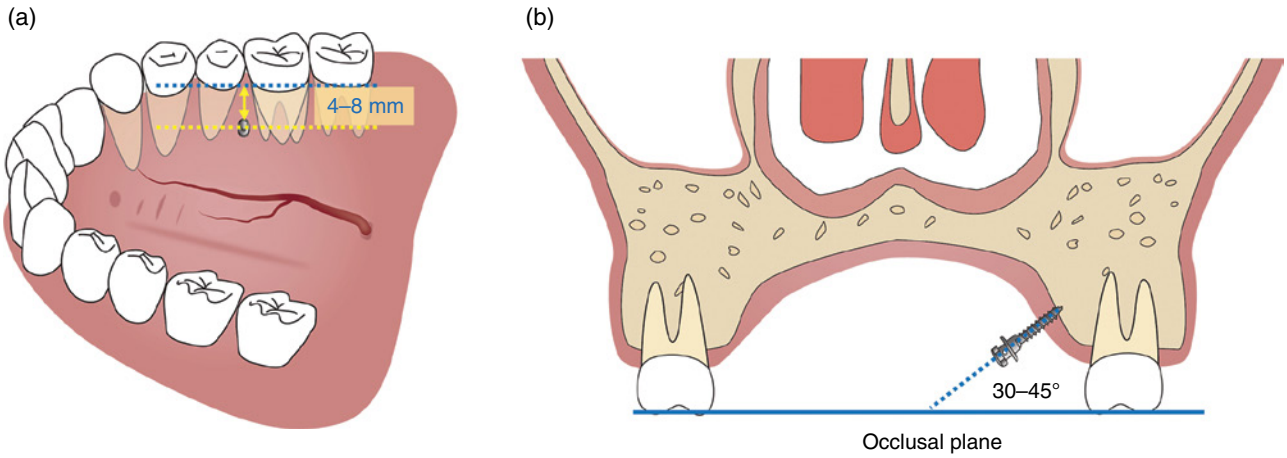


Figure 6.25 Recommended insertion site, insertion height and insertion angle for the palatal interradicular region. (a) Mini-implants are recommended to be placed at the interradicular site between the second premolar and first molar 4–8 mm apical to the CEJ. (b) The optimal insertion angle is 30–45° to the occlusal plane.

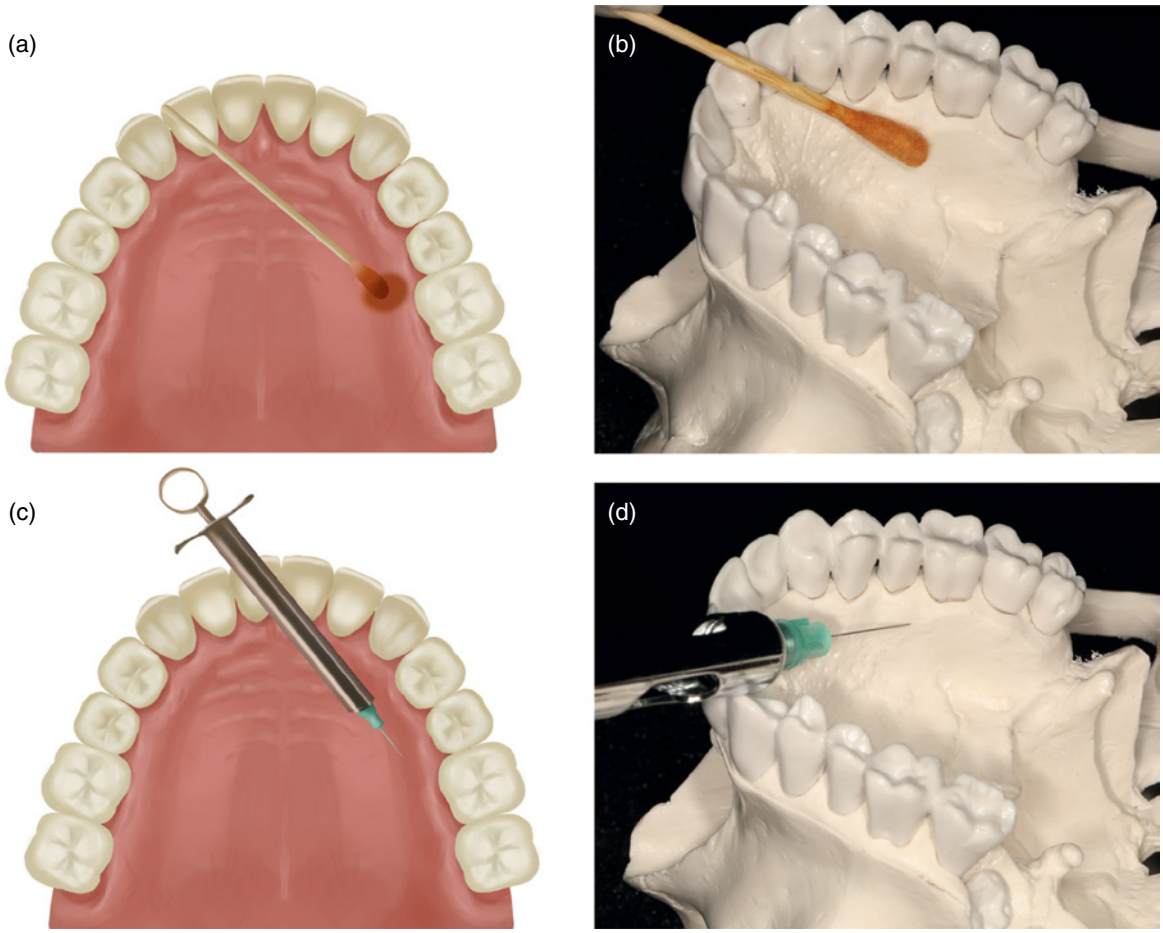


Figure 6.26 Mucosa disinfection and local infiltration anaesthesia. (a,b) Mucosa disinfection with iodophor. (c,d) Local infiltration anaesthesia.

t.me/Dr_Mouayyad_AlbtousH

anaesthetic is sufficient. As mentioned above, recommended entry points are 4–8 mm apical to the CEJ while the greater palatine vessels run at least 10 mm apically to the CEJ, rendering injection of anaesthetic around recommended entry points safe. However, considering that small branches may be present at more occlusal levels, we still recommend aspiration be performed before injecting anaesthetic to avoid vessel penetration and subsequent entry of anaesthetic into the circulation.

Third, the optimal entry point is marked with an explorer or probe at a predetermined insertion height (4–8 mm apical to CEJ) (Figure 6.27). Then, a vertical indentation is performed and the mesiodistal position of the entry point verified from the occlusal side (Figure 6.28). The entry point should be at the middle point between the two adjacent roots.

Fourth, the mini-implant is inserted through the determined entry point and the direction of the insertion is perpendicular to the tangent line of the dental arch, which should be confirmed from the occlusal view (Figure 6.29).

Lastly, the mini-implant is inserted with a contra-angle screwdriver or motor-driven handpiece. During insertion, rotation of the screwdriver is performed with the thumb, index and middle fingers of the operator's right hand, and the screwdriver should be stabilised with the operator's left hand (Figure 6.30). Otherwise, lateral displacement of the screwdriver may occur and result in mini-implant fracture. To avoid slippage of mini-implants if angled insertion technique is implemented, cortical penetration is first performed with perpendicular insertion into the bone surface, with the insertion angle being about 15–30° to the occlusal plane. Then, the mini-implant is

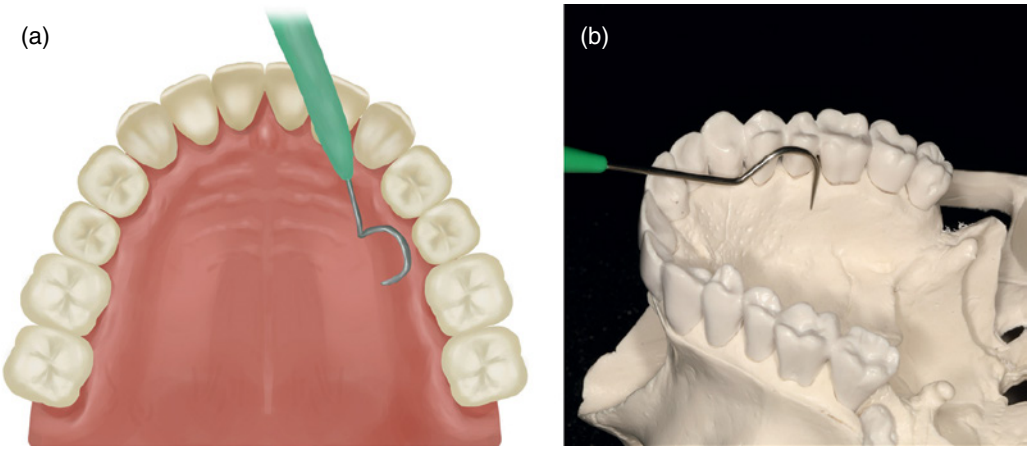


Figure 6.27 Mark the optimal entry point with an explorer. (a) Schematic illustration. (b) Skull model.

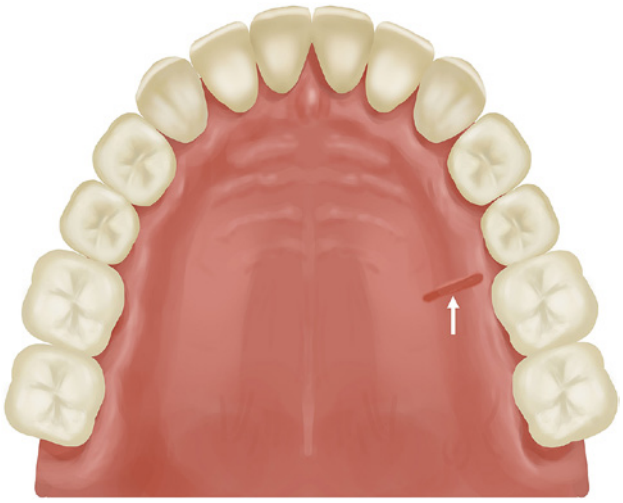


Figure 6.28 Schematic illustration showing the vertical indentation (white arrow) on the soft tissue.

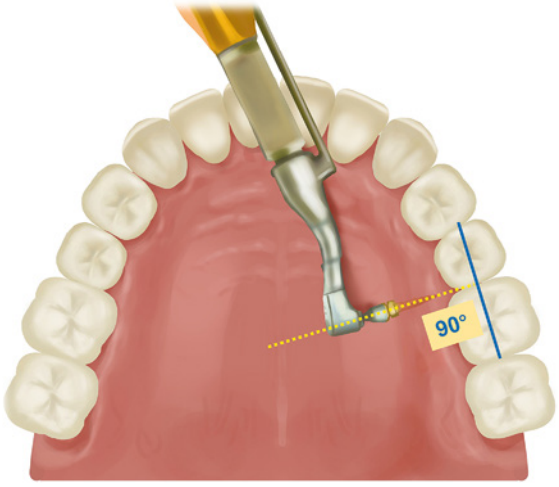


Figure 6.29 Confirmation of the insertion path from the occlusal side. The insertion path (yellow dashed line) is perpendicular to the tangent line (blue solid line) of the dental arch passing through the entry point.

t.me/Dr_Mouayyad_AlbtousH

unscrewed and the insertion angle is changed to a final one that is 30–45° to the occlusal plane (Figure 6.31). The insertion should not be stopped until firm contact is achieved between the mini-implant platform and the soft tissue. Once the insertion is complete, both the vertical and mesiodistal positions of the mini-implants should be checked.

The detailed clinical procedures of inserting a mini-implant at a palatal interradicular site is displayed in Figure 6.32.



Figure 6.30 The screwdriver is being rotated by the operator's right hand and stabilised by the left hand during insertion.

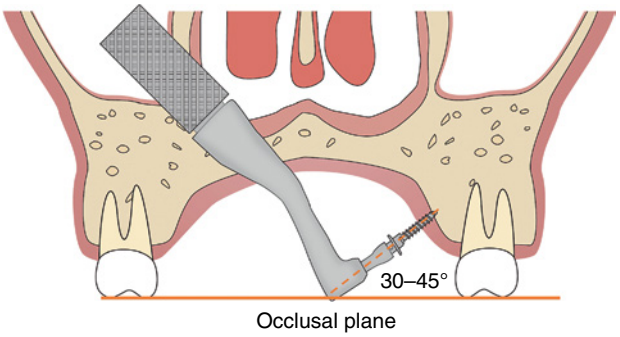


Figure 6.31 The insertion path is 30–45° to the occlusal plane.

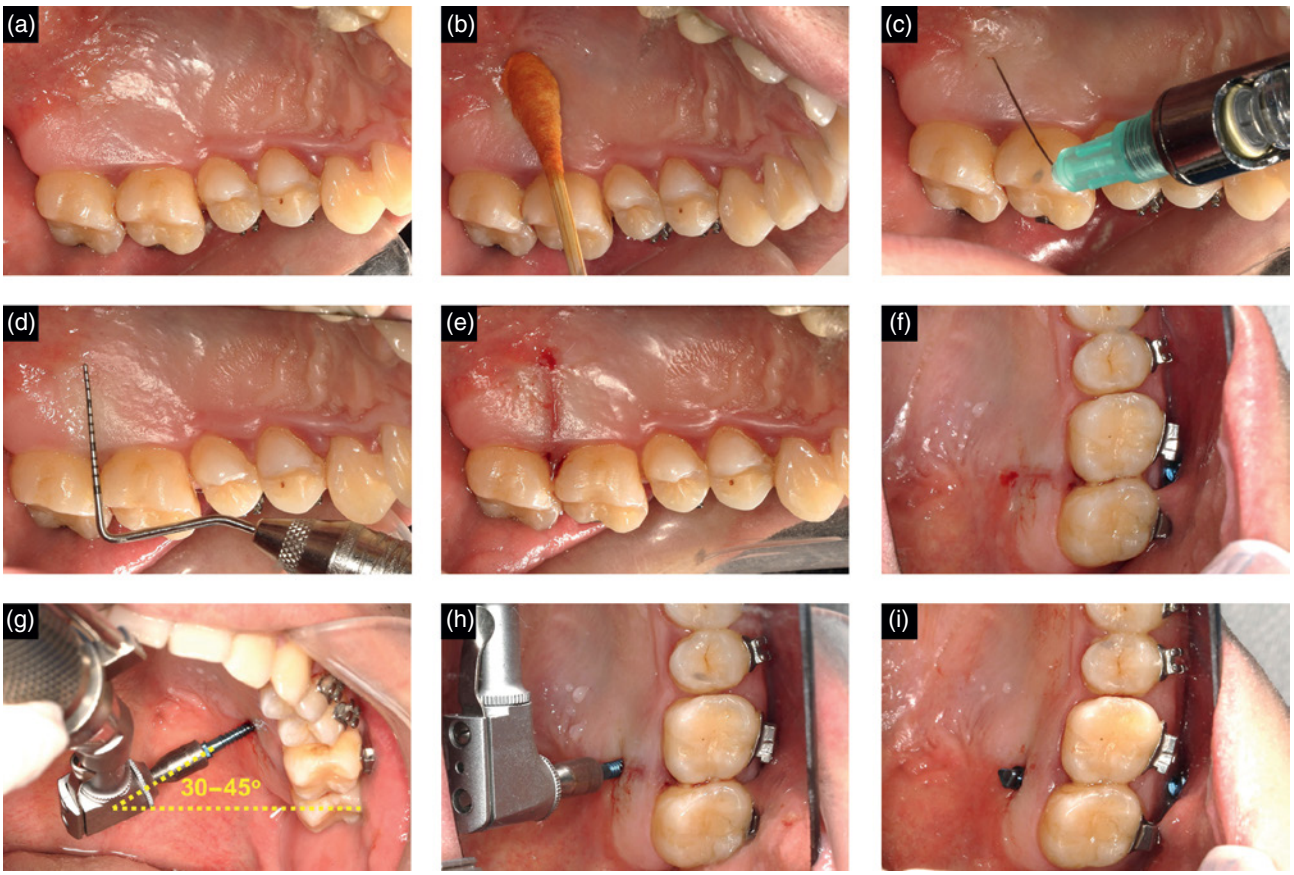


Figure 6.32 Clinical procedures of inserting a mini-implant at the palatal interradicular region. (a) Before insertion. (b) Mucosa disinfection with iodophor. (c) Local infiltration anaesthesia. (d) Mark the entry point and perform soft tissue indentation with a probe. (e) Check the vertical indentation from the palatal side. (f) Check the orientation of the vertical indentation from the occlusal side. (g) Insertion of the mini-implant with an insertion angle of 30–45° to the occlusal plane. (h) Check the insertion path from the occlusal side. (i) Postinsertion examinations.

t.me/Dr_Mouayyad_AlbtousH

6.2.5 Clinical Applications

Anterior Retraction

For premolar extraction cases, anchorage requirements are of great importance and should be considered prior to treatment. Mini-implants are indicated for patients with maximal anchorage requirements. Mini-implants placed at the palatal interradicular sites are often used for anterior retraction in conjunction with lingual appliances. Two case examples are presented below to demonstrate the clinical applications of palatal interradicular mini-implants for anterior retraction.

Case 1 A female adult presented to the orthodontic department with a chief complaint of lip protrusion.



Figure 6.33 Pretreatment photographs and radiographs.

t.me/Dr_Mouayyad_AlbtousH

Clinical examinations revealed that the patient had a bilateral Class I molar relationship, mild crowding, coincident upper and lower dental midlines, mentalis strain and protrusive facial profile (Figure 6.33). Lateral cephalometry indicated class II skeletal base (ANB = 7.1), normoclined upper incisors and labially proclined lower incisors (U1-SN = 107.1; L1-MP = 106.8), and normal mandibular angle (SN-MP = 36.5) (Table 6.2).

Based on her clinical and radiographic examinations, a treatment plan of extracting four first premolars and anterior retraction with maximal anchorage was made. The patient chose lingual orthodontic appliances. To reinforce molar anchorage, two mini-implants were inserted at the U6-U7 site and used for anterior retraction (Figure 6.34). With the aid of the palatal mini-implants, anterior retraction was achieved smoothly and successfully (Figure 6.35).

Finally, bilateral class I molar relationship was maintained with normal overjet and overbite (Figure 6.36). Owing to anterior retraction with maximal molar anchorage, the patient's facial profile was significantly improved (Figure 6.37). The pre- and posttreatment cephalometric values and superimposition are displayed in Table 6.3 and Figure 6.38.

Table 6.2 Pretreatment lateral cephalometric analysis.

Measurement	Norm	Pretreatment
Skeletal (°)		
SNA	83.0±4.0	86.9
SNB	80.0±4.0	79.7
ANB	2.0±2.0	7.1
FMA	28.0±4.0	28.7
SN-MP	35.0±4.0	36.5
Dental (°)		
U1-SN	105.7±6.3	107.1
L1-MP	97.0±7.1	106.8
FMIA	65.0±6.0	44.5
U1-L1	124.0±8.0	109.6
Soft tissue (mm)		
UL-EP	2.0±2.0	3.9
LL-EP	3.0±2.0	7.7
Wits (mm)		
Wits	–1.0	–0.5



Figure 6.34 Intraoral photographs (five months into treatment). Two mini-implants were inserted at the palatal interradicular sites between the first and second molars. Anterior retraction was achieved by applying elastomeric chains between the lingual hooks and the palatal mini-implants.

t.me/Dr_Mouayyad_AlbtousH



Figure 6.35 Intraoral photographs (nine months into treatment). Anterior retraction was almost complete with the aid of the palatal mini-implants. Note the class I molar relationship was maintained during the treatment, without molar anchorage loss.



Figure 6.36 Posttreatment photographs. Class I canine and molar relationships were maintained, with normal overjet and overbite.

t.me/Dr_Mouayyad_AlbtousH



Figure 6.37 Pretreatment versus posttreatment facial profiles.

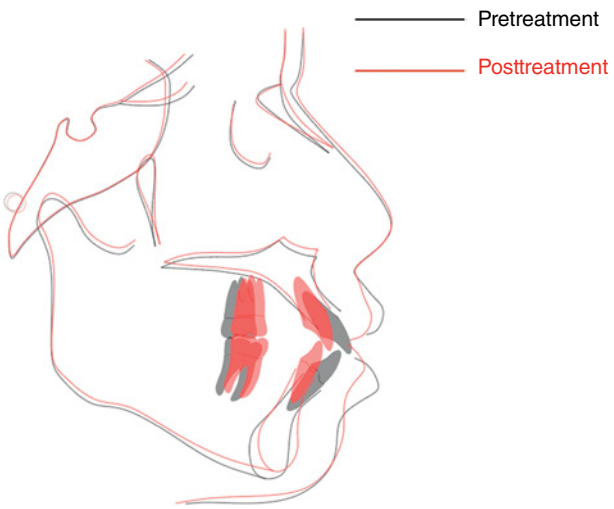


Figure 6.38 Pre- and posttreatment cephalometric superimposition.

Case 2 A female adult patient sought orthodontic treatment with a chief complaint of protrusive facial profile.[15] Her clinical examinations indicated a bilateral class I molar relationship, mild dental crowding, deep bite and protrusive facial profile (Figure 6.39). Lateral cephalometric analysis revealed that the patient had class I skeletal base (ANB = 3.6), normoclined upper incisors and labially proclined lower incisors (U1-SN = 107.2; L1-MP = 105.3), and normal mandibular plane angle (SN-MP = 31.9) (Table 6.4).

Table 6.3 Pre- and posttreatment lateral cephalometric analysis.

Measurement	Norm	Pretreatment	Posttreatment
Skeletal (°)			
SNA	83.0±4.0	86.9	84.7
SNB	80.0±4.0	79.7	79.5
ANB	2.0±2.0	7.1	5.2
FMA	28.0±4.0	28.7	28.9
SN-MP	35.0±4.0	36.5	35.4
Dental (°)			
U1-SN	105.7±6.3	107.1	95.0
L1-MP	97.0±7.1	106.8	92.0
FMIA	65.0±6.0	44.5	59.1
U1-L1	124.0±8.0	109.6	137.1
Soft tissue (mm)			
UL-EP	2.0±2.0	3.9	0.5
LL-EP	3.0±2.0	7.7	1.8
Wits (mm)			
Wits	−1.0	−0.5	−2.0

Extraction of four first premolars with subsequent anterior retraction was planned to resolve her protrusive profile. The patient chose to receive lingual brackets. To augment upper molar anchorage and facilitate anterior retraction, two palatal mini-implants were placed between the first and second molars (Figure 6.40). At the end of the orthodontic treatment, bilateral Class I molar and canine relationships were obtained, with normal overbite and overjet. Her profile aesthetics was significantly improved following the treatment (Figure 6.41). The pre- and posttreatment cephalometric values and superimposition are displayed in Table 6.5 and Figure 6.42.

t.me/Dr_Mouayyad_AlbtousH



Figure 6.39 Pretreatment photographs and radiographs. *Source:* Wang et al. [15], with permission from Elsevier.

t.me/Dr_Mouayyad_AlbtousH

Table 6.4 Pretreatment lateral cephalometric analysis.

Measurement	Norm	Pretreatment
Skeletal (°)		
SNA	83.0±4.0	83.4
SNB	80.0±4.0	79.8
ANB	2.0±2.0	3.6
FMA	28.0±4.0	24.3
SN-MP	35.0±4.0	31.9
Dental (°)		
U1-SN	105.7±6.3	107.2
L1-MP	97.0±7.1	105.3
FMIA	65.0±6.0	52.5
U1-L1	124.0±8.0	117.6
Soft tissue (mm)		
UL-EP	2.0±2.0	4.1
LL-EP	3.0±2.0	7.0
Wits (mm)		
Wits	−1.0	0

Molar Intrusion

Interradicular mini-implants in the palatal region can be used for molar intrusion in conjunction with buccal mini-implants. From the biomechanics perspective, the combination of buccal and palatal mini-implants facilitates the bodily intrusion of molars (Figure 6.43). Otherwise, if only buccal or palatal mini-implants are used for molar intrusion, inadvertent buccal tipping or lingual tipping of molars may occur (Figure 6.44). Moreover, from the occlusal view, the line connecting the buccal and palatal mini-implants should pass the centre of the molar, so that bodily intrusion of the molar can be achieved (Figure 6.45). The use of mini-implants for molar intrusion is biomechanically advantageous over a segmental archwire technique that may result in extrusion of anchorage teeth.

Molar Distalisation

Maxillary molar distalisation can be achieved through palatal interradicular mini-implants with the aid of a palatal arch between the two first molars. The palatal interradicular mini-implants can be placed at the level of the



Figure 6.40 Intraoral photographs. Two mini-implants were inserted at the palatal interradicular sites between the first and second molars. Anterior retraction was achieved by applying elastomeric chains between the archwire hooks and the palatal mini-implants. *Source:* Wang et al. [15], with permission from Elsevier.

t.me/Dr_Mouayyad_AlbtousH



Figure 6.41 Posttreatment photographs and radiographs. *Source:* Wang et al. [15], with permission from Elsevier.

t.me/Dr_Mouayyad_AlbtousH

Table 6.5 Pre- and posttreatment lateral cephalometric analysis.

Measurement	Norm	Pretreatment	Posttreatment
Skeletal (°)			
SNA	83.0±4.0	83.4	81.6
SNB	80.0±4.0	79.8	28.8
ANB	2.0±2.0	3.6	2.8
FMA	28.0±4.0	24.3	21.9
SN-MP	35.0±4.0	31.9	30.5
Dental (°)			
U1-SN	105.7±6.3	107.2	100.7
L1-MP	97.0±7.1	105.3	94.5
FMIA	65.0±6.0	52.5	63.6
U1-L1	124.0±8.0	117.6	134.3
Soft tissue (mm)			
UL-EP	2.0±2.0	4.1	1.8
LL-EP	3.012.0	7.0	3.8
Wits (mm)			
Wits	−1.0	0	−0.7

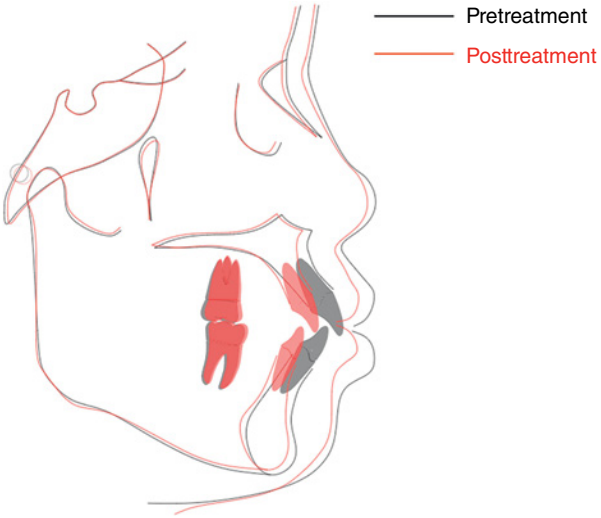


Figure 6.42 Pre- and posttreatment cephalometric superimposition.

center of resistance of the molars, so that bodily distalisation of molars can be achieved (Figure 6.46). A case example of molar distalisation through palatal interradicular mini-implants is given below.

A female adolescent presented to the orthodontic department with a chief complaint of crooked teeth and dental crowding. Her clinical examinations were indicative of severe crowding in the upper arch and mild crowding in the lower arch, with a straight facial profile. Molar and canine relationships were class II at both sides (Figure 6.47). Lateral cephalometric analysis revealed that the patient had a class II skeletal base (ANB = 4.1), retroclined upper and lower incisors (U1-SN = 91.8; L1-MP = 88.9) and high mandibular plane angle (SN-MP = 41.0) (Table 6.6).

Treatment planning was upper molar distalisation and expansion of upper and lower dental arches to resolve crowding. To achieve efficient molar distalisation, two palatal interradicular mini-implants were placed at the U5-U6 site. A palatal arch was bonded onto bilateral first molars and molar distalisation was achieved by applying closed-coil springs between the palatal arch and the mini-implants. Following molar distalisation, the labially blocked-out canines moved spontaneously into the dental arch (Figure 6.48). Then, fixed appliances were used for tooth alignment and arch levelling (Figure 6.49).

Following orthodontic treatment, class I canine and molar relationships were obtained with good buccal interdigitation (Figure 6.50). The pre- and posttreatment cephalometric values and superimposition are displayed in Table 6.7 and Figure 6.51.

t.me/Dr_Mouayyad_AlbtousH

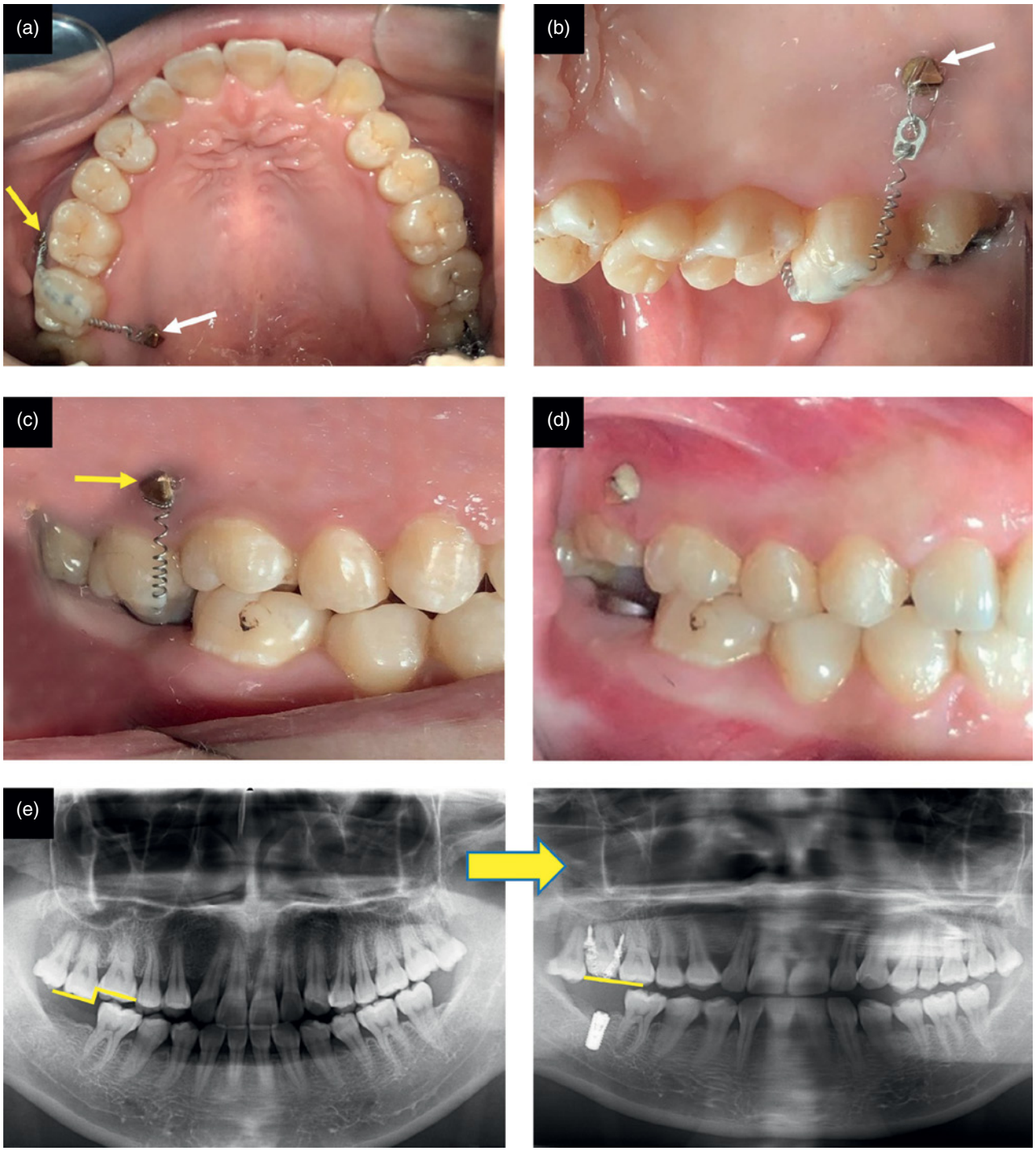


Figure 6.43 Molar intrusion with buccal and palatal mini-implants at the interradicular region. (a) Buccal (yellow arrow) and palatal (white arrow) mini-implants were inserted at the interradicular region. A closed-coil spring was employed for molar intrusion (occlusal view). (b) Palatal view. Note the palatal mini-implant (white arrow) that was inserted between the second and third molars. (c) Buccal view. Note the buccal mini-implant (yellow arrow). (d) Five months into treatment. The molar had been successfully intruded. (e) The maxillary right second molar was successfully intruded and an implant was placed at the mandibular posterior region to restore the missing mandibular right second molar.

t.me/Dr_Mouayyad_AlbtousH

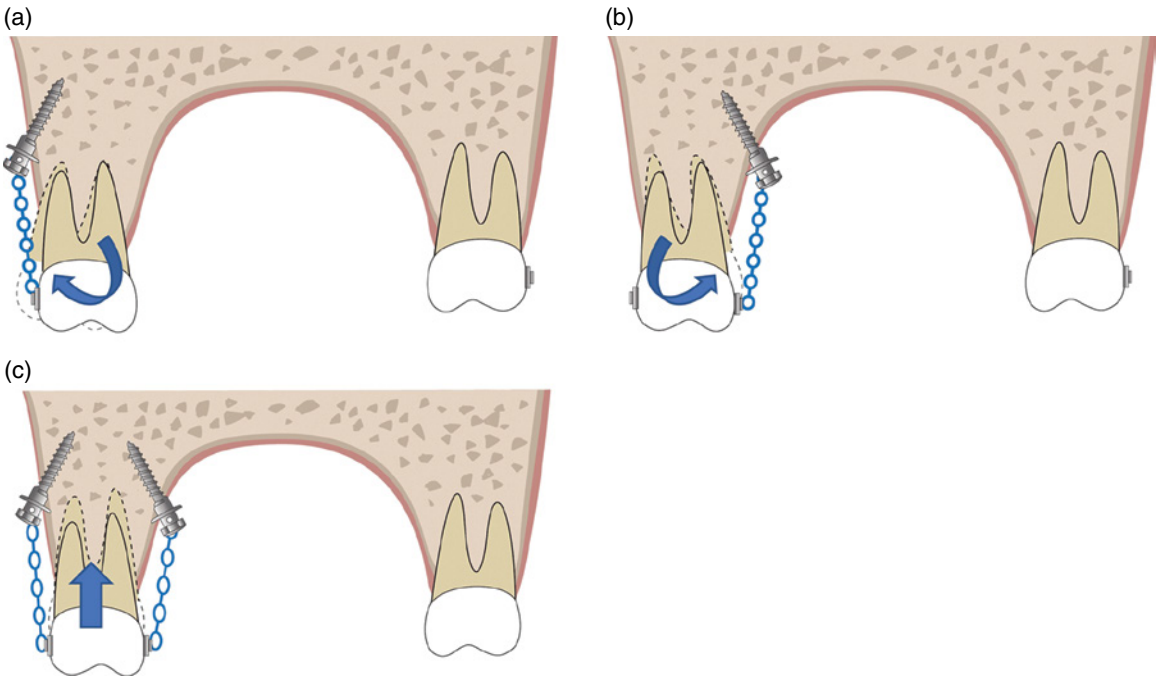
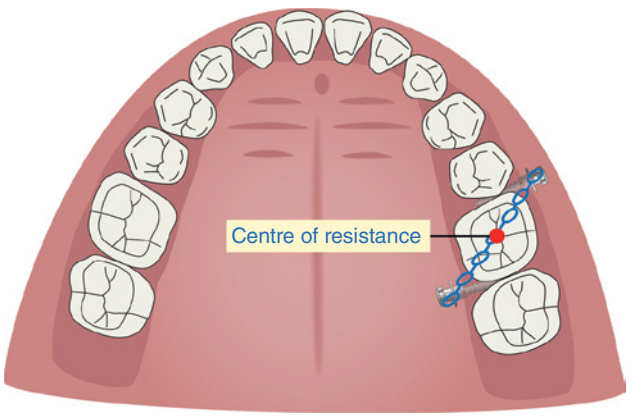


Figure 6.44 Molar intrusion with TADs. (a) A buccal mini-implant is used for molar intrusion and the molar exhibits buccal tipping during intrusion. (b) A palatal mini-implant is employed for molar intrusion and the molar is subject to lingual tipping during the intrusion. (c) Both the buccal and palatal mini-implants are utilised for molar intrusion, leading to bodily intrusion of the molar.

Figure 6.45 The line connecting the buccal and palatal mini-implants should pass through the centre of resistance (red dot) of the molar so that bodily intrusion can be achieved.



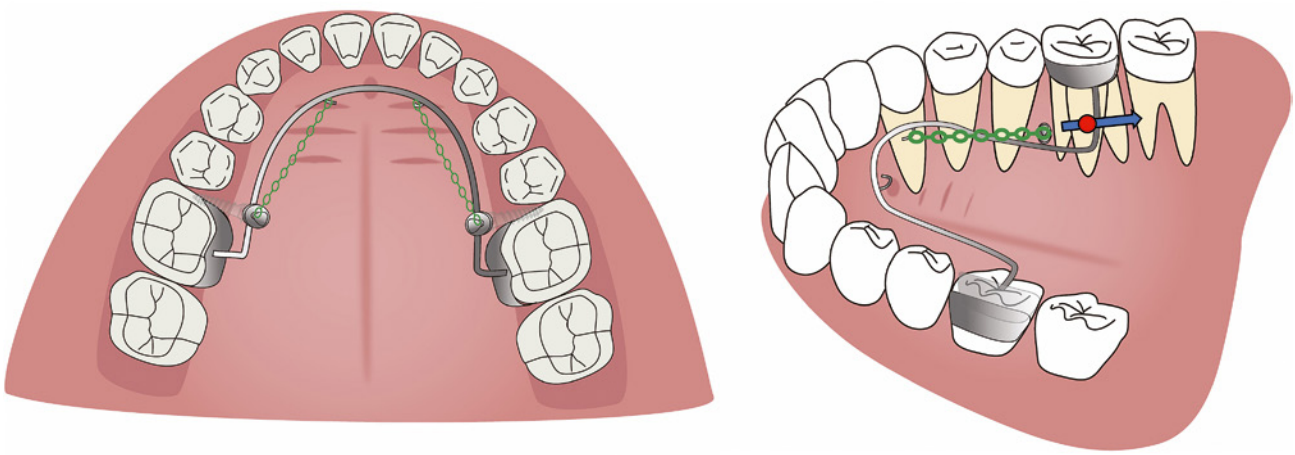


Figure 6.46 The molar distalisation force passes through the centre of resistance of the bilateral molars, leading to bodily distalisation of the molars.

t.me/Dr_Mouayyad_AlbtousH

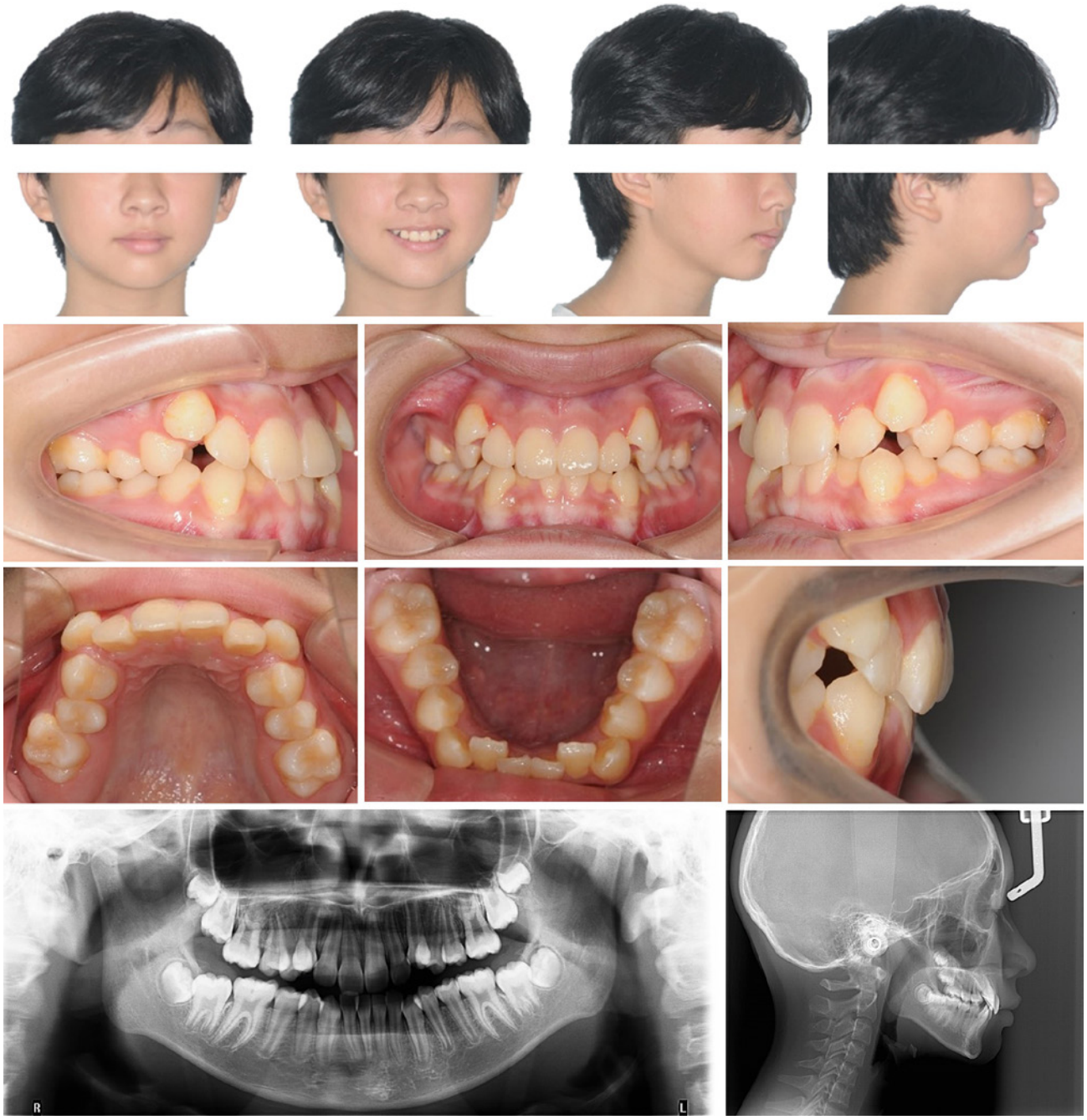


Figure 6.47 Pretreatment photographs and radiographs.

t.me/Dr_Mouayyad_AlbtousH

Table 6.6 Pretreatment lateral cephalometric analysis.

Measurement	Norm	Pretreatment
Skeletal (°)		
SNA	83.0±4.0	77.0
SNB	80.0±4.0	72.8
ANB	2.0±2.0	4.1
FMA	28.0±4.0	31.7
SN-MP	35.0±4.0	41.0
Dental (°)		
U1-SN	105.7±6.3	91.8
L1-MP	97.0±7.1	89.5
FMIA	65.0±6.0	58.8
U1-L1	124.0±8.0	137.7
Soft tissue (mm)		
UL-EP	2.0±2.0	0.7
LL-EP	3.0±2.0	1.3
Wits (mm)		
Wits	−1.0	−1.6

Molar Protraction

Molar protraction is a challenging orthodontic tooth movement that places high requirements on the anchorage teeth. If anterior teeth are employed as the anchorage, incisor retraction and lingual tipping will occur. The use of mini-implants is beneficial to augment anterior anchorage or eliminate the need to use incisors for anchorage. From the biomechanics perspectives, both buccal and palatal mini-implants should be used to offer mesialisation force. Moreover, to achieve bodily molar protraction, long hooks can be bonded onto molars so that the mesialisation force passes through the centre of resistance of the molar (Figure 6.52). Two case examples are given below.

Case 1 A male adult presented to the orthodontic department with a chief complaint of severe tooth decay of the upper left second molar (Figure 6.53). Multidisciplinary treatment plans were made for this patient. The first plan was to perform root canal therapy and subsequent crown restoration. The second plan was to extract the severely decayed second molar and perform implant restoration. The third plan was to extract the second molar and protract the third molar to substitute the second molar. The patient

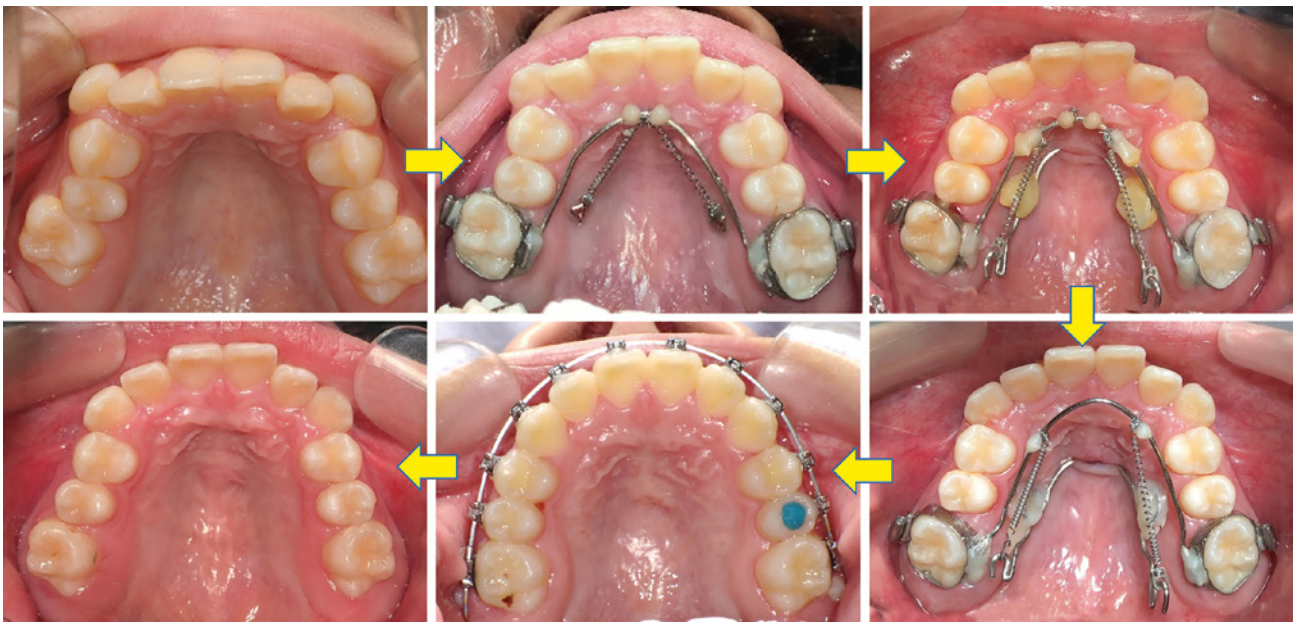


Figure 6.48 Progress of molar distalisation with the aid of mini-implants at the palatal interradicular region. With distalisation of the molars, the space was regained and the anterior crowding was resolved spontaneously.

t.me/Dr_Mouayyad_AlbtousH

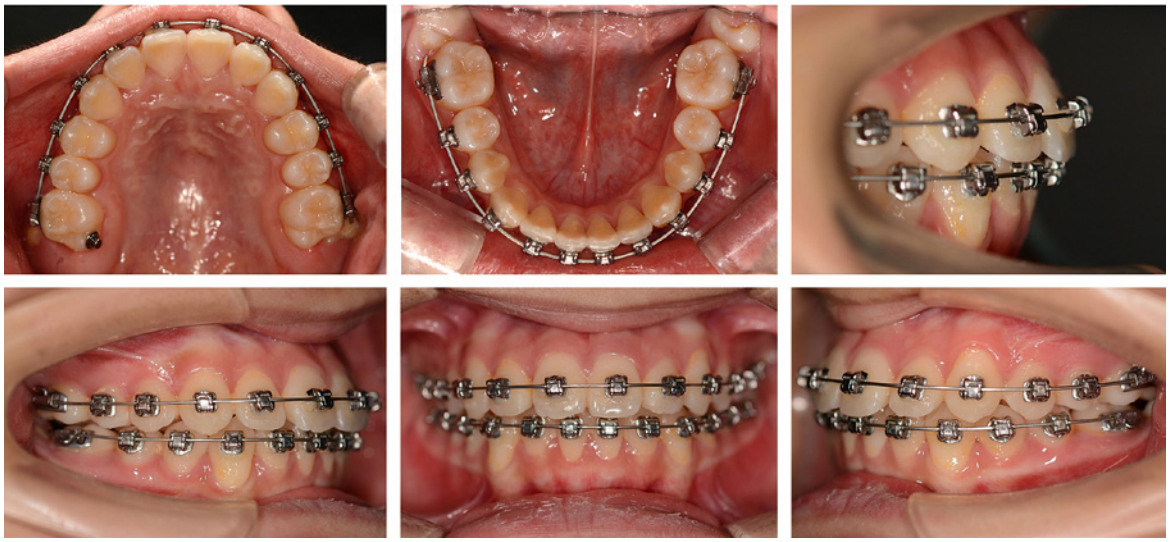


Figure 6.49 Following molar distalisation, fixed appliances were used for alignment and levelling.



Figure 6.50 Posttreatment photographs and radiographs.

t.me/Dr_Mouayyad_AlbtousH

Table 6.7 Pre- and posttreatment lateral cephalometric analysis.

Measurement	Norm	Pretreatment	Posttreatment
Skeletal (°)			
SNA	83.0±4.0	77.0	77.3
SNB	80.0±4.0	72.8	73.4
ANB	2.0±2.0	4.1	3.9
FMA	28.0±4.0	31.7	31.2
SN-MP	35.0±4.0	41.0	40.6
Dental (°)			
U1-SN	105.7±6.3	91.8	99.7
L1-MP	97.0±7.1	89.5	101.4
FMIA	65.0±6.0	58.8	47.4
U1-L1	124.0±8.0	137.7	118.4
Soft tissue (mm)			
UL-EP	2.0±2.0	0.7	1.5
LL-EP	3.0±2.0	1.3	4.1
Wits (mm)			
Wits	−1.0	−1.6	−1.6

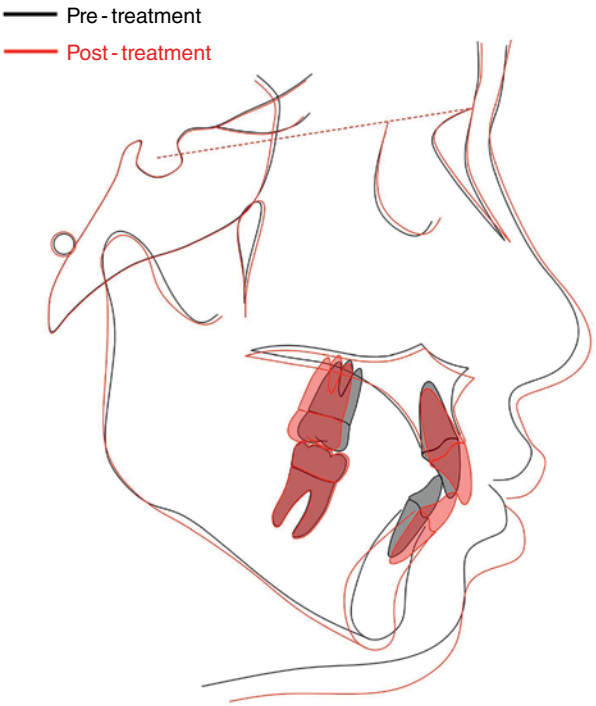


Figure 6.51 Pre- and posttreatment cephalometric superimposition.

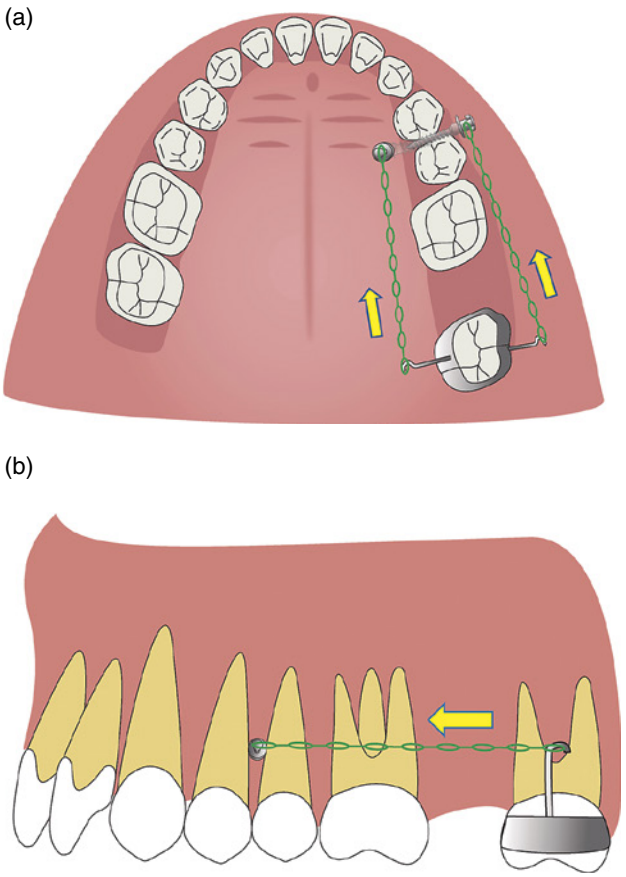


Figure 6.52 Schematic illustrations showing the biomechanics of molar protraction with two mini-implants (one at the buccal side and the other at the palatal side). (a) Occlusal view. Both mini-implants are employed for molar protraction and the protraction forces are applied at both the buccal and palatal sides. Thus, no rotation occurs during protraction. (b) Buccal view. The protraction force passes through the centre of resistance of the molar, leading to bodily protraction of the molar.

was informed of both the advantages and disadvantages of these treatment alternatives. The patient chose the third treatment plan, i.e. extraction of the second molar and protraction of the third molar.

One buccal and one palatal mini-implant were placed at the interradicular site between the first and second premolars. Two long hooks were bonded onto the third molar, with one on the buccal side and the other on the palatal side. The protraction of the third molar was achieved by applying closed-coil springs between the mini-implants and the long hooks on the third molar (Figure 6.54). Finally, the third molar was successfully protracted to substitute the second molar with good root parallelism (Figure 6.55).

Case 2 A female adult presented to the orthodontic department with a chief complaint of a missing tooth. The

t.me/Dr_Mouayyad_AlbtousH

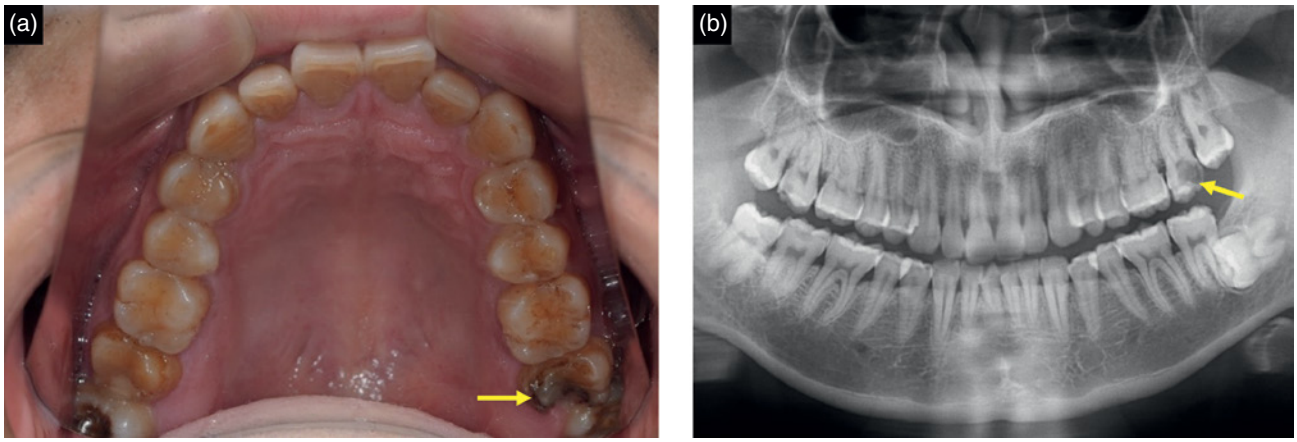


Figure 6.53 Pretreatment photograph and panoramic radiograph. (a) Intraoral photograph. The maxillary left second molar exhibited severe caries (yellow arrow). (b) Panoramic radiograph showing that the maxillary left second molar had a large area of decay (yellow arrow).



Figure 6.54 The maxillary left third molar was protracted by the two mini-implants inserted at the buccal and palatal interradicular sites. Two long hooks were bonded onto the buccal and palatal tooth surfaces of the third molar and closed-coil springs were applied between the long hooks and the mini-implants.

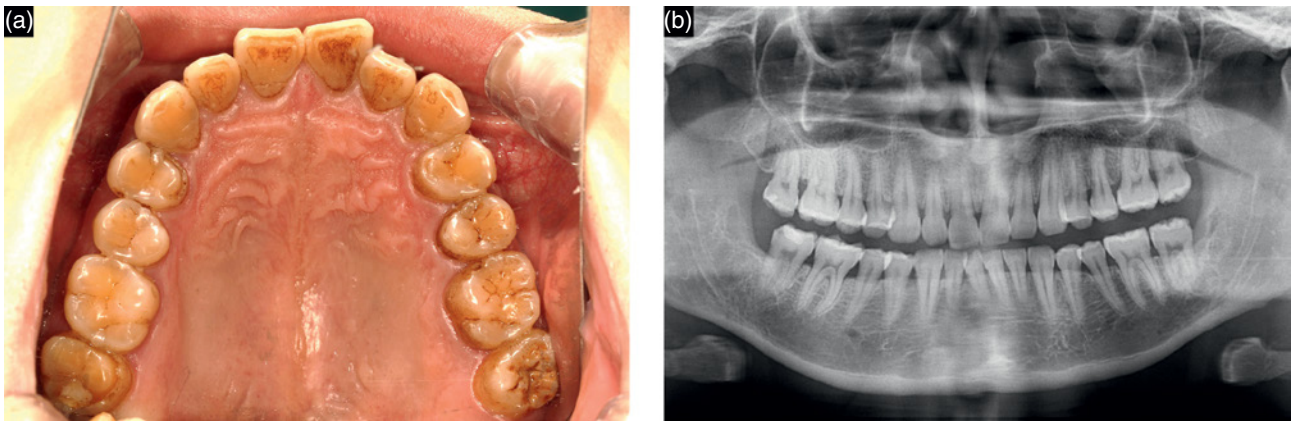


Figure 6.55 Posttreatment photograph and radiograph. (a) Intraoral photograph. (b) Panoramic radiograph.

t.me/Dr_Mouayyad_AlbtousH

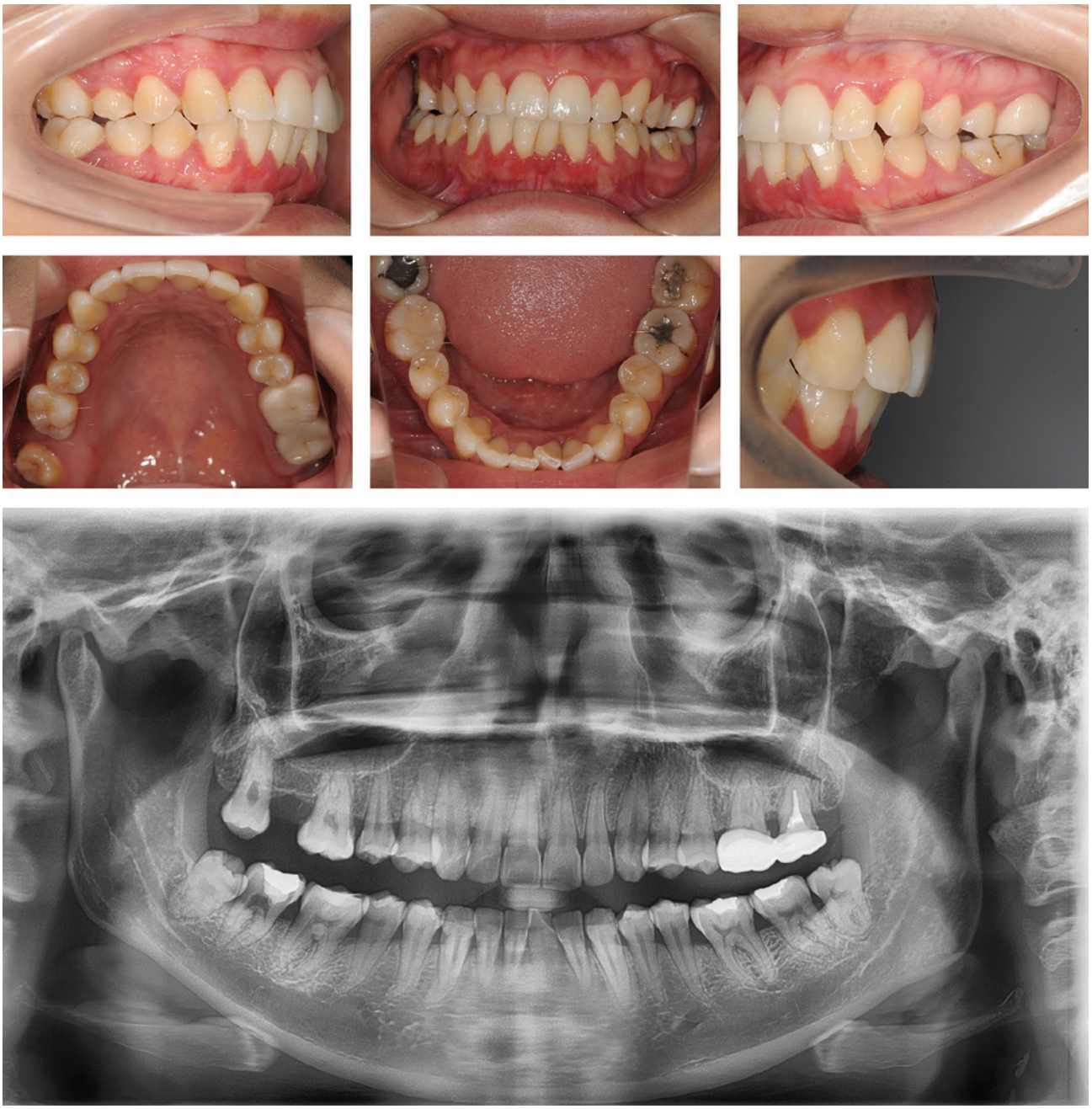


Figure 6.56 Pretreatment photographs and panoramic radiograph.

clinical and radiographic examinations revealed that she had class II canine and molar relationships on both sides, mild crowding and a missing maxillary right second molar (Figure 6.56). Following thorough discussions with the patient, protraction of the maxillary right third molar was planned to substitute the missing second molar with segmental archwire technique (Figure 6.57). The third molar was successfully protracted to substitute the missing second molar with good root parallelism, and a multi-stranded lingual retainer was utilised for retention (Figure 6.58).

t.me/Dr_Mouayyad_AlbtousH

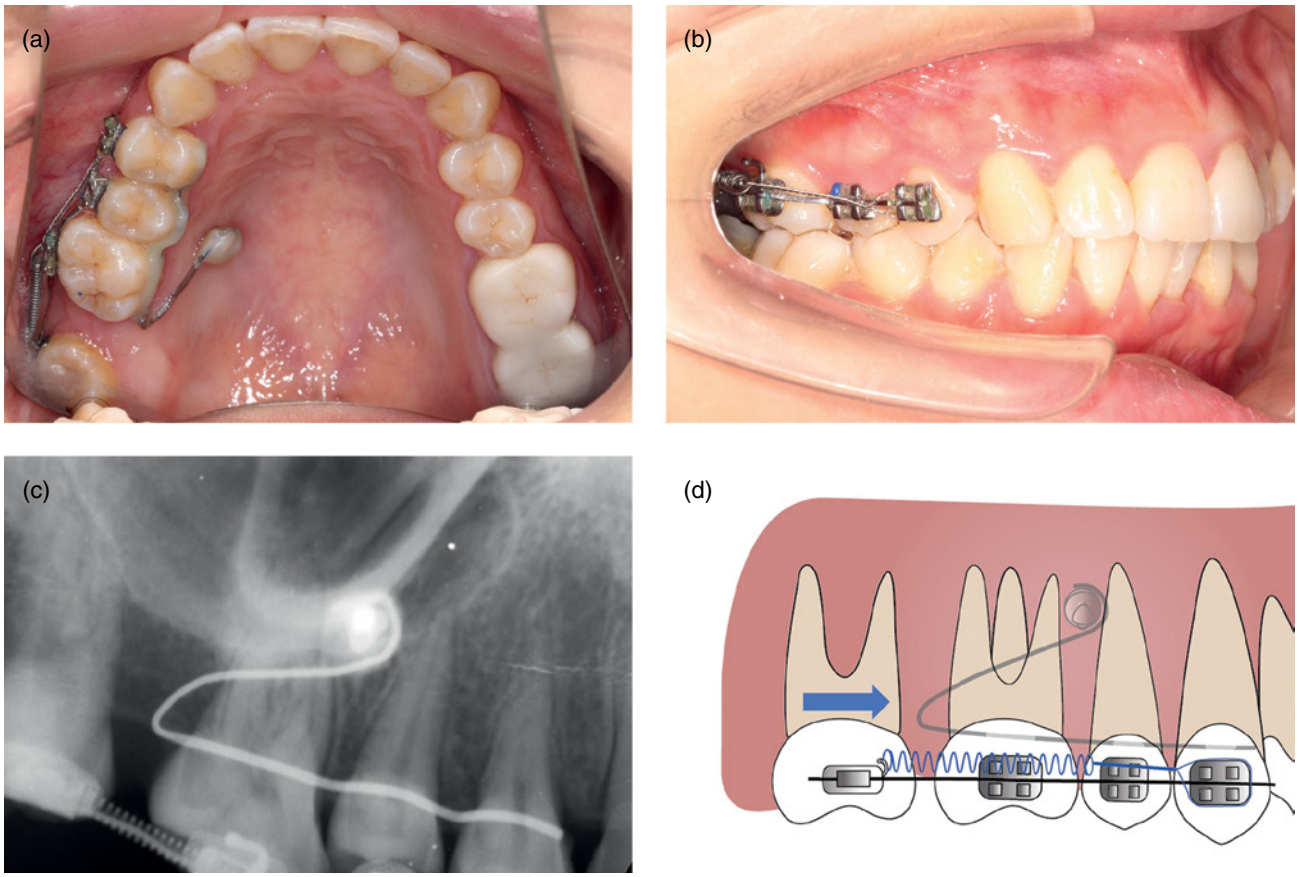


Figure 6.57 Molar protraction with a mini-implant inserted at the palatal interradicular region. (a) Occlusal view. A mini-implant was inserted at the palatal interradicular region between the second premolar and first molar. The first premolar, second premolar and first molar were fixed and stabilised by the palatal mini-implant, so that the anchorage of these teeth was reinforced. Segmental archwire technique was employed at the buccal side to protract the third molar through a closed-coil spring. (b) Buccal view. (c) Periapical radiograph showing the mini-implant and segmental archwire. (d) A schematic illustration showing the palatal mini-implant and buccal segmental archwire.

t.me/Dr_Mouayyad_AlbtousH



Figure 6.58 Posttreatment photographs and panoramic radiograph.

t.me/Dr_Mouayyad_AlbtousH

6.3 Paramedian Sites

6.3.1 Anatomical Characteristics

The paramedian region is located 2 mm laterally to the midpalatal suture and is considered to be a good alternative to palatal interradicular sites owing to its good bone quantity and quality (Figure 6.59). Moreover, this anatomical region is fully covered by keratinised and attached soft tissue, rendering soft tissue complications less likely compared with areas covered by movable mucosa. A recent systematic review revealed that the success rate of mini-implants placed at this region is as high as 95%, indicating that the paramedian region is a reliable and stable site for accommodation of mini-implants.[4] The nasal cavity is located superiorly to the paramedian region and should be considered prior to the placement of mini-implants.

To select the most appropriate insertion sites, both hard tissue and soft tissue factors as well as vital anatomical structures (nasal cavity and greater palatine neurovascular bundles) should be carefully evaluated before insertion and these will be discussed below.

Hard Tissue Factor: Cortical Thickness

Cortical thickness is recommended to be at least 1 mm so that adequate primary stability of mini-implants can be guaranteed. In the paramedian region, the cortical thickness is greater than 1 mm and is considered to be sufficient for the placement of mini-implants.[16] The cortical thickness at different sites of the paramedian region is displayed in Figure 6.60. The average value of cortical thickness becomes greater posteriorly at the 2 mm and 4 mm sites lateral to the mid palatal suture and smaller posteriorly at the 6 mm and 8 mm sites lateral to the midpalatal suture.[17] However, these differences are not of statistical or clinical significance, indicating that cortical thickness does not vary significantly among different sites in the paramedian region.[17] Generally, cortical thickness is greater in adults than in adolescents (Figure 6.61), which may partially

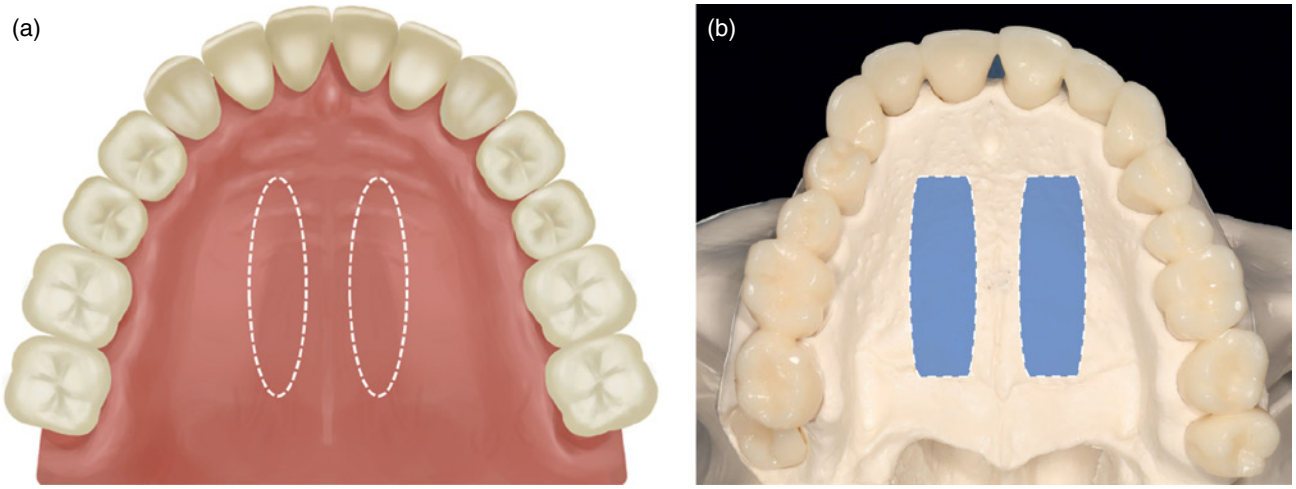


Figure 6.59 Paramedian region. (a) Schematic illustration showing the paramedian region (encircled by white dashed line). (b) A skull model showing the paramedian region (blue areas).

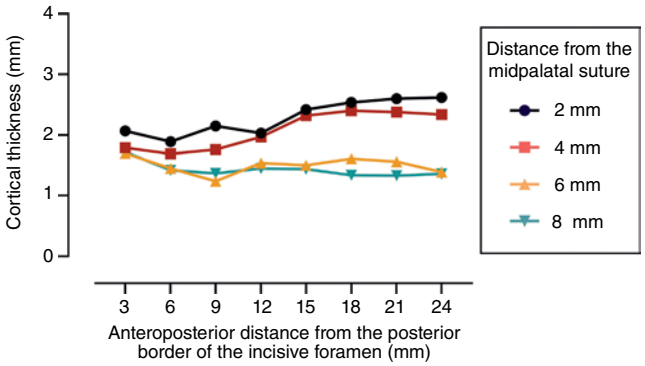


Figure 6.60 Cortical thickness at different sites of the paramedian region in adults. *Source:* Adapted from Chang et al. [17].

t.me/Dr_Mouayyad_AlbtousH

explain the higher success rate of mini-implants in adults. Nevertheless, regardless of patient age, cortical thickness is greater than 1 mm at different sites of the paramedian region. Thus, this anatomical factor need not be considered in determining the optimal insertion site, since almost all insertion sites satisfy the minimum requirements and are qualified for the placement of mini-implants.

Hard Tissue Factor: Bone Depth

Bone depth is a critical factor in choosing the most appropriate insertion site for the placement of mini-implants in the paramedian region, since bone depth varies greatly at different sites of the paramedian region.[16,18] In our previous study, we measured the bone depth (hard tissue thickness) of the palatal region and found that it varied in both anteroposterior and mediolateral dimensions (Figure 6.62).[2] Specifically, in the anteroposterior dimension, bone depth decreases from the anterior to the posterior region, with that at the first premolar region being the greatest (Figure 6.63). In the mediolateral dimension, interestingly, bone depth decreases from the midpalatal suture to the lateral region at the first molar and second molar regions, while it remains almost constant at the second premolar region and increases in the mediolateral direction for the first premolar region. Both gender and age have an impact on bone depth, with male adults exhibiting the greatest bone depth.[2]

Soft Tissue Factor: Soft Tissue Thickness

Soft tissue thickness is an important factor for the selection of optimal insertion sites. Based on our previous study,[2] soft tissue thickness increases from the median to lateral region (Figure 6.64). As displayed in Figure 6.64, soft tissue thickness is less than 3 mm at the paramedian region that is 2–4 mm lateral to the midpalatal suture while it is 4–6 mm at the region that is 10 mm lateral to the suture. Thus, mini-implants should not be placed too far away from the midpalatal suture, in order to prevent soft tissue complications. Moreover, slight differences exhibit between the first premolar region and the other three regions.

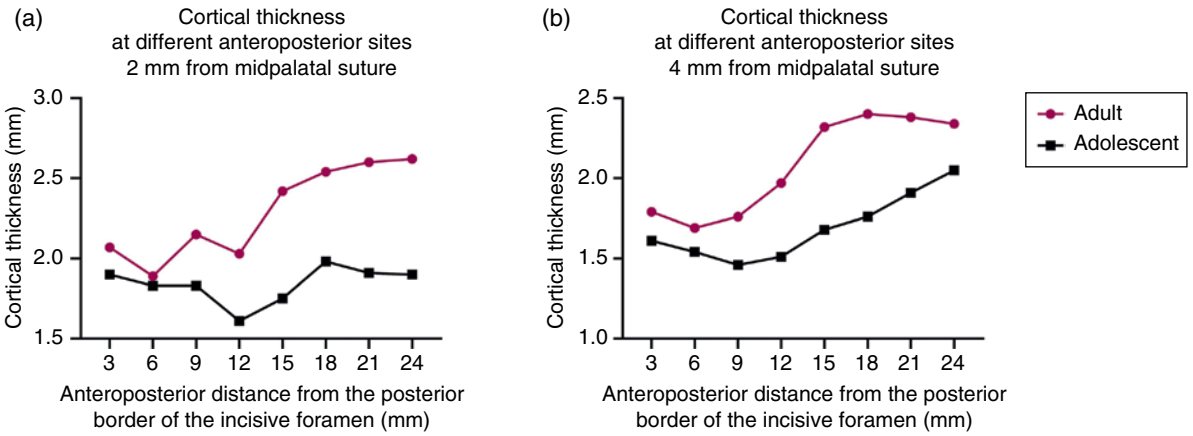
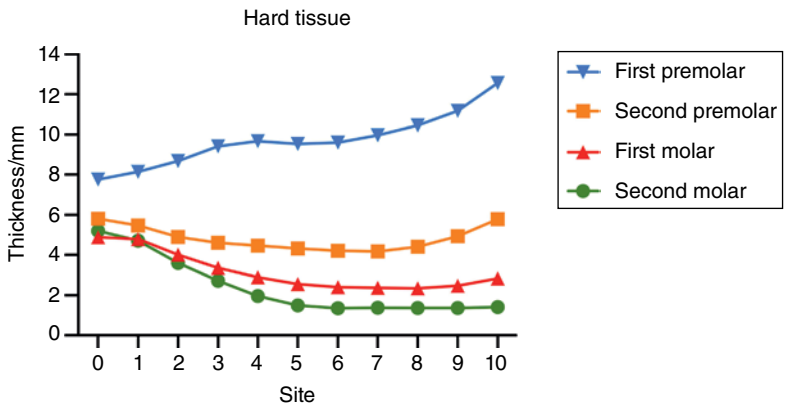


Figure 6.61 The differences of cortical thickness at different anteroposterior sites between adults and adolescents. (a) 2 mm away from the midpalatal suture. (b) 4 mm away from the midpalatal suture. *Source:* Adapted from Chang et al. [17].

Figure 6.62 Bone depth of the paramedian region at different distances (1–10 mm) lateral to the midpalatal suture at different anteroposterior sites (first premolar, second premolar, first molar and second molar). *Source:* Adapted from Lyu et al. [2].



t.me/Dr_Mouayyad_AlbtousH

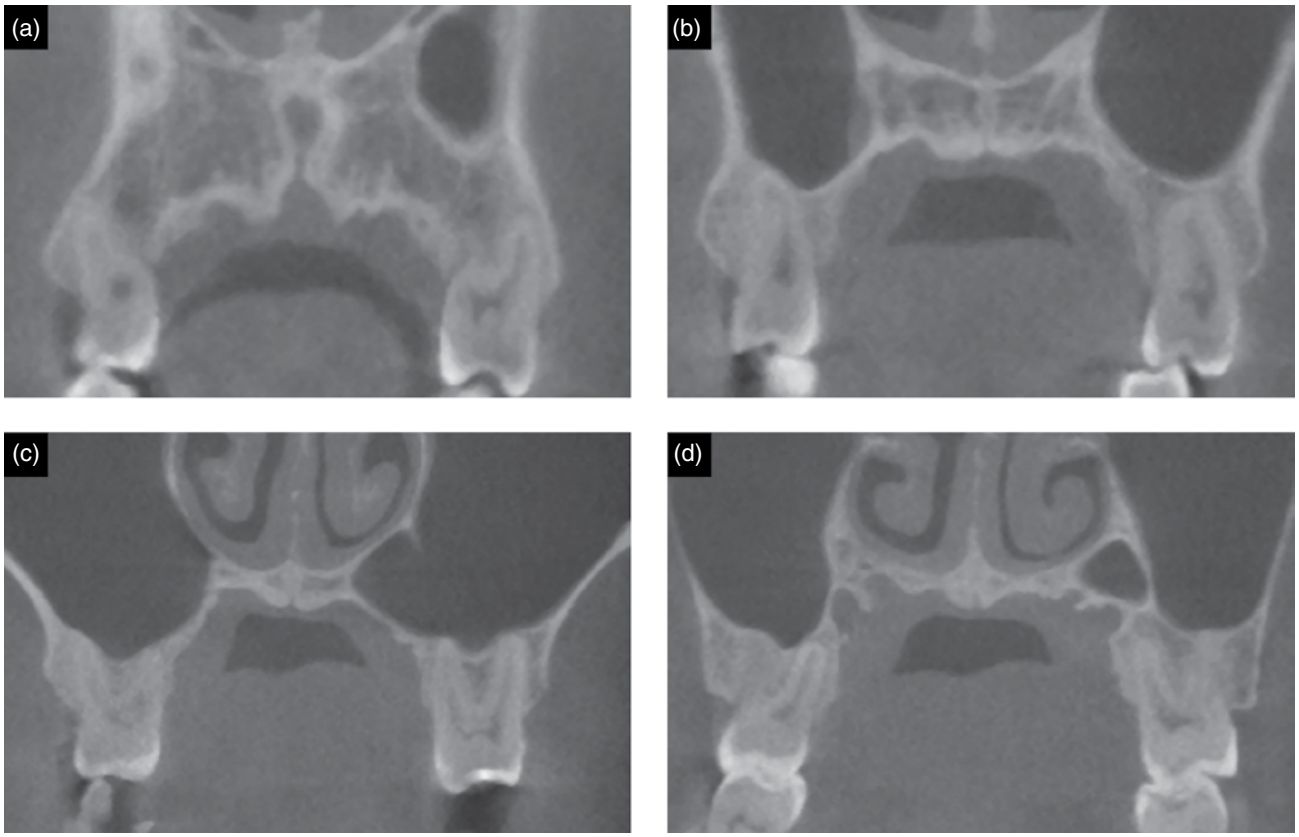


Figure 6.63 Bone depth at different anteroposterior sites. (a) First premolar region. (b) Second premolar region. (c) First molar region. (d) Second molar region.

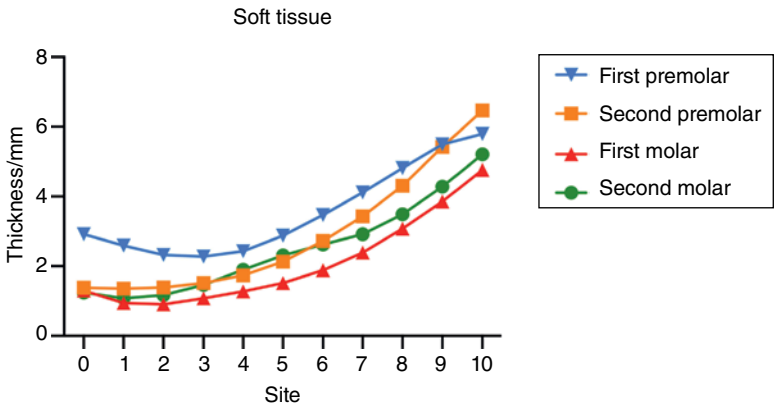


Figure 6.64 Soft tissue thickness of the paramedian region at different distances (1–10 mm) laterally to the midpalatal suture at different anteroposterior sites (first premolar, second premolar, first molar and second molar). *Source:* Adapted from Lyu et al. [2].

Vital Anatomical Structures

In the paramedian region, two vital anatomical structures, the greater palatine bundles and nasal cavity, should be taken into consideration when determining the optimal insertion sites. As mentioned above, the greater palatal neurovascular bundles exit from the greater palatine foramen that is 15 mm lateral to the midpalatal suture. Since they are mainly present in the interradicular region, placing mini-implants in the paramedian region has a low risk of damage to greater palatine vessels and nerves (Figure 6.65). Thus, injury to greater palatine bundles is not a concern for mini-implants inserted at this region.

Penetration into the nasal cavity was previously considered as a concern and it was advised to avoid penetration of the nasal cavity.[19] However, recent advances indicate that the nasal cavity should not be a concern and the resulting bicortical engagement is more biomechanically stable.[20,21] Based on our clinical experience, nasal penetration by

t.me/Dr_Mouayyad_AlbtousH

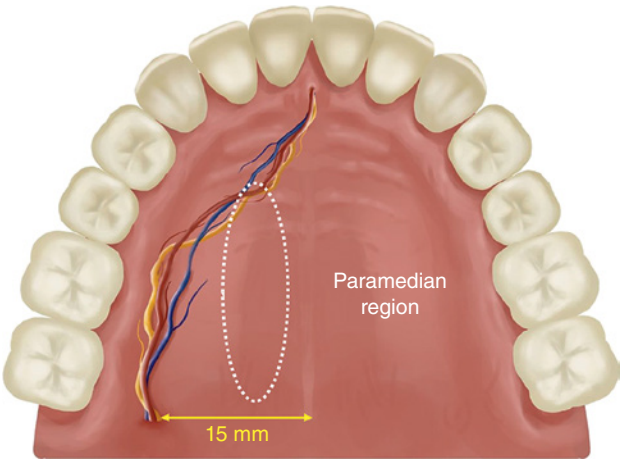


Figure 6.65 The location of the greater palatine neurovascular bundles that exit from the greater palatine foramen (15 mm laterally to the midpalatal suture). The bundles mainly travel at the lateral wall of the palatal vault.

mini-implants is often manifested as mild pain during insertion and transient nasal discomfort following insertion. Also, following insertion, up to 10% patients may experience transient sneezing that only persists for 1–2 minutes. However, if active nasal inflammation is present, nasal penetration should be avoided during insertion or the placement of mini-implants should be postponed.

Thus, unless pre-existing nasal infections are present, we recommend mini-implants be placed to penetrate the nasal cavity so that bicortical engagement can be achieved (Figure 6.66).

6.3.2 Biomechanical Considerations

Mini-implants placed at the paramedian region are versatile in satisfying different biomechanical demands. Generally, mini-implants are not resistant to rotation, tipping or pull-out. Thus, insertion angles of mini-implants should be individually designed for different biomechanical requirements. For example, if a paramedian mini-implant is used in conjunction with a buccal mini-implant to intrude molars, the long axis of the palatal mini-implant should not be parallel to the force that is applied on the mini-implant (Figure 6.67). This is biomechanically disadvantageous to the mini-implant, since the force that is applied on the mini-implant 'pulls' out the mini-implant from the palatal bone.

Auxiliary appliances are sometimes fixed onto paramedian mini-implants to offer extension arms or hooks that can reach optimal locations, so that desirable biomechanics can be offered. For example, paramedian mini-implants can be used for molar distalisation. However, the paramedian mini-implants are apical to the centre of resistance of the molars. Thus, extension hooks can be fixed onto the mini-implants and are precisely designed at the same level as the centre of resistance, so that bodily distalisation of molars can be accomplished (Figure 6.68). If the two mini-implants are in the same coronal plane, they will be subject to great tipping force that may result in mini-implant failure. Thus, the anteroposterior distance between the two mini-implants should be large enough to counteract this tipping force (Figure 6.69).

6.3.3 Selection of Optimal Insertion Sites

Both the hard tissue and soft tissue factors should be considered when determining the optimal insertion sites. The recommended hard tissue thickness (bone depth) and soft tissue thickness are greater than 4.5 mm and less than 2 mm, respectively.[2] For hard tissue thickness, the area with thickness greater than 4.5 mm is defined as optimal while that with thickness ranging from 2 mm to 4.5 mm is suboptimal. Likewise, for soft tissue thickness, the area with thickness less than 2 mm is defined as optimal while that with thickness ranging from 2 mm to 4 mm is regarded as suboptimal. Based on the data from our previous study,[2] we mapped the optimal and suboptimal areas for the placement of mini-implants at the paramedian region (Figure 6.70).

6.3.4 Insertion Techniques

Preinsertion

First, anchorage requirements and clinical procedures should be determined according to treatment goals. All the clinical details should be elaborated before insertion. For example, if mini-implant-assisted maxillary expansion is planned, the mini-implants should be placed after expansion devices are fabricated and bonded (Figure 6.71). In contrast, if molar distalisation is planned, the mini-implants should be placed first, followed by fixation of extension hooks onto the mini-implants (Figure 6.72).

t.me/Dr_Mouayyad_AlbtousH

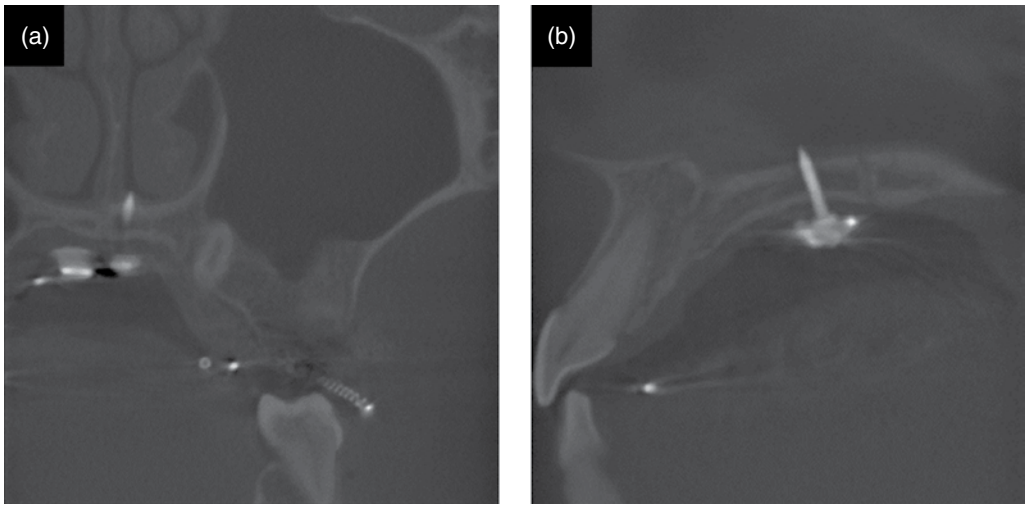


Figure 6.66 Bicortical engagement mode for the mini-implant inserted at the paramedian region. (a) Coronal section. (b) Sagittal section. Note the penetration of the nasal cavity by the mini-implant.

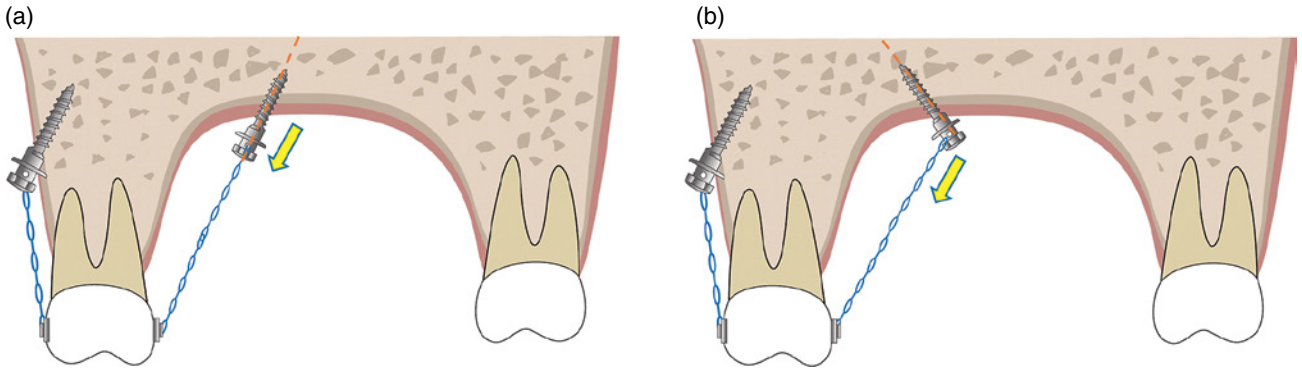


Figure 6.67 (a) Elastomeric chains are used for molar intrusion and the reciprocal pull-out force applied on the mini-implant is in parallel to the long axis of the mini-implant. The mini-implant is susceptible to failure and loosening due to its low capacity in resisting the pull-out force. (b) The reciprocal force applied on the mini-implant is in angulation with the long axis of the mini-implant. Thus, the mini-implant is more resistant to the reciprocal force.

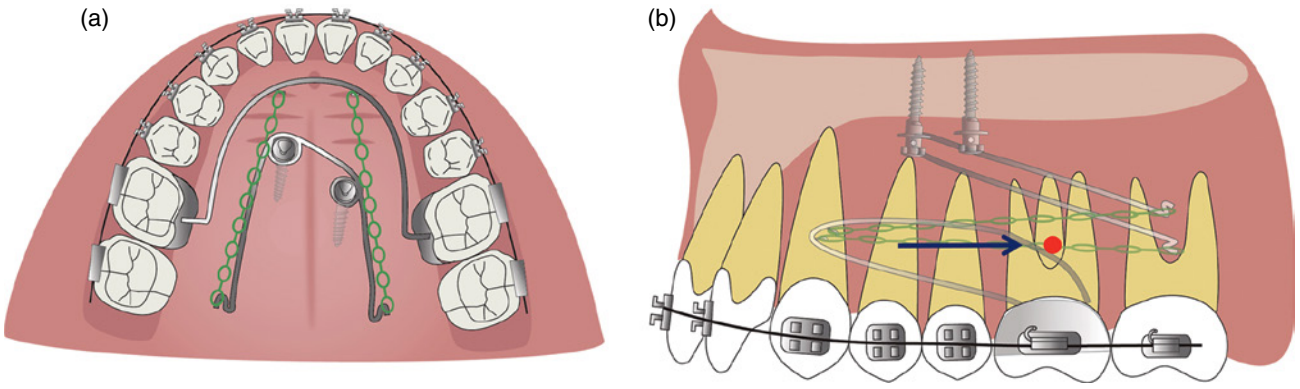


Figure 6.68 Schematic illustrations of bodily distalisation of maxillary molars with mini-implants at the paramedian region. (a) Occlusal view. (b) Buccal view. The distalisation force passes through the centre of resistance of the molars so that bodily distalisation of the molars can be achieved.

t.me/Dr_Mouayyad_AlbtousH

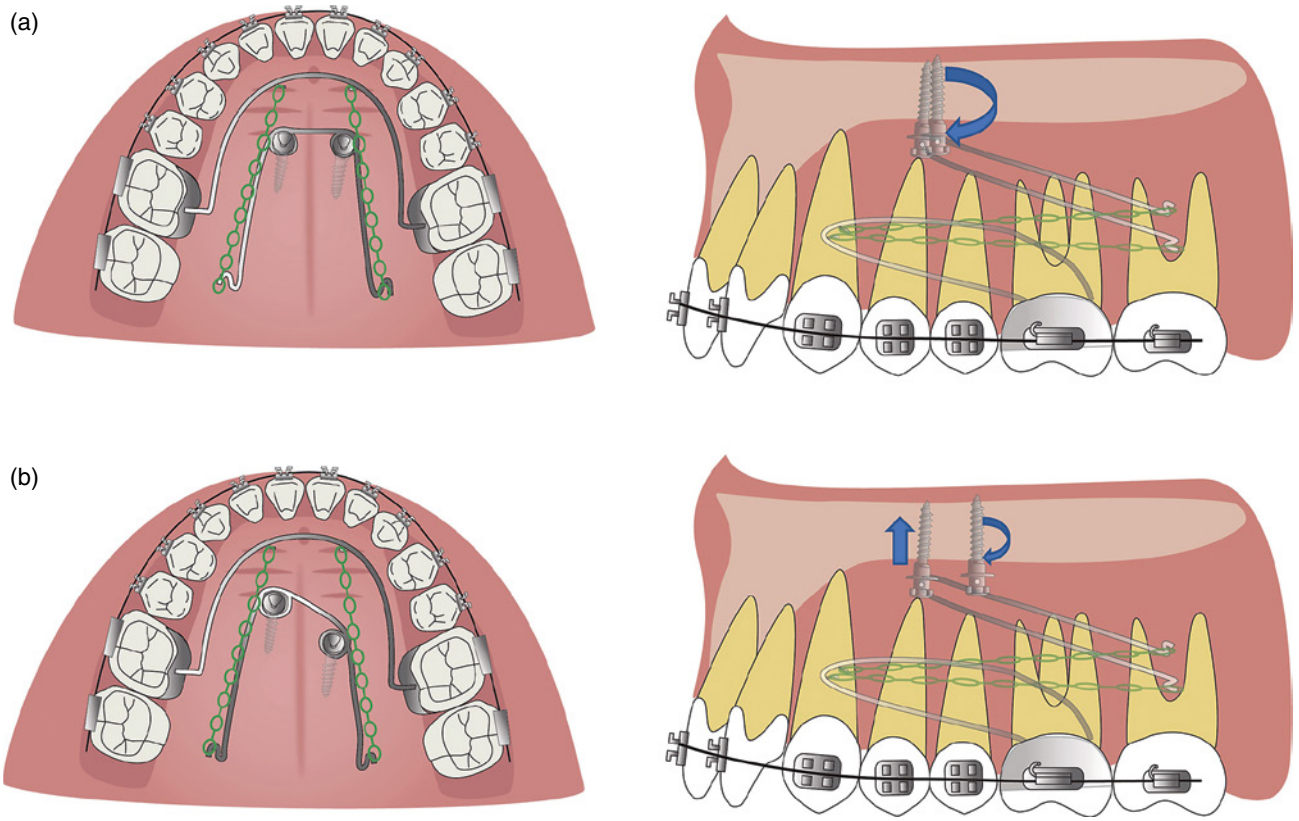


Figure 6.69 (a) Two mini-implants are placed at the same coronal plane and exhibit low capacity in resisting the reciprocal force, leading to mesial tipping of the whole palatal appliance fixed onto the mini-implants. (b) The two mini-implants are placed at different coronal planes and are more resistant to the reciprocal force. The anterior mini-implant is mainly subject to intrusion and the posterior one exhibits a small tendency of mesial tipping.

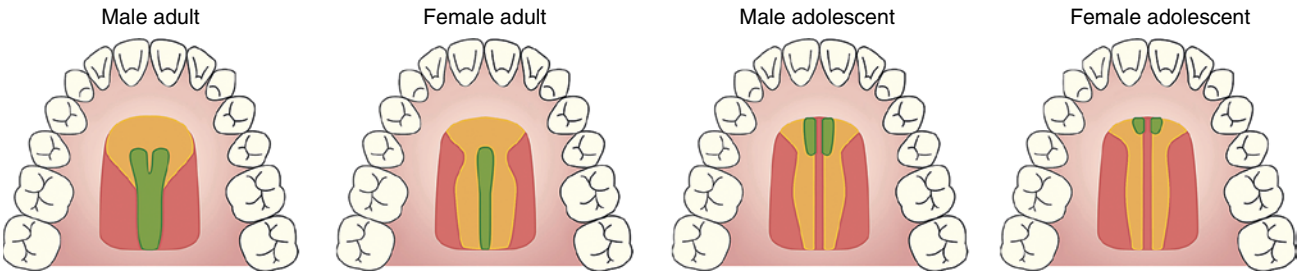


Figure 6.70 The optimal region (green), suboptimal region (yellow) and not recommended region (red) for the placement of mini-implants at the palatal region for male adults, female adults, male adolescents and female adolescents.



Figure 6.71 (a) The expansion device was fabricated before the insertion of palatal mini-implants. Before insertion, the device was tried on to test the fit. (b) Four mini-implants were inserted through the holes of the expansion device at the paramedian region. (c) Following insertion of the mini-implants, the expansion device and mini-implants were fixed through flowable resin.

t.me/Dr_Mouayyad_AlbtousH

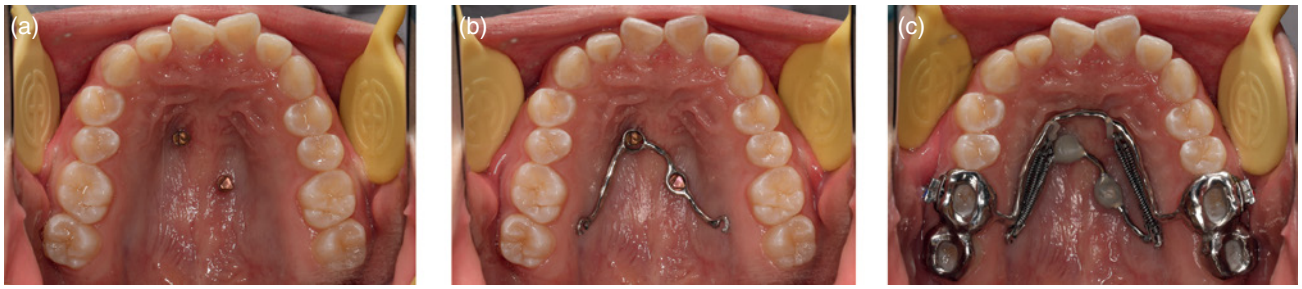


Figure 6.72 (a) Before the insertion of mini-implants. (b) Insertion of the mini-implants at the paramedian region. (c) Fixation of the extension hooks onto the mini-implants.

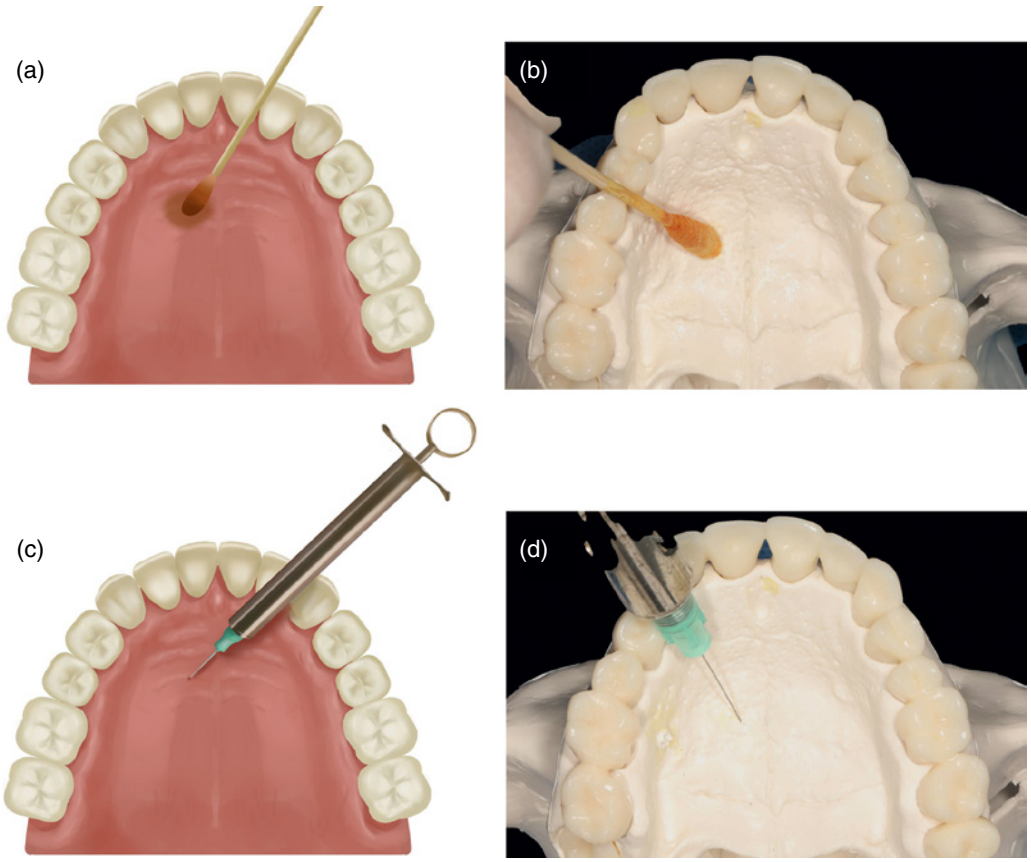


Figure 6.73 (a,b) Mucosa disinfection with iodophor. (c,d) Local infiltration anaesthesia.

Second, based on the CBCT images of the patient, the optimal insertion sites are determined. Mini-implants with appropriate lengths and diameters are selected based on hard tissue and soft tissue thickness. Furthermore, insertion angles should be determined based on different biomechanical demands.

Third, insertion guides can be designed and fabricated through 3-D techniques. This is helpful for novice or inexperienced operators to achieve accurate and precise placement of mini-implants.

Insertion

First, local infiltration anaesthesia is performed following local mucosa disinfection with iodophor (Figure 6.73). However, since the keratinised mucosa is firmly attached onto the hard palate, direct injection of infiltration anaesthetics is very painful. Thus, prior to local infiltration, topical anaesthesia is recommended. During the injection of local infiltration anaesthetics, due to the high resistance, slow injection rate is highly recommended and the injection should be stopped when soft tissue blanching is

t.me/Dr_Mouayyad_AlbtousH

observed. Soft tissue blanching is indicative of sufficient anaesthesia. Occasionally, block anaesthesia of the greater palatine nerve and nasopalatine nerve rather than local infiltration anaesthesia is indicated if mini-implants are to be placed at several dispersed sites at the paramedian region.

Second, the entry point should be marked at the predetermined site with an explorer or probe (Figure 6.74). The entry point is often marked with the upper dentition being the reference. Thus, marking the entry point with the naked eye from the chairside may lead to error since the operator's line of view is not perpendicular to the occlusal plane. This usually results in the marked entry point being distal to the desired one (Figure 6.75). Thus, we recommend operators look through a mirror reflector to locate and mark the desired entry point from the occlusal side (Figure 6.76).

Third, once the entry point is marked, the next step is to insert the mini-implant through the marked entry point. For placement of mini-implants at the paramedian region, contra-angle screwdrivers are recommended so that inserting mini-implants perpendicularly to the occlusal plane can be achieved (Figure 6.77). While the operator is rotating the screwdriver to insert the mini-implant with the right hand, the screwdriver should be stabilised by the left hand (Figure 6.78). Stabilisation of the screwdriver is very important since rotation of the contra-angle screwdriver results in lateral displacement of the screwdriver, which may lead to mini-implant fracture. Due to the thick cortical plate, it is often difficult to penetrate the cortex.

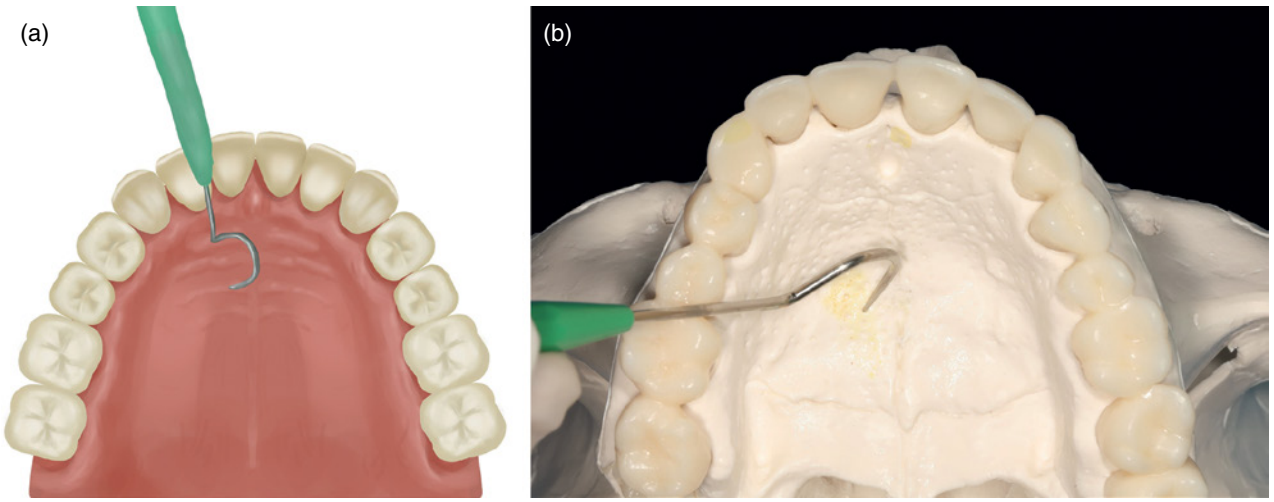
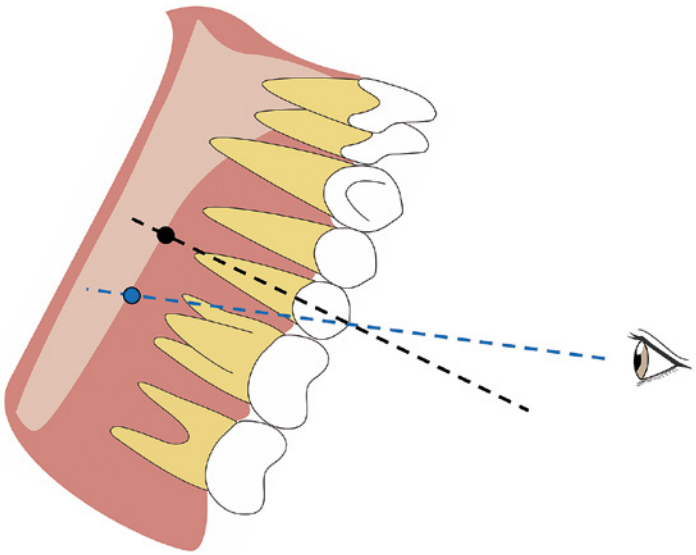


Figure 6.74 The desired entry point is marked with an explorer. (a) Illustration. (b) Skull model.

Figure 6.75 The entry point for the paramedian region is often determined in reference to the upper dentition. For example, if the desired entry point (black dot) is at the coronal plane corresponding to the second premolar, the deviated line of view may lead to a more distal location of the entry point (blue dot).



t.me/Dr_Mouayyad_AlbtousH

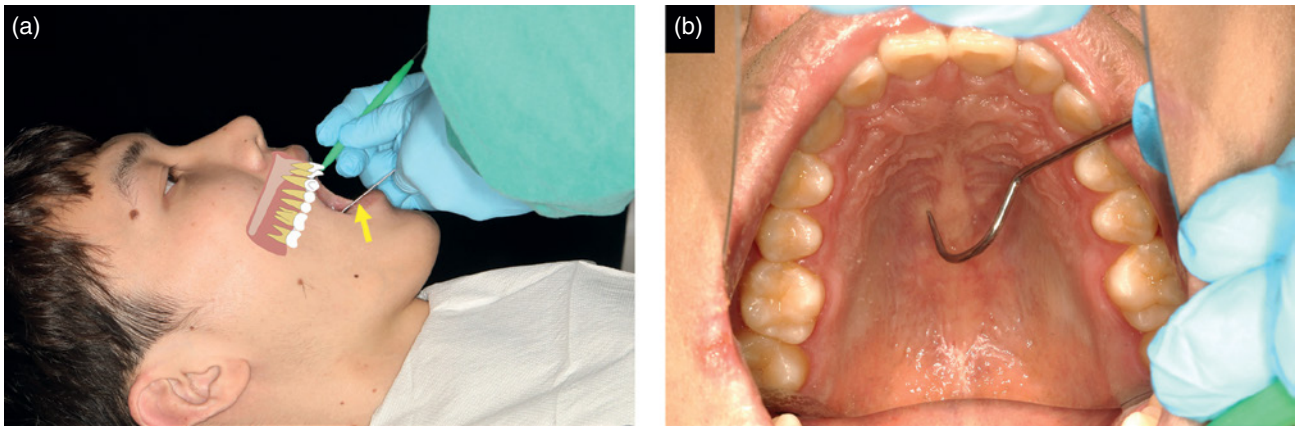


Figure 6.76 (a) A mirror reflector (yellow arrow) is used to help locate and mark the desired entry point. (b) Mark the entry point by using the mirror reflector.

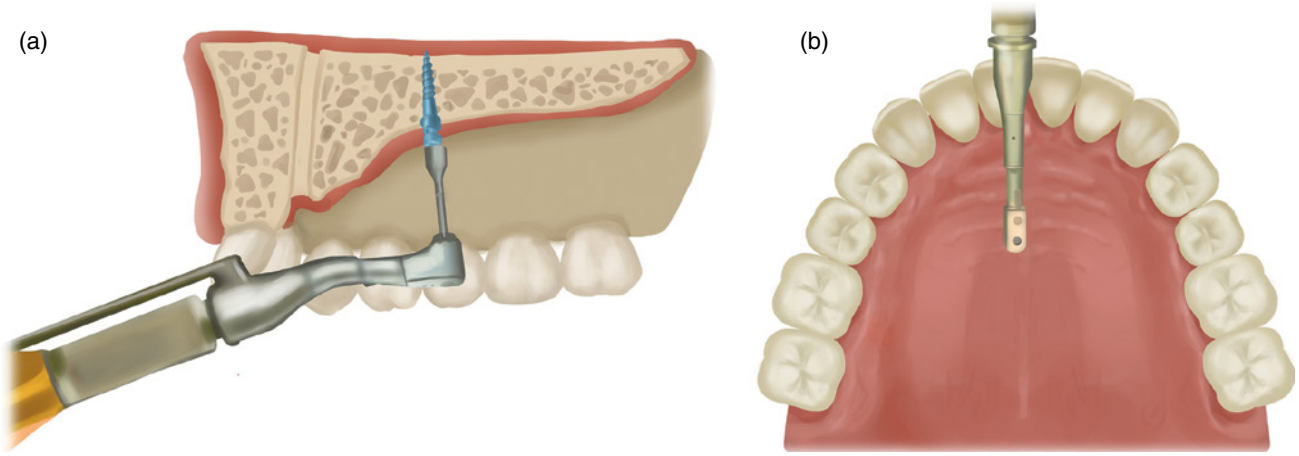


Figure 6.77 Insertion of the mini-implant into the palatal paramedian region using a contra-angle screwdriver. (a) Sagittal view. (b) Occlusal view.



Figure 6.78 Stabilisation of the screwdriver by the operator's left hand during insertion.

Thus, slight pressure can be applied on the screwdriver to facilitate cortical penetration.

Fourth, once cortical penetration is accomplished, the mini-implant is then advanced into the palatal bone slowly. During insertion, if high insertion torque is perceived, the operator should not rotate the screwdriver forcefully since this may lead to super-high insertion torque that may exceed the fracture torque of the mini-implant, resulting in fracture. If high torque is encountered, the insertion should be paused and unscrewing the mini-implants by one or two rotations is recommended. Then, the mini-implant is advanced until the mini-implant platform contacts the mucosa. Overinsertion of the mini-implant is not recommended since this may lead to submergence of the mini-implant head into soft tissue.

t.me/Dr_Mouayyad_AlbtousH

Lastly, once the insertion is complete, the operator should check the positions and orientations of the mini-implants (Figure 6.79). Also, whether the mini-implant platform is in firm contact with the mucosa should be checked. If loose contact or no contact is detected, further advancement of the mini-implant is indicated.

The detailed clinical procedures of inserting a mini-implant at the palatal paramedian region are displayed in Figure 6.80.

Postinsertion

Following the insertion of mini-implants, force loading is postponed until at least two weeks later when soft tissue healing is complete. The patient should be reassured regarding potential nasal discomfort and sneezing symptoms. Meticulous oral hygiene care is recommended with gentle brushing around the mini-implant head.

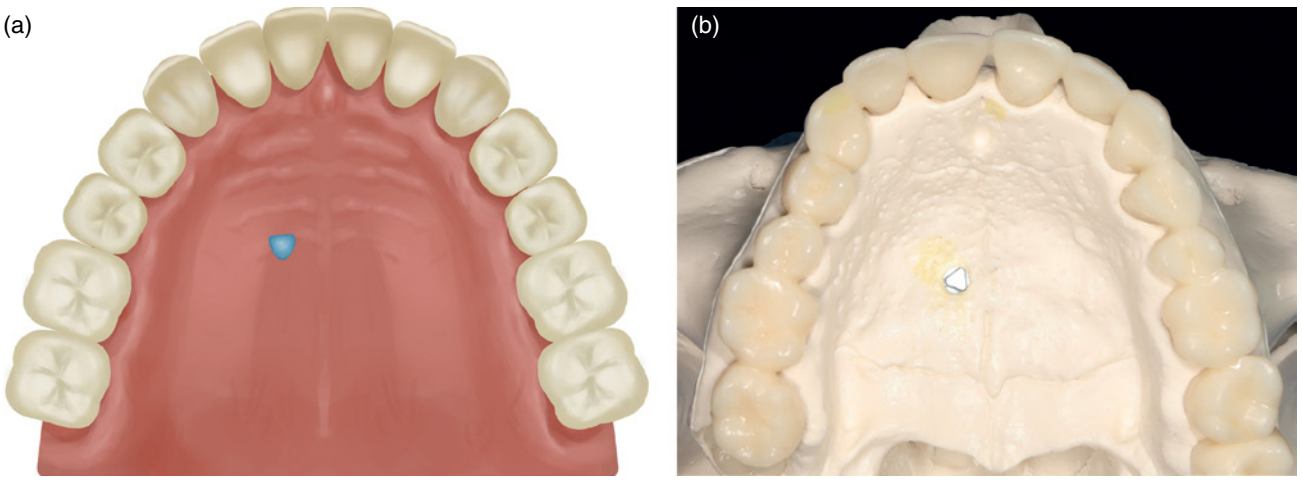


Figure 6.79 Check the position of the mini-implant from the occlusal side. (a) Illustration. (b) Skull model.

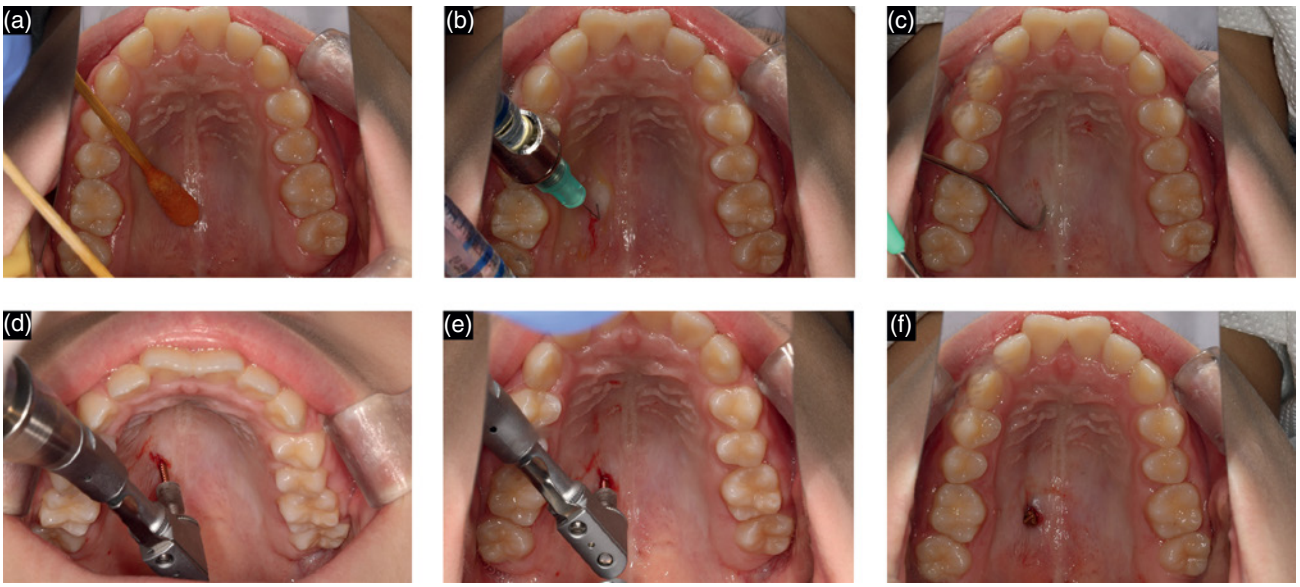


Figure 6.80 Detailed clinical procedures of inserting a mini-implant at the palatal paramedian region. (a) Mucosa disinfection with iodophor. (b) Local infiltration anaesthesia. (c) Mark the entry point with an explorer. (d) Insert the mini-implant through the marked entry point with a contra-angle screwdriver. (e) Advance the mini-implant. (f) Examination of the position and orientation of the mini-implant following insertion.

t.me/Dr_Mouayyad_AlbtousH

6.3.5 Clinical Applications

Molar Distalisation

Molar distalisation can be accomplished with two paramedian mini-implants with the aid of extension hooks fixed onto the two mini-implants. The hooks are located at the same level as the molar centre of resistance so that bodily distalisation of molars can be achieved (Figure 6.81). A case example is given below.

A female adolescent presented to the orthodontic department with a chief complaint of a missing tooth. As displayed in Figure 6.82, her clinical and radiographic examinations revealed that she had a straight facial profile with class I canine relationship on both sides. The molar relationship was class I on the left side and class II on the right side. The upper right second premolar had not erupted, which was further evidenced by the panoramic radiograph. Specifically, the root of the second premolar was underdeveloped with open apex. Mild crowding was present in the lower arch. Moreover, lateral cephalometric analysis was indicative of class II skeletal base (ANB = 4.6), normoclined upper incisors and retroclined lower incisors (U1-SN = 99.5; L1-MP = 85.9), and high mandibular plane angle (SN-MP = 39.2) (Table 6.8).

Based on her pretreatment examinations, molar distalisation of the right upper molars was planned in order to gain space for eruption of the underdeveloped second premolar. The objectives were class I canine and molar relationship on both sides, normal overjet and overbite, coincident upper and lower dental midlines.

To achieve molar distalisation, two mini-implants were placed at the palatal paramedian region. Extension hooks were fixed onto the two mini-implants and unilateral closed-coil springs were employed to deliver distalisation force (Figure 6.83). Molar distalisation was effective and sufficient space was obtained for the second premolar (Figure 6.84). Then, the second premolar was guided and tractioned into the dental arch.

Finally, as shown in Figure 6.85, the impacted second premolar was well aligned into the dental arch and in good occlusion with the opposing teeth. Class I canine and molar relationships were obtained and the straight facial profile maintained. The pre- and posttreatment cephalometric indices are presented in Table 6.9.

Molar Anchorage Reinforcement

Reinforcing molar anchorage for premolar extraction patients can be accomplished by paramedian mini-implants through a mini-implant-anchored Nance-holding arch. Usually, one paramedian mini-implant is sufficient to augment molar anchorage. Depending on the requirements of vertical control, absolute or partial fixation of the Nance-holding arch onto the mini-implant is performed. Specifically, if the vertical dimension of the lower facial third should be maintained, the Nance-holding arch is fixed onto the mini-implant with ligature wire and flowable resin. If the vertical dimension of the lower facial third should be reduced, the mini-implant is inserted through a hole on the anterior pad of the Nance-holding arch. The mini-implant is not fixed with the Nance-holding arch. In this way, the mini-implant is able to prevent mesial tipping of the molars and to permit intrusion of molars (the Nance-holding arch is able to slide upward along the mini-implant) (Figure 6.86). A case example is demonstrated below.

A male adolescent sought orthodontic treatment with a chief complaint of lip protrusion and deficient chin. As displayed in Figure 6.87, his clinical examinations revealed that he had a protrusive facial profile and chin deficiency,

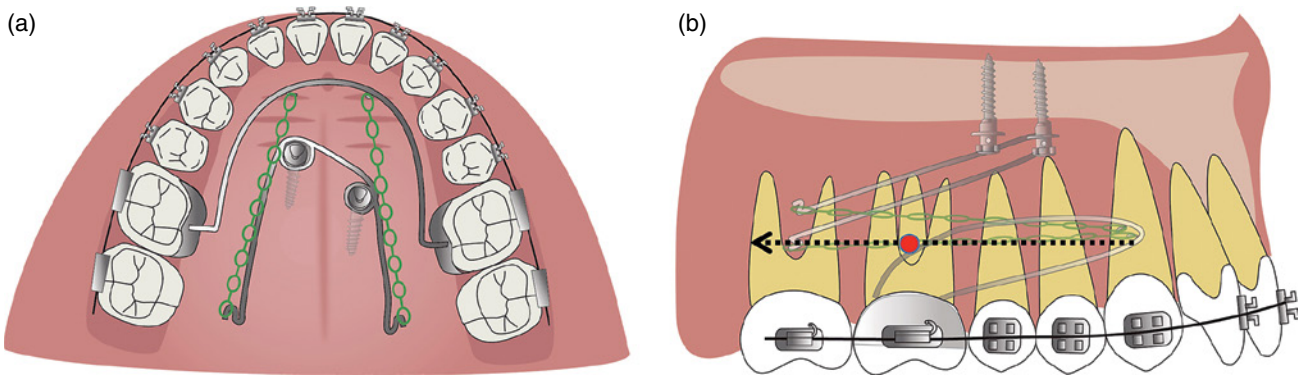


Figure 6.81 Biomechanics of molar distalisation through mini-implants at the paramedian region. (a) Occlusal view. (b) Sagittal view. Note that the distalisation force passes through the centre of resistance of the molars, so that bodily distalisation can be achieved.

t.me/Dr_Mouayyad_AlbtousH



Figure 6.82 Pretreatment photographs and radiographs.

t.me/Dr_Mouayyad_AlbtousH

Table 6.8 Pretreatment lateral cephalometric analysis.

Measurement	Norm	Pretreatment
Skeletal (°)		
SNA	83.0±4.0	85.3
SNB	80.0±4.0	80.7
ANB	2.0±2.0	4.6
FMA	28.0±4.0	29.0
SN-MP	35.0±4.0	39.2
Dental (°)		
U1-SN	105.7±6.3	99.5
L1-MP	97.0±7.1	85.9
FMIA	65.0±6.0	65.1
U1-L1	124.0±8.0	135.5
Soft tissue (mm)		
UL-EP	2.0±2.0	0.9
LL-EP	3.0±2.0	1.2
Wits (mm)		
Wits	−1.0	−3.3

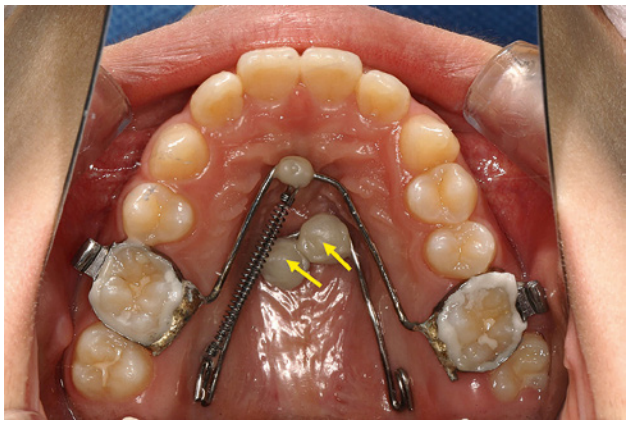


Figure 6.83 Unilateral molar distalisation through extension hooks that were fixed onto two mini-implants (yellow arrows) at the paramedian region.

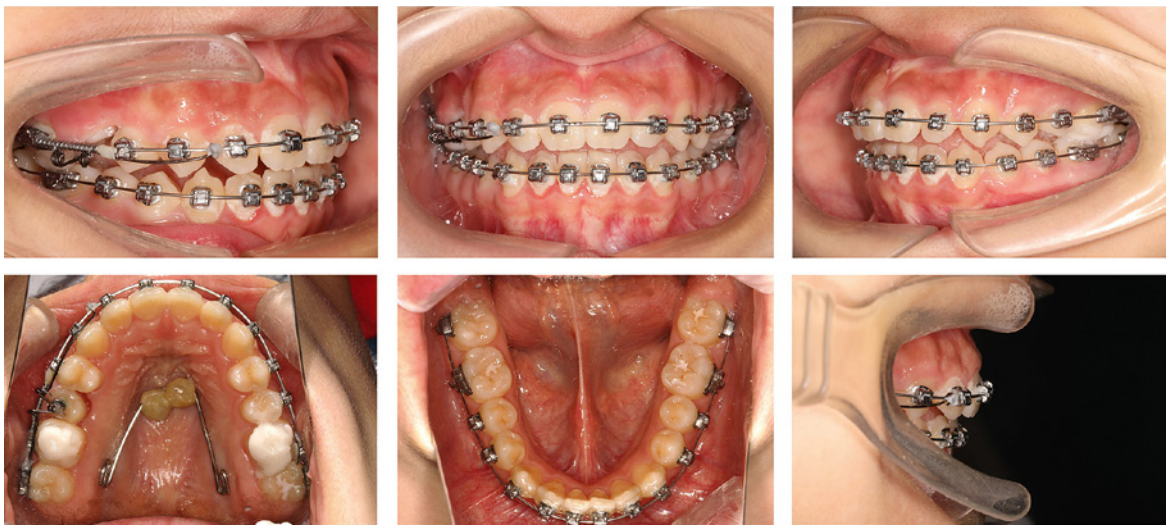


Figure 6.84 Treatment progress. Note that the maxillary right molars had been successfully distalised and the space was regained to allow orthodontic traction of the unerupted maxillary right second premolar.

t.me/Dr_Mouayyad_AlbtousH

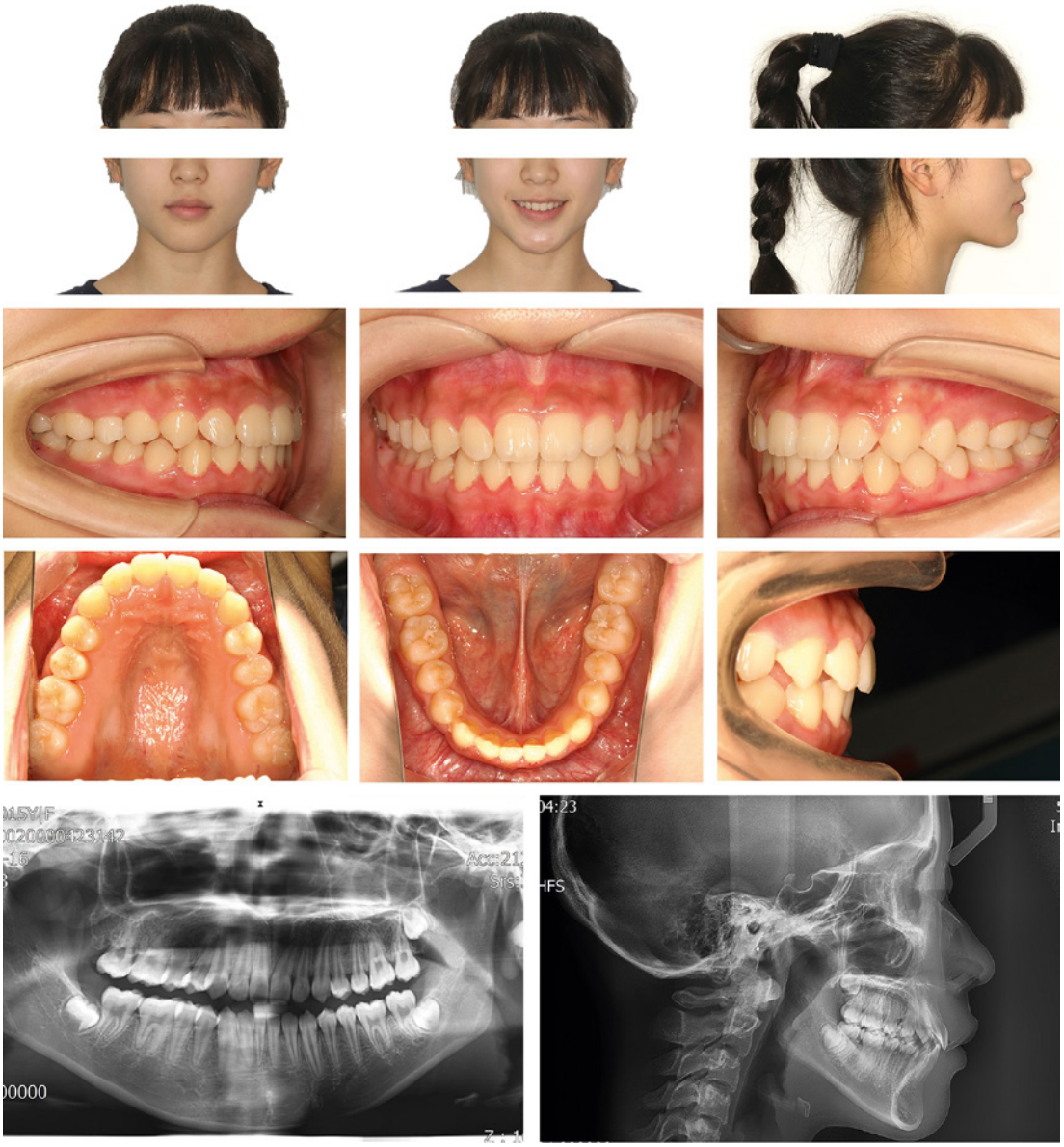


Figure 6.85 Posttreatment photographs and radiographs.

t.me/Dr_Mouayyad_AlbtousH

Table 6.9 Pre- and posttreatment lateral cephalometric analysis.

Measurement	Norm	Pretreatment	Posttreatment
Skeletal (°)			
SNA	83.0±4.0	85.3	85.1
SNB	80.0±4.0	80.7	80.7
ANB	2.0±2.0	4.6	4.4
FMA	28.0±4.0	29.0	29.8
SN-MP	35.0±4.0	39.2	39.7
Dental (°)			
U1-SN	105.7±6.3	99.5	101.3
L1-MP	97.0±7.1	85.9	88.3
FMIA	65.0±6.0	65.1	61.9
U1-L1	124.0±8.0	135.5	88.3
Soft tissue (mm)			
UL-EP	2.0±2.0	0.9	1.0
LL-EP	3.0±2.0	1.2	1.6
Wits (mm)			
Wits	−1.0	−3.3	−2.5

with class I molar relationship on both sides. Mild and moderate dental crowding was present in the upper and lower dental arches, respectively. Lateral cephalometric analysis was indicative of class II skeletal base (ANB = 4.4), normoclined upper and lower incisors (U1-SN = 107.3; L1-MP = 97.3), and high mandibular plane angle (SN-MP = 45.0) (Table 6.10).

Treatment planning was extraction of the four first premolars and subsequent anterior retraction to resolve the protrusive facial profile. Maximal molar anchorage was demanded. However, due to limited interradicular space on both the buccal and palatal sides, one paramedian mini-implant in conjunction with a Nance-holding arch was planned. Meanwhile, in consideration of the chin deficiency, molar intrusion with spontaneous mandibular anticlockwise rotation was indicated. Thus, the Nance-holding arch was only partially fixed onto the mini-implant so that molar intrusion was permitted (Figure 6.88).

Following active orthodontic treatment, bilateral canine and molar relationships were obtained. The protrusive facial profile was significantly improved and a straight facial profile was achieved with a prominent chin (Figure 6.89). Posttreatment cephalometric analysis

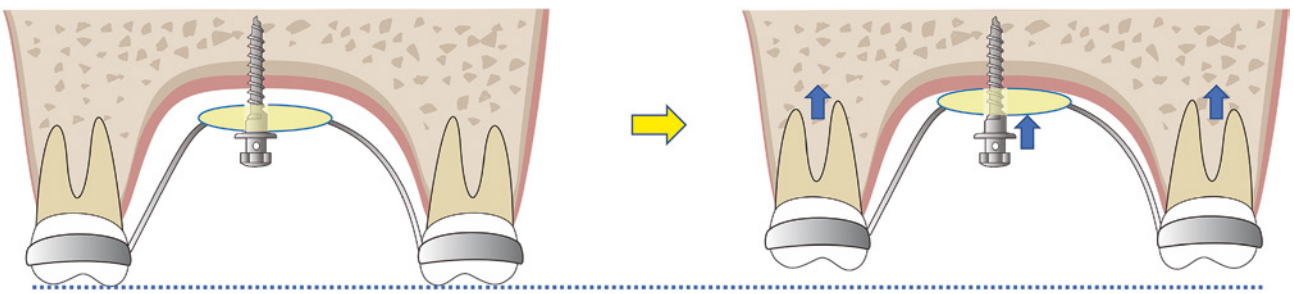


Figure 6.86 Sliding mechanisms of the Nance-holding arch along the mini-implant. The Nance-holding arch can be intruded and slid upward along the long axis of the mini-implant in response to tongue pressure, so that the molars can be intruded during the treatment.

t.me/Dr_Mouayyad_AlbtousH

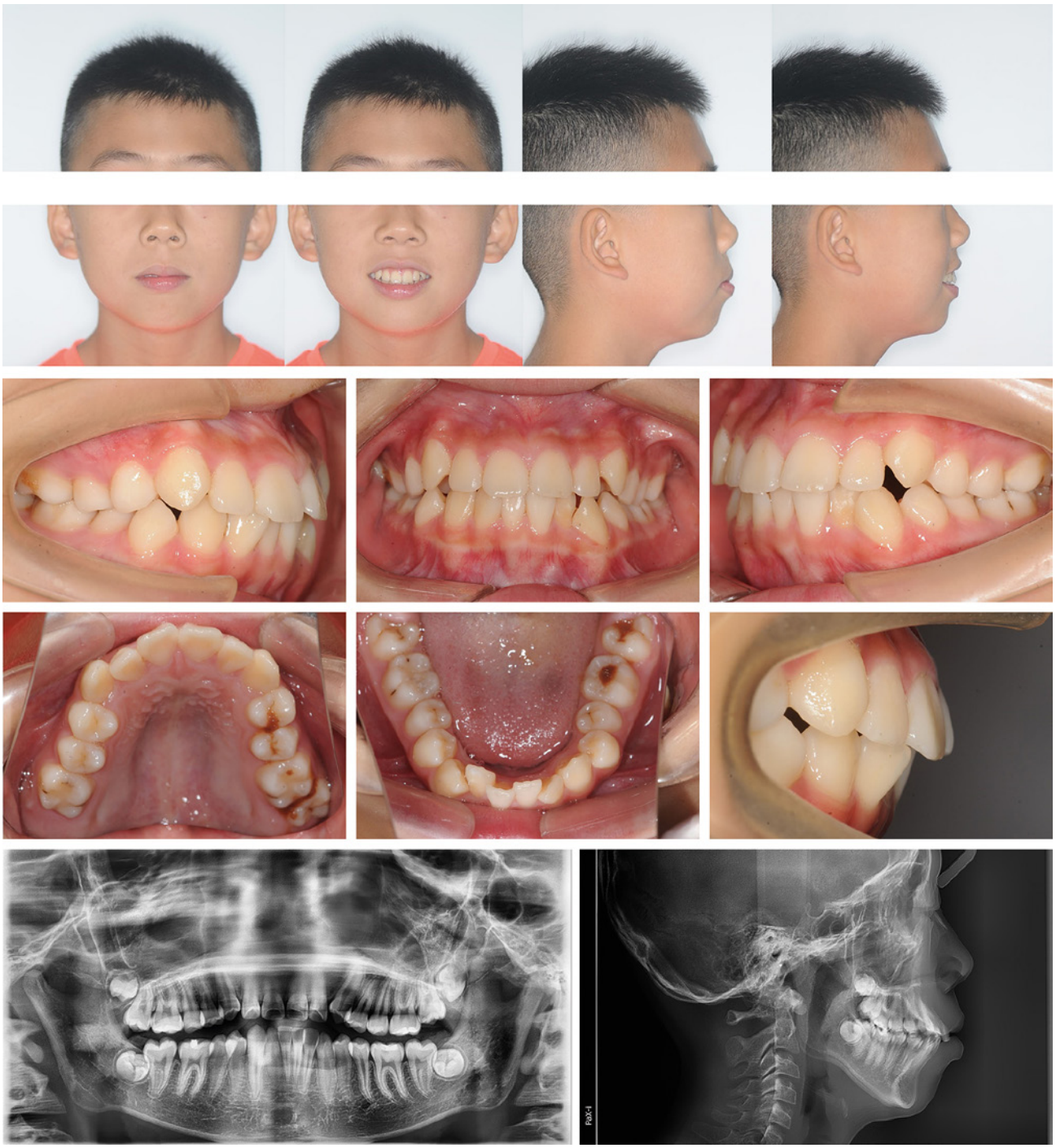


Figure 6.87 Pretreatment photographs and radiographs.

t.me/Dr_Mouayyad_AlbtousH

Table 6.10 Pretreatment lateral cephalometric analysis.

Measurement	Norm	Pretreatment
Skeletal (°)		
SNA	83.0±4.0	78.0
SNB	80.0±4.0	73.6
ANB	2.0±2.0	4.4
FMA	28.0±4.0	34.7
SN-MP	35.0±4.0	45.0
Dental (°)		
U1-SN	105.7±6.3	107.3
L1-MP	97.0±7.1	97.3
FMIA	65.0±6.0	47.9
U1-L1	124.0±8.0	110.3
Soft tissue (mm)		
UL-EP	2.0±2.0	3.8
LL-EP	3.0±2.0	7.8
Wits (mm)		
Wits	−1.0	−0.6

was indicative of mandibular anticlockwise rotation (Table 6.11).

Mini-implant-assisted Skeletal Expansion

Mini-implant-assisted skeletal expansion is often indicated for patients with a narrow maxilla. Compared to tooth-borne expansion, bone-borne maxillary expansion has greater skeletal effects and fewer dental adverse effects. Usually, four mini-implants are placed at the paramedian region, with two anterior mini-implants being placed at the first premolar region and the other two posterior mini-implants at the first molar region.

Prior to the placement of mini-implants, the optimal insertion sites for the four mini-implants should be determined based on CBCT examinations. Then, the maxillary expander is designed and fabricated with four holes through which the mini-implants are to be inserted (Figure 6.90). For adolescents, the expansion protocol is 2–3 turns/day until desired expansion is achieved. As the expansion progresses, a diastema between the two central incisors can be observed (Figure 6.91). Generally, a three-month to six-month retention period is required to stabilise the expansion effect. During the retention period, the



Figure 6.88 Treatment progress. The Nance-holding arch was partially fixed onto the mini-implant that had been inserted at the paramedian region.

t.me/Dr_Mouayyad_AlbtousH

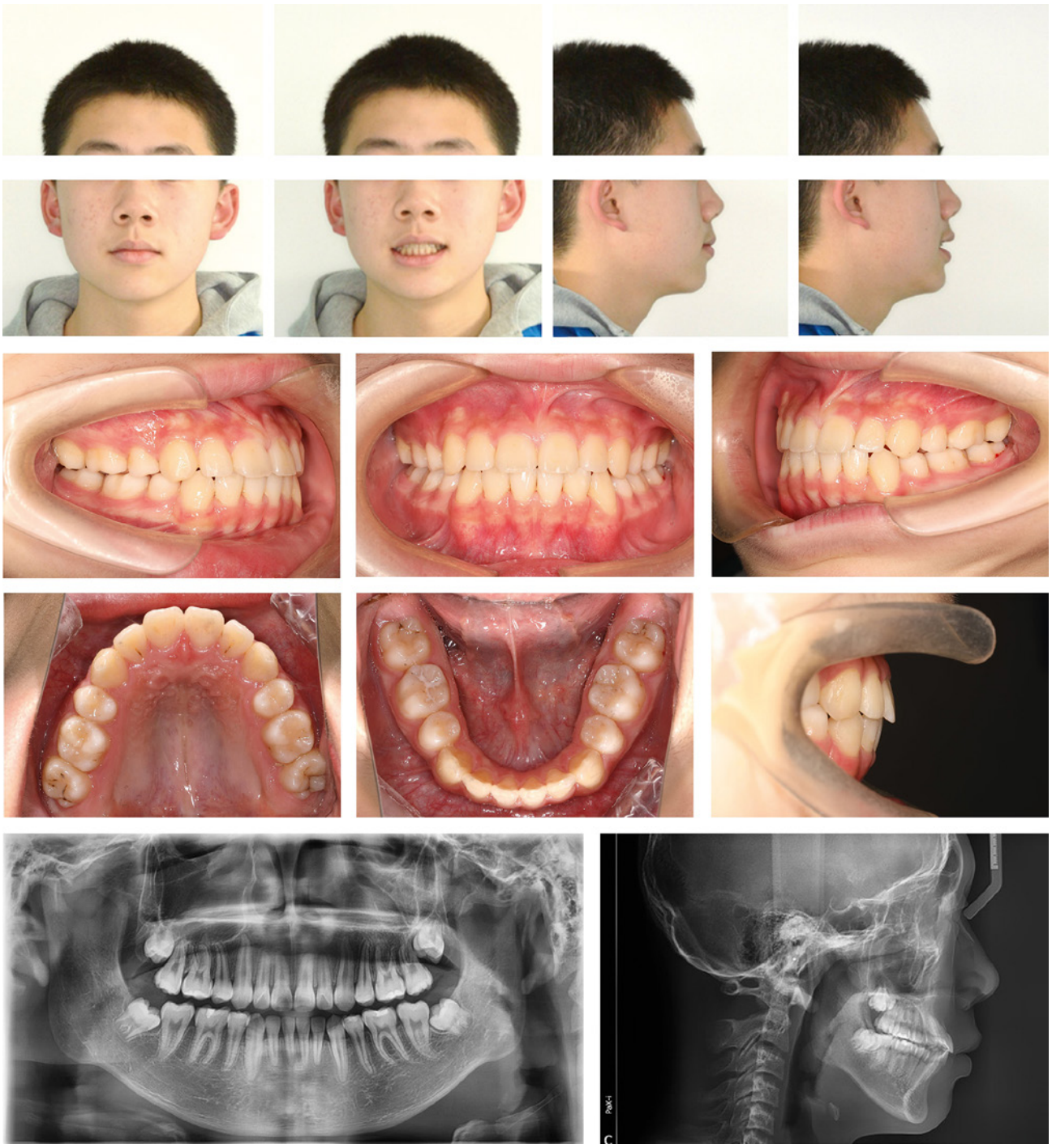


Figure 6.89 Posttreatment photographs and radiographs.

t.me/Dr_Mouayyad_AlbtousH

Table 6.11 Pre- and posttreatment lateral cephalometric analysis.

Measurement	Norm	Pretreatment	Posttreatment
Skeletal (°)			
SNA	83.0±4.0	78.0	78.5
SNB	80.0±4.0	73.6	75.5
ANB	2.0±2.0	4.4	3.0
FMA	28.0±4.0	34.7	31.0
SN-MP	35.0±4.0	45.0	40.5
Dental (°)			
U1-SN	105.7±6.3	107.3	110.8
L1-MP	97.0±7.1	97.3	113.7
FMIA	65.0±6.0	47.9	54.0
U1-L1	124.0±8.0	110.3	113.7
Soft tissue (mm)			
UL-EP	2.0±2.0	3.8	2.3
LL-EP	3.0±2.0	7.8	3.3
Wits (mm)			
Wits	–1.0	–0.6	0.3

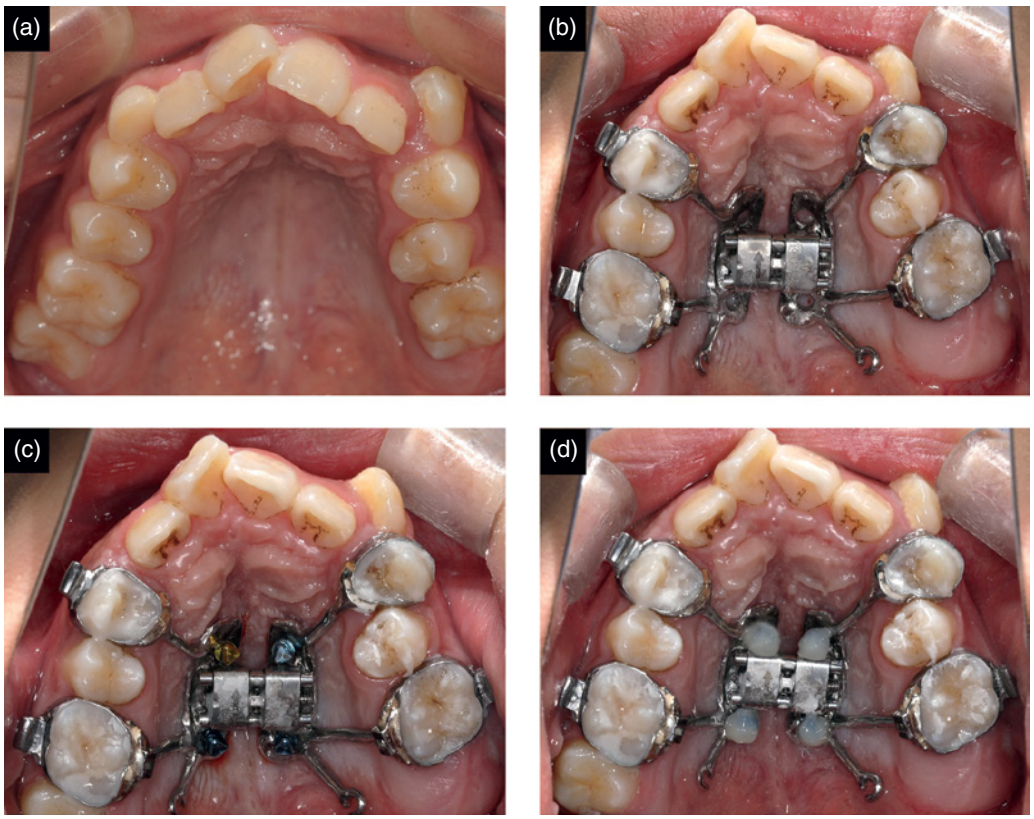


Figure 6.90 Mounting the mini-implant-assisted skeletal expansion device. (a) Before insertion. (b) Mounting the expansion device onto the dentition. (c) Insertion of four mini-implants through the designated holes on the expansion device at the palatal paramedian region. (d) Fixation of the expansion device onto the mini-implants with flowable resin.

t.me/Dr_Mouayyad_AlbtousH

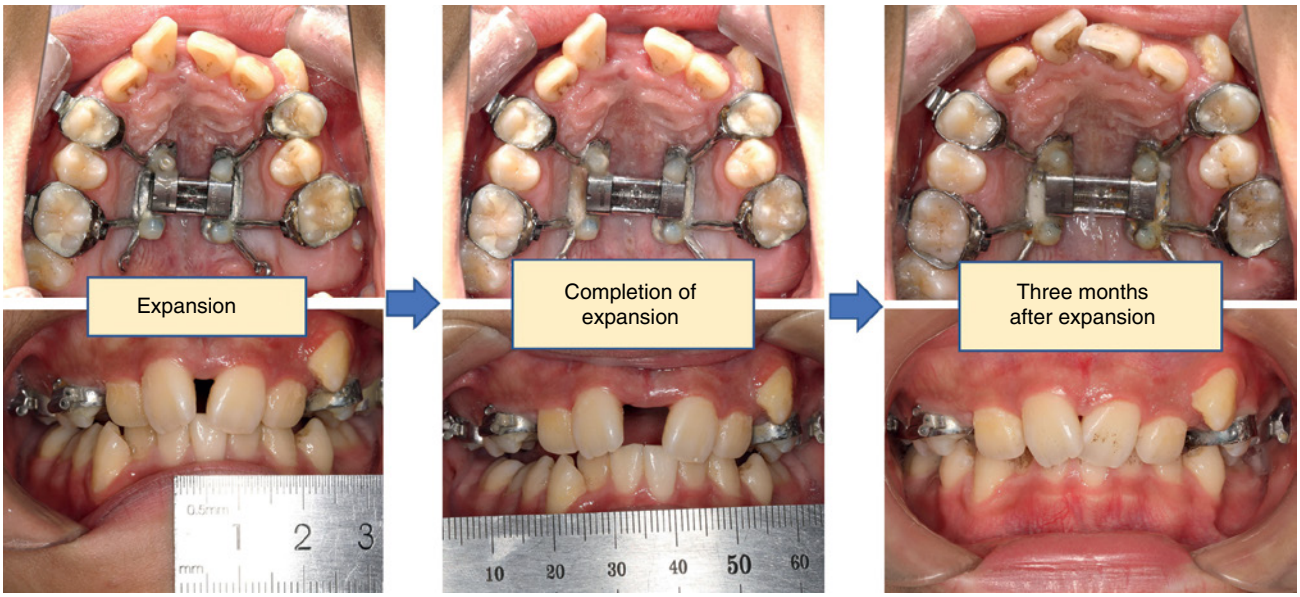


Figure 6.91 The midline diastema became bigger with the progress of the expansion and was closed spontaneously following completion of the expansion.

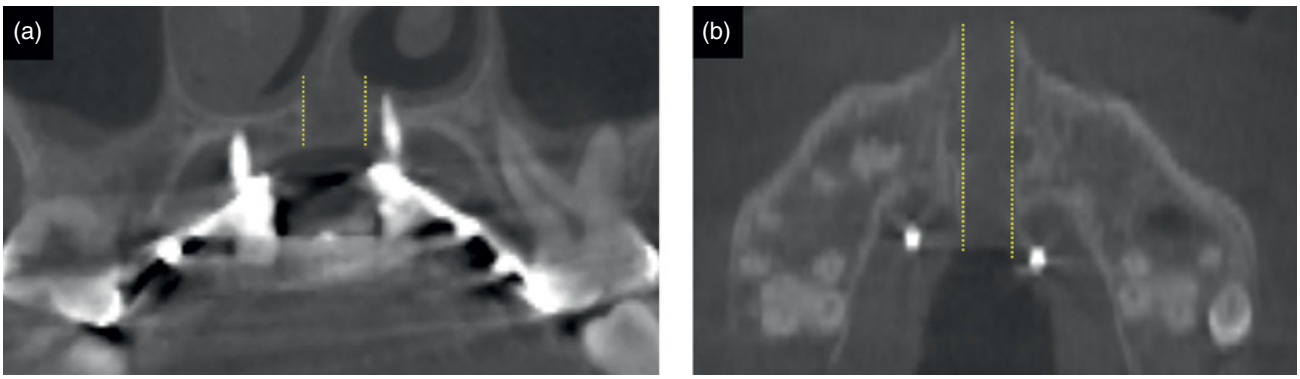


Figure 6.92 Skeletal expansion effect. Note that the maxillary suture had been effectively split and expanded. (a) Coronal view. The edges (yellow dashed lines) of the bilateral maxillae were parallel with each other in the vertical dimension. (b) Axial view. The edges (yellow dashed lines) of the bilateral maxillae were parallel with each other in the transverse dimension.

large diastema between the two central incisors is spontaneously closed due to the mesial tipping of central incisors. Due to the bone-borne nature, mini-implant-assisted skeletal expansion is very effective in skeletal expansion (Figure 6.92).

Traction of Impacted Teeth

Paramedian mini-implants can be used for traction of impacted teeth in the maxilla. They can be used for traction of impacted incisors, impacted canines, impacted premolars and even impacted molars through direct or indirect anchorage mode (Figure 6.93). A case example is given below to demonstrate the clinical application of a mini-implant for traction of an impacted molar.

A female adult was referred to the orthodontic department for multidisciplinary consultation. Radiographic examinations revealed that the left maxillary third molar was deeply impacted and impinged on the root of the

t.me/Dr_Mouayyad_AlbtousH

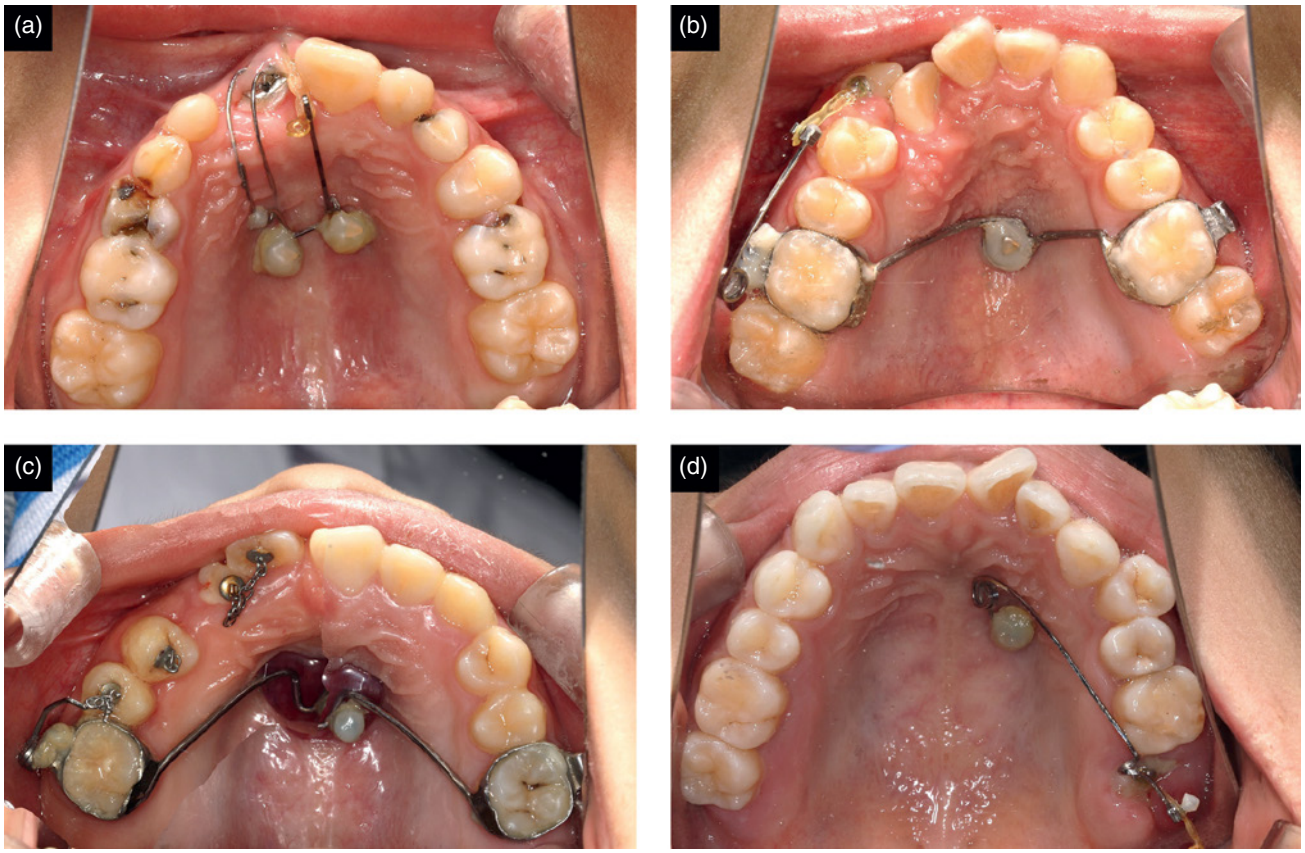


Figure 6.93 Versatile clinical applications of mini-implants at the paramedian region for orthodontic traction of impacted teeth. (a) Orthodontic traction of an impacted incisor. (b) An impacted canine. (c) Impacted premolars. (d) An impacted molar.

second molar, resulting in root resorption of the second molar with pulp involvement (Figure 6.94).[22] Four multidisciplinary treatment alternatives were planned for this patient (Figure 6.95). After thorough discussion with the patient, the patient chose the orthodontic treatment alternative, i.e. extraction of the second molar and orthodontic traction of the third molar to substitute the second molar. After extraction of the second molar and surgical exposure of the third molar, a paramedian mini-implant was inserted at the first premolar region (Figure 6.96). A cantilever spring was fixed onto the paramedian mini-implant to deliver the traction force for the impacted third molar (Figures 6.97 and 6.98). Finally, the impacted third molar was successfully tractioned down into the dental arch. The

t.me/Dr_Mouayyad_AlbtousH

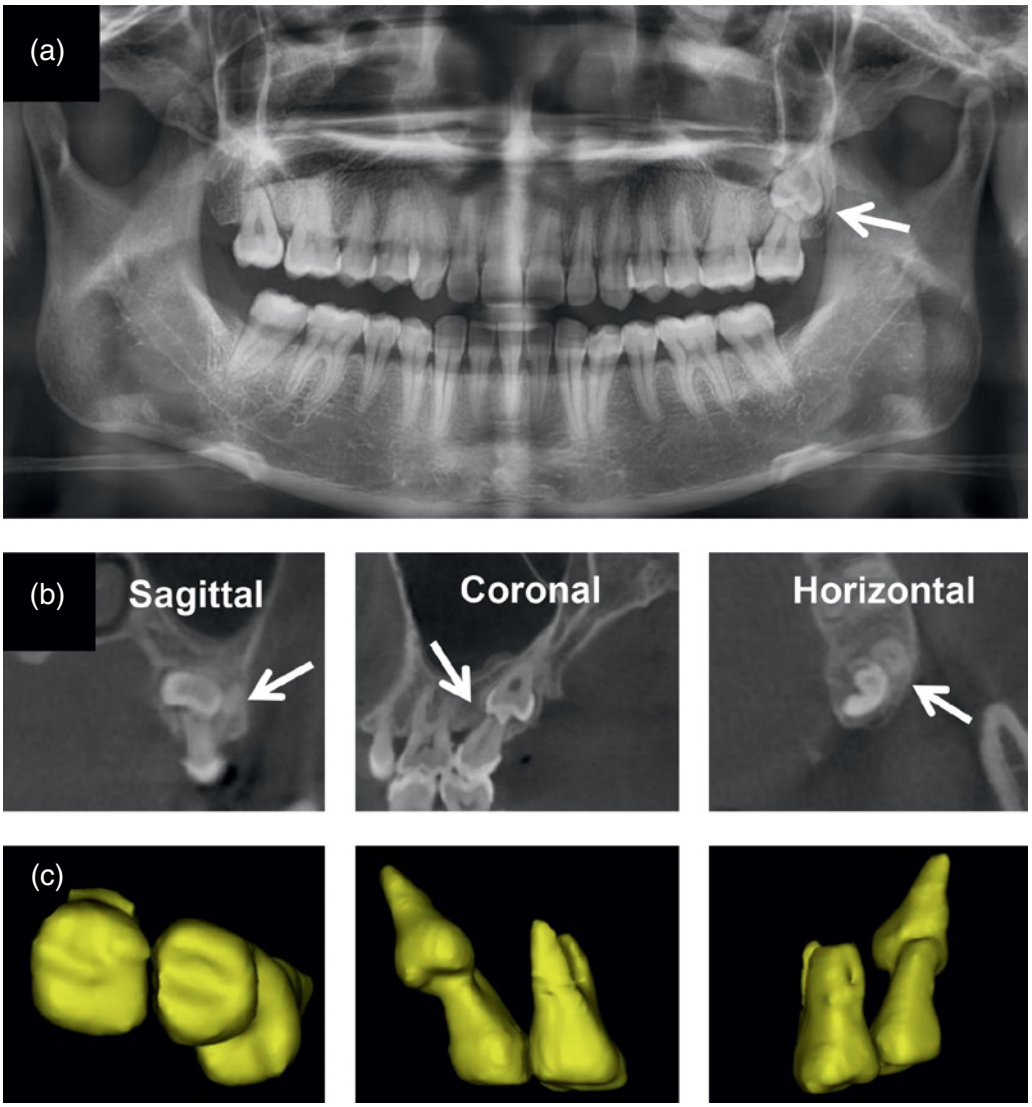


Figure 6.94 Radiographic examinations indicative of root resorption of the maxillary left second molar due to the adjacent impacted third molar. (a) Panoramic radiograph. (b) CBCT images. Note that the pulp of the second molar was involved. (c) 3-D reconstructions. *Source:* Pu et al. [22], with permission from Elsevier.

t.me/Dr_Mouayyad_AlbtousH

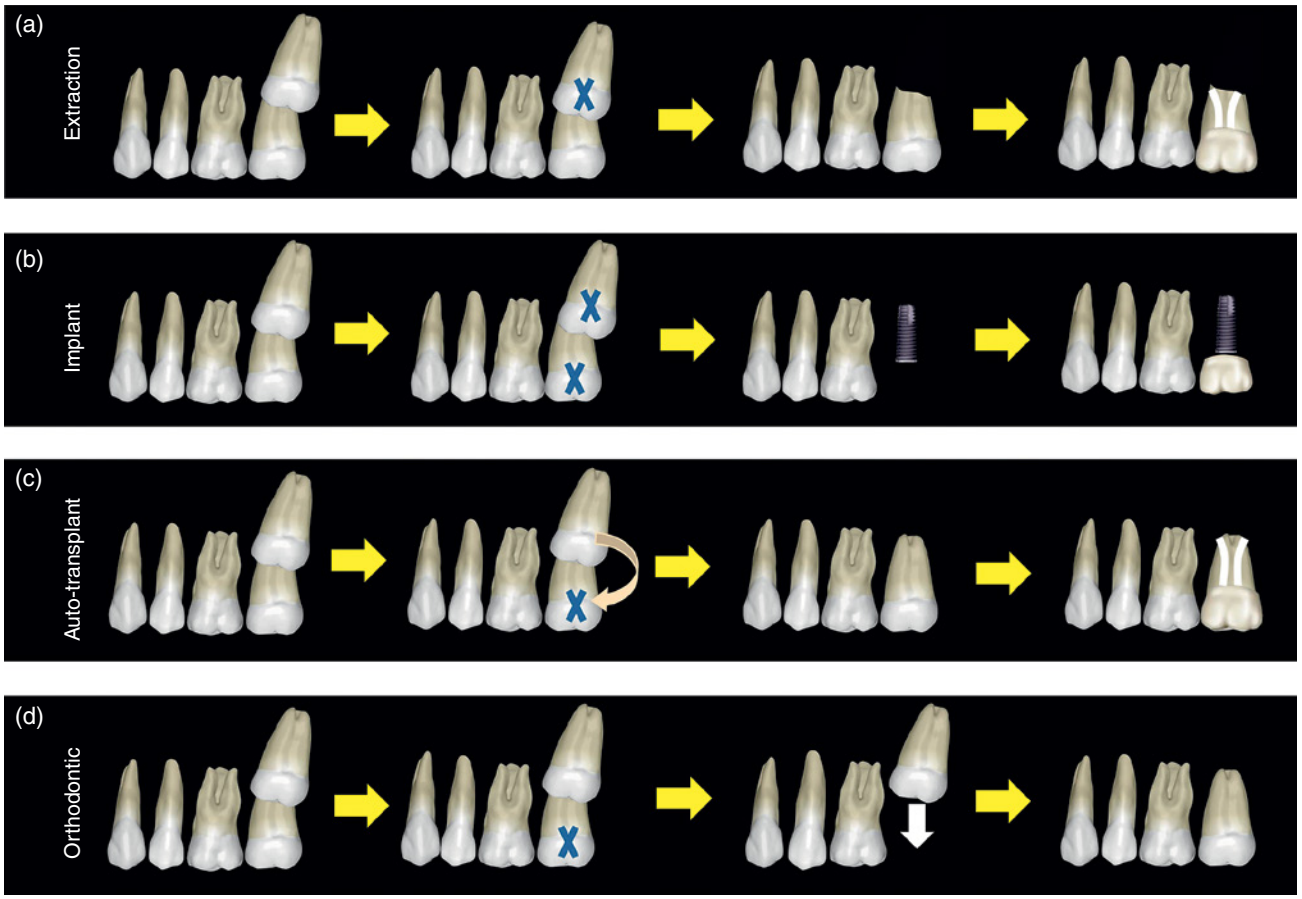


Figure 6.95 Four multidisciplinary treatment alternatives. (a) Extraction of the third molar and root canal therapy of the second molar. (b) Implant restoration of the second molar. (c) Extraction of the second molar and auto-transplantation of the third molar. (d) Extraction of the second molar and orthodontic traction of the third molar. *Source:* Pu et al. [22], with permission from Elsevier.

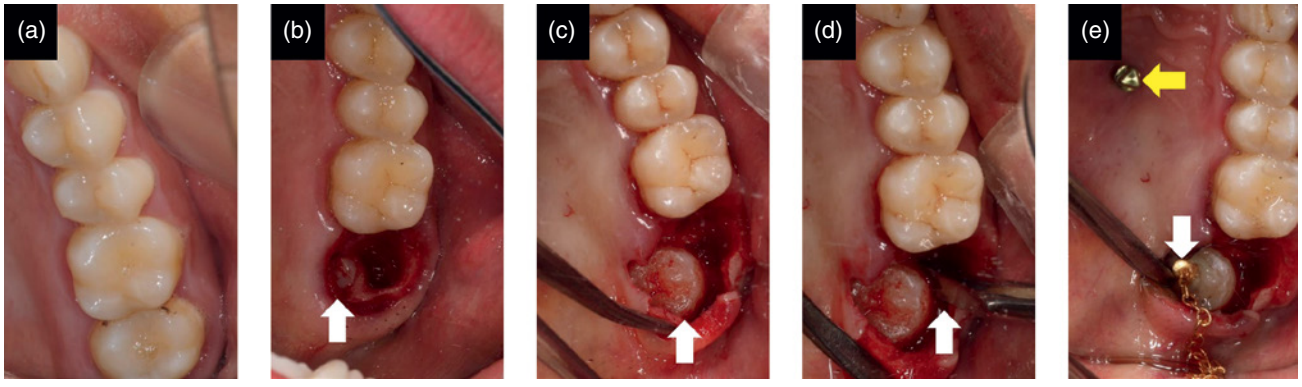


Figure 6.96 Surgical exposure of the impacted third molar. (a) Before surgery. (b) Extraction of the second molar. The impacted third molar can be partially seen (white arrow). (c) Surgical exposure of the whole contour of the impacted third molar (white arrow). (d) Subluxation of the impacted third molar with an elevator (white arrow) to rule out ankylosis. (e) Bonding a gold chain (white arrow) onto the occlusal surface of the impacted third molar and inserting a mini-implant (yellow arrow) at the paramedian region. *Source:* Pu et al. [22], with permission from Elsevier.

t.me/Dr_Mouayyad_AlbtousH

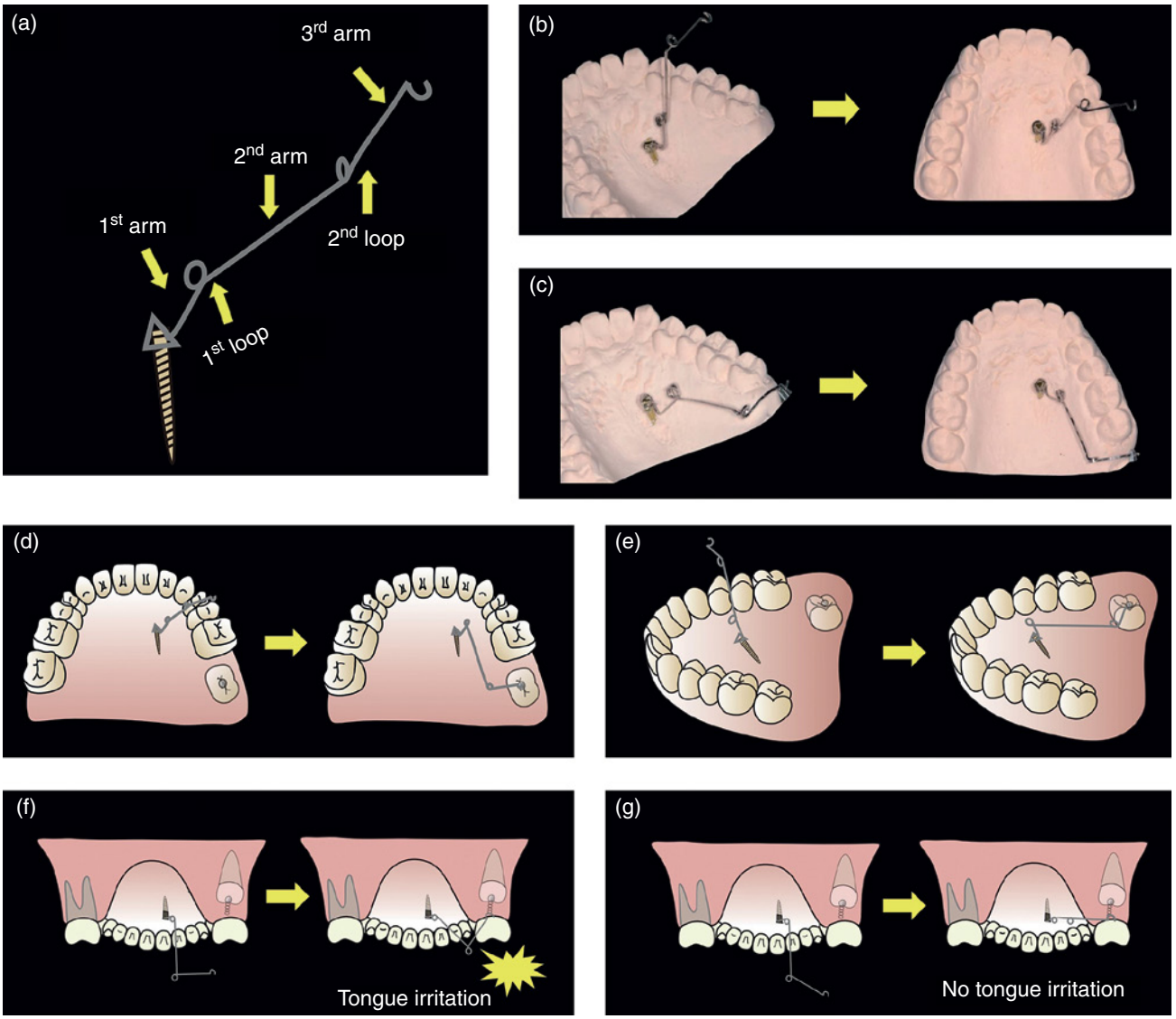


Figure 6.97 Schematic illustrations of the mini-implant-anchored cantilever spring for orthodontic traction of the impacted third molar. (a) Configuration of the cantilever spring with two loops and three arms. (b) Inactivated form of the cantilever spring shown on a dental cast. (c) Activated form of the cantilever spring. (d,e) Activation of the cantilever spring. (f,g) The spatial position of the third arm can be changed by adjusting the second loop, so that tongue irritation can be eliminated. *Source:* Pu et al. [22], with permission from Elsevier.

impacted third molar was in good occlusion with its opposing tooth (Figure 6.99).

Molar Intrusion

Molar intrusion can be achieved through one paramedian mini-implant in conjunction with one buccal mini-implant. Since the intrusion forces are applied at both the buccal and palatal sides, bodily intrusion of the molar can be achieved (Figure 6.100). The intrusion of overerupted molars can be very efficient through intrusion forces on both sides (Figure 6.101).

t.me/Dr_Mouayyad_AlbtousH

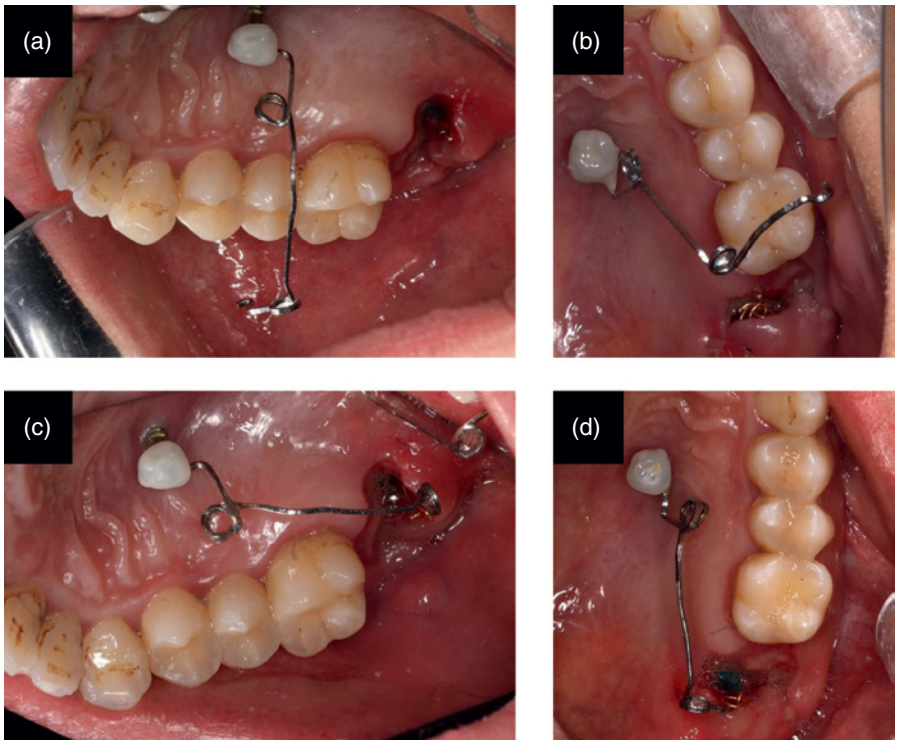


Figure 6.98 Activation of the cantilever spring intraorally. (a,b) Inactivated form. (c,d) Activated form. *Source:* Pu et al. [22], with permission from Elsevier.

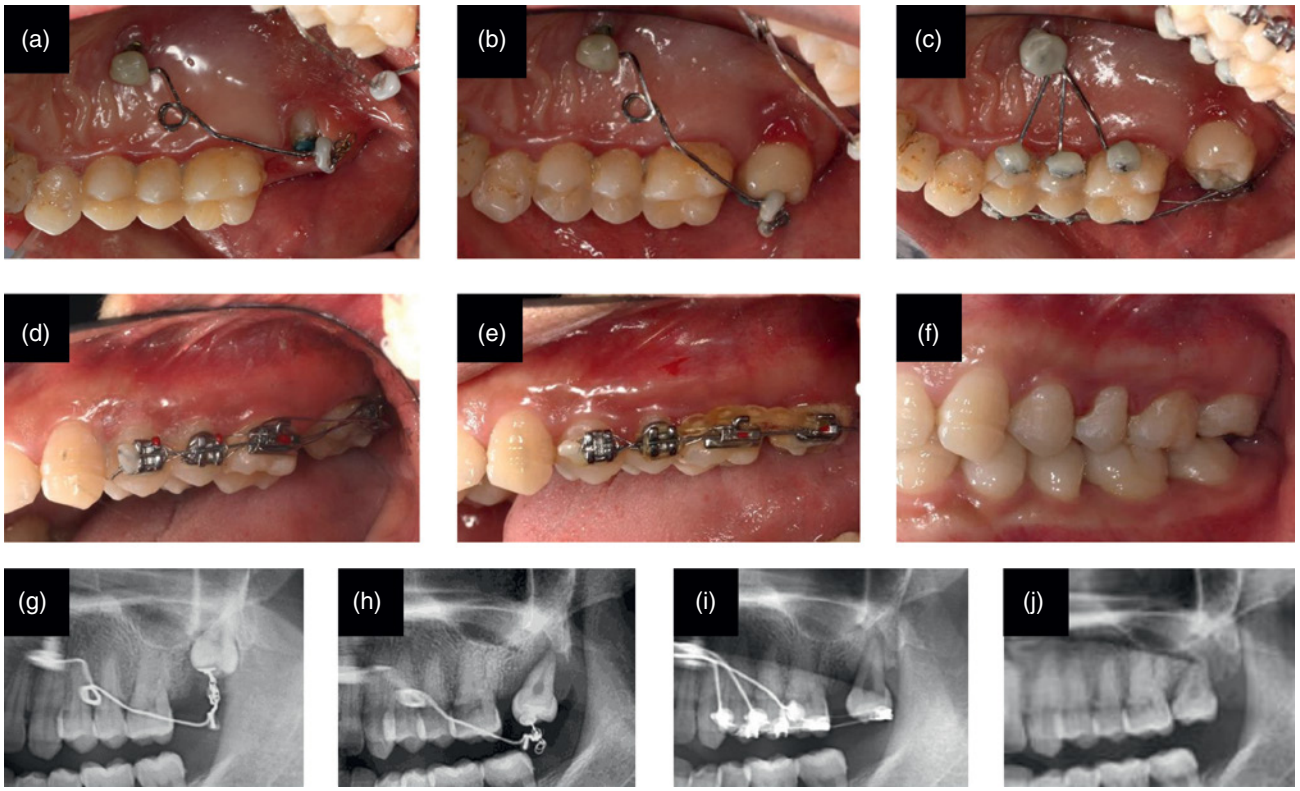


Figure 6.99 Treatment progress. (a–c) Palatal view. (d–f) Buccal view. (g–j) Panoramic radiographs. *Source:* Pu et al. [22], with permission from Elsevier.

t.me/Dr_Mouayyad_AlbtousH

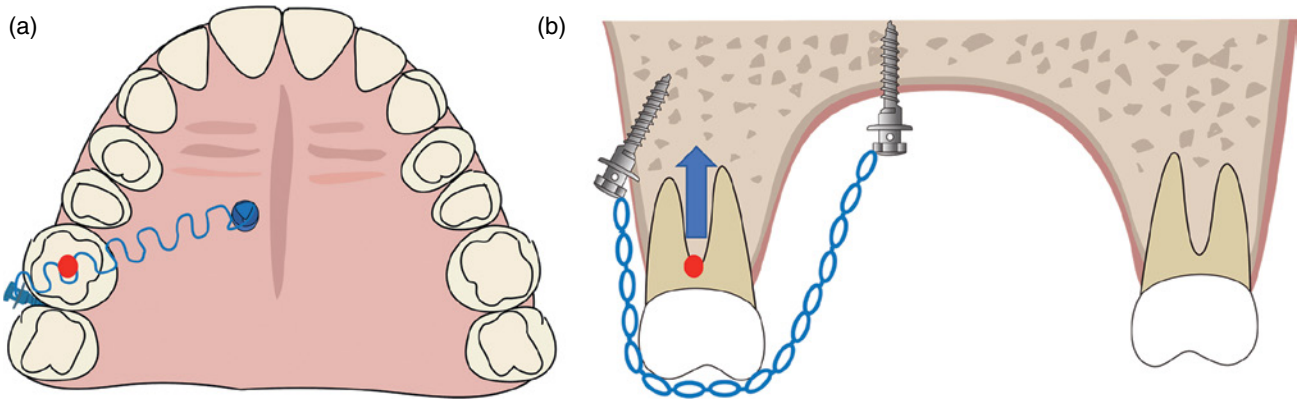


Figure 6.100 Schematic illustrations of molar intrusion using a mini-implant at the paramedian region in conjunction with a buccal mini-implant. (a) Occlusal view. (b) Coronal view.

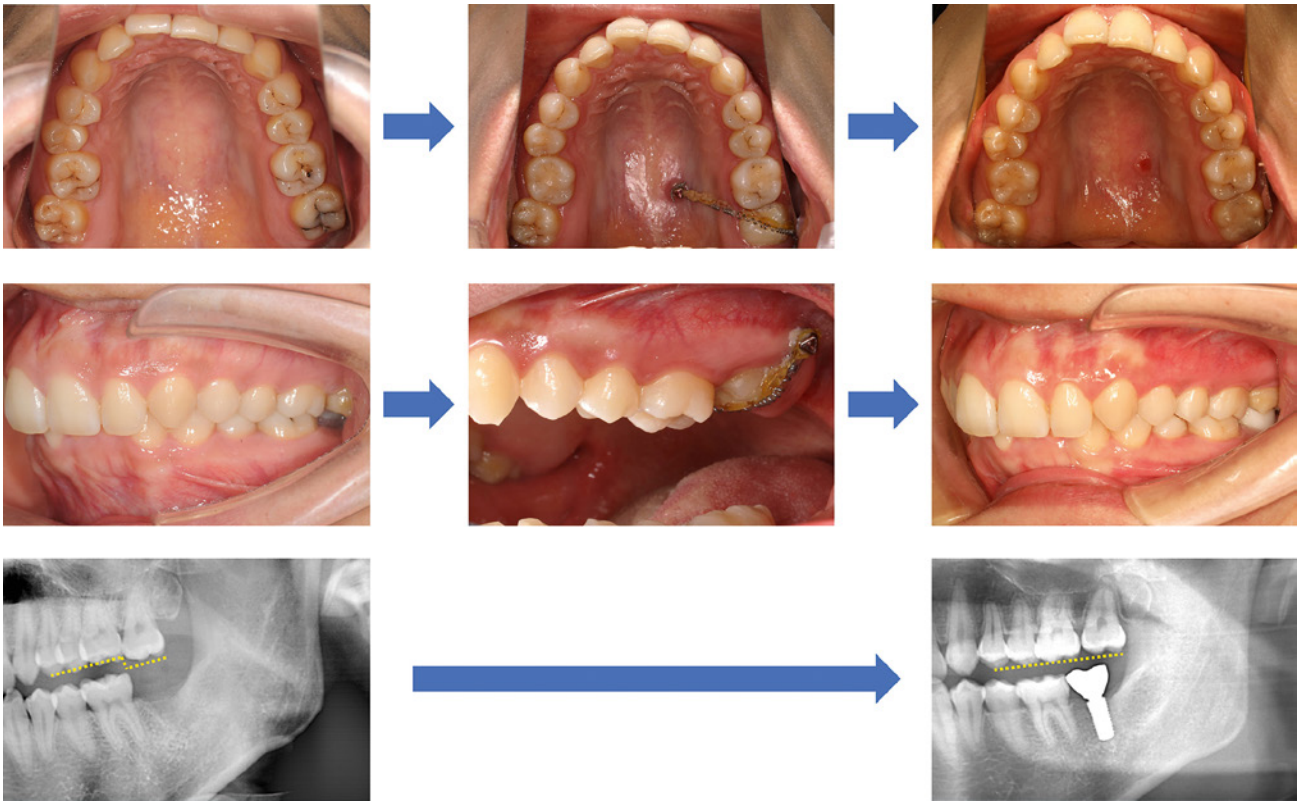


Figure 6.101 Intrusion of an overerupted molar through mini-implants that were inserted at the buccal and palatal sides.

t.me/Dr_Mouayyad_AlbtousH

6.4 Midpalatal Suture

The midpalatal suture is one of the circumaxillary sutures that function as sites of bone growth.[23-25] The midpalatal suture is initially filled with connective tissues after birth, gradually ossifies during growth and is finally united in adulthood. Specifically, the midpalatal suture takes on a 'Y' shape during infancy, changes to end-to-end junction during the juvenile period and a more tortuous interdigitated form during the adolescent period, and finally becomes obliterated and united highly calcified bone during adulthood (Figures 6.102 and 6.103).[24-26]

Fusion of the midpalatal suture begins at the posterior part and progresses anteriorly.[27] According to a classification system of midpalatal suture maturation based on suture morphology, the maturation of the suture is divided into A–C stage

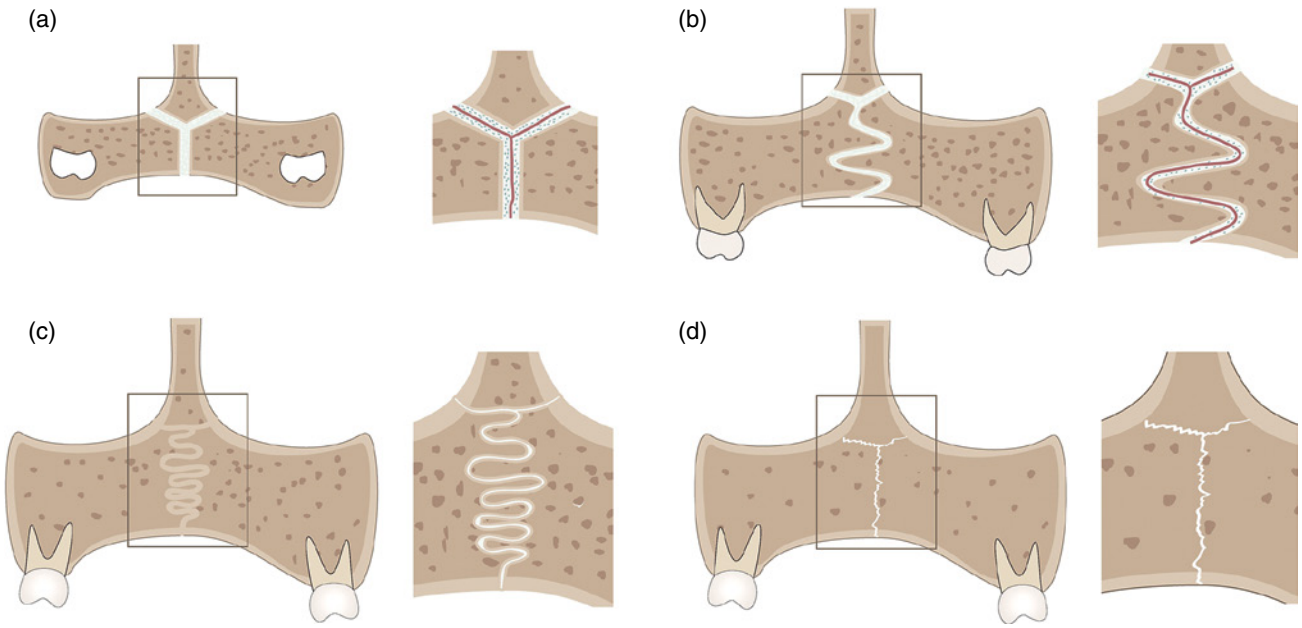


Figure 6.102 Schematic illustrations of the fusion process of the midpalatal suture. (a) Infantile phase. (b) Juvenile phase. (c) Adolescent phase. (d) Adult phase.

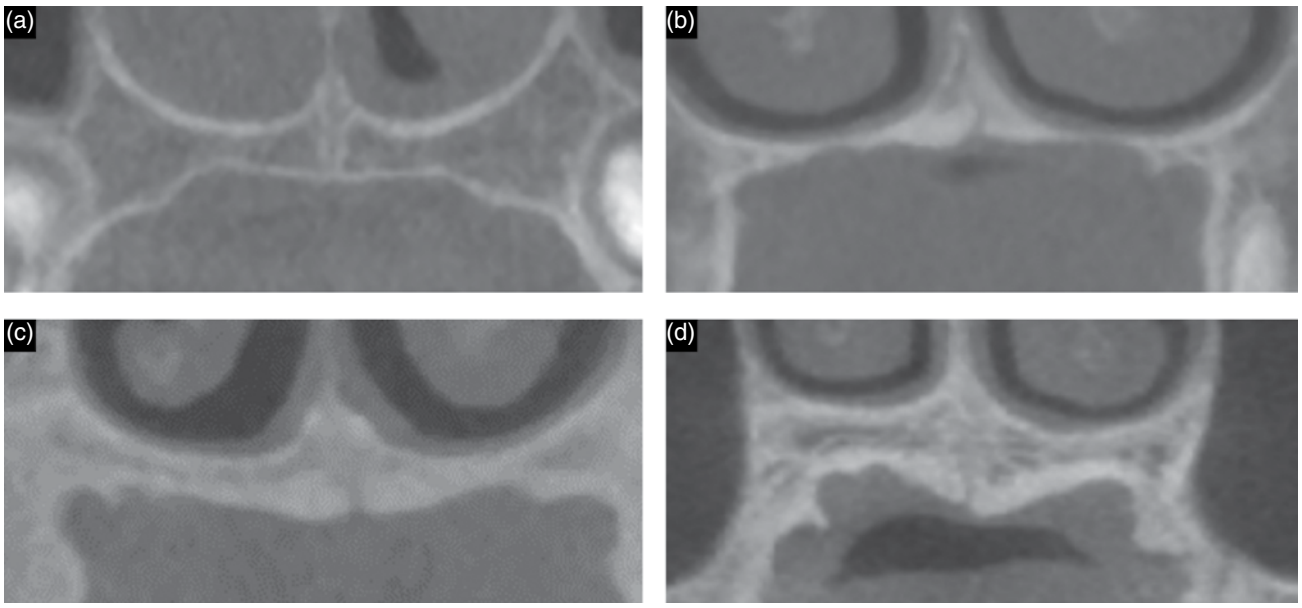


Figure 6.103 CBCT images showing the midpalatal suture at different phases. (a) Infantile phase. (b) Juvenile phase. (c) Adolescent phase. (d) Adult phase.

t.me/Dr_Mouayyad_AlbtousH

(no fusion), D stage (fusion completion in the palatal bone) and E stage (fusion completion in anterior maxilla).[28] Bone density of the midpalatal suture is low in the A–C stage and is relatively higher in the D–E stage.[29] Therefore, placement of mini-implants at the midpalatal suture should be postponed until late adolescence or adulthood. Among adults, the midpalatal suture is completed fused and highly ossified, being an ideal anatomical region for the placement of mini-implants.

6.4.1 Anatomical Features

As the halves of palatine bone and maxilla fuse at the midpalatal suture, the bone depth is adequate with thin keratinised mucosa, rendering this region ideal for mini-implant placement. The midpalatal suture that is available to mini-implant placement is located posteriorly to the incisive foramen and anteriorly to the soft palate (Figure 6.104). To determine the optimal insertion sites, both hard and soft tissue factors should be considered prior to the placement of mini-implants. Since the midpalatal suture is mainly composed of highly calcified bone that resembles cortical bone, bone depth rather than cortical thickness is a determining hard tissue factor.

Hard Tissue Factor: Bone Depth

Based on data from our previous study, we found that hard tissue thickness (bone depth) is greatest at the first premolar region and does not differ among the second premolar, first molar and second molar regions.[2] As displayed in Figure 6.105, the average bone depth exceeds 4.5 mm which

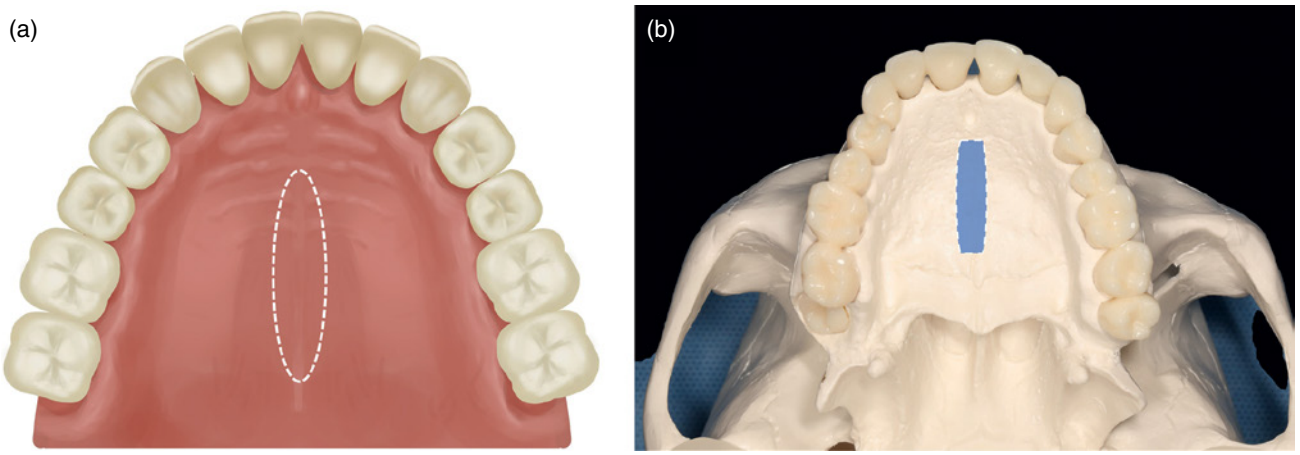


Figure 6.104 Midpalatal suture region available for the insertion of mini-implants. (a) Schematic illustration. (b) A skull model.

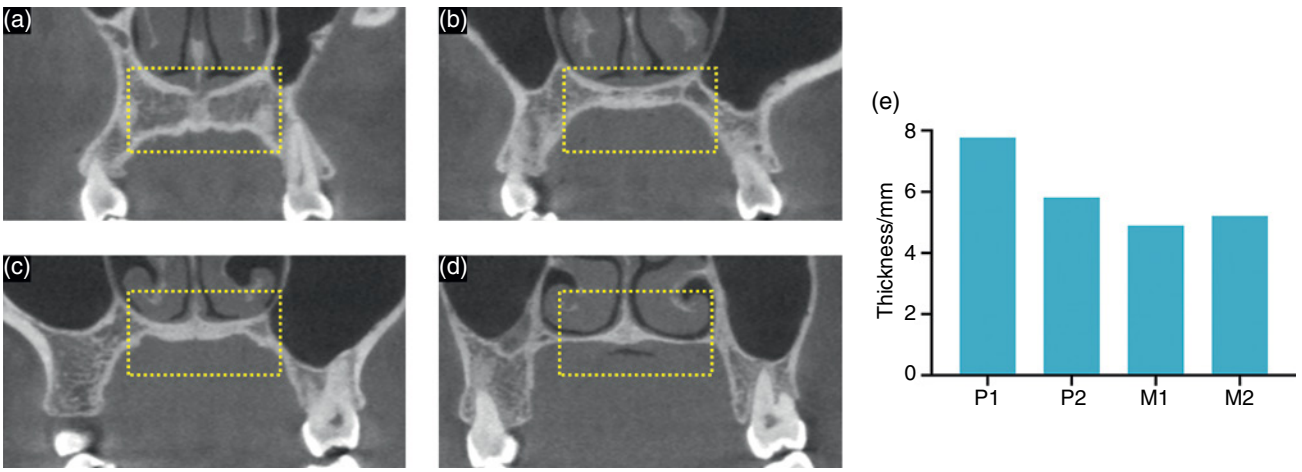


Figure 6.105 Bone depth of the midpalatal suture at different anteroposterior positions. (a) CBCT image (coronal view) showing bone depth at the coronal plane corresponding to the first premolar. (b) CBCT image (coronal view) showing bone depth at the coronal plane corresponding to the second premolar. (c) CBCT image (coronal view) showing bone depth at the coronal plane corresponding to the first molar. (d) CBCT image (coronal view) showing bone depth at the coronal plane corresponding to the second molar. (e) Comparison of bone depth at different coronal planes corresponding to the first premolar (P1), second premolar (P2), first molar (M1) and second molar (M2).

t.me/Dr_Mouayyad_AlbtousH

is considered as the minimum requirement for mini-implant placement. Thus, with regard to bone depth, all four sites can be used for the placement of mini-implants.

Soft Tissue Factor: Soft Tissue Thickness

The palatal suture is covered in thin attached and keratinised mucosa. The thickness of soft tissues gradually increases from the midline to lateral sides.[2,30] The soft tissue underlying the suture is the thinnest, ranging from 1.2 to 1.4 mm.[31,32] Based on data from our previous study, soft tissue thickness is greatest at the first premolar region (2.8 mm) and becomes constant at posterior regions (1 mm to 1.2 mm) (Figure 6.106).[2]

Vital Structures

Nasopalatine neurovascular bundles emerge from the incisive foramen located at the canine region, indicating that mini-implants should not be placed at the suture region anterior to the first premolar region. However, as the incisive canal runs downward in an anterior direction, the placement of mini-implants at the first premolar region carries a risk of canal penetration and nerve injury (Figure 6.107). Although injury to the nasopalatine nerve is not a great concern, canal penetration leads to limited bone depth and may jeopardise the primary stability of mini-implants. Thus, insertion of mini-implants at the first premolar suture region is not recommended.

6.4.2 Optimal Insertion Sites

Based on the aforementioned anatomical features of the midpalatal suture, we recommend mini-implants be placed at the midpalatal suture region distal to the first premolar region (Figure 6.108).

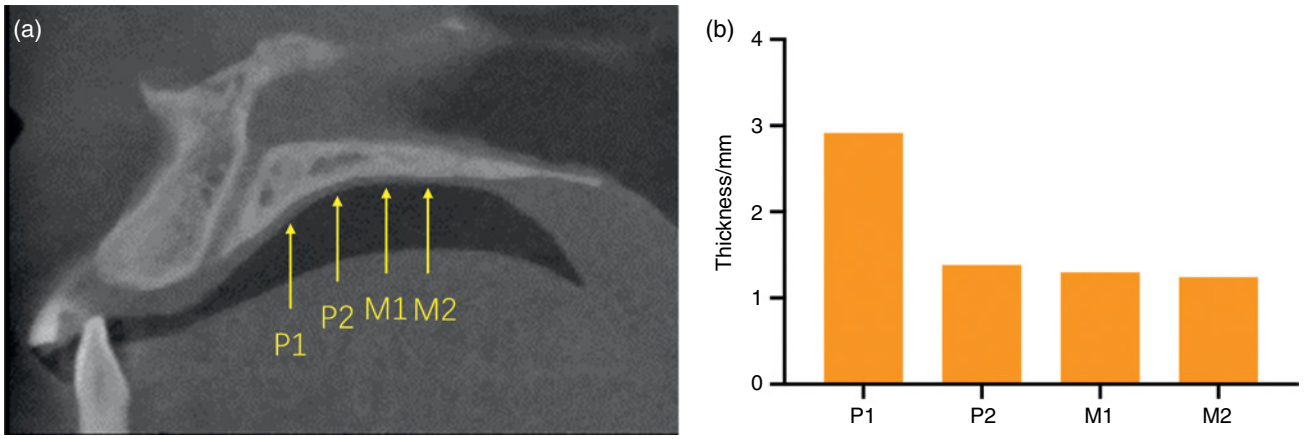


Figure 6.106 The thickness of soft tissue at the midpalatal suture region. (a) A CBCT image showing the thickness of soft tissue at different coronal planes. (b) Comparison of soft tissue thickness at different coronal planes corresponding to the first premolar (P1), second premolar (P2), first molar (M1) and second molar (M2).

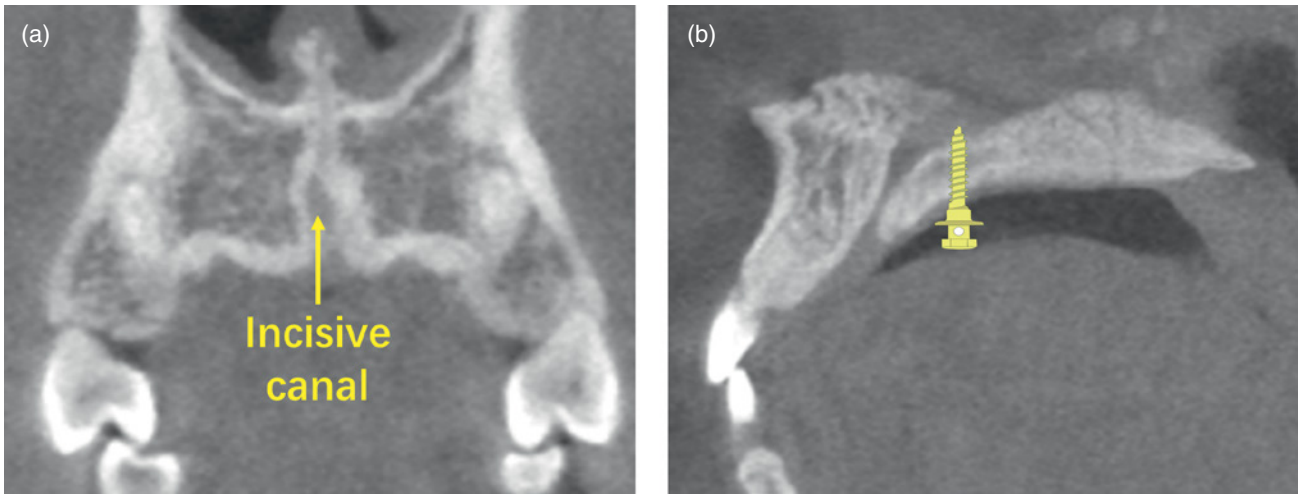


Figure 6.107 Incisive canal. (a) The incisive canal is present at the coronal plane corresponding to the first premolar among some patients. (b) Virtual placement of a simulated mini-implant at the anteroposterior position corresponding to the first premolar penetrates into the incisive canal and may cause injury to the nasopalatine neurovascular bundles.

t.me/Dr_Mouayyad_AlbtousH

6.4.3 Insertion Techniques

The insertion procedures are similar to those for the paramedian region. Briefly, following mucosa disinfection and local anaesthesia, mucosa marking is performed with a probe or explorer. Then, the mini-implant is inserted through the marked entry point using a contra-angle screwdriver. During placement of the mini-implant, the screwdriver should be stabilised to avoid lateral displacement of the shaft which may lead to mini-implant fracture. The procedures for inserting a mini-implant at the midpalatal suture region are illustrated in Figures 6.109 and 6.110.

6.4.4 Clinical Applications

Mini-implants placed at the suture region are often applied for a variety of orthodontic purposes, including molar distalisation (Figure 6.111), molar protraction (Figure 6.112) and molar intrusion (Figure 6.113).

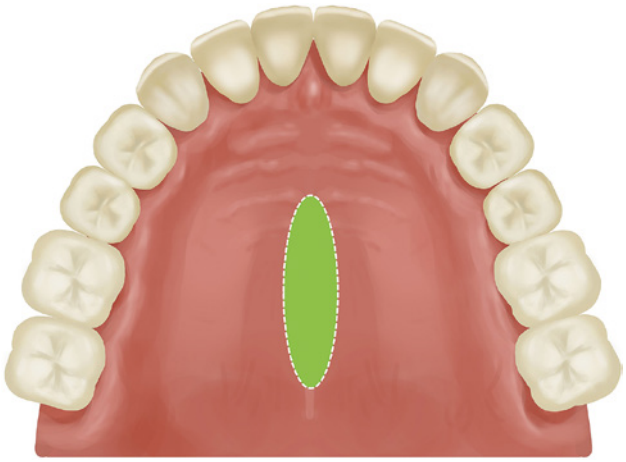


Figure 6.108 Recommended area (green area) for the insertion of mini-implants at the midpalatal suture region.

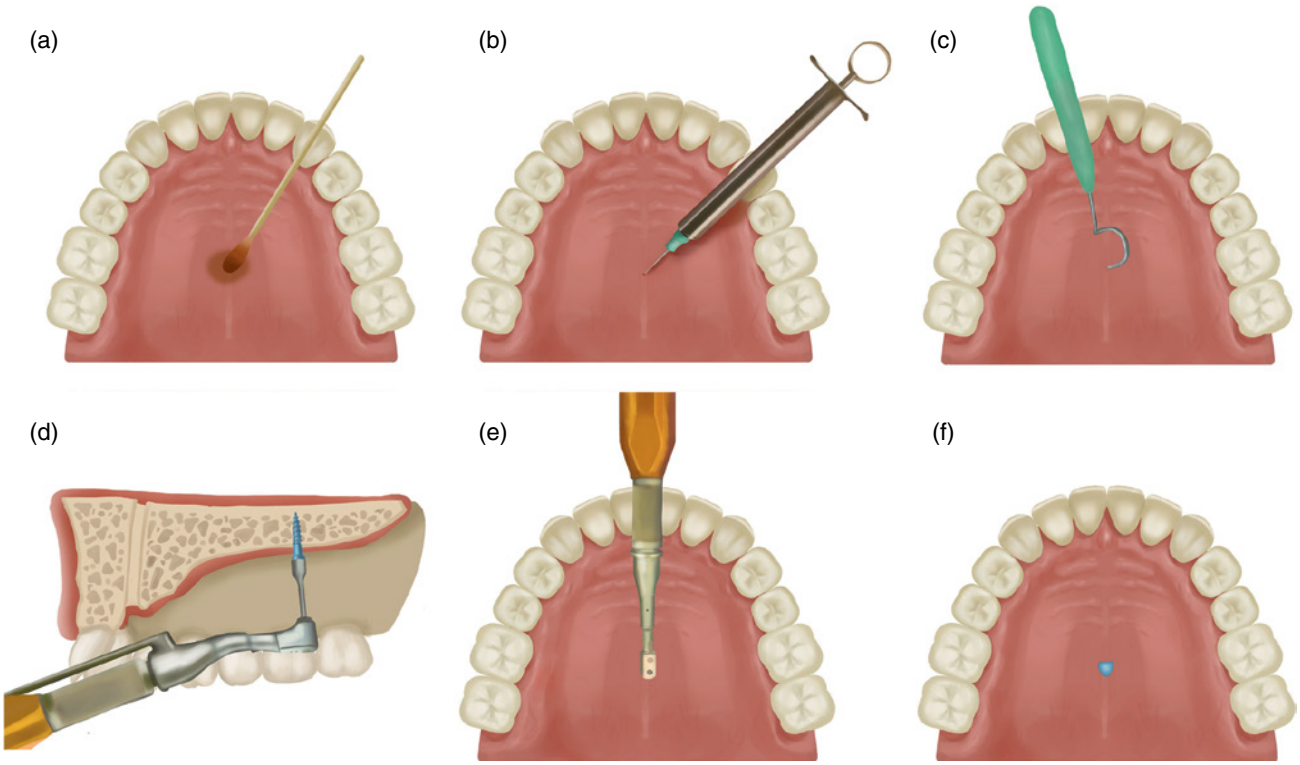


Figure 6.109 Schematic illustrations showing the detailed procedures of inserting a mini-implant at the midpalatal suture region. (a) Mucosa disinfection. (b) Local infiltration anaesthesia. (c) Mark the desired entry point with an explorer. (d) Insert a mini-implant through the designated entry point with a contra-angle screwdriver. (e) Check the orientation and position of the mini-implant from the occlusal side during insertion. (f) Postinsertion examinations.

t.me/Dr_Mouayyad_AlbtousH

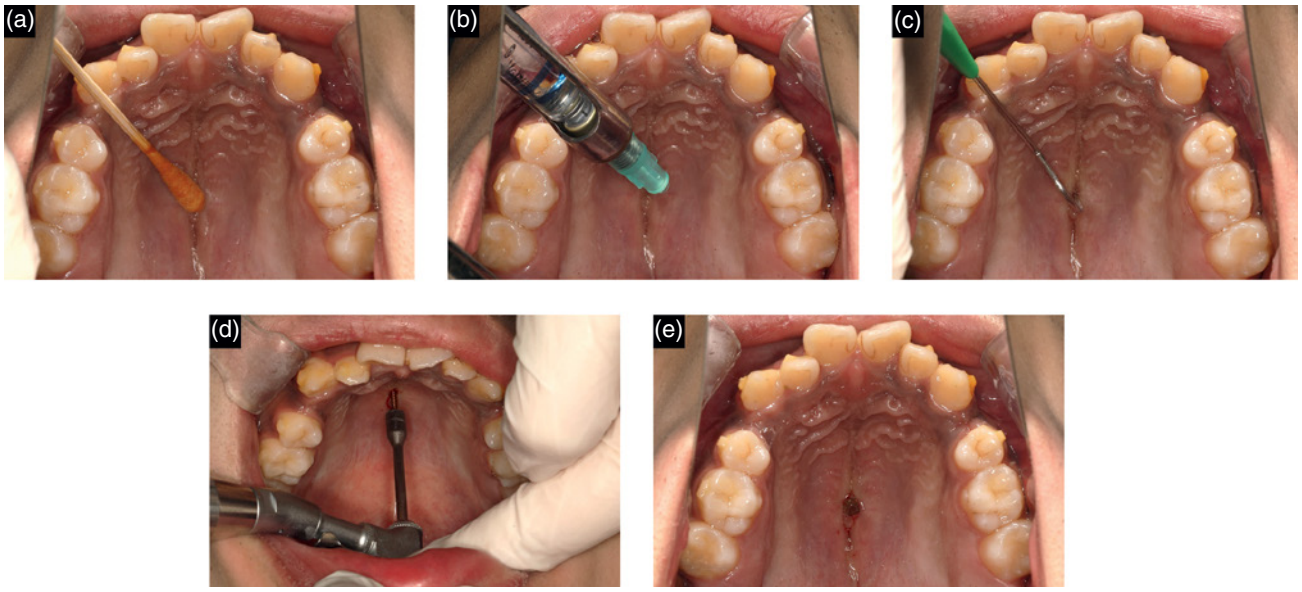


Figure 6.110 Clinical procedures of inserting a mini-implant at the midpalatal suture region. (a) Mucosa disinfection. (b) Local infiltration anaesthesia. (c) Mark the desired entry point with an explorer. (d) Insertion of the mini-implant. (e) Postinsertion examinations of the position and orientation of the mini-implant.

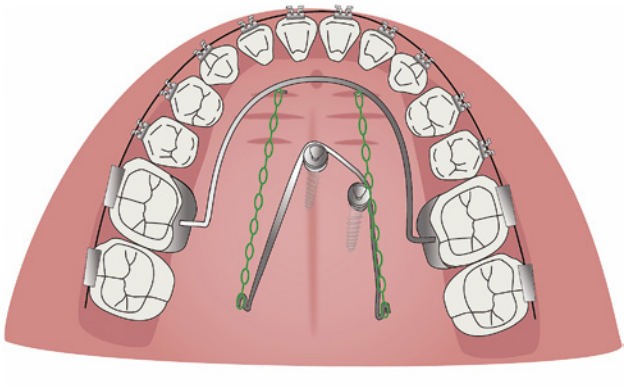


Figure 6.111 Molar distalisation.

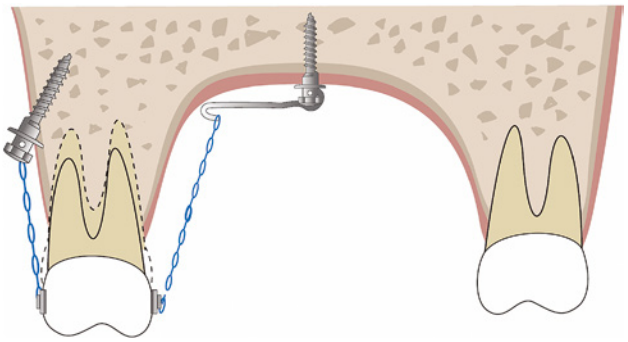
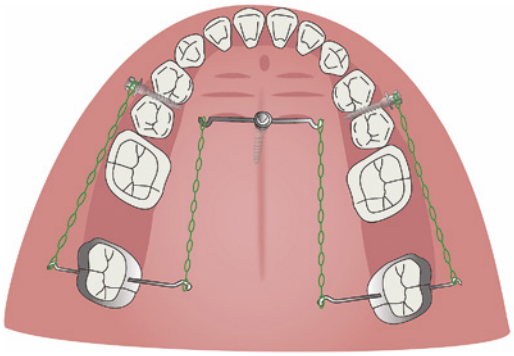


Figure 6.113 Molar intrusion.



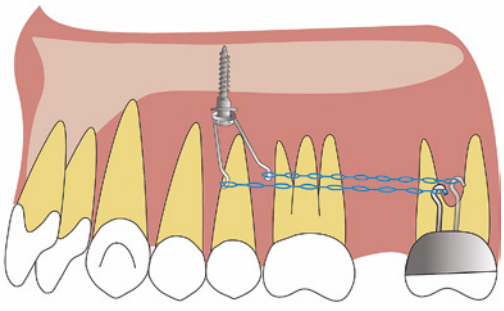


Figure 6.112 Molar protraction.

t.me/Dr_Mouayyad_AlbtousH

6.5 Summary

The palatal region is an ideal anatomical area for the placement of mini-implants owing to its sufficient bone quantity and good bone quality. Three anatomical regions are clinically available for mini-implant placement: interradicular sites, paramedian region and midpalatal suture. Injury to the greater palatine neurovascular bundles should be avoided. The three anatomical regions exhibit different features that should be carefully evaluated prior to the placement of mini-implants. Site-specific insertion procedures should be followed for the three distinct regions. Furthermore, palatal mini-implants are versatile in achieving various orthodontic and orthopaedic outcomes.

References

1 Ryu JH, Park JH, Vu Thi Thu T, Bayome M, Kim Y, Kook YA. (2012). Palatal bone thickness compared with cone-beam computed tomography in adolescents and adults for mini-implant placement. *Am. J. Orthod. Dentofacial Orthop.* 142(2): 207–212.

2 Lyu X, Guo J, Chen L et al. (2020). Assessment of available sites for palatal orthodontic mini-implants through cone-beam computed tomography. *Angle Orthod.* 90(4): 516–523.

3 Arqub SA, Gandhi V, Mehta S, Palo L, Upadhyay M, Yadav S. (2021). Survival estimates and risk factors for failure of palatal and buccal mini-implants. *Angle Orthod.* 91(6): 756–763.

4 Mohammed H, Wafaie K, Rizk MZ, Almuzian M, Sosly R, Bearn DR. (2018). Role of anatomical sites and correlated risk factors on the survival of orthodontic miniscrew implants: a systematic review and meta-analysis. *Prog. Orthod.* 19(1): 36.

5 Gurdan Z, Szalma J. (2018). Evaluation of the success and complication rates of self-drilling orthodontic mini-implants. *Niger. J. Cli.n Pract.* 21(5): 546-–52.

6 Uesugi S, Kokai S, Kanno Z, Ono T. (2018). Stability of secondarily inserted orthodontic miniscrews after failure of the primary insertion for maxillary anchorage: maxillary buccal area vs midpalatal suture area. *Am. J. Orthod. Dentofacial Orthop.* 153(1): 54–60.

7 Cassetta M, Sofan AA, Altieri F, Barbato E. (2013). Evaluation of alveolar cortical bone thickness and density for orthodontic mini-implant placement. *J. Clin. Exp. Dent.* 5(5): e245–252.

8 Ozdemir F, Tozlu M, Germec-Cakan D. (2013). Cortical bone thickness of the alveolar process measured with cone-beam computed tomography in patients with different facial types. *Am. J. Orthod. Dentofacial Orthop.* 143(2): 190–196.

9 Tepedino M, Cattaneo PM, Niu X, Cornelis MA.(2020). Interradicular sites and cortical bone thickness for miniscrew insertion: a systematic review with meta-analysis. *Am. J. Orthod. Dentofacial Orthop.* 158(6): 783–798 e720.

10 Poggio PM, Incorvati C, Velo S, Carano A. (2006) 'Safe zones': a guide for miniscrew positioning in the maxillary and mandibular arch. *Angle Orthod.* 76(2): 191–197.

11 Ahn HW, Kang YG, Jeong HJ, Park YG. (2021). Palatal temporary skeletal anchorage devices (TSADs): what to know and how to do? *Orthod. Craniofac. Res.* 24 Suppl 1: 66–74.

12 Chun YS, Lim WH. (2009). Bone density at interradicular sites: implications for orthodontic mini-implant placement. *Orthod. Craniofac. Res.* 12(1): 25–32.

13 Haddad R, Saadeh M. (2019). Distance to alveolar crestal bone: a critical factor in the success of orthodontic mini-implants. *Prog. Orthod.* 20(1): 19.

14 Tavelli L, Barootchi S, Ravidà A, Oh TJ, Wang HL. (2019). What is the safety zone for palatal soft tissue graft harvesting based on the locations of the greater palatine artery and foramen? A systematic review. *J. Oral Maxillofac. Surg.* 77(2): 271.e271–271.e279.

15 Wang X, Zhu Z, Jiang L et al. (2022). Treatment of dentoalveolar protrusion with customized lingual appliances and template-guided periodontal surgery. *AJO-DO Clin. Compan.* 2(5): 460–471.

16 Marquezan M, Nojima LI, Freitas AO et al. (2012). Tomographic mapping of the hard palate and overlying mucosa. *Braz. Oral Res.* 26(1): 36–42.

17 Chang CJ, Lin WC, Chen MY, Chang HC. (2021). Evaluation of total bone and cortical bone thickness of the palate for temporary anchorage device insertion. *J. Dent. Sci.* 16(2): 636–642.

18 Suteerapongpun P, Wattanachai T, Janhom A, Tripuwabhrut P, Jotikasthira D. (2018). Quantitative evaluation of palatal bone thickness in patients with normal and open vertical skeletal configurations using cone-beam computed tomography. *Imaging Sci. Dent.* 48(1): 51–57.

19 Giudice AL, Rustico L, Longo M, Oteri G, Papadopoulos MA, Nucera R. (2021). Complications reported with the use of orthodontic miniscrews: a systematic review. *Korean J. Orthod.* 51(3): 199–216.

t.me/Dr_Mouayyad_AlbtousH

20 Li N, Sun W, Li Q, Dong W, Martin D, Guo J. (2020). Skeletal effects of monocortical and bicortical mini-implant anchorage on maxillary expansion using cone-beam computed tomography in young adults. *Am. J. Orthod. Dentofacial Orthop.* 157(5): 651–661.

21 Lee DW, Park JH, Moon W, Seo HY, Chae JM. (2021). Effects of bicortical anchorage on pterygopalatine suture opening with microimplant-assisted maxillary skeletal expansion. *Am. J. Orthod. Dentofacial Orthop.* 159(4): 502–511.

22 Pu L, Zhou J, Yan X et al. (2022). Orthodontic traction of an impacted maxillary third molar through a miniscrew-anchored cantilever spring to substitute the adjacent second molar with severe root resorption. *J. Am. Dent. Assoc.* 153(9): 884–892.

23 White HE, Goswami A, Tucker AS. (2021). The intertwined evolution and development of sutures and cranial morphology. *Front. Cell Dev. Biol.* 9: 653579.

24 Sun Z, Lee E, Herring SW. (2004). Cranial sutures and bones: growth and fusion in relation to masticatory strain. *Anat. Rec. A Discov. Mol. Cell Evol. Biol.* 276(2): 150–161.

25 Melsen B. (1975). Palatal growth studied on human autopsy material. A histologic microradiographic study. *Am. J. Orthod.* 68(1): 42–54.

26 Cohen MM Jr. (1993). Sutural biology and the correlates of craniosynostosis. *Am. J. Med. Genet.* 47(5): 581–616.

27 Knaup B, Yildizhan F, Wehrbein H. (2004). Age-related changes in the midpalatal suture. A histomorphometric study. *J. Orofac. Orthop.* 65(6): 467–474.

28 Angelieri F, Franchi L, Cevidanes LH, Bueno-Silva B, McNamara JA Jr. (2016). Prediction of rapid maxillary expansion by assessing the maturation of the midpalatal suture on cone beam CT. *Dental Press J. Orthod.* 21(6): 115–125.

29 Abo Samra D, Hadad R. (2018). Midpalatal suture: evaluation of the morphological maturation stages via bone density. *Prog. Orthod.* 19(1): 29.

30 Yao CC, Chang HH, Chang JZ, Lai HH, Lu SC, Chen YJ. (2015). Revisiting the stability of mini-implants used for orthodontic anchorage. *J. Formos. Med. Assoc.* 114(11): 1122–1128.

31 Vu T, Bayome M, Kook YA, Han SH. (2012). Evaluation of the palatal soft tissue thickness by cone-beam computed tomography. *Korean J. Orthod.* 42(6): 291–296.

32 Parmar R, Reddy V, Reddy SK, Reddy D. (2016). Determination of soft tissue thickness at orthodontic miniscrew placement sites using ultrasonography for customizing screw selection. *Am. J. Orthod. Dentofacial Orthop.* 150(4): 651–658.

t.me/Dr_Mouayyad_AlbtousH

7

Mandibular Labial Region

Yi Yang[1], Donger Lin[1], Lingling Pu[1,2], Shizhen Zhang[1,3], Yan Wang[1], Erpan Alkam[1], and Hu Long[1]

[1] *Department of Orthodontics, State Key Laboratory of Oral Diseases and National Clinical Research Center for Oral Diseases, West China Hospital of Stomatology, Sichuan University, Chengdu, China*
[2] *Private Practice, Chengdu, China*
[3] *Faculty of Dentistry, The University of Hong Kong, Hong Kong, SAR, China*

7.1 Introduction

The mandibular labial region is an anatomical area spanning between bilateral canines. In clinical practice, this region is not as frequently used for mini-implant placement as its maxillary counterpart, probably due to limited interradicular space, especially among patients with dental crowding in the lower arches.[1] Compared with interradicular sites in the maxillary labial region, those in the mandibular labial region have higher bone density that may lead to bone damage during insertion, resulting in a higher failure rate of mini-implants in the mandible. Nevertheless, mini-implants inserted at the mandibular labial region are still clinically employed to accomplish a variety of orthodontic tooth movements (e.g. incisor intrusion and intermaxillary fixation).[2]

In this region, two anatomical areas are clinically available for the placement of mini-implants: interradicular sites and mandibular symphysis (Figure 7.1). Compared with interradicular sites, the mandibular symphysis has greater bone quantity and better bone quality and is a promising alternative anatomical area. Mini-implants placed at these two areas are most frequently used for mandibular incisor intrusion and both can be used for incisor intrusion with fixed appliances (Figure 7.2) and clear aligner (Figure 7.3). In this chapter, anatomical features, site selection and detailed insertion techniques will be presented.

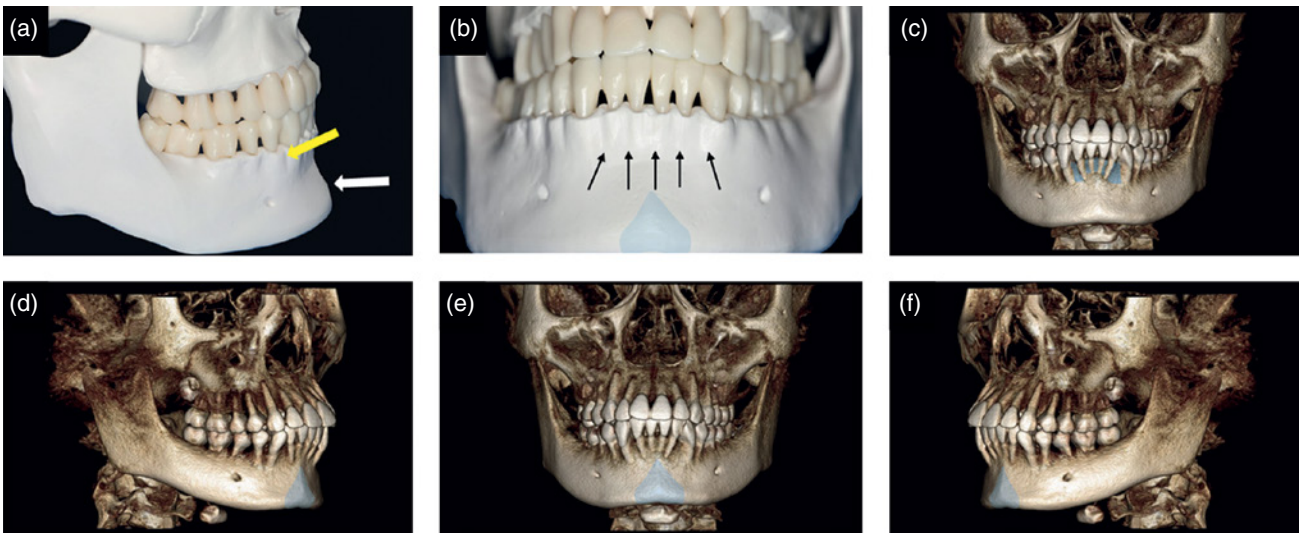


Figure 7.1 (a) Sagittal view of the mandibular labial region on a skull, including interradicular sites (yellow arrow) and mandibular symphysis (white arrow). (b) Frontal view of the mandibular labial region on a skull. Interradicular sites are indicated by the black arrows and the mandibular symphysis by the blue area. (c) The interradicular sites (blue area) are depicted on a 3-D reconstruction image. (d–f) The mandibular symphysis (blue area) is depicted on 3-D reconstruction images.

Clinical Insertion Techniques of Orthodontic Temporary Anchorage Devices, First Edition. Edited by Hu Long, Xianglong Han, and Wenli Lai.
© 2024 John Wiley & Sons Ltd. Published 2024 by John Wiley & Sons Ltd.

t.me/Dr_Mouayyad_AlbtousH

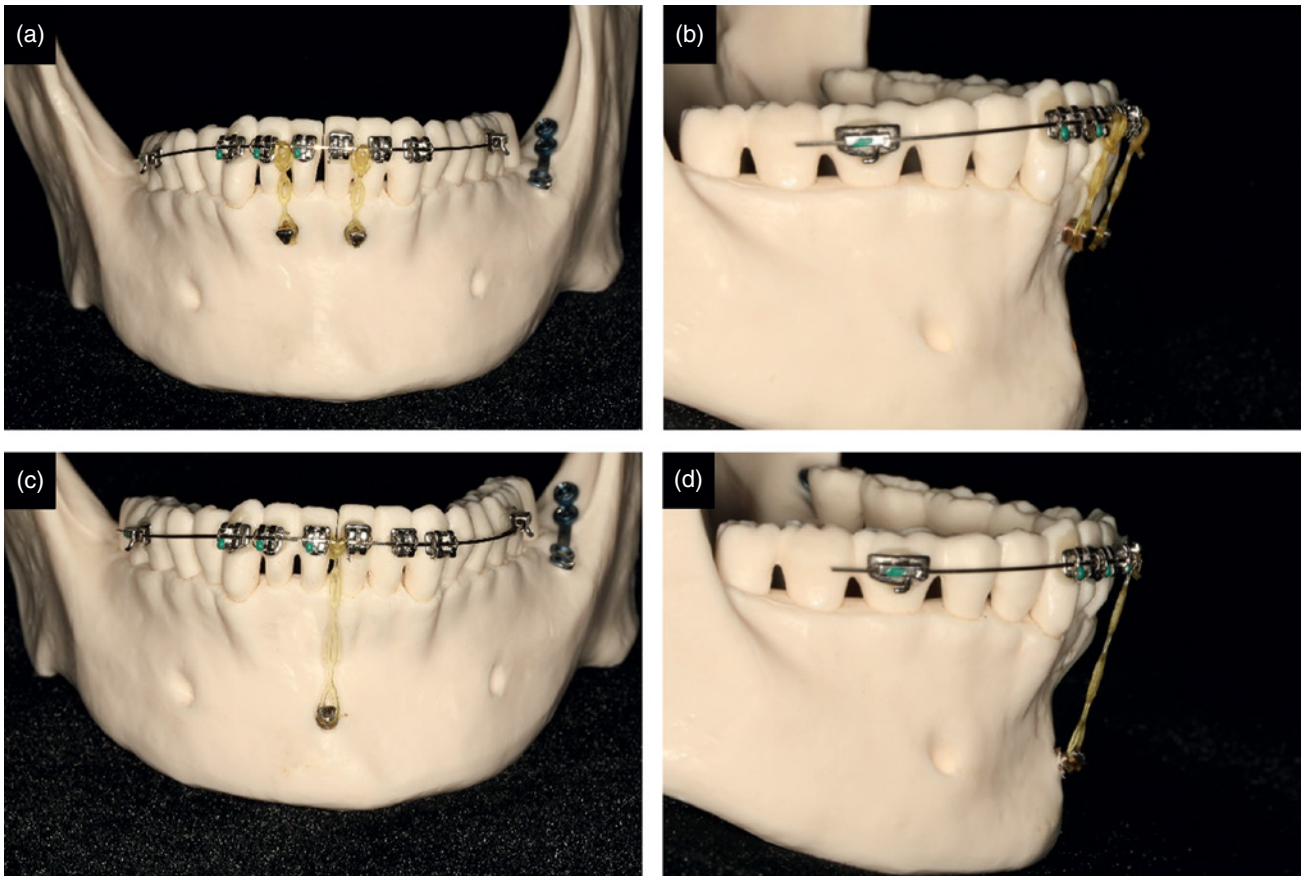


Figure 7.2 Mini-implants at the mandibular labial region for anterior intrusion with fixed appliances. (a) Mini-implants at the interradicular sites for incisor intrusion (frontal view). (b) Mini-implants at the interradicular sites for incisor intrusion (sagittal view). (c) A mini-implant at the mandibular symphysis region for incisor intrusion (frontal view). (d) A mini-implant at the mandibular symphysis region for incisor intrusion (sagittal view).

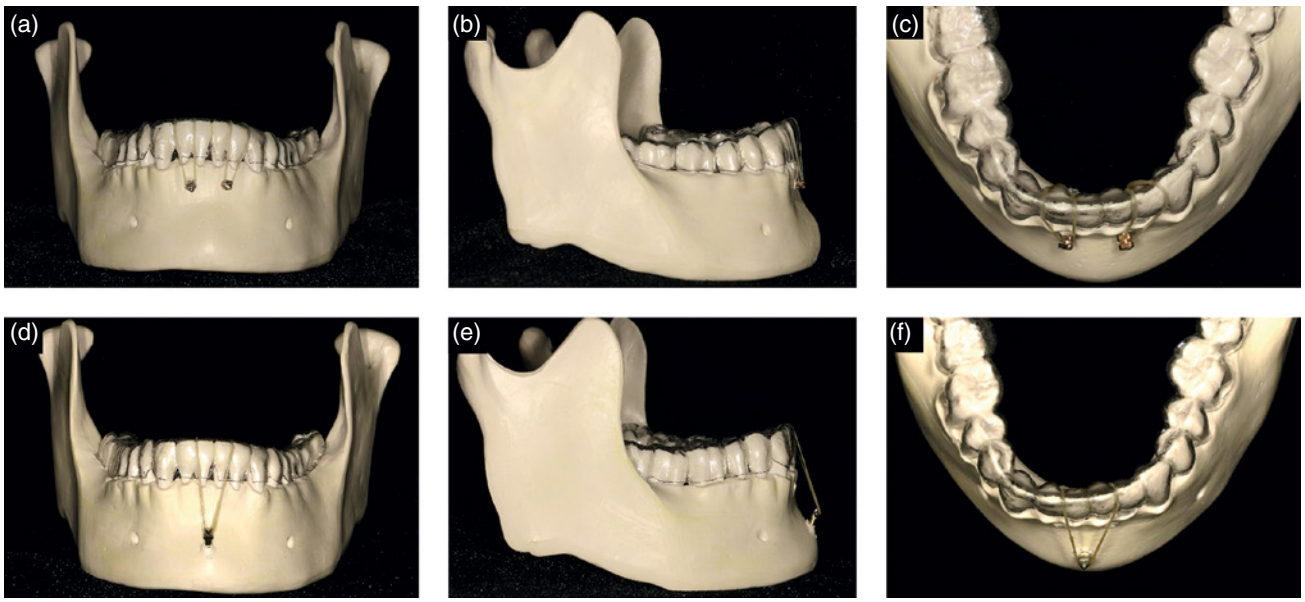


Figure 7.3 Mini-implants at the mandibular labial region for anterior intrusion with clear aligner. (a) Mini-implants at the interradicular sites for incisor intrusion (frontal view). (b) Mini-implants at the interradicular sites for incisor intrusion (sagittal view). (c) Mini-implants at the interradicular sites for incisor intrusion (occlusal view). (d) A mini-implant at the mandibular symphysis region for incisor intrusion (frontal view). (e) A mini-implant at the mandibular symphysis region for incisor intrusion (sagittal view). (f) A mini-implant at the mandibular symphysis region for incisor intrusion (occlusal view).

t.me/Dr_Mouayyad_AlbtousH

7.2 Interradicular Sites

7.2.1 Anatomical Characteristics

Interradicular sites in the mandibular labial region refer to the alveolar bone that is between two adjacent roots. There are five interradicular sites available for the placement of mini-implants and they can be divided into three anatomical sites based on their distinct anatomical features: L1-L1, L1-L2 and L2-L3 (Figure 7.4). In clinical practice, both hard tissue and soft tissue factors should be considered to select optimal sites for orthodontic mini-implants. Specifically, hard tissue factors include cortical thickness, bone depth, bone width and root prominence, while soft tissue factors are labial frenum and attached gingiva.

Hard Tissue Factor: Cortical Thickness

Cortical thickness differs among the three interradicular sites and different vertical heights.[3] Cortical thickness is similar between males and females but differs between adults and adolescents, indicating that age but not gender is an influencing factor for cortical thickness.[4] As displayed in Figure 7.5, cortical thickness at the L2-L3 site is thicker than that at the L1-L1 and L1-L2 sites, which may be attributed to higher occlusal force required at the canine region. As for insertion heights, cortical thickness increases with an increase in vertical height, indicating that greater cortical engagement is achieved if entry point is more apical. However, these differences may not be clinically significant. As is well documented, cortical thickness should be at least 1 mm so that adequate primary stability of mini-implants can be guaranteed.[5,6]

Based on average values, the requirements of cortical thickness are satisfied in almost all the interradicular sites in the mandibular labial region. However, individual variations do exist and cortical thickness may be less than 1 mm among some patients, especially for adolescents. For these patients, thorough CBCT examinations and meticulous evaluation should be implemented prior to the placement of mini-implants. If limited cortical thickness is detected, a more apical entry and angled insertion are recommended to gain greater cortical engagement (Figure 7.6).

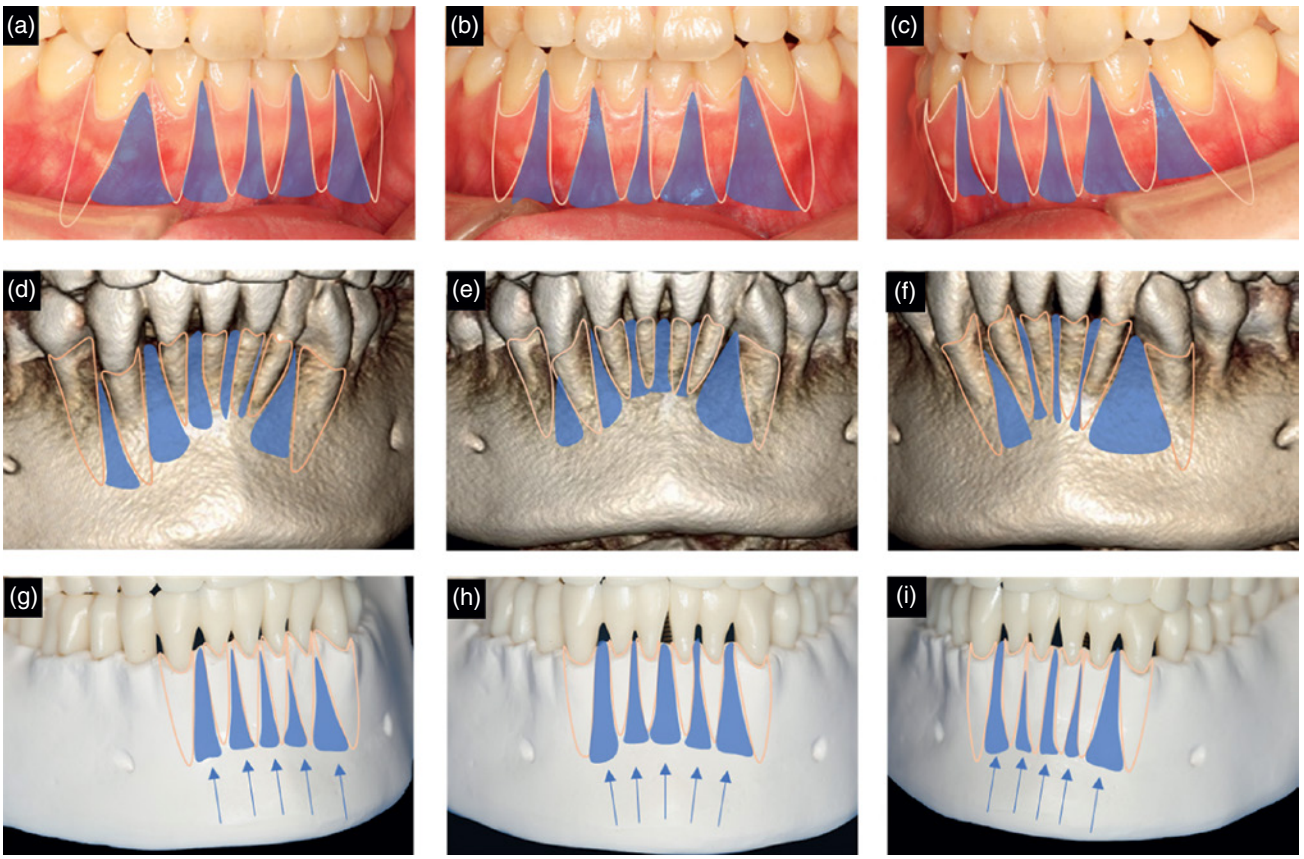


Figure 7.4 The mandibular labial interradicular sites (blue areas). (a–c) Intraoral photographs showing the interradicular sites. (d–f) Three-dimensional reconstruction images of the interradicular sites. (g–i) Interradicular sites shown on skulls.

t.me/Dr_Mouayyad_AlbtousH

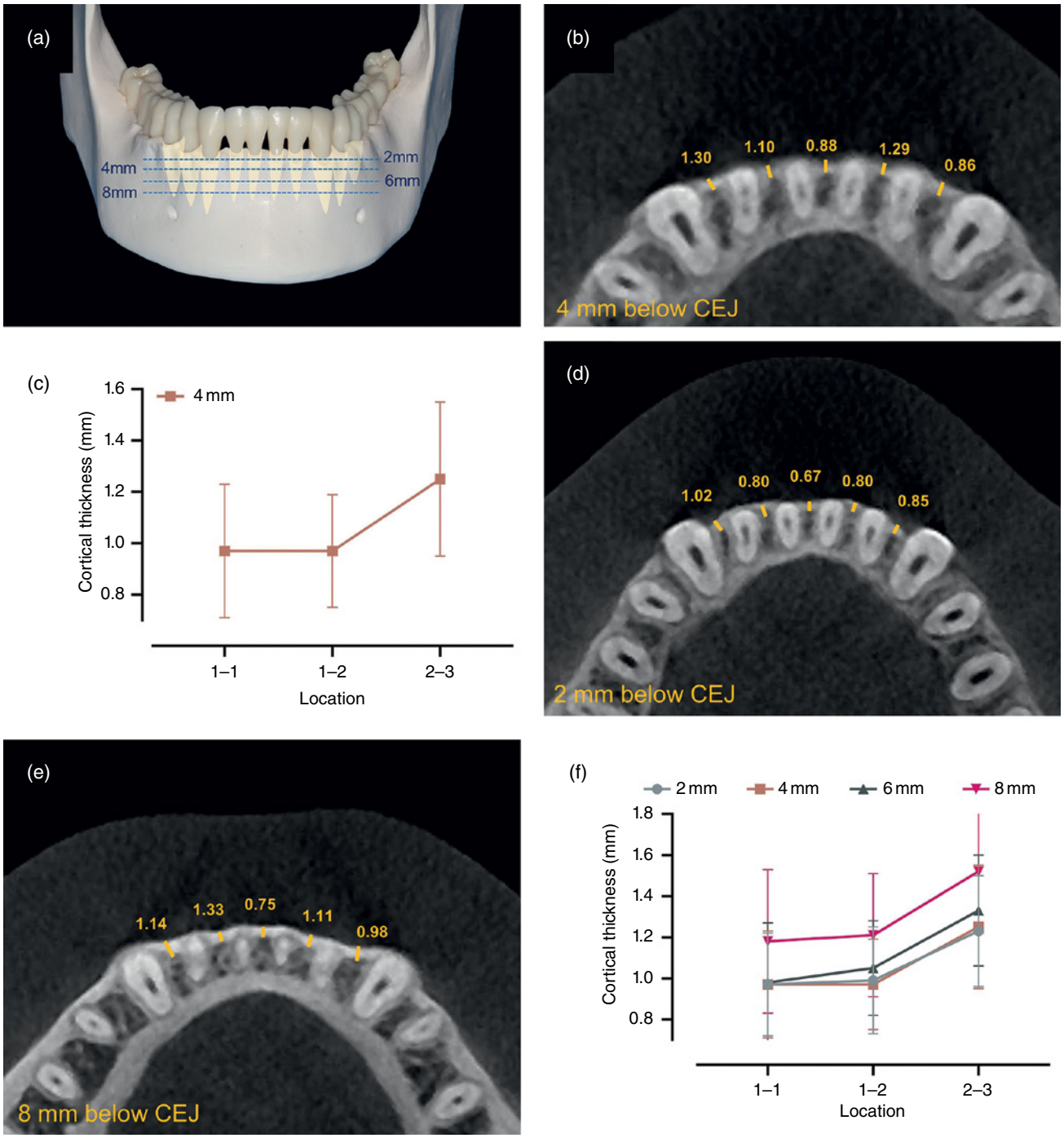


Figure 7.5 Comparison of cortical thickness at different interradicular sites and at different heights. (a) Four horizontal sections were chosen, i.e. 2mm, 4 mm, 6 mm and 8 mm below the CEJ. (b,c) The differences of cortical thickness at different interradicular sites at the 4 mm level below the CEJ. (d–f) Cortical bone thickness varies among the three interradicular sites and different heights. *Source:* Adapted from Wang et al. [3]/Frontiers Media S.A.

t.me/Dr_Mouayyad_AlbtousH

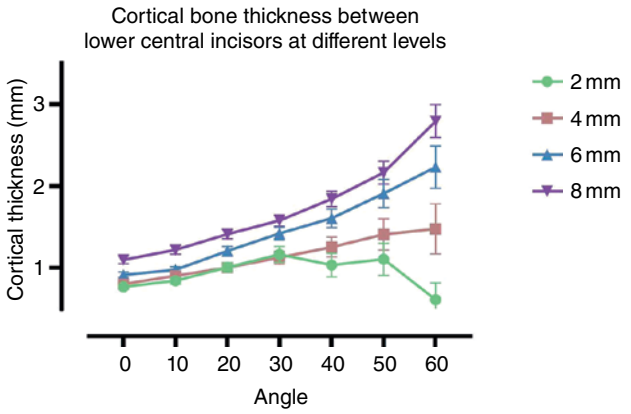


Figure 7.6 Cortical thickness of the alveolar bone between central incisors at different insertion heights and insertion angles. Cortical thickness increases with an increase in the insertion height and insertion angle. *Source:* Adapted from Zhang et al. [12].

Hard Tissue Factor: Bone Depth

Bone depth is the distance between labial and lingual cortical plates and is an important determinant factor for selection of appropriate length for mini-implants. As shown in Figure 7.7, bone depth is greatest at the L2-L3 site and smallest at the L1-L1 site, with L1-L2 being in the middle. Moreover, bone depth becomes greater with an increase in vertical height. In particular, bone depth at the 2 mm level is smaller than that at other vertical levels for all interradicular sites. Also, bone depth is similar among the other three levels (4 mm, 6 mm and 8 mm) for all the interradicular sites, except that greater bone depth is detected at the 8 mm level than at other levels (4 mm and 6 mm) for the L1-L1 site. This may be due to the bone prominence formed by the fusion of two mandibular halves at the 8 mm level. Thus, short mini-implants (6 mm length) are often recommended for mandibular labial interradicular sites.

However, among patients with limited bone depth, penetration of lingual cortical plates may be encountered in clinical practice (Figure 7.8). For these patients, more apical entry and oblique insertion can increase bone depth and may avoid the penetration of lingual cortical plates (Figures 7.9, 7.10 and 7.11).

Therefore, in terms of bone depth, we recommend that short mini-implants (6 mm) be placed at 4 mm or more apical to the CEJ with angled insertion technique.

Hard Tissue Factor: Bone Width

Bone width is the interradicular distance between two adjacent roots. Adequate bone width is required to ensure the clinical success of mini-implants, otherwise limited bone width may lead to root contact or damage that eventually results in mini-implant failure. It has been reported that inadvertent root penetration occurred due to placement of a mini-implant into mandibular labial interradicular sites with limited interradicular space.[7] As displayed in Figure 7.12, bone width is greater at the L2-L3 site than at the L1-L1 and L1-L2 sites. Moreover, bone width increases with an increase in vertical height of the entry point. Nevertheless, the average values of bone width at the L1-L1 and L1-L2 sites range from 1.4 mm to 1.8 mm, which do not satisfy the minimal requirement. Specifically, as per the 1 mm root clearance principle, bone width should be at least 3.5 mm (1 + 1.5 + 1 = 3.5) if a 1.5 mm mini-implant is used. Although bone width is greater at the L2-L3 site, this site is still not qualified for the placement of mini-implants based on average values (1.7–2.4 mm).

Thus, in terms of bone width, all three interradicular sites may not be qualified for mini-implant placement. However, fortunately, individual variations do exist in clinical practice, and sufficient bone width may be detected for certain interradicular sites at the mandibular labial region among some orthodontic patients (Figure 7.13). Likewise, more apical entry and angled insertion are recommended since greater bone width can be obtained.

Hard Tissue Factor: Root Prominence

Root prominence is more apparent in the mandibular labial region than in the maxillary counterpart (Figure 7.14). The presence of root prominence is beneficial for accurate location of the entry point. Thus, we recommend operators leverage this hard tissue factor and palpate root prominences when locating the entry points for mini-implant placement.

Soft Tissue Factor: Labial Frenum

At the L1-L1 site, labial frenum is present that originates from the mucogingival junction and extends to the movable mucosa (Figure 7.15). If mini-implants are to be placed at the interradicular site between the two central incisors, frenectomy is indicated. Otherwise, soft tissue complications may occur during (soft tissue wrapping) and following (soft tissue irritation) mini-implant insertion without frenectomy.

Soft Tissue Factor: Attached Gingiva

Since attached gingiva is fixed onto the alveolar bone, it is recommended to insert mini-implants into the attached gingiva zone, so that the likelihood of soft tissue

t.me/Dr_Mouayyad_AlbtousH

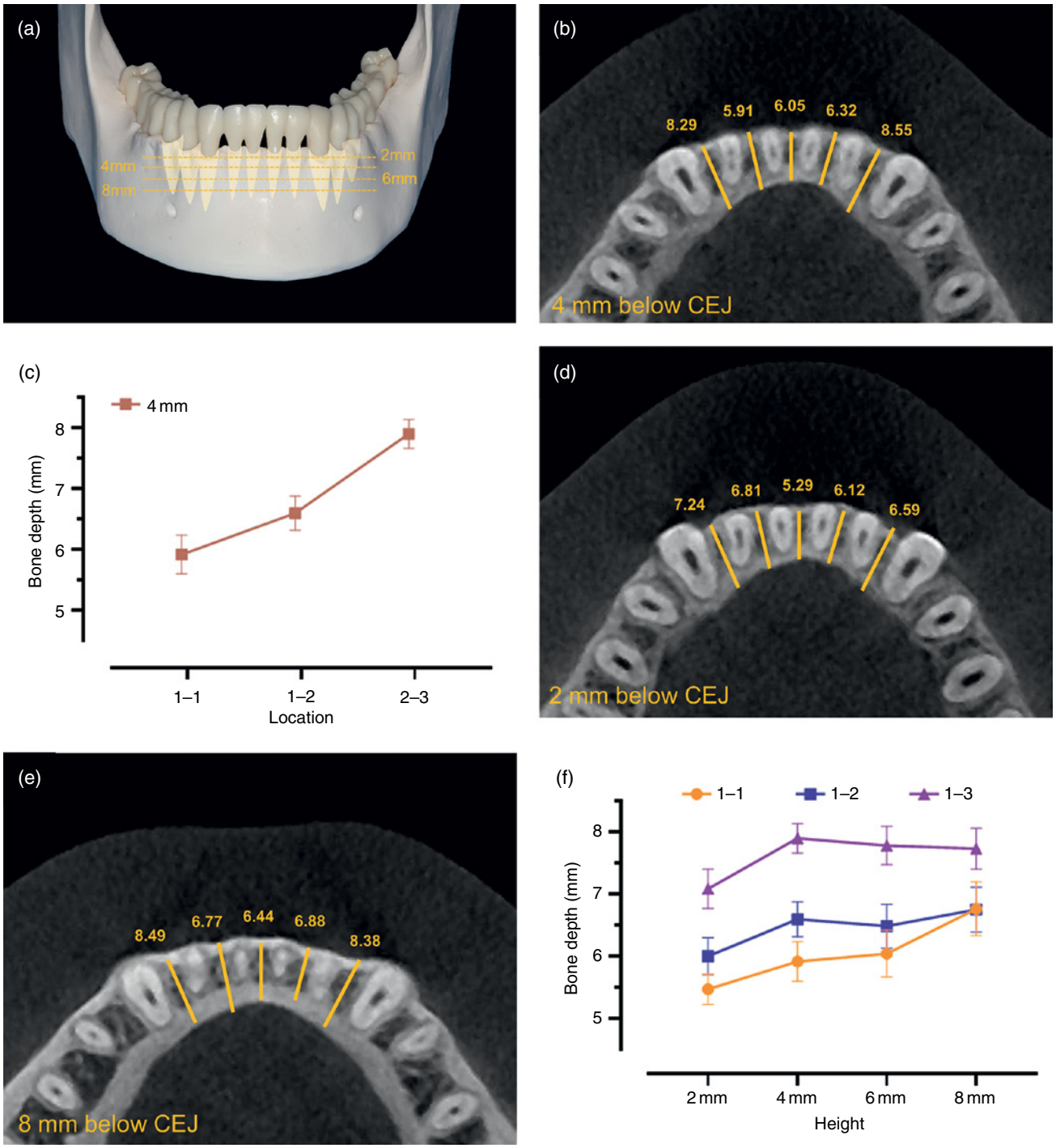


Figure 7.7 Comparison of bone depth at different interradicular sites and at different heights. (a) Four horizontal sections were chosen, i.e. 2mm, 4 mm, 6 mm and 8 mm below the CEJ. (b,c) The differences of bone depth at different interradicular sites at the 4 mm level below the CEJ. (d–f) Bone depth varies among the three interradicular sites and different heights. *Source:* Adapted from Wang et al. [3]/Frontiers Media S.A.

t.me/Dr_Mouayyad_AlbtousH

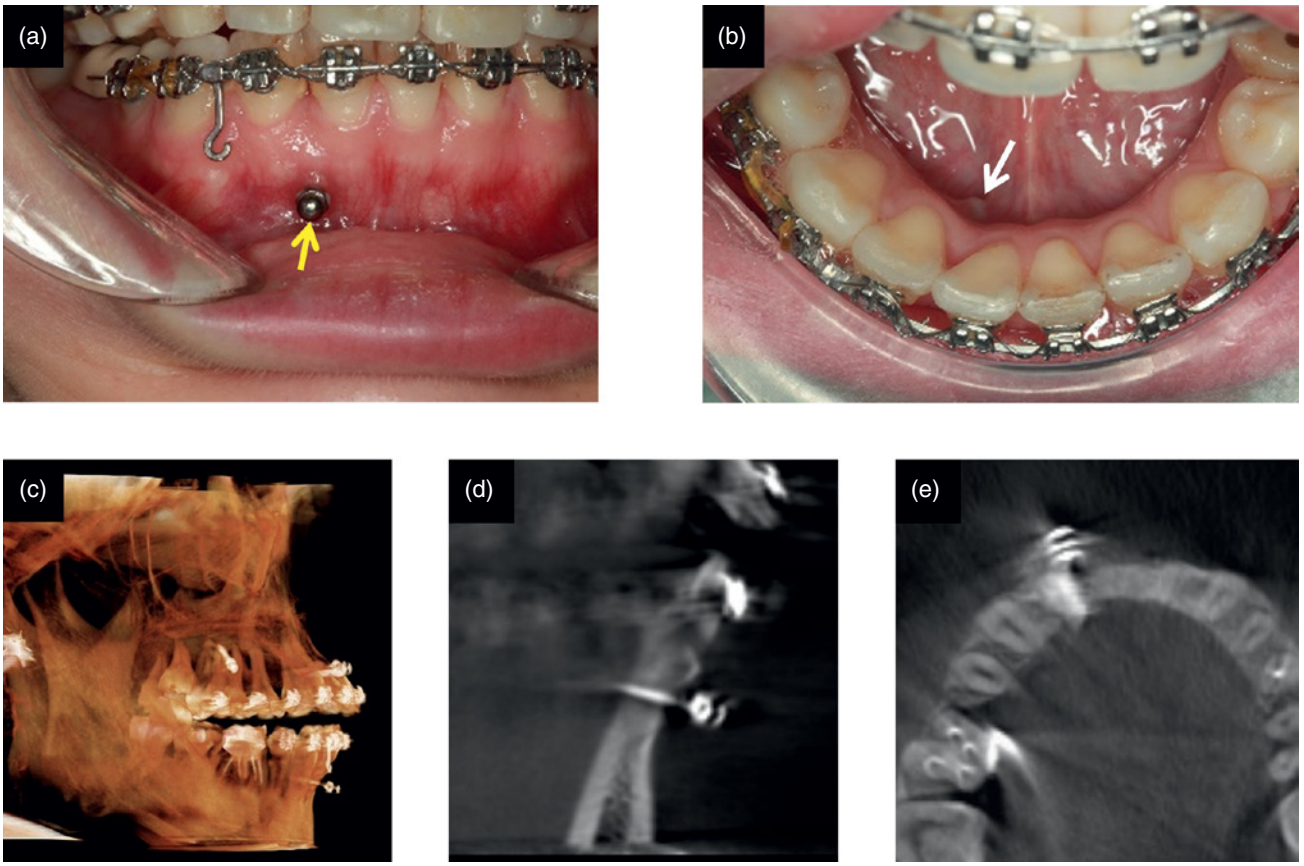


Figure 7.8 Penetration of the lingual cortex by a mini-implant. (a) The mini-implant (yellow arrow) was inserted between the mandibular right central and lateral incisors. (b) A soft tissue bulge (white arrow) that indicated penetration of the lingual cortex was detected at the lingual side between the mandibular right central and lateral incisors. (c–e) Radiographs showing the penetration of the lingual cortex by the mini-implant.



Figure 7.9 Greater bone depth can be engaged with an oblique insertion path compared to horizontal insertion through the same entry point.

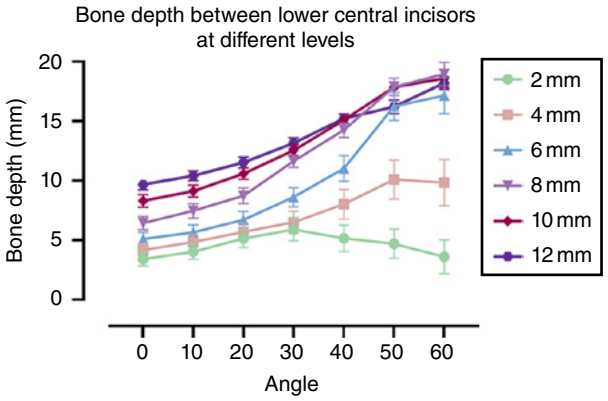


Figure 7.10 Bone depth becomes greater with an increase in insertion height and insertion angle, except for the 2 mm level below the CEJ.

t.me/Dr_Mouayyad_AlbtousH

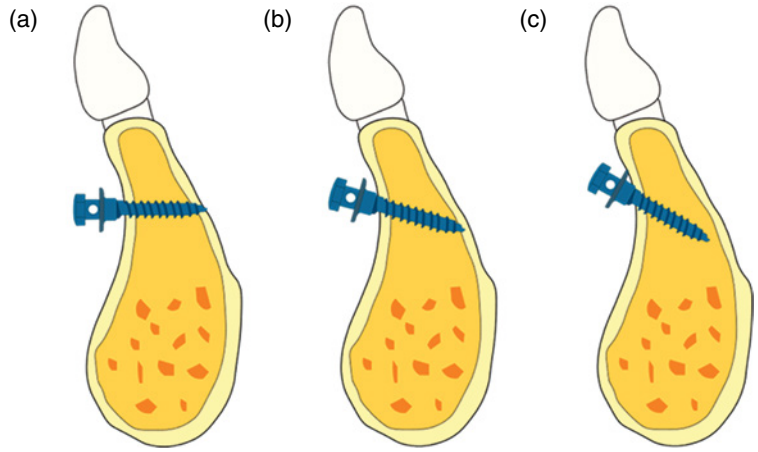


Figure 7.11 Schematic illustrations showing that greater bone depth is obtained with oblique insertion technique through the same entry point. (a) Horizontal insertion. (b) Oblique insertion (15°). (c) Oblique insertion (30°).

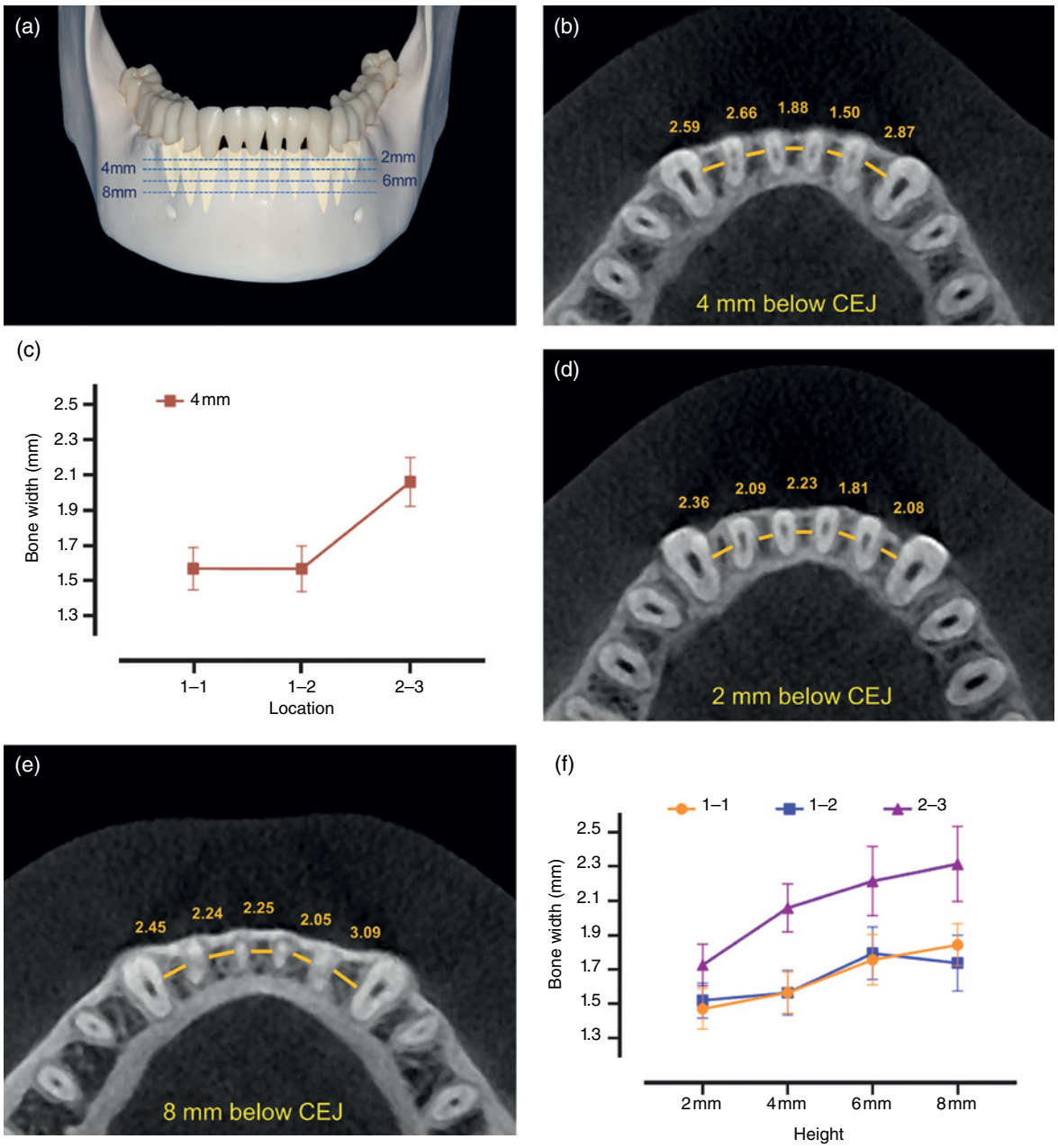


Figure 7.12 Comparison of bone width at different interradicular sites and different heights. (a) Four horizontal sections were chosen, i.e. 2 mm, 4 mm, 6 mm and 8 mm below the CEJ. (b,c) The differences of bone width at different interradicular sites at the 4 mm level below the CEJ. (d–f) Bone width varies among the three interradicular sites and different heights. *Source:* Adapted from Wang et al. [3]/Frontiers Media S.A.

t.me/Dr_Mouayyad_AlbtousH

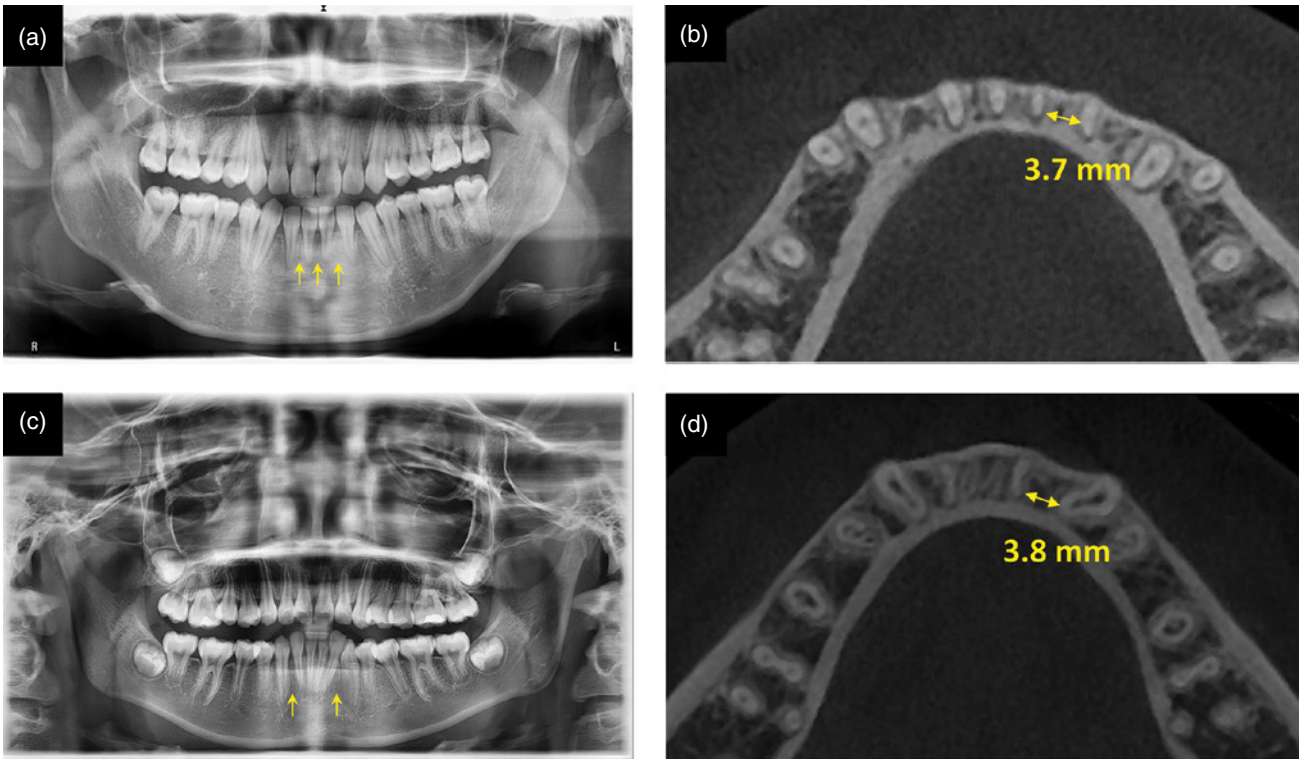


Figure 7.13 (a,b) Panoramic radiograph and CBCT image showing that the bone width in the apical region is 3.7 mm, which is qualified for insertion. (c,d) Panoramic radiograph and CBCT image showing that the bone in the apical region has a width of 3.8 mm and is eligible for insertion.



Figure 7.14 Root prominences (yellow arrows) can be visually detected at the mandibular labial region.



Figure 7.15 Mandibular labial frenum (yellow arrow).

complications and mini-implant failure can be significantly reduced. To gain greater bone quantity, mini-implants are often inserted at the apical limit of the attached gingiva (mucogingival junction) (Figure 7.16). A recent clinical study revealed that widths of attached gingiva were slightly greater in the mandibular incisor region (2.6 ± 1.1 mm) than in the canine region (2.3 ± 0.8 mm).[8] Similar results were found in another study where the averaged widths of attached gingiva were 2.9, 3.3 and 2.0 for central incisors, lateral incisors and canines, respectively.[9] However, clinical variations do exist and the optimal sites should be selected based on different widths of attached gingiva at different interradicular sites.

7.2.2 Biomechanical Perspectives

Mini-implants placed at this region are often leveraged to intrude mandibular anterior teeth. If the anterior six teeth

t.me/Dr_Mouayyad_AlbtousH

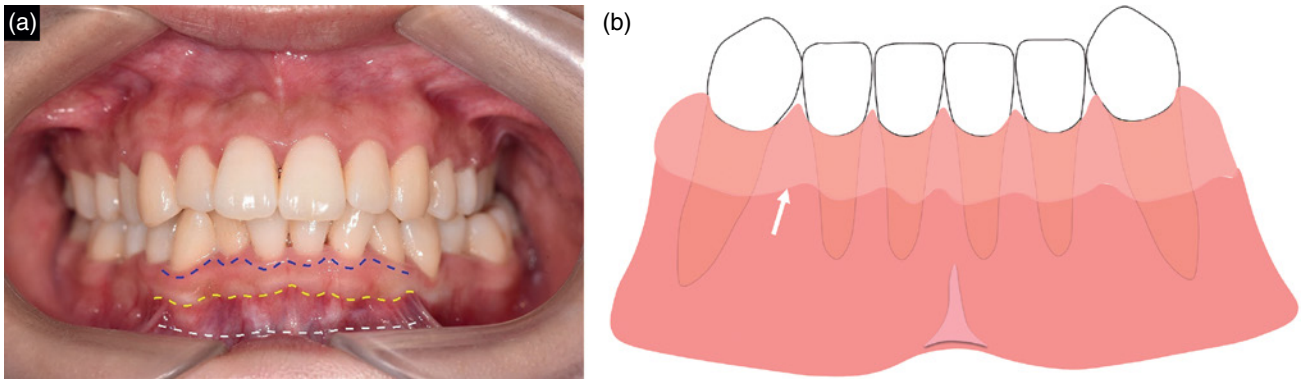


Figure 7.16 Soft tissue at the mandibular labial region. (a) Attached gingiva lies between the apical limit of the free gingiva (blue dashed line) and the mucogingival junction (yellow dashed line). Movable mucosa is between the mucogingival junction (yellow dashed line) and the vestibular sulcus (white dashed line). (b) Mini-implants are often inserted at the mucogingival junction (white arrow).

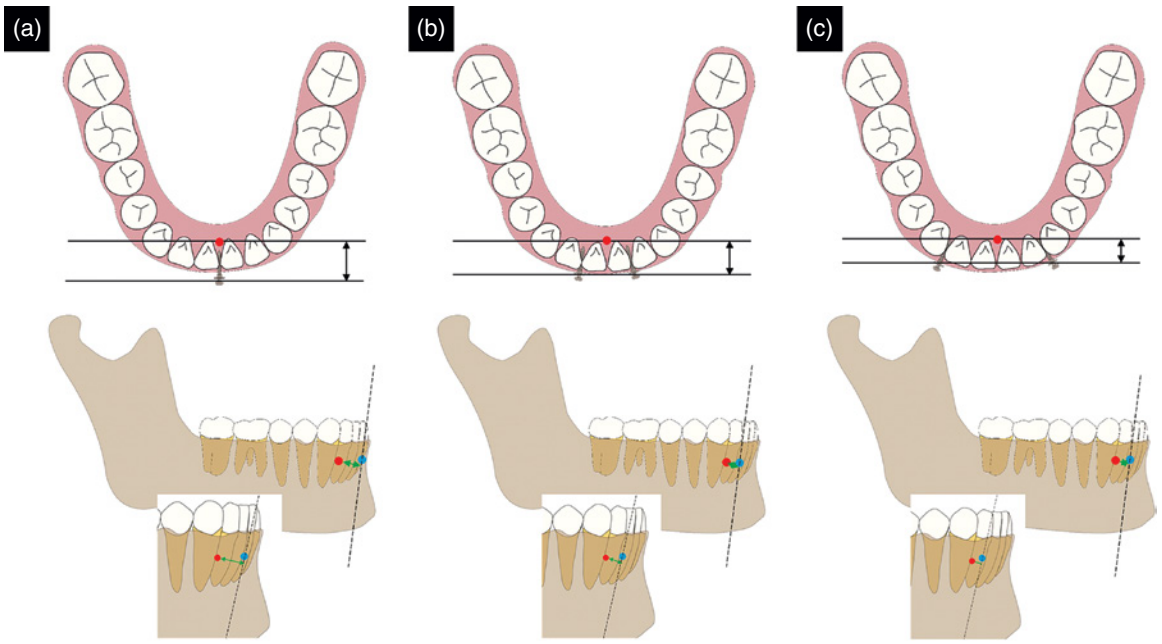


Figure 7.17 Different distances between the centres of resistance and the head of the mini-implants at different interradicular sites. (a) The mini-implant placed at the L1-L1 site. (b) L1-L2 sites. (c) L2-L3 sites.

are taken as a whole, their centre of resistance is located between the lateral incisors and canines in the sagittal plane and between the two central incisors in the transverse plane. This results in different distances between the centre of resistance and the mini-implant heads among the three interradicular sites (Figure 7.17). From the perspectives of biomechanics, different moment/force (M/F) ratios exist among the three modes, with highest and lowest M/F ratios obtained for the L1-L1 and L2-L3 sites respectively (Figure 7.18). Specifically, the L1-L1 site is recommended if both incisor proclination and intrusion are indicated, while the L2-L3 site is preferred if only intrusion is required.

7.2.3 Determining the Optimal Sites

As mentioned above, bone width is a limiting factor in selecting appropriate sites for mini-implant placement. Prior to mini-implant placement, thorough radiographic examinations and evaluations should be implemented. Mini-implants should be placed only if ample interradicular space is present. More apical entry and angled insertion

t.me/Dr_Mouayyad_AlbtousH

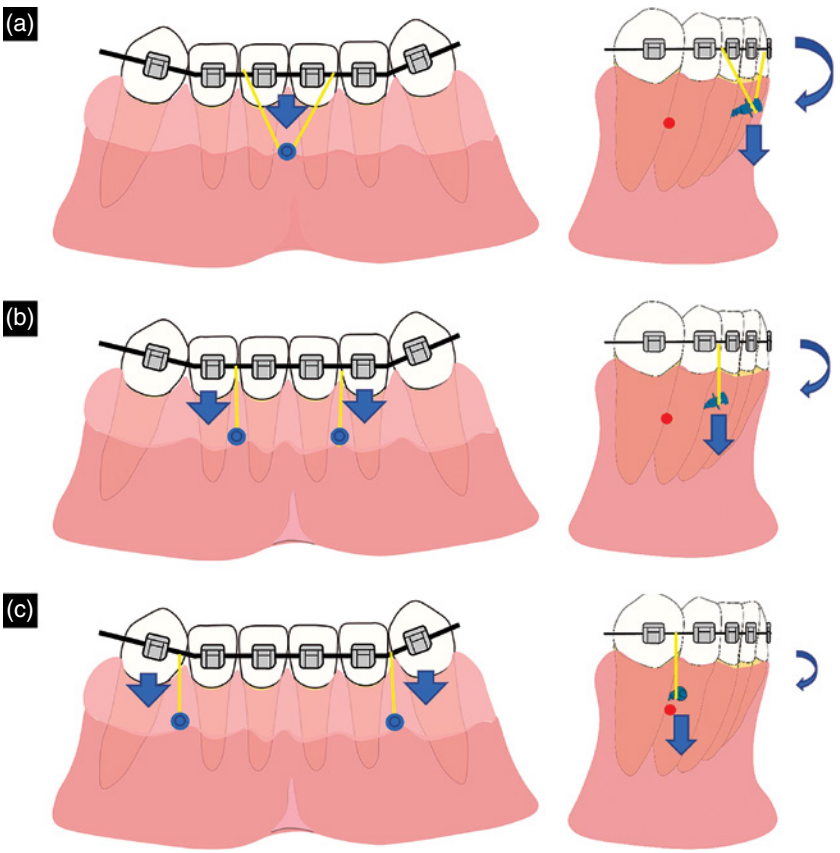


Figure 7.18 (a) The mini-implant is inserted at the L1-L1 site. The moment/force ratio is the highest. (b) The mini-implants are inserted at L1-L2 sites. (c) The mini-implants are inserted at L2-L3 sites. The moment/force ratio is the lowest.

Table 7.1 The anatomy and biomechanics of anterior interradicular sites.

		Anatomy					Biomechanics		
	Site	Bone width	Bone depth	Cortical thickness	Mucogingival height	Frenectomy	Proclination	Intrusion	M/F ratio
Mandible	1-1	Narrow	Relatively insufficient	Thin	Low	Yes	Very efficient	Efficient	High
	1-2	Narrow	Relatively insufficient	Medium	Medium	No	Efficient	Efficient	Medium
	2-3	Wide	Sufficient	Thick	High	No	Inefficient	Efficient	Low

can gain greater interradicular space and are recommended in clinical practice. As displayed in Table 7.1, anatomical characteristics and biomechanical features differ among the three anatomical sites. Unlike other anatomical regions where standard insertion protocols are available, the insertion protocols differ greatly among different individuals. However, as a general rule, the first step is to look for the interradicular site with ample bone width. Then, the entry point is determined based on the radiographic images and soft tissue features (Figure 7.19). Lastly, mini-implant placement is implemented with angled insertion (30° to the occlusal plane) to gain greater bone quantity.

7.2.4 Insertion Techniques

Once ample interradicular sites are confirmed through radiographic examination, the first step is to determine the optimal entry point and the desired insertion angle

t.me/Dr_Mouayyad_AlbtousH

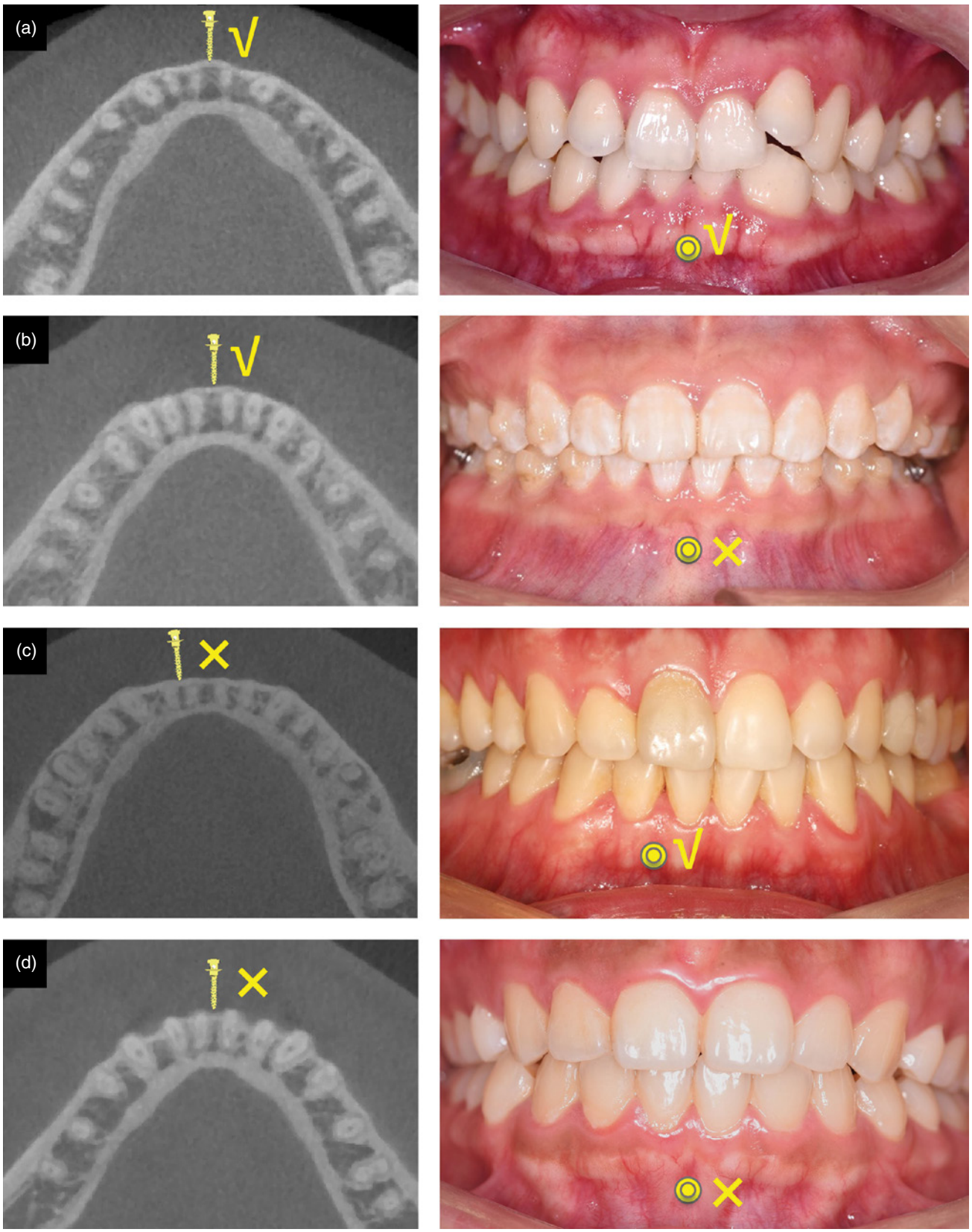


Figure 7.19 Evaluation of the qualification of both hard and soft tissues for the placement of mini-implants at mandibular interradicular sites. (a) The interradicular space (bone width) is adequate at the designated entry point. The entry point lies in the attached gingiva zone. Thus, both hard and soft tissues are qualified for the insertion of mini-implants. (b) Although the bone width is adequate for insertion, the mini-implant has to be inserted at the movable mucosa zone to meet the hard tissue requirements. Thus, this region is not qualified for the insertion of mini-implants. (c) Although the mini-implant can be inserted at the attached gingiva zone, the bone width is insufficient, precluding the insertion of mini-implants. (d) Both hard tissue and soft tissue are not qualified for the insertion of mini-implants.

t.me/Dr_Mouayyad_AlbtousH

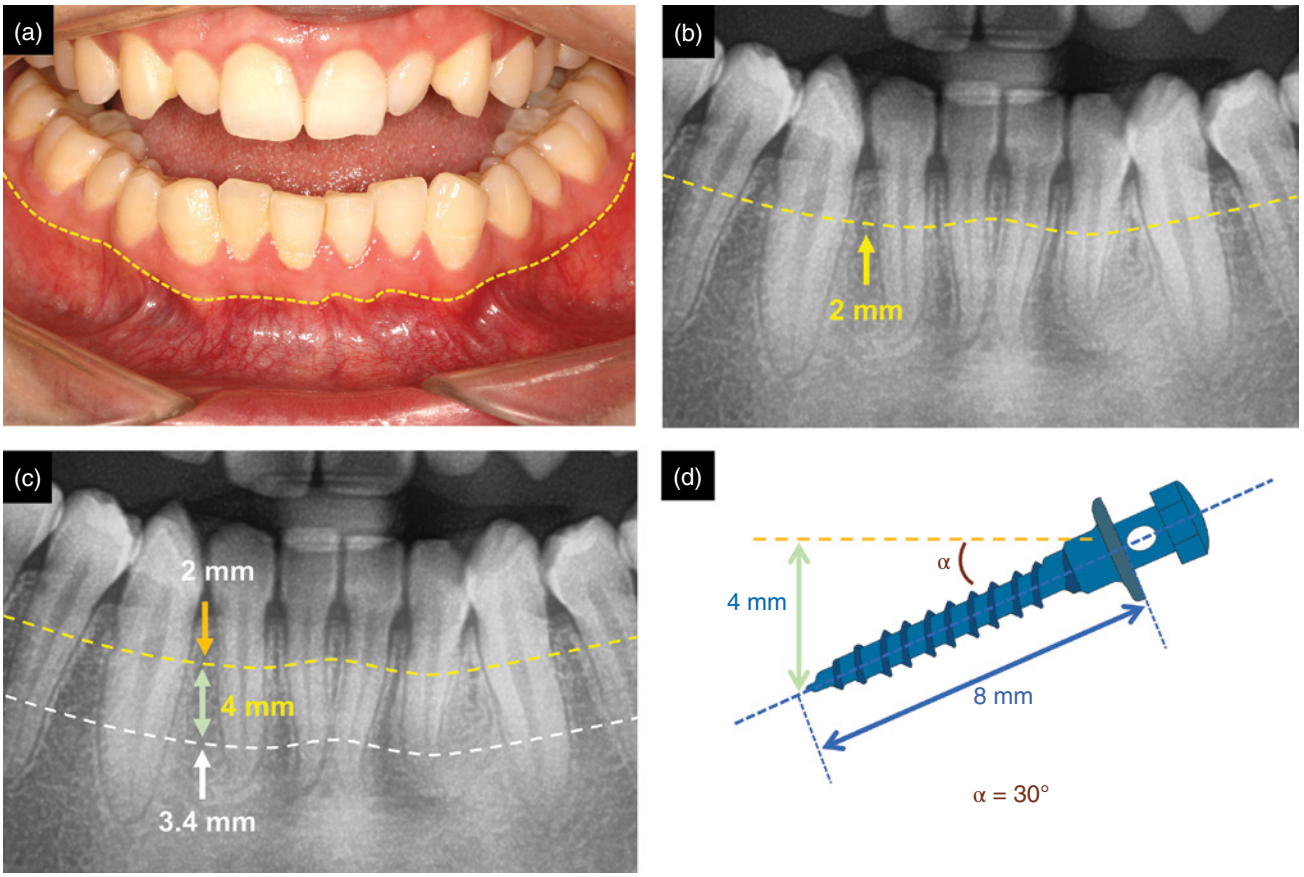


Figure 7.20 Determination of entry point and desired insertion angle based on individual data. (a) The mucogingival junction (yellow dashed line) was marked and transferred to the radiographic image. (b) Based on the marked mucogingival junction on the radiographic image, the interradicular width was 2 mm, which was inadequate for the insertion of mini-implants. (c) A greater interradicular width was sought at a more apical level and an interradicular width of 3.4 mm (adequate for insertion) was found 4 mm apical to the mucogingival junction. (d) Through mathematical calculations, the minimal insertion angle is arcsin (4/8) (30°).

based on radiographic examinations and clinical features (Figure 7.20). For interradicular sites with suboptimal interradicular space, more apical entry and greater insertion angle may be beneficial. For interradicular sites with limited space, digital techniques can be leveraged to aid in precisely determining the optimal entry point and insertion angle (Figure 7.21).

Once the optimal entry point and insertion angle are determined, the next step is to determine whether frenectomy is indicated. If the mini-implant is to be placed at the L1-L1 site, whether frenectomy should be performed is decided by the location where the labial frenum attaches. If the labial frenum attaches too coronally, frenectomy is indicated. Otherwise, frenectomy is not required if the labial frenum attaches apically to the mucogingival junction.

Second, subperiosteal infiltration anaesthesia is performed following mucosa disinfection with iodophor. The infiltration anaesthesia is limited to the mucosa but should not extend to dental roots, in order to maintain the normal sensory perception of the roots. This is to alert operators if root proximity is encountered during insertion. Thus, a limited amount (0.2–0.5 ml) of anaesthetic agent is recommended. However, if frenectomy is indicated, additional anaesthetic agent (0.5 ml) is injected submucosally to the labial frenum.

Third, the entry point is marked with a dental explorer or probe and the mesiodistal position of the marked entry point should be confirmed from the occlusal side (Figure 7.22). Root prominences can be employed to help operators locate the optimal mesiodistal position of the entry point. Specifically, operators are recommended to palpate root prominences and locate the depressions between two adjacent prominences. The midpoint of the depression indicates the optimal entry point (Figure 7.23).

Lastly, once the optimal entry point is marked and confirmed, the next step is to insert the mini-implant through

t.me/Dr_Mouayyad_AlbtousH

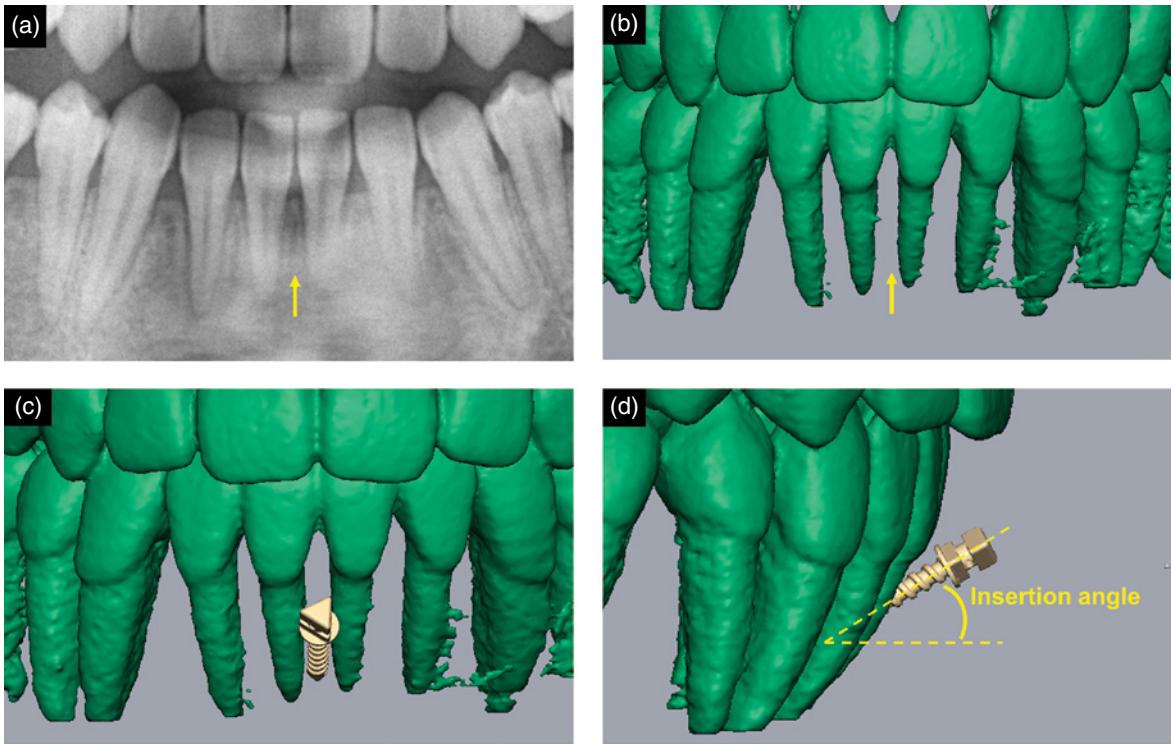


Figure 7.21 Determination of optimal entry point and insertion angle based on a 3-D reconstruction digital model. (a) 2-D radiograph image showing the designated insertion site (yellow arrow). (b) 3-D reconstruction image showing the designated insertion site (yellow arrow). (c) Virtual placement of a mini-implant into the interradicular site with oblique insertion technique and dental roots spared during insertion. (d) Measurement of the insertion angle with which the mini-implant has been virtually placed.

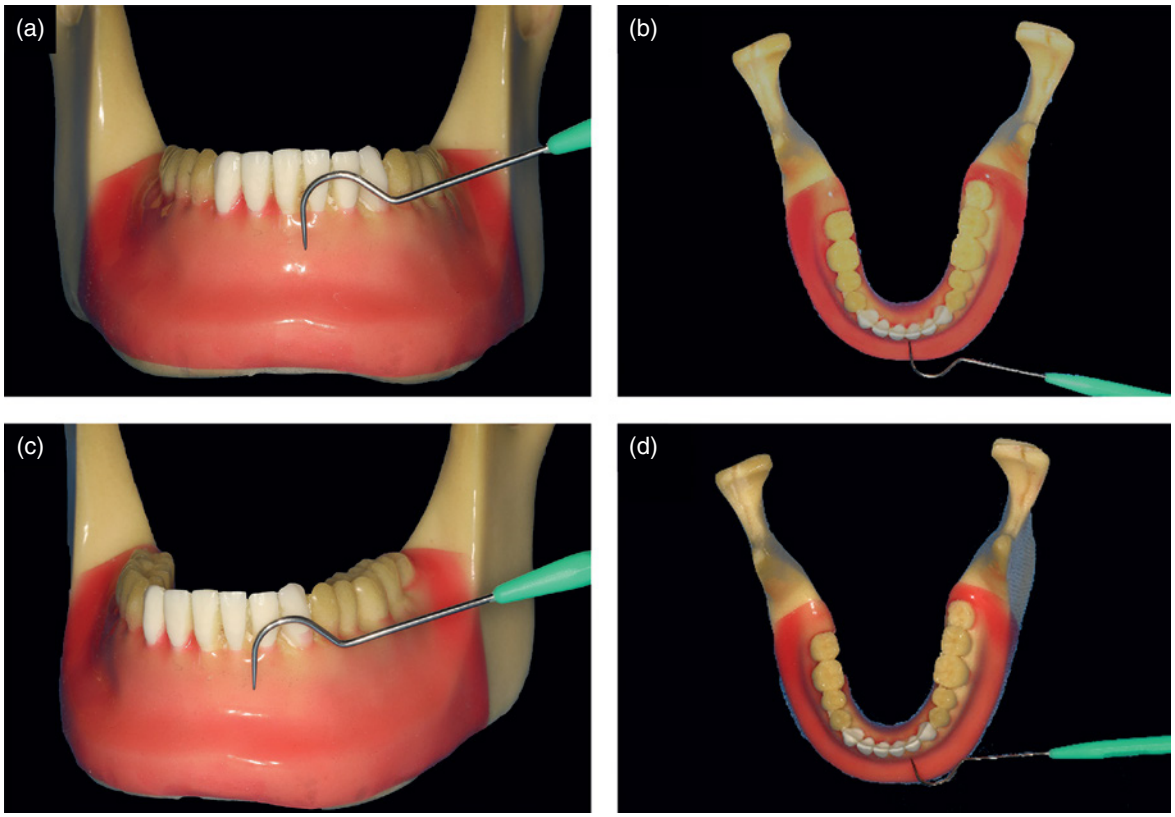


Figure 7.22 Mark the entry point with an explorer and check the mesiodistal position of the entry point from the occlusal side. (a,b) L1-L1 interradicular site. (c,d) L1-L2 interradicular site.

t.me/Dr_Mouayyad_AlbtousH

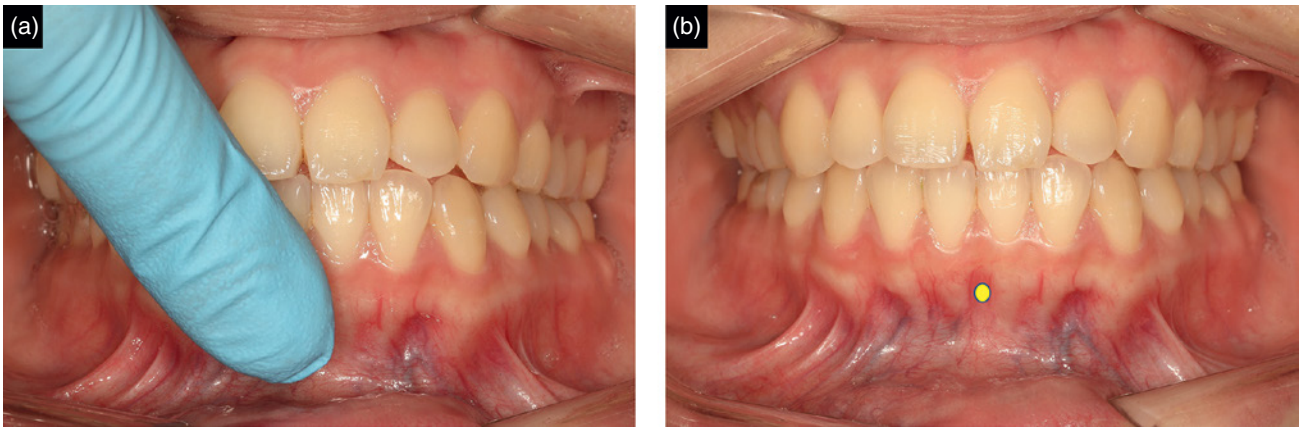


Figure 7.23 (a) Root prominences were palpated with the operator's finger to determine the depressions between root prominences. (b) The midpoint of the depression (yellow dot) is indicative of the optimal entry point.

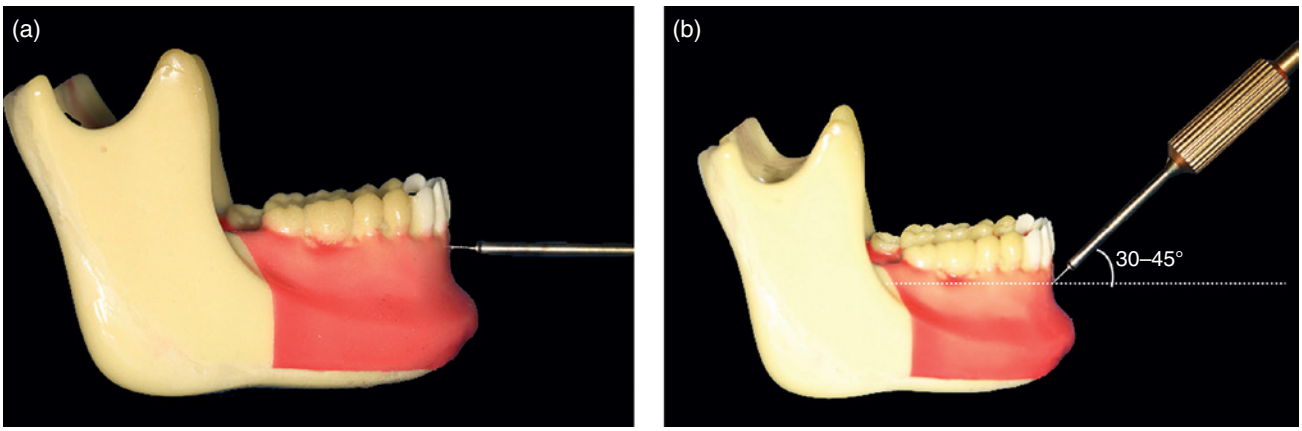


Figure 7.24 (a) A mini-implant is being inserted parallel to the occlusal plane until the cortical plate has been penetrated. (b) The mini-implant is slightly derotated and the insertion angle is changed to 30–45° to the occlusal plane.

the desired entry point. To gain greater interradicular space, angled insertion technique is often used. However, to prevent slippage during insertion, it is recommended to insert the mini-implant in parallel to the occlusal plane until cortical penetration is achieved. Then, slight derotation is performed, followed by a change of insertion angle (Figure 7.24). Due to the limitation of interradicular space in the mandibular labial region, an insertion angle of 30–45° is recommended. Once the desired insertion angle is attained, the mini-implant is inserted perpendicular to the tangent line of the dental arch through the entry point, otherwise root damage may occur (Figure 7.25).

Detailed procedures are demonstrated in a clinical case (Figure 7.26) and illustrated in Figures 7.27 and 7.28.

t.me/Dr_Mouayyad_AlbtousH

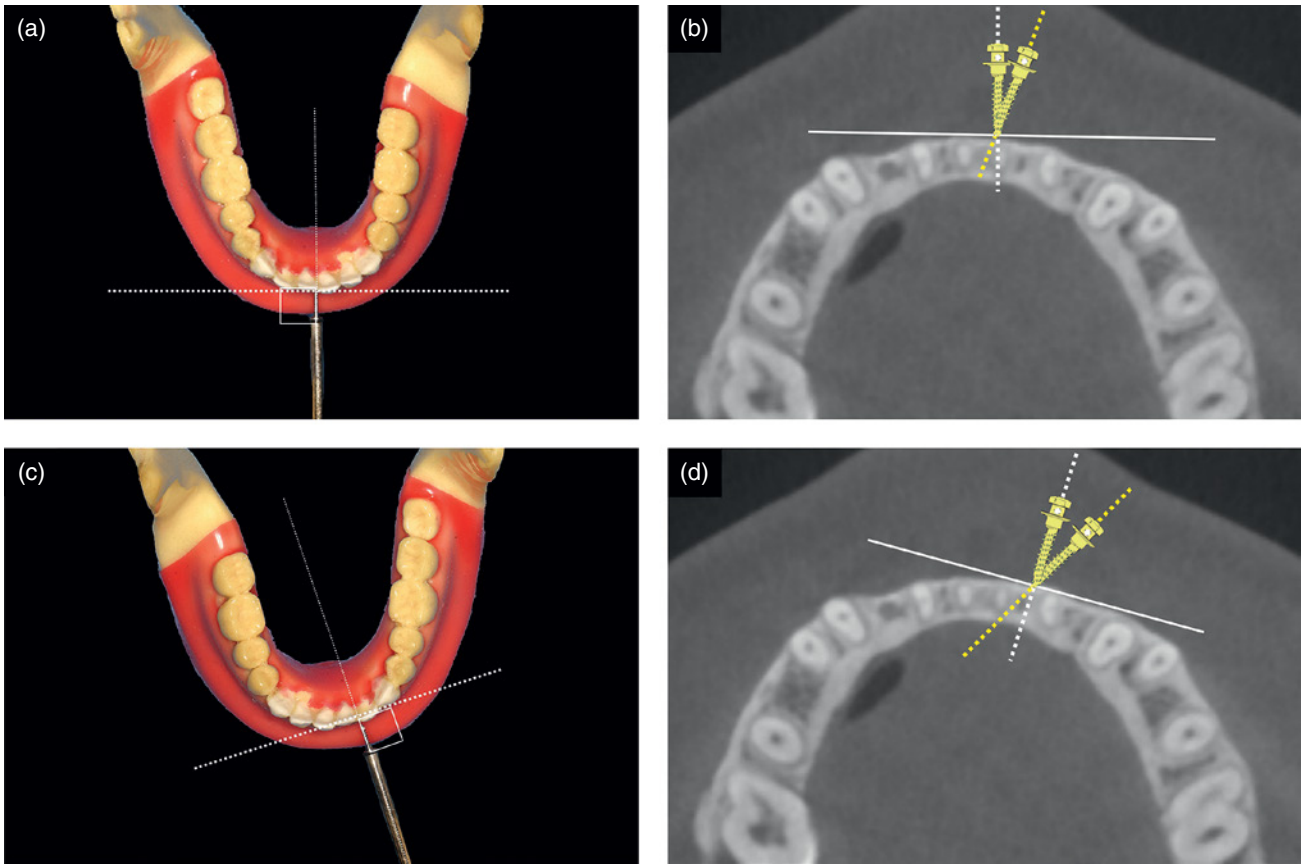


Figure 7.25 The mini-implant is recommended to be inserted perpendicularly to the tangent line of the dental arch passing through the entry point. (a) The insertion path is perpendicular to the tangent line at the L1-L1 site. (b) The recommended insertion path (white dashed line) is perpendicular to the tangent line (white solid line) while the deviated insertion path (yellow dashed line) may lead to root injury. (c) The insertion path is perpendicular to the tangent line at the L1-L2 site. (d) The recommended insertion path (white dashed line) is perpendicular to the tangent line (white solid line) while the deviated insertion path (yellow dashed line) may lead to root injury.

t.me/Dr_Mouayyad_AlbtousH

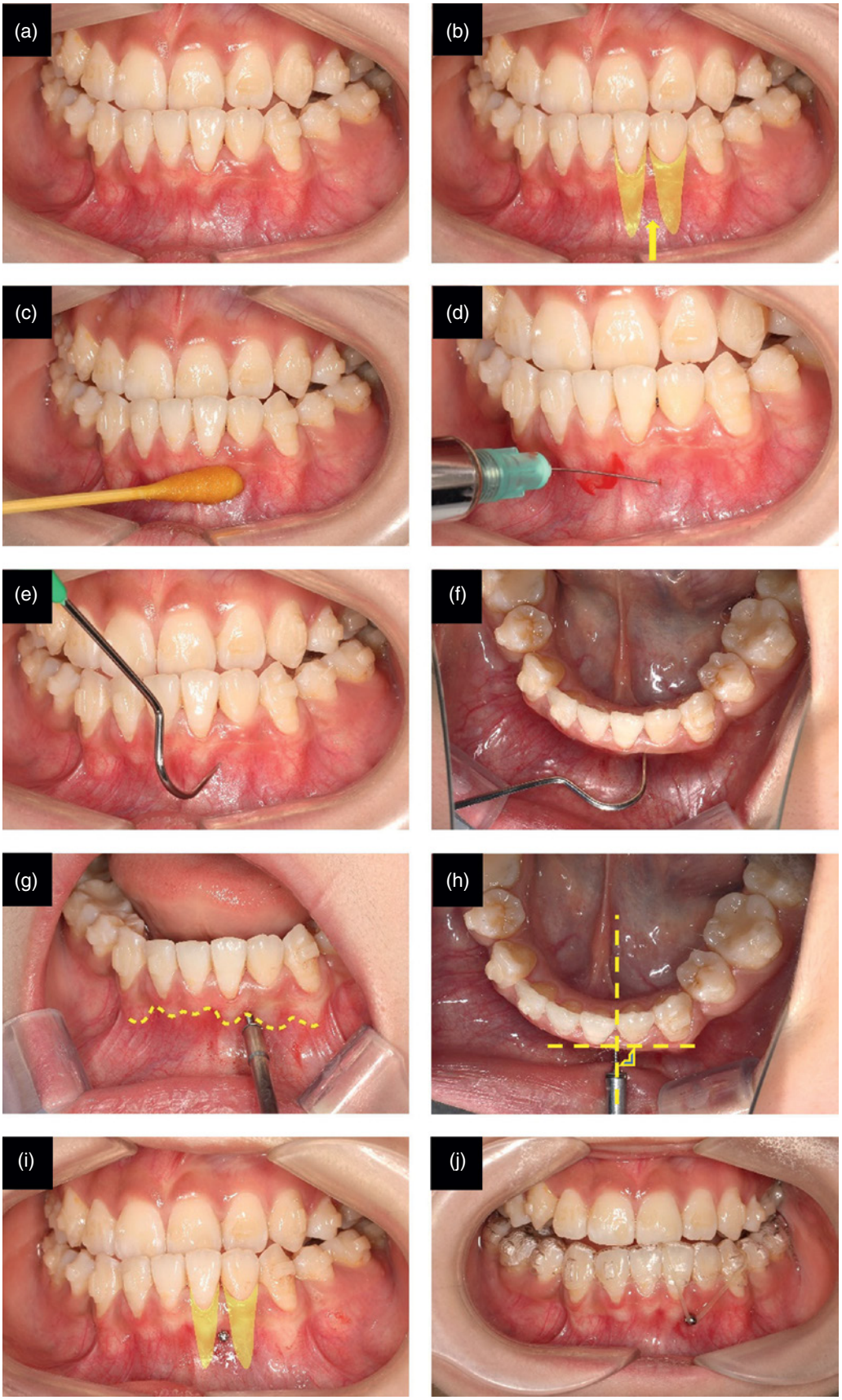


Figure 7.26 Clinical procedures of inserting a mini-implant at the mandibular interradicular region. (a,b) Evaluation of both hard and soft tissues. (c) Mucosa disinfection with iodophor. (d) Local infiltration anaesthesia. (e) Mark the desired entry point with an explorer. (f) Check the mesiodistal position of the entry point from the occlusal side. (g) Insertion of a mini-implant through the designated entry point that is at the mucogingival junction. (h) The insertion path was perpendicular to the tangent line of the arch passing through the entry point (occlusal view). (i) Postinsertion check. (j) Force loading with the mini-implant.

t.me/Dr_Mouayyad_AlbtousH

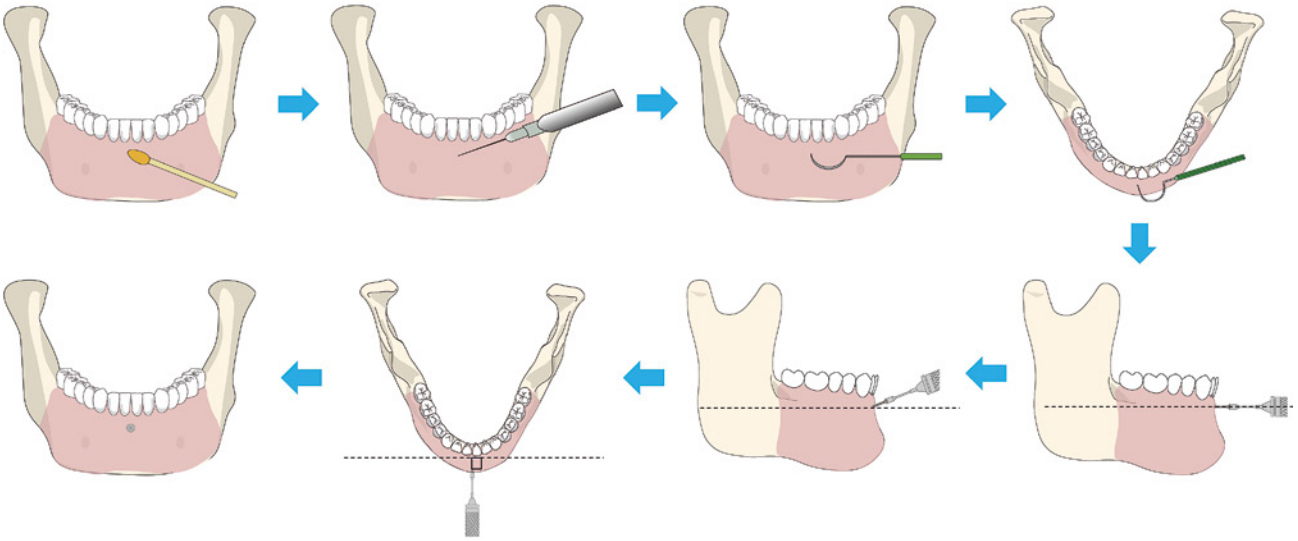


Figure 7.27 Schematic illustrations showing the detailed procedure of inserting a mini-implant at the L1-L1 interradicular site.

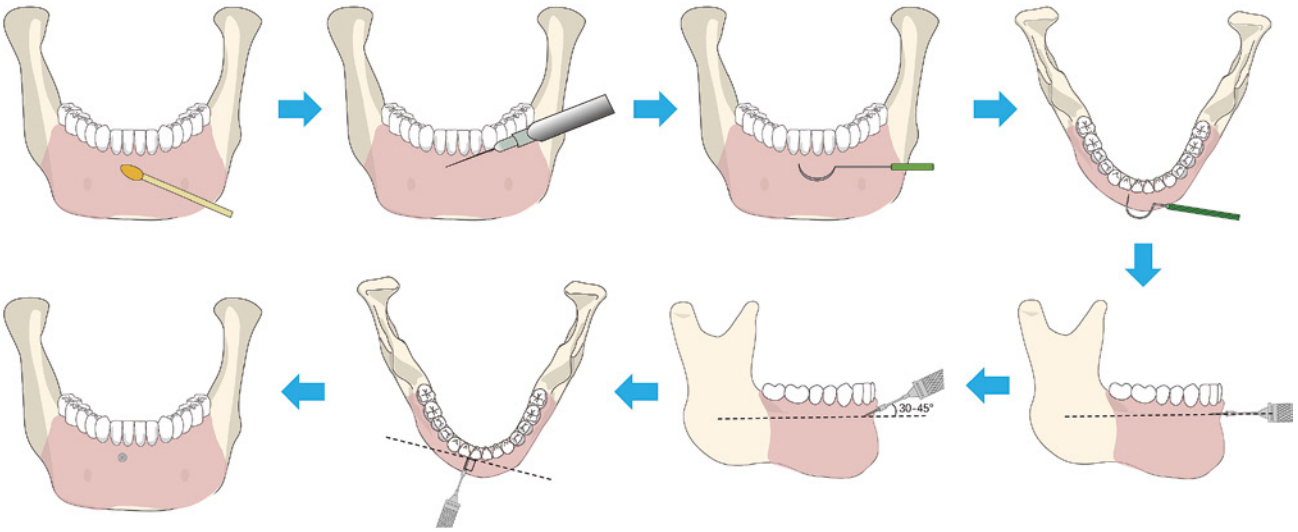


Figure 7.28 Schematic illustrations showing the detailed procedure of inserting a mini-implant at the L1-L2 interradicular site.

7.3 Mandibular Symphysis

As mentioned above, the placement of mini-implants into the mandibular labial interradicular region may not be possible due to limited interradicular space in some patients. For these patients, the mandibular symphysis is a good alternative.

The mandibular symphysis is formed by the fusion of left and right mandibular halves and, as fusion progresses, it grows anteriorly and laterally, resulting in an adequate bone protuberance labial to the mandibular incisor roots.[10,11] Thus, by definition, the mandibular symphysis is an extra-alveolar zone that is labial and apical to the mandibular incisor roots (Figure 7.29). For this anatomical region, the following hard tissue and soft tissue factors should be considered: cortical thickness, bone depth, labial frenum and soft tissue thickness.

7.3.1 Anatomical Features

Both hard tissue factors (cortical thickness and bone depth) were studied and evaluated in our previously published study.[12] As displayed in Figure 7.30, we measured both cortical thickness and bone depth at different anatomical sites,

t.me/Dr_Mouayyad_AlbtousH

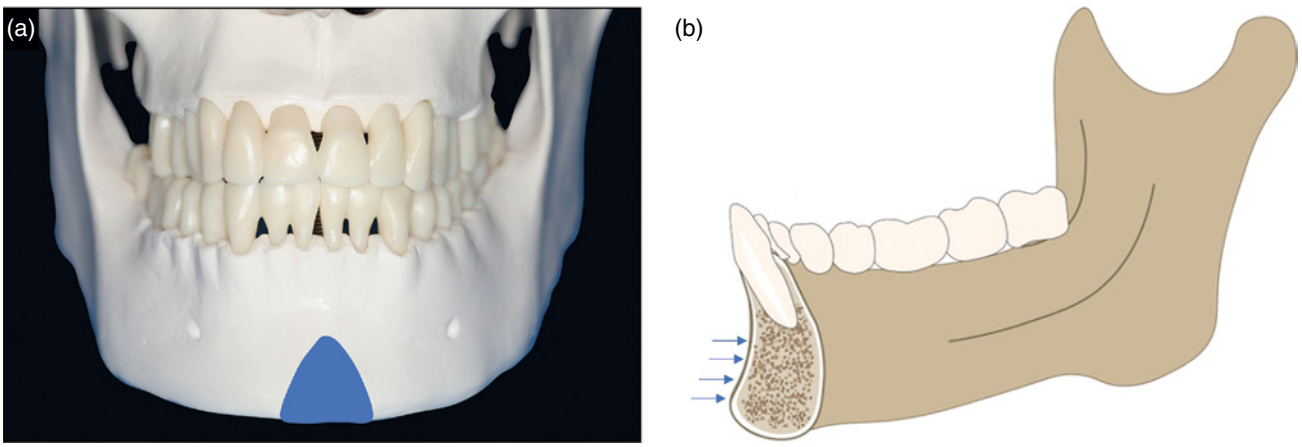


Figure 7.29 Mandibular symphysis. (a) Frontal view. The mandibular symphysis (blue area) is located apically to the mandibular incisor roots. (b) Midsagittal view. The mandibular symphysis (blue arrows) lies apically and labially to the mandibular incisor roots.

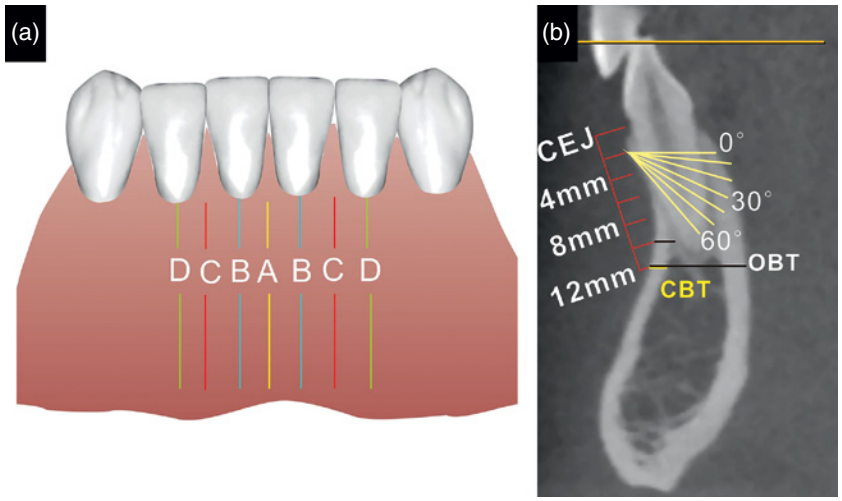


Figure 7.30 Methods of measuring cortical thickness and bone depth. (a) Different sections were chosen for the measurement. (b) A schematic diagram showing the measurement of cortical bone thickness (CBT) and overall bone thickness (OBT) at different insertion heights from the CEJ and with different insertion angles (0–60°). *Source:* Zhang et al. [12]/MDPI/CC BY 4.0.

insertion heights and insertion angles. We will describe the hard tissue characteristics based on the results of this study. In general, both cortical thickness and bone depth are greatest at the midline area and we recommend that symphyseal mini-implants be placed here. Thus, the anatomical features will be discussed only for the midline area of the mandibular symphysis.

Hard Tissue Factor: Cortical Thickness

Cortical thickness should be at least 1 mm to ensure sufficient primary stability upon which adequate secondary stability can be developed. We found that cortical thickness was influenced by vertical growth pattern and age, but not by gender (Figures 7.31 and Table 7.2). Although the differences between adults and adolescents were statistically significant, they were of no clinical significance. However, the differences among different vertical growth patterns are both statistically and clinically significant. In particular, at the 12 mm level, averaged cortical thickness was 2 mm for low-angle patients and 1.2 mm for high-angle subjects. Thus, when planning placement of mini-implants at the mandibular symphysis, vertical growth patterns should be considered.

As displayed in Figure 7.32, cortical thickness becomes greater with an increase in either the insertion height or the insertion angle. Thus, greater cortical engagement can be obtained with more apical entry and angled insertion. In terms of cortical thickness, almost all the insertion heights and insertion angles meet the requirement, except for the 2 mm level.

t.me/Dr_Mouayyad_AlbtousH

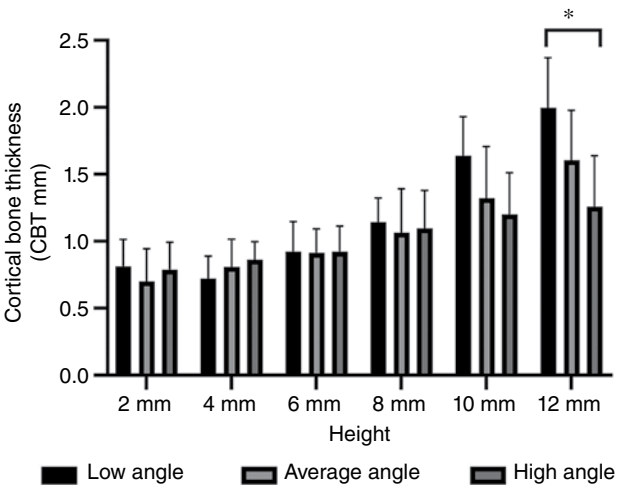


Figure 7.31 Cortical thickness varies among patients with different vertical skeletal patterns at the 12 mm level below the CEJ.

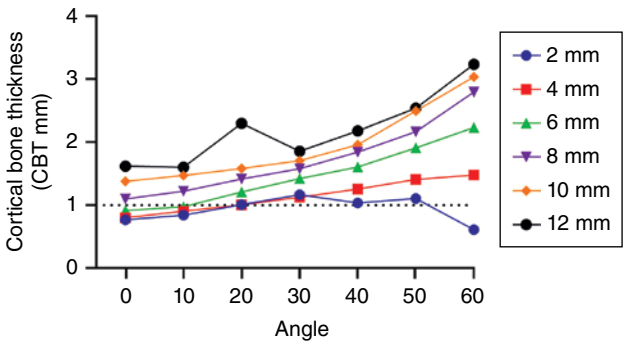


Figure 7.32 The influence of insertion height and insertion angle on cortical thickness. Cortical thickness becomes greater with an increase in either insertion height or insertion angle.

Table 7.2 Variance analysis of influence of gender and age on cortical bone thickness.

	Gender			Age		
	Males	**Females**	***p***	**Adolescents**	**Adults**	***p***
Cortical thickness (mm), mean±SD	1.35±1.06	1.33±0.90	0.271	1.31±0.89	1.38±1.09	0.001*

Table 7.3 Variance analysis of influence of gender and age on bone depth.

	Gender			Age		
	Males	**Females**	***p***	**Adolescents**	**Adults**	***p***
Bone depth (mm), mean±SD	7.65±6.93	7.57±6.28	0.393	7.56±6.76	7.67±6.55	0.272

Hard Tissue Factor: Bone Depth

Bone depth refers to the distance from the labial entry point to the contralateral lingual cortical plate. In our study, we found that neither gender nor age influenced bone depth (Table 7.3). However, vertical growth pattern did influence bone depth (Figure 7.33). Specifically, at the 12 mm level, low-angle subjects (12 mm) had greater bone depth than high-angle patients (7.5 mm). Moreover, bone depth was influenced by different insertion heights and insertion angles (Figure 7.34). Specifically, with an increase in either insertion height or insertion angle, bone depth increased, indicating that more apical entry and angled insertion are able to gain greater bone quantity. The minimum bone depth is recommended to be 5 mm and, based on this requirement, entry point should be greater than 8 mm apical to the CEJ. In terms of bone depth, if the entry point is greater than 8 mm, inserting mini-implants with all insertion angles is accepted.

t.me/Dr_Mouayyad_AlbtousH

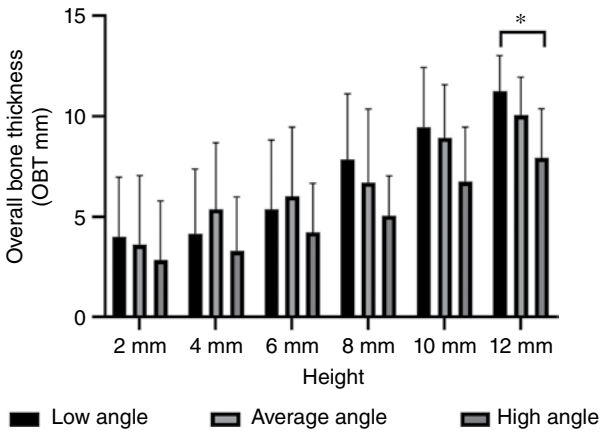


Figure 7.33 Overall bone thickness (bone depth) varies among patients with different vertical skeletal patterns at the 12 mm level.

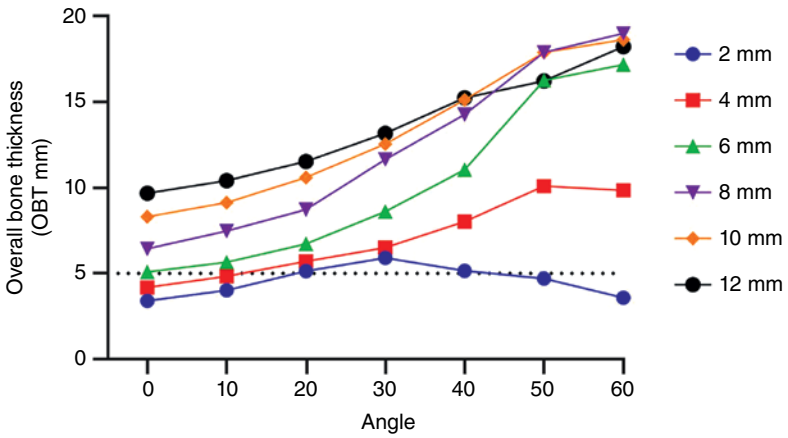


Figure 7.34 The influence of insertion height and insertion angle on overall bone thickness (bone depth). Note that the bone depth becomes greater with an increase in the insertion height or insertion angle.

Soft Tissue Factors

The mandibular symphysis is covered with thick soft tissue, with movable mucosa being the most predominant (Figure 7.35). In the midline area, the labial frenum renders soft tissue complications more likely (Figure 7.36). To prevent soft tissue wrapping around mini-implant threads during insertion, frenectomy is often indicated. Soft tissue at this region has a rich blood supply (Figure 7.37), which may result in a higher likelihood of soft tissue swelling following mini-implant placement. Thus, to obtain sufficient emergence profile, long mini-implants (10 mm or 12 mm) are recommended to avoid soft tissue complications. Moreover, insertion with an adequate angle (60^{o} to the occlusal plane) is recommended to keep the mini-implant head within the attached gingiva zone, so that soft tissue irritation can be prevented (Figure 7.38).

7.3.2 Biomechanical Considerations

Mandibular symphyseal mini-implants are able to offer intrusive force on mandibular incisors. From the sagittal dimension, this intrusive force is located labially to the centre of resistance of the six anterior teeth. Thus, simultaneous intrusion and proclination of incisors will occur (Figure 7.39). If proclination is not expected, appropriate measures should be taken to prevent incisor flaring, e.g. additional crown lingual torque.

t.me/Dr_Mouayyad_AlbtousH

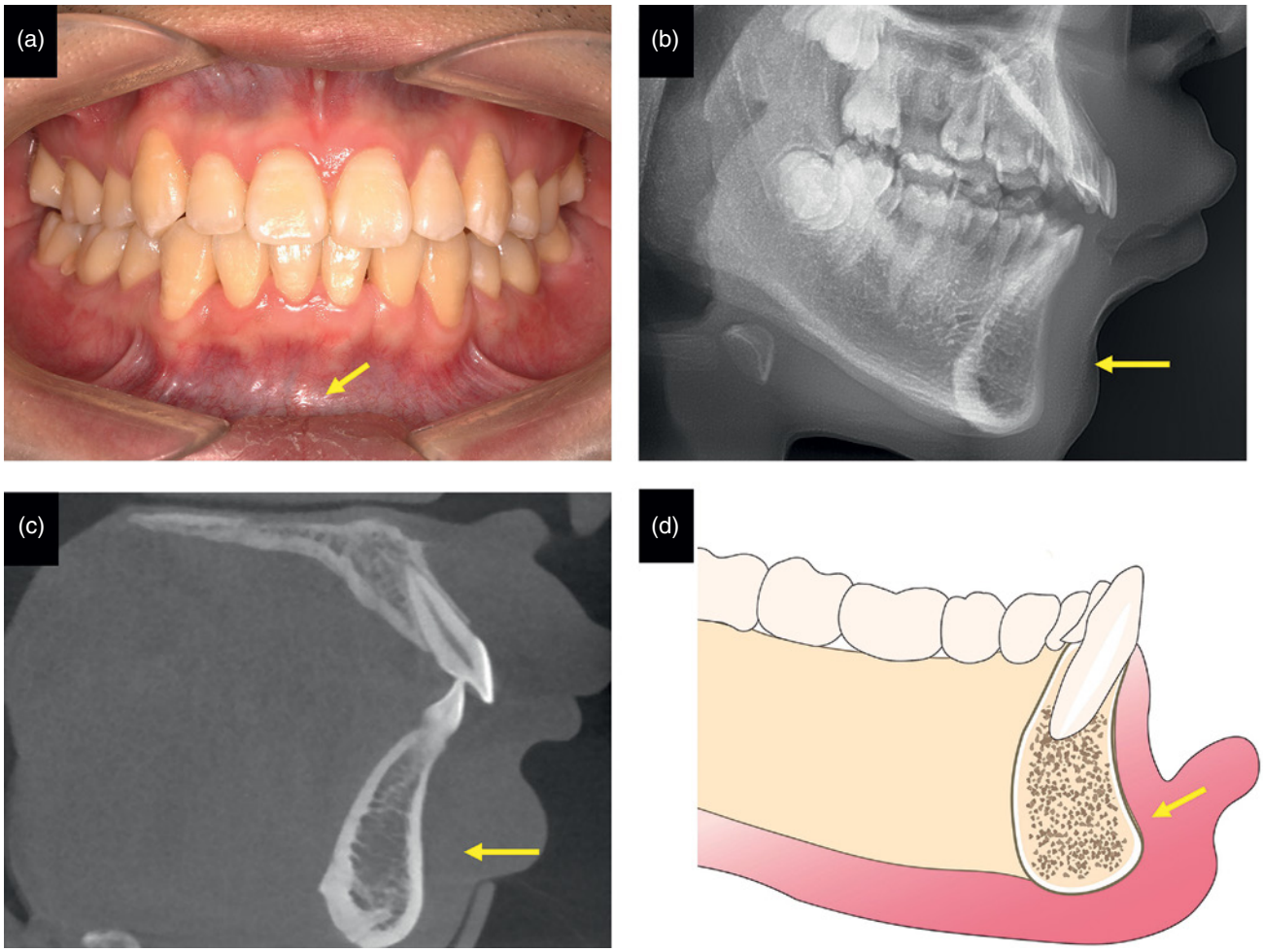


Figure 7.35 (a) Intraoral photograph showing the movable mucosa (yellow arrow) that covers the mandibular symphysis region. (b–d) Radiographs and schematic illustration showing thick soft tissue covering the mandibular symphysis region.

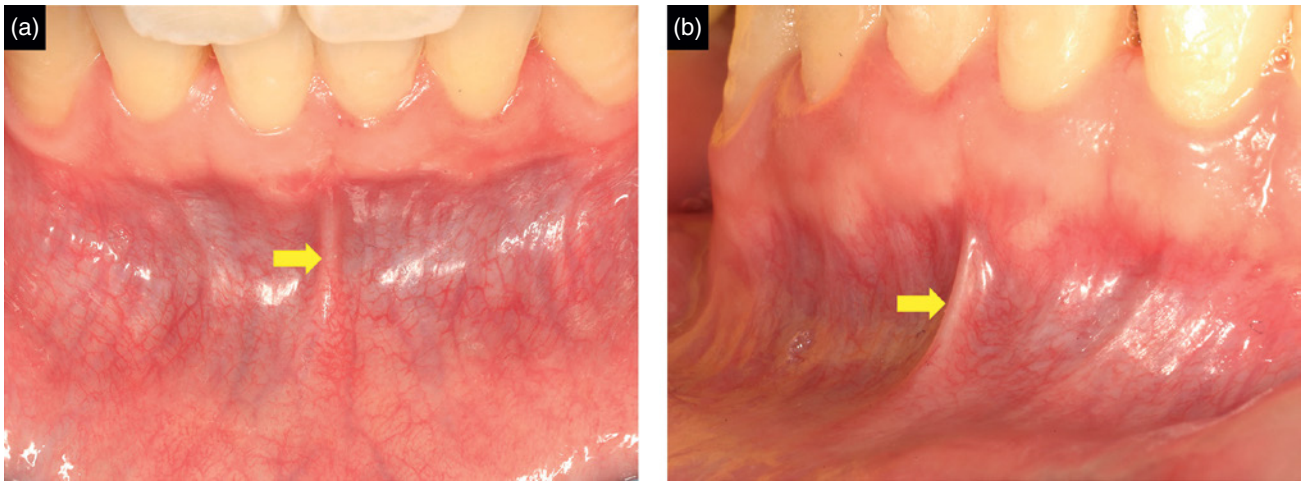


Figure 7.36 Mandibular labial frenum (yellow arrow). (a) Frontal view. (b) Frontal-oblique view.

t.me/Dr_Mouayyad_AlbtousH

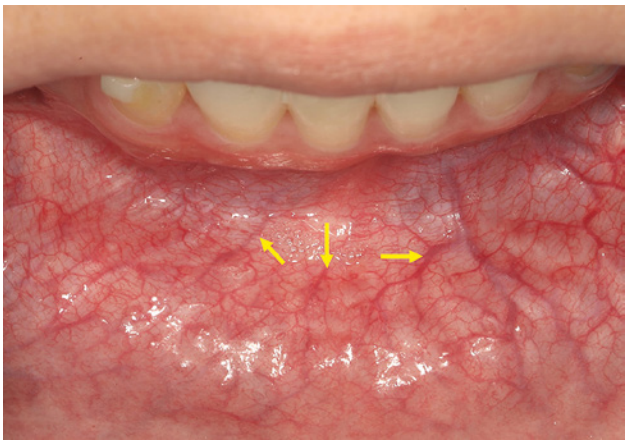


Figure 7.37 Rich blood supply at the mandibular symphysis region. The blood vessels are indicated by yellow arrows.

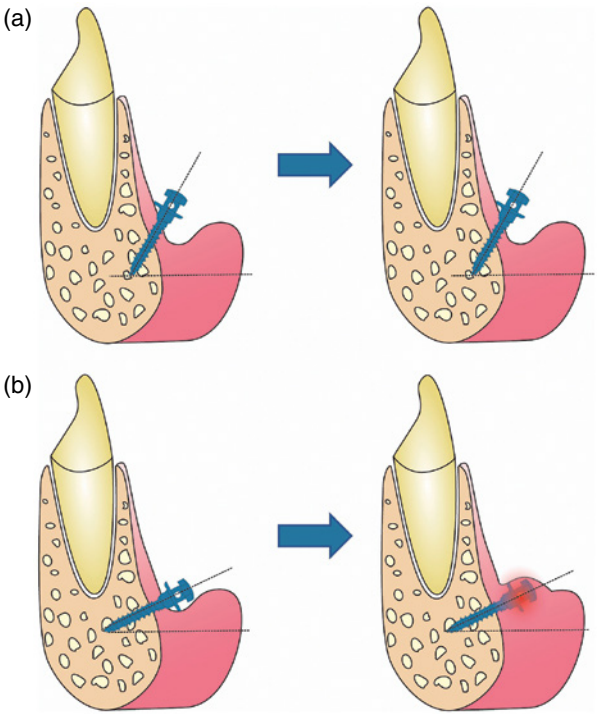


Figure 7.38 Adequate insertion angle for prevention of soft tissue complications. (a) A mini-implant is inserted with a large insertion angle (e.g. 60° to the occlusal plane) and the head of the mini-implant is located at the attached gingiva zone. No postinsertion soft tissue complications occur. (b) A mini-implant is inserted with a small insertion angle and postinsertion soft tissue irritation occurs.

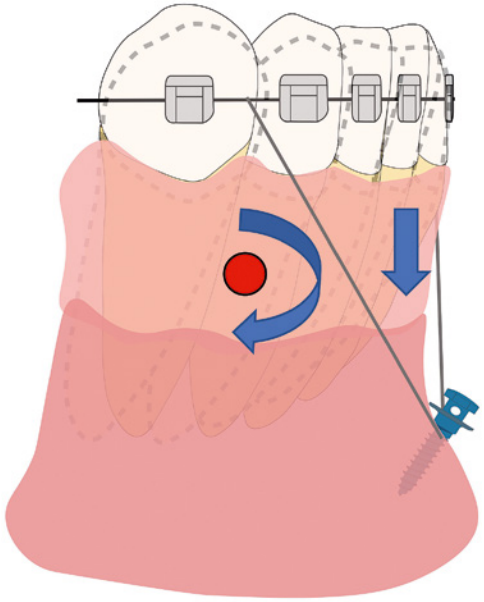


Figure 7.39 The intrusive force offered by the symphysis mini-implant passes labially to the centre of resistance of the anterior teeth. The anterior teeth are subject to simultaneous labial proclination and intrusion.

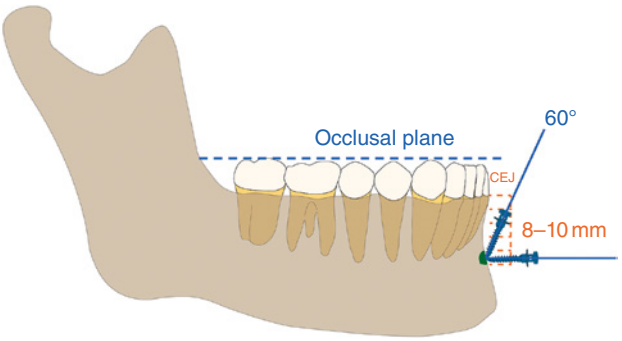


Figure 7.40 Recommended insertion height and angle for the placement of mini-implant at the mandibular symphysis region. The mini-implant should be inserted 8–10 mm apically to the CEJ with an insertion angle of 60° to the occlusal plane.

7.3.3 Selection of Optimal Sites

Based on the anatomical features described above, we recommend the following insertion parameters for the placement of mini-implants at the mandibular symphysis region: (1) entry point is 8–10 mm apical to the CEJ; (2) insertion angle is 60°; (3) long mini-implants (10 mm or 12 mm) should be used; (4) frenectomy should be implemented. The recommended insertion height and insertion angle are illustrated in Figure 7.40.

7.3.4 Insertion Techniques

First, the entry point is determined through radiographic images and clinical examinations. Generally, the entry point is located 8–10 mm apical to the CEJ of the central

t.me/Dr_Mouayyad_AlbtousH

incisors. However, individual variations do exist and individualised entry points should be determined (Figure 7.41).

Second, infiltration anaesthesia is performed following mucosal disinfection with iodophor (Figure 7.42). Both subperiosteal and submucosal anaesthesia are recommended. Due to the deep location and lack of dental roots in this anatomical region, profound anaesthesia is recommended.

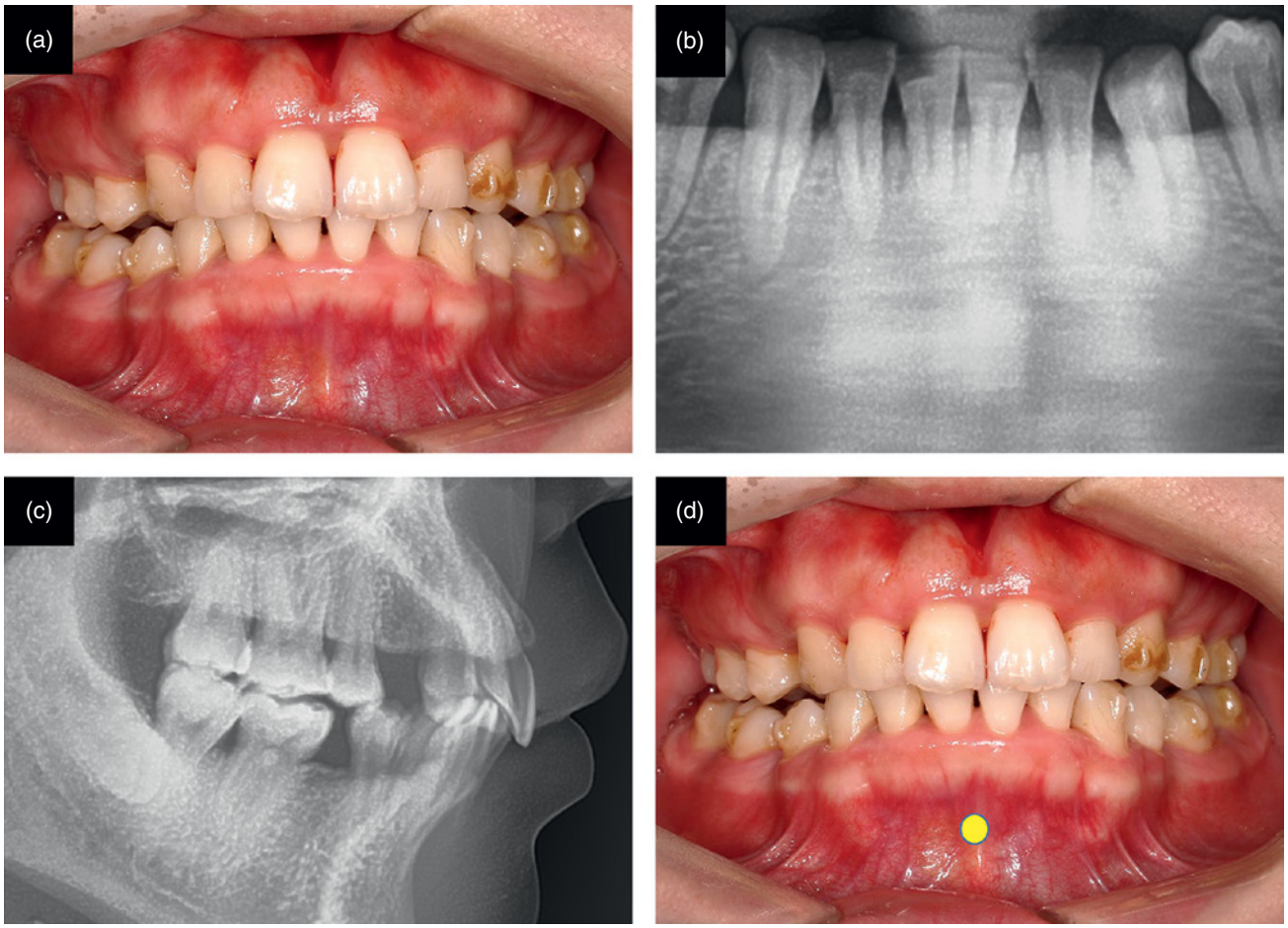


Figure 7.41 Determination of the entry point based on clinical examination and radiographs. (a) Frontal intraoral photograph showing the labial frenum and thick mucosa covering the mandibular symphysis region. (b,c) Radiographs showing the root apices of the mandibular incisors. (d) The optimal entry point (yellow dot).

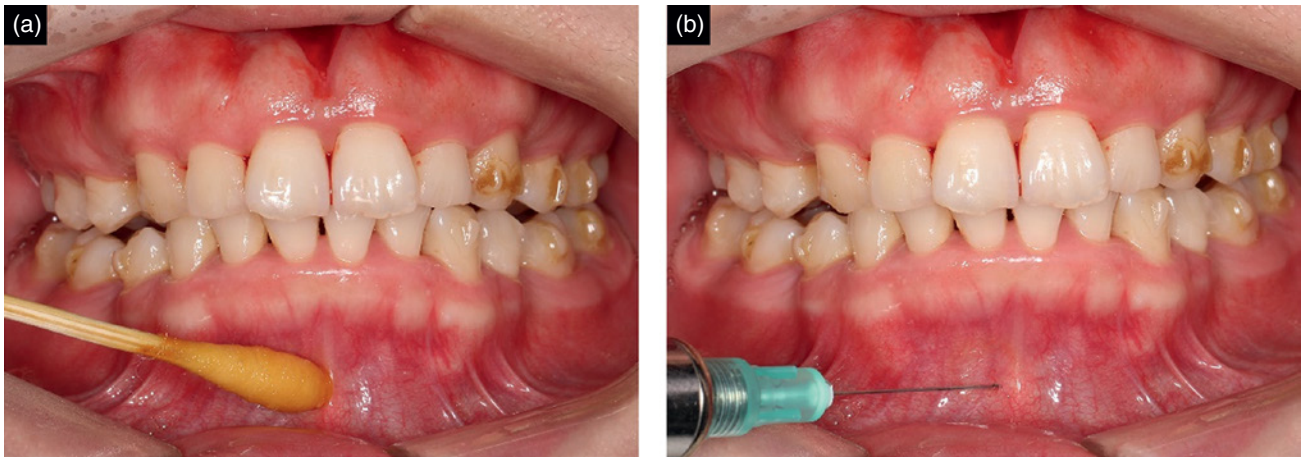


Figure 7.42 (a) Mucosa disinfection with iodophor. (b) Local infiltration anaesthesia.

t.me/Dr_Mouayyad_AlbtousH

Third, frenectomy is performed with a scalpel through a horizontal incision (Figure 7.43). Then, full-thickness flap elevation with slight soft tissue undermining is recommended to surgically expose the mandibular symphysis region (Figure 7.44). This is performed for three purposes: (1) adequate flap elevation can avoid soft tissues wrapping around mini-implant threads during insertion so that the likelihood of soft tissue complications can be reduced; (2) soft tissue undermining can reduce soft tissue tension so that the risk of postoperative soft tissue swelling can be decreased; (3) flap elevation and exposure of mandibular symphysis facilitate accurate and direct location of the entry point.

Fourth, the mini-implant is inserted through the designated entry point at the midline with recommended insertion angles. Generally, the recommended insertion angle ranges from 45° to 60°, dependent on the morphology of the mandibular symphysis. Specifically, if the mandibular symphysis is prominent, sufficient emergence profile can be attained with a coronal entry point and a small insertion angle (45°). Otherwise, the entry point should be more apical with a greater insertion angle (60°) in order to achieve adequate emergence profile for patients with a non-prominent mandibular symphysis (Figure 7.45).

The chance of mini-implant slippage is high if the implant is directly inserted with the desirable insertion angle (e.g. 60°). Thus, the mini-implant should be initially inserted through the entry point perpendicular to the bone surface for cortical penetration. Then, the insertion angle is gradually increased while the mini-implant is being



Figure 7.43 Frenectomy was performed with a scalpel through a horizontal incision.



Figure 7.44 Surgical exposure of the mandibular symphysis.

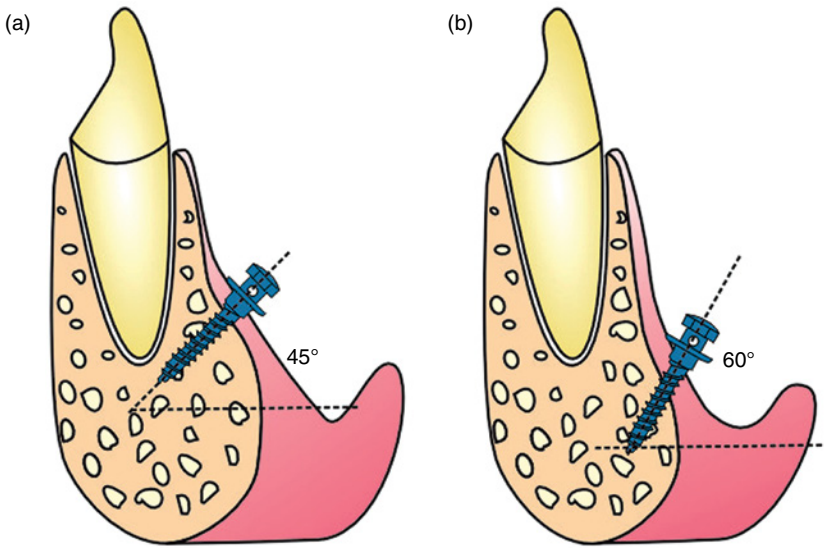


Figure 7.45 (a) For prominent mandibular symphysis, the optimal insertion angle is 45° to the occlusal plane and the entry point is recommended to be more occlusal, so that sufficient emergence profile is obtained. (b) For non-prominent mandibular symphysis, a greater insertion angle (60°) and more apical entry point are recommended.

t.me/Dr_Mouayyad_AlbtousH

advanced until the desirable insertion angle is obtained (Figure 7.46). Otherwise, due to the great insertion angle (60°), mini-implant slippage is still likely to occur if the insertion angle is abruptly changed to the desired angle after cortical penetration.

Meanwhile, during the insertion process, the operator should monitor the mesiodistal direction of the insertion and ensure that the mini-implant is advanced in line with the midsagittal plane and perpendicular to the coronal plane (Figure 7.47).

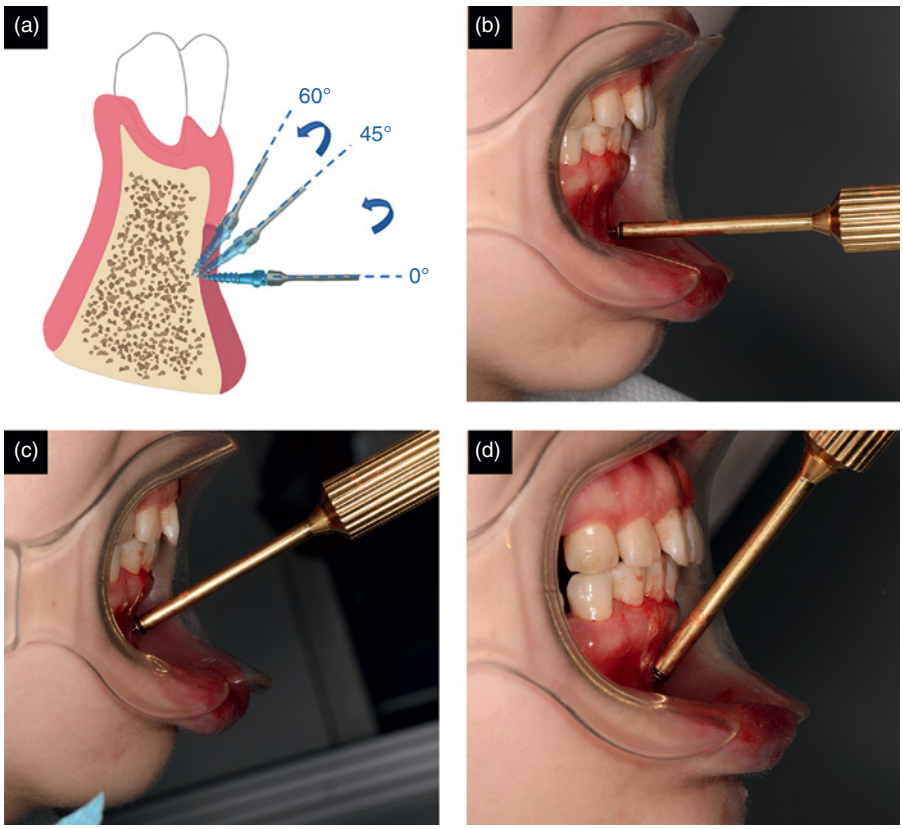


Figure 7.46 (a) A schematic illustration demonstrating the gradual increase of the insertion angle during placement of the mini-implant. (b–d) Progressive increase in the insertion angle to reach a final angle of 60° to the occlusal plane.

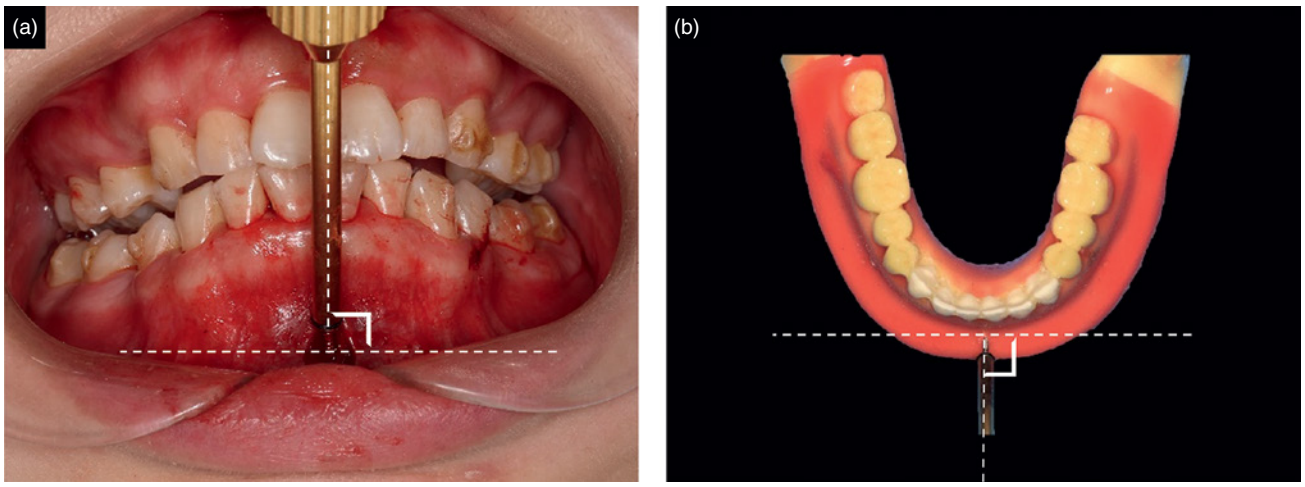


Figure 7.47 The insertion path is in line with the midsagittal plane and perpendicular to the coronal plane. (a) Frontal view. (b) Occlusal view.

t.me/Dr_Mouayyad_AlbtousH

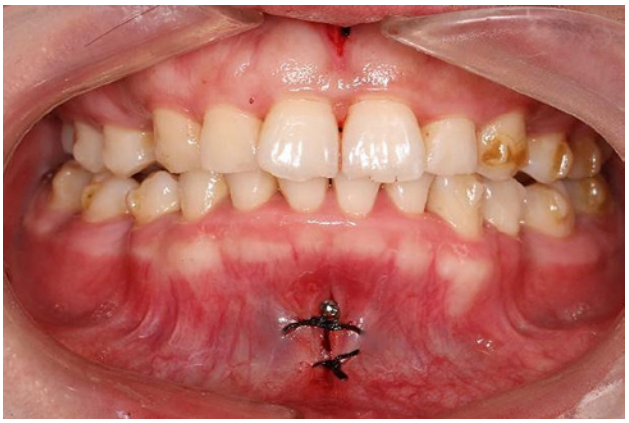


Figure 7.48 Primary closure of the flap with interrupted sutures.

Lastly, the insertion should be stopped once the platform of the mini-implant head contacts the mucosa. This is to guarantee that an adequate emergence profile is attained for ease of force loading and for prevention of postinsertion soft tissue complications. Then, primary and tension-free closure of the flap is performed with interrupted sutures (Figure 7.48).

The detailed insertion procedures are demonstrated in Figures 7.49 and 7.50.

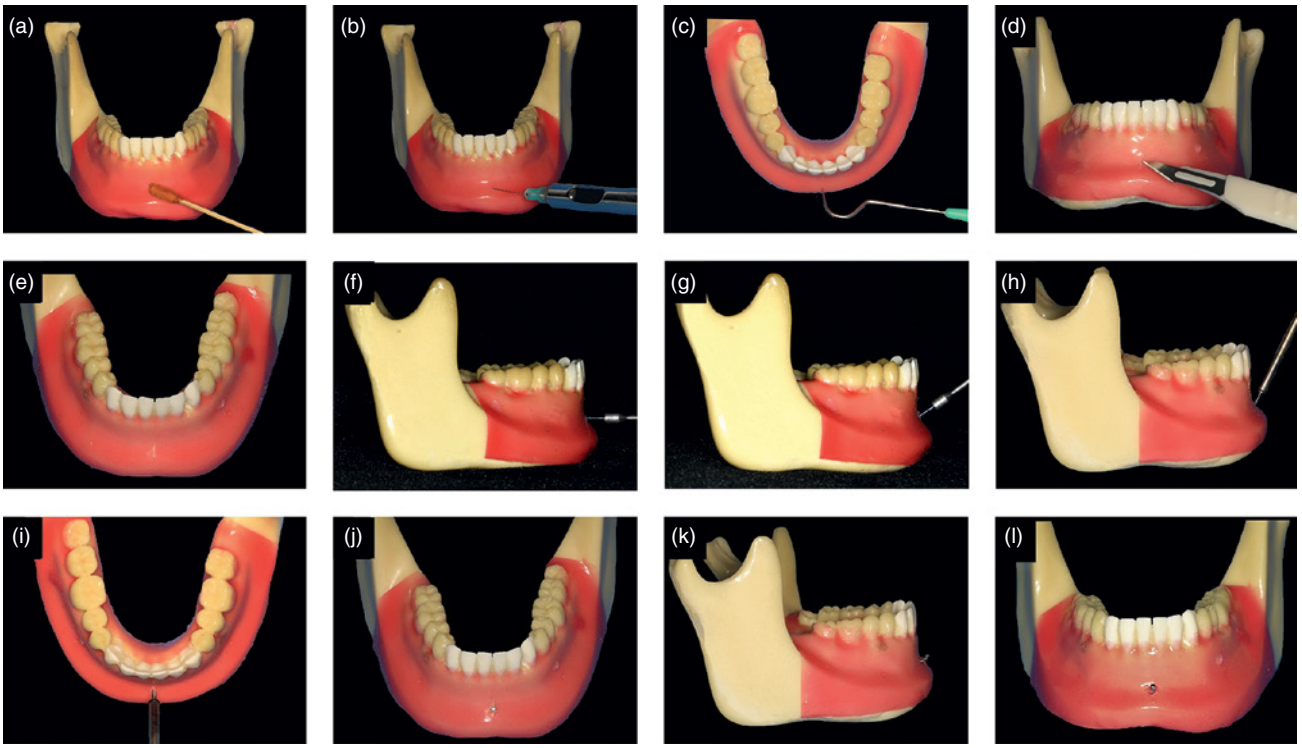


Figure 7.49 Detailed procedures of inserting a mini-implant at the mandibular symphysis region. (a) Mucosa disinfection with iodophor. (b) Local infiltration anaesthesia. (c) Marking of the entry point. (d) Mucosa incision. (e) Surgical exposure of the bone surface. (f–h) Progressive increase of the insertion angle during placement of the mini-implant. (i) Confirmation of the direction of the insertion path from the occlusal side. (j–l) Postinsertion check.

t.me/Dr_Mouayyad_AlbtousH

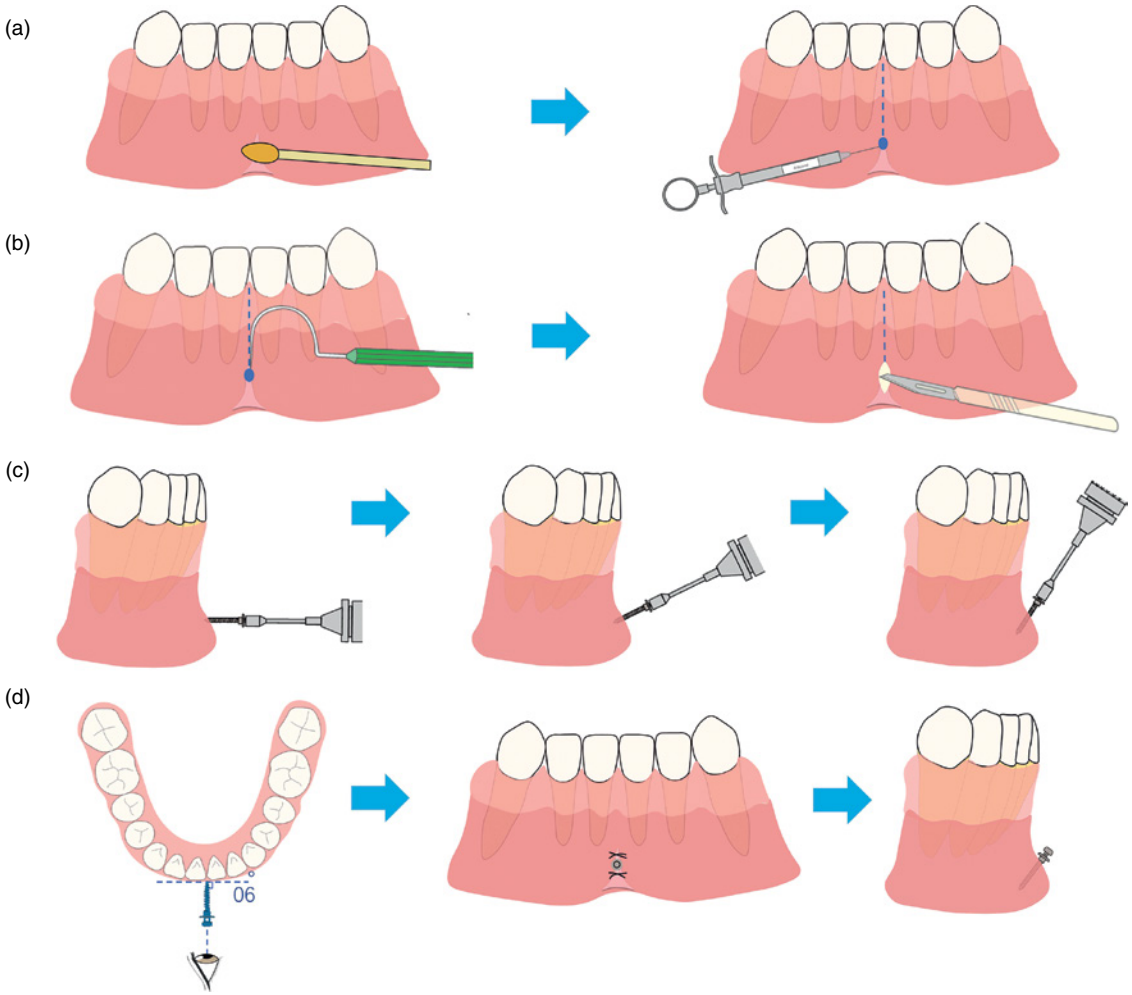


Figure 7.50 Schematic illustrations demonstrating the detailed procedures of inserting a mini-implant at the mandibular symphysis region. (a) Mucosa disinfection and local infiltration anaesthesia. (b) Soft tissue indentation, mucosa incision and exposure of the bone surface. (c) Progressive increase of the insertion angle. (d) Confirmation of the direction of the insertion path, primary suture of the flap and postinsertion examinations.

7.4 Summary

Placement of mini-implants at the mandibular labial interradicular sites should be performed with caution since interradicular space is often limited. Meticulous evaluation of pre-treatment radiographic images is of vital importance in determining the optimal entry point and desirable insertion angle. Alternatively, mandibular symphysis is a promising anatomical region with adequate bone quantity and good bone quality. Distinct insertion techniques and procedures should be followed for mini-implants to be inserted at these two regions.

References

1 Monnerat C, Restle L, Mucha JN. (2009). Tomographic mapping of mandibular interradicular spaces for placement of orthodontic mini-implants. *Am. J. Ortho.d Dentofacial Orthop.* 135(4): e421–429; discussion 428–429.

2 Purmal K, Alam M, Pohchi A, Abdul Razak N. (2013). 3D mapping of safe and danger zones in the maxilla and mandible for the placement of intermaxillary fixation screws. *PLoS One* 8(12): e84202.

t.me/Dr_Mouayyad_AlbtousH

3 Wang Y, Shi Q, Wang F. (2021). Optimal implantation site of orthodontic micro-screws in the mandibular anterior region based on CBCT. *Front. Physiol.* 12: 630859.

4 Fayed MM, Pazera P, Katsaros C. (2010). Optimal sites for orthodontic mini-implant placement assessed by cone beam computed tomography. *Angle Orthod.* 80(5):939–951.

5 Motoyoshi M, Inaba M, Ono A, Ueno S, Shimizu N. (2009). The effect of cortical bone thickness on the stability of orthodontic mini-implants and on the stress distribution in surrounding bone. *Int. J. Oral Maxillofac. Surg.* 38(1): 13–18.

6 Motoyoshi M, Yoshida T, Ono A, Shimizu N. (2007). Effect of cortical bone thickness and implant placement torque on stability of orthodontic mini-implants. *Int. J. Oral Maxillofac. Implants.* 22(5): 779–784.

7 Hwang YC, Hwang HS. (2011). Surgical repair of root perforation caused by an orthodontic miniscrew implant. *Am. J. Orthod. Dentofacial Orthop.* 139(3): 407–411.

8 Jennes ME, Sachse C, Flugge T, Preissner S, Heiland M, Nahles S. (2021). Gender- and age-related differences in the width of attached gingiva and clinical crown length in anterior teeth. *BMC Oral Health* 21(1):287.

9 Lim HC, Lee J, Kang DY, Cho IW, Shin HS, Park JC. (2021). Digital assessment of gingival dimensions of healthy periodontium. *J. Clin. Med.* 10(8).

10 Lee E, Popowics T, Herring SW. (2019). Histological development of the fused mandibular symphysis in the pig. *Anat. Rec.* 302(8): 1372–1388.

11 Coquerelle M, Bookstein FL, Braga J, Halazonetis DJ, Weber GW. (2010). Fetal and infant growth patterns of the mandibular symphysis in modern humans and chimpanzees (Pan troglodytes). *J. Anat.* 217(5): 507–520.

12 Zhang S, Wei X, Wang L et al. (2022). Evaluation of optimal sites for the insertion of orthodontic mini implants at mandibular symphysis region through cone-beam computed tomography. *Diagnostics* 12(2): 285.

t.me/Dr_Mouayyad_AlbtousH

8

Mandibular Buccal Region

Qi Fan[1], Lu Liu[1,2], Chaolun Mo[3], Xinxiong Xia[4], Yushi Zhang[1], Rui Shu[5], Liang Zhang[6,7], and Hu Long[1]

[1] *Department of Orthodontics, State Key Laboratory of Oral Diseases and National Clinical Research Center for Oral Diseases, West China Hospital of Stomatology, Sichuan University, Chengdu, China*
[2] *Department of Maxillofacial Orthognathics, Tokyo Medical and Dental University, Graduate School, Tokyo, Japan*
[3] *Department of Orthodontics, Stomatological Hospital of Guizhou Medical University, Guiyang, China*
[4] *Private Practice, Chengdu, China*
[5] *Department of Pediatric Dentistry, State Key Laboratory of Oral Diseases and National Clinical Research Center for Oral Diseases, West China Hospital of Stomatology, Sichuan University, Chengdu, China*
[6] *Department of Implantology, State Key Laboratory of Oral Diseases and National Clinical Research Center for Oral Diseases, West China Hospital of Stomatology, Sichuan University, Chengdu, China*
[7] *Center of Stomatology, West China Xiamen Hospital of Sichuan University, Xiamen, Fujian, China*

8.1 Introduction

The mandibular buccal region spans from the distal side of the mandibular canine to the distal side of the mandibular second molar and is continuous with the retromolar region and the mandibular ramus region. In this anatomical region, two continuous and overlapped sites are clinically available for the placement of mini-implants, i.e. interradicular sites and buccal shelf (Figure 8.1). Specifically, interradicular sites refer to the interradicular areas between canines and first premolars, between first and second premolars, between second premolars and first molars and between first and second molars. Moreover, the buccal shelf is the anatomical area that is located buccally to the mandibular molar roots and belongs to the extra-alveolar region. Bone quality and quantity are better and greater in the mandibular buccal region than in the maxillary counterpart region (Figure 8.2). However, a great body of evidence reveals that the failure rate of mini-implants is higher in the mandibular region than in the maxillary region.[1-3] This could be due to the higher likelihood of thermal damage during insertion and subsequent bone necrosis in the mandibular region (Figure 8.3). Thus, special care should be taken to reduce thermal and mechanical damage during the placement of mini-implants in the mandibular buccal region.

The mandibular buccal region is frequently used for the insertion of orthodontic TADs for different orthodontic purposes.[4-6] Mini-implants inserted at the mandibular buccal region are often clinically applied for a variety of orthodontic indications, e.g. anchorage reinforcement, traction of impacted molars, molar distalisation and molar intrusion (Figure 8.4).

In this chapter, anatomical characteristics, selection of insertion sites, detailed clinical insertion techniques and clinical applications of mini-implants in the mandibular buccal region (interradicular sites and buccal shelf) will be highlighted.

Clinical Insertion Techniques of Orthodontic Temporary Anchorage Devices, First Edition. Edited by Hu Long, Xianglong Han, and Wenli Lai.
© 2024 John Wiley & Sons Ltd. Published 2024 by John Wiley & Sons Ltd.

t.me/Dr_Mouayyad_AlbtousH

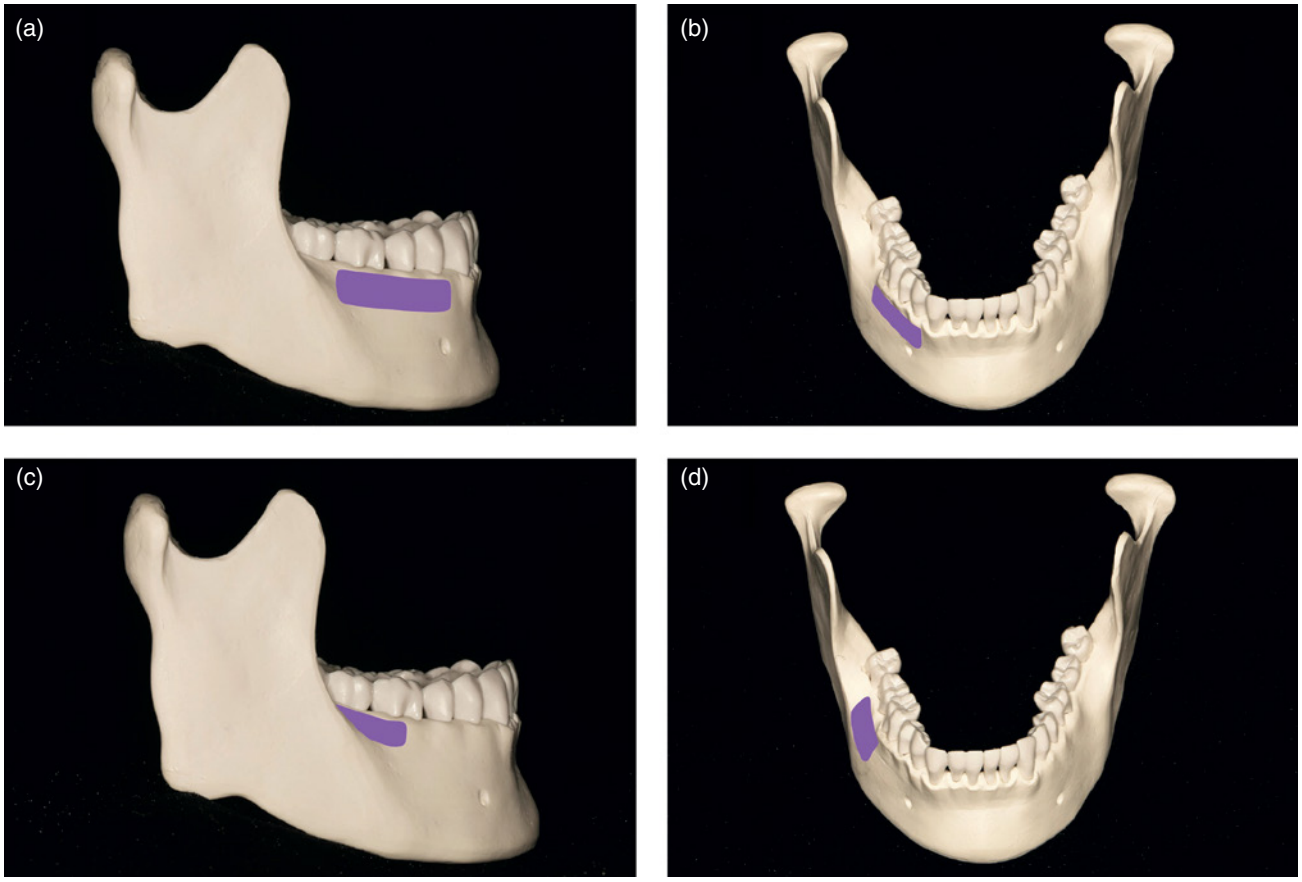


Figure 8.1 Mandibular buccal region suitable for mini-implant applications. (a,b) Interradicular region. (c,d) Buccal shelf.

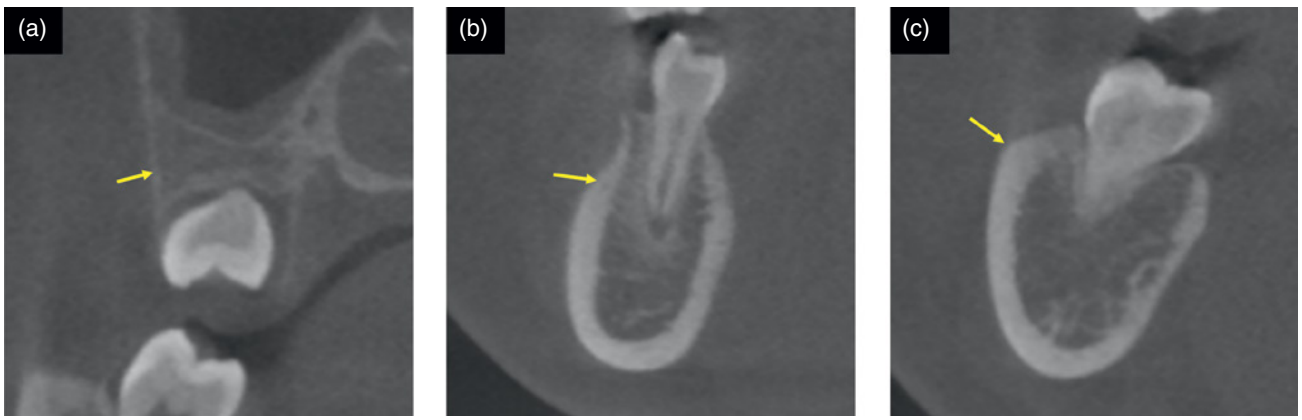


Figure 8.2 The differences of bone density and cortical thickness in the maxillary interradicular region, mandibular interradicular region and buccal shelf. (a) Maxillary alveolar bone with low bone density and thin cortex (yellow arrow). (b) Mandibular interradicular region with relatively higher bone density and thicker cortex (yellow arrow). (c) Buccal shelf with highest bone density and thickest cortex (yellow arrow).

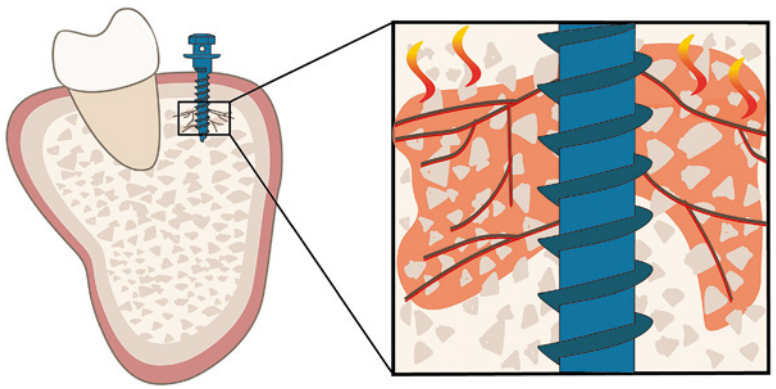


Figure 8.3 A schematic illustration showing thermal damage and necrosis during insertion.

t.me/Dr_Mouayyad_AlbtousH

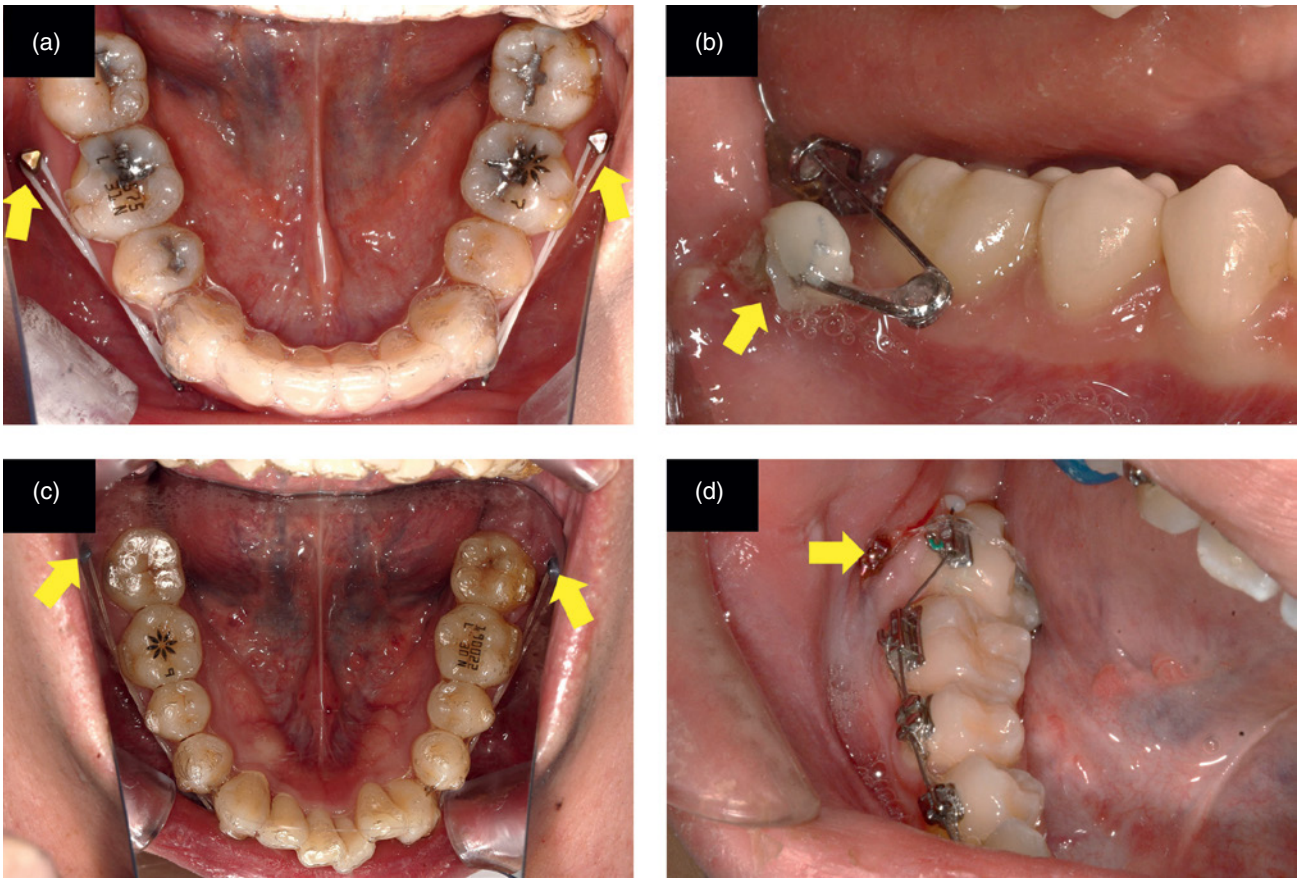


Figure 8.4 Versatile clinical applications of mini-implants (yellow arrow) at the mandibular buccal region. (a) Anchorage reinforcement. (b) Orthodontic traction (the head of the mini-implant has been covered with flowable resin). (c) Distalisation of the mandibular dentition. (d) Molar intrusion with simultaneous correction of lingual tipping.

8.2 Interradicular Sites

8.2.1 Anatomical Characteristics

Interradicular sites at the mandibular buccal region are the anatomical areas between the posterior dental roots (Figure 8.5). Compared with the maxillary buccal region, the mandibular buccal region possesses thicker bone cortex and higher trabecular bone density.[7,8] Thus, greater primary stability is often observed in the mandibular buccal region. However, owing to potential bone damage, secondary stability is lower in the mandible than in the maxilla, resulting in a lower success rate of mini-implants in the mandibular buccal region than in the maxillary counterpart. Moreover, due to the presence of mental foramina in this region, potential nerve injury should be borne in mind during mini-implant insertion and special care should be taken to avoid nerve injury. Thus, for the clinical success of mini-implants inserted at the mandibular buccal region, both hard tissue factors (i.e. cortical thickness, bone depth and bone width) and soft tissue factors (i.e. soft tissue type and buccal frenum) and vital anatomical structures (i.e. inferior alveolar neurovascular bundles and mental foramina) should be taken into consideration.

Hard Tissue Factor: Cortical Thickness

Cortical thickness is a pivotal factor in determining the primary stability of mini-implants and the optimal cortical thickness is considered to be 1–2 mm. It has been revealed that cortical thickness in the mandibular buccal region varies among subjects with different skeletal vertical patterns but not between genders.[9] Specifically, brachycephalic subjects exhibit greater cortical thickness than mesocephalic and dolichocephalic subjects. Moreover, age plays an important role in determining cortical thickness, with subjects over 12 years old possessing greater cortical thickness than those less than 12 years old.

Cortical thickness differs among different interradicular sites and increases posteriorly, with bone cortex being thickest at the L6-L7 site (Figure 8.6a–c). This indicates that greater cortical engagement can be achieved if

t.me/Dr_Mouayyad_AlbtousH

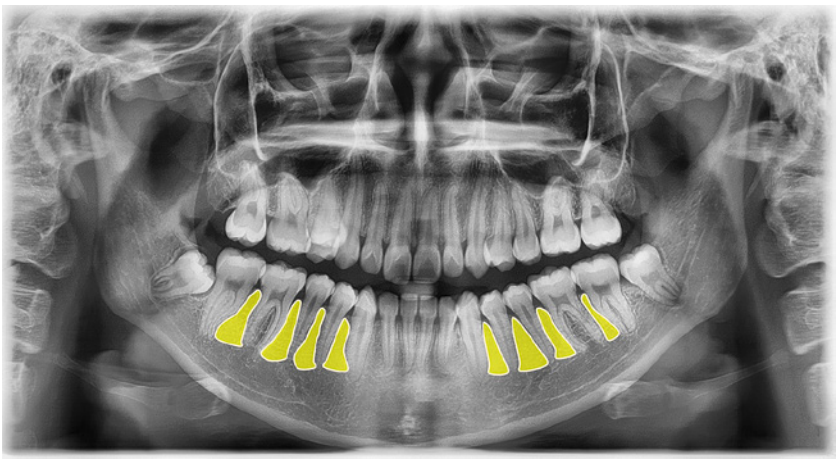


Figure 8.5 Interradicular sites at the mandibular buccal region are suitable for mini-implant insertion. The yellow areas on the panoramic radiograph illustrate the interradicular space for insertion.

insertion is located more posteriorly. Moreover, for all interradicular sites, cortical thickness increases from alveolar crest to alveolar base (Figure 8.6d–f), indicating that greater cortical thickness can be obtained if the entry point is located more apically. According to the optimal requirements of cortical thickness (1–2 mm) for the placement of mini-implants, the entry point is 2–8 mm apical to the CEJ for the L3-L4 site, the L4-L5 site and the L5-L6 site. Since cortical thickness is greater than 2 mm or even 3 mm at the L6-L7 interradicular site, this site is not recommended for mini-implant insertion unless prudent predrilling is applied, in order to reduce bone damage.

Hard Tissue Factor: Bone Depth

Bone depth is the distance between the buccal cortical plate and lingual cortical plate. As displayed in Figure 8.7, bone depth increases posteriorly, with bone depth being the least at the L3-L4 site and greatest at the L6-L7 site. Moreover, an increase in bone depth is exhibited from alveolar crest to alveolar base, suggesting that greater bone depth can be obtained if the entry point is located more apically. As per the minimum requirement of bone depth (4.5 mm) for mini-implant placement, all the interradicular sites at the mandibular buccal region are qualified for the placement of mini-implants at all insertion heights (2–8 mm). Thus, this anatomical factor need not be considered for the planning and placement of orthodontic mini-implants.

Hard Tissue Factor: Bone Width

Bone width refers to the interradicular space between two adjacent roots and is an important anatomical factor in determining the suitability of an interradicular site for mini-implant placement. As per the 1 mm root clearance principle, bone width of at least 3.5 mm is required.

Bone width differs among different interradicular sites, with the L6-L7 site exhibiting the greatest bone width (Figure 8.8).[10] Moreover, the L4-L5 site possesses greater bone width than the L5-L6 and L3-L4 sites, rendering L4-L5 as an alternative to the L6-L7 site for mini-implant placement. Moreover, as dental roots taper towards the apices, interradicular space becomes larger if the entry point is located more apically (Figures 8.8 and 8.9). Thus, bone width is influenced by both the specific interradicular site and the insertion height. According to the minimum requirement of bone width, mini-implants should be inserted 4–8 mm apical to the CEJ at the L6-L7 and L4-L5 sites, and 6–8 mm apical to the CEJ at the L5-L6 site. However, due to the limited interradicular space at the L3-L4 site and great individual variations, mini-implants should be inserted cautiously at this site and meticulous pretreatment CBCT evaluations should be implemented.

Hard Tissue Factor: Shape of Cortical Plate

The cortical plate is concave at the L3-L4 site, becomes straight at the L4-L5 and L5-L6 sites, and finally turns to be convex at the L6-L7 site (Figure 8.10). Specifically, the cortical plate is almost perpendicular (90°) to the occlusal plane at the L3-L4 site. The angle between the cortical plate and the occlusal plane becomes smaller from the L4-L5 site to the L6-L7 site. Generally, oblique insertion technique is recommended to gain greater bone engagement and reduce the likelihood of root injury. Usually, the recommended insertion angle is 30° to the normal line of the bone surface passing through the entry point (Figure 8.11). Considering the changes of the cortical plate anteroposteriorly, insertion angle is 30° to the occlusal plane at the L3-L4 site and could be greater at the other three sites (30-45° or even more).

t.me/Dr_Mouayyad_AlbtousH

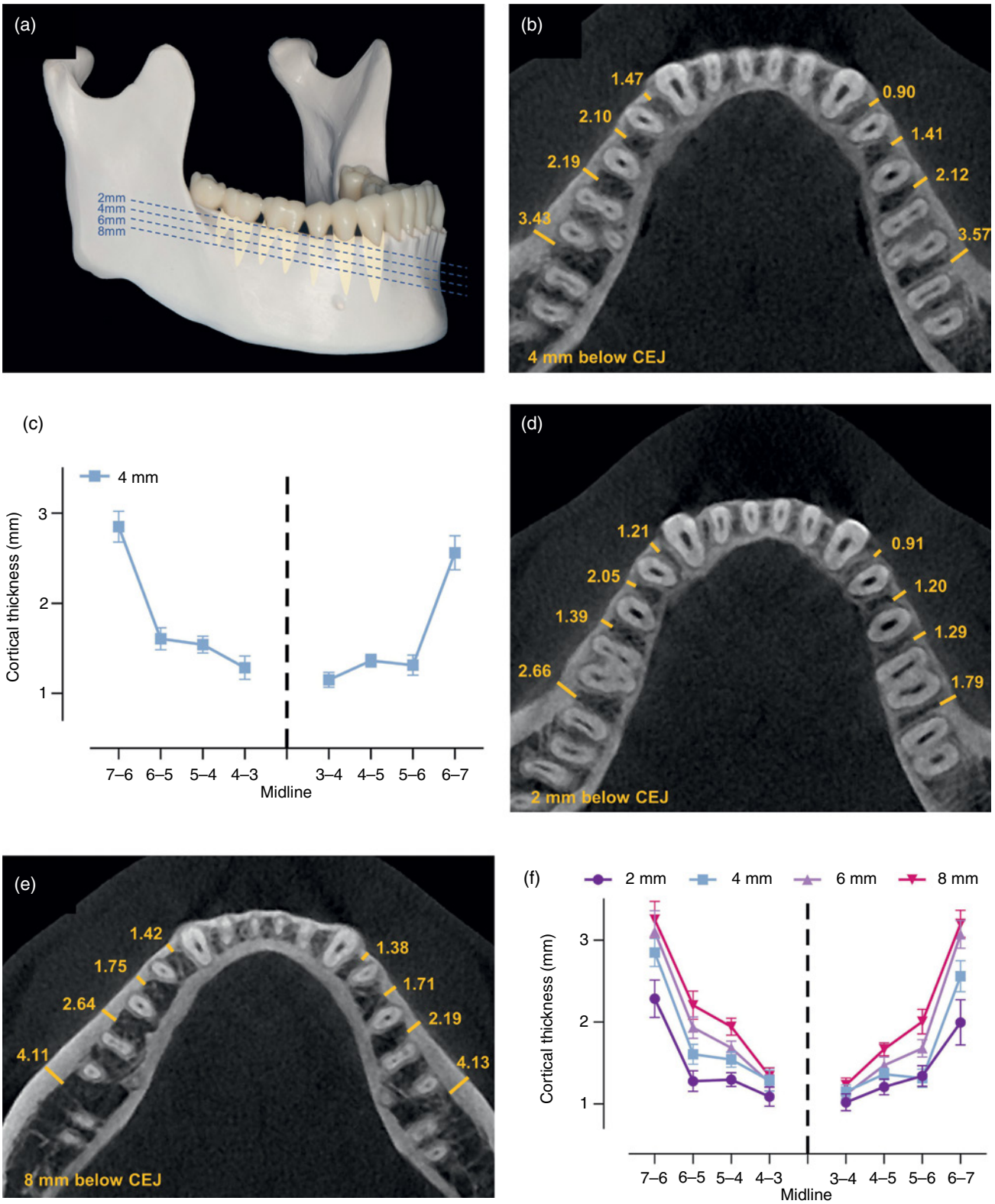


Figure 8.6 Cortical thickness among different interradicular sites and different heights. (a) An illustration of the section planes below the CEJ on the skull. (b,c) Cortical thickness among different interradicular sites at the level of 4 mm below the CEJ. (d–f) Comparisons of cortical thickness at different heights.

t.me/Dr_Mouayyad_AlbtousH

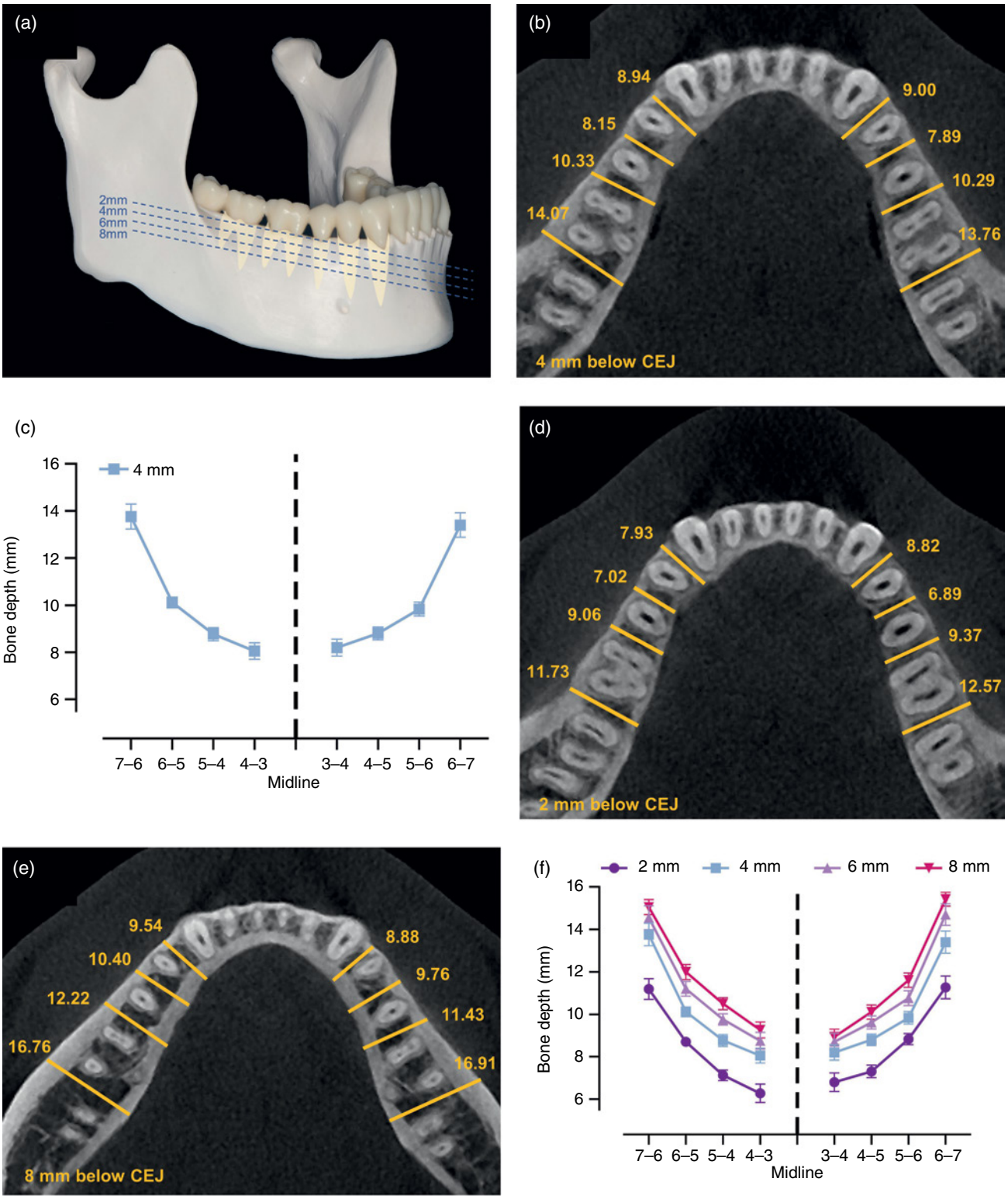


Figure 8.7 Bone depth among different interradicular sites and different heights. (a) An illustration of the section planes below the CEJ on the skull. (b,c) Bone depth among different interradicular sites at the level of 4 mm below the CEJ. (d–f) Comparisons of bone depth at different heights.

t.me/Dr_Mouayyad_AlbtousH

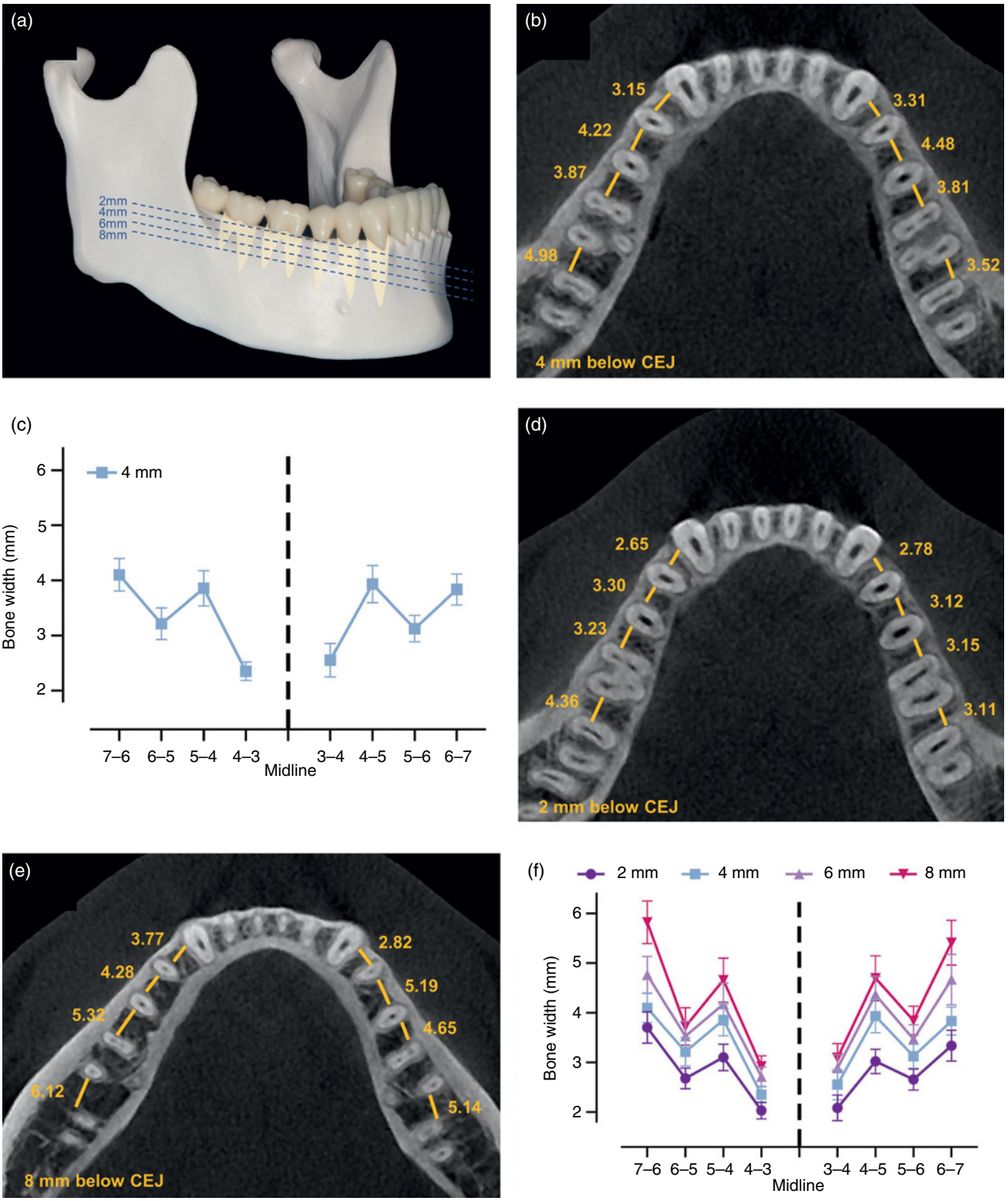


Figure 8.8 Bone width among different interradicular sites and different heights. (a) An illustration of the section planes below the CEJ on the skull. (b,c) Bone width among different interradicular sites at the level of 4 mm below the CEJ. (d–f) Comparisons of bone width at different heights.

t.me/Dr_Mouayyad_AlbtousH

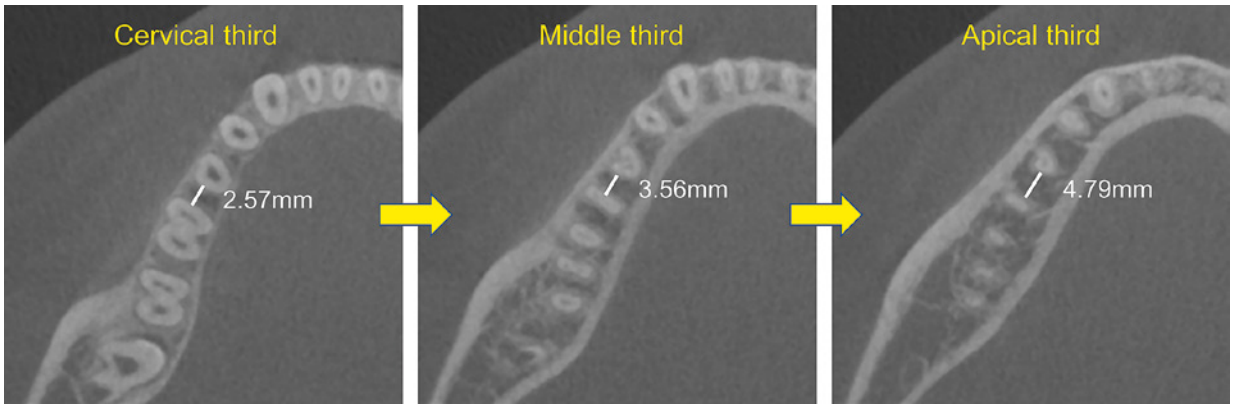


Figure 8.9 The interradicular distance increases from the cervical level to the apical level.

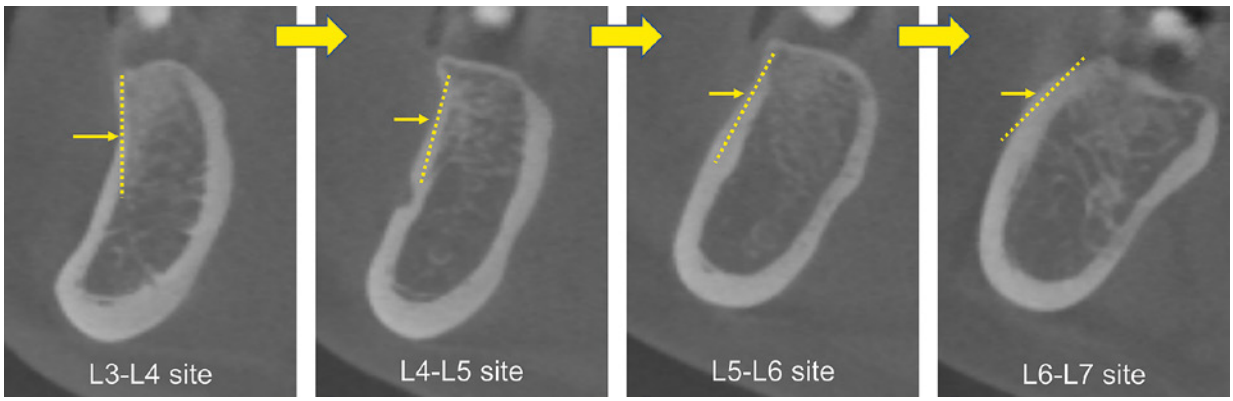


Figure 8.10 Changes in the inclination and shape of the buccal cortical plate. The cortical plate gradually becomes lingually inclined as it approaches posteriorly. The cortical plate is concave at the L3-L4 site, becomes straight at the L4-L5 and L5-L6 sites, and finally turns to be convex at the L6-L7 site.

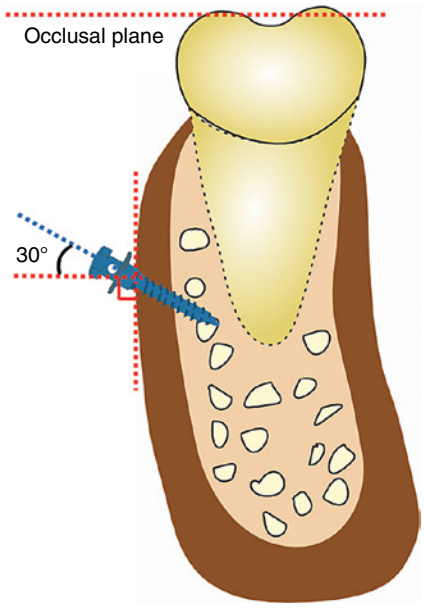


Figure 8.11 The angle between the insertion path and the normal line of the bone surface is 30°.

Soft Tissue Factor: Soft Tissue Types

Mini-implants have to pass through soft tissues before penetration into alveolar bone and judicious selection of entry points is essential for complication-free and successful application of mini-implants, otherwise soft tissue complications may lead to mini-implant failure. Ideally, the entry point is located at the attached gingiva zone where the soft tissue is keratinised and fixed onto alveolar bone (Figure 8.12). However, limited width of attached gingiva zone may be encountered in clinical practice. Among such cases, insertions close to the alveolar crest bear a high risk of mini-implant failure due to root injury. Thus, we recommend insertions be performed at the mucogingival junction or even 0.5–1 mm apical to the mucogingival junction. Moreover, angled insertion can be exploited to overcome this anatomical disadvantage (Figure 8.13).

It has been shown that, at the mandibular buccal region, the width of attached gingiva is greatest at the canine region and least at the premolar region (Figure 8.14).[11] Thus, practitioners should be cautious about placement of

t.me/Dr_Mouayyad_AlbtousH



Figure 8.12 Mini-implants should be placed at the keratinised gingiva zone that is between the white dashed line and the yellow dashed line. The movable mucosa zone lies between the yellow dashed line and the blue dashed line.

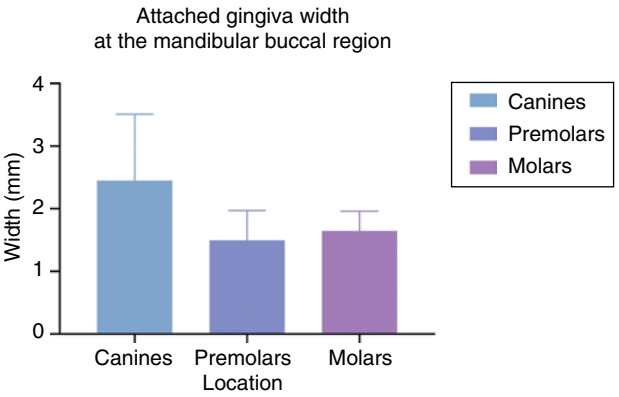


Figure 8.14 The width of attached gingiva at the mandibular buccal region. *Source:* Adapted from Bhatia et al. [11].

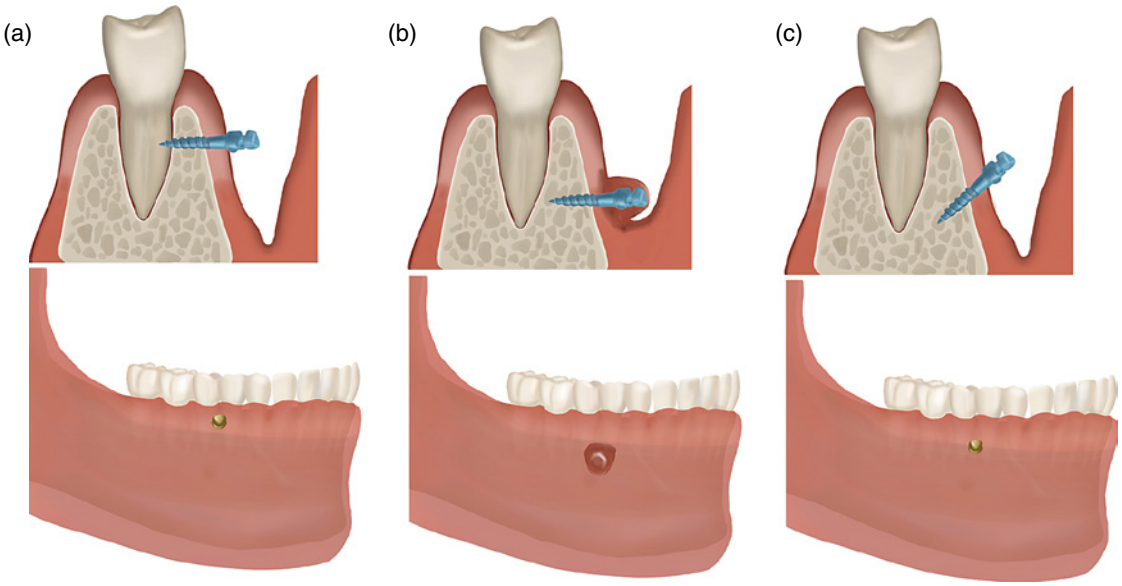


Figure 8.13 Angled insertion technique. (a) A mini-implant is inserted at the attached gingiva zone and may cause root injury due to limited interradicular space. (b) To avoid root contact, the mini-implant is inserted at a more apical level. The risk of soft tissue complications is high. (c) The mini-implant is inserted in an oblique insertion path. As the interradicular space becomes greater at more apical levels, the risk of root contact can be greatly reduced. Moreover, the head of the mini-implant remains at the attached gingiva zone and the risk of soft tissue complications is low.

mini-implants into premolar regions with limited width of attached gingiva, and angled insertion technique is recommended to overcome this disadvantage.

Soft Tissue Factor: Buccal Frenum

Buccal frenum may be observed at the L3-L4 and L4-L5 sites in some patients (Figure 8.15). On one hand, the buccal frenum may attach too coronally and interfere with the insertion of mini-implants. On the other hand, following the placement of mini-implants, the buccal frenum moves as patients perform functional movements, e.g. speaking and swallowing. This may lead to irritation of soft tissue around the heads of mini-implants. Thus, frenectomy is indicated for these two clinical scenarios.

Vital Anatomical Structures

The inferior alveolar nerve runs in the inferior alveolar canal and exits through the mental foramen, posing a risk of nerve injury for the insertion of mini-implants at the mandibular buccal region. As displayed in Figure 8.16, the

t.me/Dr_Mouayyad_AlbtousH

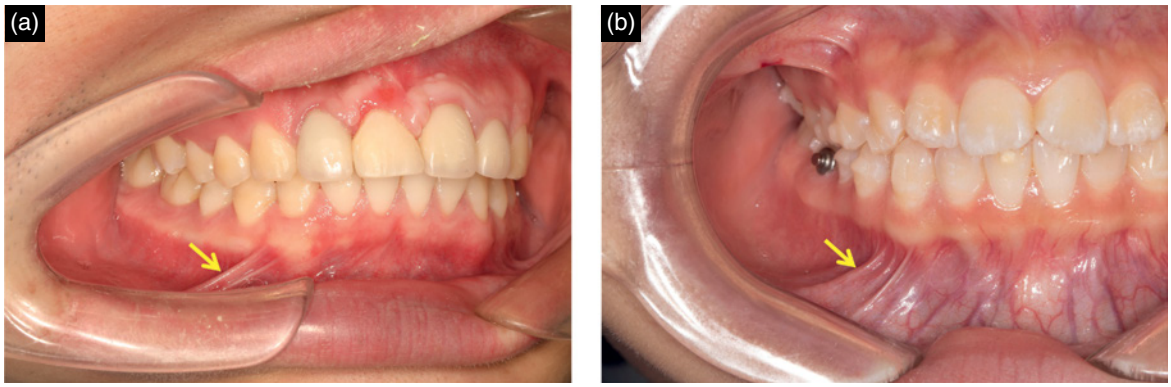


Figure 8.15 Buccal frenum. (a) The buccal frenum is present between the canine and the first premolar. (b) The buccal frenum lies between the first and second premolars.

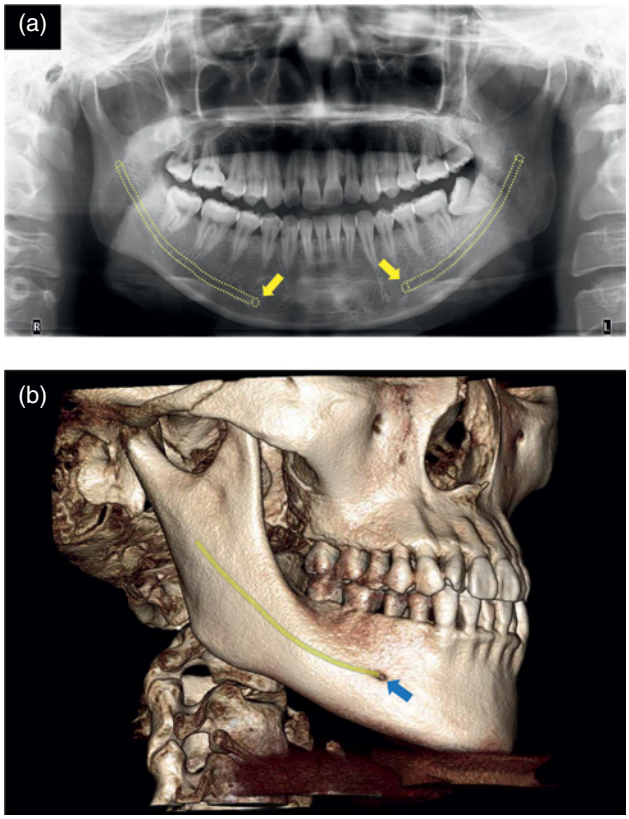


Figure 8.16 (a) The panoramic photograph shows mental foramina (yellow arrow) and mandibular canals (yellow dotted line) that are located apical to root apices. (b) A 3-D reconstruction from CBCT images showing the mental foramen (blue arrow).

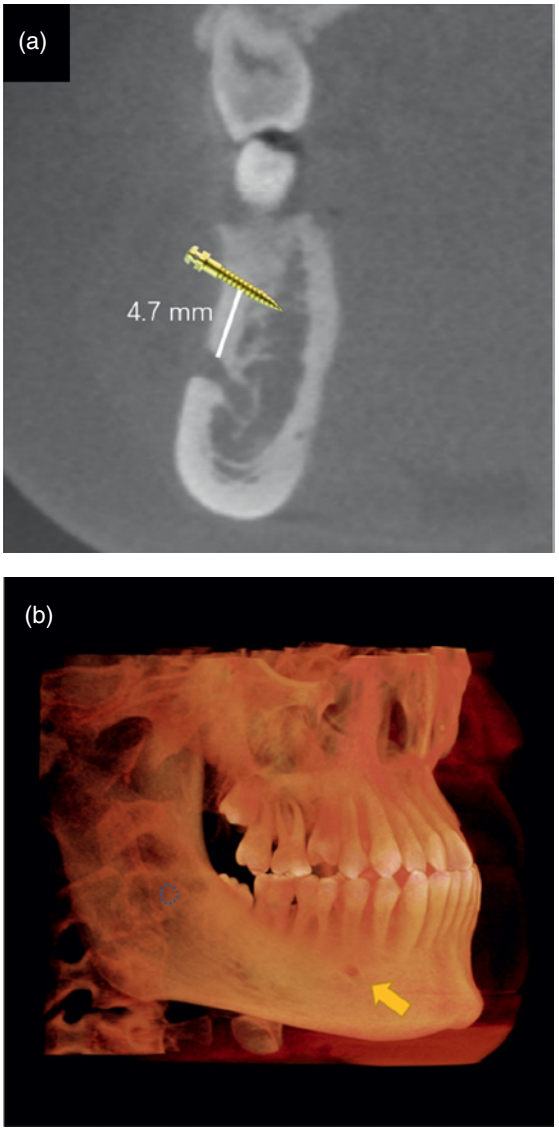


Figure 8.17 The interradicular mini-implant is inserted occlusally to the mental foramen. The distance between the entry point and the mandibular foramen is 4.7 mm. (b) 3-D reconstruction of CBCT images showing the mental foramen.

inferior alveolar canals and mental foramina are located apical to the root apices, rending insertion of mini-implants at the interradicular site to be of low risk of nerve injury. Even if mini-implants are inserted at the mental foramen zone, interradicular mini-implants are usually inserted occlusally to the mental foramen and the likelihood of nerve injury is very low, unless apical slippage of mini-implants occurs (Figure 8.17).

t.me/Dr_Mouayyad_AlbtousH

8.2.2 Biomechanical Considerations

Mini-implants are inserted at different interradicular sites to achieve versatile orthodontic tooth movements (Table 8.1). Mini-implants placed at the L3-L4 and L4-L5 sites are often exploited for molar protraction and premolar intrusion, while those placed at the L5-L6 and L6-L7 sites are applied for anterior retraction and molar intrusion. For premolar or molar intrusion, buccal tipping occurs during the intrusion process and appropriate measures (e.g. lingual arch or lingual crown torque) should be taken to avoid this adverse effect (Figure 8.18). For molar protraction, molars are susceptible to mesial tipping and intrusion that in turn result in premolar intrusion and incisor flaring (Figure 8.19a). This adverse effect can be prevented by utilising a power arm on the molar or a tip-back bend on the archwire and fixing the premolar or canine onto the mini-implant (Figure 8.19b). Furthermore, anterior retraction through mini-implants inserted at the L5-L6 or L6-L7 site may result in incisor lingual tipping and molar intrusion (Figure 8.20).

Practitioners should assess whether molar intrusion is required for the treatment plan and this biomechanical effect can be exploited if molar intrusion is indicated. Otherwise, appropriate measures should be taken to avoid this adverse effect, e.g. vertical elastics to maintain vertical positions of molars.

Table 8.1 Application of mini-implants at different interradicular sites.

Location	Application
L3-L4 and L4-L5	Molar protraction Premolar intrusion
L5-L6 and L6-L7	Anterior retraction Molar intrusion

8.2.3 Selection of Appropriate Insertion Sites

Based on hard tissue factors of the mandibular buccal interradicular region, the most appropriate interradicular sites are L6-L7 and L4-L5 where ample interradicular space is present, with insertion height being 4–8 mm apical to the CEJ. However, due to limited width of attached gingiva in the mandibular buccal region, the recommended insertion height is 4–6 mm apical to the CEJ. Angled insertion (30–45°) is recommended to keep the head of the mini-implant at the mucogingival junction zone and to take the advantage of ample interradicular space at more apical levels.

Therefore, we recommend practitioners insert mini-implants at the L6-L7 or L4-L5 site at a height of 4–6 mm apical to the CEJ, with the insertion angle being 30–45° to the occlusal plane (Figure 8.21).

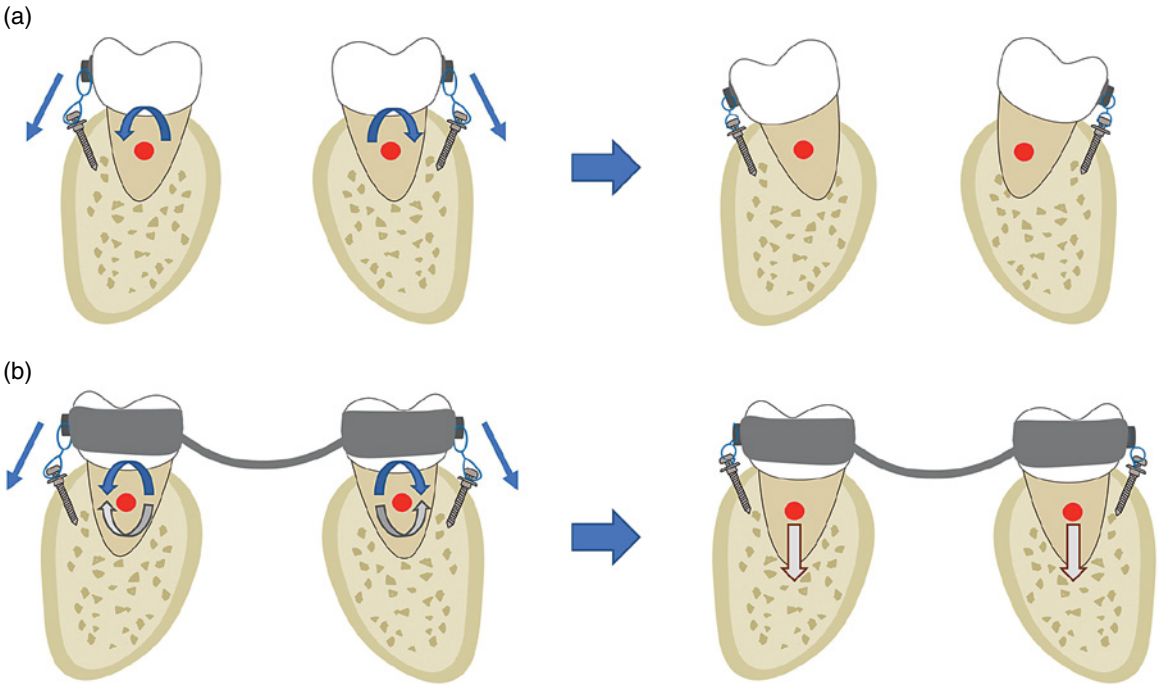


Figure 8.18 (a) As the intrusive force passes buccally to the centre of resistance, buccal tipping of the molars occurs during the intrusion process. (b) Application of the lingual arch generates a counteractive moment that prevents buccal tipping of the molars. Bodily intrusion of the molars occurs without buccal or lingual tipping.

t.me/Dr_Mouayyad_AlbtousH

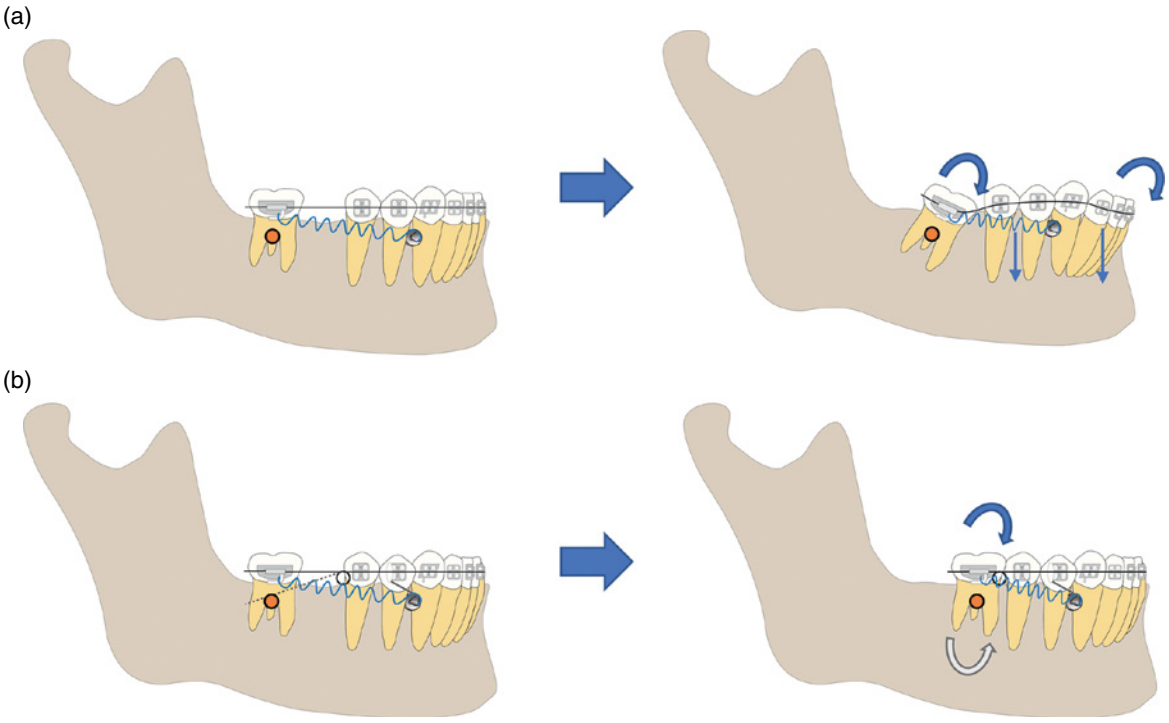


Figure 8.19 Biomechanical analysis of molar protraction. (a) As the protraction force passes occlusally to the centre of resistance, a clockwise moment is generated and the molar exhibits mesial tipping and intrusion. This in turn causes incisor labial flaring. (b) The clockwise moment generated by the protraction force is offset by the anticlockwise moment generated by the tip-back bend on the archwire. The molar is subject to bodily protraction. Moreover, to prevent incisor flaring, the second premolar is fixed onto the mini-implant with stainless steel wire.

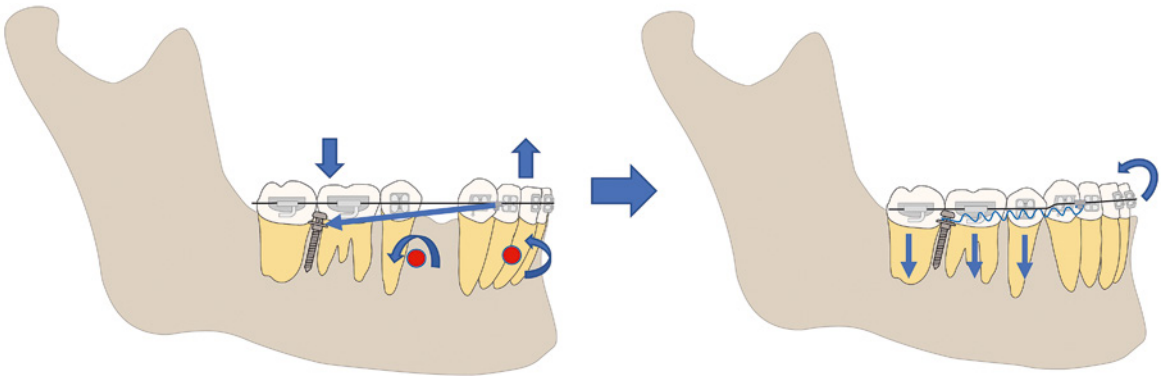


Figure 8.20 Biomechanical analysis of anterior retraction with TADs. The retraction force offered by the mini-implant passes occlusally to the centre of resistance of the mandibular dentition and generates an anticlockwise moment, leading to incisor extrusion and molar intrusion.

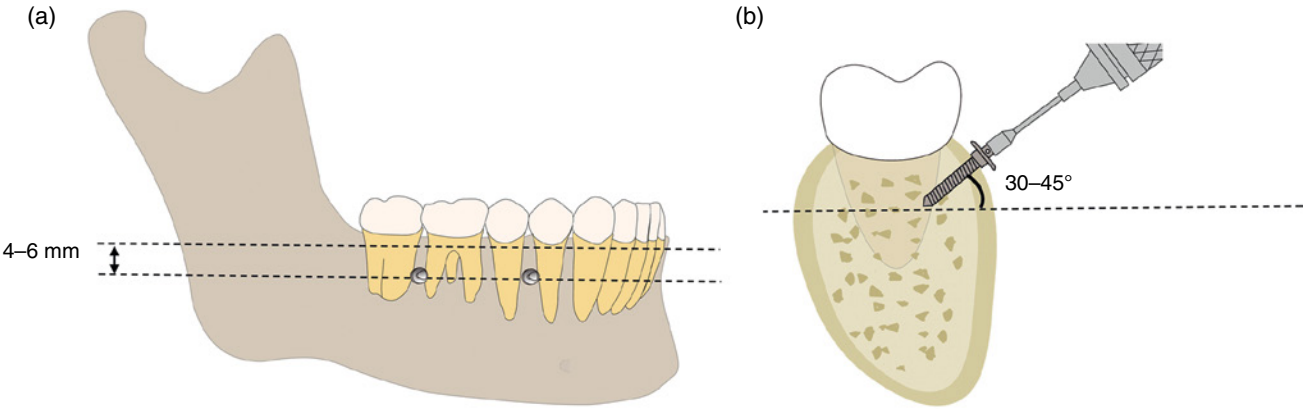


Figure 8.21 Recommended insertion height and insertion angle. (a) Mini-implants are recommended to be inserted at the L6-L7 or L4-L5 site at the insertion height of 4–6 mm apical to the CEJ. (b) The recommended insertion angle is 30–45° to the occlusal plane.

t.me/Dr_Mouayyad_AlbtousH

8.2.4 Insertion Techniques

Preinsertion

Based on anchorage requirements, biomechanical designs and treatment goals, desired interradicular sites are selected. Then, based on anatomical characteristics (both hard tissue and soft tissue factors), the optimal insertion height and angle are determined. Mini-implants with appropriate lengths and diameters should be determined. Based on mouth opening capacity and surgical access, a straight or contra-angle screwdriver is chosen prior to insertion. Moreover, for inexperienced or novice practitioners, 3-D designed and manufactured insertion guides are recommended to obtain accurate and precise insertion of mini-implants into desired positions.

Insertion

First, following mucosa disinfection with iodophor, local infiltration anaesthesia is placed (Figure 8.22). Although mini-implants are recommended to penetrate the soft tissue through the mucogingival junction, infiltration anaesthetics is not recommended to be injected at this site. Since keratinised gingiva is firmly attached and fixed onto the alveolar bone, injection of anaesthetics at the keratinised gingiva is painful. Thus, the injection point is usually 1–2 mm apical to the mucogingival junction (Figure 8.23). Moreover, in order to keep dental roots responsive to mechanical stimuli, a small amount (0.2–0.5 mL) of anaesthetics is recommended so that practitioners can be alerted when root contact occurs during insertion. Prior to infiltration anaesthesia, topical anaesthesia may be indicated for young patients or patients with dental phobia.

Adequate retraction of the cheek is recommended to stretch the mucosa so that the mucogingival junction is delineated and visible. Then, the injection syringe is inserted with the bevel facing towards the bone surface. The injection should be stopped after an appropriate amount of infiltration anaesthetic (0.2–0.5 mL) has been administered. Following the verification of satisfactory anaesthesia, patients are instructed to rinse with chlorhexidine for 30–60 seconds.

Second, the entry point is marked at the predetermined insertion site with an explorer or probe, and the mesiodistal position of the entry point should be checked and confirmed from the occlusal view (Figure 8.24). Since the operator's line of view is oblique to the insertion site, checking the entry point with naked eyes from the chairside may result in a more distal location of the entry point (Figure 8.25). Thus, the mesiodistal position of the entry point should be confirmed through the mouth mirror from the occlusal side. Moreover, a vertical indentation is made on the soft tissue so that the desired mesiodistal insertion angle can be obtained (Figure 8.26). The orientation of the vertical indentation should be checked and confirmed from both the buccal and occlusal sides.

Third, once the entry point and vertical indentation are correctly marked, the next step is to insert the mini-implant through the marked entry point. After mounting the

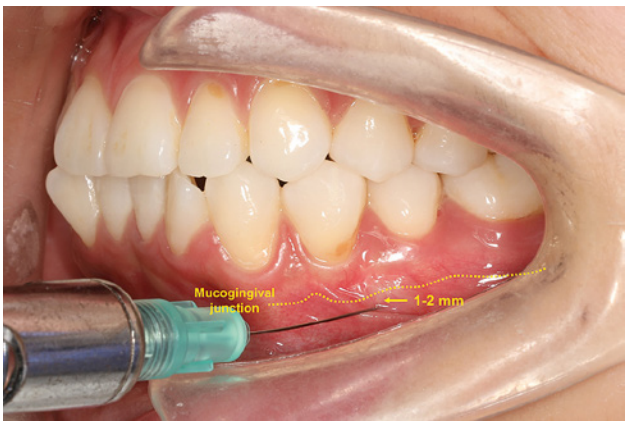


Figure 8.23 The injection point is 1–2 mm apical to the mucogingival junction.

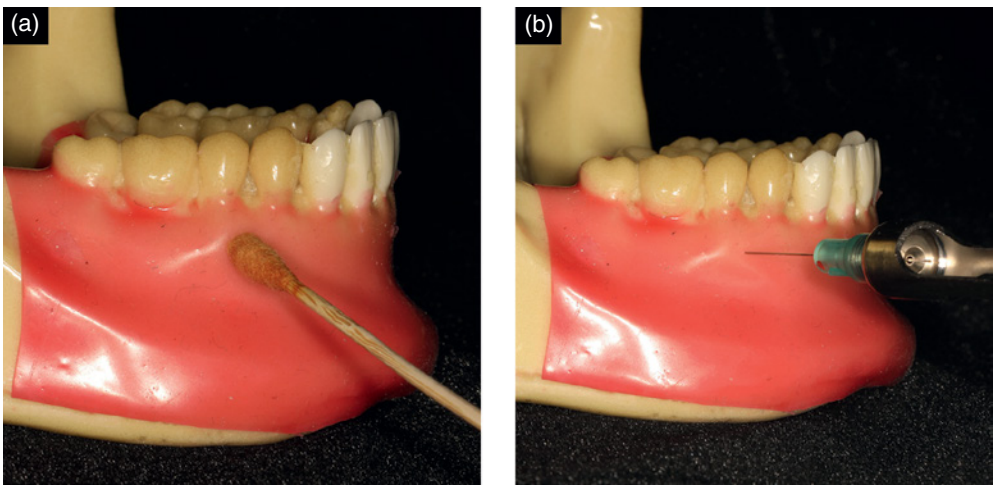


Figure 8.22 (a) Mucosa disinfection with iodophor. (b) Local infiltration anaesthesia.

t.me/Dr_Mouayyad_AlbtousH

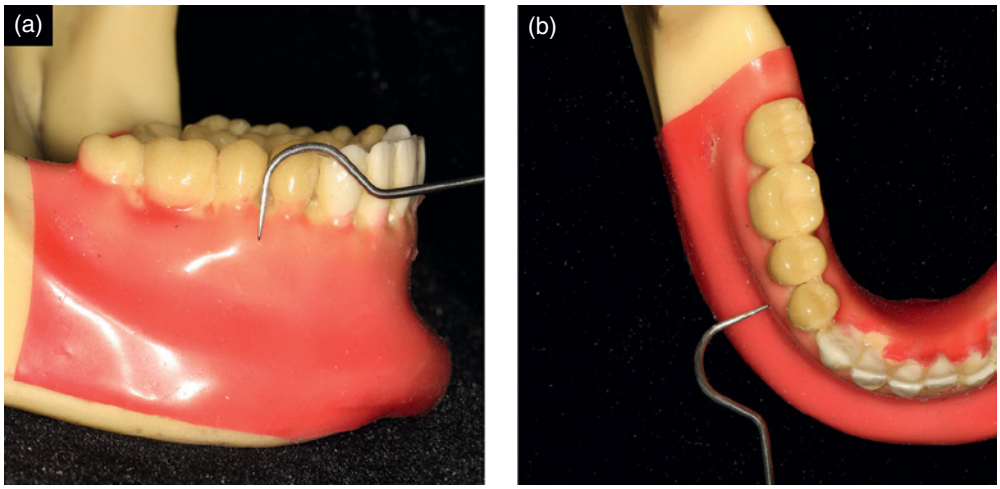


Figure 8.24 (a) The entry point is marked at the predetermined insertion site with an explorer or probe. (b) The mesiodistal position of the entry point should be checked and confirmed from the occlusal side.

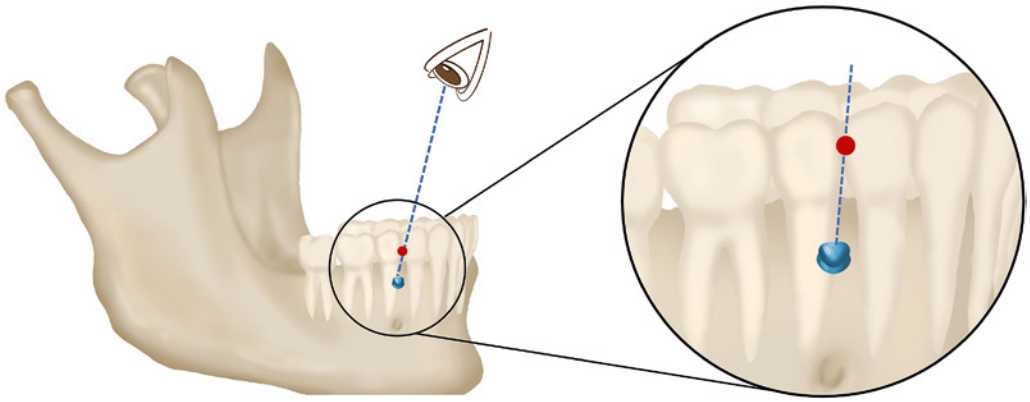


Figure 8.25 The operator's line of view is often oblique to the insertion site. Checking the entry point with the naked eye from the chairside may result in a more distal location of the entry point.

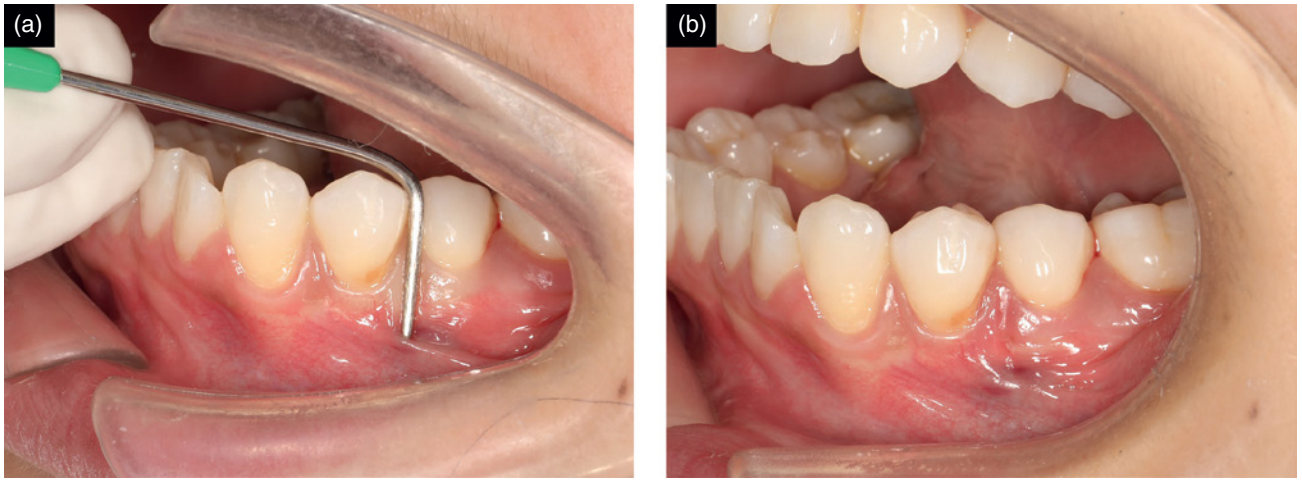


Figure 8.26 Vertical indentation of the soft tissue. (a) A vertical indentation is made on the soft tissue with an explorer. (b) The visible vertical indentation on the soft tissue.

t.me/Dr_Mouayyad_AlbtousH

mini-implant into the screwdriver, the mini-implant should be positioned perpendicularly to the bone surface and slowly advanced to penetrate the alveolar bone cortex (Figure 8.27). Due to the thick cortical plate in the mandibular buccal region, cortex penetration is more difficult than in the maxillary buccal region. Thus, slight pressure can be implemented to facilitate cortex penetration. However, the operator should slow down the rotation speed in order to avoid mechanical and thermal damage to the alveolar bone. For interradicular sites with very thick cortex (>2 mm), pilot drilling with copious saline irrigation is recommended to reduce the likelihood of bone damage.

Once the cortex is penetrated, loss of resistance may be perceived by the operator. Depending on the cortical thickness and differences of bone density between the cortical and trabecular bones, different degrees of loss of resistance can be perceived. Specifically, a strong feeling of loss of resistance may be perceived for patients with a thick and dense cortical plate. In contrast, the feeling of loss of resistance may be mild for patients with a thin cortical plate.

Fourth, once the cortex is penetrated, the mini-implant should be slightly derotated to facilitate angled insertion. If the mini-implant is not derotated, the change of insertion angle may lead to cortex or mini-implant fracture. Angled insertion is performed by inserting the mini-implant at an angle of 30–45° to the occlusal plane (Figure 8.28). Due to anatomical limitation and limited access, mini-implants are often not inserted perpendicularly to the bone surface through the entry point. Limited mouth opening and the presence of lip tension may lead to a distal orientation of mini-implant insertion (Figure 8.29). Two solutions can be employed to address this clinical problem. On one hand, patients can be instructed to decrease their mouth opening so that lip tension is reduced. On the other hand, a contra-angle screwdriver can be used to overcome this limitation,

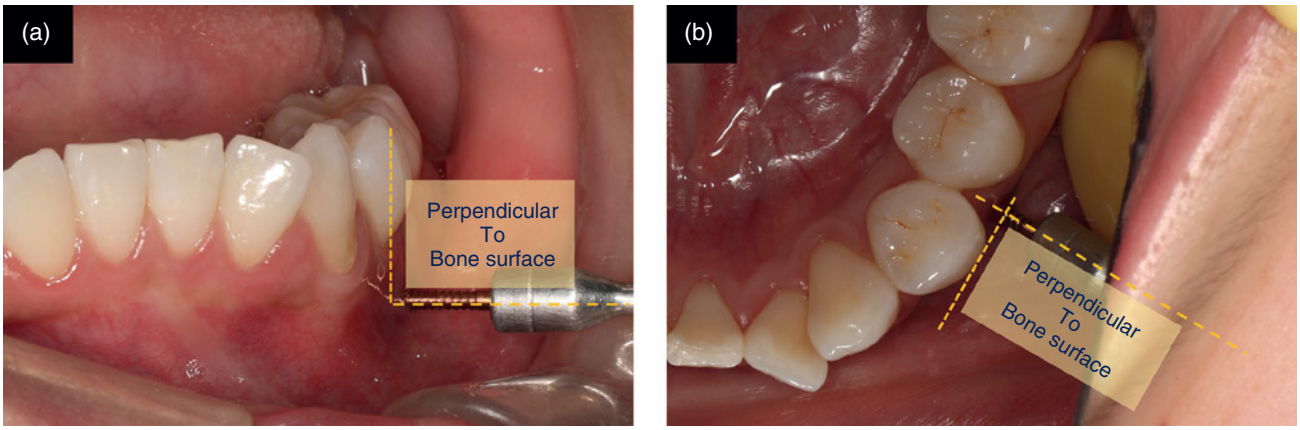


Figure 8.27 The mini-implant is inserted perpendicular to the bone surface. (a) Frontal view. (b) Occlusal view.

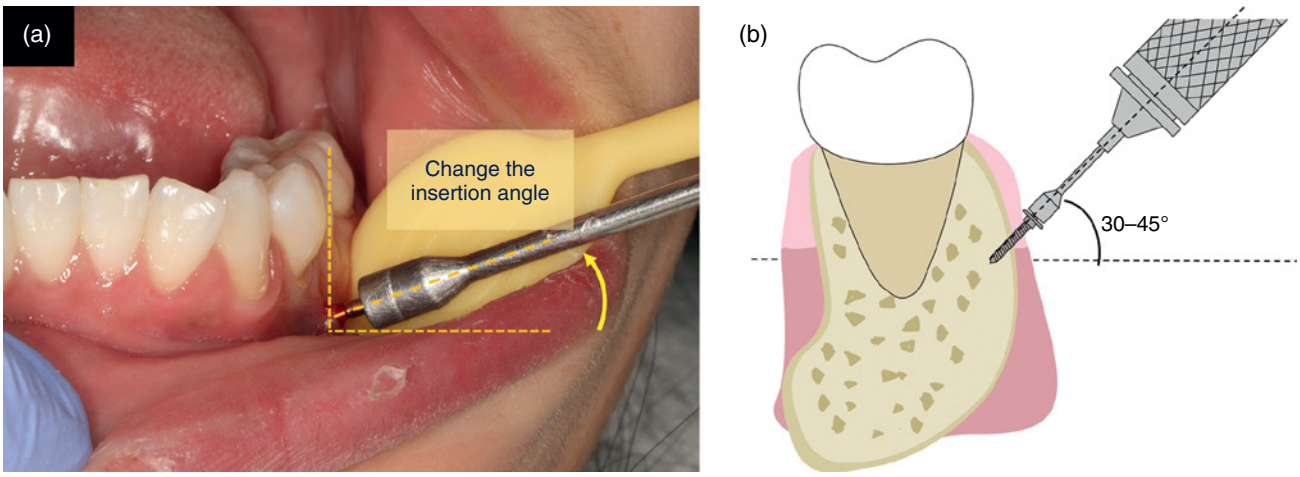


Figure 8.28 (a) The initial insertion path is perpendicular to the bone surface and parallel to the occlusal plane. Following penetration of the cortex, the insertion path is changed to reach an insertion angle of 30–45° to the occlusal plane. (b) The final insertion angle is 30–45° to the occlusal plane.

t.me/Dr_Mouayyad_AlbtousH

especially for the L6-L7 site that is the most posterior. Whichever solution is used in clinical practice, operators should check and confirm that the final insertion is perpendicular to the tangent line of the bone surface from the occlusal side (Figure 8.30).

Once the insertion angle and mesiodistal orientation are confirmed, the mini-implant is slowly inserted and advanced until the platform is in firm contact with the soft tissue (Figure 8.31). Overinsertion is prohibited since this may lead to wrapping of the mini-implant head by hyperplastic and inflamed soft tissue.

Lastly, once insertion is complete, the operator should check the position and orientation of the mini-implant. Primary stability is examined and reinsertion is recommended if primary stability is insufficient. Percussion is performed to rule out root contact.

The detailed clinical procedure of placing a mini-implant is displayed in Figures 8.32 and 8.33.



Figure 8.31 The advancement of the mini-implant is stopped once the platform of the implant is in firm contact with the soft tissue.

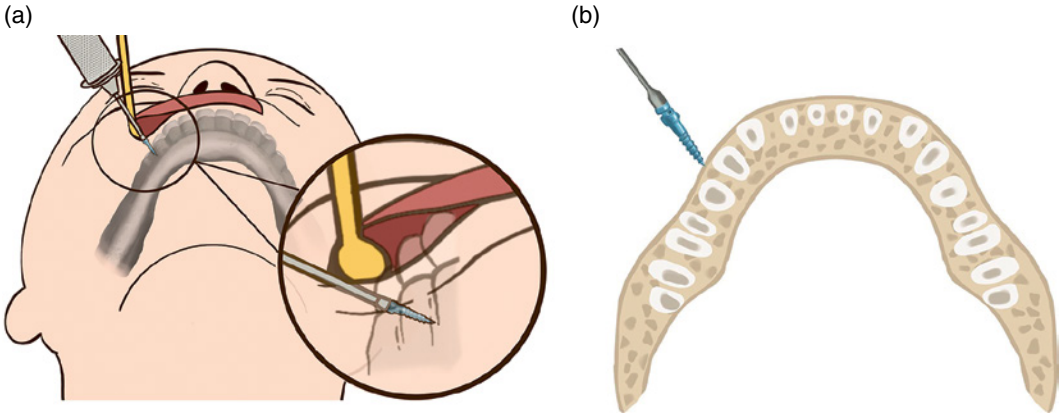


Figure 8.29 (a) Limited mouth opening and the presence of lip tension may lead to a distal orientation of mini-implant insertion. (b) The insertion path of the mini-implant is often distally oriented.

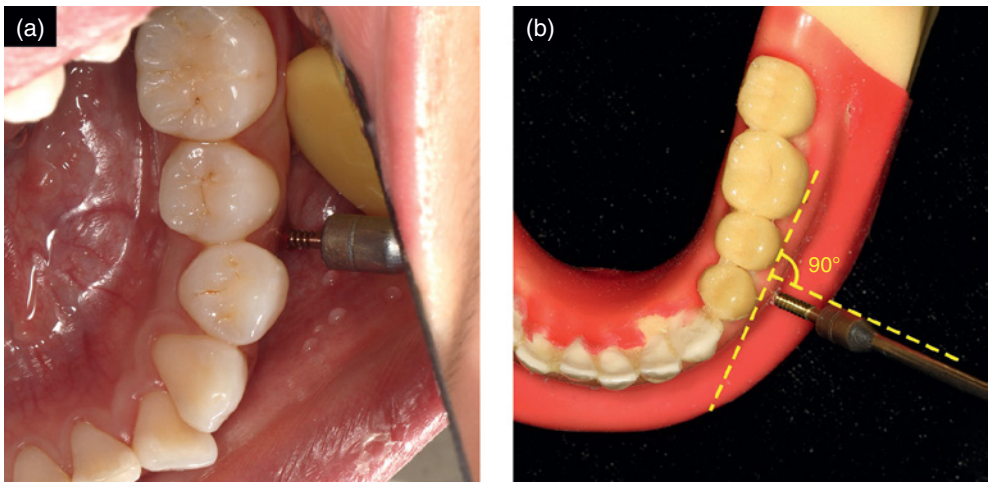


Figure 8.30 The final insertion path should be perpendicular to the tangent line of the bone surface and is checked from the occlusal side. (a) Intraoral photograph. (b) Dental model.

t.me/Dr_Mouayyad_AlbtousH

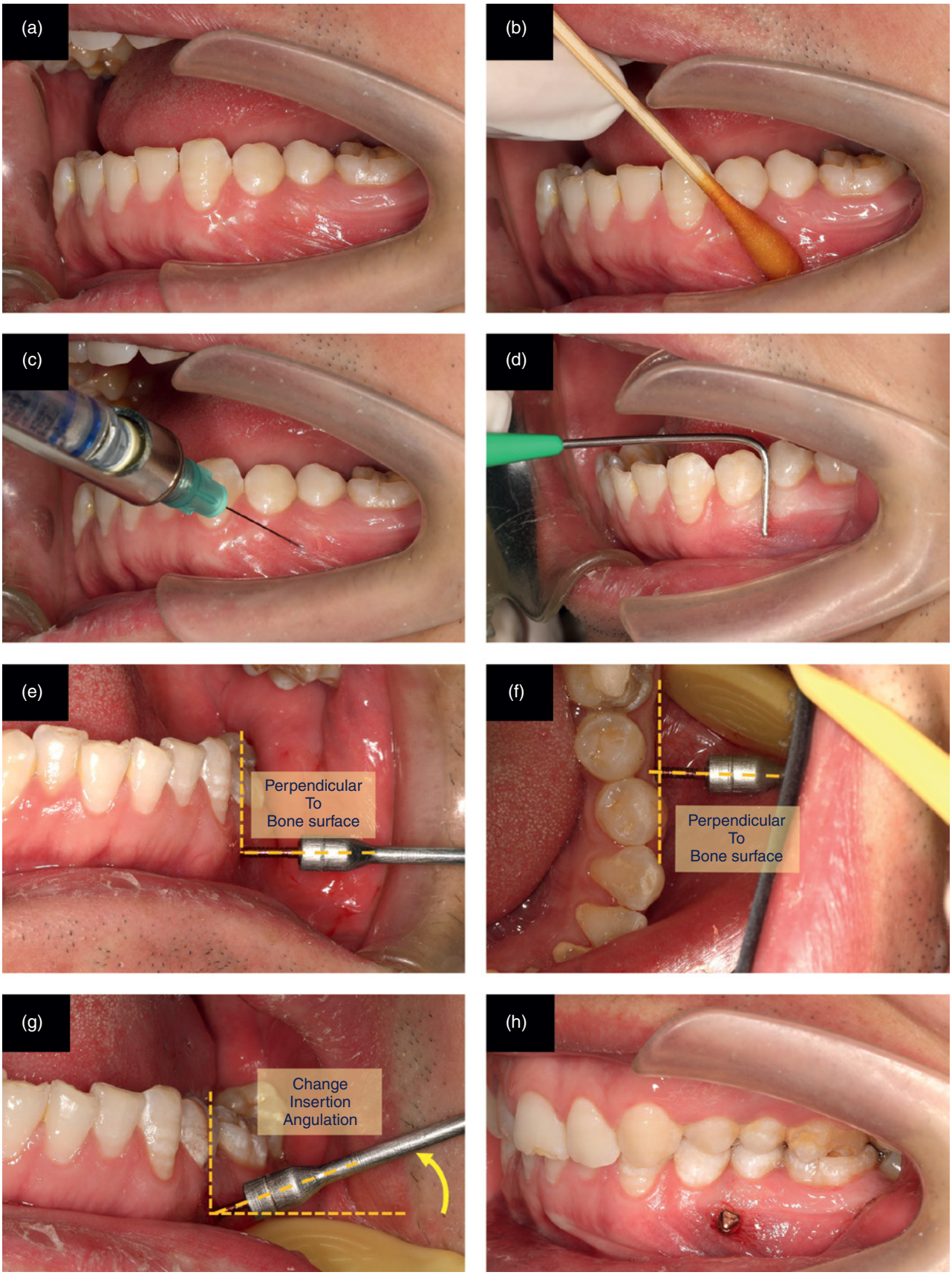


Figure 8.32 Clinical procedure for inserting a mini-implant at the mandibular buccal interradicular site. (a–c) Mucosa disinfection and local infiltration anaesthesia. (d) Perform a vertical indentation with an explorer. (e,f) Insert the mini-implant perpendicularly to the tangent line of the bone surface. (g) Change the insertion angle. (h) Postinsertion.

t.me/Dr_Mouayyad_AlbtousH

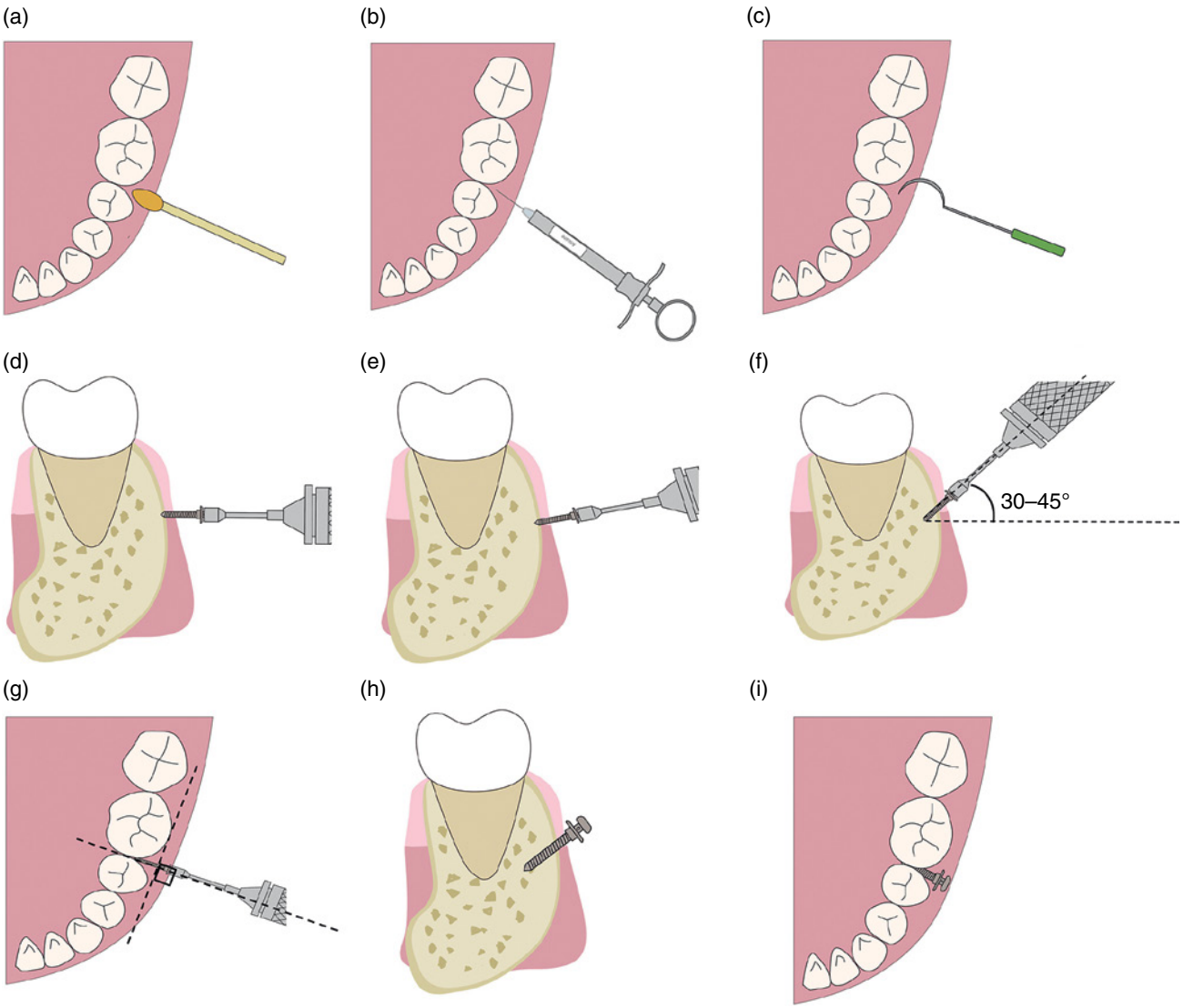


Figure 8.33 Schematic illustration of the insertion procedure. (a) Mucosa disinfection. (b) Local infiltration anaesthesia. (c) Mark the entry point with an explorer. (d) Cortex penetration. (e,f) Change the insertion path to reach a final insertion angle of 30–45° to the occlusal plane. (g) The insertion path is perpendicular to the tangent line of the bone surface. (h,i) Postinsertion.

Postinsertion

Following the placement of mini-implants, patients are instructed to maintain adequate oral hygiene. Non-steroidal anti-inflammatory drugs may be prescribed for pain relief. Force loading application should be postponed for two weeks following complete healing of soft tissues.

8.2.5 Clinical Applications

Anterior Retraction

Anterior retraction can be readily achieved by interradicular mini-implants in the mandibular buccal region. Since anterior teeth are retracted by mini-implants, molar anchorage can be reinforced and preserved. To accomplish bodily retraction, power arm is often exploited so that the retraction force passes through the centre of resistance. A case example is given below.

A female adult patient presented to the orthodontic clinic with a chief complaint of protrusive facial profile. As displayed in Figure 8.34, clinical and radiographic examinations revealed that she had a protrusive facial profile and class I canine and molar relationships on both sides. Lateral cephalometric analysis indicated that she had class I skeletal base (ANB = 2.7), normal incisor labiolingual inclinations for both the upper and lower arches (U1-SN = 108; L1-MP = 102.1), and average mandibular plane angle (SN-MP = 33.1) (Table 8.2).

Based on per-treatment examinations, extractions of four first premolars and subsequent anterior retraction were planned. Due to her protrusive facial profile, maximal molar anchorage was designed with mini-implants.

To reinforce molar anchorage and efficient incisor retraction, four mini-implants were inserted. Two upper

t.me/Dr_Mouayyad_AlbtousH

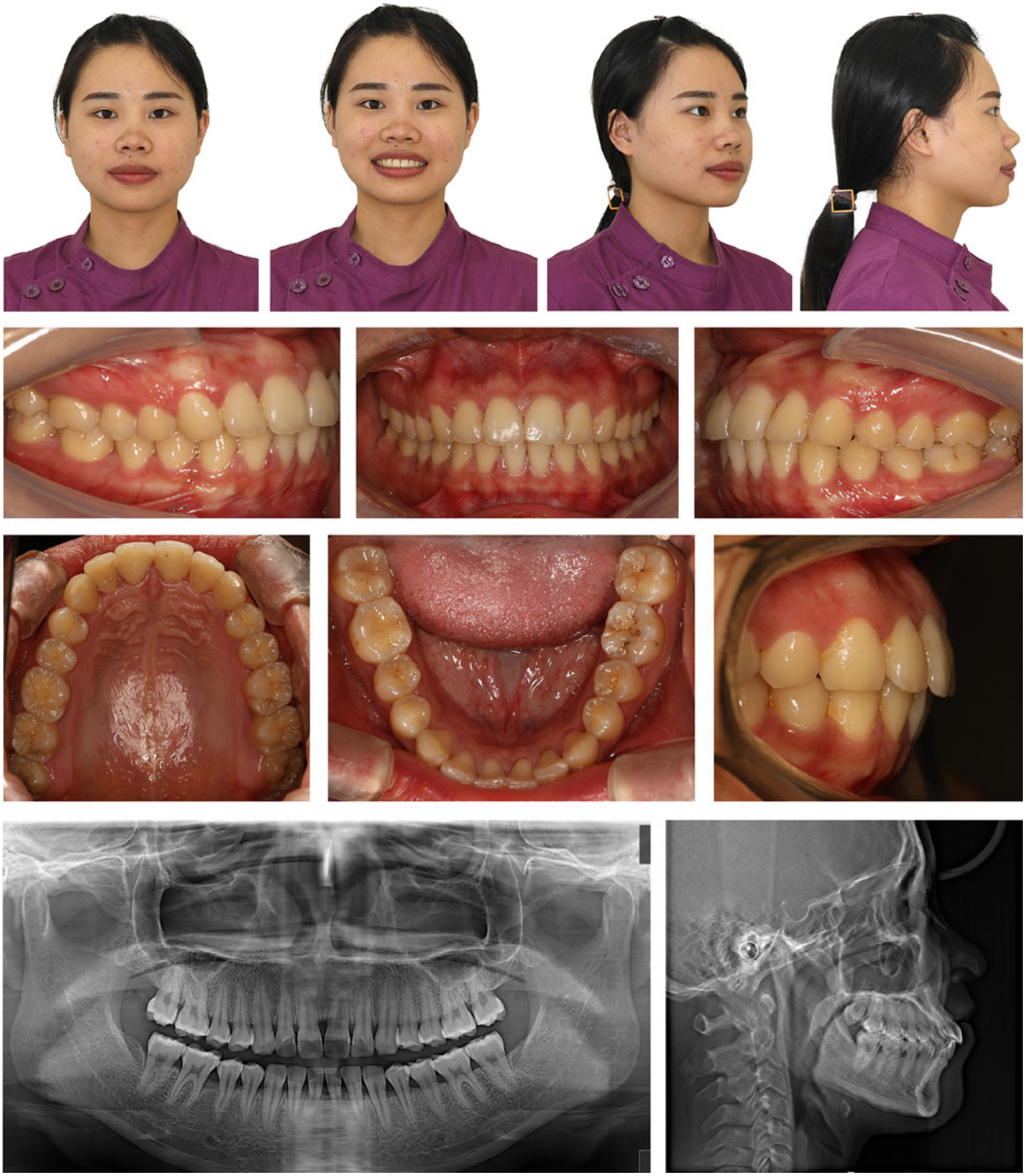


Figure 8.34 Pretreatment photographs and radiographs.

mini-implants were placed at the infrazygomatic crest region and the other two were inserted at the L6-L7 interradicular site in the mandibular buccal region (Figure 8.35). Since the incisors exhibited normal labiolingual inclinations for both the upper and lower arches, bodily retraction was required. Thus, crimpable long hooks were added onto the archwires between lateral incisors and canines, and closed-coil springs were ligated between the long hooks and mini-implants. In this way, the retraction force passed through the centres of resistance to facilitate bodily retraction of anterior teeth (Figure 8.36).

t.me/Dr_Mouayyad_AlbtousH

Table 8.2 Pretreatment lateral cephalometric analysis.

Measurement	Norm	Pretreatment
Skeletal (°)		
SNA	83.0±4.0	81.9
SNB	80.0±4.0	79.2
ANB	2.0±2.0	2.7
FMA	28.0±4.0	22.2
SN-MP	35.0±4.0	33.1
Dental (°)		
U1-SN	105.7±6.3	108.0
L1-MP	97.0±7.1	102.1
FMIA	65.0±6.0	55.7
U1-L1	124.0±8.0	116.8
Soft tissue (mm)		
UL-EP	2.0±2.0	−2.4
LL-EP	3.0±2.0	0.6

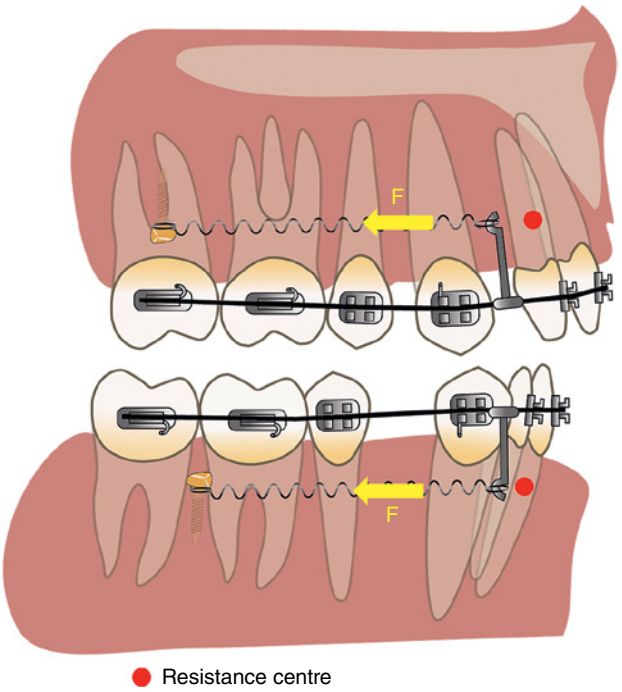


Figure 8.36 A schematic illustration showing that the application of long crimpable hooks allows the retraction forces to pass through the centres of resistance. Thus, bodily retraction of the anterior teeth is achieved.

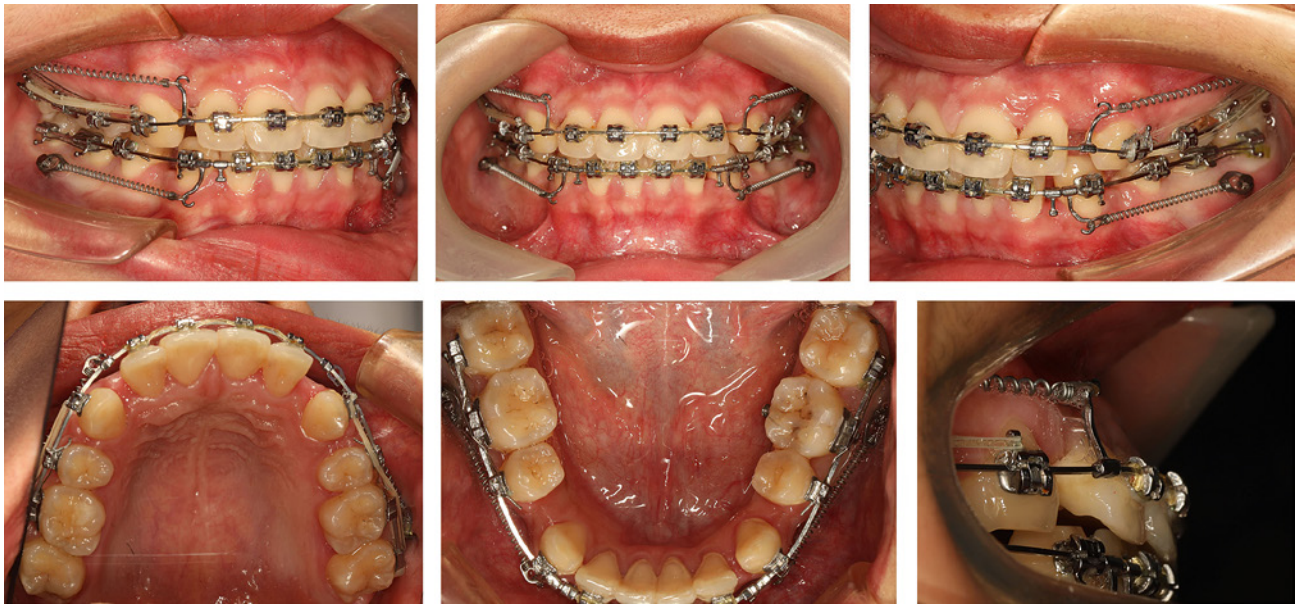


Figure 8.35 *En masse* anterior retraction with TADs. Two mini-implants were placed at the infrazygomatic crest and two were inserted at the L6-L7 buccal interradicular sites. Anterior retraction was achieved by applying closed-coil springs from the long crimpable hooks on the archwires to the mini-implants.

t.me/Dr_Mouayyad_AlbtousH



Figure 8.37 Posttreatment photographs and radiographs.

Finally, as displayed in Figure 8.37, straight facial profile was obtained with the maintenance of class I canine and molar relationships on both sides. The pretreatment and posttreatment cephalometric values are presented in Table 8.3.

Molar Protraction

Molar protraction can be achieved through mini-implants that are inserted at interradicular sites (i.e. L3-L4 and L4-L5). Molar protraction can be accomplished with an archwire or through an independent biomechanical system without archwire.

t.me/Dr_Mouayyad_AlbtousH

Table 8.3 Pre- and posttreatment lateral cephalometric analysis.

Measurement	Norm	Pretreatment	Posttreatment
Skeletal (°)			
SNA	83.0±4.0	81.9	81.8
SNB	80.0±4.0	79.2	80.0
ANB	2.0±2.0	2.7	1.8
FMA	28.0±4.0	22.2	20.4
SN-MP	35.0±4.0	33.1	32.1
Dental (°)			
U1-SN	105.7±6.3	108.0	100.3
L1-MP	97.0±7.1	102.1	88.1
FMIA	65.0±6.0	55.7	71.5
U1-L1	124.0±8.0	116.8	139.6
Soft tissue (mm)			
UL-EP	2.0±2.0	−2.4	−1.3
LL-EP	3.0±2.0	0.6	−0.3
Wits (mm)			
Wits	−1.0	−2.1	−3.4

Molar Protraction with Archwire Molars can be protracted by anterior teeth whose anchorage is reinforced by mini-implants placed at the mandibular buccal interradicular sites. A case example is presented below.

A male patient presented to the orthodontic department with a chief complaint of missing teeth. The clinical and radiographic examinations revealed that the mandibular bilateral first molars were missing and that the bilateral canine relationships were class I (Figure 8.38). Moreover, mandibular bilateral third molars were present with good root development. As displayed in Table 8.4, the lateral cephalometric analysis revealed that the patient had a class II skeletal base (ANB = 4.1), average mandibular plane angle (SN-MP = 37.4) and normal labiolingual inclination of upper and lower incisors (U1-SN = 106.2 and L1-MP = 99). The treatment plan was alignment and levelling of the dental arch and protraction of the mandibular second and third molars to substitute the first and second molars, respectively. To achieve bodily protraction of the molars, T-loops with tip-back bend were designed in the archwire (Figure 8.39). On each side, one mini-implant was inserted at the buccal interradicular site between the first and second premolars to reinforce the anchorage of the anterior teeth (Figure 8.40). The molar protraction was efficient and successful, resulting in a final good buccal interdigitation (Figure 8.41). The comparison of pre- and posttreatment cephalometric values is presented in Table 8.5.

Molar Protraction Through Albert Loop An independent biomechanical system built on a mini-implant will be elaborated below. The Albert loop appliance (one or two closing loops and one distal helical loop) can be used for molar protraction (Figure 8.42). The distal part of the loop appliance was inserted into the buccal tube and the anterior part fixed onto the mini-implant. The closing loops offer protraction force that may cause molar mesial tipping during mesial movement. The helical loop with tip-back bend offered counteractive moment in preventing mesial tipping of the molar. Thus, bodily mesial movement of the molar can be achieved. If molars exhibited mesial tipping before protraction, the tip-back moment can be increased by activating the helical loop, so that molars can be protracted and distally tipped simultaneously (Figure 8.43).

Molar Intrusion

For the intrusion of mandibular molars, only buccal mini-implants can be inserted due to anatomical limitations in the mandibular lingual side. Thus, appropriate measures should be taken to avoid buccal tipping of mandibular molars during intrusion. To overcome this biomechanical imitation, cantilevers can offer intrusive force on both the buccal and lingual sides. A case example is given below.

A patient presented to the Department of Implantology with a chief complaint of missing teeth. As displayed in Figure 8.44, clinical and radiographic examinations revealed that the maxillary left first molar and right first and second molars were missing, with overeruption of the mandibular right second molar. The treatment plan was implant restoration of the missing upper three molars. However, due to overeruption of the mandibular right second molar, implant restoration of the upper right molars was not possible. Thus, orthodontic intrusion of the right second mandibular molar was planned.

To intrude the overerupted molar, an orthodontic appliance with two cantilevers was designed, with one on the buccal side and the other on the lingual side (Figure 8.45). This appliance offered intrusive force on both sides so that bodily intrusion could be achieved. However, the intrusive force exerted on molars produced a reactive force on the first molar and premolars that may lead to their extrusion. To eliminate this adverse effect, a mini-implant was inserted at the L5-L6 interradicular site to stabilise the first molar and two premolars (Figures 8.46 and 8.47). Thus, the overerupted second molar can be efficiently intruded without extrusion of anchorage teeth.

t.me/Dr_Mouayyad_AlbtousH



Figure 8.38 Pretreatment photographs and radiographs.

t.me/Dr_Mouayyad_AlbtousH

Table 8.4 Pretreatment lateral cephalometric analysis.

Measurement	Norm	Pretreatment
Skeletal (°)		
SNA	83.0±4.0	81.6
SNB	80.0±4.0	77.5
ANB	2.0±2.0	4.1
FMA	28.0±4.0	30.2
SN-MP	35.0±4.0	37.4
Dental (°)		
U1-SN	105.7±6.3	106.2
L1-MP	97.0±7.1	99.0
FMIA	65.0±6.0	50.7
U1-L1	124.0±8.0	117.4
Soft tissue (mm)		
UL-EP	2.0±2.0	0.7
LL-EP	3.0±2.0	2.5
Wits (mm)		
Wits	−1.0	2.2

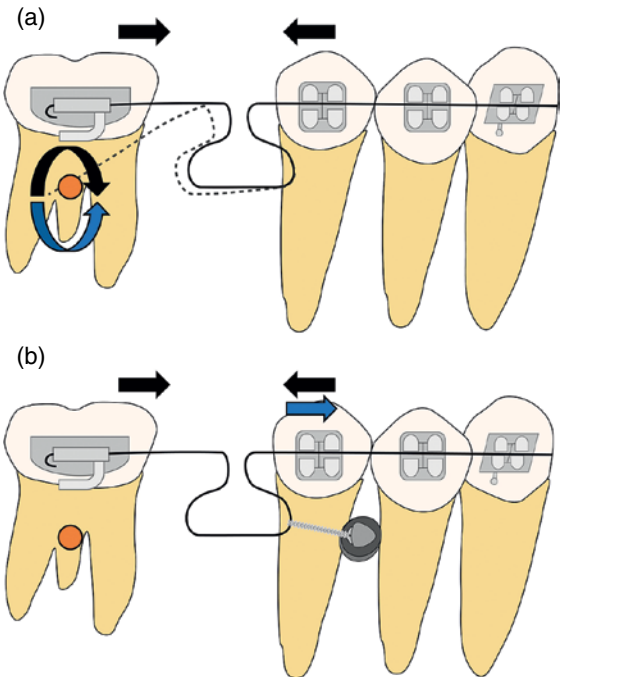


Figure 8.39 Biomechanics of molar protraction through a T-loop. (a) A T-loop with a tip-back bend is designed in the archwire. The inactivated form of the archwire is indicated by the dashed line and the activated one by the solid line. The protraction force (black arrow) applied on the molar generates a reciprocal retraction force (black arrow) on the anterior teeth. Moreover, the protraction force generates a clockwise moment (black curved arrow) on the molar, leading to mesial tipping of the molar. The mesial tipping tendency of the molar is counteracted by the anticlockwise moment (blue curved arrow) generated by the activation of the T-loop. Therefore, the net effect is bodily protraction of the molar. (b) The reciprocal retraction force (black arrow) applied on the anterior teeth is offset by the stabilisation force (blue arrow) offered by the mini-implant. Thus, the anchorage of the anterior teeth is reinforced by the mini-implant between the first and second premolars.

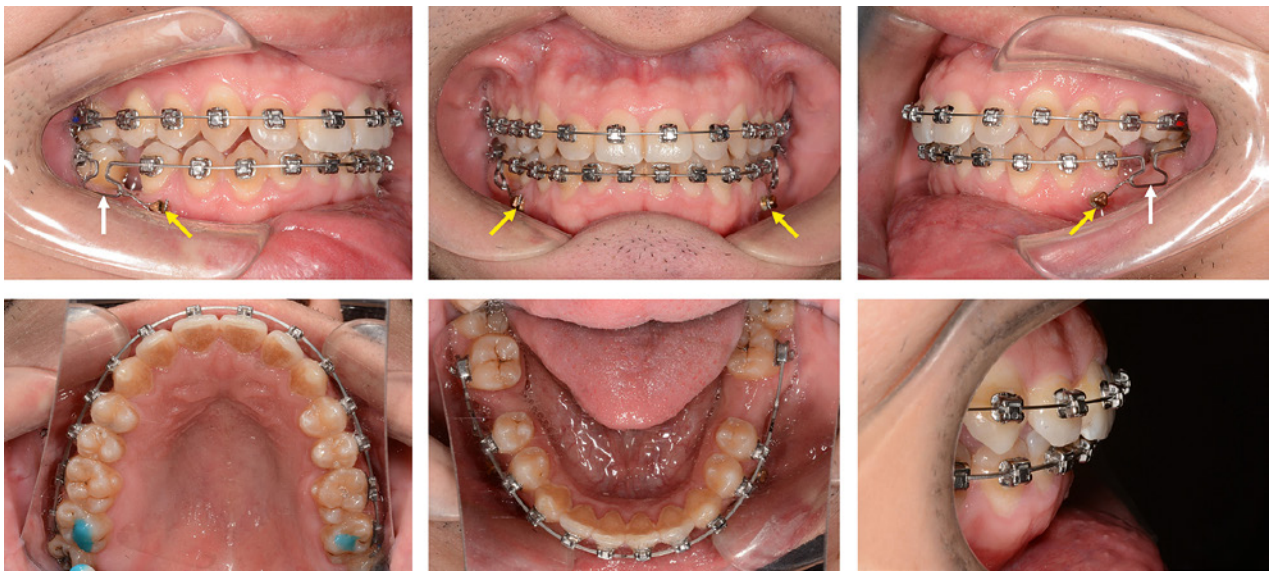


Figure 8.40 Mini-implants (yellow arrow) were placed at the buccal interradicular sites between the first and second premolars. T-loops (white arrow) were employed to protract the second molars and the mini-implants were used to reinforce the anchorage of the anterior teeth.

t.me/Dr_Mouayyad_AlbtousH

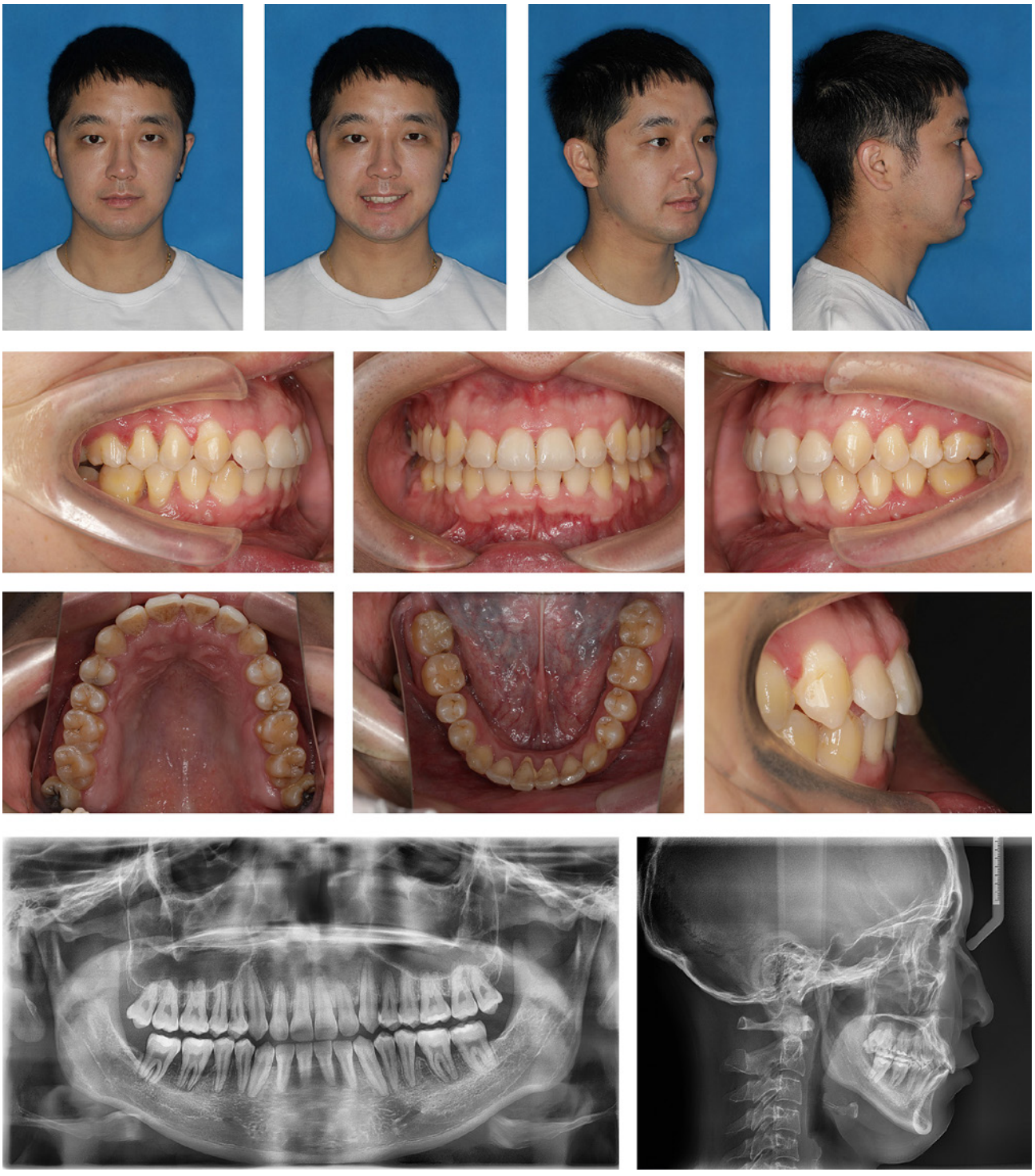


Figure 8.41 Posttreatment photographs and radiographs.

t.me/Dr_Mouayyad_AlbtousH

Table 8.5 Pre- and posttreatment lateral cephalometric analysis.

Measurement	Norm	Pretreatment	Posttreatment
Skeletal (°)			
SNA	83.0±4.0	81.6	79.1
SNB	80.0±4.0	77.5	76.7
ANB	2.0±2.0	4.1	2.4
FMA	28.0±4.0	30.2	29.8
SN-MP	35.0±4.0	37.4	37.3
Dental (°)			
U1-SN	105.7±6.3	106.2	103.2
L1-MP	97.0±7.1	99.0	99.9
FMIA	65.0±6.0	50.7	50.3
U1-L1	124.0±8.0	117.4	119.7
Soft tissue (mm)			
UL-EP	2.0±2.0	0.7	1.4
LL-EP	3.0±2.0	2.5	2.6
Wits (mm)			
Wits	−1.0	2.2	−2.4

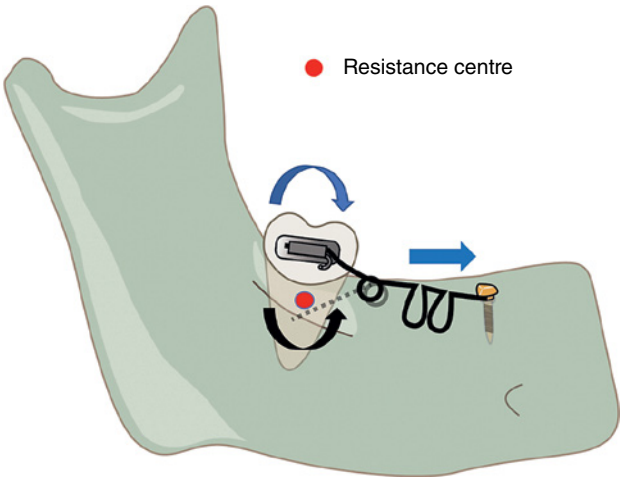


Figure 8.42 The Albert loop contains a distal helical loop that generates a tip-back anticlockwise moment and one or two closing loops that deliver protraction force. The protraction force (blue arrow) generates a clockwise moment (blue curved arrow) that in turn leads to mesial tipping of the molar. The clockwise moment generated by the closing loops is offset by the anticlockwise moment (black curved arrow) offered by the distal helical loop.

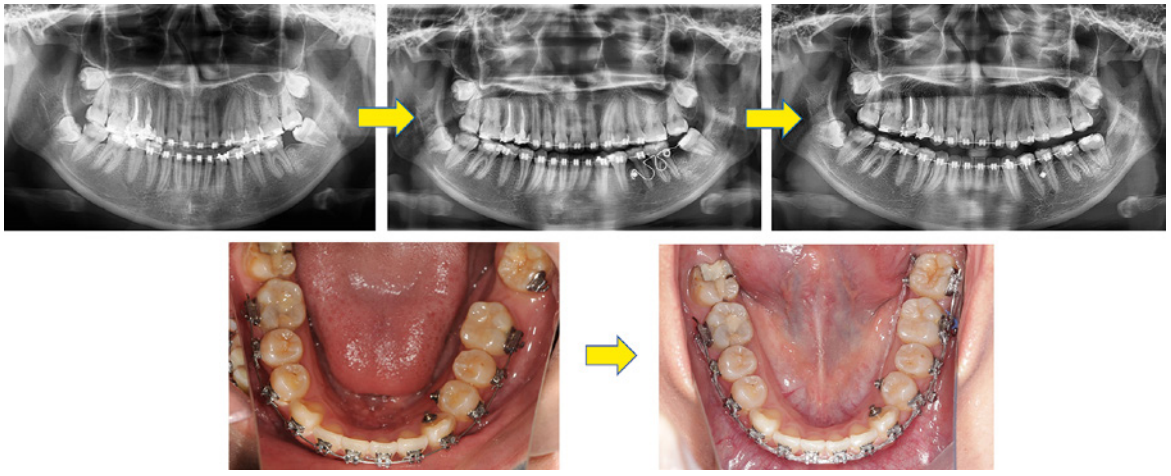


Figure 8.43 The patient presented with a missing mandibular left second molar. The mandibular left third molar was protracted through a mini-implant-anchored Albert loop. The molar was protracted efficiently with good root parallelism.

Following one year of treatment, the overerupted second molar was successfully intruded and the three missing teeth were restored with implants (Figure 8.48).

Molar Uprighting

Molar uprighting can be accomplished using a segmental archwire. By inserting an open-coil spring between mesially tipped molars and the anchorage teeth, the mesially tipped molars can be distally uprighted. However, the distal uprighting force exerted on the molar generates a reaction force that is applied on anterior anchorage teeth, resulting in mesial tip and labial proclination of the anchorage teeth (Figure 8.49). To overcome this biomechanical disadvantage, a mini-implant can be inserted at the

t.me/Dr_Mouayyad_AlbtousH



Figure 8.44 Pretreatment photographs and panoramic radiograph. Note the overerupted mandibular right second molar.

interradicular site between two premolars. The anchorage teeth can be stabilised by the mini-implant so that the adverse effect (mesial tipping and labial flaring) of the anchorage teeth can be eliminated (Figure 8.50). A case example is given below.

A female adult presented to the orthodontic department with a chief complaint of tooth irregularity. Upon examination, we found that the mandibular left second molar was mesially tipped and impacted beneath the distal undercut of the first molar (Figure 8.51). Orthodontic uprighting of the second molar was planned with a segmental archwire. To reinforce anterior anchorage, a mini-implant was placed at the L4-L5 interradicular site and segmental archwire technique was implemented from the first premolar to the second molar. The first molar was stabilised and fixed onto the mini-implant so that anterior anchorage was preserved (Figure 8.52). Following one year of orthodontic treatment, the second molar was successfully uprighted without loss of anterior anchorage (Figure 8.53).

t.me/Dr_Mouayyad_AlbtousH



Figure 8.45 The intrusion appliance contains two distal cantilevers (one on the buccal side and the other on the lingual side). (a) Occlusal view. (b) Buccal view. (c) Lingual view.

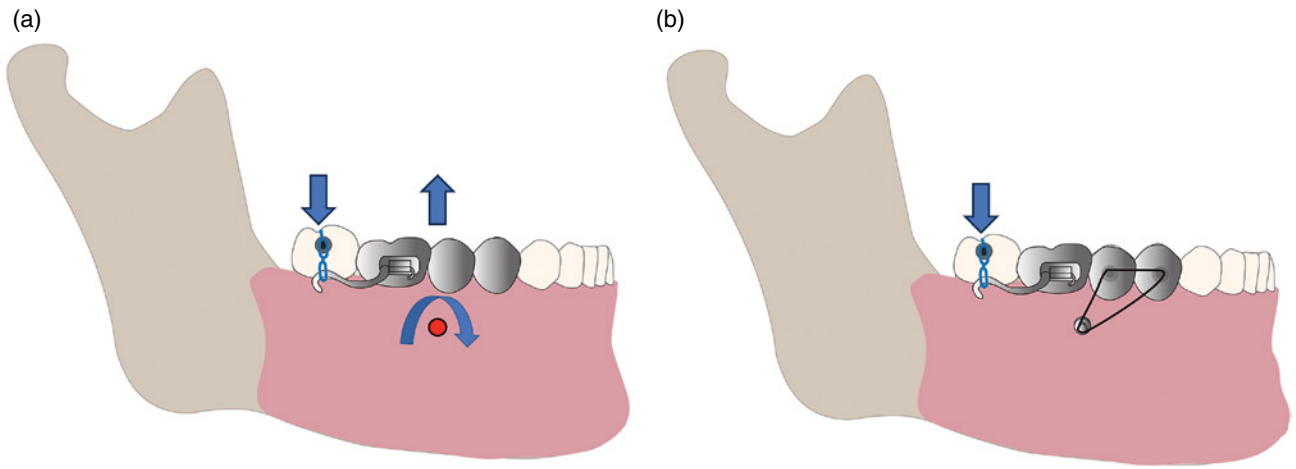


Figure 8.46 (a) The intrusive force (downward blue arrow) applied on the overerupted molar generates an extrusive force (upward blue arrow) on the anchorage teeth, leading to extrusion of the premolars and the first molar. Moreover, a clockwise moment (blue curved arrow) is generated and the anchorage tooth segment rotates around the center of resistance (red dot). (b) The anchorage teeth are stabilised by the mini-implant and extrusion of the anchorage teeth is prevented. The net effect is intrusion of the overerupted molar only.

t.me/Dr_Mouayyad_AlbtousH

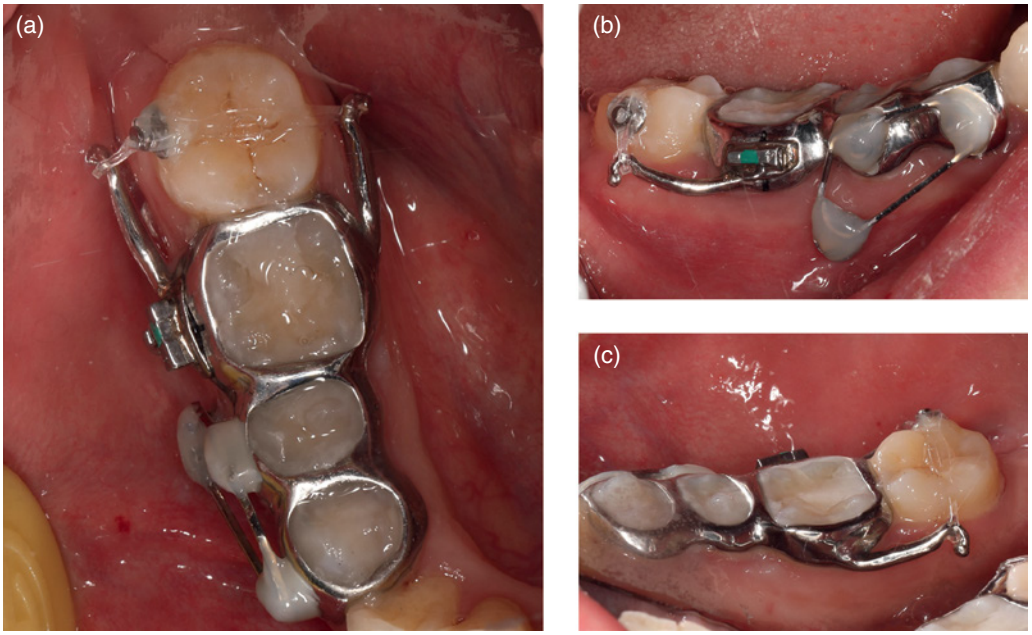
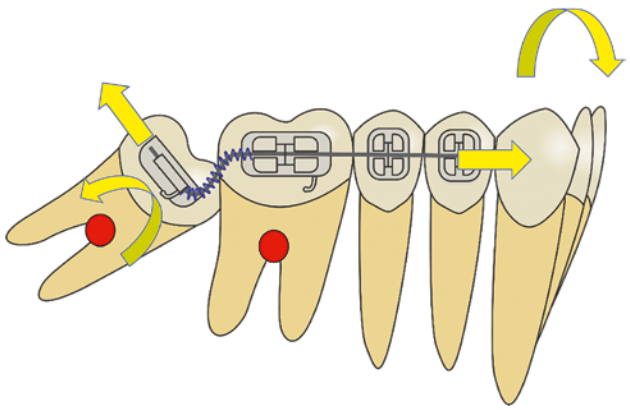


Figure 8.47 The premolars and first molar were stabilised by the buccal mini-implant. The overerupted molar was intruded by the two distal cantilevers from both the buccal and lingual sides. (a) Occlusal view. (b) Buccal view. The mini-implant was embedded by the flowable resin. (c) Lingual view.



Figure 8.48 Posttreatment photographs.

Figure 8.49 The distal uprighting force exerting on the molar generates a reaction force that is applied on the anterior anchorage teeth, resulting in mesial tip and labial proclination of the anchorage teeth.



t.me/Dr_Mouayyad_AlbtousH

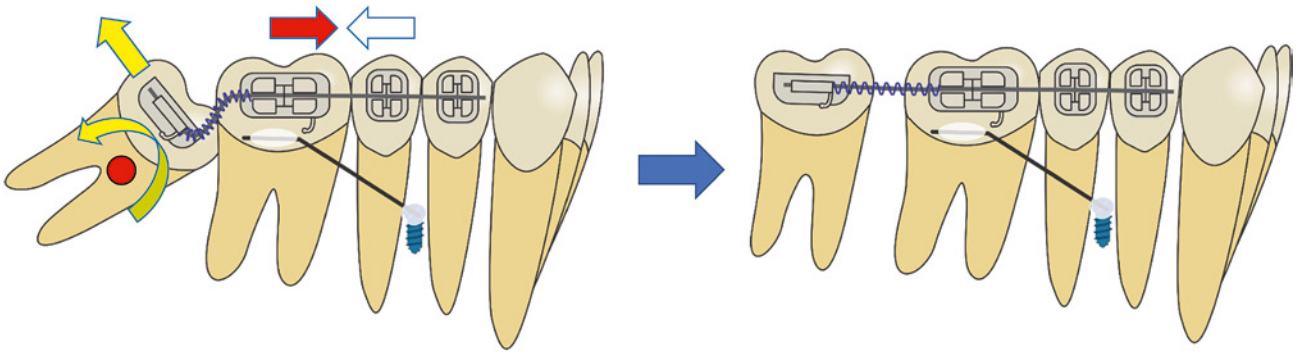


Figure 8.50 The reaction force (red arrow) applied on the anchorage teeth is counteracted by the stabilisation force (white arrow) offered by the mini-implant. The adverse effect (mesial tipping and labial flaring) of the anchorage teeth is eliminated.



Figure 8.51 Pretreatment photographs and panoramic radiograph. Note that the mandibular left second molar is mesially tipped and impacted underneath the distal undercut of the adjacent first molar.

t.me/Dr_Mouayyad_AlbtousH

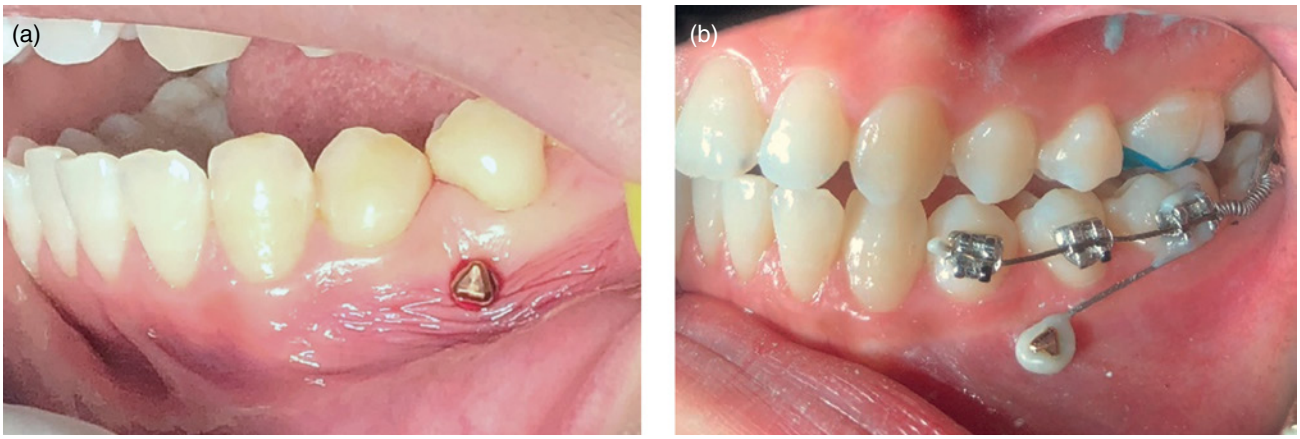


Figure 8.52 The first molar was stabilised and fixed onto the mini-implant to preserve the anchorage of the anterior teeth.



Figure 8.53 Posttreatment photographs and panoramic radiograph.

t.me/Dr_Mouayyad_AlbtousH

8.3 Buccal Shelf

8.3.1 Anatomical Characteristics

The buccal shelf is a bone plateau that lies between the alveolar crest medially and the external oblique ridge laterally. Anteroposteriorly, the buccal shelf runs from the first molar to the area beyond the distal side of the second molar, and is continuous with the retromolar region distally (Figure 8.54). The buccal shelf lies lateral to the dental roots and mini-implants are often inserted parallel to the long axis of the molar roots (Figure 8.55). Thus, by definition, the buccal shelf is considered to be an extra-alveolar region.[12] As the bone plateau of the buccal shelf widens as it approaches posteriorly, mini-implants are often inserted buccally to the second molar (Figure 8.56).[13,14] It has been shown that the success rate of mini-implants placed at the buccal shelf region is satisfactory.[15] To achieve successful application of buccal-shelf mini-implants, both hard tissue and soft tissue factors as well as vital anatomical structures should be considered in order to determine the most appropriate insertion site.

We performed a radiographic analysis based on CBCT images from 42 orthodontic patients (age range: 12–30 years) and evaluated hard tissue factors including plateau width, plateau length, plateau slope, cortical thickness and bone depth at different coronal sections (from the mesial cusp of first molars to the distal cusp of second molars) (Figure 8.57). Cortical thickness and bone depth were measured at different insertion heights (2 mm, 4 mm, 6 mm and 8 mm) and different insertion angles (from 15° to 90° with an increment of 15°) at each of the coronal sections.

Hard Tissue Factor: Plateau Features

The buccal shelf plateau is governed by three indices: length, width and slope. These indices are influenced by both sagittal and vertical skeletal patterns. Plateau length and width were greater among patients with class I and III skeletal base than those with class II skeletal base, while plateau slope was similar among patients with different sagittal skeletal patterns (Figure 8.58). Hypodivergent patients exhibited greater plateau length and width compared to normodivergent and hyperdivergent patients (Figure 8.59). Plateau slope did not differ among patients with different vertical skeletal patterns. This indicates that hyperdivergent patients with class II skeletal base have limited bone quantity at the buccal shelf region and that meticulous preinsertion CBCT examinations and prudent determination of the insertion site should be performed.

Moreover, the plateau length was similar among different coronal sections. The plateau width increased while plateau slope decreased as the coronal section approached posteriorly (Figure 8.60). As a wider and longer plateau with a smaller slope is more appropriate for the placement of mini-implants at the buccal shelf, the region lateral to the second molar or distal to the second molar is best suited for buccal shelf mini-implants.

Hard Tissue Factor: Cortical Thickness

Cortical thickness is an important factor in determining the primary stability of mini-implants. Cortical thickness is influenced by gender and vertical skeletal pattern, but not by age or sagittal skeletal pattern (Figure 8.61). Males have greater cortical thickness than females and hypodivergent and normodivergent subjects exhibit thicker cortex than hyperdivergent subjects.

Cortical thickness is primarily influenced by anatomical location (entry point).[16] Cortical thickness differs among different coronal sections, insertion heights and insertion angles (Figure 8.62). Nevertheless, cortical thickness is greater than 2 mm in almost all anatomical locations. Recommended cortical thickness ranges from 1 mm to 2 mm, since primary stability cannot be guaranteed if cortical thickness is less than 1 mm and the likelihood of bone damage is high if cortical thickness is greater than 2 mm. To reduce the risk of bone damage, pilot drilling is highly recommended prior to the placement of mini-implants in the buccal shelf region.[17] As cortical thickness is greater than 2 mm at almost all the anatomical sites in the buccal shelf region, this factor need not be considered in determining the optimal insertion site. However, pilot drilling is recommended to prevent mechanical and thermal damage to alveolar bone.

Hard Tissue Factor: Bone Depth

At the buccal shelf region, bone depth refers to the distance between the buccal cortical plate and limiting anatomical structures (i.e. lingual cortical plate, dental roots and inferior alveolar nerve). Bone depth is influenced by gender and age (Figure 8.63); adults and males exhibit greater bone depth. In addition, bone depth does not differ among different sagittal or vertical skeletal patterns (Figure 8.64). It does differ among different coronal sections and increases with increases in insertion height and angle (Figure 8.65). Since long mini-implants (10 m or longer) should be used at the buccal shelf region,[18] the minimum bone depth is 6 mm so that appropriate intra-bony to extra-bony ratio can be obtained. As displayed in Figure 8.65, setting a threshold of 6 mm results in selected insertion heights and angles suitable for the placement of mini-implants in the buccal shelf region.

t.me/Dr_Mouayyad_AlbtousH

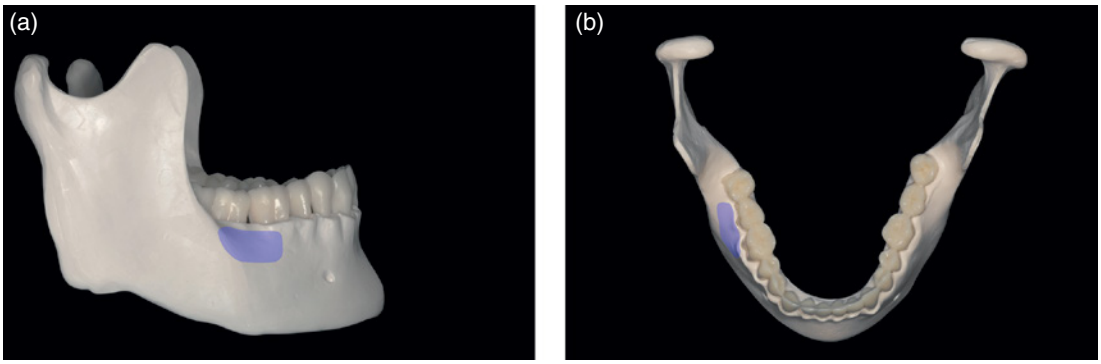


Figure 8.54 Mandibular buccal shelf (blue areas). (a) Buccal view. (b) Occlusal view.

Figure 8.55 Mini-implants inserted at the buccal shelf are parallel to the long axes of the molar roots.



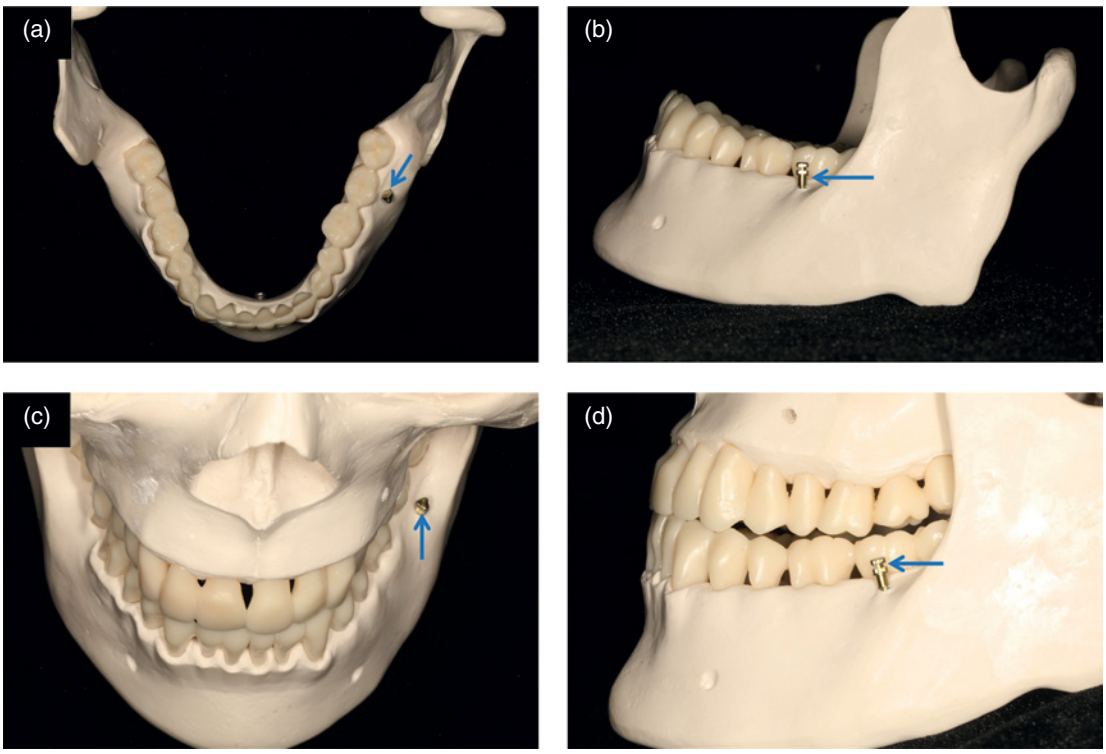


Figure 8.56 Mini-implants (blue arrows) placed at the mandibular buccal shelf region laterally to the second molar. (a) Occlusal view. (b) Buccal view. (c) Frontal oblique view. (d) Buccal view.

t.me/Dr_Mouayyad_AlbtousH

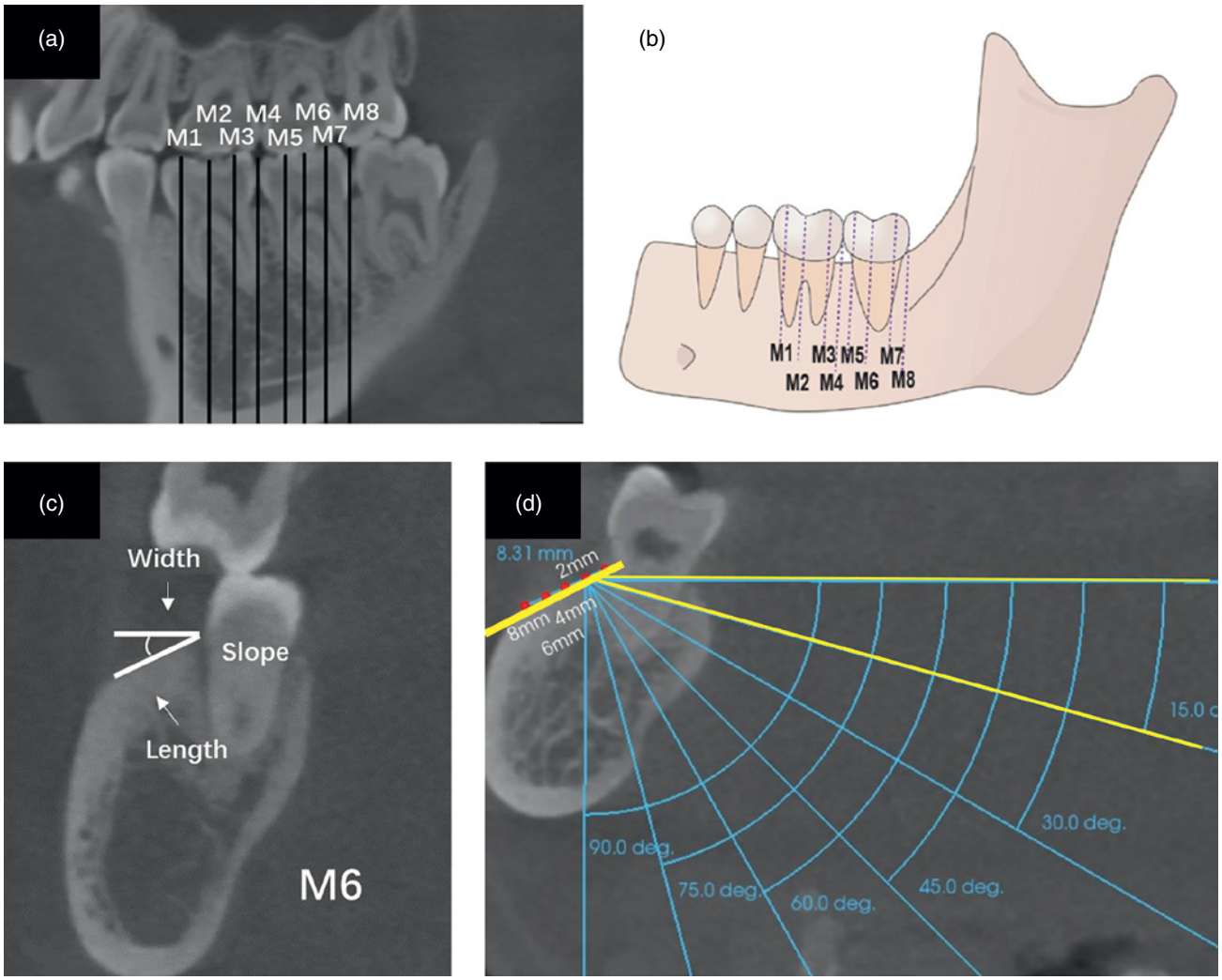


Figure 8.57 Measurement of hard tissue factors based on CBCT images. (a,b) The measurement was performed on eight coronal sections anteroposteriorly from the mesial cusp of first molars to the distal cusp of second molars. (c) The analysis evaluated the following hard tissue factors: plateau width, plateau length and plateau slope. (d) Cortical thickness and bone depth were measured at different insertion heights (2 mm, 4 mm, 6 mm and 8 mm) and different insertion angles (from 15° to 90° with an increment of 15°) at each of the aforementioned coronal sections.

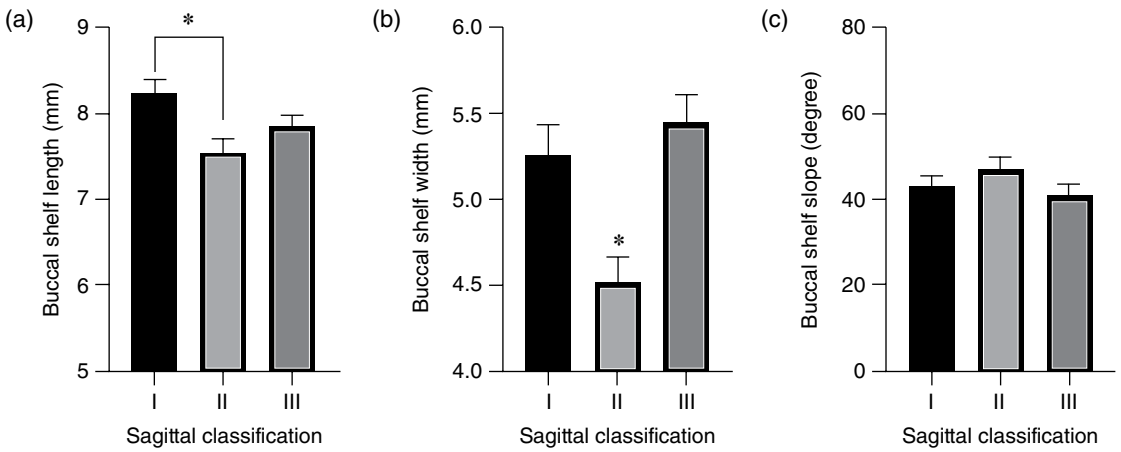


Figure 8.58 Comparison of buccal shelf length, width and slope among patients with different sagittal skeletal patterns. (a) Buccal shelf length. (b) Buccal shelf width. (c) Buccal shelf slope.

t.me/Dr_Mouayyad_AlbtousH

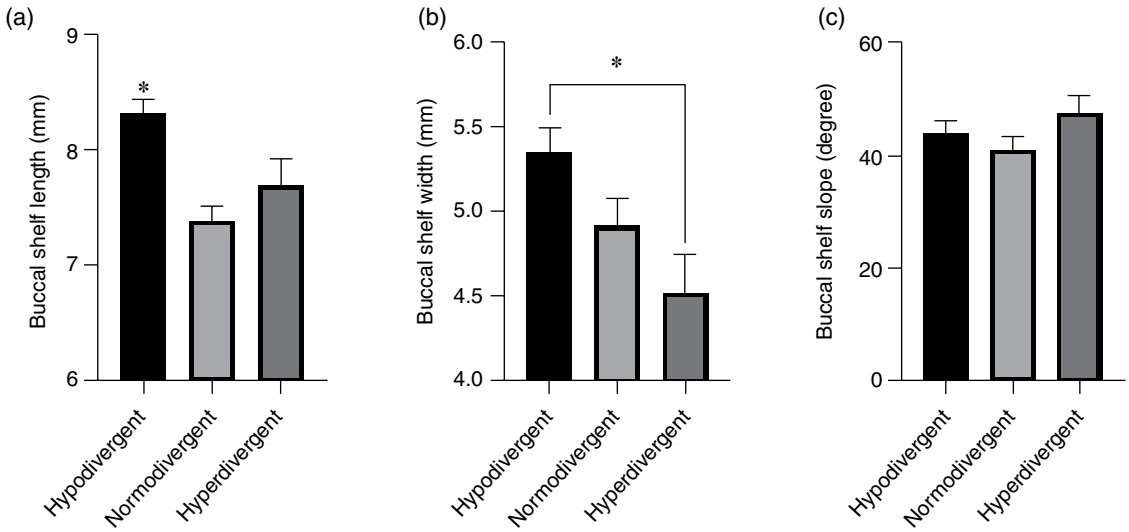


Figure 8.59 Comparison of buccal shelf length, width and slope among patients with different vertical skeletal patterns. (a) Buccal shelf length. (b) Buccal shelf width. (c) Buccal shelf slope.

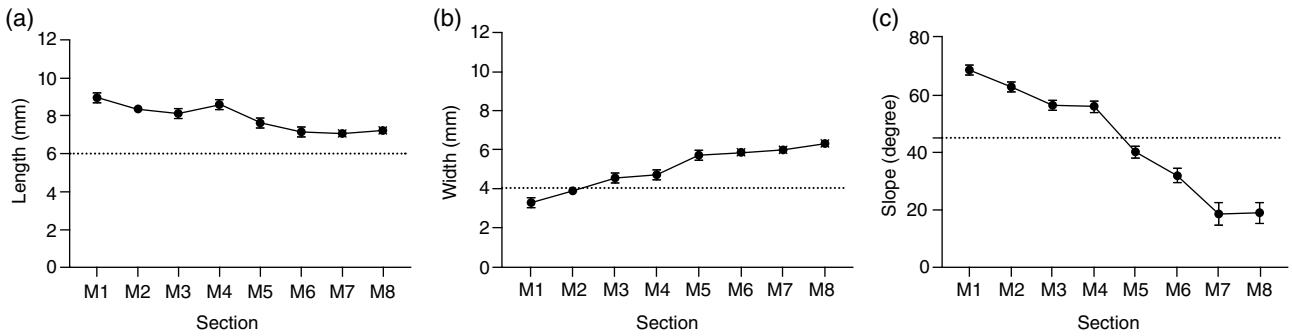


Figure 8.60 Comparison of buccal shelf length, width and slope among different coronal sections. (a) Buccal shelf length. (b) Buccal shelf width. (c) Buccal shelf slope.

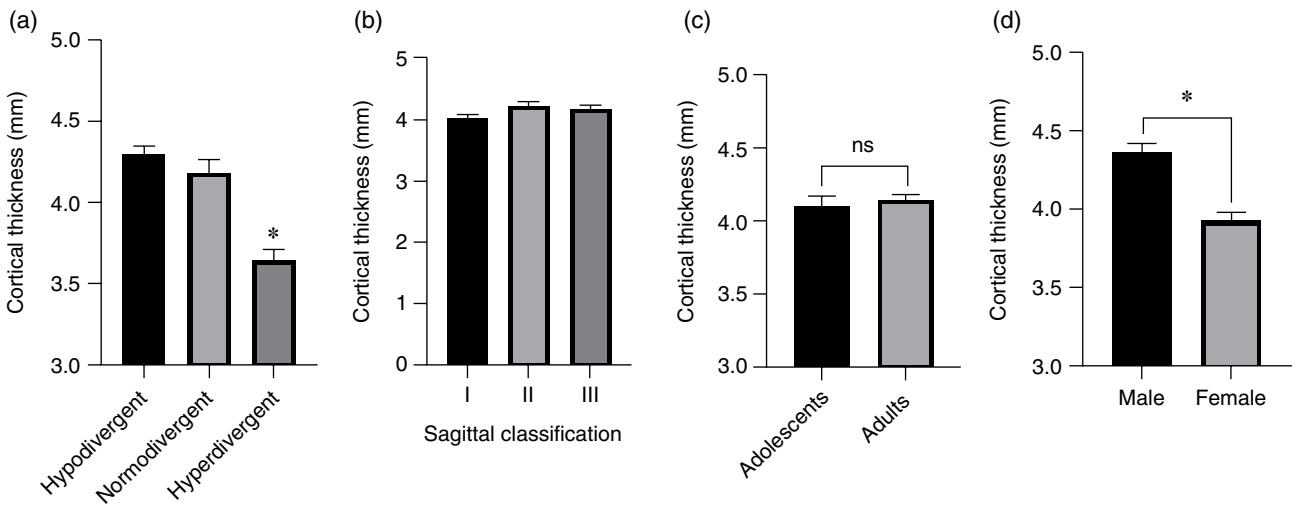


Figure 8.61 Comparison of cortical thickness (a) among different vertical skeletal patterns, (b) among different sagittal skeletal patterns, (c) between adolescents and adults, and (d) between males and females.

t.me/Dr_Mouayyad_AlbtousH

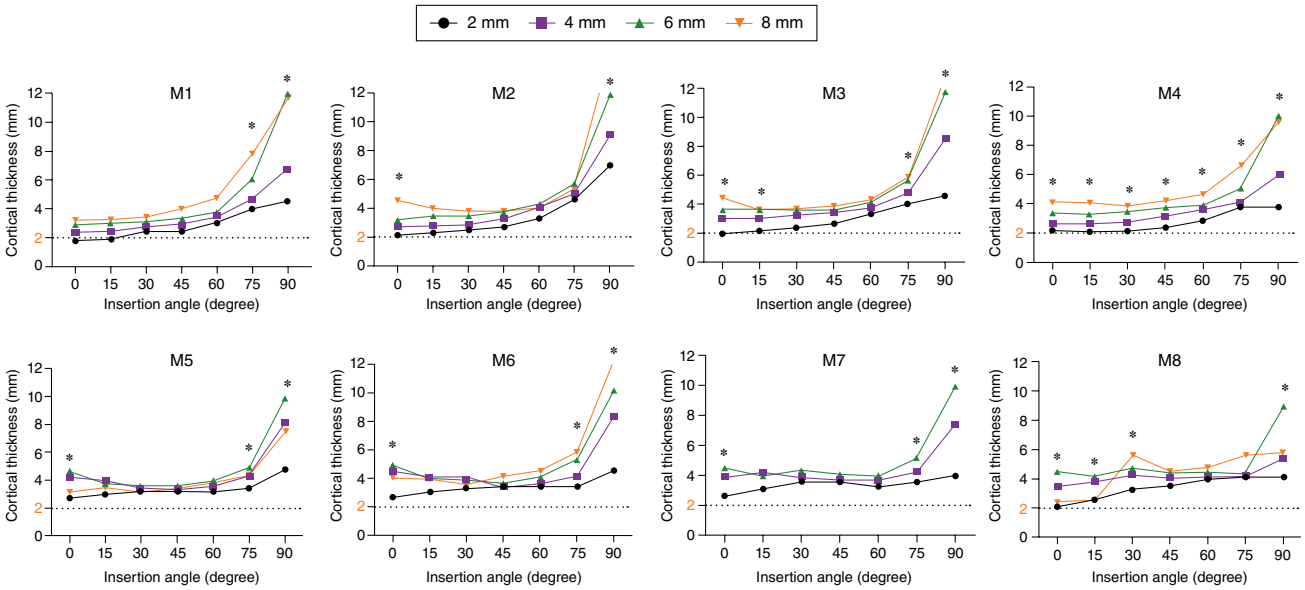


Figure 8.62 Cortical thickness differed among different coronal sections, insertion heights and insertion angles. The measuring planes were the coronal sections passing the first molar mesial buccal tip (M1), the first molar fovea (M2), the first molar distal buccal tip (M3), the distal adjacent surface of the first molar (M4), the second molar mesial buccal tip (M5), the second molar fovea (M6), the second molar distal buccal tip (M7) and the distal adjacent surface of the second molar (M8).

t.me/Dr_Mouayyad_AlbtousH

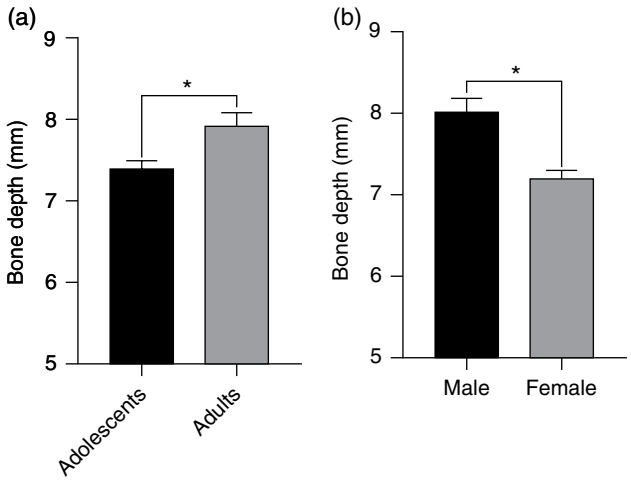


Figure 8.63 (a) Bone depth was greater in adults than in adolescents. (b) Males possess greater bone depth than females.

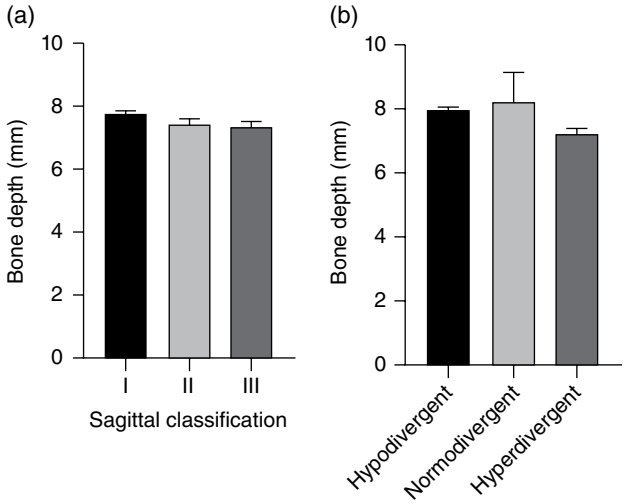


Figure 8.64 (a) Bone depth was similar among patients with different sagittal skeletal patterns. (b) Bone depth did not differ among patients with different vertical skeletal patterns.

Soft Tissue Factor: Soft Tissue Type

In the mandibular buccal shelf region, most of the soft tissue is movable mucosa and the attached gingiva is inadequate (Figure 8.66). Implantation of mini-implants into the movable mucosa zone bears a high risk of soft tissue inflammation. It has been revealed that soft tissue inflammation occurs among 26–50% of patients receiving buccal shelf mini-implants.[18] Despite the presence of soft tissue inflammation, the stability of mini-implants is not affected for 10 mm mini-implants, in contrast to 8 mm mini-implants.[18] Moreover, a clinical study revealed that success rate was similar between buccal shelf mini-implants inserted in the attached gingiva zone or movable mucosa zone. Thus, long and large mini-implants (10 mm in length and 2 mm in diameter) are recommended for the buccal shelf region, and placement in either attached gingiva or movable mucosa is acceptable.

Soft Tissue Factor: Soft Tissue Thickness

Soft tissue is very thick (>2 mm) at the mandibular buccal shelf region and the space is often limited due to the shallow vestibule (Figure 8.67). To reduce the risk of soft tissue irritation and inflammation, long mini-implants are recommended in order to obtain adequate emergence profile of mini-implants. Flapping and predrilling are indicated in order to reduce the risk of damage to soft tissue and hard tissue, respectively. The heads of mini-implants will be covered and embedded in the buccal mucosa if they are located too buccally, indicating that insertion angle should be large enough (e.g. 90°) to keep the head of the mini-implant away from the buccal mucosa.

Vital Anatomical Structure: Inferior Alveolar Nerve

The inferior alveolar nerve runs in the inferior alveolar canal and inserting mini-implants in the buccal shelf region runs the risk of nerve injury, especially for patients with missing posterior teeth.[19] A recent study revealed that the mean distance from alveolar crest to inferior alveolar canal was 15–17 mm, which decreases as the buccal shelf region approaches posteriorly.[20] Thus, for patients without missing posterior teeth, sufficient bone depth is present and the risk of nerve injury is very low for the placement of mini-implants in the buccal shelf region (Figure 8.68).

8.3.2 Biomechanical Considerations

Mini-implants inserted at the buccal shelf region are often applied for distalisation of mandibular dentition. For mandibular whole-dentition distalisation, biomechanical design is pivotal in successful treatment outcomes. As displayed in Figure 8.69, mandibular dentition distalisation is accomplished by applying an elastic powerchain or a closed-coil spring. As the distalisation force passes occlusally to the centre of resistance of the whole dentition, anticlockwise moment is generated, resulting in anticlockwise rotation of the mandibular dentition during distalisation. Moreover, as the dentition rotates in an anticlockwise direction, anterior extrusion and posterior intrusion occur. Practitioners should be aware of this movement tendency and undertake prudent biomechanical solutions.

t.me/Dr_Mouayyad_AlbtousH

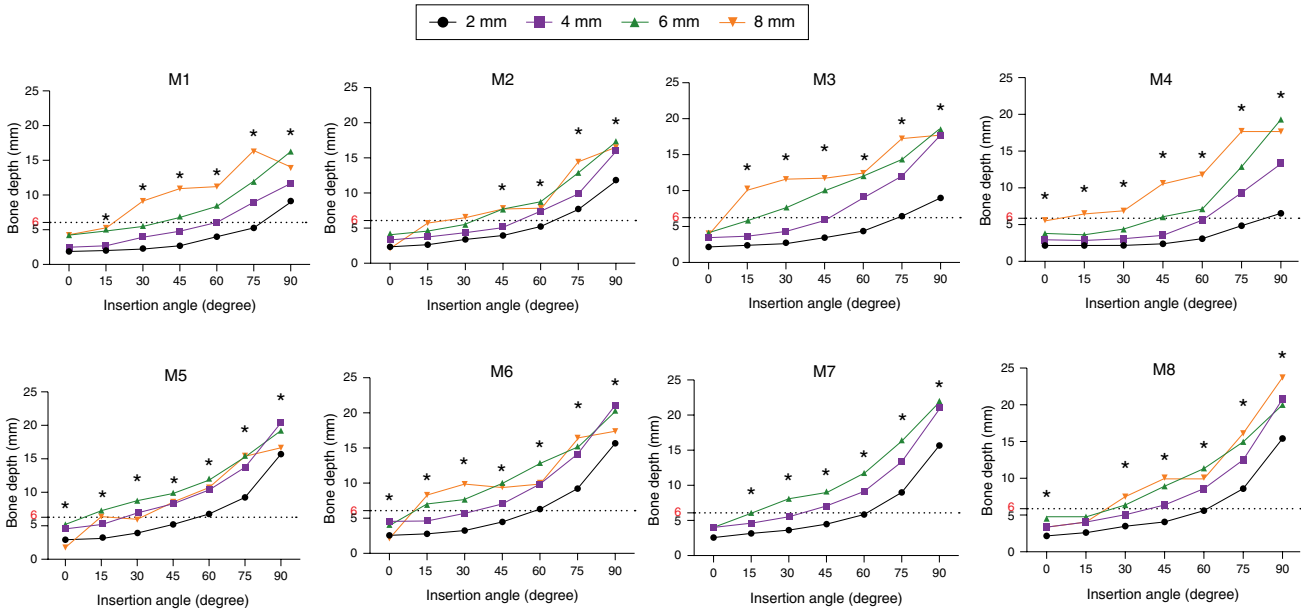


Figure 8.65 The influence of different coronal sections, insertion heights and insertion angles on bone depth. A threshold of 6 mm is set on the plots to determine the optimal insertion heights and insertion angles for each coronal section.

t.me/Dr_Mouayyad_AlbtousH

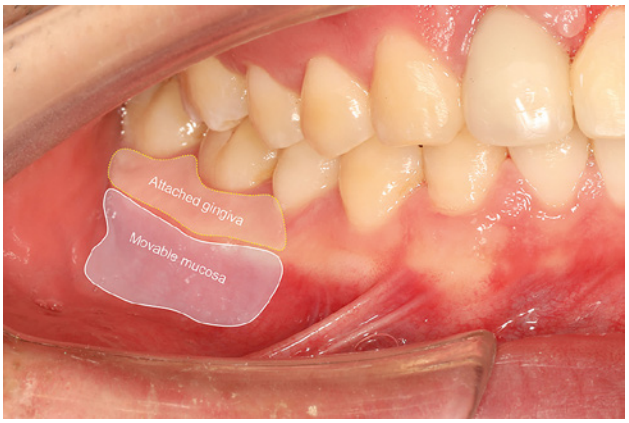


Figure 8.66 Most of the mucosa at the buccal shelf region belongs to movable mucosa and attached gingiva is insufficient.

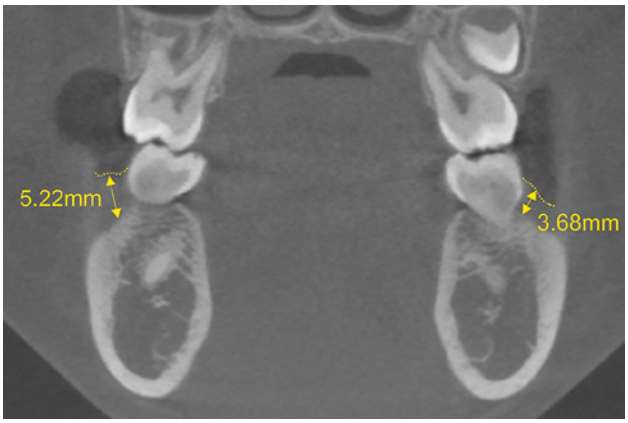


Figure 8.67 Thick soft tissue at the buccal shelf region shown on a CBCT image (coronal section).

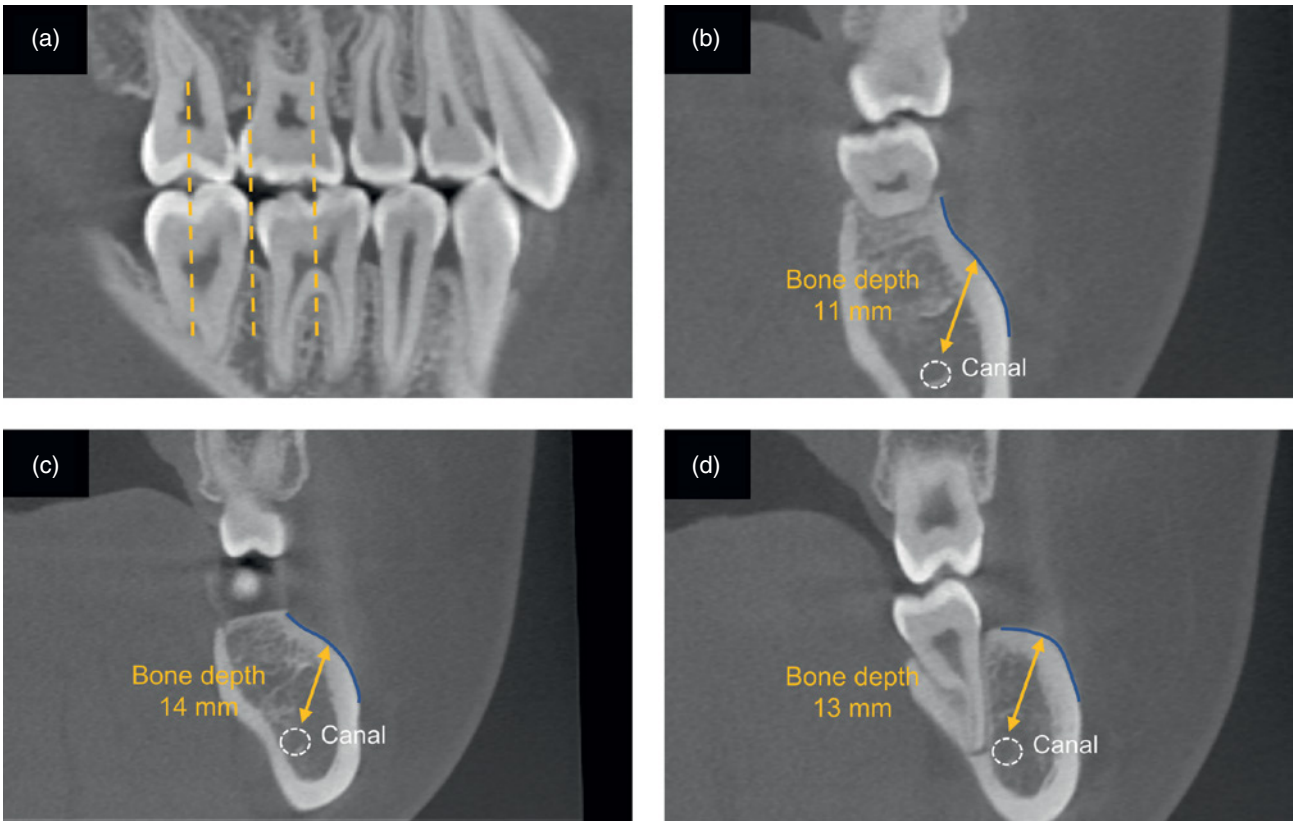


Figure 8.68 The distance between the buccal cortical plate and the inferior alveolar nerve canal. (a) Three coronal sections were selected. (b–d) The bone depth was sufficient for placing mini-implants, sparing the nerve canal at each section.

8.3.3 Selection of Appropriate Insertion Sites

To maximise the clinical success of buccal shelf mini-implants, we recommend that the optimal insertion sites meet the following anatomical requirements: (1) plateau length greater than 6 mm; (2) plateau width greater than 4 mm; (3) plateau slope less than 45°; (4) bone depth greater than 6 mm. Based on these criteria, the buccal shelf region buccal to the second molar is recommended for the placement of mini-implants.[16,17,21-23] The specific entry point is 4–6 mm buccal to the CEJ of the second molar with the insertion angle being 75–90° to the occlusal plane

t.me/Dr_Mouayyad_AlbtousH

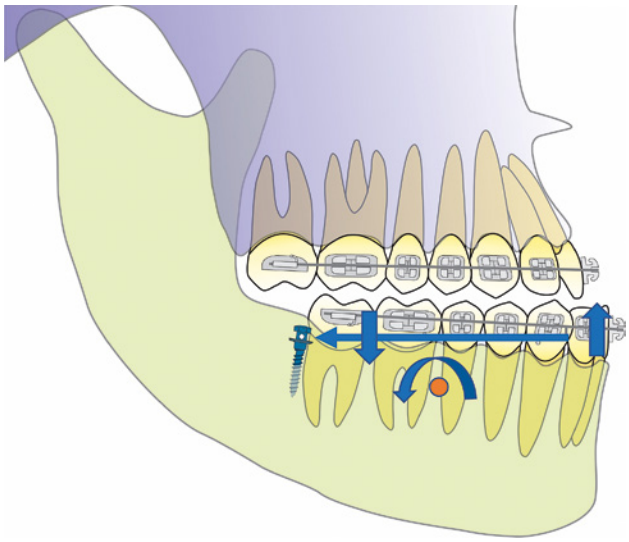


Figure 8.69 Biomechanical analysis for distalisation of the mandibular dentition. The distalisation force passes occlusally to the centre of resistance (red dot) of the mandibular dentition; an anticlockwise moment is generated, leading to extrusion of the anterior teeth and intrusion of the posterior teeth.

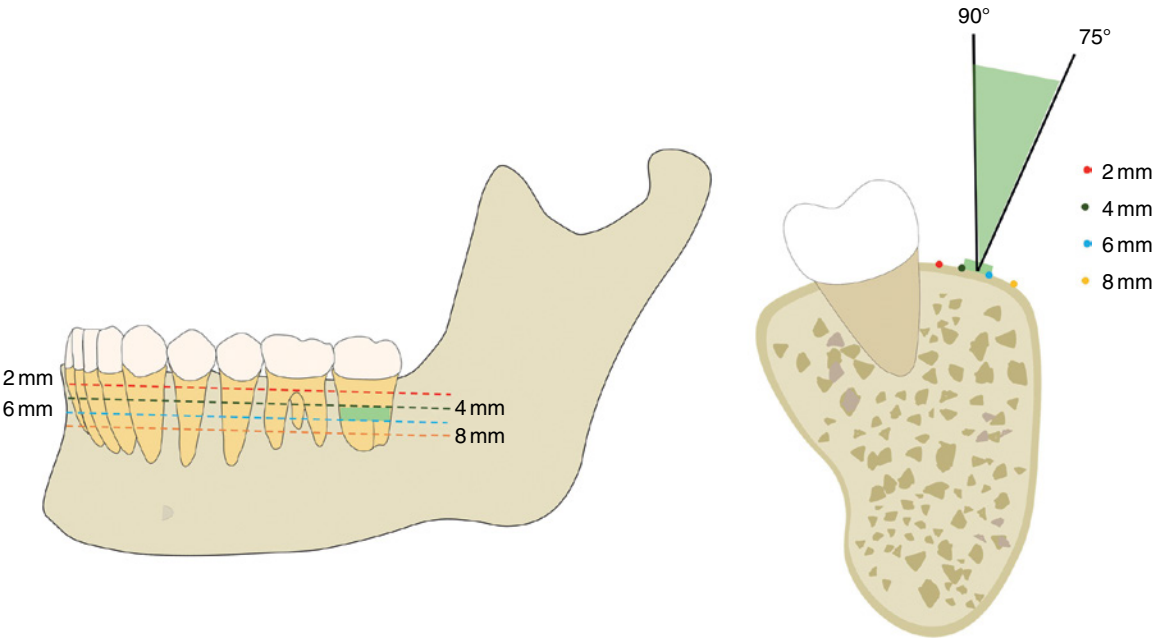


Figure 8.70 Recommended insertion sites, insertion heights and insertion angles for mini-implants at the buccal shelf region. The optimal site is 4–6 mm buccal to the CEJ of the second molar with the insertion angle being 75–90° to the occlusal plane.

(Figure 8.70). Mini-implants with adequate sizes (length 10 mm, diameter 2 mm) are recommended. Moreover, mucosal flapping and pilot drilling are highly recommended to prevent damage to both the hard and soft tissues.

8.3.4 Insertion Techniques

Preinsertion

Prior to insertion, thorough clinical examination and radiographic evaluations (CBCT is preferable) should be implemented to determine the optimal insertion sites. Insertion heights and angles should be determined based on hard and soft tissues. Then, a mini-implant analogue can be used to assess the spatial position of the mini-implant with surrounding soft tissues, in order to reduce the likelihood of soft tissue irritation following insertion.

Insertion

First, local infiltration anaesthesia is performed following mucosa disinfection with iodophor (Figure 8.71). In the buccal shelf region, no dental roots are present and the buccal cortical plate and soft tissue are very thick. Thus, adequate anaesthesia (0.5–1.0 ml) is recommended to achieve satisfactory effects. Due to the movability of the

t.me/Dr_Mouayyad_AlbtousH

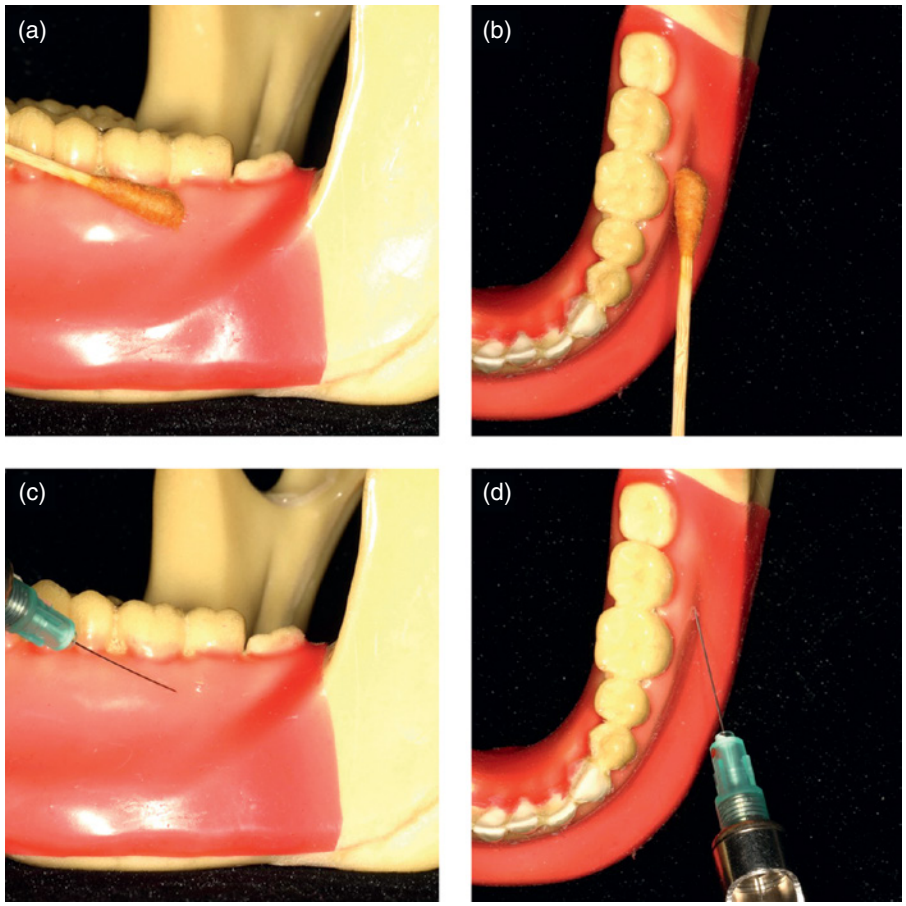


Figure 8.71 (a,b) Mucosa disinfection. (c,d) Local infiltration anaesthesia.

mucosa, the cheek should be adequately retracted and the position of the buccal mucosa should be kept stable during the whole process once the desired entry point is determined. Otherwise, the mucosa that has already been anaesthetised may move away from the desired entry point, resulting in the need for re-anaesthesia.

Second, mucosa incision and full-thickness flap elevation are performed with a scalpel and a periosteal elevator, respectively (Figures 8.72 and 8.73). A semilunar incision is performed with its convex part facing lingually (Figure 8.74). This is performed to facilitate the simultaneous retraction of the flap and buccal mucosa as well as the cheek, so that the insertion site can be adequately exposed for mini-implant placement (Figure 8.75).

Third, once the optimal insertion site is adequately exposed, the next step is to perform pilot drilling. It is recommended that the diameter of the pilot hole be 60% of that of the mini-implant.[24] Thus, for a mini-implant with a diameter of 2 mm, the diameter of the pilot hole is 1.2 mm. The pilot drilling is not required to be full depth, but should at least penetrate the whole cortical plate and reach the trabecular bone. To reduce the likelihood of both mechanical and thermal bone damage, a reduced-speed handpiece is recommended to perform pilot drilling (Figure 8.76). Moreover, during pilot drilling, copious saline irrigation is highly recommended.

Once the pilot hole is prepared, the operator should check the depth of the hole. The presence of mild bleeding in the pilot hole often heralds that the cortex has been penetrated and the trabecular bone reached.

Lastly, the last step is to insert the mini-implant through the pilot hole. Due to limited surgical access, a contra-angle reduced-speed motor-driven handpiece is recommended (Figure 8.77). Insertion should be halted once an adequate emergence profile is achieved, even if the threads have not been fully inserted into the bone (Figure 8.78).

The detailed procedures of inserting a buccal-shelf mini-implant are summarised and illustrated in Figure 8.79.

Postinsertion

Once the insertion is complete, the operator should examine the position of the mini-implant from both buccal and occlusal sides (Figure 8.80). Then, the soft tissue flap is repositioned and sutured. Sometimes, healing of soft tissue is satisfactory and suturing may not be necessary. However, patients should be instructed to maintain adequate oral hygiene. Antibiotics and non-steroidal anti-inflammatory drugs should be prescribed.

t.me/Dr_Mouayyad_AlbtousH

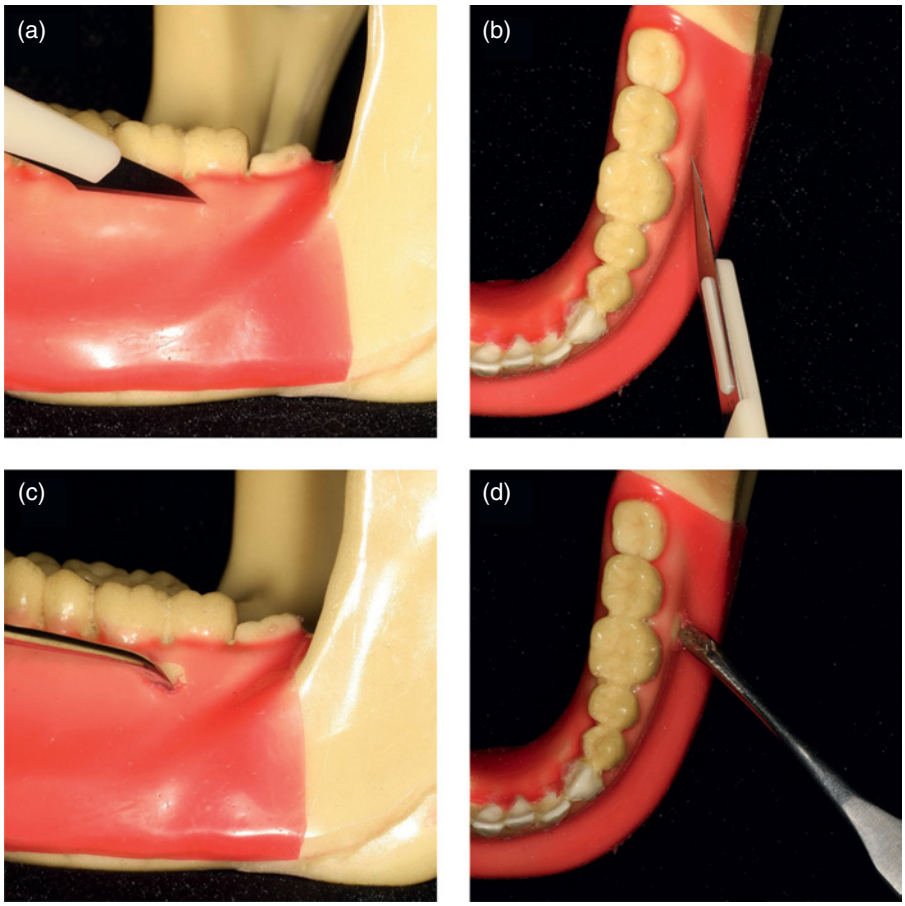


Figure 8.72 (a,b) Mucosa incision. (c,d) Flap elevation with a periosteal elevator.

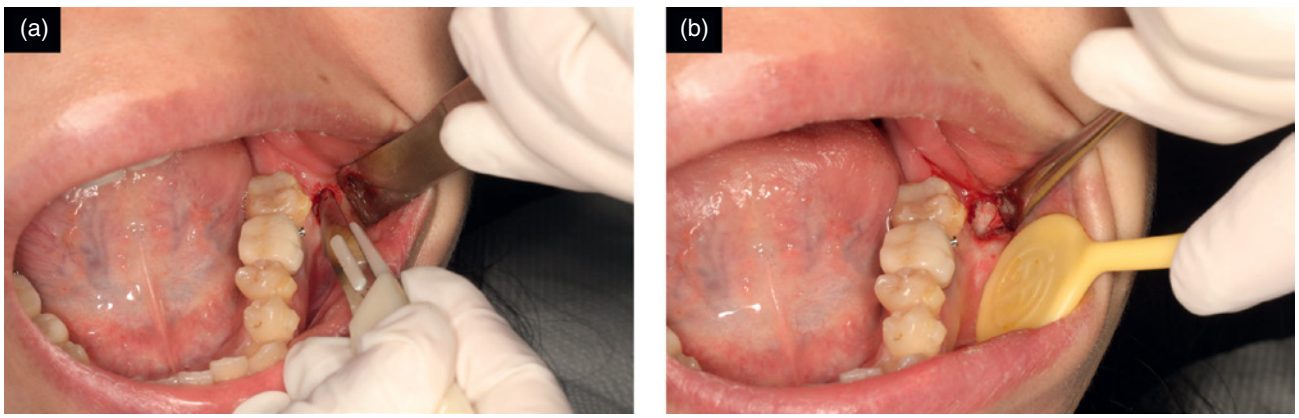


Figure 8.73 (a) Mucosa incision with a scalpel. (b) Full-thickness flap with a periosteal elevator.

t.me/Dr_Mouayyad_AlbtousH

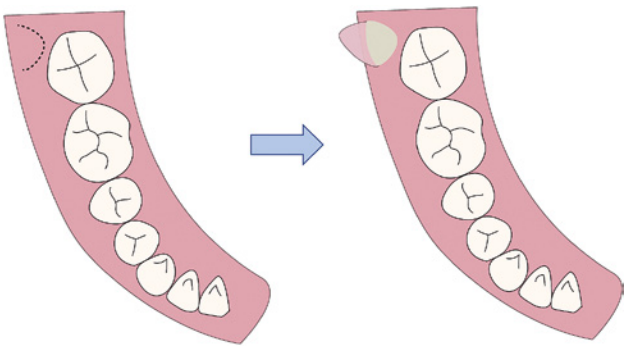


Figure 8.74 A semilunar incision is performed with its convex part facing lingually.

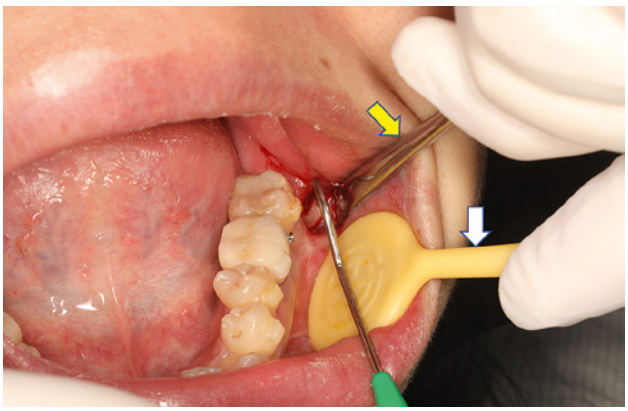


Figure 8.75 The periosteal elevator (yellow arrow) is able to retract the elevated flap and the cheek simultaneously. A mouth mirror (white arrow) can also be used for greater exposure.

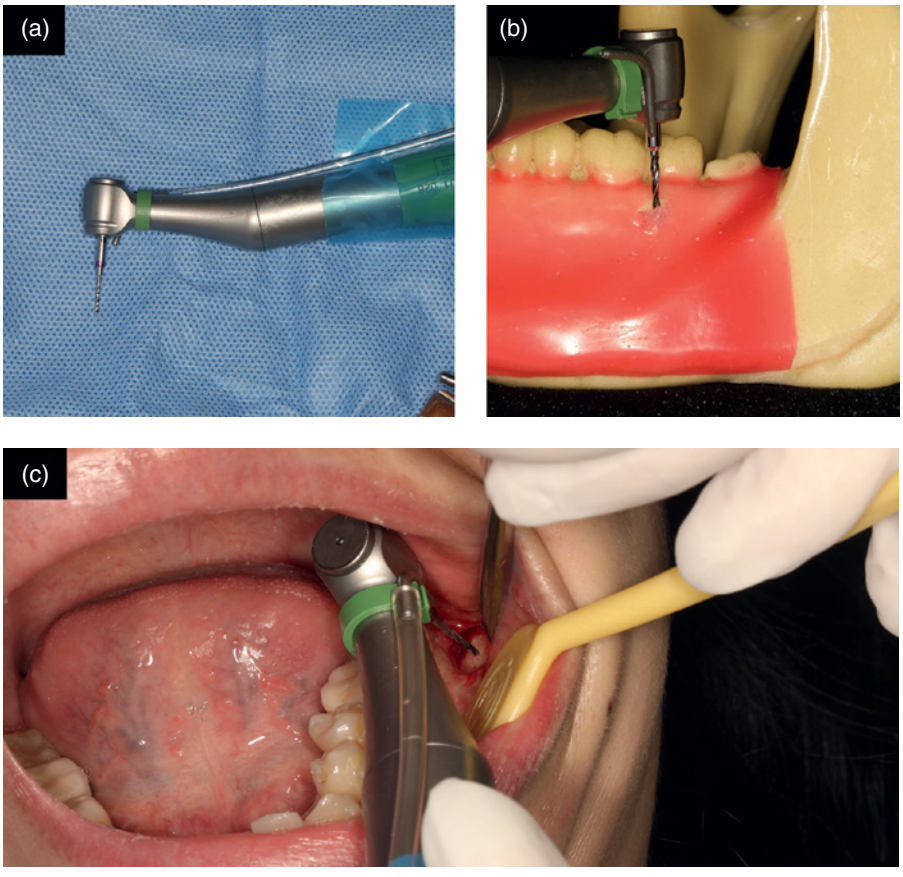


Figure 8.76 Pilot drilling with a reduced-speed handpiece. (a) A reduced-speed handpiece. (b) Pilot drilling with the reduced-speed handpiece on a skull. (c) Pilot drilling with the reduced-speed handpiece in a patient.

t.me/Dr_Mouayyad_AlbtousH

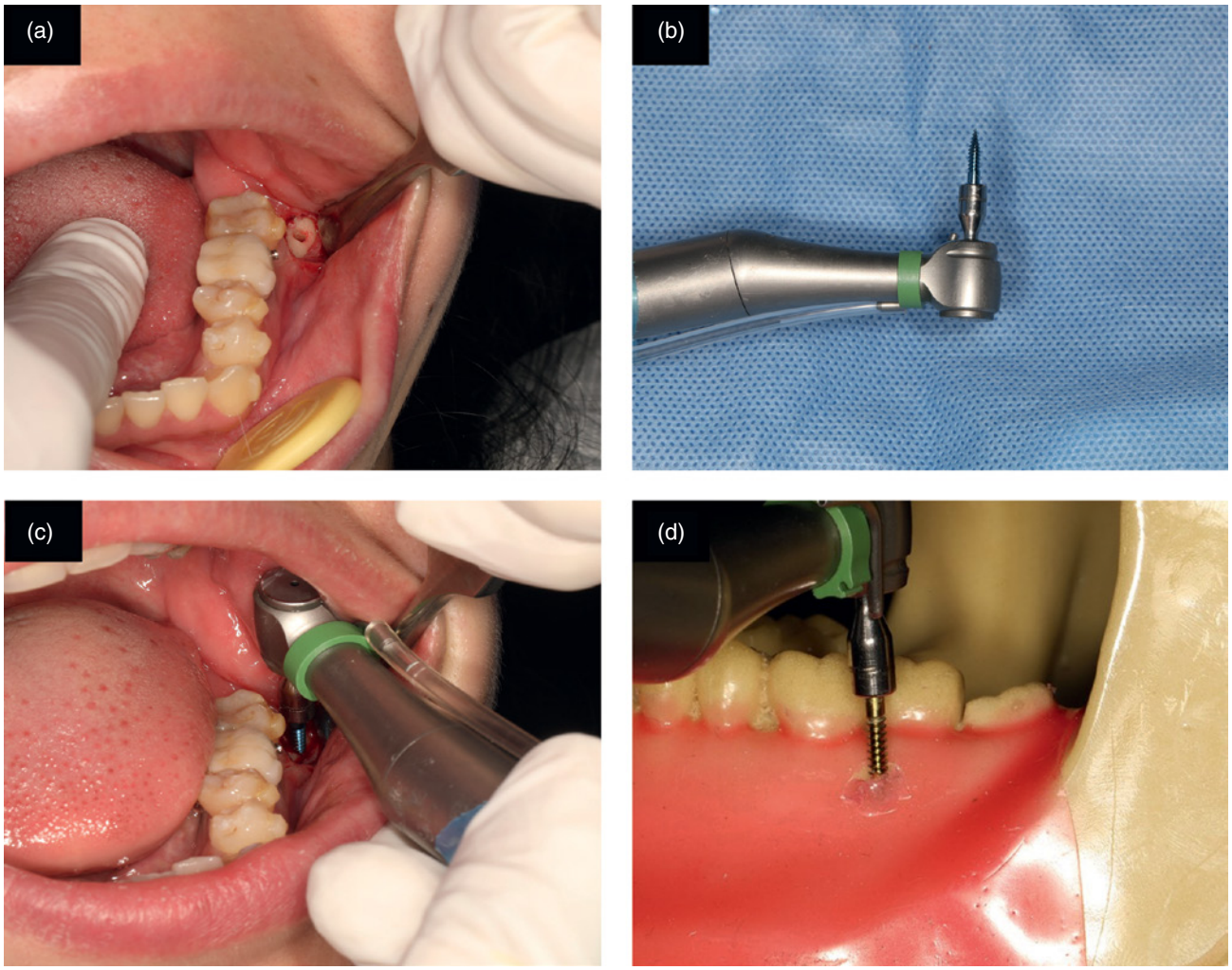


Figure 8.77 Placement of a mini-implant at the buccal shelf region. (a) The pilot hole was made ready for insertion. (b) A mini-implant was engaged into the reduced-speed handpiece. (c) Advancement of the mini-implant into the buccal shelf through the prepared pilot hole. (d) The placement of a mini-implant with the reduced-speed handpiece on a skull.



Figure 8.78 Once sufficient emergence profile was achieved, the insertion was stopped, even if the threads had not been fully inserted into the bone.

8.3.5 Clinical Applications

Mandibular Dentition Distalisation

Distalisation of the whole mandibular dentition can be readily achieved by applying an elastomeric chain or closed-coil spring between the crimpable hook on the archwire and the bilateral buccal shelf mini-implants. As mentioned above, incisor extrusion and molar intrusion occur during the distalisation process so meticulous biomechanical design is recommended. A case example is given below to demonstrate the clinical applications of buccal shelf mini-implants in mandibular dentition distalisation.

A male adult patient presented to the orthodontic department with a chief complaint of crooked teeth. Clinical and radiographic examinations revealed that the patient had

t.me/Dr_Mouayyad_AlbtousH

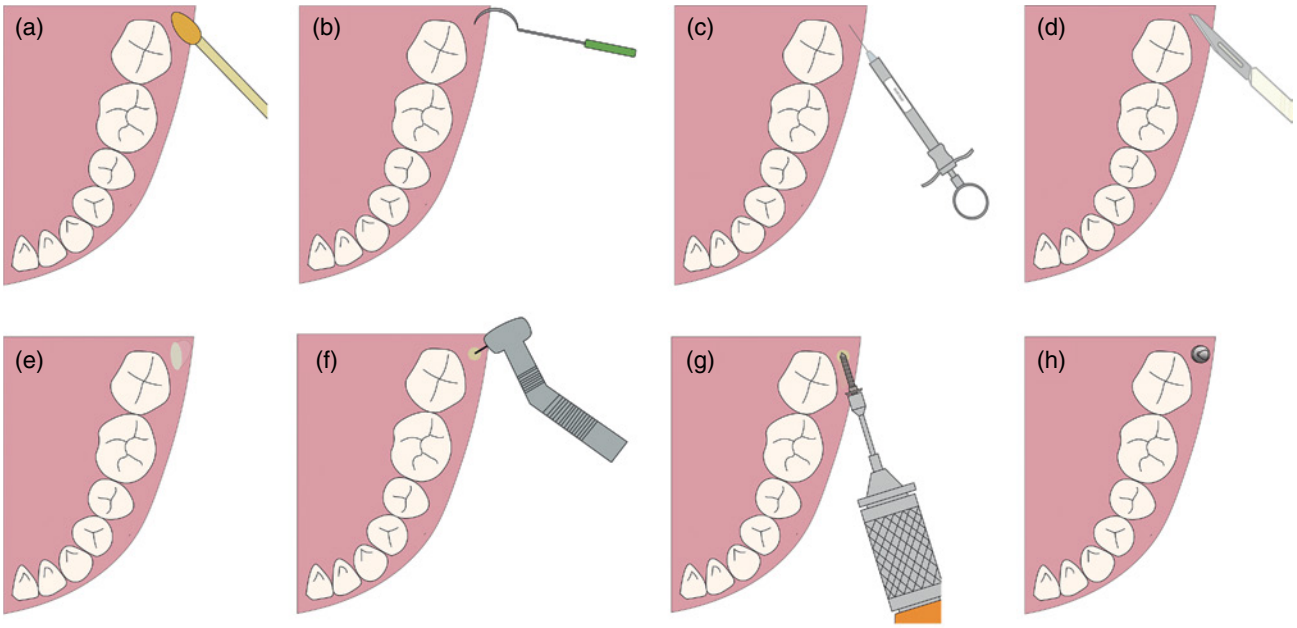


Figure 8.79 Schematic illustrations showing detailed procedures of inserting a mini-implant at the buccal shelf region. (a) Mucosa disinfection. (b) Marking of the entry point. (c) Local infiltration anaesthesia. (d) Mucosa incision. (e) Flap elevation. (f) Pilot drilling. (g) Insertion. (h) Postinsertion examinations.

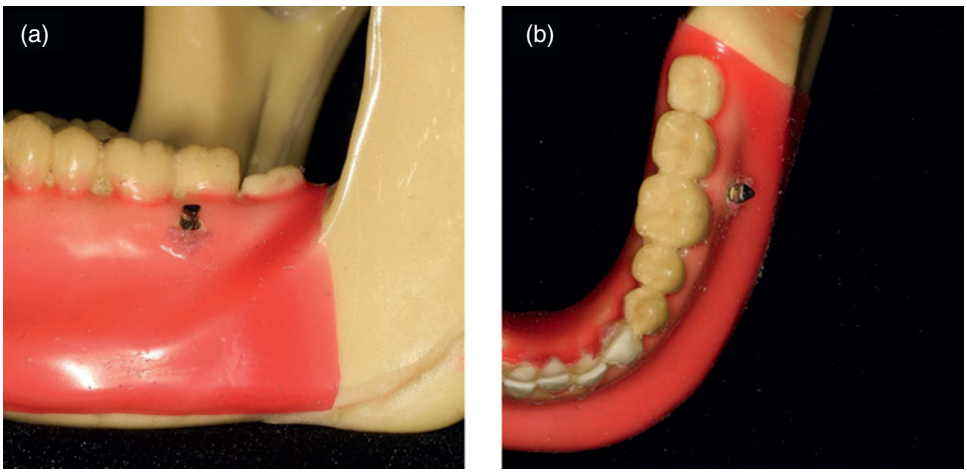


Figure 8.80 Postinsertion examinations from both (a) the buccal side and (b) the occlusal side.

cusp-to-cusp class III molar relationship on the left side and full-cusp class III molar relationship on the right side (Figure 8.81). Mild crowding and moderate crowding were present in the upper and lower arch, respectively. The maxillary right second molar had been extracted due to severe caries with the third molar being impacted. The upper and lower midlines were not coincident with shallow overbite. As displayed in Table 8.6, the cephalometric analysis was indicative of class I skeletal base (ANB = 3.2), mandibular high angle (SN-MP = 41), incisor labial proclination in the upper arch (U1-SN = 109.8) and lingual inclination of incisors in the lower arch (L1-MP = 84.1). However, the Wits value (−4.5) was indicative of class III skeletal base.

Based on the patient's pretreatment examinations and data, mandibular dentition distalisation was planned through two buccal shelf mini-implants. Since the anterior overbite was shallow, the biomechanics associated with the buccal shelf mini-implants had the tendency for molar intrusion and incisor extrusion, facilitating the correction of anterior shallow overbite. Considering that the root apex

t.me/Dr_Mouayyad_AlbtousH



Figure 8.81 Pretreatment photographs and radiographs.

t.me/Dr_Mouayyad_AlbtousH

Table 8.6 Pretreatment lateral cephalometric analysis.

Measurement	Norm	Pretreatment
Skeletal (°)		
SNA	83.0±4.0	85.9
SNB	80.0±4.0	82.7
ANB	2.0±2.0	3.2
FMA	28.0±4.0	35.8
SN-MP	35.0±4.0	41.0
Dental (°)		
U1-SN	105.7±6.3	109.8
L1-MP	97.0±7.1	84.1
FMIA	65.0±6.0	60.1
U1-L1	124.0±8.0	125.1
Soft tissue (mm)		
UL-EP	2.0±2.0	0.7
LL-EP	3.0±2.0	4.7
Wits (mm)		
Wits	−1.0	−4.5

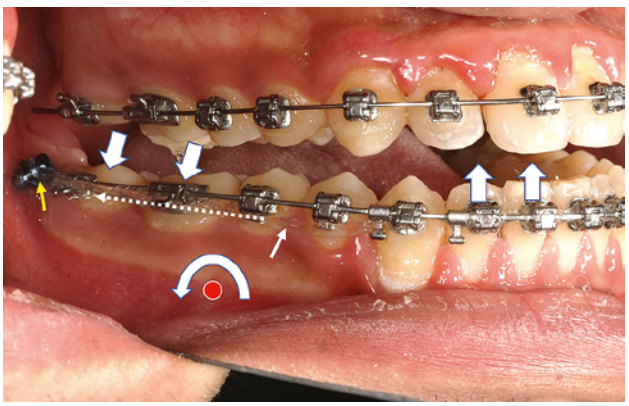


Figure 8.82 Distalisation of the mandibular dentition was achieved by applying an elastomeric chain (white arrow) between the crimpable hook on the archwire and the mini-implant (yellow arrow). The distalisation force (white dashed arrow) passes occlusally to the centre of resistance (red dot) and generates an anticlockwise moment that leads to extrusion of the incisors and intrusion of the molars.

of the maxillary right third molar had not been closed, autoeruption might be anticipated.

Following levelling and alignment, two mini-implants were placed at the buccal shelf region and elastomeric chains were applied between the crimpable hooks on the archwire and the mini-implants to offer distalisation force (Figure 8.82). As displayed in Figure 8.83, following 30 months of treatment, bilateral class I canine and molar relationships were obtained. In addition, normal overbite and coincident upper and lower midlines were achieved. The maxillary right third molar autoerupted during the orthodontic treatment and was aligned into the dental arch. Pre- and posttreatment cephalometric data are shown in Table 8.7.

Molar Uprighting

Following the loss of the mandibular first molars, mesial and lingual tipping of the second molars usually occurs. Thus, buccal shelf mini-implants inserted buccally and distally to the second molars can offer a satisfactory biomechanical solution. A case example is given below.

A female adult sought multidisciplinary treatments with a chief complaint of missing teeth. As displayed in Figures 8.84 and 8.85, the mandibular left first molar was missing and the second molar was mesially and lingual tipped. Moreover, the maxillary left second molar was buccally tipped, resulting in a Brodie bite. Following discussion with the patient, a multidisciplinary treatment plan for minor tooth movement was made: correction of the Brodie bite, extraction of the mandibular left third molar, uprighting the mandibular left second molar and implant restoration for the missing mandibular left first molar.

To achieve minor tooth movement without changing the positions of other teeth, two mini-implants were placed (Figure 8.86). One was placed at the midpalatal suture to correct the buccal tipping and extrusion of the maxillary left second molar. The other was inserted at the left buccal shelf region to offer buccal and distal force vector, so that the mesial and lingual tipping of the second molar could be readily corrected. The biomechanical analysis is displayed in Figure 8.87.

Following five months of orthodontic treatment, the buccal tipping of the maxillary left second molar was corrected and the mandibular left second molar was successfully uprighted to regain adequate space for the implant restoration of the missing mandibular left first molar (Figure 8.88). A good occlusal function was obtained following the implant restoration of the mandibular left first molar (Figures 8.89 and 8.90).

Orthodontic Traction of Impacted Teeth

Orthodontic traction of impacted teeth can be achieved through buccal shelf mini-implants with the aid of cantilever springs anchored onto the mini-implants. A case example is given below.

A female adult patient presented to the orthodontic department with a chief complaint of an impacted tooth in the lower arch. Clinical and radiographic examinations indicated that the mandibular right first premolar was impacted (Figures 8.91 and 8.92). The treatment plan was

t.me/Dr_Mouayyad_AlbtousH



Figure 8.83 Posttreatment photographs and radiographs.

t.me/Dr_Mouayyad_AlbtousH

Table 8.7 Pre- and posttreatment lateral cephalometric analysis.

Measurement	Norm	Pretreatment	Posttreatment
Skeletal (°)			
SNA	83.0±4.0	85.9	84.8
SNB	80.0±4.0	82.7	81.2
ANB	2.0±2.0	3.2	3.6
FMA	28.0±4.0	35.8	35.4
SN-MP	35.0±4.0	41.0	42.0
Dental (°)			
U1-SN	105.7±6.3	109.8	112.7
L1-MP	97.0±7.1	84.1	90.1
FMIA	65.0±6.0	60.1	54.5
U1-L1	124.0±8.0	125.1	115.1
Soft tissue (mm)			
UL-EP	2.0±2.0	0.7	0.9
LL-EP	3.0±2.0	4.7	3.5
Wits (mm)			
Wits	–1.0	–4.5	–2.6



Figure 8.84 Pretreatment photographs.

t.me/Dr_Mouayyad_AlbtousH

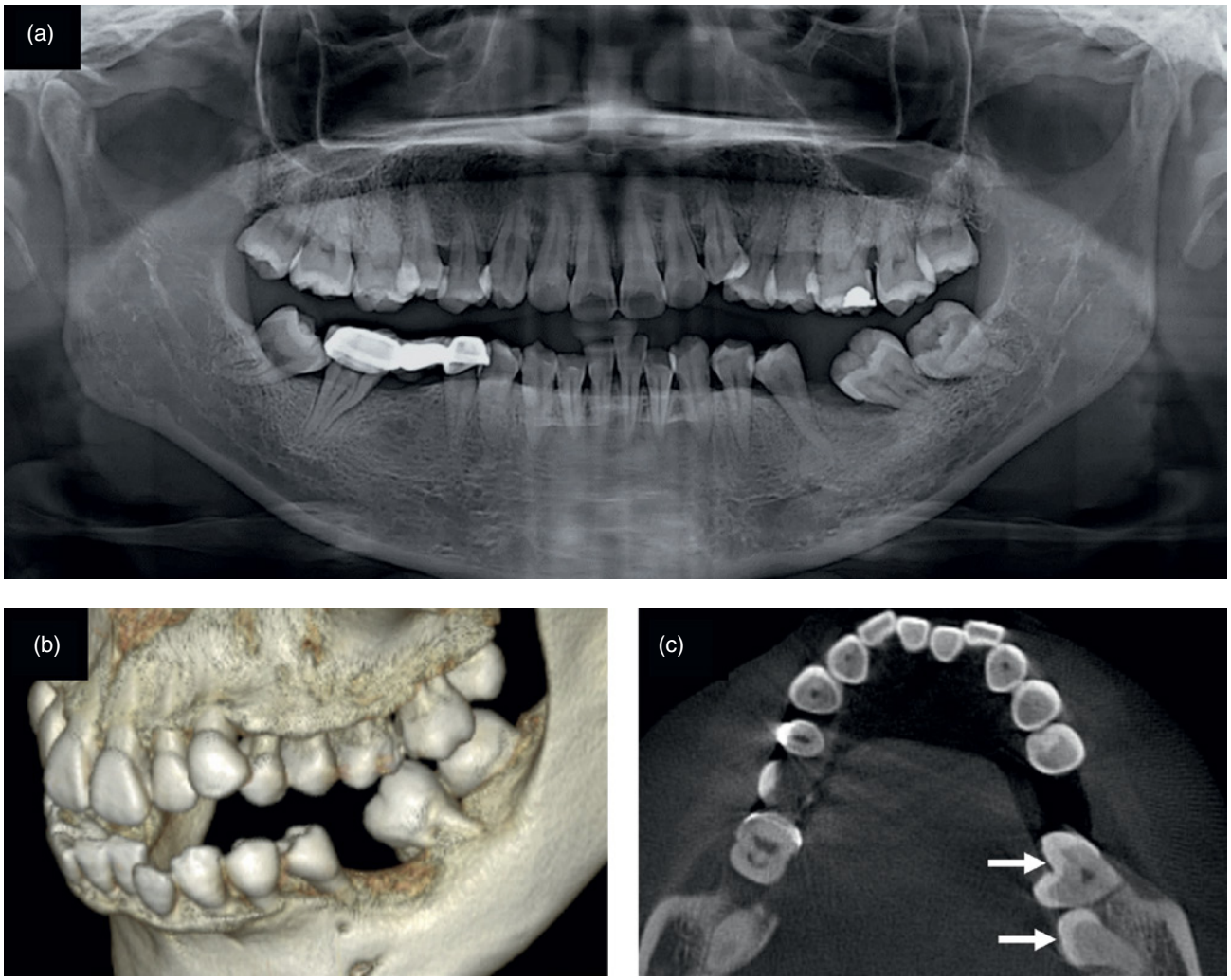


Figure 8.85 Pretreatment radiographs. (a) Panoramic radiograph. (b) CBCT 3-D reconstruction. (c) Axial view of the CBCT image. Note the lingually tipped mandibular molars (white arrow).

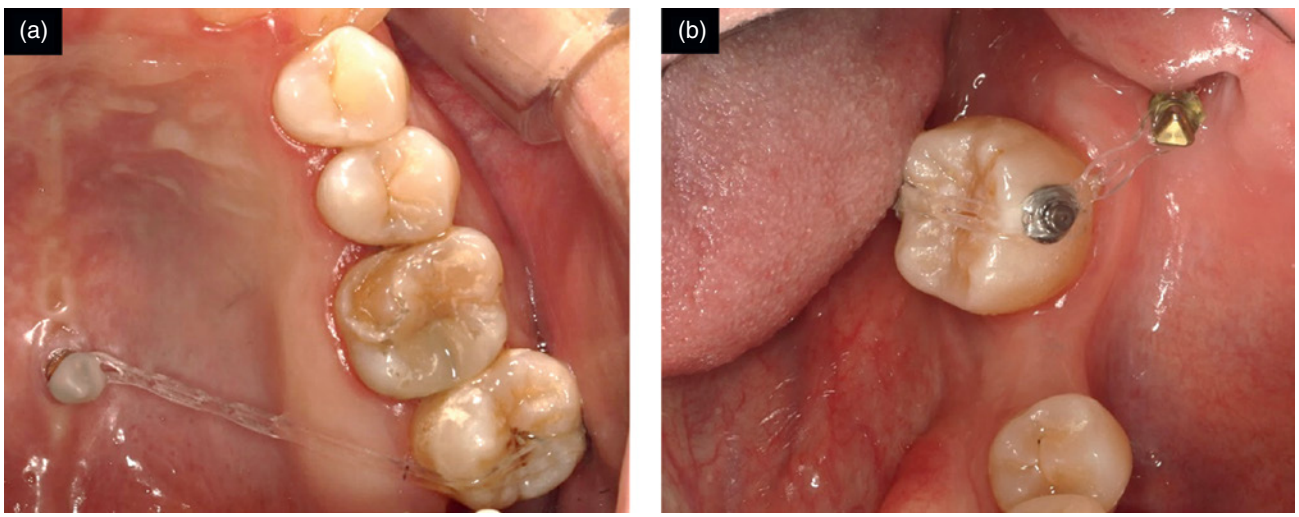


Figure 8.86 (a) A mini-implant was inserted at the midpalatal suture to correct buccal tipping and extrusion of the maxillary left second molar. (b) A mini-implant was inserted at the buccal shelf to upright the mandibular left second molar.

t.me/Dr_Mouayyad_AlbtousH

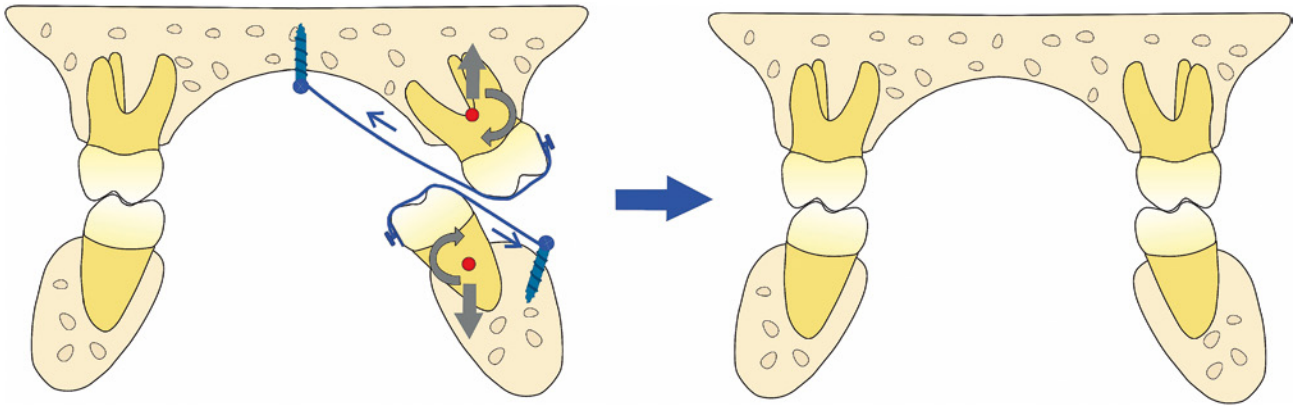


Figure 8.87 Biomechanical analysis for the correction of Brodie bite with mini-implants.

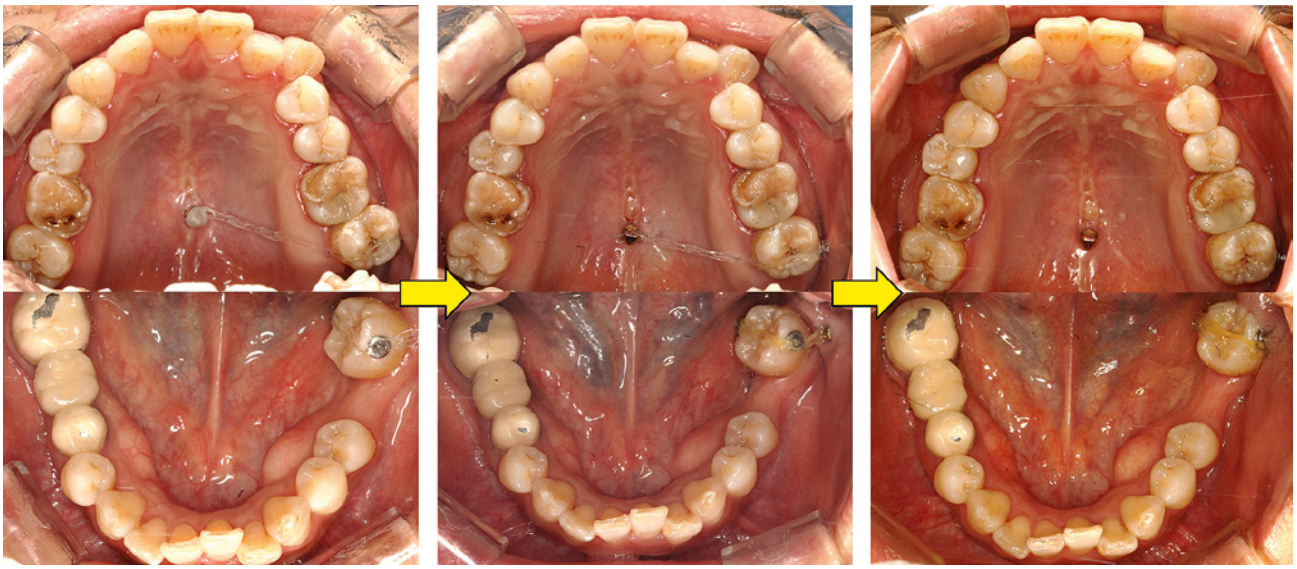


Figure 8.88 Treatment progress. Buccal tipping of the maxillary left second molar and lingual tipping of the mandibular left second molar were gradually resolved.



Figure 8.89 Posttreatment photographs.

t.me/Dr_Mouayyad_AlbtousH

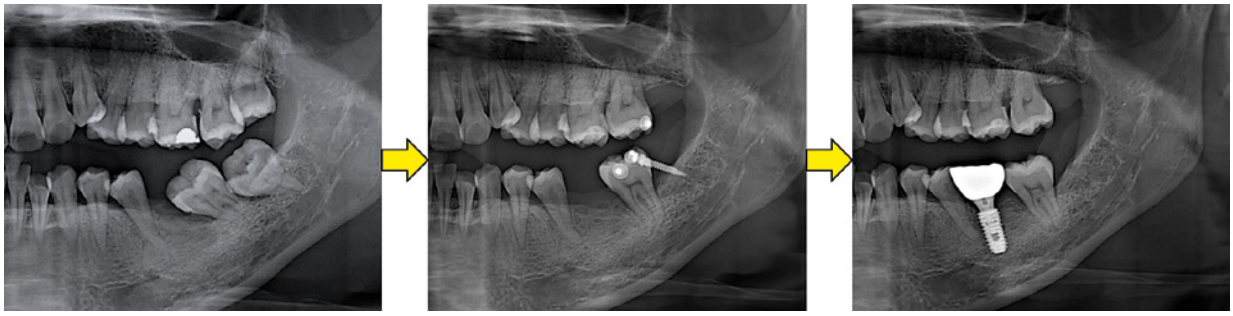


Figure 8.90 Pretreatment, progress and posttreatment radiographs.



Figure 8.91 Pretreatment intraoral photographs.

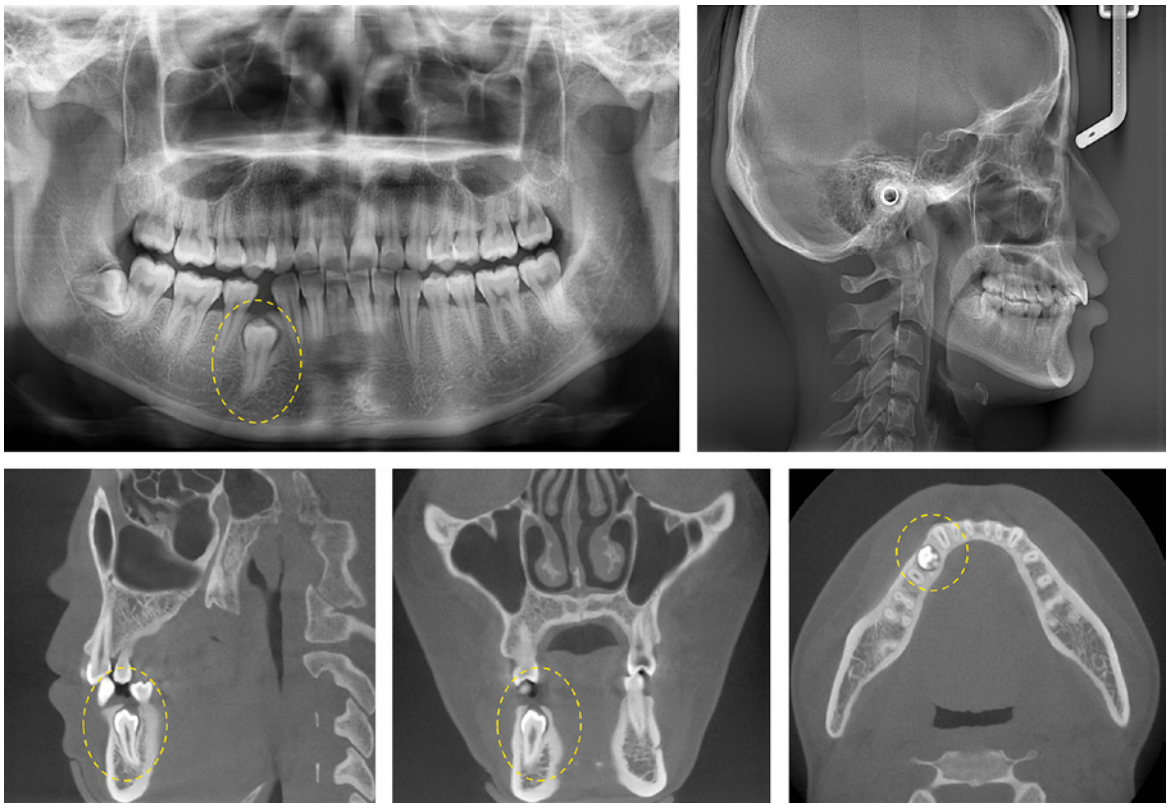


Figure 8.92 Pretreatment radiographs showing the impacted mandibular right first premolar (encircled by the yellow dashed line).

t.me/Dr_Mouayyad_AlbtousH

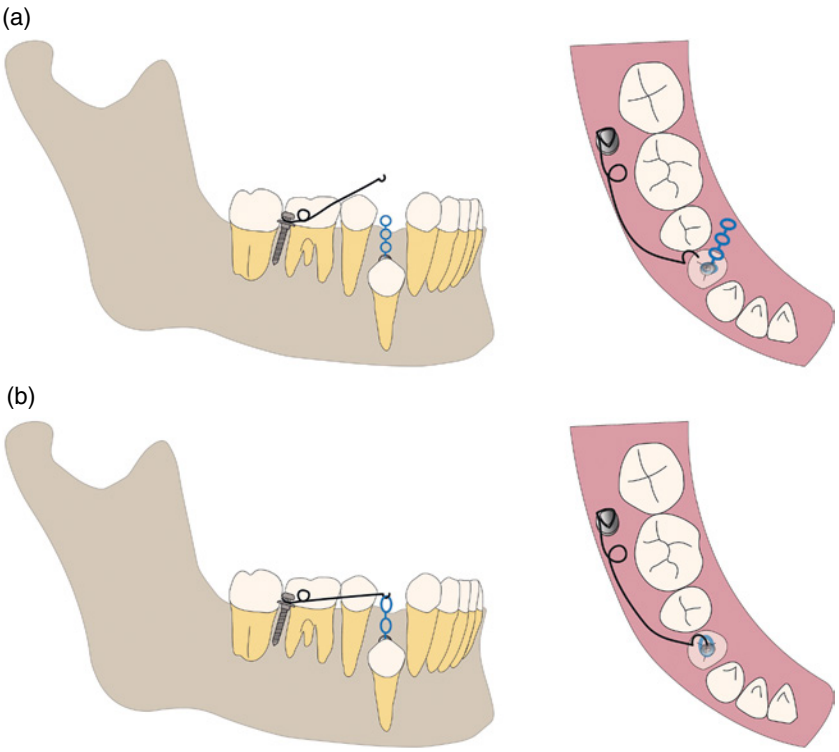


Figure 8.93 Biomechanical analysis for the mini-implant-anchored cantilever spring in the orthodontic traction of the impacted first premolar. (a) Inactivated state. (b) Activated state.

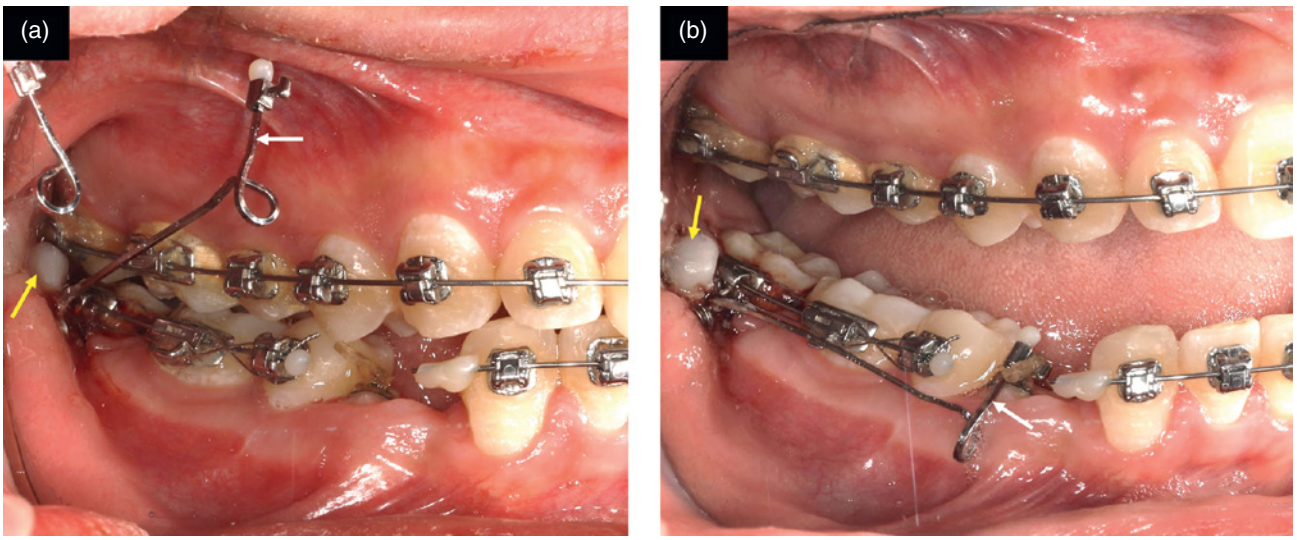


Figure 8.94 Orthodontic traction of the impacted mandibular right first premolar through a mini-implant-anchored cantilever spring. (a) Inactivated state. (b) Activated state. The cantilever spring (white arrow) was fixed onto the mini-implant through flowable resin (yellow arrow).

traction of the impacted tooth following alignment and levelling. The biomechanical system for the traction would be built on a buccal shelf mini-implant with the aid of a cantilever spring (Figure 8.93).

Following alignment and levelling of the dental arch and the space for the mandibular right first premolar being regained, a mini-implant was placed at the right buccal shelf region. A cantilever spring was fixed onto the mini-implant to offer traction force on the impacted first premolar (Figure 8.94). The impacted first premolar was successfully tractioned into occlusion with the mini-implant-anchored cantilever spring and was subsequently aligned with adjacent teeth through orthodontic archwires (Figures 8.95 and 8.96).

t.me/Dr_Mouayyad_AlbtousH

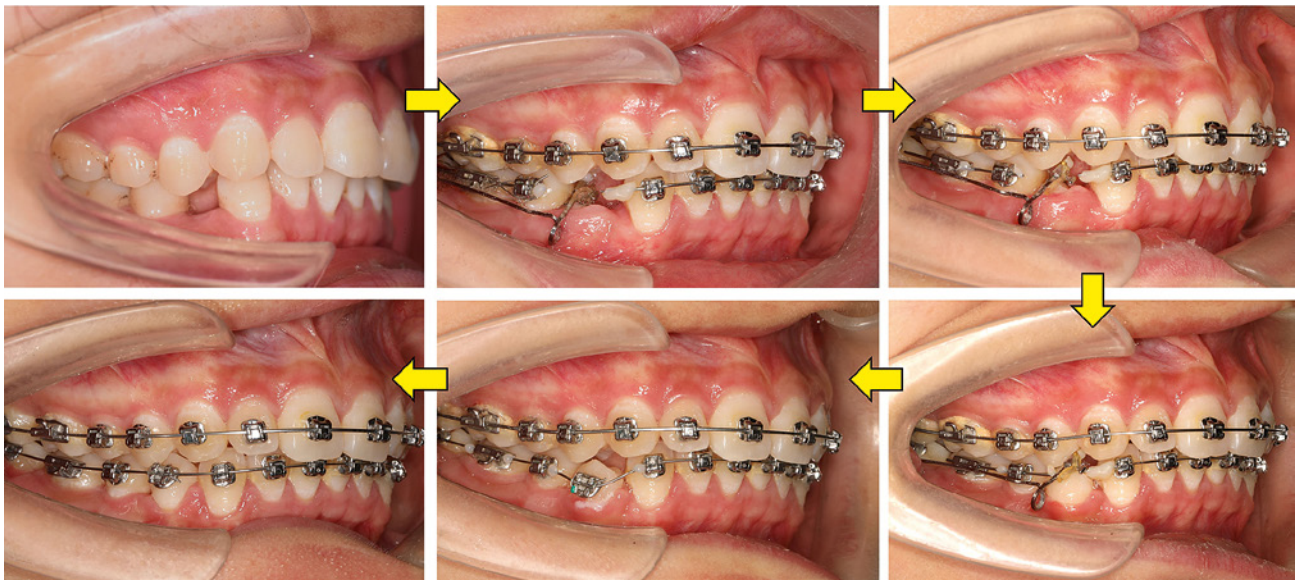


Figure 8.95 Treatment progress of the orthodontic traction of the impacted first premolar (buccal view).

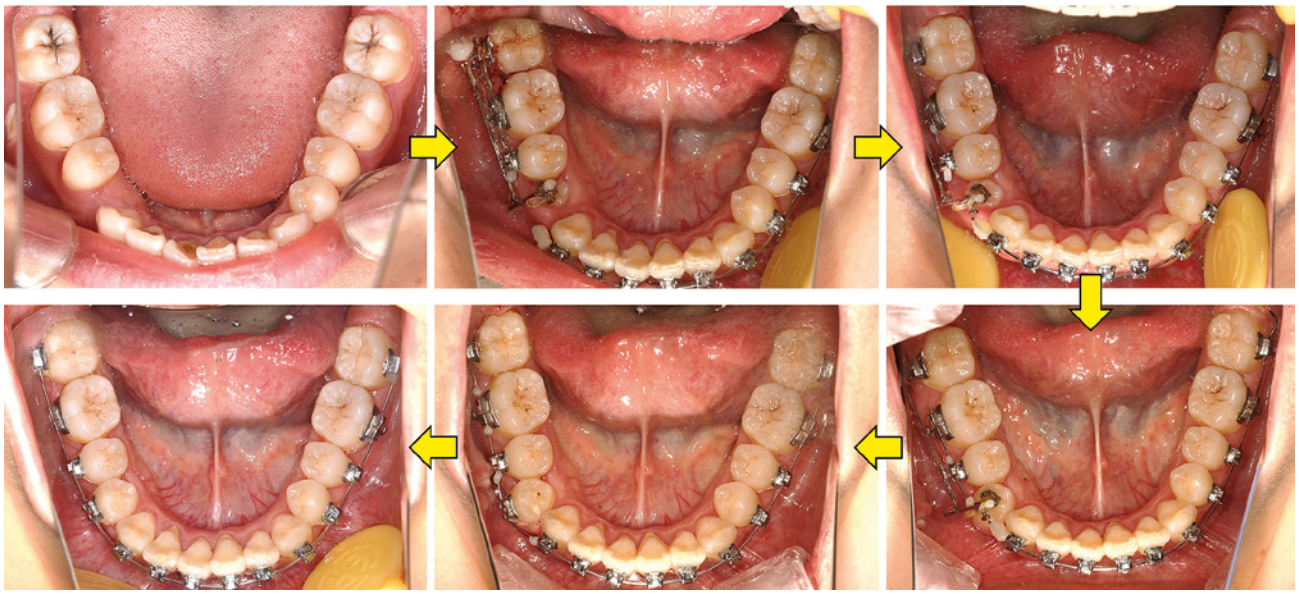


Figure 8.96 Treatment progress of the orthodontic traction of the impacted first premolar (occlusal view).

8.4 Summary

The mandibular buccal region is a desirable anatomical site for the placement of mini-implants due to its good bone quality and adequate bone quantity. Two anatomical regions are clinically available: the interradicular sites and buccal shelf. Site-specific insertion techniques and procedures should be followed to maximise the clinical success of mini-implants. Mini-implants inserted at the mandibular buccal region are versatile in accomplishing a variety of challenging orthodontic tooth movements, e.g. anterior retraction, molar protraction, molar uprighting, mandibular dentition distalisation and traction of impacted teeth.

t.me/Dr_Mouayyad_AlbtousH

References

1 Zhang S, Choi Y, Li W et al. (2022). The effects of cortical bone thickness and miniscrew implant root proximity on the success rate of miniscrew implant: a retrospective study. *Orthod. Craniofac. Res.* 25(3): 342–350.

2 Mohammed H, Wafaie K, Rizk MZ, Almuzian M, Sosly R, Bearn DR. (2018). Role of anatomical sites and correlated risk factors on the survival of orthodontic miniscrew implants: a systematic review and meta-analysis. *Prog. Orthod.* 19(1): 36.

3 Casana-Ruiz MD, Bellot-Arcis C, Paredes-Gallardo V, Garcia-Sanz V, Almerich-Silla JM, Montiel-Company JM. (2020). Risk factors for orthodontic mini-implants in skeletal anchorage biological stability: a systematic literature review and meta-analysis. *Sci. Rep.* 10(1): 5848.

4 Hakami Z, Chen PJ, Ahmida A, Janakiraman N, Uribe F. (2018). Miniplate-aided mandibular dentition distalisation as a camouflage treatment of a class III malocclusion in an adult. *Case Rep. Dent.* 2018: 3542792.

5 Yeon BM, Lee NK, Park JH, Kim JM, Kim SH, Kook YA. (2022). Comparison of treatment effects after total mandibular arch distalisation with miniscrews vs ramal plates in patients with Class III malocclusion. *Am. J. Orthod. Dentofacial Orthop.* 161(4): 529–536.

6 Freitas BV, Abas Frazao MC, Dias L, Fernandes Dos Santos PC, Freitas HV, Bosio JA. (2018). Nonsurgical correction of a severe anterior open bite with mandibular molar intrusion using mini-implants and the multiloop edgewise archwire technique. *Am. J. Orthod. Dentofacial Orthop.* 153(4): 577–587.

7 Di Stefano DA, Arosio P, Pagnutti S, Vinci R, Gherlone EF. (2019). Distribution of trabecular bone density in the maxilla and mandible. *Implant Dent.* 28(4): 340–348.

8 Ono A, Motoyoshi M, Shimizu N. (2008). Cortical bone thickness in the buccal posterior region for orthodontic mini-implants. *Int. J. Oral Maxillofac. Surg.* 37(4): 334–340.

9 Centeno ACT, Fensterseifer CK, Chami VO, Ferreira ES, Marquezan M, Ferrazzo VA. (2022). Correlation between cortical bone thickness at mini-implant insertion sites and age of patient. *Dental Press J. Orthod.* 27(1): e222098.

10 Golshah A, Salahshour M, Nikkerdar N. (2021). Interradicular distance and alveolar bone thickness for miniscrew insertion: a CBCT study of Persian adults with different sagittal skeletal patterns. *BMC Oral Health* 21(1): 534.

11 Bhatia G, Kumar A, Khatri M, Bansal M, Saxena S. (2015). Assessment of the width of attached gingiva using different methods in various age groups: a clinical study. *J. Indian Soc. Periodontol.* 19(2): 199–202.

12 Chang CCH, Lin JSY, Yeh HY. (2018). Extra-alveolar bone screws for conservative correction of severe malocclusion without extractions or orthognathic surgery. *Curr. Osteoporos. Rep.* 16(4): 387–394.

13 Gandhi V, Upadhyay M, Tadinada A, Yadav S. (2021). Variability associated with mandibular buccal shelf area width and height in subjects with different growth pattern, sex, and growth status. *Am. J. Orthod. Dentofacial Orthop.* 159(1): 59–70.

14 Vieira CAM, Damis Rodrigues R, Gomes Cardoso T, Garcia-Junior MA, Zanetta-Barbosa D. (2022). En-masse retraction of the mandibular arch with skeletal anchorage in the buccal shelf. *J. Clin. Orthod.* 56(10): 597–603.

15 Chang C, Liu SS, Roberts WE. (2015). Primary failure rate for 1680 extra-alveolar mandibular buccal shelf mini-screws placed in movable mucosa or attached gingiva. *Angle Orthod.* 85(6): 905–910.

16 Elshebiny T, Palomo JM, Baumgaertel S. (2018). Anatomical assessment of the mandibular buccal shelf for miniscrew insertion in white patients. *Am. J. Orthod. Dentofacial Orthop.* 153(4): 505–511.

17 Nucera R, Lo Giudice A, Bellocchio AM et al. (2017). Bone and cortical bone thickness of mandibular buccal shelf for mini-screw insertion in adults. *Angle Orthod.* 87(5): 745–751.

18 Sarul M, Lis J, Park HS, Rumin K. (2022). Evidence-based selection of orthodontic miniscrews, increasing their success rate in the mandibular buccal shelf. A randomized, prospective clinical trial. *BMC Oral Health* 22(1): 414.

19 Yashar N, Engeland CG, Rosenfeld AL, Walsh TP, Califano JV. (2012). Radiographic considerations for the regional anatomy in the posterior mandible. *J. Periodontol.* 83(1): 36–42.

20 Eto VM, Figueiredo NC, Eto LF, Azevedo GM, Silva AIV, Andrade I. (2023). Bone thickness and height of the buccal shelf area and the mandibular canal position for miniscrew insertion in patients with different vertical facial patterns, age, and sex. *Angle Orthod.* 93:185–194.

21 Vargas EOA, Lopes de Lima R, Nojima LI. (2020). Mandibular buccal shelf and infrazygomatic crest thicknesses in patients with different vertical facial

t.me/Dr_Mouayyad_AlbtousH

heights. *Am. J. Orthod. Dentofacial Orthop.* 158(3): 349–356.

22 Escobar-Correa N, Ramirez-Bustamante MA, Sanchez-Uribe LA, Upegui-Zea JC, Vergara-Villarreal P, Ramirez-Ossa DM. (2021). Evaluation of mandibular buccal shelf characteristics in the Colombian population: a cone-beam computed tomography study. *Korean J. Orthod.* 51(1): 23–31.

23 Sreenivasagan S, Sivakumar A. (2021). CBCT comparison of buccal shelf bone thickness in adult Dravidian population at various sites, depths and angulation – a retrospective study. *Int. Orthod.* 19(3): 471–479.

24 Uchida Y, Namura Y, Inaba M et al. (2021). Influence of pre-drilling diameter on the stability of orthodontic anchoring screws in the mid-palatal area. *J. Oral Sci.* 63(3): 270–274.

t.me/Dr_Mouayyad_AlbtousH

9

Mandibular Ramus

Qianyun Kuang[1], Qi Fan[1], Chengge Hua[2], Lingling Pu[1,3], and Hu Long[1]

[1] *Department of Orthodontics, State Key Laboratory of Oral Diseases and National Clinical Research Center for Oral Diseases, West China Hospital of Stomatology, Sichuan University, Chengdu, China*
[2] *Department of General Dentistry, State Key Laboratory of Oral Diseases and National Clinical Research Center for Oral Diseases, West China Hospital of Stomatology, Sichuan University, Chengdu, China*
[3] *Private Practice, Chengdu, China*

9.1 Introduction

The mandibular ramus was first proposed as a viable anatomical region for orthodontic TADs in 1998 and has been gaining popularity in the orthodontic community.[1,2] The mandibular ramus is not a uniplanar region but like an irregular blade, and the specific ramus region available for mini-implants is located at the bony platform between the external and internal oblique ridges (Figure 9.1). In clinical practice, ramus mini-implants are mostly employed for uprighting deeply impacted mandibular molars that are refractory to routine orthodontic biomechanics (Figure 9.2).[2,3]

9.2 Anatomical Considerations

9.2.1 Anatomical Location

The mandibular ramus is the vertical blade-shaped portion of the mandible and is continuous with the coronoid process and mandibular condyle superiorly, the mandibular body anteriorly and the mandibular angle inferiorly (Figure 9.3). Laterally, the mandibular ramus is covered by the masseter muscle that attaches to the zygomatic arch (deep head) and zygomatic process of the maxilla (superficial head) superiorly and to the mandibular angle and ramus inferiorly (Figure 9.3). Medially, the mandibular ramus is covered by the medial pterygoid muscle and inferior alveolar neurovascular bundle (Figure 9.3). The inferior alveolar neurovascular bundle enters the mandible through the mandibular foramen that lies at the centre of the medial surface of the mandibular ramus. More anteriorly, the anterior portion of the ramus medial surface is a triangular bony platform facing anteriorly and medially. The bony platform lies between the external and internal oblique ridges and is continuous inferiorly and anteriorly with the mandibular buccal shelf (Figure 9.4). Owing to its regular and flat surface, this bony platform of the anterior ramus is clinically suitable for the insertion of orthodontic TADs (Figure 9.4).

9.2.2 Hard Tissue Considerations

From the axial view, the anterior ramus platform becomes wider and faces more anteriorly from superior to inferior (Figure 9.5). The wider inferior platform renders the inferior portion of the anterior ramus more anatomically suitable for inserting mini-implants (Figure 9.5). Moreover, the inclination of the anterior ramus platform determines the direction of ramus mini-implants and the location of their heads. If inserted inferiorly, mini-implants will be anteriorly directed and buccally positioned, compared to lingually directed and lingually positioned mini-implants that are inserted superiorly (Figure 9.5). The lingually positioned mini-implants inserted superiorly are susceptible to occlusal interference with opposing maxillary third molars, especially for buccally inclined ones (Figure 9.6). Thus, for the sake of anatomical suitability, mini-implants should be inserted more inferiorly. However, from the perspectives of biomechanics, since ramus mini-implants are mostly used for uprighting impacted molars, orthodontic biomechanics will be compromised if they are inserted too inferiorly. Thus, given the trade-off between anatomy and biomechanics, we recommend ramus mini-implants be placed at

Clinical Insertion Techniques of Orthodontic Temporary Anchorage Devices, First Edition. Edited by Hu Long, Xianglong Han, and Wenli Lai.
© 2024 John Wiley & Sons Ltd. Published 2024 by John Wiley & Sons Ltd.

t.me/Dr_Mouayyad_AlbtousH

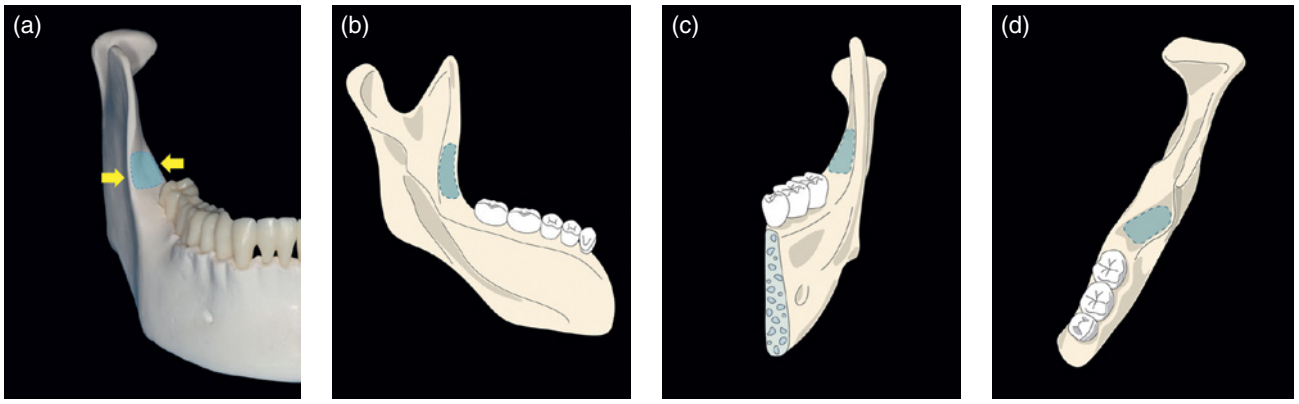


Figure 9.1 Mandibular ramus region. (a) The mandibular ramus region (encircled by the dashed line) is located at the bony platform and is between the external and internal oblique ridges (indicated by the yellow arrows). (b–d) The mandibular ramus region (grey area encircled by the dashed line).

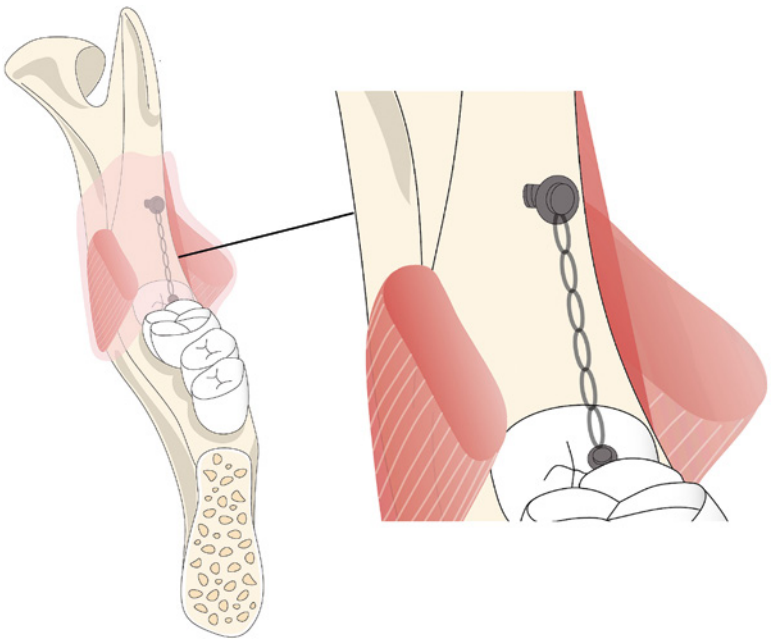


Figure 9.2 Clinical application of ramus mini-implants for uprighting deeply impacted mandibular molars.

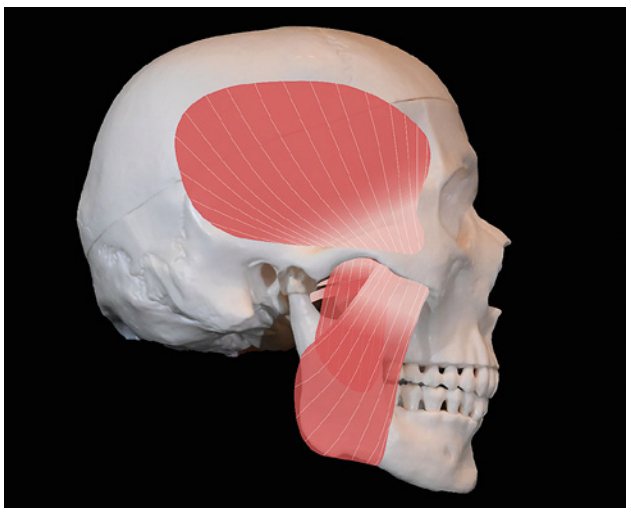


Figure 9.3 The mandibular ramus is continuous with the coronoid process and condyle superiorly and the mandibular angle inferiorly.

t.me/Dr_Mouayyad_AlbtousH

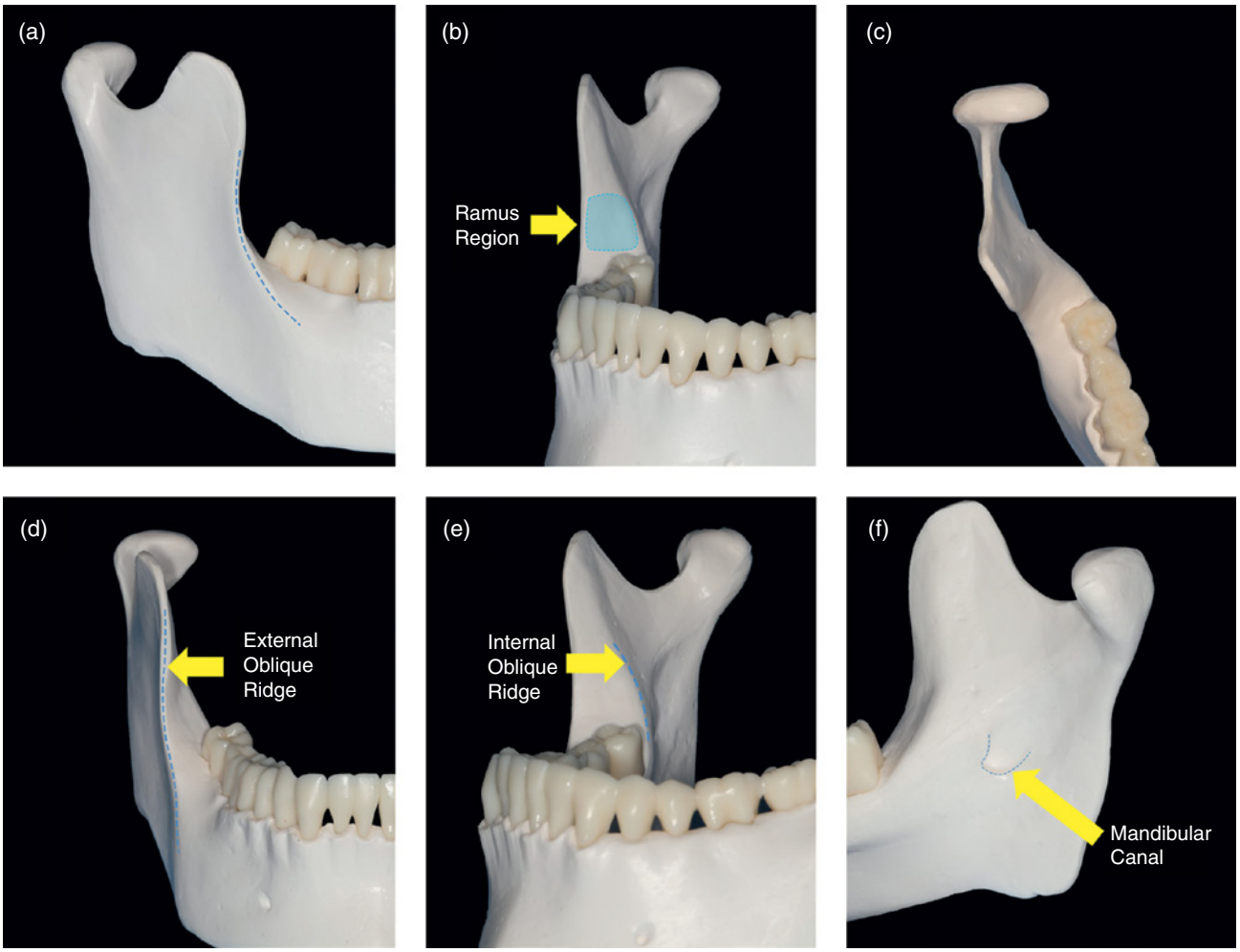


Figure 9.4 The mandibular ramus region shown on a skull. (a) Buccal view. The dashed line indicates the external oblique ridge. (b) Frontal view of the ramus region (blue area). (c) Occlusal view. (d) External oblique ridge (blue dashed line). (e) Internal oblique ridge (blue dashed line). (f) The entrance of the mandibular canal.

the vertical midpoint that is approximate 8 mm above the occlusal plane.

The mandibular ramus has excellent bone quality and quantity and has been employed in clinical practice for autogenous bone harvesting.[4,5] It harbours thick cortical bone and dense cancellous bone (Figure 9.7), justifying the need for predrilling. Based on our preliminary CBCT study, we found that cortical thickness at the mandibular ramus was above 2 mm (Figure 9.7) and that the depth of bone available for mini-implant insertion was more than 5 mm (Figure 9.7). It has been suggested that 3–5 mm bone engagement is adequate for the stability of mini-implants at the mandibular ramus region.[2] Thus, the mandibular ramus offer excellent bone quality and quantity for mini-implants.

9.2.3 Soft Tissue Considerations

The anterior ramus platform is covered by thick soft tissue composed of thick mucosa and medial pterygoid muscle (Figures 9.8 and 9.9). Although self-drilling technique without flapping has been advocated for insertion of ramus mini-implants,[3] we recommend flapping to avoid the rolling of soft tissue (especially the medial pterygoid muscle fibres) around mini-implants and the presence of necrotic soft tissue at the interface between mini-implants and alveolar bone (Figure 9.10). Otherwise, the lesion may cause prolonged soft tissue healing and even undesirable secondary stability. The thickness of soft tissue covering the anterior ramus platform is 3–5 mm, requiring mini-implants of at least 12 mm length to achieve an appropriate emergence profile.

t.me/Dr_Mouayyad_AlbtousH

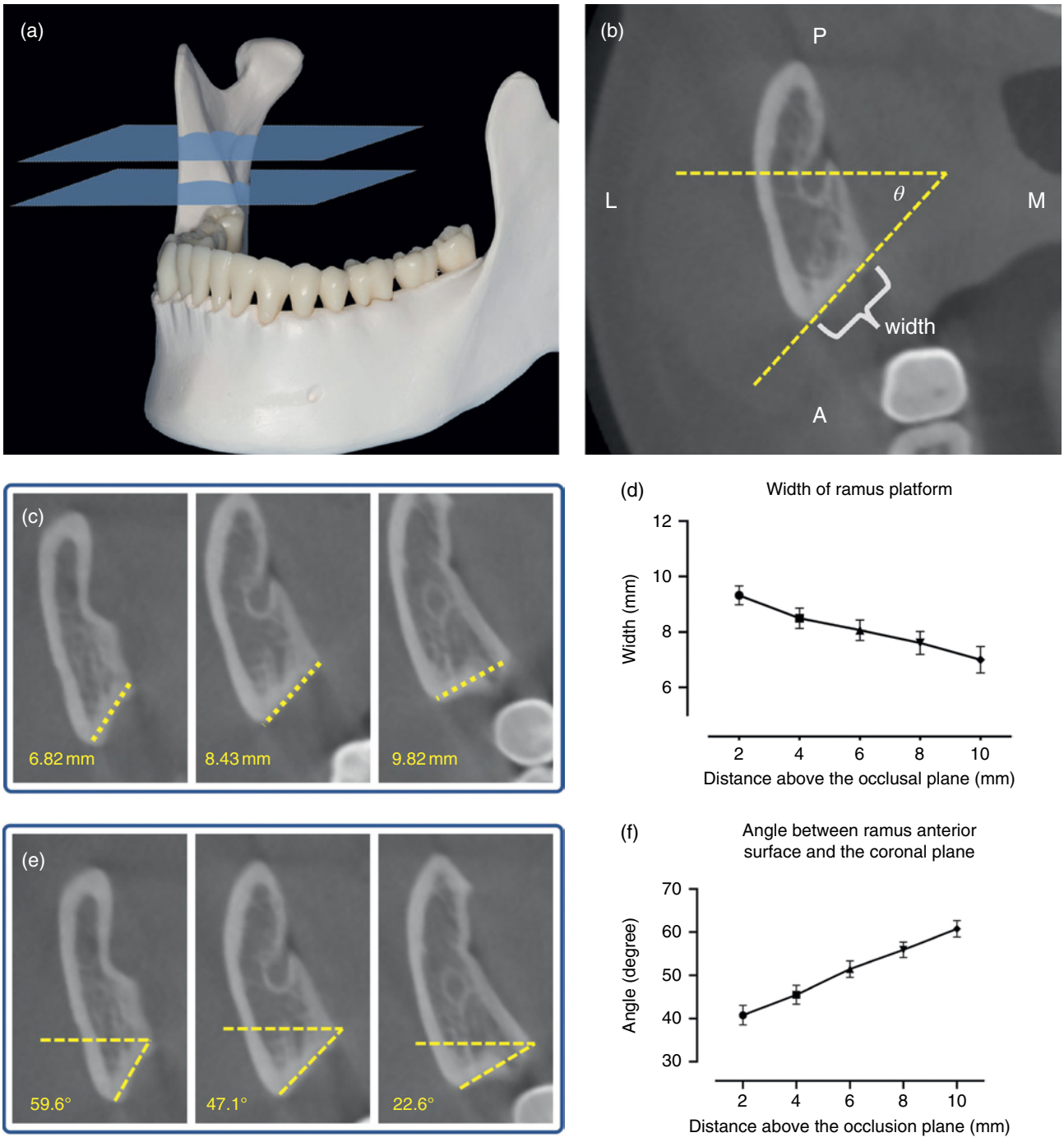


Figure 9.5 (a) Illustration of transverse sections of the mandibular ramus. (b) Axial view of the mandibular ramus. The width refers to the distance between the external and internal oblique ridges. The theta angle indicates the angle formed between the bony platform and the coronal plane. (c) Measurement of the ramus platform width. (d) Line chart of the width of the ramus platform at different heights of the ramus (in reference to the occlusal plane). (e) Measurement of the angle between the ramus anterior surface and the coronal plane at different heights of the ramus in reference to the occlusal plane. (f) Line chart of the angle between the ramus anterior surface and the coronal plane at different heights.

t.me/Dr_Mouayyad_AlbtousH

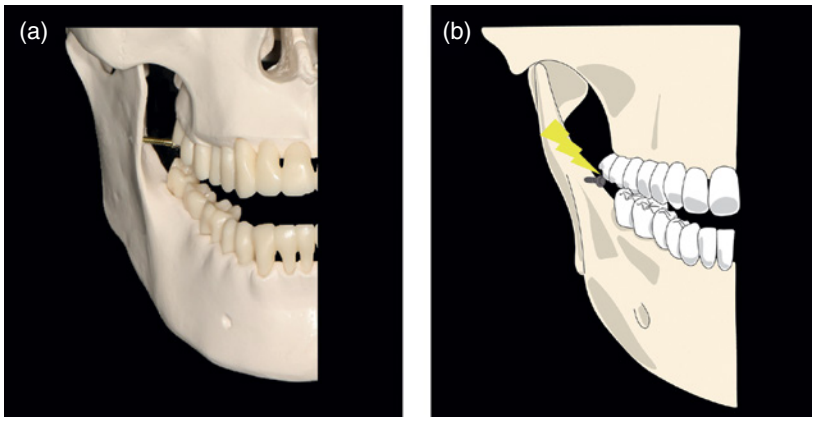


Figure 9.6 Premature contact between the ramus mini-implant and the ipsilateral maxillary third molar. (a) Skull. (b) Illustration.

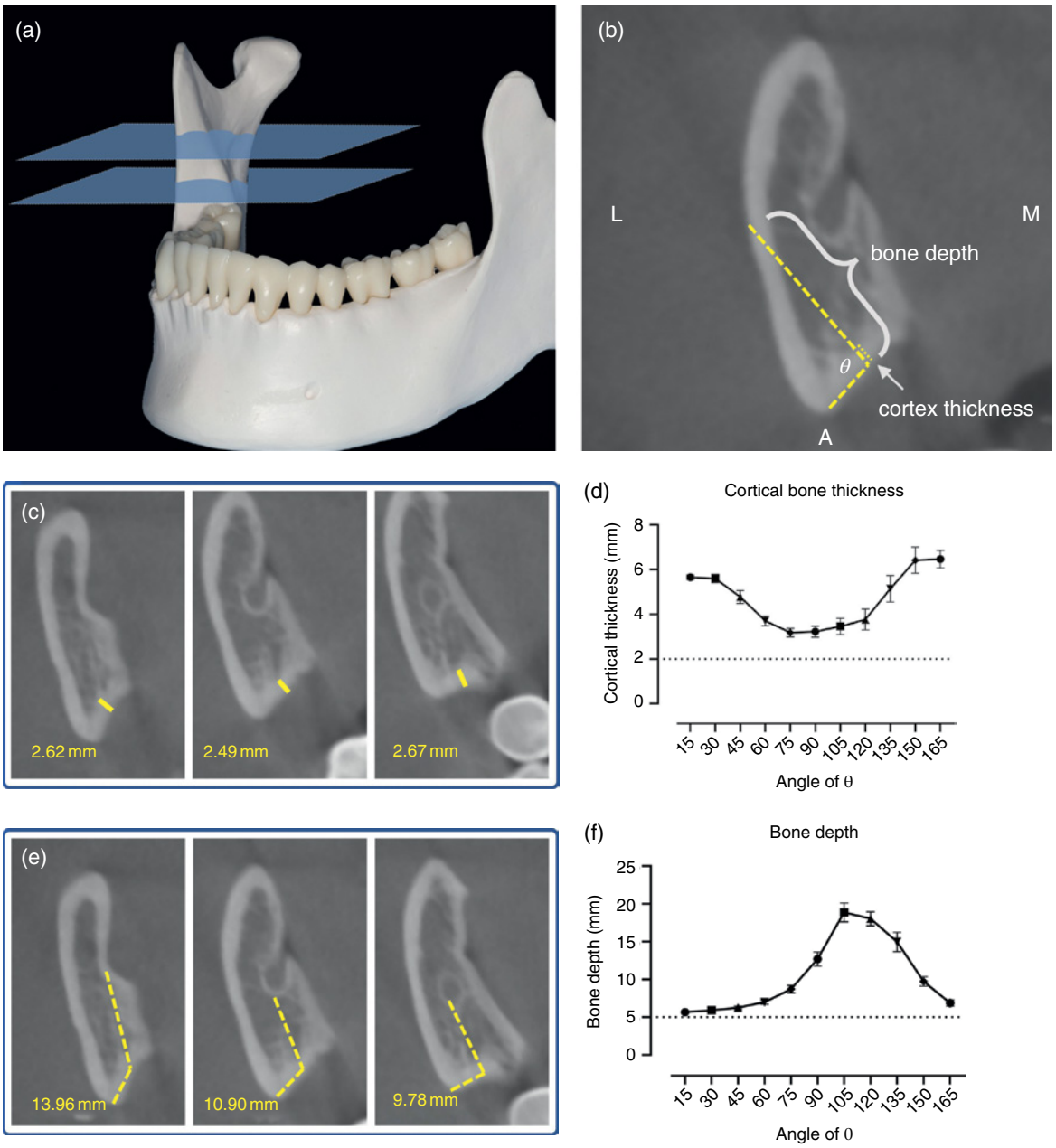


Figure 9.7 (a) Illustration of transverse sections of the mandibular ramus. (b) Axial view of the mandibular ramus by CBCT. The theta angle (insertion angle) refers to the angle formed by the ramus bone surface and the insertion path. The bone depth is defined as the distance between the insertion entry point and the contralateral cortical plate on the buccal side. Cortical thickness is the thickness of the bone cortex of the ramus platform. (c) Measurement of the cortical bone with different insertion angles (the insertion entry point is 6 mm above the occlusal plane and 4 mm medial to the external oblique ridge). (d) Line chart of cortical bone thickness with different insertion angles. (e) Measurement of bone depth with different insertion angles (the insertion entry point is 6 mm above the occlusal plane and 4 mm lingual to the external oblique ridge). (f) Line chart of bone depth at different insertion angles.

t.me/Dr_Mouayyad_AlbtousH

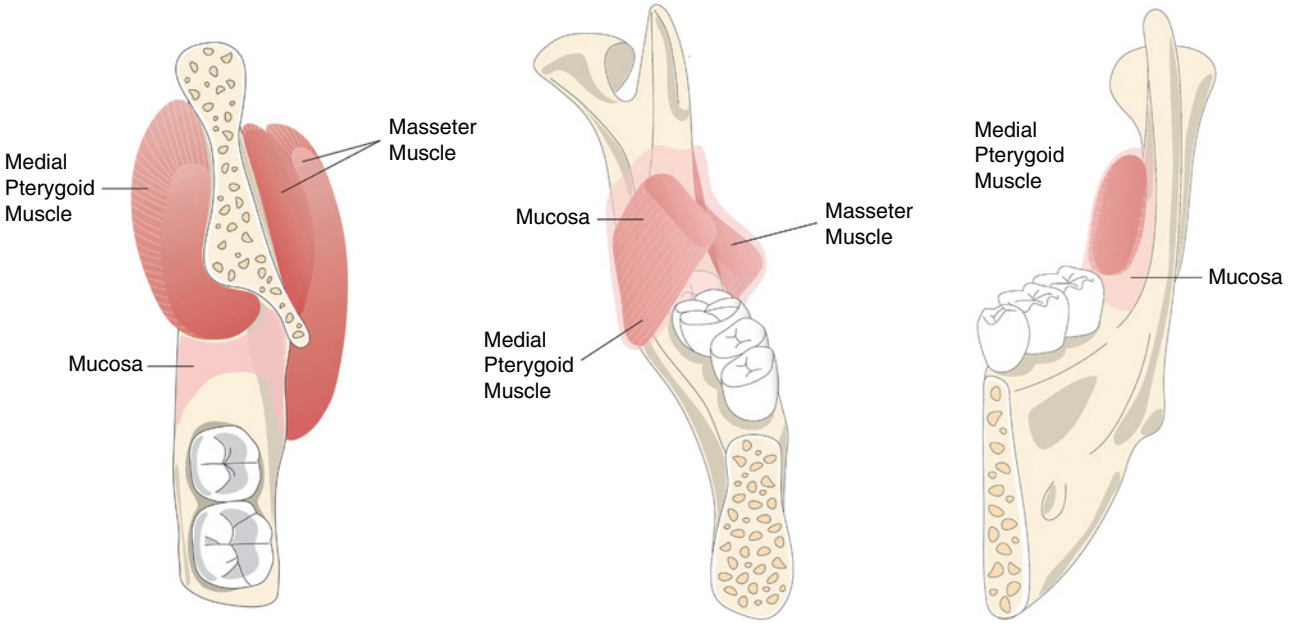


Figure 9.8 The mandibular ramus is covered by thick medial pterygoid muscle and mucosa.

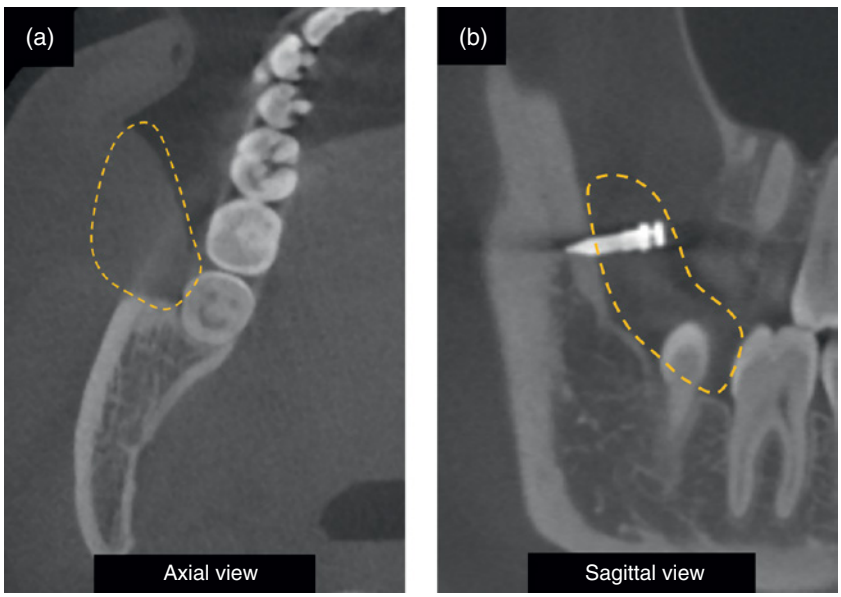


Figure 9.9 CBCT images showing the thick soft tissue covering the mandibular ramus region. (a) Axial view. The overlying soft tissue is encircled by the dashed line. (b) Sagittal view. The thick soft tissue is encircled by the dashed line. Note the soft tissue also covers the ramus mini-implant.

As mentioned above, inferior alveolar neurovascular bundles enter the mandible via the mandibular foramen located at the medial surface of the mandibular ramus. Then, the neurovascular bundles run anteriorly within the mandibular canal and exit the mandible through the mental foramen. Thus, due to the anatomical vicinity between the mandibular canal and the anterior ramus platform, injury to inferior alveolar neurovascular bundles is still likely. Our preliminary study indicated that the distance from the cortex of the anterior ramus platform to the mandibular canals is above 12 mm, suggesting that the risk of nerve injury secondary to insertion of ramus mini-implants is extremely low (Figure 9.11).

9.2.4 Optimal Insertion Sites

Optimal insertion sites should offer mini-implants with adequate bone quality and sufficient bone quantity. Moreover,

t.me/Dr_Mouayyad_AlbtousH

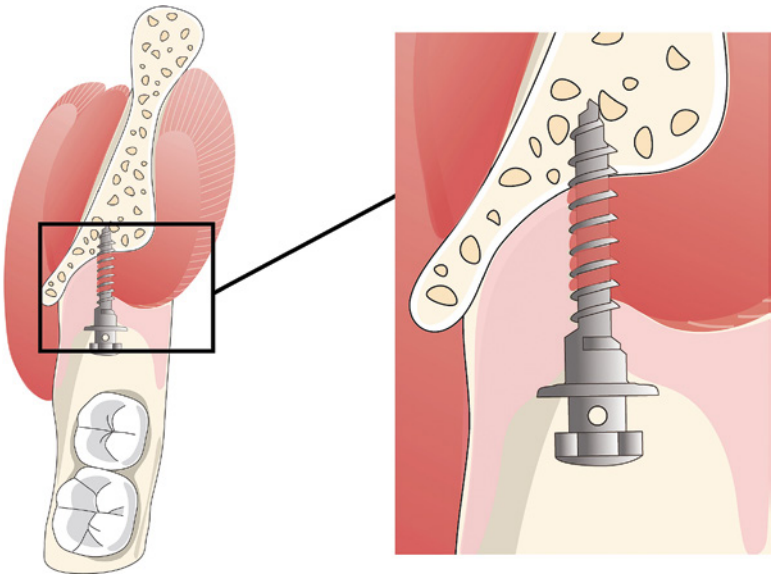


Figure 9.10 Self-drilling without flap elevation causes rolling of soft tissue (especially medial pterygoid muscle fibres) around the mini-implant.

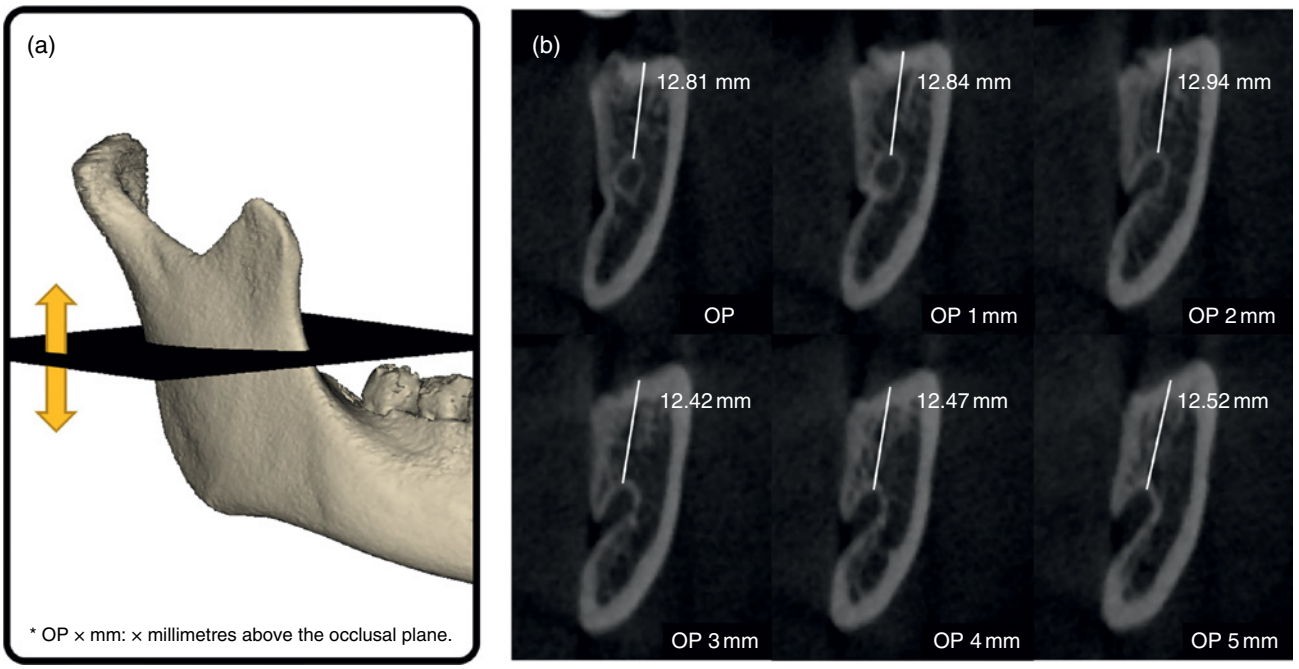


Figure 9.11 (a) Illustration of the transverse section of the mandibular ramus. (b) Measurement of the distance from the anterior ramus platform to the mandibular canal at different heights in reference to the occlusal plane.

iatrogenic injury to inferior alveolar neurovascular bundles and premature contact with opposing third molars should be avoided. In our preliminary study based on CBCT data, we defined the optimal insertion sites that meet the following requirements: (1) cortical bone thickness greater than 2 mm; (2) bone depth greater than 7 mm; (3) mini-implant tips with at least 2 mm clearance from mandibular canals; (4) mini-implant heads with at least 3.5 mm clearance from opposing third molars or mucosa of maxillary tuberosity. According to these requirements, we recommend that ramus mini-implants be inserted at a site 4–6 mm medial to the external oblique ridge and 4–8 mm above the occlusal plane with an angulation of 30–45° to the sagittal plane (Figure 9.12).

t.me/Dr_Mouayyad_AlbtousH

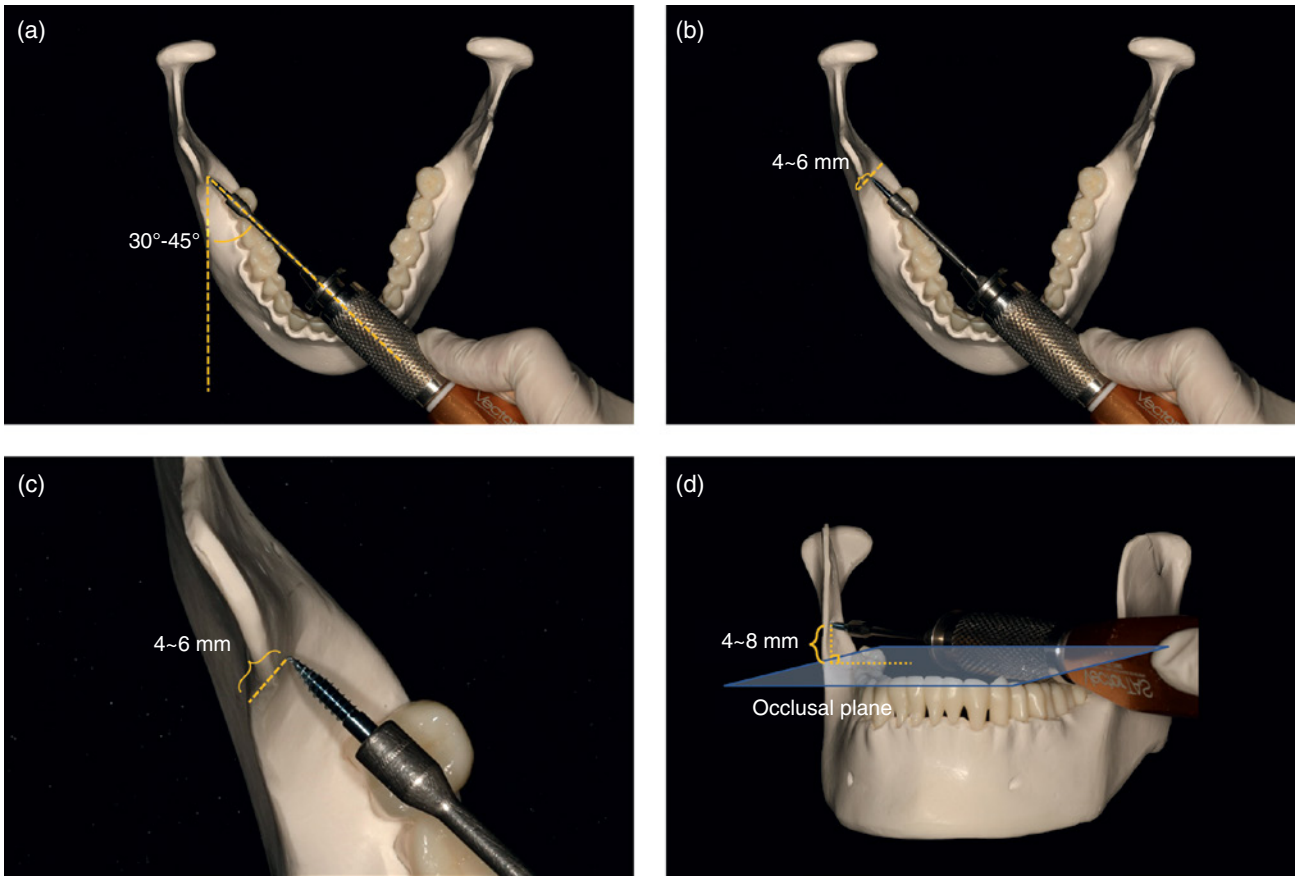


Figure 9.12 Recommended insertion technique for mandibular ramus mini-implants. (a) The optimal insertion path is 30–45° to the midsagittal plane. (b) Th entry point is 4–6 mm medial to the external oblique ridge. (c) Close-up view showing that the entry point is 4–6 mm medial to the external oblique ridge. (d) The insertion entry point is 4–8 mm above the occlusal plane.

9.3 Mini-implant Selection

Given that the bone cortex at this region is thick (>2 mm), the diameter of mini-implants should be greater than 2 mm, otherwise the risk of fracture is high, especially if self-drilling method is employed in clinical settings. To reduce the risk of mini-implant fracture and bone damage, we recommend predrilling before mini-implant insertion. Moreover, the thick soft tissue covering the mandibular ramus renders patients with ramus mini-implants susceptible to soft tissue hyperplasia that is challenging to manage and may lead to mini-implant failure.[3] Thus, mini-implants should be long enough so that soft tissue can be penetrated with adequate head exposure.

However, increasing the length of mini-implants sacrifices their resistance to fracture. Mini-implants with different materials have different resistance to fracture, with stainless steel being more resistant to fracture than titanium. It is suggested that stainless steel mini-implants (14 mm in length) be used for the ramus region.[2] However, for titanium mini-implants, this length may render them susceptible to fracture and a reduced length (12 mm) can be used in clinical practice. In our clinical experience, some of the 12 mm titanium mini-implants are embedded in soft tissue and 'closed traction' technique can be used for uprighting deeply impacted mandibular molars with excellent clinical success. The clinical success of this 'closed traction' technique is due to the superelasticity of the elastomeric module that often does not require a second activation to upright impacted molars other than the one performed during insertion surgery (Figure 9.13).

Therefore, we recommend ramus mini-implants be at least greater than 2 mm in diameter and be 12 mm

t.me/Dr_Mouayyad_AlbtousH

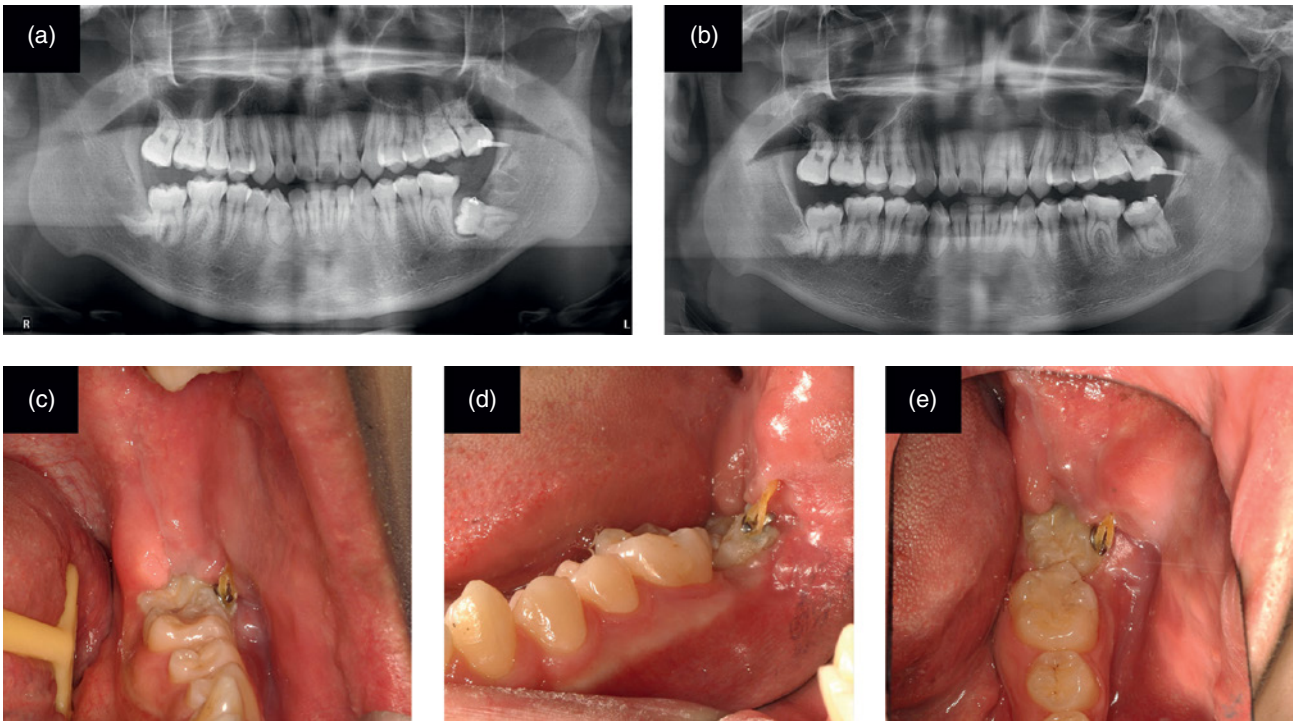


Figure 9.13 The 'closed traction' technique in clinical practice. (a) A ramus mini-implant was applied to upright the impacted mandibular left second molar with an elastic powerchain using the 'closed traction' technique. (b) Progress. Note the impacted mandibular left second molar was successfully uprighted. (c–e) Intraoral view. Note the second molar can be observed intraorally. The ramus mini-implant was fully covered by thick soft tissue.

(titanium alloy) or 14 mm (stainless steel) in length. 'Closed traction' technique can be used for uprighting deeply impacted mandibular molars for mini-implants if soft tissue hyperplasia is anticipated.

9.4 Insertion Procedure

9.4.1 Insertion Procedures

As illustrated in Figure 9.14, first, based on radiographic examinations and clinical palpation, an optimal insertion site is determined. Second, flapping surgery is performed to expose the anterior ramus bone platform and the specific site is approximately 4–8 mm the above occlusal plane. Third, once the flap is elevated, predrilling is performed to make a pilot hole. Fourth, examine whether the size of the pilot hole is adequate. Fifth, engage a mini-implant into a screwdriver and insert the mini-implant into the prepared pilot hole. Special care should be taken to avoid mini-implant fracture. At this stage, complete insertion at designated length is not required. Lastly, check the orientation and position of the mini-implant and insert the mini-implant into the ramus bone at designated depth. In general, 3–5 mm bone engagement is adequate.

9.4.2 Insertion on Skulls

The procedures of inserting a ramus mini-implant on a skull are displayed in Figure 9.15. First, locate the anterior ramus platform region that lies between the external and internal oblique ridges. Determine the specific insertion site that is 4–6 mm medial to the external ridge and 4–8 mm above the occlusal plane. Second, perform predrilling at the designated insertion site and make a pilot hole with a motor-driven handpiece. Third, insert a mini-implant into the pilot hole; the insertion is partial at this stage. The insertion angulation is 30–45° to the sagittal plane. Fourth, examine the orientation and position of the mini-implant and check premature contact with the opposing third molar. If premature contact is detected, change the orientation of the mini-implant. Lastly, finish the insertion by advancing the mini-implant to the designated depth.

t.me/Dr_Mouayyad_AlbtousH

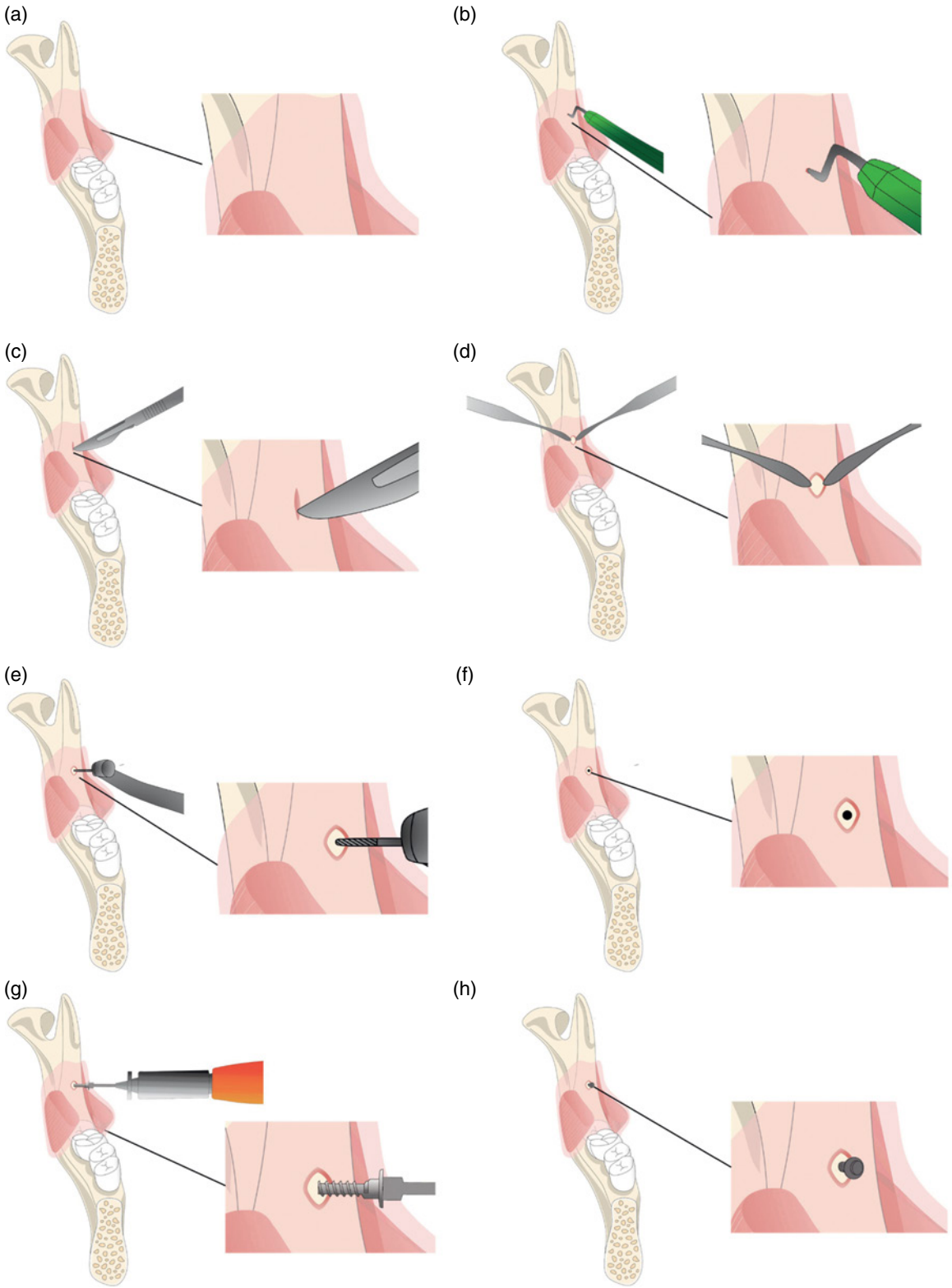


Figure 9.14 Illustrations of the insertion procedure. (a,b) Confirm an optimal insertion site. (c,d) Expose the anterior ramus bone platform following flap elevation. (e,f) Perform predrilling to obtain a pilot hole. (g,h) Insert the mini-implant into the pilot hole.

t.me/Dr_Mouayyad_AlbtousH

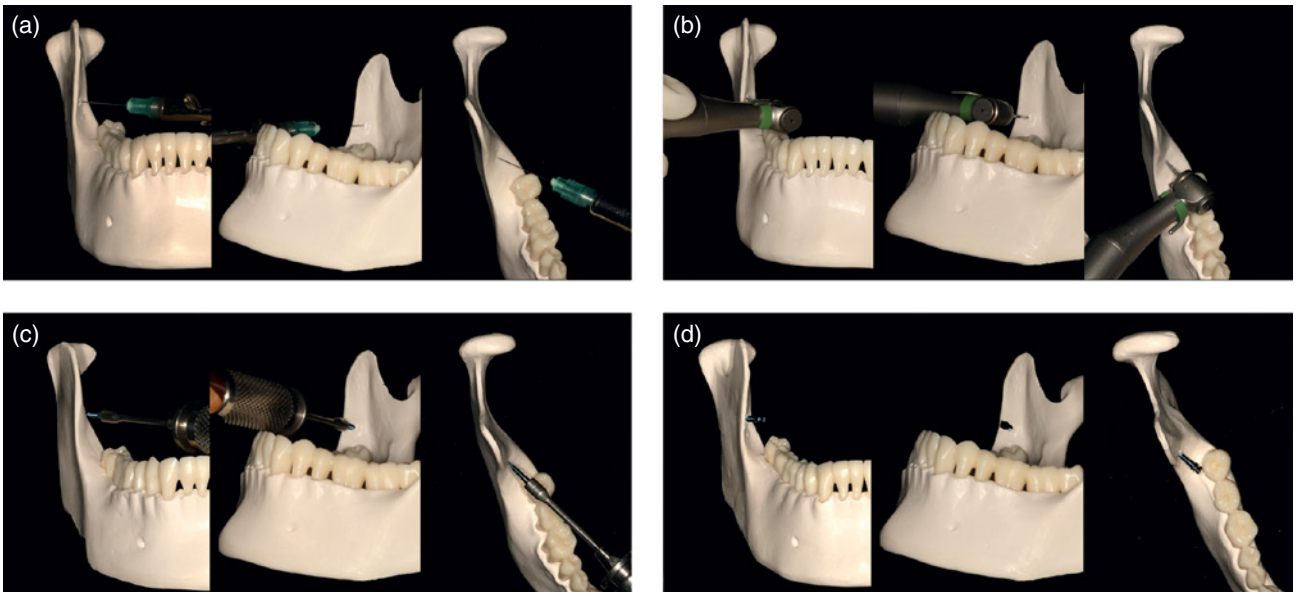


Figure 9.15 Insertion of a ramus mini-implant on a skull. (a) Local infiltration anaesthesia at the insertion site. (b) Predrilling at the designated insertion site with a reduced-speed handpiece. (c) Insert a mini-implant into the pilot hole. (d) Complete the insertion by advancing the mini-implant to the designated insertion depth.

9.4.3 Clinical Procedures

Preinsertion Preparation

Practitioners should determine the optimal insertion site for a specific patient requiring insertion of a ramus mini-implant based on radiographic examination. Patients are often anxious about the surgery, so good communication and per-insertion reassurance are necessary.

Once the patient is relaxed and surgical contradictions are ruled out, finger palpation is performed to locate the anterior ramus platform and adequate infiltration anaesthesia is executed at the predetermined insertion site. Then, ask the patient to rinse for at least 30 seconds. Practitioners should prepare the mini-implant insertion armamentaria, surgical instruments and mini-implants with appropriate sizes (12*2 mm or 14*2 mm).

Insertion

The insertion procedures for locating the insertion site and performing incision are shown in Figure 9.16. First, palpate and locate the predetermined insertion site. Second, retract soft tissue adequately to limit the mobility and thickness of soft tissue covering the bone surface so that incision can be precisely executed. Third, mucosa incision is performed with a surgical scalpel. Considering the orientation of the medial pterygoid muscle, oblique incision in line with the muscle fibre orientation is recommended (Figure 9.17). This can minimise muscle damage and reduce the likelihood of postinsertion infection and pain. The incision should be made to reach the bone surface with a first attempt. Due to the mobility of soft tissue, if the incision is made to reach the bone surface with several attempts, excessive soft tissue damage may be caused (Figure 9.18). Fourth, flap elevation is performed with periosteal elevators and the anterior ramus bone surface exposed, following by pilot drilling with a reduced-speed motor-driven handpiece with copious saline irrigation to minimise potential bone thermal necrosis.

Pilot drilling is of great importance to the success of ramus mini-implants and its three parameters should be considered: depth, size and orientation. It is not mandatory to reach full depth and pilot drilling is often performed to penetrate just the cortical bone (2–3 mm). The size of the pilot hole should be 60% of the mini-implant, indicating that a 1.2 mm pilot hole is made for 2 mm mini-implants. The orientation of pilot drilling determines that of the mini-implant. Thus, it should be determined meticulously so that enough clearance from the opposing maxillary molars will be achieved. To avoid potential bone damage due to pilot drilling orientation errors, we recommend practitioners use an explorer that is pressed against the designated insertion site to mimic a mini-implant and ask the patient to perform different mandibular movements (i.e. open, protrusion and lateral excursion) to examine whether premature contact is encountered (Figure 9.19).

t.me/Dr_Mouayyad_AlbtousH

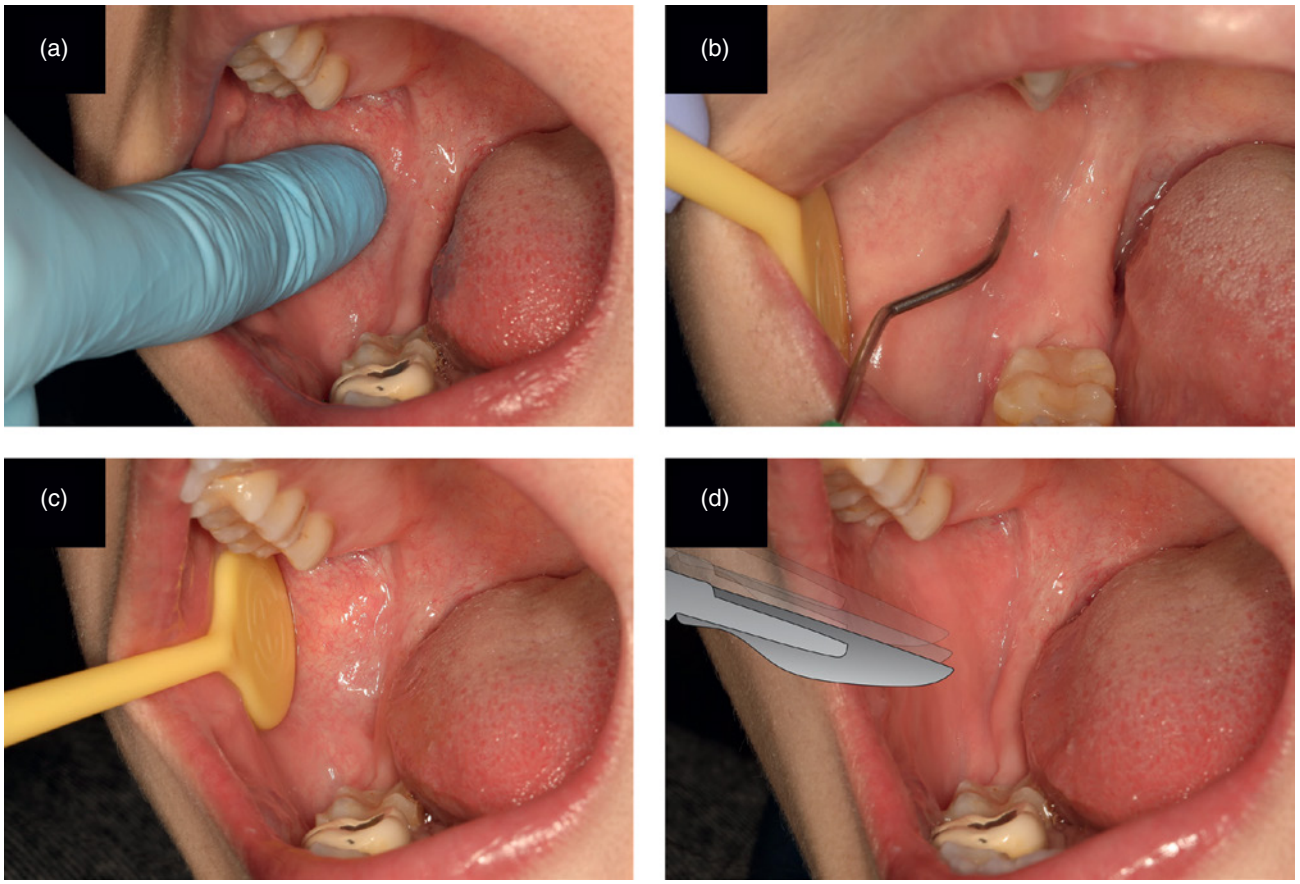


Figure 9.16 Locating the insertion site and performing incision. (a,b) Palpate and locate the predetermined insertion site. (c) Retract the soft tissue adequately to limit mobility of the soft tissue covering the bone surface. (d) Perform mucosa incision with a surgical scalpel.

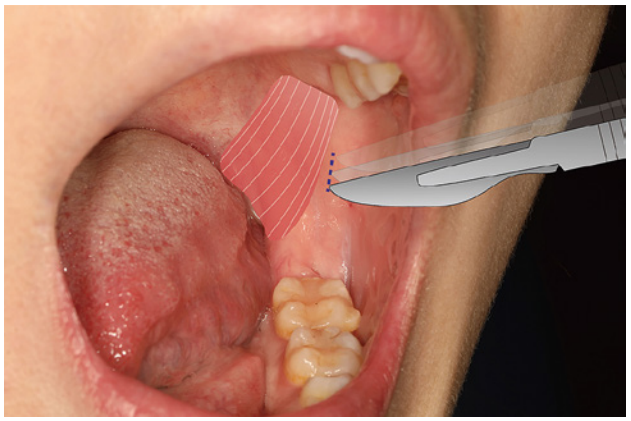


Figure 9.17 Oblique incision in line with the muscle fibre orientation is recommended to reduce excessive trauma to the medial pterygoid muscle.

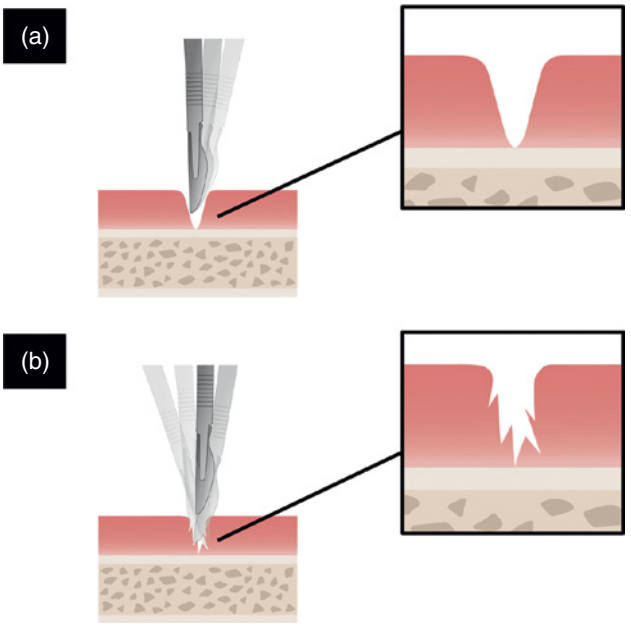


Figure 9.18 (a) The incision is made to reach the bone surface with one attempt, which minimises soft tissue trauma. (b) Excessive soft tissue damage is caused if several incision attempts are made to reach the bone surface.

t.me/Dr_Mouayyad_AlbtousH

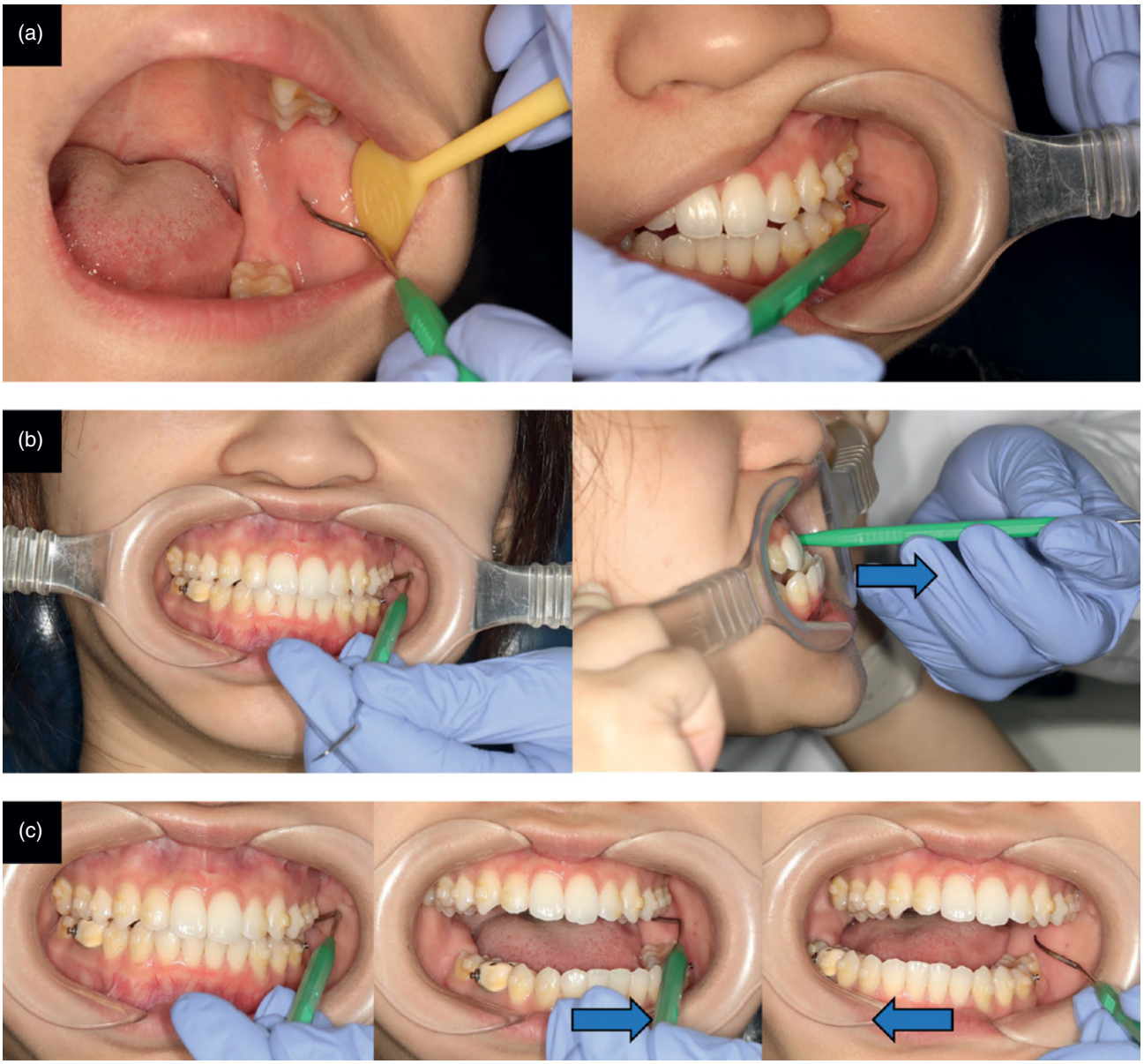


Figure 9.19 An explorer was utilised to mimic a mini-implant and the patient was instructed to perform different mandibular movements to examine whether premature contact is encountered. (a) Mouth opening. (b) Protrusion. (c) Lateral excursion.

Fifth, partially insert the mini-implant into the prepared pilot hole and ask the patient to perform mandibular movements to examine whether premature contact occurs. Lastly, finish the insertion by advancing the mini-implant to the designated insertion depth which is generally 3–5 mm. Immediate force loading can be applied with elastomeric module and suturing is performed with primary closure of the flap (Figure 9.20).

Postinsertion

Reassure the patient and instruct them to maintain meticulous oral hygiene. Antibiotics and NSAIDs can be prescribed.

9.4.4 Biomechanical Analysis

As illustrated in Figure 9.21, since the ramus mini-implant is located buccally, posteriorly and superiorly to impacted mandibular molars, a buccally, distally, occlusally directed uprighting force is applied to the impacted mandibular molar. The occlusal and distal components of the uprighting force are beneficial for molar uprighting while the buccal component is sometimes detrimental to the final position of the molar, which may require additional biomechanics.

t.me/Dr_Mouayyad_AlbtousH

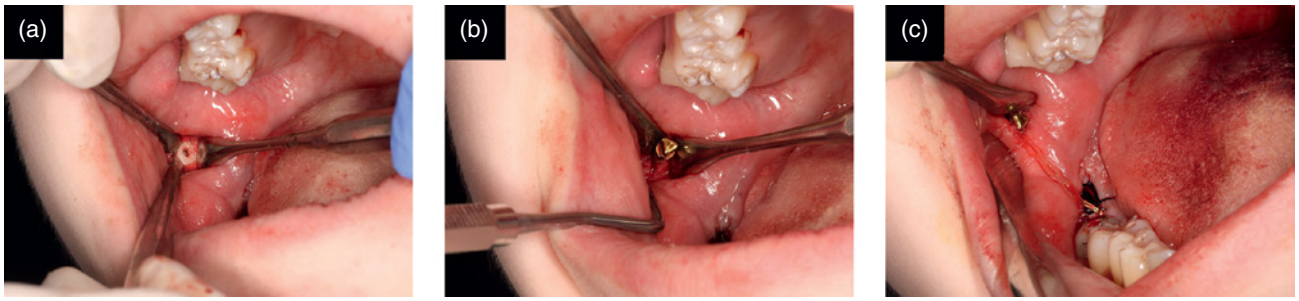


Figure 9.20 Insertion of the mini-implant. (a) Prepare a pilot hole by predrilling. (b) Insert the mini-implant into the ramus bone at designated depth. (c) Immediate force loading is applied with elastomeric module.

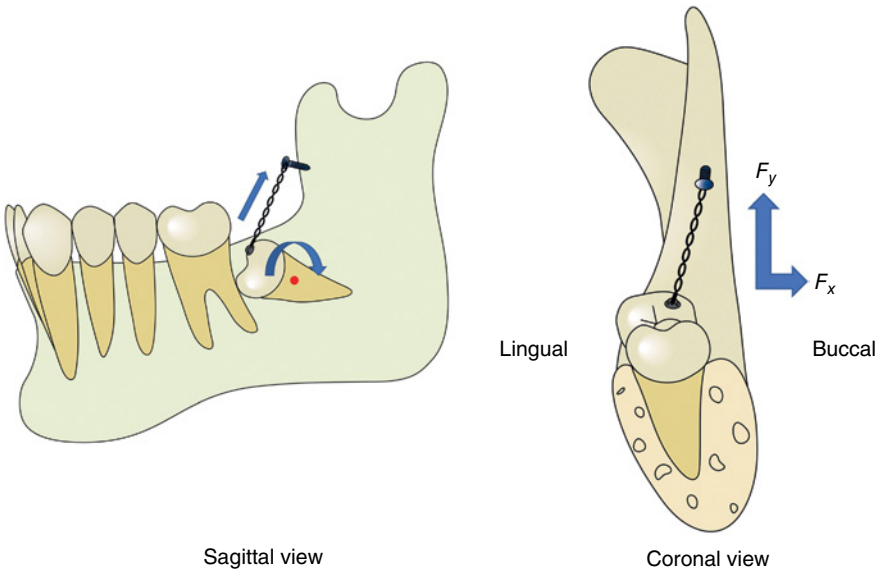


Figure 9.21 Biomechanical illustration of the orthodontic traction of an impacted molar through a ramus mini-implant. The traction force vector is distal, buccal and occlusal. An uprighting moment is generated.

9.5 Versatile Clinical Applications

9.5.1 Uprighting Mesioangulated Impacted Mandibular Second Molars

A female patient presented to the orthodontic department with a chief complaint of tooth impaction. As shown in Figure 9.22, clinical and radiographic examinations revealed that the bilateral mandibular second molars were impacted beneath the undercuts of the adjacent first molars, with the third molars lying on the distal sides of the second molars.

The treatment plan was to extract the bilateral third molars and orthodontically traction the mesioangularly impacted second molars with the aid of two mini-implants that would be inserted at the mandibular ramus region.

Two mini-implants were inserted at the left and right mandibular ramus regions. Two lingual buttons were bonded onto the crowns of the second molars, and power-chain elastics were applied between the lingual buttons and the ramus mini-implants to offer traction force. The traction force vector was distal, buccal and

t.me/Dr_Mouayyad_AlbtousH

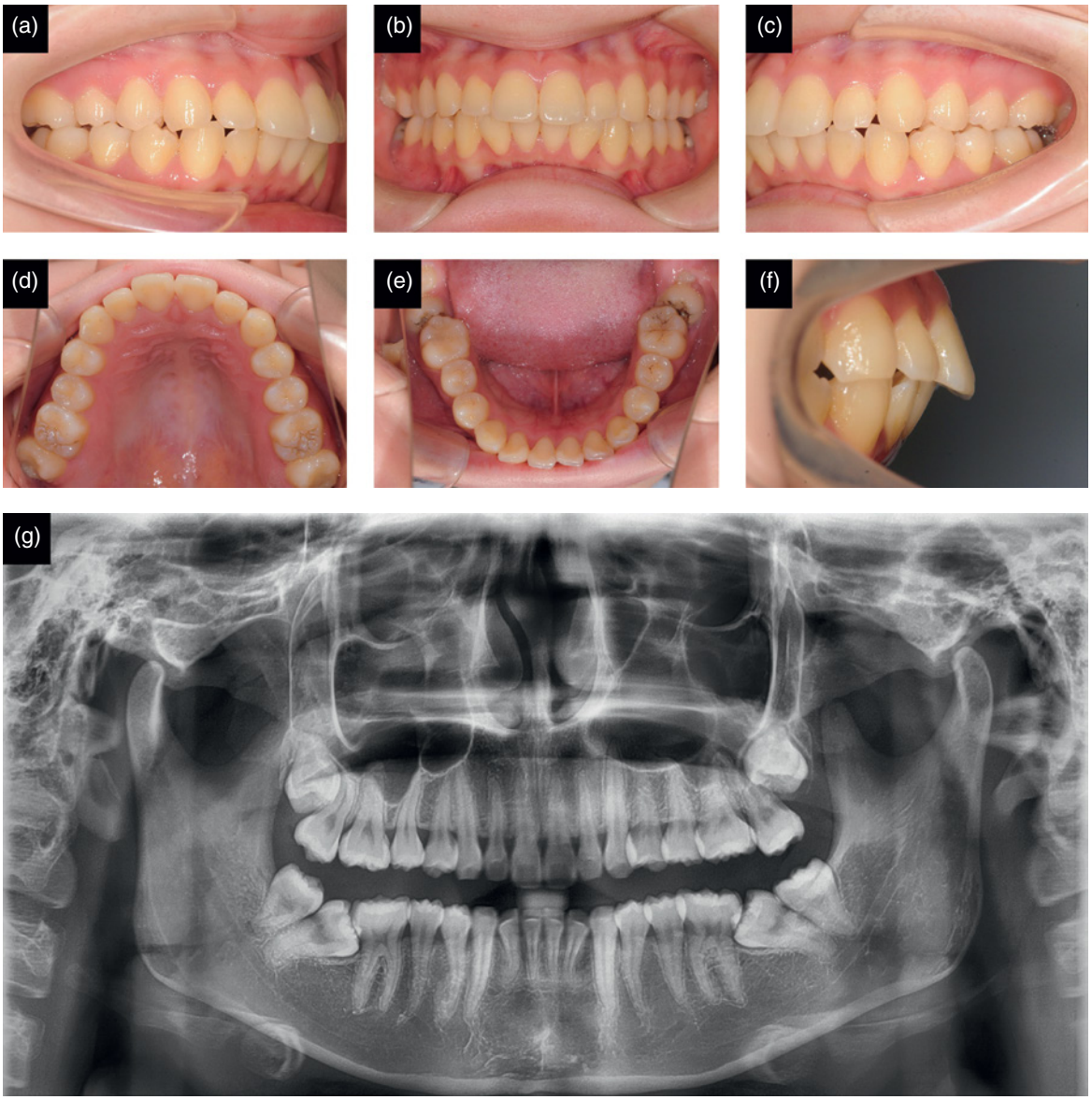


Figure 9.22 (a–f) Pretreatment intraoral photographs indicated that the mandibular left and right second molars were partially erupted. Only the distal parts of the crowns of the second molars can be observed intraorally. (g) Pretreatment panoramic radiograph revealed that the bilateral mandibular second molars were mesioangularly impacted beneath the undercuts of their adjacent first molars.

occlusal. Segmental archwire technique was implemented to align the second molars. The orthodontic traction and tooth alignment progressed smoothly and efficiently (Figure 9.23) and the treatment outcome was successful (Figure 9.24). Following the orthodontic traction of the impacted second molars, the patient would receive comprehensive orthodontic treatment of the whole dentition.

t.me/Dr_Mouayyad_AlbtousH

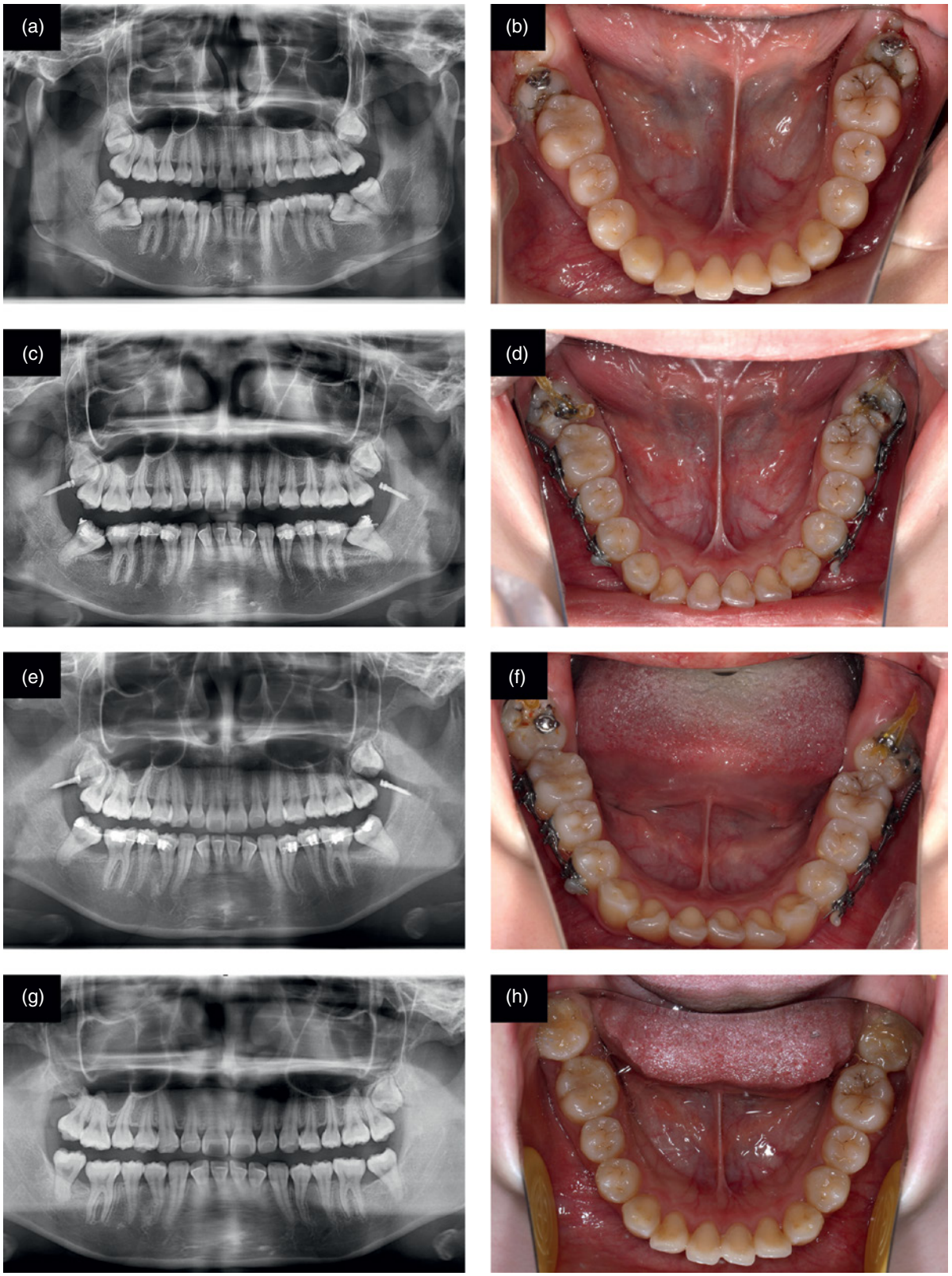


Figure 9.23 Treatment progress. (a) Pretreatment panoramic radiograph. (b) Intraoral photograph showing that two lingual buttons were bonded on the distal surface of crowns of the bilaterally impacted mandibular second molars. Powerchain elastics were applied between the lingual buttons and the ramus mini-implants for orthodontic traction. (c,d) After the impacted molars were upright until the occlusal surfaces were exposed, buttons were repositioned to the occlusal surfaces to facilitate the uprighting. Segmental archwire technique was implemented to aid in alignment. (e,f) After complete uprighting, the mandibular second molars were brought to an approximate functional position. (g,h) The first-stage treatment was completed with the bilaterally impacted mandibular second molars in functional positions. Comprehensive orthodontic treatment would be started afterwards.

t.me/Dr_Mouayyad_AlbtousH

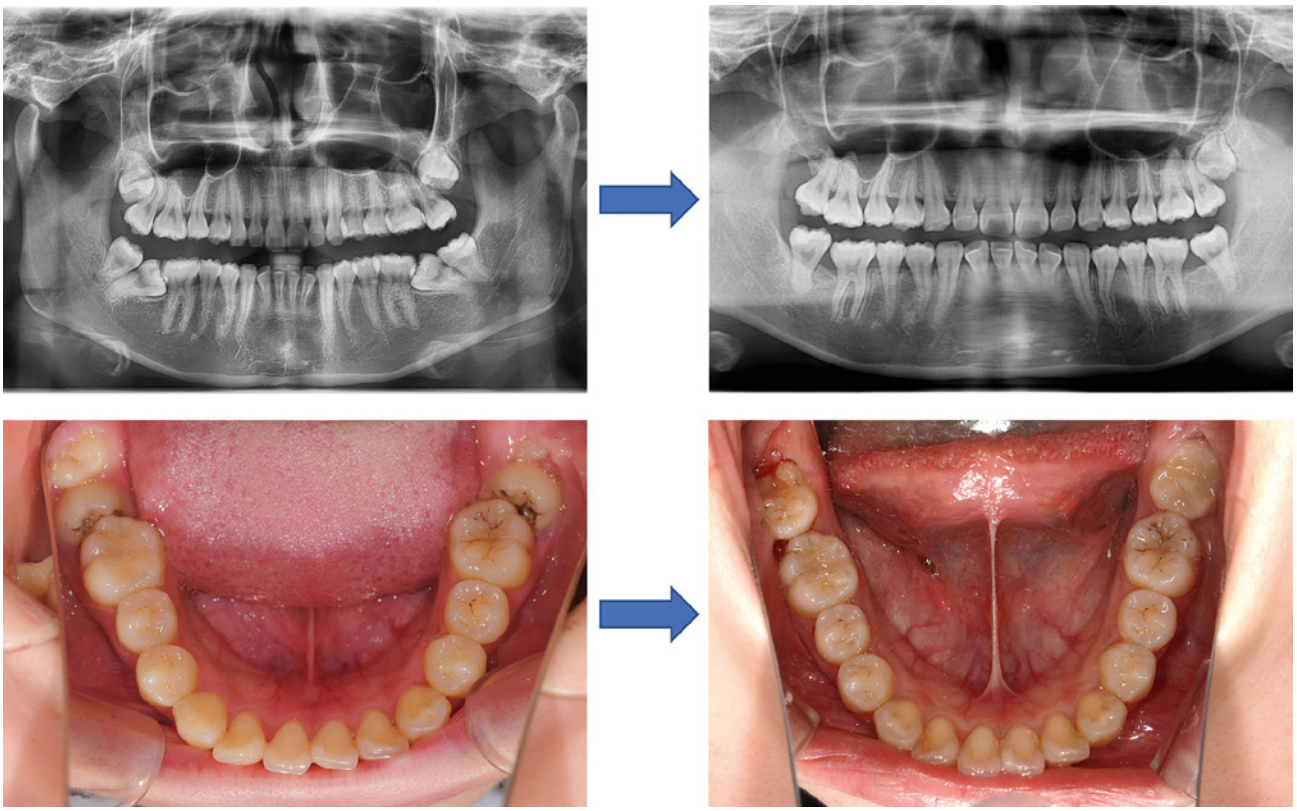


Figure 9.24 Successful treatment outcome. The bilateral mandibular second molars were successfully uprighted to the occlusal plane.

9.5.2 Orthodontic Traction of a Vertically Impacted Mandibular Second Molar

A 16-year-old male adolescent sought orthodontic treatment with a chief complaint of a missing tooth in his lower left quadrant. As displayed in Figure 9.25, clinical and radiographic examinations indicated a vertically impacted mandibular left second molar, with the adjacent third molar lying on its occlusal side. His bilateral canine and molar relationships were class II, with mild crowding in both arches.

The treatment plan was a two-stage orthodontic treatment. The first stage was to extract the mandibular left third molar and place a mini-implant at the left mandibular ramus region for orthodontic traction of the impacted second molar.

Following extraction of the mandibular left third molar, surgical exposure of the mandibular left second molar was performed to expose the whole contour of the second molar crown, so that the bony resistance was adequately removed. Then, a lingual button was bonded onto the occlusal surface of the second molar and a mini-implant was placed at the left mandibular ramus region. An elastic powerchain was applied between the lingual button and the ramus mini-implant to offer traction force for the impacted second molar. The orthodontic traction progressed smoothly and efficiently (Figure 9.26). Finally, the second molar was successfully tractioned and extruded to the occlusal plane, with good root parallelism (Figure 9.27).

9.5.3 Traction of a Lingually Angulated Impacted Mandibular Second Molar

A 20-year-old male presented with a chief complaint of anterior cross-bite. Clinical examinations revealed that the patient had anterior cross-bite and class III canine and molar relationships on both sides. Radiographic examinations indicated a lingually inclined impacted mandibular left second molar, with a mesially tipped adjacent third molar (Figure 9.28). The treatment plan was to extract the mandibular left third molar and upright the lingually inclined deeply impacted mandibular left second molar.

From the biomechanics perspective, the desired force vector should be distal, buccal and occlusal. Biomechanics generated from a ramus mini-implant was desirable for

t.me/Dr_Mouayyad_AlbtousH

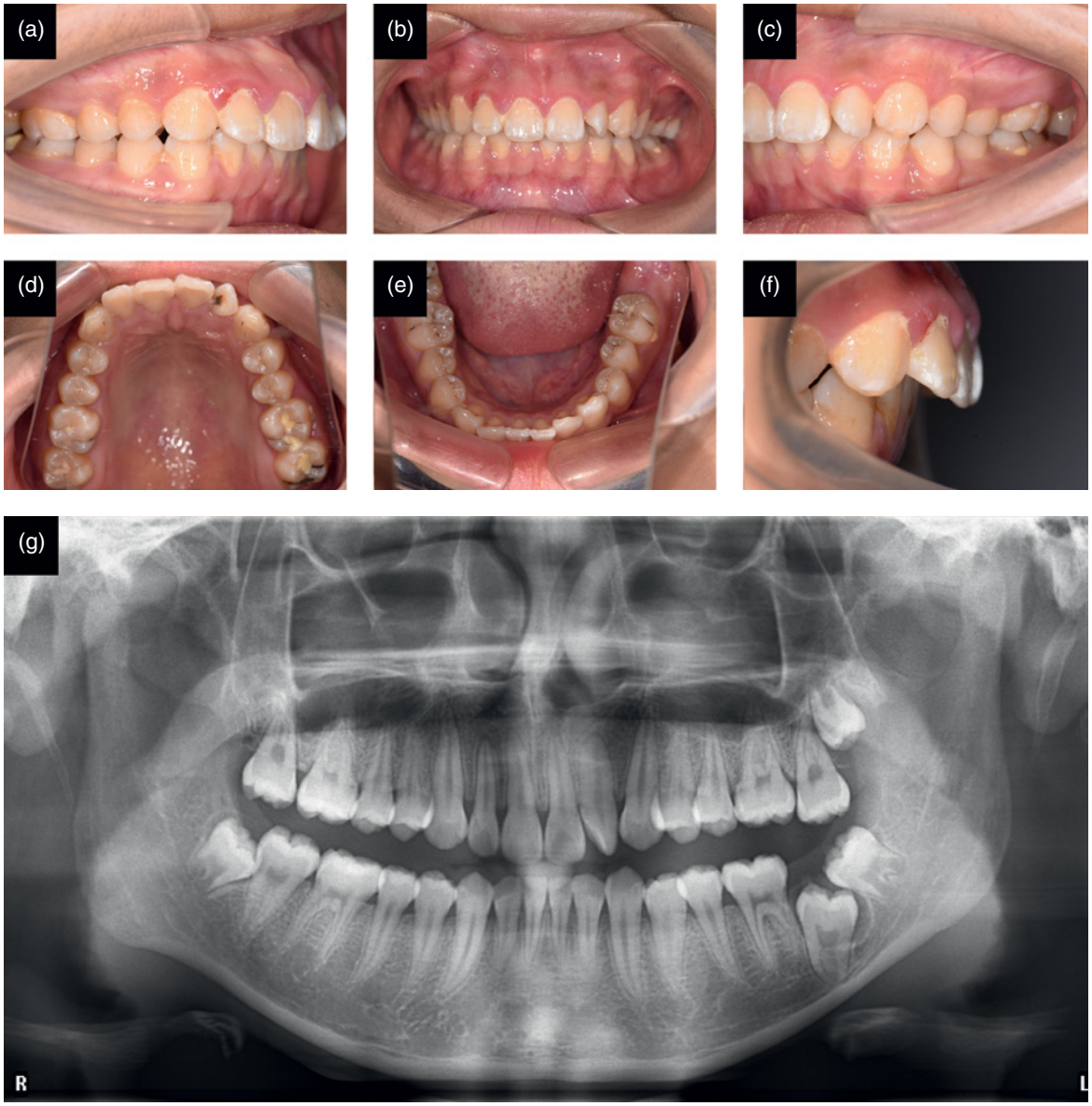


Figure 9.25 (a–f) Pretreatment intraoral photographs. The mandibular left second molar could not be observed intraorally. (g) Pretreatment panoramic radiograph revealed that the mandibular left second molar was deeply impacted with the adjacent third molar lying on its occlusal side.

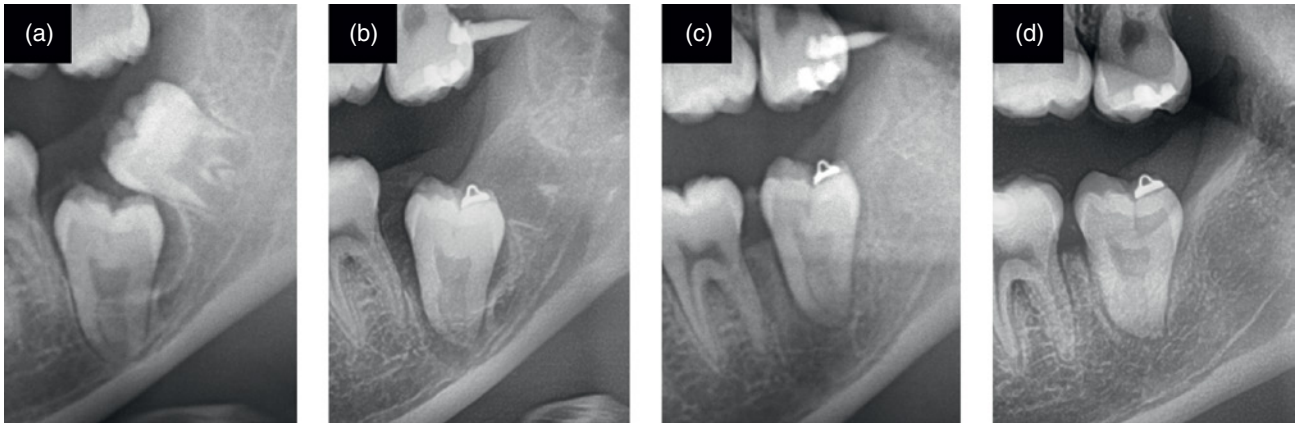


Figure 9.26 The impacted second molar was tractioned efficiently. (a) Pretreatment. (b,c) After extraction of the third molar, the second molar was tractioned through a mini-implant in the mandibular ramus. (d) The impacted second molar was extruded to the occlusal plane successfully.

t.me/Dr_Mouayyad_AlbtousH

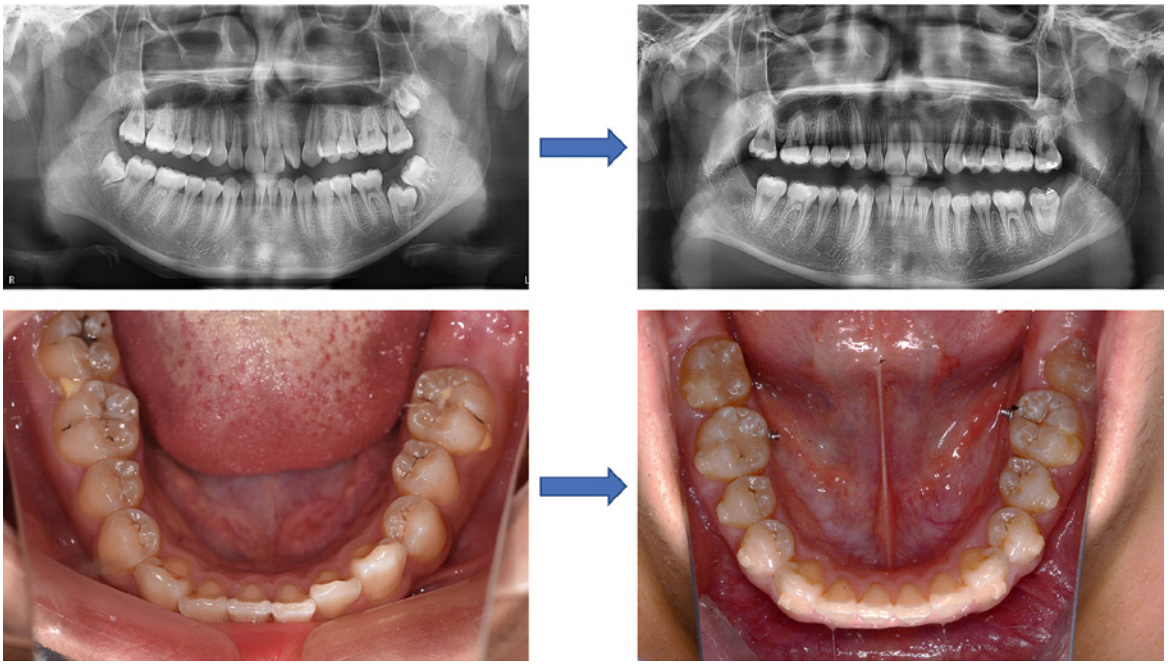


Figure 9.27 Treatment outcome. The impacted second molar was tractioned to the occlusal plane successfully with good root parallelism.

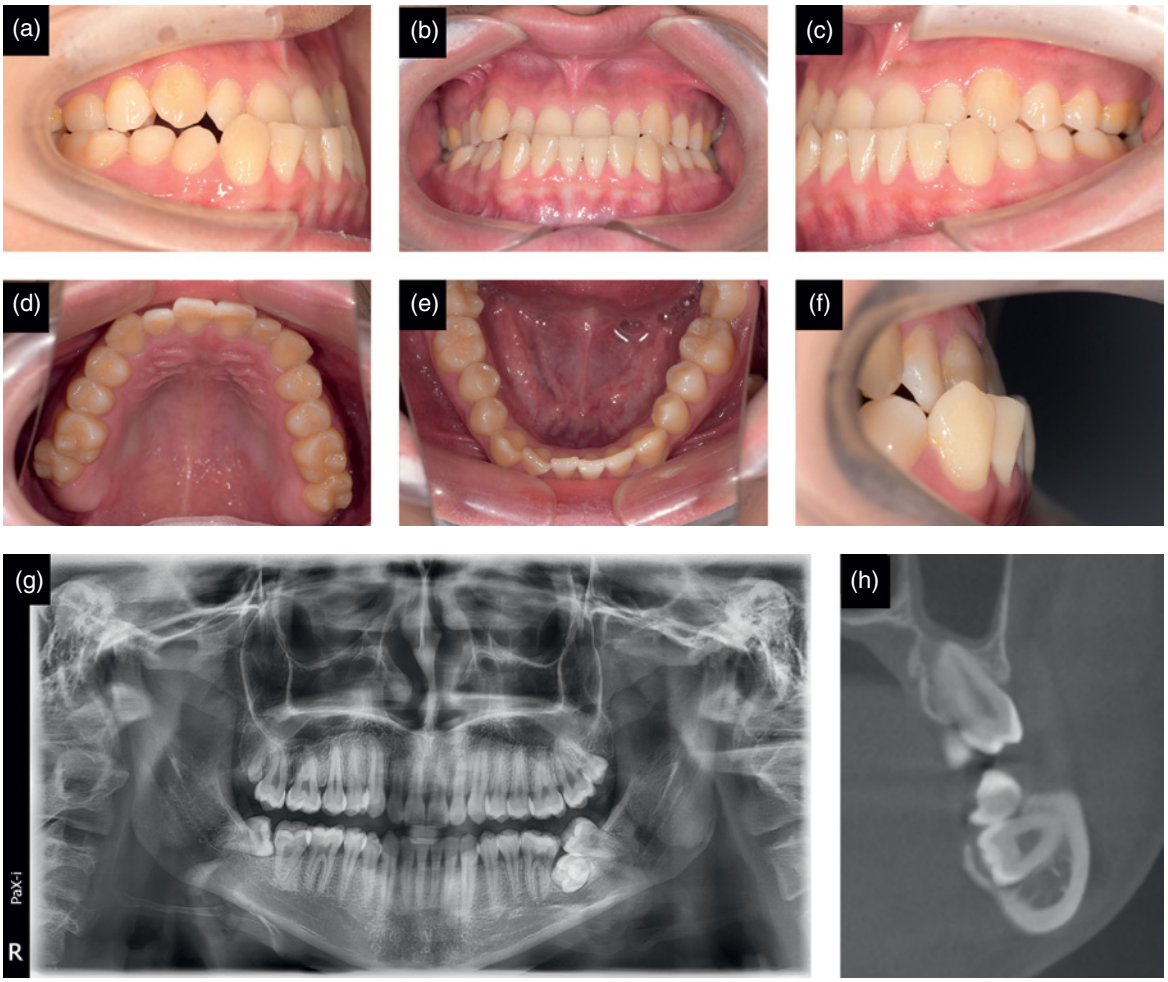


Figure 9.28 (a–f) Pretreatment intraoral photographs. The patient had anterior cross bite and class III canine and molar relationships on both sides. (g,h) The mandibular left second molar was impacted beneath the adjacent third molar that was mesially tipped.

t.me/Dr_Mouayyad_AlbtousH

orthodontic traction of the impacted second molar. Thus, the treatment plan was a combination of orthognathic surgery and orthodontic treatment. The orthodontic treatment included extraction of the maxillary first premolars, retraction of the maxillary anterior teeth, and aligning and levelling of the mandibular dental arch. The specific treatment plan for traction of the impacted second molar was to extract the mandibular left third molar and upright the impacted second molar with the aid of a ramus mini-implant.

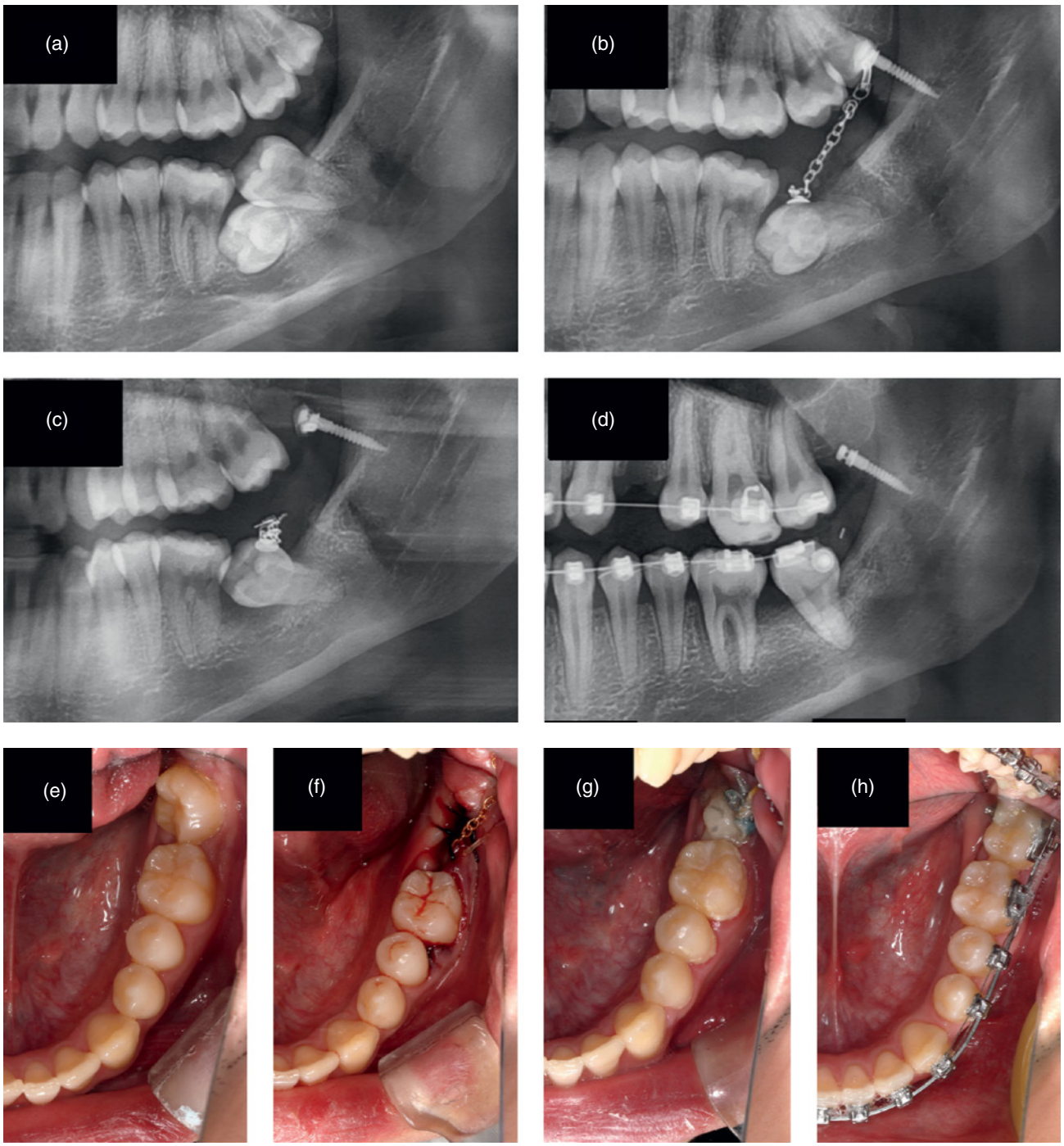


Figure 9.29 (a,e) Pretreatment. (b,f) A mini-implant was placed at the left mandibular ramus region and a gold chain was bonded onto the second molar crown. A closed-coil spring and elastic powerchain were applied for uprighting the second molar. (c,g) The gold chain and closed-coil spring were removed. (d,h) The lingually inclined impacted second molar was uprighted.

t.me/Dr_Mouayyad_AlbtousH

The mandibular left third molar was extracted under local anaesthesia, followed by surgical exposure of the adjacent second molar. To eliminate bone resistance in the process of orthodontic uprighting, the whole contour of the second molar crown was sufficiently exposed and a lingual button was bonded onto the crown of the second molar. Then, a mini-implant was inserted at the left mandibular ramus region, and a closed-coiled spring and an elastic powerchain were applied between the lingual button and the mini-implant to upright the deeply impacted second molar. The uprighting process progressed smoothly and the treatment results were satisfactory (Figures 9.29 and 9.30).

9.5.4 Traction of a Mandibular Third Molar Away from the Inferior Alveolar Canal[6]

A 25-year-old male complained of tooth crowding. The clinical and radiographic examinations indicated moderate crowding in both upper and lower arches. In particular, the mandibular left third molar was deeply impacted with a supernumerary tooth on the occlusal side (Figure 9.31). Before orthodontic treatment, extraction of the mandibular left third molar and the supernumerary tooth was planned. However, since the root of the mandibular left third molar penetrated into the inferior alveolar nerve canal, there would be a high risk of nerve injury during extraction (Figure 9.32). Thus, a treatment plan was made for orthodontic extrusion of the deeply impacted third molar away from the nerve canal before surgical extraction.

As displayed in Figure 9.33, following flap elevation under local anaesthesia, the supernumerary tooth was extracted and the mandibular left third molar was surgically exposed. Then, a lingual button was bonded onto the third molar and a mini-implant was placed at the left mandibular ramus region. Both elastic powerchain and closed-coil spring were applied for orthodontic extrusion of the impacted third molar.

Following orthodontic extrusion for four months, the third molar was successfully moved away from the nerve canal (Figure 9.34). Then, surgical extraction of the mandibular left third molar was performed and no sensory disturbance was reported by the patient (Figure 9.35). The whole procedure is illustrated in Figure 9.36.

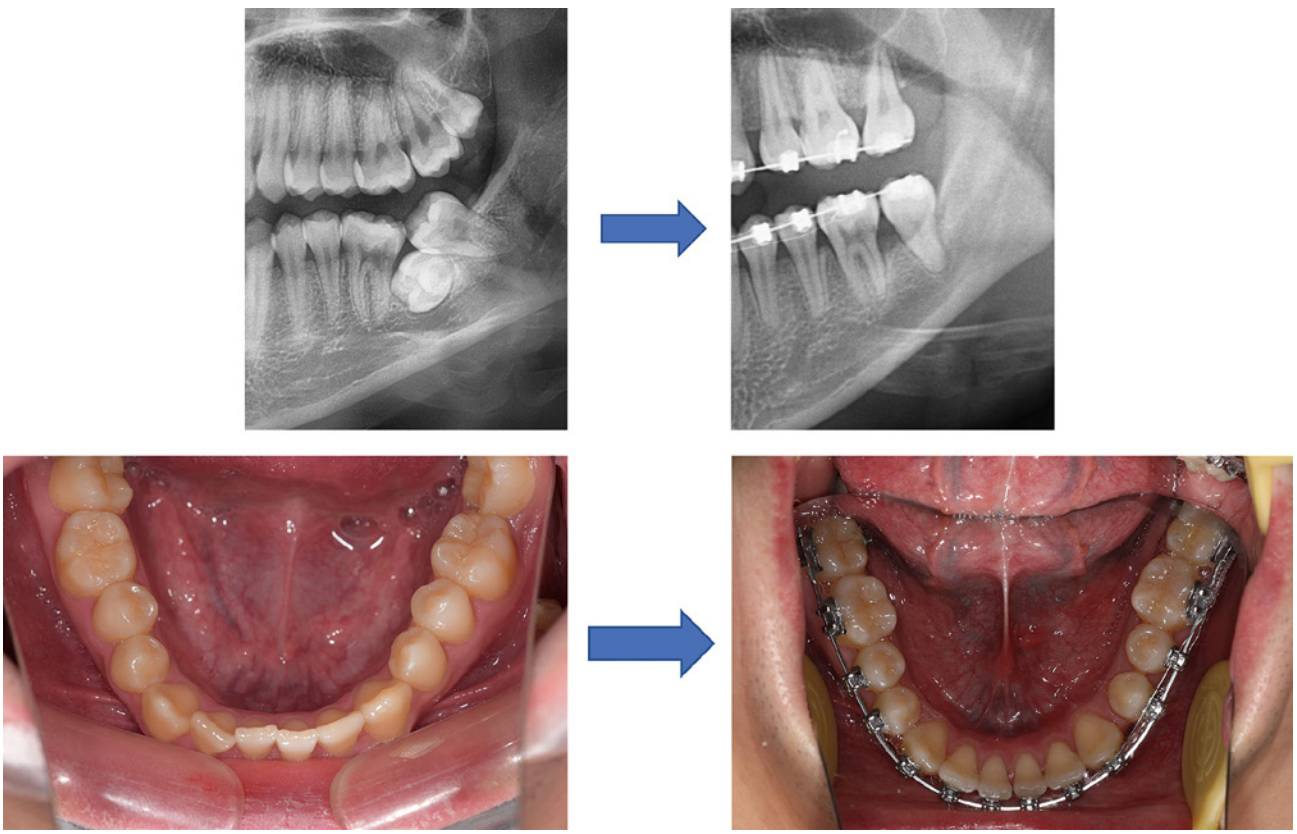


Figure 9.30 The deeply impacted mandibular left second molar was uprighted successfully with the aid of a ramus mini-implant.

t.me/Dr_Mouayyad_AlbtousH

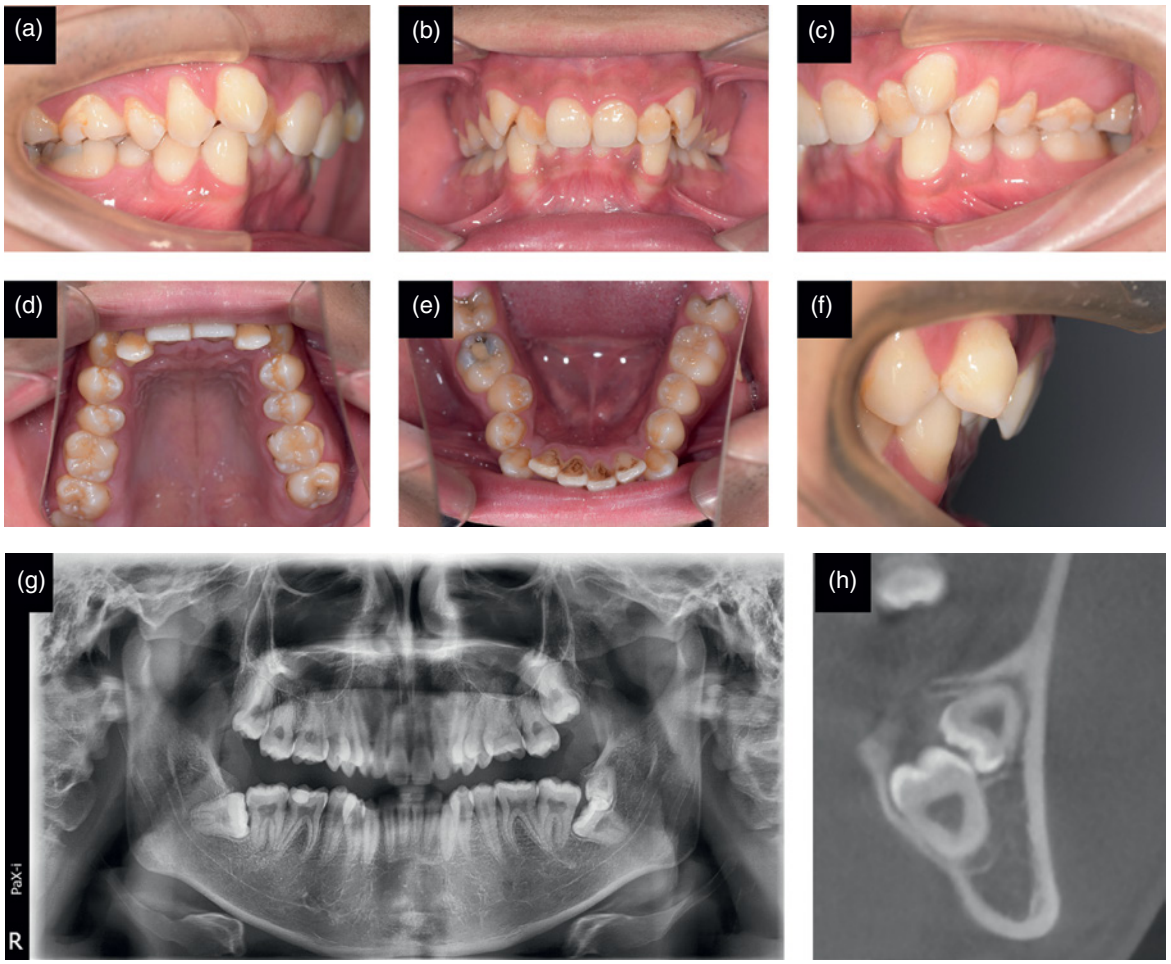


Figure 9.31 (a–f) Pretreatment intraoral photographs. (g) Panoramic radiograph indicates that the patients had a deeply impacted mandibular left third molar that was in contact with the inferior alveolar nerve canal. A supernumerary tooth was present on the occlusal side of the mandibular left third molar. (h) CBCT image (coronal view) reveals that the root of the third molar impinged on the nerve canal. *Source:* Zhou et al. [6], with permission from Quintessence Publishing.

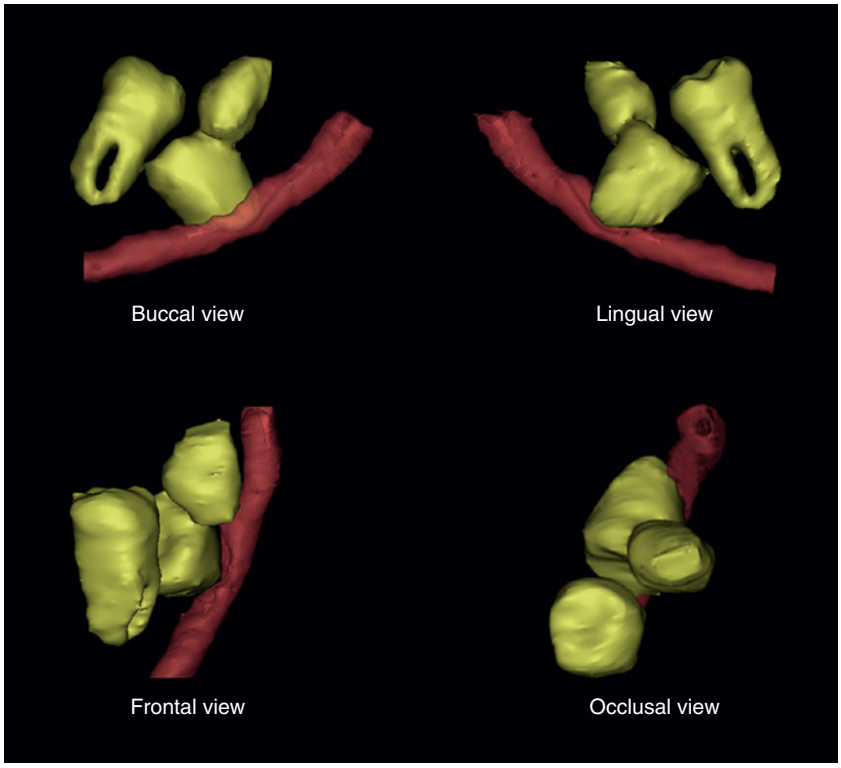


Figure 9.32 Three-dimensional reconstructed images of the spatial relationship between the tooth (38) and the inferior alveolar nerve canal. Note that the root of the third molar impinged on and penetrated into the nerve canal. *Source:* Zhou et al. [6], with permission from Quintessence Publishing.

t.me/Dr_Mouayyad_AlbtousH

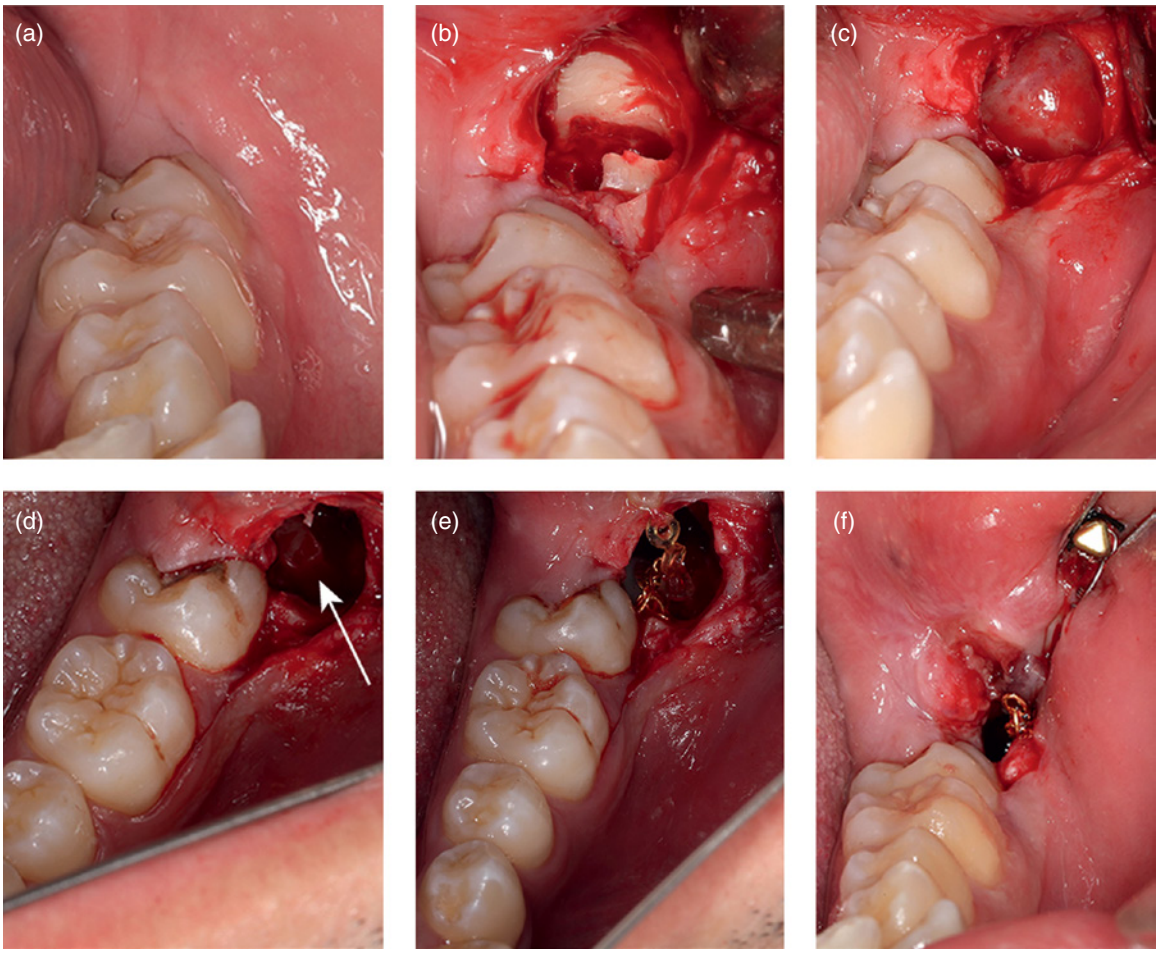


Figure 9.33 Surgical exposure and force loading through a ramus mini-implant. (a) Before surgery. (b) Following flap elevation, the supernumerary tooth was exposed and sectioned. (c) Removal of the supernumerary tooth. (d) Surgical exposure of the crown of the third molar (38) (white arrow). (e) A button was bonded onto the third molar crown (38). (f) A ramus mini-implant was inserted and an elastomeric chain was applied between the button and the mini-implant to offer traction force. *Source:* Zhou et al. [6], with permission from Quintessence Publishing.

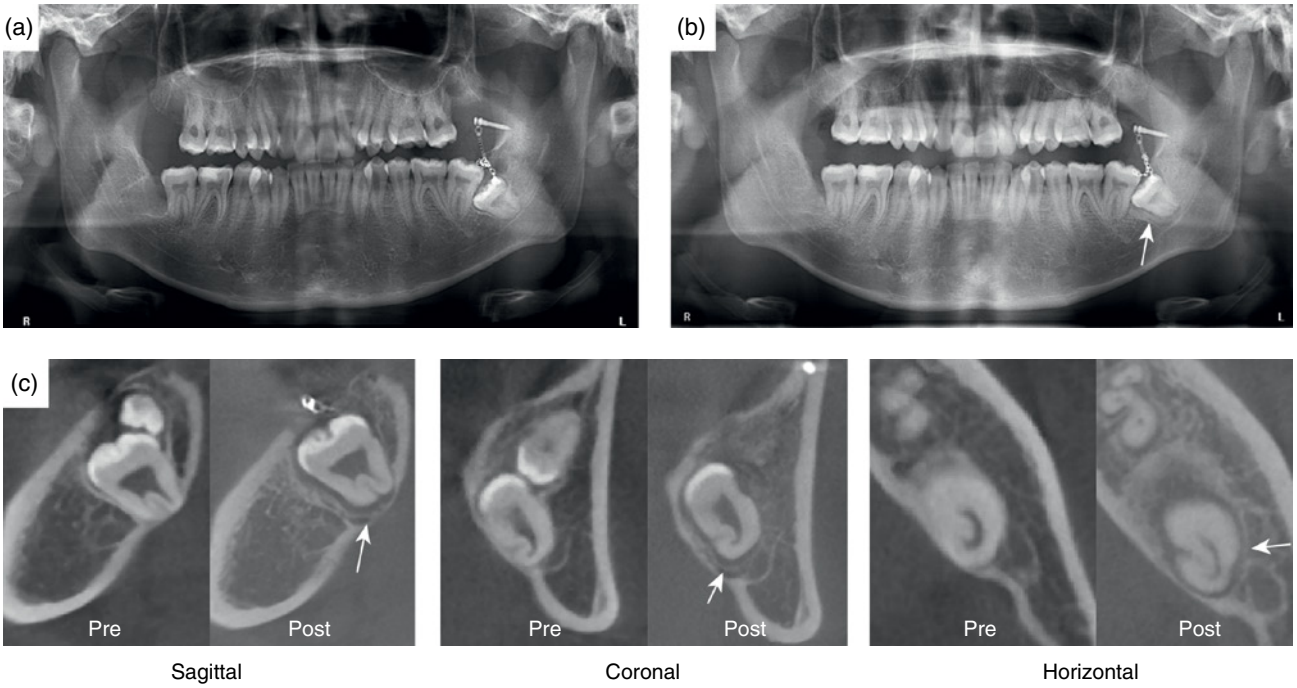


Figure 9.34 The spatial position changes of the third molar (38) before and after orthodontic traction. Note that the third molar (38) moved away from the nerve canal. (a) Panoramic radiograph showing the impacted third molar before orthodontic traction. (b) After orthodontic traction. (c) CBCT images with different section views showing the spatial relationship between the third molar and the nerve canal before versus after the orthodontic traction. *Source:* Zhou et al. [6], with permission from Quintessence Publishing.

t.me/Dr_Mouayyad_AlbtousH

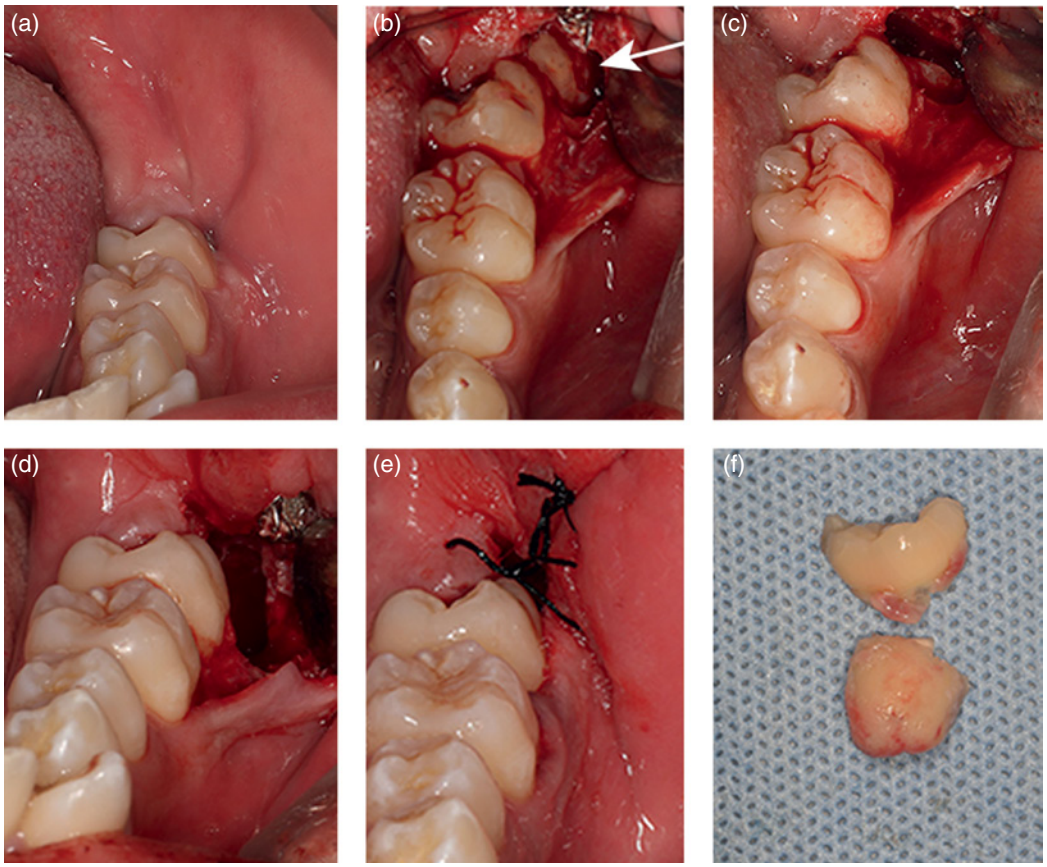


Figure 9.35 Surgical extraction of the third molar (38). (a) Before extraction. (b) Flap elevation and exposure of the third molar (38) (white arrow). (c) Crown sectioning of the third molar (38). (d) Removal of the whole tooth (38). (e) Primary suture. (f) The extracted third molar (38). *Source:* Zhou et al. [6], with permission from Quintessence Publishing.

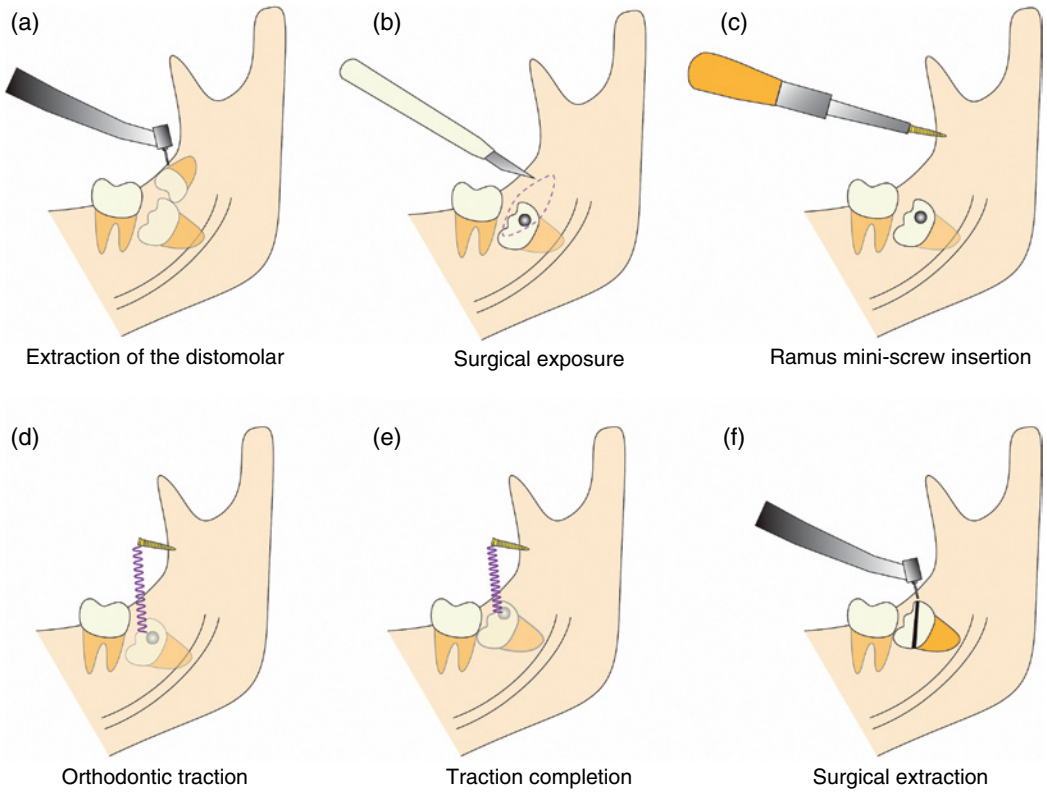


Figure 9.36 Schematic illustration of the orthodontic traction procedure. (a) Extraction of the supernumerary tooth. (b) Surgical exposure of the impacted third molar. (c) Insertion of a mini-implant into the ramus region. (d) Implementation of the orthodontic traction. (e) Following the orthodontic traction. (f) Extraction of the third molar. *Source:* Zhou et al. [6], with permission from Quintessence Publishing.

t.me/Dr_Mouayyad_AlbtousH

9.6 Summary

The mandibular ramus region is a bony platform located between the external and internal oblique ridges. We recommend that mini-implants (diameter: 2 mm; length: 12–14 mm) be inserted 4–6 mm medial to the external oblique ridge with an angulation of 30–45° with the sagittal plane at the height of 4–8 mm above the occlusal plane. Deeply impacted mandibular molars can be efficiently and predictably managed with mini-implants placed at the mandibular ramus region.

References

1 Mommaerts MY. (1998). Horizontal anchorage in the ascending ramus – a technical note. *Int. J. Adult Orthodont. Orthognath. Surg.* 13(1): 59–65.

2 Chang CH, Lin JS, Roberts WE. (2018). Ramus screws: the ultimate solution for lower impacted molars. *Semin. Orthodont.* 24(1): 135–154.

3 Chang C, Lin SY, Roberts WE. (2016). Forty consecutive ramus bone screws used to correct horizontally impacted mandibular molars. *Int. J. Orthod. Implant.* 41: 60–72.

4 Starch-Jensen T, Deluiz D, Deb S, Bruun NH, Tinoco EMB. (2020). Harvesting of autogenous bone graft from the ascending mandibular ramus compared with the chin region: a systematic review and meta-analysis focusing on complications and donor site morbidity. *J Oral Maxillofac. Res.* 11(3): e1.

5 Capelli M. (2003). Autogenous bone graft from the mandibular ramus: a technique for bone augmentation. *Int. J. Periodont. Restor. Dent.* 23(3): 277–285.

6 Zhou J, Hong H, Zhou H, Hua C, Yang Z, Lai W, Long H. Orthodontic extraction of a high-risk impacted mandibular third molar contacting the inferior alveolar nerve, with the aid of a ramus mini-screw. *Quintessence Int*. 2021; 52(6): 538–546.

t.me/Dr_Mouayyad_AlbtousH

10

The Placement of Miniplates

Lingling Pu[1,2], Yi Yang[1], Xuechun Yuan[1], Hu Long[1], and Chengge Hua[3]

[1] *Department of Orthodontics, State Key Laboratory of Oral Diseases and National Clinical Research Center for Oral Diseases, West China Hospital of Stomatology, Sichuan University, Chengdu, China*
[2] *Private Practice, Chengdu, China*
[3] *Department of General Dentistry, State Key Laboratory of Oral Diseases and National Clinical Research Center for Oral Diseases, West China Hospital of Stomatology, Sichuan University, Chengdu, China*

10.1 Introduction

The miniplate, an alternative form of orthodontic TADs, is often encountered in orthodontic practice (Figure 10.1). Anchored on skeletal bone by means of monocortical titanium screws, miniplates are indicated for orthopaedic traction to manage skeletal discrepancy (e.g. mandibular deficiency) without dental adverse effects among growing patients.[1-3] Moreover, they can be used as an alternative anchorage system when local requirements for mini-implant insertion are unsatisfactory (e.g. limited interradicular space) or as a back-up following the failure of mini-implants.

Unlike mini-implants, which are unable to withstand torsional force, miniplates can resist various types of force applications (e.g. torsional force and traction force) since they are fixed onto skeletal bone through two or three monocortical anchor screws. Well-designed biomechanics can ensure that stress is well distributed on each anchor screw, resulting in a lower failure rate of miniplates than mini-implants.[4] Thus, generally, miniplates are able to withstand force with a magnitude of 400–500 g.

Due to adequate length, the portion of a miniplate that is covered by soft tissue can be anchored apically to root apices with the other end being sufficiently exposed for force loading. This feature of miniplates helps to avoid potential root damage as well as reducing the likelihood of soft tissue irritation.

This chapter summarises the clinical features, clinical indications and insertion techniques of miniplates.

10.2 Clinical Features

10.2.1 Structure of Miniplates

The miniplate anchorage system consists of the miniplate and the corresponding anchor screws in two forms: self-tapping and self-drilling (Figure 10.2). Various shapes of miniplates are available for anatomical sites with different surface contours (Figure 10.3).

Functionally, the miniplate can be divided into three parts (Figure 10.4): the fixation part is the portion that is fixed onto the bone surface by anchor screws; the connecting part is the portion that connects the fixation part and the force-loading part; the force-loading part is the portion that penetrates the soft tissue and is exposed in the oral cavity for force application.

Depending on the quality and quantity of bone, two or three anchor screws are required for miniplate fixation. Thus, the fixation part has two or three holes through which the anchor screws can be inserted. As the diameter of the miniplate holes is between those of the screw body and the screw head, the miniplate can be fixed onto the bone surface through compression between the screw head and miniplate. The connecting part is covered beneath the soft tissue and may or may not have holes, depending on different designs. Conceivably, the connecting part with the hole design is less rigid than that without. The connecting part is continuous with the force-loading part that ends in a hook or similar configuration for functional force loading (Figure 10.5).

Clinical Insertion Techniques of Orthodontic Temporary Anchorage Devices, First Edition. Edited by Hu Long, Xianglong Han, and Wenli Lai.
© 2024 John Wiley & Sons Ltd. Published 2024 by John Wiley & Sons Ltd.

t.me/Dr_Mouayyad_AlbtousH

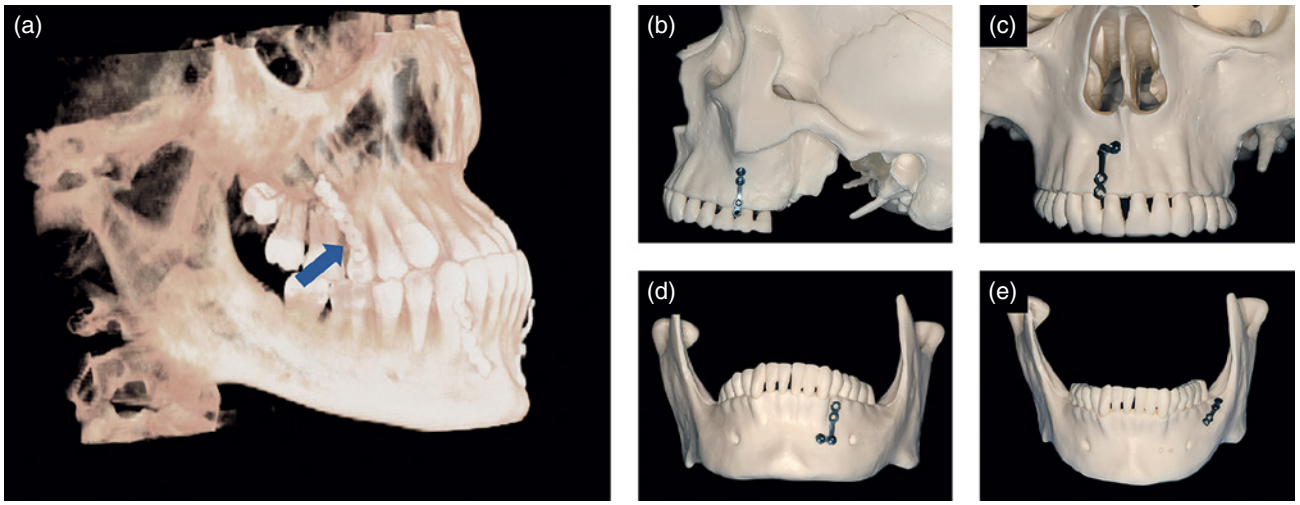


Figure 10.1 (a) Three-dimensional reconstruction image shows the miniplate placed at the zygomatic buttress (blue arrow). (b) A miniplate is inserted at the zygomatic buttress on a skull. (c) A miniplate is inserted at the piriform aperture. (d) A miniplate is inserted at the mandibular symphysis. (e) A miniplate is inserted at the retromolar region.

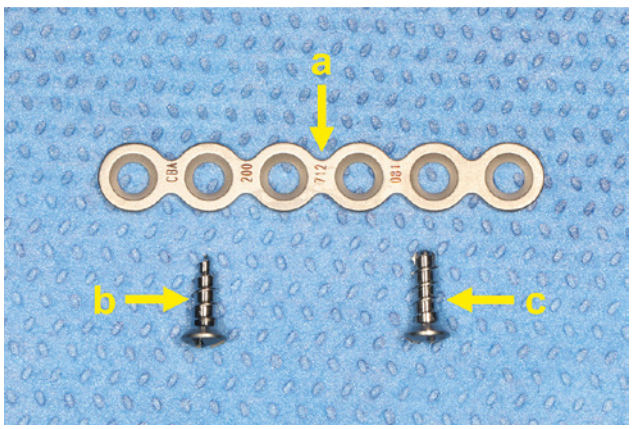


Figure 10.2 Miniplate anchorage system consists of miniplate and corresponding anchor screws. (a) Miniplate. (b) Self-drilling anchor screw. (c) Self-tapping anchor screw.

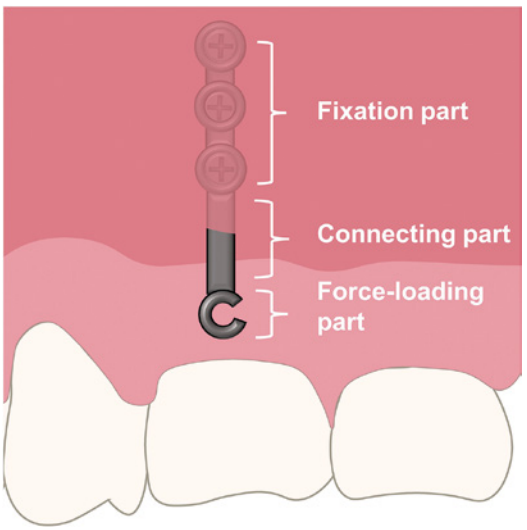


Figure 10.4 The miniplate can be divided into three continuous parts. The fixation part is the portion that is fixed onto the bone through anchor screws. The connecting part is the portion that connects the fixation part with the force-loading part that is exposed in the oral cavity and receives force loading.

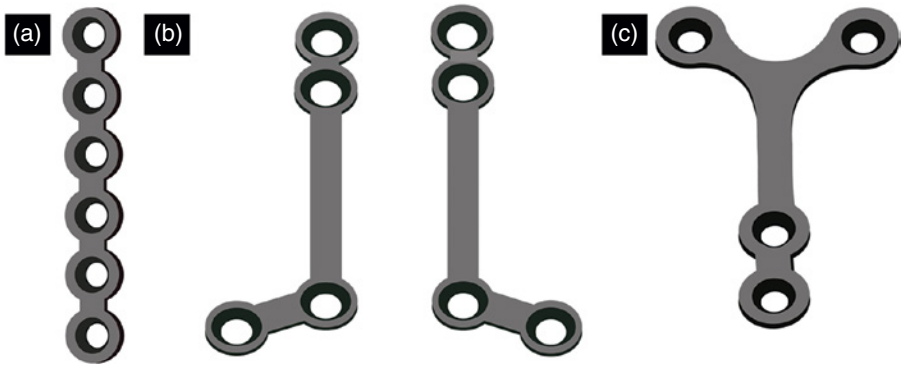


Figure 10.3 Various shapes of miniplates. (a) I-shaped miniplate. (b) L-shaped miniplates. (c) Y-shaped miniplate.

t.me/Dr_Mouayyad_AlbtousH

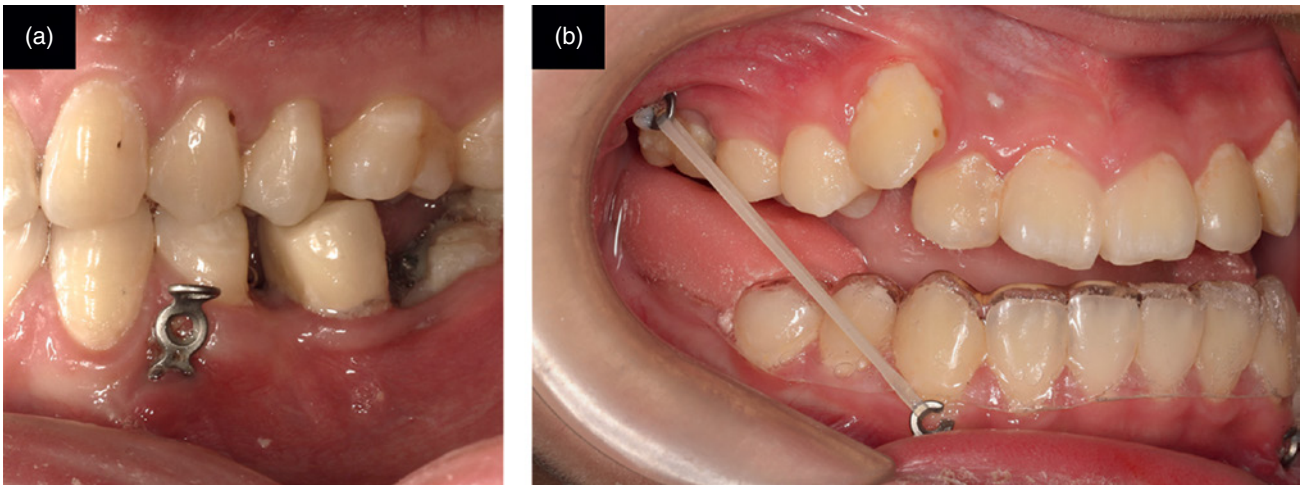


Figure 10.5 Force loading with miniplates. (a) The force-loading part of a miniplate was exposed in the oral cavity. (b) Heavy class III elastics were applied between two miniplates that ended in hooks as the force-loading parts.

10.2.2 Advantages and Disadvantages

The advantages and disadvantages of miniplates over mini-implants are summarised in Table 10.1. As miniplates are anchored onto skeletal sites through several monocortical screws, stress on miniplates generated by force applications can be well distributed onto the anchor screws. In turn, the anchor screws are fixed rigidly as a whole and can act as an anchorage for each other. Moreover, stress can be further distributed onto the bone surface through direct miniplate–bone contact. Thus, a miniplate system is able to tolerate orthopaedic force (400–500 g) or orthodontic force with simultaneous multiple vectors. In contrast, mini-implants can only resist orthodontic force (150 g) with no torsional moment.

As shown in Figure 10.6, the fixation part of miniplates is anchored onto subapical bone, where bone quality is better than interradicular alveolar bone. This may explain why miniplates have higher success rate than mini-implants.[4] Meanwhile, subapical insertion does not rely on the quality of soft tissue and is free from soft tissue limitations (e.g. insufficient width of attached gingiva). Thus, anatomical limitations of hard and soft tissues for mini-implants may not apply for miniplates, allowing miniplates to be placed at a broader range of anatomical sites than mini-implants.

As anchor screws are placed apically to root apices, the chance of root injury is largely reduced, resulting in a higher success rate than mini-implants. Moreover, as the anchor screws are away from dental roots, miniplates do not interfere with root movements, leading to a larger range of orthodontic tooth movements than mini-implants. Thus, miniplates are often indicated for orthodontic camouflage treatment for class II high-angle open bite cases demanding adequate molar intrusion.[5,6]

However, despite the advantages of miniplates, clinical application is limited by their higher cost and greater invasiveness than mini-implants. Specifically, the placement of miniplates is technique sensitive and demands collaborative teamwork of oral surgeons and orthodontists, which may lead to higher economic burden.

Table 10.1 Advantages and disadvantages of miniplates over mini-implants.

Type	Advantages	Disadvantages
Miniplates	Orthopaedic force (400-500 g)	Higher cost
	Low requirements of hard and soft tissues	Invasive surgery
	Larger range of orthodontic tooth movement	Technique-sensitive insertion
Mini-implants	Orthodontic force (150 g)	Biomechanical limitations
	Lower cost	High demands on hard and soft tissues
	Ease of insertion	

t.me/Dr_Mouayyad_AlbtousH

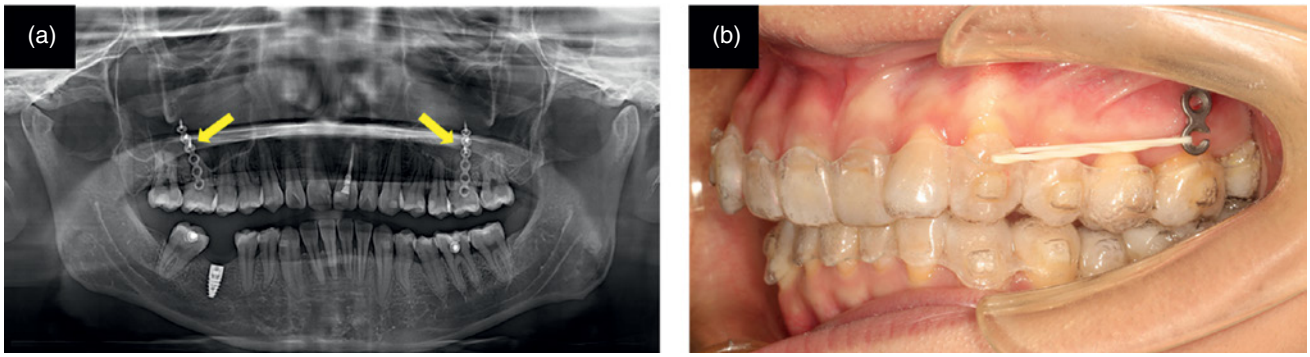


Figure 10.6 (a) Panoramic radiograph. The fixation parts of miniplates (indicated by yellow arrows) were fixed onto the subapical bone (zygomatic buttress). (b) The other end of the miniplate receives force loading. Specifically, an elastic rubber was applied between the canine aligner hook and the hook of the miniplate to aid in molar distalisation.



Figure 10.7 Flap surgery is required to place a miniplate.

Moreover, flap surgery is required to expose the subapical bone where anchor screws are inserted, which is more invasive than mini-implants (Figure 10.7). This may make both practitioners and patients reluctant to accept the use of miniplates.

10.2.3 Available Anatomical Sites

In clinical practice, available anatomical sites for miniplates are the piriform aperture, maxillary zygoma, mandibular symphysis and retromolar region (Figure 10.8). The anatomical requirements for both hard and soft tissues will be discussed below for each of these anatomical sites.

For the piriform aperture, miniplates are often placed at the lateral side, i.e. the lateral nasal wall. Generally, the hard and soft tissues satisfy the placement of miniplates at this region. However, since miniplates placed at this region are often used for maxillary protraction among patients in the mixed dentition phase, the positions of unerupted maxillary canines should be evaluated carefully prior to miniplate placement (Figure 10.9). Otherwise, tooth germs of unerupted canines may be injured.

For the maxillary zygoma, bone depth and cortical thickness should be assessed, especially for adolescents. The primary stability of anchor screws is enhanced with greater cortical thickness, while failure rate will be high if cortical thickness is less than 2 mm (Figure 10.10). Thus, cortical thickness of at least 2 mm is required for miniplate placement in the zygoma region. Moreover, the opening of the parotid gland should be detected during incision and flap elevation, and care should be taken to avoid injury of the duct of the parotid gland.

For the mandibular symphysis region, due to the high bone density and thick cortex, pilot drilling may be indicated to reduce the risk of screw fracture. Occasionally, incision and flap evaluation should be extended distally and special care should be taken to avoid injury of the mental nerve (Figure 10.11).

For the retromolar region, since the bone quality is good with adequate bone quantity, hard tissue requirements are often satisfied. Likewise, due to the thick cortex, pilot drilling may be indicated to reduce the likelihood of screw fracture.

t.me/Dr_Mouayyad_AlbtousH

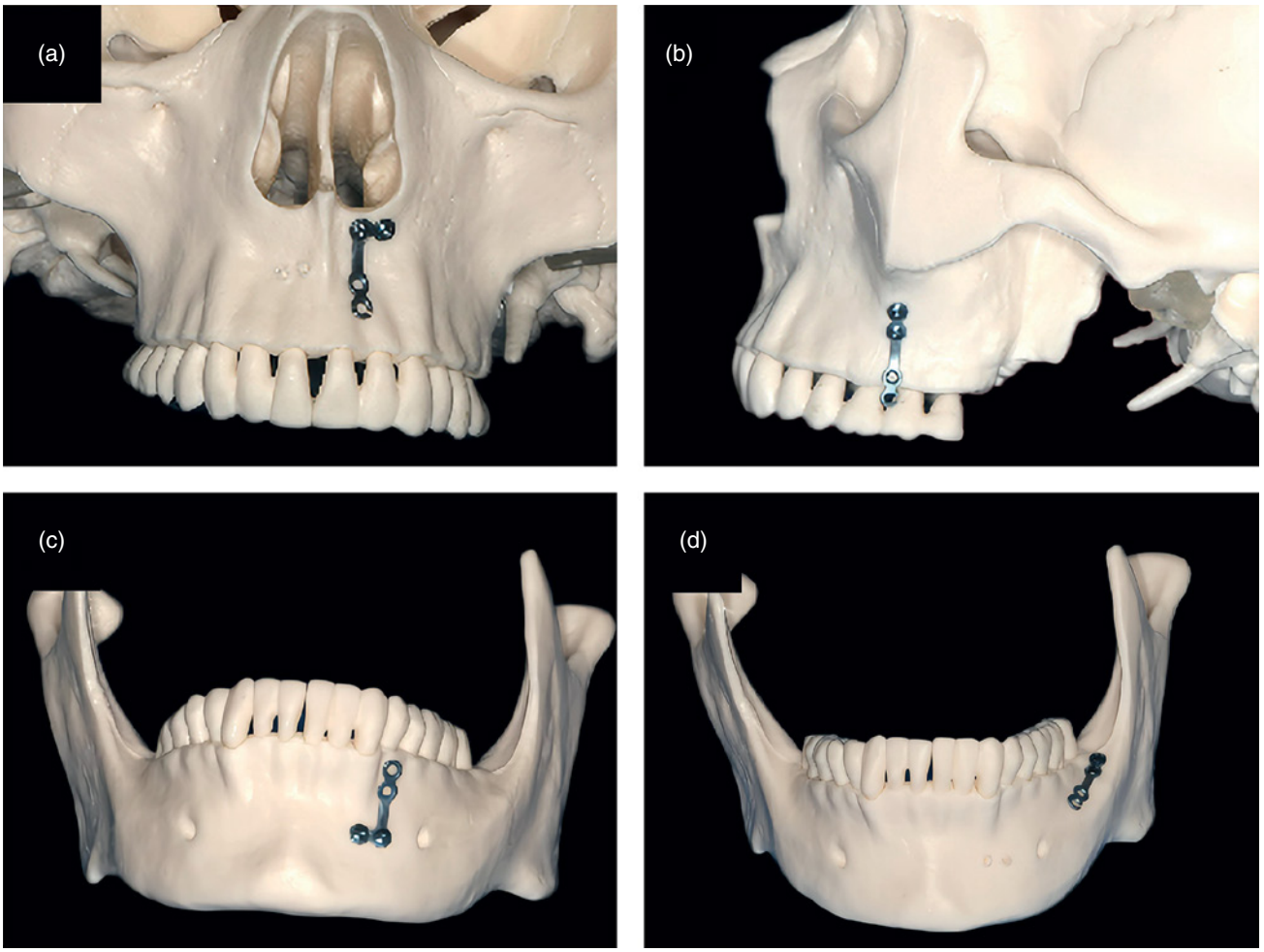


Figure 10.8 Available anatomical region for miniplates. (a) Piriform aperture. (b) Zygomatic buttress. (c) Symphysis region. (d) Retromolar region.



Figure 10.9 Unerupted canines are present in the piriform aperture region, making placement of miniplates at this region impossible.

t.me/Dr_Mouayyad_AlbtousH

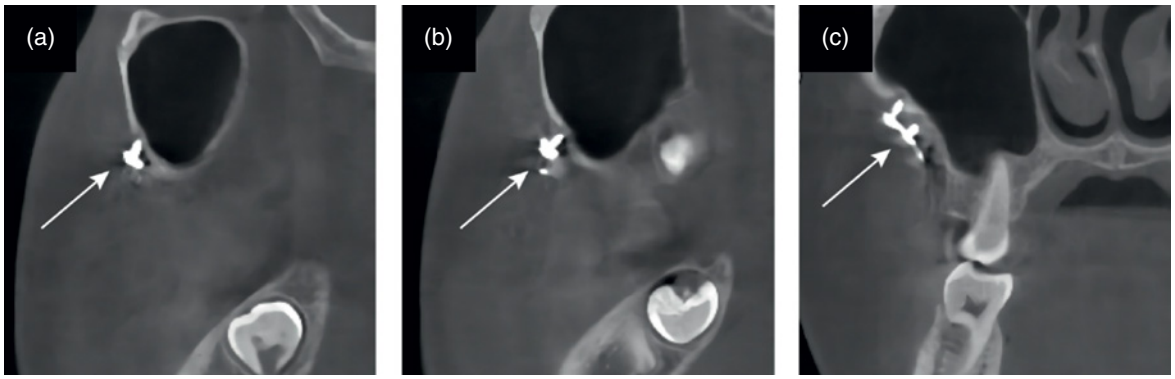


Figure 10.10 The influence of cortical thickness on miniplate stability. A miniplate was fixed at the zygomatic buttress region through three anchor screws. The cortical thickness was 1.4 mm, which was suboptimal for the insertion of anchor screws. Three months later, two anchor screws became mobile and the miniplate failed and had to be removed. (a,b) Sagittal view. (c) Coronal view. Note that the anchor screws were not firmly in contact with the bone.

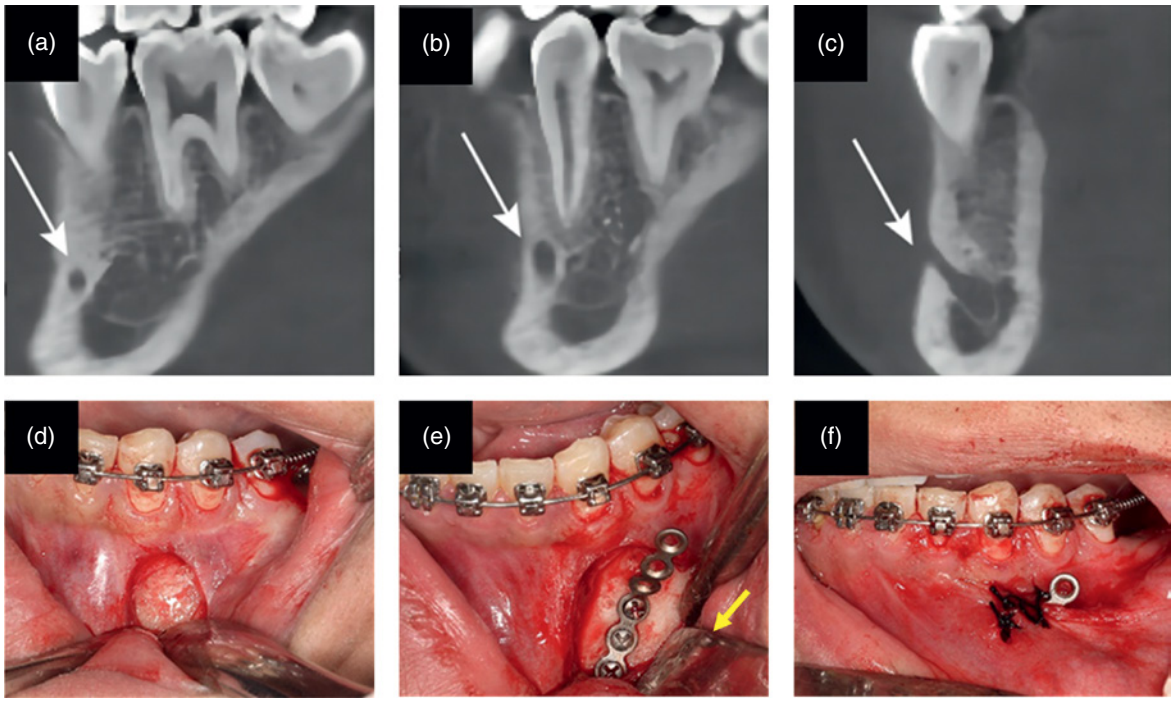


Figure 10.11 A miniplate was placed at the mandibular canine-premolar region. (a–c) CBCT images revealed that the mental foramen (white arrows) was located subapically between the first and second premolars. (d,e) Flap elevation was performed. Although the flap was extended distally, special care was taken not to injure the mental nerve. Periosteal elevators were meticulously used to retract the soft tissue distally and protect the mental nerve. (f) The flap was approximated and primary sutures were performed, leaving the force-loading part exposed in the oral cavity.

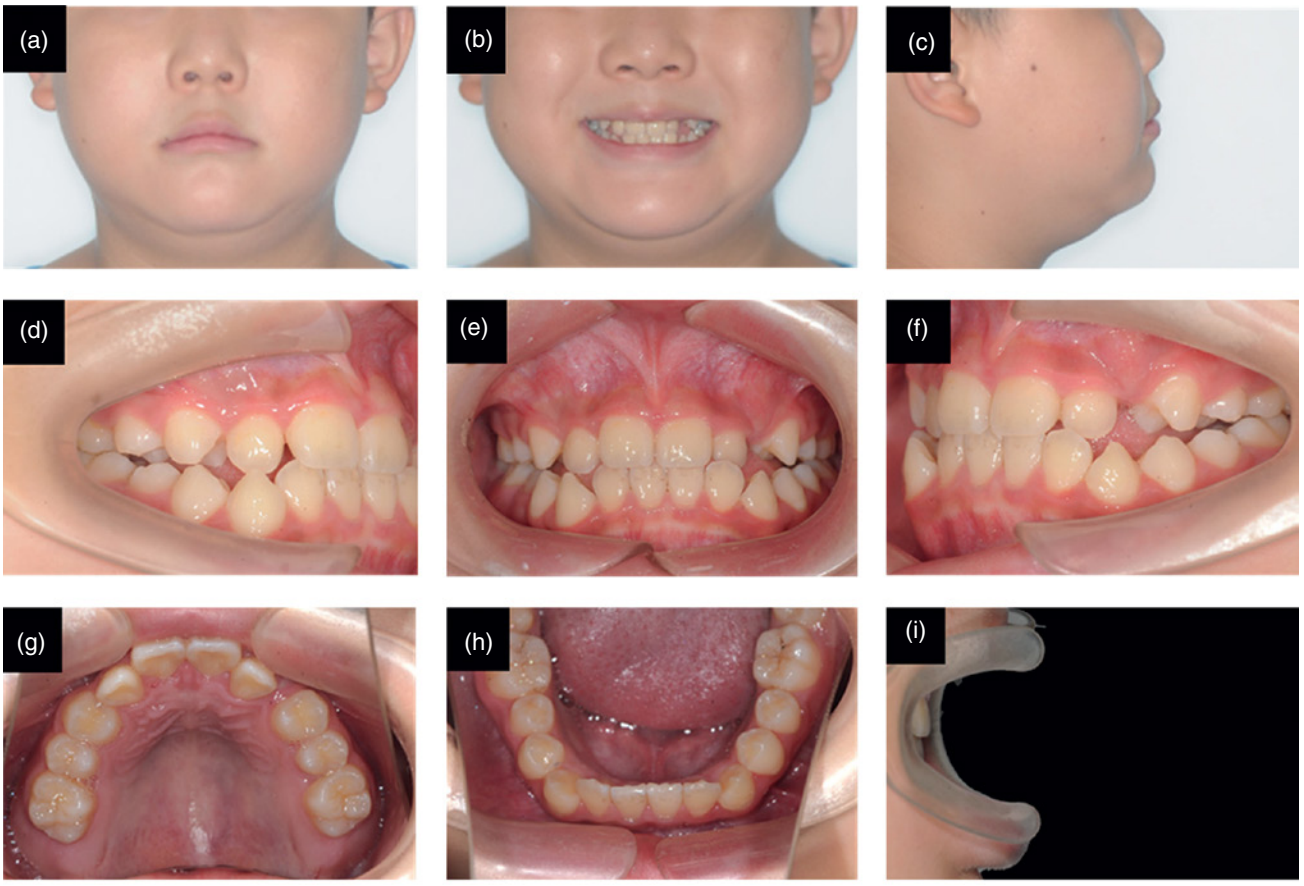
10.3 Clinical Indications

Due to their biomechanical superiority and low requirements on hard and soft tissues, miniplates are indicated in a variety of clinical situations and can achieve versatile orthopaedic and orthodontic movements. Clinical indications of miniplates will be displayed below.

10.3.1 Orthopaedic Treatment for Skeletal Discrepancy

Orthopaedic treatment is indicated for growing patients with skeletal discrepancy, especially for those before the growth spurt. By acting on skeletal sutures or growth centres, stimulation of jaw growth for the correction of

t.me/Dr_Mouayyad_AlbtousH



	Measurement	Norms	Value
Skeletal	SNA	83±3	84.3
	SNB	80±3	80.8
	ANB	3±1	3.5
	SN-MP	33±4	36.8
	Wits	−1±1	−3.7
Dental	U1-L1	125±7	136.3
	U1-SN	106±6	99
	L1-MP	97±6	87.9
Soft	UL-EP	0	−2.4
	LL-EP	0	−1.7

Figure 10.12 Pretreatment records. (a–i) Facial and intraoral photos demonstrate the concave profile and class III canine and molar relationships. (j) Lateral cephalometry. (k) Panoramic radiograph showing two unerupted maxillary canines.

skeletal discrepancy can be achieved through orthopaedic appliances. Conventional orthopaedic appliances utilise dentition and soft tissue as anchorage points to achieve desirable skeletal changes at the expense of dental adverse effects.[7,8] Thus, greater skeletal changes and fewer dental adverse effects can be obtained with absolute anchorage through miniplates.[1,9] The following case illustrates the clinical effectiveness of miniplates in maxillary protraction treatment for a growing patient.

A nine-year-old male sought orthodontic treatment with the chief complaint of edge-to-edge bite. As displayed in Figure 10.12, this patient had a concave facial profile with maxillary deficiency and obtuse nasolabial angle. He was in mixed-dentition phase with the upper two canines unerupted, which was evidenced on panoramic radiograph. Molar relationship was class III, with non-coincident upper and lower dental midlines. The lateral cephalometric radiograph revealed that ANB angle (3.5°) was normal

t.me/Dr_Mouayyad_AlbtousH

while Wits value (−3.7 mm) was indicative of class III skeletal base. This discrepancy may be attributed to the unstable N point in this patient. His upper incisors were within normal range (U1-SN: 99°) but lower incisors were retroclined (L1-MP: 87.9°). The treatment plan was maxillary protraction with the aid of an absolute anchorage system to obtain greater skeletal and fewer dental adverse effects. Thus, zygomatic miniplates were indicated for maxillary protraction for this patient.

Two miniplates were fixed onto the bilateral zygomatic bone with three anchor screws for each miniplate under local anaesthesia according to standard placement protocol that will be described explicitly below in the insertion techniques section. Maxillary protraction began two weeks following placement of miniplates. The patient was instructed to wear protraction elastics (400–500 g on each side) via facemask for 14 hours per day (Figure 10.13).

As displayed in Figure 10.14, following 18 months of active treatment, slight class II molar relationship with normal overjet and overbite was obtained. Clinically, the patient's pretreatment concave profile became a straight profile. Posttreatment ANB angle and Wits value were 5.6° and 2.3 mm. Upper and lower incisor labiolingual inclinations remained almost unchanged.

10.3.2 Anatomical Factors Undesirable for Mini-implants

As stated in Chapter 2, certain hard and soft tissue requirements should be satisfied for the placement of mini-implants. When anatomical requirements are undesirable for mini-implants, miniplates can serve as an alternative to fulfil the anchorage requirements. Two case examples are given below to demonstrate this clinical indication.

Case 1

The first case was a 30-year-old female patient with a chief complaint of crooked teeth. As presented in Figure 10.15, clinical and intraoral examinations were indicative of straight facial profile and bilateral class I molar relationship with moderate dental crowding. Lateral radiography revealed that the patient had class I skeletal base (ANB = 3.8), hyperdivergent profile (SN-MP = 42), lingual tipping of the upper incisors (U1-SN = 96) and normal inclination of the lower incisors (L1-MP = 92). Both the upper and lower third molars had erupted, except for the maxillary right one. Thus, the treatment plan was molar distalisation of both the upper and lower dentition through clear aligners with the aid of orthodontic mini-implants. Infrazygomatic and buccal mini-implants were planned to aid molar distalisation. However, as shown by the CBCT examinations, bone quality was inadequate for the placement of infrazygomatic mini-implants so zygomatic miniplates were indicated for this clinical situation.

The clear aligner treatment employed a sequential molar distalisation pattern (Figure 10.16) with elastic bands applied between precision cuts on aligners and the orthodontic TADs (miniplates for maxilla and mini-implants for mandible) (Figures 10.17 and 10.18). Specifically, the miniplates were placed at the zygomatic buttress region and the mini-implants were inserted at the buccal shelf region (Figure 10.19). Progress examinations revealed that molars had been distalised with spacing presented in the premolar regions, consistent with predicted tooth movements (Figure 10.20).

After 26 months of treatment, the first treatment stage was complete and bilateral molar class I relationship was maintained and crowding was resolved, with coincident upper and lower dental midlines (Figure 10.21).

Case 2

A 34-year-old male presented to the orthodontic department with a chief complaint of crooked teeth and one missing molar. Clinical and intraoral photos showed convex facial profile and moderate crowding in the upper arch and mild crowding in the lower dentition, with missing mandibular left first molar. Upper and lower dental midlines were inconsistent. Mandibular second and third molars were severely lingually inclined (Figure 10.22). The treatment plan was extractions of 14, 24 and 44 to resolve anterior crowding and correct dental midlines. For the lower left quadrant, molar uprighting and mesialisation was planned. The most difficult tooth movement for this patient was uprighting of the mandibular left second and third molars. One mini-implant was planned to be inserted at the left buccal shelf region to aid molar uprighting. However, as depicted in Figure 10.23, the simulation was indicative of root damage if a buccal mini-implant was inserted due to the severe lingual inclination of molars.

Since the anatomical requirements for mini-implant placement were not met, the placement of a miniplate was indicated. The miniplate was inserted buccally to the buccal shelf and aided molar uprighting with orthodontic elastics (Figure 10.24). With the aid of the miniplate, the uprighting of the mandibular left second and third molars progressed smoothly (Figure 10.25).

10.3.3 Biomechanical Advantages

As mentioned above, mini-implants cannot resist torsional force or multiple force vectors that may lead to loosening of

t.me/Dr_Mouayyad_AlbtousH

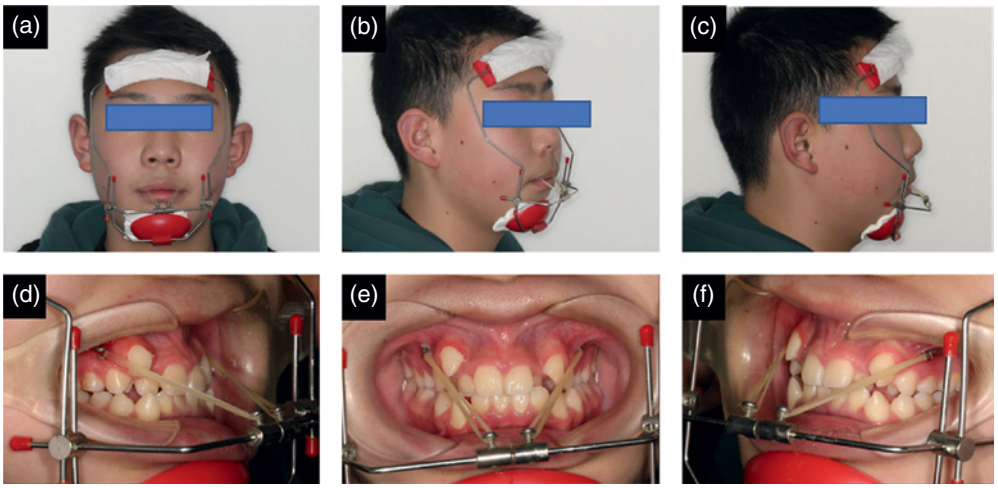
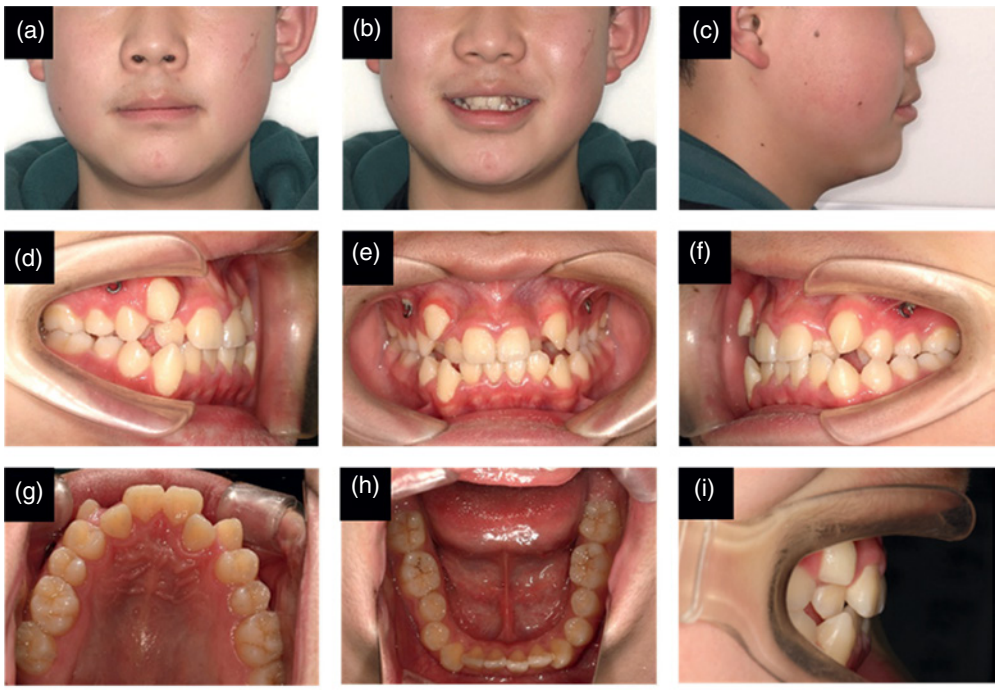
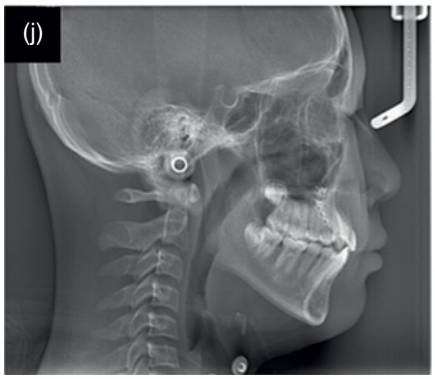


Figure 10.13 Two miniplates were placed at the zygomatic buttress region. Heavy protraction elastics (500 g on each side, for 14 h/day) were applied from the hooks of the miniplates to the protraction facemask.

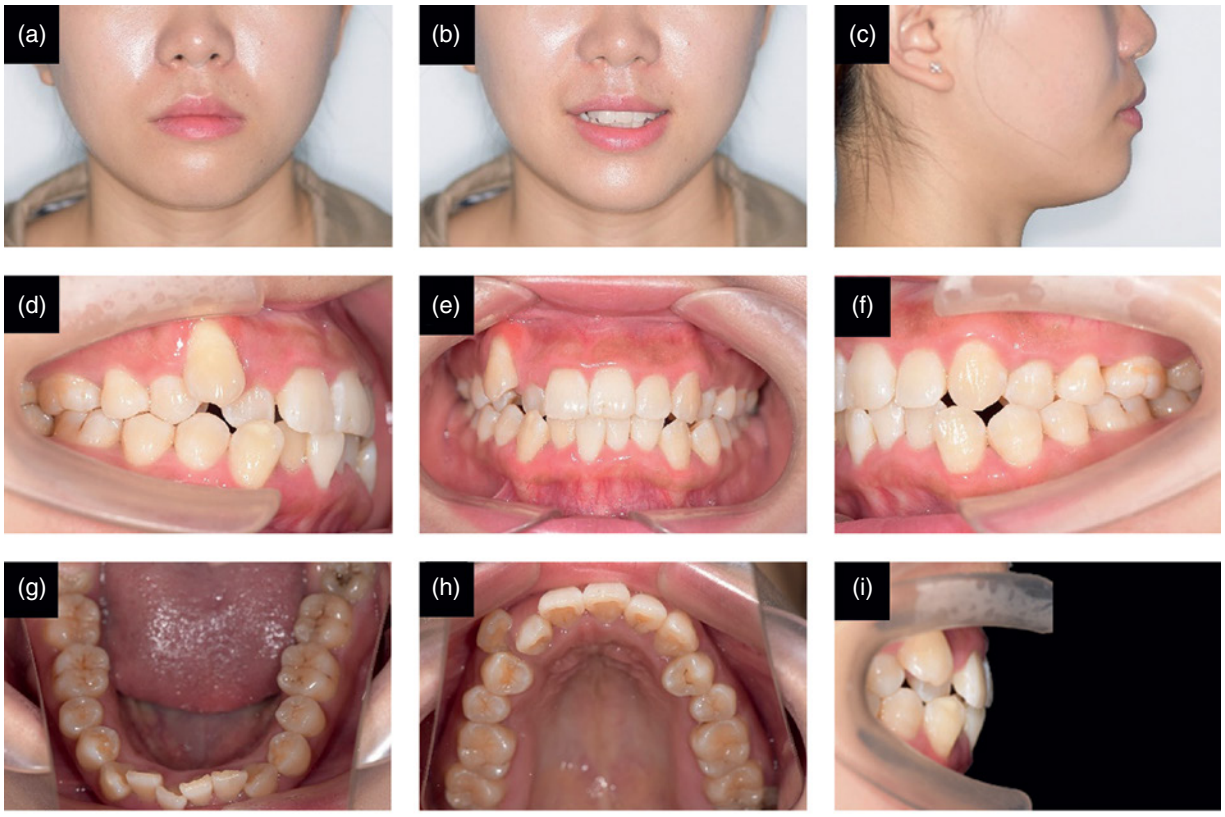




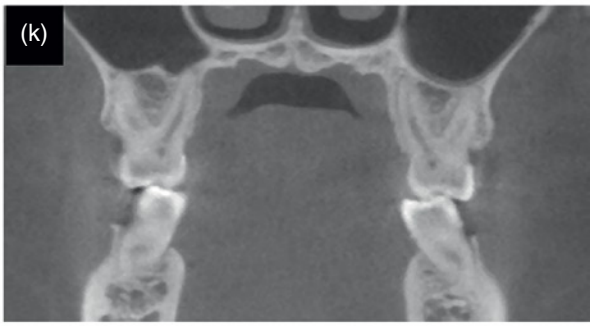
	Measurement	Norms	Pre-Value	Post-Value
Skeletal	SNA	83±3	84.3	87.4
	SNB	80±3	80.8	81.8
	ANB	3±1	3.5	5.6
Dental	SN-MP	33±4	36.8	37.1
	Wits	−1±1	−3.7	2.3
	U1-L1	125±7	136.3	132.0
	U1-SN	106±6	99	102.5
Soft	L1-MP	97±6	87.9	88.2
	UL-EP	0	−2.4	2.2
	LL-EP	0	−1.7	1.3

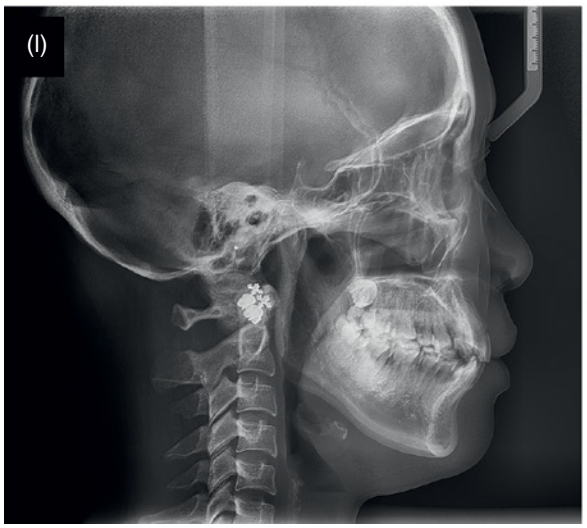
Figure 10.14 (a–i) Posttreatment records. The patient's profile was significantly improved and a straight facial profile was achieved. Class II molar relationship was achieved (slight overcorrection). (j) Lateral cephalometry. The SNA angle changed from 84.3° to 87.4°, indicating a significant maxillary advancement.

t.me/Dr_Mouayyad_AlbtousH









	Measurement	Norms	Value
Skeletal	SNA	83±4	77.0
	SNB	80±4	73.3
	ANB	3±2	3.8
	SN-MP	30±6	42.1
	Wits	0±2	–4.5
Dental	U1-L1	124±8	130.0
	U1-SN	106±6	95.6
	L1-MP	97±6	92.2
Soft	UL-EP	1±2	0.3
	LL-EP	2±2	2.5

Figure 10.15 Pretreatment records. (a–c) Pretreatment facial photographs. (d–i) Class I molar relationship on both sides, with moderate crowding in both arches. (j) Panoramic radiograph. (k) CBCT image (coronal view) indicated inadequate bone at the infrazygomatic crest region. (l) Lateral cephalometry.

t.me/Dr_Mouayyad_AlbtousH

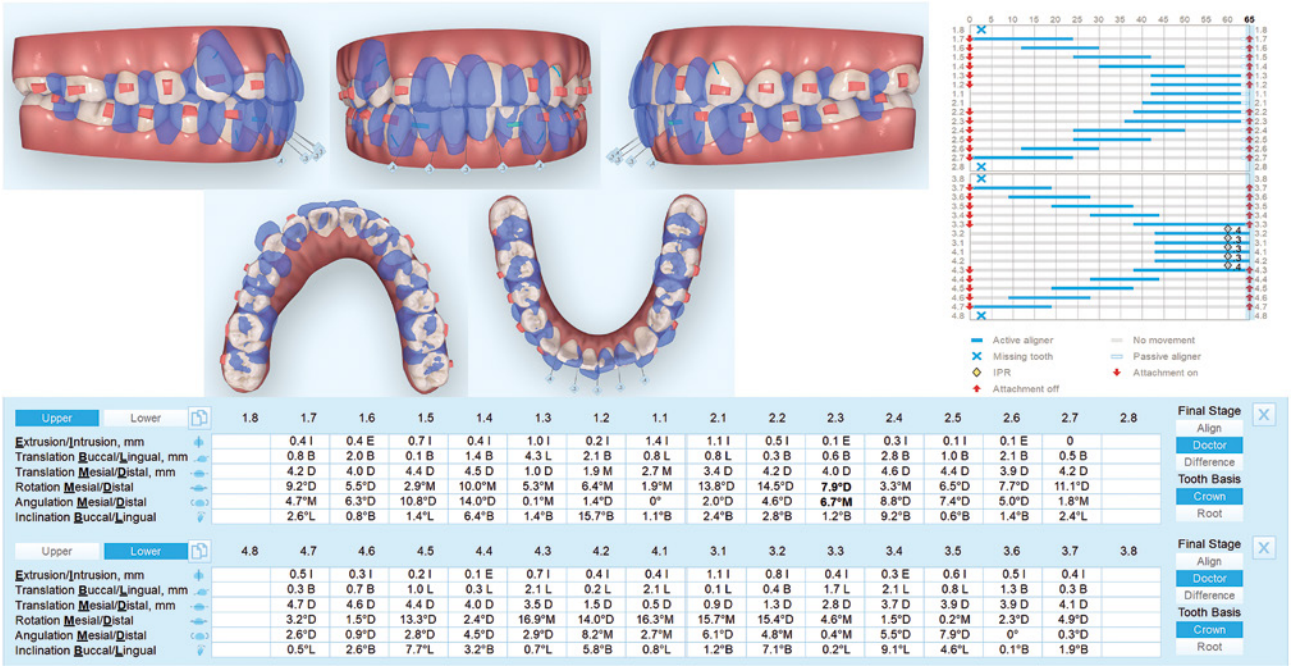


Figure 10.16 The clear aligner treatment protocol implemented a sequential molar distalisation pattern.

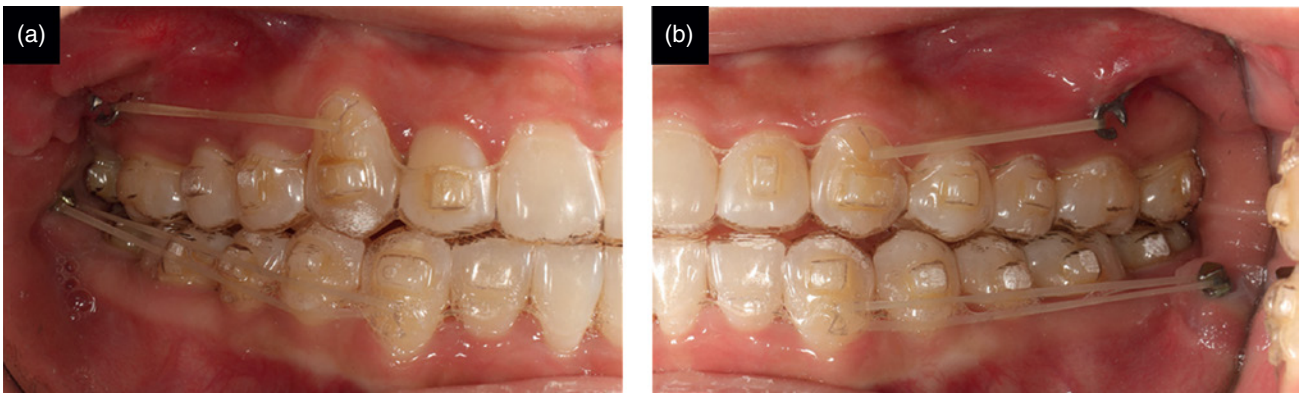


Figure 10.17 Orthodontic elastics were applied between aligner precision cuts at the canine regions and the TADs in the posterior regions. Miniplates were placed at the zygomatic buttress region for upper dentition distalisation and mini-implants were inserted at the mandibular buccal shelf region for lower dentition distalisation. (a) The right side. (b) The left side.

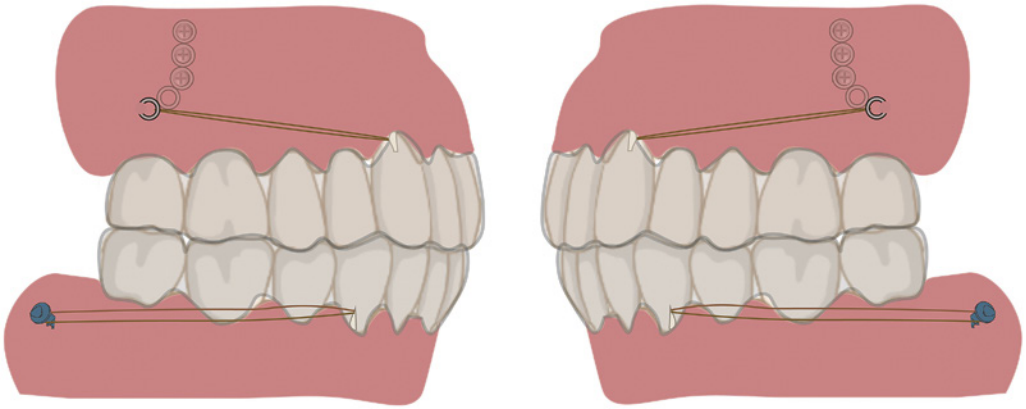


Figure 10.18 Schematic illustration showing miniplates placed at the zygomatic buttress and mini-implants inserted at the buccal shelf for molar distalisation with clear alingers.

t.me/Dr_Mouayyad_AlbtousH

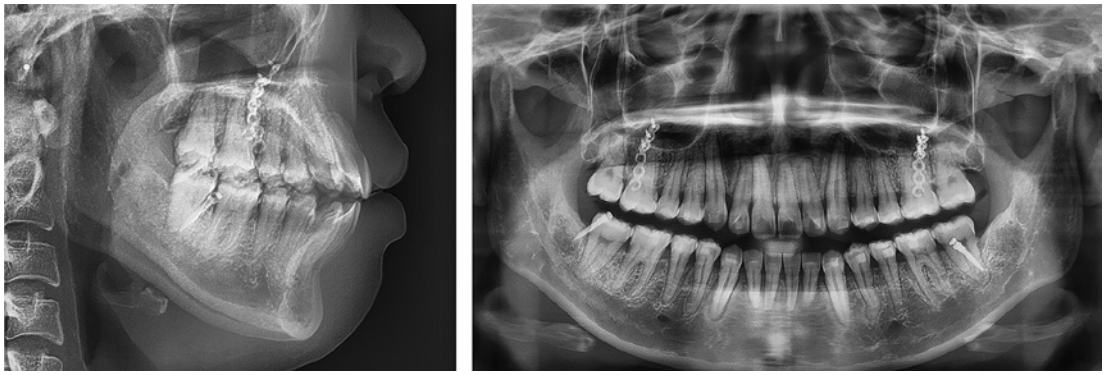


Figure 10.19 Radiographic images showing the miniplates and mini-implants.

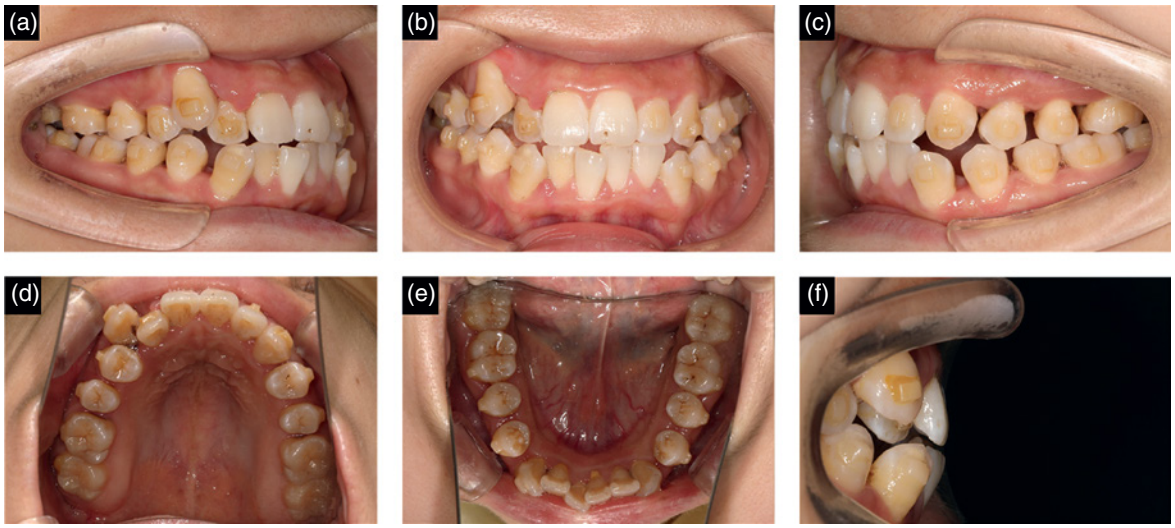


Figure 10.20 (a–f) Progress intraoral photographs. Both the upper and lower molars had been distalised, as evidenced by the spacing in the premolar region.

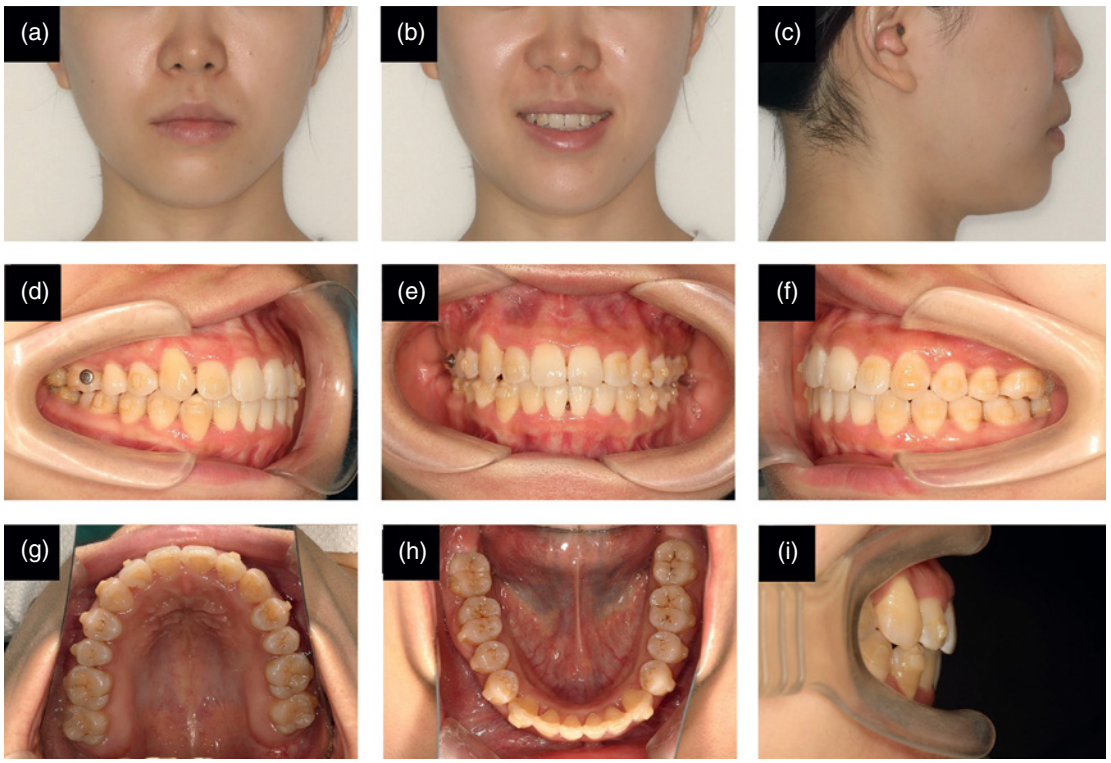


Figure 10.21 Treatment outcome after the first treatment stage. Bilateral canine and molar Class I relationship was achieved and dental crowding was resolved. (a–c) Facial photographs. (d–i) Intraoral photographs.

t.me/Dr_Mouayyad_AlbtousH

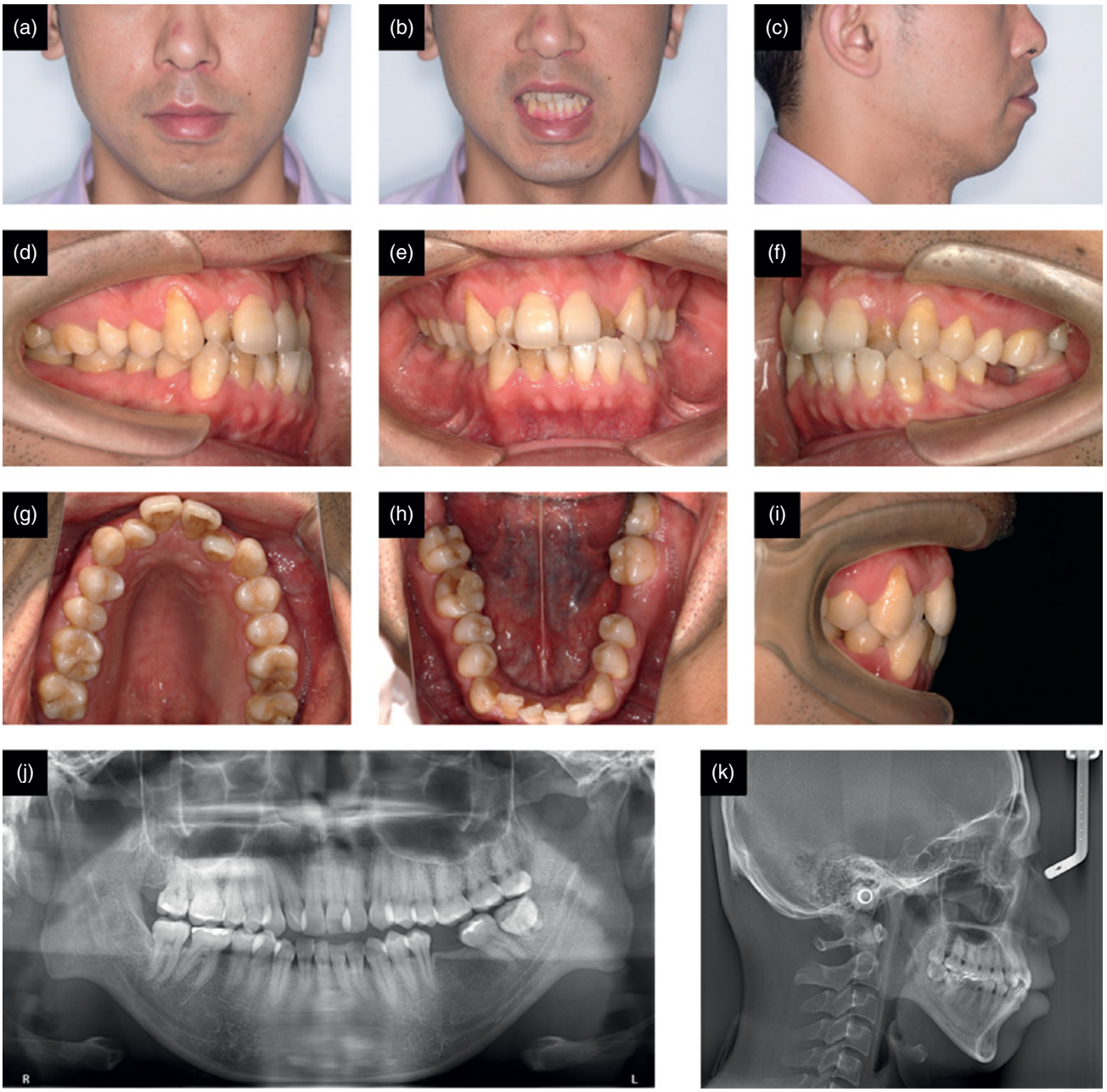
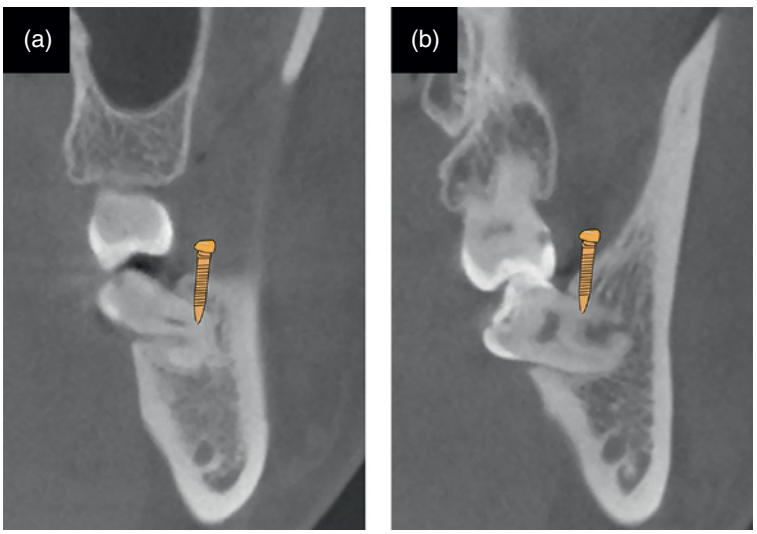


Figure 10.22 Pretreatment records. (a–c) Facial photographs. (d–i) Intraoral photographs showing dental crowding and missing mandibular left first molar. (j) Panoramic radiograph. (k) Lateral cephalometric image.

Figure 10.23 Simulation of placing a mini-implant at the buccal shelf region indicates the high risk of root injury by the mini-implant due to the severe lingual tipping of the mandibular molars. (a) CBCT image (coronal view) showing the second molar region. (b) CBCT image (coronal view) demonstrating the third molar region.



t.me/Dr_Mouayyad_AlbtousH

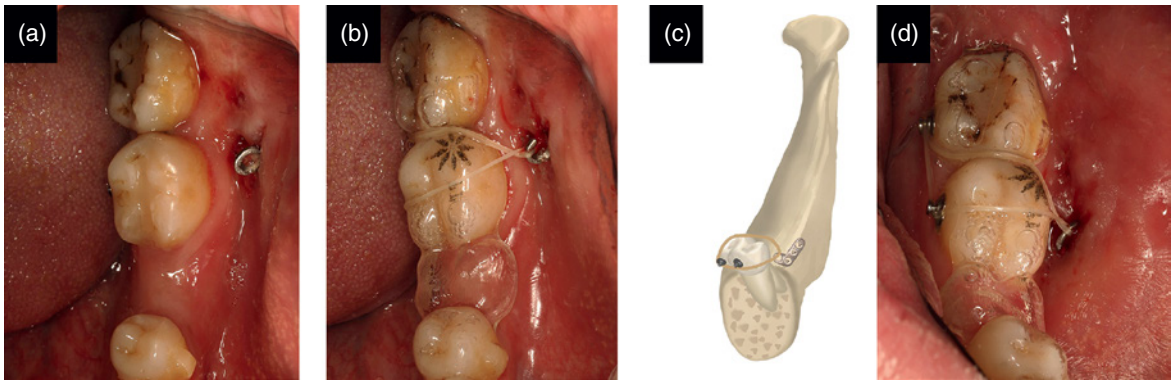


Figure 10.24 Uprighting of the lingually tipped mandibular molars was accomplished through a miniplate placed at the buccal side of the buccal shelf region. (a) After placement of the miniplate. (b) An elastic rubber was applied to aid in molar uprighting. (c) A schematic illustration. (d) The lingually tipped molars were successfully uprighted.

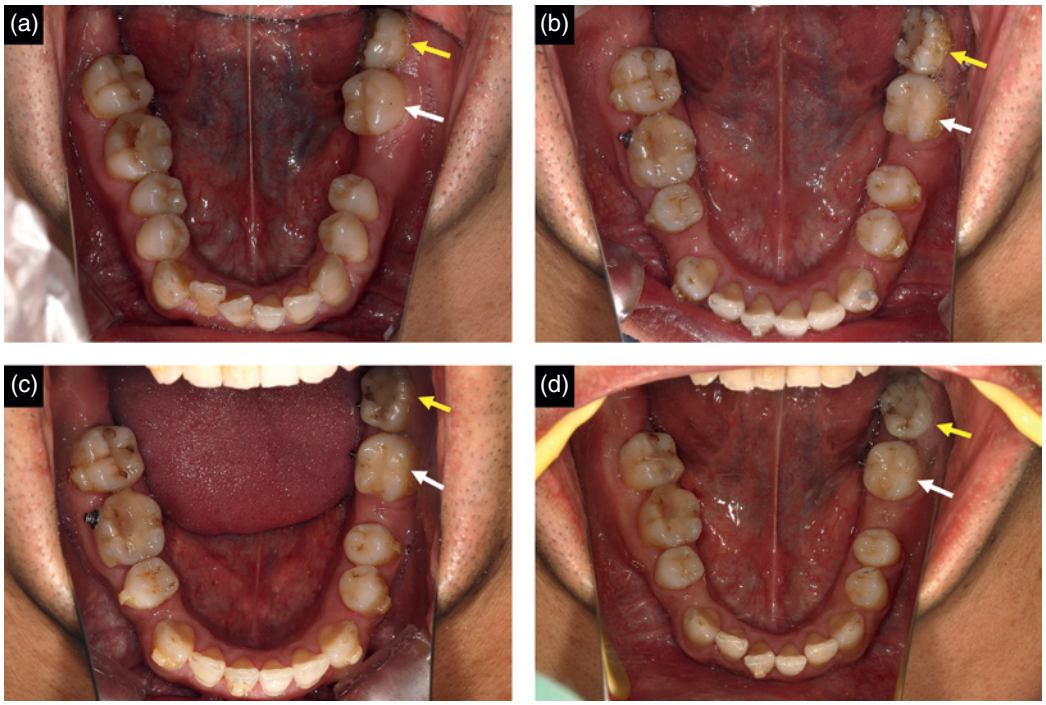


Figure 10.25 Treatment progress. The lingually inclined mandibular molars were successfully uprighted with the aid of a miniplate (the second and third molars are indicated by white and yellow arrows, respectively). (a) Pretreatment. (b) Eight months into treatment. (c) Thirteen months into treatment. (d) Twenty-two months into treatment.

mini-implants. In these clinical situations, miniplates are a good anchorage alternative. A case example is presented below.

A 31-year-old male patient sought a dental multidisciplinary consultation with a chief complaint of dental spacing and an unerupted tooth. Clinical and intraoral examinations showed that the mandibular left second premolar (35) was missing with the second molar (37) unerupted (Figure 10.26). Upper and lower dental midlines were inconsistent, with the lower one deviated to the left side. Panoramic radiograph revealed that the mandibular left second molar was mesially impacted beneath the distal

t.me/Dr_Mouayyad_AlbtousH

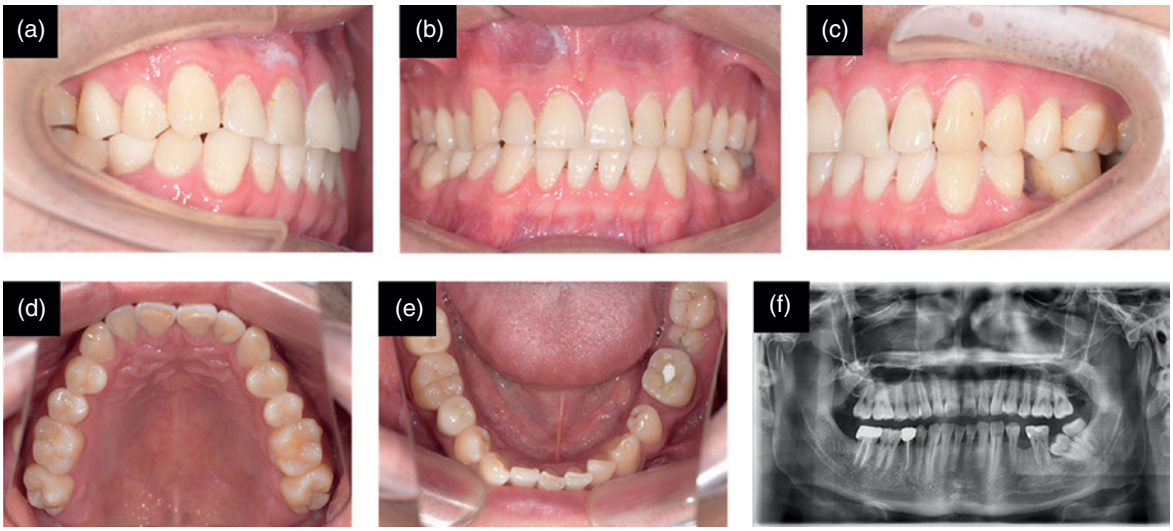


Figure 10.26 Pretreatment records. The mandibular left second premolar was missing, and the second molar was mesially impacted beneath the distal undercut of the first molar. (a–e) Intraoral photographs. (f) Panoramic radiograph.

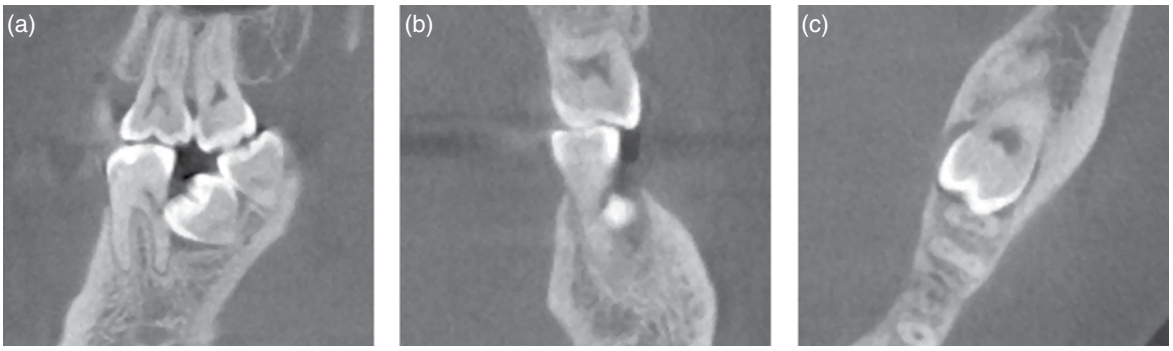


Figure 10.27 The CBCT images indicate that the impacted second molar caused resorption of the first molar with pulp involvement. (a) Sagittal view. (b) Coronal view. (c) Axial view.

undercut of the first molar. CBCT imaging revealed that the distal side of the first molar (both crown and root were involved) resorbed due to mesial impaction of the second molar and the resorption involved dental pulp (Figure 10.27). Thus, the prognosis of root canal therapy was unsatisfactory and the treatment plan was hemi-section of the first molar with removal of the distal root. The remaining mesial root would be mesialised to close the space due to the missing second premolar (35). The second molar (37) would be orthodontically tractioned mesially. Thus, insertion of a mini-implant was planned at the interradicular site between the canine and the first premolar. A cantilever spring would be employed to offer mesial and occlusal traction force for the impacted second molar. However, from the biomechanics perspective, the mini-implant was not qualified for this biomechanical demand, since the cantilever spring would exert a torsional force on the mini-implant. Thus, a miniplate that was able to withstand this torsional force was indicated for this clinical scenario.

A miniplate was placed between the canine and first premolar with the force-loading part being well adapted to offer a platform. The platform could be used to mount the cantilever spring that offered a mesial and occlusal traction force on the impacted second molar (Figure 10.28). The orthodontic traction of the second molar progressed smoothly (Figure 10.29).

t.me/Dr_Mouayyad_AlbtousH

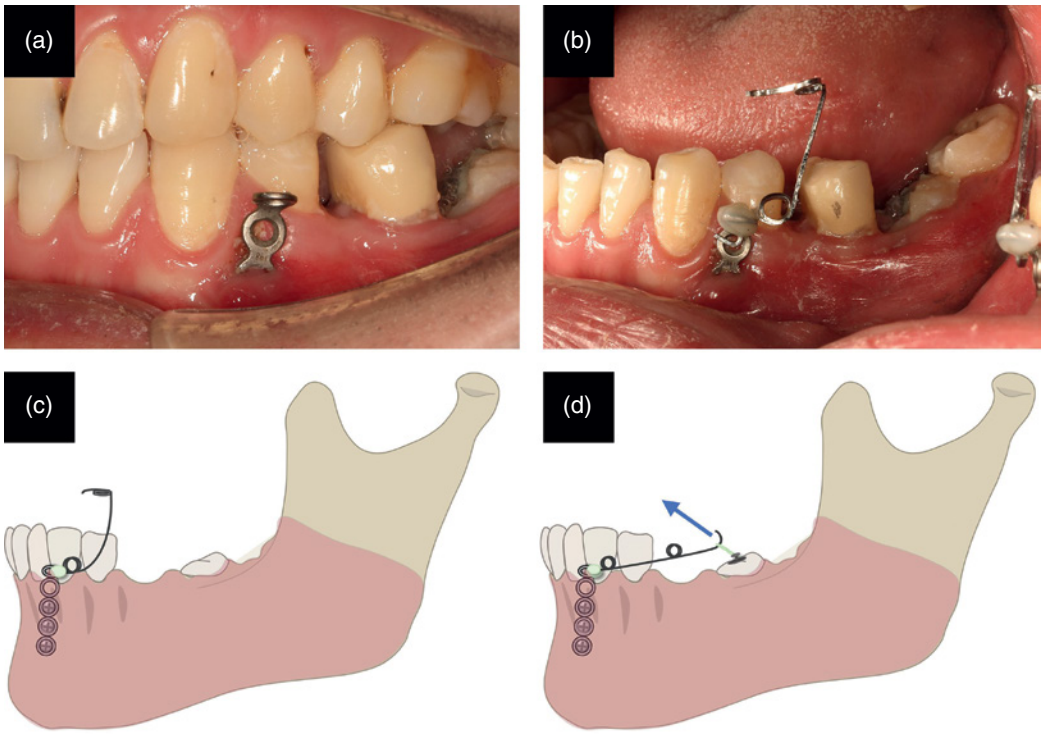


Figure 10.28 A miniplate was placed at the canine-premolar region. A cantilever loop was anchored onto the miniplate and applied to produce traction force. (a) Before fixation of the cantilever loop. (b) After fixation of the cantilever loop onto the miniplate. (c,d) Schematic illustration of the biomechanics (c: inactivated state; d: activated state).

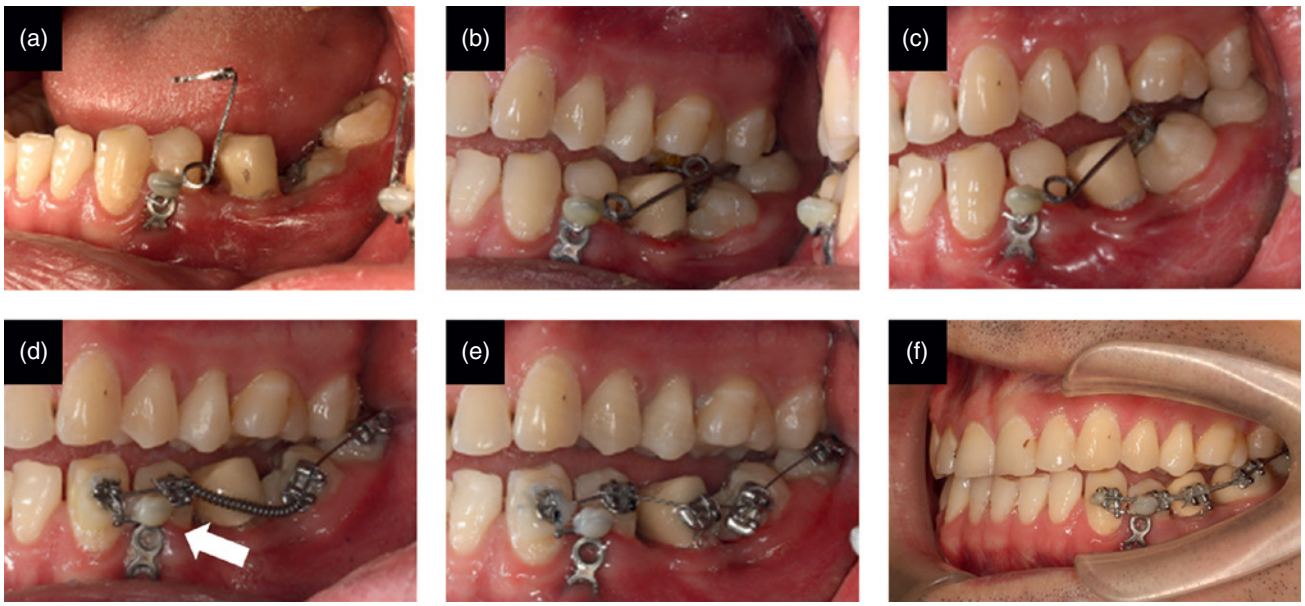


Figure 10.29 Traction of the second molar progressed smoothly. (a) Before treatment (orthodontic traction of the impacted second molar). (b) 3 months into treatment. (c) Four months into treatment. Note that the impacted second molar was successfully tractioned to the occlusal plane. (d) Six months into treatment. Segmental archwire was used for alignment. (e) Eight months into treatment. (f) Eleven months into treatment.

t.me/Dr_Mouayyad_AlbtousH

10.4 Insertion Techniques

Prior to the placement of miniplates, thorough examination should be performed to rule out any contraindication. Orthodontists and oral surgeons should have an in-depth discussion on specific anatomical sites for placement of the miniplates. Moreover, the specific spatial location and configuration of the force-loading part should be determined before insertion in order to gain a clear picture of biomechanical design.

The insertion techniques of miniplates are exemplified through a maxillary zygomatic miniplate. As illustrated in Figure 10.30, following local infiltration anaesthesia, a curved-shaped incision that is convex anteriorly is performed with a scalpel. The flap is elevated posteriorly to expose the zygomatic bone surface. Then, the specific insertion site is determined to guarantee that the force-loading part of the miniplate is located at the attached gingiva zone, so that soft tissue complications will be minimised. Insertion of anchor screws into the miniplate holes is performed with screwdrivers, followed primary suture of the flap.

Following flap elevation and exposure of bone surface, the miniplate is bent meticulously to adapt to the bone surface contour in order to achieve good contact between the miniplate and the bone surface. Note that bending should be limited to the portion that is between the holes, otherwise the miniplate may not be in good contact with the anchor screws. Alternatively, for the sake of precise bending, the miniplate can be bent pre surgically based on the 3-D-printed skeletal bone model and transferred to the predetermined location by means of a customised transfer jig.[10] Note that bending should not be performed with several attempts as this may lead to miniplate fracture.

The miniplate is fixed onto the bone surface with one anchor screw inserted into the middle hole. Note that the screw should not be completely tightened since this allows for minor rotational adjustments. For self-tapping screws, pilot drilling should be performed prior to insertion. Occasionally, even for self-drilling screws, pilot drilling may be indicated for those inserted at anatomical sites with high bone density (e.g. mandibular posterior region). Following insertion of the first screw into the middle hole, the second and third anchor screws are inserted into the upper and lower holes sequentially.

Lastly, the flap is positioned back and sutured primarily. Make sure that the force-loading part is located at the attached gingiva zone and modifications of the force-loading part can be made. For example, removing a part of the rim that forms the most occlusal hole of the miniplate gives rise to a modified hook that can be used for applying elastic bands or similar appliances.

The insertion procedures are displayed in several clinical cases (Figures 10.31 and 10.32) and in a skull with more detail (Figure 10.33).

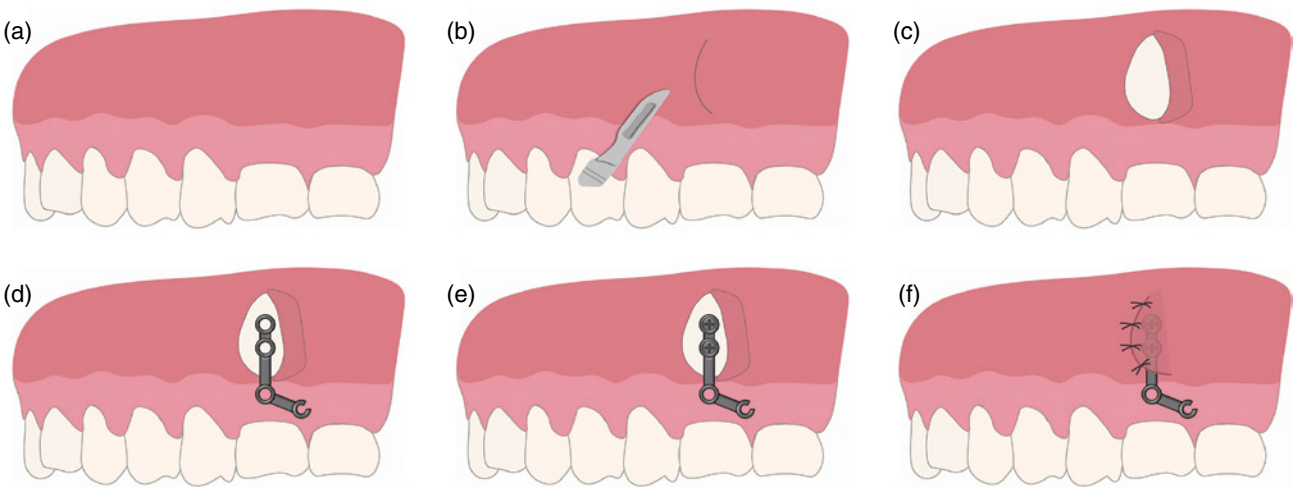


Figure 10.30 Schematic illustration of the procedures for placing a miniplate. (a) Before placement. (b) Make a semilunar or L-shaped incision with the convexity facing anteriorly. (c) Flap elevation. (d) Adjust the shape of the miniplate to make it adapt to the bone surface. (e) Fix the miniplate through two or three anchor screws. (f) Suturing.

t.me/Dr_Mouayyad_AlbtousH



Figure 10.31 Clinical procedures of placing a miniplate at the zygomatic buttress region. (a) Before placement. (b) Flap elevation. (c) Fixation of the miniplate with three anchor screws.

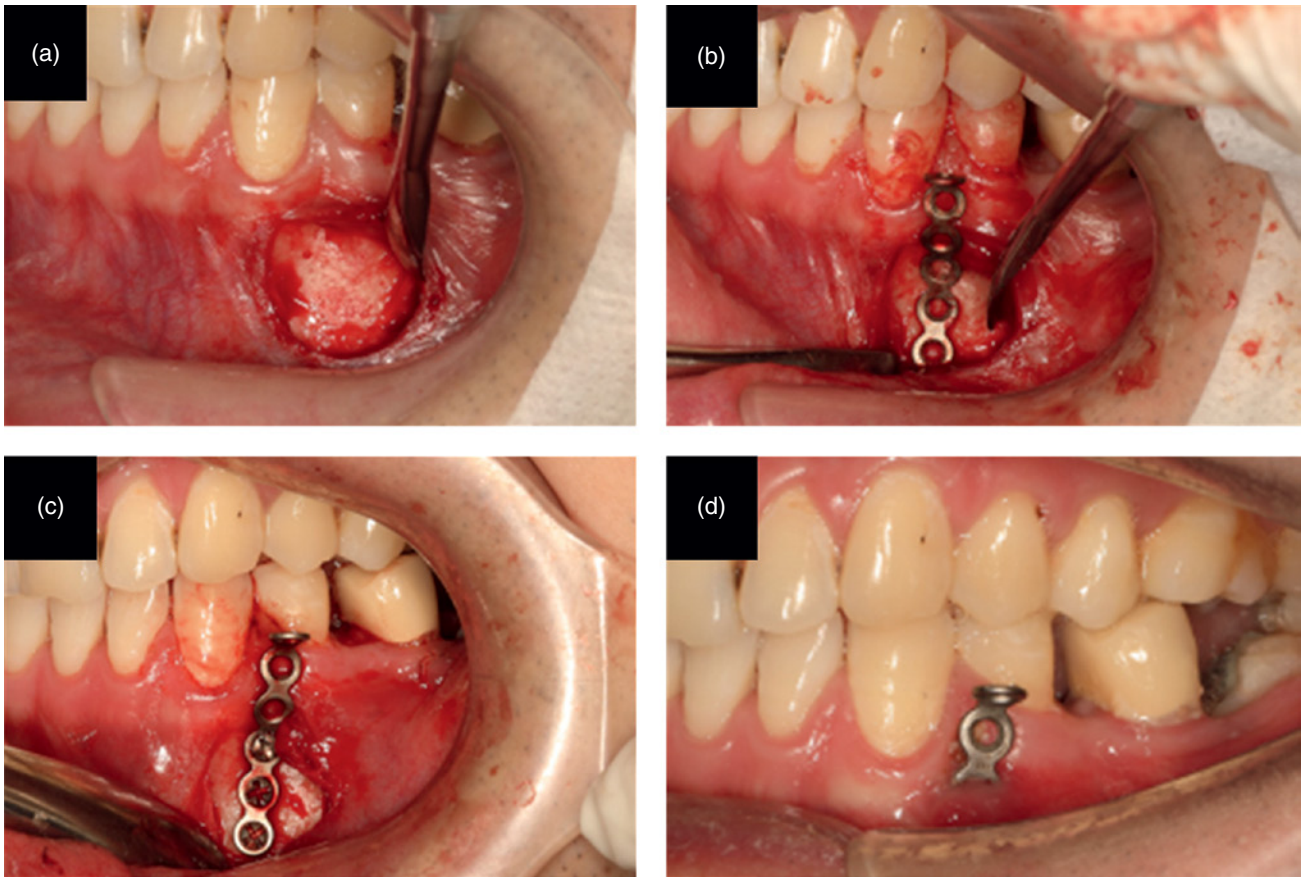


Figure 10.32 Placement of a miniplate at the mandibular canine-premolar region. (a) Flap elevation. (b) Adjust the shape of the miniplate. (c) Fixing the miniplate onto the bone with three anchor screws. (d) One week later after soft tissue healing.

t.me/Dr_Mouayyad_AlbtousH

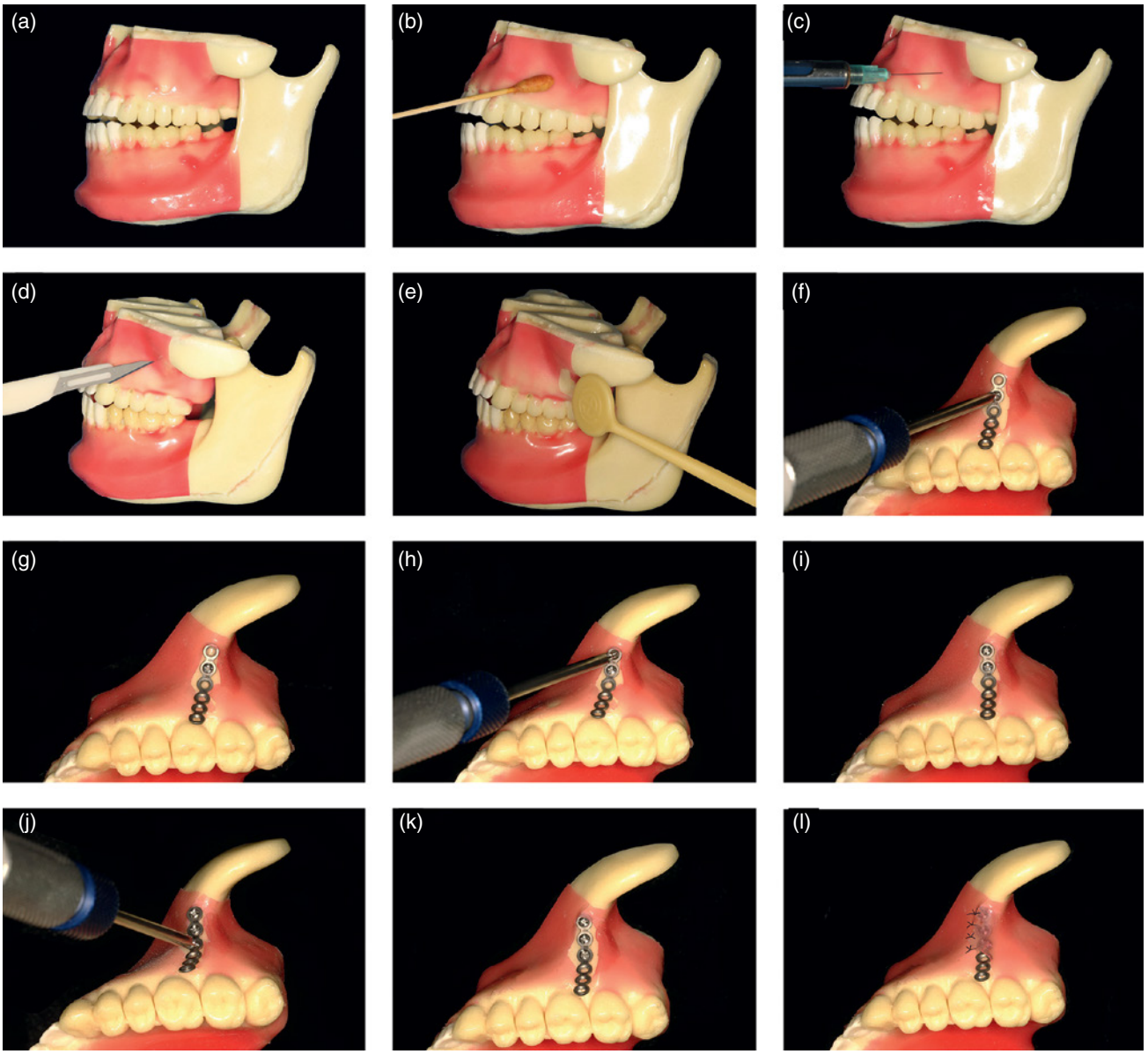


Figure 10.33 Placement of a miniplate on a skull. (a) Before placement. (b) Mucosa disinfection with iodophor. (c) Local infiltration anaesthesia. (d) Incision. (e) A semilunar flap is elevated to expose the bony surface of the zygomatic buttress region. (f,g) Insert the middle anchor screw. (h,i) The upper anchor screw is inserted. (j,k) The lower anchor screw is inserted. (l) The flap is approximated and sutured.

10.5 Removal Techniques

Miniplates can be removed once they have fulfilled their anchorage purposes. The procedures for removing miniplates are summarised below (Figure 10.34). Following local infiltration anaesthesia, an incision is made with a scalpel and flap elevation performed with a periosteal elevator to expose the miniplate and anchor screws. Then, the screws are unscrewed and removed with a screwdriver, followed by removal of the miniplate. Lastly, primary suture of the flap is performed.

Occasionally, bone apposition may occur on the miniplate and the screw heads are totally covered by the appositional bone, complicating the removal procedure (Figure 10.35). If this occurs, a piezosurgical or ultrasonic instrument can be employed to remove the bone in a minimally invasive way. Following removal of the bone, the screw heads can be exposed and removal of the miniplate can be accomplished.

t.me/Dr_Mouayyad_AlbtousH

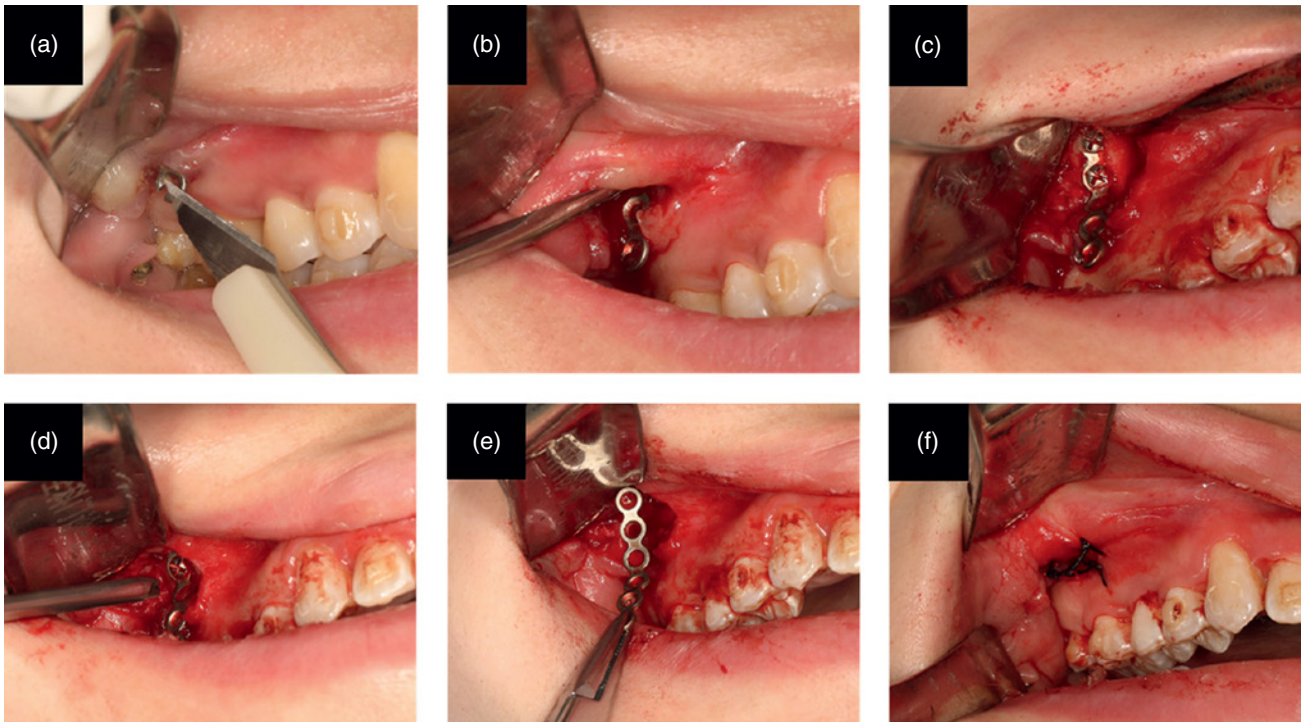


Figure 10.34 Removal technique. (a) Incision. (b,c) Elevate the flap to expose the miniplate and the anchor screws. (d) Unscrew and remove the anchor screws sequentially. (e) Remove the miniplate with a needle holder. (f) Primary suture.

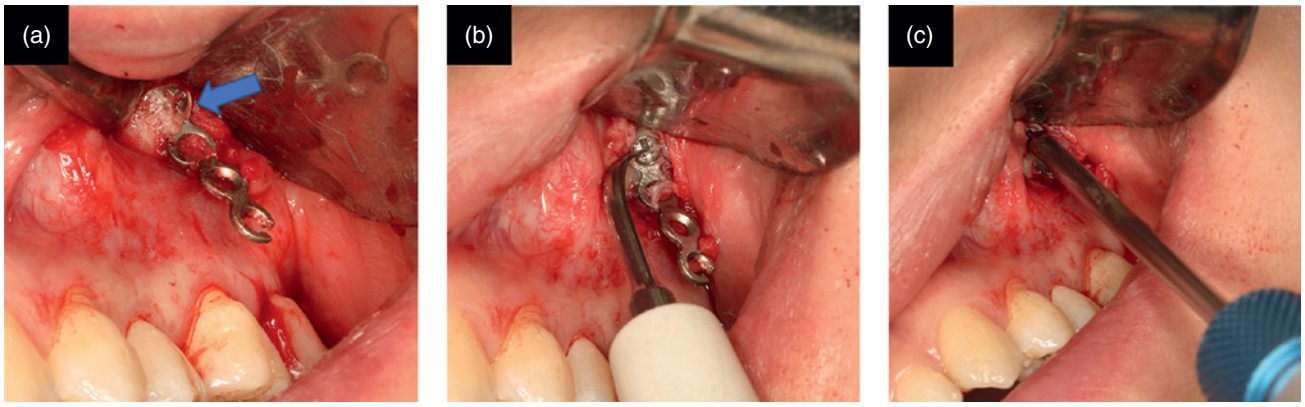


Figure 10.35 (a) Following flap elevation, the miniplate was exposed but bone apposition that fully covered the anchor screws was observed. (b) An ultrasonic kit was used to remove the bone in order to expose the anchor screws. (c) Following exposure, the anchor screws were unscrewed and removed using a screwdriver.

10.6 Summary

Miniplates, an alternative form of orthodontic TADs to mini-implants, are frequently used in clinical practice to accomplish challenging orthodontic and orthopaedic purposes. Insertion techniques of miniplates are unique, requiring flap elevation and fixation onto bone through two or three anchor screws.

t.me/Dr_Mouayyad_AlbtousH

References

1 Liu L, Zhan Q, Zhou J et al. (2021). A comparison of the effects of Forsus appliances with and without temporary anchorage devices for skeletal Class II malocclusion. *Angle Orthod.* 91(2): 255–266.

2 Jahanbin A, Shafaee H, Pahlavan H, Bardideh E, Entezari M. (2023). Efficacy of different methods of bone-anchored maxillary protraction in cleft lip and palate children: a systematic review and meta-analysis. *J. Craniofac. Surg.* 34: 875–880.

3 Kumar D, Sharma R, Arora V, Bhupali NR, Tuteja N. (2022). Evaluation of displacements and stress changes in the maxillo-mandibular complex with fixed functional appliance skeletally anchored on mandible using miniplates: a finite element study. *J. Orthod. Sci.* 11: 42.

4 de Mattos PM, Goncalves FM, Basso IB et al. (2022). Risk factors associated with the stability of mini-implants and mini-plates: systematic review and meta-analysis. *Clin. Oral Invest.* 26(1): 65–82.

5 Akan B, Unal BK, Sahan AO, Kiziltekin R. (2020). Evaluation of anterior open bite correction in patients treated with maxillary posterior segment intrusion using zygomatic anchorage. *Am. J. Orthod. Dentofacial Orthop.* 158(4): 547–554.

6 Kassem HE, Marzouk ES. (2018). Prediction of changes due to mandibular autorotation following miniplate-anchored intrusion of maxillary posterior teeth in open bite cases. *Prog. Orthod.* 19(1): 13.

7 Lee YS, Park JH, Kim J, Lee NK, Kim Y, Kook YA. (2022). Treatment effects of maxillary protraction with palatal plates vs conventional tooth-borne anchorage in growing patients with Class III malocclusion. *Am. J. Ortho.d Dentofacial Orthop.* 162(4):520–528.

8 Miranda F, Cunha Bastos JCD, Magno Dos Santos A, Janson G, Pereira Lauris JR, Garib D. (2021). Dentoskeletal comparison of miniscrew-anchored maxillary protraction with hybrid and conventional hyrax expanders: a randomized clinical trial. *Am. J. Orthod. Dentofacial Orthop.* 260(6):774–783.

9 Lee HJ, Choi DS, Jang I, Cha BK. (2022). Comparison of facemask therapy effects using skeletal and tooth-borne anchorage. *Angle Orthod.* 92(3): 307–314.

10 Hourfar J, Kanavakis G, Goellner P, Ludwig B. (2014). Fully customized placement of orthodontic miniplates: a novel clinical technique. *Head Face Med.* 10: 14.

t.me/Dr_Mouayyad_AlbtousH

11

Three-dimensional Design and Manufacture of Insertion Guides

Niansong Ye[1], Lingling Pu[2,3], Qi Fan[2], Wenqiang Ma[3], Yanqing Wu[3], Wenli Lai[2], and Hu Long[2]

[1] *Private Practice, Shanghai, China*
[2] *Department of Orthodontics, State Key Laboratory of Oral Diseases and National Clinical Research Center for Oral Diseases, West China Hospital of Stomatology, Sichuan University, Chengdu, China*
[3] *Private Practice, Chengdu, China*

11.1 Introduction

Accurate placement of orthodontic TADs is technique sensitive and places a high demand on practitioners' expertise and clinical experience. Although orthodontic mini-implants require a less complex surgical procedure than dental implants, their deviations from the optimal location have less tolerance than dental implants. This is because orthodontic mini-implants are often inserted into interradicular sites that are 3–4 mm wide and even 1 mm deviation may lead to disastrous outcomes, e.g. root damage and perforation.

With the advent of the digital era, the applications of computer-aided design and computer-aided manufacturing (CAD-CAM) have enabled practitioners to virtually insert mini-implants and to transfer the virtually designed locations of mini-implants into 'reality' through 3-D-printed insertion guides.[1] A plethora of clinical evidence has demonstrated the accuracy and clinical success of insertion guides for orthodontic mini-implants.[1-4]

In this chapter, we will mainly focus on the evolution and advantages of insertion guides for mini-implants and the procedures for 3-D design and manufacture of insertion guides.

11.2 Evolution of Insertion Guides

11.2.1 The Concept of Guided Surgery

Guided surgery refers to a surgical procedure performed with the guidance of or reference to a predetermined plan (e.g. osteotomy lines and surgical entry points). Guided surgery has revolutionised the concept of precision surgery and enables practitioners (even inexperienced ones) to obtain predictable and aesthetic surgical outcomes.[5] The clinical application of guided surgery for orthognathic surgery and dental implants preceded that for orthodontic mini-implants.

Several seminal clinical studies revealed the clinical effectiveness and safety of guided surgery for maxillofacial surgery.[6-8] Since then, guided surgery has been widely used in the field of maxillofacial surgery for a variety of conditions, e.g. LeFort I osteotomy, orthognathic jaw surgery, traumatic maxillofacial reconstruction and facial aesthetic surgery.[9-12] Guided surgery for maxillofacial surgery is often performed with the aid of a surgical guide or template whose design is based on pretreatment CBCT images. For example, an osteotomy guide is virtually designed and manufactured through 3-D printing and can be used intraoperatively to guide surgeons to perform predetermined osteotomy lines with high accuracy and prediction (Figure 11.1).

Since the introduction of modern implantology in the field of dentistry in the 1980s, practitioners have sought to place dental implants into edentulous regions with adequate bone support so that the implants are surrounded by alveolar bone and exhibit sufficient stability. However, for patients with atrophic alveolar bone where implants have to be placed, accuracy is essential and even a 1 mm error may lead to disastrous results. This is clinically presented as misplaced implants that may cause damage to vital anatomical structures (e.g. inferior alveolar nerve) or may render it difficult to place a proper prosthesis.[13,14]

Clinical Insertion Techniques of Orthodontic Temporary Anchorage Devices, First Edition. Edited by Hu Long, Xianglong Han, and Wenli Lai.
© 2024 John Wiley & Sons Ltd. Published 2024 by John Wiley & Sons Ltd.

t.me/Dr_Mouayyad_AlbtousH

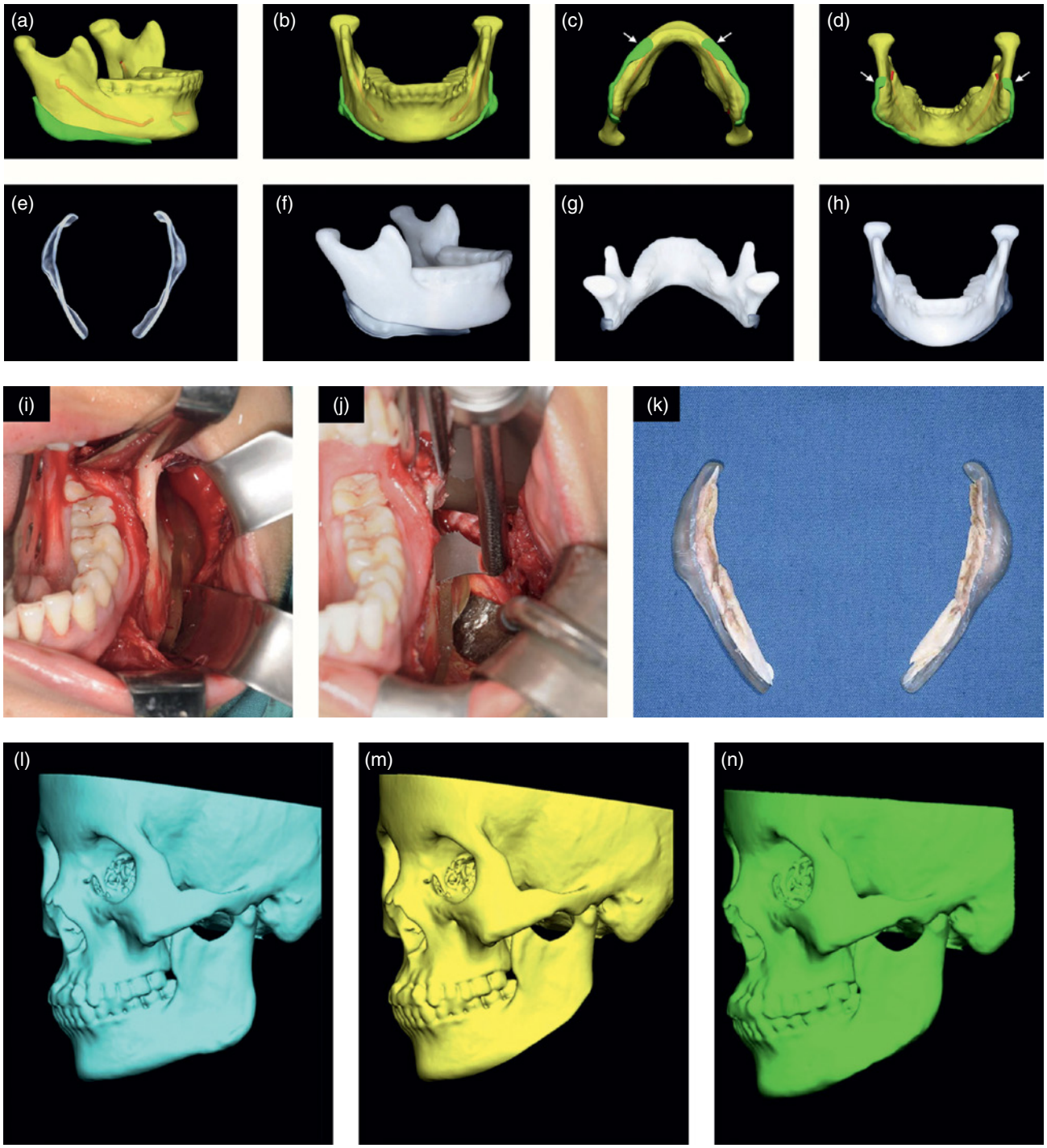


Figure 11.1 (a,b) Computer-aided design of 3D templates on the mandibular angle. (c,d) Arrows indicate the hook parts of the templates. (e–h) A pair of stereolithographic templates and a mandibular model were fabricated by the rapid prototyping technique. (i) The surgical template was positioned on the outer surface of the mandibular angle. (j) The osteotomy was easily performed with an oscillating saw along the upper edge of the template. (k) The outline of the excised mandibular angle was almost the same as that of the templates. (l) Preoperative CT image. (m) Simulated image. (n) Postoperative CT image. Note that the simulated and actual postoperative images were almost identical. Source: Ye et al. [12]/Reprinted with permission from Springer Nature.

t.me/Dr_Mouayyad_AlbtousH

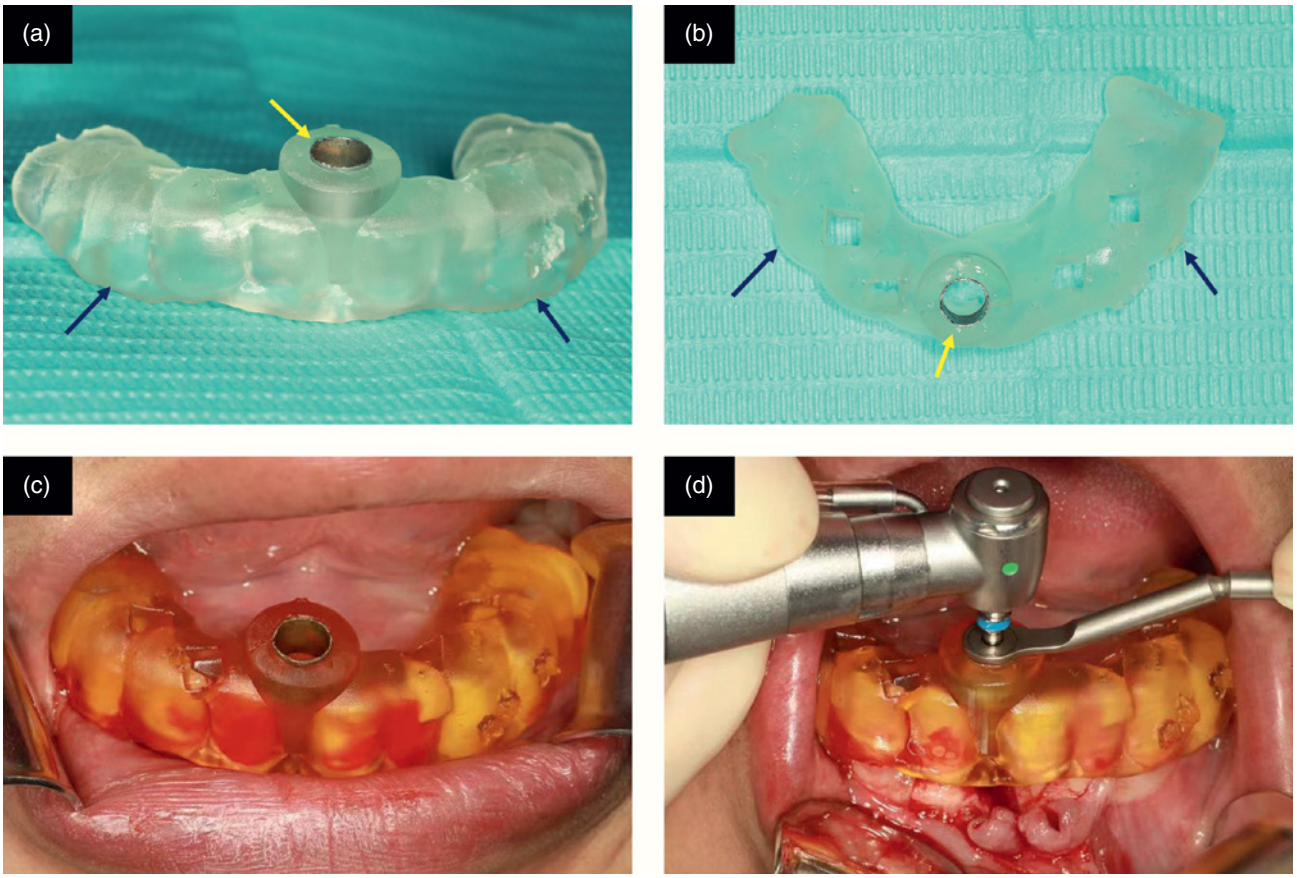


Figure 11.2 Application of an implantation guide for placing an implant. (a,b) The implantation guide is composed of a retention part (blue arrows) and a guide cylinder (yellow arrows). Note the metal sleeve at the inner surface of the guide cylinder. (c,d) The implantation guide was fitted onto the lower dentition and the implant was placed through the guide cylinder.

These clinical problems force practitioners to seek judicious resolutions. In particular, guided surgery, a promising surgical innovation, can reduce practitioners' intraoperative error and achieve highly predictable outcomes with clinical safety.[15,16] In contrast to its free-hand counterpart, guided surgery makes implant placement surgery safer, simpler and more accurate, taking less time and with a lower cost.[17-19]

An implantation guide is composed of a retention part that is supported by and fixed onto the dentition and a guide cylinder that guides the implant placement to achieve a predetermined insertion depth and insertion angle at a designated site (Figure 11.2). The successful clinical application of insertion guides for dental implants enables practitioners to translate this guided insertion concept into the placement of orthodontic mini-implants. With similar designs, insertion guides render the placement of mini-implants simpler and more accurate (Figure 11.3). We will briefly discuss the evolution of guided insertion of orthodontic mini-implants in the next section.

11.2.2 Evolution of Guided Insertion for Mini-implants

The techniques of guided insertion of mini-implants have been evolving with the development of digital technology. The insertion of orthodontic mini-implants evolved from a free-hand technique, via a wire guide technique to the current 3-D-printed insertion guide technique (Figure 11.4).

Free-hand insertion refers to the conventional insertion technique where practitioners insert orthodontic mini-implants with screwdrivers without any guidance or reference. Both a manual screwdriver and a motor-driven handpiece can be used for placement of mini-implants (Figures 11.5 and 11.6). This technique relies on practitioners' clinical expertise and fine tactile perception for accurate placement without damage to surrounding vital structures (e.g. dental roots). It has been shown that the operator's learning curve of insertion technique is a significant factor in determining the success of orthodontic

t.me/Dr_Mouayyad_AlbtousH

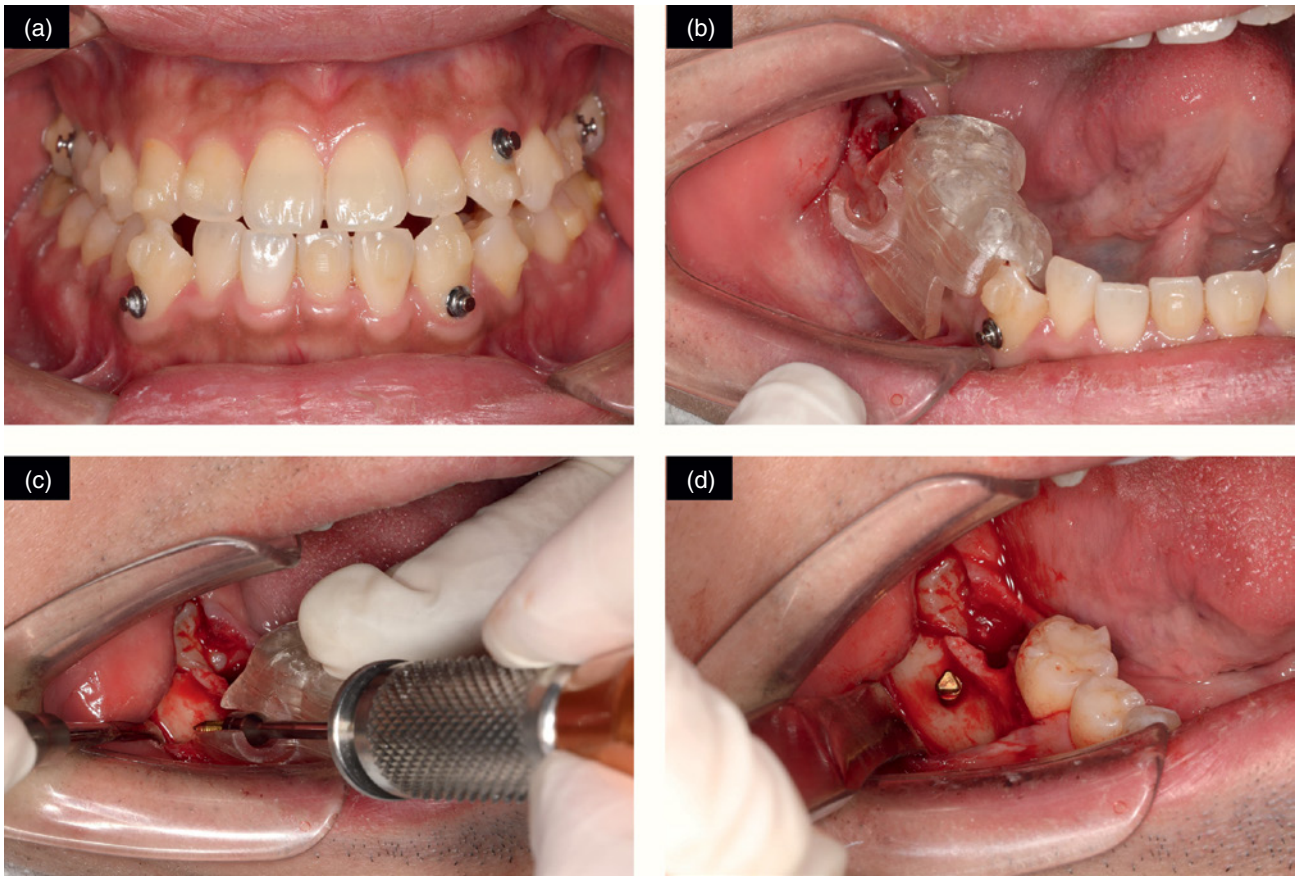


Figure 11.3 Procedures of inserting a mini-implant in the buccal shelf with the aid of an insertion guide. (a,b) Fit the insertion guide on the dentition. (c) Insert the mini-implant through the guide cylinder of the insertion guide. (d) Post insertion.

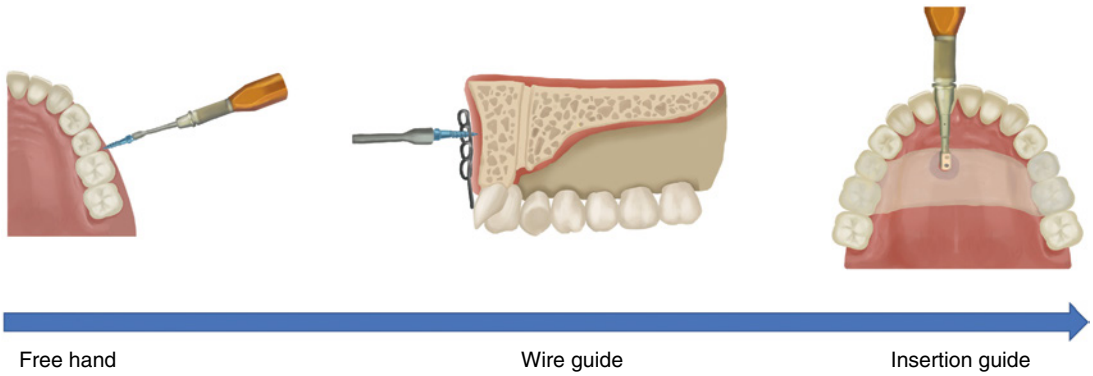


Figure 11.4 The evolution of guided insertion technique.

mini-implants.[20] Specifically, the success rate of orthodontic mini-implants increased for practitioners who performed 40+ insertions.[21] The most concerning issue for free-hand insertion is the potential manual errors that may be introduced to the actual locations of mini-implants. It has been demonstrated that practitioners tended to place mini-implants more apically and distally.[22] Thus, injudicious free-hand insertion of mini-implants may lead to deviations of mini-implants and result in root damage and eventual mini-implant failure.

To reduce the incidence of root damage for interradicular mini-implants, pioneer practitioners came up with wire guides to help ensure the accurate insertion of mini-implants into the interradicular space.[23,24] The wire guide

t.me/Dr_Mouayyad_AlbtousH

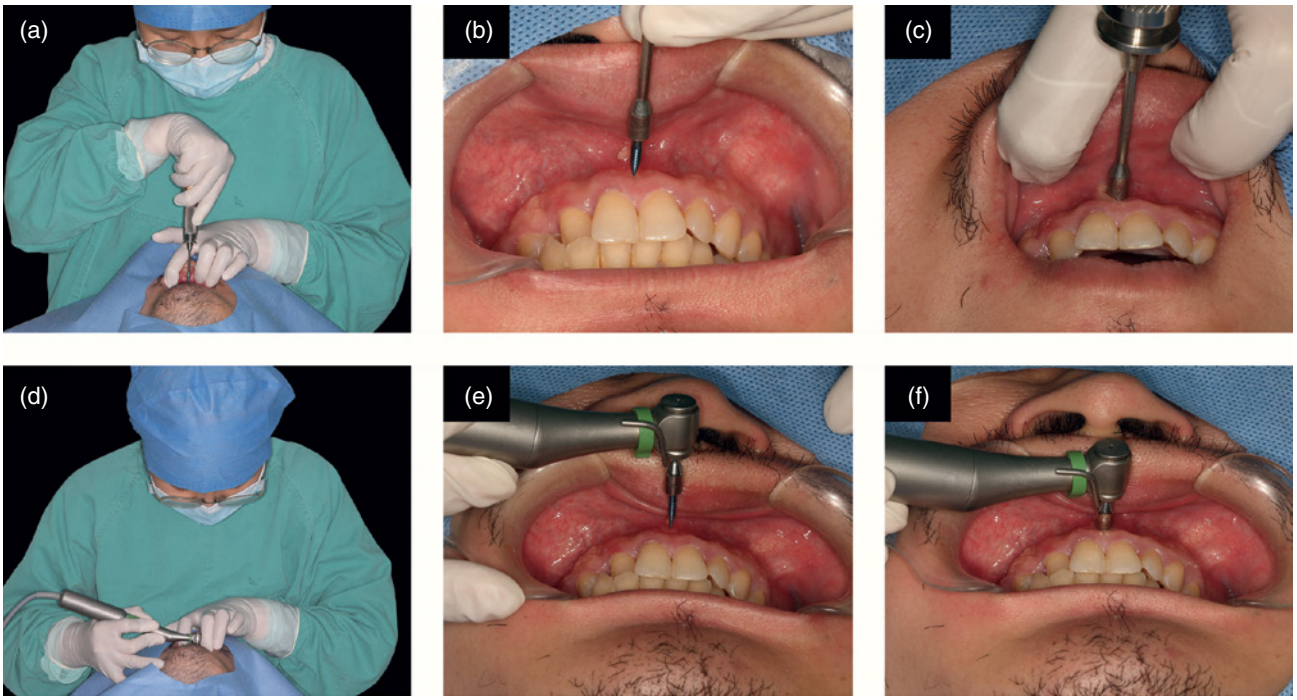


Figure 11.5 Insertion of a mini-implant at the maxillary labial interradicular site with a manual screwdriver (a–c) or a motor-driven handpiece (d–f).

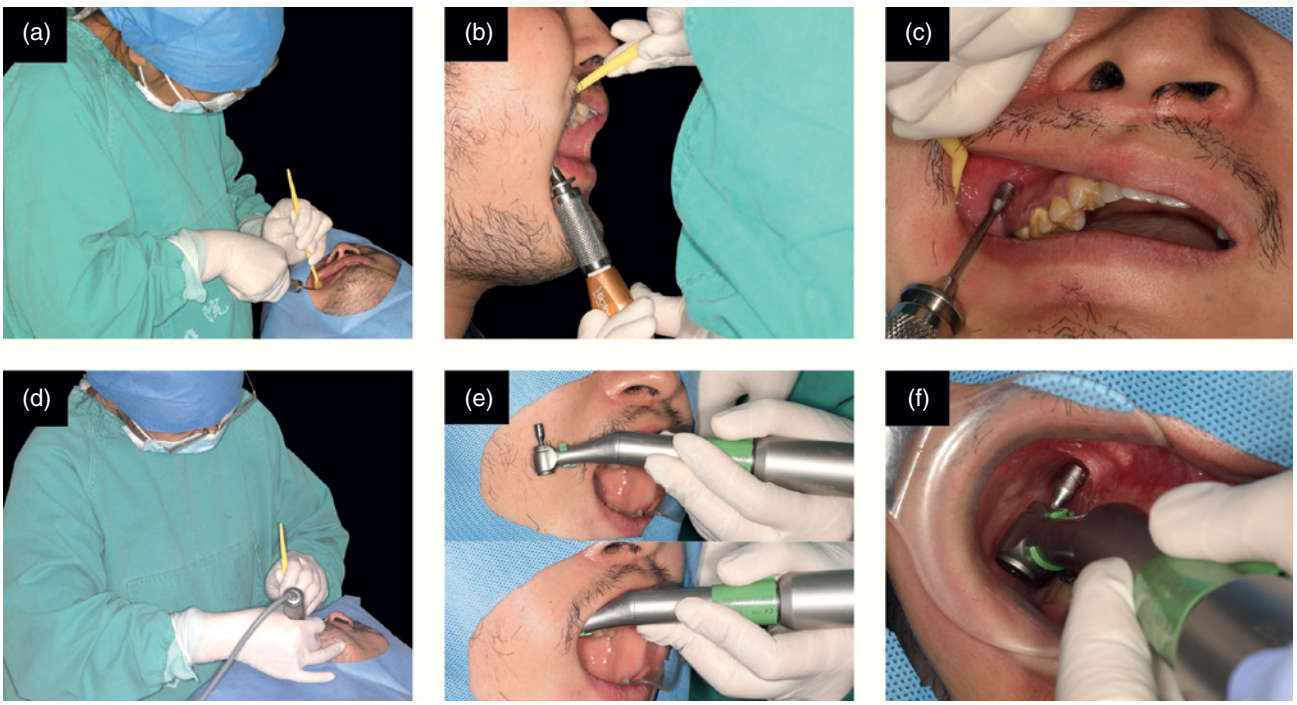


Figure 11.6 Insertion of a mini-implant at the infrazygomatic crest region via a manual screwdriver (a–c) or a motor-driven handpiece (d–f).

t.me/Dr_Mouayyad_AlbtousH

technique utilises adjustable reference wires mounted onto teeth or archwires to locate the optimal entry point for insertion. Although wire guides come in different shapes and forms, their basic configuration is similar: a supporting part and a positioning part (Figure 11.7). The clinical procedure of using wire guides for the placement of mini-implants is described below.

First, based on pretreatment radiographs, wire guides of appropriate length are fabricated and bonded onto dental casts to evaluate their suitability (Figure 11.8). Second, wire

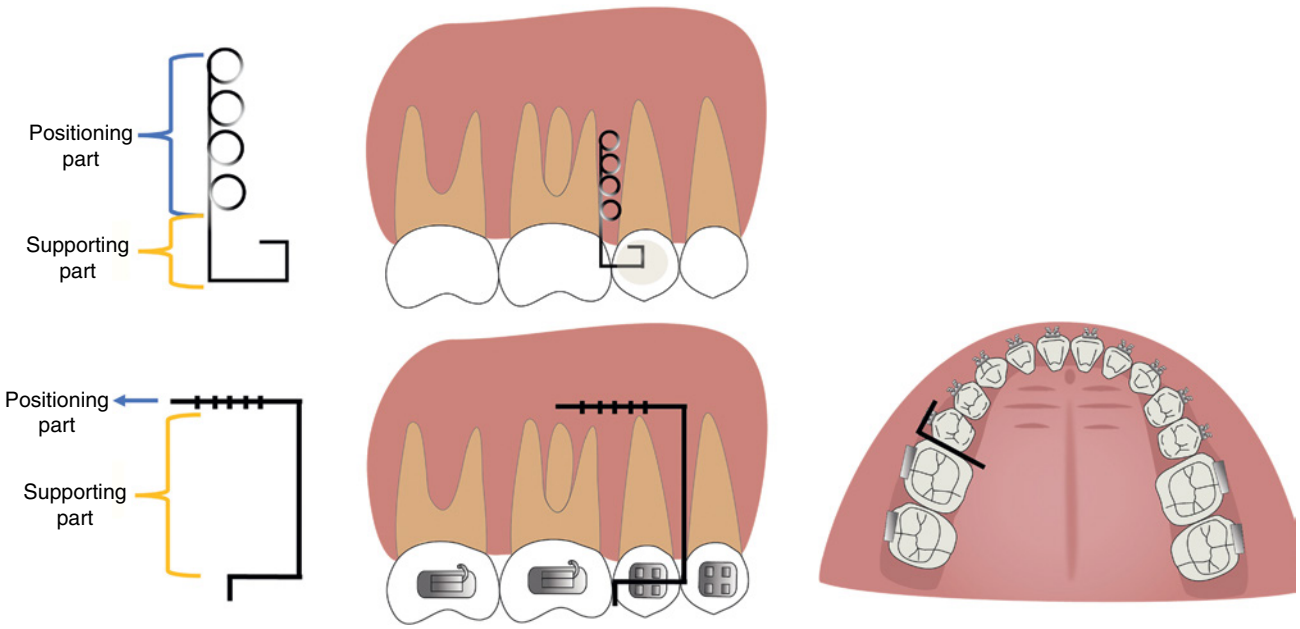


Figure 11.7 Examples of wire guides. The wire guide consists of two basic configurations, including the supporting part and the positioning part.

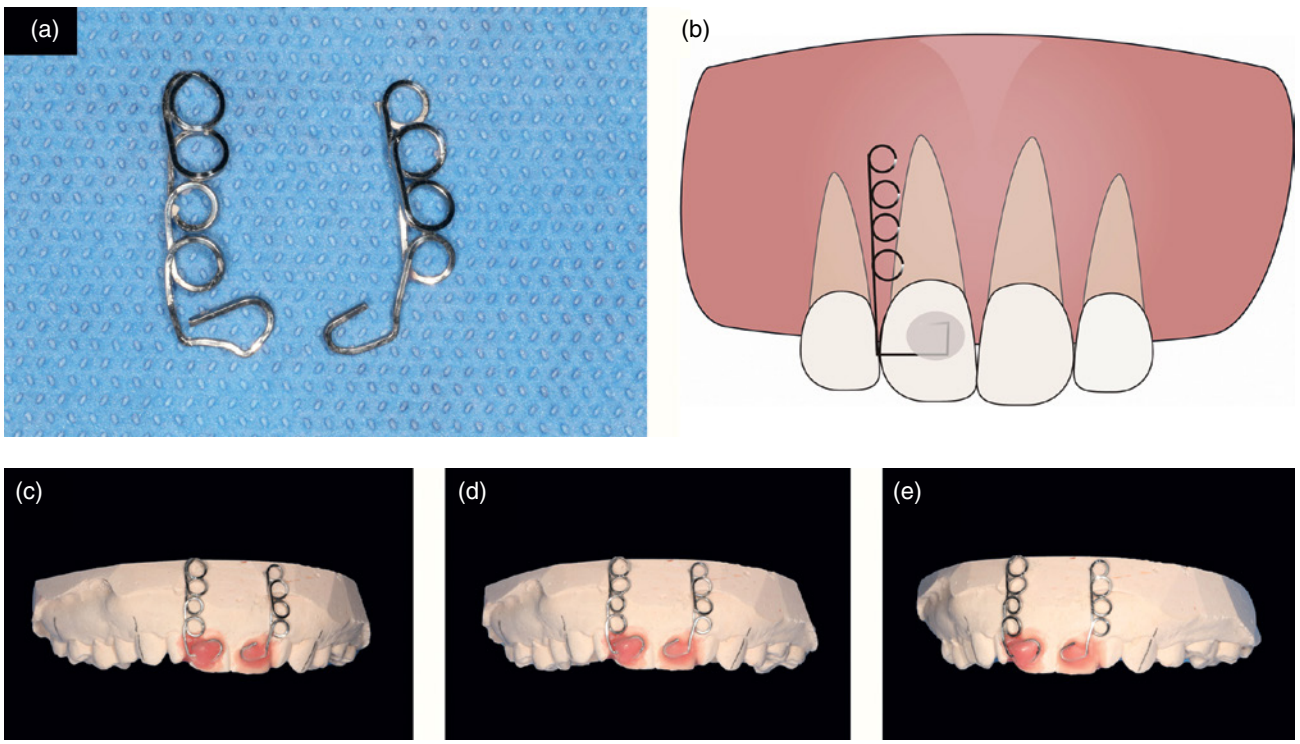


Figure 11.8 Bending wire guides on a dental cast. (a) Two wire guides with four loops were bent. (b) Schematic illustration of the wire guide. (c–e) Demonstration of wire guides on a dental cast with wax.

t.me/Dr_Mouayyad_AlbtousH

guides are bonded onto dentition or fixed onto archwires and subjected to radiographic assessment (Figure 11.9). Third, based on radiographic findings on interradicular sites with wire guides, appropriate entry points are selected and mini-implants are inserted at the selected entry points (Figures 11.10 and 11.11). Lastly, periapical radiographs are taken to examine the final location of mini-implants and rule out root proximity (Figure 11.12).

After insertion, the precise locations of mini-implants are determined by the following parameters: entry point,

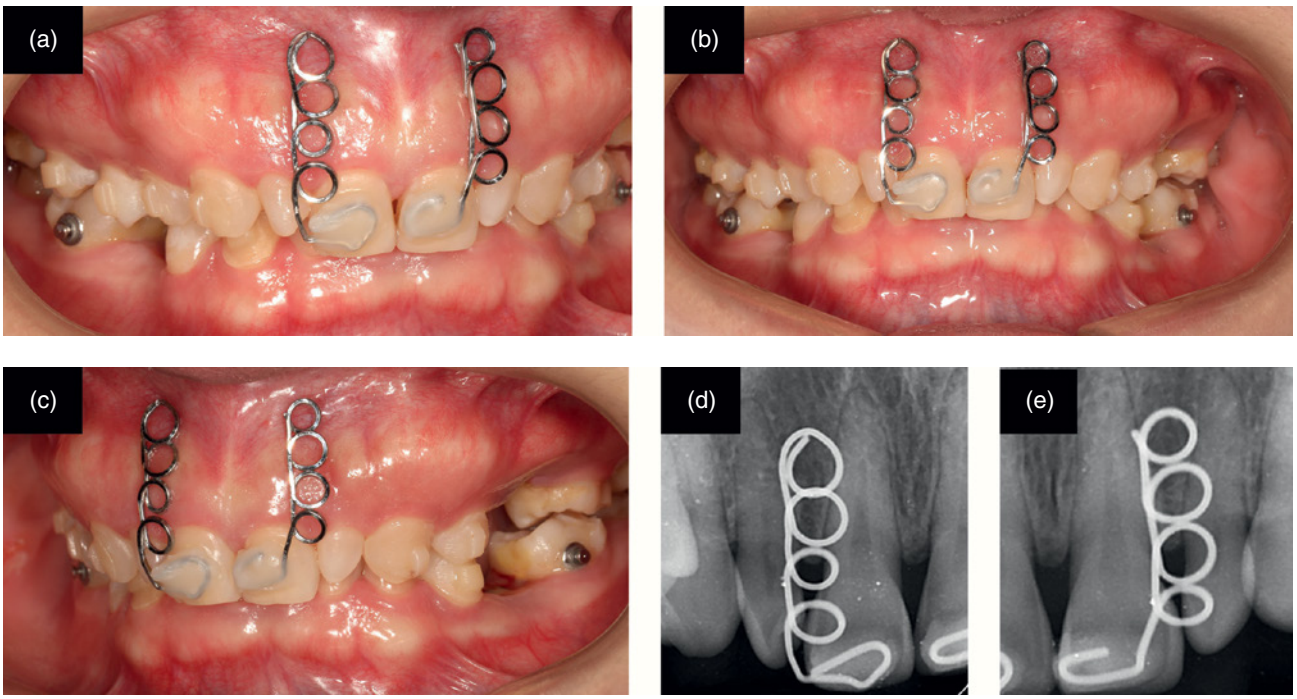


Figure 11.9 Try on the wire guides intraorally. (a–c) The wire guides were fixed onto the tooth surfaces with flowable resin. (d,e) Confirm both the vertical and mesiodistal positions of the wire loops.

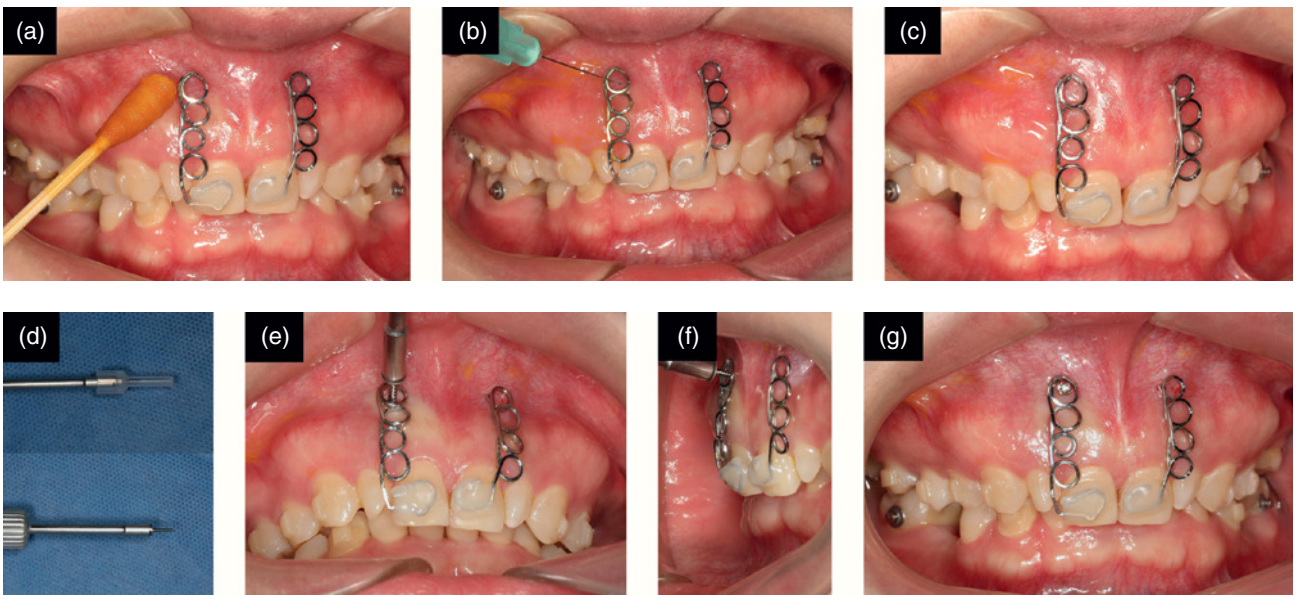


Figure 11.10 The procedures of inserting a mini-implant using wire guides. (a) Disinfection with iodophor. (b) Local anaesthesia. (c) Following anaesthesia. (d) Engage the mini-implant into the screwdriver. (e,f) Inserting the mini-implant through the most apical loop of the wire guide. (g) Post insertion.

t.me/Dr_Mouayyad_AlbtousH

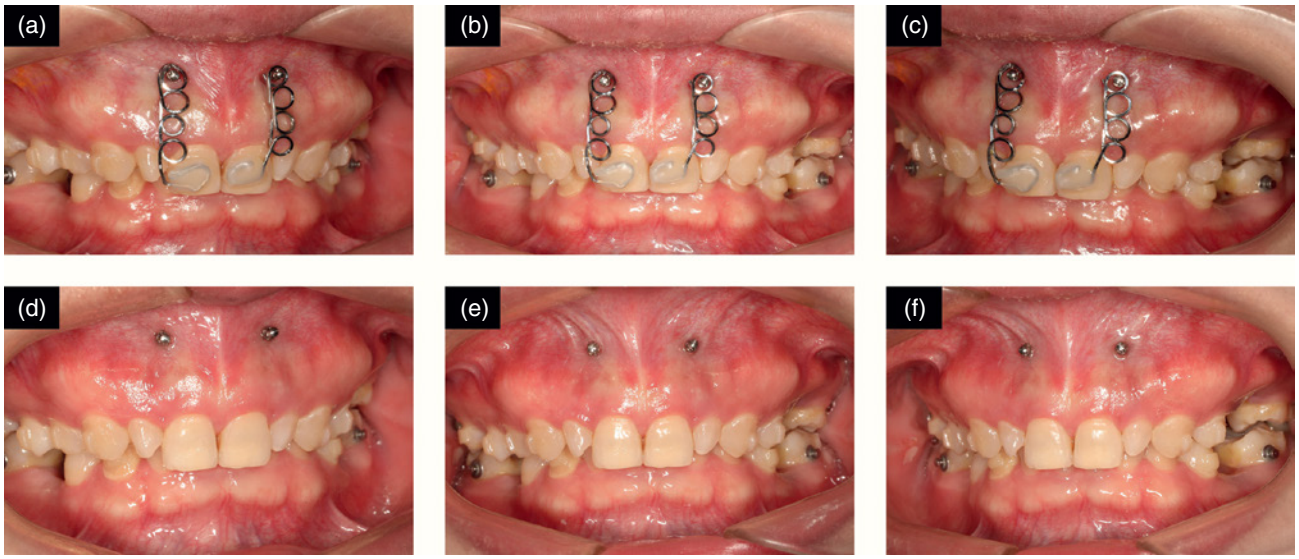


Figure 11.11 (a–c) Two mini-implants have been inserted. (d–f) The wire loops are removed following the insertion of mini-implants.

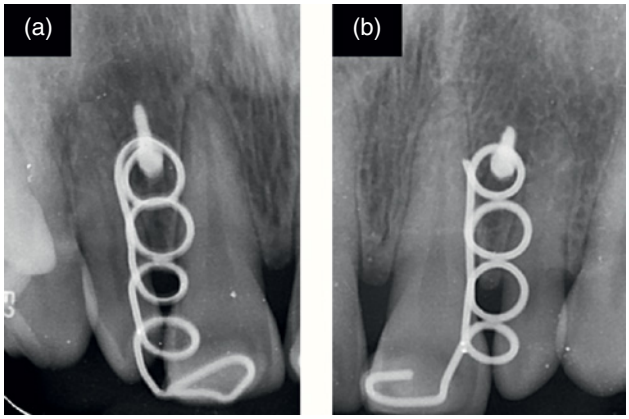


Figure 11.12 Ideal positions of bilateral mini-implants shown by orthogonal periapical radiographs.

insertion depth, insertion angulations (both mesiodistal and coronoapical). However, as displayed in Figure 11.13, only the entry point can be determined through wire guide technique while the other parameters (insertion depth and angulation) cannot be controlled. Thus, although the wire guide technique moves a step forward in increasing the precision of mini-implant insertion, its clinical applications have been limited due to its inherent drawback in controlling insertion angulation.

For better 3-D control of mini-implant location, insertion guides with 3-D CBCT images and intraoral scanning through CAD-CAM have been developed. Mini-implants are inserted virtually and insertion guides designed based on the optimal locations of mini-implants. Then, the mini-implants are transferred to the patient's mouth with the insertion guides.

An insertion guide is composed of two continuous parts: the retention part and the guide cylinder (Figure 11.14). The retention part utilises dentition and/or soft tissues for retention or stabilisation so that the insertion guide does not move during mini-implant placement. The guide cylinder is a hollow cylinder that is an integral part of the insertion guide. Depending on the design, guide cylinders may have an opening towards the occlusal or apical direction, which facilitates the change in insertion angulation during insertion or removal after insertion. The inner diameter of the guide cylinder equals or is slightly larger than the outer diameter of the screwdriver shaft, so that the screwdriver can be advanced in line with the cylinder. In this way, provided that the insertion guide is stabilised and well retained by the dentition, both the entry point and insertion angulations can be controlled with the insertion guide. Moreover, an insertion stop can be incorporated into the insertion guide, so that insertion depth can be determined. Therefore, all three parameters (entry point, insertion angulation and insertion depth) can be well controlled by insertion guides (Figure 11.15).

Lastly, through rapid prototyping technique, the designed insertion guides are 3-D printed and can be readily used for clinical placement of mini-implants (Figure 11.16).

t.me/Dr_Mouayyad_AlbtousH

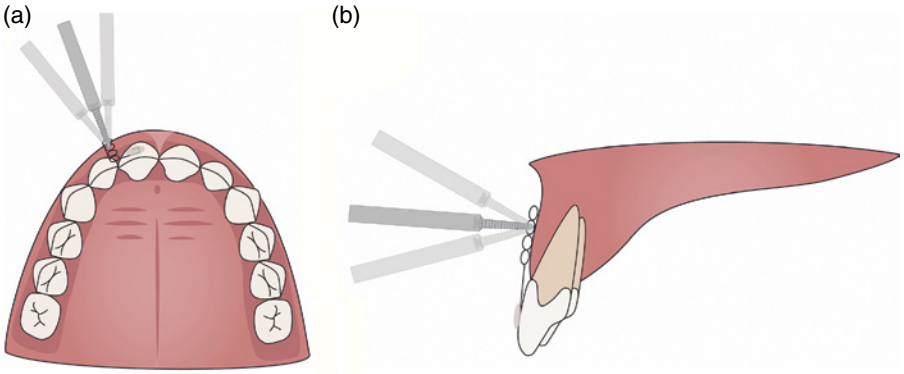


Figure 11.13 Deviated insertion directions with the use of wire guide. The wire guide is unable to secure the insertion direction which may lead to horizontal deviations (a) or vertical deviations (b).

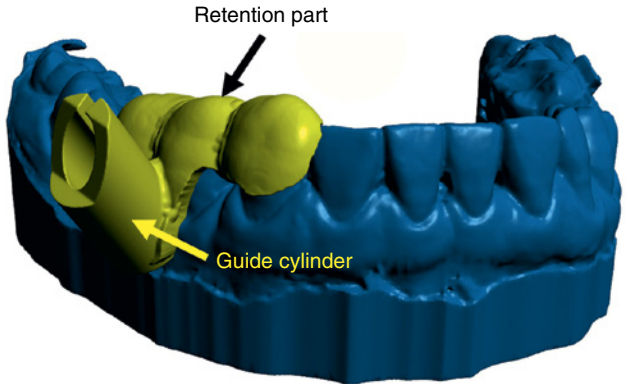


Figure 11.14 An insertion guide is composed of a retention part that is fitted onto the teeth and a guide cylinder where a mini-implant is inserted.

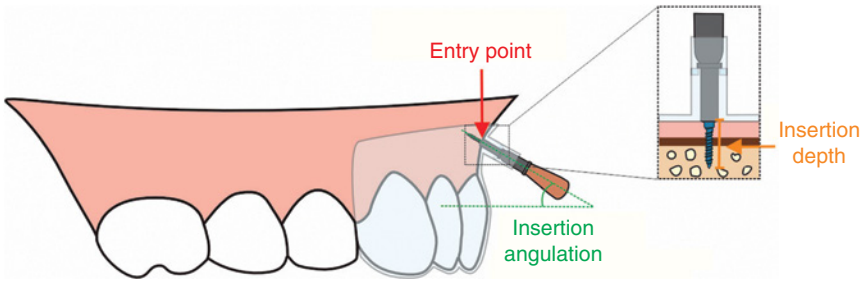


Figure 11.15 The incorporation of an insertion stop into a guide renders all the three parameters to be precisely controlled: entry point, insertion angulation and insertion depth.

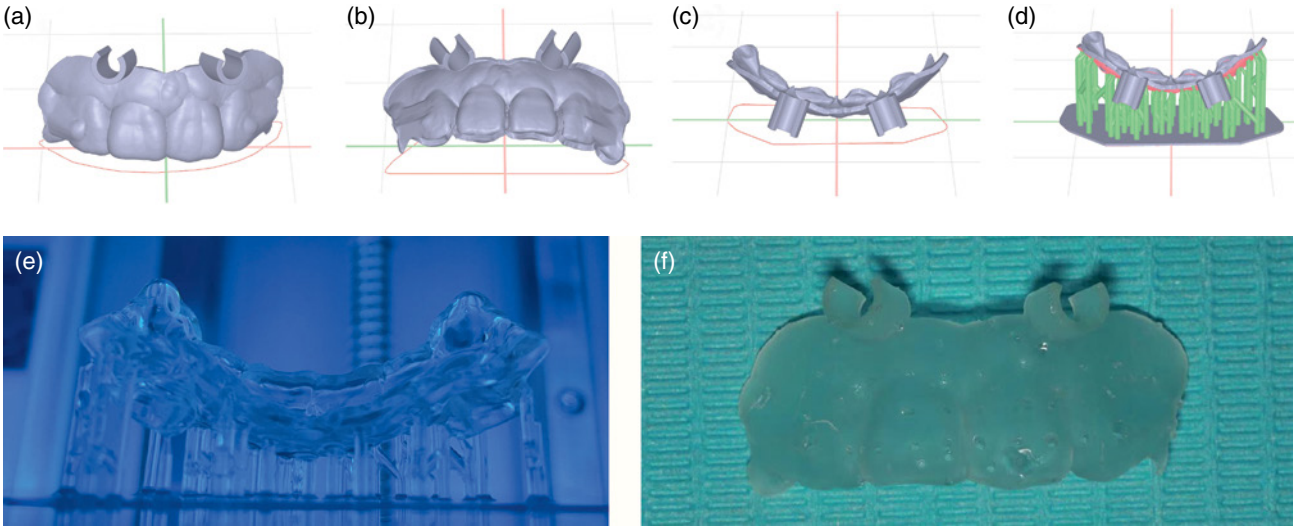


Figure 11.16 (a–d) Digital design of an insertion guide. (e) 3-D printing of the guide. (f) The printed insertion guide ready for use.

t.me/Dr_Mouayyad_AlbtousH

11.3 Advantages and Disadvantages of Insertion Guides

11.3.1 Advantages

Accuracy and Precision

Orthodontic mini-implants are often inserted into interradicular sites where root proximity is the most frequently encountered complication (Figure 11.17). The risk of root proximity is greatly increased for interradicular sites with limited space. Moreover, for anatomical sites with limited physical access (e.g. posterior interradicular sites and palatal regions), it is difficult for practitioners to manipulate the insertion from optimal directions, resulting in deviated insertion angulations and eventual root contact. A large body of evidence indicates that root proximity is a significant factor associated with mini-implant failure and that the risk of mini-implant failure doubles for every 1 mm increase in root contact.[25-29] Thus, to guarantee the clinical success of orthodontic mini-implants, root proximity or root contact should be avoided. This poses high demands for accuracy and precision in the placement of mini-implants, especially for interradicular sites with limited space. Fortunately, the accuracy and precision of inserting mini-implants have been greatly improved with the advent of insertion guides.[3]

With the insertion guide technique, practitioners can virtually design the three parameters of mini-implants on 3-D reconstructions: entry point, insertion angulation and insertion depth. As displayed in Figure 11.18, on the virtual dental model, practitioners can clearly view dental roots and virtually place the mini-implant into an optimal site. Moreover, on the model, the distance between the mini-implant and two adjacent roots can be precisely measured to guarantee a 1 mm clearance from the two adjacent roots.

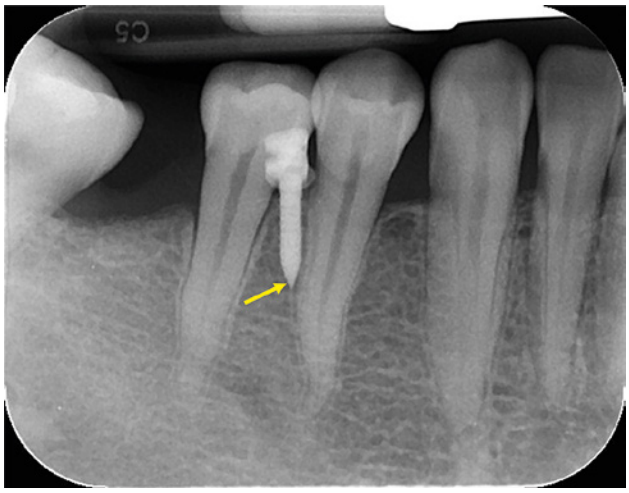


Figure 11.17 An interradicular mini-implant was misplaced and contacted the root of the first premolar. Note the root contact by the mini-implant, indicated by the yellow arrow.

Then, the determined position of the mini-implant is precisely transferred with the 3-D-printed insertion guide with high accuracy (Figures 11.19 and 11.20).

Efficiency

For free-hand insertion, numerous clinical procedures have to be performed to ensure the successful placement of mini-implants: (1) visually check the optimal entry point; (2) mark the gingiva indentation; (3) check the indentation from different directions; (4) insert a mini-implant through the entry point; (4) check the insertion angulation of the mini-implant from different directions; (5) adjust the insertion angulation during insertion. This whole procedure is time-consuming, especially for inexperienced practitioners. Moreover, for anatomical sites where direct visualisation may lead to errors, confirmation of entry point and gingiva indentation through indirect visualisation with mirrors are mandatory (Figure 11.21). This further increases the complexity of inserting mini-implants and results in extended time spent for mini-implant placement. Occasionally, when patients complain of pain during insertion, root proximity is suspected and radiographic examinations may be prescribed to rule out root proximity. This also increases the time required for mini-implant placement.

For the guided insertion technique, mini-implants can be inserted through a few clinical steps: (1) mount the insertion guide onto the dentition; (2) stabilise the insertion guide and place the mini-implant through the guide cylinder (Figure 11.22). With a predetermined entry point, insertion angulation and insertion depth, the accuracy and precision of mini-implant placement can be guaranteed. Thus, with insertion guides, mini-implants can be placed efficiently with high accuracy.

Ease of Insertion

With the free-hand insertion technique, it is often difficult for practitioners to place mini-implants at anatomical sites with limited access to manipulation, e.g. palatal region and posterior interradicular sites. Moreover, for some patients with limited mouth opening, adequate cheek retraction is required to gain access to insertion. On one hand, this causes soft tissue tension that may lead to difficulty in maintaining the optimal insertion angulation, resulting in deviations in insertion angulation and root proximity. On the other hand, retraction of soft tissue may lead to soft tissue irritation and pain and result in decreased patient compliance (Figure 11.23). In contrast, with insertion guides, it is easy for practitioners to place mini-implants through the guide cylinders using contra-angle screwdrivers without the need for adequate soft tissue retraction. Thus, applying insertion guides facilitates the placement of mini-implants into difficult-to-access anatomical sites.

t.me/Dr_Mouayyad_AlbtousH

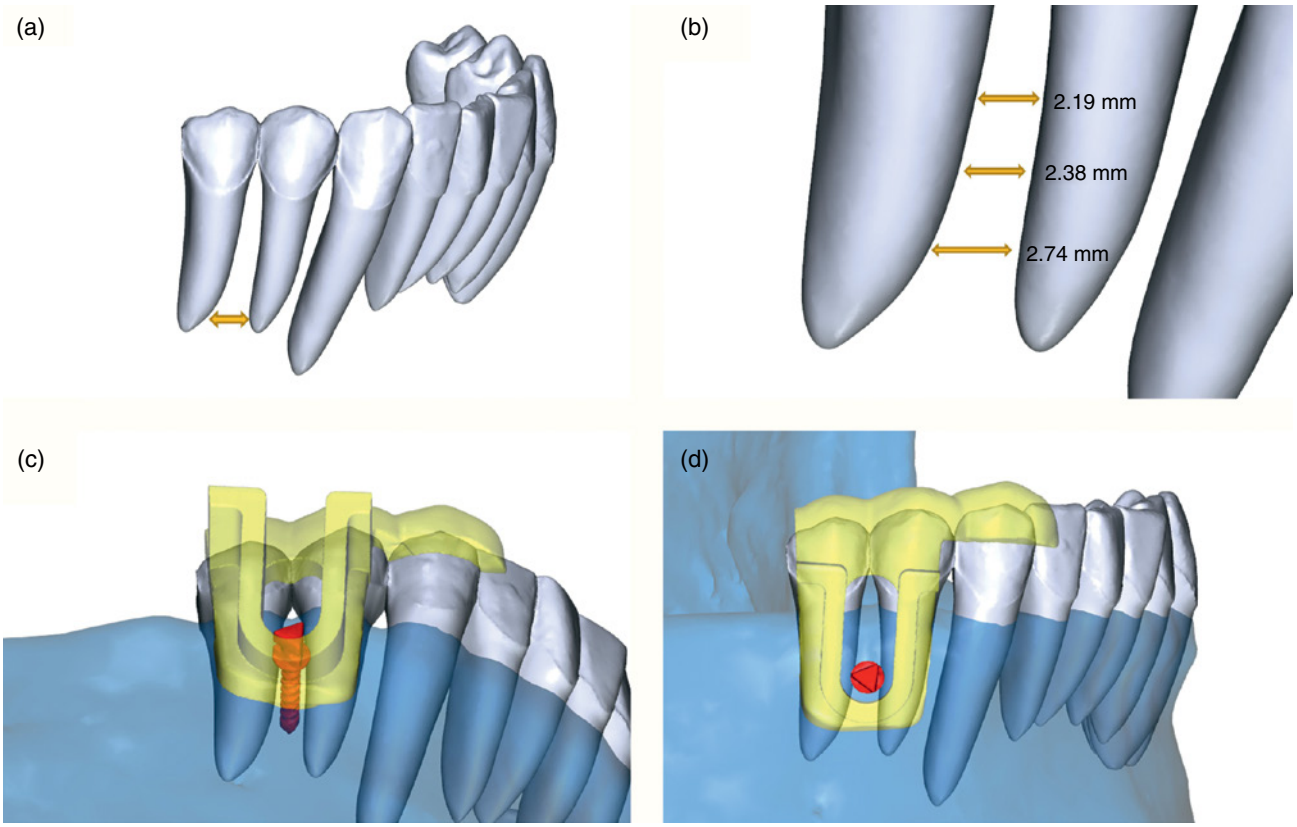


Figure 11.18 The application of a digitally designed insertion guide for an interradicular site with limited space. (a,b) Limited interradicular space makes the placement of mini-implants difficult. (c,d) Virtual placement of a mini-implant between the two roots and digital design of the insertion guide based on the final position of the mini-implant.

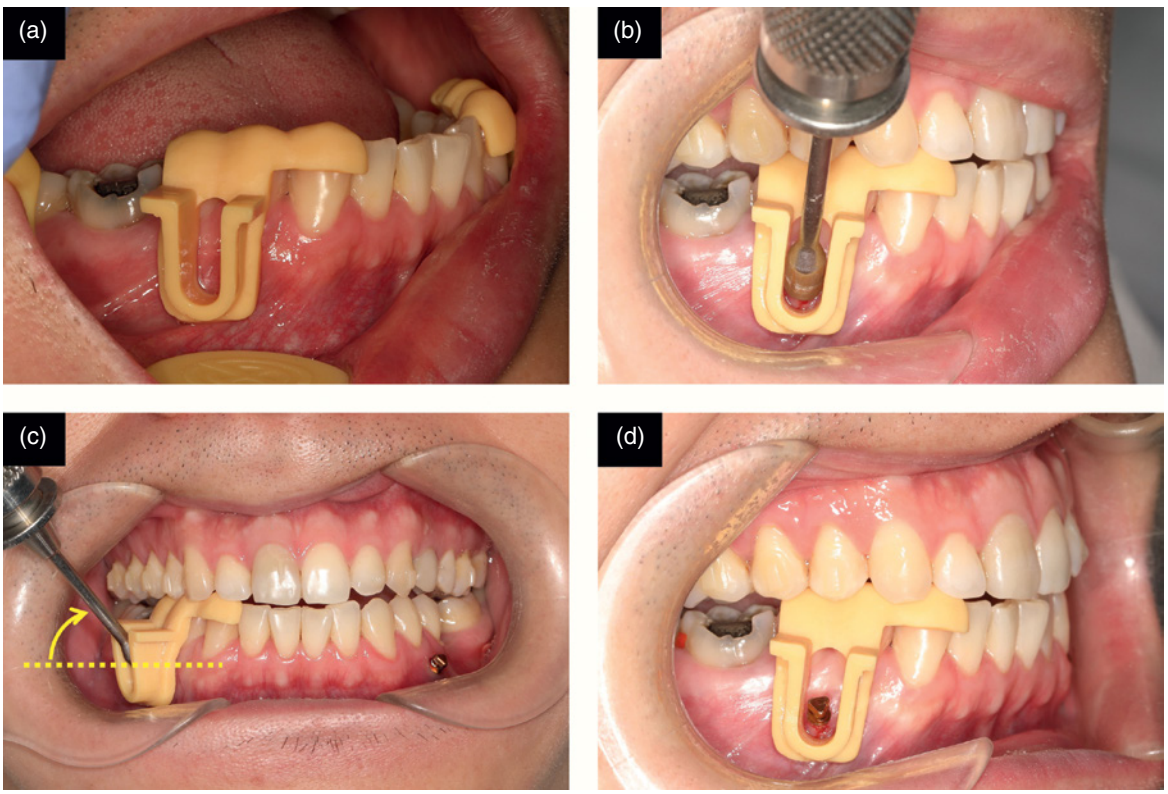


Figure 11.19 Insertion of an interradicular mini-implant using an insertion guide. (a) Engagement of the insertion guide. (b) Insertion of the mini-implant through the U-shaped guide cylinder. (c) The U-shaped guide cylinder allows a change in the insertion angle while the mini-implant is being inserted. The initial insertion path (yellow dashed line) can be changed to the final one during the insertion procedure. (d) Insertion of the mini-implant was complete and the screwdriver was disengaged.

t.me/Dr_Mouayyad_AlbtousH

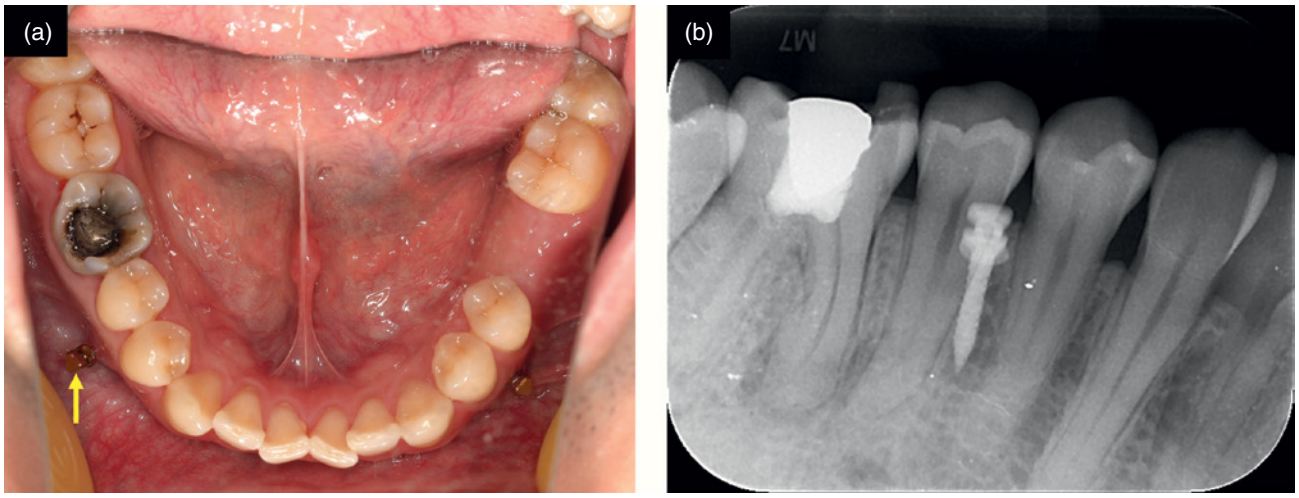


Figure 11.20 (a) Occlusal view of the mini-implant (yellow arrow). (b) Orthogonal periapical radiograph showing the correct position of the mini-implant.

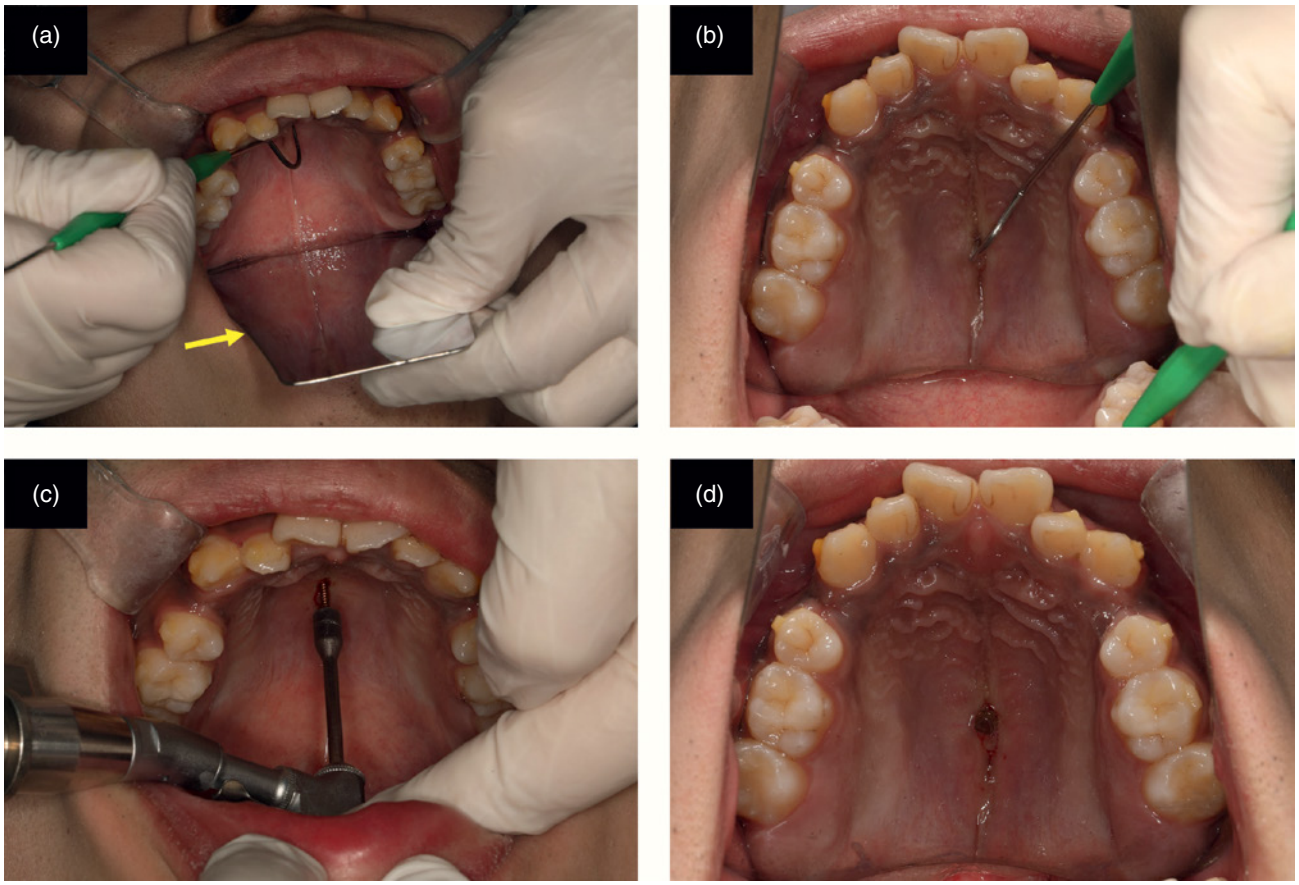


Figure 11.21 The insertion of a mini-implant at the palatal vault region. (a) Confirmation of the entry point through a mirror (yellow arrow). (b) Marking the entry point with an explorer. (c) Inserting the mini-implant with a contra-angle screwdriver through the marked entry point. (d) Post insertion.

t.me/Dr_Mouayyad_AlbtousH

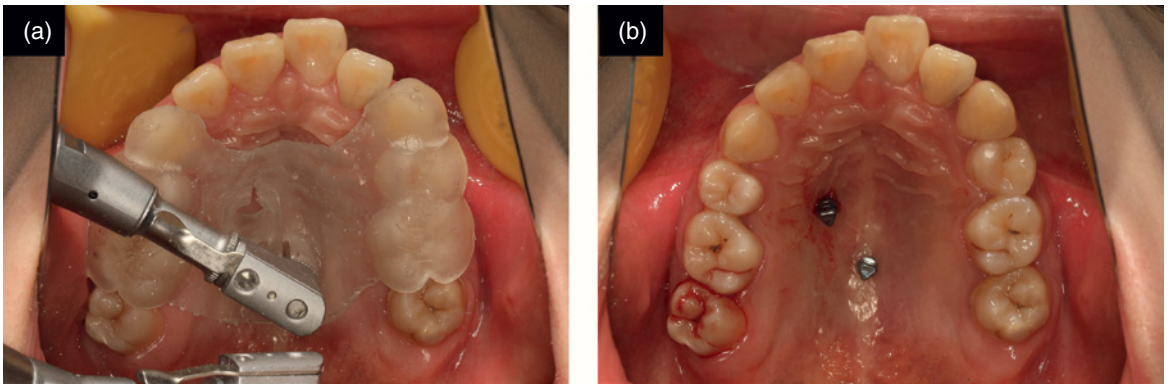


Figure 11.22 Insertion of a mini-implant at the palatal vault region through an insertion guide. (a) Insertion. (b) Post insertion.



Figure 11.23 Forceful retraction of the soft tissue for placement of a mini-implant at the mandibular buccal region may lead to pain.

11.3.2 Disadvantages

Higher Cost

The successful application of insertion guides requires a delicate multidisciplinary approach, including orthodontic treatment planning, radiographic assessment, 3-D reconstruction, 3-D virtual design and rapid prototyping. In contrast to the free-hand insertion technique, guided insertion of mini-implants poses additional economic burdens to patients, i.e. costs for CBCT, laser scanning of dental models or intraoral scanning, virtual planning software, 3-D reconstruction, virtual planning process, rapid prototyping device and 3-D printing. Thus, before making a decision on whether to apply insertion guides for a particular patient, it is important for practitioners to evaluate the cost-effectiveness of using insertion guides. For anatomical sites with ample interradicular space and ease of access, the use of guided insertion is unnecessary and free-hand insertion is indicated. However, for anatomical sites with limited interradicular space and difficult access, although guided insertion has a higher initial cost, it is more cost-effective due to higher accuracy and greater safety.

Extra Time for CAD-CAM

For patients receiving free-hand insertions, practitioners can directly insert mini-implants after radiographic assessment and only one appointment is needed. In contrast, for guided insertion of mini-implants, patients need more than two appointments.

For the first appointment, the patients receive radiographic examinations and intraoral scanning (or impression taking and subsequent laser scanning of dental casts), and are scheduled for the second appointment when guided insertion is performed for the placement of mini-implants. Between the first and second appointments, practitioners must prepare the digital dental models, virtually plan the locations of mini-implants, design the insertion guides and have the insertion guides 3-D printed. The time between the first and second appointments varies greatly among different practitioners and different clinical settings, but it generally takes 1–2 weeks. At the second appointment, it is advised to try the insertion guides onto the patient's dentition first to examine the fit between the insertion guides and dentition. Guided insertion cannot be started if the fit is unsatisfactory. Otherwise, unfitted insertion guides will lead to deviated insertions and potential damage to vital anatomical structures, e.g. dental roots. Thus, if the fit between insertion guides and dentition is not accurate, redesigning and remanufacturing of the insertion guides are required and this will take more time.

No Change During Insertion

Insertion guides can accurately and precisely transfer the virtually designed mini-implants into reality. Once the positions of mini-implants are determined on the virtual dental model, the real positions of the implants cannot be changed during the insertion procedure. Occasionally, even when the fit of the guides is confirmed prior to insertion, displacement can occur if adequate stabilisation is not guaranteed. If this occurs and deviations of mini-implants are detected during insertion, it is not possible to change the positions of mini-implants with the same insertion guide and conversion to free-hand insertion is indicated (Figure 11.24).

t.me/Dr_Mouayyad_AlbtousH

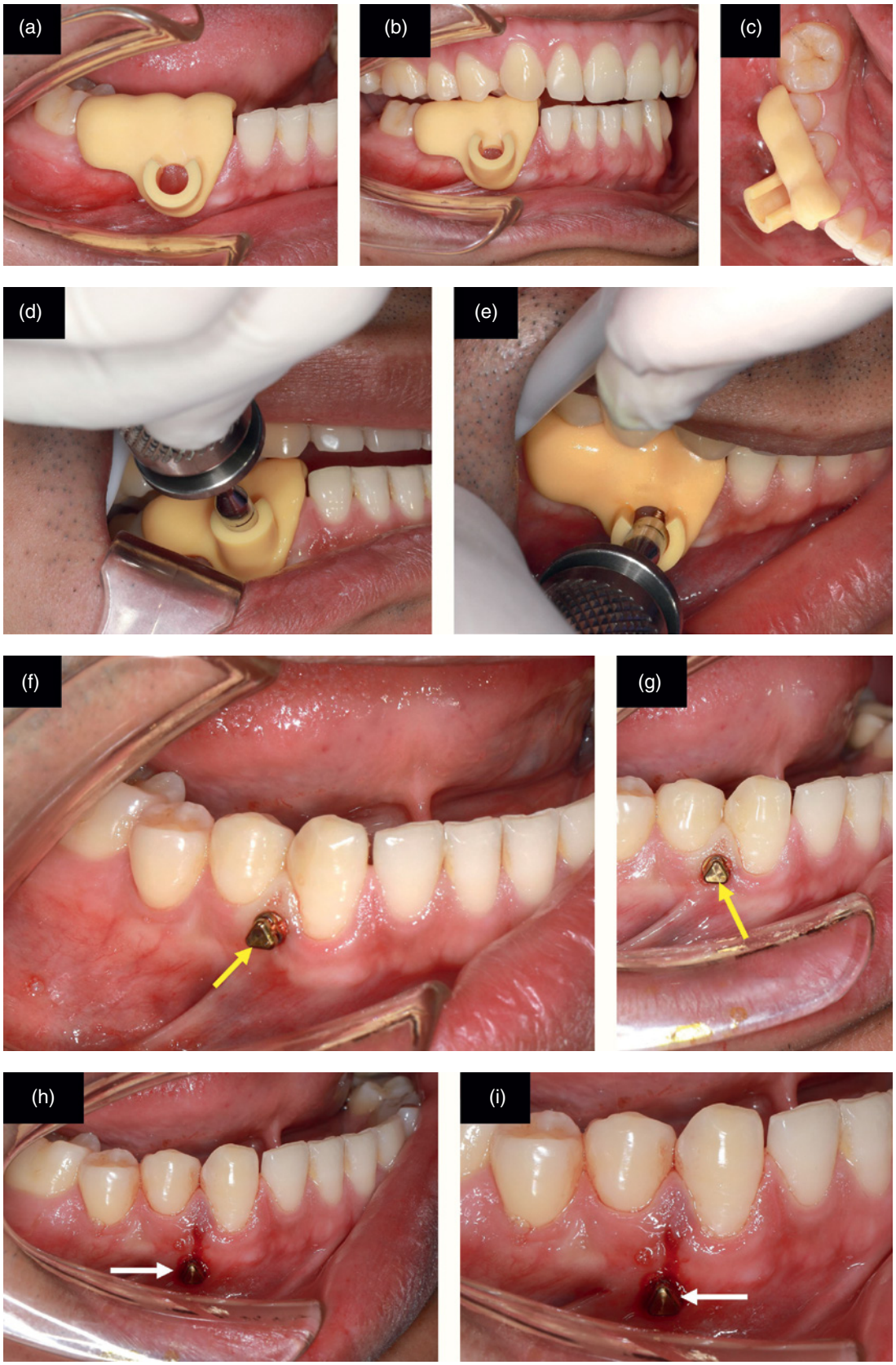


Figure 11.24 Conversion of guided insertion to free-hand insertion due to displacement of the insertion guide. (a–c) Good fit of the insertion guide. (d,e) Insertion of a mini-implant through the guide cylinder of the insertion guide. (f,g) Due to displacement of the guide during insertion, the mini-implant (yellow arrow) was misplaced and the final position was occlusal to the desired one. (h,i) The misplaced mini-implant was taken out and reinserted at the desired place (white arrow).

t.me/Dr_Mouayyad_AlbtousH

11.4 Three-dimensional Design of Insertion Guides for Mini-implants

Virtual design of insertion guides for orthodontic mini-implants demands several procedures, from obtaining 3-D digital data to the design and export of the stereolithography (STL) file. Specifically, the procedures include reconstructing a 3-D dentition model, establishing a mini-implant model, inserting mini-implants virtually, 3-D design of insertion guides and exporting the STL model of insertion guides ready for rapid prototyping. The details of each step will be discussed below.

11.4.1 Reconstructing a Three-dimensional Dentition Model

Digitalization of Dental Models

Digital data of the dentition can be obtained through either intraoral scanning or laser scanning of study models produced with silicon impression (Figures 11.25 and 11.26). The digital dental model should include not only the dentition but also soft tissue, especially the soft tissue around the planned insertion sites (Figure 11.27). Then, the digital dental model can be exported in an STL file for further processing.

Acquisition of Jaw Model

Digital data on the alveolar bone and teeth (both crowns and roots) can be acquired through CBCT (0.2 mm voxel size) and exported as DICOM ((Digital Imaging and Communications in Medicine) format files that are ready for 3-D reconstruction (Figure 11.28).

To avoid injury to dental roots, the roots and alveolar bone should be separated and differentiated in the jaw model, so that the distance between mini-implants and adjacent dental roots can be evaluated. The segmentation process can be divided into automatic and manual segmentation. For automatic segmentation, anatomical structures with different densities can be well differentiated, while those with similar density can only be differentiated through manual segmentation. Dental crowns have the highest density and soft tissues the lowest, with alveolar bone and dental roots being in the middle. Thus, based on their different densities, different thresholds for segmentations are recommended and displayed in Figure 11.29. Briefly, a segmentation threshold of 200 HU is employed to automatically exclude soft tissues and retain hard tissues (alveolar bone, dental roots and dental crowns) in the model. Then, automatic segmentation is performed to separate dental crowns from alveolar bone and roots based on a threshold of 700 HU. Lastly, due to their similar density, dental roots and alveolar bone can only be manually segmented at each layer, which is time-consuming.

The whole procedure of both automatic and manual segmentation can be conducted in Mimics® software (Materialise, Leuven, Belgium) and is illustrated in Figure 11.30. Fortunately, with the advent of artificial intelligence (AI), AI-assisted bone-root segmentation is promising in obtaining acceptably accurate results (Figure 11.31),[30] which can save time and significantly reduce manual work.

The three components (alveolar bone, dental roots and dental crowns) are registered in the same co-ordinate system and exported as STL format files for further processing.

Image Superimposition

Since insertion guides are mainly retained and supported by the dentition, digital data on the tooth surface should be of high resolution and high quality, as insertion guides produced with surface data of low quality may not fit with the dentition, leading to inaccuracy of guidance. Tooth contours that are obtained and reconstructed through CBCT are less accurate than those obtained through intraoral scanning or laser scanning of dental models (Figure 11.32).[31] Specifically, dental crowns are often enlarged by CBCT, which is attributed to the artifacts around dental crowns due to partial volume effect (Figure 11.33). Thus, digital crown data obtained through intraoral scanning should be merged with CBCT data and replace the corresponding crown data in CBCT (Figure 11.34).

To perform image merging, the surface mesh of dentition obtained through intraoral scanning is superimposed with CBCT images through the ICP (iterative closet point) algorithm in Geomagic Studio® software (Geomagic International, Morrisville, NC, USA). The following three steps are recommended to complete the superimposition process. First, three or more common reference points (e.g. central incisor embrasure and mesiobuccal cusps of first molars) are selected on both the intraorally scanned model and the CBCT model to perform a preliminary superimposition (Figure 11.35).[32] Second, the global registration function can be used to superimpose the two models as closely as possible, resulting in registration of the dental model into the CBCT model. Lastly, dental crown data obtained with CBCT are removed from this superimposed model and a final model is created containing both jaws (CBCT), facial soft tissues (CBCT), dental roots (CBCT), dental crowns (intraoral scanning) and gingivae (intraoral scanning) (Figure 11.36).

t.me/Dr_Mouayyad_AlbtousH

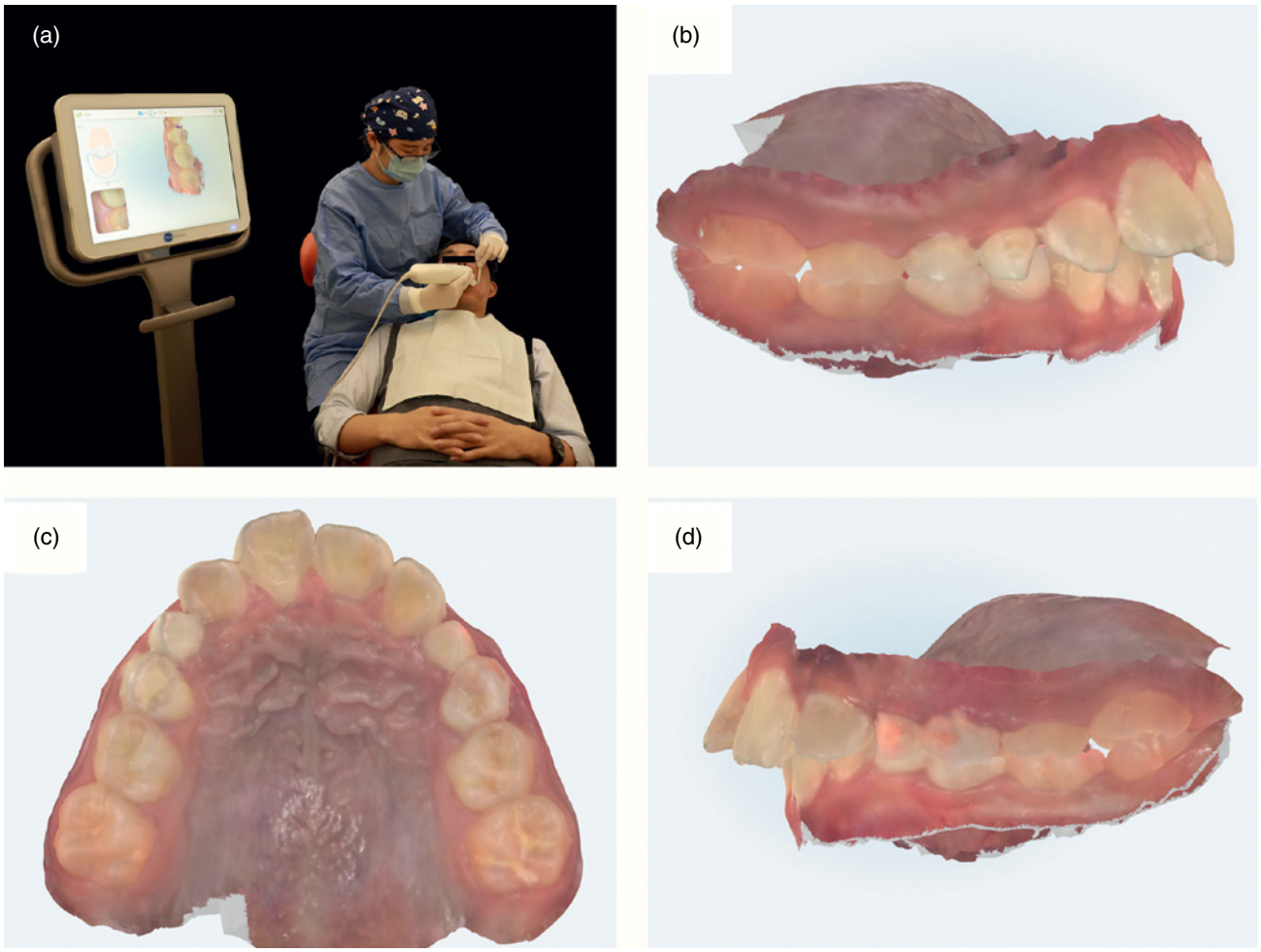


Figure 11.25 Acquisition of the digital data of dentition through intraoral scanning. (a) A practitioner is performing the intraoral scanning. (b–d) The digital data of the patient's dentition ready to be used for 3-D design of the insertion guide.

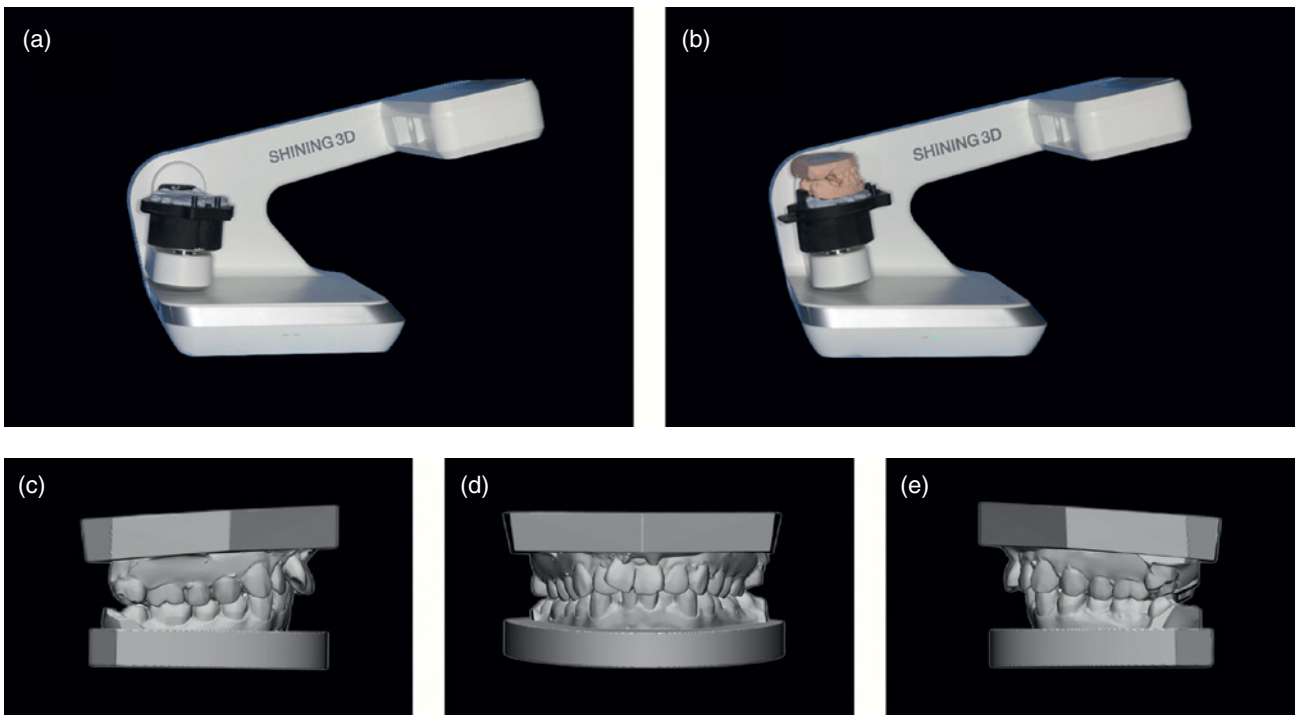


Figure 11.26 Obtaining the digital data of dentition through laser scanning of the dental casts. (a) A laser scanner. (b) The laser scanner is scanning the dental casts. (c–e) The digitalised dental model.

t.me/Dr_Mouayyad_AlbtousH

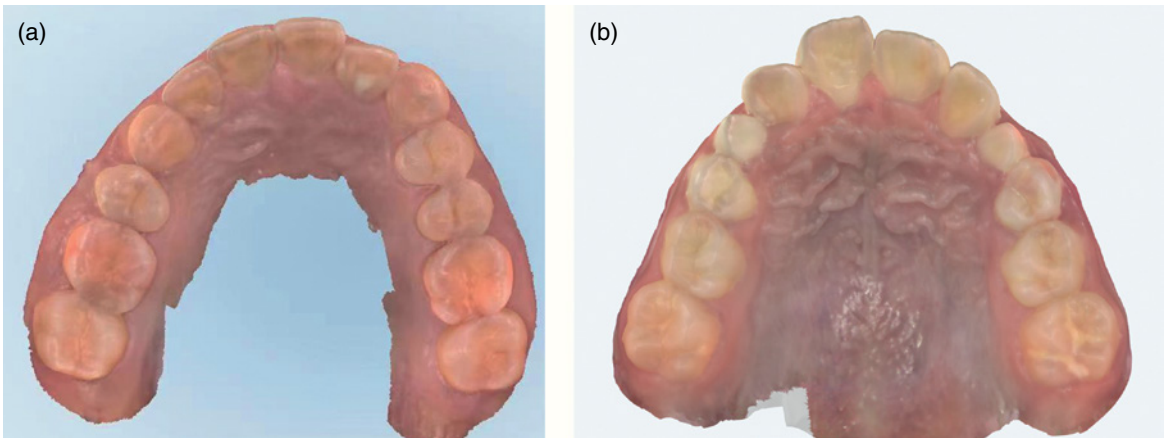


Figure 11.27 Soft tissue data is required for the design of insertion guides. (a) The upper model contains the dentition only and is not suitable for the design of an insertion guide of a palatal mini-implant. (b) The upper model contains both the dentition and the palatal vault, and can be used for the design of an insertion guide for a palatal mini-implant.

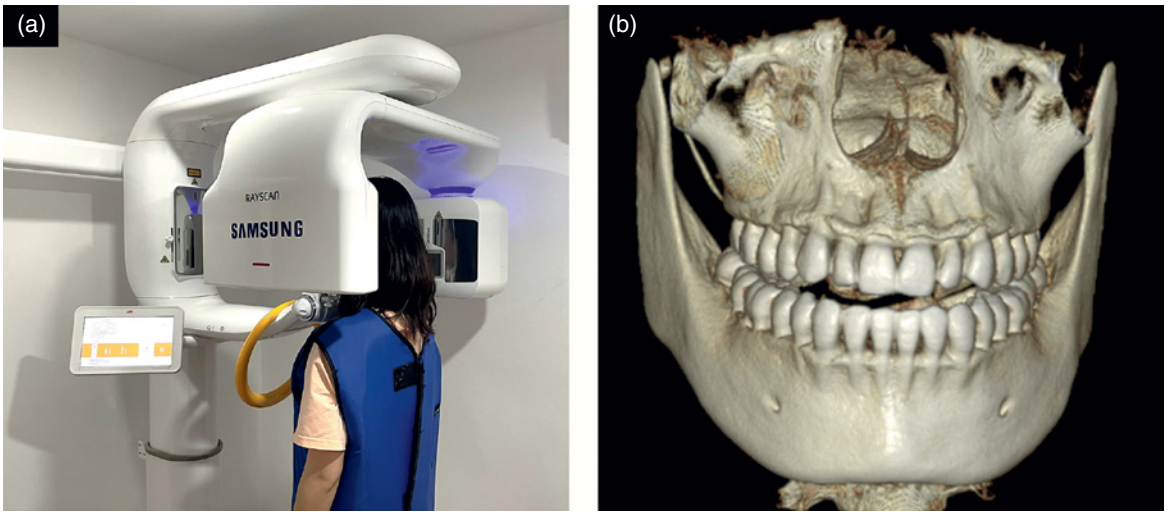
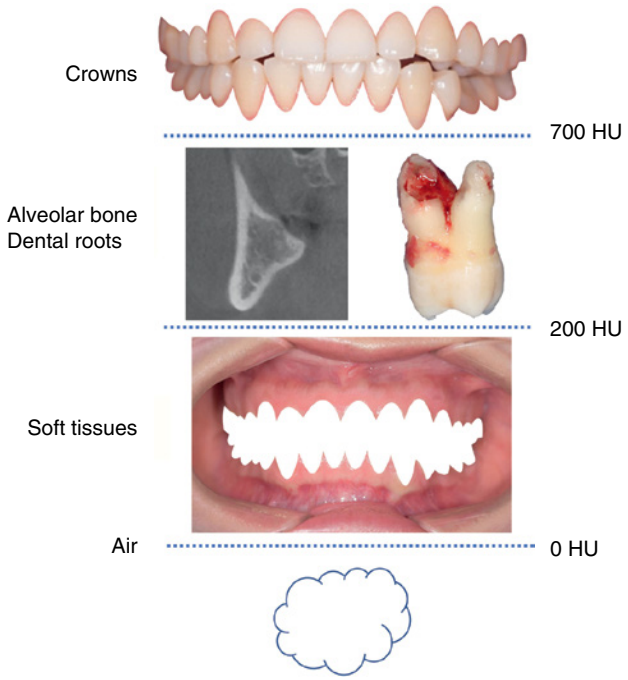


Figure 11.28 Acquisition of data on skeletal bone, alveolar bone and teeth through CBCT radiography. (a) A patient is receiving the CBCT examination. (b) 3-D reconstruction of the skeletal bone, alveolar bone and dentition based on CBCT images.

Figure 11.29 Densities of different structures in Hounsfield units (HU).



t.me/Dr_Mouayyad_AlbtousH

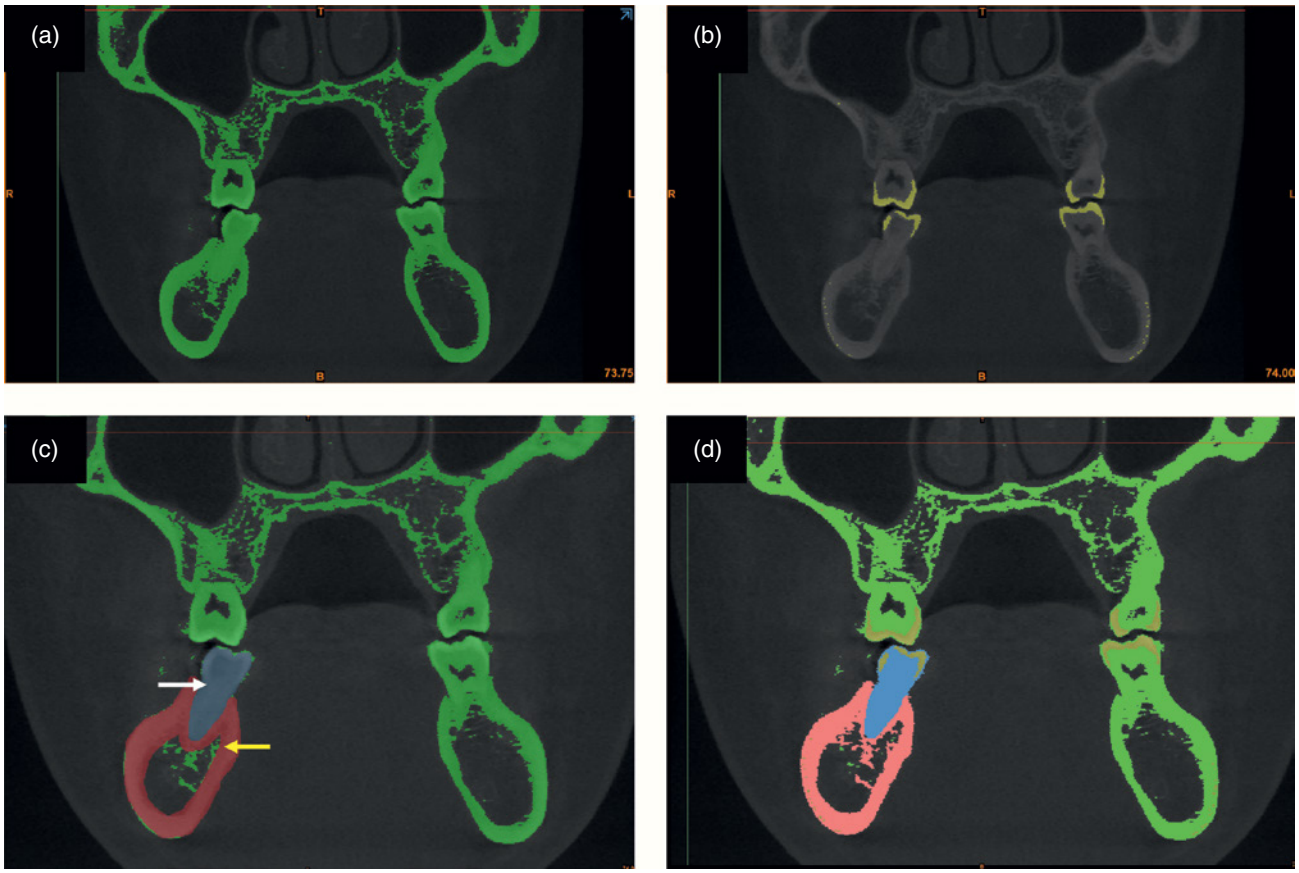


Figure 11.30 Segmentation procedures. (a) A segmentation threshold of 200 HU is employed to exclude soft tissue. (b) Dental crowns are separated through automatic segmentation at the threshold of 700 HU. (c) Separation of the dental root (white arrow) from the alveolar bone (yellow arrow) through manual segmentation. (d) Image fusion.

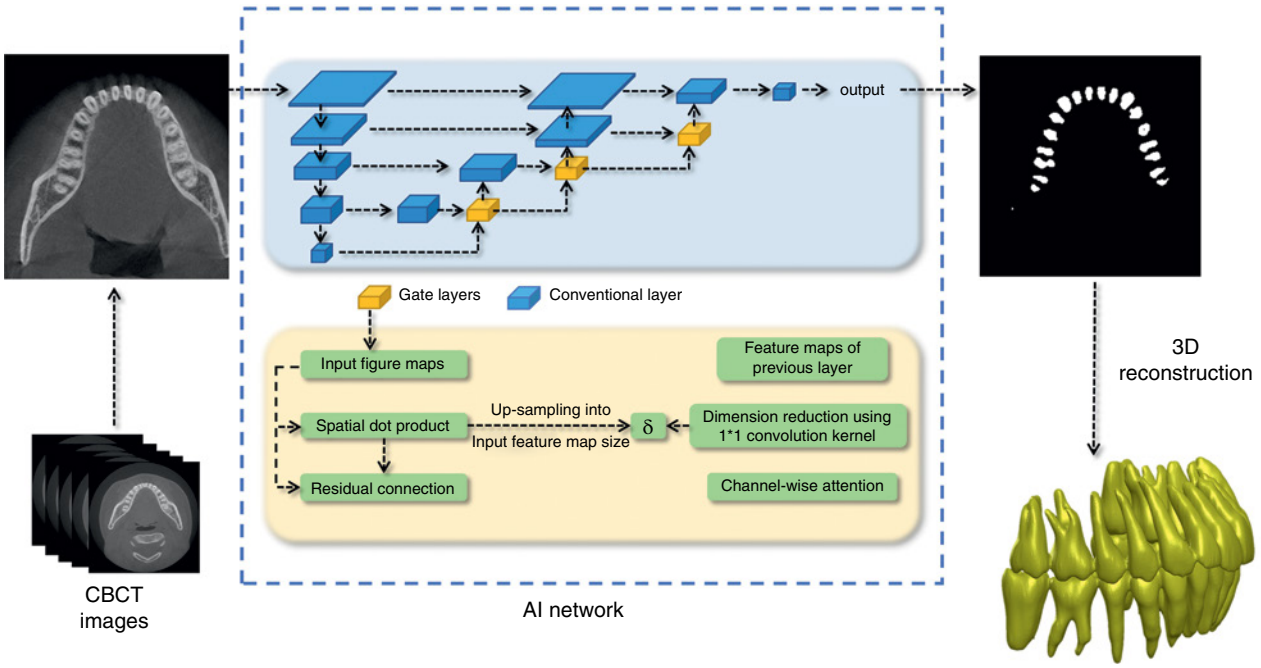


Figure 11.31 Artificial intelligence-assisted bone-root segmentation and 3-D reconstruction.

t.me/Dr_Mouayyad_AlbtousH

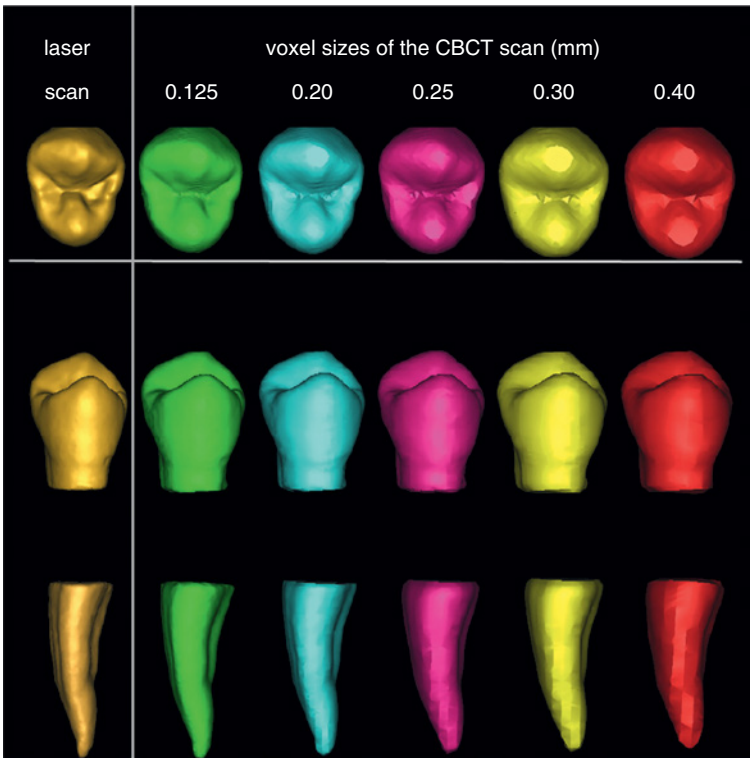
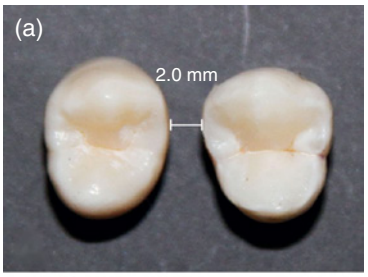
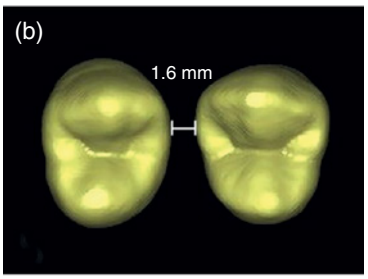
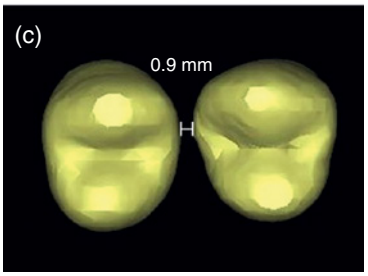
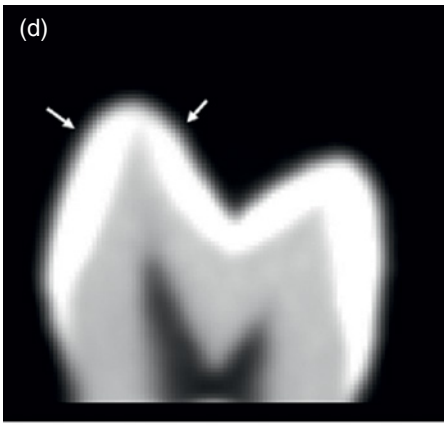


Figure 11.32 Inaccuracy of reconstructed crowns and roots from CBCT. The crown and root halves, from left to right, are laser scans (gold), 0.125 mm voxel (green), 0.20 mm voxel (cyan), 0.25 mm voxel (fuchsia), 0.30 mm voxel (yellow), and 0.40 mm voxel (red) (laser scan is the gold standard). Both the crown and root increase in size from left to right. *Source:* Ye et al. [31]/Reprinted with permission from Elsevier.









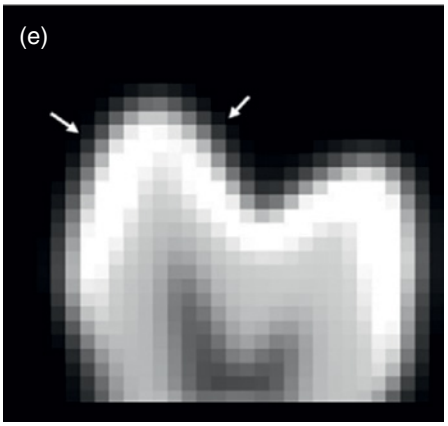


Figure 11.33 Partial volume effect causes artifacts around tooth crowns. (a) The distance between the two actual teeth. (b) The distance between the two teeth subject to 0.125 mm voxel CBCT scan. (c) The distance between the two teeth subject to 0.40 mm voxel CBCT scan. (d) 0.125 mm voxel CBCT scan image. (e) 0.40 mm voxel CBCT scan image. Note the volume of the reconstructed crowns increases with an increase in the voxel size. *Source:* Ye et al. [31]/Reprinted with permission from Elsevier.

t.me/Dr_Mouayyad_AlbtousH

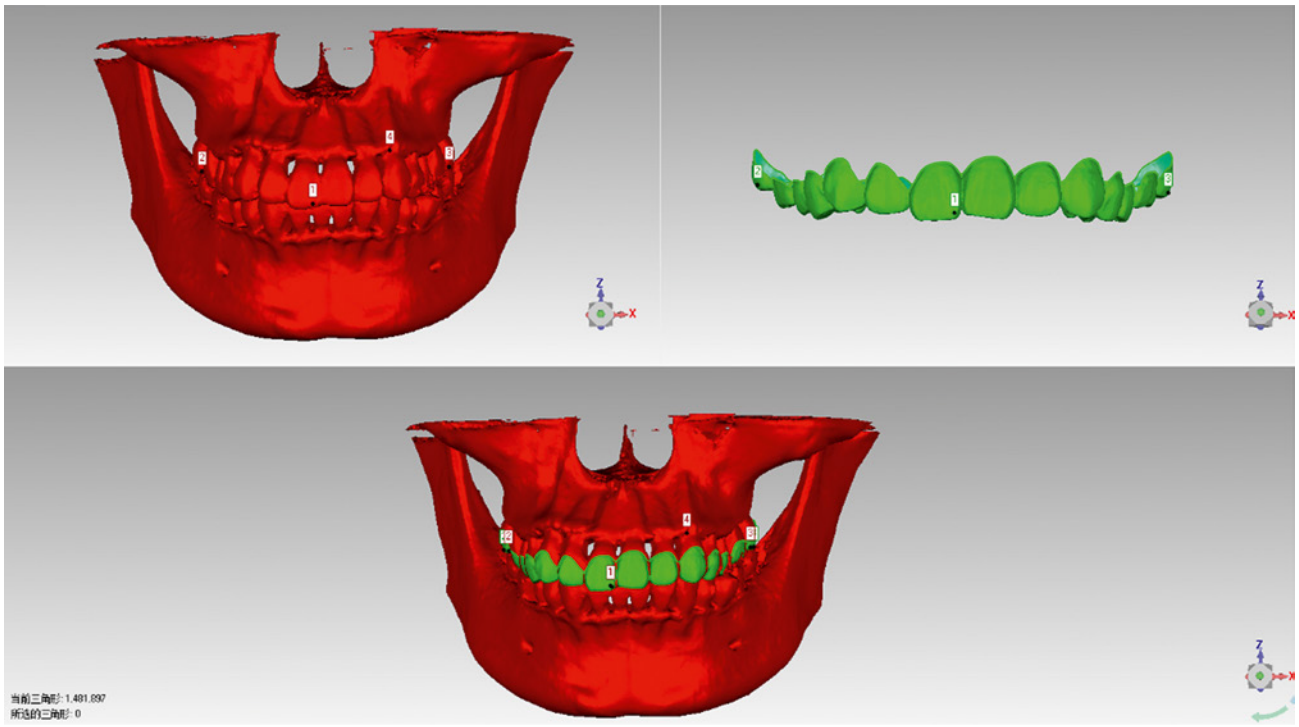


Figure 11.34 Image fusion between the CBCT data and the dentition data that are obtained from either intraoral scanning or laser scanning.

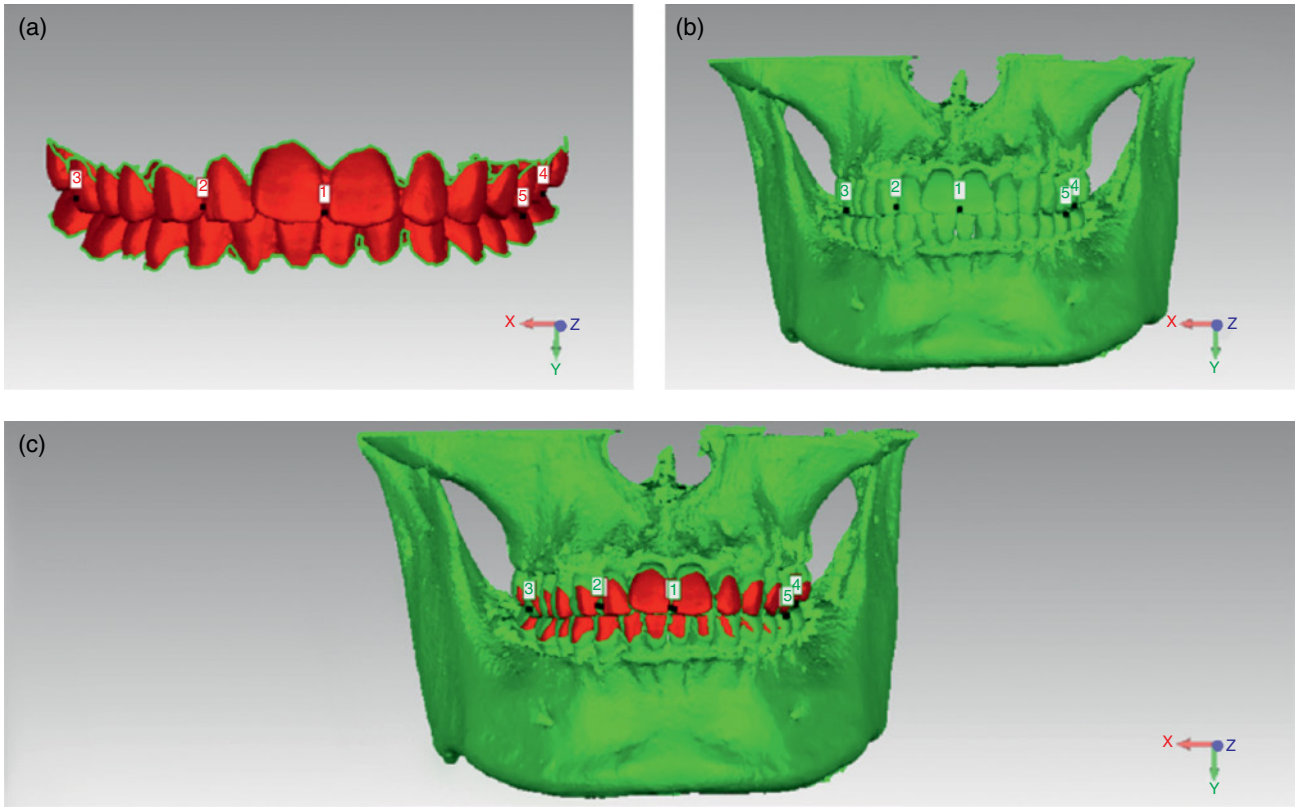


Figure 11.35 Three or more common reference points are selected on both the intraorally scanned model and the CBCT model to perform a preliminary superimposition. *Source:* Ye et al. [32]/Reprinted with permission from Elsevier.

t.me/Dr_Mouayyad_AlbtousH

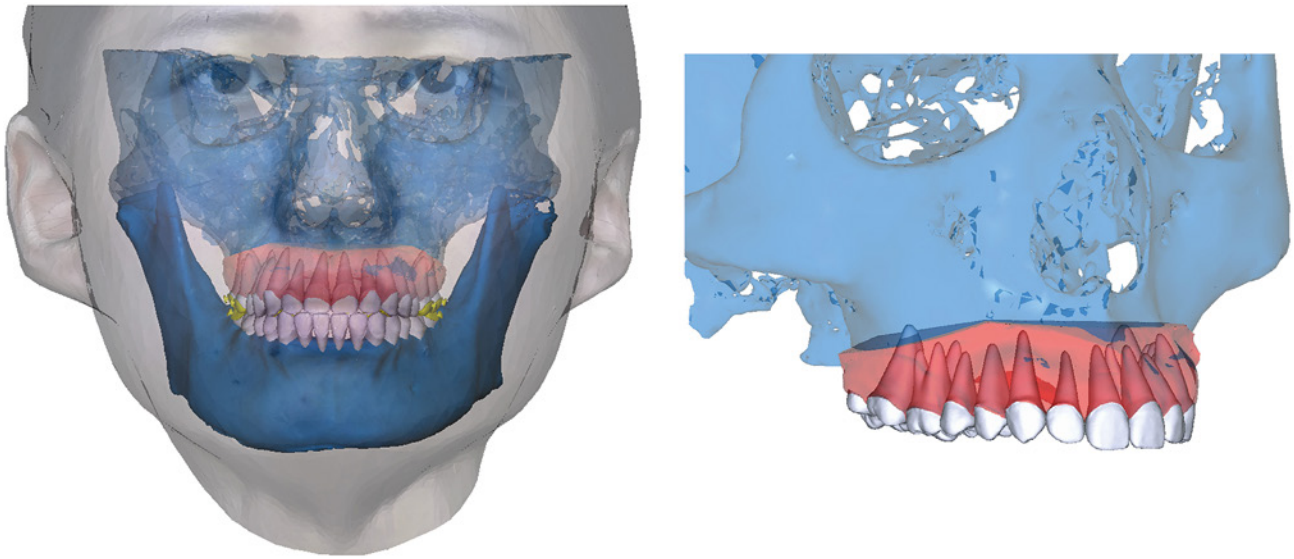


Figure 11.36 Establishment of the final model containing jaws, dental crowns, roots, gingivae, mucosa and facial soft tissues.

Model Post-processing

The presence of dental undercuts and the shrinkage of insertion guides during the curing process may cause inaccurate fitting of insertion guides. Thus, undercut block-outs and dental model offsets can avoid inaccurate fitting of insertion guides and compensate for the shrinkage of insertion guides during light curing.

Most often, insertion guides of mini-implants are designed with a combination of dentition-supported and gingiva-supported methods and the presence of dental and soft tissue undercuts may lead to inaccurate fitting of insertion guides during try-in and difficulty in removal of insertion guides, as well as soft tissue irritation. Thus, both the dental and soft tissue undercuts should be eliminated prior to the virtual design of insertion guides. To perform the block-out of undercuts, dental models are positioned with their occlusal planes in line with horizontal planes in Geomagic software and the undercut areas can be detected and blocked out in reference to the occlusal plane (Figure 11.37).

During the light-curing stage, shrinkage of the light-curing resin materials for insertion guides occurs, which may lead to inaccurate fitting and potential errors in transferring the virtual positions of mini-implants. This notion is supported by our previous study in which we found that insertion guides did not fit well if they were directly generated from the original model.[33] Moreover, we found that guides with dental offsetting through enlarging tooth contours by 0.1 mm resulted in better fit than those without (Figure 11.38).[33] Thus, dental models are offset through enlarging the whole dentition surface by 0.1 mm, creating a new dental model with a well-proportioned dentition surface (Figure 11.39).

11.4.2 Establishing the Digital Data of Mini-implants and Screwdrivers

In clinical practice, mini-implants and their corresponding screwdrivers with different dimensions are used. Thus, digital models of commonly used mini-implants and screwdriver shafts should be created, so that virtual insertion of mini-implants can be accomplished. The detailed procedures and steps are as follows.

Creating Digital Models of Mini-implants

The shapes, lengths and diameters of each part of the mini-implant are determined and measured. Then, digital models of the implant can be created in Solidworks® software (UGS Corporation, Plano, TX, USA) through reverse engineering (Figure 11.40).

Building Digital Models of Screwdrivers

The digital data of screwdriver working shafts are obtained in Solidworks software through reverse engineering in a similar way (Figure 11.40).

Creating Digital Models of Guide Cylinders

Based on the dimensions of the screwdriver working shafts, the digital data of corresponding cylinders are created. To transfer the virtual positions of mini-implants more precisely, the inner diameters of guide cylinders should be equal to or slightly greater than the outer diameters of the screwdriver working shafts (Figure 11.40).

Assembly

Finally, the mini-implant, the screwdriver working shaft and the guide cylinder can be assembled ready for the virtual placement of the mini-implant (Figure 11.40).

t.me/Dr_Mouayyad_AlbtousH

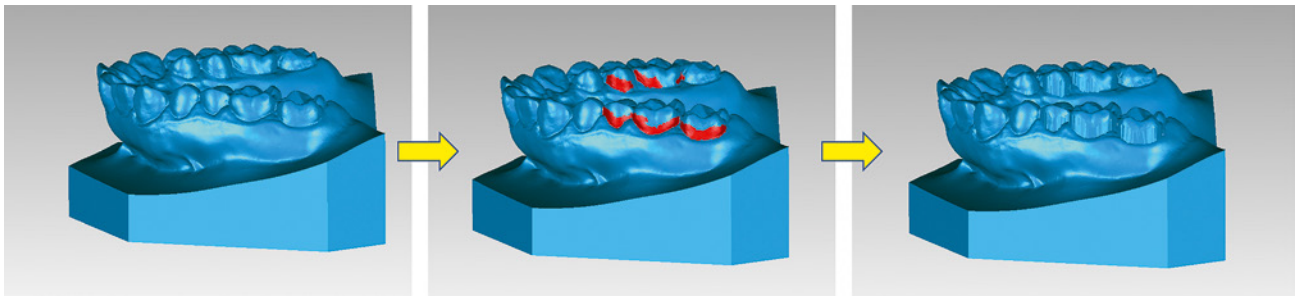


Figure 11.37 Block out the undercut of the dental model.

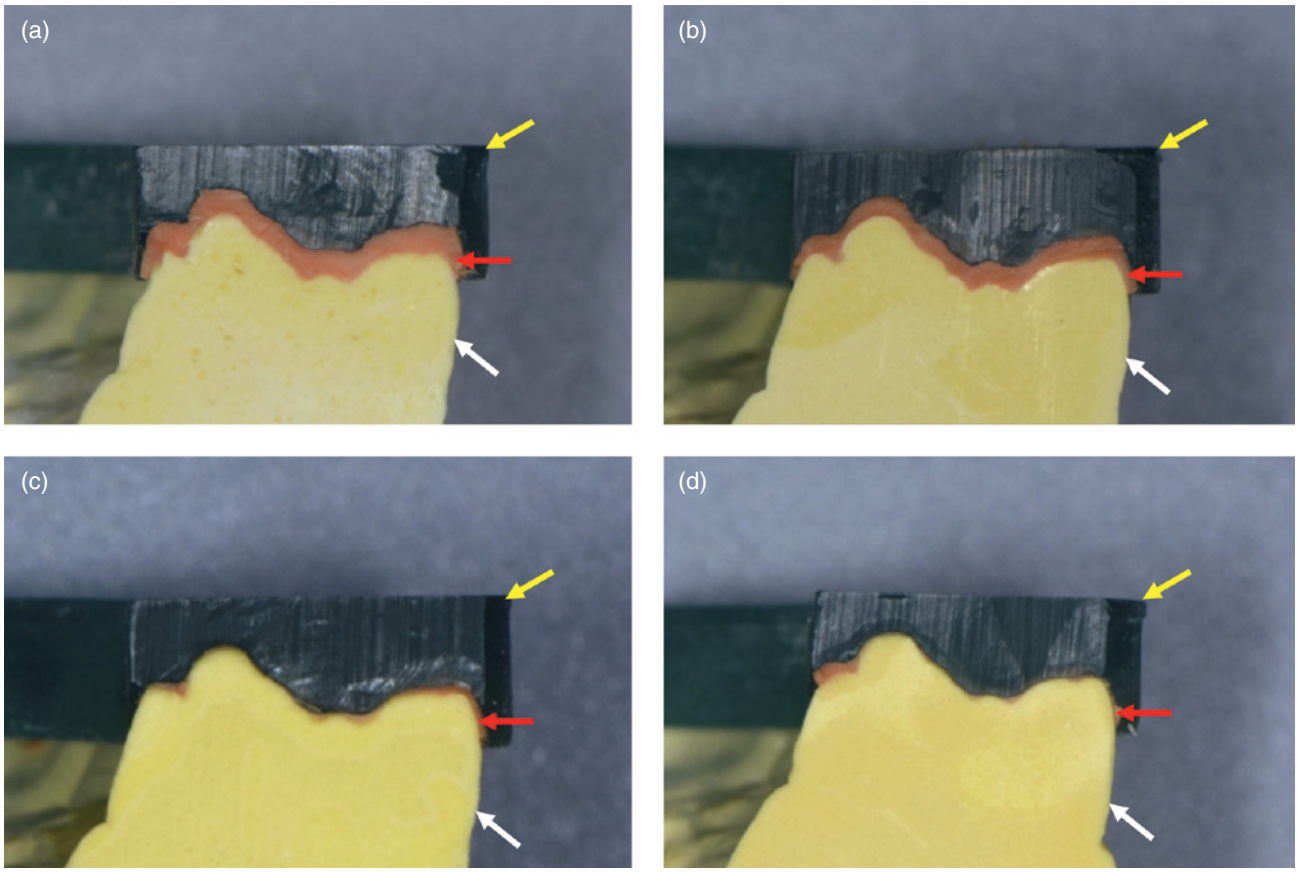


Figure 11.38 Shrinkage of resin materials due to light curing leads to inaccurate fitting of the guide and the significance of dental offset. Note the airspace represented by the impression material (red arrow) between the guide (yellow arrow) and the dental crown (white arrow) in the conditions of different levels of dental offsets. (a) 0 mm dental offset. (b) 0.05 mm dental offset. (c) 0.1 mm dental offset. (d) 0.2 mm dental offset. *Source:* Ye et al. [33]/Reprinted with permission from Elsevier.

t.me/Dr_Mouayyad_AlbtousH

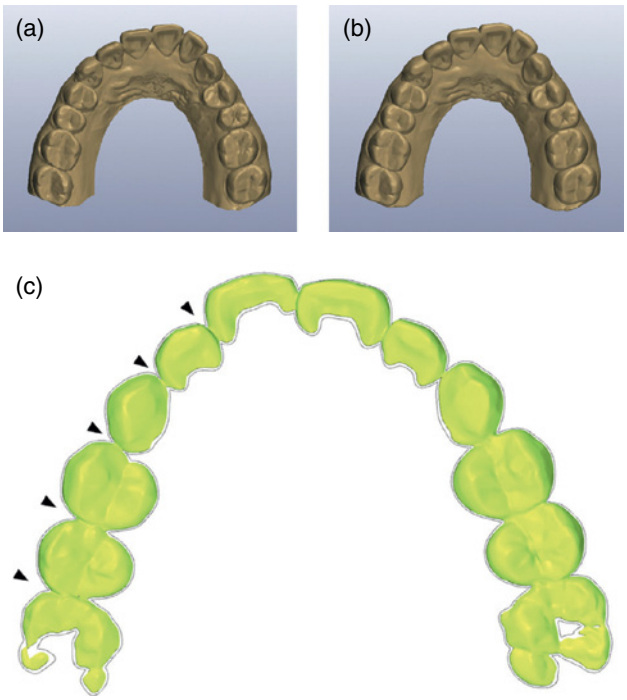


Figure 11.39 Offsetting of the dental model. (a) Initial dental model. (b) Offset dental model. (c) The initial dental model (green) and the offset model represented by the black line. The offset dental model is enlarged, especially in the interproximal areas (arrowheads). *Source:* Ye et al. [33]/Reprinted with permission from Elsevier.

11.4.3 Virtual Placement of Mini-implants

Optimal insertion sites are determined by a variety of anatomical factors and biomechanical considerations. For virtual placement of mini-implants, the following anatomical factors should be evaluated: cortical thickness, bone volume, interradicular distance, root positions and soft tissue thickness. The virtual placement of mini-implants can be performed in CAD software.

Determining an Optimal Insertion Site

Based on anatomical factors, i.e. cortical thickness, bone volume, interradicular space and soft tissue thickness, an optimal insertion site is selected and a mini-implant with appropriate diameter and length is determined (Figures 11.41 and 11.42).

Virtual Insertion of Mini-implants

Mini-implants can be virtually inserted into predetermined anatomical sites (Figure 11.43). Interradicular distances can be easily measured and root proximity can be visually detected in the software once the mini-implants are inserted (Figure 11.44). Appropriate adjustments can be made to obtain the 1 mm clearance principle and the positions and angulations of mini-implants can be adjusted in all three dimensions (Figure 11.45).

Moreover, the amount of bone engagement and the thickness of soft tissue that is penetrated by the mini-implant can be readily evaluated in the CAD software (Figure 11.46).

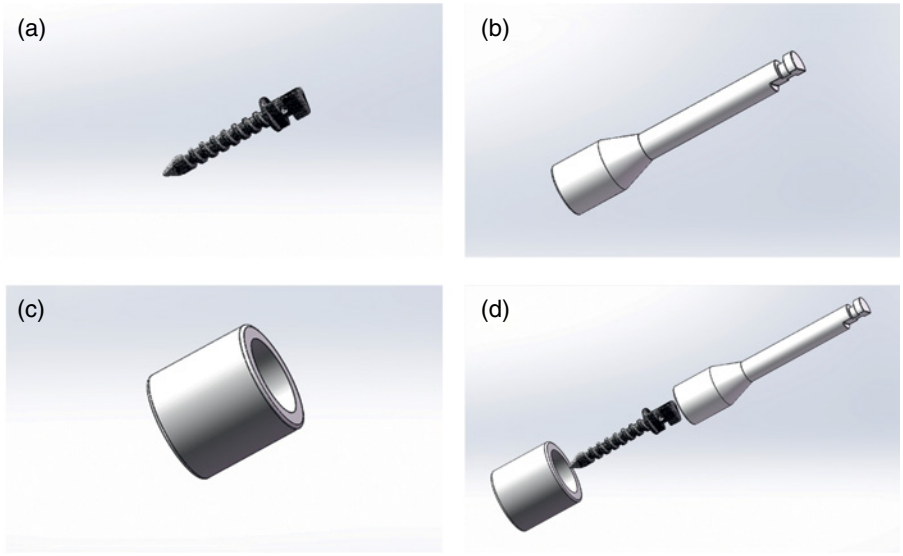


Figure 11.40 Digital models of the mini-implant system. (a) The mini-implant. (b) Working shaft of the screwdriver. (c) Guide cylinder. (d) Assembly of the system.

t.me/Dr_Mouayyad_AlbtousH

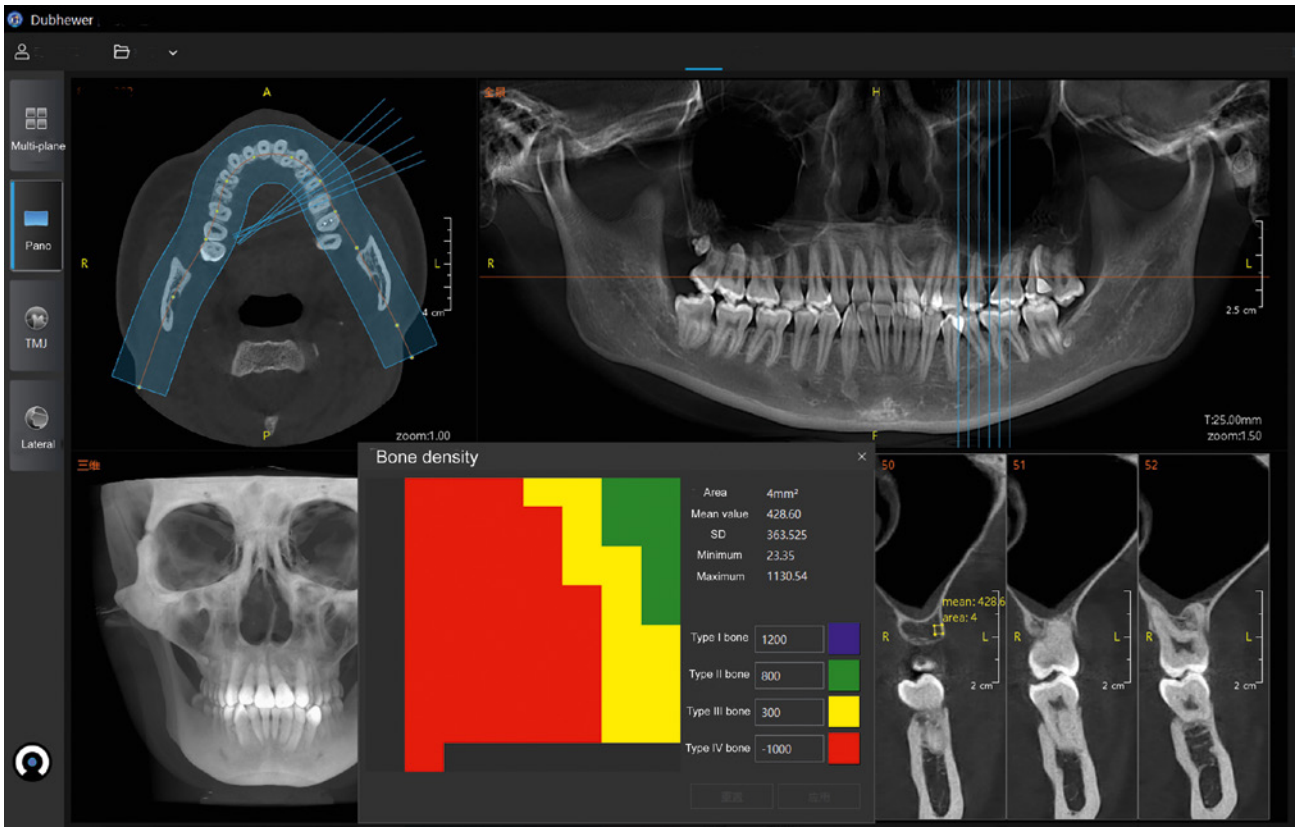


Figure 11.41 Measurement of bone depth and bone density at the implant sites.



Figure 11.42 Measurement of soft tissue thickness at the implant sites.

t.me/Dr_Mouayyad_AlbtousH

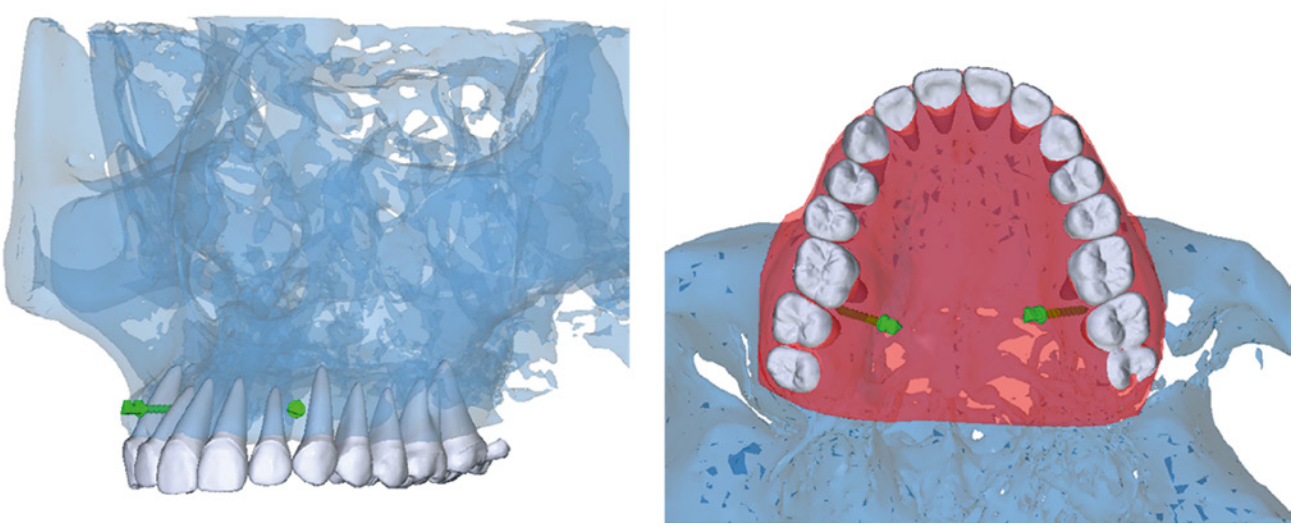


Figure 11.43 Virtual placement of mini-implants into predetermined anatomical sites.

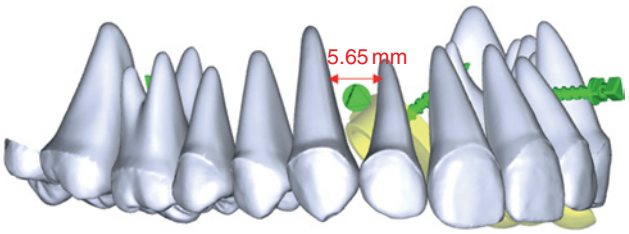


Figure 11.44 Measurement of interradicular distance and the visual detection of root proximity. The interradicular distance between the right lateral incisor and right canine is 5.65 mm which is adequate for placement of a mini-implant. Root proximity can be easily ruled out.

11.4.4 Three-dimensional Design of Insertion Guides

Insertion guides, designed based on the simulated positions of mini-implants, transfer the virtually placed mini-implants to actual anatomical sites. Accurate and stable transfer is a prerequisite for successful insertion of mini-implants with insertion guides. Thus, meticulous design of insertion guides is vital to the clinical success of guided insertion of mini-implants. The steps of designing insertion guides are discussed in detail below (Figures 11.47 and 11.48).

Determining the Area of Guide Plate on the Digital Dental Model

Based on the simulated position of the mini-implant, at least three teeth should be selected to support the guide plate. The guide plate is of vital importance since it should be stabilised on the dentition during mini-implant insertion. Thus, the guide plate should cover an adequate dentition area so that sufficient stability can be guaranteed. Moreover, the edge of the guide plate is extended from dental crowns to soft tissue. Since mini-implants are often inserted at the mucogingival junction, the edge of the guide plate should extend beyond the mucogingival junction.

Generating a Guide Plate

The guide plate model is generated with a thickness of about 2 mm based on the determined area for the guide plate, so that adequate rigidity of the plate can be guaranteed.

Generating a Guide Cylinder

An appropriate guide cylinder is generated according to the specific mini-implant that is chosen. The long axis of the guide cylinder should be consistent with that of the virtually placed mini-implant. To limit the movement of the screwdriver and to guarantee the correct insertion direction of the mini-implant, the inner diameter of the guide cylinder should be equal to or slightly greater than the outer diameter of the screwdriver working shaft. Moreover, the guide cylinder should be adequate in length, so that lateral displacement of the screwdriver and mini-implant can be avoided (Figure 11.49).

Combining the Guide Plate and Guide Cylinder

Finally, the guide plate and guide cylinder are merged and combined through Boolean operations, resulting in a final insertion guide that is ready for exporting and printing.

t.me/Dr_Mouayyad_AlbtousH

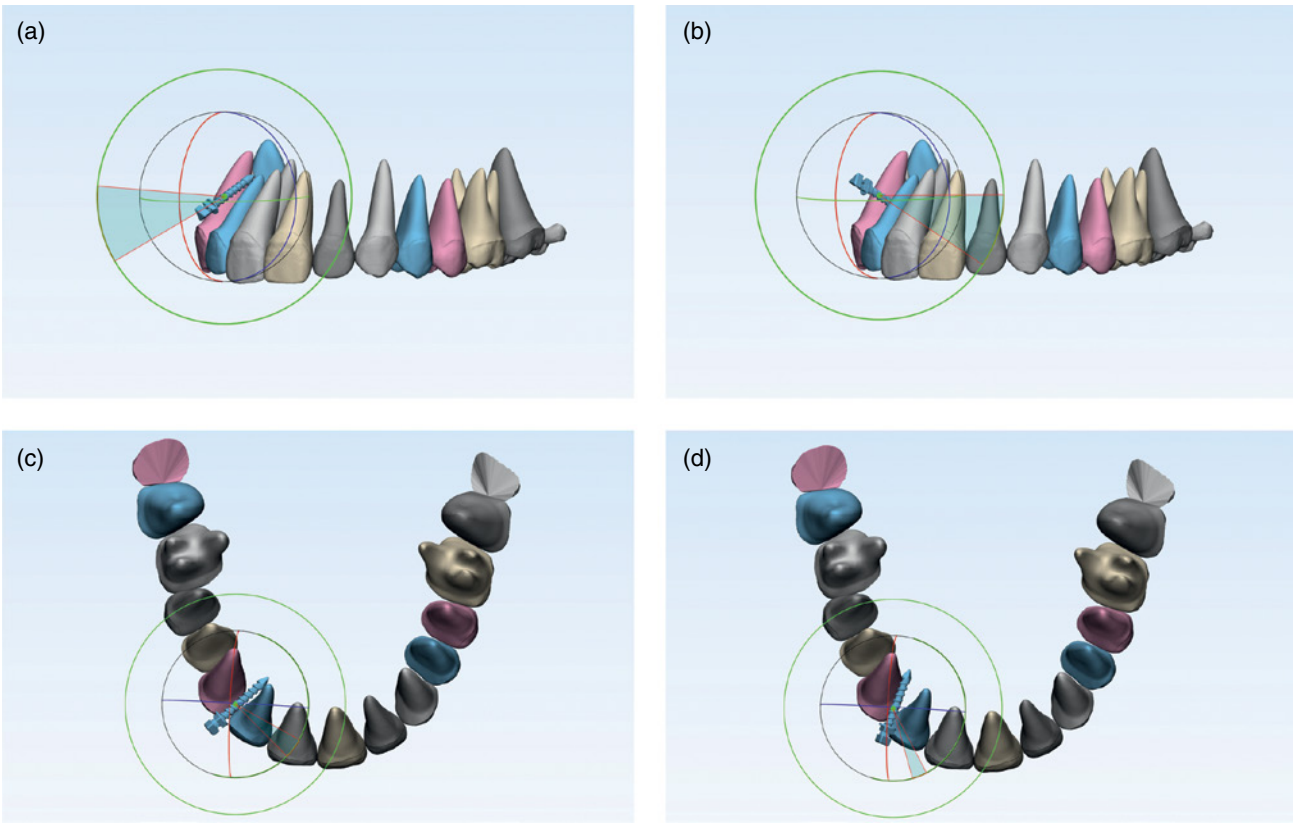


Figure 11.45 The insertion path and position of the mini-implant can be adjusted in the CAD software. (a,b) Coronoapical adjustments. (c,d) Mesiodistal adjustments.

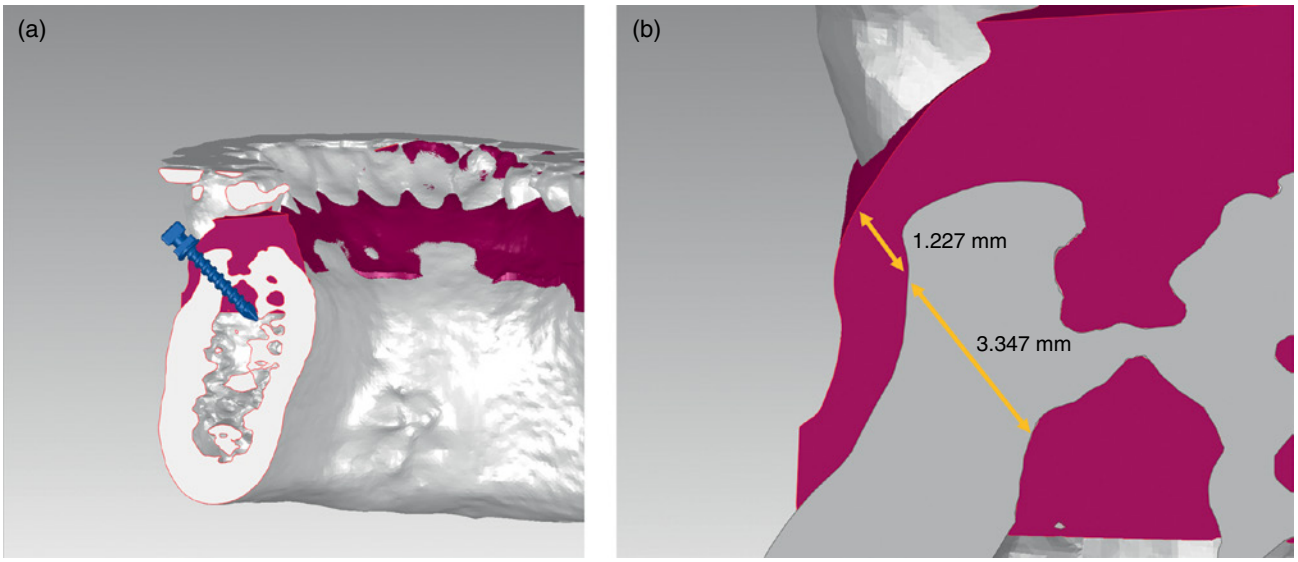


Figure 11.46 Measurement of the amount of hard and soft tissues that are penetrated by the mini-implant. (a) Coronal section showing the final position of the mini-implant. (b) The amount of hard and soft tissues penetrated by the mini-implant can be differentially measured (i.e. soft tissue engagement 1.227 mm; hard tissue engagement 3.347 mm).

t.me/Dr_Mouayyad_AlbtousH

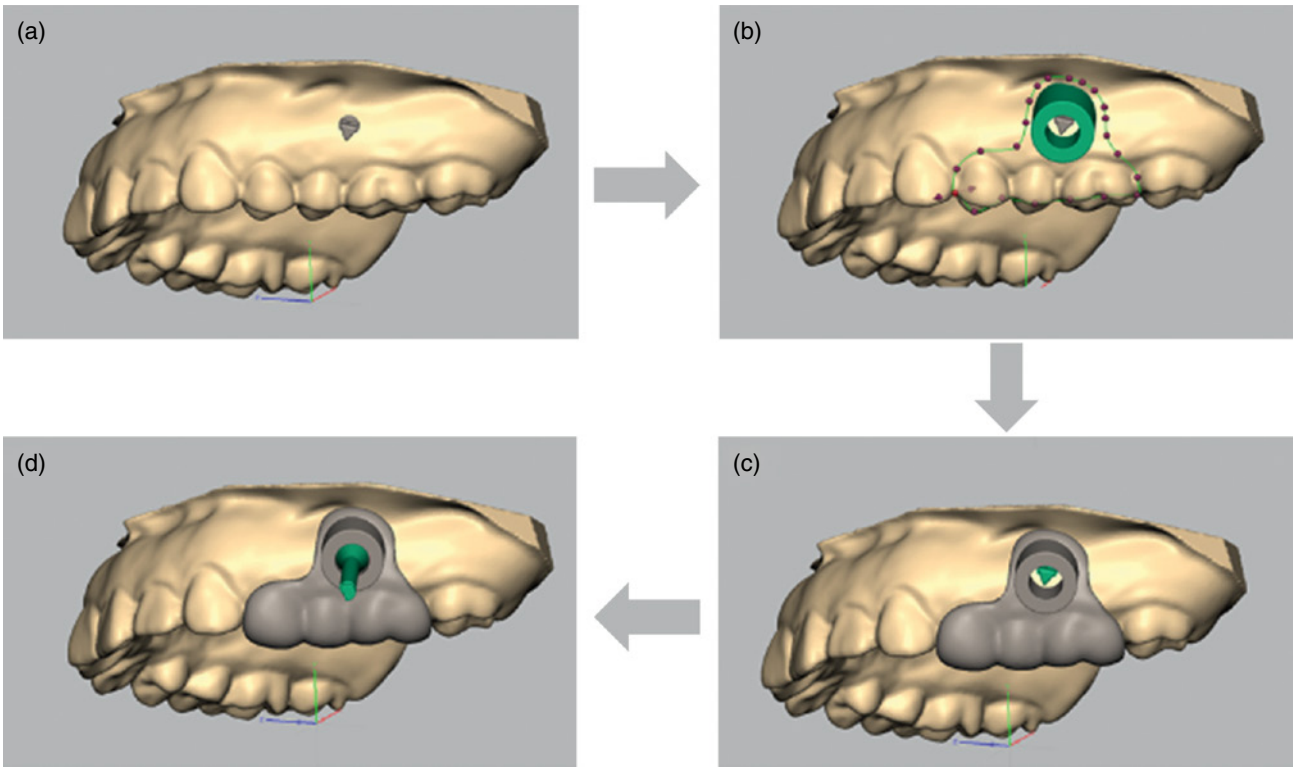


Figure 11.47 A flowchart of the digital design of an insertion guide for a buccal interradicular mini-implant. (a) Virtual insertion of a mini-implant. (b) Add a suitable guide cylinder. (c) Add the retention part of the insertion guide. (d) Confirm the appropriateness of the guide cylinder by inserting the working tip of the screwdriver.

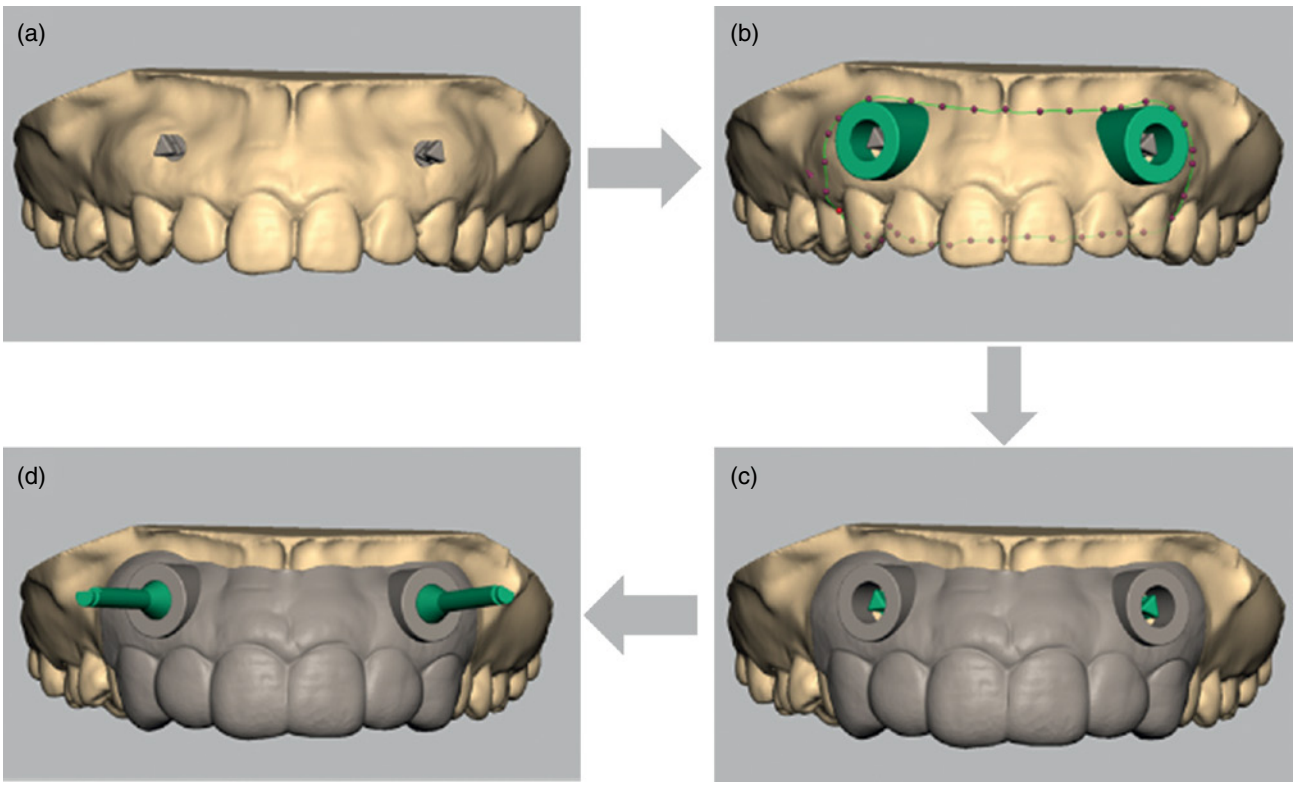


Figure 11.48 A flowchart of the digital design of an insertion guide for a labial interradicular mini-implant.

t.me/Dr_Mouayyad_AlbtousH

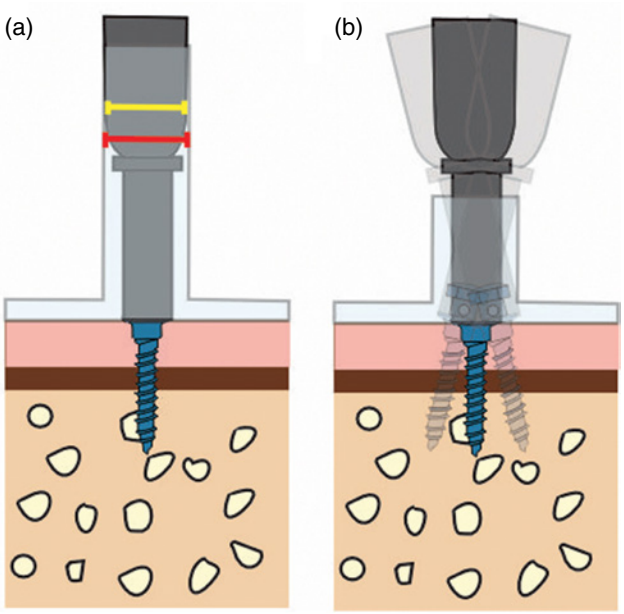


Figure 11.49 The importance of appropriate inner diameter and length of the insertion guide. (a) The inner diameter of the guide cylinder should be equal to or slightly greater than the outer diameter of the working tip of the screwdriver. (b) Lateral displacement of the screwdriver occurs if the guide cylinder is not long enough.

11.5 Manufacturing Insertion Guides

11.5.1 Exporting the STL File

Once the digital insertion guide is ready, the digital data of the insertion guide in STL format can be exported ready for 3D printing and clinical use (Figure 11.50).

11.5.2 Adding Supporting Components for the Insertion Guide

Supporting components should be added for the insertion guide to preserve its intactness and guarantee its stability during the 3-D printing (Figures 11.51 and 11.52). Special attention should be paid to the fact that supporting components cannot be added onto the inner surface of the insertion guide since this may interfere with its fitting. Moreover, the supporting components cannot be added onto the guide cylinder either, as this may cause problems when the screwdriver penetrates through it.

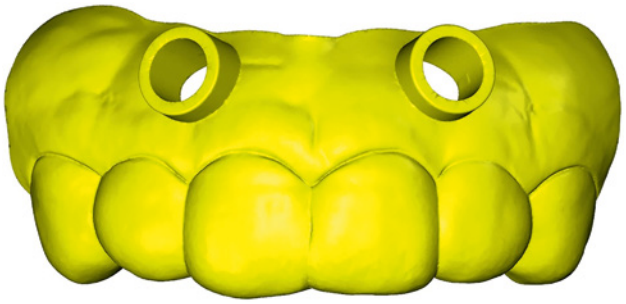


Figure 11.50 Export the STL file of the insertion guide.

11.5.3 Generating the Actual Insertion Guide Through 3-D Printing

The digital data of the insertion guide is imported into a 3-D printer (Figure 11.53). The insertion guide is printed with transparent photosensitive resin material. Meanwhile, we recommend that the dental model be printed so that the fitting of the insertion guide can be examined on the dental model prior to try-in on patient dentition.

11.5.4 Removing the Supporting Components and Polishing the Insertion Guide

Once the 3-D printing of the insertion guide is complete, the remaining resin material that has not been light cured should be washed and cleaned with ethanol and the remaining supporting components of the insertion guide should be removed through grinding and polishing (Figure 11.54).

11.5.5 Try-in on the Dental Model

Once the actual insertion guide and dental model are ready, try-in of the guide onto the model is performed to examine the fitting of the guide (Figure 11.55). Repeated try-in and removal procedures should also be performed to determine the presence of potential undercuts. Furthermore, actual placement of a mini-implant into the dental model with the insertion guide is recommended to look for any potential problem, such as inadequate stability of the guide during insertion or a high level of friction between the guide cylinder and screwdriver. If any problem is encountered at this stage, appropriate adjustments should be made and measures taken to improve the quality of the insertion guide.

t.me/Dr_Mouayyad_AlbtousH



Figure 11.51 Digital addition of supporting components for insertion guides.

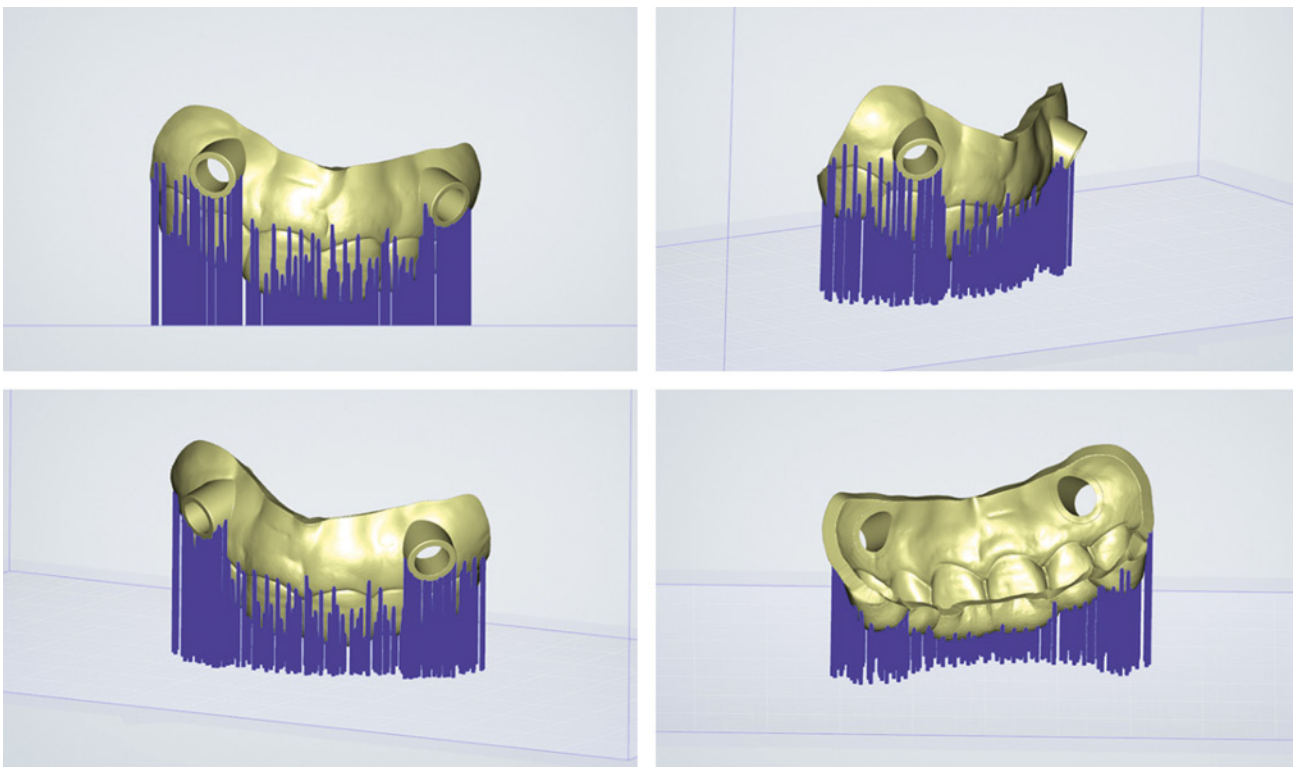


Figure 11.52 Supporting components (blue cylinders) for insertion guides.

t.me/Dr_Mouayyad_AlbtousH

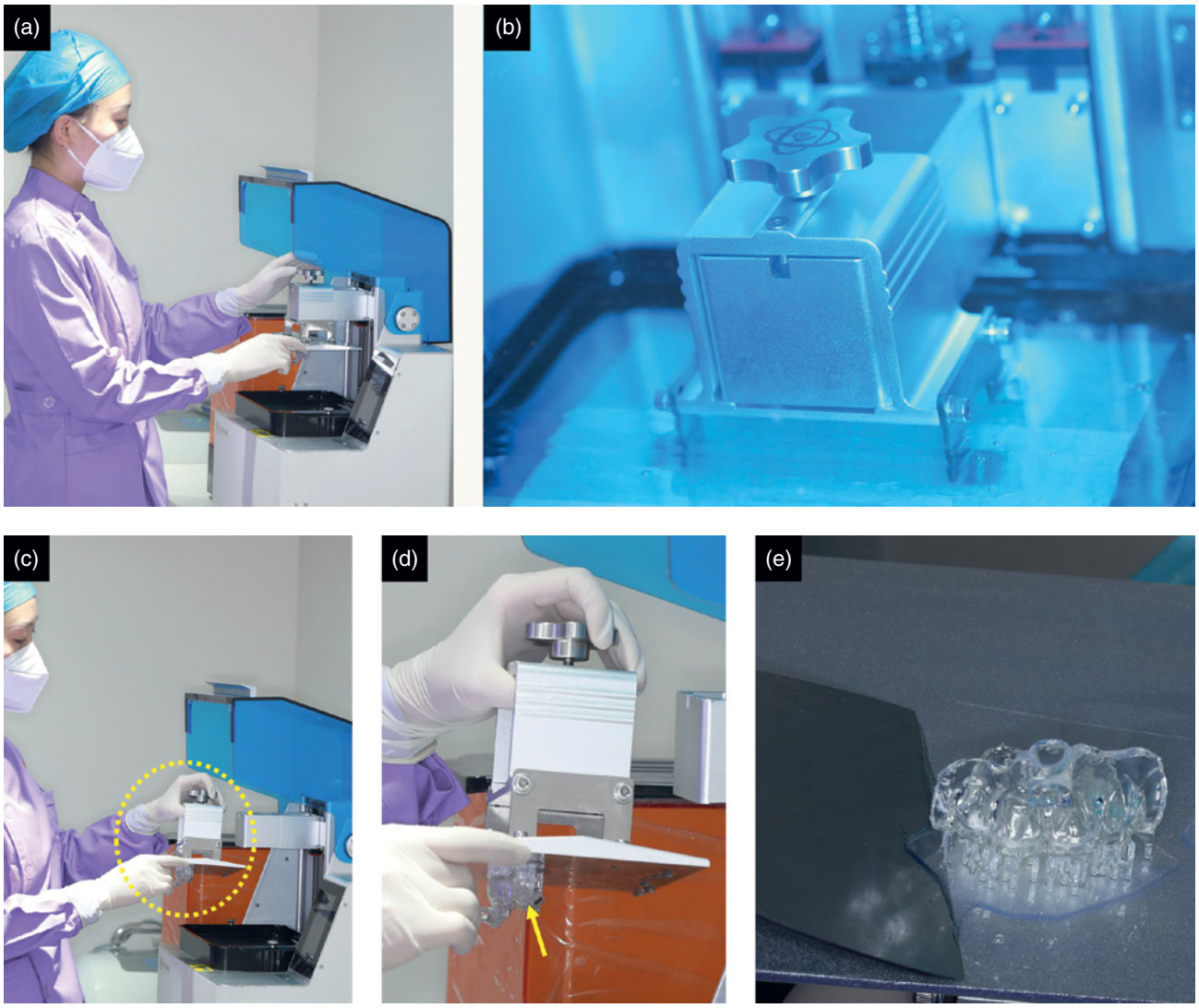


Figure 11.53 3-D printing of the insertion guide. (a) Initiate the 3-D printing process in the 3-D printer. (b) 3-D printing. (c,d) Remove the printing plate (yellow dashed circle) following printing completion. Note the printed insertion guide (yellow arrow). (e) Remove the insertion guide from the printing plate.

11.5.6 Examples of Insertion Guides for Different Anatomical Sites

Examples are shown here to demonstrate different designs of insertion guides for different anatomical sites: labial interradicular region (Figure 11.56), palatal interradicular region (Figure 11.57), buccal interradicular region (Figure 11.58), infrazygomatic crest (Figure 11.59) and buccal shelf (Figure 11.60).

t.me/Dr_Mouayyad_AlbtousH

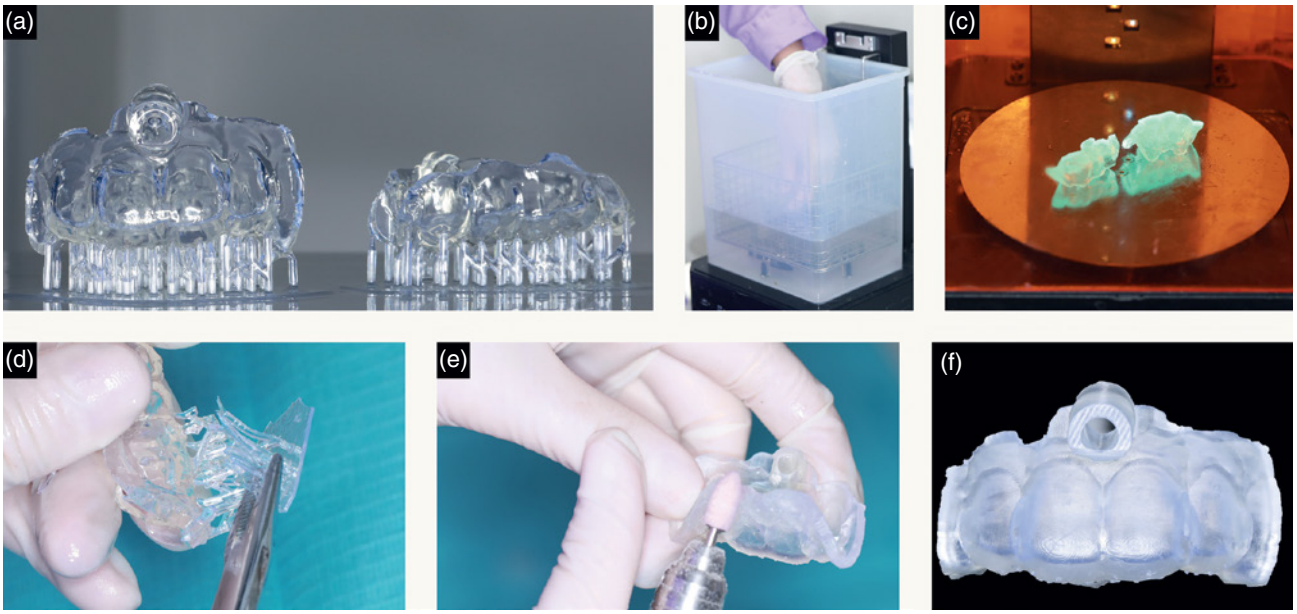


Figure 11.54 (a) Insertion guides that were removed from the printing plate following printing. (b) The remaining resin material that had not been light cured was cleaned with 95% ethanol. (c) Enhance the light curing for two minutes. (d) Remove the supporting components from the insertion guide. (e) Polish the surfaces of the insertion guide. (f) The final insertion guide ready for use.

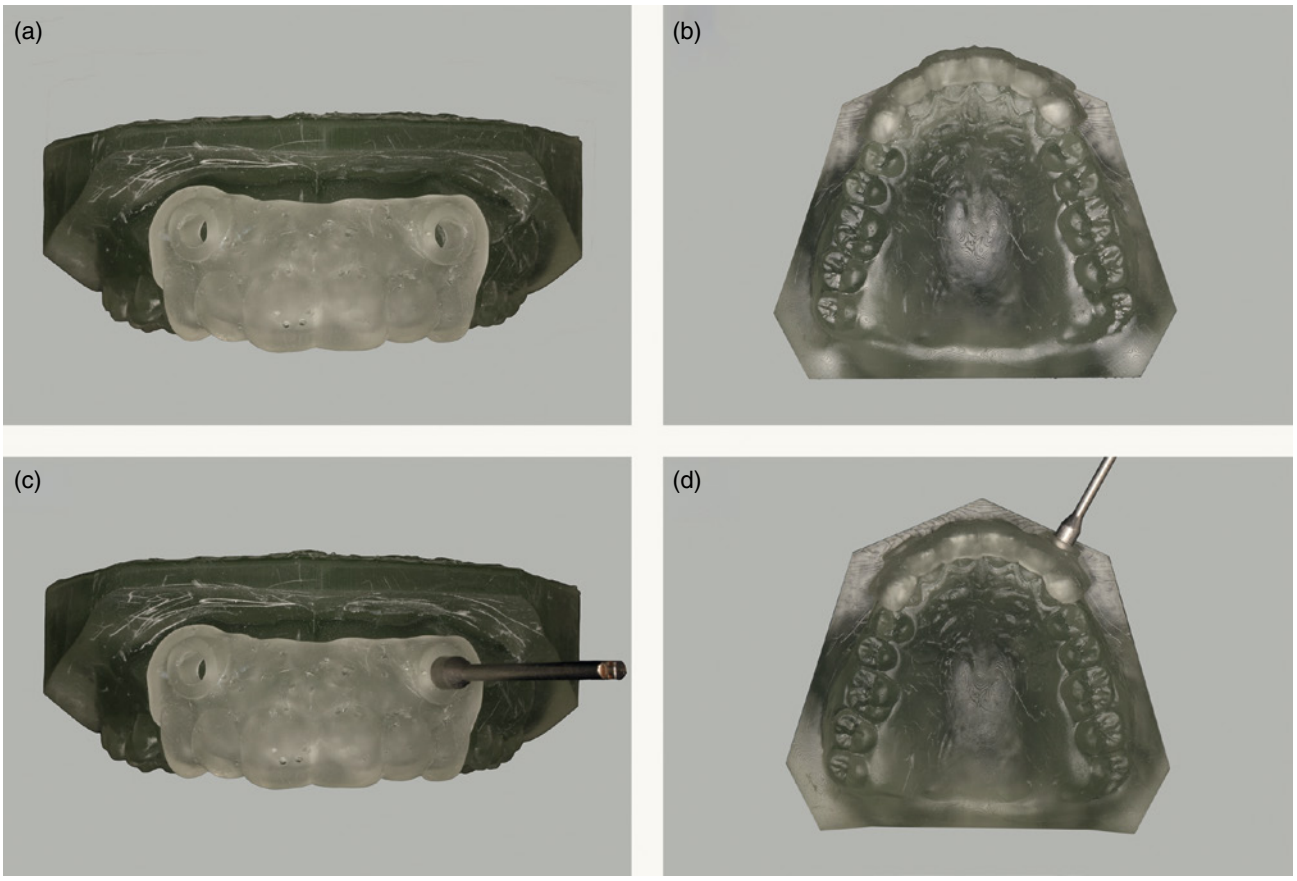


Figure 11.55 Try-in of the insertion guide. (a,b) Try the insertion guide onto the dentition. (c,d) Insertion of a mini-implant into the dental model using the insertion guide.

t.me/Dr_Mouayyad_AlbtousH

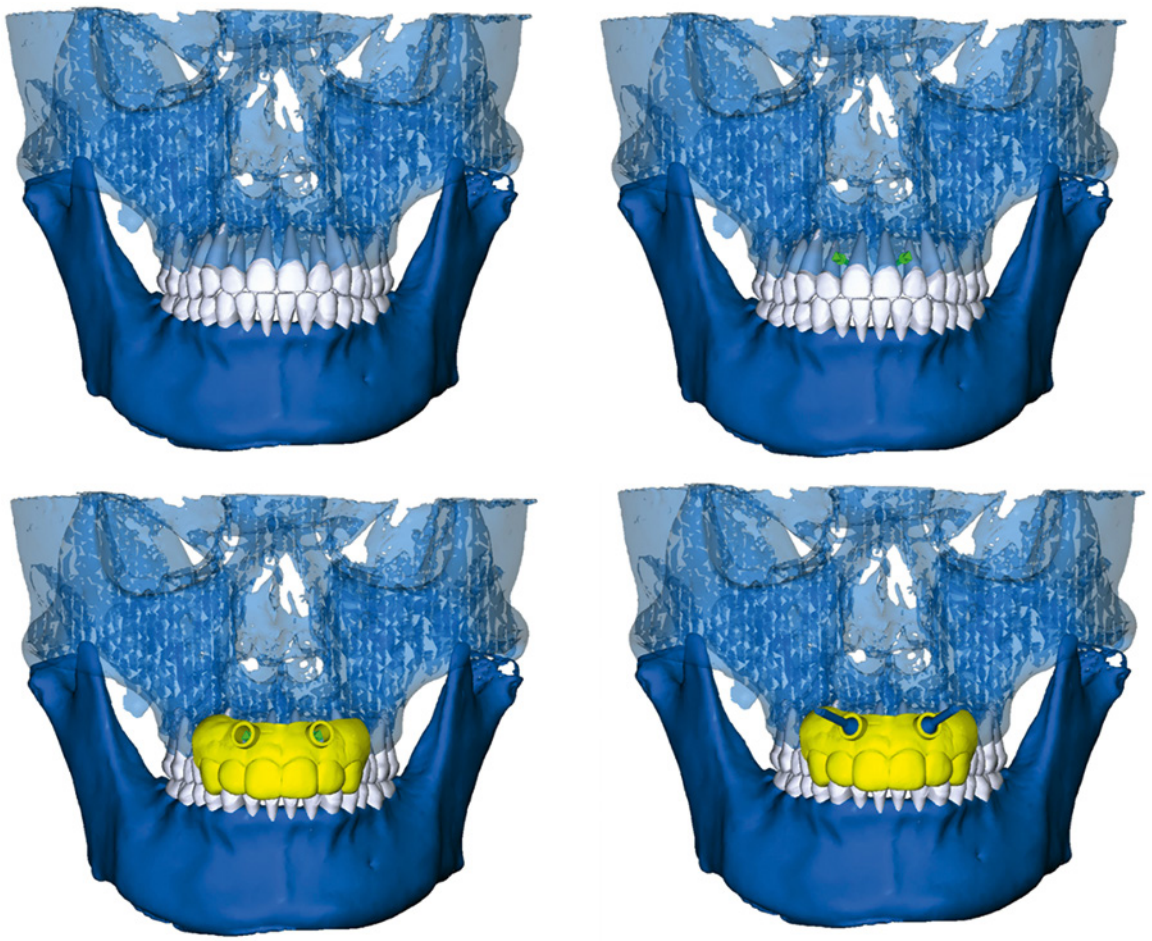


Figure 11.56 Design of an insertion guide for labial interradicular mini-implants.

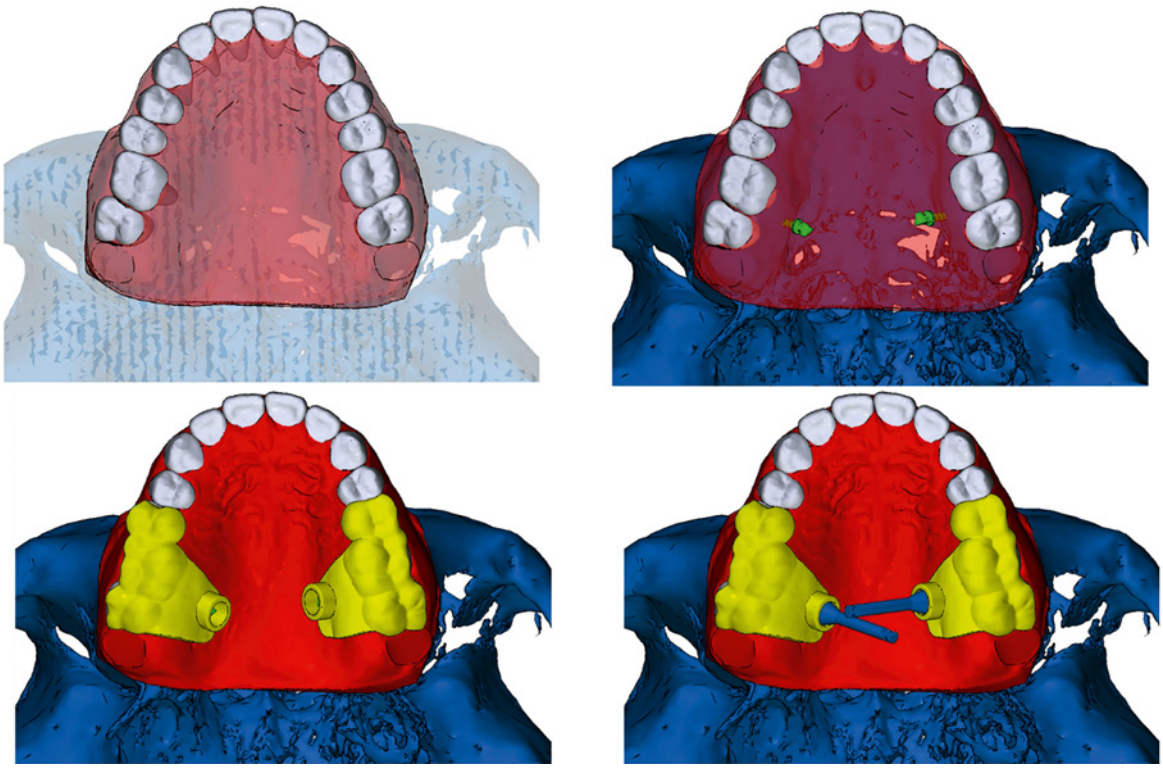


Figure 11.57 Design of insertion guides for palatal interradicular mini-implants.

t.me/Dr_Mouayyad_AlbtousH

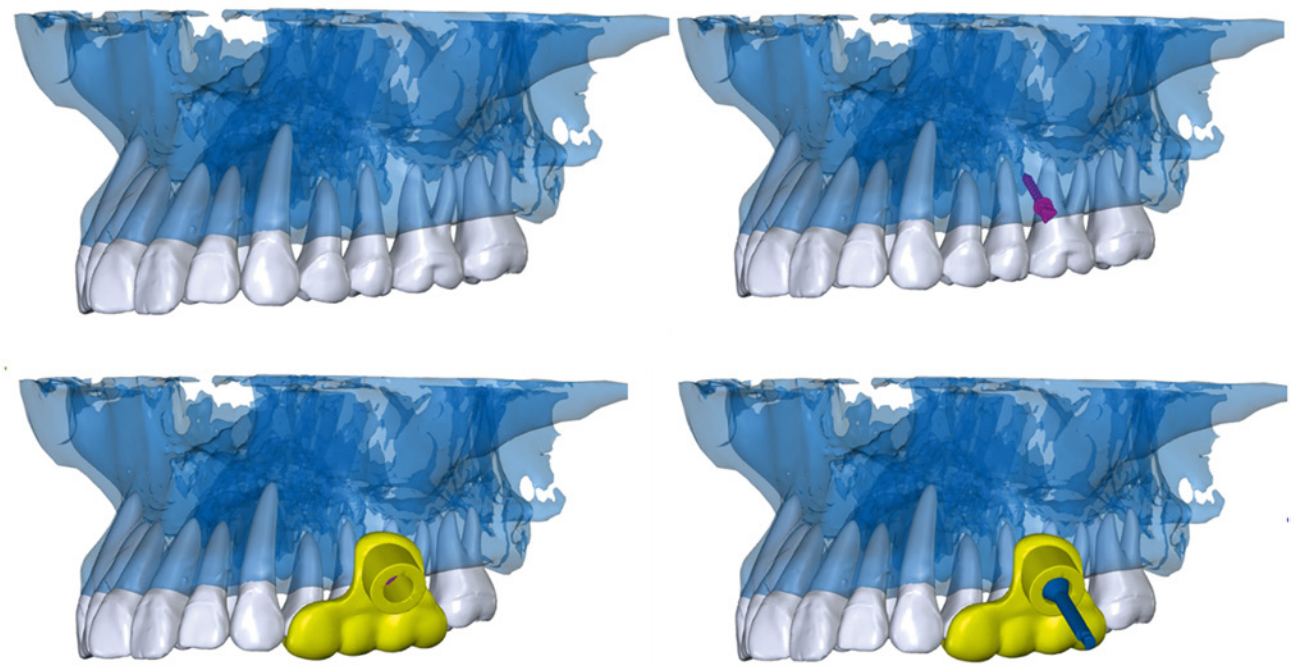


Figure 11.58 Design of an insertion guide for a buccal interradicular mini-implant.

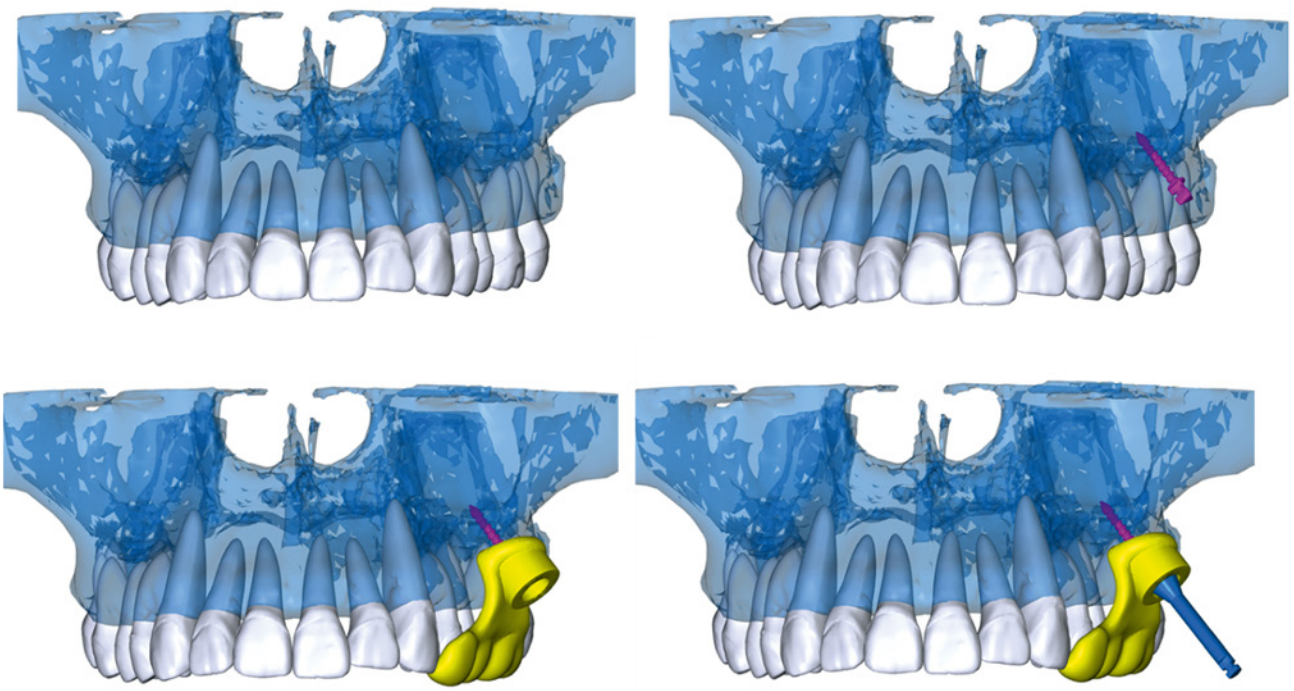


Figure 11.59 Design of an insertion guide for an infrazygomatic mini-implant.

t.me/Dr_Mouayyad_AlbtousH

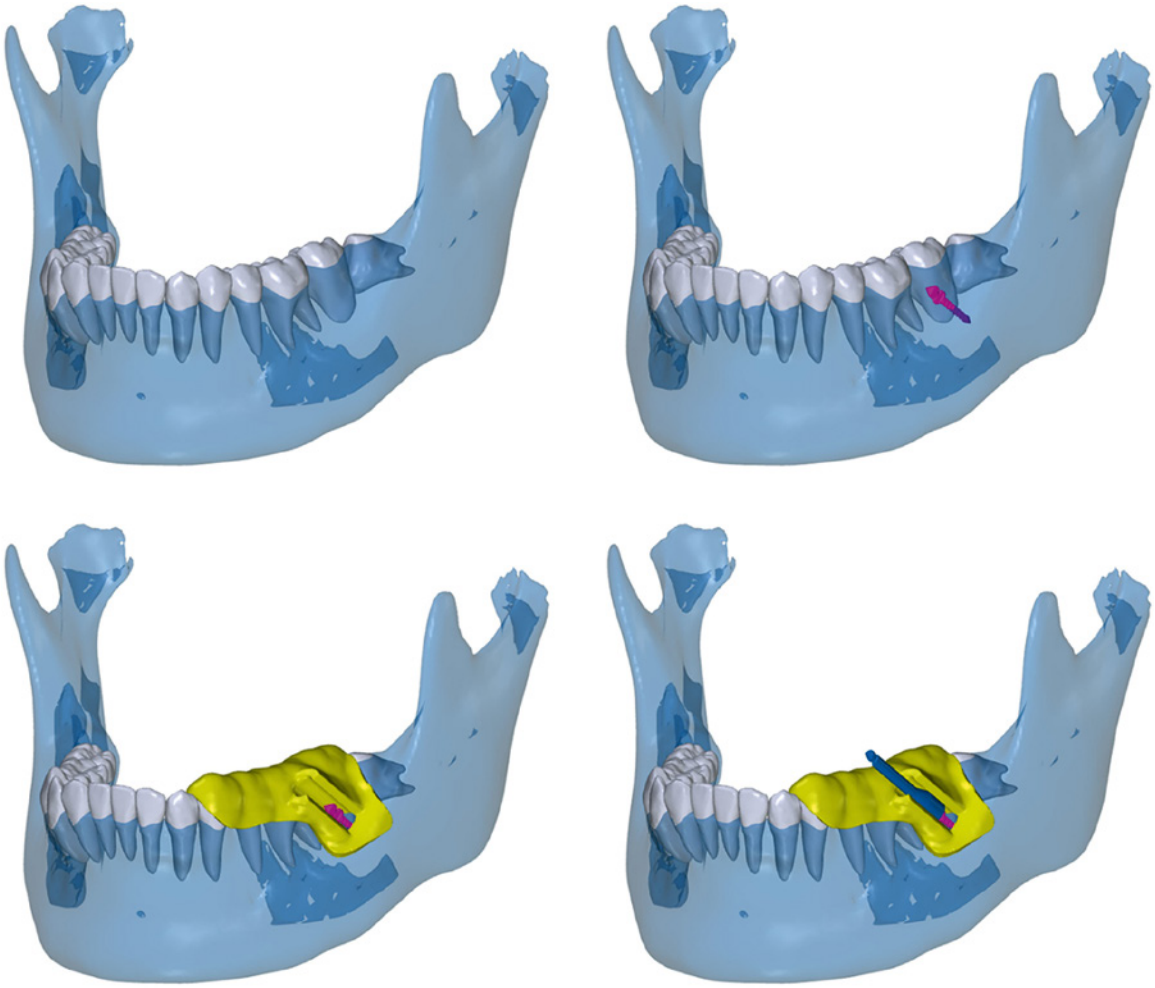


Figure 11.60 Design of an insertion guide for a buccal-shelf mini-implant.

11.6 Summary

With the advances and innovations built into insertion techniques for mini-implants, guided insertion is clinically promising in offering a more accurate, precise and efficient placement of mini-implants. The 3-D designed insertion guides are designed and produced in various procedures and steps, including obtaining a digital dentition model, establishing digital data of mini-implants and screwdrivers, virtually placing mini-implants, 3-D designing of insertion guides and manufacturing the guides through rapid prototyping. With advances in technology and development of printing materials, guided insertion of mini-implants will become more accurate, precise and efficient in future.

References

1 Wilmes B, Vasudavan S, Drescher D. (2019). CAD-CAM-fabricated mini-implant insertion guides for the delivery of a distalization appliance in a single appointment. *Am. J. Orthod. Dentofacial Orthop.* 156(1): 148–156.

2 Wilmes B, Tarraf NE, de Gabriele R, Dallatana G, Drescher D. (2022). Procedure using CAD/CAM-manufactured insertion guides for purely mini-implant-borne rapid maxillary expanders. *J. Orofac. Orthop.* 83(4): 277–284.

3 Iodice G, Nanda R, Drago S et al. (2022). Accuracy of direct insertion of TADs in the anterior palate with respect to a 3D-assisted digital insertion virtual planning. *Orthod. Craniofac. Res.* 25(2): 192–198.

t.me/Dr_Mouayyad_AlbtousH

4 Yu JJ, Kim GT, Choi YS et al. (2012). Accuracy of a cone beam computed tomography-guided surgical stent for orthodontic mini-implant placement. *Angle Orthod.* 82(2): 275–283.

5 Marchack CB, Chew LK. (2015). The 10-year evolution of guided surgery. *J. Calif Dent. Assoc.* 43(3): 131–134.

6 Hohlweg-Majert B, Schon R, Schmelzeisen R, Gellrich NC, Schramm A. (2005). Navigational maxillofacial surgery using virtual models. *World J Surg.* 29(12): 1530–1538.

7 Marmulla R, Muhling J. (2007). Computer-assisted condyle positioning in orthognathic surgery. *J. Oral Maxillofac. Surg.* 65(10): 1963–1968.

8 Pautke C, Bauer F, Tischer T et al. (2009). Fluorescence-guided bone resection in bisphosphonate-associated osteonecrosis of the jaws. *J. Oral Maxillofac. Surg.* 67(3): 471–476.

9 Seeberger R, Scherfler S, Freier K, Thiele O. (2011). Use of stereolithographic cutting guides in corrective (wedge) LeFort I osteotomy. *Br. J. Oral Maxillofac. Surg.* 49(5): e20–21.

10 Mazzoni S, Badiali G, Lancellotti L, Babbi L, Bianchi A, Marchetti C. (2010). Simulation-guided navigation: a new approach to improve intraoperative three-dimensional reproducibility during orthognathic surgery. *J. Craniofac. Surg.* 21(6): 1698–1705.

11 Tepper OM, Sorice S, Hershman GN, Saadeh P, Levine JP, Hirsch D. (2011). Use of virtual 3-dimensional surgery in post-traumatic craniomaxillofacial reconstruction. *J. Oral Maxillofac. Surg.* 69(3): 733–741.

12 Ye N, Long H, Zhu S, Yang Y, Lai W, Hu J. (2015). The accuracy of computer image-guided template for mandibular angle ostectomy. *Aesthetic Plast. Surg.* 39(1): 117–123.

13 Safi Y, Amid R, Zadbin F, Ghazizadeh Ahsaie M, Mortazavi H. (2021). The occurrence of dental implant malpositioning and related factors: a cross-sectional cone-beam computed tomography survey. *Imaging Sci. Dent.* 51(3): 251–260.

14 An JH, Park SH, Han JJ et al. (2017). Treatment of dental implant displacement into the maxillary sinus. *Maxillofac. Plast. Reconstr. Surg.* 39(1): 35.

15 Choi M, Romberg E, Driscoll CF. (2004). Effects of varied dimensions of surgical guides on implant angulations. *J. Prosthet. Dent.* 92(5): 463–469.

16 Nickenig HJ, Wichmann M, Hamel J, Schlegel KA, Eitner S. (2010). Evaluation of the difference in accuracy between implant placement by virtual planning data and surgical guide templates versus the conventional free-hand method – a combined in vivo–in vitro technique using cone-beam CT (Part II). *J. Craniomaxillofac. Surg.* 38(7): 488–493.

17 Grecchi E, Stefanelli LV, Grecchi F, Grivetto F, Franchina A, Pranno N. (2022). A novel guided zygomatic implant surgery system compared to free hand: a human cadaver study on accuracy. *J. Dent.* 119: 103942.

18 Tan PLB, Layton DM, Wise SL. (2018). In vitro comparison of guided versus freehand implant placement: use of a new combined TRIOS surface scanning, Implant Studio, CBCT, and stereolithographic virtually planned and guided technique. *Int. J. Comput. Dent.* 21(2): 87–95.

19 Afshari A, Shahmohammadi R, Mosaddad SA et al. (2022). Free-hand versus surgical guide implant placement. *Adv. Mater. Sci. Engin.* 2022: 6491134.

20 Kim YH, Yang SM, Kim S et al. (2010). Midpalatal miniscrews for orthodontic anchorage: factors affecting clinical success. *Am. J. Orthod. Dentofacial Orthop.* 137(1): 6-–72.

21 Lim HJ, Eun CS, Cho JH, Lee KH, Hwang HS. (2009). Factors associated with initial stability of miniscrews for orthodontic treatment. *Am. J. Orthod. Dentofacial Orthop.* 136(2): 236–242.

22 Kim SH, Kang SM, Choi YS et al. (2010). Cone-beam computed tomography evaluation of mini-implants after placement: is root proximity a major risk factor for failure? *Am. J. Orthod. Dentofacial Orthop.* 138(3): 264–276.

23 Pithon MM, dos Santos RL. (2010). Fabrication of an adjustable mini-screw surgical guide. *J. Orthod.* 37(2): 118–120.

24 Sharma K, Sangwan A. (2014). K.S. micro-implant placement guide. *Ann. Me.d Health Sci. Res.* 4(Suppl 3): S326–328.

25 Ikenaka R, Koizumi S, Otsuka T, Yamaguchi T. (2022). Effects of root contact length on the failure rate of anchor screw. *J. Oral Sci.* 64(3): 232–235.

26 Chen YH, Chang HH, Chen YJ, Lee D, Chiang HH, Yao CC. (2008). Root contact during insertion of miniscrews for orthodontic anchorage increases the failure rate: an animal study. *Clin. Oral Implants Res.* 19(1): 99–106.

27 Mohammed H, Wafaie K, Rizk MZ, Almuzian M, Sosly R, Bearn DR. (2018). Role of anatomical sites and correlated risk factors on the survival of orthodontic miniscrew implants: a systematic review and meta-analysis. *Prog. Orthod.* 19(1): 36.

28 Lee Y, Choi SH, Yu HS, Erenebat T, Liu J, Cha JY. (2021). Stability and success rate of dual-thread miniscrews. *Angle Orthod.* 91(4): 509–514.

29 Kuroda S, Yamada K, Deguchi T, Hashimoto T, Kyung HM, Takano-Yamamoto T. (2007). Root proximity is a major factor for screw failure in orthodontic anchorage. *Am. J. Orthod. Dentofacial Orthop.* 131(4 Suppl): S68–73.

t.me/Dr_Mouayyad_AlbtousH

30 Li Q, Chen K, Han L, Zhuang Y, Li J, Lin J. (2020). Automatic tooth roots segmentation of cone beam computed tomography image sequences using U-net and RNN. *J. Xray Sci. Technol.* 28(5): 905–922.

31 Ye N, Jian F, Xue J et al. (2021). Accuracy of in-vitro tooth volumetric measurements from cone-beam computed tomography. *Am. J. Orthod. Dentofacial Orthop.* 142(6): 879–887.

32 Ye N, Long H, Xue J, Wang S, Yang X, Lai W. (2014). Integration accuracy of laser-scanned dental models into maxillofacial cone beam computed tomography images of different voxel sizes with different segmentation threshold settings. *Oral Surg. Oral Med. Oral Pathol. Oral Radiol.* 117(6): 780–786.

33 Ye N, Wu T, Dong T, Yuan L, Fang B, Xia L. (2019). Precision of 3D-printed splints with different dental model offsets. *Am. J. Orthod. Dentofacial Orthop.* 155(5): 733–738.

t.me/Dr_Mouayyad_AlbtousH

12

Clinical Techniques for Using Insertion Guides

Lingling Pu[1,2], Qi Fan[1], Yuetian Li[1], Omar M. Ghaleb[1], Hu Long[1], and Niansong Ye[3]

[1] *Department of Orthodontics, State Key Laboratory of Oral Diseases and National Clinical Research Center for Oral Diseases, West China Hospital of Stomatology, Sichuan University, Chengdu, China*
[2] *Private Practice, Chengdu, China*
[3] *Private Practice, Shanghai, China*

12.1 Introduction

Accurate and precise insertion of orthodontic mini-implants is essential for clinical success, especially for interradicular mini-implants. The use of guides greatly improves the accuracy and precision of mini-implant insertion.[1] Specifically, the insertion site, depth and angulation that are predetermined through virtual planning can be transferred to the anatomical sites with the use of insertion guides.[2] As described in Chapter 11, errors can be introduced at each step of the process of manufacturing insertion guides (e.g. image superimposition, virtual planning and 3-D printing) and may eventually lead to deviations from the planned location. The last step of transferring the virtually planned mini-implants into actual anatomical sites is technique sensitive and not error free.

In this chapter, we will present brief clinical procedures for inserting orthodontic mini-implants using insertion guides and demonstrate relevant clinical cases.

12.2 Clinical Procedures

12.2.1 Verifying the Fit of Insertion Guides

Prior to the insertion of orthodontic mini-implants with insertion guides, the fit between the guides and printed models (and actual patients' dentitions) should be confirmed (Figure 12.1). Otherwise, precise insertion of mini-implants into virtual planned locations cannot be guaranteed. Since insertion guides are virtually designed based on 3-D dental models and printed together, insertion guides are often in good fit with 3-D printed dental models. However, occasionally, the fit between the guide and the actual dentition may be inadequate and should be checked before insertion, in order to maximise the clinical success of mini-implants. Thus, fit verification between insertion guides and dentitions will be discussed below.

First, the insertion guide is mounted onto the dentition. Unlike dentures, insertion guides do not require adequate retention since they need not withstand occlusal force. In particular, special attention should be paid to the presence of dental undercuts as these may lead to either the failure of fit-in or removal. Thus, try-in and removal of insertion guides onto the patient's dentition are repeated several times and the guides may be trimmed to guarantee the ease of performing both procedures (try-in and removal) (Figure 12.2).

Second, since insertion guides are often designed to firmly contact the soft tissue at the predetermined insertion site, the presence of large space between the guide and soft tissue may indicate an inadequate fit between the guide and the dentition (Figure 12.3), leading to deviations of actual insertion sites from those virtually planned. This is often caused by incorrect try-in path that precludes complete try-in and can be resolved by trying different paths. However, if this situation persists following several attempts, redesign and remanufacture of insertion guides may be indicated.

Lastly, apart from good fit, adequate stability of insertion guides during mini-implant placement is critical since instability may lead to incorrect insertion sites and deviated insertion paths, resulting in subsequent injury to vital anatomical structures (e.g. dental roots). During insertion, the guide is often stabilised through either patient biting or practitioner finger pressure. Thus, to test stability, patients

Clinical Insertion Techniques of Orthodontic Temporary Anchorage Devices, First Edition. Edited by Hu Long, Xianglong Han, and Wenli Lai.
© 2024 John Wiley & Sons Ltd. Published 2024 by John Wiley & Sons Ltd.

t.me/Dr_Mouayyad_AlbtousH

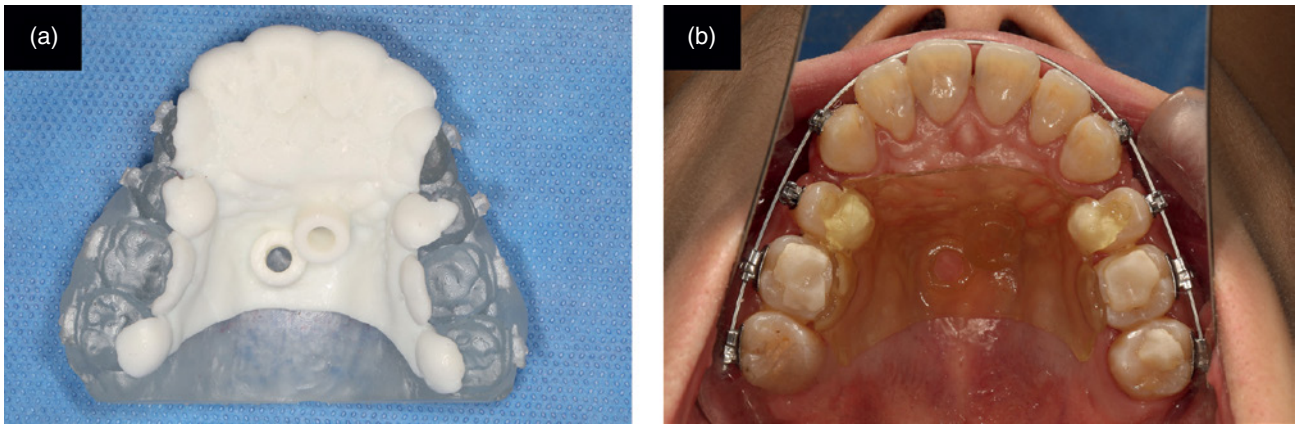


Figure 12.1 Fit verification of insertion guides prior to actual insertion. (a) Confirmation of the fit between an insertion guide and its corresponding 3-D-printed dental model. (b) Examination of the fit between an insertion guide and the patient's actual dentition.

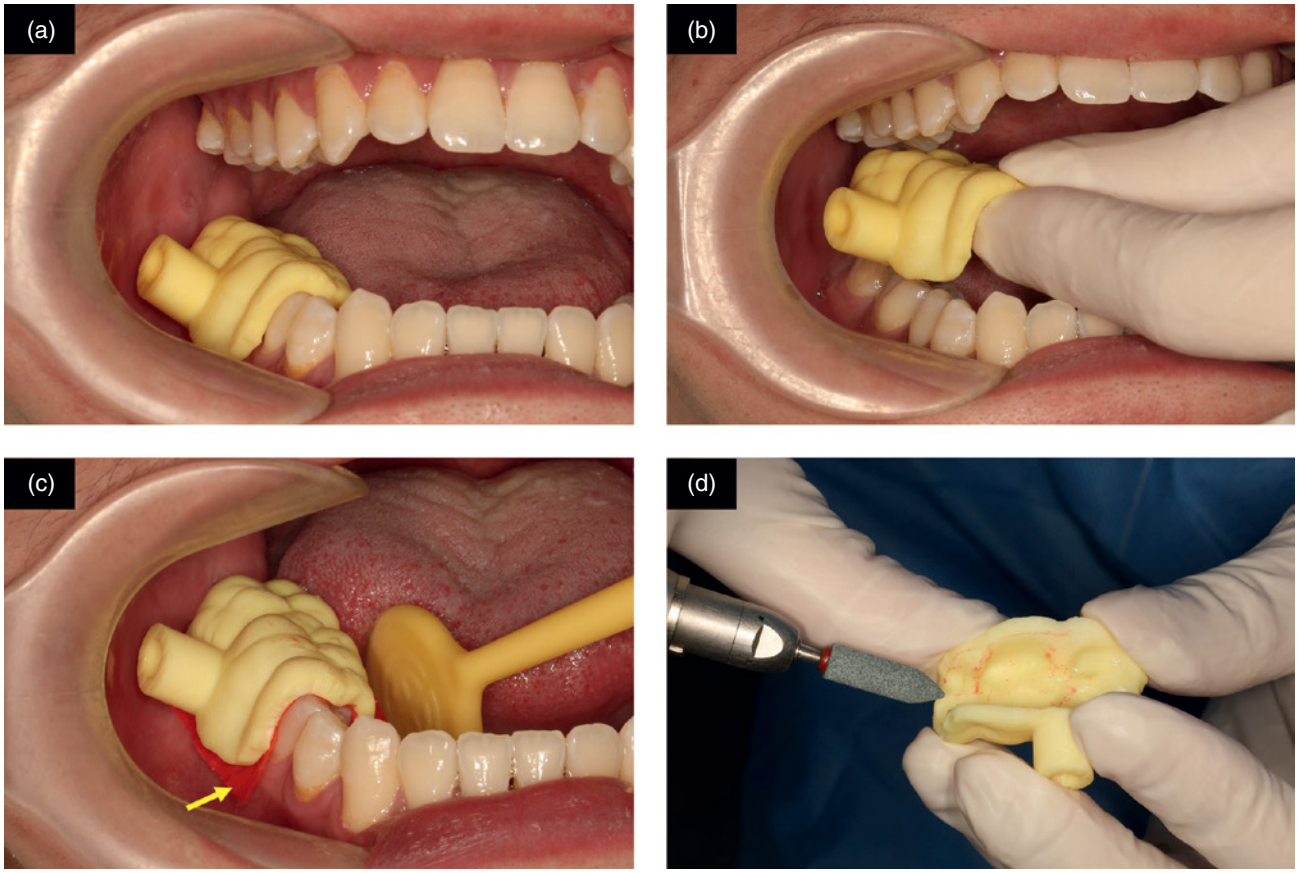


Figure 12.2 (a,b) Repeat the try-in and removal procedures intraorally. (c) If any undercut is suspected, articulation paper (yellow arrow) can be used to mark premature contact points that are preventing try-in and/or removal of the insertion guide. (d) The marked premature contact points are removed with a dental handpiece.

are often asked to bite on the insertion guide and the displacement of insertion guide before and after biting is checked (Figure 12.4a,b). Minimal or no displacement is indicative of good stability, while displacements within an unacceptable range may demand modifications of the 3-D design, such as increasing the retention surface of dentition. Alternatively, in the condition of non-biting, gentle forces that are parallel to and perpendicular to the occlusal plane are applied onto the insertion guide to determine its displacement (Figure 12.4c,d).

t.me/Dr_Mouayyad_AlbtousH



Figure 12.3 (a,b) Incomplete fit of the insertion guide is caused by an incorrect try-in path, as indicated by the large space between the insertion guide and the dentition. (c,d) Complete engagement of the insertion guide into the dentition. Note the confirmed fit between the insertion guide and the dentition.

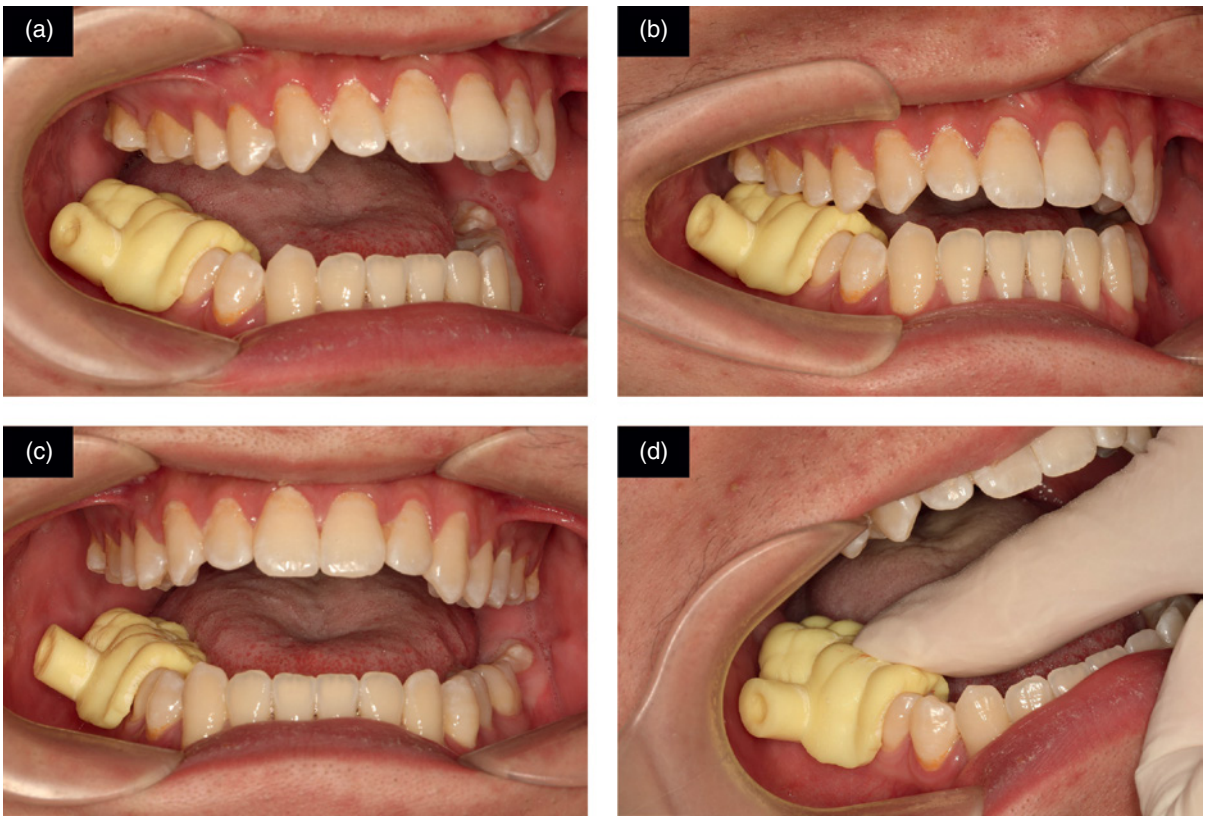


Figure 12.4 Evaluation of the stability of an insertion guide in response to biting force or a practitioner's finger pressure. (a,b) The displacement of the insertion guide is tested before and after biting. (c,d) Gentle forces that are both parallel to and perpendicular to the occlusal plane are applied onto the insertion guide to check the stability in response to finger pressure.

t.me/Dr_Mouayyad_AlbtousH

12.2.2 Anaesthesia

Precise anaesthesia can be achieved with the aid of insertion guides. However, it is not advised to inject infiltration anaesthetics directly through the guide cylinder since practitioners may be unable to verify the success of injection, especially for insertion guides with long guide cylinders (Figure 12.5). Moreover, as described in previous chapters, the amount of anaesthetic agent should be appropriate and is often determined through observing the extent of soft tissue bulging. This requires direct visual monitoring and practitioners are unable to monitor the extent of tissue bulging due to the presence of the insertion guide. Occasionally, when insertion guides are applied for anatomical sites with awkward access, it may be difficult for practitioners to inject anaesthetics through guide cylinders (Figure 12.6). Therefore, we recommend that practitioners apply topical anaesthetics prior to mounting insertion guides and mark the insertion sites (injection sites) with dental probes through the guide cylinders. Then, infiltration anaesthetics can be readily injected at the marked injection sites (Figure 12.7).

12.2.3 Inserting Mini-implants

Prior to insertion, the insertion guide should be stabilised by asking patients to bite or the practitioner can press the guide against the dentition. Then, following engagement of the mini-implant into a screwdriver, the implant is inserted through guide cylinders into the predetermined anatomical site. It is critical to ensure that the screwdriver is inserted through the guide cylinders with minimal friction, as frictional insertion indicates a deviated insertion path or incorrect insertion site. Thus, special care should be taken to ensure that the insertion path of the screwdriver is parallel to the long axis of the guide cylinder. This requires contra-angle screwdrivers to be used for anatomical sites that are difficult to access with straight screwdrivers (Figure 12.8).

During insertion, screwdrivers should not apply lateral displacement force on the insertion guide, as this may lead to lateral displacement of the guide and a deviated insertion path (Figure 12.9). Thus, screwdrivers should be stabilised by practitioners during insertion (Figure 12.10). Furthermore, in particular, after the cortex is penetrated, we recommend that screwdrivers be detached and removed temporarily, which allows practitioners to confirm the accurate insertion point through verifying whether the mini-implant is located at the centre of the guide cylinder. Eccentric location of the implant within the guide cylinder is indicative of an incorrect insertion point and adjustment should ensue.

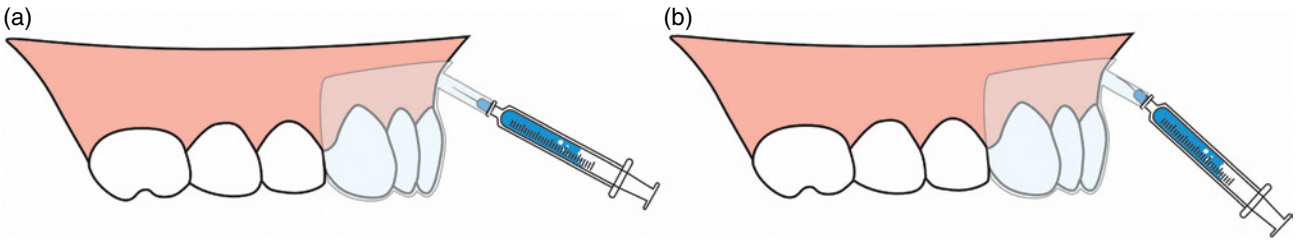


Figure 12.5 (a) The anatomical site cannot be reached by the injection needle due to the long cylinder. (b) The injection needle is stuck onto the inner wall of the cylinder and this may be mistakenly taken for successful contact with the bone surface.

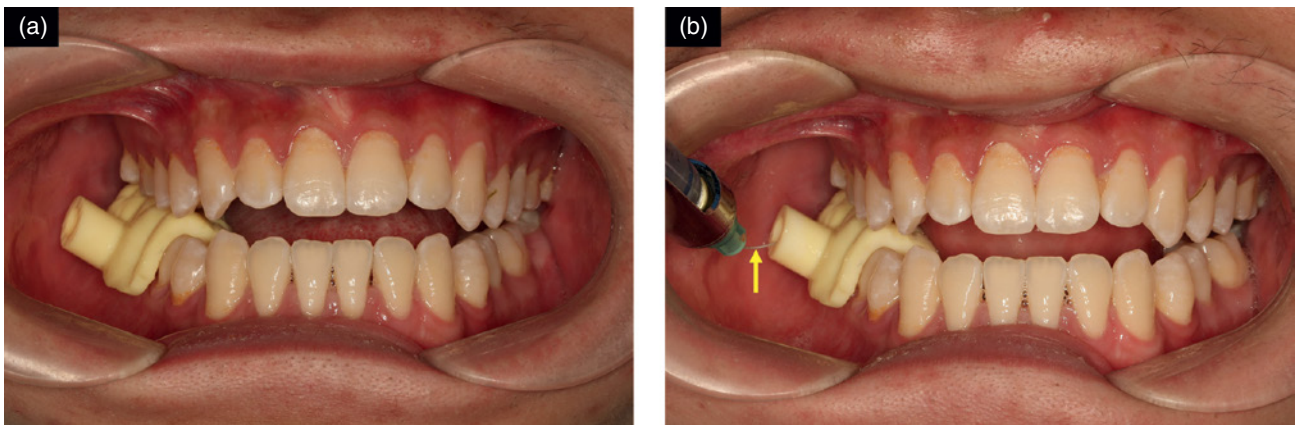


Figure 12.6 The injection of anaesthetic agent through the cylinder of an insertion guide at the buccal shelf is difficult due to awkward access to the anatomical site. (a) The insertion guide was tried in. (b) Although the injection needle was pre-bent to facilitate the injection, the direction of the injection was still difficult to control. Note the non-parallelism between the long axis of the cylinder and the injection needle (yellow arrow).

t.me/Dr_Mouayyad_AlbtousH

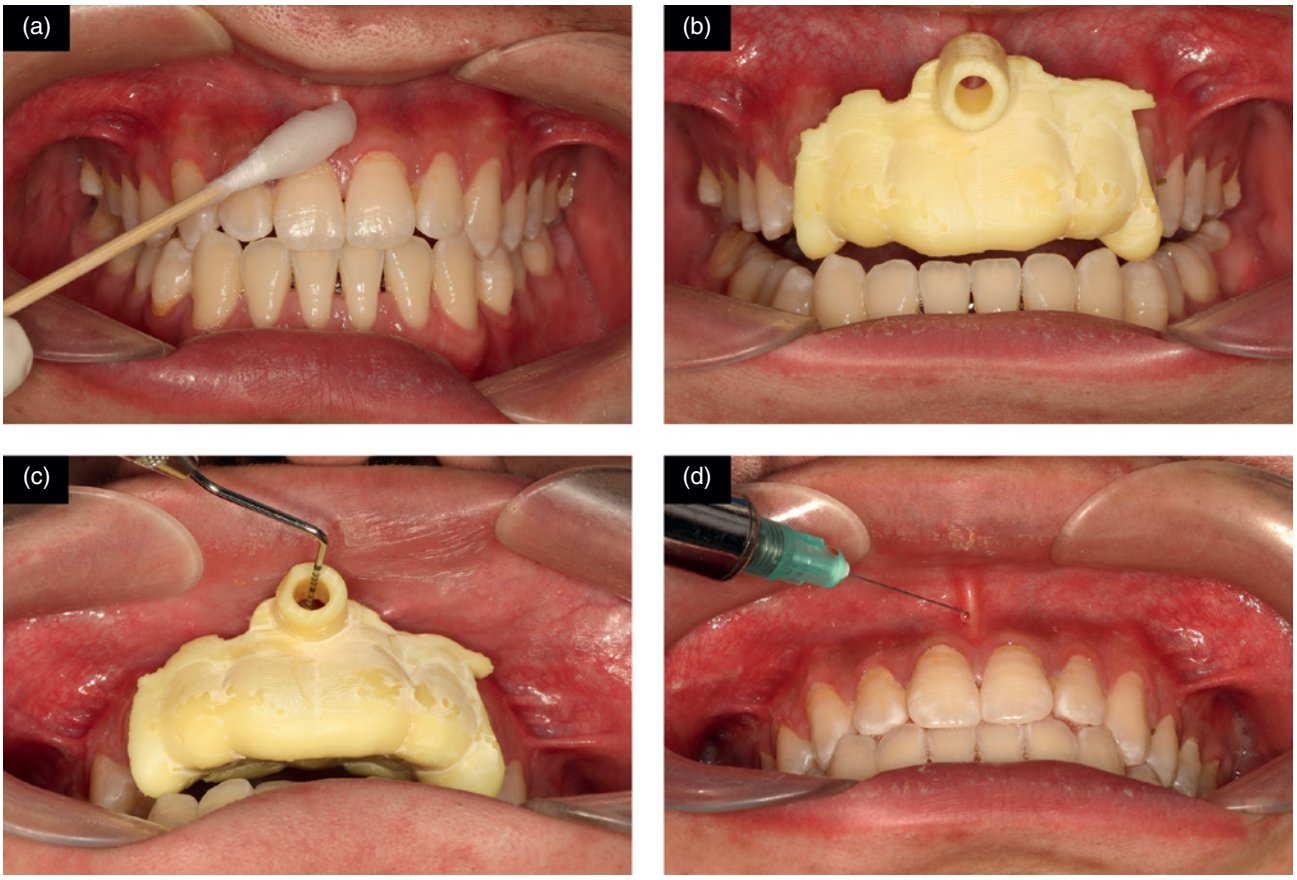


Figure 12.7 (a) Topical anaesthesia. (b) Engagement of the insertion guide. (c) Mark the injection site with a probe that is inserted into the predetermined site through the cylinder. (d) After removal of the insertion guide, infiltration anaesthesia is performed at the marked injection site.

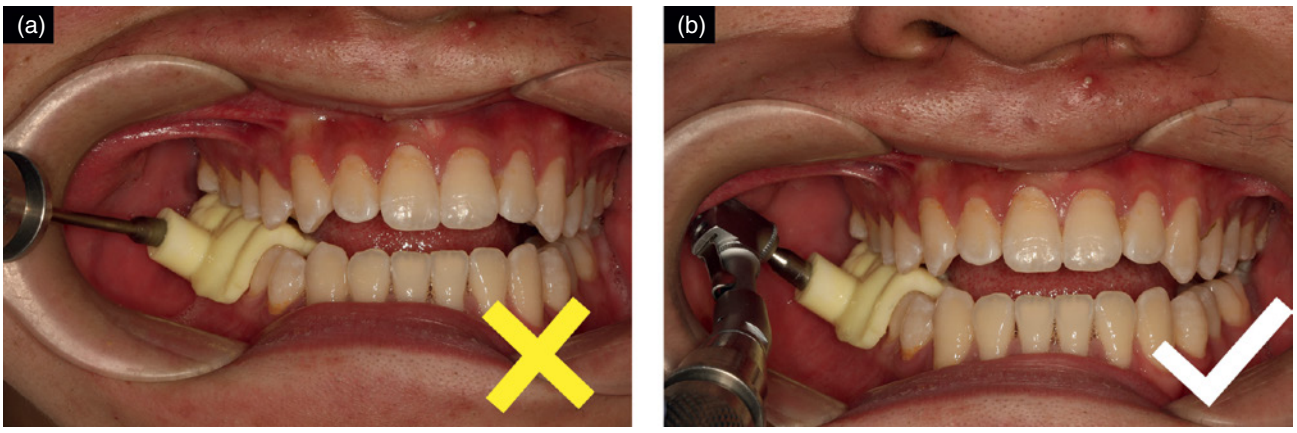
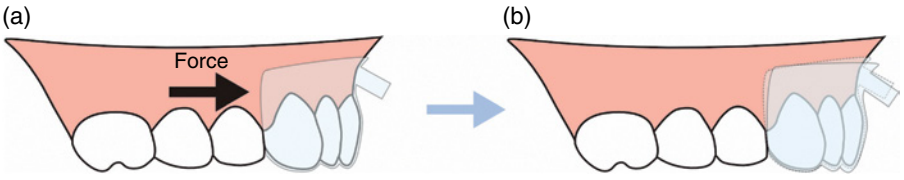


Figure 12.8 (a) The use of a straight screwdriver is not advised for the buccal shelf region that is difficult to access. Due to the presence of soft tissue resistance, the insertion path is non-parallel to the long axis of the guide cylinder. (b) A contra-angle screwdriver is recommended for the buccal shelf region so that the insertion path can be parallel to the long axis of the guide cylinder.

Figure 12.9 Lateral displacement of the insertion guide during insertion may lead to a deviated insertion path through an incorrect insertion site.



t.me/Dr_Mouayyad_AlbtousH

Depending on the design, an insertion stop may be incorporated into the insertion guide. The insertion stop is beneficial for determining the insertion depth of mini-implants so that an optimal emergence profile is achieved (Figure 12.11). If no stop is designed, practitioners should have a good sense of the insertion depth that has already been achieved and remove the insertion guide when 80–90% insertion depth is reached. Following removal of the guide, the mini-implant is further advanced consistently with the predetermined insertion path until confirmed contact between mini-implant platform and soft tissue is achieved (Figure 12.12). This procedure helps to avoid overinsertion of mini-implants. Since 80–90% insertion depth has been achieved, the insertion path is

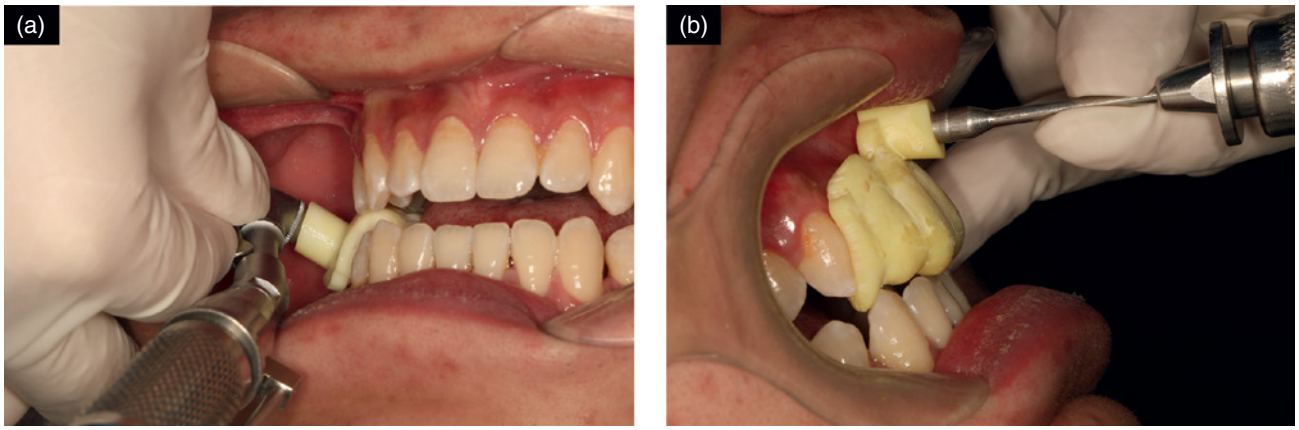


Figure 12.10 Stabilisation of the screwdriver shaft during insertion. (a) Stabilisation of a contra-angle screwdriver during insertion. (b) Stabilisation of a straight screwdriver shaft during insertion.

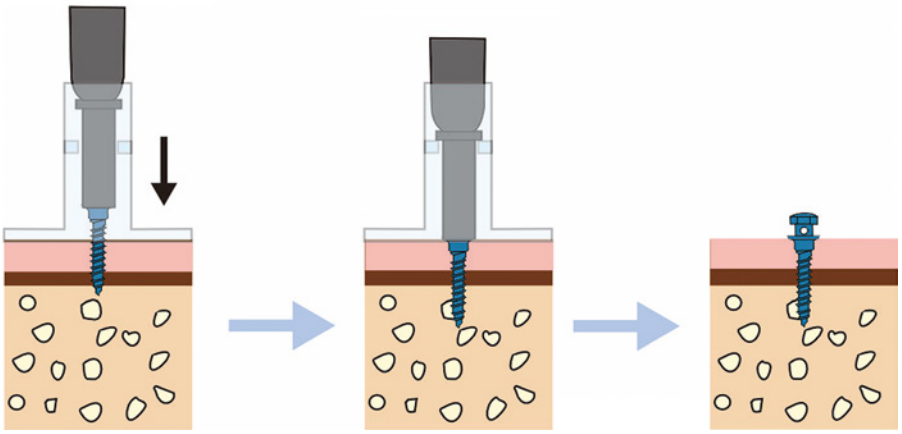


Figure 12.11 Incorporation of an insertion stop in the insertion guide facilitates the advancement of the mini-implant to a predetermined insertion depth.

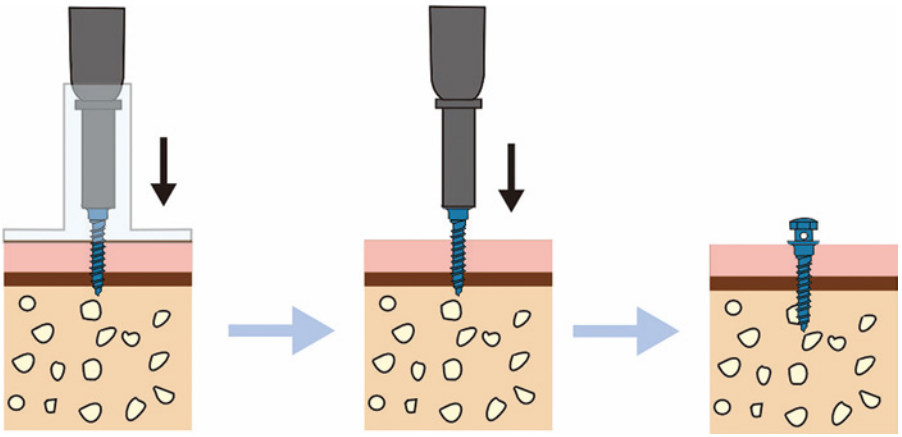


Figure 12.12 Insertion of a mini-implant with a guide without an insertion stop. The insertion guide is removed once 80–90% insertion depth has been reached and the mini-implant is further advanced without the insertion guide.

t.me/Dr_Mouayyad_AlbtousH

stable and deviations from original insertion path should not be a concern.

12.2.4 Detaching Screwdrivers and Removing Insertion Guides

The screwdriver should be detached in a direction that is in line with the long axis of the mini-implant. When difficulty of detachment is encountered, the handle and shaft of the screwdriver can be detached first, followed by removing the shaft and the insertion guide. Occasionally, when difficult detachment of the screwdriver shaft is encountered even when disassembled from the handle, gently disengaging the insertion guide may facilitate their removal since friction between shaft and guide cylinder can be reduced.

12.3 Placement of Mini-implants with Insertion Guides at Different Sites

12.3.1 Labial Interradicular Region

The labial interradicular region is readily accessible for the placement of mini-implants, allowing straight screwdrivers to be used for insertion. For the interradicular sites between two central incisors, the presence of labial frenum may interfere with the try-in of insertion guides and preclude their accurate fit. Thus, frenectomy may be indicated for patients with labial frenum. A case example is presented in Figure 12.13 to demonstrate the procedures of inserting a labial interradicular mini-implant with an insertion guide.

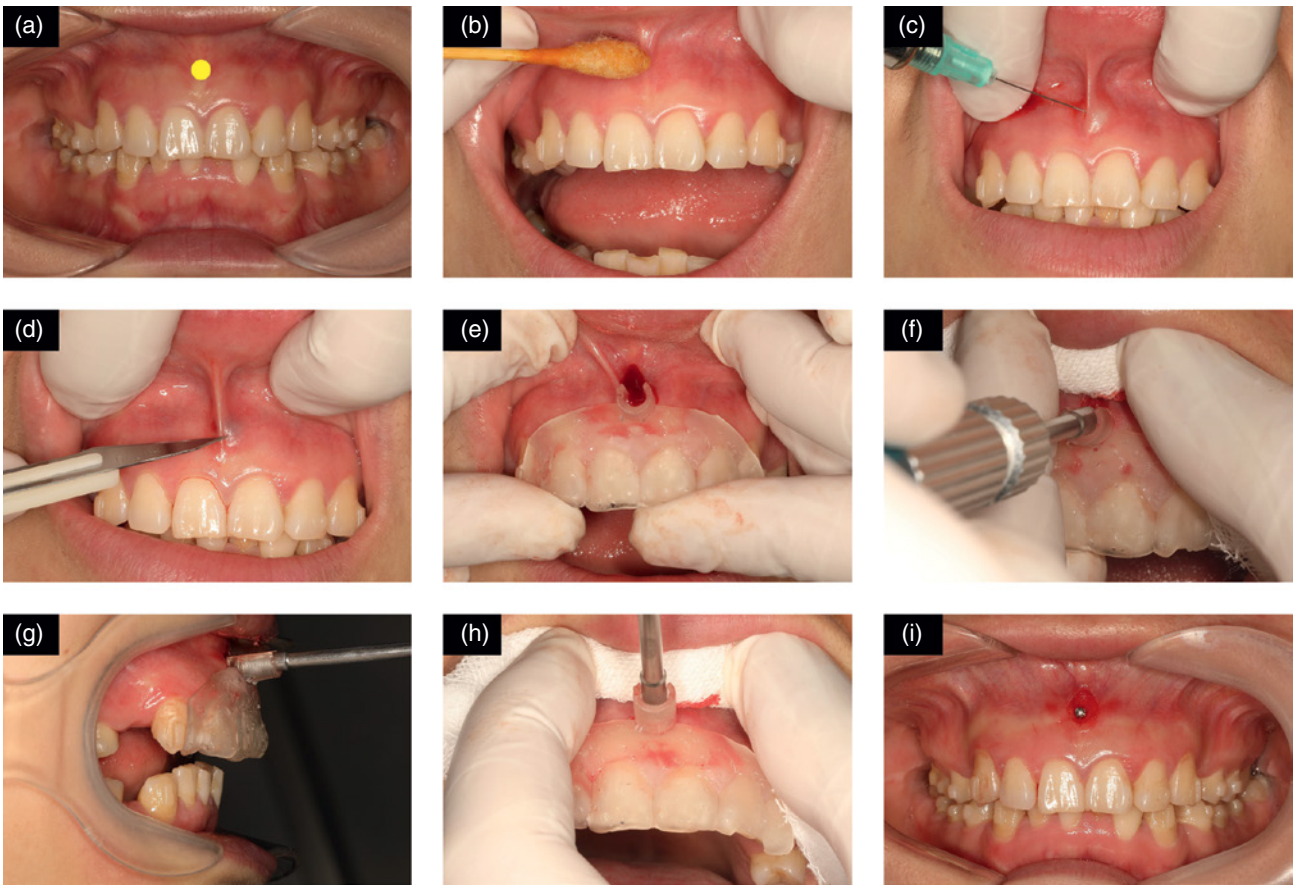


Figure 12.13 Insertion of a mini-implant at the labial interradicular region. (a) The predetermined insertion site (yellow circled area). (b) Local disinfection with iodophor. (c) Local infiltration anaesthesia. (d) Frenectomy of the labial frenum. (e) Mounting the insertion guide. (f) Insertion of the screwdriver through the guide cylinder. (g) Adjust the insertion path to confirm that it is parallel to the long axis of the guide cylinder. (h) Insertion of the mini-implant. (i) Successful insertion of the mini-implant.

t.me/Dr_Mouayyad_AlbtousH

12.3.2 Buccal Interradicular Region

The buccal interradicular region is often used for reinforcing molar anchorage among premolar extraction patients requiring maximal molar anchorage. For patients with limited interradicular space, root proximity and injury may be encountered, which eventually lead to mini-implant failure. The use of insertion guides can ensure precise insertion of mini-implants and can reduce the likelihood of iatrogenic root damage. Special attention should be paid to any additional displacement force that is exerted on insertion guides. The additional displacement force or instability of insertion guides may cause their displacement, leading to deviations from virtually planned insertion sites (Figure 12.14). Thus, insertion guides should be stabilised preferably by patients' biting force and remain free from any displacement force (Figure 12.15). Moreover, for buccal interradicular sites with limited access due to buccal soft tissues (especially for the mandibular interradicular site between molars), a contra-angle screwdriver may be needed to guarantee that the screwdriver shaft is in line with the long axis of the guide cylinder, in order to avoid any lateral displacement exerted on the insertion guide (Figure 12.16).

A case example is displayed in Figure 12.17 to demonstrate the procedure of inserting a buccal interradicular mini-implant with the aid of an insertion guide.

12.3.3 Palatal Region

As the palatal region is accessible only when patients open their mouth, stabilisation of insertion guides for palatal mini-implants can only be achieved through practitioners' finger pressure. Moreover, due to the lack of accessibility using straight screwdrivers, it is advised to use contra-angle screwdrivers for palatal mini-implants. The procedures of inserting palatal mini-implants using insertion guides are demonstrated in Figure 12.18.

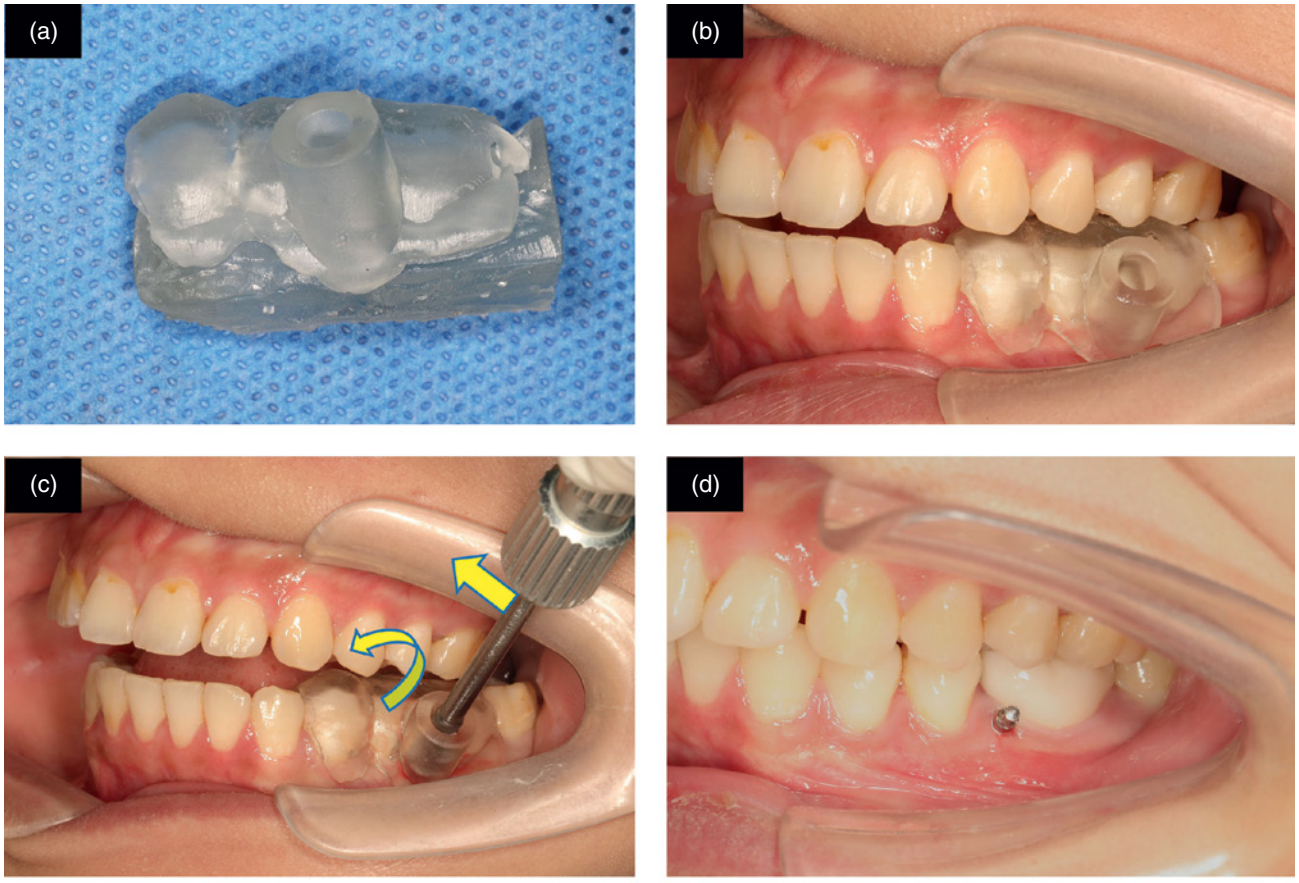


Figure 12.14 Deviated insertion of a mini-implant due to displacement of the insertion guide. (a) Try the insertion guide onto the 3-D-printed model. (b) Try the guide onto the actual dentition. (c) The insertion guide was displaced due to the instability of the screwdriver during insertion. Note that the screwdriver was not stabilised during insertion. The displacements of the screwdriver and insertion guide are indicated by the straight and curved arrows, respectively. (d,e) The actual position of the mini-implant after insertion was different compared to the virtual one. (f) Root contact was evidenced by a periapical radiograph, necessitating reimplantation.

t.me/Dr_Mouayyad_AlbtousH

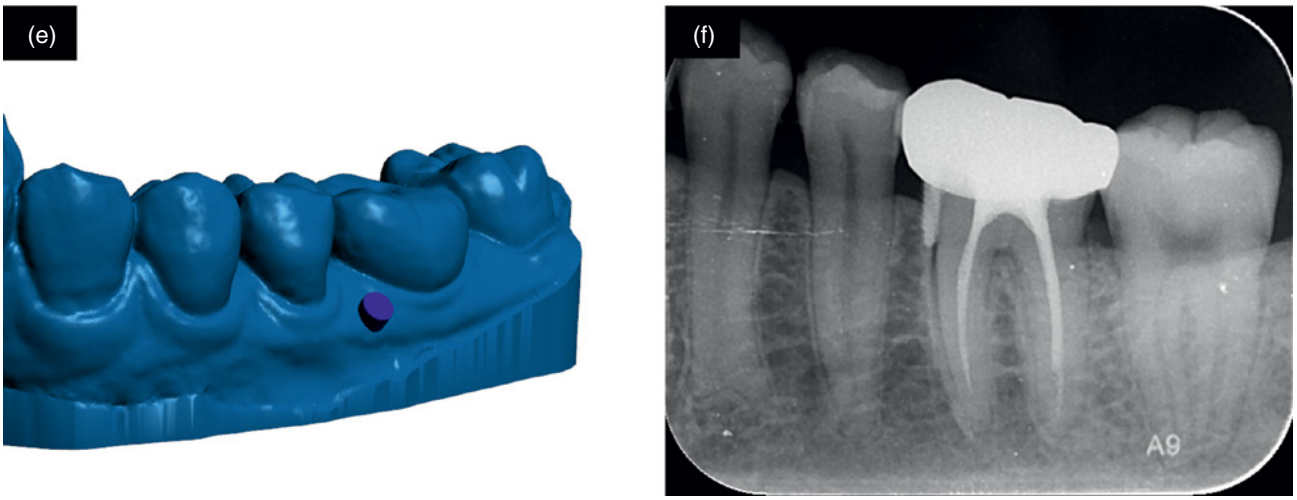


Figure 12.14 (Continued)

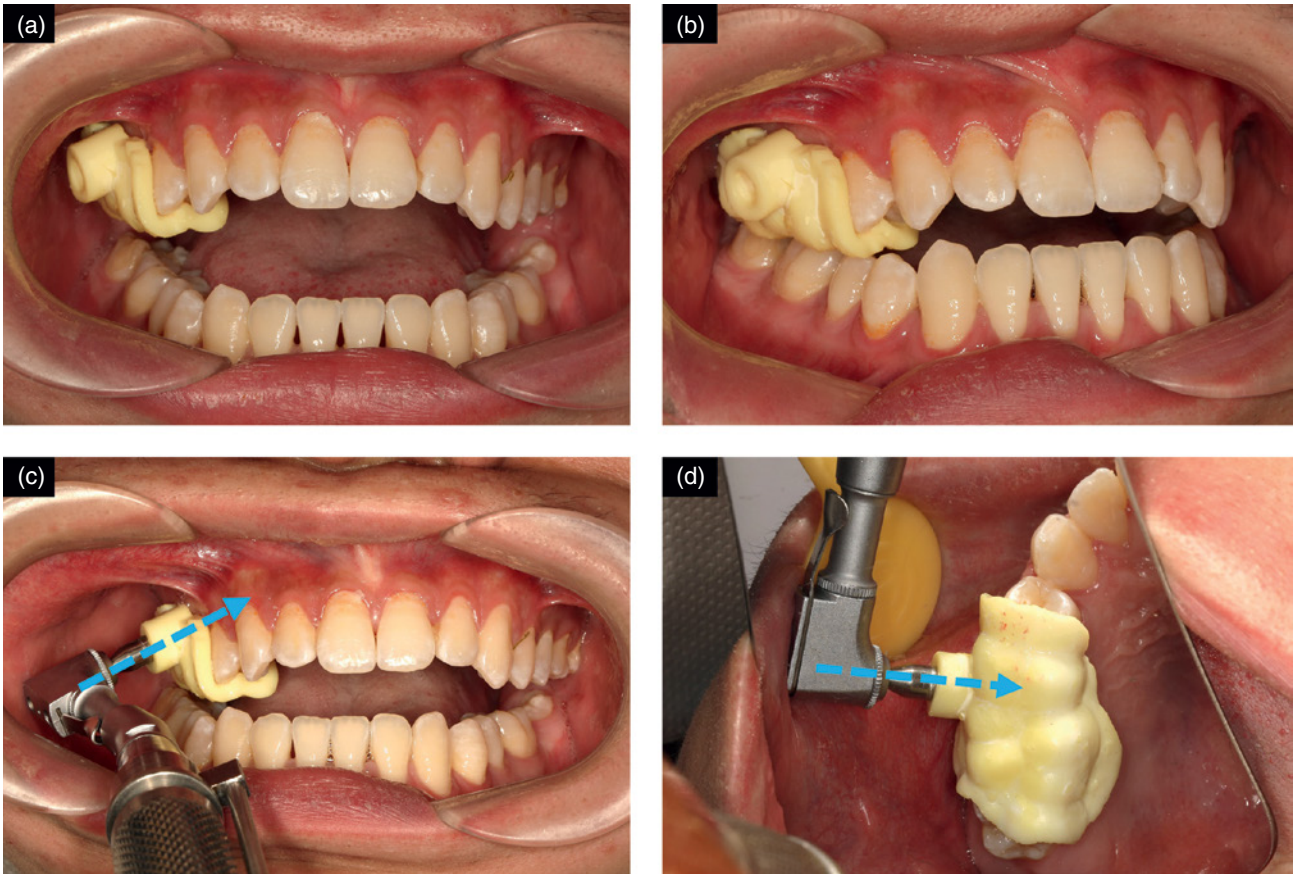


Figure 12.15 (a,b) Stabilisation of an insertion guide through the patient's biting force so that no displacement of the guide occurs. (c,d) The insertion path is parallel to the long axis of the guide cylinder and no lateral displacement force is applied

12.3.4 Buccal Shelf

The buccal shelf is a recently discovered anatomical site for the placement of orthodontic mini-implants and has the advantages of sufficient primary stability and low failure rates. However, the clinical success of buccal shelf mini-implants is jeopardised by the thick cortical bone, which may result in bone damage and compromised secondary stability. Thus, we recommend that pilot drilling be performed to reduce the risk of bone damage.

t.me/Dr_Mouayyad_AlbtousH

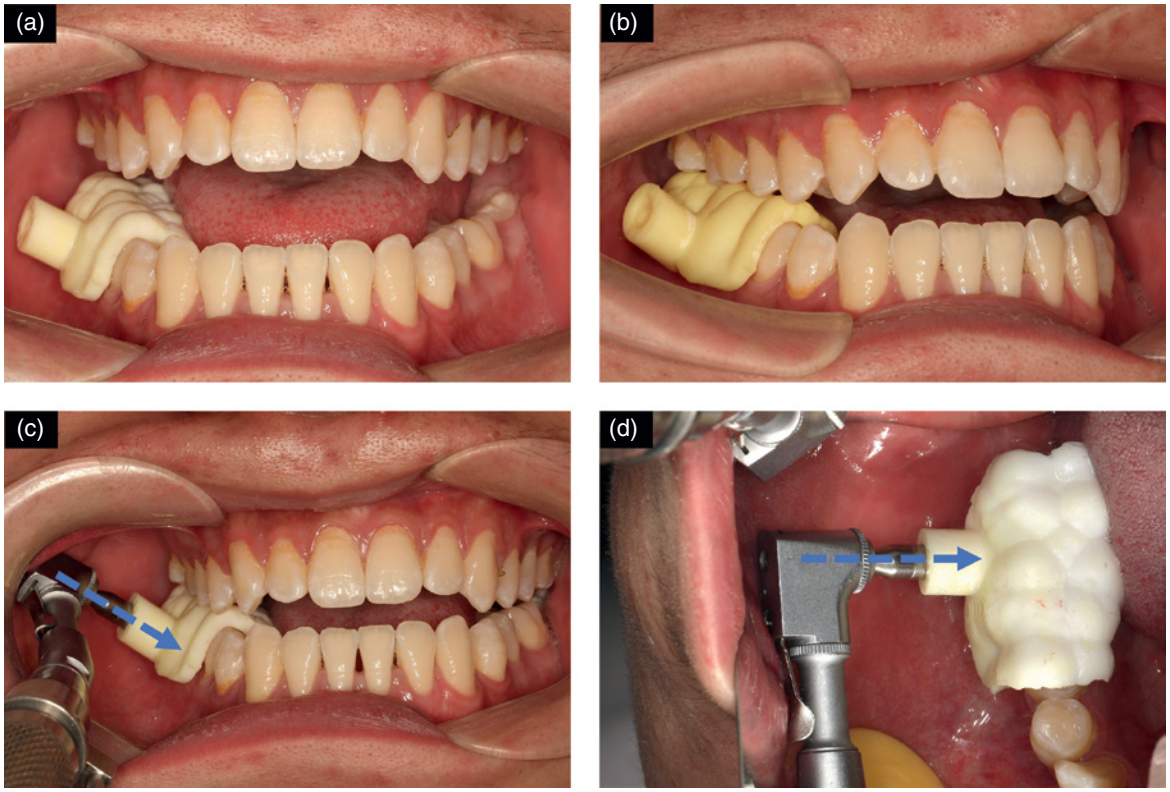


Figure 12.16 Insertion of a mini-implant with an insertion guide at the mandibular buccal interradicular region. (a) Engagement of the insertion guide. (b) Stabilisation of the insertion guide through the patient's biting. (c) Insertion of the mini-implant through the guide cylinder (frontal view). (d) Insertion of the mini-implant through the guide cylinder (occlusal view).

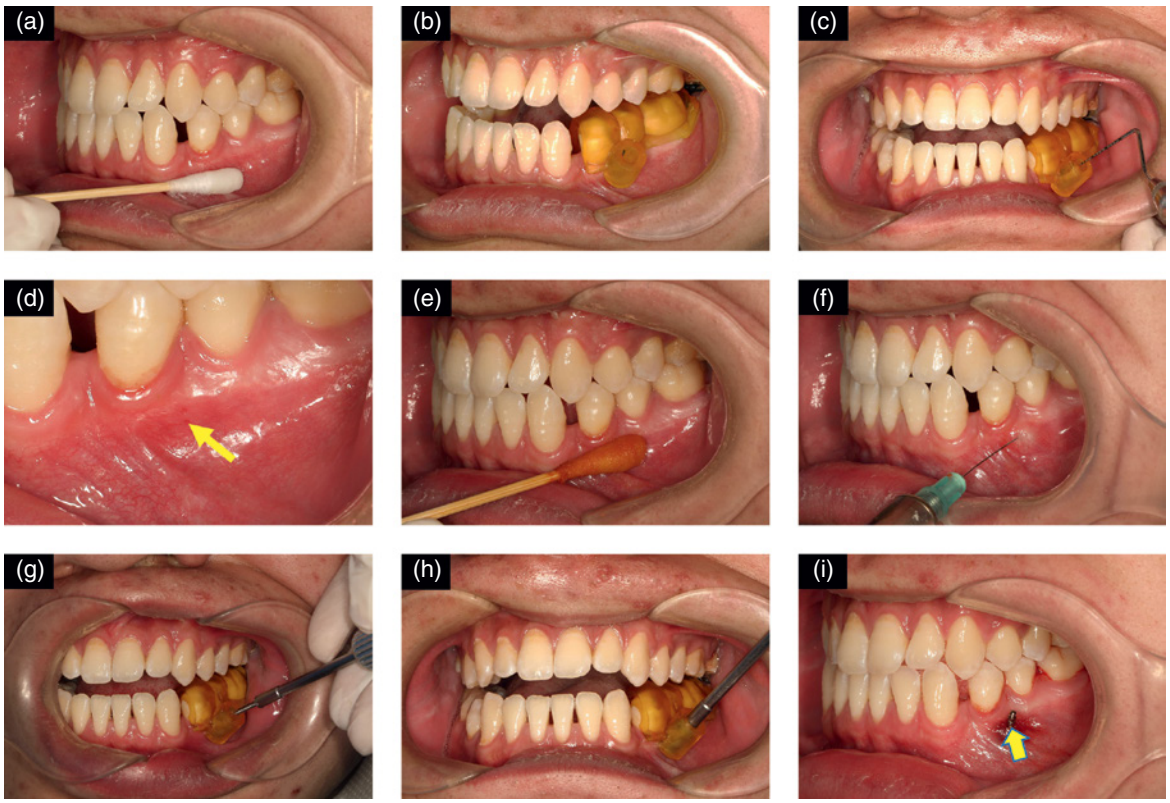


Figure 12.17 Insertion of a mini-implant at the mandibular buccal region through an insertion guide. (a) Topical anaesthesia. (b) Engagement of the insertion guide onto the dentition. (c) Marking the entry point with a probe inserted through the guide cylinder. (d) The marked entry point. (e) Local disinfection of the entry point with iodophor. (f) Local infiltration anaesthesia. (g) Insertion of the mini-implant with a screwdriver through the guide cylinder. (h) Insertion and advancement of the mini-implant. (i) Successful insertion of the mini-implant (yellow arrow).

t.me/Dr_Mouayyad_AlbtousH

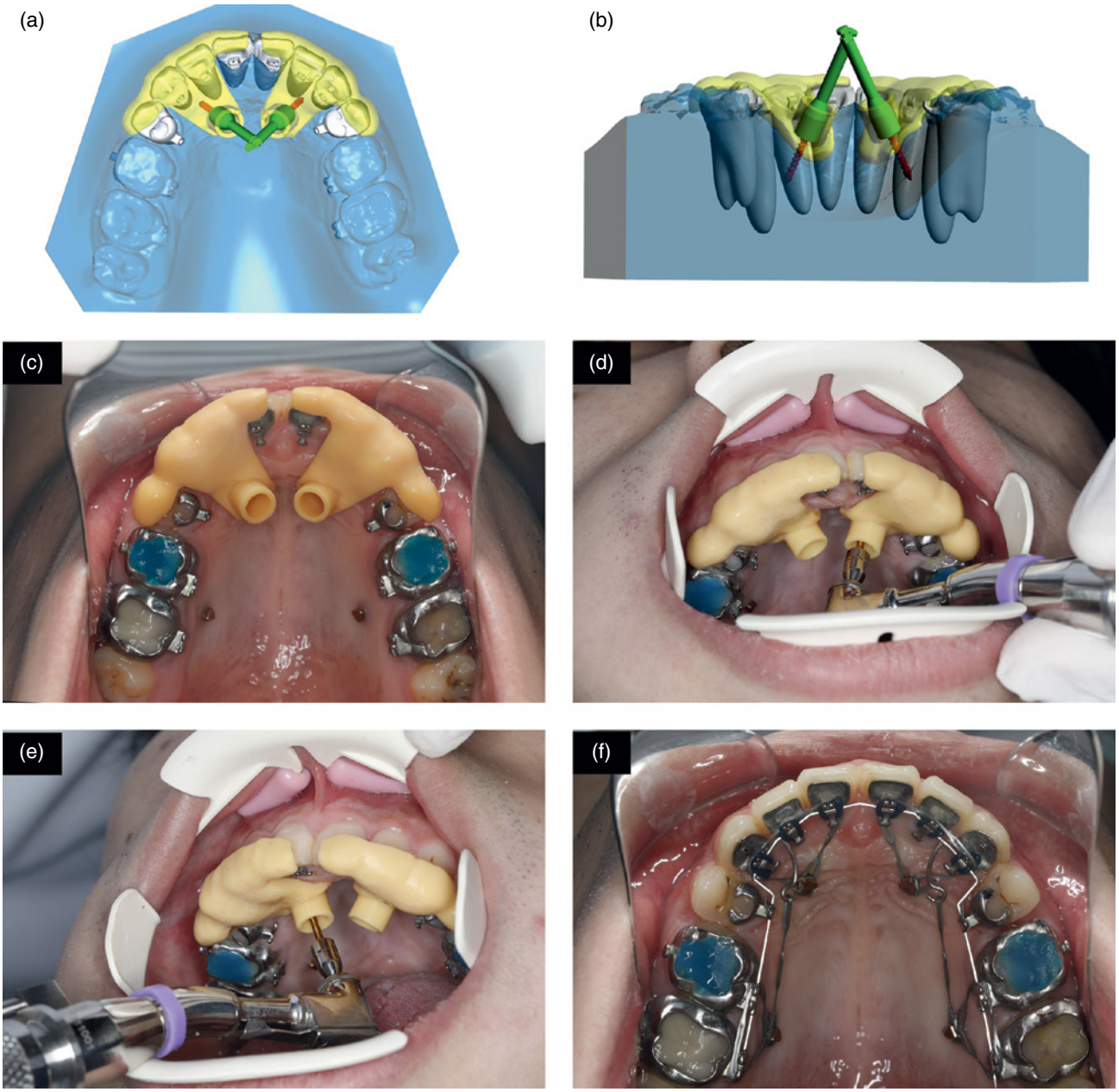


Figure 12.18 Insertion of palatal mini-implants through insertion guides. (a,b) Virtual insertion of two palatal mini-implants and design of bilateral insertion guides. (c) Mounting the insertion guides. (d) Insertion of the left palatal mini-implant through the guide cylinder. (e) Insertion of the right mini-implant. (f) Force loading on the palatal mini-implants following their insertion.

In contrast to insertion guides for other anatomical sites where soft tissue contact is designed, the insertion guides for buccal shelf mini-implants should be designed for bone contact since flap surgery and pilot drilling are indicated. Following local infiltration anaesthesia, flap elevation is performed to expose the bone surface of the buccal shelf and the insertion guide is fitted onto the dentition to create good contact with the exposed bone surface. The insertion point is marked with a contra-angle handpiece that makes a 1 mm deep pilot hole on the bone surface. Then, the insertion guide is removed and pilot drilling is continued to reach the desired depth. Lastly, the buccal shelf mini-implant is inserted through the pilot hole with the insertion guide (Figure 12.19).

The clinical procedures of inserting mini-implants into the buccal shelf are displayed in Figure 12.20.

t.me/Dr_Mouayyad_AlbtousH

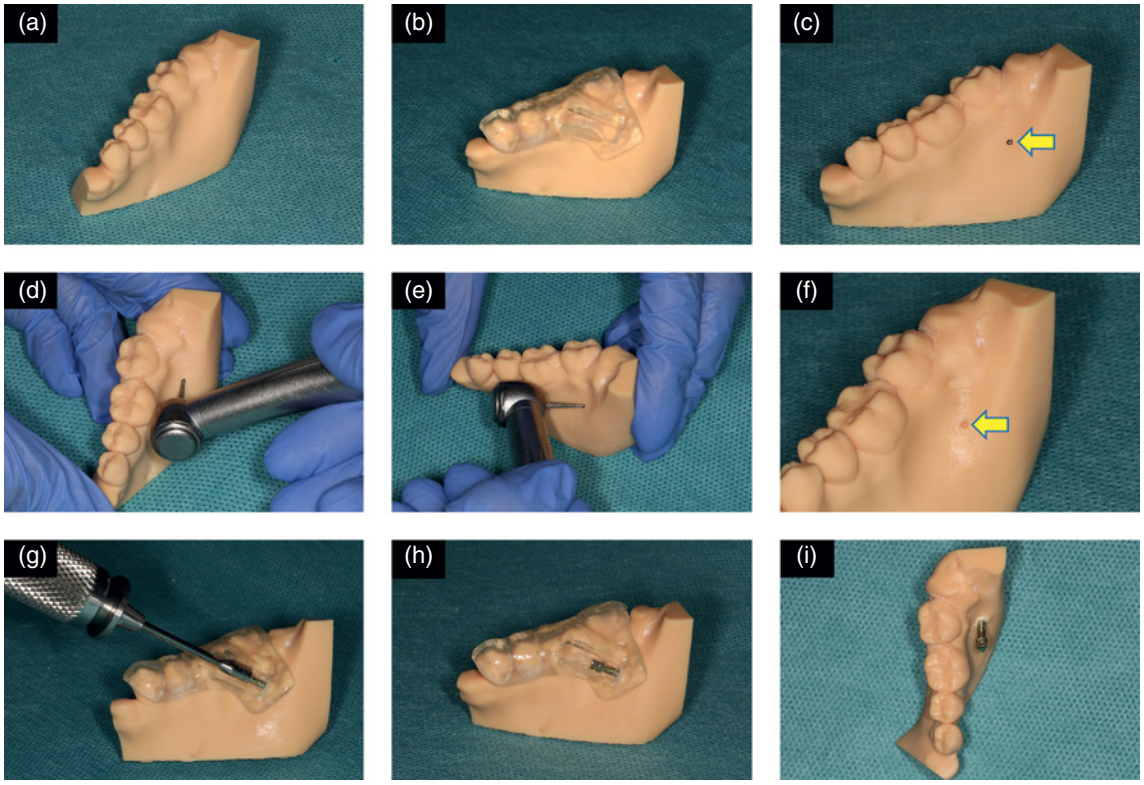


Figure 12.19 Insertion of a mini-implant at the buccal shelf region with an insertion guide on a dental model. (a) The 3-D-printed dental model. (b) Engagement of the insertion guide onto the dental model. (c) The entry point is marked. (d–f) Predrilling to make a pilot hole. (g) Insertion of the mini-implant through the guide cylinder. (h) Remove the screwdriver once the desired insertion depth is reached. (i) Removal of the insertion guide.

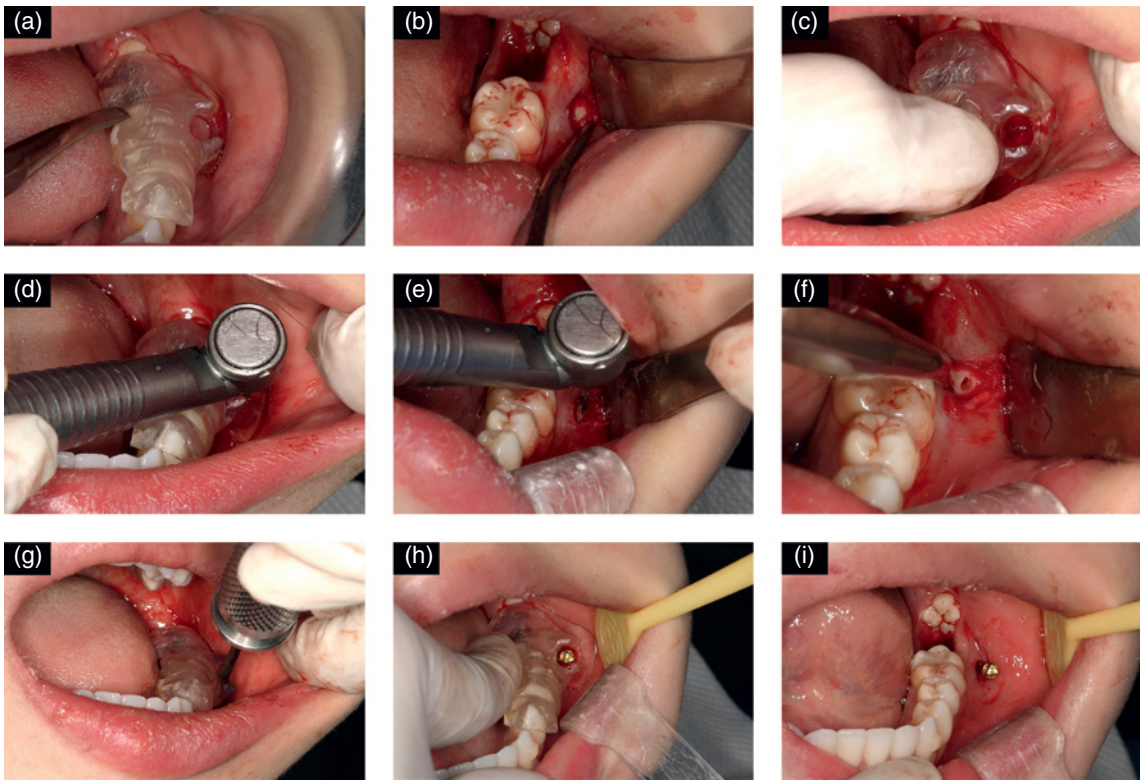


Figure 12.20 Insertion of a mini-implant at the buccal shelf region with an insertion guide. (a) Try the insertion guide onto the dentition. (b) Flap elevation to expose the bone surface of the buccal shelf. (c) Engage the insertion guide. (d,e) Predrilling is performed to make a pilot hole. (f) Verify the pilot hole after removing the insertion guide. (g) Mount the insertion guide again and insert the mini-implant through the guide cylinder with a straight screwdriver. (h) Detach the screwdriver and confirm the insertion depth and position of the mini-implant. (i) Removal of the insertion guide once desired insertion depth is reached.

t.me/Dr_Mouayyad_AlbtousH

12.4 Summary

The clinical applications of insertion guides are beneficial for the precise insertion of orthodontic mini-implants. A variety of factors may influence the accuracy of insertion guides, including the fit between insertion guides and dentition, stabilisation of insertion guides during insertion, the selection of straight or contra-angle screwdrivers and avoidance of displacement of insertion guides. Both general and site-specific principles and clinical procedures of inserting mini-implants with insertion guides have been demonstrated in this chapter.

References

1 Morea C, Hayek JE, Oleskovicz C, Dominguez GC, Chilvarquer I. (2011). Precise insertion of orthodontic miniscrews with a stereolithographic surgical guide based on cone beam computed tomography data: a pilot study. *Int. J. Oral Maxillofac. Implants.* 26(4):860–865.

2 Su L, Song H, Huang X. (2022). Accuracy of two orthodontic mini-implant templates in the infrazygomatic crest zone: a prospective cohort study. *BMC Oral Health* 22(1):252.

t.me/Dr_Mouayyad_AlbtousH

13

Root Contact

Xinyu Yan, Yan Wang, Jianru Yi, Hu Long, Xianglong Han, and Wenli Lai

Department of Orthodontics, State Key Laboratory of Oral Diseases and National Clinical Research Center for Oral Diseases, West China Hospital of Stomatology, Sichuan University, Chengdu, China

13.1 Introduction

Root contact is one of the most common complications associated with orthodontic TADs, which jeopardises the integrity of tooth structures (Figure 13.1). Tissue damage due to root contact involves periodontal tissues, cementum, dentin or even pulp (Figure 13.2). The incidence of root contact ranged from 9% to 48% among different studies (Table 13.1).[1-9] Briefly, two-thirds of the aforementioned studies reported a rate lower than 21%. The differences in

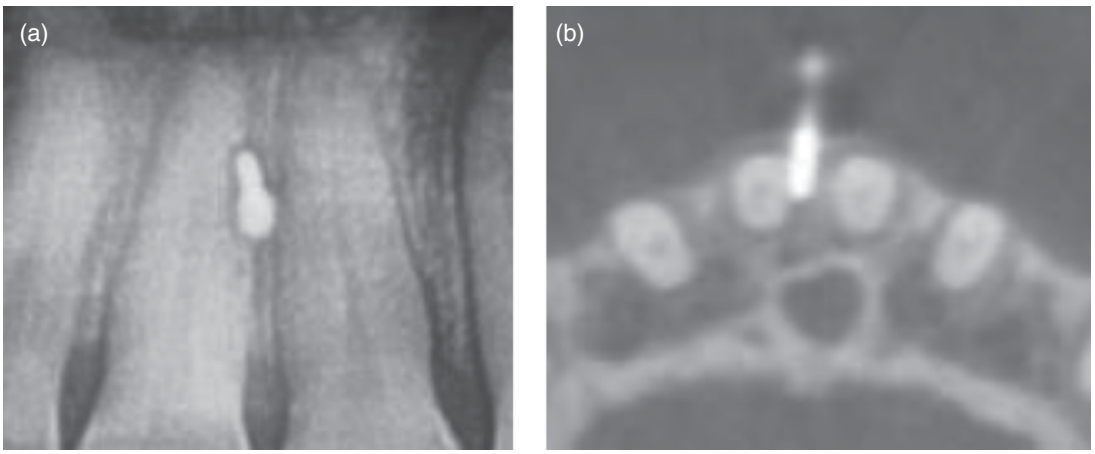


Figure 13.1 Root contact by mini-implants. (a) Periapical radiograph displaying root contact and damage by a mini-implant. (b) CBCT image (axial view) showing root contact.

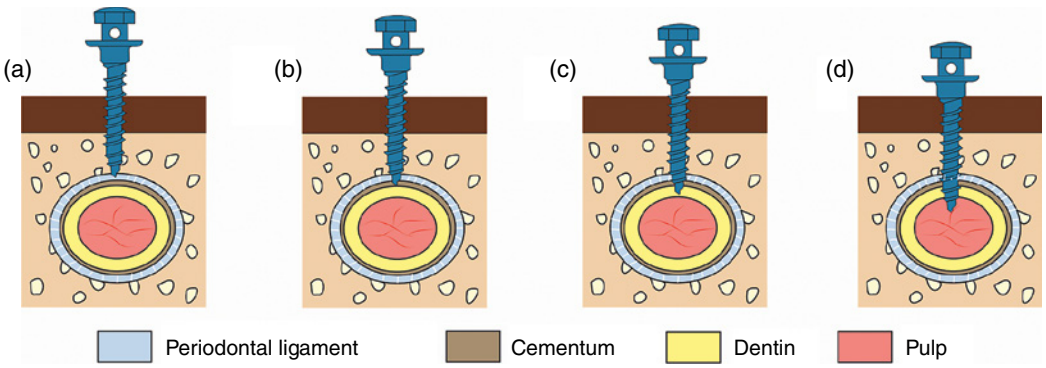


Figure 13.2 Different degrees of root damage by mini-implants. (a) Damage to periodontal ligament. (b) Injury to cementum. (c) Damage to dentin. (d) Penetration into pulp cavity.

Clinical Insertion Techniques of Orthodontic Temporary Anchorage Devices, First Edition. Edited by Hu Long, Xianglong Han, and Wenli Lai.
© 2024 John Wiley & Sons Ltd. Published 2024 by John Wiley & Sons Ltd.

t.me/Dr_Mouayyad_AlbtousH

Table 13.1 The incidence of root contact among different studies.

Study	Incidence	Insertion angles	Insertion sites	Size	Placement mode
An 2019[1]	41%	Vertical: 84–95°; horizontal: 91–101°	Buccal interradicular sites	Diameter: 2.0 mm; length: 8 mm	Self-drilling
Kim 2010[2]	30%	Vertical: 12–25°; horizontal: 5°	U5-U6 interradicular site	Diameter: 1.8 mm; length: 8.5 mm	Self-tapping
Kuroda 2007[3]	48%	N.A.		Diameter 1.3–1.5 mm, length 6–12 mm	Self-tapping
Min 2012[4]	9%	N.A.	Maxillary buccal region	Diameter: 1.2–1.3 mm; length: 8 mm	Self-drilling
Motoyoshi 2013[5]	19%	N.A.	U5-U6 interradicular site	Diameter: 1.6 mm; length: 8 mm	Both
Shigeeda 2014[6]	21%	45–60° to the tooth long axis	U5-U6 and L5-L6 interradicular sites	Diameter: 1.6 mm; length: 8 mm	Self-tapping
Shinohara 2013[7]	20%	45–60° to the tooth long axis	U5-U6 and L5-L6 interradicular sites	Diameter: 1.6 mm; length: 8 mm	Self-tapping
Son 2014[8]	20%	45–60° to the tooth long axis	U5-U6 interradicular site	Diameter: 1.6 mm; length: 8 mm	Both
Iwai 2015[9]	20%	Vertical: 45–54°; horizontal: 81–87°	U5-U6 interradicular site	Diameter: 1.6 mm; length: 8 mm	Both

root contact rate among studies can be explained by mini-implant size, insertion site, insertion angulation, insertion technique and operator experience. If root contact by mini-implants is left untreated, the mini-implants are susceptible to failure or loosening due to poor development of secondary stability.[10-12] A recent systematic review indicates that periodontal tissue, cementum and dentin may regenerate spontaneously after timely removal of mini-implants and that regeneration of damaged pulp is uncertain.[13] Thus, if mini-implants with root contact are removed in a timely manner, the overall prognosis of root contact is satisfactory and spontaneous repair is anticipated, unless pulp is involved.

13.2 Clinical Manifestations

When mini-implants are in proximity to dental roots during insertion, patients often feel sharp pain and may move their heads away to avoid further damage. This is mainly due to abundant nerve terminals in periodontal tissues but sparse nerve endings in alveolar bone (Figure 13.3). Meanwhile, operators may perceive an abrupt increase in resistance to screwdriver rotation, resulting in increased insertion torque (Figure 13.4). A large body of evidence indicates that insertion torque increases for mini-implants with root contact.[14] Thus, patient complaint of sharp pain plus operator perception of a sudden increase in resistance often herald the likelihood of root contact and appropriate measures should be taken to avoid further damage. Nevertheless, further rotation of mini-implant drivers will result in different clinical consequences according to properties of alveolar bone and mini-implants (Figure 13.5): (1) free rotation of mini-implants without further advancement; (2) mini-implant fracture; (3) root penetration.

Free rotation of mini-implants without further advancement is often encountered with poor bone quality. Alveolar bone with poor quality (i.e. limited cortical thickness and low bone density) fails to offer mini-implants adequate mechanical support to advance, resulting in free rotation of mini-implants. In contrast, alveolar bone with adequate bone quality (i.e. sufficient cortical thickness and high bone density) gives mini-implants sufficient mechanical support to advance. If the self-drilling capacity of mini-implants is inadequate, further rotation will result in bending or even fracture of the implants. Otherwise, root penetration occurs if self-drilling capacity is adequate.

t.me/Dr_Mouayyad_AlbtousH

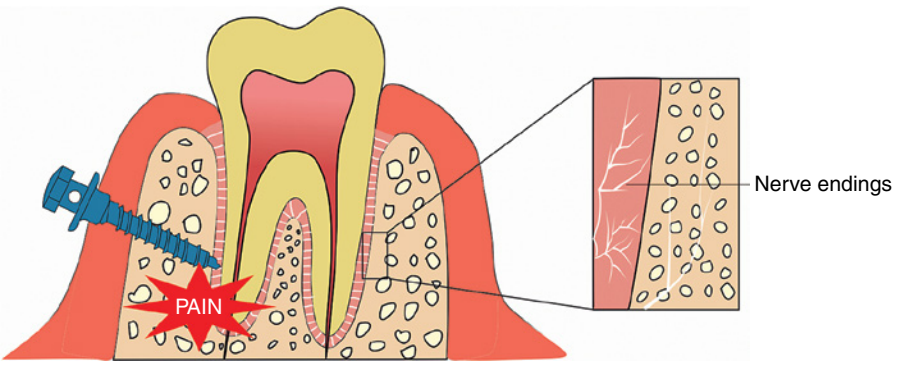


Figure 13.3 Abundant nerve endings are observed in periodontal tissues while sparse nerve terminals are seen in alveolar bone. Pain elicited by root contact is mainly perceived by nerve terminals in periodontal tissues, rather than by those in alveolar bone.

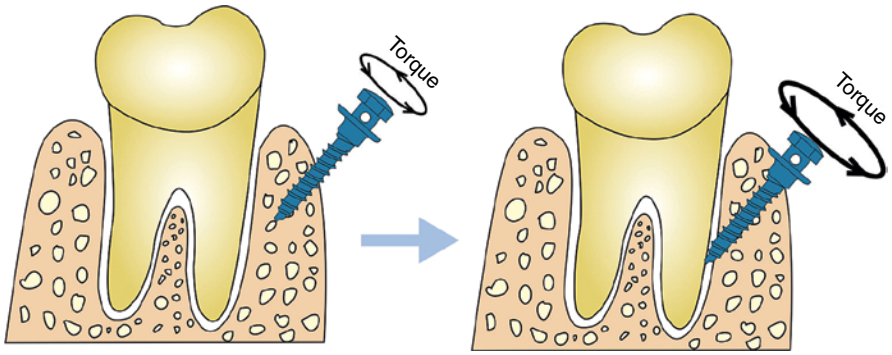


Figure 13.4 Increased insertion torque heralds root contact by mini-implants.

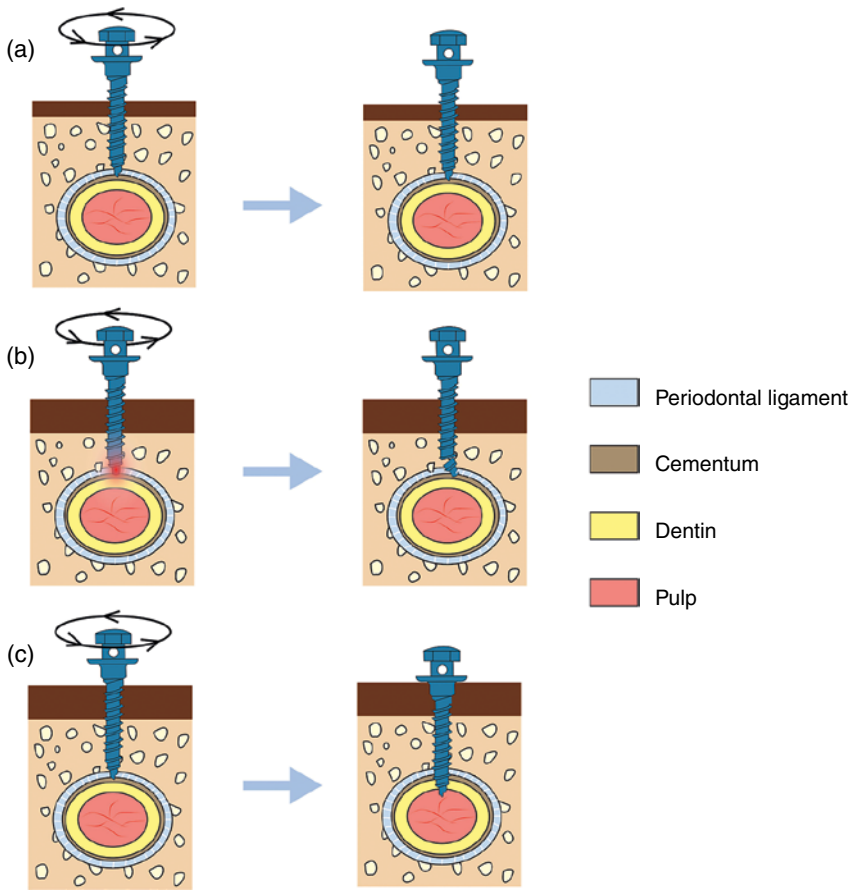


Figure 13.5 Different clinical consequences of root contact according to different properties of alveolar bone and mini-implants. (a) Free rotation of mini-implants without further advancement when the cortical bone is thin. (b) Mini-implant fracture occurs when the tip of mini-implant is blunt and the cortical bone is thick. (c) Root penetration occurs when the tip of mini-implant is sharp and the cortical bone is thick.

t.me/Dr_Mouayyad_AlbtousH

13.3 Prognosis

13.3.1 Mini-implants

When mini-implants are in proximity to dental roots, insertion torque increases abruptly due to root resistance. This increase in insertion torque plus patient complaint of sharp pain warns operators about the possibility of root contact. When root contact is suspected, percussion tests and radiographic examinations are often prescribed by prudent practitioners to establish or rule out the diagnosis. Unless forceful continued rotation of mini-implants is implemented under the circumstances of root contact, mini-implant fracture seldom occurs. In most clinical scenarios, the extent of root contact is limited so that no obvious symptoms or signs are observed, leaving mini-implants with root contact untreated. However, the long-term stability of these mini-implants is jeopardised since root contact is a major factor for mini-implant failure. Recent studies reveal that root contact accounts for up to 27% of mini-implant failure or loosening.[15-18]

To reiterate, the overall stability of mini-implants is composed of both primary stability and secondary stability. The development of secondary stability is governed by postinsertion bone remodelling processes and requires adequate primary stability (Figure 13.6). Micromovements of mini-implants due to inadequate primary stability may hinder bone remodelling and result in insufficient secondary stability (Figure 13.6). On one hand, when mini-implants are in proximity to roots, abnormally high stress is observed around the implants which may cause bone resorption where stress is concentrated (Figure 13.7).[12] On the other hand,

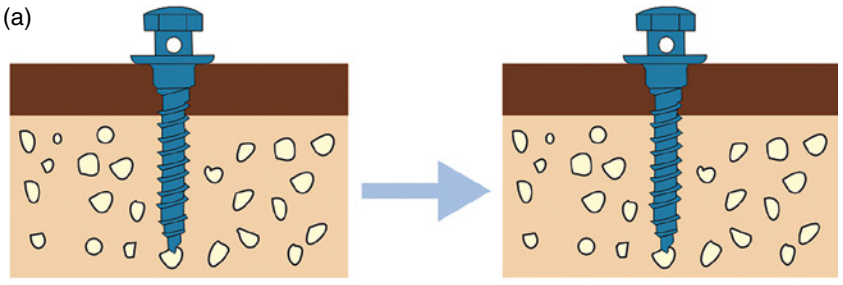


Figure 13.6 Primary stability determines subsequent alveolar bone remodelling and secondary stability. (a) Sufficient primary stability offers a suitable microenvironment for alveolar bone remodelling, resulting in adequate secondary stability. (b) Poor primary stability impairs bone remodelling, jeopardising secondary stability.

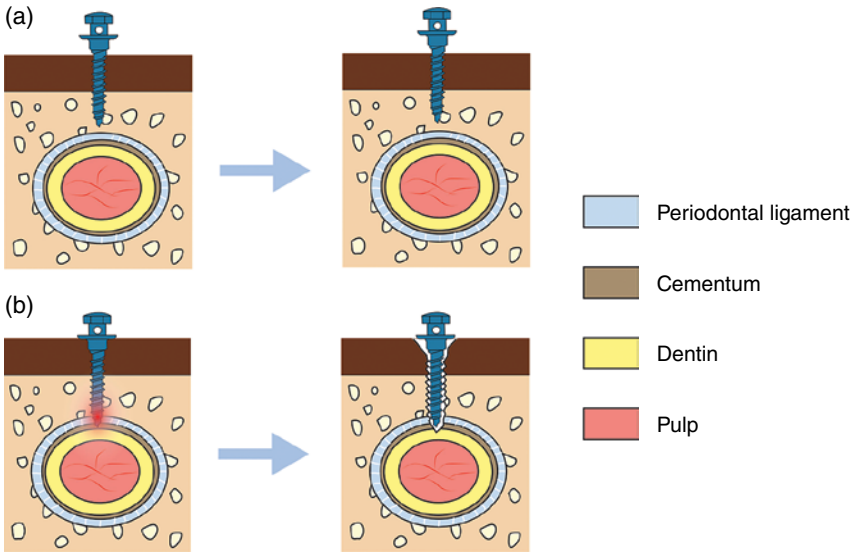


Figure 13.7 Concentrated stress is generated when root proximity occurs. (a) The mini-implant is far away from the root without concentrated stress. (b) The mini-implant contacts the root, which generates high stress at the tip and interferes with bone remodelling.

t.me/Dr_Mouayyad_AlbtousH

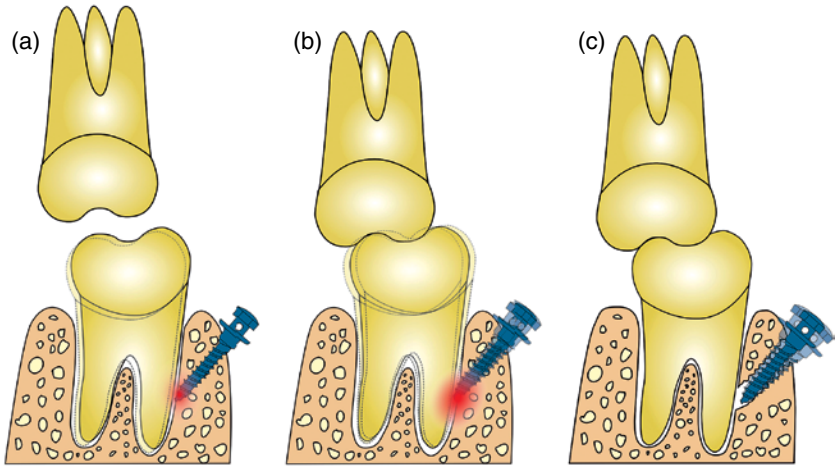


Figure 13.8 Occlusal force impairs the secondary stability of mini-implants with root contact. (a) The mini-implant touches the root with high stress concentrated at the tip. (b) Masticatory force increases the concentrated stress and jeopardises alveolar bone remodelling, leading to tooth mobility and instability of the mini-implant. (c) Under periodic masticatory force, the mini-implant becomes loose and is displaced by force loading.

periodic masticatory force can be transferred from roots to mini-implants and cause micromovements of the implants, which hinders the development of secondary stability and results in subsequent mini-implant failure (Figure 13.8).

13.3.2 Periodontal Tissues and Dental Roots

Depending on the extent of root injury, mini-implants may damage periodontal tissues, cementum, dentin and even pulp. Spontaneous repair is anticipated for minor damage to periodontal tissues, cementum and dentin, while the prognosis of pulp invasion is usually unfavourable (Figure 13.9).

After removal of mini-implants, cellular cementum is deposited to repair root damage lacunae, followed by the reorganisation of collagen fibres.[19,20] The healing of root damage is usually slower than that of alveolar bone that is repaired completely by bone formation from osteoblasts.[11] When mini-implants are not removed immediately, the healing of cementum still occurs by woven bone that is observed at the interface between the mini-implant and root.[21] However, a delay in repair or even no repair might occur if mini-implants are not removed in a timely manner.[22]

Complete repair of root damage is often achieved by the regeneration of cementum, periodontal tissue and alveolar bone.[23] However, occasionally, injured roots may display abnormal healing characterised by osteodentin formation, lack of periodontal ligament, bone degeneration and ankylosis.[24,25] Furthermore, if pulp is involved by root penetration, abnormal healing responses including pulp necrosis, ankylosis and root resorption are likely to occur.[13]

Therefore, the repair of root damage largely depends on the degree of injuries caused by mini-implants (Figure 13.10). Complete repair can be expected over time if the damage is limited to the periodontal ligament, cementum or dentin. When pulp injury occurs, abnormal responses such as pulp necrosis, ankylosis and root resorption are more likely to occur,[13,26] though pulp may still be vital in some clinical cases (especially for teeth with multiple roots) (Figure 13.11).[27]

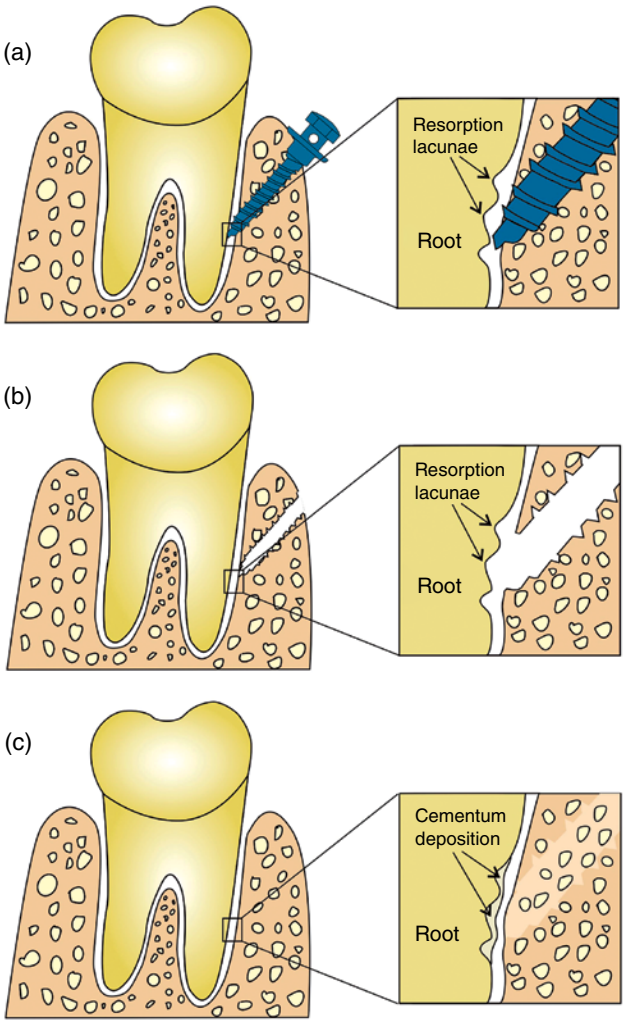


Figure 13.9 Histological responses of alveolar bone and roots to root contact. (a) Root contact of the mini-implant leads to root resorption. (b) Resorption of the root and alveolar bone occurs after removal of the mini-implant. (c) Spontaneous repair of the root and alveolar bone after a period of time.

t.me/Dr_Mouayyad_AlbtousH

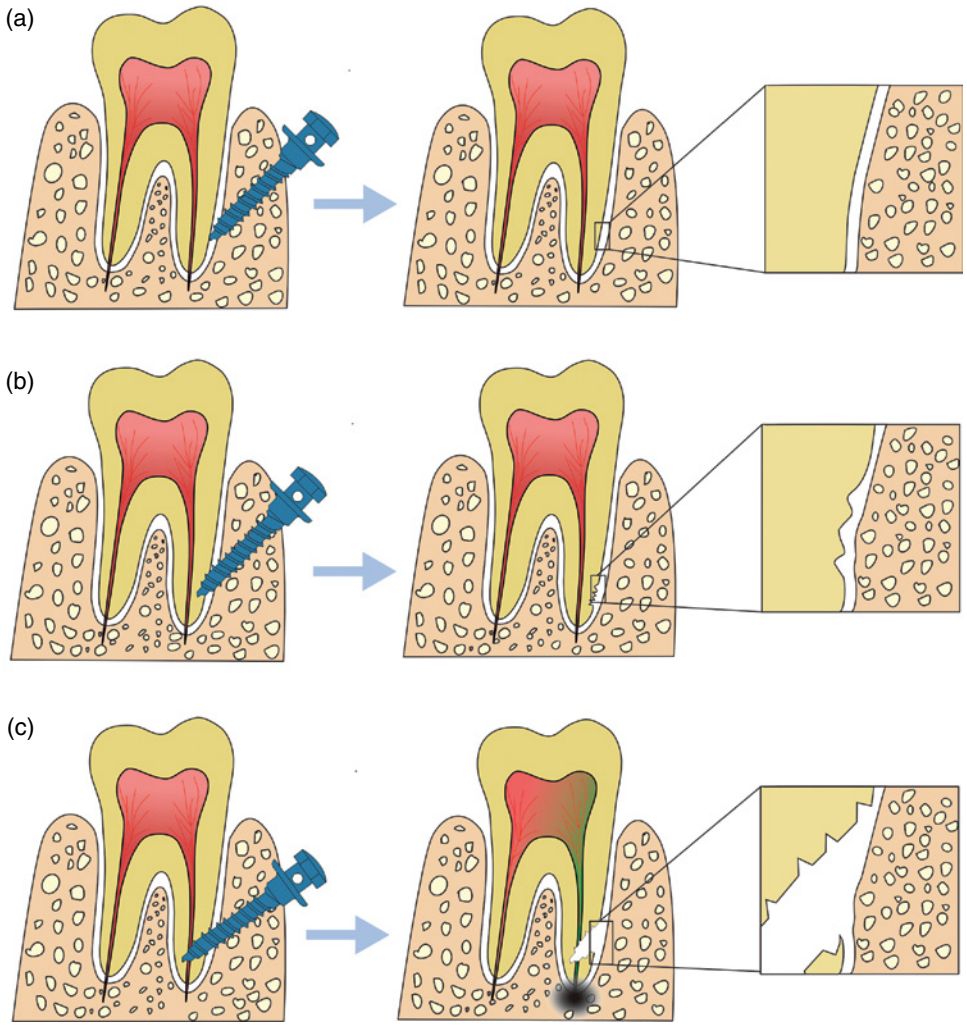


Figure 13.10 Prognosis of root contact with different degrees of injuries. (a) Almost complete repair of the periodontal tissues if damage is limited to periodontal tissues and cementum. (b) Incomplete root repair when the dentin is injured. (c) Pulp necrosis and periapical lesion occur if the damage involves the pulp.

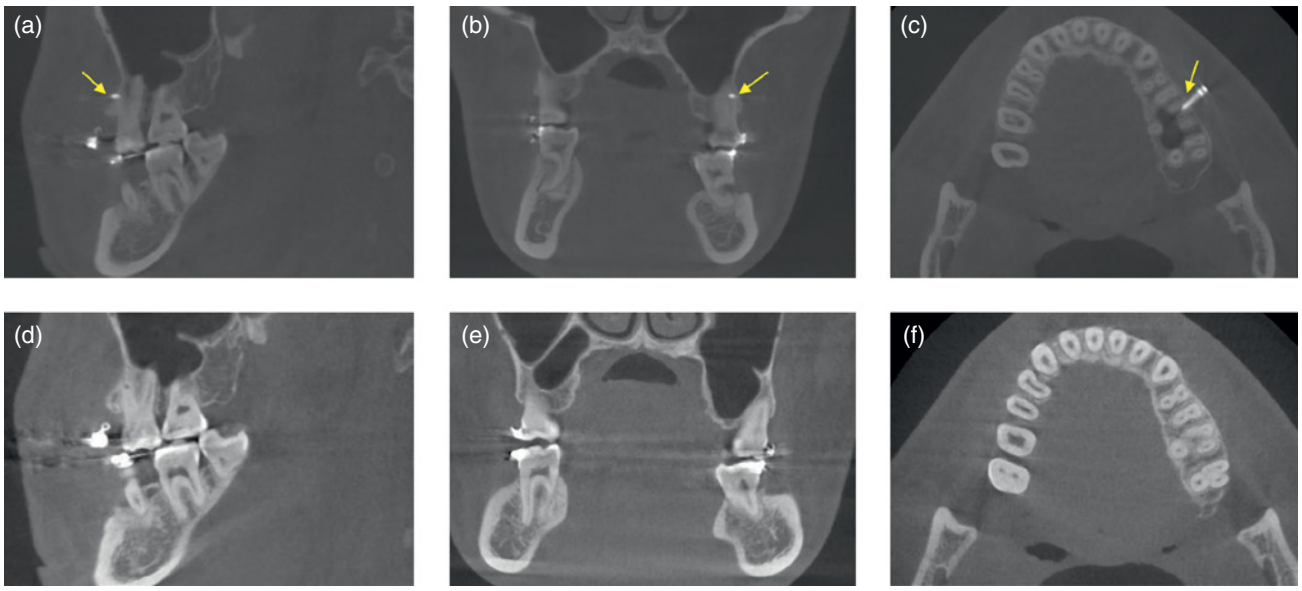


Figure 13.11 Spontaneous recovery following pulp penetration by a mini-implant. CBCT images (sagittal view) showed that the mini-implant contacted the mesiobuccal root of 26 and the mini-implant was instantly removed (a: sagittal view; b: coronal view; c: axial view). After six months, pulp vitality was revealed and CBCT images indicated no periapical lesion (d: sagittal view; e: coronal view; f: axial view). Note the 'hole' that was caused by the mini-implant penetration in the mesiobuccal root of the first molar in (d).

t.me/Dr_Mouayyad_AlbtousH

13.4 Risk Factors

13.4.1 Insertion Site

Mini-implants can be inserted into either the alveolar or extra-alveolar region. The alveolar region, also called the interradicular region (e.g. between a second premolar and a first molar), is commonly used for the insertion of mini-implants in clinical practice (Figure 13.12). In contrast, the extra-alveolar region was infrequently used but is gaining popularity in the orthodontic community due to its higher bone density. Currently, commonly used extra-alveolar regions include the infrazygomatic crest, buccal shelf, mandibular ramus, hard palate, anterior nasal spine and mandibular symphysis (Figure 13.13). Thus, the alveolar region poses higher risks of root contact than the extra-alveolar region.

13.4.2 Limited Interradicular Space

Special care should be taken to evaluate the interradicular space before insertion of mini-implants at alveolar regions. Adequate mesiodistal width between adjacent roots is a prerequisite for successful mini-implant placement in the interradicular region.[28] Mesiodistal width between two adjacent roots varies greatly among different insertion sites

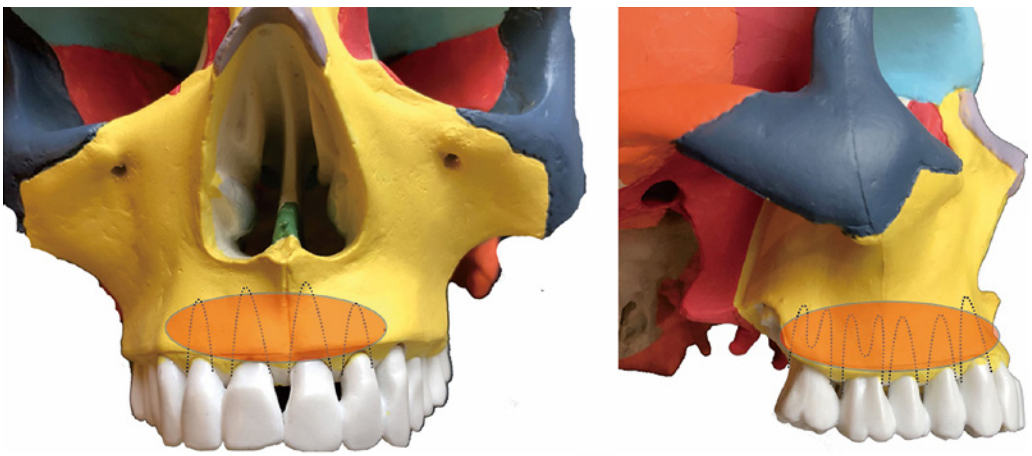


Figure 13.12 Frequently used interradicular regions for the insertion of mini-implants.

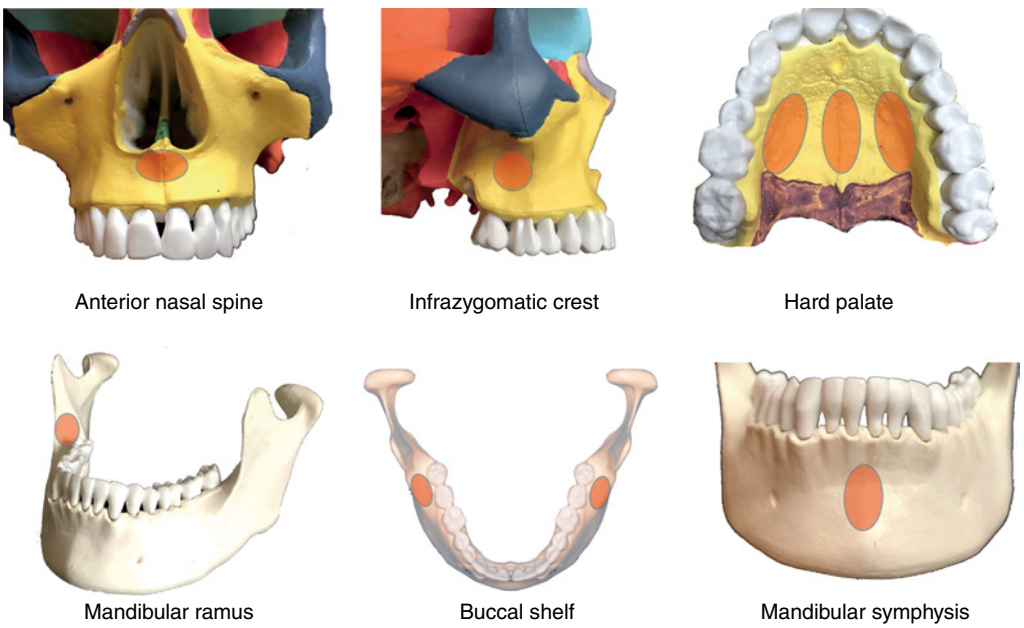


Figure 13.13 Commonly used extra-alveolar regions for insertion of mini-implants.

t.me/Dr_Mouayyad_AlbtousH

(Figure 13.14). A large body of evidence suggests that the largest mesiodistal width is between the second premolars and first molars in the maxilla and between the first and second molars in the mandible.[28-31] Moreover, greater interradicular space is detected at the palatal side than the buccal side in the maxilla (Figure 13.14).[28] However, interradicular space is smallest at the mandibular labial region,[32] so it is not recommended to insert mini-implants at this region and the mandibular symphysis may be a viable alternative.[33]

13.4.3 Insertion Height

It has been well documented that mesiodistal width increases from alveolar crest to apex.[34,35] Insertion of mini-implants at apical sites can reduce the risk of root contact, which is limited by soft tissue complications if insertion is too apical (Figure 13.15). Thus, we recommend that insertion be at the mucogingival junction.

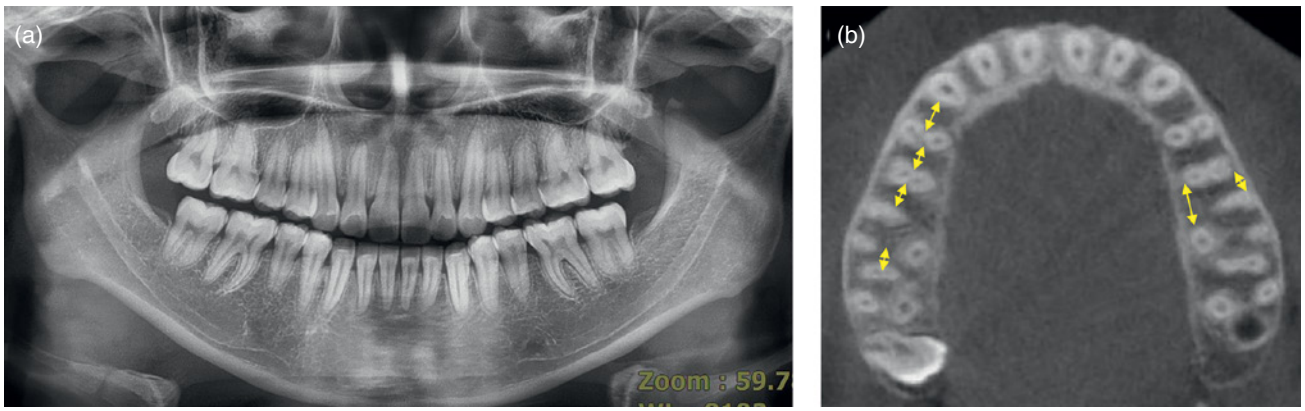


Figure 13.14 Different mesiodistal interradicular distances at buccal and palatal sides as well as at different tooth positions. (a) Mesiodistal interradicular distance varies at different tooth positions. (b) Different mesiodistal interradicular distance at different tooth positions. Less mesiodistal interradicular space is available on the buccal side than on the palatal side, particularly in the maxilla.

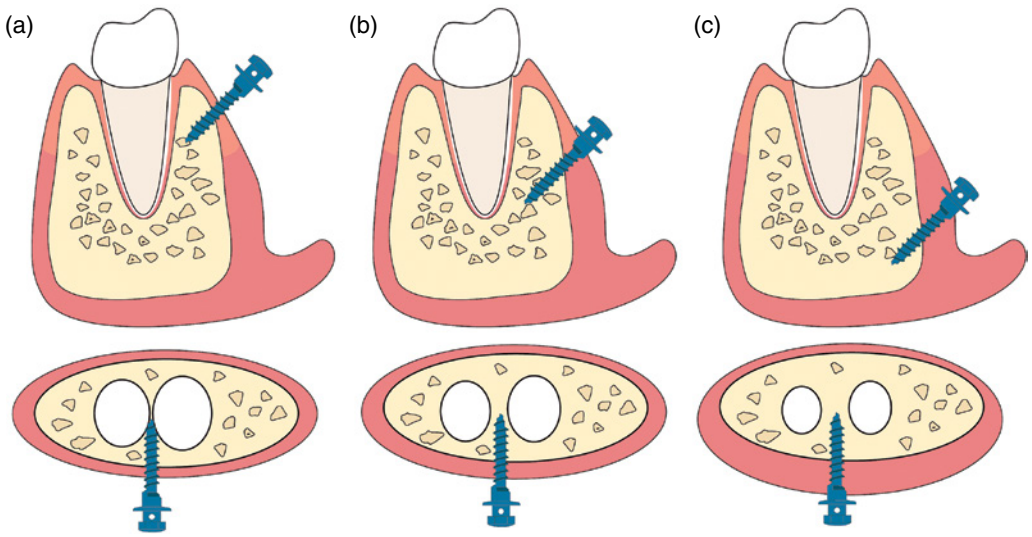


Figure 13.15 Different insertion heights of mini-implants. (a) The mesiodistal interradicular width is relatively small when the mini-implant is inserted near the alveolar crest, thus increasing the risk of root contact. (b) The mesiodistal interradicular width is adequate when the mini-implant is inserted at the mucogingival junction, thus decreasing the risk of root contact. (c) The mesiodistal interradicular width is adequate when the mini-implant is inserted at more apical sites, but the risk of soft tissue complications is increased.

t.me/Dr_Mouayyad_AlbtousH

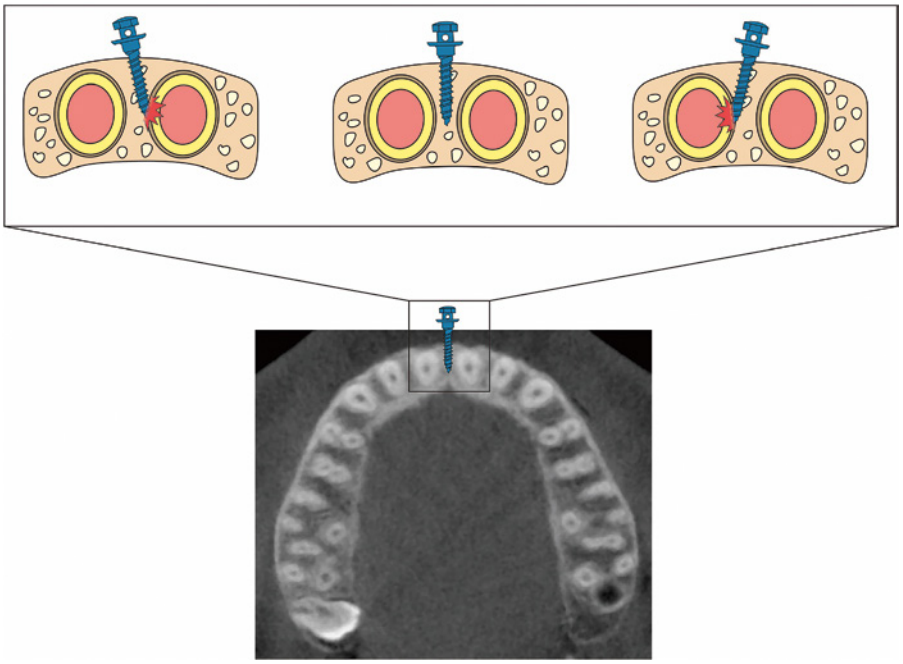


Figure 13.16 Mini-implants should be inserted at the optimal mesiodistal angle so that the risk of root contact is minimised. Mesial or distal insertion leads to root injury to the mesially or distally adjacent root.

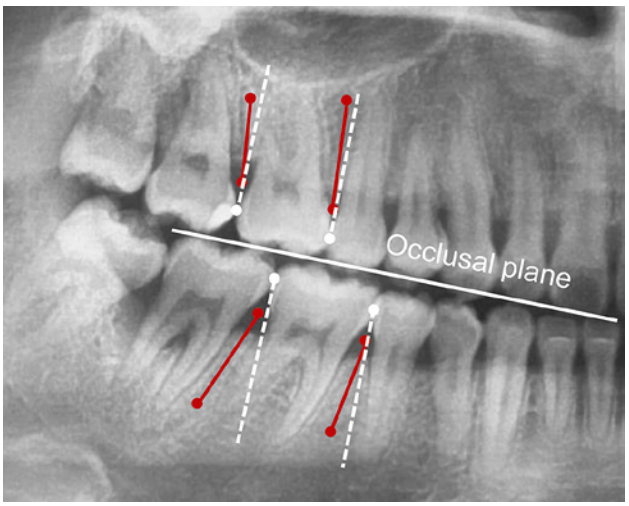


Figure 13.17 Demonstration of relative positions of midpoints between adjacent teeth. Due to the mesial tipping of posterior teeth, the midpoints between two adjacent roots (the midpoints are the points on the red lines) are often distal to the perpendicular lines (white dashed lines) to the occlusal plane passing through the contact points.

13.4.4 Insertion Angulation

Insertion angulation includes both mesiodistal angulation and cervicoapical angulation. Ideally, a mini-implant should be inserted with an optimal mesiodistal angulation that guarantees that the implant can be inserted between two adjacent roots without root contact (Figure 13.16). The midpoints between two adjacent roots are located distally to the contact point. In addition, the lines connecting the interradicular midpoints from the cervix to the apex of roots in the mandible are inclined more distally than those in the maxilla (Figure 13.17). Thus, it has been suggested that mini-implants should be inclined distally about 10–20° and placed 0.5–2.7 mm distally to the contact point to minimise root contact.[36] However, insertion of mini-implants is often distally directed at buccal interradicular sites, with the distal teeth more susceptible to root contact, especially in the right maxilla, which may be due to right-handedness.[7] Hence, the placement of mini-implants with distal angulation should be performed with caution and we recommend that CBCT be employed to determine an optimal mesiodistal angulation that results in the largest mesiodistal width (Figure 13.18).

As mentioned above, interradicular space is greater at more apical site. Thus, apically directed insertion offers a larger interradicular space and reduces the risk of root contact (Figure 13.19). However, slippage of mini-implants is likely to occur if insertion is too apically directed. Given that mini-implants with apically directed insertion (60–70° to the bone surface) exhibits the highest primary stability,[37] we recommend that implants be inserted in an apically directed angulation of 60–70°.

t.me/Dr_Mouayyad_AlbtousH

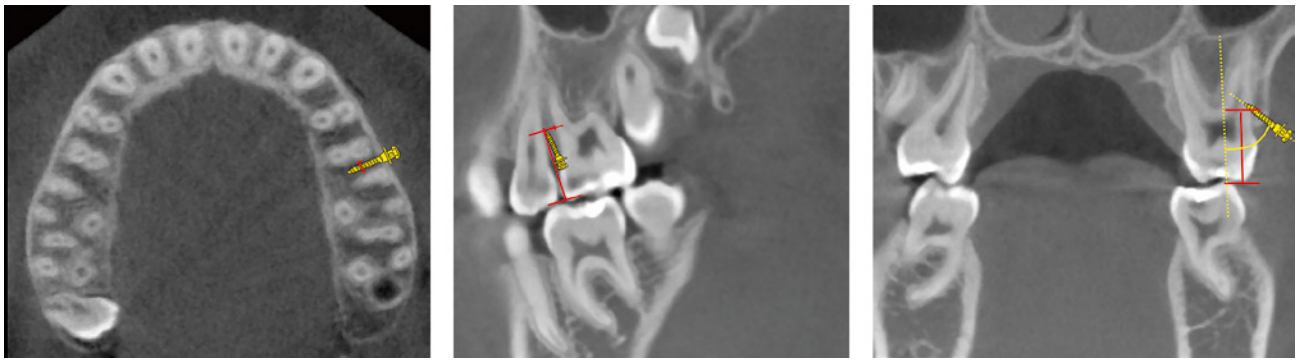


Figure 13.18 Determination of the optimal insertion site and angulation through CBCT images on axial, sagittal and coronal views.

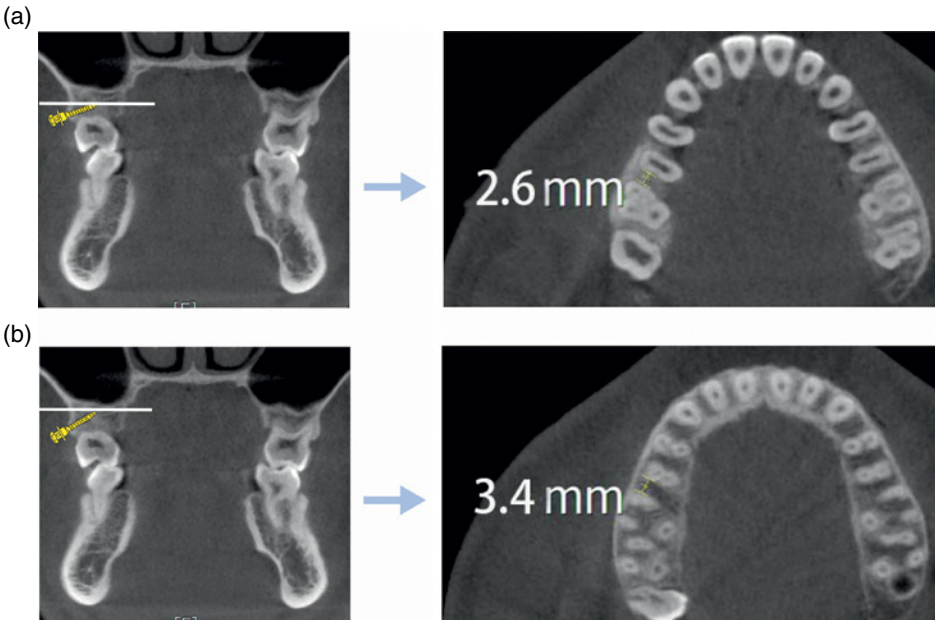


Figure 13.19 The cervicoapical insertion angle influences the risk of root contact due to different interradicular distances at different heights. (a) The mini-implant inserted at a smaller angulation reaches the level with a smaller interradicular distance (2.6 mm). (b)The mini-implant inserted at a larger angulation reaches the level with a larger interradicular distance (3.4 mm).

13.5 Prevention

13.5.1 Prudent Selection of Insertion Sites

Optimal insertion sites are determined by the combination of biomechanics-driven and anatomy-driven approaches. If both extra-alveolar and alveolar regions meet biomechanical requirements, the extra-alveolar region can be selected to reduce the risk of root contact. However, if only alveolar regions can be chosen due to anatomical limitations, those with sufficient interradicular space should be selected. Otherwise, development of interradicular space before mini-implant placement is indicated (Figure 13.20).

13.5.2 Meticulous Design of Insertion Angulation

For mini-implants to be inserted at interradicular regions, it is of great importance to design both the mesiodistal and cervicoapical insertion angulations. The optimal insertion location and angulations can be determined through clinical and radiographic data. Generally, mini-implants should be placed at the mucogingival junction level with cervicoapical angulation being 60–70° to the bony surface. The mesiodistal angulation can be determined with the largest mesiodistal width.

With advances in 3-D design and manufacture technology, insertion guides are more and more widely used to ensure precise insertion of mini-implants as planned (Figure 13.21). Mini-implants can be virtually inserted into

t.me/Dr_Mouayyad_AlbtousH

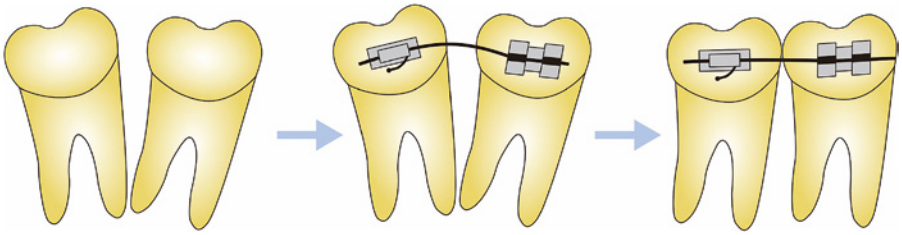


Figure 13.20 Development of interradicular space before mini-implant placement using orthodontic appliances.

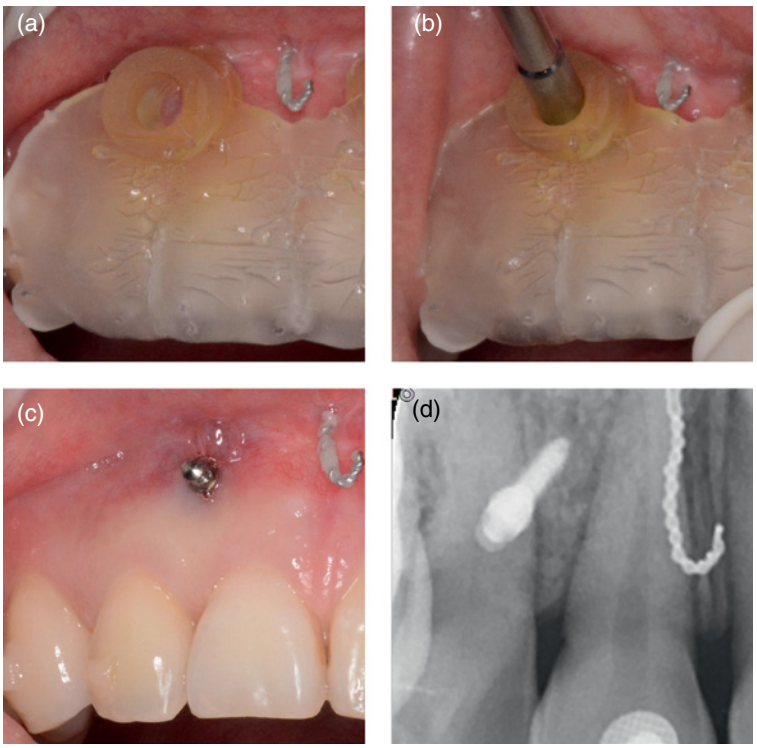


Figure 13.21 A case demonstrating the application of surgical guides for mini-implant insertion. (a) The surgical guide was tried in before mini-implant insertion. (b) Demonstration of the surgical guide during insertion of the mini-implant. (c) The mini-implant was inserted at the U1-U2 interradicular site. (d) Posttreatment periapical radiograph indicated optimal insertion between the two roots.

the interradicular region to determine the optimal location and angulation that can be transferred into patients' mouths through insertion guides. For the alveolar region with limited interradicular space, the use of insertion guides can largely reduce the risk of root contact by mini-implants.[38]

13.5.3 Appropriate Anaesthesia and Insertion Technique

Since nerve terminals are distributed richly in the mucosa, periosteum, periodontal tissues and roots but sparsely in alveolar bone, the anaesthetic region should only involve mucosa and periosteum and spare periodontal tissues and dental roots. Thus, periodontal tissues are still responsive and can alert patients if root contact occurs. Otherwise, profound anaesthesia renders periodontal tissues and dental roots unresponsive to nociceptive stimulus elicited by mini-implants (Figure 13.22).

t.me/Dr_Mouayyad_AlbtousH

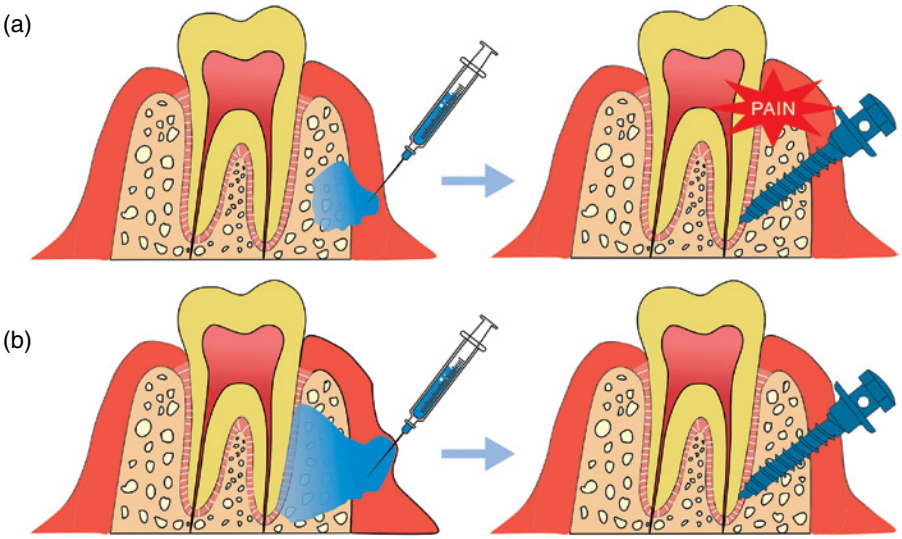


Figure 13.22 Feedback of root contact with different depth of anaesthesia infiltration. (a) If infiltration anaesthesia does not reach the periodontal tissues, pain can be perceived when root contact occurs. (b) If excessive infiltration anaesthesia is implemented and reaches the periodontal tissues, pain cannot be perceived when root contact occurs.

13.6 Management of Root Contact

If root contact is suspected in clinical practice, heralded by either patient symptoms or operator's tactile perception, further examinations (percussion test and radiographic examination) should be implemented to establish or rule out the diagnosis. Once root contact is diagnosed, timely removal of mini-implants is mandatory and the extent of damage should be evaluated based on radiographic examinations. If pulp is not involved, potential occlusal interference should be eliminated and orthodontic treatment postponed. If pulp is damaged, elimination of occlusal interference and regular pulp examinations should be executed. Orthodontic treatment can be started if pulp is vital without periapical lesion after 3–6 months. Otherwise, root canal therapy or apical surgery is indicated if pulp necrosis and periapical lesion are present. Then, orthodontic treatment can be started after recovery. The algorithm for managing root contact is displayed in Figure 13.23.

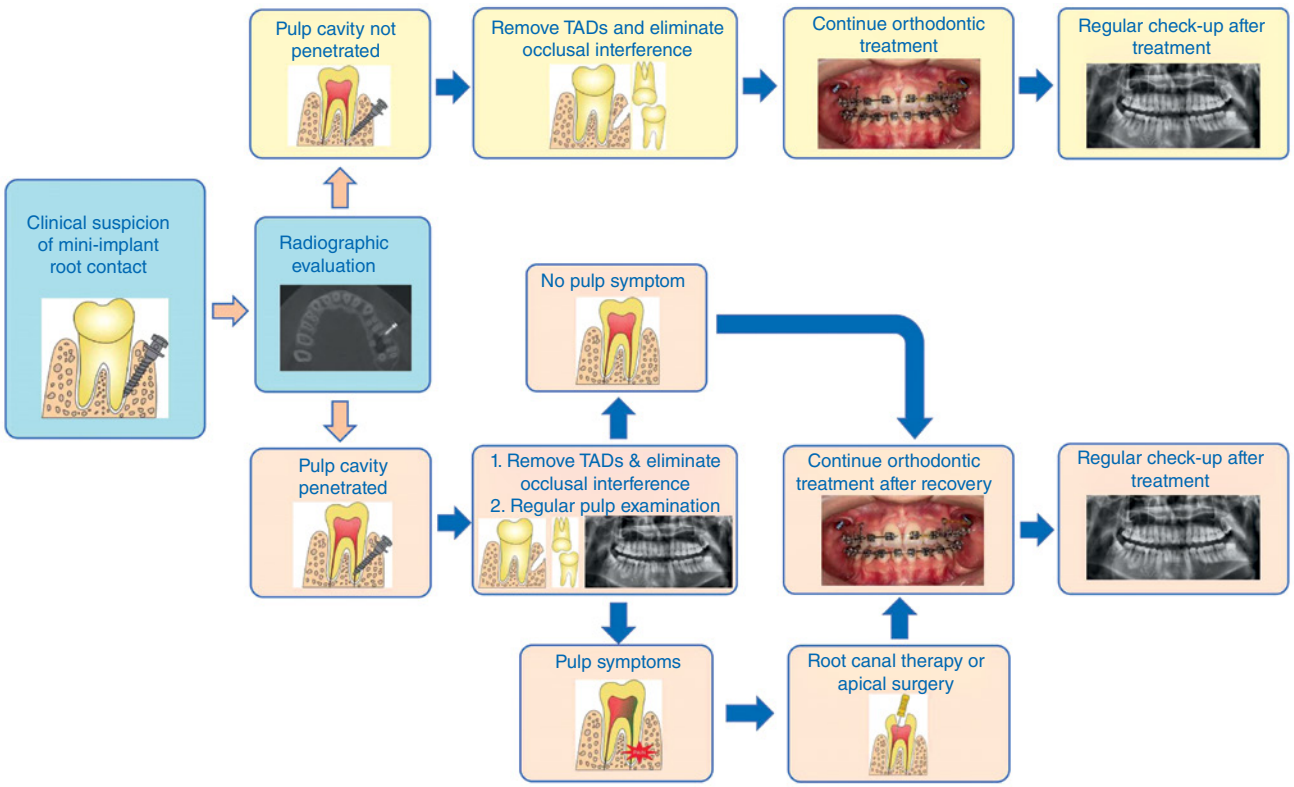


Figure 13.23 A clinical pathway for managing root contact by mini-implants.

t.me/Dr_Mouayyad_AlbtousH

13.7 Summary

Root contact is one of the most frequently encountered complications associated with the insertion of mini-implants. Depending on the severity of root injury, different prognoses are anticipated, from complete recovery to pulp necrosis and periapical lesions. A variety of factors are associated with the risk of root contact, including insertion site, insertion height, insertion angle and interradicular space. Thus, appropriate measures should be taken to minimise the risk of root contact. When root contact is encountered in clinical practice, different strategies are suggested for different severities of root damage and a clinical pathway is recommended for practitioners.

References

1 An JH, Kim YI, Kim SS, Park SB, Son WS, Kim SH. (2019). Root proximity of miniscrews at a variety of maxillary and mandibular buccal sites: reliability of panoramic radiography. *Angle Orthod.* 89(4): 611–616.

2 Kim SH, Kang SM, Choi YS, Kook YA, Chung KR, Huang JC. (2010). Cone-beam computed tomography evaluation of mini-implants after placement: is root proximity a major risk factor for failure? *Am. J. Orthod. Dentofacial Orthop.* 138(3): 264–276.

3 Kuroda S, Yamada K, Deguchi T, Hashimoto T, Kyung HM, Takano-Yamamoto T. (2007). Root proximity is a major factor for screw failure in orthodontic anchorage. *Am. J. Orthod. Dentofacial Orthop.* 131(4 Suppl): S68–73.

4 Min KI, Kim SC, Kang KH et al. (2012). Root proximity and cortical bone thickness effects on the success rate of orthodontic micro-implants using cone beam computed tomography. *Angle Orthod.* 82(6): 1014–1021.

5 Motoyoshi M, Uchida Y, Matsuoka M et al. (2014). Assessment of damping capacity as an index of root proximity in self-drilling orthodontic mini-implants. *Clin. Oral Invest.* 18(1): 321–326.

6 Shigeeda T. (2014). Root proximity and stability of orthodontic anchor screws. *J. Oral Sci.* 56(1): 59–65.

7 Shinohara A, Motoyoshi M, Uchida Y, Shimizu N. (2013). Root proximity and inclination of orthodontic mini-implants after placement: cone-beam computed tomography evaluation. *Am. J. Orthod. Dentofacial Orthop.* 144(1): 50–56.

8 Son S, Motoyoshi M, Uchida Y, Shimizu N. (2014). Comparative study of the primary stability of self-drilling and self-tapping orthodontic miniscrews. *Am. J. Orthod. Dentofacial Orthop.* 145(4): 480–485.

9 Iwai H, Motoyoshi M, Uchida Y, Matsuoka M, Shimizu N. (2015). Effects of tooth root contact on the stability of orthodontic anchor screws in the maxilla: comparison between self-drilling and self-tapping methods. *Am. J. Orthod. Dentofacial Orthop.* 147(4): 483–491.

10 Albogha MH, Kitahara T, Todo M, Hyakutake H, Takahashi I. (2016). Predisposing factors for orthodontic mini-implant failure defined by bone strains in patient-specific finite element models. *Ann. Biomed. Eng.* 44(10): 2948–2956.

11 Chen YH, Chang HH, Chen YJ, Lee D, Chiang HH, Yao CC. (2008). Root contact during insertion of miniscrews for orthodontic anchorage increases the failure rate: an animal study. *Clin. Oral Implants Res.* 19(1): 99–106.

12 Motoyoshi M, Ueno S, Okazaki K, Shimizu N. (2009). Bone stress for a mini-implant close to the roots of adjacent teeth – 3D finite element analysis. *Int. J. Oral Maxillofac. Surg.* 38(4): 363–368.

13 Gintautaite G, Kenstavicius G, Gaidyte A. (2018). Dental roots' and surrounding structures' response after contact with orthodontic mini implants: a systematic literature review. *Stomatologija* 20(3): 73–81.

14 Meursinge Reynders R, Ladu L, Ronchi L et al. (2016). Insertion torque recordings for the diagnosis of contact between orthodontic mini-implants and dental roots: a systematic review. *Syst. Rev.* 5: 50.

15 Asscherickx K, Vande Vannet B, Wehrbein H, Sabzevar MM. (2008). Success rate of miniscrews relative to their position to adjacent roots. *Eu.r J. Orthod.* 30(4): 330–335.

16 Gintautaite G, Gaidyte A. (2017). Surgery-related factors affecting the stability of orthodontic mini implants screwed in alveolar process interdental spaces: a systematic literature review. *Stomatologija* 19(1): 10–18.

17 Kang YG, Kim JY, Lee YJ, Chung KR, Park YG. (2009). Stability of mini-screws invading the dental roots and their impact on the paradental tissues in beagles. *Angle Orthod.* 79(2): 248–255.

18 Mohammed H, Wafaie K, Rizk MZ, Almuzian M, Sosly R, Bearn DR. (2018). Role of anatomical sites and correlated risk factors on the survival of orthodontic miniscrew implants: a systematic review and meta-analysis. *Prog. Orthod.* 19(1): 36.

19 Maino BG, Weiland F, Attanasi A, Zachrisson BU, Buyukyilmaz T. (2007). Root damage and repair after contact with miniscrews. *J. Clin. Orthod.* 41(12): 762–766; quiz 750.

20 Kadioglu O, Buyukyilmaz T, Zachrisson BU, Maino BG. (2008). Contact damage to root surfaces of premolars touching miniscrews during orthodontic treatment. *Am. J. Orthod. Dentofacial Orthop.* 134(3): 353–360.

t.me/Dr_Mouayyad_AlbtousH

21 Hembree M, Buschang PH, Carrillo R, Spears R, Rossouw PE. (2009). Effects of intentional damage of the roots and surrounding structures with miniscrew implants. *Am. J. Orthod. Dentofacial Orthop.* 135(3): e281–289; discussion 280–281.

22 Kim H, Kim TW. (2011). Histologic evaluation of root-surface healing after root contact or approximation during placement of mini-implants. *Am. J. Orthod. Dentofacial Orthop.* 139(6): 752–760.

23 Asscherickx K, Vannet BV, Wehrbein H, Sabzevar MM. (2005). Root repair after injury from mini-screw. *Clin. Oral Implants Res.* 16(5): 575–578.

24 Brisceno CE, Rossouw PE, Carrillo R, Spears R, Buschang PH. (2009). Healing of the roots and surrounding structures after intentional damage with miniscrew implants. *Am. J. Orthod. Dentofacial Orthop.* 135(3): 292–301.

25 Lee YK, Kim JW, Baek SH, Kim TW, Chang YI. (2010). Root and bone response to the proximity of a mini-implant under orthodontic loading. *Angle Orthod.* 80(3): 452–458.

26 Alves M Jr, Baratieri C, Mattos CT, Araujo MT, Maia LC. (2013). Root repair after contact with mini-implants: systematic review of the literature. *Eur. J. Orthod.* 35(4): 491–499.

27 Chang PE, Kim E, Jang W, Cho HY, Choi YJ. (2021). Spontaneous repair of iatrogenic root perforation by an orthodontic miniscrew: a case report. *J. Am. Dent. Assoc.* 152(3): 234–239.

28 Poggio PM, Incorvati C, Velo S, Carano A. (2006). "Safe zones": a guide for miniscrew positioning in the maxillary and mandibular arch. *Angle Orthod.* 76(2): 191–197.

29 Lim JE, Lee SJ, Kim YJ, Lim WH, Chun YS. (2009). Comparison of cortical bone thickness and root proximity at maxillary and mandibular interradicular sites for orthodontic mini-implant placement. *Orthod. Craniofac. Res.* 12(4): 299–304.

30 Sawada K, Nakahara K, Matsunaga S, Abe S, Ide Y. (2013). Evaluation of cortical bone thickness and root proximity at maxillary interradicular sites for mini-implant placement. *Clin. Oral Implants Res.* 24 Suppl A100: 1–7.

31 Park J, Cho HJ. (2009). Three-dimensional evaluation of interradicular spaces and cortical bone thickness for the placement and initial stability of microimplants in adults. *Am. J. Orthod. Dentofacial Orthop.* 136(3): e311–312; discussion 314–315.

32 Monnerat C, Restle L, Mucha JN. (2009). Tomographic mapping of mandibular interradicular spaces for placement of orthodontic mini-implants. *Am. J. Orthod. Dentofacial Orthop.* 135(4): e421–429; discussion 428–429.

33 Zhang S, Wei X, Wang L et al. (2022). Evaluation of optimal sites for the insertion of orthodontic mini implants at mandibular symphysis region through cone-beam computed tomography. *Diagnostics* 12(2): 285.

34 Monnerat C, Restle L, Mucha JN. (2009). Tomographic mapping of mandibular interradicular spaces for placement of orthodontic mini-implants. *Am. J. Orthod. Dentofacial Orthop.* 135(4): e421–429; discussion 428–429.

35 Moslemzadeh SH, Sohrabi A, Rafighi A, Kananizadeh Y, Nourizadeh A. (2017). Evaluation of interdental spaces of the mandibular posterior area for orthodontic mini-implants with cone-beam computed tomography. *J. Clin. Diagn. Res.* 11(4): ZC09–ZC12.

36 Park HS, Hwangbo ES, Kwon TG. (2010). Proper mesiodistal angles for microimplant placement assessed with 3-dimensional computed tomography images. *Am. J. Orthod. Dentofacial Orthop.* 137(2): 200–206.

37 Wilmes B, Su YY, Drescher D. (2008). Insertion angle impact on primary stability of orthodontic mini-implants. *Angle Orthod.* 78(6): 1065–1070.

38 Felicita AS. (2013). A simple three-dimensional stent for proper placement of mini-implant. *Prog. Orthod.* 14: 45.

t.me/Dr_Mouayyad_AlbtousH

14

Fractures of Orthodontic Temporary Anchorage Devices

Hong Zhou[1,2], Jing Zhou[3], Fan Jian[1], Heyi Tang[4], Jianru Yi[1], Xiaolong Li[1], and Hu Long[1]

[1] *Department of Orthodontics, State Key Laboratory of Oral Diseases and National Clinical Research Center for Oral Diseases, West China Hospital of Stomatology, Sichuan University, Chengdu, China*
[2] *Private Practice, Chengdu, China*
[3] *Department of Pediatric Dentistry, State Key Laboratory of Oral Diseases and National Clinical Research Center for Oral Diseases, West China Hospital of Stomatology, Sichuan University, Chengdu, China*
[4] *Department of Head and Neck Oncology, State Key Laboratory of Oral Diseases and National Clinical Research Center for Oral Diseases, West China Hospital of Stomatology, Sichuan University, Chengdu, China*

14.1 Introduction

Fractures of orthodontic TADs are rarely encountered in clinical practice (Figure 14.1). In contrast to microscrews used for miniplates, mini-implants are more susceptible to fracture since they are longer than microscrews. It has been reported that the overall incidence of mini-implant fracture is 1.7–3.5%, with the rate of fracture during placement (0.4–1.4%) being slightly lower than that during removal (1.4–2.2%).[1-4] Differences in the rate of mini-implant fracture during placement and removal can be attributed to the following two factors. First, practitioners are more cautious during placement and take precautions to reduce the risk of fracture, e.g. predrilling. Second, partial or full osteointegration of the mini-implant increases the likelihood of fracture during removal.

A mini-implant fractures when placement or removal torque exceeds its fracture torque.[5] The fracture torque of a mini-implant is determined by the strength of its materials, topography, length and diameter.[6-8] The fracture torque of mini-implants from different manufacturers differs. Generally, the fracture torque of an orthodontic mini-implant ranges from 9 to 35 N·cm.[5] A plethora of clinical evidence has revealed that the tip and neck are the two weakest areas of mini-implants and are most vulnerable to fracture.[1,5,9] Specifically, the fracture torque of the mini-implant tip (9–24 N·cm) is lower than that of the neck (23–35 N·cm).[5] Moreover, depending on the mini-implant and insertion site, placement torque (insertion torque) ranges from 7 to 10 N·cm.[5] This could explain why the mini-implant tip is the part where fracture occurs most frequently.

The most common placement sites for mini-implant fracture are areas with high bone density and thick cortex (Figure 14.2), e.g. palatal suture, mandibular ramus and buccal shelf.[1,2,10] Moreover, mini-implant fracture may occur when inadvertent root contact happens during placement,[11] which could be explained by the fact that roots are denser than alveolar bone. Thus, special attention should be paid to mini-implants inserted in areas of high-density bone. In order to reduce the incidence of mini-implant fracture during placement, predrilling is recommended for insertion sites with high bone density and thick cortex,[12] especially the mandibular ramus and mandibular buccal shelf.

The most frequently encountered consequences of mini-implant fractures are postinsertion pain and infection (Figure 14.3). Fortunately, these adverse events are of short duration and self-limited.

Clinical Insertion Techniques of Orthodontic Temporary Anchorage Devices, First Edition. Edited by Hu Long, Xianglong Han, and Wenli Lai.
© 2024 John Wiley & Sons Ltd. Published 2024 by John Wiley & Sons Ltd.

t.me/Dr_Mouayyad_AlbtousH

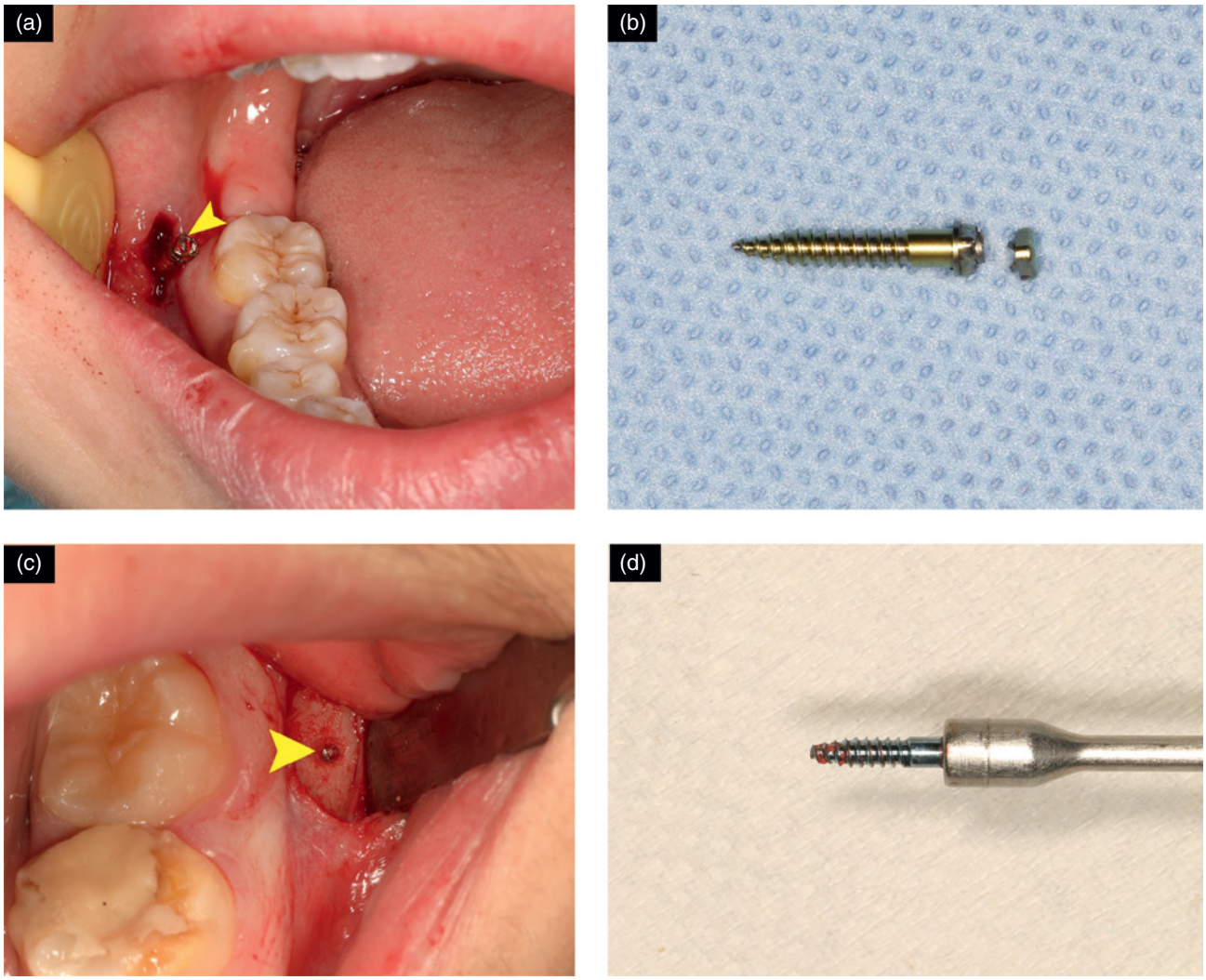


Figure 14.1 Fracture of orthodontic mini-implants during placement. (a) Fracture of an orthodontic mini-implant (yellow arrowhead) occurred during insertion into the mandibular buccal shelf. Note the fractured mini-implant body. (b) The fractured body was removed due to instability of the remaining part. (c) Fracture of a mini-implant tip (yellow arrowhead). (d) The main body of the mini-implant without the fractured tip.

t.me/Dr_Mouayyad_AlbtousH

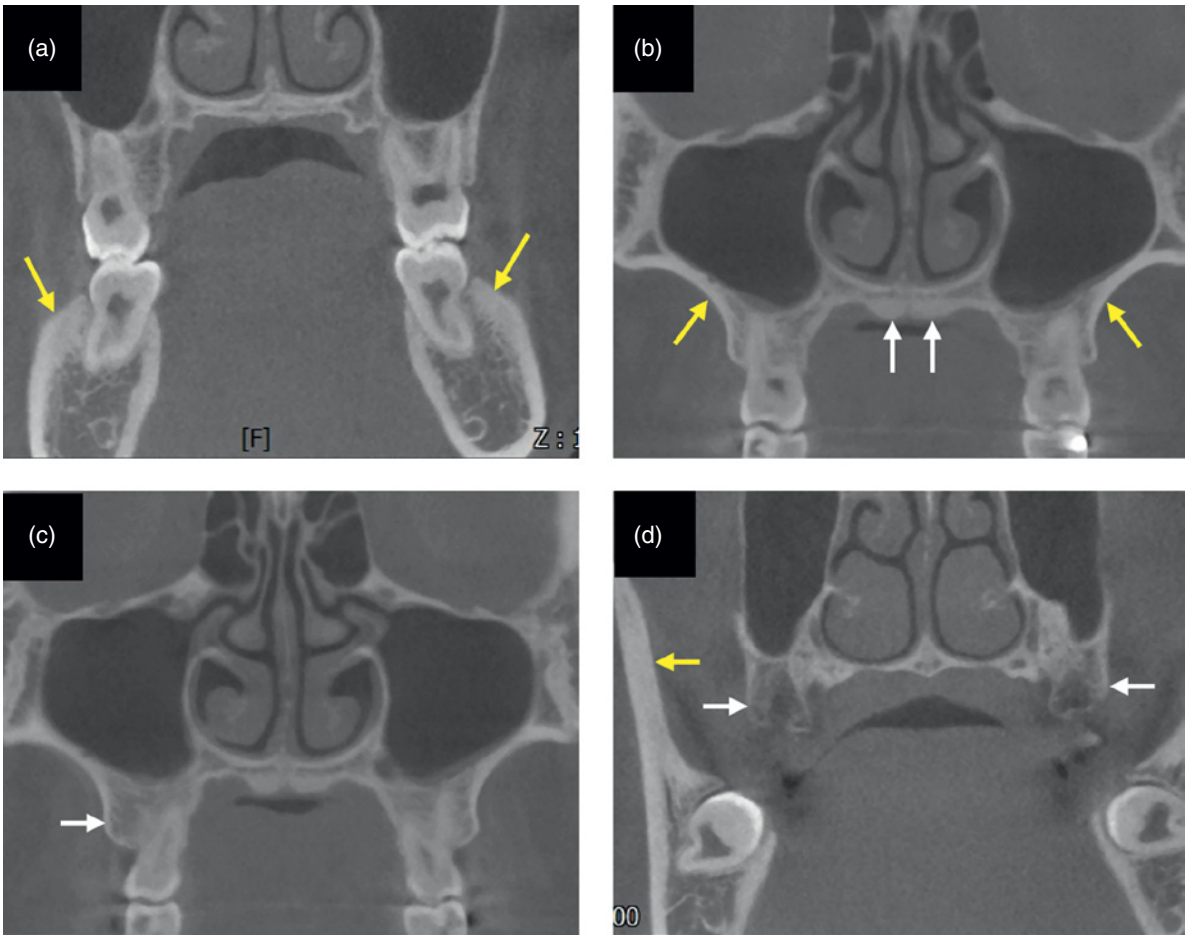
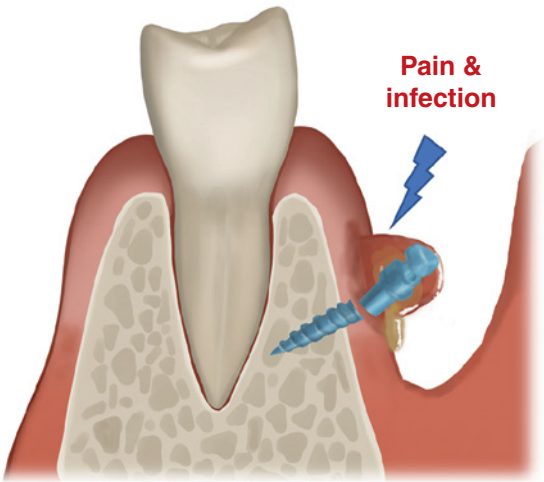


Figure 14.2 Alveolar bone and extra-alveolar bone regions with high bone density and thick cortex. (a) Buccal shelf with thick cortex, indicated by yellow arrows. (b) Infrazygomatic crest with a dense bone layer (yellow arrows) and palatal regions with thick cortex (white arrows). (c) Maxillary interradicular sites with relatively thinner cortex and lower bone density (white arrow). (d) Mandibular ramus with super-high bone density and thick cortex (yellow arrow) and maxillary tuberosity with low bone density (white arrows).

Figure 14.3 Pain and infection are the two most frequent consequences associated with mini-implant fractures.



t.me/Dr_Mouayyad_AlbtousH

14.2 Risk Factors for Mini-implant Fracture

The risk of mini-implant fracture is influenced by a variety of factors. Collectively, these risk factors can be categorised into operator-associated factors, implant-associated factors and insertion site-associated factors.

14.2.1 Operator-associated Factors

Operators' clinical skills and experience have a great impact on the success of mini-implants.[13,14] In order to avoid mini-implant fractures, placement torque should be less than fracture torque. Preinsertion evaluation of placement torque is very important. If bone density is high and the cortex is very thick, high placement torque is anticipated. For these cases, predrilling is recommended to reduce bone resistance and placement torque. Otherwise, insertion of mini-implants into high-density bone without predrilling may result in fracture (Figure 14.4). Moreover, it has been reported that self-drilling mini-implants had higher osseointegration levels than self-tapping ones,[15] suggesting that self-drilling bears a higher risk of fracture than self-tapping during removal.

During insertion, screwdrivers should be held stably, otherwise unstable insertion increases more transverse stress on the mini-implant body and makes the mini-implant susceptible to fracture (Figure 14.5). Moreover, during placement, gentle drilling with constant torque and slow speed is recommended. Otherwise, an abrupt change in drilling speed and insertion torque poses a high risk of mini-implant fracture (Figure 14.6).

After the cortex is penetrated, an abrupt change of insertion angle is not recommended. However, for some insertion sites, e.g. infrazygomatic crest, a change of angle is required to obtain an optimal position, although this increases the risk of mini-implant fracture.[16] Thus, the change of insertion angle should be gradual and operators should pay special attention to resistance during insertion. Otherwise, mini-implants are highly susceptible to fracture if the change in angulation is too abrupt (Figure 14.7).

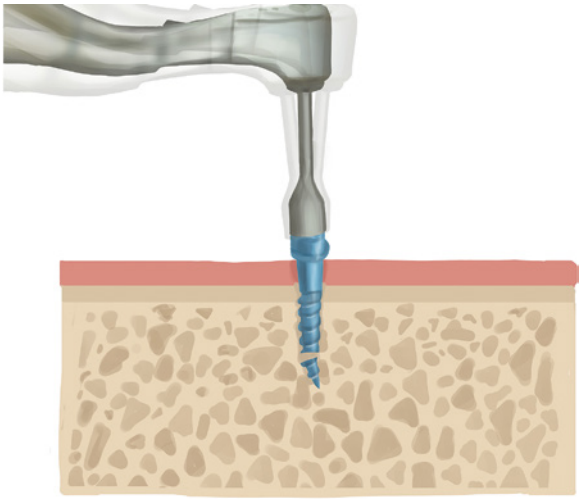


Figure 14.5 Fracture of a mini-implant due to instability of the screwdriver during insertion.

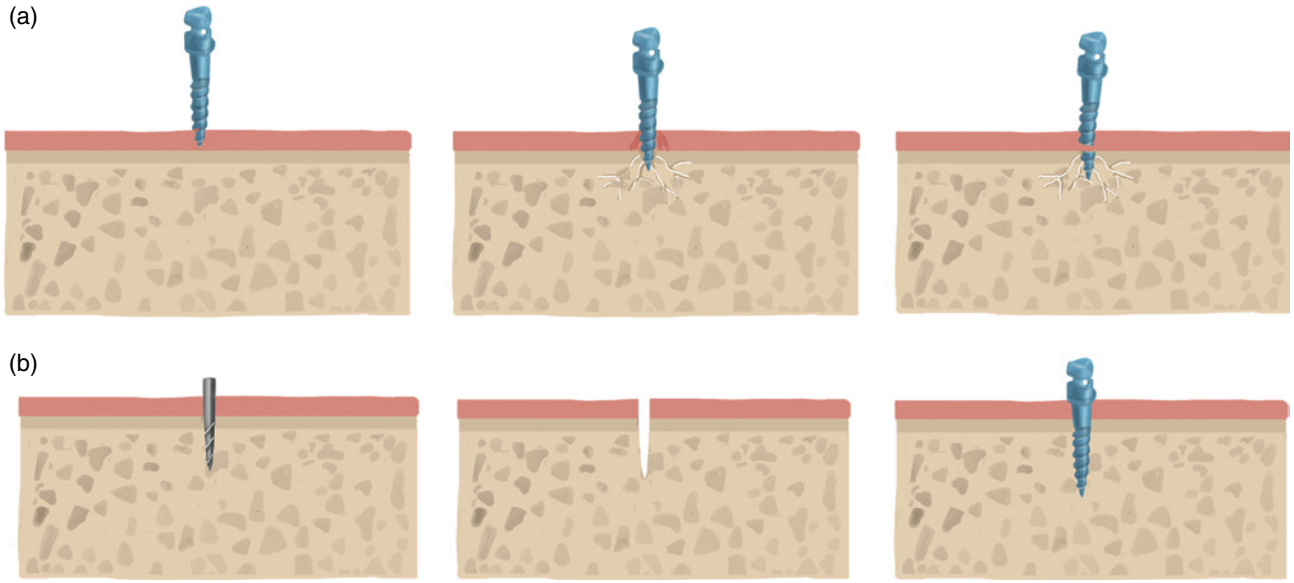


Figure 14.4 Predrilling helps to avoid mini-implant fracture for anatomical regions with high bone density. (a) A mini-implant is inserted into the mandibular buccal shelf without predrilling and fracture occurs during insertion. (b) Predrilling is performed prior to insertion. The mini-implant is inserted without fracture.

t.me/Dr_Mouayyad_AlbtousH

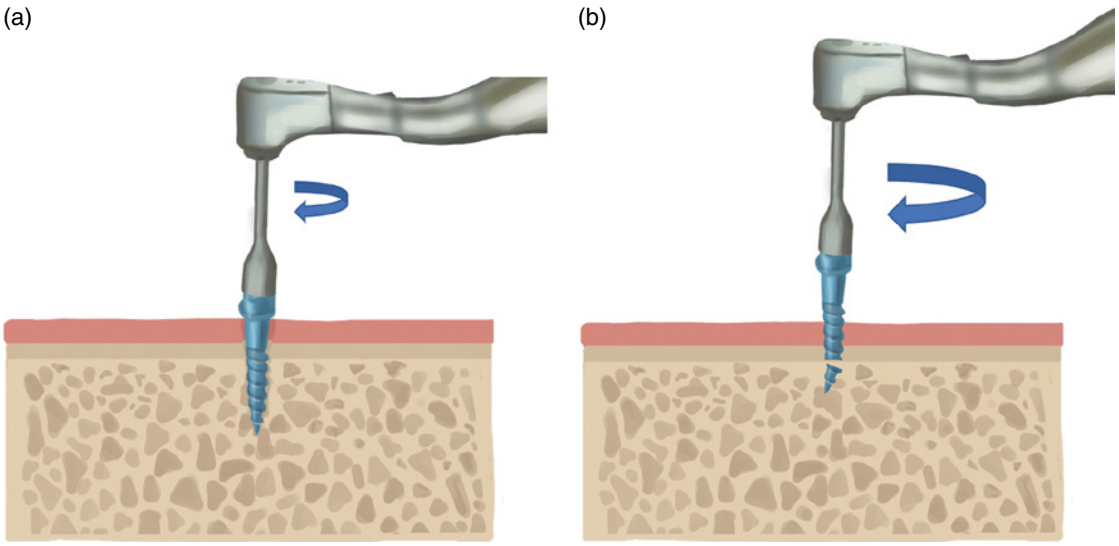


Figure 14.6 Fracture of a mini-implant due to incorrect insertion technique. (a) Gentle drilling with constant torque and low speed. (b) High drilling speed and unstable insertion torque result in mini-implant fracture.

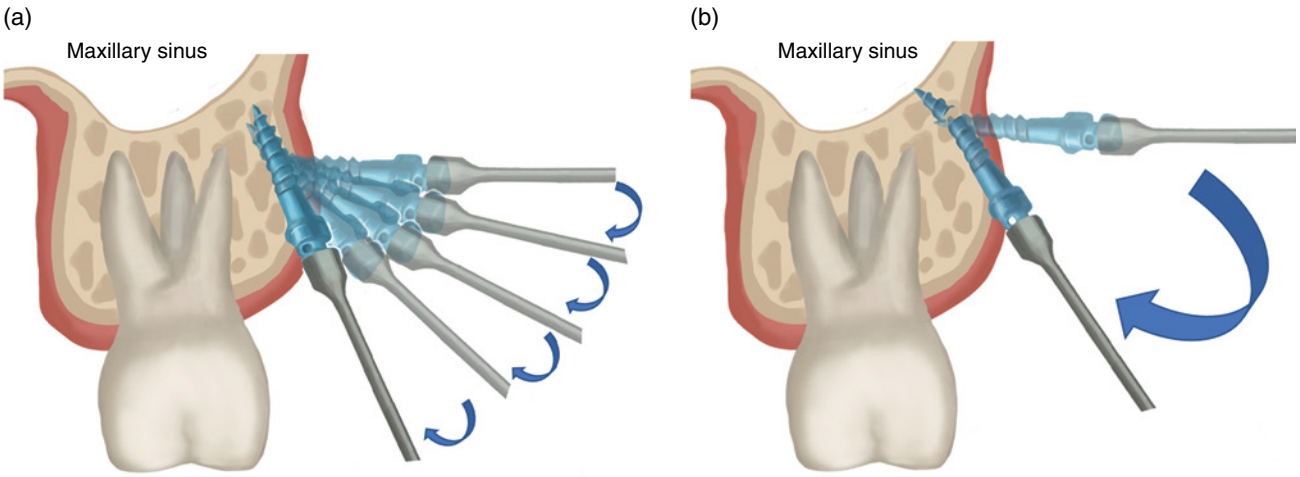


Figure 14.7 The fracture of mini-implants due to an abrupt change in insertion angle. (a) An infrazygomatic mini-implant is inserted with a gradual change in the insertion angle. (b) An abrupt change in the insertion angle leads to fracture of the mini-implant.

14.2.2 Implant-associated Factors

Fracture torque differs among mini-implants from different manufacturers.[5,17] It has been revealed that stainless steel mini-implants are more resistant to fracture than titanium alloy ones.[6] Thus, predrilling may not be required for stainless steel mini-implants for some sites with high bone density, e.g. mandibular buccal shelf and mandibular ramus.[18] It has been a concern that stainless steel mini-implants have inferior biocompatibility than titanium alloy ones, but recent studies revealed that both types of mini-implant elicit similar histological response after insertion.[19-21] Moreover, a recent randomised controlled trial suggested that the success rate of both types of mini-implants did not differ.[22] Thus, given that mini-implants of both materials have similar success rate, the greater resistance to fractures renders stainless steel implants a promising alternative to titanium alloy ones.

The risk of mini-implant fracture is influenced by geometric design. The diameter and length of mini-implants have a significant impact on fracture susceptibility. It has been shown that resistance to fracture increases with an increase in mini-implant diameter.[23] Although both placement torque and fracture torque increase with an increase in mini-implant diameter, the placement to

t.me/Dr_Mouayyad_AlbtousH

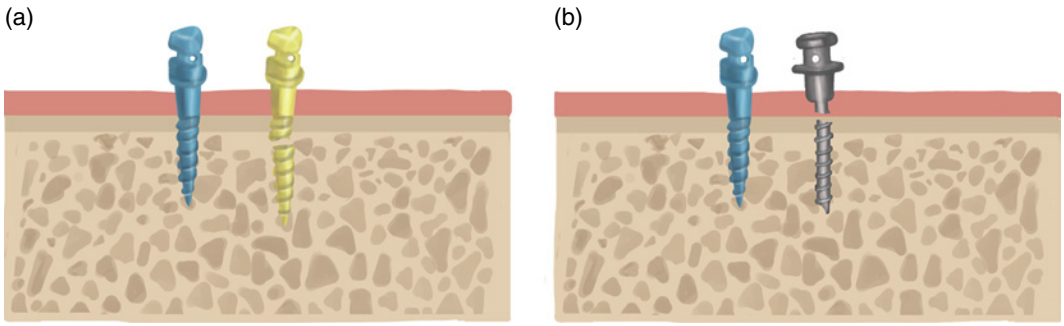


Figure 14.8 Fracture of mini-implants due to inappropriate geometric designs. (a) The two mini-implants have the same diameter but the right one is longer. An increase in mini-implant length without corresponding increase in diameter makes the mini-implant susceptible to fracture. (b) The two mini-implants have the same length but the right one has a smaller diameter, which makes it less resistant to fracture.

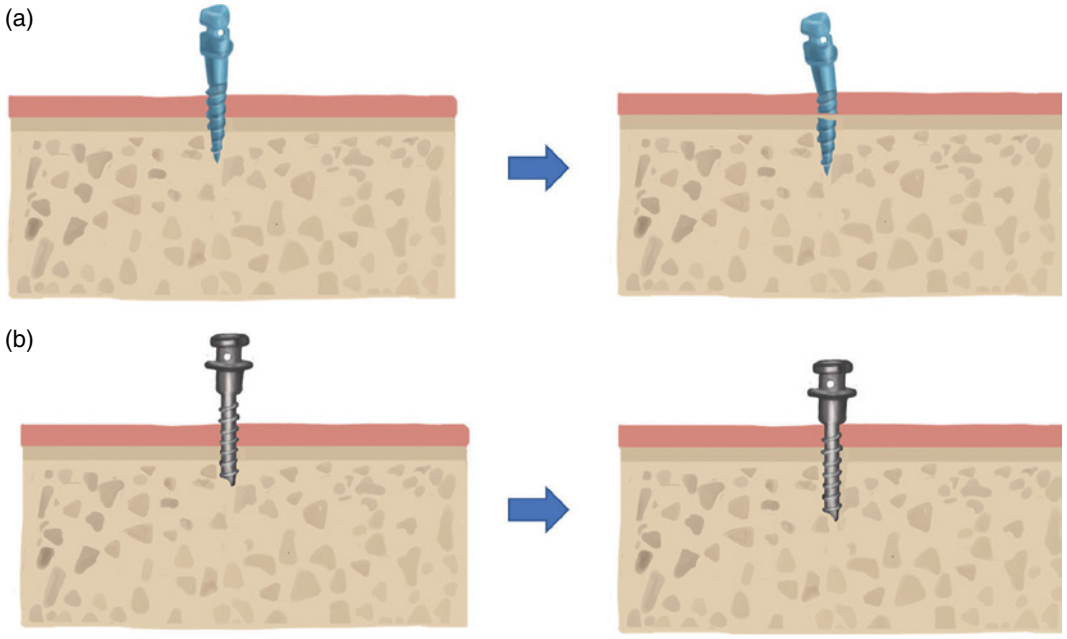


Figure 14.9 Mini-implants with two different designs exhibit differing susceptibilities to fracture. (a) A tapered mini-implant fractures at its tip during insertion. (b) A cylindrical mini-implant is inserted without fracture.

fracture torque ratio becomes lower for mini-implants with larger diameter.[24] In contrast, placement torque increases while fracture torque does not when mini-implant length increases.[8] Thus, increasing mini-implant diameter is a protective factor while increasing length renders mini-implants more vulnerable to fracture (Figure 14.8).

Shape design has a great impact on the risk of mini-implant fracture. Generally, two shape designs are common for currently available mini-implants: cylindrical and tapered. It has been revealed that the mechanical properties of cylindrical mini-implants are superior to those of tapered ones.[25] Moreover, tapered mini-implants have higher insertion torque than cylindrical mini-implants,[26] so are less resistant to fracture than cylindrical ones (Figure 14.9).[7] Since the diameter decreases for the tip part of tapered mini-implants, tapered mini-implants tend to buckle in the middle before they fracture at their tips (Figure 14.10).[7] Also, it has been reported that self-drilling mini-implants have higher osseointegration levels than self-tapping ones,[15] suggesting that self-drilling mini-implants are more vulnerable to fracture during removal.

t.me/Dr_Mouayyad_AlbtousH

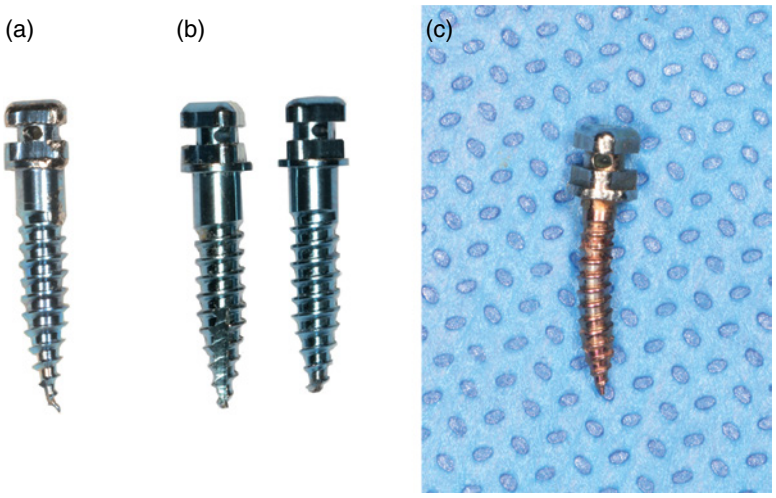


Figure 14.10 Mini-implant deformation before fracture. (a) The tip of a mini-implant was bent and was about to fracture during insertion. The operator noticed the bending of the tip and discontinued the insertion procedure. (b) The tip of the right mini-implant fractured during insertion. Compare with the complete mini-implant on the left. (c) Bending of a palatal mini-implant was noticed after removing after orthodontic treatment. The body of the mini-implant buckled in the middle and was about to fracture.

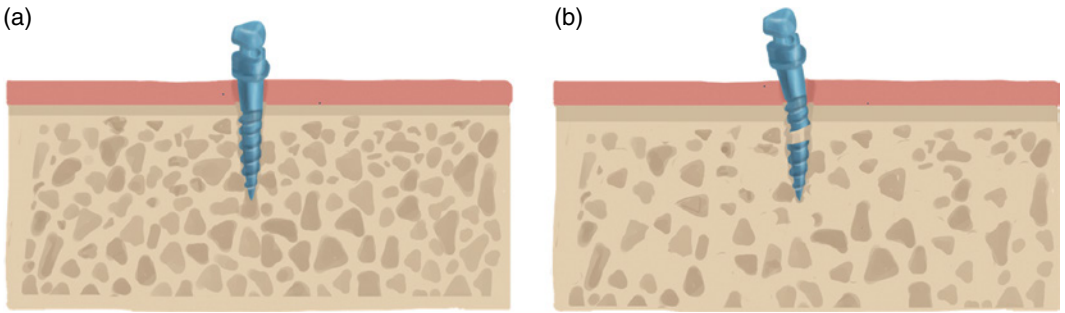


Figure 14.11 The fracture of mini-implants due to high bone density. (a) A mini-implant is inserted into a site with normal bone density without fracture. (b) A mini-implant fractures when it is inserted into a site with high bone density.

14.2.3 Insertion Site-associated Factors

Fracture torque is determined by the interaction between the mini-implant and the alveolar bone where the implant is inserted. Thus, apart from implant-associated factors, insertion site-associated factors play a major role in determining the risk of mini-implant fracture. Specifically, the risk of mini-implant fracture increases when mini-implants are placed into alveolar bone with high bone density and thick cortex (Figure 14.11).[8] Thus, for these sites, predrilling or the use of mini-implants with large diameters are recommended.[12,23]

Moreover, osseointegration of mini-implants has been demonstrated in a plethora of animal studies.[27-29] Removal torque increases if partial or complete osseointegration of mini-implants exists,[30] suggesting that osseointegration may increase the risk of fracture during removal. It has been reported that mini-implants inserted at different sites have different osseointegration levels[31] and therefore different potentials for the risk of fracture during removal (Figure 14.12).

t.me/Dr_Mouayyad_AlbtousH

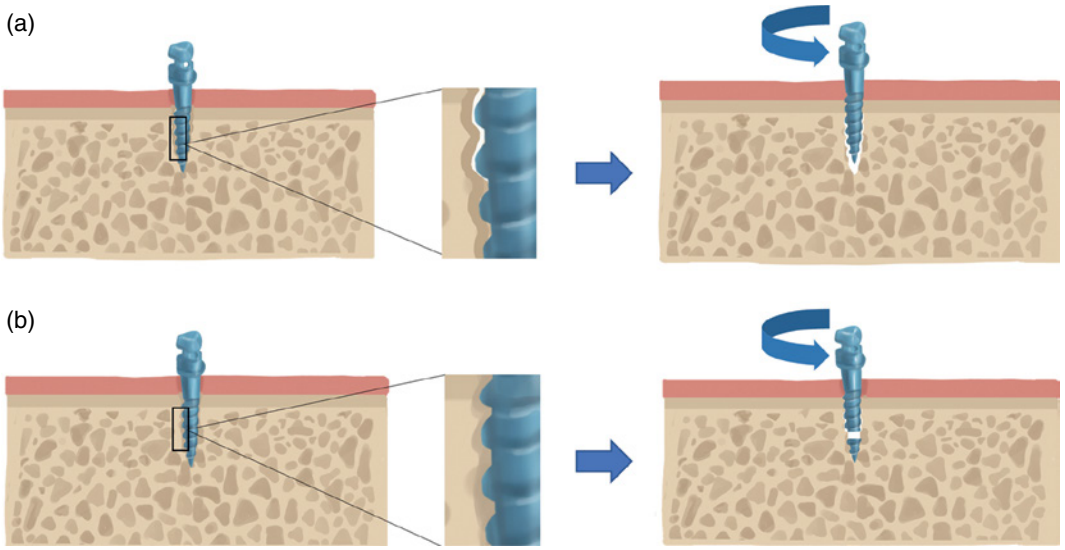


Figure 14.12 Mini-implant fracture during removal due to osseointegration. (a) Osseointegration between a mini-implant and surrounding alveolar bone is not achieved. The removal torque is normal and the mini-implant is unscrewed without fracture. (b) Osseointegration between a mini-implant and its surrounding alveolar bone is achieved. The mini-implant fractures during removal due to high removal torque that exceeds the fracture torque.

14.3 Prevention of Mini-implant Fracture

14.3.1 Prudent Selection of Insertion Sites

Before insertion, operators should carefully determine the appropriateness of insertion sites for orthodontic mini-implants and evaluate the likelihood of mini-implant fracture based on the aforementioned risk factors. To reiterate, inserting mini-implants into anatomical sites with high bone density and thick cortex should be avoided to reduce the risk of mini-implant fracture if alternative sites with normal bone density are available (Figure 14.13). If anatomical sites with high bone density and thick cortex have to be chosen due to biomechanical advantages, predrilling is indicated to reduce the risk of mini-implant fracture (Figure 14.14).

14.3.2 Judicious Selection of Appropriate Mini-implants

As mentioned above, mechanical properties differ among mini-implants with different materials and different geometric designs. Thus, the correct type of mini-implant should be carefully chosen to avoid fracture. For example, a mini-implant with large diameter should be selected for insertion at anatomical sites with high bone density and thick cortex (Figure 14.15).

14.3.3 Appropriate Insertion Techniques

Operators should employ appropriate insertion techniques for inserting mini-implants. In addition to conventional manual screwdrivers, motor-driven handpieces are available in clinical settings (Figure 14.16). For manual screwdrivers, slow and gentle drilling and constant torque with no abrupt change in insertion angle should be employed in clinical practice. In contrast to manual screwdrivers, operators are unable to receive feedback on bone resistance while inserting mini-implants with motor-driven handpieces. Thus, operators should pay special attention to insertion speed and torque value – speed should be slow and insertion torque should be less than the fracture torque of the mini-implants.

t.me/Dr_Mouayyad_AlbtousH

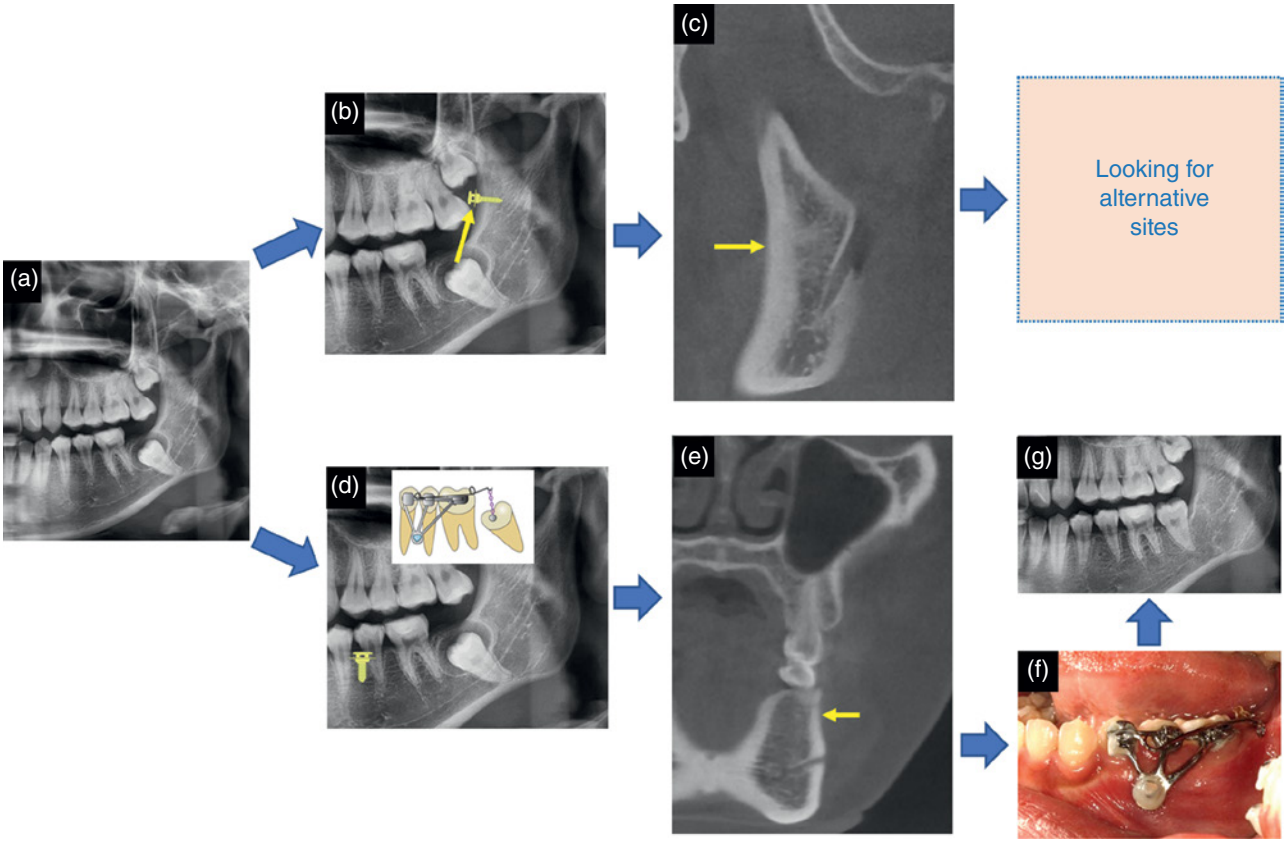
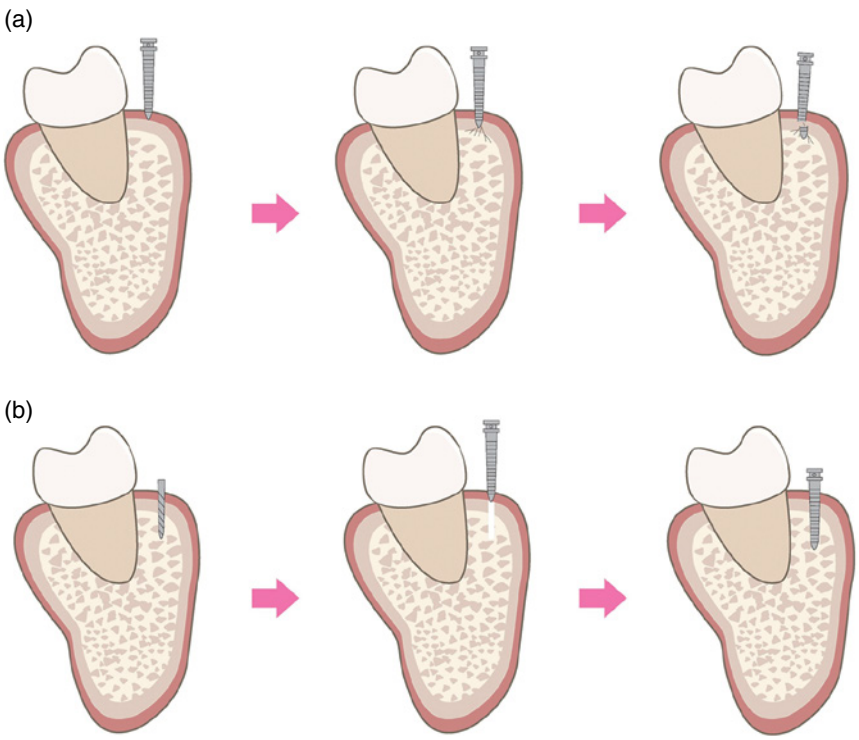


Figure 14.13 Prudent selection of an insertion site to reduce the likelihood of mini-implant fracture. (a) A mandibular left second molar was impacted. (b) The first treatment plan was to insert a mini-implant into the mandibular ramus for orthodontic traction. (c) CBCT examinations revealed that the bone cortex was very thick. In order to avoid mini-implant fracture, alternative insertion sites were planned. (d) An alternative insertion site (interradicular site between first and second premolars) was planned and an appliance with a cantilever was used for orthodontic traction. (e) CBCT examinations indicated normal cortical thickness. (f) The appliance bonded on teeth was stabilised by the mini-implant and a cantilever was used. (g) Finally, the impacted second molar was successfully tractioned to the occlusal level.

Figure 14.14 Predrilling helps to avoid mini-implant fracture for anatomical sites with high bone density. (a) A mini-implant is inserted into the mandibular buccal shelf without predrilling and fractures during insertion. (b) Predrilling is performed before inserting the mini-implant into the mandibular buccal shelf, avoiding fracture.



t.me/Dr_Mouayyad_AlbtousH

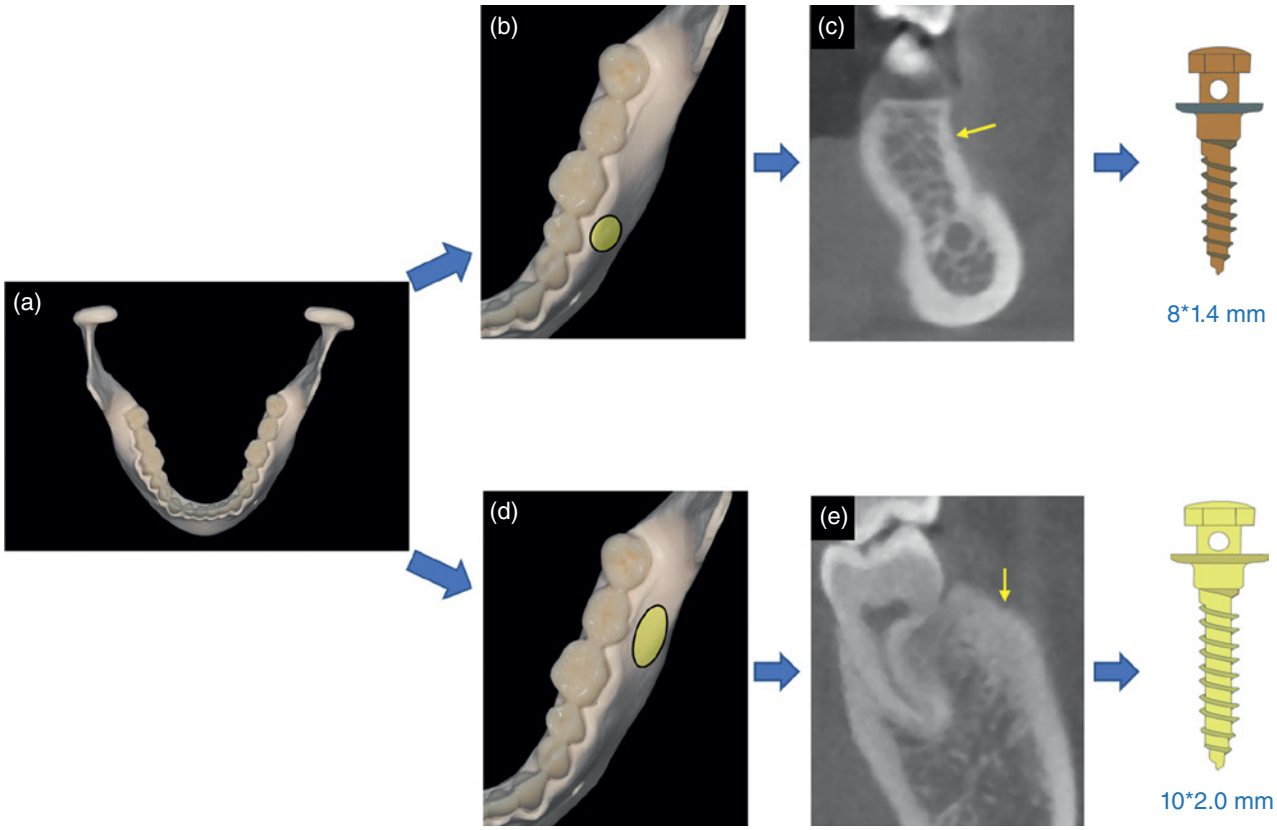


Figure 14.15 Selection of appropriate mini-implants. (a) Insertion of a mini-implant in the mandible was designed. (b) A mini-implant was planned to be inserted between the left second premolar and first molar. (c) CBCT examinations revealed that the buccal cortical thickness was within normal range. Thus, a small mini-implant (8*1.4 mm) would be used. (d) A mini-implant was designed to be inserted at the mandibular buccal shelf region. (e) Note the thick buccal cortex on a CBCT image (coronal view). Thus, a longer and larger mini-implant (10*2 mm) was selected for this site.

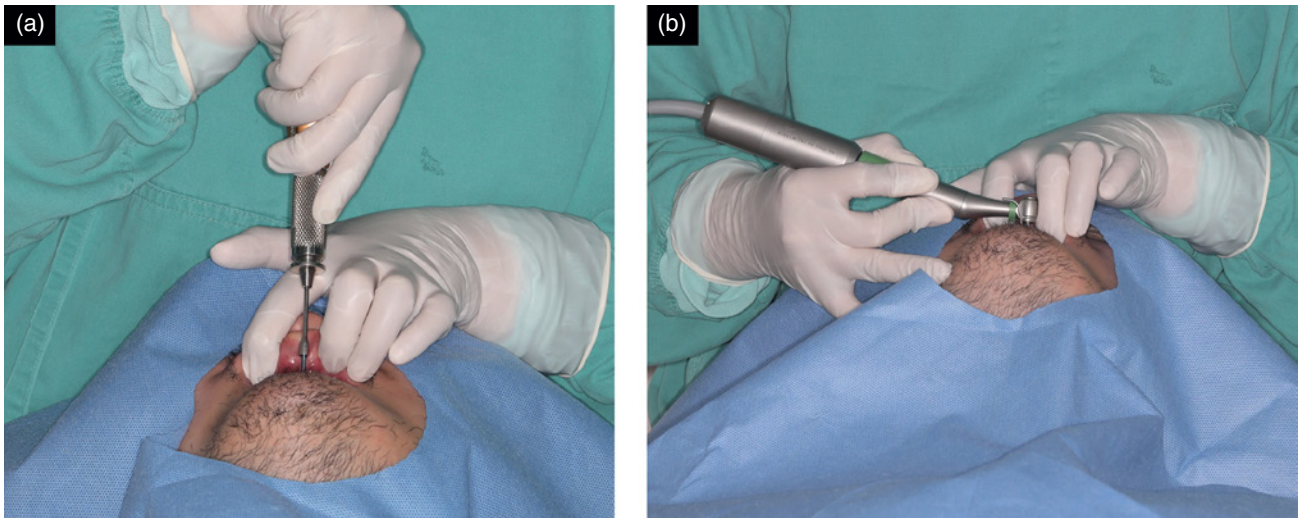


Figure 14.16 Different modalities for inserting orthodontic mini-implants. (a) Insertion using a manual screwdriver. (b) Insertion using a motor-driven handpiece.

t.me/Dr_Mouayyad_AlbtousH

14.4 Management of Mini-implant Fracture

14.4.1 Clinical Decisions in Different Clinical Scenarios

Although the incidence of mini-implant fracture is low, it does occur in clinical practice. Before insertion, the patient should be advised on the possibility of mini-implant fracture, especially when mini-implants are to be inserted into anatomical areas with high bone density or thick cortex. When mini-implant fracture is encountered during insertion or removal, operators should stay calm and reassure the patient. Depending on the fractured site of the mini-implant (i.e. neck, body or tip), different clinical decisions could be made (Figure 14.17).

When the neck of a mini-implant fractures, first check whether the main part of the mini-implant is stable. If it is stable, it could be left in the alveolar bone and be used for orthodontic force applications.

When the body of a mini-implant fractures, check whether vital structures (blood vessels and nerves) are nearby. If no vital structures are nearby, the portion remaining in the alveolar bone could be removed and a new mini-implant inserted in the vicinity.

When the tip of a mini-implant fractures, operators should inform the patient and discuss whether to remove the tiny tip of the mini-implant. If the patient agrees that the tip can stay inside the bone, the fractured tip could remain without additional surgery for removal. If the patient demands removal, an attempt should be made to remove the fractured tip. Then, a new mini-implant is placed at the same or a neighbouring site.

14.4.2 Clinical Techniques for Removing Fractured Mini-implants

Once a clinical decision has been made to remove a fractured mini-implant, radiographic examinations are required to locate the remaining part and rule out the presence of neighbouring vital anatomical structures. Following appropriate local anaesthesia, a flap is elevated to expose the fractured part. Then, circumferential bone removal is performed around the fractured part with piezosurgical tips or carbide burs. For the sake of minimal invasiveness, piezosurgery is recommended. Lastly, the fractured part is raised with elevators and removed, followed by primary suture of the flap (Figure 14.18).

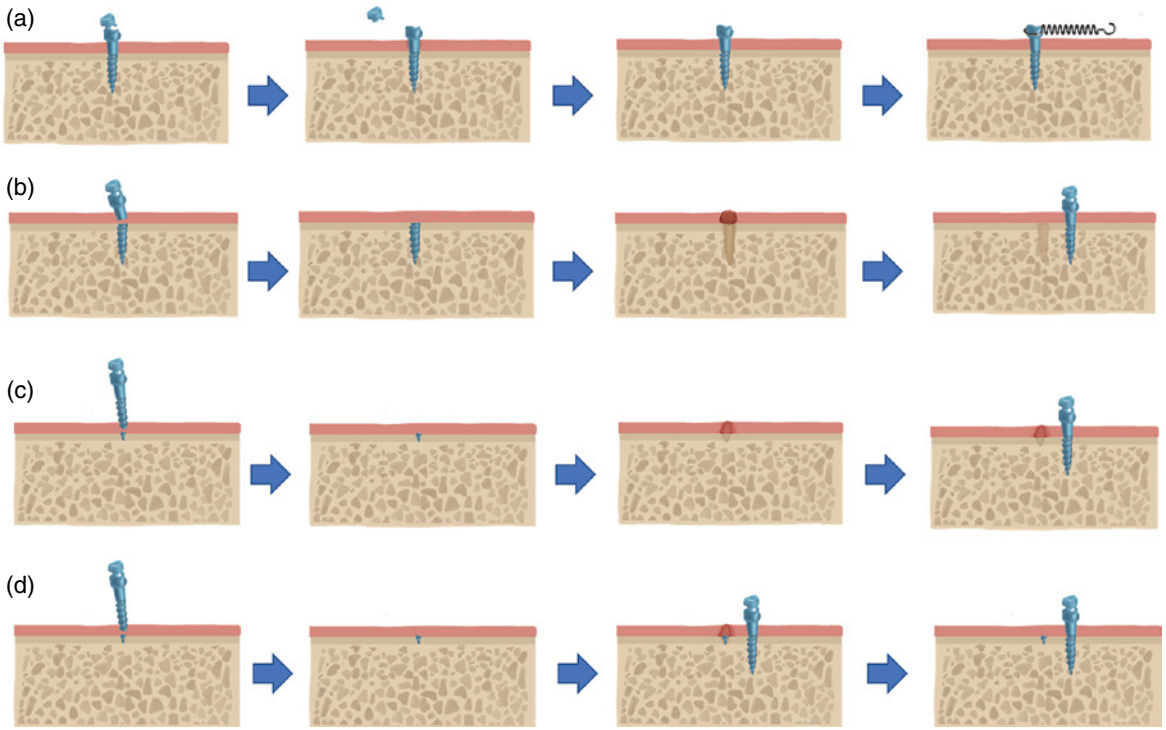


Figure 14.17 Different clinical decisions on the management of fractured mini-implants. (a) Neck fracture. If the remaining body of the mini-implant is stable, it can be applied for force loading. (b) Body fracture. The fractured mini-implant should be removed and a new one inserted at a neighbouring site. (c) Tip fracture. The fractured tip is removed and a new mini-implant is inserted at a neighbouring site. (d) Tip fracture. The fractured tip is retained and a new mini-implant is placed at a nearby site.

t.me/Dr_Mouayyad_AlbtousH

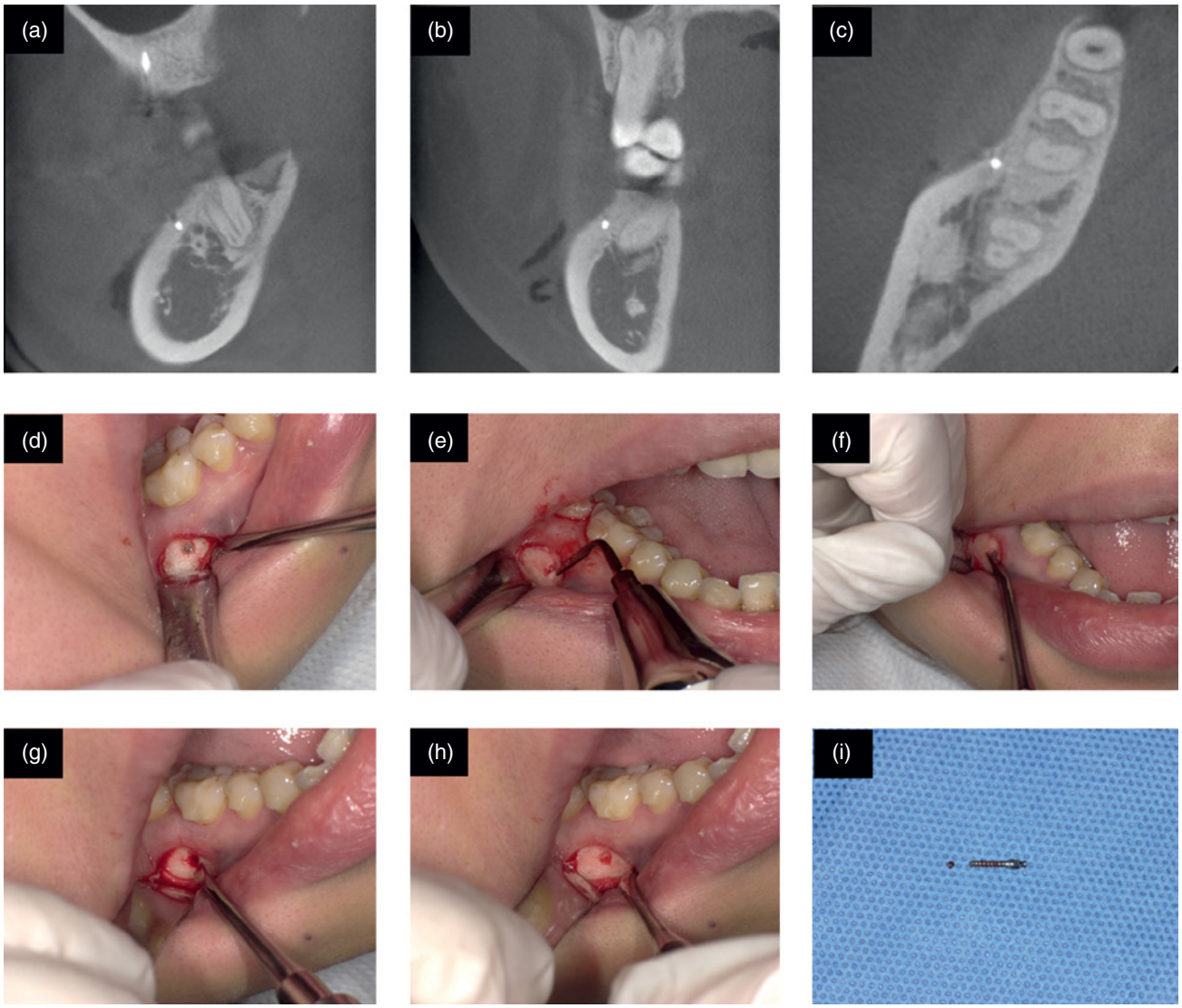


Figure 14.18 Surgical removal of a fractured mini-implant at the mandibular buccal shelf region. (a–c) A CBCT examination was prescribed to locate the fractured part. The fractured tip was inside the alveolar cortex buccal to the right first molar. (d) A flap was elevated to expose the fractured tip. (e) Circumferential bone was removed around the fractured tip through piezosurgery. (f,g) The fractured tip was raised with an elevator and removed. (h) After the fractured tip was removed, complete removal of the fractured part was confirmed. (i) The fractured tip and the remaining part of the mini-implant.

14.5 Summary

The fracture of mini-implants occurs during both insertion and removal stages when insertion torque or removal torque exceeds the fracture torque. Mini-implant facture is associated with a variety of risk factors, including operator factors, mini-implant factors and insertion site factors. Mini-implant fracture may be prevented through prudent selection of optimal insertion sites, judicious selection of appropriate mini-implants and implementation of correct insertion techniques. Depending on the location of the fracture, different clinical decisions can be made to manage fractured mini-implants.

References

1 Gurdan Z, Szalma J. (2018). Evaluation of the success and complication rates of self-drilling orthodontic mini-implants. *Niger. J. Clin. Pract.* 21(5): 546–552.

2 Suzuki EY, Suzuki B. (2011). Placement and removal torque values of orthodontic miniscrew implants. *Am. J. Orthod. Dentofacial Orthop.* 139(5): 669–678.

t.me/Dr_Mouayyad_AlbtousH

3 Park HS, Jeong SH, Kwon OW. (2006). Factors affecting the clinical success of screw implants used as orthodontic anchorage. *Am. J. Orthod. Dentofacial Orthop.* 130(1): 18–25.

4 Fah R, Schatzle M. (2014). Complications and adverse patient reactions associated with the surgical insertion and removal of palatal implants: a retrospective study. *Clin. Oral Implants Res.* 25(6): 653–658.

5 Assad-Loss TF, Kitahara-Ceia FMF, Silveira GS, Elias CN, Mucha JN. (2017). Fracture strength of orthodontic mini-implants. *Dent. Press J. Orthod.* 22(3): 47–54.

6 Barros SE, Vanz V, Chiqueto K, Janson G, Ferreira E. (2021). Mechanical strength of stainless steel and titanium alloy mini-implants with different diameters: an experimental laboratory study. *Prog. Orthod.* 22(1): 9.

7 Quraishi E, Sherriff M, Bister D. (2014). Peak insertion torque values of five mini-implant systems under different insertion loads. *J. Orthod.* 41(2): 102–109.

8 Pithon MM, Figueiredo DS, Oliveira DD. (2013). Mechanical evaluation of orthodontic mini-implants of different lengths. *J. Oral Maxillofac. Surg.* 71(3): 479–486.

9 Kravitz ND, Kusnoto B. (2007). Risks and complications of orthodontic miniscrews. *Am. J. Orthod. Dentofacial Orthop.* 131(4 Suppl): S43–51.

10 Ebenezer ES, Krishna G, Srinivasan K, Ravindran SK, Balu P, Ilangovan K. (2021). Surgical retrieval of fractured orthodontic mini-implant: a case report. *J. Sci. Dent.* 11(2): 56–60.

11 McCabe P, Kavanagh C. (2012). Root perforation associated with the use of a miniscrew implant used for orthodontic anchorage: a case report. *Int. Endod. J.* 45(7): 678–688.

12 Wilmes B, Panayotidis A, Drescher D. (2011). Fracture resistance of orthodontic mini-implants: a biomechanical in vitro study. *Eur. J. Orthod.* 33(4): 396–401.

13 Kim YH, Yang SM, Kim S et al. (2010). Midpalatal miniscrews for orthodontic anchorage: factors affecting clinical success. *Am. J. Orthod. Dentofacial Orthop.* 137(1): 66–72.

14 Luzi C, Verna C, Melsen B. (2009). Guidelines for success in placement of orthodontic mini-implants. *J. Clin. Orthod.* 43(1): 39–44.

15 Cehreli S, Arman-Ozcirpici A. (2012). Primary stability and histomorphometric bone-implant contact of self-drilling and self-tapping orthodontic microimplants. *Am. J. Orthod. Dentofacial Orthop.* 141(2): 187–195.

16 Vieira CA, Pires F, Hattori WT, de Araujo CA, Garcia-Junior MA, Zanetta-Barbosa D. (2021). Structural resistance of orthodontic mini-screws inserted for extra-alveolar anchorage. *Acta Odontol. Latinoam.* 34(1): 27–34.

17 Smith A, Hosein YK, Dunning CE, Tassi A. (2015). Fracture resistance of commonly used self-drilling orthodontic mini-implants. *Angle Orthod.* 85(1): 26–32.

18 Chang C, Liu SS, Roberts WE. (2015). Primary failure rate for 1680 extra-alveolar mandibular buccal shelf mini-screws placed in movable mucosa or attached gingiva. *Angle Orthod.* 85(6): 905–910.

19 Brown RN, Sexton BE, Gabriel Chu TM et al. (2014). Comparison of stainless steel and titanium alloy orthodontic miniscrew implants: a mechanical and histologic analysis. *Am. J. Orthod. Dentofacial Orthop.* 145(4): 496–504.

20 Bollero P, Di Fazio V, Pavoni C, Cordaro M, Cozza P, Lione R. (2018). Titanium alloy vs. stainless steel miniscrews: an in vivo split-mouth study. *Eur. Rev. Med. Pharmacol. Sci.* 22(8): 2191–2198.

21 Gritsch K, Laroche N, Bonnet JM et al. (2013). In vivo evaluation of immediately loaded stainless steel and titanium orthodontic screws in a growing bone. *PLoS One* 8(10): e76223.

22 Chang CH, Lin JS, Roberts WE. (2019). Failure rates for stainless steel versus titanium alloy infrazygomatic crest bone screws: a single-center, randomized double-blind clinical trial. *Angle Orthod.* 89(1): 40–46.

23 Dalla Rosa F, Burmann PF, Ruschel HC, Vargas IA, Kramer PF. (2016). Evaluation of fracture torque resistance of orthodontic mini-implants. *Acta Odontol. Latinoam.* 29(3): 248–254.

24 Barros SE, Janson G, Chiqueto K, Garib DG, Janson M. (2011). Effect of mini-implant diameter on fracture risk and self-drilling efficacy. *Am. J. Orthod. Dentofacial Orthop.* 140(4): e181–192.

25 Carano A, Lonardo P, Velo S, Incorvati C. (2005). Mechanical properties of three different commercially available miniscrews for skeletal anchorage. *Prog. Orthod.* 6(1): 82–97.

26 Wilmes B, Ottenstreuer S, Su YY, Drescher D. (2008). Impact of implant design on primary stability of orthodontic mini-implants. *J. Orofac. Orthop.* 69(1): 42–50.

27 Maino BG, Di Blasio A, Spadoni D et al. (2017). The integration of orthodontic miniscrews under mechanical loading: a pre-clinical study in rabbit. *Eur. J. Orthod.* 39(5): 519–527.

28 Alves A, Cacho A, San Roman F, Geros H, Afonso A. (2019). Mini implants osseointegration, molar intrusion and root resorption in Sinclair minipigs. *Int. Orthod.* 17(4): 733–743.

29 Exposto CR, Oz U, Westgate PM, Huja SS. (2019). Influence of mini-screw diameter and loading conditions on static and dynamic assessments of bone-implant contact: an animal study. *Orthod. Craniofac. Res.* 22 Suppl 1: 96–100.

30 Kim HY, Kim SC. (2016). Bone cutting capacity and osseointegration of surface-treated orthodontic mini-implants. *Korean J. Orthod.* 46(6): 386–394.

31 Zhang Q, Zhao L, Wu Y et al. (2011). The effect of varying healing times on orthodontic mini-implant stability: a microscopic computerized tomographic and biomechanical analysis. *Oral Surg. Oral Med. Oral Pathol. Oral Radiol. Endod.* 112(4): 423–429.

t.me/Dr_Mouayyad_AlbtousH

15

Soft Tissue Complications

Lin Xiang[1], Ziwei Tang[2], Jing Zhou[3], Heyi Tang[4], Hu Long[2], and Jianru Yi[2]

[1] *Department of Implantology, State Key Laboratory of Oral Diseases and National Clinical Research Center for Oral Diseases, West China Hospital of Stomatology, Sichuan University, Chengdu, China*
[2] *Department of Orthodontics, State Key Laboratory of Oral Diseases and National Clinical Research Center for Oral Diseases, West China Hospital of Stomatology, Sichuan University, Chengdu, China*
[3] *Department of Pediatric Dentistry, State Key Laboratory of Oral Diseases and National Clinical Research Center for Oral Diseases, West China Hospital of Stomatology, Sichuan University, Chengdu, China*
[4] *Department of Head and Neck Oncology, State Key Laboratory of Oral Diseases and National Clinical Research Center for Oral Diseases, West China Hospital of Stomatology, Sichuan University, Chengdu, China*

15.1 Introduction

Soft tissue remodelling actively takes place around orthodontic TADs following their placement. Soft tissue reacts to orthodontic TADs in two major ways depending on the presence of soft tissue inflammation: good adaptation and soft tissue inflammation. The incidence of soft tissue inflammation varies among different anatomical regions, different levels of oral hygiene and different types of orthodontic TADs.[1-3] The likelihood of soft tissue inflammation is 33% and 6% in the mandibular ramus and hard palate, respectively. This could be explained by the susceptibility of different types of soft tissues (keratinised vs movable tissue) to soft tissue inflammation and mini-implant loosening.[4] If mini-implants are placed at movable soft tissue, the inadequate soft tissue barrier around the mini-implant poses a high risk of soft tissue inflammation (Figure 15.1).

Mini-implants with soft tissue inflammation are more susceptible to loosening or failure.[5] Thus, meticulous care should be taken to prevent soft tissue inflammation around mini-implants, in order to maximise their clinical success.

In this chapter, we will present clinical manifestations, risk factors, prevention and treatment of soft tissue complications associated with orthodontic mini-implants.

Clinical Insertion Techniques of Orthodontic Temporary Anchorage Devices, First Edition. Edited by Hu Long, Xianglong Han, and Wenli Lai.
© 2024 John Wiley & Sons Ltd. Published 2024 by John Wiley & Sons Ltd.

t.me/Dr_Mouayyad_AlbtousH

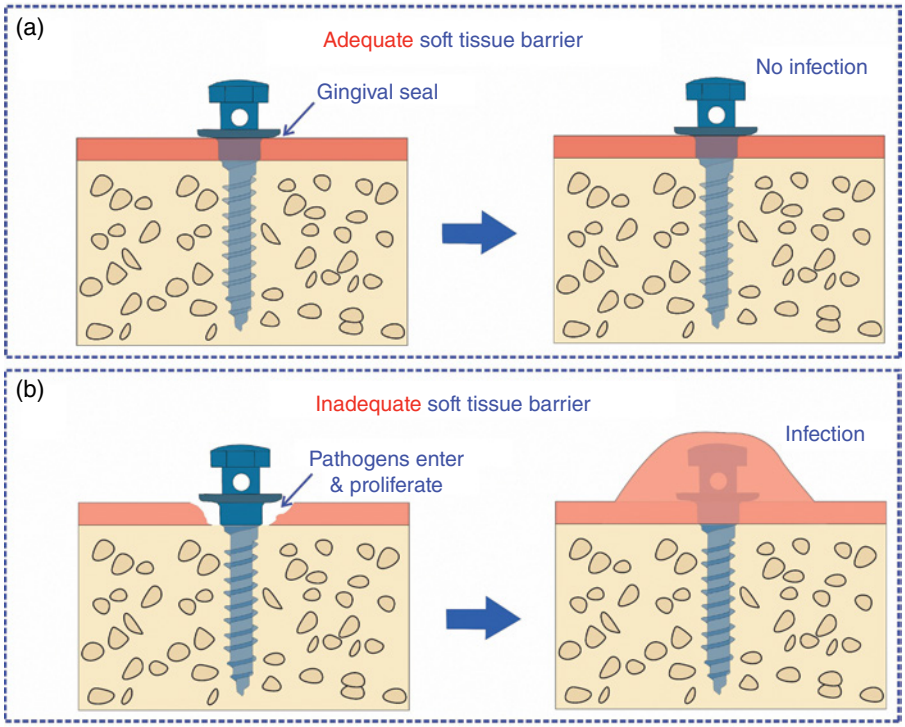


Figure 15.1 Soft tissue complications associated with orthodontic mini-implants placed at keratinised gingiva vs movable mucosa. (a) Due to good gingival seal offered by keratinised gingiva, adequate soft tissue barrier is present around the neck of the mini-implant, which could eliminate pathogen invasion and accumulation. The risk of soft tissue inflammation is low. (b) Due to the movability of the movable mucosa, soft tissue barrier is inadequate to avoid the entry of pathogens. The risk of postinsertion soft tissue inflammation is high.

15.2 Clinical Manifestations

Plaque can form around the head and neck of a mini-implant, and inflammation may occur at the gingiva–implant or mucosa–implant interface. It has been revealed that bacterial species around implants with soft tissue inflammation were similar to those in the periodontal pockets of patients with periodontitis,[6] resulting in similar clinical manifestations of soft tissue inflammation between periodontitis and peri-implantitis.[7] In clinical settings, soft tissue inflammation around mini-implants is often manifested as redness, congestion, swelling and soft tissue overgrowth. The inflamed soft tissues are of soft texture and exhibit bleeding on probing. With timely treatment, soft tissue inflammation can be resolved and reversed. However, if peri-implant inflammation persists, soft tissue inflammation could present as swelling, hyperplasia and even infection. Different types of soft tissue complications are clinically manifested, including swelling, hyperplasia, infection and lesion.

15.2.1 Soft Tissue Swelling

Soft tissue swelling occurs when peri-implant hygiene care is inadequate and is characterised by redness and hyperaemia (Figure 15.2). The swollen soft tissue may partially or fully cover the head of the mini-implant (Figure 15.3). Patients may experience local discomfort or pain that may interfere with functional movements, e.g. chewing, speech performance and swallowing. Moreover, partial or full coverage of the mini-implant by soft tissue renders force loading clinically difficult or inapplicable.

15.2.2 Soft Tissue Hyperplasia

In contrast to soft tissue swelling, soft tissue hyperplasia is characterised by gradual massive proliferation or overgrowth of firm soft tissue over time (Figure 15.4). The texture of the hyperplastic soft tissue is relatively harder than the soft tissue with swelling. Soft tissue hyperplasia is mainly due to the massive proliferation of fibrous tissue and capillary network.

t.me/Dr_Mouayyad_AlbtousH

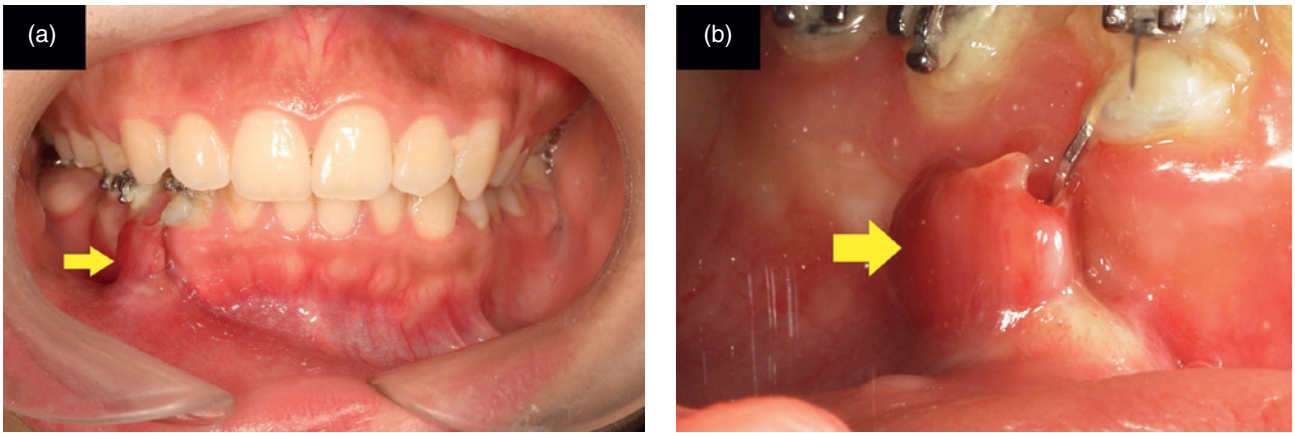


Figure 15.2 Soft tissue swelling around a mini-implant inserted at the mandibular buccal region. (a) The mini-implant is fully covered and embedded into swollen soft tissue. (b) The swollen soft tissue is characterised by redness and hyperaemia.

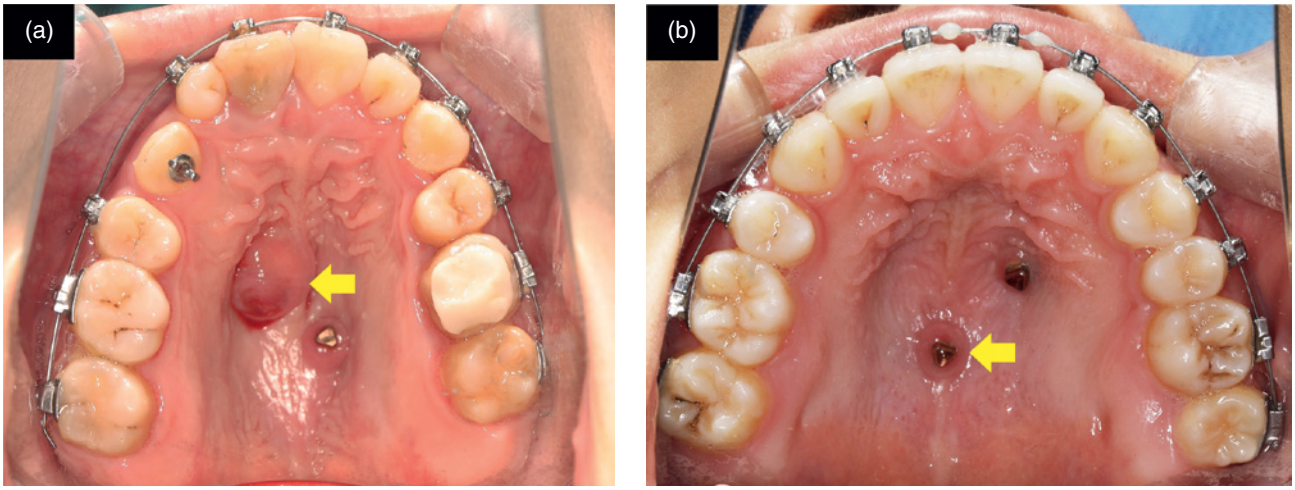


Figure 15.3 The extent of soft tissue swelling. (a) When soft tissue swelling is severe, the head of the mini-implant is fully covered and embedded into the swollen soft tissue. (b) A palatal orthodontic mini-implant is partially covered by swollen soft tissue.

15.2.3 Soft Tissue Infection

Soft tissue infection occurs if local soft tissue inflammation and bacterial infection persist. Soft tissue infection usually presents as tenderness, swelling and bleeding on probing (Figure 15.5). Soft tissue infection is often caused by local inadequate oral hygiene care and prolonged mechanical trauma. Owing to insufficient oral hygiene maintenance, prolonged bacterial infection at the mucosa–implant interface may lead to severe local infection and even pus discharge.

15.2.4 Soft Tissue Lesion

Soft tissue lesion usually occurs when mini-implants or their auxiliary appliances cause mechanical trauma to oral mucosa or gingivae. For example, prolonged use of orthodontic elastics may impinge on the gingivae or oral mucosa and cause mechanical trauma of the soft tissue (Figure 15.6). Moreover, if the extra-bony part of a mini-implant is too long, the head of the implant may cause soft tissue trauma and result in mucosa ulcer. Although soft tissue lesion is not associated with decreased

t.me/Dr_Mouayyad_AlbtousH

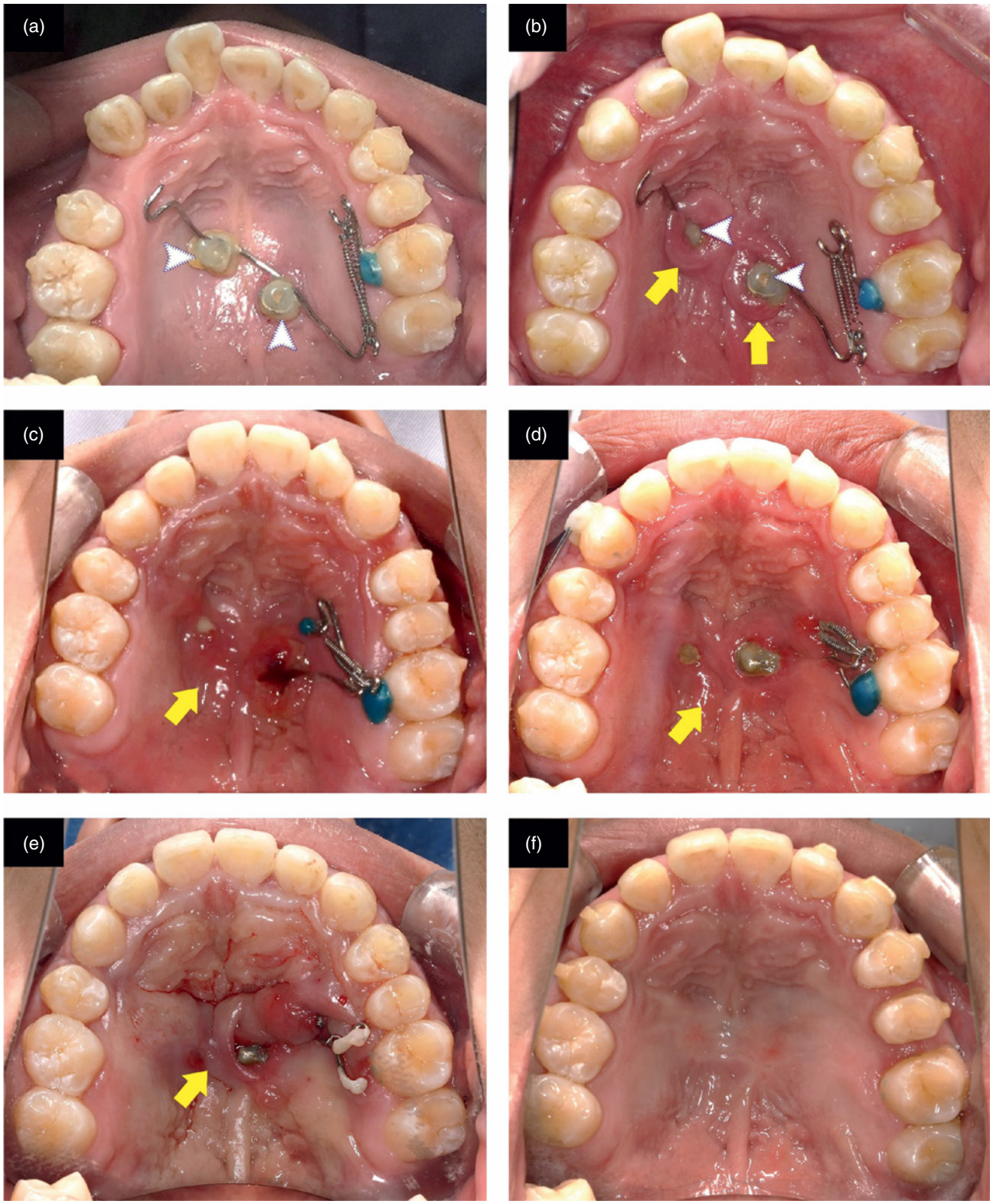


Figure 15.4 Soft tissue hyperplasia around palatal mini-implants. (a) This patient received clear aligner therapy. Two orthodontic mini-implants were placed at palatal paramedian sites. Two extension arms were fixed onto the palatal mini-implants (white arrowheads) with ligature wires and flowable resin. (b) Three months into treatment. The two mini-implants (white arrowheads) were partially covered by swollen soft tissue (yellow arrows). (c) One year into treatment. Mini-implants were fully embedded into the hyperplastic soft tissue (yellow arrow). (d) Fifteen months into treatment, the mini-implants and the distal extension arm were fully covered by the hyperplastic soft tissue (yellow arrow). (e) The hyperplastic soft tissue (yellow arrow) gradually became firm. Then, surgical excision of the hyperplastic soft tissue and removal of palatal mini-implants were implemented. (f) Six months after removal of the mini-implants and extension arms, soft tissue hyperplasia at the palatal vault subsided.

t.me/Dr_Mouayyad_AlbtousH

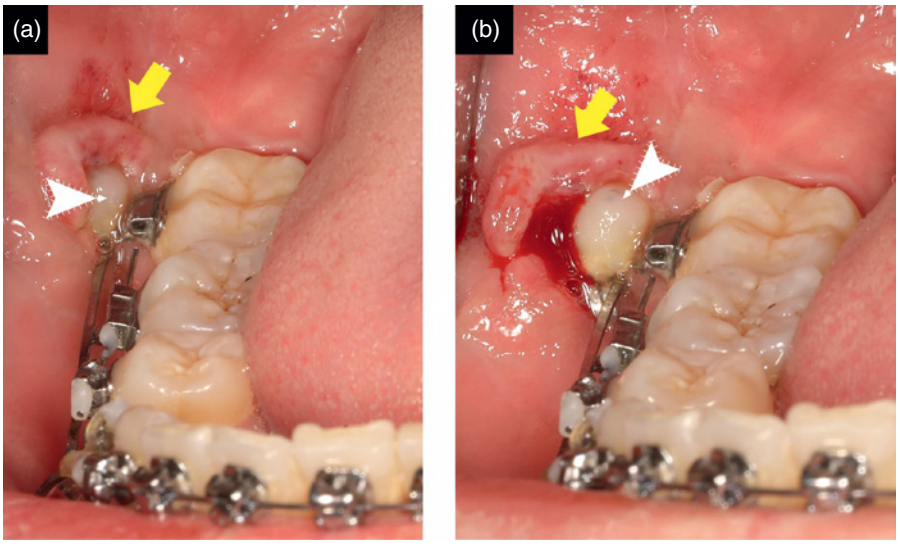


Figure 15.5 Soft tissue infection associated with an orthodontic mini-implant inserted at the mandibular buccal shelf. (a) Local soft tissue infection (yellow arrow) around a buccal shelf mini-implant. The head of the mini-implant was covered with resin build-up (white arrowhead). Note the inflamed and infected soft tissue around the mini-implant. (b) Bleeding occurred after elevating the infected soft tissue (yellow arrow) covering the head of the mini-implant (white arrowhead).

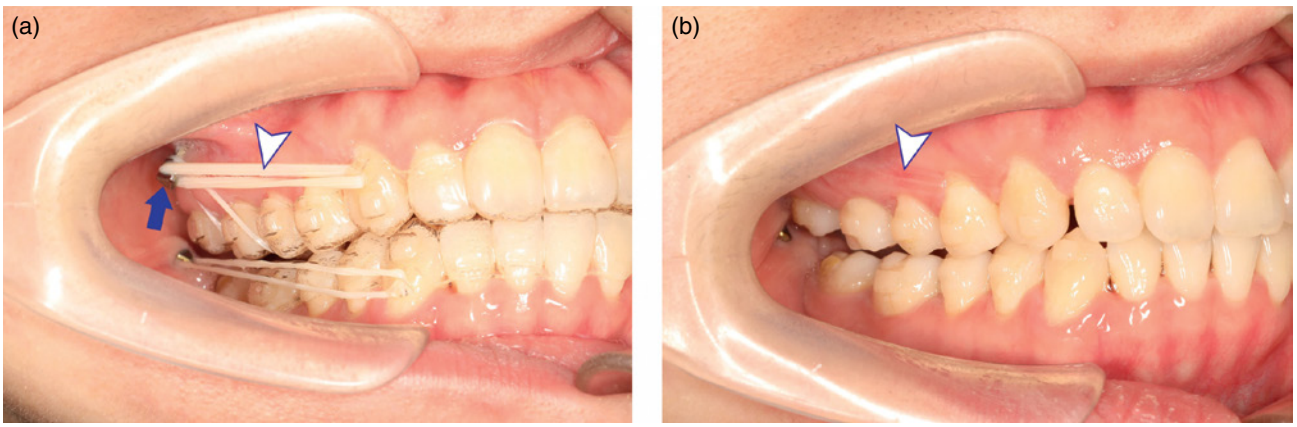


Figure 15.6 Soft tissue lesion caused by auxiliary appliances associated with orthodontic mini-implants. (a) Elastics (white arrowhead) were stretched from the canine hook to an infrazygomatic mini-implant (blue arrow). (b) The elastics impinged on soft tissue and caused a lesion (white arrowhead).

mini-implant stability, prolonged local discomfort or pain may result in decreased patient compliance. Moreover, prolonged soft tissue lesion due to physical trauma may result in soft tissue thickening or even leucoplakia.

15.3 Adverse Consequences

Persistent soft tissue complications may cause several adverse consequences, e.g. discontinuation of using mini-implants, mini-implant loosening and even facial infections.

As mentioned above, severe hyperplastic soft tissue may cover the heads of mini-implants, limiting their clinical applications (Figure 15.7a,b). If left untreated, the soft tissue hyperplasia and subsequent infections may propagate and spread into peri-implant alveolar bone, resulting in peri-implant bone resorption and mini-implant failure (Figure 15.7c). In some clinical scenarios, if local infections are severe, facial infections may occur among susceptible patients (Figure 15.7d).

t.me/Dr_Mouayyad_AlbtousH

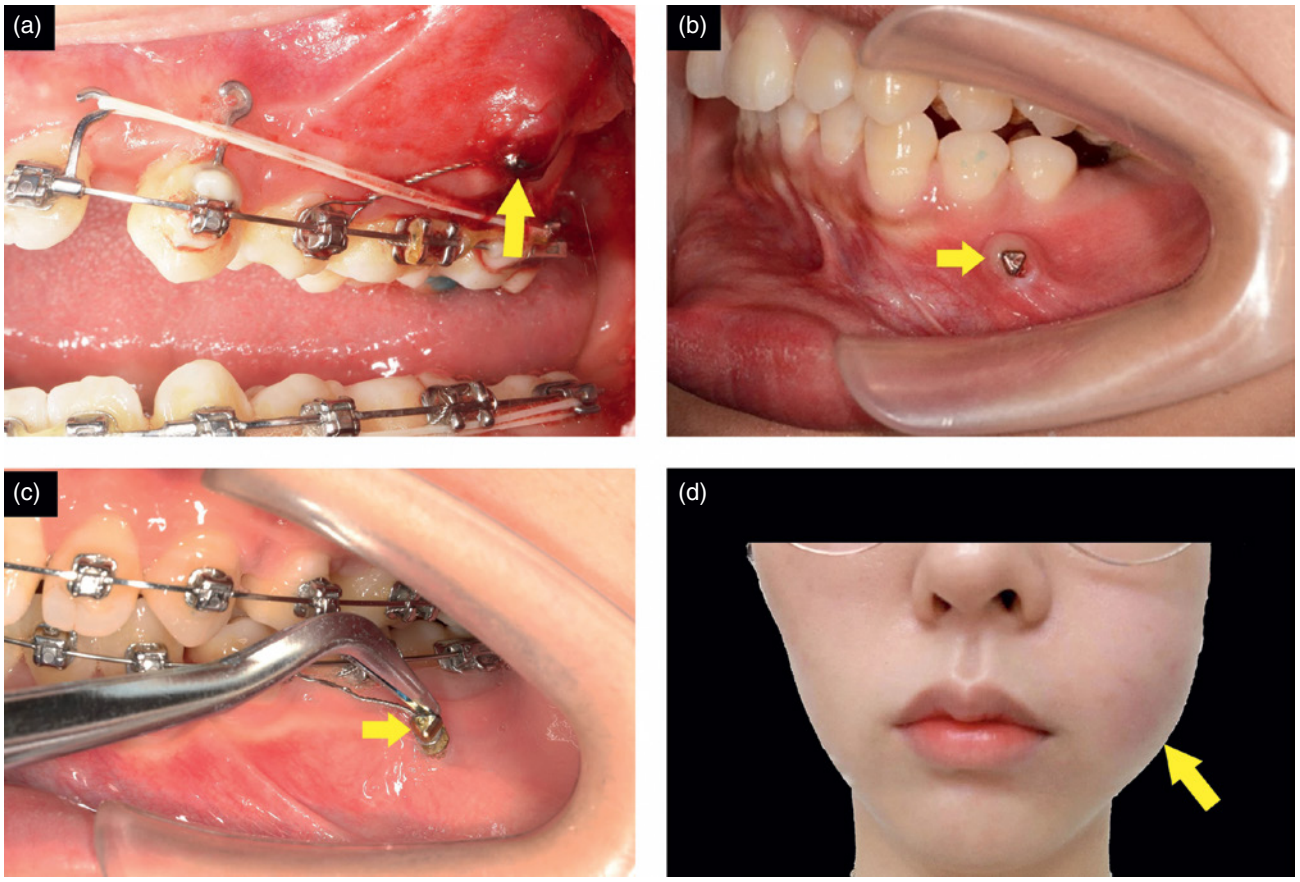


Figure 15.7 Adverse consequences due to soft tissue complications. (a,b) Soft tissue swelling and infection interfered with the clinical use of mini-implants (yellow arrow). (c) Soft tissue inflammation caused the loosening of a mini-implant (yellow arrow). (d) Soft tissue infection associated with a mini-implant caused facial infection. Note the left facial swelling (yellow arrow) of this patient.

15.4 Risk Factors

15.4.1 Patient Factors

Individual Susceptibility

Different subjects have different susceptibilities to peri-implant soft tissue complications. This may involve various factors, e.g. genetic susceptibility, body condition, bacteria and saliva flow (Figure 15.8).

Once mini-implants are inserted, both hard and soft tissues adapt to them. At the tissue–implant interface, a fine-tuning inflammatory cascade plays an important role in determining tissue reaction. Thus, individuals' genetic polymorphisms of these inflammatory mediators govern their susceptibility. Specifically, it has been revealed that interleukin gene polymorphisms are associated with peri-implantitis.[8,9]

The microbial environment differs among individuals. Once the mini-implant is inserted, it is soon covered by salivary pellicle and colonised by oral bacteria that already exist in the patient's mouth.[10] Bacteria can accumulate not only in the gingival sulcus, but also around the mini-implant. The pathogenic effects of bacteria can be suppressed by host defensive responses. It has been confirmed that clinically stable peri-implant microflora are similar to those in healthy gingival sulcus and that bacterial species did not differ between peri-implantitis and periodontitis.[6] When anaerobic bacteria and some gram-negative bacteria (e.g. *Actinobacteria*, *Prevotella intermedia*, *Porphyromonas gingivalis*, *Forsythia* and *Treponema dentis*)[11,12] dominate around mini-implants, the balance between micro-organisms and the host is broken. Then, the bacteria induce the host to produce inflammatory mediators (e.g. cytokines, interleukins and metalloproteinases),[13] resulting in soft tissue inflammation around mini-implants. Thus, bacterial level and species are defining factors for soft tissue inflammation.

Saliva contains antibacterial molecules and neutralises bacteria-generated acid that inhibits host cell metabolism. Thus, normal salivary function is an important factor in influencing peri-implant soft tissue complications.

t.me/Dr_Mouayyad_AlbtousH

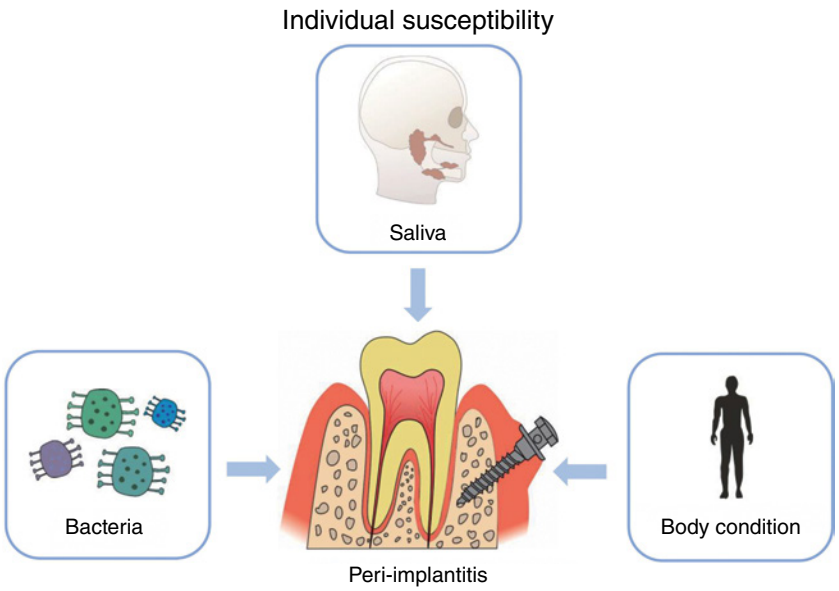


Figure 15.8 Different subjects exhibit different susceptibilities to soft tissue complications. This may involve various factors, including bacterial species, salivary function and body condition.

Furthermore, the general condition of the body is determined by endocrine, genetic, environmental and other factors, such as smoking and systemic diseases. Patients with systemic diseases (e.g. diabetes mellitus) are more prone to peri-implant soft tissue complications. Specifically, hyperglycaemia reduces the formation of microvessels in soft tissue and delays soft tissue healing, resulting in an increased chance of infection. In addition, patients with diabetes mellitus are more sensitive to the stimulation of dental plaque and are more susceptible to soft tissue inflammation.[14] Likewise, patients with some systemic diseases requiring corticosteroid administration are prone to peri-implant soft tissue complications since corticosteroid delays soft tissue healing. Therefore, we recommend that practitioners should be cautious with patients with systemic diseases.

Oral Hygiene Care

After mini-implants are inserted, a new microbial colonisation site is created.[11,15] Dental plaque is primarily an unmineralised bacterial deposit that adheres to a tooth or mini-implant surface and consists of a sticky matrix and bacteria. The matrix is mainly composed of salivary glycoproteins and bacterial extracellular polymers. Aside from oral hygiene care, the plaque adsorbed on the surface of the mini-implant is difficult to remove. Patients with insufficient oral hygiene maintenance are more likely to develop plaque around mini-implants (Figure 15.9). In addition, among patients with chronic periodontitis, the effects of plaque control are relatively poor,[16-18] which may result in the accumulation of food debris and build-up of plaque around the mini-implants. The accumulated debris and plaque irritate the surrounding soft tissue and lead to peri-implant soft tissue complications. Thus, meticulous oral hygiene care should be strictly implemented among patients following the placement of mini-implants.

Smoking

Smoking is a risk factor for soft tissue inflammation and affects both the short-term and long-term stability of orthodontic TADs. It has been revealed that the failure rate of mini-implants is significantly higher among smokers than non-smokers.[19,20] Smoking interferes with the stability of mini-implants at different phases. First of all, nicotine in tobacco influences platelet adhesion and blood viscosity and causes a delay in soft tissue healing following mini-implant placement,[21,22] resulting in a higher likelihood of microbial invasion and soft tissue inflammation. Second, nicotine interferes with protein synthesis and adhesion function of gingival fibroblasts,[23,24] which may result in incomplete gingival sealing and higher chance of soft tissue inflammation. Lastly, smoking interferes with alveolar bone remodelling by suppressing osteoblast proliferation and inhibiting osteogenic mediators.[25,26] Moreover, smoking can lead to significant loss of marginal bone around implants and may cause thread exposure and plaque accumulation,[27-29] resulting in higher risk of soft tissue inflammation and mini-implant failure. Thus, smoking cessation should be strictly implemented among patients with mini-implants installed.

t.me/Dr_Mouayyad_AlbtousH

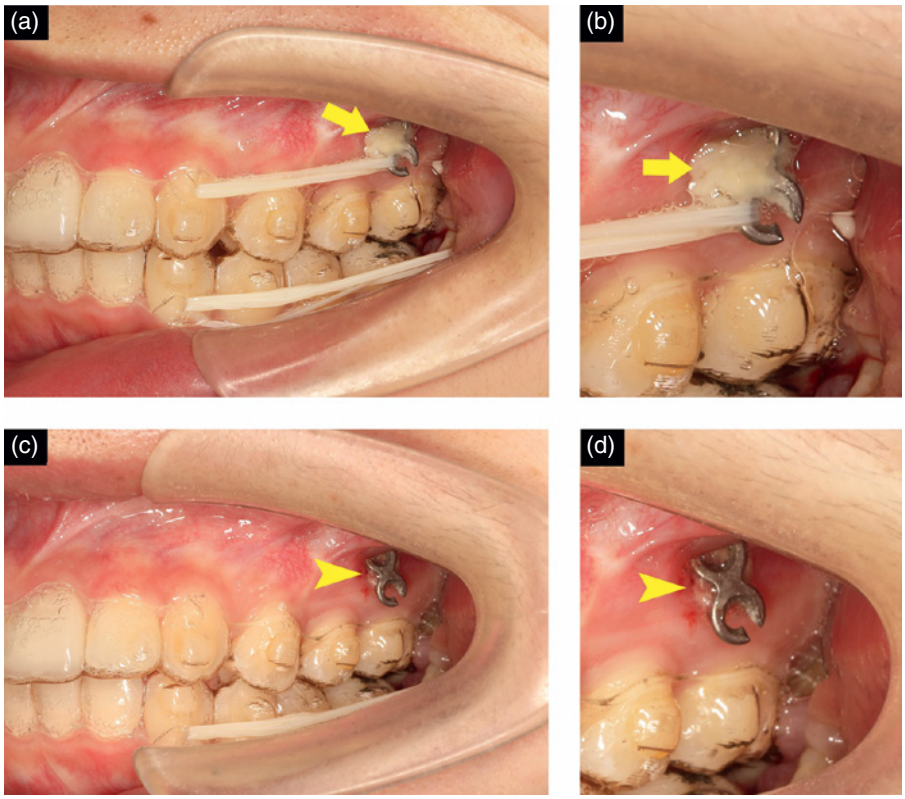


Figure 15.9 Inadequate oral hygiene. (a) A miniplate placed at the infrazygomatic crest was used to distalise maxillary molars with clear aligners. Due to inadequate oral hygiene, tartar (yellow arrow) developed around the miniplate. (b) Close-up view. Note the tartar on the miniplate (yellow arrow). (c) Tartar on the mini-plate was removed. Note the inflamed soft tissue (yellow arrowhead). (d) Close-up view.

15.4.2 Operator Factors

Position of Mini-implants

A large body of evidence indicates that peri-implant soft tissue is less susceptible to inflammation if implants are placed at the attached gingiva zone rather than the movable mucosa zone.[4,30-33] This is mainly attributed to the fact that attached gingiva is keratinised and fixed on the alveolar bone, and is more resistant to mechanical trauma or irritation than movable mucosa (Figure 15.10). Moreover, due to its movable nature, the soft tissue barrier formed by the movable mucosa is often incomplete. Microbial pathogens may enter the implant–mucosa or even the implant–bone interface, resulting in soft tissue inflammation. Thus, it is recommended to place mini-implants at the keratinised soft tissue zone (e.g. attached gingiva and palatal mucosa). However, the width of the attached gingiva is limited in some anatomical region, e.g. posterior interradicular sites. At these anatomical sites, we recommend operators exploit the most apical limit of the attached gingiva and place mini-implants at the mucogingival junction through the angled insertion technique.

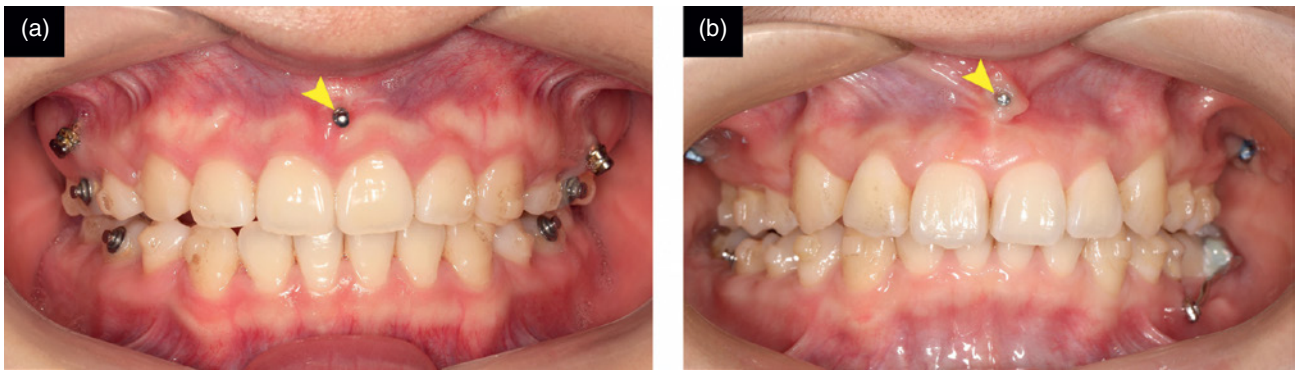


Figure 15.10 The influence of mini-implant position on soft tissue complications. (a) A labial mini-implant was placed at the mucogingival junction and its head was in the keratinised gingiva zone. No soft tissue inflammation was noted (yellow arrowhead). (b) A labial mini-implant was placed apically to the mucogingival junction and its head was in the movable mucosa zone. Note the hyperplastic soft tissue (yellow arrowhead) around the head of the mini-implant.

t.me/Dr_Mouayyad_AlbtousH

It is recommended that the insertion of a mini-implant be stopped once the platform of the mini-implant is in slightly firm contact with the corresponding soft tissue. Occasionally, operators may perform overinsertion to gain greater primary stability if adequate primary stability is not achieved. However, overinsertion may lead to the submergence of the mini-implant platform and head into the soft tissue, rendering the soft tissue susceptible to inflammation and hyperplasia (Figure 15.11). Thus, overinsertion is not recommended even if primary stability is unsatisfactory. If this clinical scenario is encountered, insertion at an alternative site or use of a larger and longer mini-implant is recommended.

Furthermore, for a specific insertion site, insertion height and angle are pivotal since judicious design of the insertion height and angle can reduce the likelihood of soft tissue complication by keeping mini-implant heads away from movable mucosa, e.g. buccal mucosa and frenum (Figure 15.12).

Force Loading

Once mini-implants are inserted, force loading can be implemented through a variety of appliances, e.g. closed-coil spings, elastic bands, elastomeric chains and cantilevers. Closed-coil springs are frequently used and they are, in most circumstances, applied between crimpable hooks on an archwire and the mini-implant. If used inappropriately, the closed-coil springs may impinge on and compress the gingiva or mucosa, resulting in soft tissue inflammation or hyperplasia (Figure 15.13). In addition, soft tissue trauma may occur if bulky appliances (e.g. cantilevers) are inappropriately designed and applied.

15.4.3 Factors Associated with the Mini-implant

Materials

Currently, two different types of mini-implant materials are used in clinical practice: titanium alloy and stainless steel. Although stainless steel implants have equal or superior biomechanical properties compared to titanium implants, a lower rate of failure and fewer complications are observed for titanium implants.[34] However, a recent systematic review reveals that the success rate does not differ between titanium alloy and stainless steel mini-implants, indicating that the materials used for mini-implants are not a major factor in determining their clinical success.[35] Moreover, current evidence fails to demonstrate the advantage of titanium implants in reducing the incidence of implant-associated infections over stainless steel implants.[36] Thus, implant materials have no or minimal effect on the risk of soft tissue complications.

Surface Properties

Surface properties (e.g. roughness, wettability and energy) of mini-implants may influence the response of soft tissue and have a significant impact on implant-associated soft tissue complications. In particular, surface roughness is an important factor in governing soft tissue response following the placement of mini-implants.

Following the insertion of mini-implants, blood emerges from the alveolar bone and comes into contact with the implant, forming an implant–blood interface that in turn recruits inflammatory cells and gingival fibroblasts to form

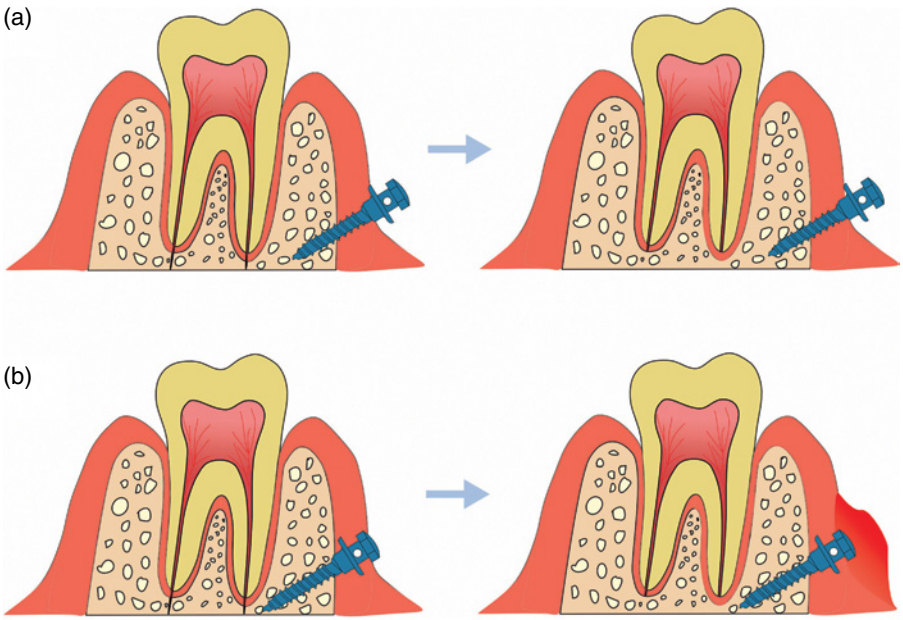


Figure 15.11 The influence of overinsertion on posttreatment soft tissue inflammation. (a) The insertion of the mini-implant is stopped once the platform is in slightly firm contact with the soft tissue. No soft tissue trauma or inflammation occur following insertion. (b) The mini-implant is overinserted into the soft tissue and overgrowth of the soft tissue occurs and the mini-implant is fully covered by the hyperplastic soft tissue.

t.me/Dr_Mouayyad_AlbtousH

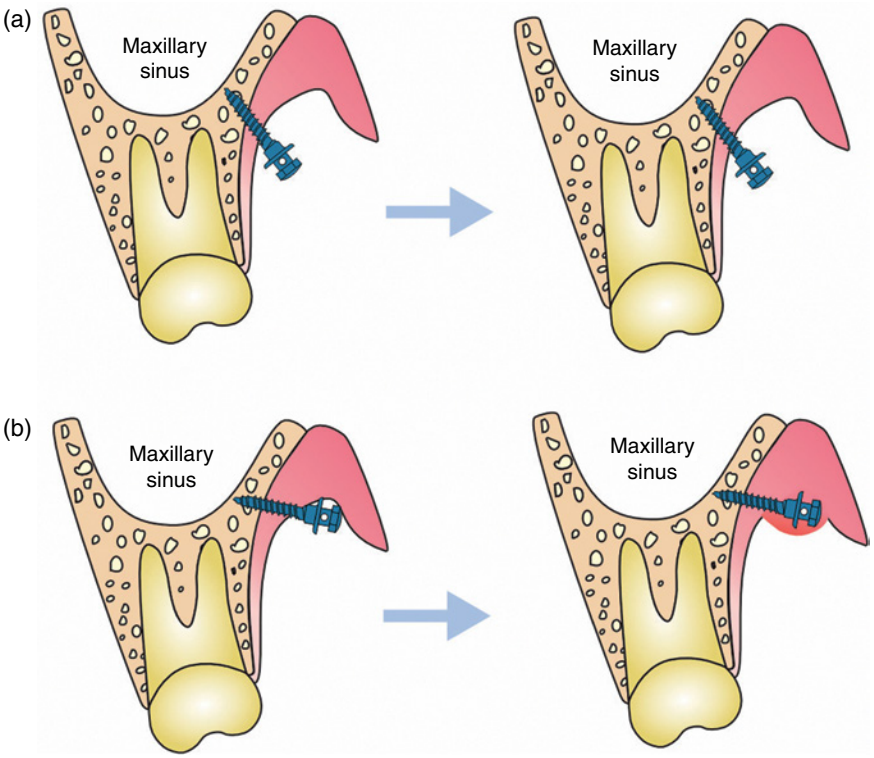


Figure 15.12 The importance of judicious design of optimal insertion height and angle for preventing soft tissue complications. (a) A mini-implant is inserted with an adequate insertion angle and the resulting position of the mini-implant head lies in the attached gingiva zone. The risk of soft tissue complications is low. (b) Inappropriate insertion height and angle lead to undesirable position of the mini-implant head that impinges on the movable mucosa, resulting in postinsertion soft tissue complications.

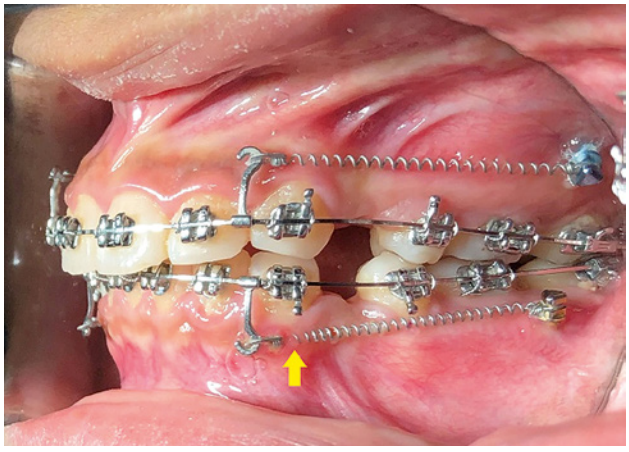


Figure 15.13 Auxiliary appliances associated with mini-implants cause soft tissue complications. The closed-coil spring in the lower arch impinged on soft tissue and caused soft tissue swelling and inflammation (yellow arrow).

an implant–cell interface.[37] Once the implant–cell interface is formed, protein adsorption and the fine-tuning release of a cascade of inflammatory mediators finally lead to soft tissue healing and sealing. If the soft tissue sealing is incomplete, the risk of postinsertion complications is high. If the surface is too smooth, the formation of blood–implant and cell–implant interfaces is difficult and the likelihood of soft tissue complications will be high due to incomplete soft tissue sealing. At the other extreme, if the mini-implant surface is too rough, although a rough surface facilitates protein adsorption and cell recruitment, mini-implants are susceptible to microbial accumulation and biofilm formation, resulting in a high risk of soft tissue complications. Thus, mini-implants should exhibit the optimum surface roughness to facilitate the formation of cell–implant interface and to prevent microbial adhesion, so that soft tissue healing is optimised and the risk of soft tissue complications is low.

t.me/Dr_Mouayyad_AlbtousH

15.5 Prevention

15.5.1 Meticulous Oral Hygiene Care

In order to reduce the incidence of soft tissue complications, meticulous oral hygiene is indispensable (Figure 15.14). Following placement of a mini-implant, soft tissue heals around the implant and forms a sulcus. Food debris and bacterial plaque can accumulate in the sulcus. If they are not sufficiently removed through daily meticulous oral hygiene, soft tissue inflammation may ensue and various forms of soft tissue complications may be manifested, i.e. inflammation, infection and hyperplasia. Patients should be instructed to mechanically brush the head and neck of mini-implants after each meal in order to remove bacterial plaque on the head and in the sulcus. In addition, regular prophylaxis is recommended.

15.5.2 Prudent Selection of Insertion Sites

Since keratinised gingiva is fixed onto alveolar bone, it is more resistant to irritation than movable mucosa. The insertion of mini-implants into the keratinised gingiva zone is associated with better soft tissue adaptation and lower likelihood of soft tissue complications.[38] This is partially because, even if adequate oral hygiene is performed, plaque accumulation is less likely at the attached gingiva as compared to movable mucosa.[39] Thus, we recommend mini-implants be placed at the keratinised and attached gingiva zone rather than at the movable mucosa zone in order to reduce the risk of soft tissue complications (Figure 15.15). Moreover, if mini-implants have to be placed at the movable mucosa zone (e.g. infrazygomatic crest) due to biomechanical considerations, mini-implants with adequate lengths should be selected so that their heads are located at the keratinised gingiva zone.

15.5.3 Sophisticated Insertion Techniques

For some insertion sites (e.g. infrazygomatic crest) covered by thick movable mucosa, orthodontic mini-implants have to be inserted through thick mucosa. Thus, the risk of post-insertion soft tissue complications is high. In these clinical

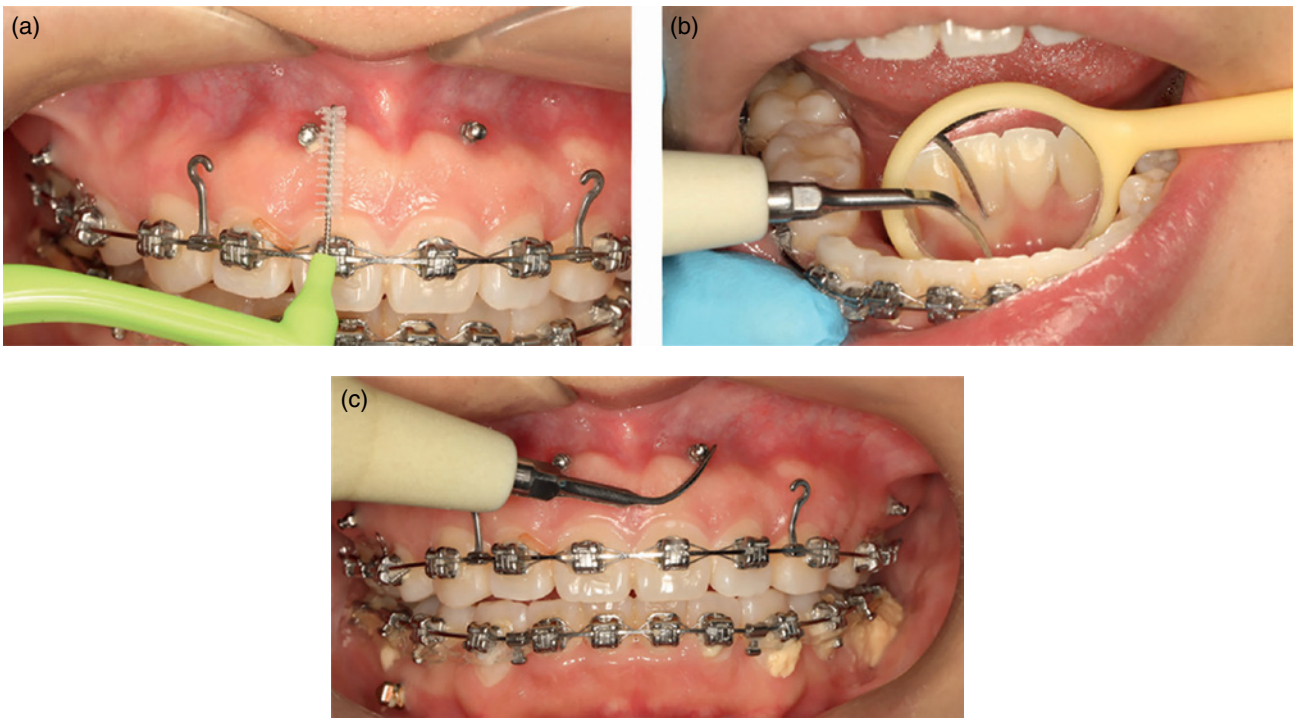


Figure 15.14 Appropriate oral hygiene care. (a) Remove food debris around the mini-implant by using an interdental brush. (b) Full-mouth ultrasonic scaling is performed during orthodontic treatment. (c) Peri-implant ultrasonic scaling is applied to remove plaque in the sulcus between the mini-implant and the soft tissue.

t.me/Dr_Mouayyad_AlbtousH

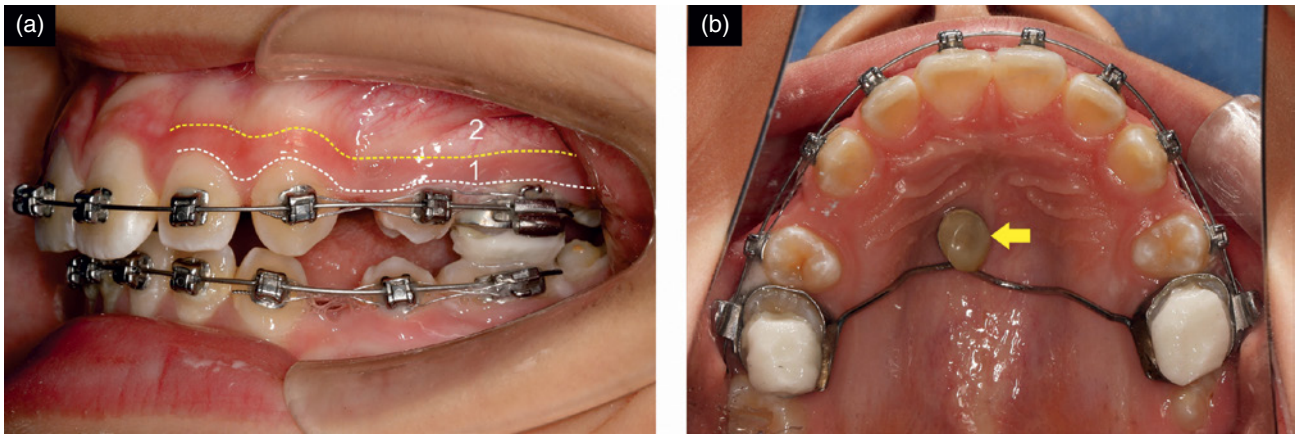


Figure 15.15 Prudent selection of an insertion site. (a) This extraction case required insertion of mini-implants to reinforce molar anchorage. The initial plan was to insert mini-implants at buccal sites (between second premolars and first molars). Note the narrow keratinised gingiva zone (the yellow and white dashed lines indicate mucogingival junction and free gingiva, respectively). If a mini-implant was placed at zone 1, it would be too occlusal and vulnerable to loosening. If the mini-implant was inserted apically (site 2), it would be in the movable mucosa zone and susceptible to postinsertion soft tissue complications. (b) The final decision was to place an orthodontic mini-implant at the palatal side (yellow arrow). Molar anchorage was augmented through a palatal bar that was fixed onto the mini-implant using flowable resin.

scenarios, angled insertion techniques and the use of long mini-implants are recommended. In this way, the heads of mini-implants are located at the keratinised gingiva zone, reducing the likelihood of soft tissue complications (Figure 15.16a–d). Moreover, extension arms or extension hooks that are fixed on mini-implant heads could be used to reduce the likelihood of soft tissue complications (Figure 15.16e–g).

15.5.4 Prevention of Excessive Soft Tissue Trauma

Soft tissue trauma occurs during penetration of soft tissue by the mini-implant and excessive trauma may result in prolonged healing and postinsertion soft tissue complications. Thus, appropriate measures should be taken to prevent excessive soft tissue trauma.

If the mini-implant is inserted at the keratinised gingiva area, penetration of the soft tissue by the mini-implant does not result in tearing and excessive trauma of the surrounding soft tissue since the keratinised gingiva is attached and fixed onto the alveolar bone. In contrast, soft tissue may wrap around the mini-implant and excessive trauma and tearing may occur if the mini-implant is placed at the movable mucosa zone. Thus, to prevent excessive soft tissue trauma, soft tissue punch or flap elevation is recommended for mini-implants that are to be placed at the movable mucosa zone.

Moreover, auxiliary appliances (e.g. closed-coil springs) may impinge and compress soft tissues and cause irritation and trauma. Appropriate measures should be taken to prevent soft tissue impingement, e.g. wrapping the closed-coil spring in a soft plastic tube and adding a power arm to keep the elastics away from the soft tissue (Figure 15.17).

t.me/Dr_Mouayyad_AlbtousH

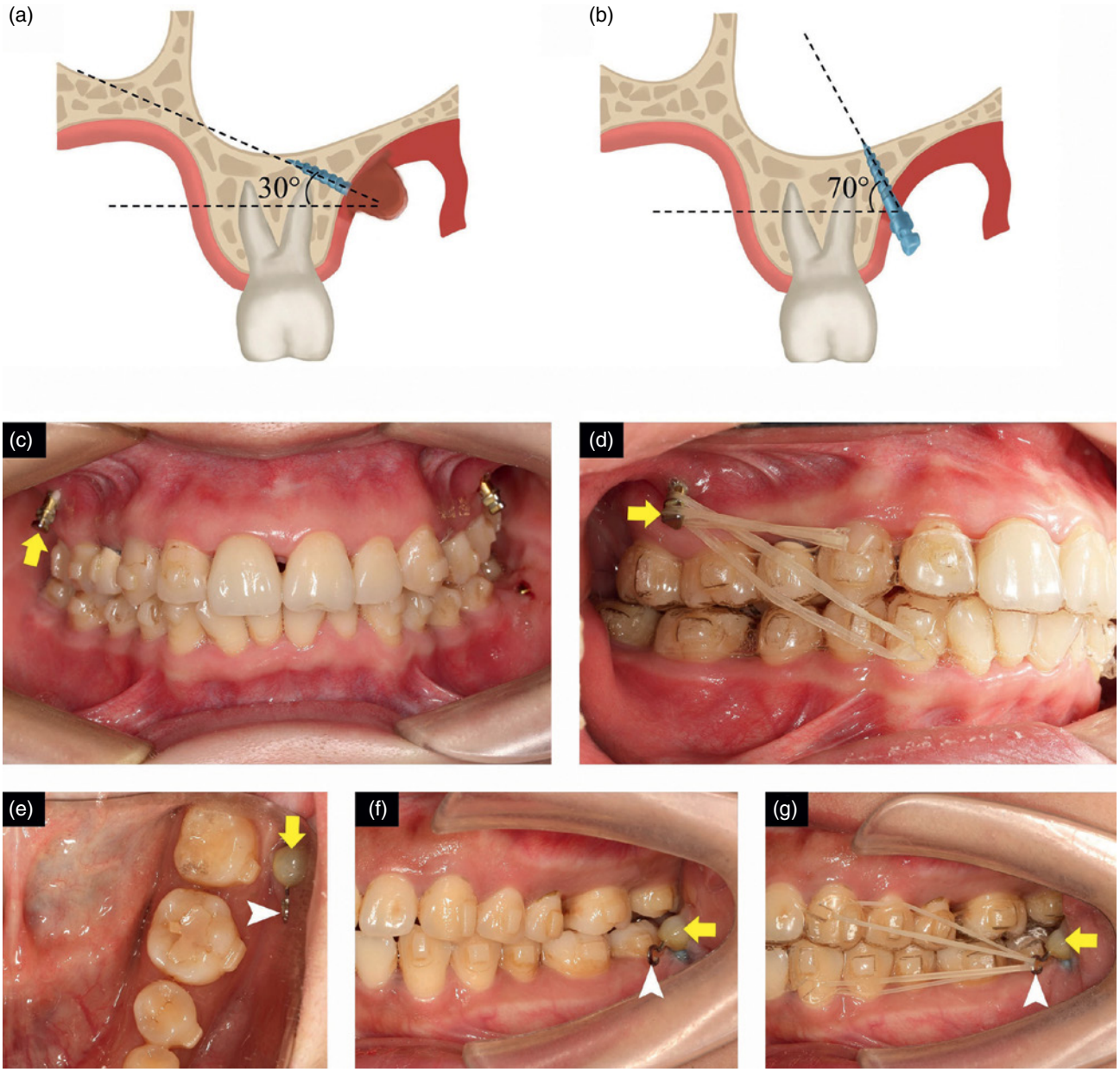


Figure 15.16 Sophisticated insertion techniques reduce the risk of soft tissue complications. (a) The infrazygomatic crest is covered with thick soft tissue, thus the heads of infrazygomatic mini-implants should be as occlusal as possible, in order to reduce the risk of soft tissue complications. Horizontal or inadequate angled insertion results in mini-implant wrapping by hyperplastic soft tissue. (b) Angled insertion technique (70° to occlusal plane) places the head of the mini-implant at the keratinised gingiva zone, reducing the likelihood of soft tissue complications. (c) Frontal view. Infrazygomatic mini-implants (yellow arrow) were inserted using angled insertion technique and their heads were located in the keratinised gingiva zone. (d) Lateral view. The infrazygomatic mini-implant (yellow arrow) was used for molar distalisation with clear aligners. (e) Buccal shelf is covered with thick soft tissue. The head of the buccal shelf mini-implant (yellow arrow) is likely to be wrapped and embedded by the overgrown soft tissue. An extension hook (white arrowhead) was fixed onto the mini-implant with ligature wire and flowable resin. (f,g) Lateral view. The extension hook (white arrowhead) was in the keratinised gingiva zone, while the head of the mini-implant (yellow arrow) was in the movable mucosa zone. Thus, the extension hook was used with elastics to deliver distalisation force with clear aligners.

t.me/Dr_Mouayyad_AlbtousH

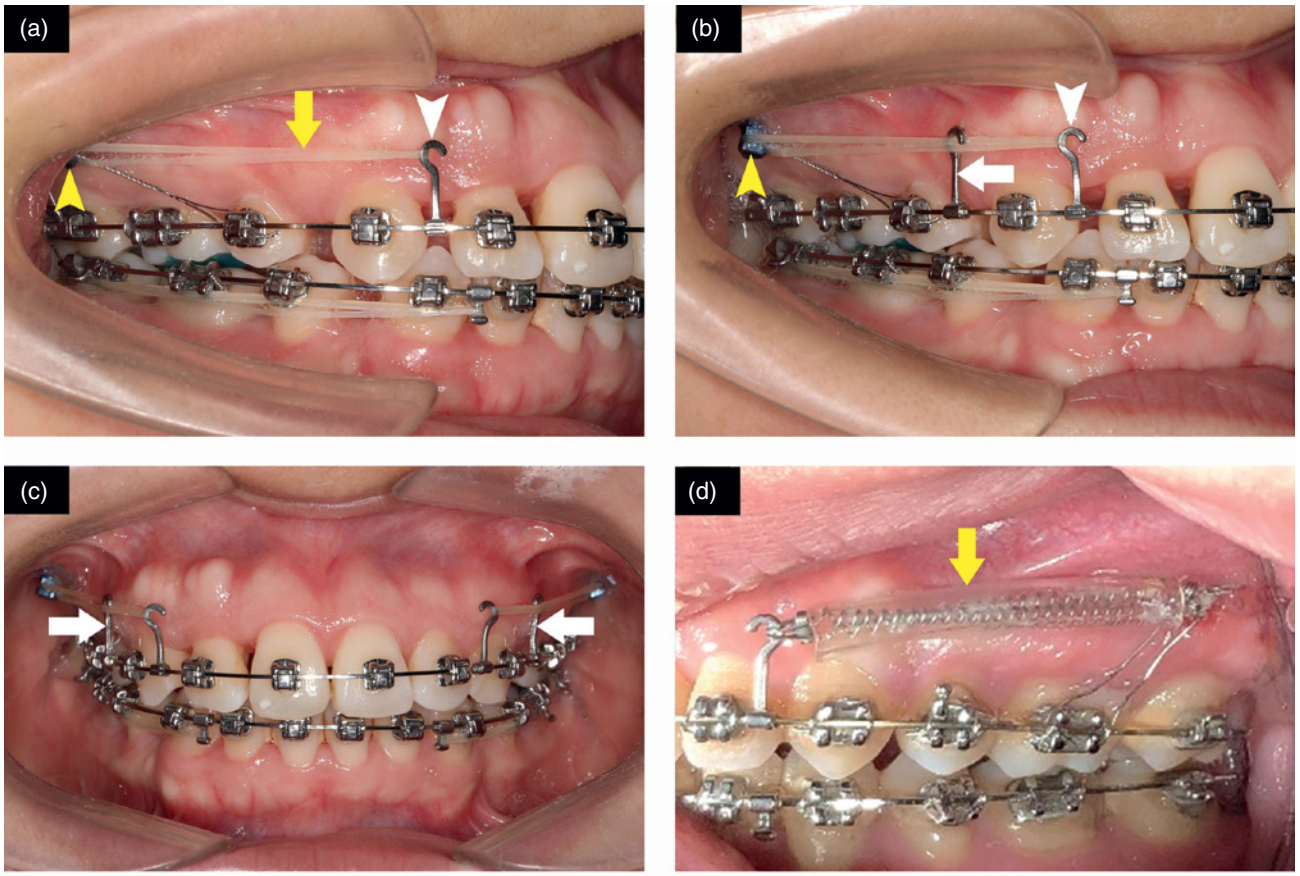


Figure 15.17 Prevention of soft tissue trauma. (a) An elastic rubber (yellow arrow) was placed between an infrazygomatic mini-implant (yellow arrowhead) and a crimpable long hook (white arrowhead). The elastic rubber impinged on the soft tissue. (b,c) An additional crimpable long hook (white arrow) was added on the archwire between the canine and second premolar to keep the elastic rubber away from the soft tissue. (d) To avoid soft tissue complications, closed-coil springs were wrapped by a plastic tube (yellow arrow) that can protect the soft tissue from trauma.

15.6 Treatment

15.6.1 Peri-implant Irrigation and Scaling

For mild soft tissue complications (e.g. mild inflammation), peri-implant irrigation and scaling are recommended to control the inflammation. As mentioned above, following mini-implant placement, soft tissue heals to form a peri-implant sulcus. Microbial plaque accumulates in the sulcus to initiate soft issue inflammation. Thus, peri-implant irrigation and scaling are performed to eliminate the anaerobic microbial plaque inside the sulcus and reduce bacterial levels, so that soft tissue inflammation can be resolved. Specifically, for peri-implant irrigation, alternate irrigation with hydrogen peroxide (3%) and chlorhexidine (0.12%) is usually performed through a syringe (Figure 15.18). Peri-implant scaling should be performed adequately to remove microbial plaque in the sulcus and around the mini-implant head (Figure 15.19).

15.6.2 Removal of Causative Factors

When soft tissue trauma is encountered due to impingement of auxiliary appliances, the appliances should be removed or moved away from the soft tissue to facilitate soft tissue healing (Figure 15.20). Moreover, protective measures can be taken to remove the causative factors. A protective plastic tube can be used to wrap a closed-coil spring that impinges on the soft tissue. Also, flowable resin can be added onto the sharp edges of mini-implants or auxiliary appliances that cause soft tissue irritation.

15.6.3 Local Debridement and Drainage

If necrotic soft tissue is present, debridement should be performed. In addition, pus should be drained if present. Irrigation with hydrogen peroxide and saline (or chlorhexidine) is recommended to help the drainage of inflammatory secretions and pus.

t.me/Dr_Mouayyad_AlbtousH

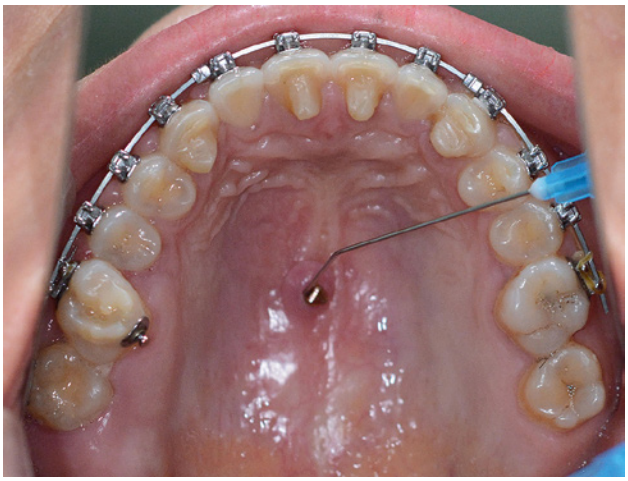


Figure 15.18 Soft tissue inflammation associated with a palatal mini-implant. The sulcus between the mini-implant and the soft tissue was alternately irrigated with hydrogen peroxide and chlorhexidine.

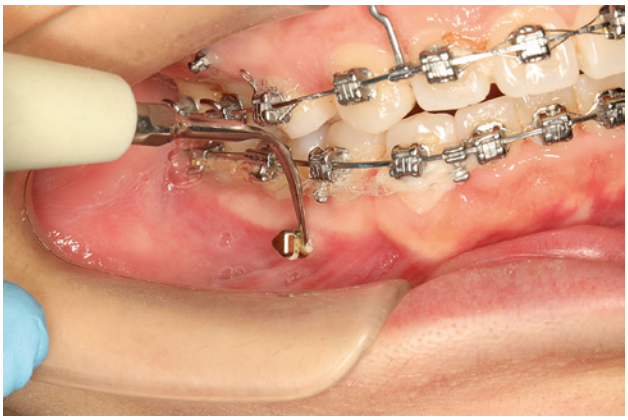


Figure 15.19 Ultrasonic scaling for a mini-implant. Ultrasonic scaling was performed to remove plaque in the sulcus formed by the mucosa and the mini-implant.

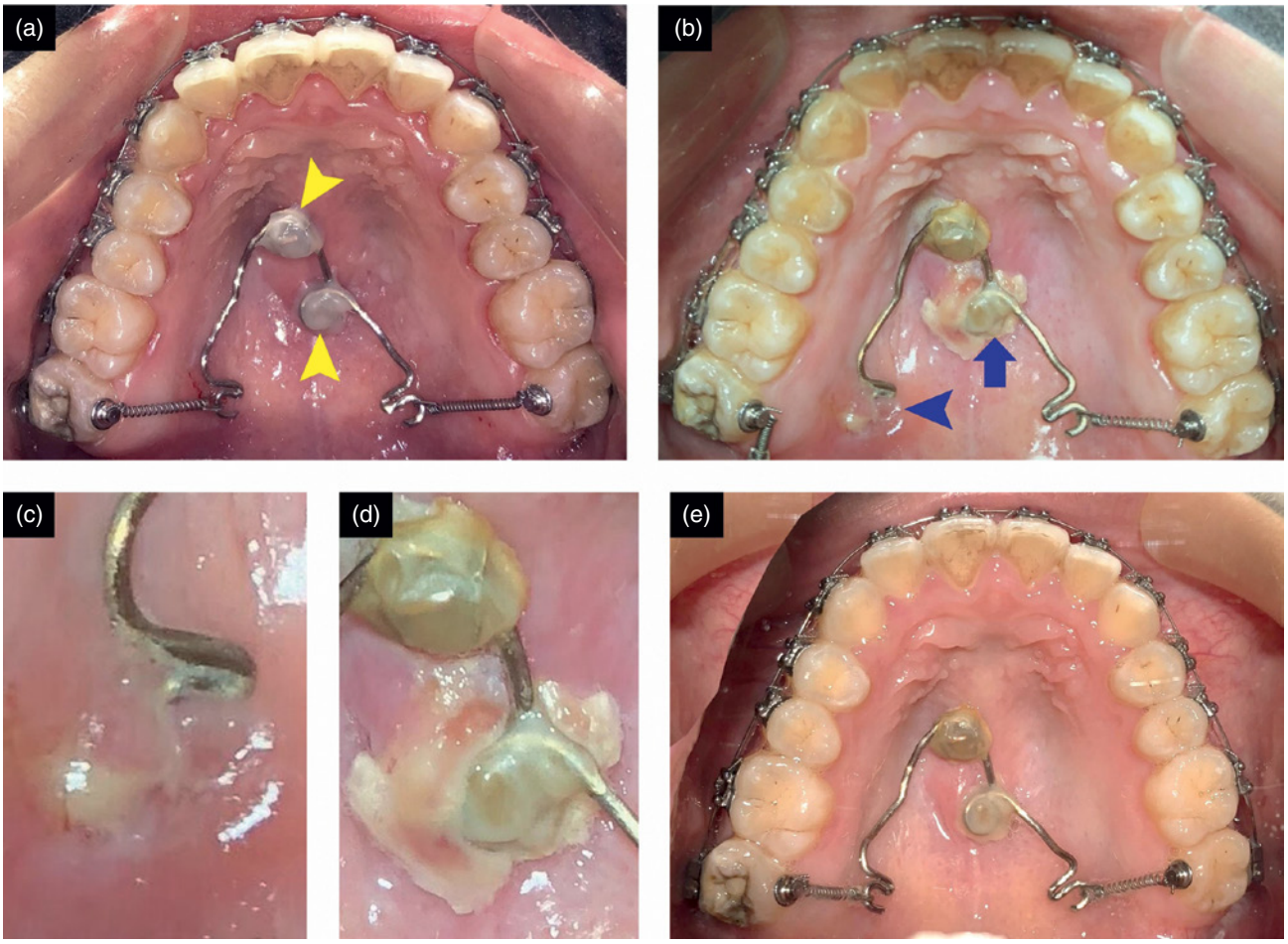


Figure 15.20 Timely removal of causative factors and local debridement and irrigation for the management of peri-implant soft tissue inflammation. (a) Two orthodontic mini-implants (yellow arrowheads) were inserted at the palatal vault. Two distal extension hooks were fixed onto the mini-implants with flowable resin for intrusion of maxillary second molars. (b) The right extension hook impinged on the palatal mucosa and caused mucosa trauma (blue arrowhead). Inflamed soft tissue around the distal mini-implant became whitish and necrotic (blue arrow). To remove the causative factor, the right extension hook was bent away from the palatal mucosa. The necrotic mucosa was excised and debrided. (c) Close-up view of the soft tissue inflammation caused by the distal extension hook. (d) Close-up view of the necrotic mucosa around the mini-implant. (e) Three days later, the soft tissue complications were resolved.

t.me/Dr_Mouayyad_AlbtousH

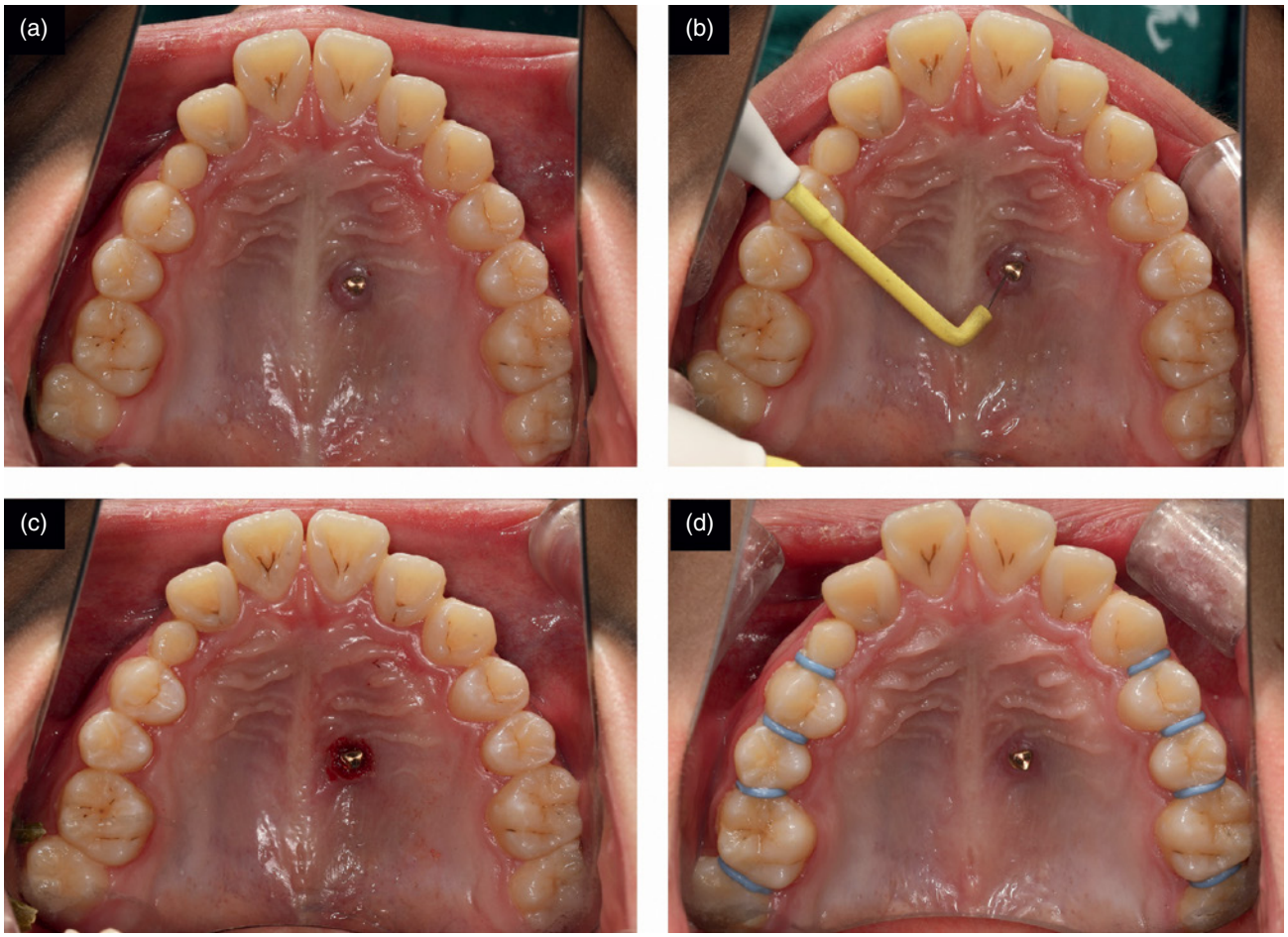


Figure 15.21 Excision of hypertrophic soft tissue around an orthodontic mini-implant. (a) Soft tissue hypertrophy around a palatal mini-implant. (b) The hypertrophic soft tissue was excised with an electrode from an electrosurgical kit. (c) Occlusal view after the excision. (d) Ten days later, the mucosa around the mini-implant had healed completely.

15.6.4 Excision of Hypertrophic Soft Tissue

Severe soft tissue hypertrophy should be surgically excised under local anaesthesia. Usually, the hyperplastic soft tissue is excised along the margins of the tissue surrounding the mini-implant (Figure 15.21). Afterwards, patients are instructed to maintain oral hygiene and use chlorhexidine mouthwash to facilitate wound healing.

15.7 Summary

Soft tissue complications associated with orthodontic TADs are not infrequently encountered in clinical practice and are manifested as swelling, hyperplasia, infection and lesion. Patient factors, operator factors and implant-associated factors influence individuals' risk of peri-implant soft tissue complications. Meticulous oral hygiene, prudent selection of insertion sites and the application of sophisticated insertion techniques can be implemented to prevent the occurrence of soft tissue complications. Furthermore, if soft tissue complications are encountered, peri-implant irrigation and scaling, the removal of causative factors, local debridement and drainage and surgical resection of hypertrophic soft tissue can be applied.

t.me/Dr_Mouayyad_AlbtousH

References

1 Gurdan Z, Szalma J. (2018). Evaluation of the success and complication rates of self-drilling orthodontic mini-implants. *Niger. J. Clin. Pract.* 21(5): 546–552.

2 Costa FO, Takenaka-Martinez S, Cota LO, Ferreira SD, Silva GL, Costa JE. (2012). Peri-implant disease in subjects with and without preventive maintenance: a 5-year follow-up. *J. Clin. Periodontol.* 39(2): 173–181.

3 Takaki T, Tamura N, Yamamoto M et al. (2010). Clinical study of temporary anchorage devices for orthodontic treatment – stability of micro/mini-screws and mini-plates: experience with 455 cases. *Bull. Tokyo Dent. Coll.* 51(3): 151–163.

4 Park HS, Jeong SH, Kwon OW. (2006). Factors affecting the clinical success of screw implants used as orthodontic anchorage. *Am. J. Orthod. Dentofacial Orthop.* 130(1): 18–25.

5 Chen YJ, Chang HH, Lin HY, Lai EH, Hung HC, Yao CC. (2008). Stability of miniplates and miniscrews used for orthodontic anchorage: experience with 492 temporary anchorage devices. *Clin. Oral Implants Res.* 19(11): 1188–1196.

6 Sato R, Sato T, Takahashi I, Sugawara J, Takahashi N. (2007). Profiling of bacterial flora in crevices around titanium orthodontic anchor plates. *Clin. Oral Implants Res.* 18(1): 21–26.

7 Roos-Jansåker AM, Renvert H, Lindahl C, Renvert S. (2006). Nine- to fourteen-year follow-up of implant treatment. Part III: factors associated with peri-implant lesions. *J. Clin. Periodontol.* 33(4): 296–301.

8 Cardoso JM, Ribeiro AC, Palos C, Proenca L, Noronha S, Alves RC. (2022). Association between IL-1A and IL-1B gene polymorphisms with peri-implantitis in a Portuguese population-a pilot study. *PeerJ.* 10: e13729.

9 Chen Z, Chen G. (2021). Interleukin-16 rs4072111 polymorphism is associated with the risk of peri-implantitis in the Chinese population. *Pharmgenomics Pers. Med.* 14: 1629–1635.

10 Prathapachandran J, Suresh N. (2012). Management of peri-implantitis. *Dent. Res. J.* 9(5): 516–521.

11 Apel S, Apel C, Morea C, Tortamano A, Dominguez GC, Conrads G. (2009). Microflora associated with successful and failed orthodontic mini-implants. *Clin. Oral Implants Res.* 20(11): 1186–1190.

12 Leonhardt A, Dahlén G, Renvert S. (2003). Five-year clinical, microbiological, and radiological outcome following treatment of peri-implantitis in man. *J. Periodontol.* 74(10): 1415–1422.

13 Gomi K, Matsushima Y, Ujiie Y et al. (2015). Full-mouth scaling and root planing combined with azithromycin to treat peri-implantitis. *Austr. Dent. J.* 60(4): 503–510.

14 Rylander H, Ramberg P, Blohme G, Lindhe J. (1987). Prevalence of periodontal disease in young diabetics. *J. Clin. Periodontol.* 14(1): 38-–3.

15 de Freitas AO, Alviano CS, Alviano DS, Siqueira JF Jr, Nojima LI, Nojima Mda C. (2012). Microbial colonization in orthodontic mini-implants. *Braz. Dent. J.* 23(4): 422–427.

16 Schwarz F, Derks J, Monje A, Wang HL. (2018). Peri-implantitis. *J. Clin. Periodontol.* 45 Suppl 20: S246–s266.

17 Derks J, Tomasi C. (2015). Peri-implant health and disease. A systematic review of current epidemiology. *J. Clin. Periodontol.* 42 Suppl 16: S158–171.

18 Monje A, Wang HL, Nart J. (2017). Association of preventive maintenance therapy compliance and peri-implant diseases: a cross-sectional study. *J. Periodontol.* 88(10): 1030–1041.

19 Bayat E, Bauss O. (2010). Effect of smoking on the failure rates of orthodontic miniscrews. *J. Orofac. Orthop.* 71(2): 117–124.

20 Lopes TF, Souza CM, Reichow AM, Melo AC, Trevilatto PC. (2019). Analysis of the association of IL4 polymorphisms with orthodontic mini-implant loss. *Int. J. Oral Maxillofac. Surg.* 48(7): 982–988.

21 Hom S, Chen L, Wang T, Ghebrehiwet B, Yin W, Rubenstein DA. (2016). Platelet activation, adhesion, inflammation, and aggregation potential are altered in the presence of electronic cigarette extracts of variable nicotine concentrations. *Platelets* 27(7): 694–702.

22 Levin L, Schwartz-Arad D. (2005). The effect of cigarette smoking on dental implants and related surgery. *Implant Dent.* 14(4): 357–361.

23 Fang Y, Svoboda KK. (2005). Nicotine inhibits human gingival fibroblast migration via modulation of Rac signalling pathways. *J. Clin. Periodontol.* 32(12): 1200–1207.

24 Snyder HB, Caughman G, Lewis J, Billman MA, Schuster G. (2002). Nicotine modulation of in vitro human gingival fibroblast beta1 integrin expression. *J. Periodontol.* 73(5): 505–510.

25 Ma L, Zwahlen RA, Zheng LW, Sham MH. (2011). Influence of nicotine on the biological activity of rabbit osteoblasts. *Clin. Oral Implants Res.* 22(3): 338–342.

26 Sayardoust S, Omar O, Norderyd O, Thomsen P. (2018). Implant-associated gene expression in the jaw bone of smokers and nonsmokers: a human study using quantitative qPCR. *Clin. Oral Implants Res.* 29(9): 937–953.

27 Nazeer J, Singh R, Suri P et al. (2020). Evaluation of marginal bone loss around dental implants in cigarette smokers and nonsmokers. A comparative study. *J. Family Med. Prim. Care* 9(2): 729–734.

t.me/Dr_Mouayyad_AlbtousH

28 Radi IA, Elsayyad AA. (2022). Smoking might increase the failure rate and marginal bone loss around dental implants. *J. Evid. Based Dent. Pract.* 22(4): 101804.

29 Lindquist LW, Carlsson GE, Jemt T. (1997). Association between marginal bone loss around osseointegrated mandibular implants and smoking habits: a 10-year follow-up study. *J. Dent. Res.* 76(10): 1667–1674.

30 Esfahanizadeh N, Daneshparvar N, Motallebi S, Akhondi N, Askarpour F, Davaie S. (2016). Do we need keratinised mucosa for a healthy peri-implant soft tissue? *Gen. Dent.* 64(4): 51–55.

31 Romanos G, Grizas E, Nentwig GH. (2015). Association of keratinised mucosa and periimplant soft tissue stability around implants with platform switching. *Implant Dent.* 24(4): 422–426.

32 Thoma DS, Gil A, Hammerle CHF, Jung RE. (2022). Management and prevention of soft tissue complications in implant dentistry. *Periodontology 2000* 88(1): 116–129.

33 Kungsadalpipob K, Supanimitkul K, Manopattanasoontorn S, Sophon N, Tangsathian T, Arunyanak SP. (2020). The lack of keratinised mucosa is associated with poor peri-implant tissue health: a cross-sectional study. *Int. J. Implant Dent.* 6(1): 28.

34 Barber CC, Burnham M, Ojameruaye O, McKee MD. (2021). A systematic review of the use of titanium versus stainless steel implants for fracture fixation. *OTA Int.* 4(3): e138.

35 Mecenas P, Espinosa DG, Cardoso PC, Normando D. (2020). Stainless steel or titanium mini-implants? *Angle Orthod.* 90(4): 587–597.

36 Tanner MC, Fischer C, Schmidmaier G, Haubruck P. (2021). Evidence-based uncertainty: do implant-related properties of titanium reduce the susceptibility to perioperative infections in clinical fracture management? *A systematic review. Infection* 49(5): 813–821.

37 Lackington WA, Fleyshman L, Schweizer P, Elbs-Glatz Y, Guimond S, Rottmar M. (2022). The response of soft tissue cells to Ti implants is modulated by blood–implant interactions. *Mater. Today Bio.* 15: 100303.

38 Bouri A Jr, Bissada N, Al-Zahrani MS, Faddoul F, Nouneh I. (2008). Width of keratinised gingiva and the health status of the supporting tissues around dental implants. *Int. J. Oral Maxillofac. Implants* 23(2): 323–326.

39 Roccuzzo M, Grasso G, Dalmasso P. (2016). Keratinised mucosa around implants in partially edentulous posterior mandible: 10-year results of a prospective comparative study. *Clin. Oral Implants Res.* 27(4): 491–496.

t.me/Dr_Mouayyad_AlbtousH

16

Failure of Orthodontic Temporary Anchorage Devices

Xinyu Yan[1], Xiaoqi Zhang[1], Jianru Yi[1], Chen Liang[2], Xi Du[1], Lingling Pu[1,2], and Hu Long[1]

[1] *Department of Orthodontics, State Key Laboratory of Oral Diseases and National Clinical Research Center for Oral Diseases, West China Hospital of Stomatology, Sichuan University, Chengdu, China*
[2] *Private Practice, Chengdu, China*

16.1 Introduction

The failure of orthodontic TADs is defined as a clinical situation in which TADs are unable to withstand orthodontic loading due to loosening or mobility (Figure 16.1). Mini-implants and miniplates are the two most frequently used orthodontic TADs. Much evidence has revealed that the failure rate of miniplates is lower than that of mini-implants.[1-3] Moreover, miniplates are considered to be a viable back-up solution for failed mini-implants among patients who still require absolute anchorage.[4] Thus, in this chapter, we will mainly discuss the failure of mini-implants.

Mini-implant failure is clinically manifested as loosening and great mobility of mini-implants when orthodontic loading is applied, which is often accompanied by peri-implant soft tissue inflammation and pain (Figure 16.2). The overall failure rate of mini-implants ranges from 1% to 56% and varies greatly among different clinical scenarios,[5-10] depending on a variety of factors, e.g. age, anatomical site, mini-implant design, first or secondary insertion and insertion techniques.[11-13] In particular, the failure rate differs among different anatomical sites (Figure 16.3) and is influenced by local bone quality and soft tissue conditions.[14-16]

In addition to soft tissue inflammation and pain, the most adverse consequence of mini-implant failure is that the implant is dislodged from alveolar bone and may be

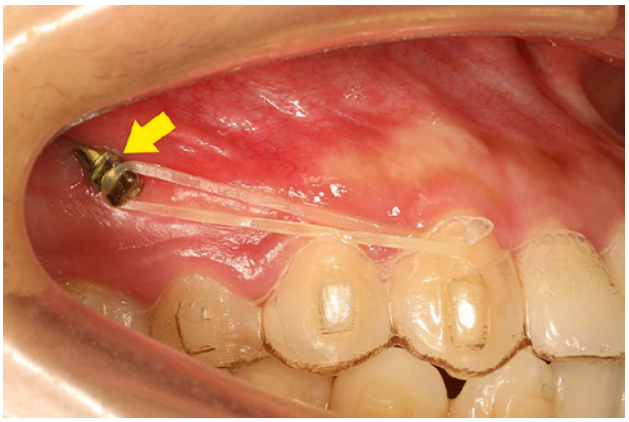


Figure 16.1 A mini-implant at the infrazygomatic crest region became loose and failed to serve as an anchorage for orthodontic elastics. Note the loose mini-implant (yellow arrow) was displaced by the elastics.

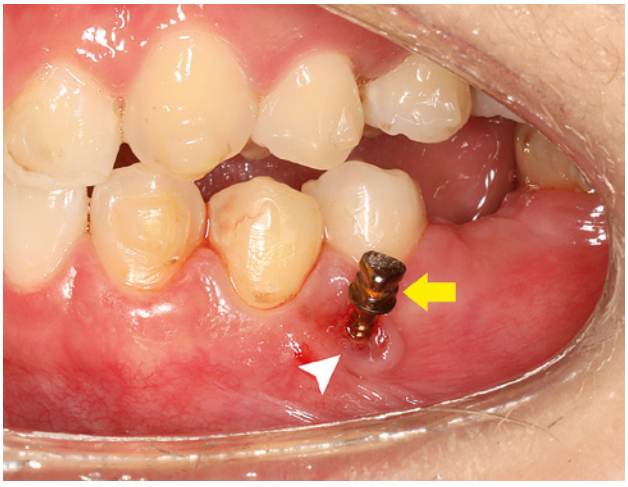


Figure 16.2 Loosening and displacement of a mini-implant (yellow arrow). Note the peri-implant soft tissue inflammation (white arrowhead).

Clinical Insertion Techniques of Orthodontic Temporary Anchorage Devices, First Edition. Edited by Hu Long, Xianglong Han, and Wenli Lai.
© 2024 John Wiley & Sons Ltd. Published 2024 by John Wiley & Sons Ltd.

t.me/Dr_Mouayyad_AlbtousH

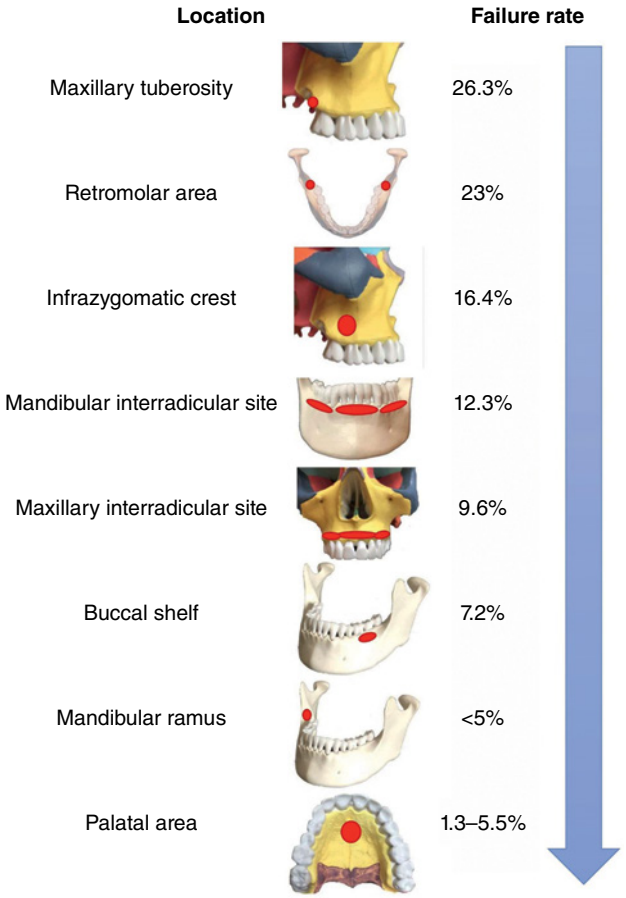


Figure 16.3 Failure rates of orthodontic mini-implants at different anatomical locations. Notably, mini-implants placed at the maxillary tuberosity and retromolar areas exhibit the highest failure rate while those inserted at the mandibular ramus and palatal areas have the lowest failure rate.

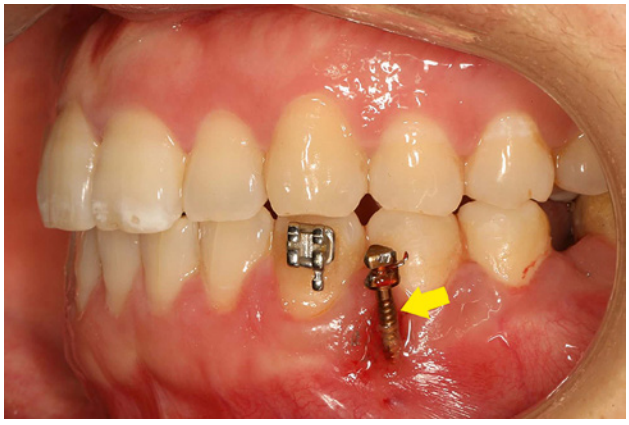


Figure 16.4 A mini-implant became loose and was dislodged from the alveolar bone. The mini-implant thread could be observed (yellow arrow).

swallowed by patients accidentally (Figure 16.4). Fortunately, an animal study has shown that all ingested mini-implants (10/10) were excreted naturally and uneventfully.[17]

16.2 Primary Stability and Secondary Stability

For mini-implants, two types of mini-implant stability have been described: primary and secondary.[18] Primary stability is the stability achieved by mechanical compression, interlocking and retention between the mini-implant and the alveolar bone. In contrast, secondary stability, also called biological stability, is accomplished by active alveolar bone healing or remodelling at the implant–bone interface. Moreover, primary stability is formed by existing bone ('old' bone) and decreases gradually after the insertion of mini-implants, while secondary stability is achieved by new bone and increases gradually after the placement of mini-implants. Thus, bone remodelling around mini-implants is a delicate process of bone resorption (decrease in primary stability) and bone apposition (increase in secondary stability). Clinical stability of mini-implants is a combination of primary and secondary stability (Figure 16.5).

To reduce the failure rate of mini-implants, both primary and secondary stability should be ensured. As mentioned above, primary stability is dependent on mechanical interlocking and retention between mini-implants and alveolar bone. Bone quality and mini-implant geometry are of great importance to primary stability (Figure 16.6). It has been well documented that primary stability is higher for mini-implants inserted at alveolar bone with higher bone density and thicker cortex.[19] In addition, higher primary stability can be obtained for longer mini-implants with larger diameters.[20,21] Therefore, in clinical practice, alveolar bone with good bone quality and mini-implants with adequate sizes should be chosen to ensure primary stability.

Primary and secondary stability are interrelated and the success of mini-implants is not only determined by primary stability.[22] Adequate primary stability offers a good basis for the development of secondary stability. Specifically, the motion of a mini-implant should be within an acceptable range to offer a suitable microenvironment for bone healing and remodelling (secondary stability). Otherwise, excessive micromovement of mini-implants results in excessive stress on the alveolar bone around the implant and interferes with bone healing and remodelling, leading to unacceptable secondary stability and mini-implant failure (Figure 16.7). Compared with cancellous bone, alveolar cortex is the principal component that resists force loading and is of more importance to primary stability. Excessive stress is present in cancellous bone around a mini-implant inserted into alveolar bone with cortical thickness less than 1 mm.[23] Thus, to ensure adequate primary stability, it is recommended that mini-implants be inserted at anatomical sites with cortical thickness equal to or greater than 1 mm by both finite element analysis and clinical studies.[23,24]

t.me/Dr_Mouayyad_AlbtousH

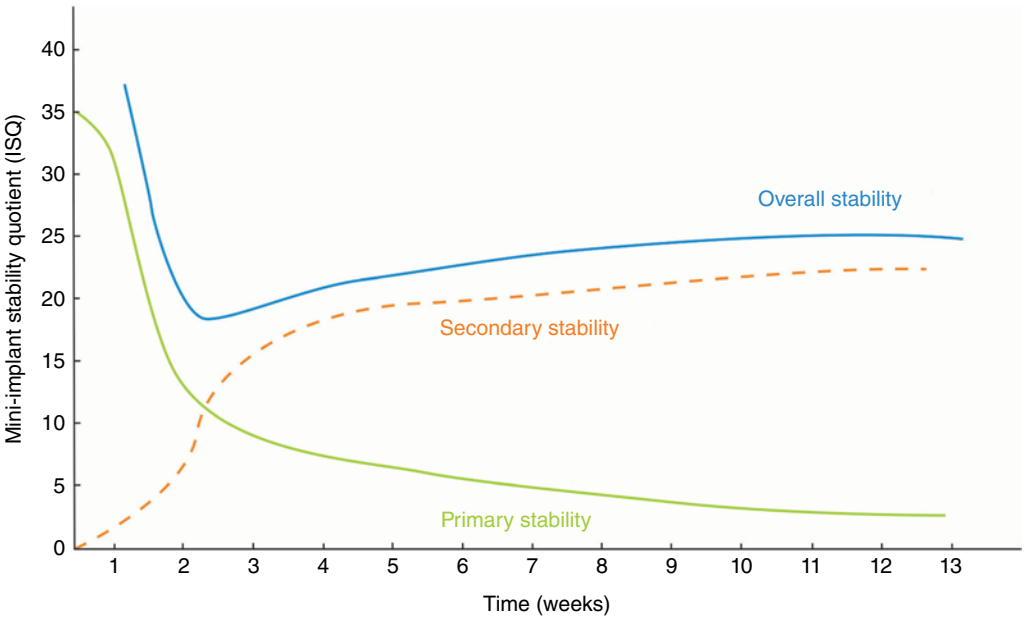


Figure 16.5 The overall stability of mini-implants is governed by both primary and secondary stability. Primary stability is greatest shortly after insertion of the mini-implant and decreases gradually thereafter. In contrast, secondary stability increases gradually following placement of the mini-implant due to alveolar bone remodelling. The overall stability, or clinical stability, is the sum of the primary and secondary stability and exhibits a 'V-pattern' change after mini-implants are inserted.

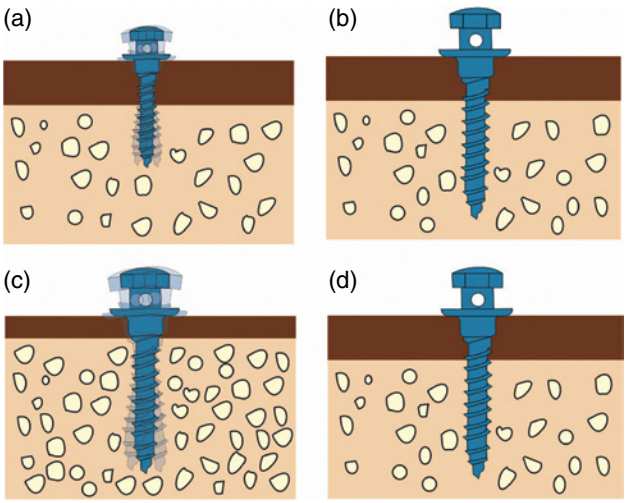


Figure 16.6 Primary stability is affected by mini-implant geometry and bone quality. Larger and longer mini-implants are more stable than smaller and shorter ones (a,b). Mini-implants inserted in bones with high density and thick cortical bone are more stable than those in alveolar bones with low density and thin cortical bone (c,d).

A paradox is often encountered in clinical practice: the success rate of mini-implants is higher in the maxilla than in the mandible. Theoretically, with higher bone density and thicker cortex in mandibular sites, both primary stability and success rate should be higher in these sites. This clinical paradox may be explained by a trade-off relationship between primary and secondary stability. During insertion of mini-implants, alveolar bone is inevitably damaged due to mechanical and thermal reasons. The damage is manifested as bone microcracks and even necrosis, resulting in undesirable secondary stability (Figure 16.8). Moreover, both mechanical and thermal damage is greater for thicker alveolar cortex (Figure 16.9).[25,26] If alveolar bone cortex is too thick, although primary stability is high, bone healing and remodelling are hindered due to excessive bone damage, resulting in poor secondary stability and even mini-implant failure. Therefore, cortical thickness is recommended to be 1–2 mm to secure an orchestrated combination of primary and secondary stabilities, resulting in optimal clinical stability of mini-implants.

t.me/Dr_Mouayyad_AlbtousH

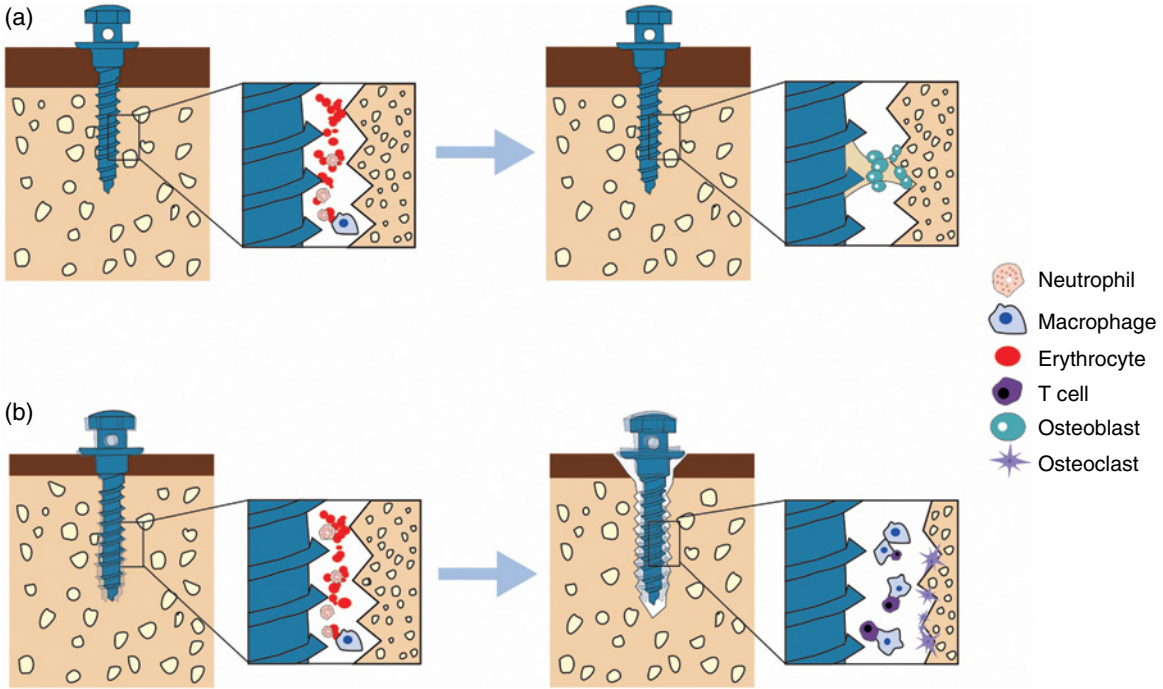


Figure 16.7 Primary stability is a prerequisite for the development of secondary stability. (a) If a mini-implant exhibits low micromovement following insertion, desired bone remodelling is anticipated and adequate secondary stability will be established. (b) If a mini-implant exhibits excessive micromovement when inserted, poor secondary stability will be generated with abnormal inflammatory reactions.

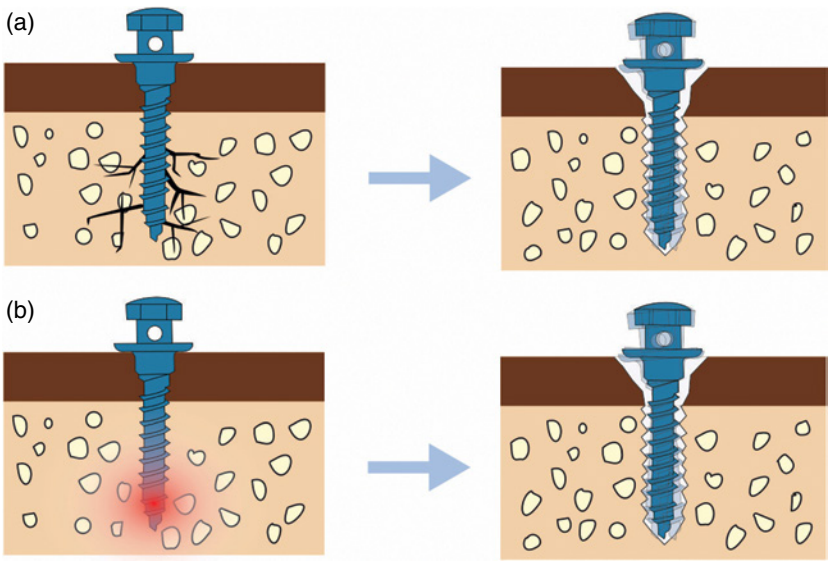


Figure 16.8 Secondary stability of mini-implants is jeopardised by mechanical and thermal damages. (a) A mini-implant associated with excessive bone cracks is subject to undesired alveolar bone remodelling and exhibits poor secondary stability. (b) A mini-implant causes thermal damage to surrounding bone and leads to unsatisfactory bone remodelling, resulting in inadequate secondary stability.

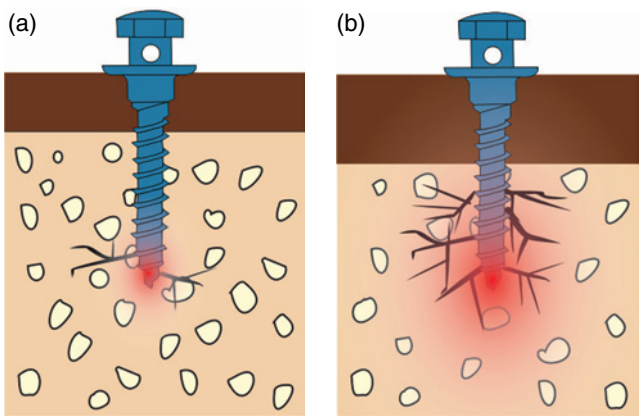


Figure 16.9 The influence of cortical thickness on the extent of thermal damage by mini-implants. (a) The mini-implant induces limited thermal damage to alveolar bone with thin cortex. (b) The mini-implant generates great thermal damage to alveolar bone with thick cortex.

t.me/Dr_Mouayyad_AlbtousH

16.3 Risk Factors

16.3.1 Patient-associated Factors

Mini-implant failure is influenced by both patient systemic factors (i.e. individual susceptibility, oral hygiene, smoking habits) and local factors (i.e. cortical thickness, cancellous bone density, soft tissue type) (Figure 16.10).

Systemic Factors

As mentioned above, following the insertion of mini-implants, active bone healing and remodelling take place at the implant–bone interface.[27] An orchestrated cascade of cytokines (i.e. IL-6) participates in this remodelling process (Figure 16.11a).[28] A large body of evidence suggesets that genetic variations (single nucleotide polymorphisms) of these cytokines were found among different patients and these genetic differences were significantly associated with mini-implant failure.[29-31] This molecular exploration explains individual susceptibility to mini-implant failure, regardless of other influencing factors. To reiterate, bone remodelling is a delicate process of bone resorption (decrease in primary stability) and bone apposition (increase in secondary stability). During the active phase of bone remodelling at the implant–bone interface, the presence of periodontal pathogens triggers excessive production of inflammatory mediators and tips the balance towards bone resorption, resulting in mini-implant failure due to inadequate bone support (Figure 16.11b).

It has been reported that more periodontal pathogens were found around failed mini-implants than healthy mini-implants.[32] This could explain why inadequate oral hygiene is a risk factor for mini-implant failure.[6,15,33] Thus, meticulous oral hygiene should be emphasised to patients following insertion of mini-implants. Moreover, since smoking renders oral hygiene maintenance difficult, smoking is also considered as a risk factor for mini-implant failure.[11,34] Furthermore, a large body of evidence reveals that mini-implant failure is associated with age, but not gender.[2,8,35]

Local Factors

An orthodontic mini-implant fails if bone support is inadequate.[36,37] The bone support is governed by both cortical thickness and cancellous bone density. In particular, cortical thickness is more important to mini-implant stability than cancellous bone density.[23] The failure rate of mini-implants is high if cortical thickness is less than 1 mm, suggesting that cortical thickness should be 1 mm to ensure adequate stability.[23] Meanwhile, as mentioned above, secondary stability is hindered if alveolar cortex is too thick. A delicate finite element analysis study revealed that 95% stress was concentrated on cortex and 5% stress on

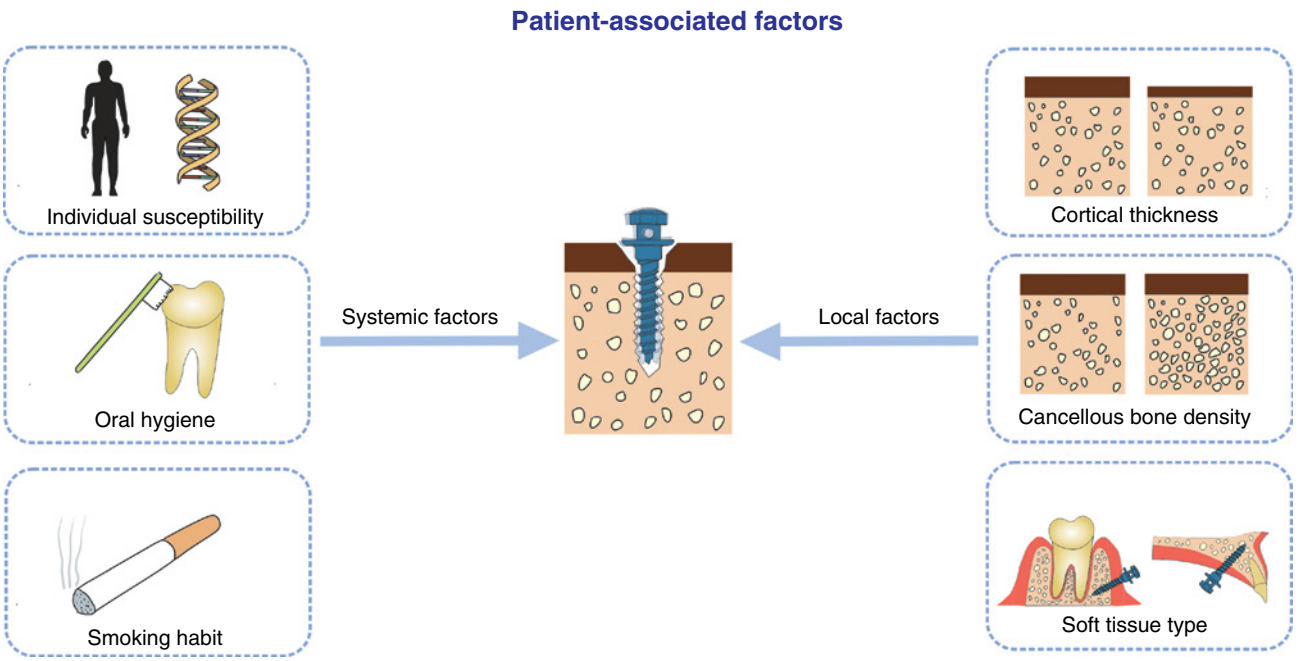


Figure 16.10 Mini-implant failure is influenced by both systemic and local factors.

t.me/Dr_Mouayyad_AlbtousH

cancellous bone when cortical thickness is 1.5 mm and that bone cortex withstands 100% stress when cortical thickness is 2 mm.[38] Given that no stress on cancellous bone fosters bone remodelling, cortical thickness greater than 2 mm is biomechanically redundant. Moreover, excessive mechanical and thermal damage may occur if cortex is too thick (Figure 16.9). Therefore, we recommend that mini-implants be inserted at anatomical sites with appropriate cortical thickness (1–2 mm). Furthermore, it has been well documented that soft tissue inflammation is a risk factor for mini-implant failure and that soft tissue type influences the success of mini-implants.[15,16] Specifically, mini-implants inserted at movable mucosa have a higher failure rate than those inserted at keratinised gingiva (Figure 16.12).[7,39] Thus, mini-implants should be inserted at the keratinised gingiva zone to minimise the risk of mini-implant failure.

16.3.2 Operator-associated Factors

Mini-implant failure is associated with a variety of operator factors, e.g. root proximity, insertion depth, insertion height and insertion angle (Figure 16.13). These factors are also associated with operator clinical experience and training.

Root Proximity

Both biomechanical and clinical studies reveal that root proximity or contact is a risk factor for mini-implant failure (Figure 16.14).[7,40,41] Mechanistically, it was revealed that alveolar bone stress is very high when mini-implants are inserted to the vicinity of dental roots,[42,43] which is not beneficial for the development of secondary stability. Moreover, when mini-implants are close to roots, the implants could be displaced by masticatory bite force, interfering with bone remodelling (secondary stability).[44-47]

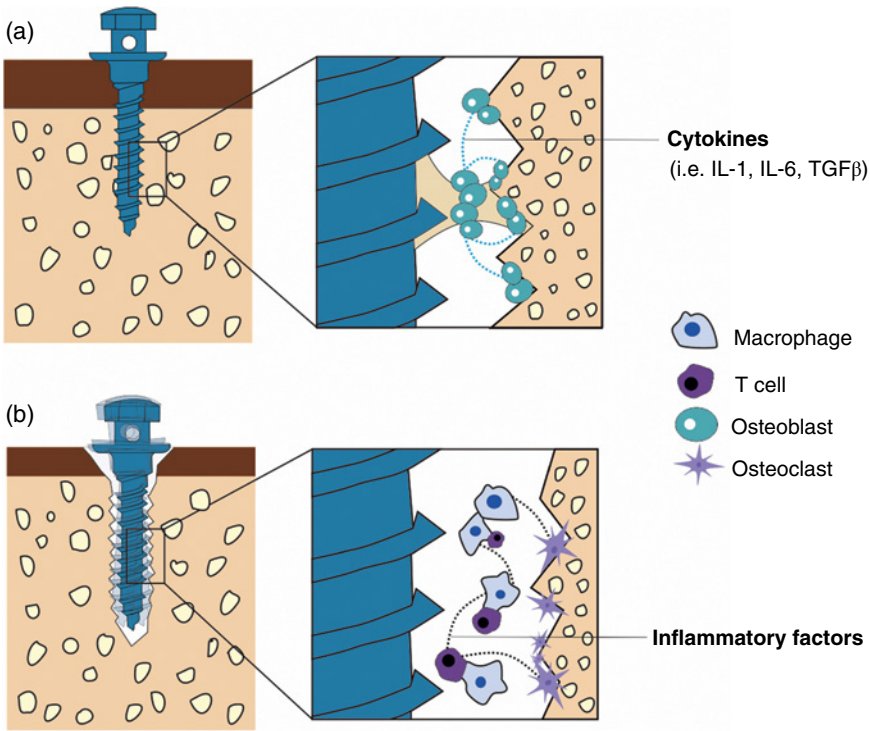


Figure 16.11 Different histological reactions determine the stability of mini-implants. (a) Satisfactory bone remodelling involves an orchestrated cascade of cytokines and results in adequate stability of the mini-implant. (b) The abnormal inflammatory reaction leads to poor stability of the mini-implant.

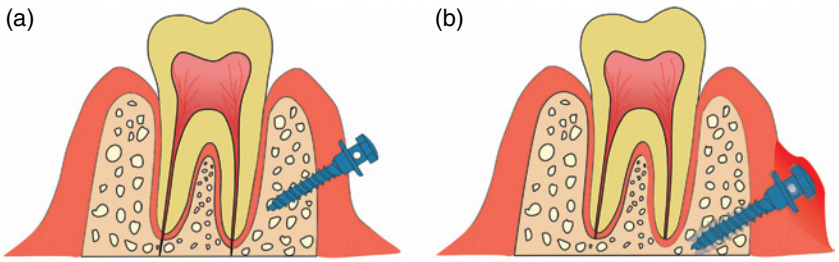


Figure 16.12 Mini-implants inserted at the movable mucosa have a higher failure rate than those inserted at the keratinised gingiva. (a) A mini-implant inserted at the attached gingiva exhibits good stability. (b) A mini-implant inserted at the alveolar mucosa exhibits poor stability and is associated with soft tissue inflammation.

t.me/Dr_Mouayyad_AlbtousH

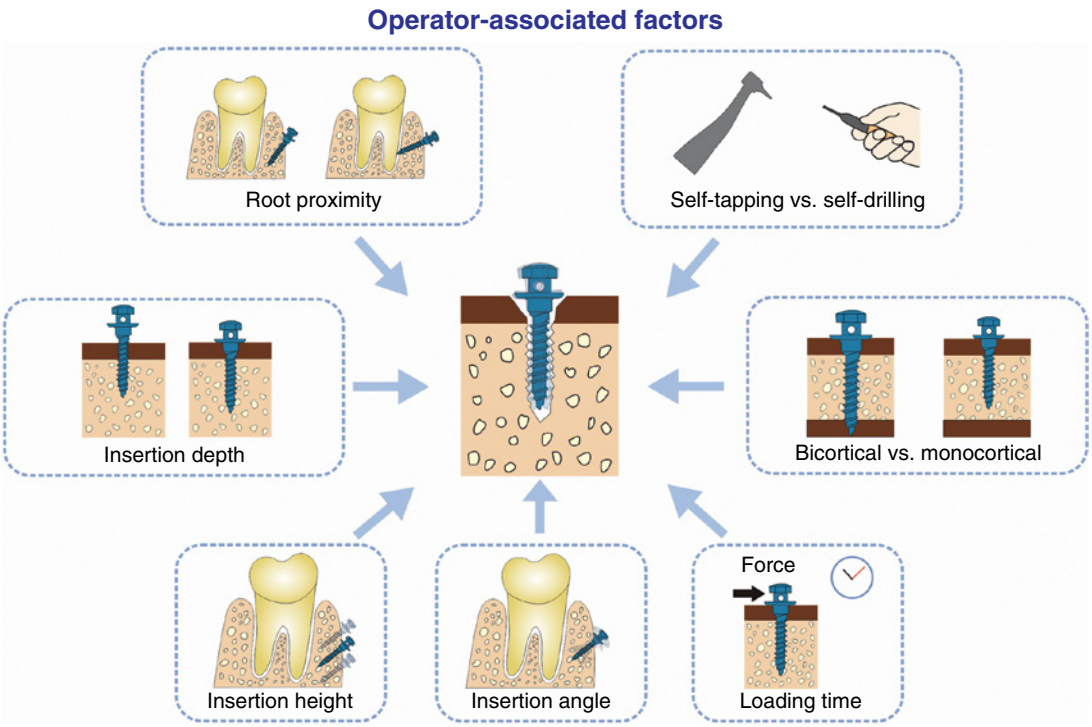
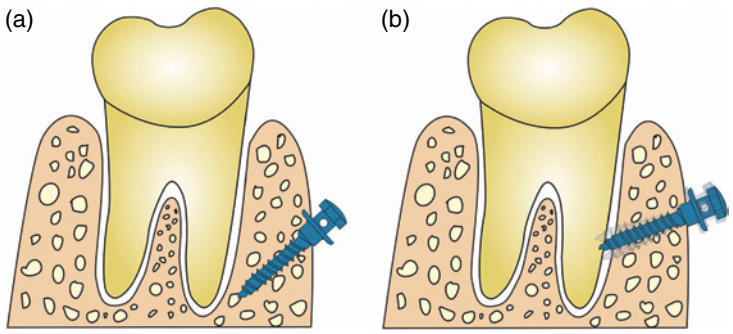


Figure 16.13 Mini-implant failure is associated with various operator factors, including root proximity, insertion depth, insertion height, insertion angle, loading time, cortical engagement and self-tapping or self-drilling.

Figure 16.14 The influence of root contact on mini-implant failure. (a) No root proximity occurs and the mini-implant exhibits sufficient stability. (b) The mini-implant with root contact displays poor stability and is susceptible to failure.



Insertion Depth

Mini-implant stability increases with increasing insertion depth, which could be explained by greater bone engagement with greater insertion depth.[48] In contrast, if insertion depth is inadequate, increased exposure length causes higher bone stress and interferes with the development of secondary stability (Figure 16.15).[49]

Insertion Height

Since interradicular space increases from cervical to apical sites, apical insertion site is beneficial to avoid root contact, thereby increasing the success rate of mini-implants.[47] Moreover, it has been shown that, regardless of root contact, the distance between implant tip and alveolar crest is negatively associated with mini-implant failure rate, probably due to higher bone quality at more apical sites (Figure 16.16).[35]

Insertion Angle

To minimise the likelihood of root proximity, angled insertion is recommended since the distance between mini-implants and roots increases significantly with increasing insertion angulation.[45] Regardless of the benefits of avoiding root contact, mini-implants subject to angled insertion (60–70° to bone surface) exhibited the highest primary stability,[46] probably due to greater cortical engagement

t.me/Dr_Mouayyad_AlbtousH

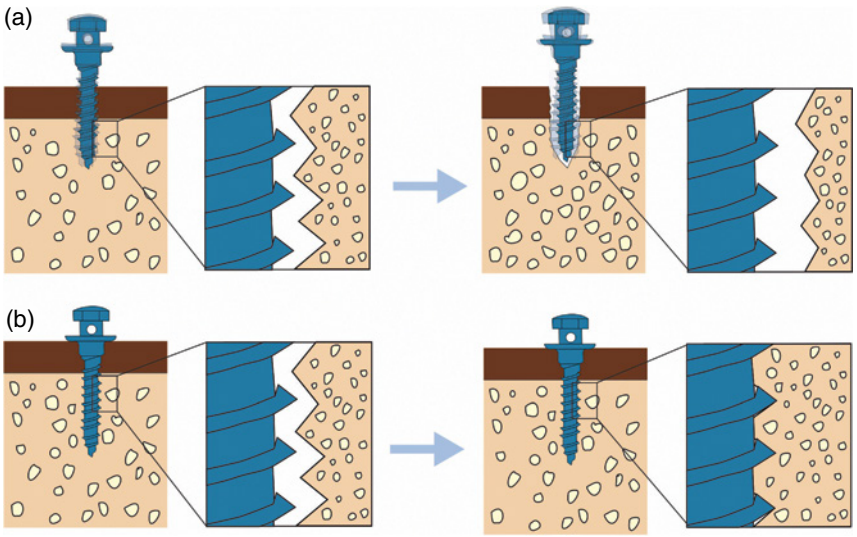


Figure 16.15 The influence of insertion depth on the stability of mini-implants. (a) The mini-implant inserted with limited depth exhibits insufficient stability, leading to poor bone remodelling and mini-implant failure. (b) The mini-implant inserted with greater depth displays adequate primary stability, resulting in adequate bone remodelling and sufficient stability.

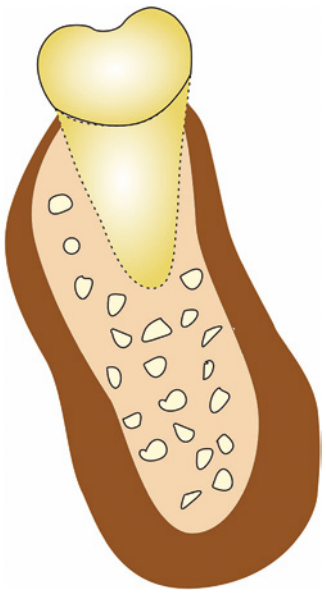


Figure 16.16 The thickness of cortical bone becomes greater from the alveolar crest to the alveolar base, hence mini-implants inserted more apically gain greater stability.

(Figure 16.17). Moreover, angled insertion (60–70° to bone surface) could significantly reduce stress on alveolar bone,[43] which is beneficial for the development of secondary stability.

Self-tapping versus Self-drilling

Our previous systematic review indicates that success rates are similar for both methods but that self-drilling mini-implants displayed a higher risk of failure when contacting with roots.[50] However, the insertion sites did not include anatomical sites with thick cortex (e.g. buccal shelf) among the included studies. This conclusion could not be generalised to these areas with high bone density and thick cortex where predrilling is recommended to reduce bone resistance and the likelihood of bone damage.[5,25,51] Moreover, a clinical study has shown that success rate of a mini-implant is highest if the diameter of its pilot hole is 60% of the mini-implant diameter. Thus, we suggest that self-tapping (pilot hole 60% of mini-implant diameter) is beneficial to reduce failure rate for mini-implants inserted at areas with high bone density and that failure rates are similar between the two methods for implants inserted at areas with average bone density.

Bicortical versus Monocortical Engagement

Bicortical engagement gives mini-implants more bone support and offers better stability and a higher success rate than monocortical engagement.[52]

Loading Time

A consensus has yet to be reached on whether immediate or delayed loading is beneficial for improving mini-implant stability.[9,53,54] We performed a clinical study comparing stability between immediate loading (0 week) and delayed loading (two weeks and four weeks). The results revealed that, although mini-implants subject to delayed loading exhibited greater stability than those subject to immediate loading during the early phase (0–4 weeks), long-term stability (three months) was not clinically different, although a statistical difference was present (Figure 16.18). This

t.me/Dr_Mouayyad_AlbtousH

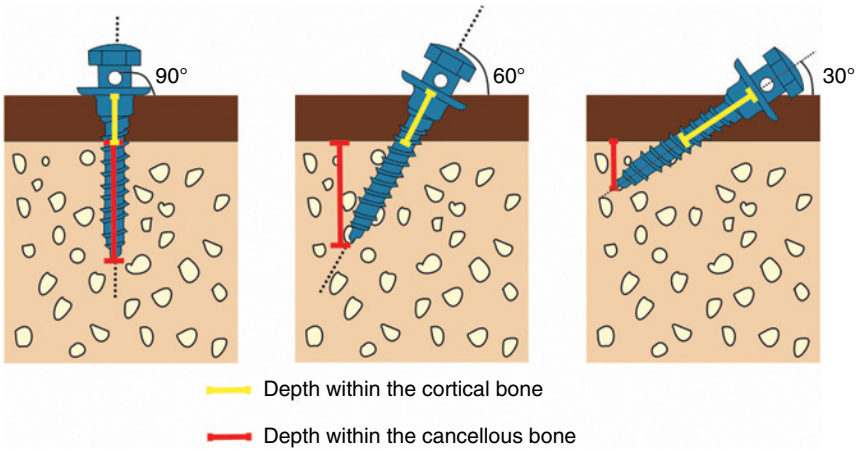


Figure 16.17 The influence of different insertion angles on stability of the mini-implant. The mini-implant inserted at 60° engages thicker cortical bone (indicated by the yellow lines) than that inserted at 90°, and engages greater trabecular bone than that inserted at 30° (indicated by red lines).

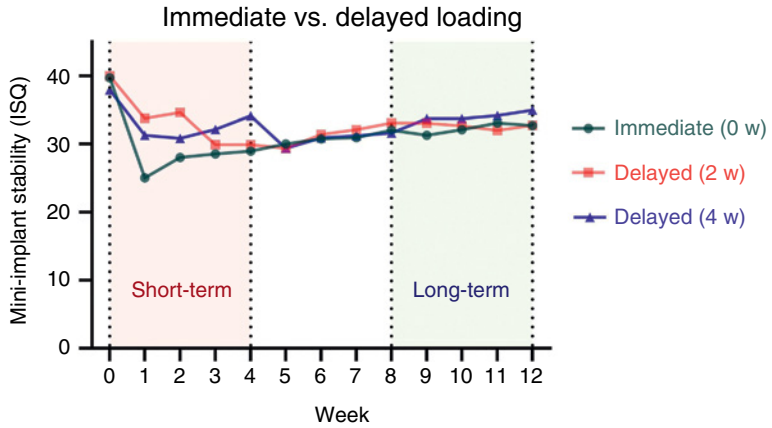


Figure 16.18 The effect of immediate loading versus delayed loading on mini-implant stability. Within the first month (short term), mini-implant stability differed among the three groups. In contrast, long-term stability did not differ clinically among the three groups, although statistical significance existed.

suggests that immediate loading and delayed loading may not differ clinically regarding stability. However, since soft tissue injury due to mini-implant insertion takes 1–2 weeks to heal, we recommend the loading of mini-implants be delayed for two weeks following placement.

16.3.3 Implant-associated Factors

Different designs of mini-implants may have an impact on failure and several implant-associated factors influence this failure, including geometry, design, shape and surface topology (Figure 16.19).

Geometry

Geometry of mini-implants includes diameter and length. *In vitro* studies have shown that primary stability of mini-implants was higher with larger and longer implants.[19,25,55] However, the benefits of increasing the size of mini-implants (diameter and length) are limited by the possibility of root contact in clinical practice. Interestingly, clinical studies revealed that the failure rate of mini-implants is not correlated with their size.[16,33,56] This contradiction could be attributed to the following two reasons. First, in clinical settings, in addition to mini-implant size, other confounding factors may also influence the failure rate and they may not be well controlled. Second, in clinical practice, only a small range of mini-implant sizes could be chosen, so the real differences of failure rate among different sizes could not be determined.

To conclude, as long as root contact can be avoided, longer and larger mini-implants should be used to minimise the failure rate in clinical practice (Figure 16.20).

Design

Thread height and thread pitch are two important parameters of mini-implants (Figure 16.21). Finite element studies have demonstrated that primary stability of mini-implants differed with different mini-implant designs (thread height and pitch).[57,58] Since the two parameters are interrelated, a finite element study has shown that the most appropriate thread height and pitch are 0.2 mm and 0.7 mm, respectively.[59]

Shape

Two shapes of mini-implants are currently available: tapered and cylindrical (Figure 16.22). Although tapered

t.me/Dr_Mouayyad_AlbtousH

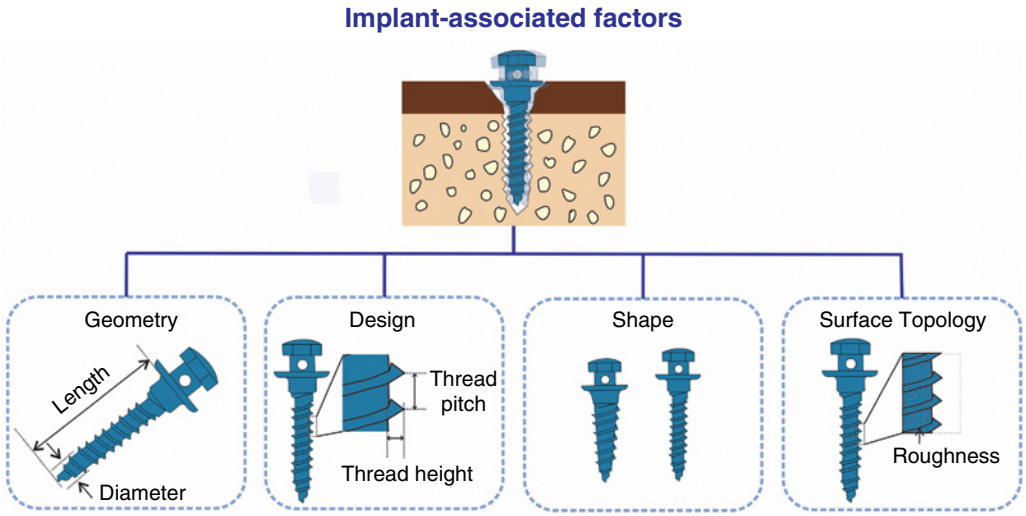


Figure 16.19 Mini-implant failure is affected by multiple implant-associated factors, including geometry, design, shape and surface topology.

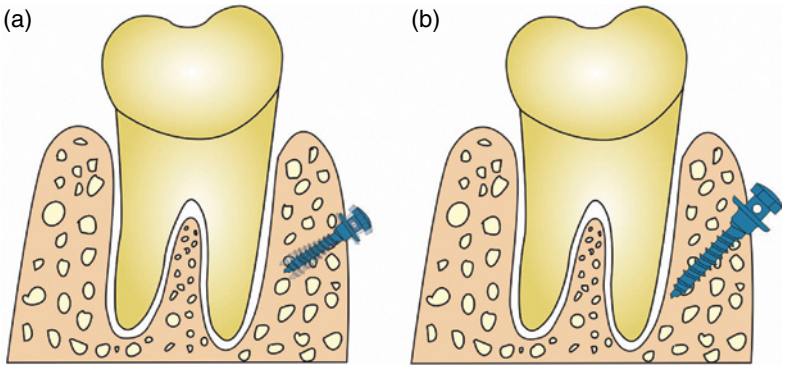


Figure 16.20 The influence of diameter and length on the stability of mini-implants. (a) A smaller and shorter mini-implant exhibits excessive mobility after placement. (b) A larger and longer mini-implant is stable following insertion.

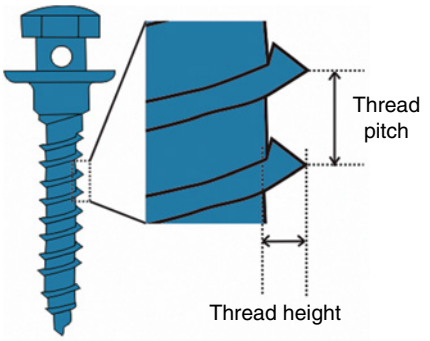


Figure 16.21 Thread height and thread pitch of mini-implants.

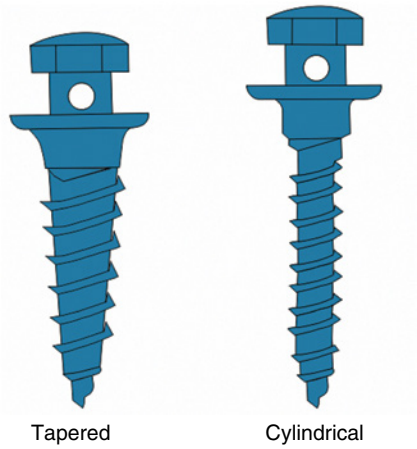


Figure 16.22 Two different shapes of mini-implants: tapered and cylindrical.

t.me/Dr_Mouayyad_AlbtousH

mini-implants have higher primary stability than cylindrical ones,[60,61] success rates are similar for the two shapes.[62,63] Nevertheless, since the tips of tapered mini-implants are smaller than those of cylindrical ones, the likelihood of root contact is lower for tapered mini-implants so they are more widely used.

Surface Topology

To improve the success rate of mini-implants, various surface modifications have been developed, e.g. increasing surface roughness. However, clinical studies reveal that success rates are similar between surface-treated and non-surface-treated mini-implants.[64,65]

16.4 Prevention of Mini-implant Failure

To prevent mini-implant failure, the following methods could be used based on the aforementioned risk factors: determining optimal insertion sites, choosing appropriate mini-implants, employing proper insertion techniques and adequate oral hygiene care (Figure 16.23).

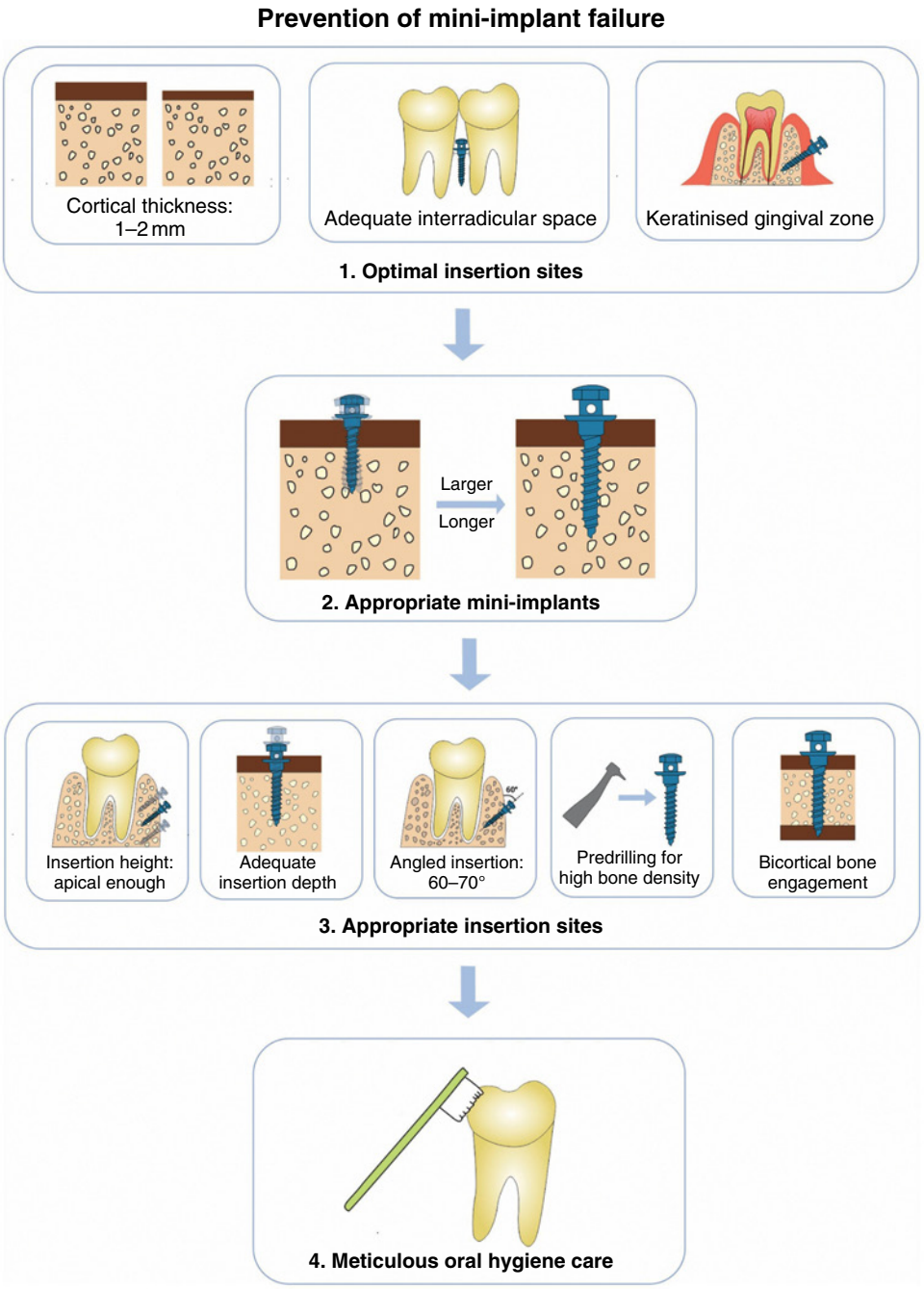


Figure 16.23 Key points for prevention of mini-implant failure.

t.me/Dr_Mouayyad_AlbtousH

16.4.1 Determining Optimal Insertion Sites

Prudent selection of an optimal insertion site is a prerequisite for the success of an orthodontic mini-implant. First, several insertion sites could be determined based on biomechanical principles. Second, based on radiographic examinations, insertion sites should meet the following biological requirements: (1) cortical thickness is 1–2 mm; (2) interradicular space is adequate; (3) insertion site lies in the keratinised gingiva zone. Third, if no insertion site can be selected to meet both the biomechanical and biological requirements, an improved insertion site might be developed. For example, if interradicular space is limited, preinsertion root divergence using segmental biomechanics is indicated.

16.4.2 Choosing Appropriate Mini-implants

For different insertion sites, mini-implants with different sizes are recommended. Operators should strictly follow the clinical recommendations. As a rule of thumb, larger and longer mini-implants should be chosen unless anatomical and biological limitations would be violated.

16.4.3 Appropriate Insertion Techniques

During insertion, operators should adhere to the recommended insertion techniques mentioned in previous chapters. In brief, the following principles should be followed: (1) insertion height should be apical enough; (2) insertion depth should be adequate; (3) angled insertion (60–70°) is recommended for interradicular space; (4) predrilling is indicated for anatomical areas with high bone density; (5) bicortical bone engagement is recommended for palatal regions and infrazygomatic crest.

16.4.4 Meticulous Oral Hygiene

Following the insertion of mini-implants, patients should be advised to maintain adequate oral hygiene. Specifically, food debris should be removed through brushing around mini-implants and plaque in the sulcus between the mini-implant and mucosa should be removed through regular prophylaxis.

16.5 Management of Mini-implant Failure

When mini-implant failure is encountered in clinical practice, practitioners should first perform a thorough examination to reveal possible reasons for mini-implant failure. If any of the aforementioned risk factors are discovered, measures should be taken to eliminate that risk factor. Based on the mobility of the failed mini-implants, the following two clinical approaches could be employed in clinical practice: (1) if the mobility of mini-implants is within an acceptable limit, the mobile mini-implant could be tightened *in situ*; (2) if mini-implants are too mobile or already dislodged, insertion of a new mini-implant or miniplate is clinically indicated.

16.5.1 Tightening Mini-implants *In Situ*

Before reinsertion of mini-implants, soft tissue inflammation should be controlled. Then, radiographic examinations should be implemented to rule out root contact or proximity. If no root proximity is detected, tightening the mini-implants *in situ* is indicated. Following resolution of the soft tissue inflammation, the loose mini-implants can be tightened *in situ* under local infiltration anaesthesia (Figure 16.24).

16.5.2 Inserting a New Mini-implant at a Neighbouring Site

If a mini-implant is too mobile or already dislodged, it should be removed first. A new mini-implant should not be inserted unless soft tissue healing is complete (Figure 16.25). Generally, soft tissue healing takes 1–2 weeks. However, both operators and patients should be warned about soft tissue scarring. It has been reported that the incidence of soft tissue scarring after removal of mini-implants is as high as 45% and that patients with flat biotype and insertion at maxillary buccal interradicular sites are more susceptible to scarring.[66]

t.me/Dr_Mouayyad_AlbtousH

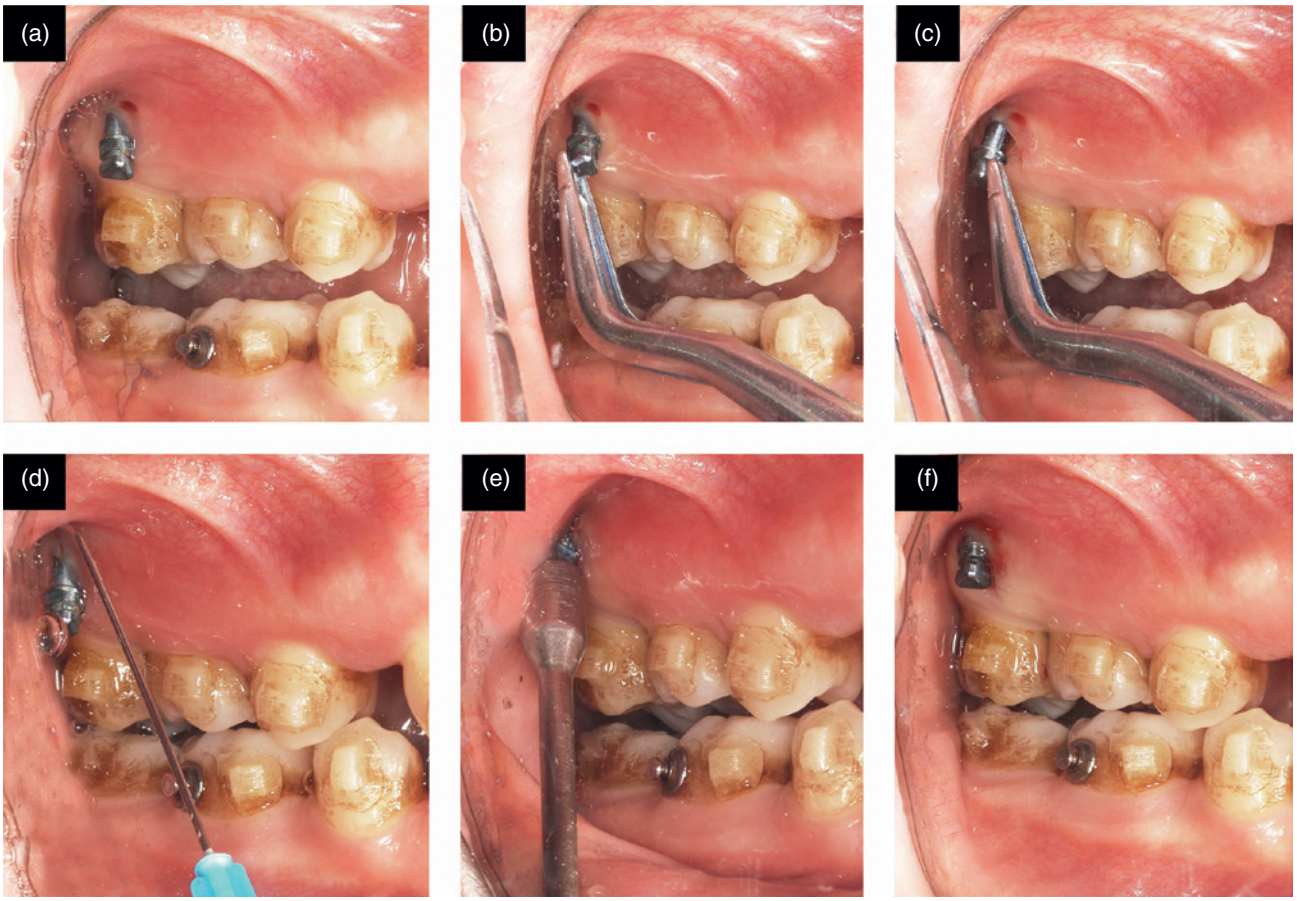


Figure 16.24 Tightening of a loose mini-implant *in situ*. (a–c) The mini-implant was loose and mobile. Note the mini-implant head can be displaced by a tweezer. (d) The peri-implant soft tissue was rinsed with chlorhexidine and local anaesthesia was applied. (e) The mobile mini-implant was tightened *in situ* with a manual mini-implant screwdriver. (f) The tightened mini-implant was stable.

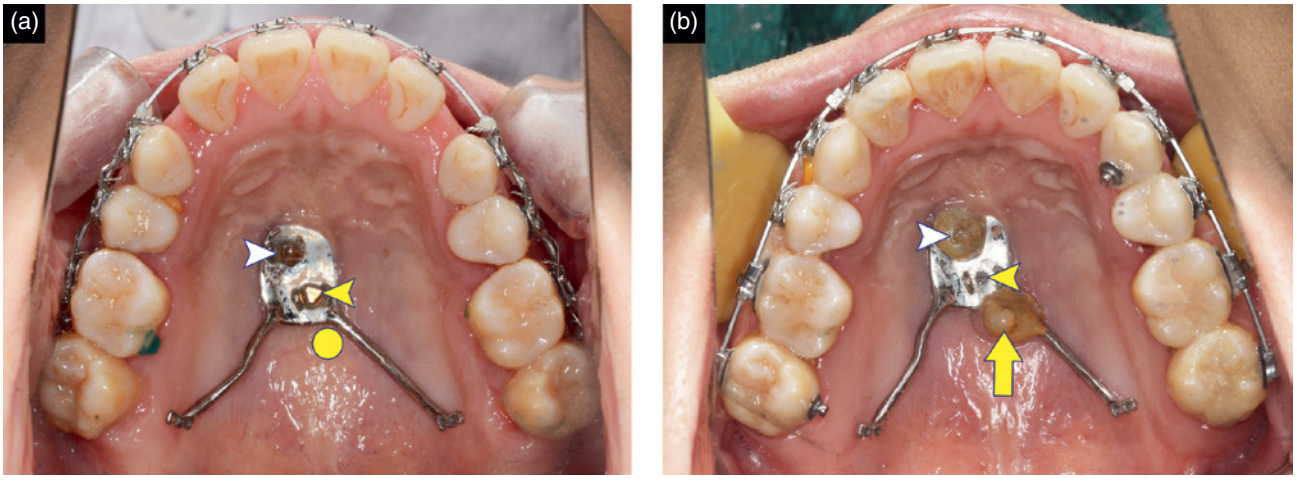


Figure 16.25 Reinsertion of a new mini-implant at a neighbouring site. (a) A palatal appliance was fixed onto the palatal vault through two mini-implants. The anterior mini-implant is indicated by the white arrowhead, the posterior one by the yellow arrowhead. However, the posterior mini-implant exhibited mobility during treatment. Thus, removal of the posterior mini-implant and reinsertion of a new one at a neighbouring site (yellow circle) was implemented. (b) The anterior mini-implant was still stable and covered by flowable resin. The hole in the palatal appliance where the original posterior mini-implant can be observed is indicated by the yellow arrowhead. A new mini-implant (covered by flowable resin, indicated by the yellow arrow) was inserted at the predetermined site to stabilise the palatal appliance.

t.me/Dr_Mouayyad_AlbtousH

16.6 Summary

Mini-implant failure is clinically manifested as loosening and failure to serve for force loading. It is associated with patient factors, operator factors and implant factors. Mini-implant failure may be prevented by selecting optimal insertion sites and appropriate mini-implants, implementing correct insertion techniques and executing meticulous oral hygiene. If mini-implant failure is encountered in clinical practice, the loose mini-implants can be tightened *in situ* if root contact is ruled out. Alternatively, new implants can be inserted at neighbouring sites to replace the loose mini-implants.

References

1 de Mattos PM, Goncalves FM, Basso IB et al. (2022). Risk factors associated with the stability of mini-implants and mini-plates: systematic review and meta-analysis. *Clin. Oral Invest.* 26(1): 65–82.

2 Yao CC, Chang HH, Chang JZ, Lai HH, Lu SC, Chen YJ. (2015). Revisiting the stability of mini-implants used for orthodontic anchorage. *J. Formos. Med. Assoc.* 114(11): 1122–1128.

3 Chen YJ, Chang HH, Huang CY, Hung HC, Lai EH, Yao CC. (2007). A retrospective analysis of the failure rate of three different orthodontic skeletal anchorage systems. *Clin. Oral Implants Res.* 18(6): 768–775.

4 Lee JH, Choo H, Kim SH, Chung KR, Giannuzzi LA, Ngan P. (2011). Replacing a failed mini-implant with a miniplate to prevent interruption during orthodontic treatment. *Am. J. Orthod. Dentofacial Orthop.* 139(6): 849–857.

5 Uchida Y, Namura Y, Inaba M et al. (2021). Influence of pre-drilling diameter on the stability of orthodontic anchoring screws in the mid-palatal area. *J. Oral Sci.* 63(3): 270–274.

6 Azeem M, Saleem MM, Liaquat A, Ul Haq A, Ul Hamid W, Masood M. (2019). Failure rates of mini-implants inserted in the retromolar area. *Int. Orthod.* 17(1): 53–59.

7 Mohammed H, Wafaie K, Rizk MZ, Almuzian M, Sosly R, Bearn DR. (2018). Role of anatomical sites and correlated risk factors on the survival of orthodontic miniscrew implants: a systematic review and meta-analysis. *Prog. Orthod.* 19(1): 36.

8 Tsai CC, Chang HP, Pan CY, Chou ST, Tseng YC. (2016). A prospective study of factors associated with orthodontic mini-implant survival. *J. Oral Sci.* 58(4): 515–521.

9 Jeong JW, Kim JW, Lee NK, Kim YK, Lee JH, Kim TW. (2015). Analysis of time to failure of orthodontic mini-implants after insertion or loading. *J. Korean Assoc. Oral Maxillofac. Surg.* 41(5): 240–245.

10 Uesugi S, Kokai S, Kanno Z, Ono T. (2017). Prognosis of primary and secondary insertions of orthodontic miniscrews: what we have learned from 500 implants. *Am. J. Orthod. Dentofacial Orthop.* 152(2): 224–231.

11 Melo AC, Andrighetto AR, Hirt SD, Bongiolo AL, Silva SU, Silva MA. (2016). Risk factors associated with the failure of miniscrews – a ten-year cross sectional study. *Braz. Oral Res.* 30(1): e124.

12 Sarul M, Minch L, Park HS, Antoszewska-Smith J. (2015). Effect of the length of orthodontic mini-screw implants on their long-term stability: a prospective study. *Angle Orthod.* 85(1): 33–38.

13 Lim HJ, Choi YJ, Evans CA, Hwang HS. (2011). Predictors of initial stability of orthodontic miniscrew implants. *Eur. J. Orthod.* 33(5): 528–532.

14 Ozdemir F, Tozlu M, Germec-Cakan D. (2013). Cortical bone thickness of the alveolar process measured with cone-beam computed tomography in patients with different facial types. *Am. J. Orthod. Dentofacial Orthop.* 143(2): 190–196.

15 Chen YJ, Chang HH, Lin HY, Lai EH, Hung HC, Yao CC. (2008). Stability of miniplates and miniscrews used for orthodontic anchorage: experience with 492 temporary anchorage devices. *Clin. Oral Implants Res.* 19(11): 1188–1196.

16 Topouzelis N, Tsaousoglou P. (2012). Clinical factors correlated with the success rate of miniscrews in orthodontic treatment. *Int. J. Oral Sci.* 4(1): 38–44.

17 Choi BH, Li J, Kim HS et al. (2007). Ingestion of orthodontic anchorage screws: an experimental study in dogs. *Am. J. Orthod. Dentofacial Orthop.* 131(6): 767–768.

18 Vilani GN, Ruellas AC, Elias CN, Mattos CT. (2015). Stability of smooth and rough mini-implants: clinical and biomechanical evaluation – an in vivo study. *Dental Press J. Orthod.* 20(5): 35–42.

19 Mohlhenrich SC, Heussen N, Winterhalder P et al. (2019). Predicting primary stability of orthodontic mini-implants, according to position, screw-size, and bone quality, in the maxilla of aged patients: a cadaveric study. *Eur. J. Oral Sci.* 127(5): 462–471.

20 Mohan S, Srinivasan D, Arumugam E, Devasahayam D, Kannan R. (2022). Effect of placement angle, diameter, length and bone density on the pull-out strength of orthodontic mini-implants: an in vitro study. *J. Orthod.* 49(2): 143–150.

21 Barros SE, Janson G, Chiqueto K, Garib DG, Janson M. (2011). Effect of mini-implant diameter on fracture risk and self-drilling efficacy. *Am. J. Orthod. Dentofacial Orthop.* 140(4): e181–192.

22 Ugarte OM, Gialain IO, de Carvalho NM et al. (2021). Can maxilla and mandible bone quality explain

t.me/Dr_Mouayyad_AlbtousH

differences in orthodontic mini-implant failures? *Biomater. Invest. Dent.* 8(1): 1–9.

23 Motoyoshi M, Inaba M, Ono A, Ueno S, Shimizu N. (2009). The effect of cortical bone thickness on the stability of orthodontic mini-implants and on the stress distribution in surrounding bone. *Int. J. Oral Maxillofac Surg.* 38(1): 13–18.

24 Motoyoshi M, Yoshida T, Ono A, Shimizu N. (2007). Effect of cortical bone thickness and implant placement torque on stability of orthodontic mini-implants. *Int. J. Oral Maxillofac. Implants.* 22(5): 779–784.

25 Mohlhenrich SC, Heussen N, Modabber A et al. (2021). Influence of bone density, screw size and surgical procedure on orthodontic mini-implant placement – part A: temperature development. *Int. J. Oral Maxillofac. Surg.* 50(4): 555–564.

26 Liu SS, Cruz-Marroquin E, Sun J, Stewart KT, Allen MR. (2012). Orthodontic mini-implant diameter does not affect in-situ linear microcrack generation in the mandible or the maxilla. *Am. J. Orthod. Dentofacial Orthop.* 142(6): 768–773.

27 Deguchi T, Yabuuchi T, Hasegawa M, Garetto LP, Roberts WE, Takano-Yamamoto T. (2011). Histomorphometric evaluation of cortical bone thickness surrounding miniscrew for orthodontic anchorage. *Clin. Implant Dent. Relat. Res.* 13(3): 197–205.

28 Long H, Wang Y, Jian F, Liao LN, Yang X, Lai WL. (2016). Current advances in orthodontic pain. *Int. J. Oral Sci.* 8(2): 67–75.

29 Giacobbo LC, Perin MAA, Pereira TM et al. (2020). RANK/RANKL/OPG gene polymorphisms and loss of orthodontic mini-implants. *Orthod. Craniofac. Res.* 23(2): 210–222.

30 Andrucioli MCD, Matsumoto MAN, Fukada SY et al. (2019). Quantification of pro-inflammatory cytokines and osteoclastogenesis markers in successful and failed orthodontic mini-implants. *J. Appl. Oral Sci.* 27: e20180476.

31 Reichow AM, Melo AC, de Souza CM et al. (2016). Outcome of orthodontic mini-implant loss in relation to interleukin 6 polymorphisms. *Int. J. Oral Maxillofac Surg.* 45(5): 649–657.

32 Garcez AS, Barros LC, Fernandes MRU, Fujii DN, Suzuki SS, Nepomuceno R. (2020). Fluorescence image and microbiological analysis of biofilm retained around healthy and inflamed orthodontic miniscrews. *Photodiagnosis Photodyn. Ther.* 30: 101707.

33 Uribe F, Mehr R, Mathur A, Janakiraman N, Allareddy V. (2015). Failure rates of mini-implants placed in the infrazygomatic region. *Prog. Orthod.* 16: 31.

34 Bayat E, Bauss O. (2010). Effect of smoking on the failure rates of orthodontic miniscrews. *J. Orofac. Orthop.* 71(2): 117–124.

35 Haddad R, Saadeh M. (2019). Distance to alveolar crestal bone: a critical factor in the success of orthodontic mini-implants. *Prog. Orthod.* 20(1): 19.

36 Marquezan M, Lima I, Lopes RT, Sant'Anna EF, de Souza MM. (2014). Is trabecular bone related to primary stability of miniscrews? *Angle Orthod.* 84(3): 500–507.

37 Wilmes B, Rademacher C, Olthoff G, Drescher D. (2006). Parameters affecting primary stability of orthodontic mini-implants. *J. Orofac. Orthop.* 67(3): 162–174.

38 Alrbata RH, Yu W, Kyung HM. (2014). Biomechanical effectiveness of cortical bone thickness on orthodontic microimplant stability: an evaluation based on the load share between cortical and cancellous bone. *Am. J. Orthod. Dentofacial Orthop.* 146(2): 175–182.

39 Xin Y, Wu Y, Chen C, Wang C, Zhao L. (2022). Miniscrews for orthodontic anchorage: analysis of risk factors correlated with the progressive susceptibility to failure. *Am. J. Orthod. Dentofacial Orthop.* 162: e192–e202.

40 Lee Y, Choi SH, Yu HS, Erenebat T, Liu J, Cha JY. (2021). Stability and success rate of dual-thread miniscrews. *Angle Orthod.* 91(4): 509–514.

41 Ikenaka R, Koizumi S, Otsuka T, Yamaguchi T. (2022). Effects of root contact length on the failure rate of anchor screw. *J. Oral Sci.* 64(3): 232–235.

42 Motoyoshi M, Ueno S, Okazaki K, Shimizu N. (2009). Bone stress for a mini-implant close to the roots of adjacent teeth – 3D finite element analysis. *Int. J. Oral Maxillofac Surg.* 38(4): 363–368.

43 Albogha MH, Kitahara T, Todo M, Hyakutake H, Takahashi I. (2016). Predisposing factors for orthodontic mini-implant failure defined by bone strains in patient-specific finite element models. *Ann. Biomed. Eng.* 44(10): 2948–2956.

44 Lee HJ, Lee KS, Kim MJ, Chun YS. (2013). Effect of bite force on orthodontic mini-implants in the molar region: finite element analysis. *Korean J. Orthod.* 43(5): 218–224.

45 Yoon JH, Cha JY, Choi YJ, Park WS, Han SS, Lee KJ. (2020). Simulation of miniscrew-root distance available for molar distalization depending on the miniscrew insertion angle and vertical facial type. *PLoS One* 15(9): e0239759.

46 Wilmes B, Su YY, Drescher D. (2008). Insertion angle impact on primary stability of orthodontic mini-implants. *Angle Orthod.* 78(6): 1065–1070.

47 Moslemzadeh SH, Sohrabi A, Rafighi A, Kananizadeh Y, Nourizadeh A. (2017). Evaluation of interdental spaces of the mandibular posterior area for orthodontic mini-implants with cone-beam computed tomography. *J. Clin. Diagn. Res.* 11(4): ZC09–ZC12.

48 Nienkemper M, Santel N, Honscheid R, Drescher D. (2016). Orthodontic mini-implant stability at different insertion depths: sensitivity of three stability measurement methods. *J. Orofac. Orthop.* 77(4): 296–303.

49 Lin TS, Tsai FD, Chen CY, Lin LW. (2013). Factorial analysis of variables affecting bone stress adjacent to the

t.me/Dr_Mouayyad_AlbtousH

orthodontic anchorage mini-implant with finite element analysis. *Am. J. Orthod. Dentofacial Orthop.* 143(2): 182–189.

50 Yi J, Ge M, Li M et al. (2017). Comparison of the success rate between self-drilling and self-tapping miniscrews: a systematic review and meta-analysis. *Eur. J. Orthod.* 39(3): 287–293.

51 Wilmes B, Panayotidis A, Drescher D. (2011). Fracture resistance of orthodontic mini-implants: a biomechanical in vitro study. *Eur. J. Orthod.* 33(4): 396–401.

52 Lee RJ, Moon W, Hong C. (2017). Effects of monocortical and bicortical mini-implant anchorage on bone-borne palatal expansion using finite element analysis. *Am. J. Orthod. Dentofacial Orthop.* 151(5): 887–897.

53 Manni A, Cozzani M, Tamborrino F, De Rinaldis S, Menini A. (2011). Factors influencing the stability of miniscrews. A retrospective study on 300 miniscrews. *Eur. J. Orthod.* 33(4): 388–395.

54 Oltramari-Navarro PV, Navarro RL, Henriques JF et al. (2013). The impact of healing time before loading on orthodontic mini-implant stability: a histomorphometric study in minipigs. *Arch. Oral Biol.* 58(7): 806–812.

55 Pithon MM, Figueiredo DS, Oliveira DD. (2013). Mechanical evaluation of orthodontic mini-implants of different lengths. *J. Oral Maxillofac. Surg.* 71(3): 479–486.

56 Wu TY, Kuang SH, Wu CH. (2009). Factors associated with the stability of mini-implants for orthodontic anchorage: a study of 414 samples in Taiwan. *J. Oral Maxillofac. Surg.* 67(8): 1595–1599.

57 Cunha AC, Freitas AO, Marquezan M, Nojima LI. (2015). Mechanical influence of thread pitch on orthodontic mini-implant stability. *Braz. Oral Res.* 29: S1806-83242015000100231.

58 Chang JZ, Chen YJ, Tung YY et al. (2012). Effects of thread depth, taper shape, and taper length on the mechanical properties of mini-implants. *Am. J. Orthod. Dentofacial Orthop.* 141(3): 279–288.

59 Ye Y, Yi W, Fan S et al. (2023). Effect of thread depth and thread pitch on the primary stability of miniscrews receiving a torque load: a finite element analysis. *J. Orofac. Orthop.* 84: 79–87.

60 Heo YY, Cho KC, Baek SH. (2012). Angled-predrilling depth and mini-implant shape effects on the mechanical properties of self-drilling orthodontic mini-implants during the angled insertion procedure. *Angle Orthod.* 82(5): 881–888.

61 Wilmes B, Ottenstreuer S, Su YY, Drescher D. (2008). Impact of implant design on primary stability of orthodontic mini-implants. *J. Orofac. Orthop.* 69(1): 42–50.

62 Yoo SH, Park YC, Hwang CJ, Kim JY, Choi EH, Cha JY. (2014). A comparison of tapered and cylindrical miniscrew stability. *Eur. J. Orthod.* 36(5): 557–562.

63 Cha JY, Takano-Yamamoto T, Hwang CJ. (2010). The effect of miniscrew taper morphology on insertion and removal torque in dogs. *Int. J. Oral Maxillofac Implants.* 25(4): 777–783.

64 Chaddad K, Ferreira AF, Geurs N, Reddy MS. (2008). Influence of surface characteristics on survival rates of mini-implants. *Angle Orthod.* 78(1): 107–113.

65 Manni A, Drago S, Migliorati M. (2022). Success rate of surface-treated and non-treated orthodontic miniscrews as anchorage reinforcement in the lower arch for the Herbst appliance: a single-centre, randomised split-mouth clinical trial. *Eur. J. Orthod.* 44(4): 452–457.

66 Jung SA, Choi YJ, Lee DW, Kim KH, Chung CJ. (2015). Cross-sectional evaluation of the prevalence and factors associated with soft tissue scarring after the removal of miniscrews. *Angle Orthod.* 85(3): 420–426.

t.me/Dr_Mouayyad_AlbtousH

Index

Numerics
3-D (three-dimensional) dentition model, reconstructing 451, 452, 453, 454, 455, 456, 457
3-D (three-dimensional) design of insertion guides, for mini-implants
  about 451, 461, 463
  combining guide plate and guide cylinder 461
  determining area of guide plate on digital dental model 461
  establishing digital data of mini-implants and screwdrivers 457
  generating guide cylinder 461, 464
  generating guide plate 461
  reconstructing three-dimensional dentition model 451, 452, 453, 454, 455, 456, 457
  virtual placement of mini-implants 459, 460, 461, 462
3-D printing, generating actual insertion guide through 464, 466

a

accuracy, as an advantage of insertion guides 446, 447–448
adverse consequences, of soft tissue complications 519, 521
age, as a basic condition 26, 27
alveolar bone 33, 34
anaesthesia
  appropriate technique for 497, 498
  for clinical procedures with insertion guides 476, 477
anatomical characteristics
  of anterior nasal spine (ANS)
    about 125, 129
    hard tissue factor: bone depth 125, 127, 130
    hard tissue factor: bone width 127, 130–131
    hard tissue factor: cortical thickness 128, 129
    soft tissue factor: labial frenum 127, 132
    soft tissue factor: mucogingival junction 127, 132, 133
  of buccal shelf of mandibular buccal region
    about 364, 365–366
    hard tissue factor: bone depth 364, 369, 370
    hard tissue factor: cortical thickness 364, 367–368
    hard tissue factor: plateau features 364, 366–367
    soft tissue factor: soft tissue thickness 369, 371
    soft tissue factor: soft tissue type 369, 371
    vital anatomical structure: inferior alveolar nerve 369, 371
  of infrazygomatic crest (IZC)
    hard tissue factor: bone depth 188, 190, 192, 190–191
    hard tissue factor: cortical thickness 188, 189
    hard tissue factor: crest shape 187–188, 187, 188
    hard tissue factor: dental roots 192, 192–193
    soft tissue factor: maxillary sinus 194, 195
    soft tissue factor: soft tissue type 192, 194
  of interradicular sites in mandibular buccal region
    about 335
    hard tissue factor: bone depth 336, 338
    hard tissue factor: bone width 336, 339–340
    hard tissue factor: cortical thickness 335–336
    hard tissue factor: shape of cortical plate 336, 340
    soft tissue factor: buccal frenum 341, 342
    soft tissue factor: soft tissue types 340–341
    vital structures 341–342
  of interradicular sites of mandibular labial region
    about 303, 304
    hard tissue factor: bone depth 307, 308–310
    hard tissue factor: bone width 307, 310–311
    hard tissue factor: cortical thickness 305, 306–307
    hard tissue factor: root prominence 307, 311
    soft tissue factor: attached gingiva 307, 311, 312
    soft tissue factor: labial frenum 307, 311
  of interradicular sites of maxillary labial region
    about 95, 98
    hard tissue factor: bone depth 99–100, 100, 101
    hard tissue factor: bone width 100–102, 102, 103, 104, 105

Clinical Insertion Techniques of Orthodontic Temporary Anchorage Devices, First Edition. Edited by Hu Long, Xianglong Han, and Wenli Lai.
© 2024 John Wiley & Sons Ltd. Published 2024 by John Wiley & Sons Ltd.

t.me/Dr_Mouayyad_AlbtousH

anatomical characteristics (*cont'd*)
hard tissue factor: cortical thickness 98–99
hard tissue factor: root prominence 103, 106
soft tissue factor: labial frenum 103, 106
soft tissue factor: mucogingival junction 103, 106
of interradicular sites on maxillary palatal region
hard tissue factor: bone depth 240–241, 241, 242
hard tissue factor: bone width 241, 243, 243, 244
hard tissue factor: cortical thickness 238–240, 239–240
hard tissue factor: inclination of cortical plate 244, 245
soft tissue factor: soft tissue thickness 246, 247
soft tissue factor: soft tissue type 246, 246
vital structures 246–248, 248
of mandibular ramus
anatomical location 389, 390, 391
hard tissue considerations 389, 391, 392–393
optimal insertion sites 394–395, 394, 396
soft tissue considerations 391, 394, 394–395
of mandibular symphysis
about 320–321
hard tissue factor: bone depth 322, 323
hard tissue factor: cortical thickness 321, 322
soft tissue factors 323, 324–325
of maxillary buccal region
about 145, 147
hard tissue factor: bone density 146, 147
hard tissue factor: bone depth 149–151
hard tissue factor: bone width 151, 153, 152–154
hard tissue factor: buccal exostosis 153, 154–155
hard tissue factor: cortical thickness 146, 148–149
soft tissue factor: buccal frenum 156, 157
soft tissue factor: soft tissue type 154–156, 155–156
of maxillary tuberosity
about 223–224, 224–225
hard tissue factor: bone density 225, 226
hard tissue factor: bone dimension 226–227, 228
hard tissue factor: cortical thickness 226, 227
soft tissue factor: soft tissue thickness 228
soft tissue factor: types of soft tissue 228
of midpalatal suture
about 297–298
hard tissue factor: bone depth 297–298
soft tissue factor: soft tissue thickness 298
vital structures 298
of paramedian sites on maxillary palatal region
about 270
hard tissue factor: bone depth 271, 272
hard tissue factor: cortical thickness 270–271
soft tissue factor: soft tissue thickness 271, 272
vital anatomical structures 272–273, 272, 273
undesirable for mini-implants 422, 424–428
anatomical location, of mandibular ramus 389, 390–391
anatomical sites
anatomy-driven paradigm
about 64, 65
mandible 68, 71, 72–74
maxilla 64, 65–68, 69–71
available for mini-plates 418, 419–420
anatomy-driven paradigm
about 56
available anatomical sites
about 64, 65
mandible 68, 71, 72–74
maxilla 64, 65–68, 69–71
general principles
about 56, 57
dental roots 56–59, 60
maxillary sinus 60, 62–63
nasal cavity 60, 64
neurovascular bundle 59–60, 61–62
ANS. *See* anterior nasal spine (ANS)
anterior intrusion, as a clinical application with infrazygomatic crest 208, 209, 217
anterior nasal spine (ANS)
anatomical features 125, 127, 132, 128–132, 133
biomechanical considerations 132, 133
clinical applications 136, 138–143
insertion techniques 134–136, 137
selection of appropriate insertion sites 132, 134
anterior retraction
as a clinical application for interradicular sites 252–269
for interradicular sites of mandibular buccal region 350–353
in sagittal dimension 11, 12, 13
applications, clinical
for anterior nasal spine 136, 138–143
for buccal shelf of mandibular buccal region
mandibular dentition distalisation 376, 377, 378, 381
molar uprighting 379, 381–384
orthodontic traction of impacted teeth 379, 384–386
for infrazygomatic crest (IAC)
anterior intrusion 208, 209, 217
molar distalisation 201, 202, 203–208, 209, 210–212, 213–214, 215
molar intrusion 209, 213, 218, 219–221
orthodontic traction of impacted teeth 214, 218, 222–223
for interradicular sites of mandibular buccal region 350–363
anterior retraction 350–353
molar intrusion 354, 358, 359, 360–361
molar protraction 353–358

t.me/Dr_Mouayyad_AlbtousH

molar uprighting 358, 359, 361–363
for interradicular sites of maxillary buccal region
en masse anterior retraction 164, 166, 167, 168, 169, 170, 171, 172–173, 174
molar intrusion 170, 171, 177–180
molar protraction 168, 170, 175–176
occlusal canting 171, 174, 180–183, 184
for interradicular sites of maxillary labial region
correction of gummy smile 118, 121–122, 123–124
correction of occlusal canting 122, 125, 126, 127, 128
incisor intrusion 114, 115, 117–118, 119–120
for interradicular sites of maxillary palatal region
anterior retraction 252–269
molar distalisation 257, 259, 261–262, 263, 264
molar intrusion 257, 260–261
molar protraction 263, 265–269
for paramedian sites
mini-implant-assisted skeletal expansion 286, 288–289
molar anchorage reinforcement 280, 284–286, 287, 288
molar distilisation 280–282, 284
molar intrusion 293, 295
traction of impacted teeth 289–293, 294
attached gingiva, as a soft tissue factor of interradicular sites of mandibular labial region 307, 311, 312

b

basic conditions
age 519, 521
gender 26, 27
biocortical engagement, monocortical engagement *versus* 540
biomechanical advantages, of mini-plates 422, 428–430
biomechanical considerations
of anterior nasal spine 132, 133
of buccal shelf in mandibular buccal region 369, 372
of interradicular sites
about 107
of mandibular buccal region 343, 344
of mandibular labial region 311, 312, 313
of mandibular symphysis 323, 325
biomechanics-driven paradigm
about 75, 76, 77
incisor intrusion 79, 80–81
maxillary molar uprighting 76, 77, 78
molar intrusion 77, 79, 80
molar protraction 82, 84, 85
orthodontic traction of impacted molars 79, 82, 83
bisphosphonates 28, 29–30
bone density
about 33, 35–36
as a hard tissue factor
of interradicular sites of maxillary buccal region 146, 147
of maxillary tuberosity 225, 226
bone depth
about 33, 35, 37, 38–39
as a hard tissue factor
of buccal shelf of mandibular buccal region 364, 369, 370
of infrazygomatic crest (IZC) 188, 190, 191, 192
of interradicular sites of mandibular labial region 307, 308–310
of interradicular sites of maxillary labial region 99–100, 101
of interradicular sites of maxillary buccal region 149–151
of mandibular symphysis in mandibular labial region 322, 323
of maxillary palatal region 240–241, 242
of midpalatal suture 297–298
bone dimension, as a hard tissue factor of maxillary tuberosity 226–227, 228
bone width
about 37, 38, 39, 40–42
as a hard tissue factor
of interradicular sites of mandibular labial region 307, 310–311
of interradicular sites of maxillary buccal region 151, 152–154
of interradicular sites of maxillary labial region 100–102, 103, 104, 105
of maxillary palatal region 241, 243, 244
Brodie bite, in transverse dimension 18, 19
buccal exostosis, as a hard tissue factor in interradicular sites of maxillary buccal region 153, 154–155
buccal frenum, as a soft tissue factor in interradicular sites of maxillary buccal region 156, 157
buccal interradicular region, placement of mini-implants with insertion guides in 480–481, 482
buccal shelf
mandibular buccal region
anatomical characteristics 364–369, 370, 371
biomechanical considerations 369, 372
clinical applications 376, 377–386
insertion techniques 160–164, 165, 166
selection of appropriate insertion sites 371–372
placement of mini-implants with insertion guides on 481, 483, 484

c

causative factors, removal of 528, 529
characteristics
drilling methods 5, 6
materials 2
morphology 4–5, 11
clinical applications
for anterior nasal spine 136, 138–143
for buccal shelf of mandibular buccal region

t.me/Dr_Mouayyad_AlbtousH

clinical applications (*cont'd*)
mandibular dentition
distalisation 376, 377, 378, 381
molar uprighting 379, 381–384
orthodontic traction of impacted teeth 379, 384–386
for infrazygomatic crest (IAC)
anterior intrusion 208, 209, 217
molar distalisation 201, 202, 203–208, 209, 210–212, 213–214, 215
molar intrusion 209, 213, 218, 219–221
orthodontic traction of impacted teeth 214, 218, 222–223
for interradicular sites of mandibular buccal region 350–363
anterior retraction 350–353
molar intrusion 354, 358, 359, 360–361
molar protraction 353–358
molar uprighting 358, 359, 361–363
for interradicular sites of maxillary buccal region
en masse anterior retraction 164, 166, 167, 168, 169, 170, 171, 172–173, 174
molar intrusion 170, 171, 177–180
molar protraction 168, 170, 175–176
occlusal canting 171, 174, 180–183, 184
for interradicular sites of maxillary labial region
correction of gummy smile 118, 121–122, 123–124
correction of occlusal canting 122, 125, 126, 127, 128
incisor intrusion 114, 115, 117–118, 119–120
for interradicular sites of maxillary palatal region
anterior retraction 252–269
molar distalisation 257, 259, 261–262, 263, 264
molar intrusion 257, 260–261
molar protraction 263, 265–269
for paramedian sites
mini-implant-assisted skeletal expansion 286, 288–289
molar anchorage reinforcement 280, 284–286, 287, 288
molar distilisation 280–282, 284
molar intrusion 293, 295
traction of impacted teeth 289–293, 294
clinical decisions, for mini-implant fractures in different clinical scenarios 511
clinical features, of mini-plates
advantages and disadvantages 417–418
available anatomical sites 418, 419–420
structure 415, 416–417
clinical indications
about 9–10
mini-plates
about 418
anatomical factors undesirable for mini-implants 422, 424–428
biomechanical advantages 422, 428–430
orthopaedic treatment for skeletal discrepancy 420, 421–422, 423
sagittal dimension 11–12, 13–14
transverse dimension 16, 18, 19
vertical dimension 12, 15–16, 17–18
clinical manifestations
of root contact 488–499
of soft tissue complications
about 516
soft tissue hyperplasia 516, 518
soft tissue infection 517, 519
soft tissue lesion 517, 519
soft tissue swelling 516, 517
clinical procedures
for inserting mini-implants
insertion of mini-implants 86, 87–89, 91
post-insertion examination 90, 91–92
preinsertion preparation 85–86, 87
for insertion guides
anaesthesia 476, 477
detaching screwdrivers 479
inserting mini-implants 476, 477–478
removing insertion guides 479
verifying fit of insertion guides 473–475
for mandibular ramus
insertion 399–401, 402
postinsertion 401
preinsertion preparation 399
for removing fractured mini-implants 511, 512
complications, potential 19–32
cortical thickness
about 37, 39, 42
as a hard tissue factor
of buccal shelf of mandibular buccal region 364, 367–368
of infrazygomatic crest (IZC) 188, 189
of interradicular sites of mandibular labial region 305, 306–307
of interradicular sites of maxillary buccal region 146, 148–149
of mandibular symphysis in mandibular labial region 322, 323
of maxillary labial region 98–99
of maxillary palatal region 238–240
of maxillary tuberosity 226, 227
cost, as a disadvantage of insertion guides 449
crest shape, as a hard tissue factor in infrazygomatic crest (IZC) 187–188

d

debridement, local 528
density, bone
about 33, 35–36
as a hard tissue factor in interradicular sites of maxillary buccal region 146, 147
as a hard tissue factor of maxillary tuberosity 225, 226
dental models, digitalization of 451, 452, 453
dental roots
as a general principle 56, 57–59, 60
as a hard tissue factor in infrazygomatic crest (IZC) 192–193

t.me/Dr_Mouayyad_AlbtousH

depth, bone
about 33, 35, 37, 38–39
as a hard tissue factor
of buccal shelf of mandibular buccal region 364, 369, 370
of infrazygomatic crest (IZC) 188, 190, 191, 192
of interradicular sites of mandibular labial region 307, 308–310
of interradicular sites of maxillar labial region 99–100, 101
of interradicular sites of maxillary buccal region 149–151
of mandibular symphysis in mandibular labial region 322, 323
of maxillary palatal region 240–241, 242
of midpalatal suture 297–298
design, as a risk factor for failure of orthodontic temporary anchorage devices 541, 542
diabetes, as a systemic disease 28, 29
digital models
creating for guide cylinders 457, 459
creating for mini-implants 457, 459
creating for screwdrivers 457, 459
dimension, bone, as a hard tissue factor of maxillary tuberosity 226–227, 228
direct anchorage, indirect anchorage *versus* 8–9
distalisation, molar
as a clinical application with infrazygomatic crest 201, 202, 203–208, 209, 210–212, 213–214, 215
for interradicular sites 257, 259, 261–262, 263, 264
for paramedian sites 280–282, 284
in sagittal dimension 11–12, 13–15
drainage, local 528
drilling methods 5, 6
drugs
bisphosphonates 28, 29–30
glucocorticoids 30, 31

e

ease of insertion, as an advantage of insertion guides 446, 449
efficiency, as an advantage of insertion guides 446, 448–449
en masse anterior retraction, for interradicular sites 164, 166, 167, 168, 169, 170, 171, 172–173, 174
evolution
of insertion guides
concept of guided surgery 437, 438, 439, 440
for mini-implants 439, 440–445
of orthodontic temporary anchorage devices 1–2, 3
extra-alveolar bone 33, 34
extrusion, in vertical dimension 16, 18

f

failure, of orthodontic temporary anchorage devices
about 533, 534, 544, 545
management of 544
prevention of 543
primary stability 534–536
risk factors
implant-associated 541–542
operator-associated 538–541
patient-associated 537–538
secondary stability 534–536
force loading, for mini-implants 523, 524
fractures, of orthodontic temporary anchorage devices
about 501–503, 512
management of mini-implant fracture
clinical decisions in different clinical scenarios 511
clinical techniques for removing fractured mini-implants 511, 512
prevention of mini-implant fracture
appropriate insertion techniques 508, 510
judicious selection of appropriate mini-implants 508, 510
prudent selection of insertion sites 508, 509
risk factors for mini-implant fracture
about 504
implant-associated factors 505–507
insertion site-associated factors 507–508
operator-associated factors 504–505

g

gender, as a basic condition 26, 27
general principles, of anatomy-driven paradigm
about 56, 57
dental roots 56, 57–59, 60
maxillary sinus 60, 62–63
nasal cavity 60, 64
neurovascular bundles 59, 60, 61–62
geometry, as a risk factor for failure of orthodontic temporary anchorage devices 541, 542
gingiva, attached, as a soft tissue factor of interradicular sites of mandibular labial region 307, 311, 312
glucocorticoids 30, 31
guide cylinders
combining with guide plate 461
creating digital models for 457, 459
generating 461, 464
guide plates
combining with guide cylinder 461
determining area of, on digital dental model 461
generating 461
guided surgery, evolution of insertion guides for 437, 438, 439, 440
gummy smile, correction of 118, 121–122, 123–124

h

habits 30, 31–32
hard tissue
about 32–33
alveolar bone and extra-alveolar bone 33, 34
bone density 33, 35–36
bone depth 33, 35, 37, 38–39
bone width 37, 38, 39, 40–42
cortical thickness 37, 39, 42
mandibular ramus 389, 391, 392–393
selection of optimal sites 39, 43

t.me/Dr_Mouayyad_AlbtousH

hard tissue factor
for buccal shelf of mandibular buccal region
bone depth 364, 369, 370
cortical thickness 364, 367–368
plateau features 364, 366–367
for infrazygomatic crest (IZC)
bone depth 188, 190, 191, 192
cortical thickness 188, 189
crest shape 187–188
dental roots 192–193
for interradicular sites of mandibular buccal region
bone depth 336, 338
bone width 336, 339–340
cortical thickness 335–336
shape of cortical plate 336, 340
for interradicular sites of mandibular labial region
bone depth 307, 308–310
bone width 307, 310–311
cortical thickness 305, 306–307
root prominence 307, 311
for interradicular sites of maxillary buccal region
bone density 146, 147
bone depth 149–151
bone width 151, 153, 152–154
buccal exostosis 153, 154–155
cortical thickness 146, 148–149
for interradicular sites of maxillary labial region
bone depth 99–100, 100, 101
bone width 100–102, 102, 103, 104, 105
cortical thickness 98–99
root prominence 103, 106
for mandibular symphysis
bone depth 322, 323
cortical thickness 321, 322
for maxillary palatal region
bone depth 240–241, 241, 242
bone width 241, 243, 243, 244
cortical thickness 238–240, 239–240
inclination of cortical plate 244, 245
for maxillary tuberosity
bone density 225, 226
bone dimension 226–227, 228
cortical thickness 226, 227
for midpalatal suture 297–298
for paramedian sites
bone depth 271, 272
cortical thickness 270–271
hyperplasia, soft tissue 516, 518
hypertrophic soft tissue, excision of 530

i

image superimposition 451, 455–457
implant-associated risk factors
of failure of orthodontic temporary anchorage devices
about 541, 542
design 541, 542
geometry 541, 542
shape 541, 542, 543
surface topology 543
of fractures of orthodontic temporary anchorage devices 505–507
incisor intrusion
biomechanics-driven paradigm 79, 80–81
in maxillary labial region 114, 115, 117–118, 119–120
in vertical dimension 16, 17
inclination of cortical plate, as a hard tissue factor of maxillary palatal region 244, 245
indications, clinical
about 9–10
mini-plates
about 418
anatomical factors undesirable for mini-implants 422, 424–428
biomechanical advantages 422, 428–430
orthopaedic treatment for skeletal discrepancy 420, 421–422, 423
sagittal dimension 11–12, 13–14
transverse dimension 16, 18, 19
vertical dimension 12, 15–16, 17–18
indirect anchorage, direct anchorage *versus* 8–9
infection, soft tissue 517, 519
infrazygomatic crest (IZC)
anatomical characteristics
about 183, 185–186
hard tissue factor: bone depth 188, 190, 191, 192
hard tissue factor: cortical thickness 188, 189
hard tissue factor: crest shape 187–188
hard tissue factor: dental roots 192–193
soft tissue factor: maxillary sinus 194, 195
soft tissue factor: soft tissue type 192, 194
biomechanical considerations 194, 195, 196
clinical applications
anterior intrusion 208, 209, 217
molar distalisation 201, 202, 203–208, 209, 210–212, 213–214, 215
molar intrusion 209, 213, 218, 219–221
orthodontic traction of impacted teeth 214, 218, 222–223
insertion techniques
insertion procedures 197–201, 202, 203
preinsertion 196, 197
selection of appropriate insertion sites 196, 197
initial procedures, for mandibular ramus 397, 398
insertion
for buccal shelf of mandibular buccal region 160–164, 165, 166
for interradicular sites of mandibular buccal region 345–350
for mandibular ramus
biomechanical analysis 401, 402
clinical procedures 399–401, 402
initial procedures 397, 398
insertion on skulls 397, 398
for paramedian sites 160–164, 165, 166
insertion angle, as a risk factor of failure of orthodontic temporary anchorage devices 539, 540, 541
insertion angulation
meticulous design of 496, 497
as a risk factor 496–498
insertion depth, as a risk factor of failure of orthodontic temporary anchorage devices 539, 540

t.me/Dr_Mouayyad_AlbtousH

insertion guides
about 437
advantages of
accuracy and precision 446, 447–448
ease of insertion 446, 449
efficiency 446, 448–449
clinical procedures
anaesthesia 476, 477
detaching screwdrivers 479
inserting mini-implants 476, 477–478
removing insertion guides 479
verifying fit of insertion guides 473–475
disadvantages
cost 449
no change during insertion 449–450
time needed for CAD-CAM 449
evolution of
concept of guided surgery 437, 438, 439, 440
for mini-implants 439, 440–445
manufacturing insertion guides
adding supporting components for insertion guide 464, 465
examples of insertion guides for different anatomical sites 466, 468–470
exporting STL file 464
generating actual insertion guide through 3-D printing 464, 466
polishing insertion guide 464, 467
removing supporting components for insertion guide 464, 467
try-in on dental model 464, 467
placement of mini-implants with insertion guides at different sites
buccal interradicular region 480–481, 482
buccal shelf 481, 483, 484
labial interradicular region 479
palatal region 480, 483
removing 479
three-dimensional design of, for mini-implants
about 451, 461, 463
combining guide plate and guide cylinder 461
determining area of guide plate on digital dental model 461
establishing digital data of mini-implants and screwdrivers 457
generating guide cylinder 461, 464
generating guide plate 461
reconstructing three-dimensional dentition model 451, 452, 453, 454, 455, 456, 457
virtual placement of mini-implants 459, 460, 461, 462
verifying fit of 473–475
insertion height, as a risk factor 494, 539, 540
insertion on skulls, mandibular ramus and 397, 398
insertion principles
about 55, 56
anatomy-driven paradigm
about 56
available anatomical sites 64–74
general principles 56–64
biomechanics-driven paradigm
about 75, 76, 77
incisor intrusion 79, 80–81
maxillary molar uprighting 76, 77, 78
molar intrusion 77, 79, 80
molar protraction 82, 84, 85
orthodontic traction of impacted molars 79, 82, 83
clinical procedures for inserting mini-implants
insertion of mini-implants 86, 87–89, 91
post-insertion examination 90, 91–92
preinsertion preparation 85–86, 87
insertion requirements
about 25, 26, 51
local requirements
about 32
hard tissue 32–40, 41–43
soft tissue 40, 43–45, 46
systemic requirements
about 26, 27
basic conditions 26, 27
drugs 28–30, 31
habits 30, 31–32
systemic diseases 28, 29
insertion site-associated risk factors 507–508
insertion sites
for anterior nasal spine 132, 134
for buccal shelf in mandibular buccal region 371–372
for interradicular sites of maxillary labial region
about 107
U1-U1 site 107–110, 111–112
U1-U2 site 110, 112–114, 115, 116
U2-U3 site 110, 112–114, 115, 116
for mandibular buccal region 343, 344
for mandibular ramus 394–395, 396
for mini-implants 459, 461, 462
prudent selection of 496, 497, 507, 508
as a risk factor 493
selecting for prevention of soft tissue complications 525, 526
insertion techniques
for anterior nasal spine 134–136, 137
appropriate 497, 498, 508, 510
for buccal shelf of mandibular buccal region
insertion 160–164, 165, 166
postinsertion 373, 377
preinsertion 372
for infrazygomatic crest (IZC)
insertion procedures 197–201, 202, 203
preinsertion 196, 197
for interradicular sites of mandibular buccal region 345–350
insertion 345–350
postinsertion 350
preinsertion 345
for interradicular sites of mandibular labial region 313–320
for interradicular sites of maxillary labial region
about 107
insertion procedures 160–164, 165, 166
preinsertion 160
U1-U1 site 107–110, 111–112
U1-U2 site 110, 112–114, 115, 116
U2-U3 site 110, 112–114, 115, 116

t.me/Dr_Mouayyad_AlbtousH

insertion techniques (*cont'd*)
for mandibular symphysis 325–330
for maxillary tuberosity
insertion procedures 229–230, 231
postinsertion 230
preinsertion 229
for mini-plates 431–433
for paramedian sites
insertion 160–164, 165, 166
postinsertion 279
preinsertion 273, 275, 276
for prevention of soft tissue complications 525, 526, 527
interradicular sites
anatomical characteristics for maxillary labial region
about 95, 98
hard tissue factor: bone depth 99–100, 101
hard tissue factor: bone width 100–102, 103, 104, 105
hard tissue factor: cortical thickness 98–99
hard tissue factor: root prominence 103, 106
soft tissue factor: labial frenum 103, 106
soft tissue factor: mucogingival junction 103, 106
anatomical characteristics of maxillary buccal region
about 145, 147
hard tissue factor: bone density 146, 147
hard tissue factor: bone depth 149–151
hard tissue factor: bone width 151, 152–154
hard tissue factor: buccal exostosis 153, 154–155
hard tissue factor: cortical thickness 146, 148–149
soft tissue factor: buccal frenum 156, 157
soft tissue factor: soft tissue type 154–156
biomechanical considerations 103, 107, 156, 157, 158
clinical applications
en masse anterior retraction 164, 166, 167, 168, 169, 170, 171, 172–173, 174
in maxillary labial region 350–363
molar intrusion 170, 171, 177–180
molar protraction 168, 170, 175–176
occlusal canting 171, 174, 180–183, 184
insertion techniques
insertion procedure 160–164, 165, 166
in maxillary labial region 107–114, 115, 116
preinsertion 160
mandibular buccal region
anatomical characteristics 335–342
biomechanical considerations 343, 344
clinical applications 350–363
insertion techniques 345–350
selection of appropriate insertion sites 343, 344
mandibular labial region
anatomical characteristics 305–311, 312
biomechanical perspectives 311, 312, 313
determining optimal sites 312, 313, 314
insertion techniques 313–320
maxillary palatal region
anatomical characteristics 238–248
biomechanical considerations 248
clinical applications 252–269
insertion techniques 248, 249–251
selection of appropriate insertion sites 248, 249
selection of appropriate insertion sites 107, 158–160
interradicular space, limited, as a risk factor 493, 494
intrusion
anterior, as a clinical application with infrazygomatic crest 208, 209, 216–217
incisor
biomechanics-driven paradigm 79, 80–81
in maxillary labial region 114, 115, 117–118, 119–120
in vertical dimension 16, 17
molar
biomechanics-driven paradigm 77, 79, 80
as a clinical application with infrazygomatic crest 209, 213, 218, 219–221
for interradicular sites of mandibular buccal region 354, 358, 359, 360–361
for interradicular sites of maxillary buccal region 170, 171, 177–180
for interradicular sites of maxillary palatal region 257, 260–261
for paramedian sites 293, 295
in vertical dimension 12, 15, 16, 17–18
IZC (infrazygomatic crest)
anatomical characteristics
about 183, 185–186
hard tissue factor: bone depth 188, 190, 191, 192
hard tissue factor: cortical thickness 188, 189
hard tissue factor: crest shape 187–188
hard tissue factor: dental roots 192–193
soft tissue factor: maxillary sinus 194, 195
soft tissue factor: soft tissue type 192, 194
biomechanical considerations 194, 195, 196
clinical applications
anterior intrusion 208, 209, 217
molar distalisation 201, 202, 203–208, 209, 210–212, 213–214, 215
molar intrusion 209, 213, 218, 219–221
orthodontic traction of impacted teeth 214, 218, 222–223
insertion techniques
insertion procedures 197–201, 202, 203
preinsertion 196, 197
selection of appropriate insertion sites 196, 197

t.me/Dr_Mouayyad_AlbtousH

j

jaw model, acquisition of 451, 453–454

l

labial frenum
  as a soft tissue factor of interradicular sites of mandibular labial region 307, 311
  as a soft tissue factor of interradicular sites of maxillary labial region 103, 106
labial interradicular region, placement of mini-implants with insertion guides in 479
lesion, soft tissue 517, 519
lingually angulated impacted mandibular second molars, traction of 405, 407–409
loading time, as a risk factor of failure of orthodontic temporary anchorage devices 540–541
local factors, as risk factors of failure of orthodontic temporary anchorage devices 537–538
local requirements
  about 32
  hard tissue 32–40, 41–43
  soft tissue 40, 43–45, 46

m

management
  of failure of orthodontic temporary anchorage devices 544–545
  of root contact 498
mandible, as an available anatomical site 68, 71–74
mandibular buccal region
  about 333, 334–335, 386
  buccal shelf
    anatomical characteristics 364–369, 370–371
    biomechanical considerations 369, 372
    clinical applications 376, 377–386
    insertion techniques 372–376, 377
    selection of appropriate insertion sites 371, 372
  interradicular sites
    anatomical characteristics 335–342
    biomechanical considerations 343, 344
    clinical applications 350–363
    insertion techniques 345–350
    selection of appropriate insertion sites 343, 344
mandibular dentition distalisation, as a clinical application for buccal shelf in mandibular buccal region 376, 377–386
mandibular labial region
  about 303–304
  interradicular sites
    anatomical characteristics 305–311, 312
    biomechanical perspectives 311, 312, 313
    determining optimal sites 312, 313, 314
    insertion techniques 313, 315–320
  mandibular symphysis
    about 320, 321
    anatomical features 320, 321–323, 324–325
    biomechanical considerations 323, 325
    insertion techniques 325–330
    selection of optimal sites 325
mandibular ramus
  about 389, 390, 413
  anatomical considerations
    anatomical location 389, 390, 391
    hard tissue considerations 389, 391, 392, 393
    optimal insertion sites 394, 395–396
    soft tissue considerations 391, 394, 395
  insertion procedure
    biomechanical analysis 401, 402
    clinical procedures 399–401, 402
    insertion procedures 397, 398
    insertion on skulls 397, 399
  mini-implant selection 396–397
  versatile clinical applications
    orthodontic traction of vertically impacted mandibular second molars 405, 406, 407
    traction of lingually angulated impacted mandibular second molar 405, 407, 408–409
    traction of mandibular third molar away from inferior alveolar canal 409, 410–412
    uprighting mesioangulated impacted mandibular second molars 402–405
mandibular symphysis, in mandibular labial region
  about 320, 321
  anatomical features 320, 321–323, 324, 325
  biomechanical considerations 323, 325
  insertion techniques 325–330
  selection of optimal sites 325
mandibular third molars away from inferior alveolar canal, traction of 409, 410–412
manifestations, clinical
  of root contact 488, 489
  soft tissue complications
    about 516
    soft tissue hyperplasia 516, 518
    soft tissue infection 517, 519
    soft tissue lesion 517, 519
    soft tissue swelling 516, 517
manufacturing insertion guides
  adding supporting components for insertion guide 464, 465
  examples of insertion guides for different anatomical sites 466, 468–470
  exporting STL file 464
  generating actual insertion guide through 3-D printing 464, 466
  polishing insertion guide 464, 467
  removing supporting components for insertion guide 464, 467
  try-in on dental model 464, 467
materials
  as a factor associated with mini-implants 523, 524
  for orthodontic temporary anchorage devices 2
maxillary arch expansion
  as an available anatomical site 64, 66–68, 69–71
  in transverse dimension 16, 18

t.me/Dr_Mouayyad_AlbtousH

maxillary buccal region
about 145, 146, 147, 232
infrazygomatic crest (IZC)
anatomical characteristics 183, 185–194, 195
biomechanical considerations 194, 195, 196
clinical applications 201, 202, 203, 204–223
insertion techniques 196, 197–201, 202, 203
selection of appropriate insertion sites 196, 197
interradicular sites
anatomical characteristics 145–146, 147, 148–156, 157
biomechanical considerations 156, 157, 158
clinical applications 164, 166, 167–183, 184, 185
insertion techniques 160–164, 165, 166
selection of appropriate insertion sites 158–160
maxillary tuberosity
anatomical characteristics 223–228
biomechanical considerations 228
clinical applications 230, 231, 232
insertion techniques 229–230, 231
selection of appropriate insertion sites 229
maxillary labial region
about 95, 96–98, 143
anterior nasal spine (ANS)
anatomical features 125, 127, 129–132, 133
biomechanical considerations 132, 133
clinical applications 136, 138–143
insertion techniques 134–136, 137
selection of appropriate insertion sites 132, 134
interradicular sites
anatomical features 95, 98–103, 104–106
biomechanical considerations 103, 107
clinical applications 114, 115, 117–125, 126, 127, 128
insertion techniques 107–114, 115, 116
selection of appropriate insertion sites 107
maxillary molar uprighting, in biomechanics-driven paradigm 76, 77, 78
maxillary palatal region
about 235–237, 301
interradicular sites
anatomical characteristics 238–248
biomechanical considerations 248
clinical applications 252–269
insertion techniques 248, 249, 250–251
selection of appropriate insertion sites 248, 249
midpalatal suture
about 296–297
anatomical features 297–298
clinical applications 299, 300
insertion techniques 299, 300
optimal insertion sites 298, 299
paramedian sites
anatomical characteristics 270–273, 274
biomechanical considerations 273, 274, 275
clinical applications 280–295
insertion techniques 273, 275–279
selection of optimal insertion sites 273, 275
maxillary sinus
as a general principle 60, 62, 63
as a soft tissue factor in infrazygomatic crest (IZC) 194
maxillary tuberosity
about 223–225
anatomical characteristics
about 223–225
hard tissue factor: bone density 225–226
hard tissue factor: bone dimension 226, 227, 228
hard tissue factor: cortical thickness 226, 227
soft tissue factor: soft tissue thickness 228
soft tissue factor: types of soft tissue 228
biomechanical considerations 228
clinical applications 230, 231–232
insertion techniques
insertion procedures 229–230, 231
postinsertion 230
preinsertion 229
selection of appropriate insertion sites 229
mechanical retention
about 5, 6, 7
direct *versus* indirect anchorage 8–9
primary stability 7–8
secondary stability 7–8
mesioangulated impacted mandibular second molars, uprighting 402–405
midpalatal suture, in maxillary palatal region
about 296–297
anatomical features 297–298
clinical applications 299, 300
insertion techniques 299, 300
optimal insertion sites 298, 299
mini-implant-assisted skeletal expansion, for paramedian sites 286, 288–289
mini-implants
about 4–5
anatomical factors undesirable for 422, 425–428
creating digital models for 457, 459
establishing digital data of 457, 459
evolution of insertion guides for mini-implants 439, 440–445
factors associated with 523, 524
inserting 85–92, 476, 477–479
judicious selection of appropriate 508, 510
management of fractures in
clinical decisions in different clinical scenarios 511
clinical techniques for removing fractured mini-implants 511, 512
placement of, with insertion guides at different sites
buccal interradicular region 480, 481, 482
buccal shelf 481, 483–484
labial interradicular region 479
palatal region 480, 483

t.me/Dr_Mouayyad_AlbtousH

position of 522–523, 524
post-insertion examination of 90, 91, 92
preinsertion preparation for 85–86, 87
prevention of fractures in
appropriate insertion techniques 508, 510
judicious selection of appropriate mini-implants 508, 510
prudent selection of insertion sites 508, 509
prognosis of 490–491
risk factors for fractures in
about 504
implant-associated factors 505–507
insertion site-associated factors 507–508
operator-associated factors 504–505
selecting 396–397
three-dimensional design and manufacture of insertion guides for
combining guide plate and guide cylinder 461
determining area of guide plate on digital dental model 461
establishing digital data of mini-implants and screwdrivers 457, 459
generating guide cylinder 461, 464
generating guide plate 461
reconstructing three-dimensional dentition model 451–457, 458, 459
virtual placement of mini-implants 459, 460–461, 462
mini-plates
about 5, 6, 415, 416, 434
clinical features
available anatomical sites 418–420
advantages and disadvantages 417–418
structure 415, 416–417
clinical indications
about 420
anatomical factors undesirable for mini-implants 422, 425–428
biomechanical advantages 422, 428–430
orthopaedic treatment for skeletal discrepancy 420–422, 423
insertion techniques 431–433
removal techniques 433–434
model post-processing 457, 458–459
molar anchorage reinforcement, for paramedian sites 280, 284–286, 287, 288
molar distalisation
as a clinical application with infrazygomatic crest 201, 202, 203, 204–223
for interradicular sites 257, 259, 261–263, 264, 265
for paramedian sites 280, 281, 282, 283, 284
in sagittal dimension 11, 12, 13
molar intrusion
biomechanics-driven paradigm 77, 79, 80
as a clinical application with infrazygomatic crest 209, 213, 214, 218–223
for interradicular sites 170, 171, 177–180, 257, 260, 261
for interradicular sites of mandibular buccal region 354, 358, 359, 360, 361
for paramedian sites 293, 295
in vertical dimension 12, 15, 16, 17
molar protraction
biomechanics-driven paradigm 82, 84–85
for interradicular sites 168, 170, 175–176, 263, 265–269
for interradicular sites of mandibular buccal region 353, 354, 355–358
in sagittal dimension 11, 12, 13, 14
molar uprighting
as a clinical application for buccal shelf in mandibular buccal region 379, 381–384
for interradicular sites of mandibular buccal region 358, 359, 361–363
monocortical engagement, biocortical engagement *versus* 540
morphology, of orthodontic temporary anchorage devices 4–5, 6
mucogingival junction, as a soft tissue factor 103, 106

n

nasal cavity, as a general principle 60, 64
neurovascular bundles, as a general principle 59, 60, 61–62
no change during insertion, as a disadvantage of insertion guides 449, 450

o

occlusal canting
correction of 122, 125, 126, 127, 128
for interradicular sites 171–173, 188–204
operator-associated risk factors
failure of orthodontic temporary anchorage devices
about 538, 539
biocortical *versus* monocortical engagement 540
insertion angle 539–540, 541
insertion depth 539, 540
insertion height 539, 540
loading time 540–541
root proximity 538, 539
self-tapping *versus* self-drilling 540
fracture of orthodontic temporary anchorage devices 504, 505–506
for soft tissue complications 522, 523–524
optimal sites
determining for interradicular sites of mandibular labial region 312–313, 314
for mandibular symphysis 323, 325
selection of 37, 43, 45–50
oral hygiene care
as a habit 31
for prevention of soft tissue complications 525, 526
orthodontic temporary anchorage devices (TADs)
about 1, 21
characteristics of
drilling methods 5, 6
materials 2
morphology 2–5

t.me/Dr_Mouayyad_AlbtousH

orthodontic temporary anchorage devices (TADs) (*cont'd*)
clinical indications for
about 9–11
sagittal dimension 9, 11–12, 13–15
transverse dimension 14–19
vertical dimension 15, 16–18
evolution of 1–3
failure of
about 534, 535, 546
management of 544
prevention of 543
primary stability 534–536, 537
risk factors 537–541, 542, 543
secondary stability 534–536, 537
fractures of
about 501, 502, 503, 512
management of mini-implant fracture 511, 512
prevention of mini-implant fracture 508, 509, 510
risk factors for mini-implant fracture 504, 505, 505–507, 508
mechanical retention of
about 5, 7
direct *versus* indirect anchorage 6, 8–9
primary stability 5–6, 8
secondary stability 5–6, 8
potential complications 19–21
orthodontic traction
of impacted molars in biomechanics-driven paradigm 82, 83
of impacted teeth
as a clinical application for buccal shelf in mandibular buccal region 214–215, 384–386
as a clinical application with infrazygomatic crest 214, 216, 222–223
of vertically impacted mandibular second molars 405, 405, 406–407
orthopaedic treatment, for skeletal discrepancy 420–421, 423, 424
osteoporosis, as a systemic disease 28

p

palatal region, placement of mini-implants with insertion guides in 480, 483
paradigms
anatomy-driven
about 55
available anatomical sites
about 62, 64
mandible 66, 71–73
maxilla 64–66, 67–68, 69–71
general principles
about 55, 56
dental roots 56–59
maxillary sinus 60, 62, 63
nasal cavity 62, 64
neurovascular bundle 59–60, 61
biomechanics-driven
about 75, 75–76, 77
incisor intrusion 79, 80–81
maxillary molar uprighting 76–77, 78
molar intrusion 77, 79, 80
molar protraction 82, 84, 85
orthodontic traction of impacted molars 82, 83
paramedian sites
insertion techniques
insertion 271, 276, 277, 278
postinsertion 279
preinsertion 273, 275, 276
maxillary palatal region
about 270
anatomical characteristics 270, 271, 270–274
biomechanical considerations 273, 274–275
clinical applications 280, 300, 280–293, 295–297
hard tissue factor: bone depth 270, 271, 276, 277
hard tissue factor: cortical thickness 270, 271
insertion techniques 271, 273, 275, 277, 278, 279
selection of optimal insertion sites 273, 275
soft tissue factor: soft tissue thickness 272
vital anatomical structures 272, 273–274
mini-implant-assisted skeletal expansion 286, 288–289
molar anchorage reinforcement 280, 286–287
molar distilisation 280, 281–282, 283, 284
molar intrusion 293, 295
traction of impacted teeth 289–294
patient-associated risk factors
failure of orthodontic temporary anchorage devices
about 537
local factors 537–538
systemic factors 537
for soft tissue complications 517, 519, 520, 521–522
peri-implant irrigation and scaling 528, 529
periodontal tissues, dental roots and 491–492, 496, 497
plateau features, as a hard tissue factor of buccal shelf of mandibular buccal region 364, 366–367
polishing insertion guides 464, 467
postinsertion
for buccal shelf of mandibular buccal region 376, 377
for interradicular sites of mandibular buccal region 350
for paramedian sites 279
precision, as an advantage of insertion guides 446, 447–448
preinsertion
for buccal shelf of mandibular buccal region 372
for interradicular sites of mandibular buccal region 345
for mandibular ramus 397, 401
for paramedian sites 273, 275, 276
prevention
of failure of orthodontic temporary anchorage devices 543–544
root contact
appropriate anaesthesia and insertion technique 497, 498
meticulous design of insertion angulation 496, 497
prudent selection of insertion sites 496, 497
soft tissue complications
meticulous oral hygiene care 525, 526

t.me/Dr_Mouayyad_AlbtousH

prevention of excessive soft tissue trauma 526–527
prudent selection of insertion sites 525, 526
sophisticated insertion techniques 525–526
primary stability 5–6, 8, 534–536, 537
procedures, clinical
for inserting mini-implants
insertion of mini-implants 86–90
post-insertion examination 90, 91
preinsertion preparation 85–86, 87
for insertion guides
anaesthesia 476, 477
detaching screwdrivers 479
inserting mini-implants 476, 477, 478–479
removing insertion guides 479
verifying fit of insertion guides 473–474, 475
mandibular ramus
insertion 397, 399, 402, 403
postinsertion 401
preinsertion preparation 399
for removing fractured mini-implants 511, 512
prognosis, of root contact
mini-implants 490, 491
periodontal tissues and dental roots 491–492, 495, 496
protraction, molar
biomechanics-driven paradigm 82, 84, 85
for interradicular sites 168–169, 175, 176, 252, 253, 275–279
for interradicular sites of mandibular buccal region 354, 356, 378–382
in sagittal dimension 12, 13–14

r

removal techniques, for mini-plates 433, 434
retraction, anterior
as a clinical application for interradicular sites 252–253, 254, 255, 256–257
for interradicular sites of mandibular buccal region 350–351, 352–353, 354
in sagittal dimension 11
risk factors
root contact
insertion angulation 495, 496
insertion height 494
insertion site 493
limited interradicular space 493–494
soft tissue complications
factors associated with mini-implants 523–524
operator factors 522–523, 522, 523, 524
patient factors 520–521, 521, 522
risk factors, implant-associated
of failure of orthodontic temporary anchorage devices
about 541, 542
design 541, 542
geometry 541, 542
shape 541, 542, 543
surface topology 543
of fractures of orthodontic temporary anchorage devices 505–506, 506–507
risk factors, operator-associated
of failure of orthodontic temporary anchorage devices
about 538, 539
biocortical *versus* monocortical engagement 540
insertion angle 539–540, 541
insertion depth 539, 540
insertion height 539, 540
loading time 540–541
root proximity 538, 539
self-tapping *versus* self-drilling 540
fracture of orthodontic temporary anchorage devices 504, 505
for soft tissue complications 522, 523, 524
risk factors, patient-associated
of failure of orthodontic temporary anchorage devices
about 537
local factors 537–538
systemic factors 537, 538
for soft tissue complications 520–521, 522
root contact
about 487–488, 488, 499
clinical manifestations 488, 489
management of 498
prevention
appropriate anaesthesia and insertion technique 497, 498
meticulous design of insertion angulation 496–497
prudent selection of insertion sites 496, 497
prognosis
mini-implants 490–491
periodontal tissues and dental roots 491, 492
risk factors
insertion angulation 495, 496
insertion height 494
insertion site 493
limited interradicular space 493–494
root prominence
as a hard tissue factor of interradicular sites in maxillary labial region 103, 106
as a hard tissue factor of interradicular sites of mandibular labial region 307, 311
root proximity, as a risk factor of failure of orthodontic temporary anchorage devices 538, 539

s

sagittal dimension, of orthodontic temporary anchorage devices 11–12, 13–15
screwdrivers
creating digital models for 457, 459
detaching 479
establishing digital data of 457, 459
secondary stability 7, 8, 534–535, 535–536
self-drilling drilling method
about 5, 6
self-tapping *versus* 540
self-tapping drilling method
about 5, 6
self-drilling *versus* 540
shape, as a risk factor for failure of orthodontic temporary anchorage devices 541, 542, 543
skeletal discrepancy, orthopaedic treatment for 420–422, 423

t.me/Dr_Mouayyad_AlbtousH

skeletal orthopaedics, in sagittal dimension 12, 15
smoking
as a habit 30, 31, 32
as a risk factor for soft tissue complications 521
soft tissue
about 40, 43
mandibular ramus 391, 394, 395
selection of optimal sites 45–50
thickness of 40, 45, 46
types of 40, 44
soft tissue complications
about 515, 516, 530
adverse consequences 519, 520
clinical manifestations
about 516, 517
soft tissue hyperplasia 516, 518
soft tissue infection 517, 519
soft tissue lesion 517, 519
soft tissue swelling 516, 517
prevention
meticulous oral hygiene care 525
prevention of excessive soft tissue trauma 526, 528
prudent selection of insertion sites 525, 526
sophisticated insertion techniques 525–526, 527
risk factors
factors associated with mini-implants 523–524
operator factors 522, 523, 524
patient factors 520–521, 522
treatment
excision of hypertrophic soft tissue 530
local debridement and drainage 528
peri-implant irrigation and scaling 528, 529
removal of causative factors 528, 529
soft tissue factor
for buccal shelf of mandibular buccal region
soft tissue thickness 369, 371
soft tissue type 369, 371
for infrazygomatic crest (IZC)
maxillary sinus 194, 195
soft tissue type 192, 194
for interradicular sites of mandibular buccal region
buccal frenum 341, 342
soft tissue types 340–341
for interradicular sites of mandibular labial region
attached gingiva 307, 311, 312
labial frenum 307, 311
for interradicular sites of maxillary buccal region
buccal frenum 156, 157
soft tissue type 154–156
for interradicular sites of maxillary labial region
labial frenum 103, 106
mucogingival junction 103, 106
for mandibular symphysis 323, 324–325
for maxillary palatal region
soft tissue thickness 246, 247
soft tissue type 246
for maxillary tuberosity
soft tissue thickness 228
types of soft tissue 228
for midpalatal suture 298
for paramedian sites 271–272
soft tissue hyperplasia 516, 518
soft tissue infection 517, 519
soft tissue lesion 517, 519
soft tissue swelling 516, 517
soft tissue thickness
about 40, 45, 46
as a soft tissue factor for midpalatal suture 298
as a soft tissue factor of buccal shelf of mandibular buccal region 369, 371
as a soft tissue factor of maxillary palatal region 246, 247
as a soft tissue factor of maxillary tuberosity 228
soft tissue type
as a soft tissue factor in infrazygomatic crest (IZC) 192, 194
as a soft tissue factor in interradicular sites of maxillary buccal region 154–156
as a soft tissue factor of buccal shelf of mandibular buccal region 369, 371
as a soft tissue factor of maxillary palatal region 246
stainless steel 2
STL file, exporting 464
structure, of mini-plates 415, 416–417
surface properties, as a factor associated with mini-implants 523–524
surface topology, as a risk factor for failure of orthodontic temporary anchorage devices 543
swelling, soft tissue 516, 517
systemic diseases
diabetes 28, 29
osteoporosis 28
systemic factors, as risk factors of failure of orthodontic temporary anchorage devices 537, 538
systemic requirements
about 26, 27
basic conditions
age 26, 27
gender 26, 27
drugs
bisphosphonates 28–29, 30
glucocorticoids 30, 31
habits 31
systemic diseases
diabetes 28, 29
osteoporosis 28

t

TADs (temporary anchorage devices)
about 1, 21
characteristics of
drilling methods 5, 6
materials 2
morphology 4–5, 6
clinical indications for
about 9, 10
sagittal dimension 11–12, 13–15
transverse dimension 16, 18–19
vertical dimension 12, 15–18
evolution of 1–2, 3
failure of
about 533, 534, 546
management of 544, 545
prevention of 543–544
primary stability 534–536
risk factors 537–543, 537–542
secondary stability 534–536
fractures of

t.me/Dr_Mouayyad_AlbtousH

about 501, 502, 503, 512
management of mini-implant fracture 511, 512
prevention of mini-implant fracture 508, 509–510
risk factors for mini-implant fracture 504–507, 505–507, 508
mechanical retention of
about 5, 6, 7
direct *versus* indirect anchorage 8–9
primary stability 7, 8
secondary stability 7, 8
potential complications 19–21
temporary anchorage devices (TADs)
about 1, 21
characteristics of
drilling methods 5, 6
materials 2
morphology 4–5, 6
clinical indications for
about 9, 10
sagittal dimension 11–12, 13–15
transverse dimension 16, 18–19
vertical dimension 12, 15–18
evolution of 1–2, 3
failure of
about 533, 534, 546
management of 544, 545
prevention of 543–544
primary stability 534–536
risk factors 537–543
secondary stability 534–536
fractures of
about 501, 502, 503, 512
management of mini-implant fracture 511, 512
prevention of mini-implant fracture 508, 509–510
risk factors for mini-implant fracture 504–507, 508
mechanical retention of
about 5, 6, 7
direct *versus* indirect anchorage 8–9
primary stability 7, 8
secondary stability 7, 8
potential complications 19–21
3-D (three-dimensional) dentition model, reconstructing 451, 452, 453, 454, 455, 456, 457, 458, 459
3-D (three-dimensional) design of insertion guides, for mini-implants
about 451, 461, 463
combining guide plate and guide cylinder 461
determining area of guide plate on digital dental model 461
establishing digital data of mini-implants and screwdrivers 457, 459
generating guide cylinder 461, 464
generating guide plate 461
reconstructing three-dimensional dentition model 451, 452, 453, 454, 455, 456, 457, 458, 459
virtual placement of mini-implants 459, 460, 461, 462
3-D printing, generating actual insertion guide through 464, 466
time needed for CAD-CAM, as a disadvantage of insertion guides 449
tissue
hard
about 32–33
alveolar bone and extra-alveolar bone 33, 34, 35
bone density 33, 35–37
bone depth 33, 34, 37, 38–39
bone width 37, 38, 40–42
cortical thickness 37, 39, 42
mandibular ramus 389, 391, 392–393
selection of optimal sites 39, 43
hard tissue factor
for buccal shelf of mandibular buccal region 364, 366–369, 370
for infrazygomatic crest (IZC) 187–192, 193
for interradicular sites of mandibular buccal region 335–336, 337–340
for interradicular sites of mandibular labial region 305, 307–311
for interradicular sites of maxillary buccal region 146, 147, 148–153, 154, 155
for interradicular sites of maxillary labial region 95, 98–103, 98, 99, 100, 101, 102, 103, 104, 105, 106
for mandibular symphysis 321–323
for maxillary palatal region 238–245
for maxillary tuberosity 225–227, 228
for midpalatal suture 297–298
for paramedian sites 270–271, 272
soft
about 40, 43
mandibular ramus 391, 394, 395
selection of optimal sites 45–50
thickness of 40, 45, 46
types of 40, 44
soft, complications with
about 515, 516, 530
adverse consequences 519, 520
clinical manifestations 516–519, 517–519
prevention 525–526, 525–528
risk factors 520–524, 521–524
treatment 528–530, 529–530
soft tissue factor
for buccal shelf of mandibular buccal region 369, 371
for infrazygomatic crest (IZC) 192, 194, 195
for interradicular sites of mandibular buccal region 340–341, 342
for interradicular sites of mandibular labial region 307, 311, 312
for interradicular sites of maxillary buccal region 154–156, 157
for interradicular sites of maxillary labial region 103, 106
for mandibular symphysis 323, 324–325
for maxillary palatal region 246, 247
for maxillary tuberosity 228
for midpalatal suture 298
for paramedian sites 271–272
soft tissue thickness
as a soft tissue factor for midpalatal suture 298

t.me/Dr_Mouayyad_AlbtousH

tissue (*cont'd*)
as a soft tissue factor of buccal shelf of mandibular buccal region 369, 371
as a soft tissue factor of maxillary palatal region 246, 247
as a soft tissue factor of maxillary tuberosity 228
soft tissue type
as a soft tissue factor in infrazygomatic crest (IZC) 192, 194
as a soft tissue factor in interradicular sites of maxillary buccal region 154–156
as a soft tissue factor of buccal shelf of mandibular buccal region 369, 371
as a soft tissue factor of maxillary palatal region 246
titanium alloy 2
traction
of impacted molars in biomechanics-driven paradigm 79, 82–83
of impacted teeth
as a clinical application for buccal shelf in mandibular buccal region 379, 384, 385, 386
as a clinical application with infrazygomatic crest 214, 218, 222–223
for paramedian sites 289–293, 294
of lingually angulated impacted mandibular second molars 405, 407–409
of mandibular third molars away from inferior alveolar canal 409, 410–412
of vertically impacted mandibular second molars 405, 406–407
transverse dimension, of orthodontic temporary anchorage devices 16, 18–19
treatment, of soft tissue complications
excision of hypertrophic soft tissue 530
local debridement and drainage 528
peri-implant irrigation and scaling 528, 529
removal of causative factors 528, 529
try-in, for insertion guides on dental model 464, 467

u

U1-U1 site 107, 109–110, 108–110, 111, 112
U1-U2 site 110, 112–114, 115, 116
U2-U3 site 110, 112–114, 115, 116
uprighting
as a clinical application for buccal shelf in mandibular buccal region 379, 381–384
for interradicular sites of mandibular buccal region 358–359, 361–363
for mesioangulated impacted mandibular second molars 402–405

v

versatile clinical applications, for mandibular ramus
orthodontic traction of vertically impacted mandibular second molars 405, 406–407
traction
of lingually angulated impacted mandibular second molar 405, 407–409
of mandibular third molar away from inferior alveolar canal 409, 410–412
uprighting mesioangulated impacted mandibular second molars 402–405
vertical dimension, of orthodontic temporary anchorage devices 12, 15–18
vertically impacted mandibular second molars, orthodontic traction of 405, 406–407
vital structures
inferior alveolar nerve and buccal shelf of mandibular buccal region 369, 371
in interradicular sites of mandibular buccal region 341–342
maxillary palatal region 246–248
midpalatal suture 298
paramedian sites 272–273
vitallium 2

w

width, bone
about 37, 38, 40–42
as a hard tissue factor
of interradicular sites of mandibular labial region 307, 310–311
of interradicular sites of maxillary buccal region 151, 153, 152–154
of interradicular sites of maxillary labial region 100–102, 102, 103, 104, 105
of maxillary palatal region 241, 243, 242, 243, 244

t.me/Dr_Mouayyad_AlbtousH